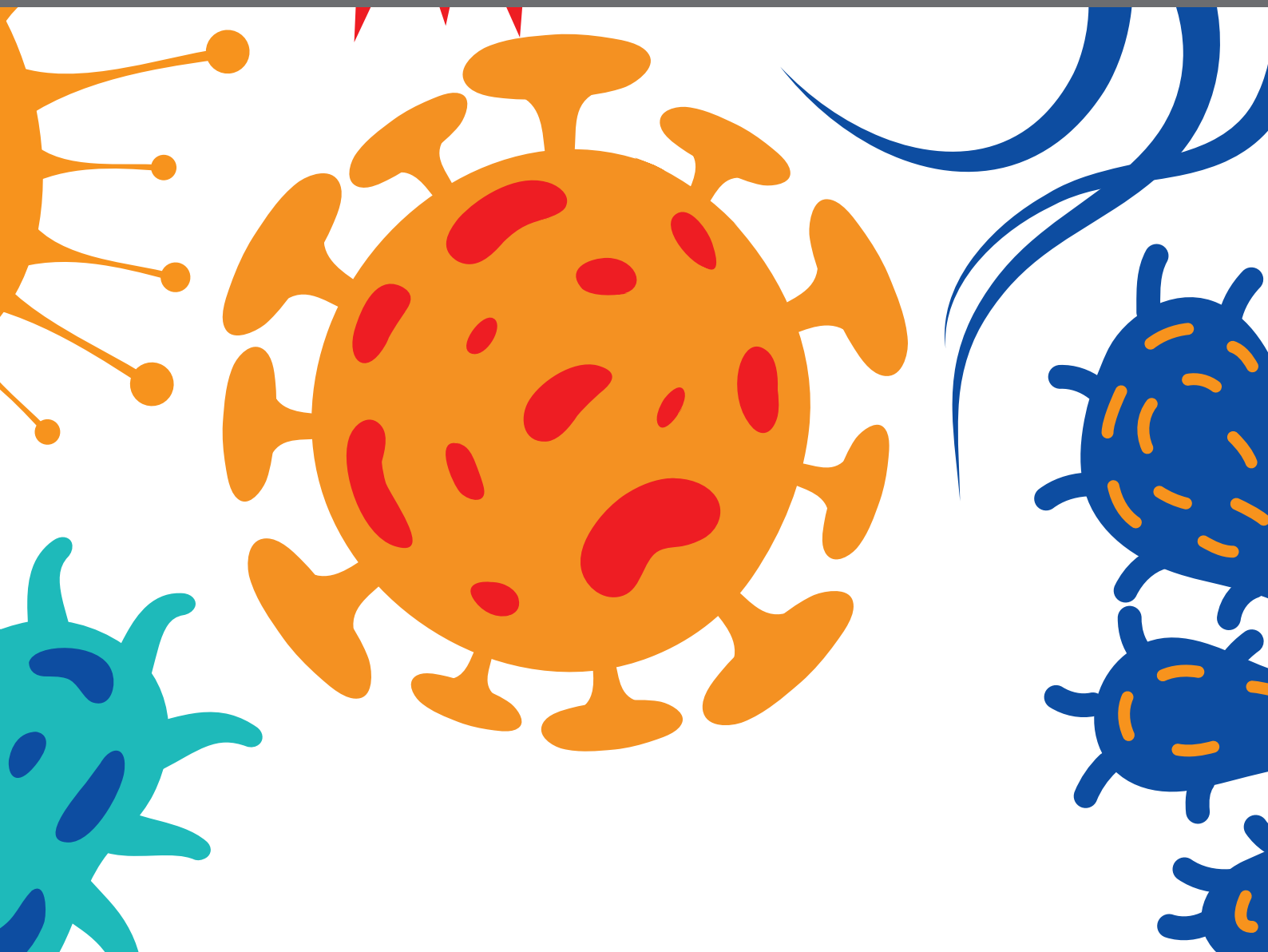




BEYOND ANTIMICROBIALS: NON-TRADITIONAL APPROACHES TO COMBATING MULTIDRUG-RESISTANT BACTERIA

EDITED BY: Natalia V. Kirienko, Laurence Rahme and You-Hee Cho
PUBLISHED IN: *Frontiers in Cellular and Infection Microbiology* and
Frontiers in Microbiology





frontiers

Frontiers eBook Copyright Statement

The copyright in the text of individual articles in this eBook is the property of their respective authors or their respective institutions or funders. The copyright in graphics and images within each article may be subject to copyright of other parties. In both cases this is subject to a license granted to Frontiers.

The compilation of articles constituting this eBook is the property of Frontiers.

Each article within this eBook, and the eBook itself, are published under the most recent version of the Creative Commons CC-BY licence.

The version current at the date of publication of this eBook is CC-BY 4.0. If the CC-BY licence is updated, the licence granted by Frontiers is automatically updated to the new version.

When exercising any right under the CC-BY licence, Frontiers must be attributed as the original publisher of the article or eBook, as applicable.

Authors have the responsibility of ensuring that any graphics or other materials which are the property of others may be included in the CC-BY licence, but this should be checked before relying on the CC-BY licence to reproduce those materials. Any copyright notices relating to those materials must be complied with.

Copyright and source acknowledgement notices may not be removed and must be displayed in any copy, derivative work or partial copy which includes the elements in question.

All copyright, and all rights therein, are protected by national and international copyright laws. The above represents a summary only. For further information please read Frontiers' Conditions for Website Use and Copyright Statement, and the applicable CC-BY licence.

ISSN 1664-8714

ISBN 978-2-88963-256-5

DOI 10.3389/978-2-88963-256-5

About Frontiers

Frontiers is more than just an open-access publisher of scholarly articles: it is a pioneering approach to the world of academia, radically improving the way scholarly research is managed. The grand vision of Frontiers is a world where all people have an equal opportunity to seek, share and generate knowledge. Frontiers provides immediate and permanent online open access to all its publications, but this alone is not enough to realize our grand goals.

Frontiers Journal Series

The Frontiers Journal Series is a multi-tier and interdisciplinary set of open-access, online journals, promising a paradigm shift from the current review, selection and dissemination processes in academic publishing. All Frontiers journals are driven by researchers for researchers; therefore, they constitute a service to the scholarly community. At the same time, the Frontiers Journal Series operates on a revolutionary invention, the tiered publishing system, initially addressing specific communities of scholars, and gradually climbing up to broader public understanding, thus serving the interests of the lay society, too.

Dedication to Quality

Each Frontiers article is a landmark of the highest quality, thanks to genuinely collaborative interactions between authors and review editors, who include some of the world's best academicians. Research must be certified by peers before entering a stream of knowledge that may eventually reach the public - and shape society; therefore, Frontiers only applies the most rigorous and unbiased reviews. Frontiers revolutionizes research publishing by freely delivering the most outstanding research, evaluated with no bias from both the academic and social point of view. By applying the most advanced information technologies, Frontiers is catapulting scholarly publishing into a new generation.

What are Frontiers Research Topics?

Frontiers Research Topics are very popular trademarks of the Frontiers Journals Series: they are collections of at least ten articles, all centered on a particular subject. With their unique mix of varied contributions from Original Research to Review Articles, Frontiers Research Topics unify the most influential researchers, the latest key findings and historical advances in a hot research area! Find out more on how to host your own Frontiers Research Topic or contribute to one as an author by contacting the Frontiers Editorial Office: researchtopics@frontiersin.org

BEYOND ANTIMICROBIALS: NON-TRADITIONAL APPROACHES TO COMBATING MULTIDRUG-RESISTANT BACTERIA

Topic Editors:

Natalia V. Kirienko, Rice University, United States

Laurence Rahme, Massachusetts General Hospital, Harvard Medical School, United States

You-Hee Cho, CHA University, South Korea

Citation: Kirienko, N. V., Rahme, L., Cho, Y.-H., eds. (2019). Beyond Antimicrobials: Non-Traditional Approaches to Combating Multidrug-Resistant Bacteria. Lausanne: Frontiers Media SA. doi: 10.3389/978-2-88963-256-5

Table of Contents

- 05 Editorial: Beyond Antimicrobials: Non-traditional Approaches to Combating Multidrug-Resistant Bacteria**
Natalia V. Kirienko, Laurence Rahme and You-Hee Cho
- 10 Novel Iron-Chelator DIBI Inhibits Staphylococcus aureus Growth, Suppresses Experimental MRSA Infection in Mice and Enhances the Activities of Diverse Antibiotics in vitro**
Maria del Carmen Parquet, Kimberley A. Savage, David S. Allan, Ross J. Davidson and Bruce E. Holbein
- 21 Attenuation of Listeria monocytogenes Virulence by Cannabis sativa L. Essential Oil**
Emanuela Marini, Gloria Magi, Gianna Ferretti, Tiziana Bacchetti, Angelica Giuliani, Armanda Pugnaroni, Maria Rita Rippo and Bruna Facinelli
- 32 Antibiofilm and Antivirulence Activities of 6-Gingerol and 6-Shogaol Against Candida albicans Due to Hyphal Inhibition**
Jin-Hyung Lee, Yong-Guy Kim, Pilju Choi, Jungyeob Ham, Jae Gyu Park and Jintae Lee
- 42 Sarconesin: Sarconesiopsis magellanica Blowfly Larval Excretions and Secretions With Antibacterial Properties**
Andrea Díaz-Roa, Manuel A. Patarroyo, Felio J. Bello and Pedro I. Da Silva Jr.
- 55 Lectin-Like Bacteriocins**
Maarten G. K. Ghequire, Başak Öztürk and René De Mot
- 66 Zinc Blockade of SOS Response Inhibits Horizontal Transfer of Antibiotic Resistance Genes in Enteric Bacteria**
John K. Crane, Muhammad B. Cheema, Michael A. Olyer and Mark D. Sutton
- 78 Morin Protects Channel Catfish From Aeromonas hydrophila Infection by Blocking Aerolysin Activity**
Jing Dong, Yongtao Liu, Ning Xu, Qiuhong Yang and Xiaohui Ai
- 87 Artificial Activation of Escherichia coli mazEF and hipBA Toxin–Antitoxin Systems by Antisense Peptide Nucleic Acids as an Antibacterial Strategy**
Marcin Równicki, Tomasz Pierńko, Jakub Czarnecki, Monika Kolanowska, Dariusz Bartosik and Joanna Trylska
- 99 Improved Biodistribution and Extended Serum Half-Life of a Bacteriophage Endolysin by Albumin Binding Domain Fusion**
Johan Seijnsing, Anna M. Sobieraj, Nadia Keller, Yang Shen, Annelies S. Zinkernagel, Martin J. Loessner and Mathias Schmelcher
- 108 In vitro and in vivo Inhibitory Activity of NADPH Against the AmpC β -Lactamase**
Jung-Hyun Na, Tae Hee Lee, Soo-Bong Park, Min-Kyu Kim, Bo-Gyeong Jeong, Kyung Min Chung and Sun-Shin Cha
- 116 Itaconimides as Novel Quorum Sensing Inhibitors of Pseudomonas aeruginosa**
Judy Fong, Kim T. Mortensen, Amalie Nørskov, Katrine Qvortrup, Liang Yang, Choon Hong Tan, Thomas E. Nielsen and Michael Givskov

- 127 ***A Novel Phage PD-6A3, and its Endolysin Ply6A3, With Extended Lytic Activity Against Acinetobacter baumannii***
Minle Wu, Kongying Hu, Youhua Xie, Yili Liu, Di Mu, Huimin Guo, Zhifan Zhang, Yingcong Zhang, Dong Chang and Yi Shi
- 139 ***Corrigendum: A Novel Phage PD-6A3, and its Endolysin Ply6A3, With Extended Lytic Activity Against Acinetobacter baumannii***
Minle Wu, Kongying Hu, Youhua Xie, Yili Liu, Di Mu, Huimin Guo, Zhifan Zhang, Yingcong Zhang, Dong Chang and Yi Shi
- 140 ***Novel Pyoverdine Inhibitors Mitigate Pseudomonas aeruginosa Pathogenesis***
Daniel R. Kirienko, Donghoon Kang and Natalia V. Kirienko
- 154 ***Exploiting the Richness of Environmental Waterborne Bacterial Species to Find Natural Legionella pneumophila Competitors***
Marie-Hélène Corre, Vincent Delafont, Anastasia Legrand, Jean-Marc Berjeaud and Julien Verdon
- 165 ***Drug Repurposing for the Treatment of Bacterial and Fungal Infections***
Andrea Miró-Canturri, Rafael Ayerbe-Algaba and Younes Smani
- 177 ***Redirecting an Anticancer to an Antibacterial Hit Against Methicillin-Resistant Staphylococcus aureus***
Hye-Jeong Jang, In-Young Chung, Changjin Lim, Sungkyun Chung, Bi-o Kim, Eun Sook Kim, Seok-Ho Kim and You-Hee Cho
- 186 ***Activity and Impact on Resistance Development of Two Antivirulence Fluoropyrimidine Drugs in Pseudomonas aeruginosa***
Francesco Imperi, Ersilia V. Fiscarelli, Daniela Visaggio, Livia Leoni and Paolo Visca
- 197 ***Recent Advances in Anti-virulence Therapeutic Strategies With a Focus on Dismantling Bacterial Membrane Microdomains, Toxin Neutralization, Quorum-Sensing Interference and Biofilm Inhibition***
Osmel Fleitas Martinez, Marlon Henrique Cardoso, Suzana Meira Ribeiro and Octavio Luiz Franco
- 221 ***Activity of a Synthetic Peptide Targeting MgtC on Pseudomonas aeruginosa Intramacrophage Survival and Biofilm Formation***
Malika Moussouni, Pauline Nogaret, Preeti Garai, Bérengère Ize, Eric Vivès and Anne-Béatrice Blanc-Potard
- 231 ***Application of Antimicrobial Peptides of the Innate Immune System in Combination With Conventional Antibiotics—A Novel Way to Combat Antibiotic Resistance?***
Maria S. Zharkova, Dmitriy S. Orlov, Olga Yu. Golubeva, Oleg B. Chakchir, Igor E. Eliseev, Tatyana M. Grinchuk and Olga V. Shamova
- 254 ***3-Benzyl-Hexahydro-Pyrrolo[1,2-a]Pyrazine-1,4-Dione Extracted From Exiguobacterium indicum Showed Anti-biofilm Activity Against Pseudomonas aeruginosa by Attenuating Quorum Sensing***
Vijay K. Singh, Avinash Mishra and Bhavanath Jha
- 268 ***The Anti-virulence Efficacy of 4-(1,3-Dimethyl-2,3-Dihydro-1H-Benzimidazol-2-yl)Phenol Against Methicillin-Resistant Staphylococcus aureus***
Nagendran Tharmalingam, Rajamohammed Khader, Beth Burgwyn Fuchs and Eleftherios Mylonakis



Editorial: Beyond Antimicrobials: Non-traditional Approaches to Combating Multidrug-Resistant Bacteria

Natalia V. Kirienko^{1*}, Laurence Rahme^{2,3,4} and You-Hee Cho^{5*}

¹ Department of BioSciences, Rice University, Houston, TX, United States, ² Department of Surgery, Massachusetts General Hospital, Harvard Medical School, Boston, MA, United States, ³ Department of Microbiology, Harvard Medical School, Boston, MA, United States, ⁴ Shriners Hospitals for Children Boston, Boston, MA, United States, ⁵ Department of Pharmacy, College of Pharmacy and Institute of Pharmaceutical Sciences, CHA University, Seongnam, South Korea

Keywords: antivirulence, phage (bacteriophage), antimicrobial peptide (AMP), quorum sensing (QS), antimicrobial resistance (AMR), novel therapeutic agents, drug repurposing and repositioning

Editorial on the Research Topic

Beyond Antimicrobials: Non-traditional Approaches to Combating Multidrug-Resistant Bacteria

OPEN ACCESS

Edited and reviewed by:

Nahed Ismail,
University of Illinois at Chicago,
United States

*Correspondence:

Natalia V. Kirienko
kirienko@rice.edu
You-Hee Cho
youhee@cha.ac.kr

Specialty section:

This article was submitted to
Clinical Microbiology,
a section of the journal
Frontiers in Cellular and Infection
Microbiology

Received: 06 September 2019

Accepted: 24 September 2019

Published: 11 October 2019

Citation:

Kirienko NV, Rahme L and Cho Y-H
(2019) Editorial: Beyond
Antimicrobials: Non-traditional
Approaches to Combating
Multidrug-Resistant Bacteria.
Front. Cell. Infect. Microbiol. 9:343.
doi: 10.3389/fcimb.2019.00343

Since the time of Galen and Hippocrates, medicine has had a slow progression, with each new advance improving the length and quality of patients' lives. By the nineteenth century, medical science had even begun to understand the concept of vaccinations and had started to make substantial inroads into the prevention of communicable diseases. Despite this, diagnosis with a bacterial infection frequently remained tantamount to a death sentence. With treatment essentially limited to supportive care, patients were left to either recover or die. But in the twentieth century, the discovery of antimicrobials changed this. It is not an overstatement to say that medical science changed forever, because this allowed the development of countless medical advances that fall under the classification of internal medicine. Ranging from simple surgeries like the removal of an inflamed appendix to the complete replacement of whole organs and organ systems, not to mention the placement of various medical devices that have improved the lives of countless patients.

Despite this, infectious diseases, including those caused by bacteria, remain the leading cause of premature death worldwide. Problematically, this trend looks as though it will worsen, as both the number and the proportion of clinically relevant bacterial strains and species exhibiting antimicrobial resistance is on the rise. For the ESKAPE pathogens (i.e., *Enterococcus faecium*, *Staphylococcus aureus*, *Klebsiella pneumoniae*, *Acinetobacter baumannii*, *Pseudomonas aeruginosa*, and *Enterobacter* spp.), not only are single and multidrug resistance common, but pandrug resistance has begun to be clinically observed (Mulani et al., 2019). Overall, for the first time in nearly a century, the spread of antimicrobial resistance has begun to lead to regressions in treatment options and the re-emergence of formerly treatable infections as real threats to community health. While the public remains largely complacent to the threat, experts in healthcare warn of the "galloping hoofbeats of the horsemen of the apocalypse" and the very real possibility that voluntary medical procedures will become a historical phenomenon within the next century, even in the developed world (Projan, 2003).

Further complicating matters, antimicrobial drug discovery has dramatically slowed over the last 20 years, with a paucity of new treatments on the market or in development pipelines.

The most obvious problem is scientific. Using the same methods to screen the same libraries leads to the same treatments, which are now ineffective. Finding new methods and new libraries is one option, but it is laborious and requires a leap of faith that the new method will be effective. A more serious problem is economic (Ventola, 2015; Renwick and Mossialos, 2018). For large pharmaceutical companies, the return on investment for antimicrobials tends to be much lower than for lifestyle medicines, which are intended for disease maintenance rather than a cure. For antimicrobials, maintenance is often impractical or impossible. Moreover, identification, development, design, regulatory approval, and marketing are necessary steps for a large pharmaceutical corporation to get a new treatment into clinics for patients. These steps can take from 5 to 20 years. Meanwhile, antimicrobial resistance frequently arises in less than five, particularly when antimicrobial stewardship (i.e., limiting antimicrobial use to last-ditch cases, preventing agricultural or household cleaner use, etc.) is not stringently maintained (Rice, 2018). Worse yet, pricing for antibiotics tends to be lower than for other drugs that have such outsized impacts on morbidity and mortality (e.g., cancer drugs). Finally, the same stewardship programs limit antibacterial use to prolong clinical utility, also artificially curtailing the market size. Cumulatively, these effects result in a monetary loss for the company.

A final obstacle is the incredible regulatory hurdles, particularly in the US, that stand in the way of companies and organizations willing to take on the burden (Metlay et al., 2006). For example, due to the transience of bacterial infections, it is often difficult to find enough patients for large-scale human trials. Another difficulty is the approval process (particularly the US FDA, the EMA has been generally more tractable) that places an undue burden of proof on pharmaceutical companies (e.g., patients only qualify as having been successfully treated if the causative bacterium is identified in complex infections like bacterial pneumonia, difficulty in demonstrating superiority of new treatments to existing therapy instead of non-inferiority to current treatments, etc.). Regulatory and legislative efforts have been initiated in the past 15 years to combat these trends, but rectification has occurred at a glacial pace (Humphries et al., 2018; Sfeir, 2018).

Clearly, it behooves us to seek out alternative mechanisms of treatment to address this growing gap. Therefore, currently there is an increased interest in alternative approaches to the treatment of drug-resistant bacteria. A number of these strategies are presented in this Research Topic.

ANTI-VIRULENCE APPROACHES

To mitigate the resistance emergence, one increasingly viable option is the discovery and development of the therapeutic chemicals that target bacterial virulence, rather than bacterial growth. In most cases (with the notable exception of immune-related pathology activated by structural components), the mere presence of bacterial cells is insufficient to trigger disease. Instead, pathogenic microorganisms produce various virulence factors that are responsible for the damage inflicted on the host. There is

mounting evidence that these pathogenic determinants are viable pharmaceutical targets; treatments that compromising one or more of these factors (i.e., anti-virulence or antipathogenic) can often largely, or even completely, mitigate disease. Anti-virulence drugs should reduce antibiotic use and, ultimately, decrease the development of antibiotic resistance, as they should not impose strong selective pressure on bacteria that favors the evolution of mechanisms of resistance and persistence. Additionally, because they do not affect bacterial cell viability, they should not disrupt beneficial microbiota. Anti-virulence compounds could serve as alternatives or adjuncts to traditional antibiotics and to potentiate their efficacy, generating even more effective treatment options in particular against multi-drug resistant pathogens and potentially viable options against pan-drug resistant bacteria.

A number of articles utilizing this approach are reported in this Research Topic. One promising virulence-associated target is the quorum-sensing (QS) systems utilized by several clinically relevant pathogens (Rutherford and Bassler, 2012; Schuster et al., 2013; Castillo-Juarez et al., 2015). Singh et al. report on the inhibitory activity of 3-benzyl-hexahydro-pyrrolo[1,2-a]pyrazine-1,4-dione on QS in *Pseudomonas aeruginosa*. Interestingly, treatment also altered biofilm architecture, compromising bacterial adherence and biofilm development. Fong et al. report on itaconimide, another novel inhibitor of Pseudomonas QS and biofilm. Perhaps unsurprisingly, inhibition of biofilm formation is another common target for the development of anti-virulent compounds (Maura et al., 2016; Francois et al., 2017; Defoirdt, 2018; Salam and Quave, 2018). This approach can also be used against opportunistic fungi. For example, Lee et al. describe antibiofilm activity for 6-geringol and 6-shogaol against *Candida albicans*. These two molecules prevented cell aggregation and inhibited the expression of several biofilm-related genes.

Both QS signaling and biofilm contribute to chronic infections. They are associated with complex regulatory switches that control large numbers of genes whose activity alters the lifestyle of the pathogen to support long-term microbial presence within a host. This is in contrast to more stereotypically acute virulence determinants (e.g., the Type 3 Secretion System, proteases, lipases, toxins, etc.) that cause consequences for which microbial presence is less relevant. Dong et al. found that the flavonoid morin inhibits the hemolytic activity of aerolysin, protecting catfish from infection with *Aeromonas hydrophila*.

Generally, drug discovery attempts have targeted chronic virulence factors. A notable exception to this is the Pseudomonas siderophore pyoverdine. Unlike many acute virulence determinants, pyoverdine plays a diverse and multifactorial role in pathogenesis, including iron acquisition (necessary for production of other virulence factors, including biofilm, and for bacterial growth) and is a transcriptional regulator of several other virulence factors and toxins (Ochsner et al., 1996; Wilderman et al., 2001; Lamont et al., 2002). In addition, it is directly cytotoxic (Kang et al., 2018). Previously, preventing pyoverdine biosynthesis has been shown to attenuate virulence in a variety of hosts, including invertebrates and mice (Meyer et al., 1996; Takase et al., 2000; Minandri et al., 2016). Here, Imperi et al. examined the limitations of this approach by selecting for

P. aeruginosa mutants resistant to one class of these inhibitors, fluoropyrimidines (Imperi et al., 2013; Kirienko et al., 2016). To circumvent this form of resistance, Kirienko et al. identified small molecules that directly inhibit pyoverdine function, rather than its production. Interestingly, these molecules are also effective against multidrug-resistant isolates of *P. aeruginosa* collected from patients with cystic fibrosis (Kang et al., 2019).

Frequently the strongest effects for anti-virulence molecule are in combination with other treatments. For example, Tharmalingam et al. demonstrated that 4-(1,3-dimethyl-2,3-dihydro-1H-S-benzimidazol-2-yl)phenol (BIP) inhibited several virulence factors of methicillin-resistant *Staphylococcus aureus* (MRSA). BIP treatment decreased MRSA virulence and sensitized bacteria to macrophage-dependent killing. Marini et al. showed that *Cannabis sativa* extracts reduced motility and biofilm formation in the food-borne pathogen *Listeria monocytogenes*. Martínez et al. reviewed a number of promising anti-virulence strategies, including disassembly of functional microdomains in bacterial membranes and toxin neutralization.

ALTERNATIVE APPROACHES: DRUG REPURPOSING, COMBINATION THERAPIES, AND NON-CONVENTIONAL BACTERICIDES

Regulatory hurdles are another stumbling block in drug discovery. Researchers have begun to propose and implement innovative strategies to practically reduce time and costs for the drug development processes. Repositioning or repurposing already approved drugs is an approach that has recently gained momentum, with the hypothesis being that the compounds may have new modes of action for which the resistance has yet to develop. Similarly, combining two or more compounds with different or synergistic mechanisms is another alternative approach to improve the efficacy of the currently available antibiotic regimens and may increase the success rate of drug repositioning as well.

In this collection, Miró-Canturri et al. reviewed the current state of knowledge regarding drug repurposing strategies for the treatment of bacterial and fungal infections. They focus on several successfully repurposed drugs, including former antihelminthic, anticancer, anti-inflammatory, immunomodulatory, and even psychopharmaceutical compounds. They have summarized their mechanisms and the status of on-going clinical trials for repurposed drugs like meloxicam, a widely available non-steroid anti-inflammatory drug. A different strategy, called drug redirecting, has been proposed by Jang et al. This strategy involves modifying a previously established chemical moiety to change its selectivity. Their example used an apoptotic inhibitor, YM155, that generates reactive-oxygen species upon entry into the target cells. By changing the substituents at the N3 position, they have optimized the antibacterial efficacy, possibly by selectively targeting the drug to Gram-positive bacterial cells, including MRSA.

Drug combination can improve treatment efficacy and reduce drug dosages to minimize side effects, as exemplified in the combination of β -lactams (e.g., clavulanic acid and amoxicillin or ticarcillin; Salerno and Cazzaniga, 2010). In this Research Topic, Na et al. investigated the inhibitory activity of a cellular metabolite, NADPH on the class C β -lactamases such as AmpC BER. Based on their previous study (Na et al., 2017), they presented a molecular docking model indicating that this dinucleotide could bind AmpC BER. Combination of NADPH with ceftazidime successfully restored sensitivity to ceftazidime-resistant bacteria in an experimental murine infection. Strengths of this approach include that it may not require new chemical discovery and may be combined with repurposing or repositioning efforts as well.

del Carmen Parquet et al. showed that an iron-chelating polymer (DIBI) suppressed a wound infection caused by MRSA. This makes intuitive sense, as iron is essential for microbial growth and survival. DIBI also increased the bactericidal activity of several antibiotics. DIBI also inhibits the growth of *Candida albicans* and increases its sensitivity to azole drugs *in vitro* and *in vivo* (Savage et al., 2018).

Another transition metal discussed here is zinc. Interestingly, Crane et al. report a surprising role for zinc in preventing the SOS response, which is required for the hypermutation-mediated generation of antibiotic resistance and the horizontal transfer of resistance genes. Both zinc acetate and zinc pyrithione were effective, with the latter being more active. This suggests another approach to mitigate bacterial resistance may be to compromise the pathways that generate it.

PHAGE-BASED APPROACHES

Recent advances in biotechnology have begun to allow the design, development, and production of new biologics with several advantages over chemical therapies. These include greater safety, potency, and specificity, potentially leading to fewer side effects. One “bioantibacterial” approach increasingly drawing favor is to revive the exploration of bacteriophages (phages) (Kim et al., 2019). The ability of phages to amplify at the site of infection and to cause the death and lysis of their bacterial targets makes it so that they can specifically eliminate an infectious bacterial strain or species without affecting the host microbiota (Abedon and Thomas-Abedon, 2010). In addition, as hosts develop resistance, phages may be able to evolve in concert to maintain their efficacy. Phages show substantial promise in a number of ways (Gorski et al., 2019; Hansen et al., 2019). One strategy practically at hand is to harness the endolysins produced by phages to degrade bacterial cell walls. For example, Wu et al. showed that the novel phage PD-6A3, and its purified endolysin Ply6A3, mitigated murine sepsis in approximately one-third of cases where clinical multi-drug resistant strains of *Acinetobacter baumannii* were tested. Seijns et al. showed that extending serum retention time, such as by fusing an albumin-binding domain to the LysK endolysin from *S. aureus* phage improved efficiency.

OTHER BIO-ANTIBACTERIAL APPROACHES

In addition to the phage-based therapies mentioned above, efforts to harness naïve or engineered antimicrobial peptides (AMPs) for clinical use have been accelerating. AMPs are generally short, positively-charged peptides that contribute to the innate immune systems of a wide variety of life forms. AMPs are conventionally thought to kill microbial pathogens directly by targeting membrane functions. Unfortunately, they are also toxic toward host cells, limiting their clinical use. Research teams are currently evaluating AMPs in clinical trials as novel anti-infectives and as immunomodulators and promoters of wound healing. Here, Zharkova et al. reported that mammalian AMPs can synergize with a variety of conventional antibiotics, including fluoroquinolones, polyketides, aminoglycosides, and β -lactams. This limits the amount of AMP needed for effective treatment, and may reduce off-target effects.

Díaz-Roa et al. report identification and characterization of an AMP isolated from a necrophagous larvae, *Sarconesiopsis magellanica*. Sarconesin, as they dubbed it, showed no sign of cytotoxicity to mammalian cells and appears to increase permeability of the target membranes and bind to DNA. Moussouni et al. present a proof-of-concept study that leverages a rationally-designed synthetic version of MgtR that targets MgtC, a virulence factor required for intracellular survival of *Salmonella* and *Mycobacterium* species (Belon et al., 2015). They showed that synthetic MgtR (based on the *Salmonella* version of the protein) compromises the function of MgtC in *P. aeruginosa*, suppressing intracellular survival and biofilm formation.

Bacteriocins are another natural product produced by bacteria to limit competition in their natural environment. These peptides are often used in a form of chemical warfare against closely related species, giving them substantial potential for development as a therapy. Ghequire et al. reviewed the therapeutic potential of one class of these proteins, lectin-like bacteriocins, or Llp, which are produced by Gram-negative proteobacteria. Unlike most bacteriocins, Llp appear to catalyze killing from the cell surface instead of requiring internalization. This trait will be useful if they are leveraged as a treatment for *Pseudomonads*, which have active export pumps that may limit the efficacy of an imported toxin.

Corre et al. used a similar approach to identify effective natural products for limiting the growth of *Legionella pneumophila*. By testing over 250 culturable bacterial isolates, they found a surprising variety of organisms that effectively limited *L.*

pneumophila growth. Although this approach, which harnesses the natural competition in the bacterial microenvironment, is not unknown, it is very effective when looking for new treatments that are more specific than have been sought in the past.

Finally, Równicki et al., describe the design and study of a peptide nucleic acid (PNA)-based treatment that exploits the MazEF-HipBA toxin-antitoxin systems in *E. coli*. They show that antisense PNAs could effectively repress translation of the antitoxin, causing bacterial death. They also showed that antisense PNAs could be used to stimulate the expression of the toxin-antitoxin system in the first place, improving the utility of the treatment. Promisingly, antisense PNAs did not seem to activate strong cytotoxicity in mammalian cells, although the effect of PNA-mRNA hybrids on the activation of the interferon response, the difficulties in delivery of PNAs into cells, and the ease of antimicrobial resistance emergence against a nucleotide-hybridization-based treatment remain concerns.

CONCLUSIONS

Although the threat of antimicrobial resistance is substantial, myriad approaches to circumvent it are currently being researched. These include classical approaches, such as searching for natural products in the environment of the pathogen and more synthetic attempts, like the discovery of new compounds with previously unknown mechanisms, rationally-mutated bacterial toxins, or even small molecules designed *ab initio* based on virtual docking screens. If some of these methods can successfully translate to therapeutic options, the bacteriological apocalypse may yet be averted.

AUTHOR CONTRIBUTIONS

All authors listed have made a substantial, direct and intellectual contribution to the work, and approved it for publication.

FUNDING

Y-HC received funding from the National Research Foundation of Korea (NRF-2017M3A9E3077204). NK, a CPRIT scholar in Cancer Research, thanks the Cancer Prevention and Research Institute of Texas (CPRIT) for their generous support, CPRIT grant RR150044. This work was also supported by the National Institutes of Health (NIAID K22AI110552 and NIGMS R35GM129294 to NK and NIAIDR01AI134857 to LR) and the Welch Foundation (C-1930 to NK).

REFERENCES

- Abedon, S. T., and Thomas-Abedon, C. (2010). Phage therapy pharmacology. *Curr. Pharm. Biotechnol.* 11, 28–47. doi: 10.2174/138920110790725410
- Belon, C., Soscia, C., Bernut, A., Laubier, A., Bleves, S., and Blanc-Potard, A. B. (2015). A macrophage subversion factor is shared by intracellular and extracellular pathogens. *PLoS Pathog.* 11:e1004969. doi: 10.1371/journal.ppat.1004969
- Castillo-Juarez, I., Maeda, T., Mandujano-Tinoco, E. A., Tomas, M., Perez-Eretza, B., Garcia-Contreras, S. J., et al. (2015). Role of quorum sensing in bacterial infections. *World J. Clin. Cases* 3, 575–598. doi: 10.12998/wjcc.v3.i7.575
- Defoidt, T. (2018). Quorum-sensing systems as targets for antiviral therapy. *Trends Microbiol.* 26, 313–328. doi: 10.1016/j.tim.2017.10.005
- Francois, B., Luyt, C. E., Stover, C. K., Brubaker, J. O., Chastre, J., and Jafri, H. S. (2017). New strategies targeting virulence factors of *Staphylococcus aureus* and *Pseudomonas aeruginosa*. *Semin. Respir. Crit. Care Med.* 38, 346–358. doi: 10.1055/s-0037-1602715

- Gorski, A., Miedzybrodzki, R., Jonczyk-Matysiak, E., Borysowski, J., Letkiewicz, S., and Weber-Dabrowska, B. (2019). The fall and rise of phage therapy in modern medicine. *Expert Opin. Biol. Ther.* doi: 10.1080/14712598.2019.1651287. [Epub ahead of print].
- Hansen, M. F., Svenningsen, S. L., Roder, H. L., Middelboe, M., and Burmolle, M. (2019). Big impact of the tiny: bacteriophage-bacteria interactions in biofilms. *Trends Microbiol.* 27, 739–752. doi: 10.1016/j.tim.2019.04.006
- Humphries, R. M., Ferraro, M. J., and Hindler, J. A. (2018). Impact of 21st Century cures act on breakpoints and commercial antimicrobial susceptibility test systems: progress and pitfalls. *J. Clin. Microbiol.* 56:e00139–18. doi: 10.1128/JCM.00139-18.
- Imperi, F., Massai, F., Facchini, M., Frangipani, E., Visaggio, D., Leoni, L., et al. (2013). Repurposing the antimycotic drug flucytosine for suppression of *Pseudomonas aeruginosa* pathogenicity. *Proc. Natl. Acad. Sci. U.S.A.* 110, 7458–7463. doi: 10.1073/pnas.1222706110
- Kang, D., Kirienko, D. R., Webster, P., Fisher, A. L., and Kirienko, N. V. (2018). Pyoverdine, a siderophore from *Pseudomonas aeruginosa*, translocates into *C. elegans*, removes iron, and activates a distinct host response. *Virulence* 9, 804–817. doi: 10.1080/21505594.2018.1449508
- Kang, D., Revtovich, A. V., Chen, Q., Shah, K. N., Cannon, C. L., and Kirienko, N. V. (2019). Pyoverdine-dependent virulence of *Pseudomonas aeruginosa* isolates from cystic fibrosis. *Front. Microbiol.* 10:2048. doi: 10.3389/fmicb.2019.02048
- Kim, B. O., Kim, E. S., Yoo, Y. J., Bae, H. W., Chung, I. Y., and Cho, Y. H. (2019). Phage-derived antibacterials: harnessing the simplicity, plasticity, and diversity of phages. *Viruses* 11:E268. doi: 10.3390/v11030268
- Kirienko, D. R., Revtovich, A. V., and Kirienko, N. V. (2016). A high-content, phenotypic screen identifies fluorouridine as an inhibitor of pyoverdine biosynthesis and *Pseudomonas aeruginosa* virulence. *mSphere* 1:e00217-16. doi: 10.1128/mSphere.00217-16
- Lamont, I. L., Beare, P. A., Ochsner, U., Vasil, A. I., and Vasil, M. L. (2002). Siderophore-mediated signaling regulates virulence factor production in *Pseudomonas aeruginosa*. *Proc. Natl. Acad. Sci. U.S.A.* 99, 7072–7077. doi: 10.1073/pnas.092016999
- Maura, D., Ballok, A. E., and Rahme, L. G. (2016). Considerations and caveats in anti-virulence drug development. *Curr. Opin. Microbiol.* 33, 41–46. doi: 10.1016/j.mib.2016.06.001
- Metlay, J. P., Powers, J. H., Dudley, M. N., Christiansen, K., and Finch, R. G. (2006). Antimicrobial drug resistance, regulation, and research. *Emerging Infect. Dis.* 12, 183–190. doi: 10.3201/eid1202.050078
- Meyer, J. M., Neely, A., Stintzi, A., Georges, C., and Holder, I. A. (1996). Pyoverdine is essential for virulence of *Pseudomonas aeruginosa*. *Infect. Immun.* 64, 518–523.
- Minandri, F., Imperi, F., Frangipani, E., Bonchi, C., Visaggio, D., Facchini, M., et al. (2016). Role of iron uptake systems in *Pseudomonas aeruginosa* virulence and airway infection. *Infect. Immun.* 84, 2324–2335. doi: 10.1128/IAI.0098-16
- Mulani, M. S., Kamble, E. E., Kumkar, S. N., Tawre, M. S., and Pardesi, K. R. (2019). Emerging strategies to combat ESKAPE pathogens in the era of antimicrobial resistance: a review. *Front. Microbiol.* 10:539. doi: 10.3389/fmicb.2019.00539
- Na, J. H., An, Y. J., and Cha, S. S. (2017). GMP and IMP are competitive inhibitors of CMY-10, an extended-spectrum class C beta-lactamase. *Antimicrob. Agents Chemother.* 61:e00098–17. doi: 10.1128/AAC.00098-17
- Ochsner, U. A., Johnson, Z., Lamont, I. L., Cunliffe, H. E., and Vasil, M. L. (1996). Exotoxin A production in *Pseudomonas aeruginosa* requires the iron-regulated pvdS gene encoding an alternative sigma factor. *Mol. Microbiol.* 21, 1019–1028. doi: 10.1046/j.1365-2958.1996.481425.x
- Projan, S. J. (2003). Why is big Pharma getting out of antibacterial drug discovery? *Curr. Opin. Microbiol.* 6, 427–430. doi: 10.1016/j.mib.2003.08.003
- Renwick, M., and Mossialos, E. (2018). What are the economic barriers of antibiotic R&D and how can we overcome them? *Expert Opin. Drug Discov.* 13, 889–892. doi: 10.1080/17460441.2018.1515908
- Rice, L. B. (2018). Antimicrobial stewardship and antimicrobial resistance. *Med. Clin. North Am.* 102, 805–818. doi: 10.1016/j.mcna.2018.04.004
- Rutherford, S. T., and Bassler, B. L. (2012). Bacterial quorum sensing: its role in virulence and possibilities for its control. *Cold Spring Harb. Perspect. Med.* 2:a012427. doi: 10.1101/cshperspect.a012427
- Salam, A. M., and Quave, C. L. (2018). Targeting virulence in *Staphylococcus aureus* by chemical inhibition of the accessory gene regulator system *in vivo*. *mSphere* 3:e00500–17. doi: 10.1128/mSphere.00500-17
- Salerno, F., and Cazzaniga, M. (2010). Therapeutic strategies and emergence of multiresistant bacterial strains. *Intern. Emerg. Med.* 5(Suppl. 1), S45–S51. doi: 10.1007/s11739-010-0447-9
- Savage, K. A., Parquet, M. C., Allan, D. S., Davidson, R. J., Holbein, B. E., Lilly, E. A., et al. (2018). Iron restriction to clinical isolates of *Candida albicans* by the novel chelator DIBI inhibits growth and increases sensitivity to azoles *in vitro* and *in vivo* in a murine model of experimental vaginitis. *Antimicrob. Agents Chemother.* 62:e02576–17. doi: 10.1128/AAC.02576-17
- Schuster, M., Sexton, D. J., Diggle, S. P., and Greenberg, E. P. (2013). Acyl-homoserine lactone quorum sensing: from evolution to application. *Annu. Rev. Microbiol.* 67, 43–63. doi: 10.1146/annurev-micro-092412-155635
- Sfeir, M. M. (2018). The GAIN Act legislation to combat antimicrobial resistance: where do we stand? *Infect. Control Hosp. Epidemiol.* 39, 1499–1500. doi: 10.1017/ice.2018.252
- Takase, H., Nitani, H., Hoshino, K., and Otani, T. (2000). Impact of siderophore production on *Pseudomonas aeruginosa* infections in immunosuppressed mice. *Infect Immun* 68, 1834–1839. doi: 10.1128/IAI.68.4.1834-1839.2000
- Ventola, C. L. (2015). The antibiotic resistance crisis: part 1: causes and threats. *P T* 40, 277–283. doi: 10.1007/978-1-4614-6435-8_102103-1
- Wilderman, P. J., Vasil, A. I., Johnson, Z., Wilson, M. J., Cunliffe, H. E., Lamont, I. L., et al. (2001). Characterization of an endoprotease (PrpL) encoded by a PvdS-regulated gene in *Pseudomonas aeruginosa*. *Infect. Immun.* 69, 5385–5394. doi: 10.1128/IAI.69.9.5385-5394.2001

Conflict of Interest: The authors declare that the research was conducted in the absence of any commercial or financial relationships that could be construed as a potential conflict of interest.

Copyright © 2019 Kirienko, Rahme and Cho. This is an open-access article distributed under the terms of the Creative Commons Attribution License (CC BY). The use, distribution or reproduction in other forums is permitted, provided the original author(s) and the copyright owner(s) are credited and that the original publication in this journal is cited, in accordance with accepted academic practice. No use, distribution or reproduction is permitted which does not comply with these terms.



Novel Iron-Chelator DIBI Inhibits *Staphylococcus aureus* Growth, Suppresses Experimental MRSA Infection in Mice and Enhances the Activities of Diverse Antibiotics *in vitro*

Maria del Carmen Parquet¹, Kimberley A. Savage¹, David S. Allan¹, Ross J. Davidson^{2,3} and Bruce E. Holbein^{1,2*}

¹ Chelation Partners Inc., Halifax, NS, Canada, ² Department of Microbiology & Immunology, Dalhousie University, Halifax, NS, Canada, ³ Queen Elizabeth II Health Sciences Centre, Nova Scotia Health Authority, Halifax, NS, Canada

OPEN ACCESS

Edited by:

Natalia V. Kirienko,
Rice University, United States

Reviewed by:

Andreas F. Haag,
University of Glasgow,
United Kingdom
Timothy J. Foster,
Trinity College, Dublin, Ireland
Manfred Nairz,
Innsbruck Medical University, Austria

*Correspondence:

Bruce E. Holbein
beholbein@sympatico.ca

Specialty section:

This article was submitted to
Antimicrobials, Resistance
and Chemotherapy,
a section of the journal
Frontiers in Microbiology

Received: 17 May 2018

Accepted: 19 July 2018

Published: 14 August 2018

Citation:

Parquet MdC, Savage KA, Allan DS,
Davidson RJ and Holbein BE (2018)
Novel Iron-Chelator DIBI Inhibits
Staphylococcus aureus Growth,
Suppresses Experimental MRSA
Infection in Mice and Enhances
the Activities of Diverse Antibiotics
in vitro. *Front. Microbiol.* 9:1811.
doi: 10.3389/fmicb.2018.01811

DIBI, a purpose-designed hydroxypyridinone-containing iron-chelating antimicrobial polymer was studied for its anti-staphylococcal activities *in vitro* in comparison to deferiprone, the chemically related, small molecule hydroxypyridinone chelator. The sensitivities of 18 clinical isolates of *Staphylococcus aureus* from human, canine and bovine infections were determined. DIBI was strongly inhibitory to all isolates, displaying approximately 100-fold more inhibitory activity than deferiprone when compared on their molar iron-binding capacities. Sensitivity to DIBI was similar for both antibiotic-resistant and -sensitive isolates, including hospital- and community-acquired (United States 300) MRSA. DIBI inhibition was primarily bacteriostatic in nature at low concentration and was reversible by addition of Fe. DIBI also exhibited *in vivo* anti-infective activity in two distinct MRSA ATCC43300 infection and colonization models in mice. In a superficial skin wound infection model, topical application of DIBI provided a dose-dependent suppression of infection along with reduced wound inflammation. Intranasal DIBI reduced staphylococcal burden by >2 log in a MRSA nares carriage model. DIBI was also examined for its influence on antibiotic activities with a reference isolate ATCC6538, typically utilized to assess new antimicrobials. Sub-bacteriostatic concentrations of DIBI resulted in Fe-restricted growth and this physiological condition displayed increased sensitivity to GEN, CIP, and VAN. DIBI did not impair antibiotic activity but rather it enhanced overall killing. Importantly, recovery growth of survivors that typically followed an initial sub-MIC antibiotic killing phase was substantially suppressed by DIBI for each of the antibiotics examined. DIBI has promise for restricting staphylococcal infection on its own, regardless of the isolate's animal source or antibiotic resistance profile. DIBI also has potential for use in combination with various classes of currently available antibiotics to improve their responses.

Keywords: iron chelator, *Staphylococcus aureus*, DIBI, antibiotic, hydroxypyridinone, deferiprone

INTRODUCTION

Staphylococcus aureus is a normal colonizer of the skin and mucosal surfaces (e.g., nares) of around 30% of healthy humans but this opportunistic pathogen also causes a range of serious wound, lung and bloodstream infections (Liu, 2009; Tong et al., 2015). Staphylococci are also prevalent in animal infections. For example, up to 80% of clinical and subclinical cases of bovine mastitis involve *S. aureus* resulting in worldwide economic losses of US \$35B/year (Hamid et al., 2017). The staphylococci are also prevalent in various infections of companion animals such as with canine otitis where it along with closely related *S. pseudintermedius* have been found in >36% of all cases (De Martino et al., 2016). The growing spread of methicillin resistant *S. aureus* (MRSA) among humans (Tong et al., 2015; Ventola, 2015) and from animals in close contact with humans such as dogs (De Martino et al., 2016) dairy cattle or pigs (Vincze et al., 2014; Hamid et al., 2017) along with the significant mortality (14%) seen with invasive human MRSA infection has led to the designation of MRSA as a serious health threat (Frieden, 2013). The prospect for developing an effective staphylococcal vaccine appears to remain poor, possibly due in part to the wide range of infections involved with this microorganism (Proctor, 2012).

Given these various factors, our dependence on antibiotic therapy for staphylococcal infections of man and animals will likely continue. Thus, there is a need for new treatment approaches to deal with the MRSA threat (Frieden, 2013; Ventola, 2015). New anti-infectives that might work on their own or also in combination with antibiotics to improve efficacy, represent a new approach. In this regard, agents that target microbial iron acquisition have been recognized for their potential (Ballouche et al., 2009; Luo et al., 2014). Microbial pathogens have broad-based and irreplaceable needs for essential iron and they must obtain sufficient iron supplies from their host during infection. A key aspect of the vertebrate host's innate defense relates to restricting availability of iron to microbes during infection (Weinberg, 2009). The two interrelated aspects of microbial iron dependence and host iron limitation during infection provide good foundations for the potential use of iron sequestering anti-infective agents that might interfere with microbial iron acquisition and/or augment host iron restriction mechanisms.

Staphylococcus aureus is very adept with iron acquisition being able to access host transferrin, lactoferrin and heme iron sources, produces its own siderophores and is also able to access xenosiderophores including deferroxamine (Hammer and Skaar, 2011 and Haley and Skaar, 2012). The recent demonstration that during experimental infection there is upregulation of the *S. aureus* FhuD2 iron acquisition receptor which binds hydroxamate xenosiderophores such as deferroxamine (Bacconi et al., 2017) is significant. Additionally, various other siderophore Fe acquisition genes are upregulated in *S. aureus* while colonizing the nares (Chaves-Moreno et al., 2016). These various findings provide strong evidence for both active host iron restriction and bacterial iron acquisition response during staphylococcal infection.

Deferoxamine (Desferal® Novartis) is used clinically to treat transfusional iron overload and its use has been associated

with increased incidence of staphylococcal infection due to the ability of this bacterium to directly access various hydroxamate siderophores including deferroxamine using its FhuD1 and FhuD2 iron acquisition systems (Hammer and Skaar, 2011; Cassat and Skaar, 2012). Deferiprone is another clinically used iron chelator that has been investigated as a potential anti-infective but it has shown relatively poor anti-staphylococcal activity with MICs typically >68 µg/ml, i.e., >0.5 mM (Huber et al., 2007; Kim and Shin, 2009; Thompson et al., 2012). Deferasirox, yet a third clinically used iron chelator displayed relatively weak activity for *S. aureus* growth inhibition *in vitro* with an MIC of 50 µg/ml, i.e., 0.13 mM (Luo et al., 2014). The relatively high concentrations of these hematologically useful iron chelators required to inhibit microbial growth, their potential use by *S. aureus* or other pathogens as iron sources, especially deferroxamine (Thompson et al., 2012) and potential issues as to their toxicity, especially deferasirox (Kontoghiorghes, 2011) have severely limited their use as prospective anti-infectives.

We hypothesized that the relatively weak antimicrobial activities of small molecule chelators such as deferiprone might be improved by incorporating similar chelator-functionality into water soluble polymers of a sufficiently larger molecular size, i.e., >1500 Da such that these compositions would still sequester iron but would be less accessible by microbes for their bound iron. This approach has led to a family of potential anti-microbial chelating compositions (Holbein et al., 2007, 2011; Holbein and Mira de Orduña, 2010; Ang et al., 2018). The antimicrobial activities and chemical properties of one such hydroxypyridinone composition, DIBI, have been reported previously (Holbein and Mira de Orduña, 2010; Ang et al., 2018; Savage et al., 2018).

Here, we report the activity of DIBI in comparison to deferiprone, its small molecule (139 Da) chemical relative, against diverse *S. aureus* clinical isolates from human, cattle and canine infections. The *in vivo* activity of DIBI against a MRSA isolate and the enhancing activity of DIBI in combination with gentamicin, ciprofloxacin, and vancomycin are also reported.

MATERIALS AND METHODS

Bacterial Strains and Cultivation

Bacterial isolates used in this study are listed in **Table 2**. Strain 38 was obtained from Mark Wilcox, University of New South Wales Australia and WBG525 was obtained from Warren Grubb, Curtin University, Australia. Isolates 12-334-07086 and 14-268-06583 were obtained from the Capital District Health Authority, Halifax, NS, Canada. The canine otitis isolates were obtained from Luisa De Martino, University of Naples, Italy. The bovine mastitis isolates were obtained from the Canadian Mastitis Culture Collection, Montreal, Canada. All isolates were routinely cultured from frozen stocks (−80°C) and maintained on Trypticase Soy Agar (TSA, Sigma-Aldrich) or Blood Agar (BA, Becton Dickinson). Liquid cultures were grown in Mueller-Hinton Broth MHB (Oxoid) or Roswell Park Memorial Institute Medium (RPMI 1640, Sigma-Aldrich)

supplemented with 2% (w/v) glucose, buffered with 0.165M 3-(*N*-morpholino)-propanesulfonic acid. Partially deferrated MHB and RPMI, extracted with FEC1 to remove excess Fe (MHB-FEC1 and RPMI-FEC1) were prepared using FEC1 as previously described (Holbein and Mira de Orduña, 2010). Cultures were grown at 35–37°C with shaking. All experiments were executed following approved biosafety and biosecurity standards (Public Health Agency of Canada) in a level 2 biosafety laboratory.

Iron-Chelators, Antimicrobials and Iron Supplementation

DIBI and FEC1 were supplied by Chelation Partners Inc. Gentamicin (GEN), ciprofloxacin (CIP), and vancomycin (VAN) (Sigma-Aldrich) were prepared as 10 mg/mL stocks in water while deferiprone (DFP) from Sigma-Aldrich was dissolved in RPMI. DIBI stocks were prepared in either water (10 mg/mL) or RPMI (200 mg/mL). Exogenous iron was added to growth media as ferric citrate (Sigma-Aldrich) in RPMI. All stock solutions were filter-sterilized (0.2 µm filter) before use.

Iron Analyses

For determination of trace elements, 10 mL samples were stabilized with 1.0% (final) ultra-high purity nitric acid and stored in acid-cleaned polycarbonate centrifuge tubes. Treated samples were kept unfrozen until analyzed to avoid the formation of iron colloids that are difficult to dissolve. The samples were number-coded prior to submission to the Trace Element Research Group, Wisconsin State Laboratory of Hygiene, University of Wisconsin-Madison, which performed analysis of 50 elements using a magnetic sector inductively coupled plasma mass spectrometry ICP-MS.

Susceptibility Testing

We grew cultures overnight in MHB-FEC1 and then tested MIC susceptibilities to DIBI, DFP, GEN, CIP and VAN in RPMI using the broth microdilution method in 96-well round-bottomed plates. MHB-FEC1 cultures were diluted to an optical density (OD₆₀₀ nm) of 0.1 and MIC plates were inoculated into RPMI at a final dilution of 1/200 (approximately $1-5 \times 10^5$ CFU/mL). Chelator and antibiotic stocks were diluted in RPMI with serial 1/2 dilutions made. Negative and positive controls were tested in parallel. MIC plates were incubated at 35°C for 48 h and the MIC value was defined as the lowest concentration of chelator or antibiotic required to inhibit visible growth at 24 h incubation. Results were also read after 48 h incubation to examine for relative duration of growth inhibition. At least two independent experiments with 2–4 replicates in each were performed.

Effect of DIBI and Media Iron Concentration on Bacterial Growth

DIBI was added at concentrations ranging from 0.01 µM (0.09 µg/mL) to 1 µM (9 µg/mL) into RPMI or RPMI-FEC1 to assess the effect of iron sequestration on growth. Ferric citrate addition was used to assess reversal on growth inhibition in RPMI-FEC1 and to cultures treated with DIBI. Cultures

were incubated at 35–37°C with shaking and OD (600 nm) readings were taken over a 24 h incubation period for replicate experiments.

Wound Infection Testing

Infection testing with BALB/c female mice using the superficial skin wound infection model first described by Kugelberg et al. (2005) with *S. aureus* ATCC43300 was performed by an external clinical research organization, Jubilant Drug Discovery and Development Services Inc. (Kirkland, QC, Canada). All animal experiments were first approved by the Institutional Ethics Committee of Jubilant Biosys Ltd., and were conducted in full accordance with the CPCSEA (India) guidelines for the use of experimental animals. Mice, 9 week old, nulliparous and non-pregnant were acclimatized for 5 days prior to use and confirmed to be healthy and free of clinical signs before use. DIBI was formulated in a cream-based vehicle at three different concentrations, 0.5, 1, and 2% (w/w). A preliminary vehicle-only sham treatment was done to both validate the model and ensure the vehicle had no effects on its own. Test DIBI creams were supplied to the animal testing facility as number-coded materials.

Staphylococcus aureus ATCC43300 was cultured in TSB overnight at 37°C with shaking. Bacteria were harvested by centrifugation, washed once, re-suspended in PBS, and OD₆₀₀ nm measurement was used to adjust the inoculum to approximately 10^{11} CFU/mL. Actual CFU of inocula were determined by plate counting. On the day of wound creation, mice were anesthetized intraperitoneally with ketamine–xylazine cocktail (100 mg/kg and 20 mg/kg, respectively), fur was shaved from a 2 cm² dorsal area and the exposed skin was stripped (7–10 successive times) using a fresh elastic adhesive bandage (3M) for each stripping. After stripping, the skin became visibly damaged and was characterized by reddening and glistening but typically there was no bleeding. Skin infection was created by applying 10 µL of bacterial cell suspension containing approximately 10^8 – 10^9 CFU onto the central area of the stripped skin wound. Uninfected control animals were prepared similarly but received no inoculum. Treatment groups received 100 mg of the appropriate test cream as applied to the central area of wound at 4 and 12 h post infection (PI) and then at each 12 h interval thereafter except there was no treatment applied within 12 h of the conclusion of the testing at day 4. Application of the 0.5, 1, and 2% DIBI creams represented dosages of 20, 40, and 80 mg/kg, respectively. All treatments were administered in a blind fashion. Skin wounds were examined prior to infection, daily and at 4d PI necropsy and were scored at 4d PI as to degree (0–4) of inflammation: 0 = no erythema; 1 = slight erythema; 2 = well-defined erythema; 3 = moderate to severe erythema and 4 = severe erythema (beet red) to eschar formation with injury at depth. Mice were euthanized with excess CO₂ and after examination the entire infected tissue including several mm of clearly visible non-infected margin was excised. For bacterial burden quantification tissues were homogenized in PBS under aseptic conditions. Viable total *S. aureus* as CFU per entire wound were determined by plate counting in duplicate on mannitol salt agar, with incubation for 48 h at

37°C. The central portion of excised tissue samples at day 4 PI from four additional mice representing each of the control wounded but non-infected and infected sham-treated groups were also harvested, fixed, paraffin-embedded, sectioned and stained with either hematoxylin/eosin (H&E) or crystal violet (CV) for histopathological examination.

Nares Carriage Testing

Infection testing with male BALB/c mice utilized the nares carriage/colonization model first described by Chhibber et al. (2014) with *S. aureus* ATCC43300 and this was also performed by Jubilant Drug Discovery and Development Services Inc. All animal experiments were first approved by the Institutional Ethics Committee of Jubilant Biosys Ltd. and were conducted in full accordance with the CPCSEA (India) guidelines for the use of experimental animals. Bacterial cultures were grown in brain heart infusion (BHI) medium after its extraction with FEC1 (performed as for MHB above) with incubation at 37°C. Overnight cultures were harvested by centrifugation at 5000 rpm, cells were resuspended and washed once with sterile PBS (pH 7.4) and then re-suspended in PBS with adjustment by dilution to approximately 10^8 CFU/mL. Plate counting to confirm inoculum CFU/mL was done on nutrient agar plates containing 1 µg/mL of GEN with incubation for 24 h at 37°C. On day -2 and day 0 mice were anesthetized by exposure to 3–5% isoflurane in an oxygen flow set at approximately 1 liter per minute and infection was initiated by nasal instillation to mice held in an upright position of 10 µL (10^6 CFU) of bacterial suspension into each nostril. Gentle mixing of the bacterial inoculum between animals ensured a uniform suspension. Mice treated at day 2 or day 2+ day 3 PI were anesthetized and treated with 10 µL/nostril of PBS (vehicle control) or 10 µL of 12.5% DIBI (w/v) in PBS, representing a DIBI treatment dosage of 100 mg/kg. On day 5 PI, mice were sacrificed by excess CO₂ in an enclosed chamber, the area around the nose was wiped with 70% alcohol and the entire nose along with the nasal bone structure was excised using sterile scissors and this was homogenized in 1 mL sterile PBS. Plate counts of serial dilutions of the tissue homogenates were made after 24 h growth on nutrient agar and nutrient agar +1 µg/mL GEN at 37°C.

DIBI Synergy With Antibiotics *in vitro*

The effects of DIBI on antibiotic activity were assessed in standard checkerboard assays and then were examined in more detail using time-kill/growth assays as follows.

Staphylococcus aureus ATCC6538 after overnight growth in MHB-FEC1 was inoculated at $1-5 \times 10^5$ CFU/mL into RPMI medium (control) and RPMI containing either antibiotic alone, DIBI alone, or the combination of DIBI and antibiotic. A sub-MIC of DIBI that provided reduced growth was first determined. GEN, CIP, and VAN were each tested at approximately $1/2-1$ MIC to ensure an initial killing phase followed by recovery growth. Cultures were incubated 48 h at 37°C during which viable bacteria were enumerated at various time points with serial dilutions in PBS and plating onto TSA or BA. Colony counts were taken following overnight incubation at 35°C. At least two

independent experiments were performed for each antibiotic and DIBI pair.

Data Analysis

Growth curves and time-kill assay curves are reported as means \pm SEM. For *in vitro* studies, data were analyzed using Two-way ANOVA with Bonferroni post-test (GraphPad Prism software). The bacterial counts for the *in vivo* results were graphed as the log₁₀ of CFU/wound and these as well as the inflammation scores are reported with their median value. For *in vivo* studies, data were analyzed using the Mann-Whitney U test, and additional One-way ANOVA and Tukey analyses were performed (GraphPad Prism software). Significant differences were defined as $p < 0.05$.

RESULTS

Establishing Low Host-Relevant Iron Availability *in vitro*

Host iron availability is very low during infection (Weinberg, 2009) and therefore we considered Fe supply in the growth medium before comparing iron chelator activities *in vitro*, i.e., to better approximate relevant *in vivo* Fe availability conditions. MHB is a complex animal protein-based standard bacteriological testing medium that is rich in iron (Girardello et al., 2012). This large excess Fe content (>8 µM, see **Table 1**) is at least 100X the reported <0.1 µM minimum Fe requirements for *S. aureus* growth (Lacasse et al., 2008). Therefore, we extracted the excess Fe content from MHB using FEC1 resin as utilized previously (Holbein and Mira de Orduña, 2010). Fe contents as well as those for other trace metals and essential cations in MHB and MHB extracted with FEC1 (MHB-FEC1) were compared along with RPMI and RPMI after FEC1 extraction (RPMI-FEC1) and these are summarized in **Table 1**.

A single shake flask contacting with FEC1 followed by its removal by filtration along with its adsorbed metals provided a large Fe removal (95%) from MHB with a residual concentration similar to that found in RPMI (i.e., <0.5 µM). Extraction of MHB or RPMI did not affect its contents of Na, K, Ca, and Mg or substantially alter other trace metals (i.e., Co, Ni) except for Mn (99% and 95% removal, respectively) as shown in **Table 1**. The Fe concentrations in both RPMI and MHB-FEC1 were sufficient for unrestricted growth with both media providing 24 h Ymax (OD600 nm) values >1 (results not shown).

Sensitivity to DIBI and Deferiprone

The MICs for DIBI and deferiprone for the 18 *S. aureus* isolates tested are shown in **Table 2**. DIBI was strongly inhibitory for all 18 isolates with a narrow overall MIC range of 1–4 µg/mL, i.e., 0.1–0.4 µM DIBI. Significantly, antibiotic-resistant hospital- and community-acquired MRSA (USA300) isolates and antibiotic-sensitive isolates all exhibited similar sensitivities to DIBI as well as to deferiprone (**Table 2**). In contrast to DIBI, deferiprone was only weakly inhibitory for all of the isolates with MICs ranging from 20 to 80 µg/mL, i.e., 0.14–0.58 mM deferiprone.

TABLE 1 | Major cations and trace metals in normal and FEC1-extracted culture media.

Medium	Major cation mgL ⁻¹				Trace metal μgL ⁻¹ (μM Fe)					
	Na	K	Ca	Mg	Fe	Mn	Cu	Co	Ni	Zn
MHB	2,523	89	5.9	6.2	488 (8.7)	16.5	31.4	0.88	33.1	757.0
MHB-FEC1	2,637	93	6.0	6.0	26.7 (0.46)	0.21	18.3	0.91	39.7	264.4
RPMI	4,493	207	19	9.9	18.7 (0.33)	1.39	13.6	0.18	2.1	35.6
RPMI-FEC1	4,418	190	17	8.8	4.6 (0.08)	0.06	0.59	0.16	1.3	7.0

Average values for $n \geq 4$ replicates; SD not shown \pm < 3%.

TABLE 2 | *Staphylococcus aureus* isolates tested and their sensitivities to Deferiprone and DIBI.

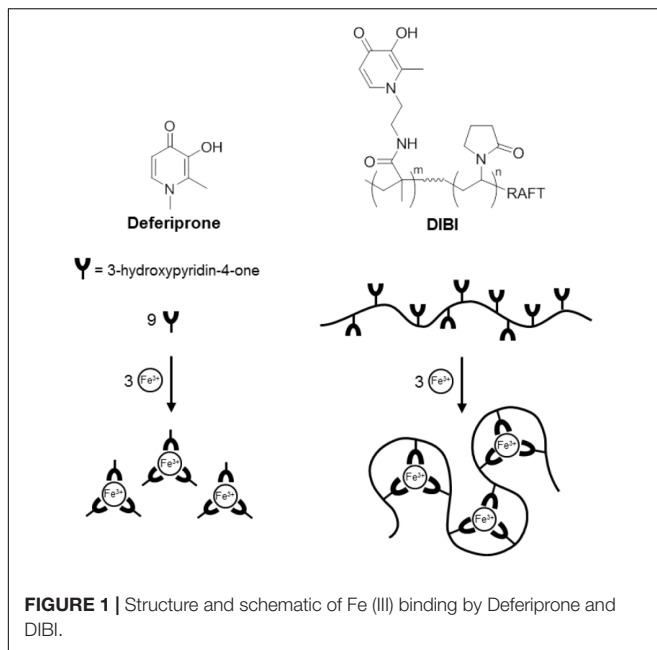
Clinical isolate	Infection source	Antibiotic resistance	MIC (24h)*			
			Deferiprone		DIBI	
			μg/mL	μM Fe capacity (3DFP-Fe)**	μg/mL	μM Fe capacity (DIBI-3Fe)**
ATCC43300	Human	MET, GEN, TOB	40	97	2	0.67
ATCCBAA1556	Human Abscess	MRSA USA 300	40	97	4	1.3
WBG525	Human Wound	MET, GEN, TOB, TET	40	97	4	1.3
14-268-06583	Human	MRSA	40	97	2	0.67
ATCC6538	Human Wound	Non-reported	40	97	4	1.3
38	Human Keratitis	Non-reported	40	97	4	1.3
ATCC25923	Human	Non-reported	20	47	1	0.33
12-334-07086	Human Bacteremia	Non-reported	20	47	2	0.67
44L	Canine otitis	ERY	20	47	2	0.67
147	Canine otitis	PEN, CLA	20	47	2	0.67
48	Canine otitis	CLA	20	47	2	0.67
44dx	Canine otitis	Non-reported	20	47	2	0.67
45R	Canine otitis	Non-reported	80	193	2	0.67
10812464	Bovine mastitis	PEN, TET	20	97	4	1.3
22301710	Bovine mastitis	ERY, OXAC, PEN	20	47	2	0.67
32308655	Bovine mastitis	ERY	20	47	2	0.67
21900341	Bovine mastitis	Non-reported	20	47	4	1.3
32101164	Bovine mastitis	Non-reported	20	47	4	1.3

*MIC, Minimum Inhibitory Concentration at 24h incubation; **, Fe capacity for MIC assuming hexadentate coordination with Chelator-Fe ratio shown (see **Figure 1**); MET, methicillin; GEN, gentamicin; TOB, tobramycin; TET, tetracycline; ERY, erythromycin; PEN, penicillin; CLA, clavulanic acid; OXAC, oxacillin; MET, TOB and OXAC are narrow spectrum and GEN, TET, ERY and PEN are broad spectrum antimicrobials. USA300 is a strain of community-associated methicillin-resistant *Staphylococcus aureus*.

The differences between DIBI and deferiprone MICs remained very large when compared more strictly on their molar iron binding capacities (**Table 2**). Both chelators are hydroxypyridinone (HPO) -containing molecules but differ in overall structure and resulting Fe binding stoichiometries as can be seen in **Figure 1**. For deferiprone, three deferiprone molecules cooperate as chelating ligands to chelate one atom of Fe with full hexadentate coordination. DIBI has a higher MW (9 kDa) and contains 9 HPO residues per molecule all of which have been shown available to bind Fe (**Figure 1** and Ang et al., 2018). Thus, a molecule of DIBI can bind three Fe molecules with full hexadentate binding while three deferiprone molecules share in the binding of one Fe. When compared as to their molar Fe binding capacities as shown in **Table 2**, DIBI still exhibited approximately 100-fold higher inhibitory activity than deferiprone (the difference range for the isolates was 36 to 288-fold).

DIBI Has Fe-Reversible Activity *in vitro*

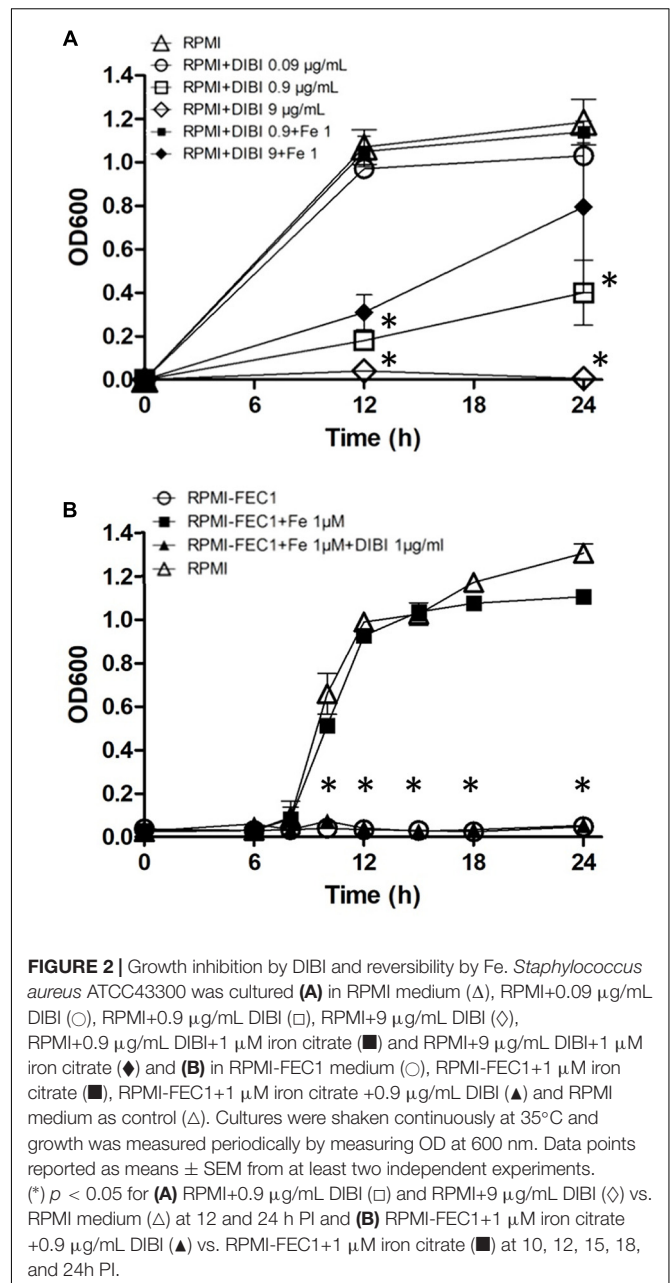
DIBI suppressed growth of *S. aureus* ATCC43300 in a dose-dependent manner (**Figure 2A**). At 0.09 μg/mL (0.01 μM) DIBI showed only a modest effect on growth with a slightly reduced Ymax compared to controls. Additions of 0.9 μg/mL or 9 μg/mL showed increased inhibition with fully suppressed growth observed at 9 μg/mL DIBI (**Figure 2A**). This complete inhibition of growth persisted for at least 36 h (results not shown). Addition of 1 μM supplemental Fe completely reversed the inhibition for cultures containing 0.9 μg/mL DIBI and it provided partial reversal in the case of DIBI at 9 μg/mL. The iron specificity of DIBI inhibition was further examined with cultures grown in RPMI-FEC1. This medium had a very low residual Fe content (0.08 μM) and this was insufficient for any growth measurable by OD600 nm. Fe addition to the RPMI-FEC1 provided a growth rate similar to RPMI control (**Figure 2B**), although the Ymax was slightly lower at 24 h. Addition of DIBI



to the Fe-supplemented RPMI-FEC1 cultures also significantly suppressed growth.

DIBI Suppresses MRSA Wound Infection

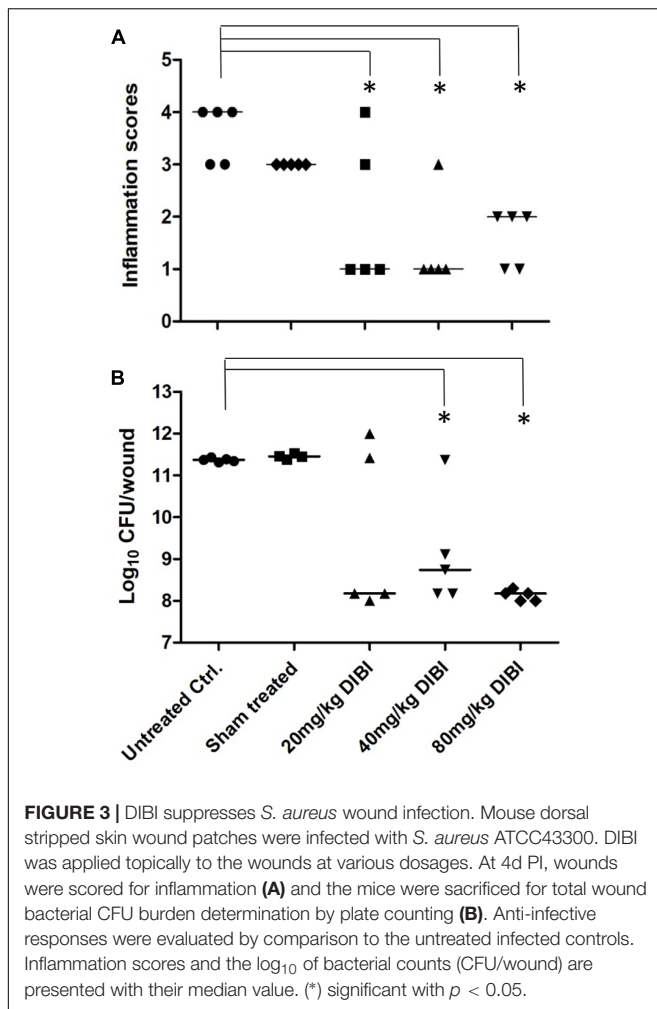
Superficial skin wounds infected with *S. aureus* ATCC43300 exhibited a pronounced infection with a 3 log increase in wound bacterial burden over the 4d study period (**Figure 3**). The results for the untreated infection were similar to those reported previously for this model (Kugelberg et al., 2005). Infection was localized to the wound site with only a mild bacteremia (<100 CFU/mL blood) found at 4d PI necropsy and the mice exhibited normal weight gains over the 4 day study period (data not shown). There was a clinically observed inflammation at the wound site that increased over the 4d study period with infected mice showing inflammation scores of approximately 3.5 out of a maximum 4 (**Figure 3A**). DIBI applied topically to the infected wounds resulted in a dose-dependent suppression of infection as evidenced both by a reduced total bacterial wound burden and a reduced inflammation score when compared to the untreated control (**Figure 3**). Sham-treated infected controls that were treated with only the vehicle, as was used for DIBI application, exhibited a similar course of infection to that of untreated infected controls. Histological examination of wounded non-infected and wounded infected sham-treated mice provided useful information as to the nature of the infection and its pathology. For wounded but non infected control mice, three of the four mice examined had no evident pathological abnormalities in H&E stained tissue sections. The one mouse that displayed wound abnormalities had no overt signs of infection (**Figure 4A**) but H&E stained tissue sections displayed multifocal epidermal necrosis with minimal neutrophilic infiltration in the hypodermis as shown in **Figure 4B**. CV stained sections from this mouse showed no bacteria within the wound (**Figure 4C**). These results were consistent with wounded non-infected mice



showing relatively fast and normal repair of their wounds over the 4 day period. In contrast, all four of the infected sham-treated mice exhibited overt signs of infection (**Figure 4D**) with wound pathology in the form of moderate to severe epidermal necrosis and with focal to diffuse edema and marked neutrophilic infiltration as observed in H&E stained sections (**Figure 4E**). CV stained sections from these infected mice showed bacterial presence within the wound, i.e., around the epidermis (**Figure 4F**).

DIBI Suppresses Nares MRSA Carriage

DIBI was also assessed for its effects on MRSA nares carriage burden following infection of mice nares with *S. aureus*

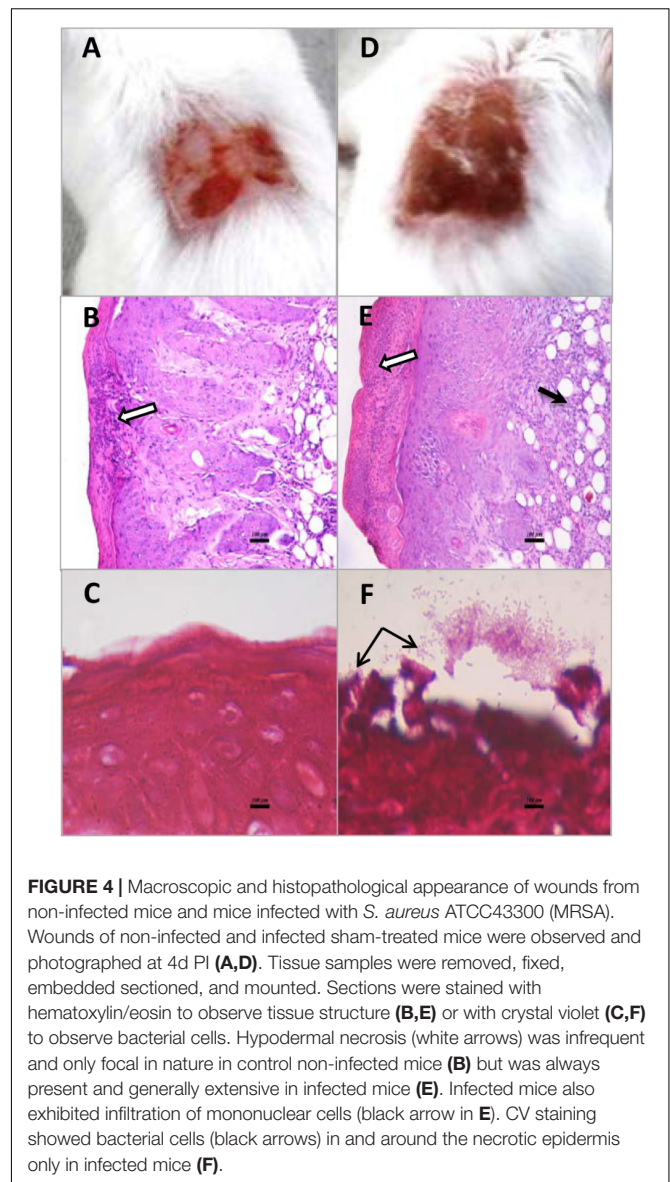


ATCC43300. Bacterial introduction by intra-nasal (IN) instillation resulted in a sustained carriage of *S. aureus* at 5 days PI and with a total nose bacterial burden of 6.6 log₁₀CFU in control infected mice (Figure 5). The control bacterial burdens were similar to those previously reported for this nares colonization model (Chhibber et al., 2014). There were no overt clinical signs of infection over the 6 day study period. *S. aureus* colonies or other resident flora were not recovered from control non-infected mice (results not shown).

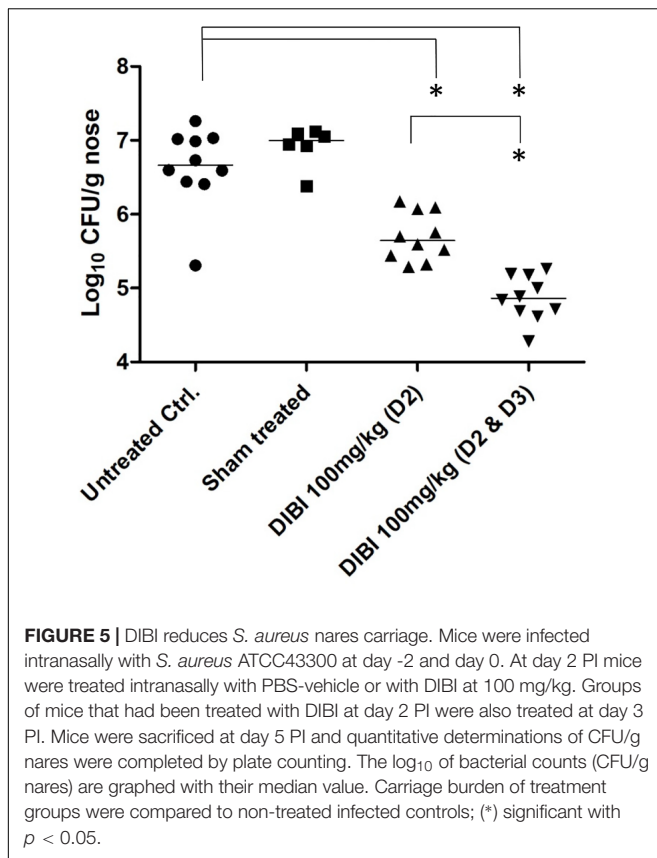
Intranasal administration of DIBI (100 mg/kg equally divided to each nostril) on day 2 PI resulted in a >1 log reduction ($p < 0.05$) in the nares bacterial burden by day 5 PI but sham treatment using only IN instillation of the PBS vehicle had no effect on the bacterial burden (Figure 5). DIBI administration on both day 2 and day 2 + 3 PI resulted in a >2 log reduction in bacterial burden by day 5 PI.

DIBI Does Not Impair but Enhances Antibiotic Activities

The possible effects of DIBI on the activities of various antibiotics representative of discrete chemical classes (aminoglycosides, fluoroquinolones, and glycopeptides) that are typically used



clinically for staphylococcal infections in humans or animals were examined. The main objectives were to determine first if DIBI might affect antibiotic killing and secondly if DIBI might affect recovery growth of bacterial survivors following a sub-lethal exposure to an antibiotic. Reference strain ATCC6538 which is often employed to assess new antimicrobials was studied. Preliminary checkerboard assays revealed FICI values of less than 0.5 suggesting synergy of DIBI with each of the antibiotics. Calculated FICIs were 0.04 for GEN, 0.04 for CIP, and 0.13 for VAN. However, we observed a growth trailing effect with DIBI when present with the antibiotics in checkerboards which made visual reading of growth/no-growth endpoints somewhat difficult. Given these limitations and the need to assess DIBI responses in a dynamic assay, we focussed on a time kill/recovery growth assay system. The initial inoculum of approximately 10⁵ CFU/mL provided sufficiently large bacterial numbers to



assess killing but yet a low enough initial inoculum to require significant replicative growth in order to reach Ymax CFU/mL values.

A concentration of DIBI providing partial inhibition of growth on its own was determined first (**Figure 6A**). DIBI added at 1 $\mu\text{g/mL}$ had no apparent effect on growth while concentrations $\geq 1.75 \mu\text{g/mL}$ reduced overall growth in a dose-dependent manner. A DIBI concentration of 1.75 $\mu\text{g/mL}$ provided an Fe-chelating capacity of approximately 0.6 μM only in slight excess of the average Fe content of RPMI (see **Table 1**). A DIBI concentration of 10 $\mu\text{g/mL}$ appeared to provide slight bactericidal activity (**Figure 6A**). Based on these results a DIBI concentration range of 1.75–2.5 $\mu\text{g/mL}$ was selected on the basis that it would result in slowed but continued growth, i.e., typical of iron-restricted growth physiology.

Similarly, CIP, GEN, and VAN concentrations were determined that provided some initial killing on their own, followed by significant recovery growth by 24–48 h post exposure (PE) (see **Figures 6B–D**). Kill/growth responses were then compared for antibiotic alone, DIBI alone and for the DIBI/antibiotic combinations all as compared to untreated control growth.

CIP at a $1/2$ MIC (0.125 $\mu\text{g/mL}$) provided short term killing followed by strong recovery growth after 4 h PE with bacterial numbers approaching those of controls by 24 h (**Figure 6B**). DIBI at 1.75 $\mu\text{g/mL}$ or 2.5 $\mu\text{g/mL}$ together with CIP did not affect initial killing by CIP. However, in the case of CIP with

2.5 $\mu\text{g/mL}$ DIBI, a continuing slow rate of killing was observed to 24 h PE and this continued to 48 h PE. DIBI at 1.75 $\mu\text{g/mL}$ with CIP resulted in a substantially reduced recovery growth after the initial killing (**Figure 6B**).

ATCC6538 treated with a $1/2$ MIC (1 $\mu\text{g/mL}$) GEN exhibited approximately a 1 log initial kill over the first 4 h followed with little change in CFU/mL to 24 h PE but then followed by >2 log CFU/mL recovery growth between 24 and 48 h PE (**Figure 6C**). DIBI at either 1.75 or 2.5 $\mu\text{g/mL}$ along with GEN resulted in an increased kill rate and overall extent of killing with little recovery growth occurring after 24 h PE in the case of the 1.75 $\mu\text{g/mL}$ DIBI/GEN combination. At the higher DIBI concentration of 2.5 $\mu\text{g/mL}$ with GEN there was further killing to 48 h PE (**Figure 6C**). There was approximately a 4 log CFU/mL difference with the DIBI/GEN combination compared to either the DIBI alone or GEN alone treatments at 48 h PE.

VAN at 1 MIC (2 $\mu\text{g/mL}$) provided only slight killing of ATCC6538 followed by strong recovery growth by 24 and 48 h PE (**Figure 6D**). DIBI at 1.75 $\mu\text{g/mL}$ with VAN provided slightly enhanced killing and fully suppressed recovery growth to 24 h PE and also to 48 h PE with evidence of slight additional killing occurring between 24 and 48 h PE (**Figure 6D**).

DISCUSSION

DIBI, an iron chelating polymer was found to be strongly inhibitory to a diverse group of *S. aureus* isolates irrespective of their animal source of origin (human, cattle or dogs) and irrespective of their antibiotic resistance characteristics. Both hospital- and community-acquired (USA300) MRSA had similar sensitivities.

DIBI also suppressed *S. aureus* infection *in vivo* when applied topically to infected superficial skin wounds or by intranasal administration to MRSA-colonized nares. A DIBI dose-dependent reduction in bacterial burdens and a reduction in wound infection-associated inflammation were observed. This evidence was consistent with DIBI sequestering host Fe within wounds or on the mucosal surfaces of the nares, i.e., host Fe supplies that would otherwise have been available to support *S. aureus* infection. The *in vivo* results are especially significant given the recent demonstration of *S. aureus* upregulating one of its key iron acquisition systems during experimental infection (Bacconi et al., 2017) revealing the bacterium is forced to compete continuously for host Fe during the course of infection. The previous finding that various Fe acquisition genes are upregulated in *S. aureus* while colonizing the nares (Chaves-Moreno et al., 2016) provides further evidence that host Fe availability is important for staphylococcal growth *in vivo* and that effective sequestration of host iron might suppress nares colonization and other infections. Our results provide evidence that the innate host iron sequestration defense mechanisms can be augmented by DIBI to better control infection.

An iron chelator such as DIBI offers potential broad utility as an alternative anti-infective for treating staphylococcal infections in man and other animals. Our ongoing investigations with canine otitis externa have shown that DIBI has stand-alone

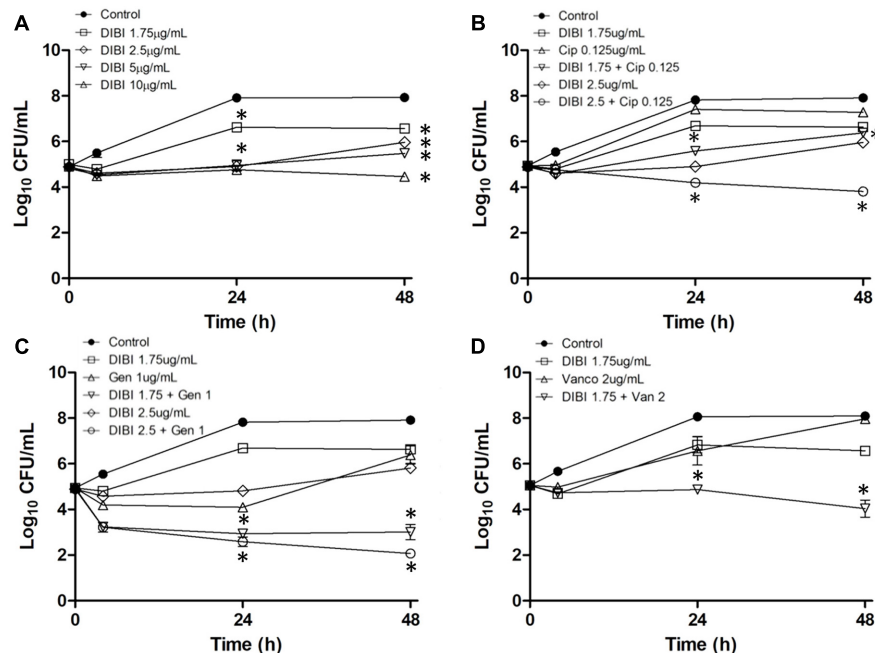


FIGURE 6 | Influence of DIBI on antibiotic killing and recovery growth. *S. aureus* ATCC6538 was inoculated at a final concentration of approximately 10^5 CFU/mL into RPMI or RPMI containing CIP, GEN, VAN, or DIBI either alone or combined with these antibiotics. Cultures were grown at 35–37°C with bacterial counts (CFU/mL) being determined at intervals over 48 h. **A:** Control (●); DIBI added at 1.75 (□); 2.5 (◇); 5 (▽) or 10 µg/mL (Δ). **B:** Control (●); DIBI 1.75 µg/mL (□); DIBI 2.5 µg/mL (◇); CIP 0.125 µg/mL (Δ); DIBI 1.75 µg/mL+CIP 0.125 µg/mL (▽) and DIBI 2.5 µg/mL+CIP 0.125 µg/mL (◇). **C:** Control (●); DIBI 1.75 µg/mL (□); DIBI 2.5 µg/mL (◇); GEN 1 µg/mL (Δ); DIBI 1.75 µg/mL+GEN 1 µg/mL (▽) and DIBI 2.5 µg/mL+GEN 1 µg/mL (◇). **D:** Control (●); DIBI 1.75 µg/mL (□); DIBI 2.5 µg/mL (◇); VAN 2 µg/mL (Δ) and DIBI 1.75 µg/mL+VAN 2 µg/mL (▽). Data points are reported as means \pm SEM. (*) $p < 0.05$ for DIBI+antimicrobial combinations vs. DIBI and antimicrobial treatments alone.

potential as a “non-antibiotic” anti-infective for treating otitis caused by *Malassezia pachydermatis* and staphylococci and also for other Gram+ and Gram– bacterial infections (unpublished results).

DIBI is a linear hydroxypyridinone-containing polymer of relatively low molecular weight (9 kDa) and it was found to have potent activity in contrast to deferiprone. Deferiprone is a small hydroxypyridinone molecule (139 Da) and a close chemical relative of DIBI with both chelators possessing identical 3-hydroxypyridin-4(1H)-one iron binding moieties. Compared on their molar iron binding capacities, DIBI was approximately 100-fold more inhibitory for *S. aureus* than deferiprone (full range of fold difference between 36 and 288-fold). This finding suggests that DIBI chelates Fe with a higher avidity than deferiprone and/or the corresponding DIBI-sequestered Fe is less available to *S. aureus* than is deferiprone-sequestered Fe. Given the larger molecular size of DIBI, it seems unlikely it would be freely transportable for intracellular uptake by microorganisms while deferiprone would presumably be available intracellularly. We have also reported enhanced growth inhibition by DIBI over deferiprone for *Candida albicans* (Savage et al., 2018) and *Acinetobacter baumannii* (Ang et al., 2018) as well as for breast cancer cells (Power Coombs et al., 2015).

Chemical characterization studies (Ang et al., 2018) have revealed that DIBI’s hydroxypyridinone groups are widely distributed on its polyvinylpyrrolidone backbone. The resulting

platform appears to provide enhanced iron chelating properties consistent with the DIBI molecule wrapping around its chelated Fe, this possibly providing some shielding of its chelated Fe atoms within the overall structure as depicted in **Figure 1**.

DIBI’s inhibitory activity was also shown to be Fe-specific and the addition of iron citrate reversed this inhibition. FEC1 treatment of the culture media was useful for investigating this aspect. FEC1 is a Fe-chelating adsorbent with identical iron chelating functionality to DIBI except that it is in the form of a crosslinked polymeric structure which is insoluble in water. FEC1 therefore provides a tool for treating a growth medium followed by its physical removal with chelated Fe (Holbein and Mira de Orduña, 2010). FEC1 removed primarily Fe and Mn from MHB and RPMI without affecting other major essential cations such as Ca and Mg. This aspect of metal selectivity has importance as previous studies of *S. aureus* Fe requirements employing deferrated media had utilized Chelex resin to extract Fe (Courcol et al., 1991), but this resin contains iminodiacetic acid metal binding groups similar to EDTA and these are much less metal selective. Consequently, Chelex® removes a variety of other cations including Ca and Mg. The lack of Fe selectivity of EDTA precludes its use as an anti-infective and also makes conclusions as to microbial metal importance using EDTA or Chelex questionable as tools.

Mn removal by FEC1 was expected and this was consistent with the known atomic similarities between Fe and Mn, as

evidenced, for example, with their similar metal reactive centers in superoxide dismutases (Miller, 2004). Mn removal from our growth media could have significance given its reported importance for *S. aureus* (Cassat and Skaar, 2012). However, we have shown that normal growth kinetics and Ymax growth yield were restored upon re-addition of only Fe to RPMI-FEC1 while deferrated RPMI-FEC1 medium without re-added Fe provided no apparent growth. Our results were consistent with DIBI being Fe-specific as well as Fe having a principal role for staphylococcal growth.

An Fe-chelating agent such as DIBI would be expected to broadly affect synthesis and regulation of a wide array of Fe-dependent microbial enzymes (e.g., ribonucleotide reductase, citrate aconitase, cytochromes, catalase, superoxide dismutase, etc) and thus, exert a generalized physiological stress on microbes. Thus, it became important to investigate DIBI's potential interaction with antibiotics given that DIBI might be administered in conjunction with these agents. A key question addressed was whether DIBI might affect the killing activity of different antibiotics. We studied three antibiotics including: GEN, an aminoglycoside class protein synthesis inhibitor; CIP a fluoroquinolone class DNA synthesis inhibitor and VAN a glycopeptide class cell wall synthesis inhibitor. Each of these antibiotics or other members of their respective families are currently used to treat staphylococcal infections in either humans or animals. Antibiotics were tested in our studies at a concentration that provided only partial initial killing followed by strong recovery growth. Antibiotic therapy typically employs a high dosage (i.e., multiple of the MIC) to ensure maximal killing but the condition of low sub-MIC antibiotic exposure with a survivor population does have clinical relevance representing a condition favoring potential microbial re-growth/infection and also a condition of possible positive selection for antibiotic resistant survivors.

For our DIBI/antibiotic interaction studies, we also deliberately provided only a sub-inhibitory amount of DIBI so as to ensure a physiological condition of Fe-restricted growth, i.e., growth restricted but not fully arrested. This physiological state of Fe-restricted growth could also have clinical relevance to infection noting that *S. aureus* has been shown to respond to *in vivo* Fe restriction through upregulation of its Fe acquisition mechanisms throughout the entire course of infection (Chaves-Moreno et al., 2016; Bacconi et al., 2017).

A small amount of DIBI (1.75–2.5 µg/mL) that was only in mild excess of that required to theoretically chelate the free Fe content of the test medium resulted in only a slight killing of the initial bacterial population followed by slow and continued growth over the 48 h study period. Fe-restricted growth resulting from this sub-MIC DIBI enhanced the overall activities of GEN, CIP, and VAN. We also observed similar responses with ATCC43300 (results not shown).

Several aspects of the observed enhancing activities of DIBI with these antibiotics are noteworthy. Importantly, DIBI did not appear to impair the initial killing activity of any of the antibiotics tested. DIBI actually increased or extended the initial antibiotic killing phase to varying degrees for each antibiotic. DIBI also appeared to either strongly restrict or fully block

recovery growth that was typically observed with a sub-MIC of antibiotic alone, i.e., re-growth following the initial killing phase from the antibiotic. The DIBI/antibiotic responses for each antibiotic thus appeared to be synergistic in nature and not just additive. DIBI promoted additional and prolonged killing by the antibiotics especially for GEN.

Our results showing DIBI enhancement of VAN activity were in general agreement with the previous report that the iron chelator deferasirox enhanced VAN activity against MRSA (Luo et al., 2014). However, their reported enhancement *in vitro* required 50 µg/mL deferasirox corresponding to 70 µM Fe binding capacity (noting two molecules of deferasirox coordinate one Fe atom). Our VAN enhancement by DIBI required only 1.75 µg/mL DIBI corresponding to only 0.52 µM Fe binding capacity. Thus, DIBI was >125 times more active to enhance VAN than had been reported for deferasirox. Deferiprone has also been studied as to its potential antibiotic enhancing activities against *S. aureus* (Richter et al., 2017). Deferiprone alone at 20 mM (2.8 mg/mL) did not enhance CIP or GEN anti-biofilm activity in an artificial wound model but when present with gallium-protoporphyrin it did enhance CIP activity. The Ga-heme, being a nonfunctional analog for Fe-heme, in *S. aureus*, appeared to have exerted additional Fe requirement stress on the bacteria (Richter et al., 2017). The earlier demonstration that the host defense iron sequestering protein lactoferrin enhances penicillin G activity for *S. aureus* isolated from bovine mastitis (Diarra et al., 2002) provides additional evidence that Fe limitation has potential for improving antibiotic responses.

It seems reasonable that repair of antibiotic-effected damage might first be required so as to then enable subsequent regrowth and replication, and these repair mechanisms would likely include Fe-dependent enzymes. Restriction of microbial essential Fe by DIBI might then generally affect this essential bacterial repair for recovery/regrowth. Interestingly, the three antibiotics studied have widely different bacterial targets and modes of action. The present results and others showing that DIBI enhances clearance of *Candida albicans* infection by fluconazole (Savage et al., 2018) suggest DIBI enhancement of antimicrobial activity might be broad-based with potential for improving antibiotic responses for various microbial infections. Our ongoing studies are investigating the effects of DIBI *in vivo* both on its own and in combination with antibiotics for anti-infective therapy of both Gram positive and Gram negative bacterial infections.

AUTHOR CONTRIBUTIONS

All authors listed have made a substantial, direct and intellectual contribution to the work, and approved it for publication.

FUNDING

This work was supported in part by the Government of Canada through its Atlantic Canada Opportunities Agency and the National Research Council of Canada through its Industrial Research Assistance Program.

REFERENCES

- Ang, M. T. C., Gumbau-Brisa, R., Allan, D. S., McDonald, R., Ferguson, M. J., Holbein, B. E., et al. (2018). DIBI, a 3-hydroxypyridin-4-one chelator iron-binding polymer with enhanced antimicrobial activity. *Med. Chem. Commun.* 9, 1206–1212. doi: 10.1039/c8md00192h
- Bacconi, M., Haag, A. F., Chiarot, E., Donato, P., Bagnoli, F., Delany, I., et al. (2017). In vivo analysis of *Staphylococcus aureus*-infected mice reveals differential temporal and spatial expression patterns of flhD2. *Infect. Immun.* 85, e270–17. doi: 10.1128/IAI.00270-17
- Ballouche, M., Cornelis, P., and Baysse, C. (2009). Iron metabolism: a promising target for antibacterial strategies. *Recent Pat. Antiinfect. Drug Discov.* 4, 190–205. doi: 10.2174/157489109789318514
- Cassat, J. E., and Skaar, E. P. (2012). Metal ion acquisition in *Staphylococcus aureus*: overcoming nutritional immunity. *Semin. Immunopathol.* 34, 215–235. doi: 10.1007/s00281-011-0294-4
- Chaves-Moreno, D., Wos-Oxley, M. L., Jáuregui, R., Oxley, A. P. A., and Pieper, D. H. (2016). Exploring the transcriptome of *Staphylococcus aureus* in its natural niche. *Nat. Sci. Rep.* 6:33174. doi: 10.1038/srep33174
- Chhibber, S., Gupta, P., and Kaur, S. (2014). Bacteriophage as effective decolonising agent for elimination of MRSA from anterior nares of BALB/c mice. *BMC Microbiol.* 14:212. doi: 10.1186/s12866-014-0212-8
- Courcol, R. J., Lambert, P. A., Fournier, P., Martin, G. R., and Brown, M. R. W. (1991). Effects of iron depletion and sub-inhibitory concentrations of antibodies on siderophore production by *Staphylococcus aureus*. *J. Antimicrob. Chemother.* 28, 663–668. doi: 10.1093/jac/28.5.663
- De Martino, L., Nocera, F. P., Mallardo, K., Nizza, S., Masturzo, E., Fiorita, F., et al. (2016). An update on microbiological causes of canine otitis in Campania region Italy. *Asian Pac. J. Trop. Biomed.* 6, 384–389. doi: 10.1016/j.apjtb.2015.11.012
- Diarra, M. S., Petitclerc, D., and Lacasse, P. (2002). Effect of lactoferrin in combination with penicillin on the morphology and the physiology of *Staphylococcus aureus* isolated from bovine mastitis. *J. Dairy Sci.* 85, 1141–1149. doi: 10.3168/jds.S0022-0302(02)74176-3
- Frieden, T. R. (2013). *Antimicrobial Resistance Threats in the United States*. Atlanta, GA: Centers for Disease Control and Prevention.
- Girardello, R., Bispo, P. J. M., Yamanaka, T. M., and Galesa, A. C. (2012). Cation concentration variability of four distinct Mueller-Hinton agar brands influences polymyxin B susceptibility results. *J. Clin. Microbiol.* 50, 2414–2418. doi: 10.1128/JCM.06686-11
- Haley, K. P., and Skaar, E. P. (2012). A battle for iron: host sequestration and *Staphylococcus aureus* acquisition. *Microbes Infect.* 14, 217–227. doi: 10.1016/j.micinf.2011.11.001
- Hamid, S., Bhat, M. A., Mir, I. A., Taku, A., Badroo, G. A., Nazki, S., et al. (2017). Phenotypic and genotypic characterization of methicillin-resistant *Staphylococcus aureus* from bovine mastitis. *Vet. World* 10, 363–367. doi: 10.14202/vetworld.2017.363-367
- Hammer, N. D., and Skaar, E. P. (2011). Molecular mechanisms of *Staphylococcus aureus* iron acquisition. *Annu. Rev. Microbiol.* 65, 129–147. doi: 10.1146/annurev-micro-090110-102851
- Holbein, B. E., Feng, M., Huber, A. L., and Kidby, D. K. (2011). Metal chelating compositions and methods for controlling growth or activities of a living cell or organism. US20160038604A1.
- Holbein, B. E., Huber, A. L., Brenner, T., and Mira de Orduña, R. (2007). Increased fluconazole susceptibility in *Candida albicans* through iron deprivation by a new chelator, DIBI. *ASM Toronto*
- Holbein, B. E., Mira, and de Orduña, R. (2010). Effect of trace iron levels and iron withdrawal by chelation on the growth of *Candida albicans* and *Candida vini*. *FEMS Microbiol. Lett.* 307, 19–24. doi: 10.1111/j.1574-6968.2010.01956.x
- Huber, A. L., Grubb, W. B., Mira, de Orduña, R., and Holbein, B. E. (2007). JMS11, a new iron chelator but not deferiprone, greatly reduces resistance of clinical *Staphylococcus aureus* isolates to antibiotics. *ASM Toronto*
- Kim, C. M., and Shin, S. H. (2009). Effect of iron-chelator deferiprone on the in vitro growth of staphylococci. *J. Korean Med. Sci.* 24, 289–295. doi: 10.3346/jkms.2009.24.2.289
- Kontoghiorghes, G. J. (2011). A record of 1320 suspect, deferiasirox-related, patient deaths reported in 2009: insufficient toxicity testing, low efficacy and lack of transparency may endanger the lives of iron loaded patients. *Hemoglobin* 35, 301–311. doi: 10.3109/03630269.2011.576906
- Kugelberg, E., Norstro, T., Petersen, T. K., Duvold, T., Andersson, D. I., and Hughes, D. (2005). Establishment of a superficial skin infection model in mice by using *Staphylococcus aureus* and *Streptococcus pyogenes*. *Antimicrob. Agents Chemother.* 49, 3435–3441. doi: 10.1128/AAC.49.8.3435-3441.2005
- Lacasse, P., Lauzon, K., Diarra, M. S., and Petitclerc, D. (2008). Utilization of lactoferrin to fight antibiotic-resistant mammary gland pathogens. *J. Anim. Sci.* 86, 66–71. doi: 10.2527/jas.2007-0216
- Liu, G. Y. (2009). Molecular pathogenesis of *Staphylococcus aureus* infection. *Pediatr. Res.* 65(5 pt 2), 71R–77R. doi: 10.1203/PDR.0b013e31819d44d
- Luo, G., Spellberg, B., Gebremariam, T., Lee, H., Xiong, Y. Q., French, S. W., et al. (2014). Combination therapy with iron chelation and vancomycin in treating murine staphylococemia. *Eur. J. Clin. Microbiol. Infect. Dis.* 33, 845–851. doi: 10.1007/s10096-013-2023-5
- Miller, A.-F. (2004). Superoxide dismutases: active sites that save but a protein that kills. *Curr. Opin. Chem. Biol.* 8, 162–168. doi: 10.1016/j.cbpa.2004.02.011
- Power Coombs, M. R., Grant, T., Greenshields, A. L., Arsenault, D. J., Holbein, B. E., and Hoskin, D. W. (2015). Inhibitory effect of iron withdrawal by chelation on the growth of human and murine mammary carcinoma and fibrosarcoma cells. *Exp. Mol. Pathol.* 99, 262–270. doi: 10.1016/j.yexmp.2015.07.008
- Proctor, R. A. (2012). Challenges for a universal *Staphylococcus aureus* vaccine. *Clin. Infect. Dis.* 54, 1179–1186. doi: 10.1093/cid/cis033
- Richter, K., Thomas, N., Zhang, G., Prestidge, C. A., Coenye, T., Wormald, P.-J., et al. (2017). Deferiprone and gallium-protoporphyrin have the capacity to potentiate the activity of antibiotics in *Staphylococcus aureus* small colony variants. *Front. Cell. Infect. Microbiol.* 7:280. doi: 10.3389/fcimb.2017.00280
- Savage, K. A., Parquet, M. d. C., Allan, S., Davidson, R. J., Holbein, B. E., Lilly, E. A., et al. (2018). Iron restriction to clinical isolates of *Candida albicans* by the novel chelator DIBI inhibits growth and increases sensitivity to azoles *in vitro* and *in vivo* in a murine model of experimental vaginitis. *Antimicrob. Agents Chemother.* 62:e02576-17. doi: 10.1128/AAC.02576-17
- Thompson, M. G., Corey, B. W., Si, Y., Craft, D. W., and Zurawski, D. V. (2012). Antibacterial activities of iron chelators against common nosocomial pathogens. *Antimicrob. Agents Chemother.* 56, 5419–5421. doi: 10.1128/AAC.01197-12
- Tong, S. Y. C., Davis, J. S., Eichenberger, E., Holland, T. L., and Fowlwer, V. G. (2015). *Staphylococcus aureus* infections: epidemiology, pathophysiology, clinical manifestations and management. *Clin. Microbiol. Rev.* 28, 603–661. doi: 10.1128/CMR.00134-14
- Ventola, C. L. (2015). The antibiotic resistance crisis part1: causes and threats. *Pharmacol. Ther.* 40, 277–283.
- Vincze, S., Stamm, I., Kopp, P. A., Hermes, J., Adlhoch, C., Semmler, T., et al. (2014). Alarming proportions of methicillin-resistant *Staphylococcus aureus* (MRSA) in wound samples from companion animals, Germany 2010–2012. *PLoS One* 9:e85656. doi: 10.1371/journal.pone.0085656
- Weinberg, E. D. (2009). Iron availability and infection. *Biochim. Biophys. Acta* 1790, 600–605. doi: 10.1016/j.bbagen.2008.07.002

Conflict of Interest Statement: BH has a beneficial interest in Chelation Partners Inc., that has contributed financially to this study. MdCP, KS, and DA are employees of Chelation Partners Inc., RD has no conflicts or competing interests in relation to this study.

Copyright © 2018 Parquet, Savage, Allan, Davidson and Holbein. This is an open-access article distributed under the terms of the Creative Commons Attribution License (CC BY). The use, distribution or reproduction in other forums is permitted, provided the original author(s) and the copyright owner(s) are credited and that the original publication in this journal is cited, in accordance with accepted academic practice. No use, distribution or reproduction is permitted which does not comply with these terms.



Attenuation of *Listeria monocytogenes* Virulence by *Cannabis sativa* L. Essential Oil

Emanuela Marini¹, Gloria Magi¹, Gianna Ferretti², Tiziana Bacchetti³, Angelica Giuliani⁴, Armanda Pugnali⁴, Maria Rita Rippo⁴ and Bruna Facinelli^{1*}

¹ Unit of Microbiology, Department of Biomedical Sciences and Public Health, Polytechnic University of Marche, Ancona, Italy, ² Department of Clinical Sciences, Polytechnic University of Marche, Ancona, Italy, ³ Department of Life and Environmental Sciences, Polytechnic University of Marche, Ancona, Italy, ⁴ Division of Pathology, Department of Clinical and Molecular Sciences, Polytechnic University of Marche, Ancona, Italy

OPEN ACCESS

Edited by:

You-Hee Cho,
CHA University, South Korea

Reviewed by:

Arun K. Bhunia,
Purdue University, United States
Tânia Aparecida Tardelli Gomes,
Federal University of São Paulo, Brazil

*Correspondence:

Bruna Facinelli
b.facinelli@univpm.it

Received: 17 May 2018

Accepted: 31 July 2018

Published: 22 August 2018

Citation:

Marini E, Magi G, Ferretti G, Bacchetti T, Giuliani A, Pugnali A, Rippo MR and Facinelli B (2018) Attenuation of *Listeria monocytogenes* Virulence by *Cannabis sativa* L. Essential Oil. *Front. Cell. Infect. Microbiol.* 8:293. doi: 10.3389/fcimb.2018.00293

Anti-virulence strategies are being explored as a novel approach to combat pathogens. Such strategies include inhibition of surface adhesion, tissue invasion, toxin production, and/or interference with the gene regulation of other virulence traits. *Listeria monocytogenes*, the causative agent of listeriosis, is a facultative intracellular food pathogen characterized by a wide distribution in the environment. Its ability to persist within biofilms and to develop resistance to sanitizers is the cause of significant problems in food processing plants and of steep costs for the food industry. In humans, the treatment of listeriosis is hampered by the intracellular location of listeriae and the poor intracellular penetration of some antibiotics. Eleven *L. monocytogenes* isolates from patients who were diagnosed with invasive listeriosis in Italy in 2014–2016 were studied. This *in vitro* and *in vivo* study explored the antibacterial and anti-virulence properties of a steam-distilled essential oil of *Cannabis sativa* L., which is being intensively investigated for its high content in powerful bioactive phytochemicals. Susceptibility experiments demonstrated a moderate bactericidal activity of the essential oil (Minimum Bactericidal Concentration > 2048 µg/mL). Assessment of the effects of sublethal concentrations of the essential oil on *L. monocytogenes* virulence traits demonstrated a significant action on motility. Listeriae were non-motile after exposure to the essential oil. Light and scanning electron microscopy documented aggregates of listeriae with the flagella trapped inside the cluster. Real-time RT-PCR experiments showed downregulation of flagellar motility genes and of the regulatory gene *prfA*. The ability to form biofilm and to invade Caco-2 cells was also significantly reduced. *Galleria mellonella* larvae infected with *L. monocytogenes* grown in presence of sublethal concentrations of the essential oil showed much higher survival rates compared with controls, suggesting that the extract inhibited tissue invasion. Food contamination with *L. monocytogenes* is a major concern for the food industry, particularly for plants making ready-to-eat and processed food. The present work provides a baseline in the study of the anti-virulence properties of the *C. sativa* essential oil against *L. monocytogenes*. Further studies are needed to understand if it could be used as an alternative agent for the control of *L. monocytogenes* in food processing plants.

Keywords: *Cannabis sativa*, essential oil, sublethal concentrations, *Listeria monocytogenes*, virulence, motility, cell invasion, biofilm

INTRODUCTION

In recent years, the use of plant products as alternative/adjunct antimicrobial agents to control pathogenic microorganisms has been attracting mounting interest. Anti-virulence strategies are being explored as a novel approach to combat bacterial pathogens; such approaches include inhibition of surface adhesion, tissue invasion, toxin production, and/or interference with the gene regulation of other virulence traits (Rasko and Sperandio, 2010). A major group of plant antimicrobial compounds is represented by essential oils (EO), complex mixtures of volatile secondary metabolites belonging to different chemical families including terpenes, alcohols, ethers, aldehydes, and phenols (Cannas, 2016). The antimicrobial activity of EO and their components has been known for millennia. More recently, synergy between EO components and antibiotics has been demonstrated against antibiotic-resistant pathogens (Langeveld et al., 2014). In contrast, the knowledge of the effects of EO on bacterial virulence is still very limited (Nazzaro et al., 2013; Silva et al., 2016).

Cannabis sativa L. (Cannabaceae), an annual species that has spread from its native range in central Asia to Europe and Africa, is one of the earliest domestic plants in the history of mankind and has been grown and selected for thousands of years for a multiplicity of purposes, like a source of food, fuel, paper, and building material, as a textile fiber, and as a remedy in folk medicine (Andre et al., 2016). The plant is a source of several bioactive compounds including psychoactive substances such as cannabinoids (the most important being Δ^9 -tetrahydrocannabinol, Δ^9 -THC), terpenoids, flavonoids, and polyunsaturated fatty acids. In the late 1930s, the psychotropic effects due to Δ^9 -THC led to a ban on its cultivation worldwide. In recent years, selection of some genotypes containing low Δ^9 -THC concentrations ($\leq 0.2\%$ w/v) has led to a lifting of the ban; the plant can now be grown legally (Holler et al., 2008) and used for research purposes.

Listeria monocytogenes, a Gram-positive, facultative intracellular pathogen with a wide environmental distribution, is the causative agent of human and animal listeriosis (Freitag et al., 2009). The disease is the most lethal zoonosis in the EU (fatality rate, 20%), affecting particularly immunocompromised and elderly individuals (EFSA and ECDC, 2016). Infection of the human host is commonly via the oral route, through ingestion of contaminated food, although transplacental transmission during gestation also occurs. Severe *L. monocytogenes* infection include septicaemia, meningitis, endocarditis, and spontaneous abortion (McDougal and Sauer, 2018). Infection requires bacterial internalization into host cells, intracellular survival, and spread into neighboring cells, which enable bacterial diffusion from the primary site of infection, usually the bowel, to the liver, the spleen, and on to peripheral blood and eventually the brain. A limited subset of serotypes (i.e., 1/2a, 1/2b, and 4b) is responsible for the bulk of clinical cases worldwide (Kathariou, 2002); the serotype most frequently associated with listeriosis outbreaks, particularly in Europe and North America, is 1/2a (Lomonaco et al., 2015). *L. monocytogenes* is intrinsically resistant to broad-spectrum cephalosporin antibiotics (Krawczyk-Balska and

Markiewicz, 2016) and shows acquired resistance to other drugs. Treatment with aminopenicillin or benzylpenicillin, alone or combined with an aminoglycoside, is currently the gold standard antibiotic therapy for *L. monocytogenes* infections (Thønnings et al., 2016). However, listeriae are difficult to eradicate, due to their intracellular location and the poor intracellular penetration of these drugs. Their ability to persist within biofilms and to develop resistance to sanitizers is the cause of significant problems in food processing plants and of steep costs for the food industry (Colagiorgi et al., 2017; Boqvist et al., 2018).

The virulence of *L. monocytogenes* relies on highly effective mechanisms of invasion and spread, which ensure its intracellular lifecycle (Vázquez-Boland et al., 2001; Freitag et al., 2009; Radoshevich and Cossart, 2018). Host cell invasion is either via phagocytosis or receptor-mediated endocytosis, facilitated by the bacterial surface proteins internalins InlA (*inlA*) and InlB (*inlB*) (Chen et al., 2017). Recently, Drolia et al. have demonstrated that *Listeria* adhesion protein (LAP) induces intestinal epithelial barrier dysfunction contributing to bacterial translocation from the intestinal lumen, across the gut epithelium (Drolia et al., 2018). *L. monocytogenes* is initially trapped in a phagocytic vacuole and subsequently secretes the cholesterol-dependent pore-forming toxin listeriolysin O (LLO; *hly*) and two phospholipases C (PlcA and PlcB), resulting in vacuole rupture and escape of bacteria into cytosol (Chen et al., 2017). In this phase, an actin assembly-inducing protein (ActA; *actA*) promotes actin-based motility and cell-to-cell spread (Chen et al., 2017). These processes are closely regulated, mainly by the transcriptional regulator PrfA (*prfA*), which is activated by host infection (de las Heras et al., 2011). Recent progress highlights that *L. monocytogenes*, which has long been a model for cytosolic pathogens, is also capable of residing in vacuoles, in a slow/non-growing state (Bierne et al., 2018).

Flagellum-based motility and biofilm formation have also been implicated in virulence (Josenhans and Suerbaum, 2002; Duan et al., 2013). The biosynthesis of flagella is temperature-dependent, since most *L. monocytogenes* strains produce flagella and are motile only at temperatures of 30°C and less (Peel et al., 1988). Flagellum-mediated motility is critical both for initial surface attachment and subsequent biofilm formation (Lemon et al., 2007).

The purpose of this study was to investigate the *in vitro* and *in vivo* antibacterial and anti-virulence properties of an EO extracted from a legal *C. sativa* L. variety against *L. monocytogenes* isolates collected from patients diagnosed with invasive listeriosis in central Italy in 2014–2016.

MATERIALS AND METHODS

Strains and Growth Media

A total number of 11 *L. monocytogenes* isolates collected from the blood or cerebrospinal fluid (CSF) of patients diagnosed with invasive listeriosis in Ancona province (Italy) from 2014 to 2016 were investigated in the study (Table 1). The 2015 and 2016 isolates had already been characterized in terms of antibiotic resistance phenotype and molecular typing/genetic relatedness (Marini et al., 2016).

Blood agar base (BAB) supplemented with 5% sheep blood, Müller-Hinton agar (MHA) supplemented with 5% sheep blood, Müller-Hinton cation-adjusted broth (CAMHB) supplemented with 3% laked sheep blood, brain heart infusion (BHI) agar and broth, Tryptone Soya Broth (TSB), and Luria Bertani (LB) agar and broth (all from Oxoid, Basingstoke, UK) were used in the study. Isolates were maintained in glycerol at -70°C and subcultured twice on BAB before testing.

Extraction and Characterization of *C. sativa* L. Essential Oil

EO was extracted from the French monoecious variety Futura 75, which is grown in the countryside around Ancona. Fresh inflorescences and leaves were steam-distilled by the Associazione Produttori Piante Officinali (APPO Marche, Ancona, Italy). Gas chromatography/mass spectrometry (GC-MS) identification of EO components was performed by Agenzia Servizi Settore Agroalimentare delle Marche (ASSAM, Ancona, Italy).

Susceptibility Tests

The minimum inhibitory concentration (MIC), i.e., the lowest EO concentration inhibiting visible bacterial growth after incubation, was determined in blood-supplemented CAMHB by the microdilution method according to Clinical and Laboratory Standards Institute (CLSI) guidelines (Clinical Laboratory Standards Institute, 2017). The minimum bactericidal concentration (MBC), i.e., the lowest EO concentration killing 99.9% of the inoculum, was determined by plating 10 μL of each microdilution on blood-supplemented MHA followed by overnight incubation at 37°C . All experiments were performed in triplicate.

Motility Assays

Motility of *L. monocytogenes* in presence of the *C. sativa* EO was assessed by the “umbrella test” in semi-solid agar stabbed with the strains and incubated overnight at 30°C . Detection of

an umbrella-like growth about 0.5 cm below the agar surface indicated a positive test. Motility was also assessed by measuring the diameter of the growth zone with respect to control bacteria on 0.3% soft agar plates inoculated with 10 μL of a broth culture and incubated overnight at 30°C .

Flagella Stain

L. monocytogenes incubated at 30°C in presence of the *C. sativa* EO were examined by light microscopy (LM). Flagella were visualized using BD Flagella Stain Droppers (Becton Dickinson, Milano, Italy), a procedure that demonstrates bacterial flagella and their arrangement on the cell.

Scanning Electron Microscopy Examination

For morphological studies, *L. monocytogenes* cells grown on BAB agar at 30°C with and without the *C. sativa* EO were fixed overnight in 2.5% glutaraldehyde in 0.1 M sodium cacodylate buffer (pH 7.4) at 4°C and washed with the same buffer supplemented with 7% sucrose. Samples were left to adhere on glass slides covered with 0.01% poly-L-lysine solution (Sigma

TABLE 2 | List of primers used in the study.

Gene	Primer	Sequence (5' - 3')	Product size
16S	rDNA 16s-F	AGGTGGGGATGACGTCAAAT	138 bp
	rDNA 16s-R	GCAGCCTACAATCCGAACCTG	
prfA	prfA-RT-F	GACCGCAAATAGAGCCAAGC	122 bp
	prfA-RT-R	ACTGAGCAAGAATCTTACGCAC	
flaA	flaA-RT-F	GGCTGCTGAAATGTCCGAAA	90 bp
	flaA-RT-R	ATTTGCGGTGTTTGTTTG	
motA	motA-RT-F	GGTTACGTACTTTGAGCGCC	137 bp
	motA-RT-R	AAACGTTCTTCCACAACCCG	
motB	motB-RT-F	CGTTCTGTTCCTCCAGTT	103 bp
	motB-RT-R	ATATGCTTGATTGCCTGCCG	

TABLE 1 | *L. monocytogenes* strains used in the study and their characteristics.

Strain #	Date of isolation	Source	Serotype	MBC ($\mu\text{g/mL}$)			Biofilm producer
				EO	α -pinene	Myrcene	
60551	2014	Blood	4b	>2048	1024	2048	Weak
66785	"	"	1/2a	"	>2048	"	Strong
75227	"	"	1/2b	"	1024	"	Moderate
82468	"	"	1/2a	"	2048	"	Strong
97885	"	"	4b	"	>2048	"	Moderate
02470	2015	"	1/2a	"	"	>2048	Strong
09707	"	"	1/2c	"	"	2048	Moderate
56053	"	"	1/2a	"	1024	"	Moderate
31829	"	"	"	"	2048	"	Moderate
77660	2016	CSF	4b	"	1024	"	Moderate
80466	"	Blood	1/2a	"	2048	"	Moderate

CSF, cerebrospinal fluid; MBC, minimum bactericidal concentration.

Aldrich, Milano, Italy), postfixed in 1% OsO₄ in 0.1 M sodium cacodylate buffer for 2 h at 4°C, washed with the same buffer, dehydrated with EtOH, and critical point dried. Samples were mounted on aluminum stubs by graphite glue (Sigma Aldrich) and coated with a thin (20 Å) gold film using an EMITECH K550 (Ashford, England) sputtering device. Scanning electron microscopy (SEM) observations were performed with a Zeiss Supra 40 apparatus.

RNA Extraction and Real-Time Quantitative Reverse Transcription PCR (RT-qPCR) on *prfA*, *flaA*, *motA*, and *motB*

The effect of the EO on the expression of *L. monocytogenes* virulence genes was investigated using real time RT-PCR. Strains were grown in presence of EO at 30°C in TSB, and total RNA was extracted using GenElute total RNA Purification kit (Sigma Aldrich). cDNA synthesis was performed using the Quantitect Reverse Transcription kit (Qiagen, Hilden, Germany) and synthesized cDNA was used as the RT-qPCR template. The amplification product was detected using SYBR Green reagents (SYBR Green JumpStar Taq ReadyMix, Sigma Aldrich) by Rotor-Gene (Qiagen). The primers for each gene are reported in Table 2. Data were normalized to the endogenous control (16S rRNA) and the level of candidate gene expression between treated and untreated samples was compared to study relative gene expression and the effect of EO on each gene.

Biofilm Formation Assays

Biofilm formation was evaluated as previously described (Marini et al., 2015). Briefly, bacteria were grown overnight in TSB containing 1% glucose at 30°C. Overnight bacterial suspensions were prepared to yield final inocula of $\sim 1 \times 10^8$ colony-forming units (CFU)/mL; then 200 μ L aliquots of the bacterial suspension were inoculated into 96-well microtitre plates at least in triplicate. After 24-h incubation, wells were washed 3 times in phosphate-buffered saline (PBS), dried for 1 h at 60°C, and stained with Hucker's crystal violet. After three washes in sterile water, wells were inoculated with 100 μ L of 95% EtOH and shaken for 10 min. Biofilm formation was quantified by measuring absorbance at 690 nm with a Multiscan Ascent apparatus (Thermo Scientific, Waltham, MA, USA). The optical density (OD) cut-off (OD_c) was defined as 3 standard deviations above the mean OD of the negative control, represented by non-inoculated wells containing TSB (Stepanovic et al., 2000). Strains were classified as non-producers (OD \leq OD_c), weak producers (OD_c < OD \leq 2 \times OD_c), moderate producers (2 \times OD_c < OD \leq 4 \times OD_c), or strong producers (OD > 4 \times OD_c). The biofilm-forming strain *S. epidermidis* ATCC 35984 was used as a positive control (Christensen et al., 1985). In some assays, biofilm formation was evaluated in presence of the *C. sativa* EO. Briefly, overnight bacterial suspensions were prepared to yield final inocula of $\sim 2 \times 10^8$ CFU/mL. Then, 100 μ L of bacterial culture and 100 μ L of different EO concentrations were added to each well of a 96-well microplate. Wells containing 100 μ L of the bacterial suspension and 100 μ L TSB without EO were the positive controls. After incubation, biofilm formation was evaluated as described above. All experiments were performed in triplicate.

Caco-2 Invasion Assays

The human colon carcinoma Caco-2 cell line (ATCC HTB37) (Rousset, 1986) was used in cell invasion experiments. Cells were routinely cultured in Modified Eagle Medium (MEM; Gibco, New York, NY, USA) supplemented with 1% (v/v) L-glutamine, 1% (v/v) non-essential amino acids and 10% (v/v) fetal calf serum (both from Gibco) in 50 mL (25 cm²) plastic tissue culture flasks (Corning Costar, Milano, Italy) at 37°C in an atmosphere containing 5% CO₂. Monolayers were trypsinized and adjusted to a concentration of 2.5×10^5 cells/mL in culture medium; 1 mL

TABLE 3 | GC-MS analysis of the *C. sativa* EO.

Components	%
Tricyclene	0.63
α -thujene	0.09
α-pinene	19.20
Camphene	0.65
β-pinene	4.34
Myrcene	17.17
δ -3-carene	0.60
α -phellandrene	0.15
Limonene	1.81
β -phellandrene	0.86
1,8-cineole	1.06
p-cymene	1.52
Trans- β -ocimene	2.28
γ -terpinene	0.12
Terpinolene	4.50
Neo-allo-ocimene	0.14
Camphor	5.78
Borneol	1.15
Terpinen-4-ol	0.28
α -terpinene	0.46
Cuminol	0.64
Verbenone	0.95
Bornyl acetate	0.56
Ethyl hexanoate	0.08
Iso-caryophyllene	0.94
β-caryophyllene	15.31
Allo-aromadendrene	0.11
Trans- β -farnesene	1.11
α-humulene	3.68
γ -selinene	0.28
β -selinene	1.35
α -selinene	1.08
Valencene	1.22
Caryophyllene-oxide	3.27
α -bisabolol	0.61

Components present at greater than 3% are indicated by bold font.

cell suspension was dispensed into each 22-mm well of a 12-well tissue culture plate and incubated 4 days to obtain confluent monolayers (Facinelli et al., 1998).

Invasion experiments were performed using *L. monocytogenes* strains grown in presence of the *C. sativa* EO. Briefly, after overnight growth in BHI broth supplemented with EO, listeriae were resuspended in PBS to OD_{550} 0.6 ± 0.02 . Then, 1 mL of the suspension, suitably diluted in MEM, was added to each well to obtain a multiplicity of infection of about 30 bacteria/cell. Penetration was allowed to occur for 1 h at 37°C in 5% CO₂. Then monolayers were washed 3 times and covered with 2 mL MEM containing a bactericidal concentration of gentamicin (10 µg/mL), to kill extracellular bacteria. After 2 h at 37°C in 5% CO₂ air, cells were washed 3 times and lysed in 1 mL Triton X-100 (0.1% in cold sterile water). The CFU of viable bacteria were counted by plating suitable dilutions of the lysates on BHI agar and incubating them for 36–48 h at 37°C. Data are expressed as a percentage of initial

inoculum of viable bacteria. Experiments were carried out in triplicate.

Cytopathogenic Effects on Caco-2 Monolayers

The ability of listeriae to cause cytopathogenic effects (CPE) in Caco-2 monolayers was evaluated by the trypan blue exclusion assay (Gibco), which measures cell viability (Facinelli et al., 1998). Briefly, Caco-2 monolayers grown in slide flasks (Corning Costar) were infected with bacterial strains grown with and without the *C. sativa* EO, as described above. Control monolayers received MEM without bacteria. At the end of the infection period (1 h), the supernatant was removed and monolayers were washed and covered with MEM supplemented with gentamicin (10 µg/mL). After overnight incubation at 37°C in 5% CO₂, 1 mL of a 0.4% trypan blue solution was added to the culture medium and cells were kept at room temperature for 30 min. Finally, the culture medium with the dye was removed and monolayers were examined with a Leica DMRB microscope (Leica Microsystems, Wetzlar, Germany) using a 10 × objective.

Galleria mellonella Survival Assays

Final instar larvae (~300 mg) of the greater wax moth *G. mellonella* were purchased from a local vendor, stored in the dark at 15°C, and used within 7 days. Larvae were rinsed with 70% EtOH before injection using a standard protocol (Mukherjee et al., 2010). Ten larvae were randomly allocated to different treatment groups: positive control (larvae inoculated with *L. monocytogenes*); test group (larvae injected with *L. monocytogenes* grown in presence of the *C. sativa* EO); negative control (larvae that were not injected); PBS control (larvae injected with PBS). Before infection, bacteria were washed and resuspended in PBS at the appropriate cell density (5×10^7 CFU/mL); then, 50 µL of the inoculum was injected into the larval haemocoel via the left proleg using a microsyringe (Mukherjee et al., 2010). After injection, larvae were incubated at 30°C in sterile Petri plates. The number of dead larvae was scored at 24 h intervals for 6 days. Larvae were considered dead when they turned black and failed to react to touch. Three separate experiments were conducted. *G. mellonella* survival data were plotted using the Kaplan-Meier method.

Statistics

Data are mean \pm standard deviation (SD). Differences between groups were assessed using GraphPad Prism, version 5 (GraphPad Software Inc., San Diego, CA, USA) by a paired Student's *t*-test (biofilm, cell invasion and real time RT-PCR experiments) and the log-rank (Mantel-Cox) test (*G. mellonella* survival assays). $P \leq 0.05$ indicated statistical significance.

RESULTS

GC-MS Analysis of the *C. sativa* EO

GC-MS analysis of the *C. sativa* EO, obtained from the Futura 75 genotype by steam distillation, identified 35 compounds, which accounted for 95% of the whole GC profile (Table 3). Most were sesquiterpenes found at very low concentrations, except

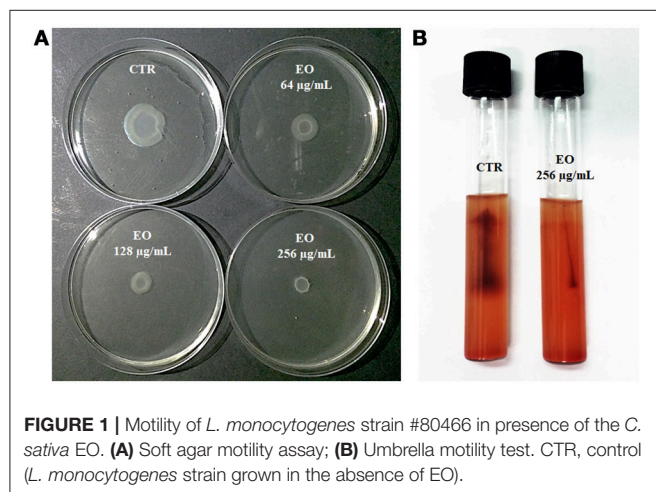


FIGURE 1 | Motility of *L. monocytogenes* strain #80466 in presence of the *C. sativa* EO. (A) Soft agar motility assay; (B) Umbrella motility test. CTR, control (*L. monocytogenes* strain grown in the absence of EO).

TABLE 4 | Motility of *L. monocytogenes* grown in presence of the *C. sativa* EO.

Strain #	Zone of motility (mm)		% reduction
	CTR	EO (256 µg/mL)	
60551	18.0 \pm 0.6	5.0 \pm 0.0*	72.2
66785	21.0 \pm 5.2	4.7 \pm 0.6*	77.6
75227	9.7 \pm 0.6	4.3 \pm 0.6*	55.7
97885	10.0 \pm 1.0	5.0 \pm 0.0*	50.0
82468	23.3 \pm 1.2	6.7 \pm 0.6*	71.2
02470	22.3 \pm 3.8	7.3 \pm 0.6*	67.3
09707	23.0 \pm 5.3	5.0 \pm 0.0*	78.3
56053	21.3 \pm 6.7	5.3 \pm 0.6*	75.1
31829	14.0 \pm 1.0	5.0 \pm 1.0*	64.3
77660	23.3 \pm 6.7	4.7 \pm 0.6*	79.8
80466	14.0 \pm 1.7	5.0 \pm 0.0*	64.3

Values are mean of two independent experiments. Asterisks indicate significant values compared with control ($p \leq 0.05$). CTR, control (*L. monocytogenes* strains grown in the absence of EO).

for β -caryophyllene (15.31%) and α -humulene (3.68%). Myrcene (17.17%), α -pinene (19.20%), and β -pinene (4.34%) were the main monoterpenes.

Susceptibility of *L. monocytogenes* Strains to the *C. sativa* EO and Its Main Components

The antimicrobial activity (MIC and MBC) of the total EO, α -pinene, and myrcene was determined against all tested strains. Only the MBC values are reported, because the MIC values were difficult to interpret due to turbidity (Table 1). The MBC of the whole EO and of myrcene were $\geq 2048 \mu\text{g/mL}$, whereas those of α -pinene ranged from 1024 to $> 2048 \mu\text{g/mL}$, suggesting that both components contribute to the bactericidal activity of the extract against the *L. monocytogenes* strains.

Reduced Flagellar Motility in Presence of the *C. sativa* EO

L. monocytogenes motility was first evaluated by measuring colony diameter and by the “umbrella motility test” after growth on soft agar containing a sublethal concentration (256 $\mu\text{g/mL}$) of the *C. sativa* EO (Figures 1A,B). A significant, concentration-dependent, reduction in colony diameter (from 50.0 to 79.8 %) was observed in all strains (Table 4, Figure 1A). Moreover, strains grown in presence of 256 $\mu\text{g/mL}$ of the extract did not show the typical umbrella-like growth

(Figure 1B). LM examination after flagella staining showed that, unlike control strains, the listeriae incubated with 256 $\mu\text{g/mL}$ of the *C. sativa* EO formed aggregates with the flagella trapped inside the cluster (Figure 2A). SEM observation confirmed these findings and demonstrated that there were fewer flagella in the extract-incubated strains (Figure 2B).

Downregulation of *prfA*, *flaA*, *motA*, and *motB* in *L. monocytogenes* Exposed to the *C. sativa* EO

Investigation of the relative expression levels of *prfA*, *flaA*, *motA* and *motB* genes, after growth in the presence of *C. sativa* EO at 256 $\mu\text{g/mL}$, by a real-time RT-PCR assay, demonstrated a 3.3, 8.1, and 16.8 reduction in the expression levels of *prfA*, *motA* and *motB*, respectively, ($p = 0.0541$, $p = 0.0819$, and $p = 0.0569$, respectively). Interestingly, the relative expression of *flaA* also demonstrated a significant 241.5 reduction ($p = 0.0002$) (Figure 3).

Effects of the *C. sativa* EO on *L. monocytogenes* Biofilm Formation

All 11 *L. monocytogenes* strains were found to be biofilm producers: 4 strains (#66785, #02470, #09707, and #82468) were strong producers, 6 (#56053, #31829, #77660, #97885, #75227, and #80466) were moderate producers, and one (#60551) was a weak producer. To evaluate the ability

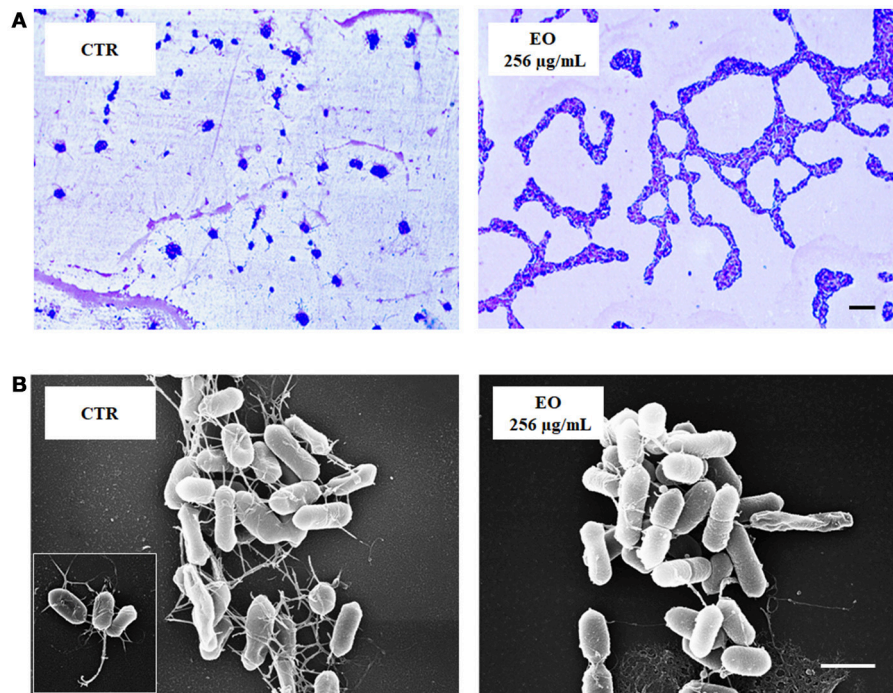


FIGURE 2 | LM and SEM images of *L. monocytogenes* strain #80466 grown in presence of the *C. sativa* EO. **(A)** LM images after staining with Flagella Stain Droppers (magnification: 1000 \times ; bar, 5 μm): flagella are stained in pink red; **(B)** SEM images (bar, 1 μm). Insert, “bouquet” of listeriae. CTR, control (*L. monocytogenes* strain grown in the absence of EO).

of the EO to interfere with biofilm formation, all strains were tested for biofilm production in presence of sublethal (256, 128, and 64 $\mu\text{g/mL}$) EO concentrations. A reduction in biofilm production was induced by all concentrations in all strains. The 256 $\mu\text{g/mL}$ concentration reduced biofilm

production by 25–69%; a similar reduction was observed with 128 $\mu\text{g/mL}$ (from 32 to 73%) and 64 $\mu\text{g/mL}$ (from 15 to 65%) (**Figure 4**). Except #60551 (weak producer), all the moderate/strong biofilm producers became weak producers at all EO concentrations.

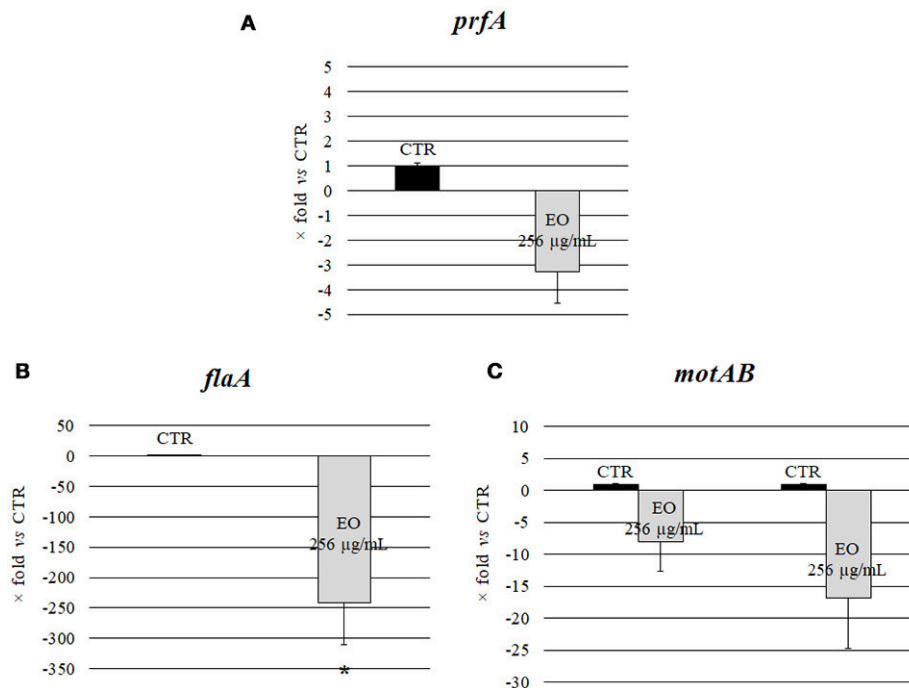


FIGURE 3 | Expression of motility genes of *L. monocytogenes* strain #80466 grown in presence of the *C. sativa* EO. Gene expression was normalized to the expression of the 16S rRNA gene in the same conditions compared to the control and is presented as x-fold: **(A)** *prfA*; **(B)** *flaA*; **(C)** *motA* and *motB*. Mean values and standard deviations of three experiments. Asterisks indicate significant values compared with control ($p \leq 0.05$). CTR, control (*L. monocytogenes* strain grown in the absence of EO).

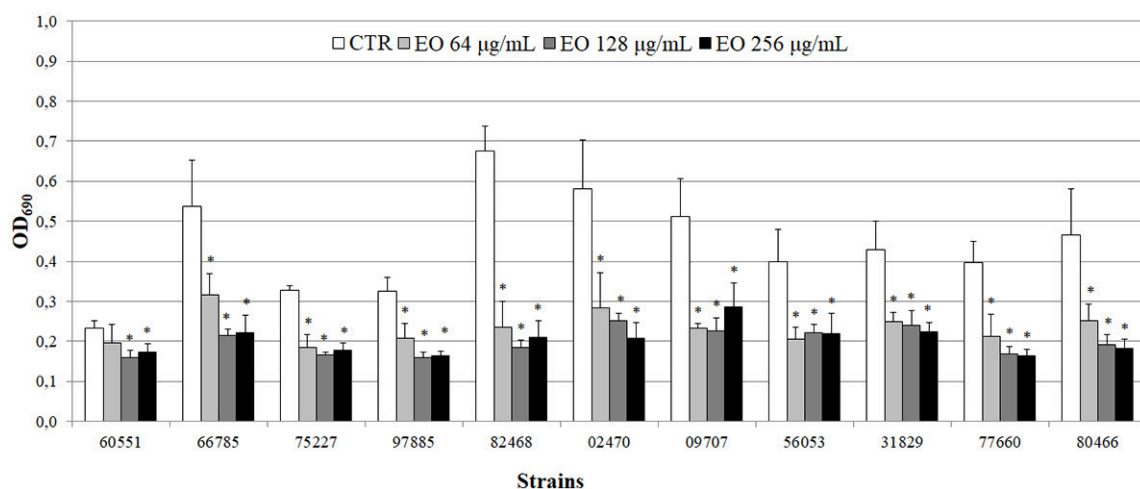


FIGURE 4 | Biofilm production by *L. monocytogenes* in presence of the *C. sativa* EO. Exposure to the three EO concentrations resulted in a shift to a lower producer type in all but one (#60551) of the 11 strains. Values are mean $\text{OD}_{690} \pm \text{SD}$ of three experiments. Asterisks indicate significant values ($p \leq 0.05$) compared with control (*L. monocytogenes* strain grown in the absence of EO).

Effects of Exposure of *L. monocytogenes* Strains to the *C. sativa* EO on Caco-2 Cell Invasion Efficiency and CPE

Preliminary Caco-2 infection experiments were conducted to ascertain the ability of *L. monocytogenes* strains to enter Caco-2 cells in the gentamicin survival test. Three strains were excluded from further experiments due to low invasion efficiency; the other 8 strains, which showed an invasion efficiency up to 4.1% of the initial inoculum, were used in infection inhibition experiments. Remarkably, the invasion efficiency of Caco-2 cells by 7/8 strains was strongly reduced (from 25.9 to 97%) when bacteria were grown in presence of 256 µg/mL of the *C. sativa* EO (Figure 5).

The viability of infected Caco-2 cells was assessed with trypan blue, which stains dead cells but is actively excluded from viable eukaryotic cells. The test demonstrated a dramatic CPE reduction in *L. monocytogenes* strains grown in presence of 256 µg/mL of the *C. sativa* EO (Figure 6), in particular, the monolayers infected with the extract-exposed strains were actually indistinguishable from the uninfected monolayers, whereas the CPE of control monolayers, i.e., those infected with strains grown without the EO, took the form of large, almost contiguous, stained areas.

Survival of *G. mellonella* Larvae Infected With *L. monocytogenes* Grown in Presence of the *C. sativa* EO

The ability of a sublethal concentration of the *C. sativa* EO to attenuate *L. monocytogenes* virulence was tested *in vivo* using the *G. mellonella* model. Larvae were infected with *L. monocytogenes* strains grown with and without (control) 256 µg/mL of the *C. sativa* EO. Larvae were considered

dead when they turned black and did not respond to touch. On day 6 after infection with listeriae, larval mortality was about 50% in the group infected with the strains grown without the EO whereas, remarkably, survival rates greater than 90% ($p = 0.0009$) were seen in the group infected with the strains grown with the EO (Figures 7A,B). PBS (negative control) did not result in larval mortality (data not shown).

DISCUSSION

C. sativa L. has been a source of food, fuel, paper, and building materials, a textile fiber, and a folk medicine remedy for thousands of years, and was eventually abandoned due to its high content in psychotropic compounds. Currently, industrial varieties containing low Δ^9 -THC concentrations are being studied for their powerful bioactive phytochemicals (Andre et al., 2016).

The antibacterial activity of freshly extracted EO from industrial *C. sativa* varieties has been assessed by Nissen et al. (2010) against Gram-positive and Gram-negative bacteria, mostly food-borne pathogens. In this study, GC-MS analysis of the EO obtained by distillation of the inflorescences and leaves of the variety Futura 75 disclosed a chemical composition similar to the one reported by Nissen et al. (2010) for this variety. Susceptibility experiments, carried out by the microdilution method, demonstrated that the EO and its two main components, α -pinene and myrcene, showed moderate bactericidal activity against clinical strains of *L. monocytogenes*.

The study also evaluated the effects of sublethal concentrations of the *C. sativa* EO on *L. monocytogenes* virulence traits such as motility, biofilm production, and cell

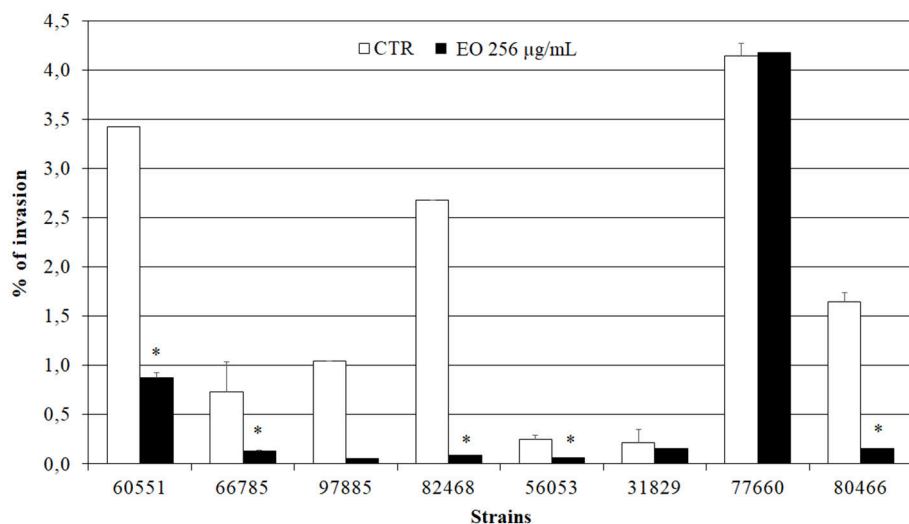
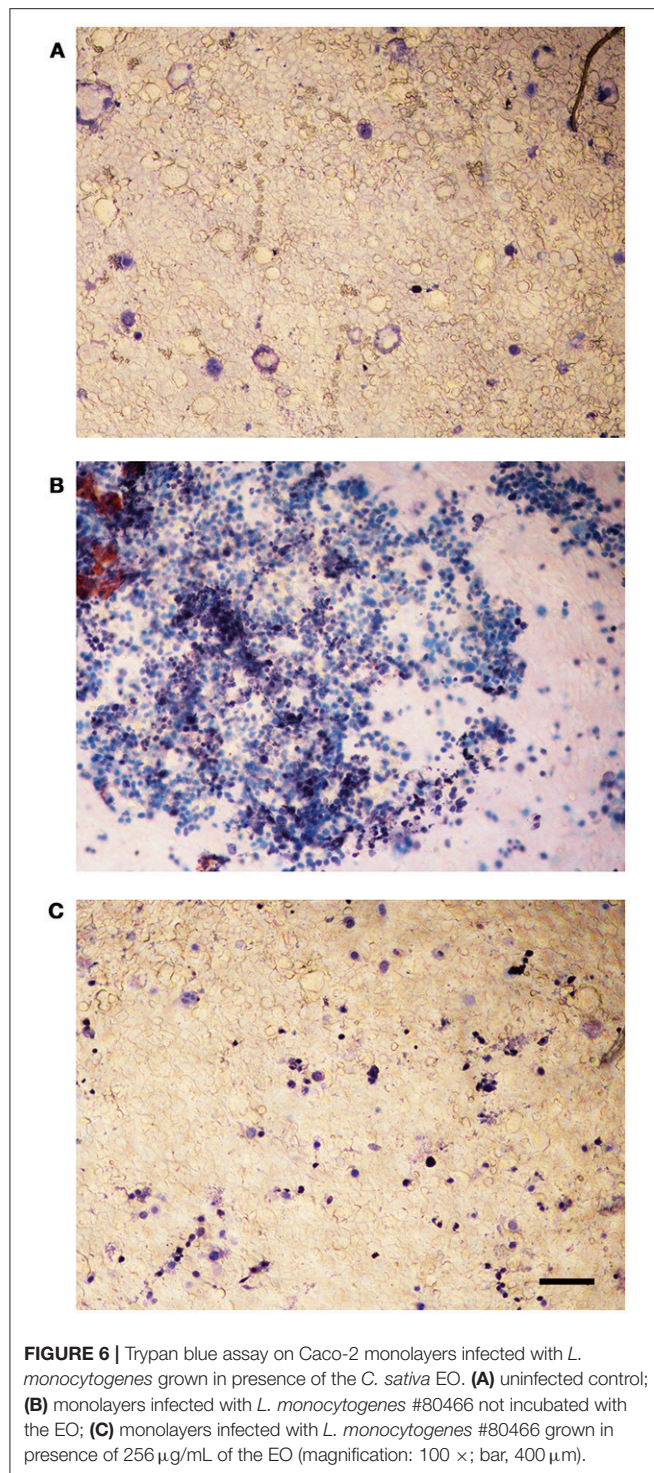


FIGURE 5 | Caco-2 cell invasion by *L. monocytogenes* strains grown in presence of the *C. sativa* EO. Data are expressed as percentage (compared with the initial inoculum) of viable bacteria recovered after 2 h incubation with gentamicin (gentamicin survival test). Each column is the mean of three experiments. Asterisks indicate significant values ($p \leq 0.05$) compared with control (*L. monocytogenes* strains grown in the absence of EO).



invasion. Motility was assessed by phenotypic (umbrella and soft agar motility assay) and molecular (real time RT-PCR) approaches and by LM and SEM observation. Both motility tests demonstrated that, after growth in presence of the *C. sativa* EO, all listerial strains became non-motile. Remarkably, flagella staining of treated cells showed aggregates of listeriae with

the flagella trapped inside the aggregates; SEM demonstrated that the flagella were adherent to the cell rather than free, as in control specimens. Real time RT-PCR experiments showed a downregulation of flagellar motility genes *flaA* (encoding flagellin) and *motA* and *motB* (encoding a part of the flagellar motor). A reduced expression levels of *prfA*, the transcriptional activator of genes involved in cell invasion, intracellular surviving, and spreading to neighboring cells, was also demonstrated after growth in the presence of *C. sativa* EO. Inhibition of *L. monocytogenes* motility by natural products has also been reported with trans-cinnamaldehyde from *Cinnamomum zeylandicum*, carvacrol, and thymol, the main components of oregano and thyme EO (Upadhyay et al., 2012). In the Gram-negative pathogens *Salmonella* Typhimurium and *Escherichia coli* O157:H7, carvacrol affects motility through loss of flagellum functionality (Inamuco et al., 2012) and inhibition of flagellin synthesis (Burt et al., 2007), respectively.

Since flagella and flagellum-mediated motility are important virulence traits of *L. monocytogenes* for initial surface attachment and subsequent biofilm formation (Lemon et al., 2007) as well as for cell invasion (Dons et al., 2004), we tested the hypothesis that a reduction of motility by sublethal concentrations of the *C. sativa* EO would affect biofilm-forming and cell invasion ability. The hypothesis was successfully demonstrated. Remarkably, the number of intracellular listeriae (gentamicin survival test) was almost zero when Caco-2 cells were infected with listeriae exposed to the EO and their viability was unaffected (trypan blue test). The present results therefore clearly demonstrate that sublethal concentrations of the *C. sativa* EO can affect the virulence of *L. monocytogenes* *in vitro*.

In vivo experiments using *G. mellonella* larvae as a model (Rakic Martinez et al., 2017) were performed to establish whether incubation of listeriae with sublethal concentrations of the *C. sativa* EO would prevent larval infection. The test has recently emerged as a promising model to assess the virulence of numerous human pathogens, including *L. monocytogenes*. In our study, larvae infected with *L. monocytogenes* grown in presence of sublethal EO concentrations showed a significantly higher survival compared with larvae infected with untreated listeriae. Thus, the *in vivo* experiments confirmed the protective activity of the *C. sativa* EO against *L. monocytogenes* infection.

Since LLO production is critical to *L. monocytogenes* pathogenesis in *G. mellonella* (Joyce and Gahan, 2010) we could hypothesize that the protective activity of the *C. sativa* EO is due to the attenuation of this virulence factor.

Targeting microbial virulence rather than survival is an exciting novel strategy with the potential to reduce the evolutionary pressure for the development of resistance. Food contamination by *L. monocytogenes* remains a major concern for the food processing industry, particularly the plants making ready-to-eat and processed food. The present work provides a baseline in the study of the anti-virulence properties of the EO of *C. sativa* against *L. monocytogenes*. Further studies are needed to understand if it could be used as an alternative agent for the control of *L. monocytogenes* in food processing plants.

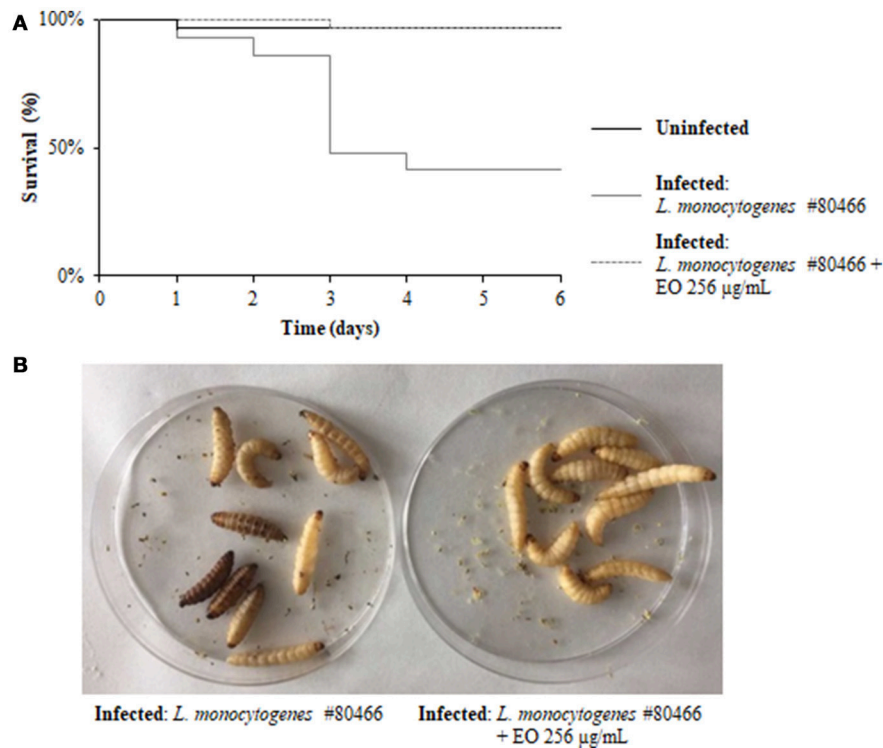


FIGURE 7 | Survival of *G. mellonella* larvae infected with *L. monocytogenes* strain #80466 grown in presence of the *C. sativa* EO. **(A)** Kaplan-Meier survival curves of *G. mellonella* larvae after 6 days from injection with *L. monocytogenes* strain #80466 are shown. No more than one control larvae injected with PBS died in any given trial (data not shown); **(B)** Dead (black and motionless) and viable (yellowish and moving) larvae.

AUTHOR CONTRIBUTIONS

BF, GM, and EM conceived the study. BF, GM, EM, AP, and MR designed the experiments. GM, EM, AP, and AG performed the experiments. BF, GM, EM, AP, GF, TB, MR, and AG analyzed the data. BF, GM, and EM wrote the paper. All authors approved the manuscript.

FUNDING

This study was supported by the Project: Plant compounds to fight bacterial antibiotic resistance and virulence:

searching for bioactive molecules among the agricultural biodiversity of the Marche Region. ERC Field LS6 - 43.000,00 €. Progetto strategico di ricerca di Ateneo 2016 (UNIVPM-DiSBSP) Coordinator: Bruna Facinelli; staff members: Armanda Pugnaroni, Gianna Ferretti, and Tiziana Bacchetti.

ACKNOWLEDGMENTS

The authors are grateful to Dr. Enrica Cimarelli, President of APPO Marche, for providing the *C. sativa* L. essential oil.

REFERENCES

- Andre, C. M., Hausman, J. F., and Guerriero, G. (2016). *Cannabis sativa*: the plant of the thousand and one molecules. *Front. Plant Sci.* 7:19. doi: 10.3389/fpls.2016.00019
- Bierne, H., Milohanic, E., and Kortebe, M. (2018). To be cytosolic or vacuolar: the double life of *Listeria monocytogenes*. *Front. Cell. Infect. Microbiol.* 8:136. doi: 10.3389/fcimb.2018.00136
- Boqvist, S., Söderqvist, K., and Vågsholm, I. (2018). Food safety challenges and one Health within Europe. *Acta Vet. Scand.* 60:1. doi: 10.1186/s13028-017-0355-3
- Burt, S. A., van der Zee, R., Koets, A. P., de Graaff, A. M., van Knapen, F., Gastra, W., et al. (2007). Carvacrol induces heat shock protein 60 and inhibits synthesis of flagellin in *Escherichia coli* O157:H7. *Appl. Environ. Microbiol.* 73, 4484–4490. doi: 10.1128/AEM.00340-07
- Cannas, S. (2016). Chemical composition, cytotoxicity, antimicrobial and antifungal activity of several essential oils. *Nat. Prod. Res.* 30, 332–339. doi: 10.1080/14786419.2015.1060592
- Chen, G. Y., Pensinger, D. A., and Sauer, J. D. (2017). *Listeria monocytogenes* cytosolic metabolism promotes replication, survival, and evasion of innate immunity. *Cell. Microbiol.* 19:e12762. doi: 10.1111/cmi.12762
- Christensen, G. D., Simpson, W. A., Younger, J. J., Baddour, L. M., Barrett, F. F., Melton, D. M., et al. (1985). Adherence of coagulase-negative staphylococci to plastic tissue culture plates: a quantitative model for the adherence of staphylococci to medical devices. *J. Clin. Microbiol.* 22, 996–1006.
- Clinical and Laboratory Standards Institute (2017). *Performance Standards for Antimicrobial Susceptibility Testing*, 27th Edn. CLSI (Suppl.) M100. Wayne, PA: USA.

- Colagiorgi, A., Bruini, I., Di Ciccio, P. A., Zanardi, E., Ghidini, S., and Ianieri, A. (2017). *Listeria monocytogenes* biofilms in the wonderland of food industry. *Pathogens* 6:41. doi: 10.3390/pathogens6030041
- de las Heras, A., Cain, R. J., Bielecka, M. K., and Vázquez-Boland, J. A. (2011). Regulation of listeria virulence: PrfA master and commander. *Curr. Opin. Microbiol.* 14, 118–127. doi: 10.1016/j.mib.2011.01.005
- Dons, L., Eriksson, E., Jin, Y., Rottenberg, M. E., Kristensson, K., Larsen, C. N., et al. (2004). Role of flagellin and the two-component CheA/CheY system of *Listeria monocytogenes* in host cell invasion and virulence. *Infect. Immun.* 72, 3237–3244. doi: 10.1128/IAI.72.6.3237-3244.2004
- Drolia, R., Tenguria, S., Durkes, A. C., Turner, J. R., and Bhunia, A. K. (2018). *Listeria* adhesion protein induces intestinal epithelial barrier dysfunction for bacterial translocation. *Cell Host Microbe*. 23, 470–484. doi: 10.1016/j.chom.2018.03.004
- Duan, Q., Zhou, M., Zhu, L., and Zhu, G. (2013). Flagella and bacterial pathogenicity. *J. Basic Microbiol.* 53, 1–8. doi: 10.1002/jobm.201100335
- EFSA and ECDC (2016). The European Union summary report on trends and sources of zoonoses, zoonotic agents and food-borne outbreaks in 2015. *EFSA J.* 14:4634. doi: 10.2903/j.efsa.2016.4634
- Facinelli, B., Giovanetti, E., Magi, G., Biavasco, F., and Varaldo, P. E. (1998). Lectin reactivity and virulence among strains of *Listeria monocytogenes* determined *in vitro* using the enterocyte-like cell line Caco-2. *Microbiology* 144, 109–118. doi: 10.1099/00221287-144-1-109
- Freitag, N. E., Port, G. C., and Miner, M. D. (2009). *Listeria monocytogenes*-from saprophyte to intracellular pathogen. *Nat. Rev. Microbiol.* 7, 623–628. doi: 10.1038/nrmicro2171
- Holler, J. M., Bosy, T. Z., Dunkley, C. S., Levine, B., Past, M. R., and Jacobs, A. (2008). $\Delta 9$ -tetrahydrocannabinol content of commercially available hemp products. *J. Anal. Toxicol.* 32, 428–432. doi: 10.1093/jat/32.6.428
- Inamuco, J., Veenendaal, A. K., Burt, S. A., Post, J. A., Tjeerdsma-van Bokhoven, J. L., Haagsman, H. P., et al. (2012). Sub-lethal levels of carvacrol reduce *Salmonella* Typhimurium motility and invasion of porcine epithelial cells. *Vet. Microbiol.* 157, 200–207. doi: 10.1016/j.vetmic.2011.12.021
- Josenhans, C., and Suerbaum, S. (2002). The role of motility as a virulence factor in bacteria. *Int. J. Med. Microbiol.* 291, 605–614. doi: 10.1078/1438-4221-00173
- Joyce, S. A., and Gahan, C. G. (2010). Molecular pathogenesis of *Listeria monocytogenes* in the alternative model host *Galleria mellonella*. *Microbiology* 156, 3456–3468. doi: 10.1099/mic.0.040782-0
- Kathariou, S. (2002). *Listeria monocytogenes* virulence and pathogenicity, a food safety perspective. *J. Food Prot.* 65, 1811–1829. doi: 10.4315/0362-028X-65.11.1811
- Krawczyk-Balska, A., and Markiewicz, Z. (2016). The intrinsic cephalosporin resistome of *Listeria monocytogenes* in the context of stress response, gene regulation, pathogenesis and therapeutics. *J. Appl. Microbiol.* 120, 251–265. doi: 10.1111/jam.12989
- Langeveld, W. T., Veldhuizen, E. J., and Burt, S. A. (2014). Synergy between essential oil components and antibiotics: a review. *Crit. Rev. Microbiol.* 40, 76–94. doi: 10.3109/1040841X.2013.763219
- Lemon, K. P., Higgins, D. E., and Kolter, R. (2007). Flagellar motility is critical for *Listeria monocytogenes* biofilm formation. *J. Bacteriol.* 189, 4418–4424. doi: 10.1128/JB.01967-06
- Lomonaco, S., Nucera, D., and Filippello, V. (2015). The evolution and epidemiology of *Listeria monocytogenes* in Europe and the United States. *Infect. Genet. Evol.* 35, 172–183. doi: 10.1016/j.meegid.2015.08.008
- Marini, E., Magi, G., Mingoa, M., Pugnali, A., and Facinelli, B. (2015). Antimicrobial and anti-virulence activity of capsaicin against erythromycin-resistant, cell-invasive Group A Streptococci. *Front. Microbiol.* 6:1281. doi: 10.3389/fmicb.2015.01281
- Marini, E., Magi, G., Vincenzi, C., Manso, E., and Facinelli, B. (2016). Ongoing outbreak of invasive listeriosis due to serotype 1/2a *Listeria monocytogenes*, Ancona province, Italy, January 2015 to February 2016. *Euro Surveill.* 21:17. doi: 10.2807/1560-7917.ES.2016.21.17.30217
- McDougal, C. E., and Sauer, J. D. (2018). *Listeria monocytogenes*: the impact of cell death on infection and immunity. *Pathogens* 7:8. doi: 10.3390/pathogens7010008
- Mukherjee, K., Altincicek, B., Hain, T., Domann, E., Vilcinskas, A., and Trinad, C. (2010). *Galleria mellonella* as a model system for studying *Listeria* pathogenesis. *Appl. Environ. Microbiol.* 76, 310–317. doi: 10.1128/AEM.01301-09
- Nazzaro, F., Fratianni, F., De Martino, L., Coppola, R., and De Feo, V. (2013). Effect of essential oils on pathogenic bacteria. *Pharmaceuticals* 6, 1451–1474. doi: 10.3390/ph6121451
- Nissen, L., Zatta, A., Stefanini, I., Grandi, S., Sgorbati, B., Biavati, B., et al. (2010). Characterization and antimicrobial activity of essential oils of industrial hemp varieties (*Cannabis sativa* L.). *Fitoterapia* 81, 413–419. doi: 10.1016/j.fitote.2009.11.010
- Peel, M., Donachie, W., and Shaw, A. (1988). Temperature-dependent expression of flagella of *Listeria monocytogenes* studied by electron microscopy, SDS-PAGE and western blotting. *J. Gen. Microbiol.* 134, 2171–2178.
- Radosheвич, L., and Cossart, P. (2018). *Listeria monocytogenes*: towards a complete picture of its physiology and pathogenesis. *Nat. Rev. Microbiol.* 16, 32–46. doi: 10.1038/nrmicro.2017.126
- Rakic Martinez, M., Wiedmann, M., Ferguson, M., and Datta, A. R. (2017). Assessment of *Listeria monocytogenes* virulence in the *Galleria mellonella* insect larvae model. *PLoS ONE*. 12:e0184557. doi: 10.1371/journal.pone.0184557
- Rasko, D. A., and Sperandio, V. (2010). Anti-virulence strategies to combat bacteria-mediated disease. *Nat. Rev. Drug Dis.* 9, 117–128. doi: 10.1038/nrd3013
- Rousset, M. (1986). The human colon carcinoma cell lines HT-29 and Caco-2: two *in vitro* models for the study of intestinal differentiation. *Biochimie*. 68, 1035–1040. doi: 10.1016/S0300-9084(86)80177-8
- Silva, L. N., Zimmer, K. R., Macedo, A. J., and Trentin, D. S. (2016). Plant natural products targeting bacterial virulence factors. *Chem. Rev.* 116, 9162–9236. doi: 10.1021/acs.chemrev.6b00184
- Stepanovic, S., Vukovic, D., Dakic, I., Savic, B., and Svabic-Vlahovic, M. (2000). A modified microtiter-plate test for quantification of staphylococcal biofilm formation. *J. Microbiol. Methods*. 40, 175–179. doi: 10.1016/S0167-7012(00)00122-6
- Thønnings, S., Knudsen, J. D., Schonheyder, H. C., Søgaard, M., Arpi, M., Gradel, K. O., et al. (2016). Antibiotic treatment and mortality in patients with *Listeria monocytogenes* meningitis or bacteraemia. *Clin. Microbiol. Infect.* 22, 725–730. doi: 10.1016/j.cmi.2016.06.006
- Upadhyay, A., Johnny, A. K., Amalaradjou, M. A., Ananda Baskaran, S., Kim, K. S., and Venkitanarayanan, K. (2012). Plant-derived antimicrobials reduce *Listeria monocytogenes* virulence factors *in vitro*, and down-regulate expression of virulence genes. *Int. J. Food Microbiol.* 157, 88–94. doi: 10.1016/j.ijfoodmicro.2012.04.018
- Vázquez-Boland, J. A., Kuhn, M., Berche, P., Chakraborty, T., Domínguez-Bernal, G., Goebel, W., et al. (2001). *Listeria* pathogenesis and molecular virulence determinants. *Clin. Microbiol. Rev.* 14, 584–640. doi: 10.1128/CMR.14.3.584-640.2001

Conflict of Interest Statement: The authors declare that the research was conducted in the absence of any commercial or financial relationships that could be construed as a potential conflict of interest.

Copyright © 2018 Marini, Magi, Ferretti, Bacchetti, Giuliani, Pugnali, Rippo and Facinelli. This is an open-access article distributed under the terms of the Creative Commons Attribution License (CC BY). The use, distribution or reproduction in other forums is permitted, provided the original author(s) and the copyright owner(s) are credited and that the original publication in this journal is cited, in accordance with accepted academic practice. No use, distribution or reproduction is permitted which does not comply with these terms.



Antibiofilm and Antivirulence Activities of 6-Gingerol and 6-Shogaol Against *Candida albicans* Due to Hyphal Inhibition

Jin-Hyung Lee^{1†}, Yong-Guy Kim^{1†}, Pilju Choi², Jungyeob Ham², Jae Gyu Park^{3*} and Jintae Lee^{1*}

¹ School of Chemical Engineering, Yeungnam University, Gyeongsan, South Korea, ² Natural Products Research Institute, Korea Institute of Science and Technology, Gangneung, South Korea, ³ Advanced Bio Convergence Center, Pohang Technopark Foundation, Pohang, South Korea

OPEN ACCESS

Edited by:

You-Hee Cho,
CHA University, South Korea

Reviewed by:

Hee-Deung Park,
University of Wisconsin-Madison,
United States
Qing-shan Shi,
Guangdong Institute of
Microbiology (CAS), China

*Correspondence:

Jae Gyu Park
jaepark@pohangtp.org
Jintae Lee
jtlee@ynu.ac.kr

[†]These authors have contributed
equally to this work

Received: 07 June 2018

Accepted: 07 August 2018

Published: 28 August 2018

Citation:

Lee J-H, Kim Y-G, Choi P, Ham J, Park JG and Lee J (2018) Antibiofilm and Antivirulence Activities of 6-Gingerol and 6-Shogaol Against *Candida albicans* Due to Hyphal Inhibition. *Front. Cell. Infect. Microbiol.* 8:299. doi: 10.3389/fcimb.2018.00299

Candida albicans is an opportunistic pathogen and responsible for candidiasis. *C. albicans* readily forms biofilms on various biotic and abiotic surfaces, and these biofilms can cause local and systemic infections. *C. albicans* biofilms are more resistant than its free yeast to antifungal agents and less affected by host immune responses. Transition of yeast cells to hyphal cells is required for biofilm formation and is believed to be a crucial virulence factor. In this study, six components of ginger were investigated for antibiofilm and antivirulence activities against a fluconazole-resistant *C. albicans* strain. It was found 6-gingerol, 8-gingerol, and 6-shogaol effectively inhibited biofilm formation. In particular, 6-shogaol at 10 μ g/ml significantly reduced *C. albicans* biofilm formation but had no effect on planktonic cell growth. Also, 6-gingerol and 6-shogaol inhibited hyphal growth in embedded colonies and free-living planktonic cells, and prevented cell aggregation. Furthermore, 6-gingerol and 6-shogaol reduced *C. albicans* virulence in a nematode infection model without causing toxicity at the tested concentrations. Transcriptomic analysis using RNA-seq and qRT-PCR showed 6-gingerol and 6-shogaol induced several transporters (*CDR1*, *CDR2*, and *RTA3*), but repressed the expressions of several hypha/biofilm related genes (*ECE1* and *HWP1*), which supported observed phenotypic changes. These results highlight the antibiofilm and antivirulence activities of the ginger components, 6-gingerol and 6-shogaol, against a drug resistant *C. albicans* strain.

Keywords: antivirulence, biofilm, *C. albicans*, gingerol, hyphae, shogaol

INTRODUCTION

Candida albicans is an opportunistic pathogen normally present on skin and mucous membranes, such as, those of the vagina, mouth, and rectum. *C. albicans* colonizes host tissues and various indwelling medical devices (Ramage et al., 2005; Sardi et al., 2013) and readily develops biofilms on biotic and abiotic surfaces that are intrinsically resistant to conventional antifungal therapeutics and the host immune system (Nobile et al., 2006b). *C. albicans* can grow as oval budding yeasts, pseudohyphae, or true hyphae. For biofilm development, yeast cells initially attach to a surface, and this is then followed by germ tube formation and hyphal transition, and mature biofilms are typically formed within 24 h (Nobile et al., 2006b). The transition of yeast cells to hyphal cells

appears to regulate biofilm maturation, and hyphal transition is considered a crucial virulence factor in *Candida* infections (Carradori et al., 2016). Also, many clinical isolates of *C. albicans* exhibit drug resistance against commercial antifungals, such as azoles and polyenes, which are used to treat candidiasis (Tobudic et al., 2010; Taff et al., 2013; Sandai et al., 2016). Hence, novel antivirulence drugs not prone to the development of antifungal resistance, are required to eradicate *C. albicans* biofilms and virulence.

Phytochemicals are important sources for antimicrobial and antibiofilm agents against drug resistant microorganisms (Nascimento et al., 2000). Recently, several studies have demonstrated ginger components have antibiofilm activities against pathogenic bacteria, such as, ginger water extract against *Pseudomonas aeruginosa* (Kim and Park, 2013) and against *Salmonella Typhimurium* and *Escherichia coli* (Khiralla, 2015), and zingerone (Kumar et al., 2013), raffinose (Kim et al., 2016a), 6-gingerol (Kim et al., 2015), and 6- and 8-gingerol analogs (Choi et al., 2017) against *P. aeruginosa*. However, the antibiofilm activities of ginger components have not been studied in any yeast species.

In this study, the antibiofilm activities of six ginger components, namely, 6-gingerol, 8-gingerol, 10-gingerol, 6-shogaol, 8-shogaol, and 10-shogaol, were initially investigated against antifungal-resistant *C. albicans* strain. Two active compounds 6-gingerol and 6-shogaol were further evaluated with respect to hyphal and virulence inhibition. Scanning electron microscopy (SEM) and confocal laser scanning microscopy (CLSM) were used to investigate the effects of 6-gingerol and 6-shogaol on morphological changes, biofilm formation, and on the hyphal growth of *C. albicans*. The molecular basis of the alterations in *C. albicans* physiology upon exposure to 6-gingerol and 6-shogaol was also investigated using RNA-seq and qRT-PCR. In addition, an *in vivo* *Caenorhabditis elegans* model was used to confirm the antivirulence efficacies of 6-gingerol and 6-shogaol. This is the first report to be issued regarding the use of 6-gingerol or 6-shogaol to inhibit *C. albicans* biofilm formation and hyphal formation and to reduce the virulence of this pathogen.

MATERIALS AND METHODS

Strains and Medium

In this study, we used fluconazole resistant *C. albicans* strain DAY185 (minimum inhibitory concentration >1,024 µg/ml). *C. albicans* was maintained in potato dextrose agar (PDA) or potato dextrose broth (PDB). The gingerols and shogaols (6-gingerol, 8-gingerol, 10-gingerol, 6-shogaol, 8-shogaol, and 10-shogaol) used in this study were purchased from Sigma-Aldrich (St. Louis, USA) and dissolved in dimethyl sulfoxide (DMSO). DMSO was used as a negative control for all experiments and the concentration of DMSO in media did not exceed 0.1% (vol/vol), which did not affect the antibiofilm or antivirulence activities. Cell growths and turbidities were measured using spectrophotometer (UV-160, Shimadzu, Japan) at 620 nm.

Assays for Biofilm Formation

Candida biofilms were developed on 96-well polystyrene plates, as previously reported (Lee et al., 2011). Briefly, a 2-day single colony was inoculated into 25 ml of PDB and incubated overnight at 37°C. Overnight cultures at an initial turbidity of 0.1 at 600 nm were then inoculated into PDB (final volume 300 µl) with or without a gingerol or a shogaol, and incubated for 24 h without shaking at 37°C. Biofilm cells that adhered to the 96-well plates were stained with 0.1% crystal violet (Sigma-Aldrich, St. Louis, USA) for 20 min, washed repeatedly with sterile distilled water, and resuspended in 95% ethanol. Plates were read at 570 nm and results are presented as the averages of at least six repetitions.

Confocal Laser Scanning Microscopy Assay of Biofilm Formation

C. albicans biofilms were grown on 96-well plates with or without 6-gingerol or 6-shogaol without shaking for 24 h. Planktonic cells were then removed by washing with water three times, and biofilms were stained with carboxyfluorescein diacetate succinimidyl ester (a minimally fluorescent lipophile; Invitrogen, Molecular Probes, Inc, Eugene, USA) (Lee et al., 2016). Plate bases were then visualized using an (a 488 nm) Ar laser (emission 500 to 550 nm) under a confocal laser microscope (Nikon Eclipse Ti, Tokyo), and COMSTAT biofilm software (Heydorn et al., 2000) was then used to calculate biovolumes (µm³ µm⁻²), mean biofilm thicknesses (µm), and substratum coverages (%). Two independent cultures were performed under each experimental condition and at least 10 random positions were assayed.

Observation of *C. albicans* Colony Morphologies on Solid Media

A freshly prepared glycerol stock of *C. albicans* was used to streak on PDA plates supplemented with and without 6-gingerol or 6-shogaol. Plates were then incubated for 7 days at 37°C and temporal changes in colony morphologies were observed using an iRISTM Digital Cell Imaging System (Logos Bio Systems, Korea).

Hyphal Assay in Liquid Media

Cell aggregation was analyzed as previously described (Zelante et al., 2012). Briefly, *C. albicans* cells were inoculated into 2 ml of PDB medium or RPMI-1640 medium at density of 10⁵ CFU/ml in 14 ml test tubes with or without 6-gingerol or 6-shogaol and incubated at 37°C for 24 h with shaking at 250 rpm. Cell cultures (2 ml) were then transferred into glass-bottom dishes and observed. Aggregated cells were visualized in bright field using the iRISTM Digital Cell Imaging System (Logos Bio Systems, Korea) at a magnification of 4x. At least, four independent experiments were conducted.

Microscopic Imaging of Hyphal Formation

Scanning electron microscopy (SEM) was used to observe the morphologies of biofilm cells attached to a nylon membrane, as previously described (Kim et al., 2016b). Briefly, a nylon

membrane was cut into 0.5×0.5 cm pieces and placed in 96-well plates containing *C. albicans* grown with or without 6- gingerol or 6-shogaol and incubated for 24 h at 37°C. Cells that adhered to the nylon membrane were fixed with glutaraldehyde (2.5%) and formaldehyde (2%) for 24 h and then post-fixed using osmium, dehydrated with an ethanol series (50, 70, 80, 90, 95, and 100%), and isoamyl acetate. After critical-point drying, cells were examined and imaged using a S-4100 scanning electron microscope (Hitachi, Japan) at a voltage of 15 kV.

RNA Isolation for RNA-Seq and Quantitative Real-Time PCR (qRT-PCR)

For transcriptomic analyses, 25 ml of *C. albicans* at an initial turbidity of 0.1 at OD₆₀₀ was inoculated into PDB in 250 ml Erlenmeyer flasks and incubated for 4 h at 37°C with agitation (250 rpm) in the presence or absence of 6- gingerol (50 µg/ml) or 6-shogaol (10 µg/ml). To prevent RNA degradation, RNase inhibitor (RNAlater, Ambion, TX, USA) was added to cells. Total RNA was isolated using a hot acidic phenol method (Amin-ul Mannan et al., 2009), and RNA was purified using a Qiagen RNeasy mini Kit (Valencia, CA, USA).

RNA-Seq and RNA Library Preparation and Sequencing

For RNA-Seq, a RNA library was constructed using the SMARTer Stranded RNA-Seq Kit (Clontech Laboratories, Inc., USA). Briefly, 2 µg of total RNA was incubated with magnetic beads decorated with oligo-dT and then RNAs, other than mRNA, were removed using washing solution. Library production was initiated by the random hybridization of starter/stopper heterodimers to poly(A) RNA bound to the magnetic beads. These starter/stopper heterodimers contained Illumina-compatible linker sequences. A single-tube reverse transcription and ligation reaction extended the starter to the next hybridized heterodimer, where the newly-synthesized cDNA insert was ligated to the stopper. Second strand synthesis was performed to release the library from the beads, and the library was then amplified. Barcodes were introduced when the library was amplified. High-throughput sequencing was performed by paired-end 100 sequencing using HiSeq 2500 (Illumina, Inc., USA).

RNA-Seq Data Analysis

mRNA-Seq reads were mapped using TopHat software (Trapnell et al., 2009) in order to obtain the alignment file. Differentially expressed genes were identified based on counts from unique and multiple alignments using Bedtools (Quinlan and Hall, 2010). RT (Read Count) data were processed by Quantile normalization using Bioconductor (Gentleman et al., 2004). The alignment files also were used to assemble transcripts, estimate their abundances, and to detect the differential expressions of genes or isoforms using Cufflinks. FPKM (fragments per kilobase of exon per million fragments) was used to determine the expression levels of gene regions. Gene classification was based on the results of searches performed using DAVID (<http://david.abcc.ncifcrf.gov/>). The RNA-seq data were deposited at NCBI Gene Expression Omnibus and are accessible through

accession number GSE117201. Differentially expressed gene study was analyzed with the DEG analysis method in ExDEGA (Excel based Differentially Expressed Gene Analysis) tool and classified by biological processes. Gene ontology analysis was performed at QuickGO (www.ebi.ac.uk/QuickGO/). KEGG (Kyoto Encyclopedia of Genes and Genomes) pathway analyses of the RNA-seq data were performed with the KEGG Mapper tool (http://www.genome.jp/kegg/tool/map_pathway2.html).

qRT-PCR

qRT-PCR was used to determine the expressions of hyphae-related genes (*ALS1*, *ALS3*, *ECE1*, *ECM38*, *EED1*, *EFG1*, *HYR1*, *HWPI*, *RBT1*, *SAP4*, and *UME6*). The specific primers and housekeeping gene (*RDN18*) used for qRT-PCR are listed in **Supplementary Table S2**. The qRT-PCR method used was as described by Kim et al. (2016b), and performed using SYBR Green master mix (Applied Biosystems, Foster City, USA) and an ABI StepOne Real-Time PCR System (Applied Biosystems). At least two independent cultures were used.

Antivirulence and Toxicity Assays Using the *Caenorhabditis elegans* Model

For the antivirulence assay, we used *C. elegans* strain *fer-15 (b26); fem-1 (hc17)*, as previously described (Manoharan et al., 2017a). Briefly, synchronized adult worms were fed on *C. albicans* lawns for 4 h at 25°C and then collected after washing three times with M9 buffer. Approximately 30 worms were then added to each well of 96-well plates containing PDB medium (300 µl) with or without 6- gingerol (10 or 50 µg/ml) or 6-shogaol (10 or 50 µg/ml). Assay plates were then incubated for 4 days at 25°C without shaking. For toxicity assays, 30 non-infected worms were pipetted into single wells of a 96-well dish containing M9 buffer and solutions of 6- gingerol or 6-shogaol were added to final concentrations of (0, 100, 200, or 500 µg/ml) without *C. albicans*. Plates were then incubated for 4 days at 25°C without shaking. Three independent experiments were performed in triplicate. Results are expressed as percentages of live worms (survival), as determined by responses to platinum wire touching after incubation for 4 days. Observations were made using an iRISTM Digital Cell Imaging System (Logos Bio Systems, Korea).

Statistical Analysis

Replication numbers for assays are provided above and results are expressed as means ± standard deviations. The statistical analysis was performed by one-way ANOVA followed by Dunnett's test using SPSS version 23 (SPSS Inc., Chicago, IL, USA). *P*-values of < 0.05 were regarded significant.

RESULTS

Inhibitory Effects of Gingerols and Shogaols on *C. albicans* Biofilm Formation

Initially, we investigated whether three gingerols (6- gingerol, 8- gingerol, and 10- gingerol) and three shogaols (6-shogaol, 8-shogaol, and 10-shogaol) affect biofilm formation by fluconazole-resistant *C. albicans* DAY185, cell growth was also measured

in the presence of these agents. Of the six compounds, 6-gingerol, 8-gingerol, and 6-shogaol significantly reduced biofilm formation at concentrations of 10, 50, and 100 $\mu\text{g/ml}$, while 10-gingerol, 8-shogaol, and 10-shogaol at 100 $\mu\text{g/ml}$ had no effect (Figure 1). In particular, 6-shogaol most significantly inhibited biofilm formation in a dose-dependent manner (Figure 1D). Specifically, 6-shogaol inhibited biofilm formation by 85, 94, and 94% at concentrations of 10, 50, and 100 $\mu\text{g/ml}$, respectively (Figure 1D). In addition, 6-gingerol and 8-gingerol at 50 $\mu\text{g/ml}$ inhibited biofilm formation by 88 and 80%, respectively (Figures 1A,B). It appeared the antibiofilm activities of gingerols and shogaols were related to the number of carbon side chains as larger carbon side chain numbers appeared to decrease antibiofilm activity in 10-gingerol, 8-shogaol, and 10-shogaol (Figures 1C,E,F). Notably, none of the three gingerols or three shogaols at concentrations up to 100 $\mu\text{g/ml}$ inhibited the planktonic cell growth of *C. albicans* (Figures 1A–F).

The antifungal activities of 6-gingerol and 6-shogaol were investigated by measuring minimum inhibitory concentrations (MIC), and for 6-gingerol and 6-shogaol MICs were 1000 $\mu\text{g/ml}$ and > 2000 $\mu\text{g/ml}$, respectively, against *C. albicans* DAY185. These results support the notion that biofilm formation by *C. albicans* was effectively inhibited by the antibiofilm activities of 6-gingerol and 6-shogaol and not by their fungicidal activities. Furthermore, the observed biofilm inhibition in the absence of any effect on planktonic cell growth suggests that unlike conventional fungicides, 6-gingerol and 6-shogaol may be less prone to the development of drug resistance.

Confocal laser microscope images showed that *C. albicans* formed dense biofilms in non-treated control samples, and that in the presence of 6-gingerol or 6-shogaol biofilm cellular densities and thicknesses were dramatically reduced (Figure 2A). Biofilm reduction was further confirmed by COMSTAT analysis, which showed 6-gingerol at 50 $\mu\text{g/ml}$ and 6-shogaol at 10 $\mu\text{g/ml}$ significantly reduced biofilm biomass, average thickness, and substrate coverage (Figure 2B). Specifically, biofilm biomass, thickness, and substrate coverage were reduced by 6-shogaol by more than 95% vs. the untreated control.

6-Gingerol and 6-Shogaol Inhibited Hyphal Growth and Cell Aggregation

To examine the effects of 6-gingerol and 6-shogaol on *C. albicans* morphology, a temporal observation of *C. albicans* colonies on potato dextrose agar (PDA) was performed and scanning electron microscope (SEM) was also used. Whereas hyphal protrusions from colonies of untreated *C. albicans* were observed after 3 days of incubation, in the presence of 6-shogaol at 10 $\mu\text{g/ml}$ suppressed hyphal protrusions for 7 days (Figure 3A). Furthermore, 6-shogaol at 10 $\mu\text{g/ml}$ was found to more effectively suppress hyphal protrusions than 6-gingerol at 50 $\mu\text{g/ml}$. SEM analysis also confirmed 6-gingerol and 6-shogaol substantially suppressed hyphal formation. As shown in Figure 3B, non-treated biofilms consisted predominately of hyphae and few pseudohyphae, where biofilms grown in the presence of 6-gingerol or 6-shogaol had shorter hyphae and more yeast cells.

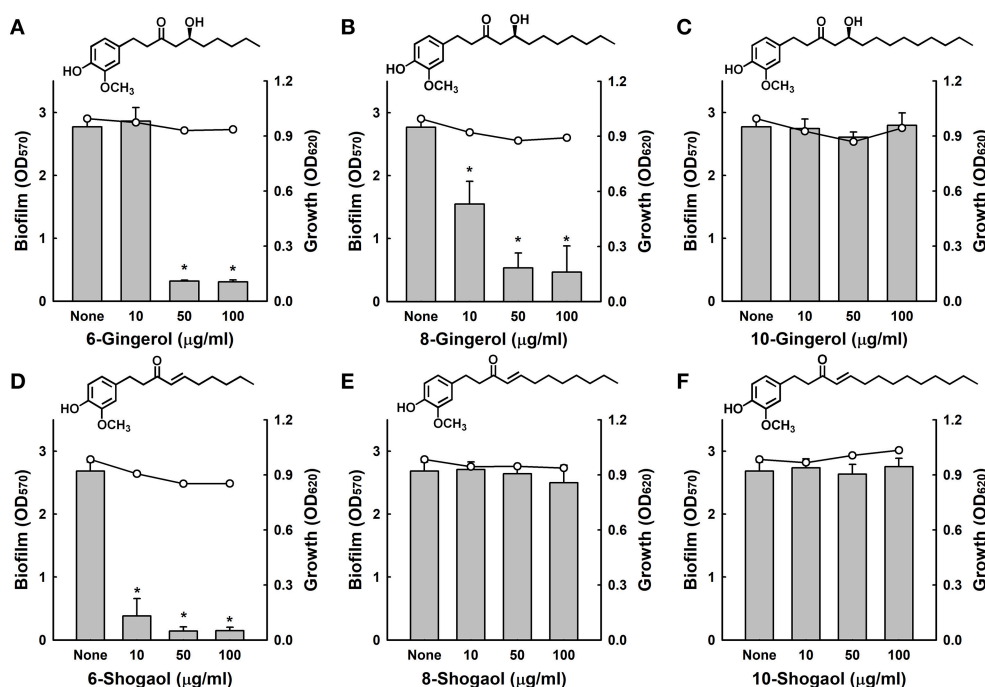


FIGURE 1 | Antibiofilm activities of gingerols and shogaols against *C. albicans*. The antibiofilm activities of three gingerols (A–C) and three shogaols (D–F) against *C. albicans* DAY185 in PDB medium were determined after culture for 24 h. Bars indicate biofilm formation and lines indicate planktonic cell growth. The chemical structures of gingerols and shogaols are shown. * $P < 0.05$ vs. non-treated controls. None; non-treated control.

It is generally believed yeast-to-hypha-transition and cell aggregation are prerequisites of biofilm development by *C. albicans* (Chandra et al., 2001). In liquid potato dextrose broth (PDB) medium, hyphal inhibition was evident in the presence of 6-gingerol or 6-shogaol and more marked in the presence of 6-shogaol (Figure 4A). Another hyphal assay was performed using RPMI-1640 medium, which promotes hyphal formation (Kucharikova et al., 2011). After incubation for 24 h, mostly hyphae and large cell aggregations entangled by hyphae were observed in the control sample whereas treatment with 6-gingerol or 6-shogaol resulted in much smaller cell aggregations in a dose-dependent manner (Figure 4B). Furthermore, hyphal and cell aggregation results were in-line with the observed antibiofilm activities of 6-gingerol and 6-shogaol. Taken together, these results show 6-gingerol and 6-shogaol both potentially inhibited hyphal formation and cell aggregation, and thus, suggest these two agents reduced biofilm formation by *C. albicans*.

Differential Gene Expressions by 6-gingerol and 6-shogaol

The molecular bases of the effects of 6-gingerol or 6-shogaol on biofilm formation and hyphal growth were investigated by RNA-seq and qRT-PCR. RNA-seq was first used to determine differential gene expressions in untreated sample and treated samples. Genes differentially expressed by at least 2-fold were selected and sorted into four functional categories including biofilm and hyphae-related genes or virulence-related genes (Supplementary Table S1). Overall, expression trends were similar after treatment with 6-gingerol at 50 µg/ml or 6-shogaol at 10 µg/ml. However, in view of the concentrations used 6-shogaol clearly had a greater effect than 6-gingerol. The addition of 6-gingerol significantly altered the expressions of 125 genes by more than 2-fold; 37 genes were up-regulated and 88 genes were down-regulated. Similarly, the addition of 6-shogaol significantly altered the expressions of 78 genes; 29 genes were up-regulated and 49 genes were down-regulated.

Notably, these expressional changes involved various biofilm- and hypha-related genes (Supplementary Table S1). Specifically, *HWPI* (hyphal cell wall protein, also known as *ECE2*) and *ECE1* (hypha-specific protein) were repressed by 6-gingerol or 6-shogaol by more than 7- and 2-fold, respectively, and *CDR1* and *CDR2* (multidrug transporter) and *RTA3* (lipid-translocating exporter) were up-regulated by 6-gingerol or 6-shogaol more than 4-fold. qRT-PCR was used to confirm gene expressional changes of highly differentially expressed loci in the 6-gingerol and 6-shogaol RNA-seq experiments. qRT-PCR for 15 selected genes showed differential changes in expression that generally concurred with RNA-seq assay results (Figure 5). For 6-shogaol experiment, RNA-seq and qRT-PCR showed the genes were repressed to similar extents, i.e., 10-fold vs. 20-fold for *CDR1*, 3-fold vs. 2-fold for *CHT2*, 12-fold vs. 9-fold for *HWPI*, 6-fold vs. 9-fold for *RTA3*, respectively. Similarly, 6-gingerol down-regulated the expression of *HWPI* and *CHT2*, and upregulated *CDR1* and *RTA3*. Nevertheless, the expressions of other biofilm and hyphae-related genes (*ALS1*, *ALS3*, *EFG1*, *HYR*, *PDR16*, *RBT1*, *SNQ2*,

TEC1, and *UME6*) were unaffected by 6-gingerol or 6-shogaol. Taken together, RNA-seq and qRT-PCR results showed that 6-gingerol and 6-shogaol significantly altered the expressions of some hypha-specific (*HWPI* and *ECE1*), biofilm-related (*HWPI* and *RTA3*) and multidrug transporter (*CDR1* and *CDR2*) related genes.

6-Gingerol and 6-Shogaol Rescued Nematodes Infected With *C. albicans*

We examined whether 6-gingerol or 6-shogaol could affect *C. albicans* virulence in a *Caenorhabditis elegans* nematode model, which is an accepted alternative to mammalian models (Tampakakis et al., 2008). *C. albicans* infection caused 45% *C. elegans* fatality in 4 days. However, > 80% of nematodes survived in the presence of 6-gingerol or 6-shogaol at 50 µg/ml (Figures 6A,B). To investigate the chemical toxicities of 6-gingerol and 6-shogaol, non-infected nematodes were exposed to different concentrations of the two agents. We found 6-gingerol and 6-shogaol at concentrations up to 500 µg/ml were not toxic to *C. elegans* (Figure 6C). These results show that both 6-gingerol and 6-shogaol effectively promoted the survival of infected nematodes and that they had no toxic effects on the nematode.

DISCUSSION

Current study shows for the first time that the ginger components 6-gingerol and 6-shogaol reduce biofilm formation by a drug-resistant *C. albicans* strain by inhibiting hyphae growth and cell aggregation, and reduced fungal virulence.

Ginger (*Zingiber officinale* (L.) Rosc) has been used as a spice and herbal medicine for over 2000 years. Its roots and extracts contain polyphenol compounds, such as, gingerols, shogaols, paradols, gingerdiols, and zingerone, which have considerable antioxidant activity (Si et al., 2018). Fresh ginger contains about 4% of 6-gingerol by weight but almost no 6-shogaol. However, 6-shogaol is easily produced by dehydrating 6-gingerol using drying processes (Chen et al., 1986; Jolad et al., 2004). 6-Gingerol and 6-shogaol have been reported to be effective treatments for metabolic syndrome, cardiovascular disease, dementia, arthritis, diabetes, osteoporosis, cancers, and infectious diseases (Ali et al., 2008; Kim et al., 2010). The antibacterial activities of gingerols and shogaols have been also studied (Park et al., 2008). More recently, the antibiofilm activities of 6-gingerol (Kim et al., 2015) and 6- and 8-gingerol analogs (Choi et al., 2017) against *P. aeruginosa* have been reported. Interestingly, 6-gingerol inhibited biofilm formation of both *P. aeruginosa* (Kim et al., 2015) (Choi et al., 2017) and *C. albicans* without affecting the planktonic cell growth and showed no chemical toxicity. 6-Gingerol including its analogs interfere the quorum sensing system in *P. aeruginosa*, while 6-gingerol and 6-shogaol suppressed hyphal growth in this study.

Of the six gingerol and shogaol compounds studied in the present study, 6-gingerol and 6-shogaol most effectively reduced *C. albicans* biofilm formation (Figure 1) and 6-shogaol most

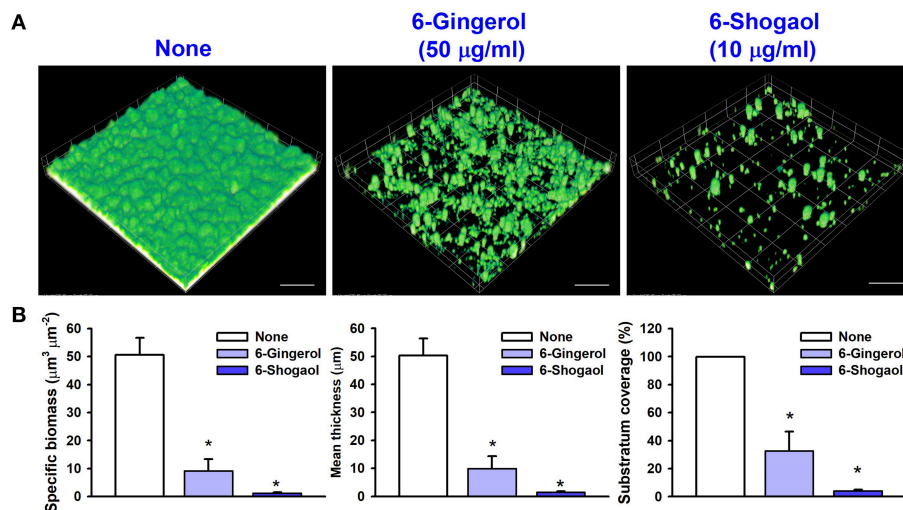


FIGURE 2 | Microscopic observations of the inhibitory effects of 6-gingerol and 6-shogaol on biofilms. Biofilm formation by *C. albicans* on polystyrene plates was observed in the presence of 6-gingerol at 50 µg/ml or 6-shogaol at 10 µg/ml by confocal laser microscopy (A). Scale bars represent 100 µm. Biofilm formation was quantified by using COMSTAT (B). **P* < 0.05 vs. non-treated controls. None; non-treated control.

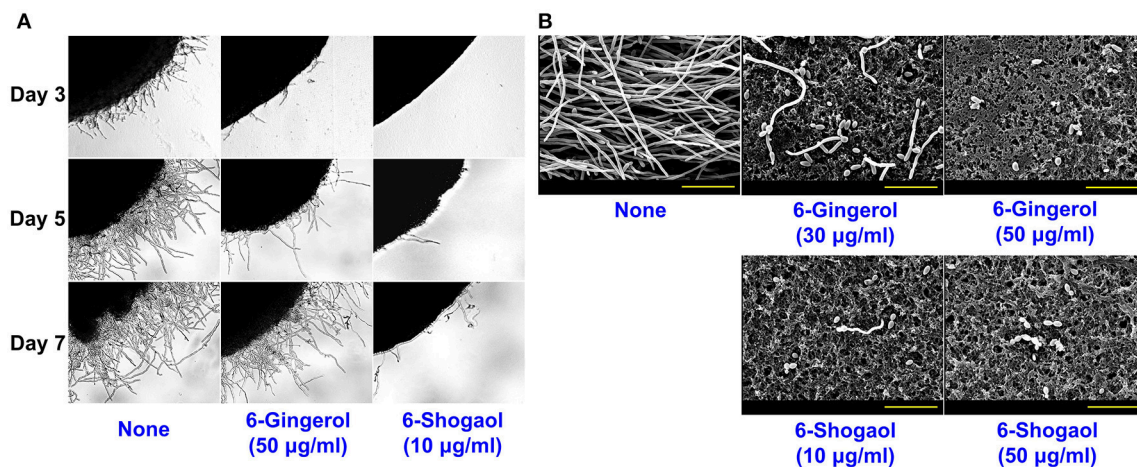


FIGURE 3 | Effects of 6-gingerol and 6-shogaol on the hyphal morphogenesis of *C. albicans*. *C. albicans* morphology on solid media (A). *C. albicans* was streaked on PDA solid plates in the absence or presence of 6-gingerol or 6-shogaol. Colony morphologies were observed during incubation for 7 days at 37°C. Inhibitions of hyphal growths by 6-gingerol or 6-shogaol in *C. albicans* biofilms were visualized by SEM (B). The scale bar represents 30 µm. None; non-treated control.

inhibited biofilm formation, hyphae growth, cell aggregation, and fungal virulence (Figures 1–5). It has been reported on several occasions that the biological potency of 6-shogaol is greater than that of 6-gingerol, and interestingly, these compounds differ structurally by the presence of a hydroxyl moiety in 6-gingerol and double bond on the carbon side chain of 6-shogaol (Figures 1A,D). The presence of this hydroxyl moiety has been previously reported to importantly influence proinflammatory gene activation (Isa et al., 2008). Furthermore, 6-shogaol has been reported to have a markedly stronger anti-tumorigenic effect than 6-gingerol (Wu et al., 2010). Previous studies have suggested α,β -unsaturated carbonyls are susceptible to

nucleophilic addition reactions with thiols, such as, glutathione, the most abundant nonprotein thiol *in vivo* (Boyland and Chasseaud, 1968). The transcriptomic analysis conducted in the present study showed 6-gingerol at 50 µg/ml resulted in similar changes in global gene expression as those induced by 6-shogaol at 10 µg/ml (Figure 5), which indicates 6-gingerol and 6-shogaol act at the transcriptional level. We suggest that the structural difference between 6-gingerol and 6-shogaol influence the abilities of these to influence the expressions of hyphae-regulatory genes in the hyphae signaling pathway. Also, we have observed the antibiofilm and antihyphae activities of 8-gingerol (Supplementary Figures S1, S2) and the action mode of

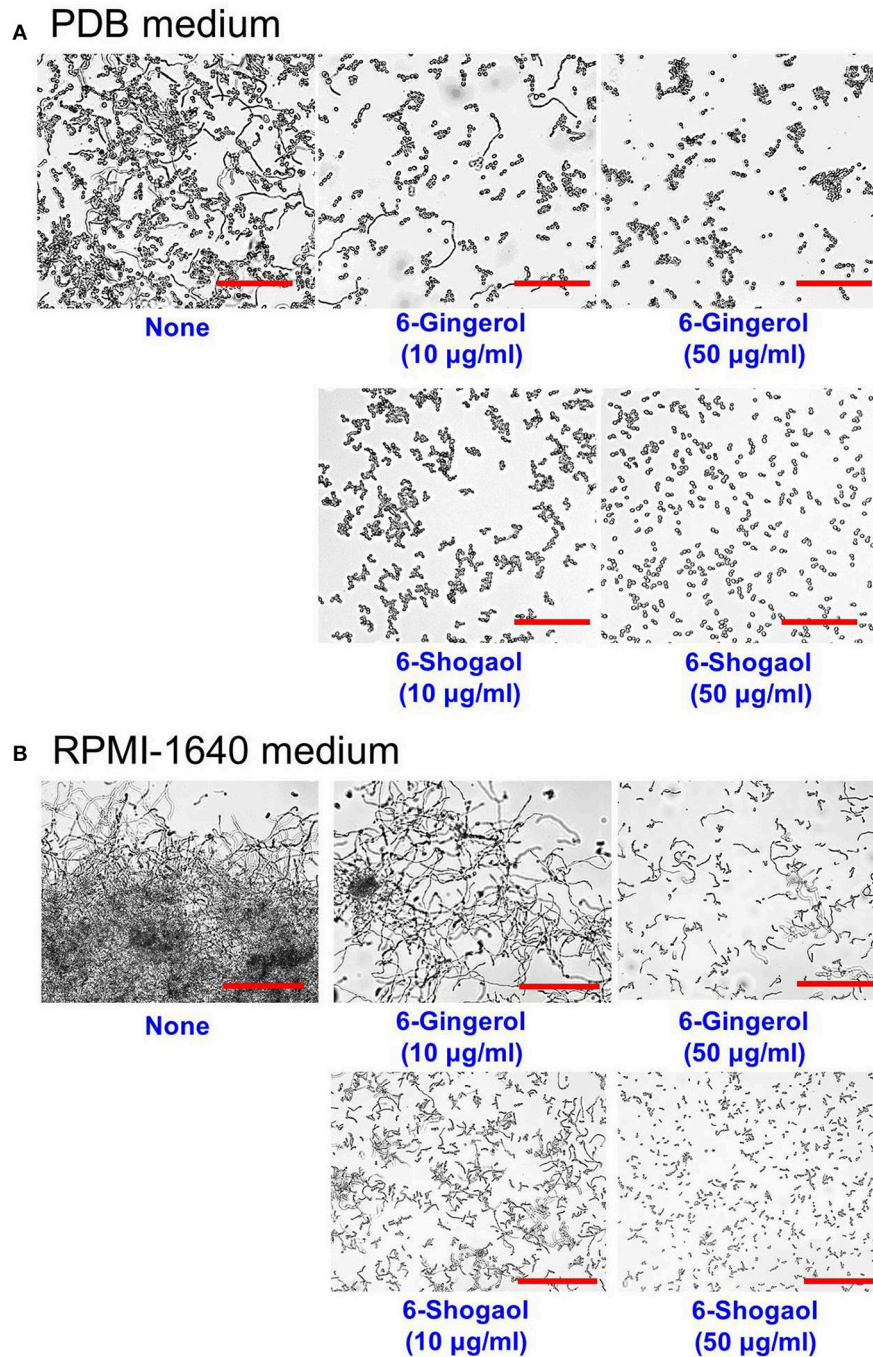


FIGURE 4 | Inhibitions of hyphal filamentation and aggregation by 6-gingerol and 6-shogaol in liquid medium. Inhibitions of hyphal filamentation in PDB medium **(A)** and in RPMI medium **(B)**. *C. albicans* cells were grown for 24 h in PDB medium or RPMI-1640 medium in the absence or presence of 6-gingerol or 6-shogaol. Hyphae were visualized after incubation for 24 h. The scale bar represents 200 μ m. None; non-treated control.

8-gingerol is probably similar to that of 6-gingerol and 6-shogaol in *C. albicans*.

In the present study, we found the transcriptional levels of several hyphae-specific and biofilm-related genes were significantly altered by 6-gingerol and by 6-shogaol (**Supplementary Table S1**). Gene ontology analysis showed that

6-gingerol and 6-shogaol regulated expression of genes involving membrane components, transport proteins, pathogenesis, stress, and biofilm formation (**Supplementary Figure S3**). KEGG analysis showed that 6-gingerol and 6-shogaol are similarly associated with several metabolisms such as glycerophospholipid, meiosis, ABC transport, and carbon

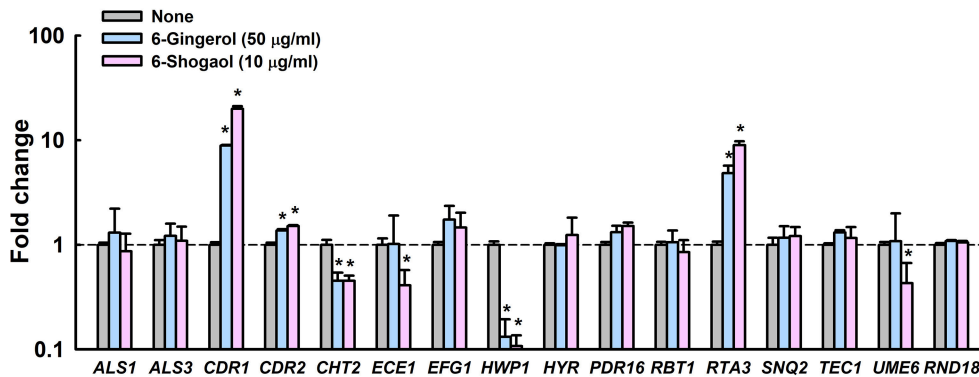


FIGURE 5 | Transcriptional profiles of *C. albicans* cells treated with or without 6-gingerol or 6-shogaol. *C. albicans* was cultivated with or without 6-gingerol at 50 µg/ml or 6-shogaol at 10 µg/ml for 4 h with shaking at 250 rpm. Transcriptional profiles were obtained by qRT-PCR. Fold changes represent changes in the transcriptions of treated vs. untreated *C. albicans*. The experiment was performed in duplicate (six qRT-PCR reactions were performed per gene). **P* < 0.05 vs. non-treated controls (None).

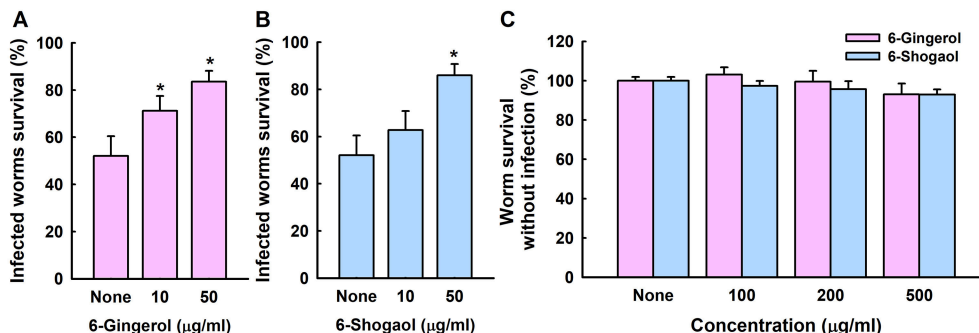


FIGURE 6 | Effects of 6-gingerol and 6-shogaol on *C. albicans* infected *C. elegans*. Nematode survival after exposure to *C. albicans* for 4 days in the presence of 6-gingerol (A) or 6-shogaol (B). The toxicities of 6-gingerol and 6-shogaol were determined by treating non-infected nematodes for 4 days (C). None indicates non-treated controls. Worm survival was determined based on movement. **p* < 0.05 vs. non-treated controls.

metabolism (Supplementary Figure S4). Most noticeably, *HWP1* and *ECE1* were down-regulated, and *ECE1* is essential for hyphal development and its expression has been shown to be correlated with cell elongation and biofilm formation (Nobile et al., 2006a). The down-regulations of *HWP1* and *ECE1* by 6-gingerol or 6-shogaol are consistent with their observed effects on biofilm formation and hyphal development. *HWP1* encodes a hyphal wall protein that is essential for hyphal development (Nobile et al., 2006b) and intercellular adherence (Orsi et al., 2014). Previously, we reported that camphor and fenchyl alcohol from cedar leaf oil (Manoharan et al., 2017b) and alizarin from the roots of the madder genus (Manoharan et al., 2017a) inhibit *C. albicans* biofilm formation by reducing hyphal formation by suppressing the gene expressions of *HWP1* and *ECE1*. Thus, it appears that the ability to reduce hyphal formation is not rare in the plant kingdom and that this offers a practical means of inhibiting biofilm formation by *C. albicans*.

On the other hand, both 6-gingerol and 6-shogaol upregulated the expressions of *CDR1* (*Candida* drug resistance, multidrug transporter) and *RTA3* (lipid-translocating exporter) about

10-fold. *CDR1* is a major ABC transporter, and in a previous study, *CDR1* mRNA levels were found to be positively correlated with an increase in azole resistance in *C. albicans* isolates and to be up-regulated during biofilm formation (White, 1997). Ramage et al. reported *CDR1* mutant was highly susceptible to fluconazole when growing planktonically but retained the resistant phenotype during biofilm growth (Ramage et al., 2002). On the other hand, the *RTA3* gene encodes Rta1 p-like lipid-translocating exporter and its expression was found to be positively associated with *CDR1* expression (Whaley et al., 2016). Hence, it is possible that *C. albicans* strives to pump out 6-gingerol and 6-shogaol, which might increase azole-resistance in *C. albicans* when azole antifungal agent(s) and 6-gingerol or 6-shogaol are co-administrated.

The emergence of multidrug resistant *Candida* strains has driven investigations on alternative antifungal agents, and antivirulence and antibiofilm agents have attracted considerable research interest. The present study shows that the antibiofilm effects of 6-gingerol and 6-shogaol on fluconazole-resistant *C. albicans* DAY185 are due to the prevention of yeast-hyphal

transition and not to the inhibition of fungal growth. Also, 6-gingerol and 6-shogaol effectively reduced *C. albicans* virulence *in vivo* in a *Caenorhabditis elegans* model with minimal chemical toxicity under the conditions used. In conclusion, 6-gingerol and 6-shogaol have the antibiofilm and antivirulence activities against a drug resistant *C. albicans*.

AUTHOR CONTRIBUTIONS

J-HL, Y-GK, JGP, and JL designed research, performed experiments, and analyzed the data. PC, JH, and JGP provided materials. J-HL and JL wrote the manuscript. All authors read and approved the final manuscript.

REFERENCES

- Ali, B. H., Blunden, G., Tanira, M. O., and Nemmar, A. (2008). Some phytochemical, pharmacological and toxicological properties of ginger (*Zingiber officinale* Roscoe): a review of recent research. *Food Chem. Toxicol.* 46, 409–420. doi: 10.1016/j.fct.2007.09.085
- Amin-ul Mannan, M., Sharma, S., and Ganesan, K. (2009). Total RNA isolation from recalcitrant yeast cells. *Anal. Biochem.* 389, 77–79. doi: 10.1016/j.ab.2009.03.014
- Boyland, E., and Chasseaud, L. F. (1968). Enzymes catalysing conjugations of glutathione with alpha-beta-unsaturated carbonyl compounds. *Biochem. J.* 109, 651–661. doi: 10.1042/bj1090651
- Carradori, S., Chimenti, P., Fazzari, M., Granese, A., and Angiolella, L. (2016). Antimicrobial activity, synergism and inhibition of germ tube formation by *Crocus sativus*-derived compounds against *Candida* spp. *J. Enzyme Inhib. Med. Chem.* 31, 189–193. doi: 10.1080/14756366.2016.1180596
- Chandra, J., Kuhn, D. M., Mukherjee, P. K., Hoyer, L. L., McCormick, T., and Ghannoum, M. A. (2001). Biofilm formation by the fungal pathogen *Candida albicans*: development, architecture, and drug resistance. *J. Bacteriol.* 183, 5385–5394. doi: 10.1128/JB.183.18.5385-5394.2001
- Chen, C.-C., Rosen, R. T., and Ho, C.-T. (1986). Chromatographic analyses of isomeric shogaol compounds derived from isolated gingerol compounds of ginger (*zingiber officinale* roscoe). *J. Chromatogr. A* 360, 175–184. doi: 10.1016/S0021-9673(00)91660-1
- Choi, H., Ham, S. Y., Cha, E., Shin, Y., Kim, H. S., Bang, J. K., et al. (2017). Structure-activity relationships of 6-and 8-gingerol analogs as anti-biofilm agents. *J. Med. Chem.* 60, 9821–9837. doi: 10.1021/acs.jmedchem.7b01426
- Gentleman, R. C., Carey, V. J., Bates, D. M., Bolstad, B., Dettling, M., Dudoit, S., et al. (2004). Bioconductor: open software development for computational biology and bioinformatics. *Genome Biol.* 5:R80. doi: 10.1186/gb-2004-5-10-r80
- Heydorn, A., Nielsen, A. T., Hentzer, M., Sternberg, C., Givskov, M., Ersboll, B. K., et al. (2000). Quantification of biofilm structures by the novel computer program COMSTAT. *Microbiology* 146, 2395–2407. doi: 10.1099/00221287-146-10-2395
- Isa, Y., Miyakawa, Y., Yanagisawa, M., Goto, T., Kang, M. S., Kawada, T., et al. (2008). 6-Shogaol and 6-gingerol, the pungent of ginger, inhibit TNF-alpha mediated downregulation of adiponectin expression via different mechanisms in 3T3-L1 adipocytes. *Biochem. Biophys. Res. Commun.* 373, 429–434. doi: 10.1016/j.bbrc.2008.06.046
- Jolad, S. D., Lantz, R. C., Solyom, A. M., Chen, G. J., Bates, R. B., and Timmermann, B. N. (2004). Fresh organically grown ginger (*Zingiber officinale*): composition and effects on LPS-induced PGE2 production. *Phytochemistry* 65, 1937–1954. doi: 10.1016/j.phytochem.2004.06.008
- Khiralla, G. M. (2015). Antibiofilm and anti-adhesive effects of ginger against some food-related pathogens. *J. Food Res. Technol.* 3, 87–96.
- Kim, H. S., Cha, E., Kim, Y., Jeon, Y. H., Olson, B. H., Byun, Y., et al. (2016a). Raffinose, a plant galactoside, inhibits *Pseudomonas aeruginosa* biofilm formation via binding to LecA and decreasing cellular cyclic diguanylate levels. *Sci. Rep.* 6:25318. doi: 10.1038/srep25318

ACKNOWLEDGMENTS

This research was supported by the Basic Science Research Program through the NRF funded by the Ministry of Education (2018R1D1A3B07040699 to J-HL and 2018R1D1A1B07044288 to JL), and by the Priority Research Centers Program through the NRF funded by the Ministry of Education (2014R1A6A1031189).

SUPPLEMENTARY MATERIAL

The Supplementary Material for this article can be found online at: <https://www.frontiersin.org/articles/10.3389/fcimb.2018.00299/full#supplementary-material>

- Kim, H. S., Lee, S. H., Byun, Y., and Park, H. D. (2015). 6-Gingerol reduces *Pseudomonas aeruginosa* biofilm formation and virulence via quorum sensing inhibition. *Sci. Rep.* 5:8656. doi: 10.1038/srep08656
- Kim, H. S., and Park, H. D. (2013). Ginger extract inhibits biofilm formation by *Pseudomonas aeruginosa* PA14. *PLoS ONE* 8:e76106. doi: 10.1371/journal.pone.0076106
- Kim, M. K., Chung, S. W., Kim, D. H., Kim, J. M., Lee, E. K., Kim, J. Y., et al. (2010). Modulation of age-related NF-κB activation by dietary zingerone via MAPK pathway. *Exp. Gerontol.* 45, 419–426. doi: 10.1016/j.exger.2010.03.005
- Kim, Y.-G., Lee, J.-H., Gwon, G., Kim, S.-I., Park, J. G., and Lee, J. (2016b). Essential oils and eugenols inhibit biofilm formation and the virulence of *Escherichia coli* O157:H7. *Sci. Rep.* 6:36377. doi: 10.1038/srep36377
- Kucharikova, S., Tournu, H., Lagrou, K., Van Dijck, P., and Bujdakova, H. (2011). Detailed comparison of *Candida albicans* and *Candida glabrata* biofilms under different conditions and their susceptibility to caspofungin and anidulafungin. *J. Med. Microbiol.* 60, 1261–1269. doi: 10.1099/jmm.0.032037-0
- Kumar, L., Chhibber, S., and Harjai, K. (2013). Zingerone inhibit biofilm formation and improve antibiofilm efficacy of ciprofloxacin against *Pseudomonas aeruginosa* PAO1. *Fitoterapia* 90, 73–78. doi: 10.1016/j.fitote.2013.06.017
- Lee, J.-H., Cho, M. H., and Lee, J. (2011). 3-Indolylacetoneitrile decreases *Escherichia coli* O157:H7 biofilm formation and *Pseudomonas aeruginosa* virulence. *Environ. Microbiol.* 13, 62–73. doi: 10.1111/j.1462-2920.2010.02308.x
- Lee, J.-H., Kim, Y.-G., Ryu, S. Y., and Lee, J. (2016). Calcium-chelating alizarin and other anthraquinones inhibit biofilm formation and the hemolytic activity of *Staphylococcus aureus*. *Sci. Rep.* 6:19267. doi: 10.1038/srep19267
- Manoharan, R. K., Lee, J.-H., Kim, Y.-G., and Lee, J. (2017a). Alizarin and chrysazin inhibit biofilm and hyphal formation by *Candida albicans*. *Front. Cell. Infect. Microbiol.* 7:447. doi: 10.3389/fcimb.2017.00447
- Manoharan, R. K., Lee, J.-H., and Lee, J. (2017b). Antibiofilm and antihyphal activities of cedar leaf essential oil, camphor, and fenchone derivatives against *Candida albicans*. *Front. Microbiol.* 8:1476. doi: 10.3389/fmicb.2017.01476
- Nascimento, G. G. F., Locatelli, J., Freitas, P. C., and Silva, G. L. (2000). Antibacterial activity of plant extracts and phytochemicals on antibiotic-resistant bacteria. *Braz. J. Microbiol.* 31, 247–256. doi: 10.1590/S1517-83822000000400003
- Nobile, C. J., Andes, D. R., Nett, J. E., Smith, F. J., Yue, F., Phan, Q. T., et al. (2006a). Critical role of Bcr1-dependent adhesins in *C. albicans* biofilm formation *in vitro* and *in vivo*. *PLoS Pathog.* 2:e63. doi: 10.1371/journal.ppat.0020063
- Nobile, C. J., Nett, J. E., Andes, D. R., and Mitchell, A. P. (2006b). Function of *Candida albicans* adhesin Hwp1 in biofilm formation. *Eukaryot. Cell* 5, 1604–1610. doi: 10.1128/EC.00194-06
- Orsi, C. F., Borghi, E., Colombari, B., Neglia, R. G., Quaglini, D., Ardizzoni, A., et al. (2014). Impact of *Candida albicans* hyphal wall protein 1 (HWP1) genotype on biofilm production and fungal susceptibility to microglial cells. *Microb. Pathog.* 69–70, 20–27. doi: 10.1016/j.micpath.2014.03.003
- Park, M., Bae, J., and Lee, D. S. (2008). Antibacterial activity of [10]-gingerol and [12]-gingerol isolated from ginger rhizome against periodontal bacteria. *Phytother. Res.* 22, 1446–1449. doi: 10.1002/ptr.2473

- Quinlan, A. R., and Hall, I. M. (2010). BEDTools: a flexible suite of utilities for comparing genomic features. *Bioinformatics* 26, 841–842. doi: 10.1093/bioinformatics/btq033
- Ramage, G., Bachmann, S., Patterson, T. F., Wickes, B. L., and Lopez-Ribot, J. L. (2002). Investigation of multidrug efflux pumps in relation to fluconazole resistance in *Candida albicans* biofilms. *J. Antimicrob. Chemother.* 49, 973–980. doi: 10.1093/jac/dkf049
- Ramage, G., Saville, S. P., Thomas, D. P., and Lopez-Ribot, J. L. (2005). *Candida* biofilms: an update. *Eukaryot. Cell* 4, 633–638. doi: 10.1128/EC.4.4.633-638.2005
- Sandai, D., Tabana, Y. M., Ouweini, A. E., and Ayodeji, I. O. (2016). Resistance of *Candida albicans* biofilms to drugs and the host immune system. *Jundishapur J. Microbiol.* 9:e37385. doi: 10.5812/jjm.37385
- Sardi, J. C., Scorzoni, L., Bernardi, T., Fusco-Almeida, A. M., and Mendes Giannini, M. J. (2013). *Candida* species: current epidemiology, pathogenicity, biofilm formation, natural antifungal products and new therapeutic options. *J. Med. Microbiol.* 62, 10–24. doi: 10.1099/jmm.0.045054-0
- Si, W. H., Chen, Y. P., Zhang, J. H., Chen, Z. Y., and Chung, H. Y. (2018). Antioxidant activities of ginger extract and its constituents toward lipids. *Food Chem.* 239, 1117–1125. doi: 10.1016/j.foodchem.2017.07.055
- Taff, H. T., Mitchell, K. F., Edward, J. A., and Andes, D. R. (2013). Mechanisms of *Candida* biofilm drug resistance. *Future Microbiol.* 8, 1325–1337. doi: 10.2217/fmb.13.101
- Tampakakis, E., Okoli, I., and Mylonakis, E. (2008). A *C. elegans*-based, whole animal, *in vivo* screen for the identification of antifungal compounds. *Nat. Protoc.* 3, 1925–1931. doi: 10.1038/nprot.2008.193
- Tobudic, S., Lassnigg, A., Kratzer, C., Graninger, W., and Presterl, E. (2010). Antifungal activity of amphotericin B, caspofungin and posaconazole on *Candida albicans* biofilms in intermediate and mature development phases. *Mycoses* 53, 208–214. doi: 10.1111/j.1439-0507.2009.01690.x
- Trapnell, C., Pachter, L., and Salzberg, S. L. (2009). TopHat: discovering splice junctions with RNA-Seq. *Bioinformatics* 25, 1105–1111. doi: 10.1093/bioinformatics/btp120
- Whaley, S. G., Tsao, S., Weber, S., Zhang, Q., Barker, K. S., Raymond, M., et al. (2016). The RTA3 gene, encoding a putative lipid translocase, influences the susceptibility of *Candida albicans* to fluconazole. *Antimicrob. Agents Chemother.* 60, 6060–6066. doi: 10.1128/AAC.00732-16
- White, T. C. (1997). Increased mRNA levels of ERG16, CDR, and MDR1 correlate with increases in azole resistance in *Candida albicans* isolates from a patient infected with human immunodeficiency virus. *Antimicrob. Agents Chemother.* 41, 1482–1487.
- Wu, H., Hsieh, M. C., Lo, C. Y., Bin Liu, C., Sang, S. M., Ho, C. T., et al. (2010). 6-Shogaol is more effective than 6-gingerol and curcumin in inhibiting 12-O-tetradecanoylphorbol 13-acetate-induced tumor promotion in mice. *Mol. Nutr. Food Res.* 54, 1296–1306. doi: 10.1002/mnfr.200900409
- Zelante, T., Iannitti, R. G., De Luca, A., Arroyo, J., Blanco, N., Servillo, G., et al. (2012). Sensing of mammalian IL-17A regulates fungal adaptation and virulence. *Nat. Commun.* 3:683. doi: 10.1038/ncomms1685

Conflict of Interest Statement: The authors declare that the research was conducted in the absence of any commercial or financial relationships that could be construed as a potential conflict of interest.

Copyright © 2018 Lee, Kim, Choi, Ham, Park and Lee. This is an open-access article distributed under the terms of the Creative Commons Attribution License (CC BY). The use, distribution or reproduction in other forums is permitted, provided the original author(s) and the copyright owner(s) are credited and that the original publication in this journal is cited, in accordance with accepted academic practice. No use, distribution or reproduction is permitted which does not comply with these terms.



Sarconesin: *Sarconesiopsis magellanica* Blowfly Larval Excretions and Secretions With Antibacterial Properties

Andrea Díaz-Roa^{1,2,3}, Manuel A. Patarroyo^{4,5}, Felio J. Bello^{6,7} and Pedro I. Da Silva Jr.^{1,3*}

¹ Laboratório Especial de Toxinologia Aplicada, Instituto Butantan, São Paulo, Brazil, ² PhD Programme in Biomedical and Biological Sciences, Universidad del Rosario, Bogotá, Colombia, ³ Biomedical Sciences Institute, Universidade de São Paulo, São Paulo, Brazil, ⁴ Molecular Biology and Immunology Department, Fundación Instituto de Inmunología de Colombia, Bogotá, Colombia, ⁵ Basic Sciences Department, School of Medicine and Health Sciences, Universidad del Rosario, Bogotá, Colombia, ⁶ Faculty of Agricultural and Livestock Sciences, Program of Veterinary Medicine, Universidad de La Salle, Bogotá, Colombia, ⁷ Medicine Faculty, Universidad Antonio Nariño, Bogotá, Colombia

OPEN ACCESS

Edited by:

You-Hee Cho,
CHA University, South Korea

Reviewed by:

Dong-Chan Oh,
Seoul National University,
South Korea
Yoonkyung Park,
Chosun University, South Korea

*Correspondence:

Pedro I. Da Silva Jr.
pedro.junior@butantan.gov.br;
peisjr@gmail.com

Specialty section:

This article was submitted to
Antimicrobials, Resistance
and Chemotherapy,
a section of the journal
Frontiers in Microbiology

Received: 21 June 2018

Accepted: 03 September 2018

Published: 28 September 2018

Citation:

Díaz-Roa A, Patarroyo MA, Bello FJ
and Da Silva PI Jr (2018) Sarconesin:
Sarconesiopsis magellanica Blowfly
Larval Excretions and Secretions With
Antibacterial Properties.
Front. Microbiol. 9:2249.
doi: 10.3389/fmicb.2018.02249

Larval therapy (LT) is an alternative treatment for healing chronic wounds; its action is based on debridement, the removal of bacteria, and stimulating granulation tissue. The most important mechanism when using LT for combating infection depends on larval excretions and secretions (ES). Larvae are protected against infection by a spectrum of antimicrobial peptides (AMPs); special interest in AMPs has also risen regarding understanding their role in wound healing since they degrade necrotic tissue and kill different bacteria during LT. *Sarconesiopsis magellanica* (Diptera: Calliphoridae) is a promising medically-important necrophagous fly. This article reports a small AMP being isolated from *S. magellanica* ES products for the first time; these products were obtained from third-instar larvae taken from a previously-established colony. ES were fractionated by RP-HPLC using C18 columns for the first analysis; the products were then lyophilised and their antimicrobial activity was characterized by incubation with different bacterial strains. These fractions' primary sequences were determined by mass spectrometry and *de novo* sequencing; five AMPs were obtained, the Sarconesin fraction was characterized and antibacterial activity was tested in different concentrations with minimum inhibitory concentrations starting at 1.2 μ M. Potent inhibitory activity was shown against Gram-negative (*Escherichia coli* D31, *E. coli* DH5 α , *Salmonella enterica* ATCC 13314, *Pseudomonas aeruginosa* 27853) and Gram-positive (*Staphylococcus aureus* ATCC 29213, *S. epidermidis* ATCC 12228, *Micrococcus luteus* A270) bacteria. Sarconesin has a significant similarity with Rho-family GTPases which are important in organelle development, cytoskeletal dynamics, cell movement, and wound repair. The data reported here indicated that Sarconesin could be an alternative candidate for use in therapeutics against Gram-negative and Gram-positive bacterial infections. Our study describes one peptide responsible for antibacterial activity when LT is being used. The results shown here support carrying out further experiments aimed at validating *S. magellanica* AMPs as novel resources for combating antibacterial resistance.

Keywords: antimicrobial peptide, *Sarconesiopsis magellanica*, sarconesin, larval therapy, insect peptide

INTRODUCTION

Larval therapy (LT) involves applying sterile larvae (usually Diptera from the Calliphoridae family) to an infected non-healing wound (Raposio et al., 2017); its action is based on four mechanisms: removing necrotic tissue (debridement), disinfecting microorganisms, including methicillin-resistant *Staphylococcus aureus* (MRSA) (Robinson, 1935; Mumcuoglu, 2001; Bexfield et al., 2004; Nigam et al., 2010), inhibiting and eradicating biofilms (van der Plas et al., 2008; Cazander et al., 2009; Gottrup and Jorgensen, 2011) and stimulating granulation tissue for enhancing healing (Church, 1996; Thomas A.M. et al., 1999; Sherman et al., 2000; Mumcuoglu, 2001; Wolff and Hansson, 2005; Spilisbury et al., 2008).

It has been proposed that larvae release antimicrobial ingredients into wounds in response to infection; some of these ingredients are low molecular weight bacteriostatic compounds, such as p-hydroxybenzoic acid, p-hydroxyphenylacetic acid, dioxopiperazine proline (Huberman et al., 2007) and an enigmatic compound (C₁₀H₁₆N₆O₉) known as seraticin (Nigam et al., 2010). Other compounds are antimicrobial peptides (AMPs) originating from the immune system that, when applied into wounds, contribute to their healing (Thomas A.M. et al., 1999; Bexfield et al., 2004). Such insect peptides belong to the dipteracin, cecropin, and defensin groups (Hoffmann and Hetru, 1992; Bulet and Stocklin, 2005). Lucifensin is one of the well characterized AMPs; it is derived from *Lucilia sericata* larvae and has been found as a constituent of larval excretions and secretions (ES) (Cеровsky et al., 2010). This molecule was originally isolated from *Lucilia sericata* larval intestine, later being detected in the salivary glands, fat body and haemolymph. However, it has been shown that it is the larval immune system which induces the production of these substances in the fat body when activated in response to an infectious environment (Valachova et al., 2013) for its rapid release into the haemolymph.

Insects respond to bacterial attacks by rapidly producing AMPs which have a broad spectrum of activity against Gram-positive and Gram-negative bacteria, and against fungi; more recently, it has been demonstrated that AMPs have activity against some parasites and viruses (Yi et al., 2014). Insect-isolated AMPs can be classified on the basis of their sequence and structural characteristics into three categories: linear peptides which can form an alpha-helical structure and contain no cysteine residues, such as cecropins; cyclic peptides containing disulphide bridges, such as defensins; and linear peptides having remarkable contents of one or two amino acid (aa) residues, mostly proline and/or glycine (e.g., pyrocoricins and dipteracins) (Bulet et al., 1999).

These peptides are conserved host immune system evolutionary components forming part of the first line of defense against infections and have been identified in almost all life forms. Insect isolates make up the most abundant group of more than 2,798 AMPs listed in the antimicrobial peptide database¹. AMPs are synthesized in the fat body (the equivalent of the liver in mammals), epithelial cells and certain

haemolymph cells (the equivalent of mammalian blood), and spread throughout the body by this medium for counteracting infection. Most of these peptides are cationic AMPs having a molecular mass of less than 5 kDa (Brown and Hancock, 2006). In contrast to conventional antibiotics, AMPs do not induce microbial resistance and require only a short time to induce microorganism death (Yeaman and Yount, 2003).

Microorganisms' resistance to antibiotics represents an ever-increasing difficulty; such situation becomes even more relevant in relation to chronic wounds which are difficult to heal in patients suffering underlying disease (such as diabetes and cardiovascular failure). Polymicrobial colonization by different bacterial strains often occurs in this type of lesion, forming a biofilm, thereby making them more difficult to treat, control and/or eradicate. Recent studies (O'Meara et al., 2014) have demonstrated that conventional antibiotics do not promote chronic wound healing, in addition to generating resistance in bacteria, which is why their general use has been questioned for treating the bacteria colonizing this type of wound. There is thus a need to introduce new or re-emerging strategies which may be effective against microorganisms in chronic, necrotic and infected wounds which do not respond to antibiotic therapy.

Identifying and characterizing antibacterial compounds involved in larval ES during LT is the starting point for the search and typing of natural molecules in insects, mainly dipterans from the Calliphoridae family (Yeaman and Yount, 2003). AMPs have been isolated from purified larvae in just *L. sericata* (Cеровsky et al., 2010), *L. cuprina* (El Shazely et al., 2013), and *Calliphora vicina* (Chernysh et al., 2015) whilst lucifensins have been isolated from larvae, purified, characterized and evaluated. They have been shown to be mainly effective against Gram-positive bacteria, such as MRSA and its strains (Andersen et al., 2010; Cеровsky and Bem, 2014). Amongst the most recent studies on antimicrobial peptides isolated from flies from the Calliphoridae family different to those obtained from larval ES, it is worth mentioning a study by Yakovlev et al. (2017) (Yakovlev et al., 2017), who studied the presence of AMPs in the culture medium from both fat bodies and haemocytes derived of *Calliphora vicina* larvae. They demonstrated that both cell types synthesized and released an AMPs complex to the culture medium, corresponding to defensins, cecropins, dipteracins, and proline-rich peptides. In another study, AMPs extracted from *C. vicina* larval haemolymph were applied in environments extremely contaminated by germs forming biofilms (under *in situ* and *in vitro* conditions), exhibiting strong destructive activity of the matrix and of bacteria adhered to it, these bacteria were resistant to conventional antibiotics, such as *Escherichia coli*, *Staphylococcus aureus*, and *Acinetobacter baumannii* (Gordya et al., 2017). Likewise, this AMP complex containing a combination of defensins, cecropins, dipteracins and proline-rich peptides, and interacting synergistically with antibiotics of various classes, produced a much stronger action on the bacterial strains (*Staphylococcus aureus*, *Escherichia coli*, *Pseudomonas aeruginosa*, *Klebsiella pneumoniae*, and *Acinetobacter baumannii*) and the biofilm materials, when compared with the antibacterial effect on the same strains in a model of planktonic cultures (Chernysh et al., 2018).

¹<http://aps.unmc.edu/AP/main.php>

The *S. magellanica* species has been reported in Argentina (Mariluís and Mulieri, 2003), Bolivia, Chile, Ecuador and Perú (Pape et al., 2004); Mariluís and Peris have described it as being present in areas over 900 masl (Mariluís and Peris, 1984). In Colombia, it is found in Boyacá and Cundinamarca departments (Hardy, 1966). *S. magellanica* was reported as the first species colonizing decomposing pigs in Bogotá (an animal bio-model similar to that of humans) (Goff, 2001). Its antibacterial activity has been confirmed, giving better results than those for *L. sericata* (Díaz-Roa et al., 2014) and it has already been evaluated regarding LT, leading to good effects concerning diabetic wound cicatrization (Cruz-Saavedra et al., 2016) and in *Leishmania* lesions (Cruz-Saavedra et al., 2016).

This study was thus aimed at characterizing a novel AMP purified from *S. magellanica* ES. The antimicrobial activity of the peptide so obtained against various Gram-positive and Gram-negative bacteria was also evaluated.

MATERIALS AND METHODS

Adult *S. magellanica* Capture and Colony Maintenance

Insect capture and colony maintenance followed a previously described procedure (Díaz-Roa et al., 2014). Adult *S. magellanica* forms were captured in the mountainous part of Bogotá's Parque Nacional; the park is located 2,600 masl (4°37'8.90N; 74°3'27.73W). Entomological nets were used for collecting insects which were then stored alive in glass flasks for being transported to the Universidad del Rosario's Medical and Forensic Entomology laboratory. The specimens were kept in 45 × 45 × 45 cm Gerber cages at 20–25°C, with 60–70% relative humidity and a 12/12 h photoperiod. The adult forms were fed on a sugar solution (carbohydrate source) and pigs' liver as protein feed necessary for providing continuity for the biological cycle (Rueda et al., 2010); after adults had laid eggs on the liver they were placed in a glass flask with a liver slice until maggots hatched. The maggots were kept in this flask throughout the 3 instars until they reached the pre-pupa stage; they were then put in a flask containing sand until the adults emerged to be released in the same cages to continue the cycle. Third instar maggots were used for extracting their ES.

Extracting *S. magellanica* ES

S. magellanica-derived ES were collected from third instar larvae, following a previously described procedure (van der Plas et al., 2008); about 200 larvae were used in each assay. Third-instar larvae were incubated with a bacterial suspension (OD₅₉₅ = 0.5) of each selected strain to activate the immune system and enhance the expression of products having antibacterial activity (Kawabata et al., 2010; Jiang et al., 2012). They were then placed in a 15 mL Falcon tube and disinfected by adding 0.5% formaldehyde for 5 min followed by replacing this solution with 0.5% hypochlorite with constant shaking for the same amount of time and washed with sterile PBS; 2 mL sterile PBS was then added to the larvae which were incubated at 25°C for 1 h. The larval ES mixture was

removed by using a syringe and placed in another tube to continue centrifuging at 13,000 g at 4°C for 10 min. The precipitate was discarded and the supernatant with the ES was sterilized by filtering through a 0.22 µm membrane and stored at –70°C.

Peptide Purification

ES were partially purified by Sep-Pak C18 disposable columns for the first analysis; bound material was eluted with 80% acetonitrile (ACN) in acidified water and freeze-dried. *S. magellanica* hydrophobic ES (80%) were then lyophilised and reconstituted in 2mL trifluoroacetic acid (0.05% TFA). ES were purified by semi-preparative reverse-phase high-performance liquid chromatography (RP-HPLC) using a C18 Jupiter column (10 µm; 300A; 10mm × 250mm) at 2mL/min flow rate, as previously described (Hou et al., 2011). Fractions were collected manually, absorbance being monitored at 225nm. Each fraction's antibacterial activity was then determined. RP-HPLC (1mL/min flow rate) was then used with fractions having antibacterial activity, using an analytical C18 Jupiter column (10 µm; 300A; 4,6mm × 250mm). The Sarconesin gradient was open, ACN concentration ranging from 44% to 54%. Absorbance was monitored at 225nm, fractions were collected manually and antibacterial activity was tested.

Antimicrobial Assays

A liquid growth inhibition assay was used for evaluating the fractions' antibacterial activity (Bulet, 2008; Wiegand et al., 2008). Lyophilised fractions were suspended in 500 µL Mili Q water; the assay was carried out using 96-well sterile plates. 20 µL of the fractions were aliquoted into each well with 80 µL of the bacterial dilution, to 100 µL final volume. Bacteria were cultured in poor nutrient broth (PB) (1.0 g peptone in 100 mL of water containing 86 mM NaCl at pH 7.4; 217 mOsm). Exponential growth phase cultures were diluted to 5 × 10⁴ CFU/mL (DO = 0.001) final concentration (Hetru and Bulet, 1997; Bulet, 2008; Poppel et al., 2015). Sterile water and PB were used as growth control, and streptomycin was used as growth inhibition control. Microtitre plates were incubated for 18 h at 30°C; growth inhibition was determined by measuring absorbance at 595 nm. The assay for determining the minimum concentration of peptide required to achieve 100% growth inhibition was performed using a serial dilution in 96-well sterile plates at 100 µL final volume (Silva et al., 2000; Lorenzini et al., 2003; Riciluca et al., 2012); 20 µL stock solution was used in each microtitre plate well at twofold serial dilution and added to 80 µL of the bacterial dilution. The strains used were *Staphylococcus aureus* ATCC 29213, *S. epidermidis* ATCC 12228, *Escherichia coli* D31, *E. coli* DH5α, *Pseudomonas aeruginosa* 27853, *Salmonella enterica* ATCC 13314, and *Micrococcus luteus* A270. Microbial growth was measured by monitoring optical density at 595 nm and assays were performed in triplicate (PerkinElmer Victor 3TM 1420 multilabel counter). The bacterial growth curve of *S. aureus* with Sarconesin MIC and 1/2 MIC was measured every 15 min for 1 h and then every hour for 12 h. Graph was background-corrected by subtracting the OD₅₉₅ of medium without bacteria (Velema et al., 2013; Magi et al., 2015).

Cytotoxicity (CC)

The toxicity of Sarconesin peptide against VERO cells (African green monkey kidney fibroblast) was evaluated. Cells were obtained from the American Type Culture Collection (ATCC CCL81; Manassas, VA, United States) and maintained in DMEM culture medium, supplemented with 10% heat-inactivated calf serum. CC was determined using the MTT colorimetric assay. Briefly, the cells were seeded in 96-well plates (2×10^5 cells/well) and cultured for 24 h at 37°C in a humidified atmosphere containing 5% CO₂. Eight two-fold serial dilutions of peptide were performed with DMEM to give solutions with final concentrations ranging from 4, 7 to 600 µM. Varying concentrations were added and allowed to react with the cells for 48 h, followed by the addition of 20 µL MTT (5 mg/mL in PBS) for another 4 h at 37°C. Formazan crystals were dissolved by adding 150 µL isopropanol and incubating at room temperature until all crystals were dissolved. Absorbance at 550 nm was measured using a microplate ELISA reader. Cell survival was calculated using the following formula: survival (%) = (A550 of peptide-treated cells/A550 of peptide-untreated cells)*100 (Sayegh et al., 2016).

Haemolytic Activity

Fresh human red blood cells (hRBCs) were washed 3 times with PBS (35 mM phosphate buffer, 0.15 M NaCl, pH 7.4) by centrifugation for 7 min at $1000 \times g$, and resuspended in PBS to a final 4% (v/v) concentration. Sarconesin solutions (serial 2-fold dilutions in PBS) were added to 100 µL hRBC suspension to a final 200 µL volume, and incubated for 1 h at 37°C. Hemoglobin release was monitored by measuring the supernatant absorbance at 405 nm with a Microplate ELISA Reader. The haemolysis percentage was expressed in relation to a 100% lysis control (erythrocytes incubated with 0.1% Triton X-100); PBS was used as a negative control (Nan et al., 2012; Chaparro and da Silva, 2016).

Mass Spectrometry

Active antibacterial fractions were analyzed by mass spectrometry LC-MS/MS on a LTQ-Orbitrap Velos (Thermo Scientific) coupled to an Easy-nLCII liquid nano-chromatography system (Thermo Scientific). The chromatographic step involved using 5 µL of each sample automatically on a C18 pre-column (100 µm I.D. \times 50 mm; Jupiter 10 µm, Phenomenex Inc., Torrance, California, United States) coupled to a C18 analytical column (75 µm I.D. \times 100 mm; ACQUA 5 µm, Phenomenex Inc.). The eluate was electro-sprayed at 2 kV and 200°C in positive ion mode. Mass spectra were acquired by FTMS analyser; full scan (MS1) involved using 200–2,000 m/z (60,000 resolution at 400 m/z) as mass scan interval with the instrument operated in data dependent acquisition mode, the five most intense ions per scan being selected for fragmentation by collision induced dissociation. The minimum threshold for selecting an ion for a fragmentation event (MS2) was set to 5,000 cps.

The dynamic exclusion time used was 15 s, repeating at 30 s intervals.

Bioinformatics

The MS/MS peak list files were submitted to an in-house version of the MASCOT server (Matrix Science, United States) and screened against the Uniprot database. PEAKS 8.5 (Bioinformatics Solutions Inc., Waterloo, Ontario, Canada) *de novo* sequencing/database search software was used for establishing sequences. Analysis involved 10 ppm error tolerance for precursor ions and 0.6 Da for fragment ions. Oxidation was considered a variable modification.

The Sarconesin sequence was analyzed for similarities with the *L. sericata* and *L. cuprina* genome and transcriptome and also with other proteins registered in the National Center for Biotechnology (NCBI) public database, using the Basic Local Alignment Search Tool (BLASTp), with default parameters² (Altschul et al., 1997). The sequences' physical-chemical parameters were calculated using the PepCalc tool³. Gene Runner was used for nucleotide translation to protein and Seaview (Gouy et al., 2010) and Boxshade⁴ was used for making and formatting alignments' shaded background. The Chimera structure prediction tool (accessed through the European Bioinformatics Institute⁵ was used for obtaining the three-dimensional (3D) images of secondary structure.

Circular Dichroism (CD)

The far-UV (190–250nm) CD spectrum of the peptide was recorded in a Jasco J810 spectropolarimeter (Jasco Inc., Japan) at 25°C and in a 0.1cm path length quartz cell. All CD spectra were recorded after accumulation of 4 runs and smoothed using a FFT (Fast Fourier Transform) filter to minimize background effects. The solvents used in the experiment were pure water and 10, 30 and 50% v/v solutions of 2,2,2 trifluoroethanol (TFE) in water.

Mechanism of Action

Membrane Integrity and Esterase Activity

Mid-log phase *E. coli* cells (2×10^8 CFU/mL) were incubated with or without MIC peptide solution at 37°C. The bacterial membrane integrity was measured by fluorometry and microscopy using propidium iodide (PI) to 60 µM final concentration in the dark for 15 min, followed by measuring fluorescence with excitation/emission wavelengths of 485/620 nm (Faisal et al., 2016). For Esterase activity, 180 µL were transferred to a 96-well black plate which was added 20 µL of 250 µM 5(6)-Carboxyfluorescein diacetate (CFDA), incubated in dark for 30 min, followed by measurement of fluorescence with excitation/emission wavelengths of 485/535 nm (Nocker et al., 2011; Yang et al., 2017). PI microscope slides, were made by depositing drops of melted agarose 1% (w/v); after placing 20 µL of the cells onto solidified agar pad for immobilisation, the

²<http://blast.ncbi.nlm.nih.gov/> [accessed April 23, 2018]

³<http://pepcalc.com/> [accessed April 30, 2018]

⁴http://www.ch.embnet.org/software/BOX_form.html

⁵<http://www.ebi.ac.uk/thornton-srv/databases/profunc/> [accessed April 30, 2018]

dried culture was covered with a glass coverslip and observed under a microscope (Carretero et al., 2018). Microscopy was performed using a Leica TCS SP8 confocal laser scanning microscope, the images were processed with Leica software LAS X.

DNA Staining

Treated and untreated bacterial cells were fixed on a slide, permeabilised with ethanol, and stained with 4',6-diamidino-2-phenylindole (DAPI) to visualize the DNA using a confocal microscope.

Gel Retardation Assay

The binding of Sarconesin to *E. coli* DH5 α genomic DNA was evaluated by a gel retardation assay (Teng et al., 2014). *E. coli* genomic DNA was extracted following the method of Landry et al. (1993). Seven two-fold increasing amounts of Sarconesin peptide (3.1 to 200 μ M) were incubated for 1 hour with 500 ng of genomic DNA. The mixture was incubated for 1 hour at room temperature and analyzed by electrophoresis on a 0.8% agarose gel (Yang et al., 2017).

Statistical Analysis

All statistical analyses were performed using GraphPad Prism software (version 7.00). Bacterial growth curve after Sarconesin

treatment was compared to the untreated control using a one-way ANOVA ($\alpha = 0.05$). Statistical comparison of combination treatment in toxicity assays was done using a one-way ANOVA ($\alpha = 0.05$) with Dunnett's multiple comparisons test.

RESULTS

Peptide Purification

ES material, analyzed by RP-HPLC, was lyophilised, suspended in water and antibacterial activity was tested. Antibacterial activity was quantified by plate growth inhibition assay using a Gram-positive *M. luteus* A270 bacteria as test-organism (Figure 1). Five of these fractions had antibacterial activity. Fractions 2, 3, 4, and 5 had anti-*P. aeruginosa* activity whilst the other compounds having no activity against *P. aeruginosa* were tested against the Gram-positive *M. luteus*. Activity was found in fraction 1; fractions having antimicrobial activity were eluted at 8.1, 50.9, 51.7, 52.1, and 64.9 min and chromatographed again in the same system with an analytic C18 column. All antimicrobial fractions were analyzed by mass spectrometry; when compared through a preliminary database search, just fraction 3 showed homogeneity with Diptera proteins. Purification of this fraction revealed the 3.2 molecule, having antibacterial activity against *M. luteus*.

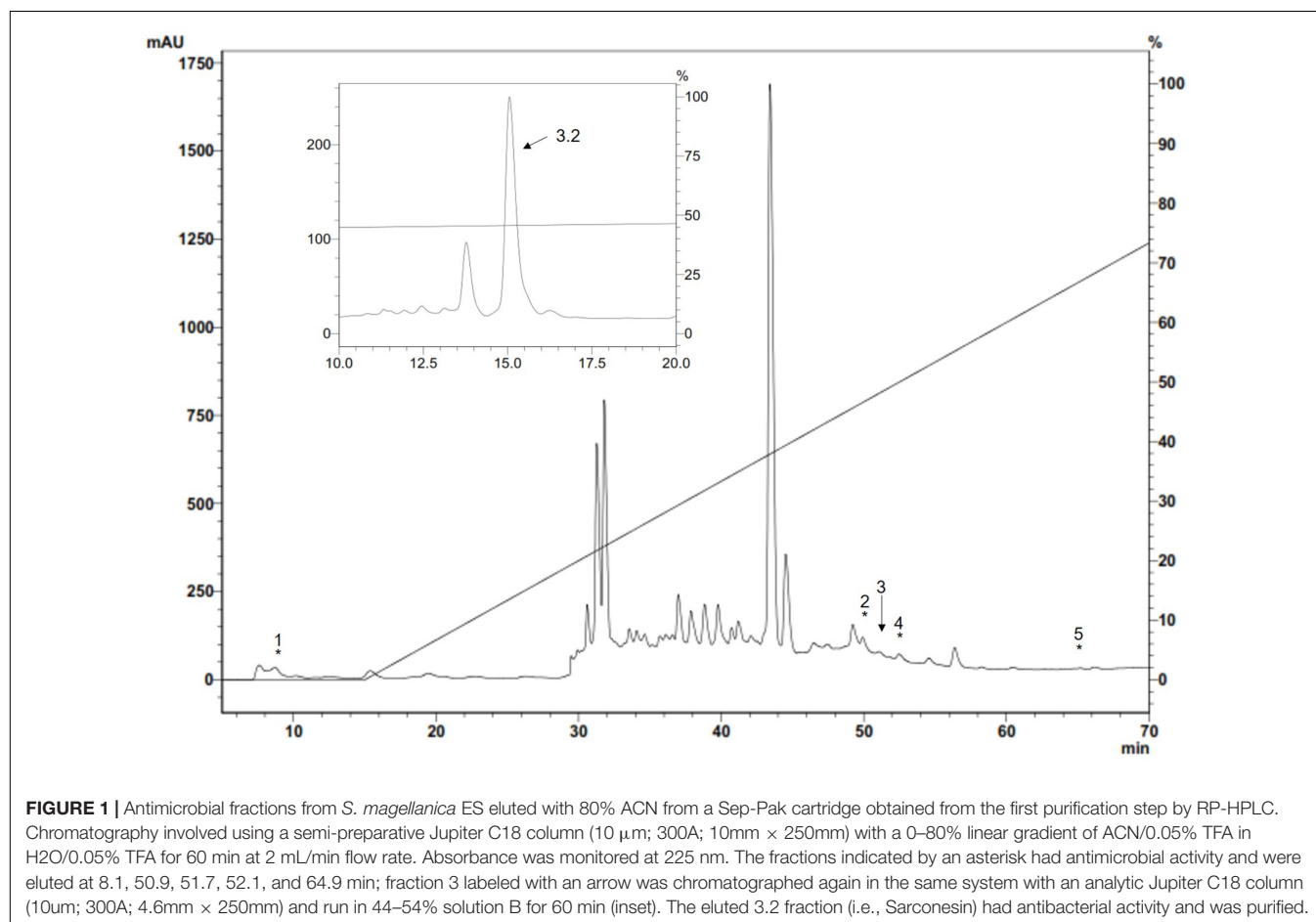


TABLE 1 | MIC, minimum inhibitory concentration; MIC refers to the concentration needed for achieving 100% inhibition of growth.

	Strain	Sarconesin MIC
Gram +	<i>M. luteus</i> A270	4.7 μ M
	<i>S. aureus</i> ATCC 29213	1.2 μ M
	<i>S. epidermidis</i> ATCC 12228	1.2 μ M
Gram –	<i>P. aeruginosa</i> ATCC 27853	4.7 μ M
	<i>E. coli</i> D31	2.4 μ M
	<i>E. coli</i> DH5 α	2.4 μ M
	<i>S. enterica</i> ATCC 13314	2.4 μ M

Antimicrobial Assays

The peptides were studied regarding their potential for inhibiting Gram-positive and Gram-negative bacterial growth. Sarconesin MIC was the same (4.7 μ M) for *M. luteus* A270 and *P. aeruginosa* ATCC 27853; minimum MIC (1.2 μ M) was obtained for *S. aureus* ATCC 29213 and *S. epidermidis* ATCC 12228, and *E. coli* D31 and DH5 α MIC was 2.4 μ M (Table 1). Sarconesin MIC exhibited its effect in the exponential phase of *S. aureus* growth curve, which was reached after more than 180 min, incubation with $1/2$ MIC showed a decrease of the bacterial growth (Figure 2A).

Toxicity

The CC activity of Sarconesin was tested against the Vero cell line (Figure 2B). No sign of CC was observed with Sarconesin, even at the highest tested concentration, i.e., 600 μ M. The viability of the cells was approximately 92% after exposure to Sarconesin. Selectivity index was not calculated as no CC50 values were found in the maximum evaluated concentrations. A very low (< 2%) haemolytic activity was observed upon incubating human red blood cells with Sarconesin at the highest concentration tested (600 μ M) (Figure 2C).

Mass Spectrometry

Mass spectrometry analysis of the Sarconesin fraction revealed a molecule having a mass of 1,471.84 Da. The complete Sarconesin aa sequence obtained by PEAKS *de novo* sequencing revealed a 13 aa sequence having a post-translational modification (PTM): TPm(+ 16)LLVGTKLDLR. Collision-induced dissociation spectrum from mass/charge (m/z) of its double charged ion gave $[M + 2H]^2 +$, m/z 736.9266 (Figure 3). Characterizing the peptide's primary structure with the MASCOT tool gave the TPFLLVGTQIDLR sequence.

Knowing the sequence, proteomic, and peptidomic bioinformatics tools were used for predicting Sarconesin's significant physicochemical characteristics. ExPASy's (SIB Bioinformatics Resource Portal) PepDraw and Pep-Calc.com sequence analysis yielded a potential peptide isoelectric point (pI), molar extinction coefficient and net charge (Table 2). The peptide was predicted to have one Asp negatively-charged aa residue and a positively-charged Arg residue, thereby contributing to the peptide's neutral characteristics (0 net charge). Four of the 13 aa were predicted to be hydrophobic

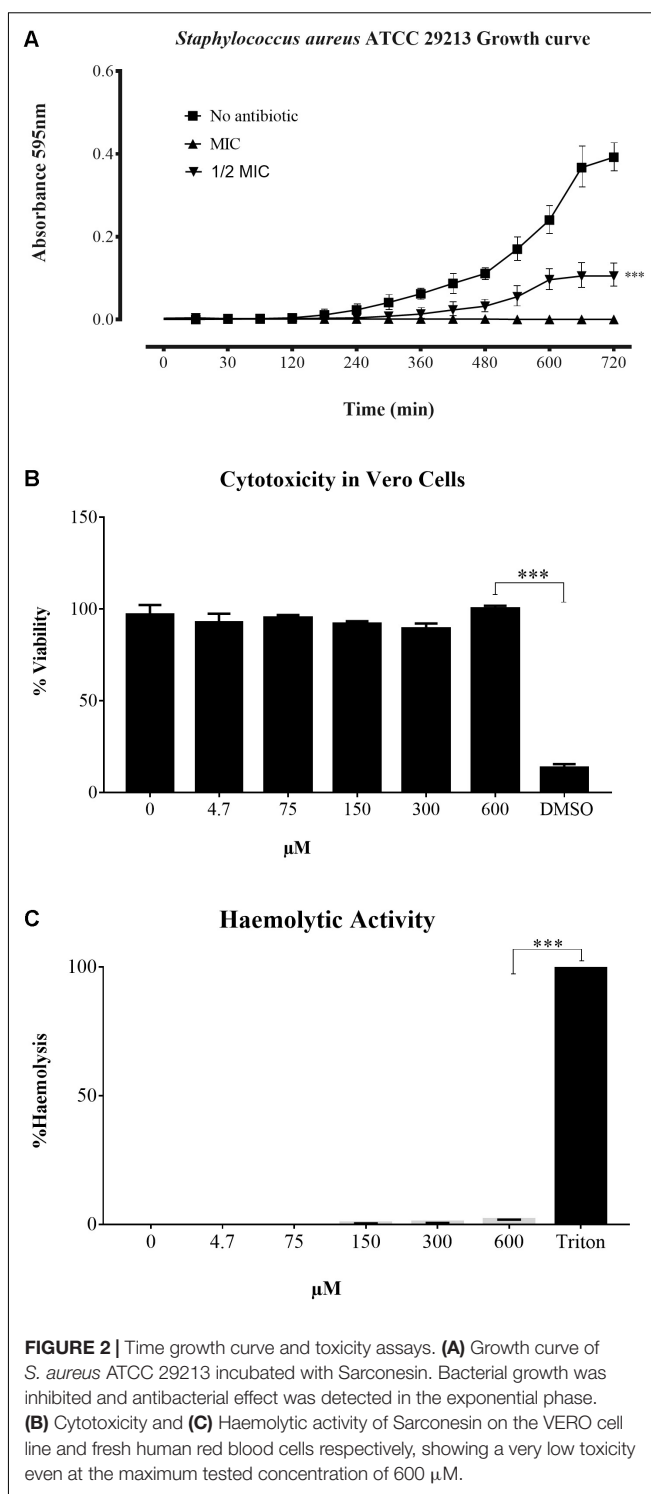


FIGURE 2 | Time growth curve and toxicity assays. **(A)** Growth curve of *S. aureus* ATCC 29213 incubated with Sarconesin. Bacterial growth was inhibited and antibacterial effect was detected in the exponential phase. **(B)** Cytotoxicity and **(C)** Haemolytic activity of Sarconesin on the VERO cell line and fresh human red blood cells respectively, showing a very low toxicity even at the maximum tested concentration of 600 μ M.

(1 Ile, 3 Leu), suggesting poor water solubility for Sarconesin. ExPASy's ProtParam tool predicted that the peptide would remain intact for up to 7.2 h in mammalian reticulocytes (*in vivo*), >20 h in yeast and >10 h in the Gram-negative bacterium *E. coli* (*in vivo*). This was likely due to the presence of a Thr (T) residue at the N-terminus.

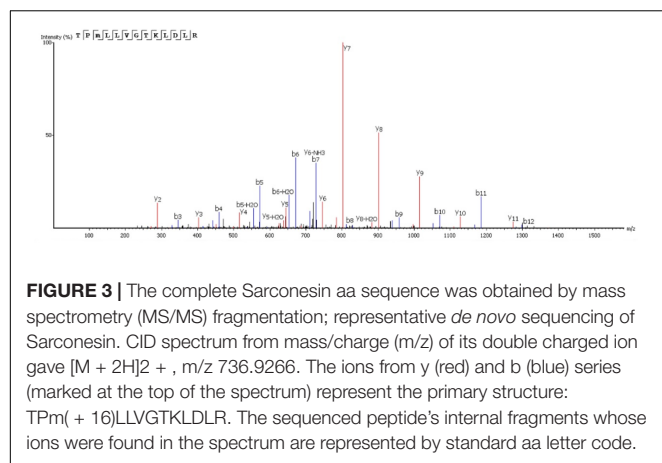


TABLE 2 | Physicochemical parameters calculated using ExPASy PepDraw and Pep-Calculator (accessed April 30th 2018).

Peptide properties		
Sequence:	TPFLLVGTQIDLR	
Length:	13	
Mass:	1471.8372	
Isoelectric point (pI):	6.42	
Net charge at pH 7:	0	
Hydrophobicity:	+ 8.87 Kcal*mol ⁻¹	
Estimated solubility:	poor water solubility	
Extinction coefficient 1:	0 M ⁻¹ *cm ⁻¹	

Protein Model

A search for TPFLLVGTQIDLR in databases found matches with cell division control protein 42 (CDC42) sequences from humans, cows and fruit flies, having 100% sequence similarity. All sequences are referred to by their NCBI accession numbers⁶ to minimize confusion: CDC42 cell division control protein 42 homologue OS = *Bos taurus* (Q2KJ93), CDC42_HUMAN Chain A, structure of the Rho Family Gtp-binding protein Cdc42 in complex with the multifunctional regulator Rhogdi (gi| 7245832| 1DOA_A), CDC42_DROME CDC42 homologue OS = *Drosophila melanogaster* GN = Cdc42 PE = 1 SV = 1 (P40793). The BLASTp 2.6.1 + tool for comparing the sequence obtained with those for other *Lucilia* species proteins found 69% identity with a similar sequence previously report as a Ras-related protein Rac1 [*Lucilia cuprina*, another blowfly from the Calliphoridae family]: GenBank: KNC23156.1.

Sarconesin sequence was sought in the genomes and transcriptomes reported for *L. cuprina* (genome ASM118794V1, transcriptome SRX907163) and *L. sericata* (genome ASM101483V1, transcriptome ERX614478, 3-4 day pupa transcriptome SRX087348). Sarconesin was found in all of them (*L. sericata* genome scaffold JXPF01028806.1 and transcriptomes ERR658157.22222021.1 and pupa SRR350018.17744834.1. *L. cuprina* genome scaffold JRES01000256.1 and transcriptome SRR1853100.27006533.2 (accessed May 16th, 2018) (Figure 4A).

The exon containing Sarconesin in the JXPF01028806.1 scaffold (GenBank) was located and compared to other proteins by Blastp for determining which organisms had the greatest similarity with the gene. It was shown that this gene was mainly present in other Diptera species (*Stomoxys calcitrans* XP_013103099.1, *Drosophila sechellia* XP_002039460.1, *Musca domestica* XP_005189222.1, *Anopheles gambiae* CAA93820.1, and *Ceratitis capitata* XP_004518385.1), having 100% similarity. It was established that Sarconesin formed part of a CDC42 conserved domain (Figure 4B). The Sarconesin model was built using CDC42's known structure (PDB ID: 1DOA) since it has 100% identity with bovine CDC42 and a PDB model is available. Figure 4C shows the homology model constructed for Sarconesin.

Circular Dichroism (CD)

CD deconvolution software was not suitable for peptide analysis, since it was designed for larger proteins (Bochicchio and Tamburro, 2002), so the peptide's secondary structure analysis was thus made in a qualitative way, by comparing with CD spectra obtained from known secondary structures of the literature. CD spectra of the peptide were obtained at 25°C, in water and in TFE/water ranging from 0 to 50% v/v (Figure 5). In water, the CD spectrum showed a strong negative band around 208 nm and a moderate positive band around 190 nm. As TFE concentration increased, the negative band became less intense and the positive band became more intense and a shoulder between 220 and 230 nm appeared. TFE has the property of aggregating itself around peptide molecules promoting the displacement of the solvation layer, thereby favoring the formation of intra-peptide hydrogen bonds, stabilizing the peptide's secondary-structure. CD spectra features suggested a mixture of 3_{10} -Helix and α -Helix conformations (Berova et al., 2012). In water, the 3_{10} -Helix proportion was favored and as the TFE concentration in solution increased, the α -Helix contribution also increased, suggesting that the α -Helix conformation could be predominant in low dielectric environment, like in a phospholipidic membrane.

Mechanism of Action

Membrane Integrity and Esterase Activity

The red fluorescent dye propidium iodide (PI), which is kept on the outside of intact membranes, can penetrate damaged cell membranes and intercalate into nucleic acids. The fluorescence intensity of PI indicates the level of cell membrane integrity. In the absence of peptide, cells exhibited no PI staining, indicating that membranes were intact (Figures 6, 7). After treatment with Sarconesin, the percentage of PI-permeable *E. coli* cells increased. This suggested that the inner membrane of *E. coli* was disrupted after treatment with Sarconesin. Also, an alteration in the esterase activity when compared with bacteria control was observed.

DNA Staining

Neither untreated bacteria nor Sarconesin-treated bacteria showed DNA fluorescence, indicating that DNA was not denatured with Sarconesin treatment (Figure 7).

⁶<https://www.ncbi.nlm.nih.gov/>

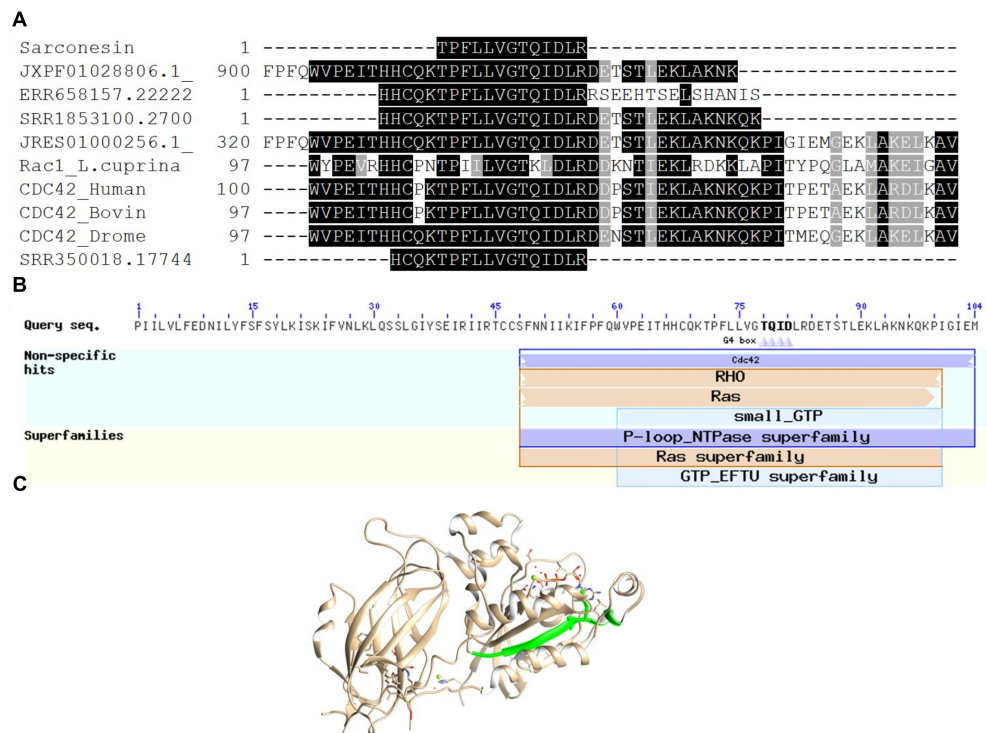


FIGURE 4 | Sarconesin alignment and protein model. **(A)** Sarconesin multiple sequence alignment against selected proteins. (<https://www.ncbi.nlm.nih.gov/>): CDC42 cell division control protein 42 homologue OS = *Bos taurus* (Q2KJ93), CDC42_HUMAN Chain A, structure of the Rho family Gtp-binding protein Cdc42 in complex with the multifunctional regulator Rhogdi (gi| 7245832| 1DOA_A), CDC42_DROME Cdc42 homologue OS = *Drosophila melanogaster* GN = Cdc42 PE = 1 SV = 1 (P40793), Ras-related protein Rac1 [*Lucilia cuprina*] GenBank: KNC23156.1. Sarconesin has 100% sequence similarity with CDC proteins and 69% with Rac from *L. cuprina*. Translated sequences from *L. sericata*. Genome scaffold (JXPF01028806.1), transcriptomes ERR658157.22222021.1 and pupa SRR350018.17744834.1 genome scaffold (JRES01000256.1) and *L. cuprina* transcriptome SRR1853100.27006533.2. **(B)** Conserved domains found in JXPF01028806.1 *L. sericata* Blastp, showing Sarconesin a conserved residue from CDC42 domain. **(C)** Representative model of human CDC42 (PDB ID: 1DOA_A). Sarconesin is encrypted in a site between residues 111 and 123 (green), which folds as a β -sheet.

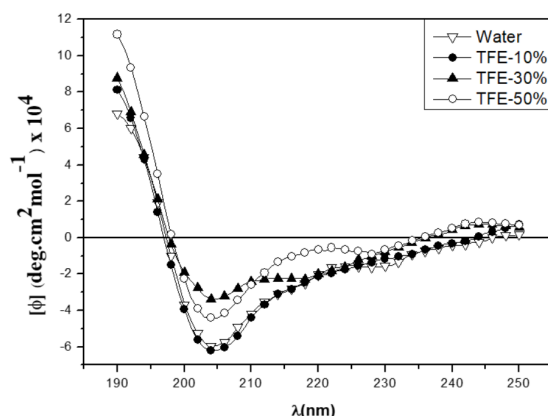


FIGURE 5 | CD spectra of the Sarconesin peptide in water and different TFE/Water proportions.

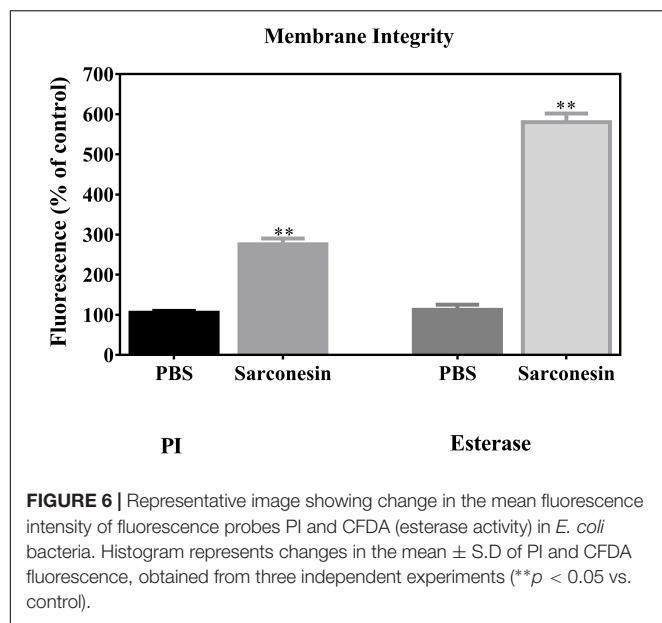
DNA Gel Movement Retardation

In an attempt to clarify the molecular mechanism of action, DNA-binding properties of Sarconesin were examined by analysing

electrophoretic migration of DNA. The migration of *E. coli* genomic DNA suppressed by Sarconesin at 50, 100, and 200 μ M (Figure 8). This result indicated that Sarconesin can bind to bacterial DNA.

DISCUSSION

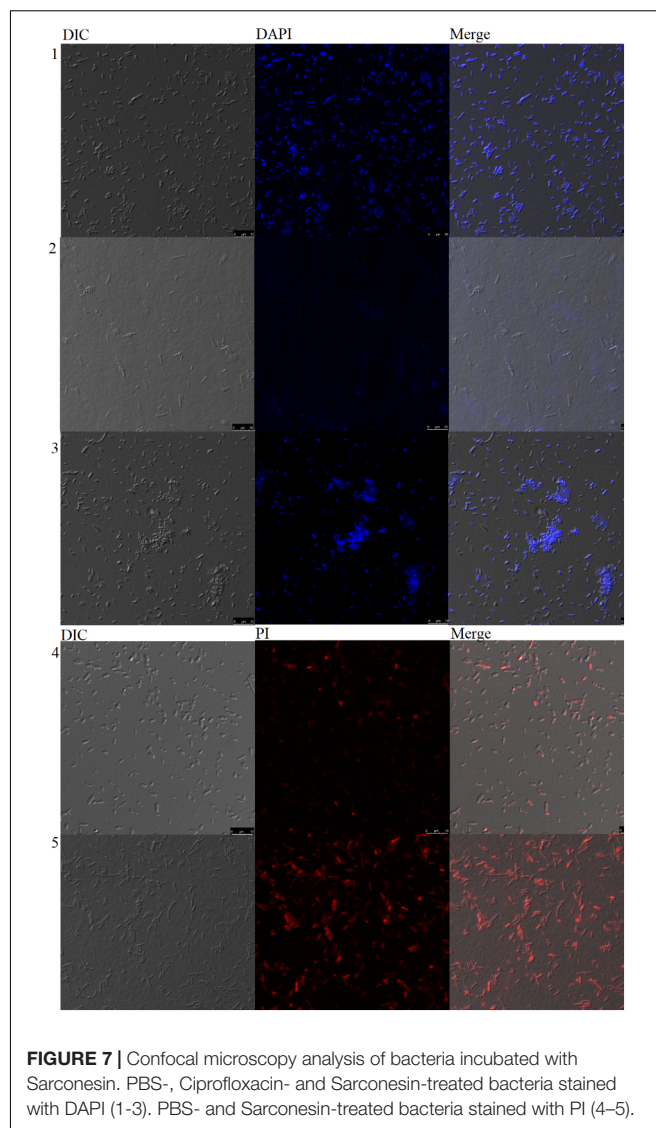
Bacterial resistance against antibiotics has created special interest in searching for new compounds as potential antimicrobial drugs which might be more effective in developing new therapeutic tools (Chernysh et al., 2015). The present work led to finding a new sequence from *S. magellanica*; its antibacterial activity was screened and its biochemical and structural properties were elucidated by sequence homology. One AMP responsible for the antibacterial activity previously reported in *S. magellanica* was found (Díaz-Roa et al., 2014). Sarconesin was seen to have 1,471.8372 Da mass and similarity with Cdc42 and Rac proteins; the AMP was embedded in a site between human Cdc42 residues 111 and 123, folding as a β -sheet. A search for the peptide in AMPs database did not reveal any similarity with previously reported AMPs; however, this new peptide could be part of the family of linear AMPs (Giuliani et al., 2006).



The MIC obtained for Sarconesin in this study suggested a potent activity, similar to that previously reported for other peptides that are active below a 32 $\mu\text{g/mL}$ concentration (Cézar et al., 2011), also, the thanatin peptide has shown a MIC below 2.5mM, which highlights that Sarconesin required less peptide to inhibit bacterial growth (Bulet et al., 1999). This further supports the importance of new effective substances, knowing that several bacteria do become resistant after some days or even hours of exposure (Giacometti et al., 1999). Also, the growth curve of *S. aureus* showed that Sarconesin has effect in less than 180 min of incubation. It should be stressed that the fractions having antibacterial activity were absent in the peaks having the greatest absorbance; this has already been observed in other work where defensin, dipterin (Chernysh et al., 2015) and lucifensin have been detected in very tiny peaks (Cеровsky et al., 2010).

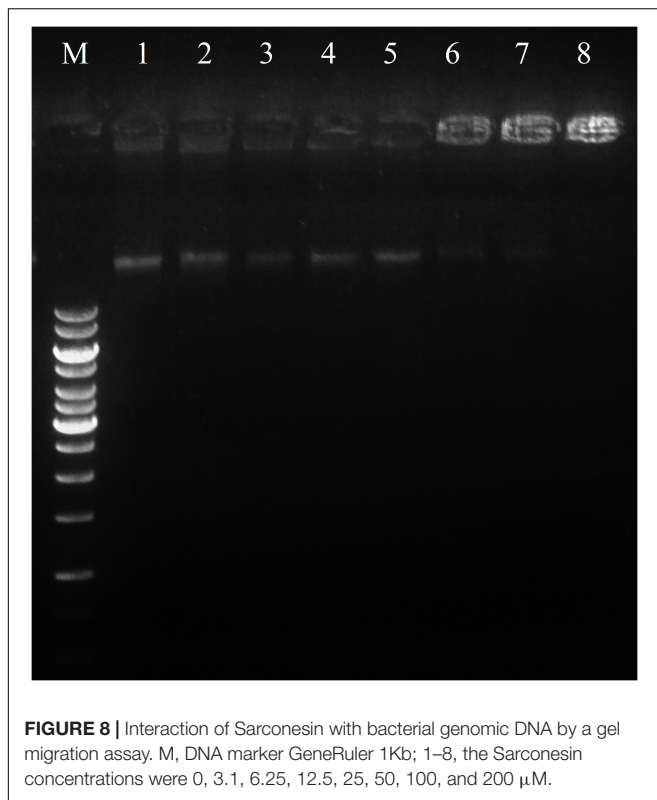
Sarconesin has C-terminal R and N-terminal T residues, when a search by homology was made, a K residue was found immediately before the N-terminal T, suggesting that it might be targeted by trypsin-like activity (Chay Pak Ting et al., 2011). The peptide obtained could have resulted from the presence of some proteases and other enzymes in the ES, taking into account that our experimental procedure did not involve trypsin treatment (Nigam et al., 2010); it has already been reported that ES have trypsin and chymotrypsin in their content (Sandeman et al., 1990; Telford et al., 2011). Sarconesin could be a product of processing the Cdc42 or Rac protein and have other functions in the blowfly related to cell cycle; the derived Sarconesin also has antibacterial activity. It is worth emphasizing that Rac's antimicrobial activity has not been reported before in Calliphoridae blowflies.

As Sarconesin was also present in *S. scrofa* and the flies' food supplement was liver, it could be possible to assume that the peptide was a subproduct of CDC42 from *S. scrofa* and not



from *S. magellanica*. However, the presence of Sarconesin in the transcriptome and genome of other *Lucilia* species showed that this peptide is present in such blowflies, maybe as a sub-product of Diptera. Indeed, multi-omics studies of maggots for larval therapy usually involve using insects fed on bovine liver (Sze et al., 2012; Anstead et al., 2015). The Sarconesin peptide was also present in studies with maggots fed on sheep blood agar as supplement (Poppel et al., 2015; Franta et al., 2016). This exon was also searched in through blast to discard whether it had greater similarity with Diptera species than with *S. scrofa*. It was found to be more similar with Diptera species having different feeding habits and was also associated with a CDC42 conserved domain. Sarconesin was also found in pupa transcriptome having no contact with liver residue, showing that this peptide's origin could most likely be from the fly.

ES pH is usually 8–8.5 (i.e., in *Phaenicia sericata*) (Erdmann, 1987; Thomas S. et al., 1999) because of a waste product



(ammonia), since ammonia increases wound pH, resulting in alkaline conditions which are unfavorable for many bacterial species (van der Plas et al., 2008; Cazander et al., 2009). Sarconesin's net charge would thus be negative as Sarconesin is present in ES and knowing that a protein's net charge is positive at pH below pI (Shaw et al., 2001) (Table 2). This makes Sarconesin an anionic peptide in normal conditions in ES. The mechanism of action regarding bacteria could involve translocation across the membrane (the common mode of action for anionic peptides) (Phoenix et al., 2013), knowing that AMPs can function as direct antimicrobial compounds (Diamond et al., 2009) and also as effector molecules induced upon microbial infection (Zhang et al., 2013).

Sarconesin has 100% sequence similarity with different organisms' CDC42 protein and 69% identity with RAC from *L. cuprina*. Both proteins form part of the Rho-family GTPases (Wennerberg and Der, 2004); Sarconesin may have a similar intracellular mechanism of action, knowing that this protein's expression activates growth factors (Higuchi et al., 2001) and acts as a molecular switch by responding to exogenous and/or endogenous signals, relaying such signals to activate an intracellular biological pathway's downstream components (Johnson, 1999). As the PI assay showed, Sarconesin was confirmed to have a membrane disruption mechanism that has already been reported for other AMPs due to electrostatic interactions, which can be probably followed by hydrophobic patches' insertion into the non-polar interior of the membrane bilayer (Khamis et al., 2015), having a barrel-stave model for the channel pore similar to Alamethicin

that, as Sarconesin, has a 3_{10} -helix conformation (Nagao et al., 2015). Some morphological changes on bacteria were observed in Sarconesin PI experiment (Figure 7), these most likely occurred when the antimicrobial agent attacked the cell membrane, as has been previously reported by Hyde (Hyde et al., 2006).

Sarconesin induced the release of 6-carboxyfluorescein, indicating an effect resulting from a transient destabilization of the bilayer upon initial interaction, a similar effect previously reported for the magainin-2 peptide (Oren and Shai, 1998). The bacterial DNA, when incubated with Sarconesin and DAPI, did not show degradation and the gel retardation assay showed that Sarconesin strongly bound to DNA *in vitro*, thus suggesting the possibility of inhibiting intracellular functions via interference with DNA (Shi et al., 2016).

The selectivity index was not established, nevertheless, no CC was found. These findings would point toward the existence of an appreciable selectivity of this compound against bacteria and, therefore, this observation may be an indicator of their safety as drugs for mammalian organisms. To verify whether the peptide was able to disrupt human erythrocyte membranes in an attempt to evaluate the peptide's future pharmacological potential, a haemolytic assay was performed, where the peptide displayed a very low (<2%) haemolytic activity in a 600 μ M final concentration. The haemolytic activity decreased to 0% in a concentration ranging between 600 and 300 μ M (Figure 2C). As expected, the peptide has no relevant toxic potential, even when tested a concentration 128 times higher than the *M. luteus* and *P. aeruginosa* MIC (i.e., 4.7 μ M), based on the fact that Sarconesin is identical with a conserved domain from CDC42, molecule present in different human cells that acts as a molecular switch in the control of a variety of eukaryotic processes (Johnson, 1999).

Sarconesin may also have implications for wound healing. It has previously been reported in cell culture that ES from other necrophagous flies increase fibroblast proliferation for wound healing (Polakovícova et al., 2015). Also, specifically Sarconesin has been previously reported as an angiogenesis biomarker of recovery after acute kidney injury, so could be a good candidate for future wound evaluation activities (Titulaer, 2013). The Rho family also has wound-healing properties and the role of GTPases in epithelial remodeling during wound-healing and epithelial-mesenchymal transitions has also been previously reported (Van Aelst and Symons, 2002). There is also evidence that Cdc42 plays a major role in wound healing, regarding host defense against infection (Lee et al., 2013). Previously identified natural AMPs from insects are produced by bacteria, fungi, numerous invertebrates, vertebrates, and plants and are usually associated with killing microbes, although they could also be involved in wound repair, inflammation, chemotaxis, and cytokine activity (Ratcliffe et al., 2014).

This article reports, for the first time, a small antimicrobial peptide which is a member of a new Rho family; it contains 13 residues and is active against Gram-positive and Gram-negative bacteria. The native peptide was purified from *S. magellanica* by RP-HPLC and characterized by amino acid sequencing. Further studies aimed at evaluating its activity against other bacteria,

fungi, viruses, and parasites are needed, as well as ascertaining its mechanism of action and investigating its action in wound healing.

DATA AVAILABILITY

The datasets analyzed during the current study are available from the corresponding author on reasonable request.

AUTHOR CONTRIBUTIONS

AD-R carried out the design, conduct of the study, and wrote the manuscript. FB, MP, and PJ contributed to the idea, revised the manuscript and helped data interpretation and supervised the work. All authors read and approved the final manuscript.

REFERENCES

- Altschul, S. F., Madden, T. L., Schaffer, A. A., Zhang, J., Zhang, Z., Miller, W., et al. (1997). Gapped BLAST and PSI-BLAST: a new generation of protein database search programs. *Nucleic Acids Res.* 25, 3389–3402. doi: 10.1093/nar/25.17.3389
- Andersen, A. S., Sandvang, D., Schnorr, K. M., Kruse, T., Neve, S., Joergensen, B., et al. (2010). A novel approach to the antimicrobial activity of maggot debridement therapy. *J. Antimicrob. Chemother.* 65, 1646–1654. doi: 10.1093/jac/dkq165
- Anstead, C. A., Korhonen, P. K., Young, N. D., Hall, R. S., Jex, A. R., Murali, S. C., et al. (2015). *Lucilia cuprina* genome unlocks parasitic fly biology to underpin future interventions. *Nat. Commun.* 6:7344. doi: 10.1038/ncomms8344
- Berova, N., Polavarapu, P. L., Nakanishi, K., and Woody, R. (2012). *Comprehensive Chiroptical Spectroscopy: Applications in Stereochemical Analysis of Synthetic Compounds, Natural Products, and Biomolecules*. Hoboken, NJ: John Wiley & Sons, Inc. doi: 10.1002/9781118120392
- Bexfield, A., Nigam, Y., Thomas, S., and Ratcliffe, N. A. (2004). Detection and partial characterisation of two antibacterial factors from the excretions/secretions of the medicinal maggot *Lucilia sericata* and their activity against methicillin-resistant *Staphylococcus aureus* (MRSA). *Microbes Infect.* 6, 1297–1304. doi: 10.1016/j.micinf.2004.08.011
- Bochicchio, B., and Tamburro, A. M. (2002). Polyproline II structure in proteins: identification by chiroptical spectroscopies, stability, and functions. *Chirality* 14, 782–792. doi: 10.1002/chir.10153
- Brown, K. L., and Hancock, R. E. (2006). Cationic host defense (antimicrobial) peptides. *Curr. Opin. Immunol.* 18, 24–30. doi: 10.1016/j.coi.2005.11.004
- Bulet, P. (2008). Strategies for the discovery, isolation, and characterization of natural bioactive peptides from the immune system of invertebrates. *Methods Mol. Biol.* 494, 9–29. doi: 10.1007/978-1-59745-419-3_2
- Bulet, P., Hetru, C., Dimarcq, J. L., and Hoffmann, D. (1999). Antimicrobial peptides in insects: structure and function. *Dev. Comp. Immunol.* 23, 329–344. doi: 10.1016/S0145-305X(99)00015-4
- Bulet, P., and Stocklin, R. (2005). Insect antimicrobial peptides: structures, properties and gene regulation. *Prot. Pept. Lett.* 12, 3–11. doi: 10.2174/0929866053406011
- Carretero, G. P. B., Saraiva, G. K. V., Cauz, A. C. G., Rodrigues, M. A., Kiyota, S., Riske, K. A., et al. (2018). Synthesis, biophysical and functional studies of two BP100 analogues modified by a hydrophobic chain and a cyclic peptide. *Biochim. Biophys. Acta* 1860, 1502–1516. doi: 10.1016/j.bbame.2018.05.003
- Cazander, G., Van Veen, K. E., Bernards, A. T., and Jukema, G. N. (2009). Do maggots have an influence on bacterial growth? A study on the susceptibility of strains of six different bacterial species to maggots of *Lucilia sericata* and their excretions/secretions. *J. Tissue Viab.* 18, 80–87. doi: 10.1016/j.jtv.2009.02.005
- Cerovsky, V., and Bem, R. (2014). Lucifensins, the insect Defensins of biomedical importance: the story behind maggot therapy. *Pharmaceuticals* 7, 251–264. doi: 10.3390/ph7030251
- Cerovsky, V., Zdarek, J., Fucik, V., Monincova, L., Voburka, Z., and Bem, R. (2010). Lucifensin, the long-sought antimicrobial factor of medicinal maggots of the blowfly *Lucilia sericata*. *Cell Mol. Life Sci.* 67, 455–466. doi: 10.1007/s00018-009-0194-0
- Cézard, C., Silva-Pires, V., Mullié, C., and Sonnet, P. (2011). *Antibacterial Peptides: A Review Science against Microbial Pathogens: Communicating Current Research And Technological Advances*, ed. A. Méndez-Vilas, Badajoz: Formatex Research Center.
- Chaparro, E., and da Silva, P. I. J. (2016). Lacrain: the first antimicrobial peptide from the body extract of the Brazilian centipede *Scolopendra viridicornis*. *Int. J. Antimicrob. Agents* 48, 277–285. doi: 10.1016/j.ijantimicag.2016.05.015
- Chay Pak Ting, B. P., Mine, Y., Juneja, L. R., Okubo, T., Gauthier, S. F., and Pouliot, Y. (2011). Comparative composition and antioxidant activity of Peptide fractions obtained by ultrafiltration of egg yolk protein enzymatic hydrolysates. *Membranes* 1, 149–161. doi: 10.3390/membranes1030149
- Chernysh, S., Gordya, N., and Suborova, T. (2015). Insect antimicrobial peptide complexes prevent resistance development in bacteria. *PLoS One* 10:e0130788. doi: 10.1371/journal.pone.0130788
- Chernysh, S., Gordya, N., Tulin, D., and Yakovlev, A. (2018). Biofilm infections between Scylla and Charybdis: interplay of host antimicrobial peptides and antibiotics. *Infect Drug Resist.* 11, 501–514. doi: 10.2147/IDR.S157847
- Church, J. C. (1996). The traditional use of maggots in wound healing, and the development of larva therapy (biosurgery) in modern medicine. *J. Altern. Complement. Med.* 2, 525–527. doi: 10.1089/acm.1996.2.525
- Cruz-Saavedra, L., Díaz-Roa, A., Gaona, M. A., Cruz, M. L., Ayala, M., Cortes-Vecino, J. A., et al. (2016). The effect of *Lucilia sericata*- and *Sarconesiopsis magellanica*-derived larval therapy on *Leishmania panamensis*. *Acta Trop.* 164, 280–289. doi: 10.1016/j.actatropica.2016.09.020
- Diamond, G., Beckloff, N., Weinberg, A., and Kisich, K. O. (2009). The roles of antimicrobial peptides in innate host defense. *Curr. Pharm. Des.* 15, 2377–2392. doi: 10.2174/138161209788682325
- Díaz-Roa, A., Gaona, M. A., Segura, N. A., Suarez, D., Patarroyo, M. A., and Bello, F. J. (2014). *Sarconesiopsis magellanica* (Diptera: Calliphoridae) excretions and secretions have potent antibacterial activity. *Acta Trop.* 136, 37–43. doi: 10.1016/j.actatropica.2014.04.018
- El Shazely, B., Veverka, V., Fucik, V., Voburka, Z., Zdarek, J., and Cerovsky, V. (2013). Lucifensin II, a defensin of medicinal maggots of the blowfly *Lucilia cuprina* (Diptera: Calliphoridae). *J. Med. Entomol.* 50, 571–578. doi: 10.1603/ME12208
- Erdmann, G. R. (1987). Antibacterial action of Myiasis-causing flies. *Parasitol. Today* 3, 214–216. doi: 10.1016/0169-4758(87)90062-7

FUNDING

This work was supported by the Colombian Science, Technology, and Innovation Department (Colciencias) through Colciencias-UAN agreement FP44842-384-2016 (Project code No. 125371250687). Funding was also received from the São Paulo Research Foundation (FAPESP) Grants 13/07467-1 to CeTICS-CEPID and from the Brazilian National Technological and Scientific Development Council (CNPq) Grant 472744/2012-7. AD-R received support through Colciencias grant (convocatoria 617, Colombia).

ACKNOWLEDGMENTS

We would like to thank Jason Garry for correcting the English, Abraham Espinoza-Culupú and Flávio Lopes Alves for their diligent help with part of the experimental work.

- Faisal, M., Saquib, Q., Alatar, A. A., Al-Khedhairi, A. A., Ahmed, M., Ansari, S. M., et al. (2016). Cobalt oxide nanoparticles aggravate DNA damage and cell death in eggplant via mitochondrial swelling and NO signaling pathway. *Biol. Res.* 49:20. doi: 10.1186/s40659-016-0080-9
- Franta, Z., Vogel, H., Lehmann, R., Rupp, O., Goesmann, A., and Vilcinskis, A. (2016). Next generation sequencing identifies five major classes of potentially therapeutic enzymes secreted by *Lucilia sericata* medical maggots. *Biomed. Res. Int.* 2016:8285428. doi: 10.1155/2016/8285428
- Giacometti, A., Cirioni, O., Barchiesi, F., Fortuna, M., and Scalise, G. (1999). In-vitro activity of cationic peptides alone and in combination with clinically used antimicrobial agents against *Pseudomonas aeruginosa*. *J. Antimicrob. Chemother.* 44, 641–645. doi: 10.1093/jac/44.5.641
- Giuliani, A., Pirri, G., and Nicoletto, S. F. (2006). Antimicrobial peptides: an overview of a promising class of therapeutics. *Curr. Med. Chem.* 2, 2449–2466.
- Goff, M. L. (2001). *A Fly for the Prosecution: How Insect Evidence Helps Solve Crimes*. Cambridge, MA: Harvard University Press, 225.
- Gordya, N., Yakovlev, A., Kruglikova, A., Tulin, D., Potolitsina, E., Suborova, T., et al. (2017). Natural antimicrobial peptide complexes in the fighting of antibiotic resistant biofilms: *Calliphora vicina* medicinal maggots. *PLoS One* 12:e0173559. doi: 10.1371/journal.pone.0173559
- Gottrup, F., and Jorgensen, B. (2011). Maggot debridement: an alternative method for debridement. *Eplasty* 11:e33.
- Gouy, M., Guindon, S., and Gascuel, O. (2010). SeaView Version 4: a multiplatform graphical user interface for sequence alignment and phylogenetic tree building. *Mol. Biol. Evol.* 27, 221–224. doi: 10.1093/molbev/msp259
- Hardy, D. E. (1966). *A Catalogue of the Diptera of the Americas south of the United States*. Museu de Zoologia, Departamento de Zoologia, Universidade de São Paulo. São Paulo: Departamento de Zoologia, Secretaria da Agricultura do Estado de São Paulo.
- Hetru, C., and Bulet, P. (1997). Strategies for the isolation and characterization of antimicrobial peptides of invertebrates. *Methods Mol. Biol.* 78, 35–49. doi: 10.1385/0-89603-408-9:35
- Higuchi, M., Masuyama, N., Fukui, Y., Suzuki, A., and Gotoh, Y. (2001). Akt mediates Rac/Cdc42-regulated cell motility in growth factor-stimulated cells and in invasive PTEN knockout cells. *Curr. Biol.* 11, 1958–1962. doi: 10.1016/S0960-9822(01)00599-1
- Hoffmann, J. A., and Hetru, C. (1992). Insect defensins: inducible antibacterial peptides. *Immunol. Today* 13, 411–415. doi: 10.1016/0167-5699(92)90092-L
- Hou, F., Li, J., Pan, P., Xu, J., Liu, L., Liu, W., et al. (2011). Isolation and characterisation of a new antimicrobial peptide from the skin of *Xenopus laevis*. *Int. J. Antimicrob. Agents* 38, 510–515. doi: 10.1016/j.ijantimicag.2011.07.012
- Huberman, L., Gollop, N., Mumcuoglu, K. Y., Breuer, E., Bhusare, S. R., Shai, Y., et al. (2007). Antibacterial substances of low molecular weight isolated from the blowfly, *Lucilia sericata*. *Med. Vet. Entomol.* 21, 127–131. doi: 10.1111/j.1365-2915.2007.00668.x
- Hyde, A. J., Parisot, J., McNichol, A., and Bonev, B. B. (2006). Nisin-induced changes in *Bacillus* morphology suggest a paradigm of antibiotic action. *Proc. Natl. Acad. Sci. U.S.A.* 103, 19896–19901. doi: 10.1073/pnas.0608373104
- Jiang, K.-C., Sun, X.-J., Wang, W., Liu, L., Cai, Y., Chen, Y.-C., et al. (2012). Excretions/Secretions from bacteria-pretreated maggot are more effective against *Pseudomonas aeruginosa* Biofilms. *PLoS One* 7:e49815. doi: 10.1371/journal.pone.0049815
- Johnson, D. I. (1999). Cdc42: an essential Rho-type GTPase controlling eukaryotic cell polarity. *Microbiol. Mol. Biol. Rev.* 63, 54–105. doi: 10.1385/0-89603-44\break08-9:35
- Kawabata, T., Mitsui, H., Yokota, K., Ishino, K., Oguma, K., and Sano, S. (2010). Induction of antibacterial activity in larvae of the blowfly *Lucilia sericata* by an infected environment. *Med. Vet. Entomol.* 24, 375–381. doi: 10.1111/j.1365-2915.2010.00902.x
- Khamis, A. M., Essack, M., Gao, X., and Bajic, V. B. (2015). Distinct profiling of antimicrobial peptide families. *Bioinformatics* 31, 849–856. doi: 10.1093/bioinformatics/btu738
- Landry, B. S., Dextraze, L., and Boivin, G. (1993). Random amplified polymorphic DNA markers for DNA fingerprinting and genetic variability assessment of minute parasitic wasp species (Hymenoptera: Mymaridae and Trichogrammatidae) used in biological control programs of phytophagous insects. *Genome* 36, 580–587. doi: 10.1139/g93-078
- Lee, K., Boyd, K. L., Parekh, D. V., Kehl-Fie, T. E., Baldwin, H. S., Brakebusch, C., et al. (2013). Cdc42 promotes host defenses against fatal infection. *Infect. Immun.* 81, 2714–2723. doi: 10.1128/IAI.01114-12
- Lorenzini, D. M., Da Silva, P. I. Jr., Fogaca, A. C., Bulet, P., and Daffre, S. (2003). Acanthoscurrin: a novel glycine-rich antimicrobial peptide constitutively expressed in the hemocytes of the spider *Acanthoscurria gomesiana*. *Dev. Comp. Immunol.* 27, 781–791. doi: 10.1016/S0145-305X(03)00058-2
- Magi, G., Marini, E., and Facinelli, B. (2015). Antimicrobial activity of essential oils and carvacrol, and synergy of carvacrol and erythromycin, against clinical, erythromycin-resistant Group A Streptococci. *Front. Microbiol.* 6:165. doi: 10.3389/fmicb.2015.00165
- Mariluis, J., and Mulieri, P. (2003). The distribution of the Calliphoridae in Argentina (Diptera). *Revista de la Sociedad Entomológica Argentina* 62, 85–97.
- Mariluis, J. C., and Peris, S. V. (1984). Datos para una sinopsis de los Calliphoridae neotropicales. *EOS Revista Española de Entomología* 40, 67–86.
- Mumcuoglu, K. Y. (2001). Clinical applications for maggots in wound care. *Am. J. Clin. Dermatol.* 2, 219–227. doi: 10.2165/00128071-200102040-00003
- Nagao, T., Mishima, D., Javkhantugs, N., Wang, J., Ishioka, D., Yokota, K., et al. (2015). Structure and orientation of antibiotic peptide alamethicin in phospholipid bilayers as revealed by chemical shift oscillation analysis of solid state nuclear magnetic resonance and molecular dynamics simulation. *Biochim. Biophys. Acta* 1848, 2789–2798. doi: 10.1016/j.bbmem.2015.07.019
- Nan, Y. H., Bang, J.-K., Jacob, B., Park, I.-S., and Shin, S. Y. (2012). Prokaryotic selectivity and LPS-neutralizing activity of short antimicrobial peptides designed from the human antimicrobial peptide LL-37. *Peptides* 35, 239–247. doi: 10.1016/j.peptides.2012.04.004
- Nigam, Y., Dudley, E., Bexfield, A., Bond, A. E., Evans, J., and James, J. (2010). “The physiology of wound healing by the medicinal maggot, *Lucilia sericata*,” in *Advances in Insect Physiology*, Vol. 39, ed. S. J. Simpson (London: Academic Press Ltd-Elsevier Science Ltd.), 39–81.
- Nocker, A., Caspers, M., Esveld-Amanatidou, A., Van Der Vossen, J., Schuren, F., Montijn, R., et al. (2011). Multiparameter viability assay for stress profiling applied to the food pathogen *Listeria monocytogenes* F2365. *Appl. Environ. Microbiol.* 77, 6433–6440. doi: 10.1128/AEM.00142-11
- O'Meara, S., Al-Kurdi, D., Ologun, Y., Ovington, L. G., Martyn-St James, M., and Richardson, R. (2014). Antibiotics and antiseptics for venous leg ulcers. *Cochrane Database Syst. Rev.* 14:CD003557. doi: 10.1002/14651858.CD003557.pub5
- Oren, Z., and Shai, Y. (1998). Mode of action of linear amphipathic α -helical antimicrobial peptides. *Pept. Sci.* 47, 451–463. doi: 10.1002/(SICI)1097-0282(1998)47:6<451::AID-BIP4>3.0.CO;2-F
- Pape, T., Wolff, M., and Amat, E. (2004). Los califóridos, éstridos, rinofóridos y sarcófagos (Diptera: Calliphoridae, Oestridae, Rhinophoridae y Sarcophagidae) de Colombia. *Biota Colombiana* 5, 201–208.
- Phoenix, D. A., Dennison, S. R., and Harris, F. (2013). Anionic antimicrobial peptides. *Antimicrob. Pept.* 10, 585–606. doi: 10.1002/9783527652853.ch9783527652853
- Polakovícova, S., Polak, S., Kuniakova, M., Cambal, M., Caplovícova, M., Kozanek, M., et al. (2015). The effect of salivary gland extract of *Lucilia sericata* maggots on human dermal fibroblast proliferation within collagen/hyaluronan membrane in vitro: transmission electron microscopy study. *Adv. Skin Wound Care* 28, 221–226. doi: 10.1097/01.ASW.0000461260.03630.a0
- Poppel, A. K., Vogel, H., Wiesner, J., and Vilcinskis, A. (2015). Antimicrobial peptides expressed in medicinal maggots of the blow fly *Lucilia sericata* show combinatorial activity against bacteria. *Antimicrob. Agents Chemother.* 59, 2508–2514. doi: 10.1128/AAC.05180-14
- Raposo, E., Bortolini, S., Maistrello, L., and Grasso, D. A. (2017). Larval therapy for chronic cutaneous ulcers: historical review and future perspectives. *Wounds* 29, 367–373.
- Ratcliffe, N., Azambuja, P., and Mello, C. B. (2014). Recent advances in developing insect natural products as potential modern day medicines. *Evid. Based Complement. Alternat. Med.* 2014:904958. doi: 10.1155/2014/904958
- Ricilica, K. C., Sayegh, R. S., Melo, R. L., and Silva, P. I. Jr. (2012). Rondonin an antifungal peptide from spider (*Acanthoscurria rondoniae*) haemolymph. *Results Immunol.* 2, 66–71. doi: 10.1016/j.rinim.2012.03.001
- Robinson, W. (1935). Stimulation of healing in non-healing wounds by allantoin in maggot secretions and of wide biological distribution. *J. Bone Joint Surg. Am.* 17, 267–271.

- Rueda, L. C., Ortega, L. G., Segura, N. A., Acero, V. M., and Bello, F. (2010). *Lucilia sericata* strain from Colombia: experimental colonization, life tables and evaluation of two artificial diets of the blowfly *Lucilia sericata* (Meigen) (Diptera: Calliphoridae), Bogota, Colombia strain. *Biol. Res.* 43, 197–203. doi: 10.4067/S0716-97602010000200008
- Sandeman, R. M., Feehan, J. P., Chandler, R. A., and Bowles, V. M. (1990). Tryptic and chymotryptic proteases released by larvae of the blowfly, *Lucilia cuprina*. *Int. J. Parasitol.* 20, 1019–1023. doi: 10.1016/0020-7519(90)90044-N
- Sayegh, R. S., Batista, I. F., Melo, R. L., Riske, K. A., Daffre, S., Montich, G., et al. (2016). Longipin: an Amyloid Antimicrobial Peptide from the Harvestman *Acutisoma longipes* (Arachnida: Opiliones) with preferential affinity for anionic vesicles. *PLoS One* 11:e0167953. doi: 10.1371/journal.pone.0167953
- Shaw, K. L., Grimsley, G. R., Yakovlev, G. I., Makarov, A. A., and Pace, C. N. (2001). The effect of net charge on the solubility, activity, and stability of ribonuclease Sa. *Protein Sci.* 10, 1206–1215. doi: 10.1110/ps.440101
- Sherman, R. A., Hall, M. J., and Thomas, S. (2000). Medicinal maggots: an ancient remedy for some contemporary afflictions. *Annu. Rev. Entomol.* 45, 55–81. doi: 10.1146/annurev.ento.45.1.55
- Shi, W., Li, C., Li, M., Zong, X., Han, D., and Chen, Y. (2016). Antimicrobial peptide melittin against *Xanthomonas oryzae* pv. *oryzae*, the bacterial leaf blight pathogen in rice. *Appl. Microbiol. Biotechnol.* 100, 5059–5067. doi: 10.1007/s00253-016-7400-4
- Silva, P. I. Jr., Daffre, S., and Bulet, P. (2000). Isolation and characterization of gomesin, an 18-residue cysteine-rich defense peptide from the spider *Acanthoscurria gomesiana* hemocytes with sequence similarities to horseshoe crab antimicrobial peptides of the tachyplesin family. *J. Biol. Chem.* 275, 33464–33470. doi: 10.1074/jbc.M001491200
- Spilsbury, K., Cullum, N., Dumville, J., O'meara, S., Petherick, E., and Thompson, C. (2008). Exploring patient perceptions of larval therapy as a potential treatment for venous leg ulceration. *Health Expect.* 11, 148–159. doi: 10.1111/j.1369-7625.2008.00491.x
- Sze, S. H., Dunham, J. P., Carey, B., Chang, P. L., Li, F., Edman, R. M., et al. (2012). A de novo transcriptome assembly of *Lucilia sericata* (Diptera: Calliphoridae) with predicted alternative splices, single nucleotide polymorphisms and transcript expression estimates. *Insect Mol. Biol.* 21, 205–221. doi: 10.1111/j.1365-2583.2011.01127.x
- Telford, G., Brown, A. P., Kind, A., English, J. S., and Pritchard, D. I. (2011). Maggot chymotrypsin I from *Lucilia sericata* is resistant to endogenous wound protease inhibitors. *Br. J. Dermatol.* 164, 192–196. doi: 10.1111/j.1365-2133.2010.10081.x
- Teng, D., Wang, X., Xi, D., Mao, R., Zhang, Y., Guan, Q., et al. (2014). A dual mechanism involved in membrane and nucleic acid disruption of AvBD103b, a new avian defensin from the king penguin, against *Salmonella enteritidis* CVCC3377. *Appl. Microbiol. Biotechnol.* 98, 8313–8325. doi: 10.1007/s00253-014-5898-x
- Thomas, A. M., Harding, K. G., and Moore, K. (1999). The structure and composition of chronic wound eschar. *J. Wound Care* 8, 285–287. doi: 10.12968/jowc.1999.8.6.25881
- Thomas, S., Andrews, A. M., Hay, N. P., and Bourgoise, S. (1999). The antimicrobial activity of maggot secretions: results of a preliminary study. *J. Tissue Viab.* 9, 127–132. doi: 10.1016/S0965-206X(99)80032-1
- Titulaer, M. K. (2013). Candidate biomarker discovery for angiogenesis by automatic integration of Orbitrap MS1 spectral- and X!Tandem MS2 sequencing information. *Genomics Proteomics Bioinformatics* 11, 182–194. doi: 10.1016/j.gpb.2013.02.002
- Valachova, I., Bohova, J., Palosova, Z., Takac, P., Kozanek, M., and Majtan, J. (2013). Expression of lucifensin in *Lucilia sericata* medicinal maggots in infected environments. *Cell Tissue Res.* 353, 165–171. doi: 10.1007/s00441-013-1626-6
- Van Aelst, L., and Symons, M. (2002). Role of Rho family GTPases in epithelial morphogenesis. *Genes Dev.* 16, 1032–1054. doi: 10.1101/gad.978802
- van der Plas, M. J., Jukema, G. N., Wai, S. W., Dogterom-Ballering, H. C., Lagendijk, E. L., Van Gulpen, C., et al. (2008). Maggot excretions/secretions are differentially effective against biofilms of *Staphylococcus aureus* and *Pseudomonas aeruginosa*. *J. Antimicrob. Chemother.* 61, 117–122. doi: 10.1093/jac/dkm407
- Vealema, W. A., Van Der Berg, J. P., Hansen, M. J., Szymanski, W., Driessen, A. J. M., and Feringa, B. L. (2013). Optical control of antibacterial activity. *Nat. Chem.* 5, 924–928. doi: 10.1038/nchem.1750
- Wennerberg, K., and Der, C. J. (2004). Rho-family GTPases: it's not only Rac and Rho (and I like it). *J. Cell Sci.* 117, 1301–1312. doi: 10.1242/jcs.01118
- Wiegand, I., Hilpert, K., and Hancock, R. E. (2008). Agar and broth dilution methods to determine the minimal inhibitory concentration (MIC) of antimicrobial substances. *Nat. Protoc.* 3, 163–175. doi: 10.1038/nprot.2007.521
- Wolff, H., and Hansson, C. (2005). Rearing larvae of *Lucilia sericata* for chronic ulcer treatment—an improved method. *Acta Derm. Venereol.* 85, 126–131. doi: 10.1080/00015550510025533
- Yakovlev, A. Y., Nesin, A. P., Simonenko, N. P., Gordya, N. A., Tulin, D. V., Kruglikova, A. A., et al. (2017). Fat body and hemocyte contribution to the antimicrobial peptide synthesis in *Calliphora vicina* R.-D. (Diptera: Calliphoridae) larvae. *In Vitro Cell Dev. Biol. Anim.* 53, 33–42. doi: 10.1007/s11626-016-0078-1
- Yang, N., Liu, X., Teng, D., Li, Z., Wang, X., Mao, R., et al. (2017). Antibacterial and detoxifying activity of NZ17074 analogues with multi-layers of selective antimicrobial actions against *Escherichia coli* and *Salmonella enteritidis*. *Sci. Rep.* 7:3392. doi: 10.1038/s41598-017-03664-2
- Yeaman, M. R., and Yount, N. Y. (2003). Mechanisms of antimicrobial peptide action and resistance. *Pharmacol. Rev.* 55, 27–55. doi: 10.1124/pr.55.1.2
- Yi, H. Y., Chowdhury, M., Huang, Y. D., and Yu, X. Q. (2014). Insect antimicrobial peptides and their applications. *Appl. Microbiol. Biotechnol.* 98, 5807–5822. doi: 10.1007/s00253-014-5792-6
- Zhang, Z., Wang, J., Zhang, B., Liu, H., Song, W., He, J., et al. (2013). Activity of antibacterial protein from maggots against *Staphylococcus aureus* in vitro and in vivo. *Int. J. Mol. Med.* 31, 1159–1165. doi: 10.3892/ijmm.2013.1291

Conflict of Interest Statement: The authors declare that the research was conducted in the absence of any commercial or financial relationships that could be construed as a potential conflict of interest.

Copyright © 2018 Díaz-Roa, Patarroyo, Bello and Da Silva. This is an open-access article distributed under the terms of the Creative Commons Attribution License (CC BY). The use, distribution or reproduction in other forums is permitted, provided the original author(s) and the copyright owner(s) are credited and that the original publication in this journal is cited, in accordance with accepted academic practice. No use, distribution or reproduction is permitted which does not comply with these terms.



Lectin-Like Bacteriocins

Maarten G. K. Ghequire^{1*}, Başak Öztürk^{2†} and René De Mot^{1‡}

¹ Centre of Microbial and Plant Genetics, KU Leuven, Leuven, Belgium, ² Leibniz-Institut DSMZ-Deutsche Sammlung von Mikroorganismen und Zellkulturen, Braunschweig, Germany

OPEN ACCESS

Edited by:

Natalia V. Kirienko,
Rice University, United States

Reviewed by:

Marina G. Kalyuzhanaya,
San Diego State University,
United States
Rhys William Grinter,
University of Birmingham,
United Kingdom

*Correspondence:

Maarten G. K. Ghequire
maarten.ghequire@kuleuven.be;
maarten.ghequire@biw.kuleuven.be
orcid.org/0000-0002-5577-7277

[†]orcid.org/0000-0002-8687-3210

[‡]orcid.org/0000-0002-0030-9441

Specialty section:

This article was submitted to
Antimicrobials, Resistance
and Chemotherapy,
a section of the journal
Frontiers in Microbiology

Received: 25 July 2018

Accepted: 23 October 2018

Published: 12 November 2018

Citation:

Ghequire MGK, Öztürk B and
De Mot R (2018) Lectin-Like
Bacteriocins.
Front. Microbiol. 9:2706.
doi: 10.3389/fmicb.2018.02706

Bacteria produce a diverse array of antagonistic compounds to restrict growth of microbial rivals. Contributing to this warfare are bacteriocins: secreted antibacterial peptides, proteins and multi-protein complexes. These compounds typically eliminate competitors closely related to the producer. Lectin-like bacteriocins (LlpAs) constitute a distinct class of such proteins, produced by *Pseudomonas* as well as some other proteobacterial genera. LlpAs share a common architecture consisting of two B-lectin domains, followed by a short carboxy-terminal extension. Two surface-exposed moieties on susceptible *Pseudomonas* cells are targeted by the respective lectin modules. The carboxy-terminal domain binds D-rhamnose residues present in the lipopolysaccharide layer, whereas the amino-terminal domain interacts with a polymorphic external loop of the outer-membrane protein insertase BamA, hence determining selectivity. The absence of a toxin-immunity module as found in modular bacteriocins and other polymorphic toxin systems, hints toward a novel mode of killing initiated at the cellular surface, not requiring bacteriocin import. Despite significant progress in understanding the function of LlpAs, outstanding questions include the secretion machinery recruited by lectin-like bacteriocins for their release, as well as a better understanding of the environmental signals initiating their expression.

Keywords: LlpA, L-type pyocin, BAM complex, protein antibiotic, bacterial antagonism

INTRODUCTION

Pseudomonads produce a diverse set of antagonism-mediating compounds that assist the elimination of rival microorganisms. A major subset of molecules contributing to this microbial fight are bacteriocins, ribosomally encoded antibacterial peptides and proteins that target bacteria closely related to the producing strain (Ghequire and De Mot, 2014). Bacteriocins assigned to different classes, based on molecular size and architecture, have been identified in a variety of *Pseudomonas* species (Lavermicocca et al., 2002; Parret et al., 2003, 2005; Barreteau et al., 2009; Fischer et al., 2012; Godino et al., 2015; Hockett et al., 2015). To date, research has primarily focused on *Pseudomonas aeruginosa* bacteriocins (termed pyocins) (Michel-Briand and Bayse, 2002). The bacteriocin armamentarium owned by pseudomonads varies from strain to strain (Ghequire and De Mot, 2014; Sharp et al., 2017). For different classes of bacteriocins, an evolutionary advantage has been demonstrated for bacteria secreting such compounds (Inglis et al., 2014; Ghoul et al., 2015; Godino et al., 2015; Dorosky et al., 2017; Príncipe et al., 2018).

Four main groups of *Pseudomonas* bacteriocins have been identified so far, all of which equally occur in other bacterial genera: tailocins, modular bacteriocins, B-type microcins and lectin-like bacteriocins (**Supplementary Table S1**). (i) Tailocins resemble contractile (R-type) or flexible (F-type) bacteriophage tails (Ghequire and De Mot, 2015; Scholl, 2017). Acquired from different phage

sources, these high molecular-weight particles are synthesized from large gene clusters and are functional stand-alone units, lacking an accompanying phage head structure. (ii) Modular (S-type) bacteriocins represent a heterogeneous group of polymorphic toxins, and include a receptor-binding domain, a moiety assisting in membrane passage of target cells and a toxin domain (Ghequire and De Mot, 2014; Jamet and Nassif, 2015; Sharp et al., 2017). Self-inhibition due to toxin activity in bacteriocin producers is avoided by co-expression of dedicated immunity genes. These immunity partners form specific and high-affinity complexes with their cognate toxin domains, or reside in the cytoplasmic membrane to temporarily inhibit toxin activity during secretion (Rasouliha et al., 2013; Joshi et al., 2015; Ghequire et al., 2017b). To gain access to targeted pseudomonads, S-type bacteriocins take advantage of TonB-dependent outer-membrane proteins (White et al., 2017). (iii) B-type microcins are post-translationally modified peptides, interfering with DNA gyrase (Meteliev et al., 2013). (iv) Lectin-like (further abbreviated as L-type) bacteriocins are composed of two monocot mannose-binding lectin domains and represent a fourth major class of *Pseudomonas* bacteriocins (Parret et al., 2003), with an unknown mode of action. In this review, we provide an overview summarizing current knowledge on the latter bacteriocin type, with emphasis on outstanding research questions.

A SUGAR-BINDING TANDEM DESIGNED TO KILL

Originally identified in banana rhizosphere isolate *Pseudomonas putida* BW11M1 (recently reclassified as *Pseudomonas mosselii* BW11M1) (Parret et al., 2003; Ghequire et al., 2016), the first lectin-like bacteriocin was termed LlpA (lectin-like putidacin A), and shown to possess selective genus-specific antagonistic activity, characteristic of bactericidal action. Later, LlpA bacteriocins were characterized in a number of other *Pseudomonas* species as well: *Pseudomonas protegens* (Parret et al., 2005), *Pseudomonas syringae* (Ghequire et al., 2012a) and *P. aeruginosa* (Ghequire et al., 2014; McCaughey et al., 2014) (Table 1). These bacteriocins are called “lectin-like” because all share an organization comprising two “monocot mannose-binding lectin” (MMBL) domains (B-lectin, Pfam PF01453), instead of a toxin-immunity module that is usually present in bacteriocins of similar size. The B-lectin domain is abundant in (monocot) plants (Van Damme et al., 1991; Pang et al., 2003; Gao et al., 2011; Pereira et al., 2015), but has also been found in fish (Tsutsui et al., 2003; de Santana Evangelista et al., 2009; Park et al., 2016; Arasu et al., 2017), fungi (Fouquaert et al., 2011; Shimokawa et al., 2012), slime molds (Barre et al., 1999) and sponges (Wiens et al., 2006). In those organisms a variety of antagonistic functions have been assigned to these lectins, including antifungal, antiviral and nematocidal activities (Ghequire et al., 2012b; Wu and Bao, 2013). A lectin-type bacteriocin with a distinct domain organization has been identified in a Gram-positive bacterium: albusin B of *Ruminococcus albus* 7 targets *Ruminococcus flavefaciens*, and consists of a B-lectin

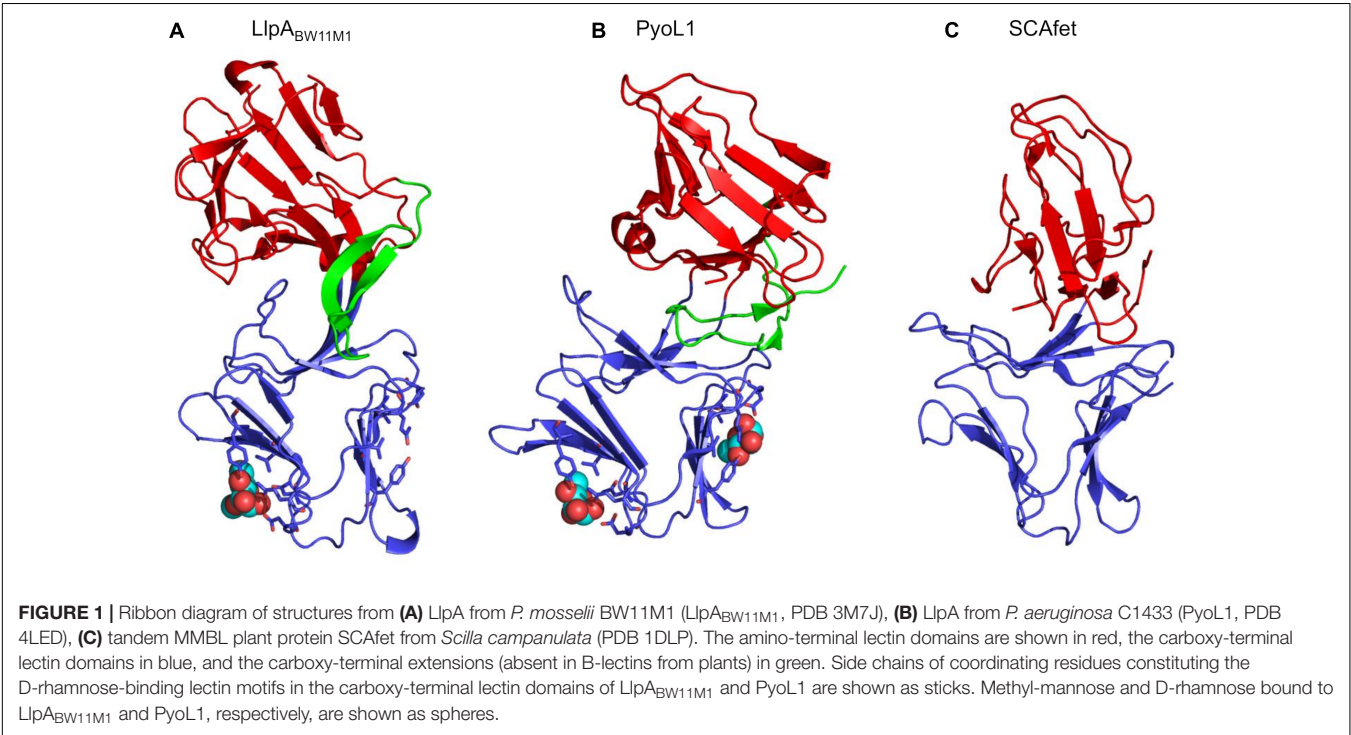
domain followed by a peptidase M15 domain (PF08291) (Chen et al., 2004). Genes encoding albusin B-like proteins have been retrieved in many other *R. albus* strains (Azevedo et al., 2015).

The 3D structure of LlpA from strain BW11M1 (LlpA_{BW11M1}) confirmed the architecture of two B-lectin domains as studied in monocot plants (Wright et al., 2000). Each module is stabilized by a central tryptophan triad. A short β -hairpin extension is present at the carboxy-terminus (Figure 1), but is absent from plant lectins (Ghequire et al., 2013b). The two domains form a rigid tandem due to β -strand swapping and intramolecular interactions (Figure 1). Such swapping can be equally noticed in dimers of single-domain MMBLs and tandem MMBLs from plants, though the relative orientation of each of the lectin domains in LlpAs may differ compared to (dimeric and tandem) MMBLs from plants (discussed in more detail in Ghequire et al., 2013b; McCaughey et al., 2014) (Figure 1). Plant B-lectin modules contain three carbohydrate-binding motifs with a consensus sequence QxDxNxVxY (Ghequire et al., 2012b; Wu and Bao, 2013), most of which are usually active, whereas these lectin motifs are often harder to discern in LlpAs (Ghequire et al., 2014). Motif conservation is mainly present in LlpA's carboxy-terminal lectin domain. Sugar-binding properties are indeed linked to the latter domain, since intact QxDxNxVxY lectin motifs proved necessary to obtain a fully active bacteriocin. Nevertheless the affinity of LlpA_{BW11M1} for D-mannose and oligomannosides was observed to be quite low (Ghequire et al., 2013b), raising doubts about its biological significance. This issue was resolved after elucidating the structure of a lectin-like bacteriocin from cystic fibrosis isolate *P. aeruginosa* C1433, pyocin L1, that targets *P. aeruginosa* model strain PAO1 (McCaughy et al., 2014) (Figure 1). This L-type bacteriocin adopts a similar fold as LlpA_{BW11M1}, but rather than binding D-mannose, pyocin L1 displays a much higher affinity for D-rhamnose, a 6-deoxy-D-mannose that is omnipresent in the common polysaccharide antigen (CPA) of *P. aeruginosa* (Lam et al., 2011). Two lectin motifs in the carboxy-terminal domain of pyocin L1 were ultimately shown to assist in this D-rhamnose binding, which equally appeared to be the case for LlpA_{BW11M1} (McCaughy et al., 2014). Following crystal soaks of LlpA_{BW11M1} with D-mannose, it was initially unclear whether one or two lectin motifs contributed to the protein's sugar-binding properties (Ghequire et al., 2013b). More recently a third LlpA, LlpA_{Pf-5} from *P. protegens* Pf-5, was equally found to depend on CPA for cellular killing (Ghequire et al., 2018b), suggesting that CPA likely is a common receptor among *Pseudomonas* LlpAs for target cell attachment. Carbohydrates present in O-antigen-specific lipopolysaccharide (LPS) are also used for cell surface docking by the tail fibers of R-type tailocins (Köhler et al., 2010; Kocincová and Lam, 2013; Ghequire et al., 2015; Buth et al., 2018), and some modular pyocins equally bind to CPA for target anchoring (McCaughy et al., 2016a). From a bacteriocin producer point of view, such targeting of LPS is a very attractive and effective strategy, since competitors become more susceptible to killing by detergents and permeable to antibiotics when attempting to escape from bacteriocin killing by LPS assembly loss (Ruiz et al., 2006; Falchi et al., 2018).

TABLE 1 | Overview of functionally characterized proteobacterial LlpA bacteriocins.

Species	Strain	LlpA name	Size (AA)	Locus tag	Target spectrum	Reference
<i>Burkholderia cenocepacia</i>	AU1054	LlpA1 _{AU1054} (or, LlpA _{Bcen_1091})	277 ^a	Bcen_1091	Select bacteria belonging to <i>Burkholderia cepacia</i> complex, including several <i>B. ambifaria</i> strains	Ghequire et al., 2013a
	TAtI-371	LlpA88	277 ^a	SAMN05443026_0088	Same target spectrum as LlpA1 _{AU1054}	Rojas-Rojas et al., 2018
<i>P. aeruginosa</i>	C1433	PyoL1	256	CDG56231	Select <i>P. aeruginosa</i> strains	Ghequire et al., 2014; McCaughey et al., 2014
<i>P. aeruginosa</i>	62	PyoL2	256	P997_04049	Select <i>P. aeruginosa</i> strains	Ghequire et al., 2014
<i>P. aeruginosa</i>	BWHPSA007	PyoL3	269 ^a	Q020_03570	Select <i>P. aeruginosa</i> strains	Ghequire et al., 2014
<i>P. mosselii</i>	BW11M1	LlpA _{BW11M1} (or, LlpA _{BW})	276	AXZ07_RS10630	Mainly <i>P. syringae</i> (select strains), also some <i>P. fluorescens</i> and <i>P. putida</i> isolates	Parret et al., 2003; Ghequire et al., 2012a; McCaughey et al., 2014
<i>P. protegens</i>	Pf-5	LlpA1 (or, LlpA1 _{Pf-5})	280	PFL_1229	Mainly isolates belonging to the <i>P. fluorescens</i> species group	Parret et al., 2005; Ghequire et al., 2012a
		LlpA2 (or, LlpA2 _{Pf-5})	280	PFL_2127	Same target spectrum as LlpA1 _{Pf-5}	Parret et al., 2005
<i>P. syringae</i> pv. <i>syringae</i>	642	LlpA _{Pss642}	290	COO_RS0109380	Select strains belonging to species groups of <i>P. aeruginosa</i> , <i>P. fluorescens</i> , <i>P. putida</i> , <i>P. syringae</i>	Ghequire et al., 2012a
<i>Xanthomonas citri</i> pv. <i>malvacearum</i>	LMG 761	LlpA _{Xcm761}	248 ^a	XAC0868	Select <i>Xanthomonas</i> strains	Ghequire et al., 2012a

^asize of the mature protein after cleavage of predicted Sec-dependent signal peptide.

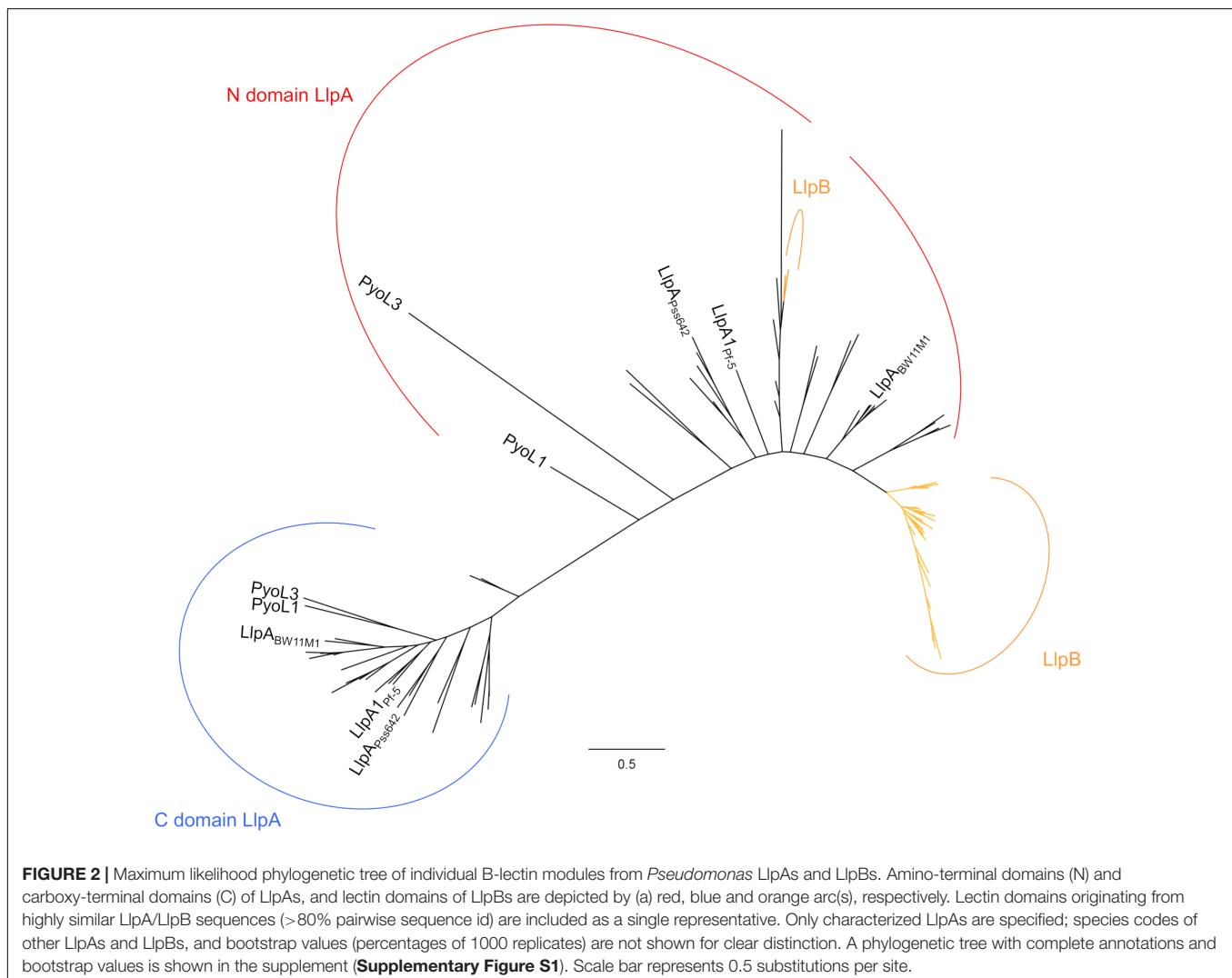


Via activity/specificity assays using engineered LlpA chimeras, it was further found that the amino-terminal lectin domain of LlpA accounts for target selection, regardless of the LPS-binding carboxy-terminal lectin module being present (Ghequire et al., 2013b). Phylogenetic analysis of individual lectin domains of characterized and putative LlpAs shows a clear clustering of each of the domains (**Figure 2** and **Supplementary Figure S1**) (Ghequire et al., 2012b, 2014), which is in support of this domain-function dichotomy. Comparatively higher sequence conservation of the carboxy-terminal lectin domains [48% pairwise amino acid (AA) sequence identity (seq id)] results in a tighter clustering and advocates a more general function of the C-terminal lectin domain with regard to CPA binding (see above). Conversely, the amino-terminal domains have diverged more (~39% pairwise AA seq id), and apparently evolved to hit different subsets of pseudomonads. Highly similar lectin-like pyocins PyoL1 and PyoL2 (86% pairwise AA seq id) display a divergent target spectrum, and differential bacteriocin residues primarily cluster at one patch of their amino-terminal lectin domains (Ghequire et al., 2014), which

again supports the target-selective function of the amino-terminal lectin domain.

VANDALIZING AN ESSENTIAL OUTER-MEMBRANE PROTEIN ASSEMBLY MACHINERY

Mutants of *P. aeruginosa* PAO1 defective in CPA biosynthesis do not become fully resistant to pyocin L1 killing (McCaughey et al., 2014). This suggests that a second receptor for L-type bacteriocin bactericidal action has to exist. Since CPA binding on its own cannot account for a cell death mechanism and given the lack of a distinct toxin domain, as present in modular bacteriocins, this was also expected. Recently, it was found that spontaneous mutants of *P. fluorescens* Pf0-1 become resistant to LlpA_{1Pf-5} killing when mutated in a surface-exposed loop of outer membrane protein (OMP) insertase BamA (Ghequire et al., 2018b). This essential protein consists of five polypeptide transport-associated (POTRA) domains and a

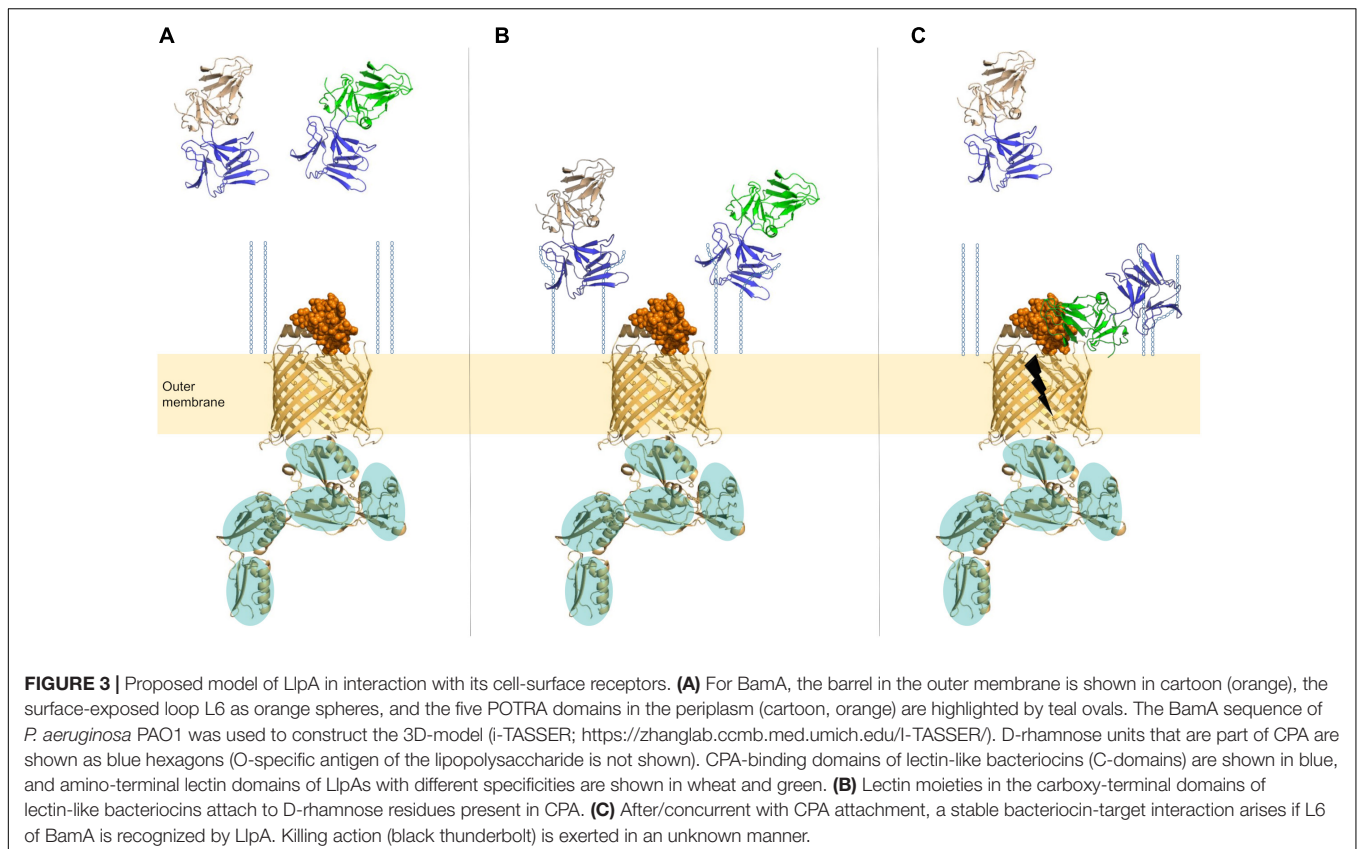


carboxy-terminal β -barrel in the outer membrane, and interacts with lipoproteins BamB, BamC, BamD and BamE to constitute the BAM complex (Leyton et al., 2015; Noinaj et al., 2017). This machinery acts as the main catalyst for the insertion of new OMPs in the outer-membrane layer, with a key function attributed to BamA to partially unzip and create an open gate for a nascent OMP (Noinaj et al., 2014). The surface-exposed side of BamA is covered by three large loops (loops 4, 6, and 7) forming a dome-like structure (Ni et al., 2014). Mutations (single nucleotide polymorphisms, small in-frame deletions) in loop 6 (L6), allowed escape from LlpA_{1Pf-5} killing. In a similar experimental set-up using the reference strain PAO1, mutations in this same BamA loop were detected for spontaneous mutants resistant to PyoL1 killing (Ghequire et al., 2018b).

Depending on the *Pseudomonas* species group of interest, conservation in BamA may be moderate to very high. In *P. aeruginosa* in particular, BamA sequence conservation is nearly perfect, except for surface-exposed L6, the same loop in which mutations yielding bacteriocin resistance were detected. Furthermore, only a limited set of L6 sequence variants seem to exist in nature, that vary depending on the *Pseudomonas* species (group). Interestingly, a strong correlation between L6 sequence type and susceptibility to a certain LlpA was demonstrated for pyocins L1 and L2, and LlpA_{BW11M1} (Ghequire et al., 2018b). BamA indeed appears to be the key selectivity partner of LlpAs, since susceptibility to a particular LlpA is conferred

upon an otherwise LlpA-resistant *Pseudomonas* by expression of a BamA with the corresponding LlpA-compatible L6 loop. LlpA producers escape from self-inhibition by expressing a BamA equipped with a different L6 than the one they are targeting (Ghequire et al., 2018b), an elegant mechanism preventing kin killing without the need for an immunity protein. Whereas modular bacteriocins typically display species-specific antagonism (Barreteau et al., 2009; Ghequire and De Mot, 2014; Godino et al., 2015; Ghequire et al., 2017a; Hockett et al., 2017), lectin-like bacteriocins (may) show genus-specific killing, which is explained by the occurrence of certain L6 sequence types in different *Pseudomonas* species (Ghequire et al., 2012a, 2018b). Taken together, the variation in surface-exposed loops of BamA proteins explains why different LlpAs target different subsets of pseudomonads. An interesting observation is that some effectors of contact-dependent growth inhibition (CDI) systems – polymorphic toxins released via a Type V secretion system mediating cell death by cell-to-cell contact (Willett et al., 2015; Chassaing and Cascales, 2018) – equally take advantage of BamA as a surface receptor (Aoki et al., 2008). As is the case for LlpAs, sequence polymorphism of BamA was found to determine susceptibility, although depending on two surface-exposed loops, L6 and L7 (Ruhe et al., 2013).

At this point, the molecular details of the interaction between LlpA and (L6 of) BamA remain elusive, and therefore it is currently unclear how exactly LlpA impairs the BAM function.



It should be underlined that BamA is a dynamic protein given its role in OMP assembly: the integration of (a) new β -sheet(s) of a nascent OMP requires a destabilized and structurally rearranged seam of the BamA β -barrel (Doerner and Sousa, 2017). Conceivably, LlpA may impair the function of this lateral gate/exit pore located at the outer-membrane-periplasm interface by hindering structural reorganization, subsequently leading to a (lethal) downstream stress response (Figure 3). A role for the carboxy-terminal extension of LlpAs may also be anticipated since this stretch contains a number of hydrophobic residues that may mimic an elongated β -sheet (Figure 1) (Ghequire et al., 2013b; McCaughey et al., 2014). These residues may occupy BamA's lateral pore, ultimately locking its function. LlpA's rigid nature and the targeting of an essential protein strongly advocate a killing-upon-contact mechanism, in contrast to the killing-following-uptake of the more flexible S-type pyocins; the latter need partial unfolding to penetrate target cells via the β -barrel of TonB-dependent transporters and deliver their toxin load (White et al., 2017). A second unanswered issue concerns the observation that some (mainly fluorescent) *Pseudomonas* are killed by different LlpAs (Ghequire et al., 2012a). Interestingly, a second *bamA* can be retrieved in the genomes of some *Pseudomonas*, often (but not exclusively) belonging to the *P. fluorescens* group (Heinz and Lithgow, 2014). The physiological role of this BamA paralog remains undisclosed. The presence of a different L6 sequence type in this second BamA may explain the susceptibility of some *Pseudomonas* to different LlpAs, though this is subject to experimental verification.

LlpA: A PROMISING PROTEIN ANTIBIOTIC FOR BACTERIOCIN COCKTAILS?

Their high potency, biodegradability and selective action makes bacteriocins a promising drug lead (Behrens et al., 2017; Ghequire and De Mot, 2018). Envisaging their therapeutic use, several mid-sized pyocins – including lectin-like bacteriocins – have been tested in a murine model of acute lung infection, and their high efficacy was demonstrated (McCaughy et al., 2016b). Interestingly, lectin-like pyocins are also amenable to large-scale production in plants (Paškevičius et al., 2017). The narrow spectrum of activity of bacteriocins nevertheless requires that several of these protein antibiotics are combined in a cocktail to guarantee coverage of the species diversity (Behrens et al., 2017). At this point it remains to be assessed (i) whether L-type pyocins could constitute a stable ingredient for such a cocktail, and (ii) whether the (low) mutation rate of L6 in BamA resulting in bacteriocin resistance (Ghequire et al., 2018b) is physiologically relevant, and whether this has any effect on bacterial fitness. Given the essential role of the BAM complex, several other therapeutic strategies are currently explored to interfere with its function, such as via monoclonal antibodies (Storek et al., 2018), peptides (Mori et al., 2012; Hagan et al., 2015) or peptidomimetic antibiotics (Urfer et al., 2016).

PATCHY DISTRIBUTION OF LECTIN-LIKE BACTERIOCIN GENES

Lectin-like bacteriocin genes can be retrieved in genomes of virtually all *Pseudomonas* species, although sequence identity between LlpA homologs may be as low as 23% (pairwise AA identity among LlpAs), even if they originate from the same species (Supplementary Figure S2). The sole notable exception is *P. aeruginosa* in which L pyocins display high sequence similarity. Pyocins L1 and L2 share 86% amino acid sequence identity but exhibit a different target spectrum, coupled to the targeting of different BamA subsets (see above). Homology searches reveal the occurrence of a putative pyocin L4 in a small set of *P. aeruginosa* strains (e.g., in *P. aeruginosa* env100) that resembles pyocins L1 and L2 well (82 and 91% AA sequence identity, respectively). Possibly, pyocin L4 targets yet another L6 sequence type of BamA. On the contrary, pyocin L3 is much more diverged (~26% sequence identity to L1/L2/L4). Overall, L pyocins can be retrieved in ~4% of the assembled *P. aeruginosa* genomes, and a similar percentage (~5%) of strains from other *Pseudomonas* species carry an *llpA* bacteriocin gene in their genome. LlpAs appear to occur more frequently in plant-associated and soil-dwelling *Pseudomonas*, which may reflect a possible ancestral relationship with MMBL lectins from monocot plants. With few exceptions, *Pseudomonas* isolates only host one L-type bacteriocin gene in their genome, if any (Ghequire and De Mot, 2014). The latter observation strongly contrasts with modular S-type bacteriocins for which usually multiple representatives, albeit with different receptor-binding/toxin domain combinations, are present within a single *Pseudomonas* genome (Loper et al., 2012; Ghequire and De Mot, 2014; Sharp et al., 2017; Beaton et al., 2018). Bacteriocin sequences from strains encoding two LlpAs are usually dissimilar (30–52% pairwise AA id), arguing against a duplication event.

Genes encoding (putative) L-type bacteriocins have been recruited to a variety of loci, but are often present in tailocin and prophage clusters (Ghequire et al., 2015; Wang et al., 2016). As cargo genes, these *llpA* genes may spread via horizontal gene transfer. Lectin-like bacteriocin genes are hallmarked by a lower than host-average G + C content, a feature they share with modular bacteriocins (Mavrodi et al., 2009; Loper et al., 2012; Dingemans et al., 2016; Ghequire et al., 2017a,b; Ghequire and Öztürk, 2018). In general no clear correlation between LlpA phylogeny and *Pseudomonas* taxonomy can be made (except for *P. aeruginosa*, Supplementary Figure S2). Together with the observation that LlpA action may surpass species boundaries (Ghequire et al., 2012a), this further complicates the introduction of a thoughtful (re)classification of L-type bacteriocins. This lack of phylogeny-taxonomy correlation is reflected in the spectrum of BamA L6 variants that is not confined to species boundaries.

In addition to *Pseudomonas*, LlpA-like bacteriocins have also been described in another γ -proteobacterial genus, *Xanthomonas* (Ghequire et al., 2012a) and in the β -proteobacterium *Burkholderia* (Ghequire et al., 2013a; Rojas-Rojas et al., 2018) (Table 1), and putative L-type bacteriocins can also be detected in (select) genomes of a number of other genera, such as *Chromobacterium* and *Caballeronia* (both β -proteobacteria),

though it remains unclear whether these proteins are bactericidal molecules as well. It also remains to be investigated whether LPS and BamA equally serve as receptors in susceptible strains of *Xanthomonas* and *Burkholderia*. D-rhamnose was previously detected as a constituent in lipopolysaccharides of *Xanthomonas* (Molinaro et al., 2003) and *Burkholderia* (Vinion-Dubiel and Goldberg, 2003; Karapetyan et al., 2006), although sugar-binding affinity for another oligosaccharide cannot be excluded a priori. Also in genomes of δ -proteobacteria (such as *Chondromyces*), Bacteroidetes (*Chryseobacterium*, *Spirosoma*, etc.) and diverse actinobacteria (*Arthrobacter*, *Pseudonocardia*, etc.), genes encoding a tandem MMBL protein can be retrieved. Furthermore, MMBL domains are often fused to one or more distinct domains, as highlighted earlier (Ghequire et al., 2012b). Overall, lectin-like bacteriocins seem confined to rather limited bacterial genera, thus representing a highly specialized tool, particularly apt for interbacterial warfare in plant-associated niches.

LlpB: A MINIMIZED LECTIN-LIKE BACTERIOCIN?

In *Pseudomonas* genomes, a second type of B-lectin proteins can be discerned (Ghequire et al., 2012b) (**Supplementary Table S1**). These proteins, tentatively termed LlpBs, only host a single lectin domain, equally followed by a carboxy-terminal extension as is the case for LlpAs (size of ~166 AA for LlpBs vs. ~278 AA for LlpAs). The lectin domains of most of these LlpBs cluster on a distinct branch associated with the LlpA amino-terminal domain clade (**Figure 2** and **Supplementary Figure S1**). Characteristic to B-lectins, these LlpBs consistently host a tryptophan triad and three potential sugar-binding motifs, one of which is well conserved and may be involved in carbohydrate binding. Antagonistic tests with select recombinant LlpB demonstrate that these proteins indeed display bactericidal action (Ghequire, 2013). Possibly the LPS-binding and target-selective function of LlpBs are condensed in a single lectin domain. One question arising is whether *llpA* genes evolved from *llpB* genes, or vice versa, or whether *llpA* and *llpB* genes were acquired independently. Overall, *llpB* genes can be retrieved in a variety of *Pseudomonas* species, but they appear to be absent from *P. aeruginosa* genomes. Similar to *llpA* genes, *llpB* genes are also present as cargos in tailocin or prophage clusters, for example in *Pseudomonas libanensis* DSM 17149 and *P. fluorescens* FF9, respectively, although this coupling appears to be much rarer.

SECRETION WITH A SACRIFICE?

With the exception of a small subset of L-type pyocins (pyocin L3 and highly similar sequences) and *Burkholderia/Xanthomonas* representatives (Ghequire et al., 2014), LlpAs are not preceded by a Sec-dependent signal sequence motif to facilitate their secretion from producer cells. The same is true for S-type modular bacteriocins in *Pseudomonas* (Ghequire and De Mot,

2014), raising the question how these proteins can be released from producer cells? Group A colicin genes – encoding modular bacteriocins from *Escherichia coli* – are joined by a lysis module, typically located downstream of the bacteriocin gene, and these lipoprotein-encoding genes are co-expressed along with the colicins. For group B colicins, as is the case for *Pseudomonas* bacteriocins, a lysis gene is lacking (Cascales et al., 2007). However, for these colicins in particular it was found that the cellular release may be mediated by a prophage lysis module encoded elsewhere in the genome (Nedialkova et al., 2016; van Raay and Kerr, 2016). Conceivably, a similar strategy may be followed by LlpAs and other *Pseudomonas* bacteriocins as well, although this remains to be explored. The observation that L-type and other bacteriocin genes can often be retrieved within or in close proximity of tailocin and prophage gene clusters may facilitate co-expression of bacteriocin genes and lysis modules and co-inheritance, suggestive of such lysis “piggybacking” (Mavrodi et al., 2009; Loper et al., 2012; Ghequire et al., 2015, 2018a; Wang et al., 2016). Regardless of the mechanism used, the expression of lysis genes poses a burden on producer cells. For this reason, it is expected that only part of a *Pseudomonas* cell population secretes lectin-like bacteriocins, as demonstrated in *E. coli* for a colicin A/E2/E7 competition model (Bayramoglu et al., 2017).

STRESS-TRIGGERED RETALIATION?

The environmental cues controlling expression of L-type bacteriocins remain poorly understood to date. For LlpA from *P. mosselii* BW11M1 (Parret et al., 2003), and LlpA_{Pf-5} and LlpA_{2Pf-5} from *P. protegens* Pf-5 (Parret et al., 2005), constitutive expression was observed, though it should be emphasized that bacteriocin-expression conditions may vary from strain to strain. Following exposure to UV light, LlpA_{BW11M1} expression is significantly enhanced. Similar observations have been made for several other (*Pseudomonas*) bacteriocins as well (Ghazaryan et al., 2014; Godino et al., 2015; Hockett and Baltrus, 2017; Turano et al., 2017), and such DNA-damaging conditions (e.g., via mitomycin C treatments) constitute a common strategy to induce bacteriocin overproduction. Screening of a *P. mosselii* BW11M1 transposon mutant library revealed that LlpA expression is reduced in a *recA* and *spoT* mutant background, confirming the UV-light-induced expression of LlpA (de los Santos et al., 2005). Following DNA-damaging treatment, RecA is activated leading to a stress response, which includes the activation of S-type pyocin expression in *P. aeruginosa* (Michel-Briand and Baysse, 2002; Ghequire and De Mot, 2014). Therefore, L-type bacteriocin expression may depend (in part) on a general regulatory mechanism triggering bacteriocin expression in pseudomonads. Similarly, colicins also depend on a SOS system to initiate their expression, mediated by LexA. This protein controls two overlapping SOS boxes, which prevents untimely colicin expression and cell lysis (Gillor et al., 2008; Žgur-Bertok, 2012; Fornelos et al., 2016).

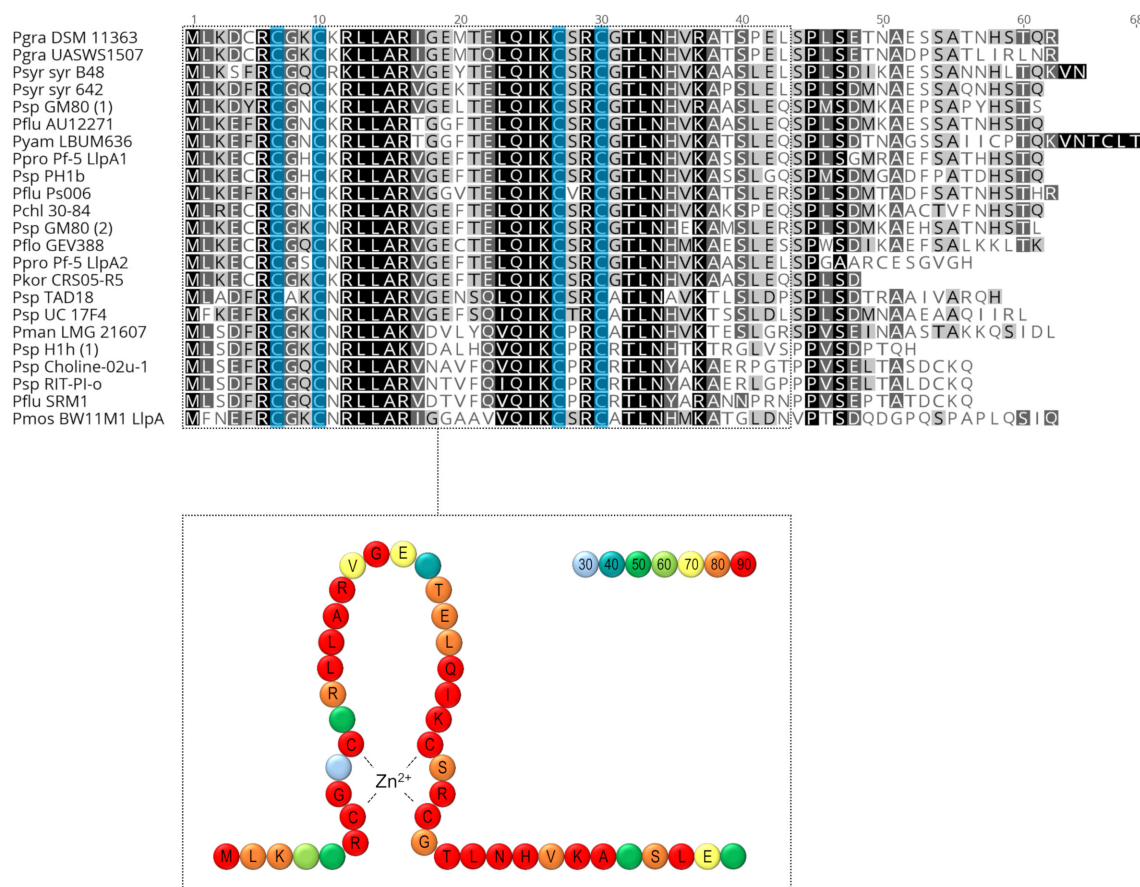


FIGURE 4 | Multiple sequence alignment of *Pseudomonas* Com proteins (<90% pairwise AA sequence identity), encoded by genes preceding *lfpA* genes.

Differential shading reflects the sequence conservation. The conserved zinc-coordinating cysteine residues are highlighted in blue. In case two LlpAs are present in a single strain, preceding Com proteins (if present) are specified with (1) and (2). The zinc-finger domains (PF10122) of these Com proteins are marked by a dotted box and a schematic representation of the sequence conservation within this domain is shown under the alignment. Amino acids are depicted by beads and colored according to the (weighted) degree (%) of sequence conservation (legend) (AA sequences of all *lfpA*-preceding Com proteins were included). In case sequence conservation is 70% or higher, the corresponding amino acid is identified inside the dot. The backbone of the scheme corresponds to the Com protein of the phage Mu. Pchl, *Pseudomonas chlororaphis*; Pflu, *Pseudomonas fluorescens*; Pgra, *Pseudomonas graminis*; Pkor, *Pseudomonas koreensis*; Pman, *Pseudomonas mandelii*; Pmos, *Pseudomonas mosselii*; Ppro, *Pseudomonas protegens*; Psp, *Pseudomonas* sp.; Psyr syr, *Pseudomonas syringae* pv. *syringae*; Pyam, *Pseudomonas yamanorum*.

With the exception of *P. aeruginosa*, a large majority of L-type bacteriocin genes (~90%) are preceded by a short gene encoding a putative zinc-finger-like protein (PF10122) (Ghequire et al., 2015), which is often not annotated in *Pseudomonas* genomes. Hallmarked by four conserved cysteine residues, this ~60-AA protein is homologous to Com, a translational activator protein of bacteriophage Mu that initiates expression of the *mom* operon (Hattman et al., 1991; Witkowski et al., 1995). The amino-terminal region, which includes the coordinating cysteine residues, is largely conserved, whereas the Com tail may vary significantly in length (Figure 4). An interesting observation is that non-L-type bacteriocin genes present as tailocin cargos in pseudomonads may equally be preceded by such a *com*-like gene (Ghequire et al., 2015). Furthermore, in some strains that is also the case for the lytic enzyme that is part of the tailocin lysis cassette. *Com*-linked genes also appear in other *Pseudomonas* contexts, for instance, in

P. syringae this gene is (often) linked to glycosyl hydrolase genes, including levansucrase homologs (Srivastava et al., 2012). The more general (regulatory) role of this Com protein remains to be explored.

CONCLUDING REMARKS

Following the identification of the first lectin-like bacteriocin with a tandem lectin module architecture in a *P. mosselii* isolate, multiple LlpA representatives have been studied in a variety *Pseudomonas* species and other genera, largely facilitated by an ongoing release of genome sequencing data. The structure of LlpA, and the subsequent identification of CPA and BamA in particular as target receptors, are indicative of a novel killing mechanism that does not require protein import as observed for modular S-type bacteriocins. Undoubtedly a careful

assessment of the interaction between LlpA and BamA will shed further light on the interference process exerted by these bacteriocins. Future research also needs to clarify the regulatory features for expression of this unusual group of bacteriocins, and elucidate how their secretion is accomplished. Given that the B-lectin module is present in proteins with different domain organizations, other lectin-like bacteriocin types likely exist.

AUTHOR CONTRIBUTIONS

MG, BÖ, and RDM wrote the manuscript. All authors revised and approved the manuscript.

REFERENCES

- Aoki, S. K., Malinverni, J. C., Jacoby, K., Thomas, B., Pamma, R., Trinh, B. N., et al. (2008). Contact-dependent growth inhibition requires the essential outer membrane protein BamA (YaeT) as the receptor and the inner membrane transport protein AcrB. *Mol. Microbiol.* 70, 323–340. doi: 10.1111/j.1365-2958.2008.06404.x
- Arasu, A., Kumaresan, V., Palanisamy, R., Arasu, M. V., Al-Dhabi, N. A., Ganesh, M. R., et al. (2017). Bacterial membrane binding and pore formation abilities of carbohydrate recognition domain of fish lectin. *Dev. Comp. Immunol.* 67, 202–212. doi: 10.1016/j.dci.2016.10.001
- Azevedo, A. C., Bento, C. B., Ruiz, J. C., Queiroz, M. V., and Mantovani, H. C. (2015). Distribution and genetic diversity of bacteriocin gene clusters in rumen microbial genomes. *Appl. Environ. Microbiol.* 81, 7290–7304. doi: 10.1128/AEM.01223-15
- Barre, A., Van Damme, E. J., Peumans, W. J., and Rougé, P. (1999). Homology modelling of the core domain of the endogenous lectin comitin: structural basis for its mannose-binding specificity. *Plant Mol. Biol.* 39, 969–978. doi: 10.1023/A:1006133527621
- Barreteau, H., Bouhss, A., Fourgeaud, M., Mainardi, J. L., Touzé, T., Gérard, F., et al. (2009). Human- and plant-pathogenic *Pseudomonas* species produce bacteriocins exhibiting colicin M-like hydrolase activity towards peptidoglycan precursors. *J. Bacteriol.* 191, 3657–3664. doi: 10.1128/JB.01824-08
- Bayramoglu, B., Toubiana, D., van Vliet, S., Inglis, R. F., Shnerb, N., and Gillor, O. (2017). Bet-hedging in bacteriocin producing *Escherichia coli* populations: the single cell perspective. *Sci. Rep.* 7:42068. doi: 10.1038/srep42068
- Beaton, A., Lood, C., Cunningham-Oakes, E., MacFadyen, A., Mullins, A. J., Bestaw, W. E., et al. (2018). Community-led comparative genomic and phenotypic analysis of the aquaculture pathogen *Pseudomonas baetica* a390T sequenced by Ion semiconductor and Nanopore technologies. *FEMS Microbiol. Lett.* 365:fny069. doi: 10.1093/femsle/fny069
- Behrens, H. M., Six, A., Walker, D., and Kleanthous, C. (2017). The therapeutic potential of bacteriocins as protein antibiotics. *Emerg. Top. Life Sci.* 1, 65–74. doi: 10.1042/ETLS20160016
- Buth, S. A., Shneider, M. M., Scholl, D., and Leiman, P. G. (2018). Structure and analysis of R1 and R2 pyocin receptor-binding fibers. *Viruses* 10:E427. doi: 10.3390/v10080427
- Cascales, E., Buchanan, S. K., Duché, D., Kleanthous, C., Llobès, R., Postle, K., et al. (2007). Colicin biology. *Microbiol. Mol. Biol. Rev.* 71, 158–229. doi: 10.1128/MMBR.00036-06
- Chassaing, B., and Cascales, E. (2018). Antibacterial weapons: targeted destruction in the microbiota. *Trends Microbiol.* 26, 329–338. doi: 10.1016/j.tim.2018.01.006
- Chen, J., Stevenson, D. M., and Weimer, P. J. (2004). Albusin B, a bacteriocin from the ruminal bacterium *Ruminococcus albus* 7 that inhibits growth of *Ruminococcus flavefaciens*. *Appl. Environ. Microbiol.* 70, 3167–3170. doi: 10.1128/AEM.70.5.3167-3170.2004
- de los Santos, P. E., Parret, A. H., and De Mot, R. (2005). Stress-related *Pseudomonas* genes involved in production of bacteriocin LlpA. *FEMS Microbiol. Lett.* 244, 243–250. doi: 10.1016/j.femsle.2005.01.049

FUNDING

MG is a postdoctoral fellow from FWO Vlaanderen (12M4618N). This work was supported by the FWO Vlaanderen under Grants 1523116N, 1525618N, and 1529718N (to MG). The funders had no role in study design, data collection and interpretation, or the decision to submit the work for publication.

SUPPLEMENTARY MATERIAL

The Supplementary Material for this article can be found online at: <https://www.frontiersin.org/articles/10.3389/fmicb.2018.02706/full#supplementary-material>

- de Santana Evangelista, K., Andrich, F., Figueiredo de Rezende, F., Niland, S., Cordeiro, M. N., Horlacher, T., et al. (2009). Plumieribetin, a fish lectin homologous to mannose-binding B-type lectins, inhibits the collagen-binding alpha1beta1 integrin. *J. Biol. Chem.* 284, 34747–34759. doi: 10.1074/jbc.M109.002873
- Dingemans, J., Ghequire, M. G., Craggs, M., De Mot, R., and Cornelis, P. (2016). Identification and functional analysis of a bacteriocin, pyocin S6, with ribonuclease activity from a *Pseudomonas aeruginosa* cystic fibrosis clinical isolate. *Microbiologyopen* 5, 413–423. doi: 10.1002/mbo3.339
- Doerner, P. A., and Sousa, M. C. (2017). Extreme dynamics in the BamA β -Barrel seam. *Biochemistry* 56, 3142–3149. doi: 10.1021/acs.biochem.7b00281
- Dorosky, R. J., Yu, J. M., Pierson, L. S. III, and Pierson, E. A. (2017). *Pseudomonas chlororaphis* produces two distinct R-tailocins that contribute to bacterial competition in biofilms and on roots. *Appl. Environ. Microbiol.* 83:e00706-17. doi: 10.1128/AEM.00706-17
- Falchi, F. A., Maccagni, E. A., Puccio, S., Peano, C., De Castro, C., Palmigiano, A., et al. (2018). Mutation and suppressor analysis of the essential lipopolysaccharide transport protein LptA reveals strategies to overcome severe outer membrane permeability defects in *Escherichia coli*. *J. Bacteriol.* 200:e00487-17. doi: 10.1128/JB.00487-17
- Fischer, S., Godino, A., Quesada, J. M., Cordero, P., Jofré, E., Mori, G., et al. (2012). Characterization of a phage-like pyocin from the plant growth-promoting rhizobacterium *Pseudomonas fluorescens* SF4c. *Microbiology* 158, 1493–1503. doi: 10.1099/mic.0.056002-0
- Fornelos, N., Browning, D. F., and Butala, M. (2016). The use and abuse of LexA by mobile genetic elements. *Trends Microbiol.* 24, 391–401. doi: 10.1016/j.tim.2016.02.009
- Fouquaert, E., Peumans, W. J., Gheysen, G., and Van Damme, E. J. (2011). Identical homologs of the *Galanthus nivalis* agglutinin in *Zea mays* and *Fusarium verticillioides*. *Plant Physiol. Biochem.* 49, 46–54. doi: 10.1016/j.plaphy.2010.09.018
- Gao, Z. M., Zheng, B., Wang, W. Y., Li, Q., and Yuan, Q. P. (2011). Cloning and functional characterization of a GNA-like lectin from Chinese Narcissus (*Narcissus tazetta* var. *Chinensis* Roem). *Physiol. Plant* 142, 193–204. doi: 10.1111/j.1399-3054.2011.01449.x
- Ghazaryan, L., Tonoyan, L., Ashhab, A. A., Soares, M. I., and Gillor, O. (2014). The role of stress in colicin regulation. *Arch. Microbiol.* 196, 753–764. doi: 10.1007/s00203-014-1017-8
- Ghequire, M. (2013). *Protein-mediated killing among bacteria: structure and function of prokaryotic MMBL lectins*. Ph.D. thesis, University of Leuven, Leuven, 127.
- Ghequire, M. G., and De Mot, R. (2014). Ribosomally encoded antibacterial proteins and peptides from *Pseudomonas*. *FEMS Microbiol. Rev.* 38, 523–568. doi: 10.1111/1574-6976.12079
- Ghequire, M. G., and De Mot, R. (2015). The tailocin tale: peeling off phage tails. *Trends Microbiol.* 23, 587–590. doi: 10.1016/j.tim.2015.07.011
- Ghequire, M. G., De Canck, E., Wattiau, P., Van Winge, I., Loris, R., Coenye, T., et al. (2013a). Antibacterial activity of a lectin-like *Burkholderia cenocepacia* protein. *Microbiologyopen* 2, 566–575. doi: 10.1002/mbo3.95

- Ghequire, M. G., Dillen, Y., Lambrichts, I., Proost, P., Wattiez, R., and De Mot, R. (2015). Different ancestries of R tailocins in rhizospheric *Pseudomonas* isolates. *Genome Biol. Evol.* 7, 2810–2828. doi: 10.1093/gbe/evv184
- Ghequire, M. G., Dingemans, J., Pirnay, J. P., De Vos, D., Cornelis, P., and De Mot, R. (2014). O serotype-independent susceptibility of *Pseudomonas aeruginosa* to lectin-like pyocins. *Microbiologyopen* 3, 875–884. doi: 10.1002/mbo3.210
- Ghequire, M. G., Garcia-Pino, A., Lebbe, E. K., Spaepen, S., Loris, R., and De Mot, R. (2013b). Structural determinants for activity and specificity of the bacterial toxin LlpA. *PLoS Pathog.* 9:e1003199. doi: 10.1371/journal.ppat.1003199
- Ghequire, M. G., Kemland, L., Anoz-Carbonell, E., Buchanan, S. K., and De Mot, R. (2017a). A natural chimeric *Pseudomonas* bacteriocin with novel pore-forming activity parasitizes the ferrichrome transporter. *mBio* 8:e01961-16. doi: 10.1128/mBio.01961-16
- Ghequire, M. G., Kemland, L., and De Mot, R. (2017b). Novel immunity proteins associated with colicin M-like bacteriocins exhibit promiscuous protection in *Pseudomonas*. *Front. Microbiol.* 8:93. doi: 10.3389/fmicb.2017.00093
- Ghequire, M. G., Li, W., Proost, P., Loris, R., and De Mot, R. (2012a). Plant lectin-like antibacterial proteins from phytopathogens *Pseudomonas syringae* and *Xanthomonas citri*. *Environ. Microbiol. Rep.* 4, 373–380. doi: 10.1111/j.1758-2229.2012.00331.x
- Ghequire, M. G., Loris, R., and De Mot, R. (2012b). MMBL proteins: from lectin to bacteriocin. *Biochem. Soc. Trans.* 40, 1553–1559. doi: 10.1042/BST20120170
- Ghequire, M. G., Swings, T., Michiels, J., Gross, H., and De Mot, R. (2016). Draft genome sequence of *Pseudomonas putida* BW11M1, a banana rhizosphere isolate with a diversified antimicrobial armamentarium. *Genome Announc.* 4:e00251-16. doi: 10.1128/genomeA.00251-16
- Ghequire, M. G. K., Buchanan, S. K., and De Mot, R. (2018a). The ColM Family, polymorphic toxins breaching the bacterial cell wall. *mBio* 9:e02267-17. doi: 10.1128/mBio.02267-17
- Ghequire, M. G. K., and De Mot, R. (2018). Turning over a new leaf: bacteriocins going green. *Trends Microbiol.* 26, 1–2. doi: 10.1016/j.tim.2017.11.001
- Ghequire, M. G. K., and Öztürk, B. (2018). A colicin M-type bacteriocin from *Pseudomonas aeruginosa* targeting the HxuC heme receptor requires a novel immunity partner. *Appl. Environ. Microbiol.* 84:e00716-18. doi: 10.1128/AEM.00716-18
- Ghequire, M. G. K., Swings, T., Michiels, J., Buchanan, S., and De Mot, R. (2018b). Hitting with a BAM: selective killing by lectin-like bacteriocins. *mBio* 9:e02138-17. doi: 10.1128/mBio.02138-17
- Ghoul, M., West, S. A., Johansen, H. K., Molin, S., Harrison, O. B., Maiden, M. C., et al. (2015). Bacteriocin-mediated competition in cystic fibrosis lung infections. *Proc. Biol. Sci.* 282:1814. doi: 10.1098/rpsb.2015.0972
- Gillor, O., Vriezen, J. A., and Riley, M. A. (2008). The role of SOS boxes in enteric bacteriocin regulation. *Microbiology* 154, 1783–1792. doi: 10.1099/mic.0.2007/016139-0
- Godino, A., Príncipe, A., and Fischer, S. (2015). A *ptsP* deficiency in PGPR *Pseudomonas fluorescens* SF39a affects bacteriocin production and bacterial fitness in the wheat rhizosphere. *Res. Microbiol.* 167, 178–189. doi: 10.1016/j.resmic.2015.12.003
- Hagan, C. L., Wzorek, J. S., and Kahne, D. (2015). Inhibition of the β -barrel assembly machine by a peptide that binds BamD. *Proc. Natl. Acad. Sci. U.S.A.* 112, 2011–2016. doi: 10.1073/pnas.1415955112
- Hattman, S., Newman, L., Murthy, H. M., and Nagaraja, V. (1991). Com, the phage Mu mom translational activator, is a zinc-binding protein that binds specifically to its cognate mRNA. *Proc. Natl. Acad. Sci. U.S.A.* 88, 10027–10031. doi: 10.1073/pnas.88.22.10027
- Heinz, E., and Lithgow, T. (2014). A comprehensive analysis of the Omp85/TpsB protein superfamily structural diversity, taxonomic occurrence, and evolution. *Front. Microbiol.* 5:370. doi: 10.3389/fmicb.2014.00370
- Hockett, K. L., and Baltrus, D. A. (2017). Use of the soft-agar overlay technique to screen for bacterially produced inhibitory compounds. *J. Vis. Exp.* 119:e55064. doi: 10.3791/55064
- Hockett, K. L., Clark, M., Scott, S., and Baltrus, D. A. (2017). Conditionally redundant bacteriocin targeting by *Pseudomonas syringae*. *bioRxiv* [Preprint]. doi: 10.1101/167593
- Hockett, K. L., Renner, T., and Baltrus, D. A. (2015). Independent co-option of a tailed bacteriophage into a killing complex in *Pseudomonas*. *mBio* 6:e00452. doi: 10.1128/mBio.00452-15
- Inglis, R. F., West, S., and Buckling, A. (2014). An experimental study of strong reciprocity in bacteria. *Biol. Lett.* 10:20131069. doi: 10.1098/rsbl.2013.1069
- Jamet, A., and Nassif, X. (2015). New Players in the toxin field: polymorphic toxin systems in bacteria. *mBio* 6:e00285-15. doi: 10.1128/mBio.00285-15
- Joshi, A., Grinter, R., Josts, I., Chen, S., Wojdyla, J. A., Lowe, E. D., et al. (2015). Structures of the ultra-high-affinity protein-protein complexes of pyocins S2 and AP41 and their cognate immunity proteins from *Pseudomonas aeruginosa*. *J. Mol. Biol.* 427, 2852–2866. doi: 10.1016/j.jmb.2015.07.014
- Karapetyan, G., Kaczynski, Z., Iacobellis, N. S., Evidente, A., and Holst, O. (2006). The structure of the O-specific polysaccharide of the lipopolysaccharide from *Burkholderia gladioli* pv. *agraricola*. *Carbohydr. Res.* 341, 930–934. doi: 10.1016/j.carres.2006.02.010
- Kocincová, D., and Lam, J. S. (2013). A deletion in the *wapB* promoter in many serotypes of *Pseudomonas aeruginosa* accounts for the lack of a terminal glucose residue in the core oligosaccharide and resistance to killing by R3-pyocin. *Mol. Microbiol.* 89, 464–478. doi: 10.1111/mmi.12289
- Köhler, T., Donner, V., and van Delden, C. (2010). Lipopolysaccharide as shield and receptor for R-pyocin-mediated killing in *Pseudomonas aeruginosa*. *J. Bacteriol.* 192, 1921–1928. doi: 10.1128/JB.01459-09
- Lam, J. S., Taylor, V. L., Islam, S. T., Hao, Y., and Kocincová, D. (2011). Genetic and functional diversity of *Pseudomonas aeruginosa* lipopolysaccharide. *Front. Microbiol.* 2:118. doi: 10.3389/fmicb.2011.00118
- Lavermicocca, P., Lonigro, S. L., Valerio, F., Evidente, A., and Visconti, A. (2002). Reduction of olive knot disease by a bacteriocin from *Pseudomonas syringae* pv. *ciccaronei*. *Appl. Environ. Microbiol.* 68, 1403–1407. doi: 10.1128/AEM.68.3.1403-1407.2002
- Leyton, D. L., Belousoff, M. J., and Lithgow, T. (2015). The β -barrel assembly machinery complex. *Methods Mol. Biol.* 1329, 1–16. doi: 10.1007/978-1-4939-2871-2_1
- Loper, J. E., Hassan, K. A., Mavrodi, D. V., Davis, E. W. II, Lim, C. K., Shaffer, B. T., et al. (2012). Comparative genomics of plant-associated *Pseudomonas* spp.: insights into diversity and inheritance of traits involved in multitrophic interactions. *PLoS Genet.* 8:e1002784. doi: 10.1371/journal.pgen.1002784
- Mavrodi, D. V., Loper, J. E., Paulsen, I. T., and Thomashow, L. S. (2009). Mobile genetic elements in the genome of the beneficial rhizobacterium *Pseudomonas fluorescens* Pf-5. *BMC Microbiol.* 9:8. doi: 10.1186/1471-2180-9-8
- McCaughey, L. C., Grinter, R., Josts, I., Roszak, A. W., Waløen, K. I., Cogdell, R. J., et al. (2014). Lectin-like bacteriocins from *Pseudomonas* spp. utilise D-rhamnose containing lipopolysaccharide as a cellular receptor. *PLoS Pathog.* 10:e1003898. doi: 10.1371/journal.ppat.1003898
- McCaughey, L. C., Josts, I., Grinter, R., White, P., Byron, O., Tucker, N. P., et al. (2016a). Discovery, characterisation and in vivo activity of pyocin SD2, a protein antibiotic from *Pseudomonas aeruginosa*. *Biochem. J.* 473, 2345–2358. doi: 10.1042/BCJ20160470
- McCaughey, L. C., Ritchie, N. D., Douce, G. R., Evans, T. J., and Walker, D. (2016b). Efficacy of species-specific protein antibiotics in a murine model of acute *Pseudomonas aeruginosa* lung infection. *Sci. Rep.* 6:30201. doi: 10.1038/srep30201
- Metelev, M., Serebryakova, M., Ghilarov, D., Zhao, Y., and Severinov, K. (2013). Structure of microcin B-like compounds produced by *Pseudomonas syringae* and species specificity of their antibacterial action. *J. Bacteriol.* 195, 4129–4137. doi: 10.1128/JB.00665-13
- Michel-Briand, Y., and Baysse, C. (2002). The pyocins of *Pseudomonas aeruginosa*. *Biochimie* 84, 499–510. doi: 10.1016/S0300-9084(02)01422-0
- Molinaro, A., Silipo, A., Lanzetta, R., Newman, M. A., Dow, J. M., and Parrilli, M. (2003). Structural elucidation of the O-chain of the lipopolysaccharide from *Xanthomonas campestris* strain 8004. *Carbohydr. Res.* 338, 277–281. doi: 10.1016/S0008-6215(02)00433-0
- Mori, N., Ishii, Y., Tateda, K., Kimura, S., Kouyama, Y., Inoko, H., et al. (2012). A peptide based on homologous sequences of the β -barrel assembly machinery

- component BamD potentiates antibiotic susceptibility of *Pseudomonas aeruginosa*. *J. Antimicrob. Chemother.* 67, 2173–2181. doi: 10.1093/jac/dks174
- Nedialkova, L. P., Sidstedt, M., Koepfel, M. B., Spriewald, S., Ring, D., Gerlach, R. G., et al. (2016). Temperate phages promote colicin-dependent fitness of *Salmonella enterica* serovar Typhimurium. *Environ. Microbiol.* 18, 1591–1603. doi: 10.1111/1462-2920.13077
- Ni, D., Wang, Y., Yang, X., Zhou, H., Hou, X., Cao, B., et al. (2014). Structural and functional analysis of the β -barrel domain of BamA from *Escherichia coli*. *FASEB J.* 28, 2677–2685. doi: 10.1096/fj.13-248450
- Noinaj, N., Gumbart, J. C., and Buchanan, S. K. (2017). The β -barrel assembly machinery in motion. *Nat. Rev. Microbiol.* 15, 197–204. doi: 10.1038/nrmicro.2016.191
- Noinaj, N., Kuszak, A. J., Balusek, C., Gumbart, J. C., and Buchanan, S. K. (2014). Lateral opening and exit pore formation are required for BamA function. *Structure* 22, 1055–1062. doi: 10.1016/j.str.2014.05.008
- Pang, Y. Z., Shen, G. A., Liao, Z. H., Yao, J. H., Fei, J., Sun, X. F., et al. (2003). Molecular cloning and characterization of a novel lectin gene from *Zephyranthes candida*. *DNA Seq.* 14, 163–167. doi: 10.1080/1042517031000089450
- Park, H. J., Jeong, J. M., Bae, J. S., Kim, J. W., An, C. M., Min, B. H., et al. (2016). Molecular cloning and expression analysis of a new lily-type lectin in the rock bream, *Oplegnathus fasciatus*. *Dev. Comp. Immunol.* 65, 25–30. doi: 10.1016/j.dci.2016.06.014
- Parret, A. H., Schoofs, G., Proost, P., and De Mot, R. (2003). Plant lectin-like bacteriocin from a rhizosphere-colonizing *Pseudomonas* isolate. *J. Bacteriol.* 185, 897–908. doi: 10.1128/JB.185.3.897-908.2003
- Parret, A. H., Temmerman, K., and De Mot, R. (2005). Novel lectin-like bacteriocins of biocontrol strain *Pseudomonas fluorescens* Pf-5. *Appl. Environ. Microbiol.* 71, 5197–5207. doi: 10.1128/AEM.71.9.5197-5207.2005
- Paškevičius, S., Starkevič, U., Misiūnas, A., Vitkauskienė, A., Gleba, Y., and Ražanskienė, A. (2017). Plant-expressed pyocins for control of *Pseudomonas aeruginosa*. *PLoS One* 12:e0185782. doi: 10.1371/journal.pone.0185782
- Pereira, P. R., Winter, H. C., Vericimo, M. A., Meagher, J. L., Stuckey, J. A., Goldstein, I. J., et al. (2015). Structural analysis and binding properties of isoforms of tarin, the GNA-related lectin from *Colocasia esculenta*. *Biochim. Biophys. Acta* 1854, 20–30. doi: 10.1016/j.bbapap.2014.10.013
- Príncipe, A., Fernandez, M., Torasso, M., Godino, A., and Fischer, S. (2018). Effectiveness of tailocins produced by *Pseudomonas fluorescens* SF4c in controlling the bacterial-spot disease in tomatoes caused by *Xanthomonas vesicatoria*. *Microbiol. Res.* 21, 94–102. doi: 10.1016/j.micres.2018.05.010
- Rasouliha, B. H., Ling, H., Ho, C. L., and Chang, M. W. (2013). A predicted immunity protein confers resistance to Pyocin S5 in a sensitive strain of *Pseudomonas aeruginosa*. *Chembiochem* 14, 2444–2446. doi: 10.1002/cbic.201300410
- Rojas-Rojas, F. U., Salazar-Gómez, A., Vargas-Díaz, M. E., Vásquez-Murrieta, M. S., Hirsch, A. M., De Mot, R., et al. (2018). Broad-spectrum antimicrobial activity by *Burkholderia cenocepacia* TATL-371, a strain isolated from the tomato rhizosphere. *Microbiology* 164, 1072–1086. doi: 10.1099/mic.0.000675
- Ruhe, Z. C., Wallace, A. B., Low, D. A., and Hayes, C. S. (2013). Receptor polymorphism restricts contact-dependent growth inhibition to members of the same species. *mBio* 4:e00480-13. doi: 10.1128/mBio.00480-13
- Ruiz, N., Kahne, D., and Silhavy, T. J. (2006). Advances in understanding bacterial outer-membrane biogenesis. *Nat. Rev. Microbiol.* 4, 57–66. doi: 10.1038/nrmicro1322
- Scholl, D. (2017). Phage tail-like bacteriocins. *Annu. Rev. Virol.* 4, 453–467. doi: 10.1146/annurev-virology-101416-041632
- Sharp, C., Bray, J., Housden, N. G., Maiden, M. C. J., and Kleanthous, C. (2017). Diversity and distribution of nuclease bacteriocins in bacterial genomes revealed using Hidden Markov Models. *PLoS Comput. Biol.* 13:e1005652. doi: 10.1371/journal.pcbi.1005652
- Shimokawa, M., Fukudome, A., Yamashita, R., Minami, Y., Yagi, F., Tateno, H., et al. (2012). Characterization and cloning of GNA-like lectin from the mushroom *Marasmius oreades*. *Glycoconj. J.* 29, 457–465. doi: 10.1007/s10719-012-9401-6
- Srivastava, A., Al-Karablieh, N., Khandekar, S., Sharmin, A., Weingart, H., and Ullrich, M. S. (2012). Genomic distribution and divergence of levansucrase-coding genes in *Pseudomonas syringae*. *Genes* 3, 115–137. doi: 10.3390/genes3010115
- Storek, K. M., Auerbach, M. R., Shi, H., Garcia, N. K., Sun, D., Nickerson, N. N., et al. (2018). Monoclonal antibody targeting the beta-barrel assembly machine of *Escherichia coli* is bactericidal. *Proc. Natl. Acad. Sci. U.S.A.* 115, 3692–3697. doi: 10.1073/pnas.1800043115
- Tsutsui, S., Tasumi, S., Suetake, H., and Suzuki, Y. (2003). Lectins homologous to those of monocotyledonous plants in the skin mucus and intestine of pufferfish, *Fugu rubripes*. *J. Biol. Chem.* 278, 20882–20889. doi: 10.1074/jbc.M301038200
- Turano, H., Gomes, F., Barros-Carvalho, G. A., Lopes, R., Cerdeira, L., Netto, L. E. S., et al. (2017). Tn6350, a novel transposon carrying pyocin S8 genes encoding a bacteriocin with activity against carbapenemase-producing *Pseudomonas aeruginosa*. *Antimicrob. Agents Chemother.* 61:e00100-17. doi: 10.1128/AAC.00100-17
- Urfer, M., Bogdanovic, J., Lo Monte, F., Moehle, K., Zerbe, K., Omasits, U., et al. (2016). A peptidomimetic antibiotic targets outer membrane proteins and disrupts selectively the outer membrane in *Escherichia coli*. *J. Biol. Chem.* 291, 1921–1932. doi: 10.1074/jbc.M115.691725
- Van Damme, E. J., Kaku, H., Perini, F., Goldstein, I. J., Peeters, B., Yagi, F., et al. (1991). Biosynthesis, primary structure and molecular cloning of snowdrop (*Galanthus nivalis* L.) lectin. *Eur. J. Biochem.* 202, 23–30. doi: 10.1111/j.1432-1033.1991.tb16339.x
- van Raay, K., and Kerr, B. (2016). Toxins go viral: phage-encoded lysis releases group B colicins. *Environ. Microbiol.* 18, 1308–1311. doi: 10.1111/1462-2920.13246
- Vinion-Dubiel, A. D., and Goldberg, J. B. (2003). Lipopolysaccharide of *Burkholderia cepacia* complex. *J. Endotoxin Res.* 9, 201–213. doi: 10.1179/096805103225001404
- Wang, D., Yu, J. M., Dorosky, R. J., Pierson, L. S. III, and Pierson, E. A. (2016). The phenazine 2-hydroxy-phenazine-1-carboxylic acid promotes extracellular DNA release and has broad transcriptomic consequences in *Pseudomonas chlororaphis* 30-84. *PLoS One* 11:e0148003. doi: 10.1371/journal.pone.0148003
- White, P., Joshi, A., Rassam, P., Housden, N. G., Kaminska, R., Goult, J. D., et al. (2017). Exploitation of an iron transporter for bacterial protein antibiotic import. *Proc. Natl. Acad. Sci. U.S.A.* 114, 12051–12056. doi: 10.1073/pnas.1713741114
- Wiens, M., Belikov, S. I., Kaluzhnaya, O. V., Krasko, A., Schröder, H. C., Perovic-Ottstadt, S., et al. (2006). Molecular control of serial module formation along the apical-basal axis in the sponge *Lubomirskia baicalensis*: silicateins, mannose-binding lectin and mago nashi. *Dev. Genes Evol.* 216, 229–242. doi: 10.1007/s00427-005-0047-2
- Willett, J. L., Ruhe, Z. C., Goulding, C. W., Low, D. A., and Hayes, C. S. (2015). Contact-dependent growth inhibition (CDI) and CdiB/CdiA two-partner secretion proteins. *J. Mol. Biol.* 427, 3754–3765. doi: 10.1016/j.jmb.2015.09.010
- Witkowski, R. T., Hattman, S., Newman, L., Clark, K., Tierney, D. L., Penner-Hahn, J., et al. (1995). The zinc coordination site of the bacteriophage Mu translational activator protein, com. *J. Mol. Biol.* 247, 753–764. doi: 10.1016/S0022-2836(05)80153-6
- Wright, L. M., Reynolds, C. D., Rizkallah, P. J., Allen, A. K., Van Damme, E. J., Donovan, M. J., et al. (2000). Structural characterisation of the native fetuin-binding protein *Scilla campanulata* agglutinin: a novel two-domain lectin. *FEBS Lett.* 468, 19–22. doi: 10.1016/S0014-5793(00)01109-1
- Wu, L., and Bao, J. K. (2013). Anti-tumor and anti-viral activities of *Galanthus nivalis* agglutinin (GNA)-related lectins. *Glycoconj. J.* 30, 269–279. doi: 10.1007/s10719-012-9440-z
- Žgur-Bertok, D. (2012). Regulating colicin synthesis to cope with stress and lethality of colicin production. *Biochem. Soc. Trans.* 40, 1507–1511. doi: 10.1042/BST20120184

Conflict of Interest Statement: The authors declare that the research was conducted in the absence of any commercial or financial relationships that could be construed as a potential conflict of interest.

Copyright © 2018 Ghequire, Öztürk and De Mot. This is an open-access article distributed under the terms of the Creative Commons Attribution License (CC BY). The use, distribution or reproduction in other forums is permitted, provided the original author(s) and the copyright owner(s) are credited and that the original publication in this journal is cited, in accordance with accepted academic practice. No use, distribution or reproduction is permitted which does not comply with these terms.



Zinc Blockade of SOS Response Inhibits Horizontal Transfer of Antibiotic Resistance Genes in Enteric Bacteria

John K. Crane^{1*}, Muhammad B. Cheema¹, Michael A. Olyer¹ and Mark D. Sutton²

¹ Division of Infectious Diseases, Department of Medicine, Jacobs School of Medicine and Biomedical Sciences, University at Buffalo, Buffalo, NY, United States, ² Department of Biochemistry, Jacobs School of Medicine and Biomedical Sciences, University at Buffalo, Buffalo, NY, United States

OPEN ACCESS

Edited by:

You-Hee Cho,
Cha University, South Korea

Reviewed by:

Chulhee Choi,
Chungnam National University,
South Korea
Yang Zhang,
University of Pennsylvania,
United States

*Correspondence:

John K. Crane
jcrane@buffalo.edu

Specialty section:

This article was submitted to
Clinical Microbiology,
a section of the journal
Frontiers in Cellular and Infection
Microbiology

Received: 01 August 2018

Accepted: 05 November 2018

Published: 21 November 2018

Citation:

Crane JK, Cheema MB, Olyer MA and
Sutton MD (2018) Zinc Blockade of
SOS Response Inhibits Horizontal
Transfer of Antibiotic Resistance
Genes in Enteric Bacteria.
Front. Cell. Infect. Microbiol. 8:410.
doi: 10.3389/fcimb.2018.00410

The SOS response is a conserved response to DNA damage that is found in Gram-negative and Gram-positive bacteria. When DNA damage is sustained and severe, activation of error-prone DNA polymerases can induce a higher mutation rate than is normally observed, which is called the SOS mutator phenotype or hypermutation. We previously showed that zinc blocked the hypermutation response induced by quinolone antibiotics and mitomycin C in *Escherichia coli* and *Klebsiella pneumoniae*. In this study, we demonstrate that zinc blocks the SOS-induced development of chloramphenicol resistance in *Enterobacter cloacae*. Zinc also blocked the transfer of an extended spectrum beta-lactamase (ESBL) gene from *Enterobacter* to a susceptible *E. coli* strain. A zinc ionophore, zinc pyrithione, was ~100-fold more potent than zinc salts in inhibition of ciprofloxacin-induced hypermutation in *E. cloacae*. Other divalent metals, such as iron and manganese, failed to inhibit these responses. Electrophoretic mobility shift assays (EMSAs) revealed that zinc, but not iron or manganese, blocked the ability of the *E. coli* RecA protein to bind to single-stranded DNA, an important early step in the recognition of DNA damage in enteric bacteria. This suggests a mechanism for zinc's inhibitory effects on bacterial SOS responses, including hypermutation.

Keywords: antibiotic resistance, RecA, electrophoretic mobility shift assay, *Enterobacter cloacae*, extended spectrum beta lactamase, CTX-M27, Zinc pyrithione

INTRODUCTION

The term “SOS response” as descriptor of a bacterial reactions to DNA damage was coined about 1975, the same year that the ship Edmund Fitzgerald sank in Lake Superior without sending out an SOS distress call. The SOS response triggers a constellation of changes in the bacterial cell, including cellular elongation, suspension of cell division, induction of DNA repair pathways, induction of latent bacteriophages, expression of bacteriophage-encoded toxins, and increased expression of error-prone DNA polymerases (Goodman, 2002). The latter underlies the increased mutation rate observed when the SOS response is strongly induced.

Recently, several laboratories showed that sublethal concentrations of certain SOS-inducing antibiotics induced resistance to other, unrelated antibiotics (Kohanski et al., 2010; Song et al., 2016; Bunnell et al., 2017). Their work and that of others have led to increased interest in whether SOS inhibitors could block emergence of antibiotic resistance (Nautiyal et al., 2014; Alam et al., 2016).

We initially became interested in the SOS response because of its role in inducing the expression of the Shiga toxins in Shiga-toxigenic *Escherichia coli* (STEC), because antibiotics induce production of the Shiga toxins Stx1 and Stx2, resulting in a worsening of the disease. Since previous work showed that zinc inhibited Stx production in STEC, we wondered if zinc's inhibitory effects were mediated by inhibition of the SOS response, and found that indeed they were (Crane et al., 2014). Indeed, zinc's inhibitory effects on the SOS response also blocked hypermutation in *E. coli* and *Klebsiella* strains (Bunnell et al., 2017).

Beaber et al. previously showed that induction of the SOS response with mitomycin C or ciprofloxacin dramatically increased the rate of horizontal antibiotic resistance transfer from *E. coli* to *Vibrio cholerae*, and from one strain of *V. cholerae* to another (Beaber et al., 2003). In this study, we first tested whether the inhibitory effects of zinc salts on SOS also extended to another member of the Enterobacteriaceae family, *Enterobacter cloacae*. We next tested whether zinc ionophores, such as A23187 or zinc pyrithione, would show increased potency against the hypermutation response. We also tested whether zinc could block the transfer of antibiotic resistance from *Enterobacter* to a susceptible *E. coli* recipient strain. Zinc salts and zinc pyrithione blocked hypermutation in *E. cloacae* and zinc also blocked horizontal transfer of β -lactam resistance to another, unrelated *E. coli* strain. Last, we developed an electrophoretic mobility shift assay (EMSA) to determine if metals blocked binding of RecA to ssDNA. We demonstrated that zinc, but not other divalent metals, blocked the ability of RecA to bind to ssDNA in this EMSA.

MATERIALS AND METHODS

Materials

Mitomycin C, ciprofloxacin (cipro), chloramphenicol (chloramph), zinc acetate, zinc pyrithione, A23187, agarose, ATP, ATP- γ -S, Sypro Orange protein stain, and copper phthalocyanine tetrasulfonate were from Sigma-Aldrich (St. Louis, MO). Gradient-impregnated antibiotic test strips were purchased from Liofilchem, Inc., (Abruzzi, Italy, and Waltham, MA). Copper pyrithione was from Combi-Blocks, San Diego, CA, while ceftazidime (ceftaz) was purchased from TCI, Tokyo, Japan. DMEM-F12 medium was from Gibco, Inc., Grand Island, NY, a subsidiary of Thermo-Fisher. DNase I was from Worthington Biochemical Corp., Lakewood, NJ. Purified RecA protein was purchased from New England Biolabs (NEB, Boston, MA). Blue Juice loading dye, SYBR-Safe DNA dye, and the 100 bp DNA ladder were from the Invitrogen division of Thermo-Fisher.

Bacterial Strains Used. Bacterial strains are described in Table 1.

Hypermutation in *E. cloacae* Bacteria

As previously described, bacteria were grown overnight in LB broth at 37°C with 300 rpm shaking, then subcultured into DMEM-F12 broth medium for induction of hypermutation. The DMEM/F12 medium was supplemented with 18 mM NaHCO₃

and 25 mM additional HEPES, pH 7.4, but omitted serum and antibiotics. The usual dilution from overnight was 1:100 into DMEM-F12, but this was varied if needed. After 75 min, the culture was divided into separate tubes and ciprofloxacin was added to a concentration equivalent to 1/2 to 3/4 of the MIC for that strain. Differences in the concentration of ciprofloxacin used resulted in differences in the antibiotic resistance frequencies observed. Metals such as zinc were added at this time, and incubation was continued with 300 rpm shaking. Four hours after initiation of the subculture, the culture turbidities were measured as OD₆₀₀ on a spectrophotometer, and serial dilutions were quickly plated onto LB agar to measure the total bacterial counts in each condition. In addition, 100–200 μ L of undiluted culture was plated in triplicate onto plates of LB + 20 mg/L (20 μ g/mL) chloramphenicol, a concentration 5 times the MIC of *E. cloacae*. Antibiotic resistance frequencies were calculated as the (CFU of antibiotic resistant colonies/mL) \div (CFU of total colonies/mL). In some cases, the antibiotic resistance frequency was multiplied by 10e6 and expressed as “chloramphenicol resistance frequency per million” as previously shown, and in other cases these results were converted to a logarithmic scale. When zero colonies were observed on any of the triplicate plates, the lower limit of detection was calculated as if 1 colony had been observed; this was often the case in the control cultures, i.e., bacteria not exposed to any SOS-inducing antibiotic.

Cross-Species (Horizontal) Transfer of Antibiotic Resistance

In order to test for the transfer of genetic material from the ceftaz^R *E. cloacae* to Chloramph^R fluorescent *E. coli* strain EC43, or vice versa, both strains were grown up in LB broth overnight, then both were subcultured into DMEM-F12 liquid medium. After 75 min, ciprofloxacin was added at the appropriate concentrations for each strain. At this time, metals such as zinc were also added. At the 4 h time point, the culture turbidities were read as OD₆₀₀, and then dilutions were made in order to determine the total number of bacteria of each species in their separate cultures. Bacteria were then mixed in a 1:1 ratio, centrifuged at 1,600 g for 10 min, and then the bacteria were allowed to stand on the bench top at room temperature. After the bacteria had incubated together in the centrifuged pellets, the pellets were resuspended, and then plated on LB + 6 μ g/mL ceftazidime and 20 μ g/mL chloramphenicol, and the plates were inspected on the UV transilluminator box for double-resistant, green-fluorescing colonies. In pilot experiments, we tested mixing the two bacterial strains for 3, 4, and 6 h, but we never observed any transconjugant colonies at these durations of bacterial contact. Finally, we therefore allowed the centrifuged bacterial mixtures to stand on the bench top at room temperature for 20 h, and with this longer duration we did observe putative transconjugant colonies, meaning double-resistant, green-fluorescing colonies. Putative transconjugant colonies were picked and re-streaked on LB with ceftazidime + chloramphenicol. Biochemical tests were next performed to determine if the putative transconjugant colonies were *E. coli* that had gained resistance to ceftazidime, or *E. cloacae* that

TABLE 1 | Description of bacterial strains used.

	Description	Ciprofloxacin MIC on DMEM, mg/L	Chloramphenicol MIC on LB agar, mg/L	Ceftazidime MIC on LB agar, mg/L	Comments
ENTEROBACTER STRAINS					
<i>Enterobacter cloacae</i> E_clo_Niagara	Wild-type, clinical isolate, bloodstream infection, ESBL	0.064	4	6 on LB; ≥ 16 on Muller-Hinton	"ESBL" or extended spectrum beta-lactamase producer; + for <i>bla</i> _{CTX-M27}
BAA-1143	ATCC type strain	0.006	8	96	AmpC chromosomal beta-lactamase; from Microbiologics, St. Cloud, MN
<i>E. coli</i> STRAINS					
<i>E. coli</i> EC43	O157:H7 (pGFP-UV-Chloramph ^R). Expresses green fluorescent protein (GFP) from plasmid; Chloramphenicol-resistant.	0.008	>40	0.064	Microbiologics, St. Cloud, MN; traceable to FDA strain ESC1177

had developed chloramphenicol resistance and also acquired the plasmid expressing GFP. The biochemical tests done to distinguish *Enterobacter* from *E. coli* included indole production, acid production by the Methyl Red test, Voges-Proskauer test for acetoin production, and streaking on eosin methylene blue (EMB) agar. In all cases the putative transconjugants were *E. coli* that had become resistant to ceftazidime.

Testing for Beta-Lactamase-Encoding Genes in *Enterobacter* and in *E. coli* Transconjugants

We extracted total DNA from *Enterobacter* E_clo_Niagara and from the putative *E. coli* transconjugants that had acquired β -lactam resistance using the AllPrep Bacterial DNA Kit from Qiagen (Hilden, Germany and Waltham, MA) according to the manufacturer's instructions. Purified DNA was sent to ID Genomics, Seattle, WA, for PCR detection of the extended spectrum β -lactamase genes. PCR assays using broad-range primers initially identified the β -lactamase as a member of CTX-M family, and then specific primers indicated the β -lactamase was a CTX-M27. This "head start" from ID Genomics allowed us to then conduct our own PCR assays.

PCR Detection of CTX-M27 in *E. cloacae* and in Putative *E. coli* Transconjugants/Transformants

Plasmid DNA was prepared from the donor strain, E_clo_Niagara, recipient strain EC43, and from the putative transconjugant *E. coli* strains that emerged from the inter-species gene transfer experiments, using Qiagen Midi-Plasmid preparation kits (Waltham, MA). Primer pairs directed against the gene *bla*_{CTX-M27}, encoding the extended spectrum beta-lactamase CTX-M27, were used for PCR and are shown in Table 2A. PCR was conducted on a Bio-Rad CFX96 real-time PCR machine using Bio-Rad iTaq Universal SYBR Green Master Mix in a final volume of 20 μ L; Primer concentration was 0.5 μ M, and 5 μ L of the plasmid DNA prepared from each strain

TABLE 2 | Oligonucleotides used.

(A) PCR primers used to amplify plasmid DNA for CTX-M27 beta lactamase.

Primers	Amplicon size, b.p.	Comment
Forward CTGGAGAAAAGCAGCGGAG	158	From (Szczepanowski et al., 2009), Supplemental Data
Reverse TGCTTTTGCCTTCACTCTG		
Forward GCGACAATACCGCCATGAAC	257	Designed using Primer BLAST tool based on Accession No. AY156923, from Bonnet (2004) (https://www.ncbi.nlm.nih.gov/)
Reverse CGTATTGCCTTTGAGCCACG		

(B) Fluorescently labeled oligonucleotide used for electrophoretic mobility shift assay.

This 38-mer oligonucleotide was labeled at the 5' end with 6-FAM (fluorescein)
GGCCACGCGTCGACTAGTACTTTT TTTT TTTT TTTT TTTT

was used as the template for 35–39 PCR cycles using a 3-Step amplification protocol.

Electrophoretic Mobility Shift (EMSA; "Gel-Shift") Assay for RecA Binding to ssDNA

Purified RecA protein from NEB was used for EMSA along with 10X Assay buffer (Tris acetate, pH 7.8, with magnesium) supplied by the manufacturer. To test for binding to ssDNA, a fluorescently labeled oligonucleotide was purchased from Integrated DNA Technologies, Inc., Coralville, IA. This 38-mer oligonucleotide was labeled at the 5' end with 6-FAM (fluorescein) and the sequence is shown in Table 2B.

To test for RecA-DNA binding, we first did pilot experiments to determine how much fluorescent oligonucleotide was needed to produce a visible fluorescent band on agarose gels. We found that using 5 μ M fluorescent oligonucleotide gave a visible band when 15 μ L were loaded on an agarose gel. We next did pilot

experiments to determine what molar ratio of RecA protein to oligonucleotide was needed to observe any gel shift.

The binding assay was carried out in duplicate or triplicate in 15 μ L final volume in conical-bottomed 96-well plates kept on ice during reagent addition. The fluorescent oligonucleotide in assay buffer was added first, followed by zinc or other metals added to final concentrations of 0.1–1 μ M. In addition, ATP or ATP- γ -S was added as noted to achieve a final concentration of 0.3 mM. Last, RecA protein was added from a concentrated stock to achieve the appropriate ratio relative to ssDNA. This ratio was varied to obtain RecA: oligonucleotide ratios of 2:1 to 5:1, as indicated in the Figure Legends. After addition of RecA, the plate was moved to the 37° incubator where it was sandwiched between pre-warmed metal blocks to speed heat transfer to the samples, and binding was allowed to proceed for 15 min. After the incubation, 2 μ L of 10 X “Blue Juice” loading dye was added to the samples, and then samples were loaded into the wells of an agarose gel (1.5% agarose in 1 X TAE buffer, with SYBR-Safe DNA stain added to be able to visualize the DNA ladder).

Electrophoresis was carried out at 135 V for 35 min. After electrophoresis, the gel was visualized on the Gel-Doc E-Z fluorescent imager (Bio-Rad) using the Blue illuminator plate and the settings for SYBR Green, which also work for fluorescein. In some experiments, zinc or other metals were added to the agarose gel at the same concentration as that added to the binding assay. In this case, we used plastic rulers cut to the correct length in order to have some samples running in gel lanes with metal incorporated into the gel itself (**Supplemental Figure 1**). For quantitation, the image files from the Gel-Doc EZ were “inverted” to produce dark bands on a light background, then quantitated using Un-Scan-It Gel software for the MacIntosh computer (Silk Scientific, Orem, UT).

Measurement of Extracellular DNA

DNA released into culture supernatants by SOS-inducing treatments was measured in a UV spectrophotometer by A_{260}/A_{280} ratio.

Statistical Analysis

Data shown are means \pm SD. Tests of significance were by analysis of variance (ANOVA), using Dunnett's test for multiple comparisons. Graphs were produced using GraphPad Prism (San Diego, CA).

RESULTS

Testing for Induction of Hypermutation in *Enterobacter cloacae* Strain E_clo_Niagara

Initial experiments were performed to see if ciprofloxacin could induce hypermutation to the unrelated antibiotic, chloramphenicol, in E_clo_Niagara. For these experiments we used a chloramphenicol concentration five times the starting MIC for this strain. **Figure 1A** shows that a sublethal concentration of ciprofloxacin did greatly increase the chloramphenicol resistance frequency in this strain, and this increase was reversed by zinc acetate in a dose-dependent fashion. As previously observed, however, 200 μ M zinc acetate

was needed to observe strong inhibition of the mutator response (**Figure 1A**). In addition to zinc, CuSO₄ and CoCl₂ also were able to inhibit the hypermutation response (**Figure 1B**), but they were less potent than zinc, as we previously observed with *E. coli* and *Klebsiella* (Bunnell et al., 2017). In contrast to zinc, iron (as FeSO₄), and manganese did not inhibit ciprofloxacin-induced hypermutation (**Figure 1C**; data not shown for MnCl₂). Interestingly, gallium nitrate also had a mild inhibitory effect on ciprofloxacin-induced hypermutation, even though gallium is a trivalent rather than divalent element.

We next tested whether metal ionophores, such as A23187, or zinc pyrithione, could improve the potency of zinc against the hypermutation response. Our results with A23187 plus zinc were unexpectedly negative, because A23187 alone, in the absence of any metal, consistently increased ciprofloxacin-induced mutation to chloramphenicol resistance (**Supplemental Figure 2A**, middle bar). Compared to zinc acetate alone, the addition of 100 μ M A23187 unexpectedly reduced the potency of zinc (dose-response curve shifted to the right, **Supplemental Figure 2B**). These results may be consistent with A23187 acting more as a zinc chelator than as a zinc ionophore in E_clo_Niagara. Indeed, most of the literature on A23187 in bacterial systems has been with Gram-positive rather than Gram-negative bacteria, and it may be that A23187 is unable to conduct zinc across the double membranes of enteric Gram-negative bacteria.

Despite the unexpected results with A23187 + zinc, zinc pyrithione (ZPT) showed much more promise as an inhibitor of SOS-induced hypermutation. ZPT inhibited ciprofloxacin-induced hypermutation at concentrations near 1 μ M (**Figures 2A,B**). While copper pyrithione (CuPT) is often viewed as more toxic to living cells than ZPT (Bao et al., 2014), we found that ZPT was \sim 4-fold more potent than CuPT in its ability to inhibit bacterial growth (**Figure 2C**). Similarly, ZPT was better than CuPT in blocking the mutator response (**Figure 2D**). Direct comparison of zinc acetate to ZPT showed that ZPT was \sim 100 fold (2 logs) more potent than zinc acetate in inhibition of SOS-induced hypermutation (**Figures 2E,F**). The high potency of ZPT against the SOS response might allow the effects of zinc to be exploited in situations where concentrations of zinc acetate as high as 0.2 mM cannot be achieved.

Testing for Horizontal, Inter-species Gene Transfer in Enteric Bacteria

Having shown that the SOS response could be induced in E_clo_Niagara, we next tested whether SOS induction could trigger transfer of antibiotic resistance elements between species, as shown by Beaber et al. (2003). In contrast to the study by Beaber et al., who worked with *V. cholerae*, an organism that is naturally competent for uptake of extracellular DNA, *E. coli* and related enterics are not naturally competent, and although they can take up DNA from the environment, such DNA is often degraded and used as food rather than incorporated into their genomes (Finkel and Kolter, 2001; Chen and Dubnau, 2004; Palchevskiy and Finkel, 2006). Therefore, it was unclear whether

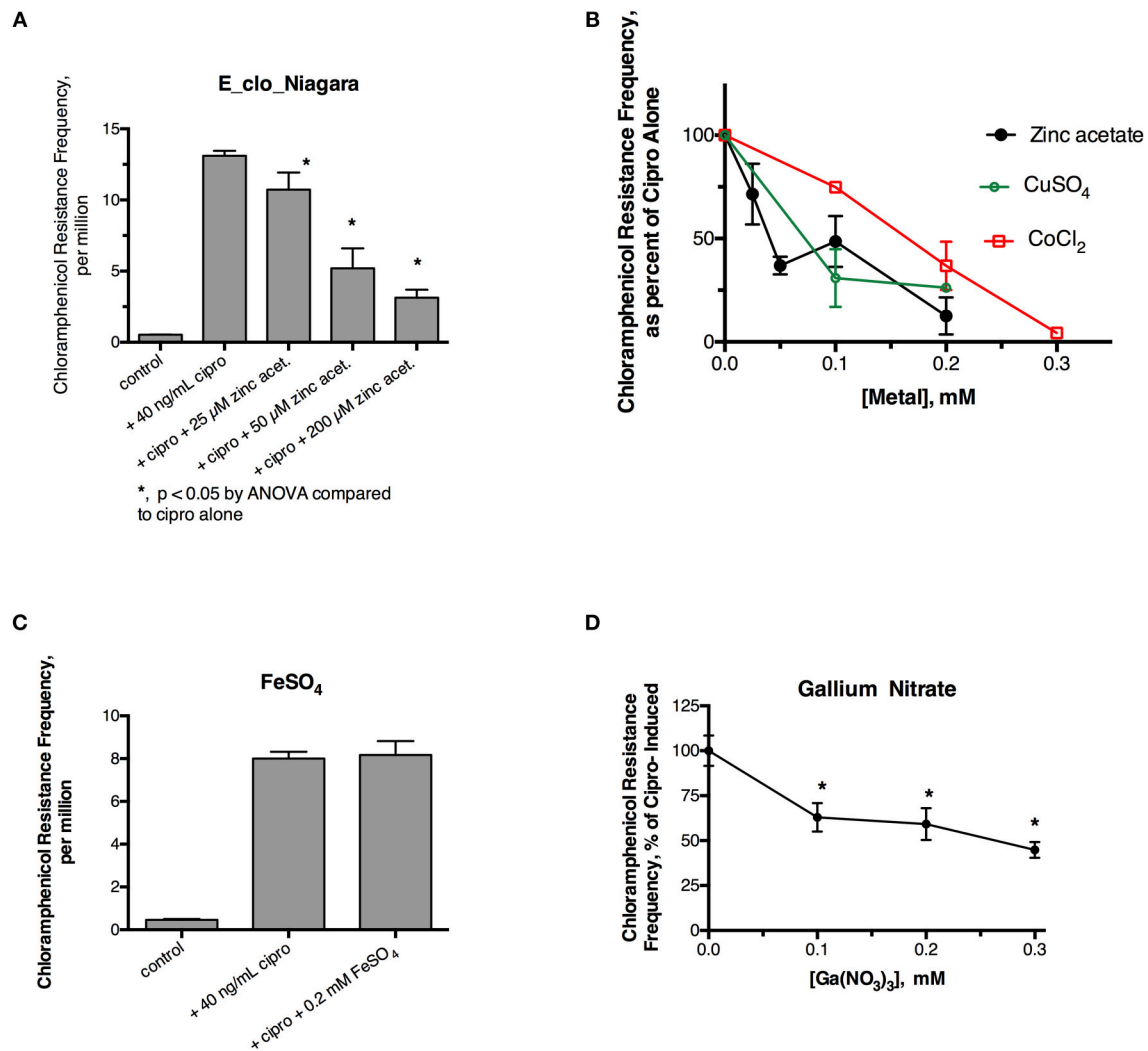


FIGURE 1 | Effect of zinc and other metals on ciprofloxacin-induced hypermutation in *E_clo_Niagara*. **(A)** Effect of ciprofloxacin and zinc on the chloramphenicol resistance frequency in *E_clo_Niagara*. **(B)** Comparison of zinc with CuSO₄ and CoCl₂ on ciprofloxacin-induced mutation frequency. To allow comparison of separate experiments, the results were expressed as a percent of the ciprofloxacin-induced mutation frequency for each experiment, then averaged. Each line on the graph shows the mean \pm SD of at least two separate experiments. **(C)** Lack of effect of FeSO₄ on ciprofloxacin-induced hypermutation. **(D)** Effect of gallium (III) nitrate on ciprofloxacin-induced hypermutation in *E_clo_Niagara*. *Significant compared to cipro alone by ANOVA; graph shown is the Mean \pm SD of 3 separate experiments, expressed as % of cipro-induced.

the findings of Beaber et al. on SOS and horizontal gene transfer would apply to a different microbial system.

We tested whether the β -lactamase of *Enterobacter E_clo_Niagara* could be transferred to a susceptible STEC *E. coli* strain, EC43. EC43 also possessed its own plasmid, encoding the green fluorescence protein (GFP) and resistance to chloramphenicol. As described in section Materials and Methods, we induced the SOS response in each bacterial strain, then mixed together the 2 strains of bacteria at a 1:1 ratio, and, after allowing the mixtures to incubate for increasing periods of time, then plated aliquots on LB agar + chloramphenicol + ceftazidime. Plates were examined on the UV transilluminator box for green-fluorescing colonies resistant to both antibiotics.

In initial experiments where the *E_clo_Niagara* and EC43 were allowed to co-mingle for 3, 4, or 6 h before plating on antibiotic selective agar, no green fluorescing colonies were observed on the double-antibiotic plates. When the 2 species of bacteria were allowed to co-incubate for 20 h, however, green colonies resistant to both antibiotics were observed in the condition in which the SOS-response was induced with ciprofloxacin (Figure 3 and Supplemental Figure 3A). Addition of 0.2 mM zinc acetate blocked the appearance of the putative transconjugants when zinc was added to both bacteria along with ciprofloxacin (Figure 3A). Identification of the double-resistant, green colonies showed them to be *E. coli* that had acquired resistance to ceftazidime, rather than *E_clo_Niagara* that had

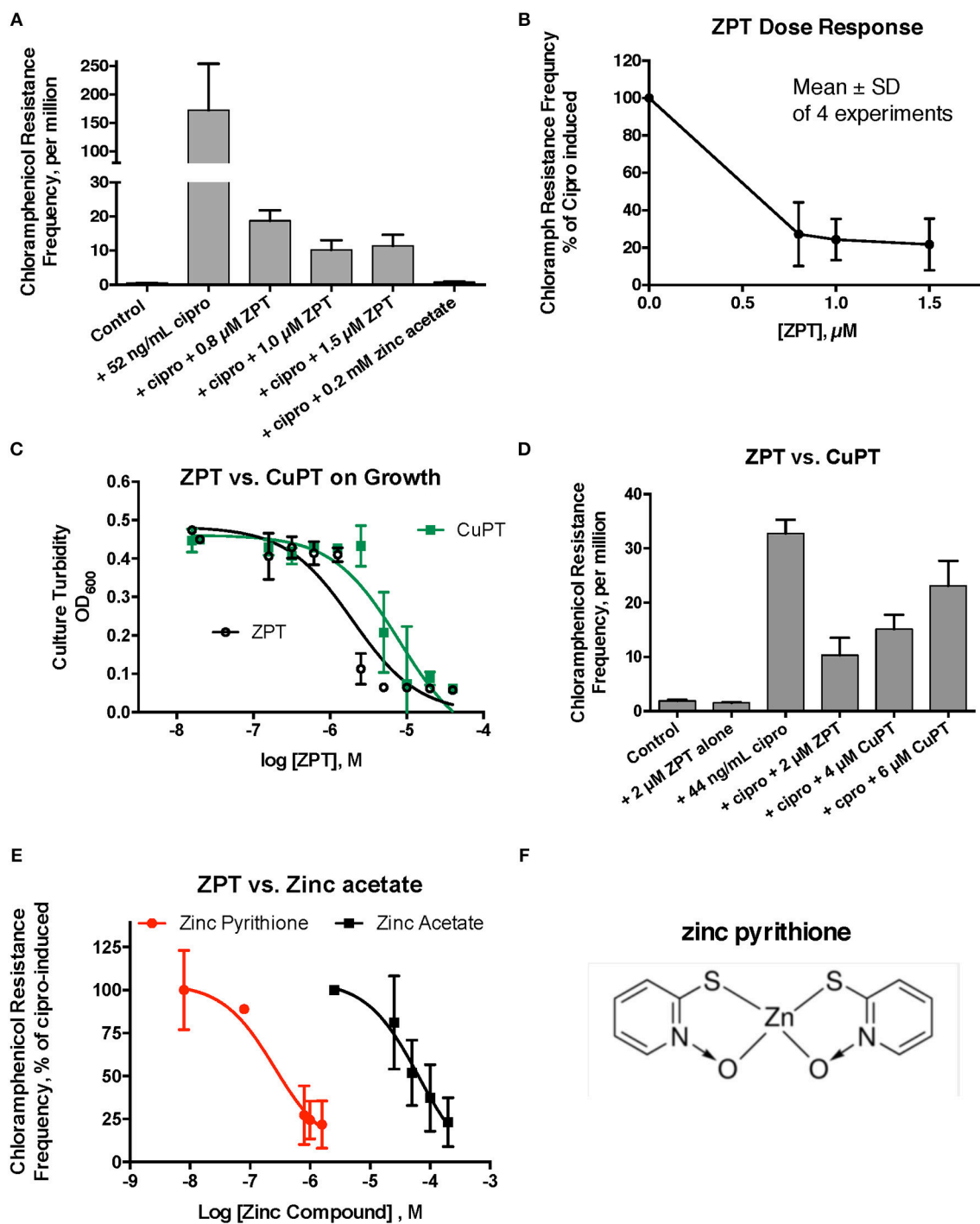


FIGURE 2 | Effect of zinc pyrithione (ZPT) on ciprofloxacin-induced mutation response in *E_clo_Niagara*. ZPT is also known as 1-hydroxypyridine-2-thione zinc salt. **(A)** Dose-response relationship of ZPT on ciprofloxacin-induced mutation to chloramphenicol resistance, showing a single representative experiment. **(B)** Dose-response relationship of the ZPT on chloramphenicol resistance frequency, showing combined results from 4 separate experiments. ZPT at concentrations greater than or equal to 0.8 μ M produced statistically significant reductions in chloramphenicol resistance frequency in **(A,B)** (< 0.05). **(C)** Comparison of ZPT and copper pyrithione (CuPT) on growth of *E_clo_Niagara*. **(D)** Comparison of ZPT and CuPT on inhibition of chloramphenicol resistance. Although 2 μ M CuPT produced a partial inhibition of hypermutation, higher concentrations of CuPT showed a paradoxical increase back toward the ciprofloxacin-induced level; this was due to increased killing of bacteria at 4–6 μ M, resulting in a drop in the denominator value (total counts). **(E)** Dose response relationship of zinc compounds in inhibition of mutation to chloramphenicol resistance, expressed on a log scale. ZPT curve is the mean \pm SD of 4 experiments, while the zinc acetate curve is the mean \pm SD of 7 separate experiments. **(F)** Chemical structure of zinc pyrithione.

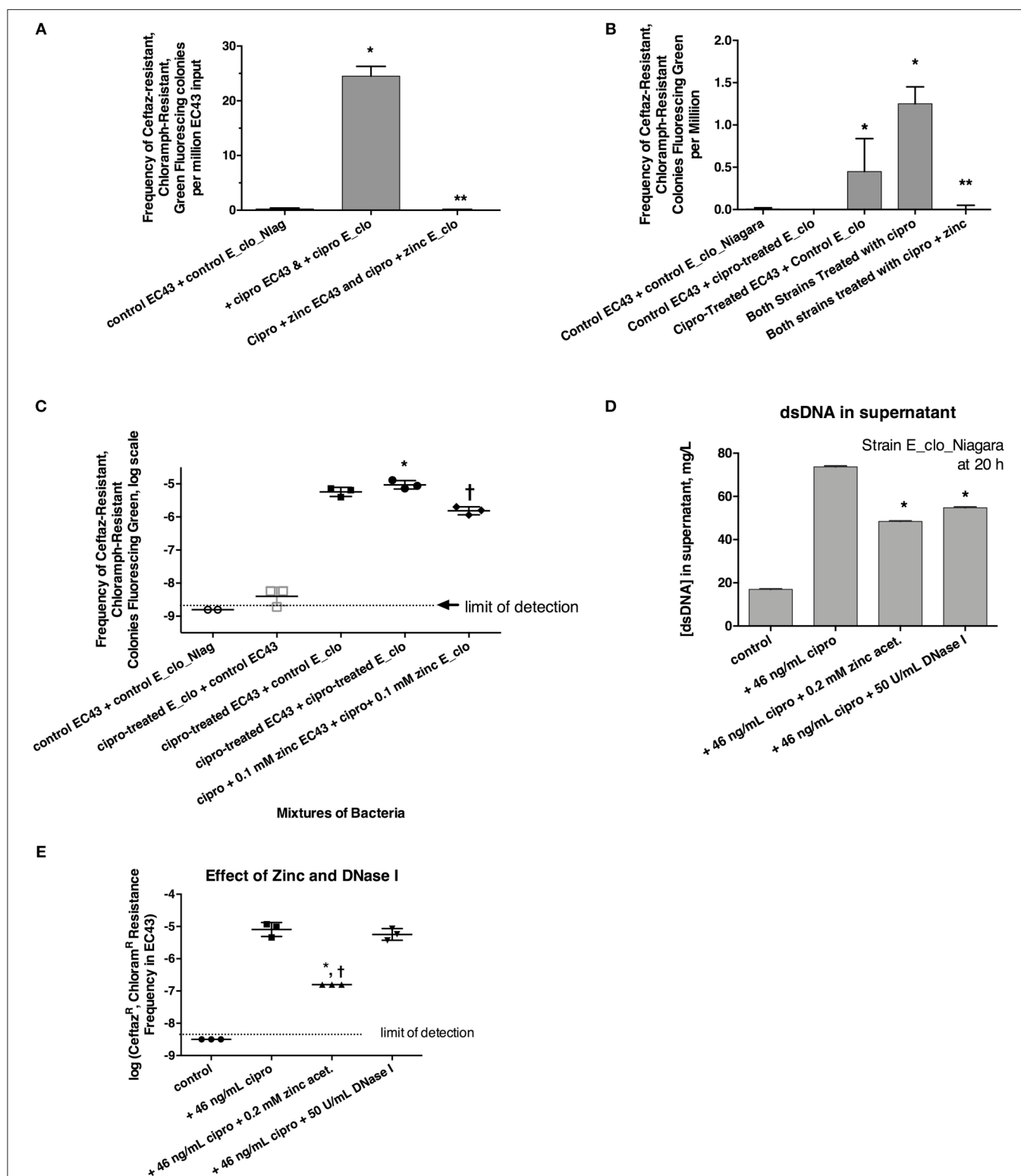


FIGURE 3 | Role of the SOS response in horizontal transfer of beta-lactam resistance from *E. coli* strain EC43 to susceptible *E. coli* strain *E. coli*. **(A)** Induction and inhibition of inter-species gene transfer. *E. coli* strain EC43 and *E. coli* strain *E. coli* were both treated separately with ciprofloxacin to induce the SOS response, then mixed and allowed to co-incubate for 20 h. The mixtures were plated on LB + ceftazidime + chloramphenicol, and examined under UV light for green fluorescent colonies resistant to both antibiotics. Since the colonies fitting the above description all tested as being *E. coli*, not Enterobacter, the frequency of emergence of such colonies was calculated relative to the number of EC43 bacteria placed into the original mixture. Zinc acetate concentration was 0.2 mM; *significantly increased compared to (Continued)

FIGURE 3 | control, **significantly decreased compared to the conditions receiving ciprofloxacin. **(B)** Effect of ciprofloxacin applied to *E_clo_Niagara* alone, *E. coli* EC43 alone, or both strains, on the horizontal gene transfer. The concentration of zinc used in **(B)**, far-right column, was 0.2 mM; *significantly increased compared to control, **significantly decreased compared to the conditions receiving ciprofloxacin. **(C)** Effect of ciprofloxacin and zinc on horizontal gene transfer, with the transconjugant frequency expressed on a log scale. 0.1 mM zinc was used in panel C; *significantly increased compared to control, †significantly decreased compared to the conditions receiving ciprofloxacin. **(D)** Effect of zinc and DNase I on release of double-stranded DNA into culture supernatant; *significantly decreased compared to the plus cipro condition. **(E)** Effect of zinc and DNase I on frequency of emergence of putative transconjugants (green fluorescing colonies resistant to both antibiotics), showing that zinc, but not DNase, blocked the transfer of beta-lactam resistance to the *E. coli* strain. *significantly decreased compared to the condition receiving ciprofloxacin alone. †There were no Ceftaz^R, Chloram^R *E. coli* colonies in the zinc-treated group, so the data points shown are calculated as if 1 colony had appeared.

acquired the plasmid encoding GFP and the chloramphenicol resistance marker. Control experiments with EC43 alone, not mixed with *E_clo_Niagara*, failed to show ciprofloxacin-induced acquisition of ceftazidime resistance (zero colonies observed in 10 separate experiments, all done in triplicate).

We next induced the SOS response in EC43 and *E_clo_Niagara* separately to try to determine if SOS induction was more important in the donor strain or the recipient strain. When only the donor strain, *E_clo_Niagara*, was treated with ciprofloxacin, putative transconjugants remained rare (**Figures 3B,C**, respectively). When only *E. coli* EC43 was subjected to SOS induction with ciprofloxacin, putative transconjugants were regularly observed in substantial numbers (**Figures 3B,C**). The greatest frequency of transconjugants was observed, however, when both the donor and the recipient strain were treated with ciprofloxacin (**Figures 3B,C**). Zinc acetate consistently blocked the SOS-induced transfer of β -lactam resistance phenotype. When the zinc concentration was reduced to 0.1 mM, however, the reversal of the SOS response was only partial (**Figure 3C**, right-hand set of points).

In the course of these experiments, we noted that induction of the SOS with ciprofloxacin, followed by a 20 h incubation, was accompanied by a release of DNA into the supernatant (**Figure 3D**; similar results were obtained with strain EC43 as well; data not shown). During the 20 h incubation, bacterial counts of both strains increased ~ 3 -fold compared to the counts at the 4 h collection point, for both the antibiotic-treated and untreated conditions. Therefore, the DNA release observed is not due to massive die-off of bacteria during the 20 h incubation. Addition of zinc acetate and DNase I both significantly reduced the amount of DNA detectable in bacterial supernatants (**Figure 3D**). Therefore, we tested whether addition of exogenous DNase I would block the horizontal transfer of β -lactam resistance to EC43. As shown in **Figure 3E**, DNase I had no effect on the frequency of appearance of the double-resistant transconjugant colonies in this assay, while zinc again showed its strong inhibitory effect. This also hinted that, although release of DNA into the supernatant occurred during our 20 h incubation, transfer of relevant DNA encoding antibiotic resistance likely does not occur by bulk release of DNA into the culture medium, but instead may require direct cell-to-cell contact.

The experiments of **Figure 3** showed that the beta-lactam resistant phenotype from *E_clo_Niagara*, could be transferred to a susceptible *E. coli* strain when the SOS response was induced. We next tested whether we could detect the gene encoding the resistance had indeed been transferred to the recipient strain. The extended spectrum beta-lactamase (ESBL) gene family is

large, but the ID Genomics company helped us narrow our focus to *bla*_{CTX-M27}. Using this knowledge, we constructed two sets of primers directed against CTX-M27 (section Materials and Methods and **Table 2**). PCR with both sets of primers revealed that DNA encoding CTX-M27 was present in the donor strain *E_clo_Niagara* and in the *E. coli* transconjugants, but not present in parental *E. coli* strain EC43. Quantitative PCR analysis from a typical experiment showed that the number of cycles to threshold, C_t , for amplification from the plasmid preparations from the various strains were: *E_clo_Niagara*: 28.0 ± 0.7 ; EC43: NA (no amplification); Transconjugant 1: 32.2 ± 1.0 ; Transconjugant 2, 27.3 ± 0.5 ; and Transconjugant 3, 35.8 ± 0.3 , using the first set of primers shown in **Table 2**. Similar results were observed using the second set of primers as well.

RecA-ssDNA-Zinc Interactions

Previously, we showed that zinc blocked the SOS-induced cleavage of the LexA repressor in live *E. coli* bacterial cells, and zinc also blocked RecA-mediated LexA cleavage in a cell-free assay using purified bacterial proteins plus cofactors (Bunnell et al., 2017). That previous work strongly suggested that zinc acted on RecA, as previously suggested by other authors (Lee and Singleton, 2004), but left open a narrow possibility that zinc might act on LexA, or on the protein-protein interface where RecA binds to LexA, possibly interfering with LexA's own proteolytic cleavage. To determine if zinc had effects on RecA alone, in the absence of LexA, we performed EMSAs using fluorescein-tagged ssDNA and purified RecA to see if zinc influenced the ability of RecA to bind to ssDNA (Svingen et al., 2001). **Figure 4A** shows the effect of adding increasing amounts of RecA protein in the presence of a fixed, 5 μ M concentration of fluorescent 38-mer ssDNA oligonucleotide. A marked upward shift in mobility was noted in the presence of 10 μ M RecA (lanes 4–6, 2:1 molar ratio of RecA to ssDNA), and the proportion of ssDNA migrating in this slower, upper band increased as the ratio of RecA to ssDNA was increased (**Figure 4A**, lanes 7–14). **Figure 4A** shows the results obtained in the absence of ATP- γ -S, but experiments in the presence of 0.3 mM ATP- γ -S were also performed, and the densitometry scans of the fluorescence images, with and without ATP- γ -S, are shown in **Figure 4B**. Addition of zinc markedly reduced the proportion of ssDNA migrating as the upper band, and increased the amount of ssDNA in the original, unbound position (black arrows). Gels scans of **Figure 4C** and a parallel experiment done in the absence of ATP- γ -S are shown in **Figure 4D**. As shown in **Figure 4D**, the inhibitory effects of zinc on RecA binding were enhanced in the presence of ATP- γ -S, consistent with the

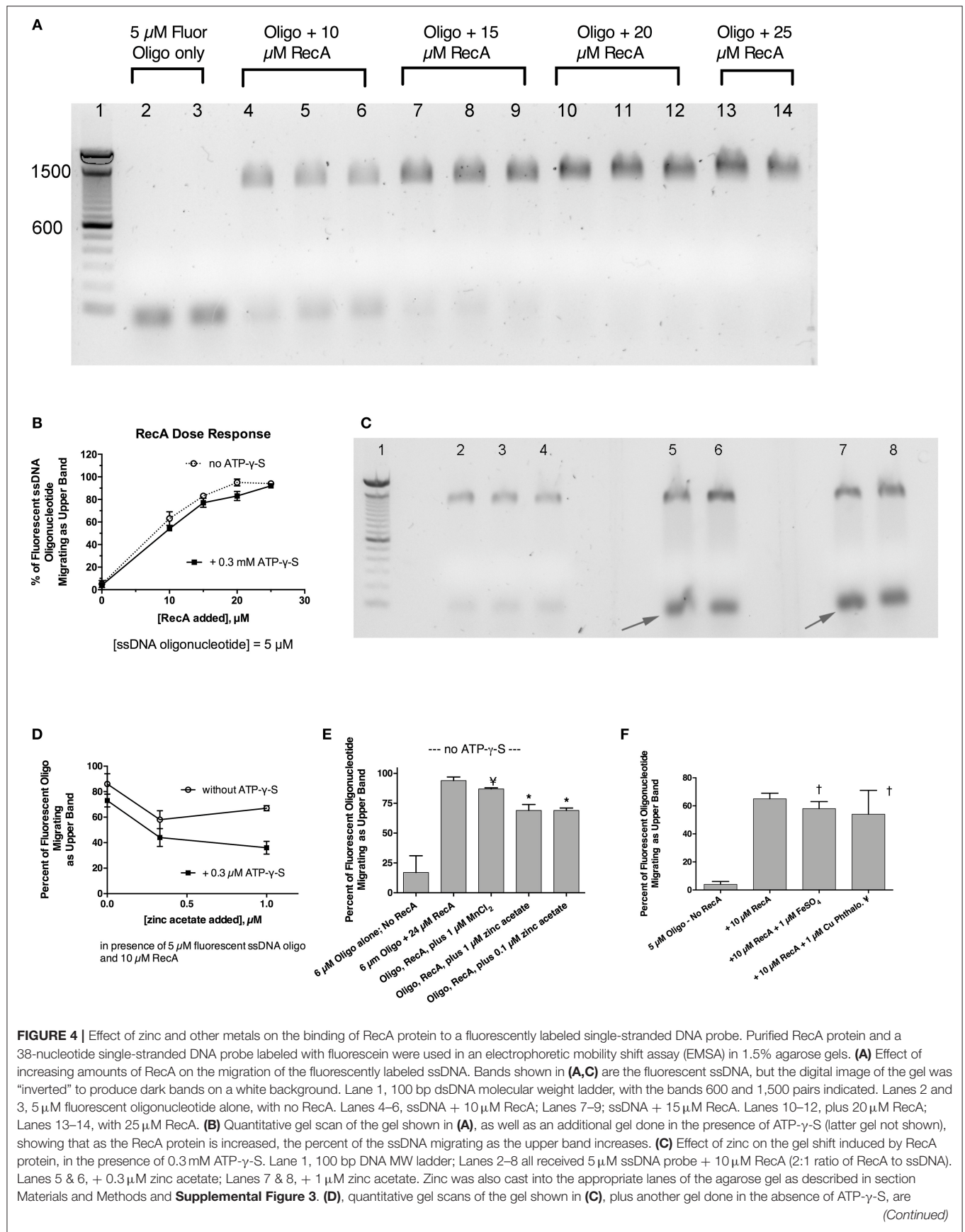


FIGURE 4 | graphed as a function of the concentration of added zinc. **(E)** Comparison of the effect of zinc on the gel shift assay, in contrast with the lack of effect of MnCl_2 . With RecA added to achieve a 4:1 ratio relative to ssDNA, the inhibitory effect of $1\ \mu\text{M}$ zinc was still evident, while $1\ \mu\text{M}$ MnCl_2 failed to inhibit the RecA-induced upward shift in the migration of the ssDNA probe; N.S. , not significant compared to Oligo + RecA, by ANOVA; *significant compared to Oligo + RecA; $p < 0.01$ by ANOVA. **(F)** Lack of effect of $1\ \mu\text{M}$ FeSO_4 and $1\ \mu\text{M}$ copper phthalocyanine tetrasulfonate (CuP), reported to be a RecA inhibitor, on the gel shift induced by RecA. N.S. Not significant compared to RecA alone by ANOVA.

known role of ATP and ATP- γ -S in supporting the dissociation of bound RecA monomers from the ssDNA nucleofilament (Wigle et al., 2006). The inhibitory effects of zinc on RecA binding persisted even when higher concentrations of RecA were used in the assay (**Figure 4E**; 4:1 ratio of RecA to ssDNA). In contrast to the inhibitory effects of zinc, manganese did not inhibit ssDNA binding to RecA (**Figure 4E**), and neither did $1\ \mu\text{M}$ FeSO_4 (**Figure 4F**). Surprisingly, the newly discovered RecA inhibitor, copper phthalocyanine tetrasulfonate, also failed to inhibit RecA-ssDNA binding in this assay (**Figure 4F**). The $1\ \mu\text{M}$ concentration used in **Figure 4F**, however, was lower than the $10\text{--}15\ \mu\text{M}$ concentrations used in the report by Alam et al. however (Alam et al., 2016). Nevertheless, **Figure 4** shows that RecA binding to ssDNA can be readily detected using a fluorescently labeled oligonucleotide in agarose gels, and that zinc inhibits RecA binding to ssDNA at low, $1\ \mu\text{M}$ concentrations, while iron, manganese, and a phthalocyanine tetrasulfonate compound did not. In addition, although zinc acts to block RecA-induced LexA cleavage (Bunnell et al., 2017), the presence of LexA is not necessary to observe the effects of zinc *in vitro*. Our results suggest that zinc blocks LexA cleavage by preventing the formation of the active RecA-ATP-ssDNA nucleofilament.

DISCUSSION

Although the SOS response has been discussed in the molecular biology literature for over 40 years (Radman, 1975), appreciation of the role of the SOS pathway in generation of antibiotic resistance has been very slow to percolate into the fields of clinical microbiology and infectious diseases. Recently, however, several laboratories have shown that sublethal concentrations of antibiotics can not only induce the SOS response, but also trigger the emergence of resistance to other, unrelated antibiotics (Kohanski et al., 2010; Song et al., 2016). In addition, our laboratory and others have shown that SOS-induced hypermutation, resulting in the emergence of antibiotic resistance, can be triggered by a wider array of compounds than classical inducers such as mitomycin C, ciprofloxacin, and UV light. The SOS response is induced in *E. coli* by oxidant stress and by a wide variety of drugs used in human and veterinary medicine, including some antiviral drugs, cancer chemotherapy agents, antimetabolites, arsenic compounds, the herbicide paraquat, and many other antibiotics, including those used for growth promotion in farm animals (Baharoglu and Mazel, 2011; Bunnell et al., 2017). We began studying zinc because it is an inhibitor of Shiga toxin (Stx) production in STEC, but later learned that zinc was blocking the SOS response itself, not just Stx toxin release. We showed that zinc, but not most other metals tested, blocked SOS-induced hypermutation to antibiotics such as rifampin and trimethoprim, in *E. coli* and

Klebsiella pneumoniae (Bunnell et al., 2017). As expected from the work of others (Cirz and Romesberg, 2006; Recacha et al., 2017), the hypermutation response, and zinc's inhibitory effects on SOS-induced mutation were dependent on RecA, a key sensor of DNA damage and initiator of the SOS response (Bunnell et al., 2017).

In this study, we first tested whether the inhibitory effects of zinc could be observed in another member of the Enterobacteriaceae family, *E. cloacae*. Zinc blocked ciprofloxacin-induced hypermutation, reducing the emergence of chloramphenicol resistance, while cobalt, copper, and gallium showed similar, but weaker activity (**Figure 1**). We also showed that a zinc ionophore, zinc pyrithione (ZPT), blocked SOS-induced hypermutation with an inhibitory concentration 50% (IC_{50}) ~ 100 -fold lower than zinc salts. This high potency compares favorably with other RecA inhibitors that have been proposed (Lee et al., 2005; Wigle et al., 2009; Alam et al., 2016). Although ZPT can have some toxicity toward mammalian cells (Priestley and Brown, 1980), it has been cleared by the United States Food and Drug Administration (FDA) for use on the skin at concentrations up to 0.25% ($7.8\ \text{mM}$) in “leave on” products such as lotions, and 2% ($63\ \text{mM}$) in “rinse-off” products such as shampoos (Schwartz, 2016). Older literature on ZPT tended to focus on its antifungal effects (Pierard-Franchimont et al., 2002; Reeder et al., 2011), but more recent reports emphasize the activity of ZPT against bacteria as well (Schwartz, 2016).

Inspired by the work of Beaber et al., we tested whether induction of the SOS response would trigger horizontal gene transfer from a β -lactam resistant, ESBL-producing *Enterobacter* strain to a sensitive *E. coli* strain. We were able to demonstrate transfer of the β -lactamase gene to the *E. coli* EC43 strain after a prolonged, 20 h, co-incubation. Although we have referred to the newly-resistant EC43 colonies as “putative transconjugants,” we have not conclusively shown that the mechanism of transfer of the β -lactamase is by conjugation. Jung tested a panel of 15 *Enterobacter aerogenes* strains for their ability to conjugate with *E. coli* and found only 1 of the 15 strains capable of doing so (Jung, 2014). Indeed, when we tested for transfer of the AmpC chromosomal β -lactamase from a different *E. cloacae* strain (BAA-1143) to EC43, putative transconjugants were either much rarer, or, in some experiments, not observed at all (data not shown). The rare transconjugants observed with strain BAA-1143 as the donor were also unstable genetically, and gradually lost their β -lactam resistance with repeated passage.

PCR analysis of the *E. coli* transconjugants that had acquired ceftazidime resistance revealed that the CTX-M27 beta-lactamase gene was present in the plasmid DNA. Therefore, it may be more accurate to describe these resistant *E. coli* strains as transformants (Chen and Dubnau, 2004) rather than as transconjugants. Classically, conjugation proceeds via transfer of ssDNA via a

conjugation pilus to the recipient strain, whereas transformation (such as by electroporation) is usually more efficient with double-stranded plasmid DNA. McCollister et al. recently described *in vivo* acquisition of the CTX-M27 plasmid by a *Salmonella enterica* strain in a relapsed infection (McCollister et al., 2016). In that case, the patient's *Salmonella* strain was initially susceptible to the 3rd-generation cephalosporins and the patient was treated with ceftriaxone. After relapse, however, the *Salmonella* strain was resistant to ceftriaxone, and comparison of the two strains allowed the investigators to determine that the *Salmonella* had acquired the CTX-M27 beta-lactamase, incorporated into a plasmid. The resistance element in *Salmonella* could be transferred back into a susceptible *E. coli* strain, where it also was located on a plasmid. Although we have not conducted the detailed DNA sequencing done by McCollister et al., we believe that our results may reflect a similar process, but with gene transfer between *E. cloacae* and *E. coli*. Notably, beta-lactam antibiotics such as ceftriaxone do induce the SOS response (Drago et al., 2004; Maiques et al., 2006), and so SOS induction could have played a role in the *in vivo* transfer of the resistance gene in the GI tract of the patient described by McCollister et al. It is also notable that the work of McCollister et al. (2016) and Beaber et al. (2003), and the work in this study all used wild-type enteric pathogens in their studies of DNA transfer between species. Over-reliance on highly passaged laboratory strains of *E. coli* in the past may have prevented earlier recognition of these phenomena.

Although DNA, especially ssDNA, is often degraded upon entry into *E. coli* cells via the competence (Com) gene locus (Finkel and Kolter, 2001; Palchevskiy and Finkel, 2006), it is possible that when the SOS is induced, RecA becomes abundant enough that it is able to catalyze recombination of ssDNA with the recipient cell's DNA before the newly acquired DNA is degraded (Beaber et al., 2003). If so, this would explain why transfer of the β -lactam resistance was greatest when the SOS response was induced in the recipient as well as the donor strain (Figures 3B,C). While the mechanism of the DNA transfer is not clear, what is clear is that transfer is triggered by the SOS response, and that the transfer is strongly inhibited by zinc, raising the possibility that zinc compounds could be used to block horizontal transfer of antibiotic resistance in situations where this gene transfer would be undesirable.

Other authors have suggested that a good way to exploit RecA inhibitors under development would be to reverse pre-existing antibiotic resistance, i.e., in strains already resistant to antibiotics such as the quinolones (Alam et al., 2016; Recacha et al., 2017).

We suggest that a more effective strategy would be to use RecA inhibitors, including zinc compounds, to prevent the emergence of resistance in situations where sensitive microbes are still present, but induction of the SOS response would be expected or inevitable, such as when UV light, ionizing radiation, cytotoxic cancer chemotherapy, or other SOS-inducing drugs are used (Rutala et al., 2010).

Although zinc-containing RecA inhibitors show promise for preventing emergence of antibiotic resistance, a concern is whether zinc resistance could emerge as a bacterial counter-measure. Zinc resistance seems to be uncommon in bacteria, but has been reported (McHugh et al., 1975; Hau et al., 2017). Therefore, if RecA inhibitors are ever adopted for use in human or veterinary medicine, animal agriculture, or food processing, prudence and stewardship in use of these RecA inhibitors may become as necessary as prudence and stewardship in the use of antibiotics themselves.

AUTHOR CONTRIBUTIONS

MC did the initial hypermutation experiments with *E. cloacae* and began the inter-species gene transfer experiments. MO did all of the experiments with zinc ionophores. JC completed inter-species gene transfer experiments, performed the EMSA's, the PCR experiments, and wrote the manuscript. MS helped design experiments, reviewed the manuscript, and made helpful critiques.

FUNDING

This work was supported by funds from the Dept. of Internal Medicine, University at Buffalo, and by support from the CLIMB UP program for the summer stipend for MO.

ACKNOWLEDGMENTS

We thank Elena Rechkina, Ph.D., ID Genomics, for help in determining the type of β -lactamase present in *E. cloacae*. We also thank Eric DeCoursey for assistance in ordering supplies and reagents.

SUPPLEMENTARY MATERIAL

The Supplementary Material for this article can be found online at: <https://www.frontiersin.org/articles/10.3389/fcimb.2018.00410/full#supplementary-material>

REFERENCES

- Alam, M. K., Alhazmi, A., Decoteau, J. F., Luo, Y., and Geyer, C. R. (2016). RecA inhibitors potentiate antibiotic activity and block evolution of antibiotic resistance. *Cell Chem. Biol.* 23, 381–391. doi: 10.1016/j.chembiol.2016.02.010
- Baharoglu, Z., and Mazel, D. (2011). *Vibrio cholerae* triggers SOS and mutagenesis in response to a wide range of antibiotics: a route towards multiresistance. *Antimicrob. Agents Chemother.* 55, 2438–2441. doi: 10.1128/AAC.01549-10
- Bao, V. W., Lui, G. C., and Leung, K. M. (2014). Acute and chronic toxicities of zinc pyrrhione alone and in combination with copper to the marine copepod *Tigriopus japonicus*. *Aquat. Toxicol.* 157, 81–93. doi: 10.1016/j.aquatox.2014.09.013
- Beaber, J. W., Hochhut, B., and Waldor, M. K. (2003). SOS response promotes horizontal dissemination of antibiotic resistance genes. *Nature* 427, 72–74. doi: 10.1038/nature02241

- Bonnet, R. (2004). Growing group of extended-spectrum β -lactamases: the CTX-M enzymes. *Antimicrob. Agents Chemother.* 48, 1–14. doi: 10.1128/AAC.48.1.1-14.2004
- Bunnell, B. E., Escobar, J. F., Bair, K. L., Sutton, M., and Crane, J. (2017). Zinc blocks SOS-induced hypermutation via inhibition of RecA in *Escherichia coli*. *PLoS ONE* 12:e0178303. doi: 10.1371/journal.pone.0178303
- Chen, I., and Dubnau, D. (2004). DNA uptake during bacterial transformation. *Nat. Rev. Microbiol.* 2:241. doi: 10.1038/nrmicro844
- Cirz, R. T., and Romesberg, F. E. (2006). Induction and inhibition of ciprofloxacin resistance-conferring mutations in hypermutator bacteria. *Antimicrob. Agents Chemother.* 50, 220–225. doi: 10.1128/AAC.50.1.220-225.2006
- Crane, J. K., Broome, J. E., Reddinger, R. M., and Werth, B. B. (2014). Zinc protects against shiga-toxicogenic *Escherichia coli* by acting on host tissues as well as on bacteria. *BMC Microbiol.* 14:145. doi: 10.1186/1471-2180-14-145
- Drago, L., De Vecchi, E., Nicola, L., Tocalli, L., and Gismondo, M. R. (2004). Effect of moxifloxacin on bacterial pathogenicity factors in comparison with amoxicillin, clarithromycin and ceftriaxone. *J. Chemother.* 16, 30–37. doi: 10.1179/joc.2004.16.1.30
- Finkel, S. E., and Kolter, R. (2001). DNA as a nutrient: novel role for bacterial competence gene homologs. *J. Bacteriol.* 183, 6288–6293. doi: 10.1128/JB.183.21.6288-6293.2001
- Goodman, M. F. (2002). Error-prone repair DNA polymerases in prokaryotes and eukaryotes. *Annu. Rev. Biochem.* 71, 17–50. doi: 10.1146/annurev.biochem.71.083101.124707
- Hau, S. J., Frana, T., Sun, J., Davies, P. R., and Nicholson, T. L. (2017). Zinc Resistance within swine-associated methicillin-resistant *Staphylococcus aureus* isolates in the United States is associated with multilocus sequence type lineage. *Appl. Environ. Microbiol.* 83:e00756-17. doi: 10.1128/AEM.00756-17
- Jung, C. M. (2014). Dissemination of bacterial fluoroquinolone resistance in two multidrug-resistant enterobacteriaceae. *J. Mol. Microbiol. Biotechnol.* 24, 130–134. doi: 10.1159/000362278
- Kohanski, M. A., Depristo, M. A., and Collins, J. J. (2010). Sublethal antibiotic treatment leads to multidrug resistance via radical-induced mutagenesis. *Mol. Cell* 37, 311–320. doi: 10.1016/j.molcel.2010.01.003
- Lee, A. M., Ross, C. T., Zeng, B.-B., and Singleton, S. F. (2005). A molecular target for suppression of the evolution of antibiotic resistance: inhibition of the *Escherichia coli* RecA protein by N6-(1-Naphthyl)-ADP. *J. Med. Chem.* 48, 5408–5411. doi: 10.1021/jm050113z
- Lee, A. M., and Singleton, S. F. (2004). Inhibition of the *Escherichia coli* RecA protein: zinc (II), copper (II) and mercury (II) trap RecA as inactive aggregates. *J. Inorg. Biochem.* 98, 1981–1986. doi: 10.1016/j.jinorgbio.2004.08.018
- Maiques, E., Úbeda, C., Campoy, S., Salvador, N., Lasa, Í., Novick, R. P., et al. (2006). β -Lactam antibiotics induce the SOS response and horizontal transfer of virulence factors in *Staphylococcus aureus*. *J. Bacteriol.* 188, 2726–2729. doi: 10.1128/JB.188.7.2726-2729.2006
- McCollister, B., Kotter, C. V., Frank, D. N., Washburn, T., and Jobling, M. G. (2016). Whole genome sequencing identifies *in vivo* acquisition of a blaCTX-M-27-encoding IncFII transmissible plasmid as the cause of ceftriaxone treatment failure for an invasive *Salmonella enterica* serovar Typhimurium infection. *Antimicrob. Agents Chemother.* 60, 7224–7235. doi: 10.1128/AAC.01649-16
- McHugh, G. L., Moellering, R., Hopkins, C., and Swartz, M. (1975). *Salmonella typhimurium* resistant to silver nitrate, chloramphenicol, and ampicillin: a new threat in burn units? *Lancet* 305, 235–240. doi: 10.1016/S0140-6736(75)91138-1
- Nautiyal, A., Patil, K. N., and Muniyappa, K. (2014). Suramin is a potent and selective inhibitor of *Mycobacterium tuberculosis* RecA protein and the SOS response: RecA as a potential target for antibacterial drug discovery. *J. Antimicrob. Chemother.* 69, 1834–1843. doi: 10.1093/jac/dku080
- Palchevskiy, V., and Finkel, S. E. (2006). *Escherichia coli* competence gene homologs are essential for competitive fitness and the use of DNA as a nutrient. *J. Bacteriol.* 188, 3902–3910. doi: 10.1128/jb.01974-05
- Pierard-Franchimont, C., Goffin, V., Decroix, J., and Pierard, G. E. (2002). A multicenter randomized trial of ketoconazole 2% and zinc pyrithione 1% shampoos in severe dandruff and seborrheic dermatitis. *Skin Pharmacol. Appl. Skin Physiol.* 15, 434–441. doi: 10.1159/000066452
- Priestley, G. C., and Brown, J. C. (1980). Acute toxicity of Zinc pyrithione to human skin cells *in vitro*. *Acta Derm. Venereol.* 60, 145–148.
- Radman, M. (1975). “SOS repair hypothesis: phenomenology of an inducible DNA repair which is accompanied by mutagenesis,” in *Molecular Mechanisms for Repair of DNA*, eds P. C. Hanawalt and R. B. Setlow (Boston, MA: Springer), 355–367.
- Recacha, E., Machuca, J., Díaz de Alba, P. D., Ramos-Güelfo, M., Docobo-Pérez, F., Rodríguez-Beltrán, J., et al. (2017). Quinolone resistance reversion by targeting the SOS response. *mBio* 8:e00971-17. doi: 10.1128/mBio.00971-17
- Reeder, N. L., Xu, J., Youngquist, R. S., Schwartz, J. R., Rust, R. C., and Saunders, C. W. (2011). The antifungal mechanism of action of zinc pyrithione. *Brit. J. Dermatol.* 165(Suppl. 2), 9–12. doi: 10.1111/j.1365-2133.2011.10571.x
- Rutala, W. A., Gergen, M. F., and Weber, D. J. (2010). Room decontamination with UV radiation. *Infect. Control Hospital Epidemiol.* 31, 1025–1029. doi: 10.1086/656244
- Schwartz, J. R. (2016). Zinc pyrithione: a topical antimicrobial with complex pharmaceuticals. *J. Drugs Dermatol.* 15, 140–144.
- Song, L. Y., Goff, M., Davidian, C., Mao, Z., London, M., Lam, K., et al. (2016). Mutational consequences of ciprofloxacin in *Escherichia coli*. *Antimicrob. Agents Chemother.* 60, 6165–6172. doi: 10.1128/aac.01415-16
- Svingen, R., Takahashi, M., and Åkerman, B. (2001). Gel-shift assays: migrative dissociation of a RecA-oligonucleotide complex during electrophoresis in hydroxyethylated agarose gels. *J. Phys. Chem. B* 105, 12879–12893. doi: 10.1021/jp011674e
- Szczepanowski, R., Linke, B., Krahn, I., Gartemann, K.-H., Gützkow, T., Eichler, W., et al. (2009). Detection of 140 clinically relevant antibiotic-resistance genes in the plasmid metagenome of wastewater treatment plant bacteria showing reduced susceptibility to selected antibiotics. *Microbiology* 155, 2306–2319. doi: 10.1099/mic.0.028233-0
- Wigle, T. J., Lee, A. M., and Singleton, S. F. (2006). Conformationally selective binding of nucleotide analogues to *Escherichia coli* RecA: a ligand-based analysis of the RecA ATP binding site. *Biochemistry* 45, 4502–4513. doi: 10.1021/bi052298h
- Wigle, T. J., Sexton, J. Z., Gromova, A. V., Hadimani, M. B., Hughes, M. A., Smith, G. R., et al. (2009). Inhibitors of RecA activity discovered by high-throughput screening: cell-permeable small molecules attenuate the SOS response in *Escherichia coli*. *J. Biomol. Screen.* 14, 1092–1101. doi: 10.1177/1087057109342126

Conflict of Interest Statement: The authors declare that the research was conducted in the absence of any commercial or financial relationships that could be construed as a potential conflict of interest.

Copyright © 2018 Crane, Cheema, Olyer and Sutton. This is an open-access article distributed under the terms of the Creative Commons Attribution License (CC BY). The use, distribution or reproduction in other forums is permitted, provided the original author(s) and the copyright owner(s) are credited and that the original publication in this journal is cited, in accordance with accepted academic practice. No use, distribution or reproduction is permitted which does not comply with these terms.



Morin Protects Channel Catfish From *Aeromonas hydrophila* Infection by Blocking Aerolysin Activity

Jing Dong^{1,2}, Yongtao Liu^{1,2}, Ning Xu^{1,2}, Qihong Yang^{1,2} and Xiaohui Ai^{1,2*}

¹ Yangtze River Fisheries Research Institute, Chinese Academy of Fishery Sciences, Wuhan, China, ² Key Laboratory of Control of Quality and Safety for Aquatic Products, Ministry of Agriculture, Beijing, China

OPEN ACCESS

Edited by:

Natalia V. Kiriienko,
Rice University, United States

Reviewed by:

Durg Vijai Singh,
Institute of Life Sciences (ILS), India
Iddya Karunasagar,
Nitte University, India

*Correspondence:

Xiaohui Ai
aixh@yfi.ac.cn

Specialty section:

This article was submitted to
Infectious Diseases,
a section of the journal
Frontiers in Microbiology

Received: 11 September 2018

Accepted: 05 November 2018

Published: 21 November 2018

Citation:

Dong J, Liu Y, Xu N, Yang Q and
Ai X (2018) Morin Protects Channel
Catfish From *Aeromonas hydrophila*
Infection by Blocking Aerolysin
Activity. *Front. Microbiol.* 9:2828.
doi: 10.3389/fmicb.2018.02828

Aeromonas hydrophila (*A. hydrophila*) is an opportunistic bacterial pathogen widely distributed in the environments, particular aquatic environment. The pathogen can cause a range of infections in both human and animals including fishes. However, the application of antibiotics in treatment of *A. hydrophila* infections leads to the emergence of resistant strains. Consequently, new approaches need to be developed in fighting this pathogen. Aerolysin, the chief virulence factor produced by pathogenic *A. hydrophila* strains has been employed as target identifying new drugs. In our present study, we found that morin, a flavonoid without anti-bacterial activity isolated from traditional Chinese medicine, could directly inhibit the hemolytic activity of aerolysin. To determine the binding sites and the action of mechanism of morin against AerA, several assays were performed. Ser36, Pro347, and Arg356 were identified as the main binding sites affecting the conformation of AerA and resulted in block of the heptameric formation. Moreover, morin could protect Vero cells from cell injury mediated by aerolysin. *In vivo* study showed that morin could provide a protection to channel catfish against *A. hydrophila* infection. These results demonstrated that morin could be developed as a promising candidate for the treatment of *A. hydrophila* infections by decreasing the pathogenesis of *A. hydrophila*.

Keywords: *Aeromonas hydrophila*, aerolysin, morin, anti-virulence, antibiotics

INTRODUCTION

Aeromonas hydrophila (*A. hydrophila*) is a gram-negative aquatic bacterium widely distributed in aquatic water worldwide leading to a number of diseases in fish (Grim et al., 2014). Outbreak of *A. hydrophila* infections resulted in high mortality and severe economic losses to the aquaculture industry all over the world (Zhang et al., 2018). Moreover, the pathogen can transmit from diseased fish, contaminated water or uncooked food to human (Rama Devi et al., 2016). Although *A. hydrophila* is not a typical pathogen for human, it has been reported to be responsible for a range of infections including septicemia, wound infections, burn-associated sepsis, and respiratory tract infections (Santos et al., 1999; Casabianca et al., 2015). Antibiotics are the main approach in the treatment of infections caused by bacterium (Dong et al., 2017a). However, the abuse of antibiotics in aquaculture leads to emergence of antibiotic resistance and environmental pollution (Zhang et al., 2015; Stratev and Odeyemi, 2016). The spread of antibiotic resistance can reduce the effect of antibiotics in the treatment of infections caused *A. hydrophila* and is a potential threaten to

human health (Stratev and Odeyemi, 2016). Therefore, there is an urgent need for new approaches against *A. hydrophila* infections.

As is known, pathogenic *A. hydrophila* can produce a number of virulence factors including proteases, hemolysin (HlyA), aerolysin (AerA), enterotoxins, and acetylcholinesterase which contribute to the pathogenicity of the bacterium (Bi et al., 2007). AerA, a pore forming toxin with hemolytic, cytotoxic and enterotoxic activities produced by all pathogenic *A. hydrophila* strains, plays a critical role in the pathogenicity of *A. hydrophila* and has been identified as a marker of pathogenic *A. hydrophila* strains (Howard and Buckley, 1982; Abrami et al., 2003). The toxin was secreted as a 52 kDa precursor without activity named proaerolysin (pAerA), then the toxin can be activated after cleaving a flexible 43-residue loop near the C-terminus by trypsin or furin (Abrami and van Der Goot, 1999; Iacovache et al., 2011). After binding on the glycosylphosphatidylinositol (GPI) anchor of target cells, the toxin is concentrated and promote forming oligomerization with channel pore that can insert into the membrane (Iacovache et al., 2006). AerA is one of the most well-known and characterized pore forming toxins, previous studies have shown that AerA is the main virulence factor of *A. hydrophila* (Wu and Guo, 2010).

Morin (Figure 1A), a Flavonoid can be isolated from several traditional Chinese medicine, has a series of biological activities such as antioxidant, anti-apoptotic, and anti-inflammatory activity (Huang et al., 2014). In this paper, we found that morin, without anti-*A. hydrophila* activity, could inhibit the hemolytic activity by hindering the heptameric formation of AerA. Then the binding sites were calculated by molecular dynamics simulations and validated by fluorescence quenching assay. Moreover, we demonstrated that morin could protect Vero cells from AerA mediated injury and decrease the mortality of channel catfish (*Ictalurus punctatus*) infected with *A. hydrophila*.

MATERIALS AND METHODS

Micro-Organism and Reagents

Aeromonas hydrophila strain XS-91-4-1 was isolated from diseased *Hypophthalmichthys molitrix* XS-91-4-1 was cultured in brain heart infusion (BHI) medium at 28°C for experiments described below. Morin (purity > 98%) and enrofloxacin (purity > 98%) were obtained from National Institutes for Food and Drug Control (Beijing, China). Stock solutions of both drugs were prepared in dimethyl sulfoxide (DMSO, Sigma-Aldrich, St. Louis, MO, United States). For *in vivo* study, morin was dissolved in sterile PBS. The minimum inhibitory concentrations (MIC) of morin and enrofloxacin were determined by broth micro-dilution method recommended by Clinical and Laboratory Standards Institute [CLSI] (2009).

Growth Curves

Aeromonas hydrophila strain XS-91-4-1 was cultured in BHI medium at 28°C to obtain optical density at 600 nm (OD_{600 nm}) of 0.3, and then the culture was aliquoted into a 100-ml flask and

a series of morin with a final concentration of 0, 4, 8, 16, 32, and 64 µg/mL were added. The mixture was further cultured for 5 h at 28°C. Cell growth was evaluated by recording the OD_{600 nm} values at intervals of 30 min using a spectrophotometer.

Hemolytic Assays

Hemolytic activities were performed using purified AerA and supernatants of *A. hydrophila* co-cultured with different concentrations of morin ranging from 1 to 8 µg/mL. Hemolytic assays were performed according to previous reports (Dong et al., 2013; Dong et al., 2017a). For hemolytic assay of co-cultured supernatant, 100 µL of trypsin treated supernatants were combined with 25 µL defibrinated sheep red blood cells (5×10^6 cells/ml) in hemolytic buffer (20 mM Tris, 150 mM NaCl, pH 7.2). For hemolytic activity of purified AerA, 2 µL of concentrated protein were added into 975 µL hemolytic buffer, 25 µL defibrinated sheep red blood cells were added after incubation at 37°C for 15 min. Following centrifugation, the hemolytic activities of the mixtures were determined by measuring the absorption at 543 nm after further incubated at 37°C for 20 min. Morin-free group was served as 100% hemolytic control.

Western Blot Analysis

Western blot assay was performed as reported elsewhere (Dong et al., 2013). In brief, *A. hydrophila* strain XS-91-4-1 was incubated at 28°C in BHI medium with morin at concentrations of 1, 2, 4, and 8 µg/mL to OD_{600 nm} = 1.5. Supernatants of the culture were centrifuged and the supernatants were used for sodium dodecyl sulfate (SDS)-polyacrylamide (12%) gel electrophoresis, BHI medium was employed as negative control. Then a semi-dry transfer cell was used to transfer the proteins onto a polyvinylidene fluoride membrane. After blocking the membrane with 3% skim milk for 60 min at room temperature, an anti-aerolysin primary polyclonal antibody was incubated with the membrane at 1:1000 dilution overnight at 4°C, and followed incubating with a HRP-conjugated secondary goat anti-rabbit antiserum (diluted 1:5000) for 1 h. The blots were then treated with ECL western blotting detection reagents.

Molecular Docking and Molecular Dynamics

The binding mode between the morin and the pAerA was analyzed by molecular docking method using AutoDock Vina 1.1.2 (Trott and Olson, 2010). The crystal structure of the pAerA (PDB ID: 1PRE) was obtained from Protein Data Bank¹. The structure of morin was drawn by ChemBioDraw Ultra 12.0 and ChemBio3D Ultra 12.0 software. The files for docking were generated by the AutoDockTools 1.5.6 package (Sanner, 1999; Morris et al., 2009). Structures of morin were prepared for docking by merging non-polar hydrogen atoms and defining rotatable bonds. The search grid of the pAerA was identified as center_x: 9.973, center_y: 49.913, and center_z: 27.774 with dimensions size_x: 47.25, size_y: 47.25, and size_z: 47.25. The

¹<http://www.rcsb.org/pdb/home/home.do>

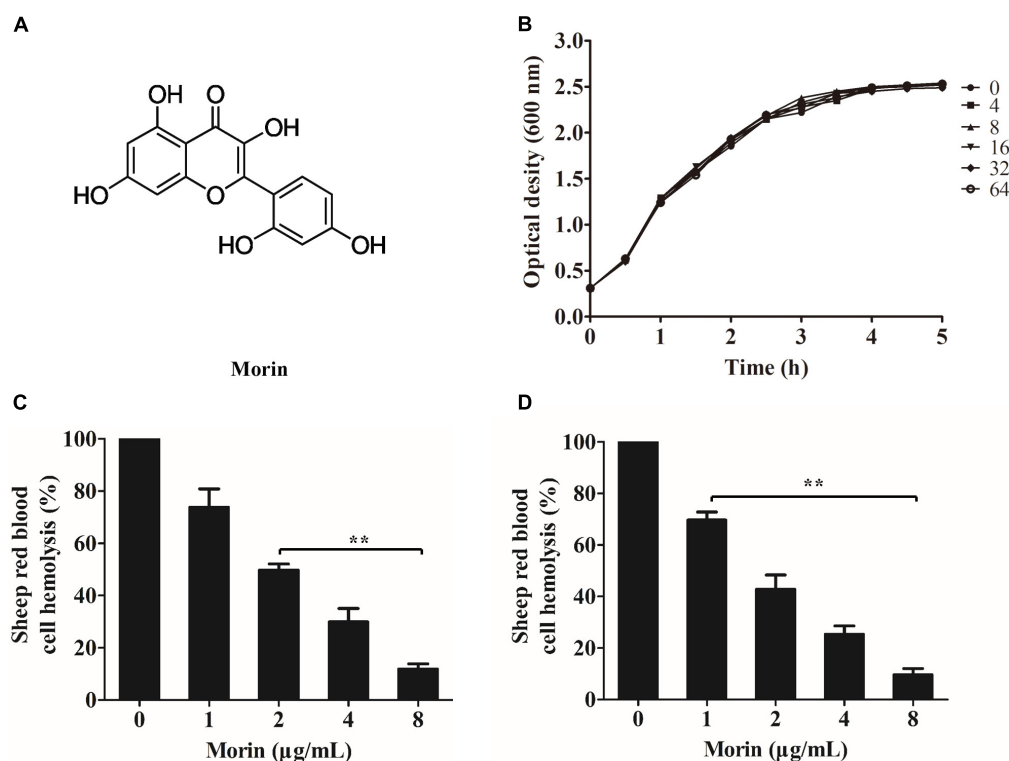


FIGURE 1 | Morin inhibits the hemolytic activity induced by AerA. **(A)** Chemical structure of morin. **(B)** Growth curves of *A. hydrophila* strain XS-91-4-1 co-cultured with different concentrations of morin. **(C)** Inhibition of hemolytic activity of *A. hydrophila* supernatants co-cultured with morin. **(D)** The inhibitory effect of morin against purified AerA. Data shown in panels **(C,D)** were presented as mean value \pm SD of three independent assays. * $p < 0.05$ and ** $p < 0.01$ when compared with the drug-free supernatants or AerA.

exhaustive value was set to 20 to improve the accuracy of the docking. Then the docking results were modified by performance of an MD study.

MD simulations of docked pose were performed by the Amber 14 and AmberTools 15 programs on Dell Precision T5500 workstation as described previously (Gotz et al., 2012; Pierce et al., 2012; Salomon-Ferrer et al., 2013). The automatic topologies, parameters and calculation of partial charges were generated by ACPYPE, a tool based on ANTECHAMBER (Wang et al., 2004, 2006; Sousa da Silva and Vranken, 2012). Then, morin was prepared by forcefield “leaprc.gaff,” while “leaprc.ff14SB” was employed for the preparation of pAerA. The “SolvateOct” command with the minimum distance was performed to put the reaction system in a rectangular box with TIP3P water. The pAerA–morin system was first energy relaxed by 2000 steps of steepest descent and conjugate gradient energy minimization, and then the solvated complex was equilibrated by a 500 ps of heating, and 500 ps of density equilibration with weak restraints. At last, 40 ns of MD simulations were carried out.

Mutagenesis of the pAerA Protein

Plasmid encoding wild-type (WT) pAerA was constructed as we reported previously (Dong et al., 2017b). Plasmid encoding S36A-pAerA, P347A-pAerA, and R356A-pAerA were conducted according to the instruction of the QuikChange

site-directed mutagenesis kit (Stratagene, CA, United States) from WT-pAerA plasmid. Prime pairs for the mutant were listed in **Supplementary Table 1**. Then protein expression and purification were performed according to previous report (Dong et al., 2017b). Proteins were concentrated in storage buffer (25 mM Tris, 150 mM NaCl, pH 9.0) to avoid oligomerization by ultrafiltration. Trypsin was added in to purified proteins for activation by cleaving 43 residues at the C-terminal of the protein. After incubation at room temperature for 10 min, the reaction was stopped by addition of a 10-fold excess of trypsin/chymotrypsin inhibitor (Abrami and van Der Goot, 1999). Activated proteins were stored at -80°C for further applications.

Binding Affinity Determination of WT-AerA and Mutants

The binding constants (K_A) of morin to WT-AerA and mutants were determined by the fluorescence quenching method using a Cary Eclipse fluorescence spectrophotometer (Agilent Technologies, Santa Clara, CA, United States) as described previously (Jurasekova et al., 2009; Ibrahim et al., 2010). Briefly, A 280-nm excitation wavelength with a 5-nm band-pass and a 345-nm emission wavelength with a 10-nm band-pass were set up for the fluorescence spectrofluorimetry measurement.

Inhibition of Oligomerization

Inhibition of oligomerization was performed as described previously. In brief, WT-AerA was mixed with morin at the same mol ratio as performed in hemolytic assays, the mixtures with a volume of 20 μ L were incubated at 37°C for 15 min. Then 1 μ L 1 M Hepes were added to each sample to match the pH (pH < 8) of oligomerization. The mixtures were then loaded onto 8% SDS-PAGE gels for electrophoresis after incubated at 4°C for 1 h.

Cell Viability Assays

Vero cells were obtained from the American Tissue Culture Collection (ATCC) and were cultured in DMEM supplemented with 10% fetal bovine serum at 37°C with 5% CO₂ in a humidified incubator. Cells with a density of 1.5×10^5 per well were seeded into 96-well cell culture plates. After incubated for 16 h at 37°C with 5% CO₂, cells were co-cultured with 100 μ L of AerA at a concentration of 1 μ g/mL and indicated concentrations of morin at 37°C for 24 h. All assays were performed in triplicate measurements.

The determinations of cell viability were performed by lactate dehydrogenase (LDH) release using a Cytotoxicity Detection Kit and live/dead assay with a live (green)/dead (red) reagent. Dead cells were stained by propidium iodide with a fluorescent-red dye, while live cells were stained by calcein AM with a fluorescent-green dye. Cell images were taken by a confocal laser scanning microscope (Nikon, Japan). LDH activity was determined on a microplate reader (Tecan, Austria).

Ethics Statement

All animal assays were carried out according to the experimental practices and standards developed by the Animal Welfare and Research Ethics Committee at Yangtze River Fisheries Research Institute. All the assays were approved and supervised by the animal care committee (Permit No. 20171105-009C).

Channel Catfish Model Infected With *A. hydrophila*

Channel catfish weighing 200 ± 5 g were separated into three groups and maintained in 100 L glass aquaria tanks at 28°C for 15 days before infection. Channel catfish were infected with *A. hydrophila* by injecting 200 μ L XS-91-4-1 suspension intraperitoneally. Fish injected with sterile PBS served as negative control. Infected channel catfish were administered with 25 mg/kg of morin or PBS 6 h postinfection and at 12-h intervals for 3 days. For negative control, fish were administered with PBS at the same intervals. Each group contains 10 channel catfish. The death of each group were monitored every day for 8 days.

Statistical Analysis

The experimental data were compared by independent Student's *t*-test with SPSS 14.0 statistical software (SPSS Inc., Chicago, IL, United States). Survival rate of channel catfish was analyzed with Kaplan-Meier test, log-rank test was carried out to analyze the

significance of different groups. A *p*-value <0.05 was considered to be statistically significant.

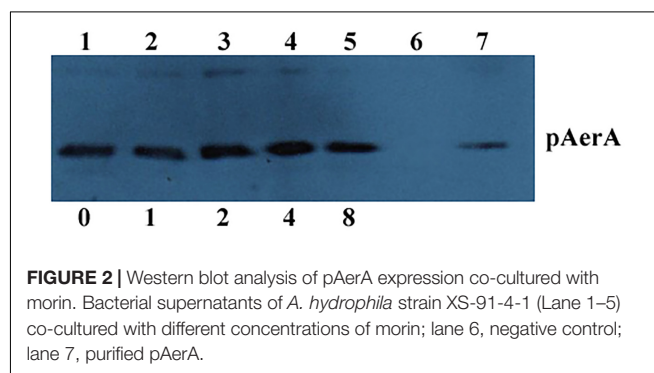
RESULTS

Morin Inhibits the Hemolytic Activity of AerA

Minimum inhibitory concentrations and growth curves were performed to evaluate the influence of morin on the growth of *A. hydrophila*. According to the results of MICs, morin had no evident inhibitory effect on *A. hydrophila* XS-91-4-1 strain, while the MIC of enrofloxacin was 4 μ g/mL. Moreover, the results of growth curves with different concentrations of morin showed that morin could not influence the growth of *A. hydrophila* XS-91-4-1 strain from the concentration of 4–64 μ g/mL (Figure 1B). In the present paper, we found that morin could not affect the expression of pAerA (Figure 2), but could inhibit the hemolytic activity of *A. hydrophila* XS-91-4-1 when co-cultured with definite concentrations of morin (Figure 1C). Before analysis, the concentrations of total protein in supernatants were determined by a BCA protein assay kit. The concentrations were 1.45, 1.42, 1.44, 1.36, and 1.47 mg/mL for the strain co-cultured with morin at concentrations of 0, 1, 2, 4, and 8 μ g/mL, respectively. Furthermore, the hemolytic activity of purified AerA could be inhibited in a dose-dependent manner (Figure 1D). When treated with 8 μ g/mL morin, the hemolytic activities of supernatant and purified AerA were significantly decreased to 11.86 and 9.62%, respectively. Thus, it is infer that morin can inhibit the activity of AerA directly according to these findings.

Determination of Binding Sites by Molecular Dynamics

The AutoDock Vina 1.1.2 and Amber 14 software package were employed to analyze the potential binding mode of AerA–morin complex using molecular docking and molecular dynamics simulation methods. According to the docking results, the binding mode of AerA–morin complex was determined by 40-ns molecular dynamics simulations. As shown in Supplementary Figure 1, the root-mean-square deviation (RMSD) values of the initial structure of pAerA were calculated to confirm the dynamic stability and the rationality. The protein structures of



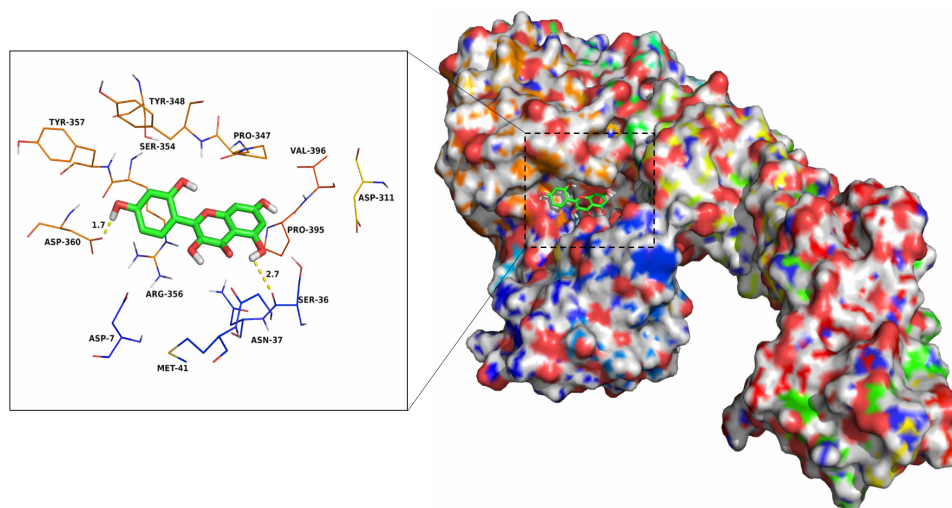


FIGURE 3 | The predicted binding mode of morin in pAerA binding pocket obtained from MD simulation.

the two systems were stabilized during the 40-ns simulation (**Supplementary Figure 1**).

The flexibility of residues between pAerA–morin complex and free pAerA were determined by the root mean square fluctuations (RMSF). As shown in **Supplementary Figure 2**, the difference of flexibilities in the binding site of pAerA was described in the absence or presence of morin. Compared with the free pAerA, a smaller degree of flexibility with a RMSF of less than 3 Å was discovered at the majority of the residues positions 91–470 in the pAerA, which suggested that the residues binding to morin became more rigid. While a big degree of flexibility with the RMSF values nearly reached to 13 Å was found at the position 2–90, which indicated that the residues became more flexible when binding to morin.

The electrostatic, *Van der Waals*, solvation, and total contribution of the residues to the binding free energy were analyzed using the MMGBSA method to evaluate the binding sites and contribution of residues to the system. The per residue interaction free energies were separated into *Van der Waals* (ΔE_{vdw}), electrostatic (ΔE_{ele}), solvation (ΔE_{sol}), and total contribution (ΔE_{total}). In the pAerA–morin complex, the residue Asp-360 have a strong electrostatic (ΔE_{ele}) contribution, with the value of <-9.0 kcal/mol (**Supplementary Figure 3**). Detailed analysis showed that the residue Asp-360 is oriented to the phenyl group of the morin, and electrostatic interaction exist, leading to the anion- π interaction and one strong hydrogen bond interaction (bond length: 1.7 Å) between the pAerA and the morin (**Figure 3**). In addition, the residues Pro-347 and Arg-356, with the ΔE_{vdw} of <-2.0 kcal/mol, have an appreciable *Van der Waals* interactions with the morin because of the close proximity between the residues and the morin. Except for the residues Ser-36, Ser-354, and Asp-360, *Van der Waals* interactions was found to be the major decomposed energy, apparently through hydrophobic interactions (i.e., Met-41, Pro-347, Pro-395, and Val-396). In addition, the total binding free energy for the

pAerA–morin complex calculated according to the MMGBSA approach, and the an estimated binding free energy (ΔG_{bind}) of -14.4 kcal/mol was found for morin, which revealed that morin could strongly bind to and interact with the binding site of the pAerA. Moreover, to confirm the main binding sites of morin–AerA system, ΔG_{bind} of morin binding to active site of AerA was calculated (**Table 1**). In summary, the above molecular simulations explained the interactions between morin and proaerolysin, which provided useful information for identification of the pAerA inhibitors.

Determination of the Mechanism of Morin Inhibiting the Activity of AerA

The fluorescence quenching assay was performed to confirm the results of molecular dynamics. As shown in **Table 1**, ΔG_{bind} of morin is the highest with WT-AerA, followed by Arg356A mutant, Pro347A mutant, and then Ser36A mutant, which suggesting that the ability of morin binding with WT-AerA is the strongest among all types of proteins. Similar results of the binding constants (K_A) and the number of binding sites (n) between morin and proteins calculated by the fluorescence quenching method were obtained, indicating that findings obtained by the computational methods could be used for further research. Moreover, the oligomerization assay were carried out to analyze the mechanism of morin inhibiting the

TABLE 1 | The binding free energy (ΔG_{bind}) based on a computational method and the values of the binding constants (K_A) based on the fluorescence-quenching method.

	WT-AerA	R356A	P347A	S36A
ΔG_{bind} (kcal/mol)	−14.4	−2.64	−2.18	−1.16
K_A (1×10^4) L mol ^{−1}	12.2	7.74	6.19	0.88
n	1.0998	1.0254	1.0305	0.8539

activity of AerA. As expected, morin could reduce the production of heptamer in a dose-dependent manner (Figure 4). When the mol ratio of AerA and morin reached to 1:600, no visible heptamer was observed. Moreover, the hemolytic activities of the mutants were determined, the results showed that there was no evident difference between WT-AerA and mutants (data not shown). The results indicates that mutations do not affect the formation of heptamer. Taken together, when morin binds to WT-AerA, the conformation of AerA was changed (Supplementary Figures 1, 2) and resulted in the decrease of heptamer.

Morin Protects Vero Cells From Cell Injury Induced by AerA

It is reported that AerA can target to a number of mammalian cells, such as fibroblast like cells, lymphocytes, granulocytes, erythrocytes, and epithelial cells (Abrami et al., 2003). As reported previously, Vero cells were widely used in the measurement toxicity of aerolysin (Dong et al., 2017b). Therefore, Vero cells were employed to investigate the protective effects of morin against AerA mediated cell injury. Vero cells were stained with the live/dead reagent after incubation with AerA and indicated concentrations of morin. Then cell viability was monitored by a confocal laser scanning microscope. As shown in Figure 5A, live cells were exhibited to be green, while dead cells were red (Figure 5B). When co-cultured with AerA and 8 $\mu\text{g/mL}$ morin, no evident cell death was observed (Figure 5C). Moreover, the

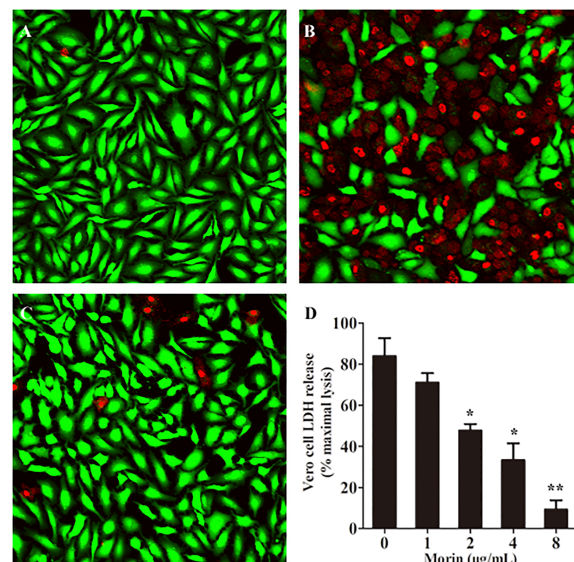


FIGURE 5 | Morin protects Vero cells from AerA-induced cell injury. Vero cells were stained with live (green)/dead (red) reagent and were captured by a confocal laser scanning microscope after treated with AerA with the presence or absence of morin. A fluorescent-red dye stained dead cells, while a fluorescent-green dye stained live cells. (A) untreated cells; (B) cells treated with AerA in the absence of morin; (C) cells treated with AerA in the presence of 8 $\mu\text{g/mL}$ morin; and (D) LDH release by Vero cells when treated with AerA and indicated concentrations of morin. All were presented as mean value \pm SD of three independent experiments. * $p < 0.05$ and ** $p < 0.01$ when compared with the drug-free group.

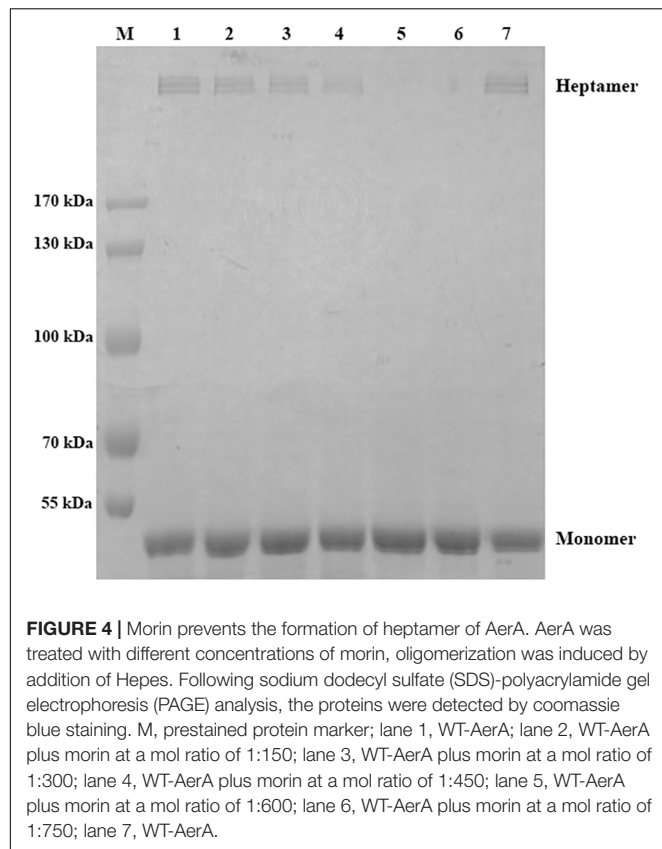


FIGURE 4 | Morin prevents the formation of heptamer of AerA. AerA was treated with different concentrations of morin, oligomerization was induced by addition of Hepes. Following sodium dodecyl sulfate (SDS)-polyacrylamide gel electrophoresis (PAGE) analysis, the proteins were detected by coomassie blue staining. M, prestained protein marker; lane 1, WT-AerA; lane 2, WT-AerA plus morin at a mol ratio of 1:150; lane 3, WT-AerA plus morin at a mol ratio of 1:300; lane 4, WT-AerA plus morin at a mol ratio of 1:450; lane 5, WT-AerA plus morin at a mol ratio of 1:600; lane 6, WT-AerA plus morin at a mol ratio of 1:750; lane 7, WT-AerA.

cell viability was determined by measuring the release of LDH in each sample. As expected, morin could protect Vero cells from AerA mediated cell injury in a dose dependent manner from concentrations of 1–8 $\mu\text{g/mL}$ (Figure 5D). These findings demonstrated that morin could provide an *in vitro* protection to Vero cells against AerA induced cell injury.

Morin Protects Channel Catfish From *A. hydrophila* Infection

According to previous studies, the pathogenicity of *A. hydrophila* strains lacking of *aerA* gene was significantly reduced, which revealed that AerA played an important role in *A. hydrophila* infections (Chakraborty et al., 1987). Our results have shown that morin could significantly reduce the hemolytic activity of AerA and protect Vero cells from cell injury mediated by AerA *in vitro*, which indicated that morin had potent protective effect against infections caused by *A. hydrophila* *in vivo*. Thus, an infection model of channel catfish was established to investigate the *in vivo* therapeutic effect of morin. Channel catfish infected with *A. hydrophila* (3×10^7 CFU per fish) were then treated with either 25 mg/kg morin or sterilized PBS as control. As shown in Figure 6, deaths were observed 24 h postinfection. Skin of fish infected with *A. hydrophila* alone exhibited swelling and ulcers. Fish administered with PBS resulted in 90% death, while 30% of fish treated with 25 mg/kg morin (Figure 6). In conclusion,

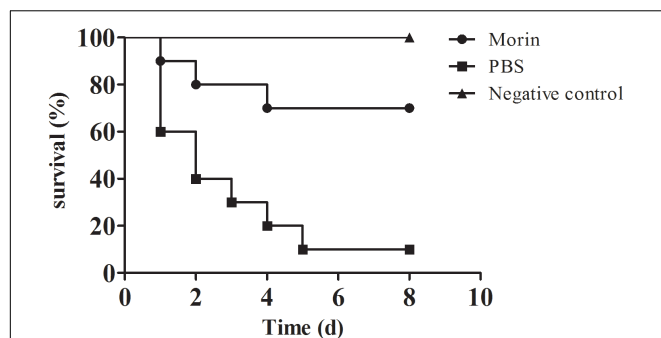


FIGURE 6 | Morin treatment reduce the mortality of channel catfish infected with *A. hydrophila*. Infected channel catfish were administered with 25 mg/kg morin or PBS as positive control, the mortality of channel catfish was monitored for 8 days. The mortality for morin-treated group is significantly different from group for positive control when analyzed by log-rank test ($p = 0.026$ for morin-treated group).

morin could significantly reduce the mortality of channel catfish infected with *A. hydrophila* ($p = 0.026$).

DISCUSSION

Large amount of antibiotics were discovered and used for the treatment of human infectious diseases, as well as for animal husbandry and aquaculture since the discovery of penicillin (Nikaido, 2009). Though the discovery and application of antibiotics reduced the mortality of infectious diseases to some extent, the abuse of antibiotics brought up new challenges. Following the stress of antibiotics on the life of bacterial pathogens, drug resistant, even multi-resistant strains were emerged. The spread of antibiotic resistance resulted in failure of antibiotic treatment. *A. hydrophila*, a typical pathogenic strain of aquatic environment, has been recognized as a human pathogen responsible for several diseases in human and other terrestrial animal worldwide (Stratev and Odeyemi, 2016). Because of the rapid development of aquaculture and the widespread use of antibiotics, multi-resistant *A. hydrophila* strains were isolated to be resistant to several antibiotics, including quinolones and tetracycline which are frequently used in aquaculture (Deng et al., 2014). The increasing incidence of *A. hydrophila* resistance has become a new public health concern. Thus, novel strategies to control bacterial infections caused by resistant *A. hydrophila* are urgently needed (Defoirdt et al., 2011). Anti-virulence therapy, targeting on virulence expression, activity, or regulation rather than inhibiting the growth of bacteria, has been introduced and was well investigated (Clatworthy et al., 2007). Pore-forming toxins (PFTs) are one of the most common bacterial extracellular proteins and are critical for the pathogenicity in a mount of bacteria, such as *Staphylococcus aureus* (*S. aureus*), *Streptococcus pneumoniae* (*S. pneumoniae*), *A. hydrophila*, *Clostridium perfringens* (*C. perfringens*), and *Escherichia coli* (*E. coli*) (Los et al., 2013). PFTs have been identified as unique targets for novel drugs against these pathogens because of their universal presence (Los et al., 2013).

Studies using PFTs as target have shown significant effect against bacterial infections both *in vitro* and *in vivo* (Dong et al., 2013; Li et al., 2015; Song et al., 2016).

As is known, the pathogenesis of *A. hydrophila* was contributed by expression and secretion of extracellular virulence factors (Singh et al., 2013). Among them, two different kinds of PFTs named AerA and HlyA play important roles in infections caused by *A. hydrophila*. According to previous studies, the hemolytic activity was eliminated only when both HlyA (*hlyA*) and AerA (*aerA*) gene were double mutated (Wong et al., 1998). Moreover, the *hlyA* and *aerA* gene were identified in all the virulent *A. hydrophila* strains (Heuzenroeder et al., 1999). Consequently, AerA and HlyA were recognized as potent targets in identifying novel drugs (Dong et al., 2017a). Several works have determined the structure of AerA and mechanism of forming pore (Parker et al., 1994; Degiacomi et al., 2013). AerA is a member of toxins containing a high percentage of β -sheet. Following binding on the membranes of target cells, the heptamer with a 2 nm channel pore was formed which resulted in ion fluxes leading to cell death (Abrami et al., 2000; Bischofberger et al., 2016). Moreover, previous studies have shown that the pathogenesis of *A. hydrophila* strain mutated *aerA* to a mouse model was significantly decreased compared with the WT strain (Chakraborty et al., 1987). All these findings revealed that AerA could be chosen as a convincing target in drug discovery.

There have been several successful attempts identifying small molecules inhibiting the activity or expression of AerA and antibodies. In our previous study, we found that magnolol isolated from traditional Chinese medicine could significantly reduce the mortality of channel catfish infected with *A. hydrophila* via inhibiting the transcription of *aerA* (Dong et al., 2017a). In this paper, another natural compound named morin was identified that could directly inhibit the activity of AerA. Morin has been reported that could reduce the mortality of mice from pneumonia caused by *S. aureus* by blocking the activity of α -toxin produced by *S. aureus* (Wang et al., 2015). Similar results were has been identified that morin could reduce the *Streptococcus suis* pathogenicity in a mice model by neutralizing the activity of suilysin (Li et al., 2017). However, the effect of morin on *A. hydrophila* is not investigated. Compared with four kinds of indolo[3,2-*b*]quinoline, compounds against the activity of aerolysin-like hemolysin (ALH) produced by *A. sobria*, the mechanism and binding site of morin inhibiting AerA were determined using molecular dynamics and fluorescence quenching methods (Takahashi et al., 2016). Moreover, the *in vivo* effect against *A. hydrophila* infection has been evaluated by a channel catfish model. As expected, 25 mg/kg morin could provide a protection of 70% to fish infected with *A. hydrophila*. Rosmarinic acid has been reported that could inhibit the hemolysis induced by *A. hydrophila* supernatant by down-regulate the transcription of *aerA* and *ahh1* (Rama Devi et al., 2016). The inhibiting dose of rosmarinic acid was much higher than morin in this report, but several factors regulated by the quorum sensing system was suppressed and similar *in vivo* effect was achieved (Rama Devi et al., 2016). Some metal ions such as Zinc, cupric, and cadmium have been identified as inhibitors of hemolysis caused

by AerA. However, the inhibition only occurred when continuous ions were presented, which limited the application under field conditions (Avigad and Bernheimer, 1976). Another approach against AerA is vaccine. Several different types of vaccines have been identified in recent years. Although some of them showed higher protective effects against *A. hydrophila* infections than small molecules, the protection against different *A. hydrophila* isolates needs to be further studied (Anuradha et al., 2010). Although these findings have shown a convincing results against *A. hydrophila* both *in vitro* and *in vivo*, more efforts are still needed before morin can be used in aquaculture farming and human clinic. Moreover, the risk of *A. hydrophila* infections after antibiotic treatment has not been clarified, thus antibiotic treatment combined with morin is not recommended before any experimental data was carried out. Despite this, the findings provided a new approach in identifying novel drugs against *A. hydrophila* infections. Collectively, it is reasonable to infer that morin may be a potential agent for the treatment of infections caused by resistant *A. hydrophila*.

REFERENCES

- Abrami, L., Fivaz, M., Glauser, P. E., Sugimoto, N., Zurzolo, C., and Van Der Goot, F. G. (2003). Sensitivity of polarized epithelial cells to the pore-forming toxin aerolysin. *Infect. Immun.* 71, 739–746. doi: 10.1128/IAI.71.2.739-746.2003
- Abrami, L., Fivaz, M., and Van Der Goot, F. G. (2000). Adventures of a pore-forming toxin at the target cell surface. *Trends Microbiol.* 8, 168–172. doi: 10.1016/S0966-842X(00)01722-4
- Abrami, L., and van Der Goot, F. G. (1999). Plasma membrane microdomains act as concentration platforms to facilitate intoxication by aerolysin. *J. Cell Biol.* 147, 175–184. doi: 10.1083/jcb.147.1.175
- Anuradha, K., Foo, H. L., Mariana, N. S., Loh, T. C., Yusoff, K., Hassan, M. D., et al. (2010). Live recombinant *Lactococcus lactis* vaccine expressing aerolysin genes D1 and D4 for protection against *Aeromonas hydrophila* in tilapia (*Oreochromis niloticus*). *J. Appl. Microbiol.* 109, 1632–1642. doi: 10.1111/j.1365-2672.2010.04789.x
- Avigad, L. S., and Bernheimer, A. W. (1976). Inhibition by zinc of hemolysis induced by bacterial and other cytolytic agents. *Infect. Immun.* 13, 1378–1381.
- Bi, Z. X., Liu, Y. J., and Lu, C. P. (2007). Contribution of AhvR to virulence of *Aeromonas hydrophila* J-1. *Res. Vet. Sci.* 83, 150–156. doi: 10.1016/j.rvsc.2007.01.003
- Bischofberger, M., Iacovache, I., Boss, D., Naef, F., Van Der Goot, F. G., and Molina, N. (2016). Revealing assembly of a pore-forming complex using single-cell kinetic analysis and modeling. *Biophys. J.* 110, 1574–1581. doi: 10.1016/j.bpj.2016.02.035
- Casabianca, A., Orlandi, C., Barbieri, F., Sabatini, L., Di Cesare, A., Sisti, D., et al. (2015). Effect of starvation on survival and virulence expression of *Aeromonas hydrophila* from different sources. *Arch. Microbiol.* 197, 431–438. doi: 10.1007/s00203-014-1074-z
- Chakraborty, T., Huhle, B., Hof, H., Bergbauer, H., and Goebel, W. (1987). Marker exchange mutagenesis of the aerolysin determinant in *Aeromonas hydrophila* demonstrates the role of aerolysin in *A. hydrophila*-associated systemic infections. *Infect. Immun.* 55, 2274–2280.
- Clatworthy, A. E., Pierson, E., and Hung, D. T. (2007). Targeting virulence: a new paradigm for antimicrobial therapy. *Nat. Chem. Biol.* 3, 541–548. doi: 10.1038/nchembio.2007.24
- Clinical and Laboratory Standards Institute [CLSI] (2009). *Methods for Dilution Antimicrobial Susceptibility Tests for Bacteria That Grow Aerobically—Eighth Edition: Approved Standard M07-A8*. Wayne, PA: CLSI.
- Defoirdt, T., Sorgeloos, P., and Bossier, P. (2011). Alternatives to antibiotics for the control of bacterial disease in aquaculture. *Curr. Opin. Microbiol.* 14, 251–258. doi: 10.1016/j.mib.2011.03.004
- Degiacomi, M. T., Iacovache, I., Pernot, L., Chami, M., Kudryashev, M., Stahlberg, H., et al. (2013). Molecular assembly of the aerolysin pore reveals a swirling membrane-insertion mechanism. *Nat. Chem. Biol.* 9, 623–629. doi: 10.1038/nchembio.1312
- Deng, Y. T., Wu, Y. L., Tan, A. P., Huang, Y. P., Jiang, L., Xue, H. J., et al. (2014). Analysis of antimicrobial resistance genes in *Aeromonas* spp. isolated from cultured freshwater animals in China. *Microb. Drug Resist.* 20, 350–356. doi: 10.1089/mdr.2013.0068
- Dong, J., Ding, H., Liu, Y., Yang, Q., Xu, N., Yang, Y., et al. (2017a). Magnolol protects channel catfish from *Aeromonas hydrophila* infection via inhibiting the expression of aerolysin. *Vet. Microbiol.* 211, 119–123. doi: 10.1016/j.vetmic.2017.10.005
- Dong, J., Ruan, J., Xu, N., Yang, Y. B., and Ai, X. H. (2017b). Expression, purification, and characterization of hemolytic toxin from virulent *Aeromonas hydrophila*. *J. World Aquacult. Soc.* 48, 531–536. doi: 10.1111/jwas.12351
- Dong, J., Qiu, J., Zhang, Y., Lu, C., Dai, X., Wang, J., et al. (2013). Oroxylin A inhibits hemolysis via hindering the self-assembly of alpha-hemolysin heptameric transmembrane pore. *PLoS Comput. Biol.* 9:e1002869. doi: 10.1371/journal.pcbi.1002869
- Gotz, A. W., Williamson, M. J., Xu, D., Poole, D., Le Grand, S., and Walker, R. C. (2012). Routine microsecond molecular dynamics simulations with AMBER on GPUs. 1. *Gener. Born. J. Chem. Theory Comput.* 8, 1542–1555. doi: 10.1021/ct200909j
- Grim, C. J., Kozlova, E. V., Ponnusamy, D., Fitts, E. C., Sha, J., Kirtley, M. L., et al. (2014). Functional genomic characterization of virulence factors from necrotizing fasciitis-causing strains of *Aeromonas hydrophila*. *Appl. Environ. Microbiol.* 80, 4162–4183. doi: 10.1128/AEM.00486-14
- Heuzenroeder, M. W., Wong, C. Y., and Flower, R. L. (1999). Distribution of two hemolytic toxin genes in clinical and environmental isolates of *Aeromonas* spp.: correlation with virulence in a suckling mouse model. *FEMS Microbiol. Lett.* 174, 131–136. doi: 10.1111/j.1574-6968.1999.tb13559.x
- Howard, S. P., and Buckley, J. T. (1982). Membrane glycoprotein receptor and hole-forming properties of a cytolytic protein toxin. *Biochemistry* 21, 1662–1667. doi: 10.1021/bi00536a029
- Huang, P., Hu, P., Zhou, S. Y., Li, Q., and Chen, W. M. (2014). Morin inhibits sortase A and subsequent biofilm formation in *Streptococcus mutans*. *Curr. Microbiol.* 68, 47–52. doi: 10.1007/s00284-013-0439-x
- Iacovache, I., Degiacomi, M. T., Pernot, L., Ho, S., Schiltz, M., Dal Peraro, M., et al. (2011). Dual chaperone role of the C-terminal propeptide in folding and oligomerization of the pore-forming toxin aerolysin. *PLoS Pathog.* 7:e1002135. doi: 10.1371/journal.ppat.1002135

AUTHOR CONTRIBUTIONS

JD and XA conceived the project. JD, XA, and YL designed the experiments. YL, NX, and QY performed the experiments. JD and XA wrote the paper and all authors made the editorial input.

FUNDING

This work is supported by the National Natural Science Foundation of China (No. 31702368) and China Agriculture Research System (CARS-49).

SUPPLEMENTARY MATERIAL

The Supplementary Material for this article can be found online at: <https://www.frontiersin.org/articles/10.3389/fmicb.2018.02828/full#supplementary-material>

- Iacovache, I., Paumard, P., Scheib, H., Lesieur, C., Sakai, N., Matile, S., et al. (2006). A rivet model for channel formation by aerolysin-like pore-forming toxins. *EMBO J.* 25, 457–466. doi: 10.1038/sj.emboj.7600959
- Ibrahim, N., Ibrahim, H., Kim, S., Nallet, J. P., and Nepveu, F. (2010). Interactions between antimalarial indolone-N-oxide derivatives and human serum albumin. *Biomacromolecules* 11, 3341–3351. doi: 10.1021/bm100814n
- Jurasekova, Z., Marconi, G., Sanchez-Cortes, S., and Torreggiani, A. (2009). Spectroscopic and molecular modeling studies on the binding of the flavonoid luteolin and human serum albumin. *Biopolymers* 91, 917–927. doi: 10.1002/bip.21278
- Li, G., Lu, G., Qi, Z., Li, H., Wang, L., Wang, Y., et al. (2017). Morin attenuates *Streptococcus suis* pathogenicity in mice by neutralizing suilysin activity. *Front. Microbiol.* 8:460. doi: 10.3389/fmicb.2017.00460
- Li, H., Zhao, X., Wang, J., Dong, Y., Meng, S., Li, R., et al. (2015). beta-sitosterol interacts with pneumolysin to prevent *Streptococcus pneumoniae* infection. *Sci. Rep.* 5:17668. doi: 10.1038/srep17668
- Los, F. C., Randis, T. M., Aroian, R. V., and Ratner, A. J. (2013). Role of pore-forming toxins in bacterial infectious diseases. *Microbiol. Mol. Biol. Rev.* 77, 173–207. doi: 10.1128/MMBR.00052-12
- Morris, G. M., Huey, R., Lindstrom, W., Sanner, M. F., Belew, R. K., Goodsell, D. S., et al. (2009). AutoDock4 and AutoDockTools4: automated docking with selective receptor flexibility. *J. Comput. Chem.* 30, 2785–2791. doi: 10.1002/jcc.21256
- Nikaido, H. (2009). Multidrug resistance in bacteria. *Annu. Rev. Biochem.* 78, 119–146. doi: 10.1146/annurev.biochem.78.082907.145923
- Parker, M. W., Buckley, J. T., Postma, J. P., Tucker, A. D., Leonard, K., Pattus, F., et al. (1994). Structure of the *Aeromonas* toxin proaerolysin in its water-soluble and membrane-channel states. *Nature* 367, 292–295. doi: 10.1038/367292a0
- Pierce, L. C., Salomon-Ferrer, R., Augusto, F. D. O. C., Mccammon, J. A., and Walker, R. C. (2012). Routine access to millisecond time scale events with accelerated molecular dynamics. *J. Chem. Theory Comput.* 8, 2997–3002. doi: 10.1021/ct300284c
- Rama Devi, K., Srinivasan, R., Kannappan, A., Santhakumari, S., Bhuvaneswari, M., Rajasekar, P., et al. (2016). In vitro and in vivo efficacy of rosmarinic acid on quorum sensing mediated biofilm formation and virulence factor production in *Aeromonas hydrophila*. *Biofouling* 32, 1171–1183. doi: 10.1080/08927014.2016.1237220
- Salomon-Ferrer, R., Gotz, A. W., Poole, D., Le Grand, S., and Walker, R. C. (2013). Routine microsecond molecular dynamics simulations with AMBER on GPUs. 2. explicit solvent particle mesh ewald. *J. Chem. Theory Comput.* 9, 3878–3888. doi: 10.1021/ct400314y
- Sanner, M. F. (1999). Python: a programming language for software integration and development. *J. Mol. Graph. Model.* 17, 57–61.
- Santos, J. A., Gonzalez, C. J., Otero, A., and Garcia-Lopez, M. L. (1999). Hemolytic activity and siderophore production in different *Aeromonas* species isolated from fish. *Appl. Environ. Microbiol.* 65, 5612–5614.
- Singh, V., Chaudhary, D. K., Mani, I., Jain, R., and Mishra, B. N. (2013). Development of diagnostic and vaccine markers through cloning, expression, and regulation of putative virulence-protein-encoding genes of *Aeromonas hydrophila*. *J. Microbiol.* 51, 275–282. doi: 10.1007/s12275-013-2437-x
- Song, M., Li, L., Li, M., Cha, Y., Deng, X., and Wang, J. (2016). Apigenin protects mice from pneumococcal pneumonia by inhibiting the cytolytic activity of pneumolysin. *Fitoterapia* 115, 31–36. doi: 10.1016/j.fitote.2016.09.017
- Sousa da Silva, A. W., and Vranken, W. F. (2012). ACPYPE – AnteChamber PYthon parser interface. *BMC Res Notes* 5:367. doi: 10.1186/1756-0500-5-367
- Stratev, D., and Odeyemi, O. A. (2016). Antimicrobial resistance of *Aeromonas hydrophila* isolated from different food sources: a mini-review. *J. Infect. Public Health* 9, 535–544. doi: 10.1016/j.jiph.2015.10.006
- Takahashi, E., Fujinami, C., Kuroda, T., Takeuchi, Y., Miyoshi, S., Arimoto, S., et al. (2016). Indolo[3,2-b]quinoline derivatives suppressed the hemolytic activity of beta-pore forming toxins, aerolysin-like hemolysin produced by *Aeromonas sobria* and alpha-hemolysin produced by *Staphylococcus aureus*. *Biol. Pharm. Bull.* 39, 114–120. doi: 10.1248/bpb.b15-00708
- Trott, O., and Olson, A. J. (2010). AutoDock vina: improving the speed and accuracy of docking with a new scoring function, efficient optimization, and multithreading. *J. Comput. Chem.* 31, 455–461.
- Wang, J., Wang, W., Kollman, P. A., and Case, D. A. (2006). Automatic atom type and bond type perception in molecular mechanical calculations. *J. Mol. Graph. Model.* 25, 247–260. doi: 10.1016/j.jmkgm.2005.12.005
- Wang, J., Wolf, R. M., Caldwell, J. W., Kollman, P. A., and Case, D. A. (2004). Development and testing of a general amber force field. *J. Comput. Chem.* 25, 1157–1174. doi: 10.1002/jcc.20035
- Wang, J., Zhou, X., Liu, S., Li, G., Shi, L., Dong, J., et al. (2015). Morin hydrate attenuates *Staphylococcus aureus* virulence by inhibiting the self-assembly of alpha-hemolysin. *J. Appl. Microbiol.* 118, 753–763. doi: 10.1111/jam.12743
- Wong, C. Y., Heuzenroeder, M. W., and Flower, R. L. (1998). Inactivation of two haemolytic toxin genes in *Aeromonas hydrophila* attenuates virulence in a suckling mouse model. *Microbiology* 144(Pt 2), 291–298. doi: 10.1099/00221287-144-2-291
- Wu, Q., and Guo, Z. (2010). Glycosylphosphatidylinositols are potential targets for the development of novel inhibitors for aerolysin-type of pore-forming bacterial toxins. *Med. Res. Rev.* 30, 258–269. doi: 10.1002/chin.201024225
- Zhang, M., Yan, Q., Mao, L., Wang, S., Huang, L., Xu, X., et al. (2018). KatG plays an important role in *Aeromonas hydrophila* survival in fish macrophages and escape for further infection. *Gene* 672, 156–164. doi: 10.1016/j.gene.2018.06.029
- Zhang, Q. Q., Ying, G. G., Pan, C. G., Liu, Y. S., and Zhao, J. L. (2015). Comprehensive evaluation of antibiotics emission and fate in the river basins of China: source analysis, multimedia modeling, and linkage to bacterial resistance. *Environ. Sci. Technol.* 49, 6772–6782. doi: 10.1021/acs.est.5b00729

Conflict of Interest Statement: The authors declare that the research was conducted in the absence of any commercial or financial relationships that could be construed as a potential conflict of interest.

Copyright © 2018 Dong, Liu, Xu, Yang and Ai. This is an open-access article distributed under the terms of the Creative Commons Attribution License (CC BY). The use, distribution or reproduction in other forums is permitted, provided the original author(s) and the copyright owner(s) are credited and that the original publication in this journal is cited, in accordance with accepted academic practice. No use, distribution or reproduction is permitted which does not comply with these terms.



Artificial Activation of *Escherichia coli mazEF* and *hipBA* Toxin–Antitoxin Systems by Antisense Peptide Nucleic Acids as an Antibacterial Strategy

Marcin Równicki^{1,2}, Tomasz Pieńko^{1,3}, Jakub Czarnecki^{4,5}, Monika Kolanowska^{1,6}, Dariusz Bartosik⁴ and Joanna Trylska^{1*}

¹ Centre of New Technologies, University of Warsaw, Warsaw, Poland, ² College of Inter-Faculty Individual Studies in Mathematics and Natural Sciences, University of Warsaw, Warsaw, Poland, ³ Department of Drug Chemistry, Faculty of Pharmacy with the Laboratory Medicine Division, Medical University of Warsaw, Warsaw, Poland, ⁴ Department of Bacterial Genetics, Institute of Microbiology, Faculty of Biology, University of Warsaw, Warsaw, Poland, ⁵ Unit of Bacterial Genome Plasticity, Department of Genomes and Genetics, Pasteur Institute, Paris, France, ⁶ Genomic Medicine, Medical University of Warsaw, Warsaw, Poland

OPEN ACCESS

Edited by:

Natalia V. Kirienko,
Rice University, United States

Reviewed by:

Ilana Kolodkin-Gal,
Weizmann Institute of Science, Israel
Chew Chieng Yeo,
Sultan Zainal Abidin University,
Malaysia

*Correspondence:

Joanna Trylska
joanna@cent.uw.edu.pl

Specialty section:

This article was submitted to
Antimicrobials, Resistance
and Chemotherapy,
a section of the journal
Frontiers in Microbiology

Received: 13 September 2018

Accepted: 08 November 2018

Published: 26 November 2018

Citation:

Równicki M, Pieńko T,
Czarnecki J, Kolanowska M,
Bartosik D and Trylska J (2018)
Artificial Activation of *Escherichia coli*
mazEF and *hipBA* Toxin–Antitoxin
Systems by Antisense Peptide
Nucleic Acids as an Antibacterial
Strategy. *Front. Microbiol.* 9:2870.
doi: 10.3389/fmicb.2018.02870

The search for new, non-standard targets is currently a high priority in the design of new antibacterial compounds. Bacterial toxin–antitoxin systems (TAs) are genetic modules that encode a toxin protein that causes growth arrest by interfering with essential cellular processes, and a cognate antitoxin, which neutralizes the toxin activity. TAs have no human analogs, are highly abundant in bacterial genomes, and therefore represent attractive alternative targets for antimicrobial drugs. This study demonstrates how artificial activation of *Escherichia coli mazEF* and *hipBA* toxin–antitoxin systems using sequence-specific antisense peptide nucleic acid oligomers is an innovative antibacterial strategy. The growth arrest observed in *E. coli* resulted from the inhibition of translation of the antitoxins by the antisense oligomers. Furthermore, two other targets, related to the activities of *mazEF* and *hipBA*, were identified as promising sites of action for antibacterials. These results show that TAs are susceptible to sequence-specific antisense agents and provide a proof-of-concept for their further exploitation in antimicrobial strategies.

Keywords: antimicrobial strategies, bacterial toxin–antitoxin systems, peptide nucleic acid (PNA), antisense oligonucleotides, *Escherichia coli mazEF* and *hipBA* targets

INTRODUCTION

Antibiotics are essential medicines used to prevent and treat otherwise incurable bacterial infections (Coates and Hu, 2007). However, the combination of widespread usage of antibiotics and bacterial evolution have decreased their efficacy, and stimulated the emergence of antibiotic-resistant bacteria (Fair and Tor, 2014). The traditional answer to this problem has been the introduction of new, improved versions of existing antibiotics that can kill the resistant bacterial mutants. However, simple molecular variants of commonly used antibiotics are becoming less effective

in overcoming bacterial resistance mechanisms (Ventola, 2015a). The identification of new non-traditional targets for antimicrobials is therefore critical in combating infectious diseases caused by evolving pathogens (Ventola, 2015b).

Many bacteria contain toxin-antitoxin systems (TAs), usually composed of two genes that encode (i) a stable toxin that targets an essential cellular process, and (ii) a labile antitoxin that counteracts the activity of the toxin (Harms et al., 2018). These genetic modules are widely distributed in bacterial genomes, including clinical pathogens, but are not found in eukaryotes (Hayes and Van Melder, 2011; Fernandez-Garcia et al., 2016; Lee and Lee, 2016). This makes them promising targets for the development of novel antibacterials (Kirkpatrick et al., 2016).

TAs have been divided into six classes, depending on the nature and the mode of action of the antitoxin molecule (Page and Peti, 2016). Type II TAs have been the most extensively characterized (Ma et al., 2015; Chan et al., 2016; Rocker and Meinhart, 2016). In this class, both the toxin and the antitoxin are proteins (Lobato-Márquez et al., 2016). Two particularly well studied type II TAs are *mazEF* (Hazan et al., 2004; Schuster et al., 2013; Tripathi et al., 2014) and *hipBA* (Schumacher et al., 2009; Germain et al., 2013; Kaspy et al., 2013). In the *mazEF* TAs family, the MazF toxin is an endoribonuclease, which cleaves mRNA at three-, five-, or seven-base recognition sequences in different bacteria resulting in translation inhibition (Yamaguchi and Inouye, 2009; Yamaguchi et al., 2012; Schifano et al., 2016). This cleavage occurs independently of both the ribosome and translation, and it is inhibited by the MazE antitoxin (Kędzierska and Hayes, 2016). In the *hipBA* TAs family, the HipA toxin targets the glutamyl-tRNA synthetase (GltX) involved in tRNA synthesis (Germain et al., 2013). The overproduction of HipA affects the integrity of *E. coli* cells and induces their lysis (Kędzierska and Hayes, 2016). The HipA toxin is neutralized by forming a complex with the HipB antitoxin (Wen et al., 2014). The *mazEF* and the *hipBA* loci are present in the chromosomes of many bacteria (Fu et al., 2009; Rothenbacher et al., 2012; Fernandez-Garcia et al., 2016), but their function has mainly been studied in *E. coli* (Hazan et al., 2004; Schumacher et al., 2009).

The artificial activation of TAs has potential as an antimicrobial strategy (Lioy et al., 2010; Shapiro, 2013; Verma et al., 2015; Kim et al., 2018). To test this concept we have used antisense oligonucleotides to try to alter TAs activity and arrest the growth of bacteria (Figure 1). Antisense oligonucleotides bind to nucleic acids in a sequence-specific manner by Watson-Crick base pairing, and can affect the function of targeted mRNAs and silence genes (Dias and Stein, 2002). Due to the rapid degradation of natural oligonucleotides in the intracellular environment, chemically modified oligonucleotides, such as peptide nucleic acids (PNA), have been successfully used as silencing agents (Rasmussen et al., 2007). PNA is a DNA analog with a pseudo-peptide backbone composed of repeating *N*-(2-aminoethyl) glycine units linked by amide bonds (Nielsen et al., 1991). PNA oligomers show enhanced nuclease and protease resistance, improved binding affinity with natural nucleic acids, and negligible toxicity to eukaryotic cells (Good et al., 2001).

Typically, antibacterial PNAs have been targeted against mRNAs of essential genes (Good et al., 2001; Nekhotiaeva et al., 2004; Patenge et al., 2013) or functional ribosomal sites (Hatamoto et al., 2009; Górka et al., 2016; Kulik et al., 2017). Earlier problems with the delivery of PNAs to bacterial cells have been solved by conjugating them to various carriers, such as cell penetrating peptides (CPP) (Abushahba et al., 2016) or vitamin B₁₂ (Równicki et al., 2017).

In this study, we have investigated three innovative strategies related to the use of TAs and associated proteins as targets for antibacterial molecules (Figure 1). To the best of our knowledge, such approaches have not been reported so far. The first strategy was the artificial activation of the *E. coli* MazF and HipA toxins by using antisense PNA oligomers to inhibit the translation of the corresponding antitoxins (MazE and HipB, respectively, Figure 1A). The second strategy involved the indirect activation of the MazF toxin by inducing thymine starvation. This was achieved by silencing the *thyA* gene encoding thymidylate synthase, an enzyme involved in folic acid metabolism, which has been shown to interfere with *mazEF*-mediated growth inhibition (Figure 1B) (Engelberg-Kulka et al., 2005). The third strategy was to mimic the action of the HipA toxin by silencing the *gltX* gene encoding its cellular target glutamyl-tRNA synthase (Figure 1C).

To test these novel strategies, we first designed and synthesized antisense PNAs and evaluated their antimicrobial effectiveness by determining the minimal inhibitory concentration (MIC) for three strains of *E. coli*: a K-12 wild-type strain, the pathogenic strain O157:H7 (Łoś et al., 2008) and the extended spectrum β -lactamase-producing strain WR3551/98 (Baraniak, 2002) (Supplementary Table 1). Second, we examined the decay of the target mRNAs after treatment with different PNA concentrations, using reverse transcription real-time quantitative PCR (RT-qPCR). Third, we checked for any synergistic interactions between the *mazEF*-targeted PNAs and selected antibiotics (trimethoprim and sulfamethoxazole) by determining the fractional inhibitory concentration (FIC). Finally, we assessed the cytotoxicity of the oligonucleotides to eukaryotic cells in an assay using human embryonic kidney-293 cells (HEK-293).

RESULTS

Selection of Targets for PNA Oligomers

Based on the predicted secondary and tertiary structures of the targeted mRNAs, four antisense PNA sequences were designed (Table 1). Their complementary sequences overlapped the most favorable mRNA sites that covered the translation start codon (Dryselius et al., 2003; Deere et al., 2005) and lacked stable secondary structures such as stem-loops or hairpins (Rasmussen et al., 2007).

To validate the sequence homology of the PNA target sites in *E. coli* O157:H7 and WR3551/98, these regions were amplified by PCR using specific primers (Supplementary Table 2) and sequenced. All sequences were identical in the three *E. coli* strains, excluding any possibility that mutation of the mRNA target sites for the PNAs might cause decreased susceptibility. To deliver the PNAs into

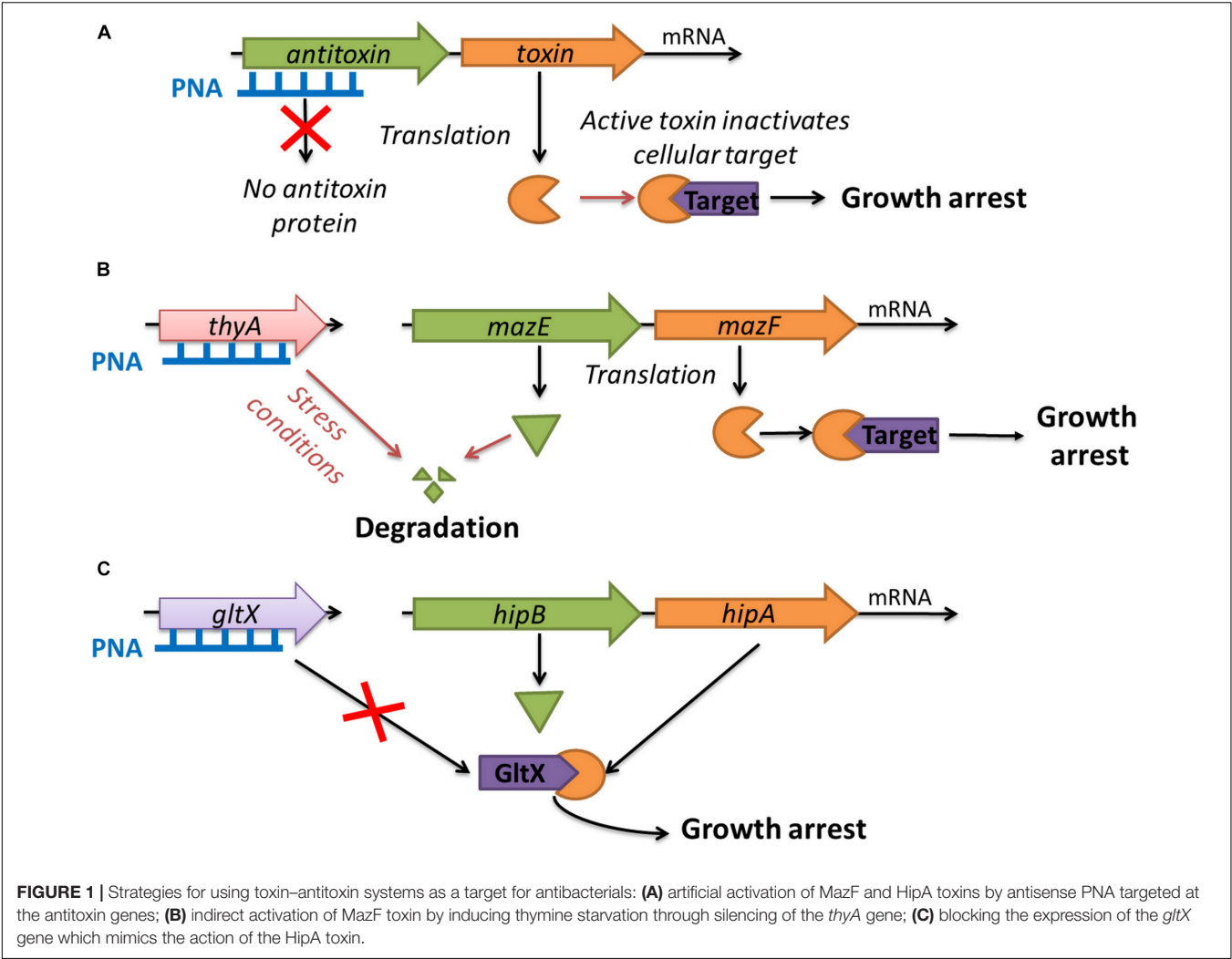


FIGURE 1 | Strategies for using toxin–antitoxin systems as a target for antibacterials: **(A)** artificial activation of MazF and HipA toxins by antisense PNA targeted at the antitoxin genes; **(B)** indirect activation of MazF toxin by inducing thymine starvation through silencing of the *thyA* gene; **(C)** blocking the expression of the *gltX* gene which mimics the action of the HipA toxin.

TABLE 1 | PNAs used in this study.

TA system	Name	Target	Sequence
			(N _{term} –C _{term})*
mazEF	anti-mazE PNA	mazE	(KFF) ₃ K-cataacccttc
	anti-thyA PNA	thyA	(KFF) ₃ K-tcatggttcctc
hipBA	anti-hipB PNA	hipB	(KFF) ₃ K-catgtcatacg
	anti-gltX PNA	gltX	(KFF) ₃ K-gattttcatg
–	PNAnc	Control	(KFF) ₃ K-tccattgtctgc
			non-complementary sequence

To increase water solubility, each PNA has a lysine residue at the C-terminus. *lower case letters indicate the PNA sequence.

cells, we used a cell-penetrating peptide (KFF)₃K, which was covalently linked to each PNA oligomer via an AEEA (aminoethoxyethoxyacetic acid) linker. (KFF)₃K is the most widely used cell-penetrating peptide for achieving PNA entry into *E. coli* cells (Eriksson et al., 2002; Bendifallah et al., 2006).

As a negative control, a random PNA (PNAnc) unrelated to the target sequences was used (Table 1). See Materials and Methods for detailed synthesis protocols.

Escherichia coli Growth Inhibition by Sequence-Specific PNAs

To evaluate the potential of antisense PNAs to inhibit the growth of *E. coli* strains, the minimal inhibitory concentrations (MIC) of the compounds were determined. All tested PNAs inhibited *E. coli* growth. First, the MICs for the (KFF)₃K-PNAs targeted to antitoxins were measured.

The MIC of the anti-mazE PNA was 16 μM for all three *E. coli* strains (Figure 2, top), while the anti-hipB PNA prevented the growth of *E. coli* K-12 at a concentration of 8 μM and *E. coli* WR3551/98 at 16 μM (Figure 2, bottom). In *E. coli* O157:H7, the antimicrobial activity of anti-hipB PNA was observed only up to 8 h of exposure (Figure 2, bottom). Therefore, the MIC was recorded as being >16 μM.

Next, the antisense PNAs to the two TAs-associated target genes were tested (Table 1). The anti-thyA PNA had lower activity

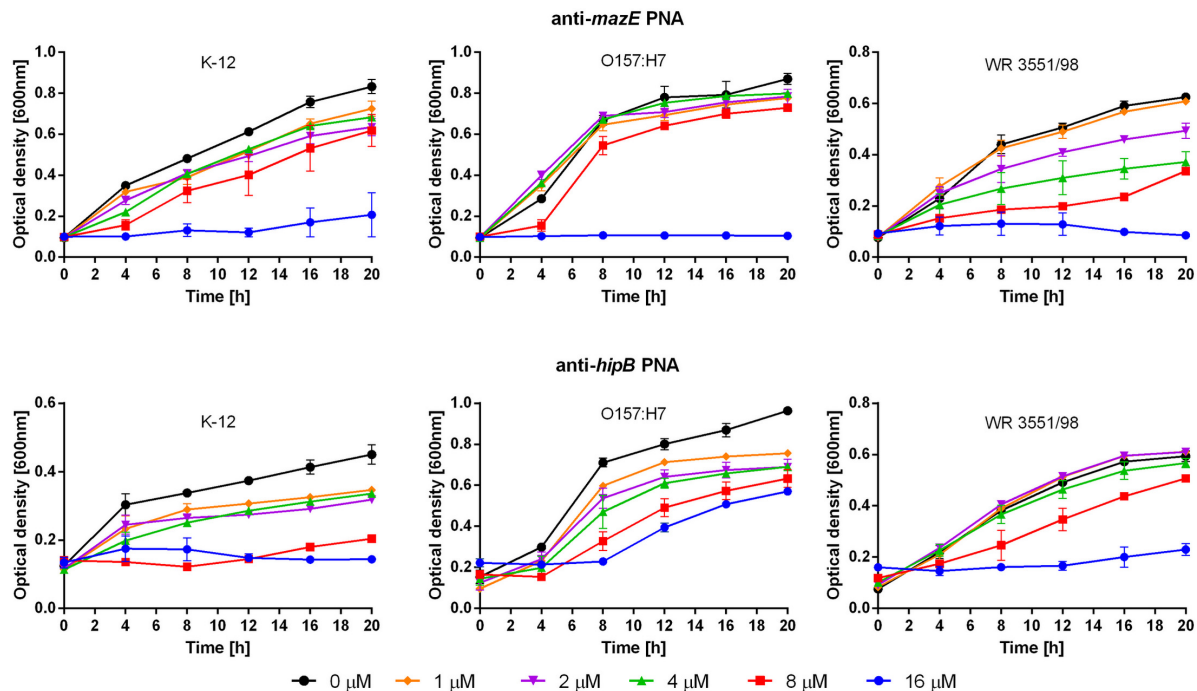


FIGURE 2 | Growth inhibition after treatment with the anti-*mazE* (top) and anti-*hipB* (bottom) PNAs. Error bars represent the mean \pm SEM, $n = 3$. For all strains the differences between 0 and 16 μM concentrations at 20 h are statistically significant with $P < 0.001$.

against *E. coli* K-12 (MIC $> 16 \mu\text{M}$) than against the strains O157:H7 and WR3551/98 (MIC = 16 μM) (Figure 3, top). After treatment with anti-*gltX* PNA, the growth of *E. coli* K-12, O157:H7, and WR3551/98 was prevented at MICs of 4, 16, and 1 μM , respectively (Figure 3, bottom).

To control for specificity of the interaction of the sequence-specific PNAs, the non-complementary PNanc was tested (Table 1). No growth inhibition was observed following the addition of the (KFF)₃K-PNanc at concentrations of up to 16 μM (Supplementary Figure 1A). Addition of the (KFF)₃K peptide alone at concentrations above 16 μM also failed to cause any significant reduction in *E. coli* growth (Supplementary Figure 1B).

To confirm that the observed growth inhibition was a consequence of toxin action, we used *E. coli* mutants lacking either the *mazF* (K-12 MG1655 ΔmazF) or *hipA* (JW1500-2 ΔhipA) toxin genes (Supplementary Table 1). The ΔmazF mutant was treated with anti-*mazE* PNA and the ΔhipA mutant with anti-*hipB* PNA. No growth inhibition of these mutant strains was observed following treatment with the corresponding PNAs at concentrations of up to 16 μM (Supplementary Figure 2). This result verified that the activity of the MazF and HipA toxins was the main cause of growth inhibition after treatment with the specific PNAs.

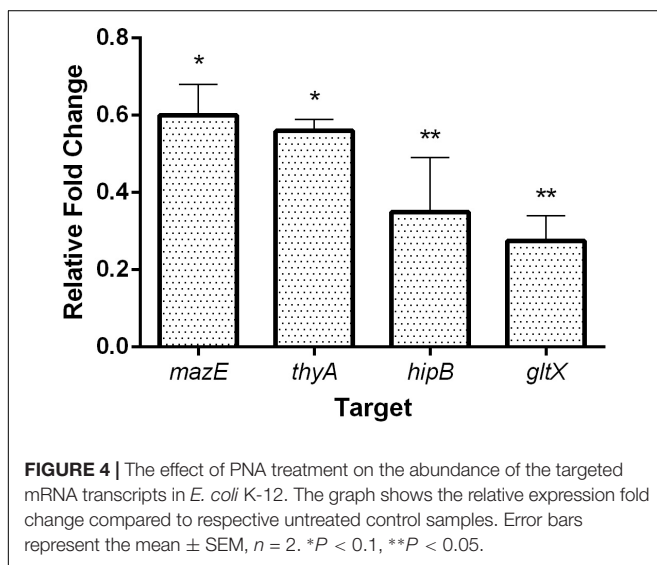
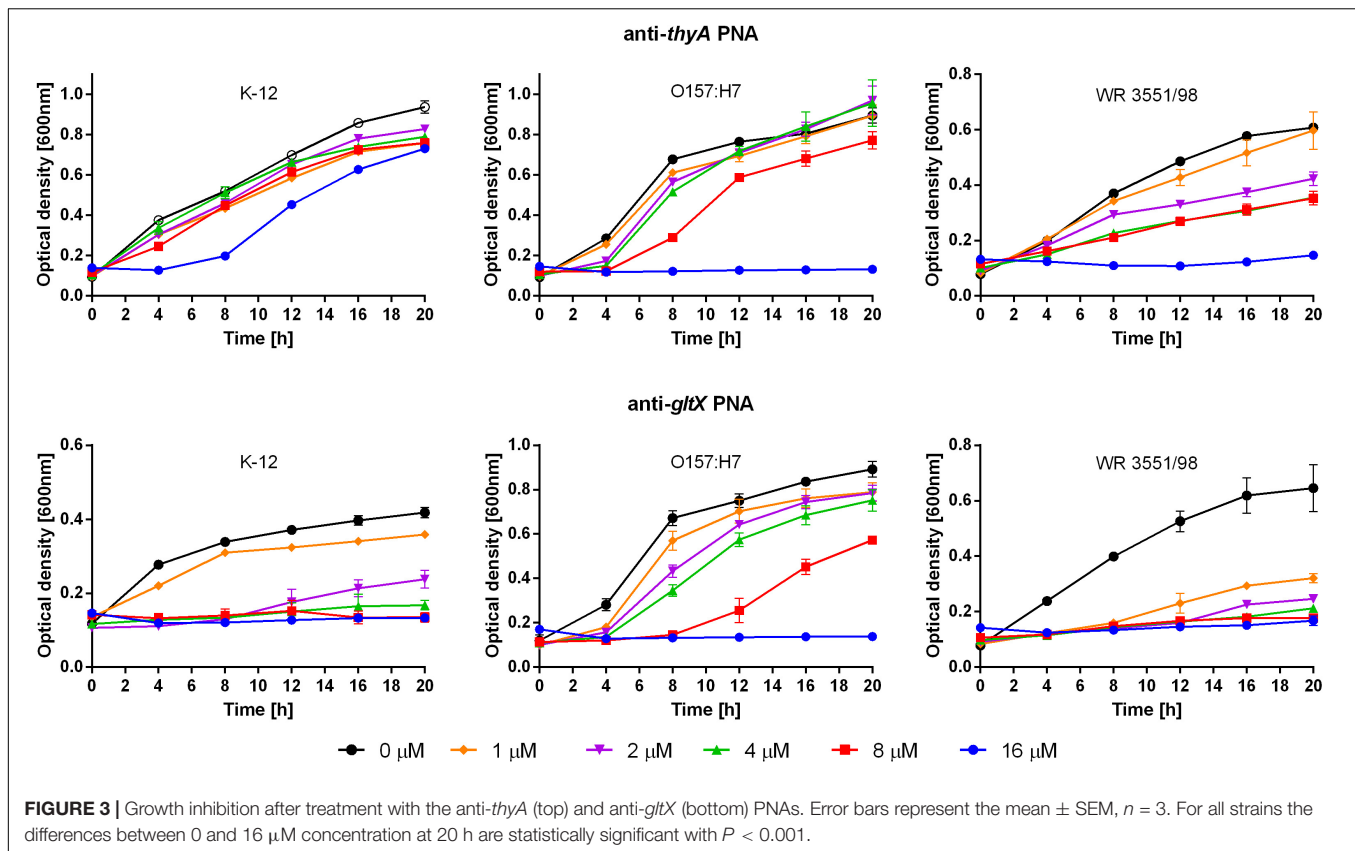
Effect of PNAs on Corresponding Gene Transcripts

We further tested whether the reduction in growth of *E. coli* upon treatment with sequence-specific PNAs was reflected in

the changes of the corresponding gene transcript levels. To determine the level of the targeted mRNAs, the quantitative reverse transcription polymerase chain reaction (qRT-PCR) was used (Figure 4). *E. coli* K-12 cultures were treated with sub-MIC concentrations of each respective PNA and the level of mRNAs was compared to untreated control samples. Upon treatment with 8 μM anti-*mazE* PNA, the amount of *mazE* transcript was reduced to 60% (Figure 4). The level of *thyA* mRNA was reduced to 55% after treatment with 16 μM anti-*thyA* PNA. Similarly, the level of *hipB* and *gltX* transcripts was diminished to 40 and 35%, respectively, after treatment with sub-MIC concentrations (4 μM anti-*hipB* and 1 μM anti-*gltX*) of corresponding PNAs (Figure 4). We also monitored the mRNA levels of the *mazF* and *hipA* toxin genes. Treatment with PNA conjugates targeting these antitoxin genes did not influence the relative *mazF* and *hipA* mRNA levels detected by qRT-PCR (Supplementary Figure 3).

Antimicrobial Synergy Between PNAs and Antibiotics

It has been demonstrated that the antibiotics trimethoprim and sulfonamide induce thymine starvation by inhibiting folic acid metabolism, and this triggers *mazEF*-mediated cell death in *E. coli* (Engelberg-Kulka et al., 2004). Because folic acid metabolism inhibitors and the *mazEF*-targeted PNAs (anti-*mazE* and anti-*thyA*, Table 1) have related targets (Figure 5A), we sought to determine whether they act synergistically against *E. coli* O157:H7. The combinatory effects of antibiotics and PNAs were examined in checkerboard



assays and quantified by the calculation of FIC indices. Following this protocol, the MIC for each compound was determined independently, and subsequently this was repeated for each concentration of the PNA combined with each concentration of the antibiotic (Figure 5B). The combinations of anti-*mazE* PNA/trimethoprim (Figure 5B1) and PNAs/sulfamethoxazole (Figures 5B2, B4) presented an interaction of indifference.

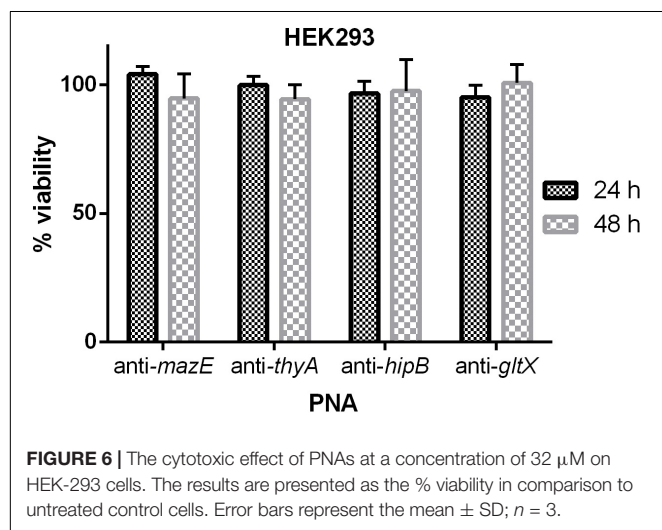
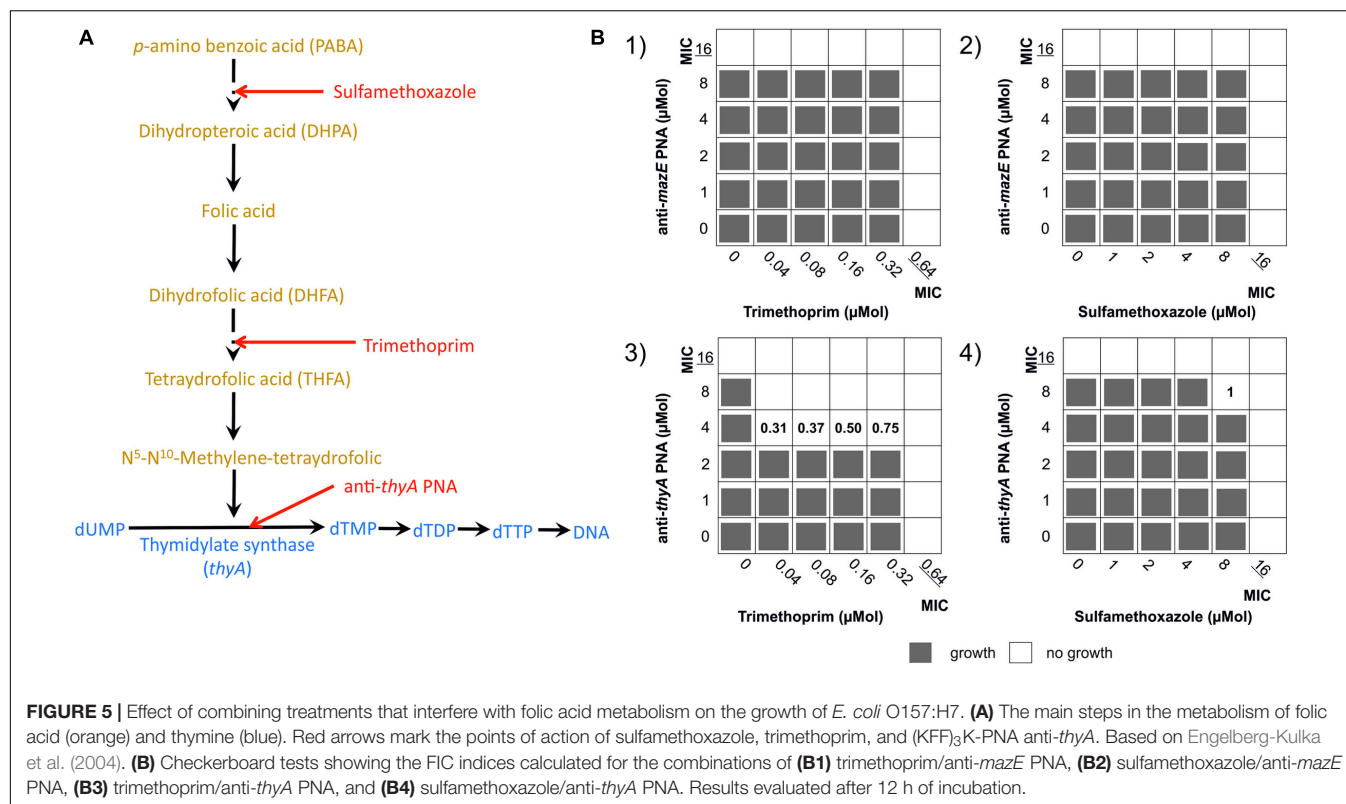
However, the combination of anti-*thyA* PNA with trimethoprim resulted in a highly synergistic interaction ($\text{FIC}_i = 0.31$; Figure 5B3).

Influence of PNAs on Human Cells

The cytotoxic effect of the tested $(\text{KFF})_3\text{K}$ -PNA conjugates on human embryonic kidney cells 293 (HEK-293) was evaluated. For these experiments the $(\text{KFF})_3\text{K}$ -PNA conjugates were applied at a concentration of 32 μM . No significant impact on cell viability was observed after 24 or 48 h of treatment compared to untreated control cells (Figure 6).

DISCUSSION

The exploitation of TAs in antibacterial strategies via artificial activation of the toxin has been proposed (Shapiro, 2013; Williams and Hergenrother, 2014; Chan et al., 2015), but there have been no experimental data to support this idea until now. The results of this study provide a proof-of-concept for the use of bacterial TAs as novel targets for antimicrobial compounds. Operons encoding the targeted TAs, *mazEF* and *hipBA*, conserved in both laboratory and pathogenic *E. coli* strains (Fernandez-Garcia et al., 2016), were found to be promising candidates for antisense-based antibacterials. A reduction in *E. coli* growth was obtained by inhibiting the expression of the *mazE* and *hipB* antitoxins using PNA oligomers targeting their mRNAs.



To the best of our knowledge, artificial activation of toxins by antisense oligonucleotides has never been attempted as an antibacterial strategy (Narenji et al., 2017). PNAs have been tested as antibacterials, typically by targeting the expression of essential genes. The TAs genes are non-essential, and this might explain why the MICs obtained in this study are slightly higher than those previously reported for PNAs (Dryselius et al., 2003, 2005; Nikravesh et al., 2007). On the other hand, these MIC values are comparable with those reported for cases where essential sites

on ribosomal RNA were targeted (Hatamoto et al., 2009; Górska et al., 2016; Kulik et al., 2017).

Furthermore, we tested PNAs specific for two additional targets related to the activities of *mazEF* and *hipBA*. First, we targeted the *thyA* gene in order to induce thymine starvation and as a consequence indirectly activate the MazF toxin. The other target was the *gltX* gene encoding glutamyl-tRNA synthase, the enzyme inhibited by HipA toxin. The assumption was that lowering the concentration of GltX should result in fatal effects for the bacterial cell, similar to those observed in the case of the HipA-mediated inactivation. Both approaches were successful, showing that multiple antimicrobial strategies might be based on the action of TAs.

With the PNAs targeted to inhibit the translation of the *thyA* and *gltX* transcripts, *E. coli* WR3551/98 turned out to be the most susceptible strain. This observation is consistent with a previous report that extended-spectrum beta-lactamase (ESBL)-producing *E. coli* strains are more susceptible to an anti-*rpoD* PNA than the wild-type strain (Bai et al., 2012). Furthermore, the obtained MICs for the anti-*thyA* and anti-*gltX* PNAs are generally comparable with those reported for PNAs targeting essential genes. For example, in the studies employing *E. coli* K-12, the MIC of a PNA targeting the *acpP* gene was 1 μ M (Nikravesh et al., 2007), while those of PNAs against the *fabI* and *fabD* genes were both 3 μ M (Dryselius et al., 2005). Overall, *E. coli* O157:H7 was the least susceptible to the PNAs tested in this study. This observation may be due to the diverse genetic background of the *E. coli* strains and consequently different expression levels of the target genes in response to respective PNAs. Another possible

reason could be due to the differences in the structure of the lipopolysaccharide in *E. coli* strains, which is a known limiting factor for antimicrobial PNA action (Good et al., 2000).

Antisense silencing using PNA in bacteria leads to translational repression via steric blocking of the ribosome assembly on the mRNA (Rasmussen et al., 2007). As a consequence, such non-translated transcripts are degraded (Dryselius et al., 2006; Goh et al., 2009). Therefore, the effectiveness of antisense silencing can be estimated by quantifying mRNA abundance (Kurupati et al., 2007). Note, that the qRT-PCR experiments were performed on the *E. coli* K-12 strain and not on O157:H7 or WR3551/98 strains. This was mostly because the yield and quality of the RNA (which are critical in qRT-PCR analysis), isolated from *E. coli* O157:H7, were much lower than the RNA isolated from *E. coli* K-12. Although there are differences in the response of the tested *E. coli* strains to different PNA oligomers, the tendency is similar in the O157:H7 and WR3551/98 strains as compared to K-12. We thus used wild-type *E. coli* K-12 as a background in all qRT-PCR experiments.

We detected a significant reduction in the levels of the targeted mRNAs upon treatment with the complementary PNAs (Figure 4), confirming their sequence-specific binding to these transcripts. Similar observations have been reported in various bacterial species, e.g., in *Streptococcus pyogenes* where the application of anti-*gyrA* PNA decreased the *gyrA* mRNA level to about 50% of the untreated control value (Patenge et al., 2013). In *E. coli* the level of *acpP* mRNA was diminished to about 60% of the control following treatment with anti-*acpP* PNA (Nikravesh et al., 2007). To demonstrate the absence of off-target activity of the tested PNAs, the levels of the mRNAs for the *mazF* and *hipA* toxin genes were monitored after treatment with PNA conjugates targeting the corresponding antitoxin genes. The transcript levels of these toxin genes remained unchanged as compared to the untreated control samples (Supplementary Figure 3). Since the antitoxin and toxin genes are organized in operons, we presume that disruption of translation of the former does not totally prevent translation of the latter. Although the genes are co-transcribed as a single mRNA, the toxin gene carries its own ribosome binding site located within the upstream antitoxin gene (Chan et al., 2012).

The use of synergistic antibiotic/non-antibiotic combinations is a promising option for maximizing the therapeutic effect against problematic drug-resistant pathogens (Schneider et al., 2017). Moreover, the combination of agents makes the emergence of resistance in bacteria less likely (Doern, 2014). The *in vitro* effectiveness of the combined application of antisense PNAs and traditional antibiotics has already been demonstrated for several bacterial pathogens such as *Campylobacter jejuni* (Mu et al., 2013), *Streptococcus pyogenes* (Patenge et al., 2013), *Staphylococcus aureus*, and *E. coli* (Dryselius et al., 2005). However, in all these reports, the authors described synergistic antimicrobial effects for the combinations of drugs sharing the same targets. In addition, Patenge et al. (2013) also showed synergy between agents independent of the targeted pathways.

The combination of trimethoprim and sulfamethoxazole (cotrimoxazole) is commonly used in clinical treatment because

of their impedance of two sequential steps in folic acid synthesis (Figure 5A) (Bushby, 1975; Harvey, 1982). Since both agents trigger *mazEF*-mediated growth inhibition (Engelberg-Kulka et al., 2004), synergistic interactions with the *mazEF*-targeted PNAs were expected. However, we found strong synergy only for the combination of anti-*thyA* PNA and trimethoprim (Figure 5B3). The combination of the same anti-*thyA* PNA and sulfamethoxazole resulted in an interaction of indifference (Figure 5B4). This observation is interesting with regard to the mechanism of synergy. All three agents act on the same metabolic pathway (Figure 5A), but the synergistic effect was observed only for two combinations, i.e., trimethoprim/sulfamethoxazole and trimethoprim/anti-*thyA* PNA. Dryselius et al. (2005) tested combinations of PNAs and drugs against the folate biosynthesis pathway in *E. coli* and *S. aureus*. Surprisingly, they found synergy when sulfamethoxazole, which targets the dihydropteroate synthase (FolP), was combined with anti-*folP* PNA. However, they did not observe synergy when the anti-*folP* PNA was combined with trimethoprim, which targets dihydrofolate reductase (FolA). Similarly, the combination of anti-*folA* PNA and trimethoprim showed synergy but the sulfamethoxazole/anti-*folA* PNA combination showed indifference (Dryselius et al., 2005). Further investigation is required to understand these drug interactions, but the results of this and previous studies show how combinations of PNAs and antibiotics can be applied to help decipher mechanisms of drug action.

PNA oligonucleotides are generally considered to have negligible toxicity for eukaryotic cells (Good et al., 2001; Evers et al., 2015). However, whether or not PNAs elicit toxic effects is highly dependent on their sequence composition and the presence of a transporter vehicle (Pandey et al., 2009; Rozners, 2012; Zeng et al., 2016). We demonstrated that treatment of HEK-293 cells with the designed PNAs at a concentration of 32 μ M did not cause significant cytotoxicity. This observation is consistent with those reported previously (Sharma et al., 2017). However, another study found that 2-aminopyridine-modified PNAs and their peptide conjugates were not cytotoxic up to 10 μ M, but toxicity occurred at higher concentrations (Hnedzko et al., 2017). For this reason, confirmation that PNA-peptide conjugates are not toxic to mammalian cells is crucial before their therapeutic use is considered.

Two potential undesirable effects of artificial activation of TAs are bacterial persistence and biofilm formation (Lewis, 2007; Díaz-Orejas et al., 2017). The precise mechanism of persister formation is currently unknown (Formation et al., 2017), but according to previous reports, only overexpression of the toxin induces persistence (Pedersen et al., 2002; Lewis, 2008; Harrison et al., 2009; Wood et al., 2013). The PNAs employed in the present study did not lead to overexpression of the toxin (Supplementary Figure 3), so we speculate that the risk of dormant cell formation is relatively low. On the other hand, there is evidence that toxin-antitoxin modules are not the only factors that contribute to the formation of persister cells (Fisher et al., 2017). The deletion of multiple TAs reduces persisters but does not fully abolish their presence (Kint et al., 2012; Chowdhury et al., 2016). It is possible that there is heterogeneity within the persister

population, with several different pathways contributing to the formation of persister cells. Furthermore, we speculate that the artificial activation of *E. coli* TAs by antisense PNA oligomers could induce the stringent response. This phenomenon is a bacterial response to stress conditions, e.g., amino-acid starvation (Cashel et al., 1996). The stringent response has been described as an important mechanism for the persister formation as a reaction to a diauxic growth (Amato and Brynildsen, 2015). However, how the formulation of persister cells is connected to this stress response is still unknown. Persister cells are present in each population prior to any treatment with antibacterial agent. Therefore, further investigation is required to determine the exact roles of central metabolism and toxin-antitoxin modules in the formation of persisters. In the future, we plan to determine whether artificial activation of TAs by PNAs influences persister formation and if it triggers the stringent response.

MATERIALS AND METHODS

Target Site Selection

The genome sequence of *E. coli* K-12 was obtained from the KEGG database (Ogata et al., 1999). For secondary and tertiary structure prediction of the targeted mRNAs, the Mfold (Zuker, 2003), and RNAComposer (Popenda et al., 2012) software were used, respectively. To ensure target specificity of PNAs, the target sites were examined for uniqueness within the *E. coli* K-12 genome using the on-line search tools GenoList (Lechat et al., 2008) and RiboScanner (Górska et al., 2016), with special consideration given to the start codon region that includes the consensus Shine-Dalgarno sequence.

Reagents and Conditions for (KFF)₃K-AEEA-PNA Synthesis

Commercial reagents and solvents were used as received from the supplier. NovaSyn®TG Sieber resin for PNA synthesis was obtained from Merck and Fmoc/Bhoc-protected PNA monomers (Fmoc-PNA-A(Bhoc)-OH, Fmoc-PNA-G(Bhoc)-OH, Fmoc-PNA-C(Bhoc)-OH, Fmoc-PNA-T-OH) from Panagene and Link Technologies Ltd. Fmoc-AEEA-OH was purchased from Link Technologies Ltd. N α -Fmoc protected L-amino acids (Fmoc-Lys(Boc)-OH, Fmoc-Phe-OH) were obtained from Sigma-Aldrich. Preparative chromatography was performed using C18 reversed-phase silica gel 90 Å (Sigma-Aldrich) with redistilled water and HPLC grade MeCN as eluents with the addition of HPLC grade trifluoroacetic acid (TFA) (0.1% v/v solution). The following conditions were used for HPLC: column – Eurospher II 100–5 C18, 250 mm Å – 4.6 mm with a precolumn; pressure – 230 bar; flow rate – 4.5 ml/min; room temperature; detection – UV/Vis at a wavelength of 267 nm.

Synthesis of (KFF)₃K-AEEA-PNA Conjugates

The conjugates of (KFF)₃K with PNA connected via an aminoethylethanolamine linker (AEEA) were in-house

synthesized manually using the Fmoc solid-phase methodology at 10 μ mol scale. The syntheses were conducted using 9-Fmoc-amino-xanthen-3-yloxy TG resin with amine group loading of 190 μ mol/g. This resin carries a linker, which yields a C-terminal amide upon TFA cleavage of the PNA. In all syntheses, Lys was the first monomer attached to the resin. PNA oligomers were synthesized using a 2.5-fold molar excess of the Fmoc/Bhoc-protected PNA monomers. To activate the monomers, we used a 2-(1H-7-azabenzotriazole-1-yl)-1,1,3,3-tetramethyluronium hexafluorophosphate (HATU), N-methylmorpholine (NMM), and 2,6-lutidine (0.7:1:1.5) mixture in DMF/NMP (1:1, v/v) solution. Coupling of the activated compounds was carried out two times for 30 min each. The Fmoc group was removed with 20% (v/v) piperidine in DMF (2 mm \times 2 min). After the PNA oligomer synthesis and N-terminal Fmoc deprotection, Fmoc-AEEA-OH was attached to the N-terminus. Then, the N-terminal Fmoc was removed, and amino acids were coupled to yield the (KFF)₃K peptide. We used a 3-fold and 1.5-fold molar excess of Fmoc-AEEA-OH and the Fmoc-protected amino acids (Fmoc-Lys(Boc)-OH, Fmoc-Phe-OH) in the respective couplings performed two times for each substrate (for 60 and 40 min, respectively). The reagents were activated with HATU and the addition of HOAt and collidine (1:1:2) and N,N-dimethylpyridin-4-amine (DMAP) as a catalyst, in DMF/NMP (1:1, v/v) solution. The Fmoc groups of Fmoc-AEEA-OH and amino acids were deprotected using 20% (v/v) piperidine in DMF in two cycles (5 and 15 min). All of the protecting groups were removed and cleavage of the (KFF)₃K-AEEA-PNA conjugates from the resin was accomplished by treatment with a TFA/triisopropylsilane/m-cresol (95:2.5:2.5; v/v/v) mixture for 60 min. The crude products were precipitated with cold diethyl ether, collected by centrifugation, decanted, lyophilized, and subsequently purified by RP-HPLC. The HPLC methods and molecular masses are shown in **Supplementary Table 3**, and the RP-HPLC chromatograms and MS spectra of the purified products in **Supplementary Figures 4–8**.

Bacterial Strains and Growth Conditions

The strains used in this study are listed in **Supplementary Table 1**. All strains were grown in LB or LA medium at 37°C. When necessary, the media were supplemented with kanamycin (50 μ g/ml), chloramphenicol (20 μ g/ml), sucrose (10% w/v), or diaminopimelic acid (DAP, 0.3 mM). For susceptibility tests, the strains were grown in cation-adjusted Mueller Hinton Broth (Difco) at 37°C with shaking.

PCR for Sequencing

Bacterial gDNA was extracted from cell pellets using a Bacterial & Yeast Genomic DNA Purification Kit (EURx, Poland) according to the manufacturer's instructions. Based on the *E. coli* K-12 MG1655 genome sequence (RefSeq assembly accession: GCF_000005845.2) appropriate oligonucleotide primers were designed (**Supplementary Table 2**) for the amplification of fragments of the genes overlapping the targeted sequences. The PCR products were purified and sequenced.

Genetic Manipulations and Strain Construction

DNA manipulations were performed using standard procedures, and according to the manufacturer's instructions included in kits for DNA isolation and PCR (Phusion, Thermo Fisher Scientific). Deletion of the *E. coli* K-12 MG1655 *mazF* gene was performed using the gene replacement method (Pósfai et al., 1999). The plasmid for the mutagenesis [pDS132-*mazFKm* was generated by the Gibson assembly procedure (Gibson et al., 2009)]. The DNA fragments used for the assembly were amplified by PCR using the following primer pairs: (i) *mazF1/mazF2* and *mazF3/mazF4* – amplification of DNA fragments flanking the *mazF* gene using MG1655 genomic DNA as template, (ii) KML/KMR – amplification of the kanamycin resistance gene from plasmid pMSB1 (Dziewit et al., 2011), and (iii) *pds132X/pds132Y* – amplification of mobilizable vector pDS132 carrying the *sacB* gene enabling counter-selection with sucrose (Philippe et al., 2004). The assembled plasmid was transformed into *E. coli* DH5 α pir cells, carrying the *pir* gene required for pDS132 replication. Isolated pDS132-*mazFKm* plasmid DNA was then used to transform *E. coli* strain β 2163 (carrying the *pir* gene) and a single transformant was used as a donor in a bi-parental mating with strain MG1655 (without the *pir* gene) as the recipient. The Δ *mazF* mutant colonies (in which the *mazF* gene was replaced by the kanamycin resistance gene following homologous recombination between the flanking regions) were selected on LA medium containing kanamycin and sucrose. The deletion was confirmed by PCR using primers *LmazFspr/RmazFspr* and sequencing of the amplified DNA fragment.

Minimal Inhibitory Concentrations

The minimal inhibitory concentrations (MICs) of the antibiotics, (KFF)₃K-PNAs and free (KFF)₃K were determined by broth microdilution according to Clinical and Laboratory Standards Institute method M07-A10 (CLSI, 2015). Each MIC was scored as the lowest concentration that prevented visibly detectable growth. Cells were cultured in Mueller-Hinton Broth (MHB) to exponential phase and diluted to $\sim 5 \times 10^5$ CFU/ml. Aliquots of the cell suspensions were added to the wells of sterile 96-well plates containing dilutions of the tested agents and these plates were incubated at 37°C in a microplate reader for 20 h. During incubation, the optical density at 600 nm (OD₆₀₀) of the culture in each well was measured at 10-min intervals. Before each measurement, the plate was briefly shaken to suspend the cells. Each experiment was performed on at least three independent biological replicates.

RNA Isolation and Quantitative Reverse Transcription Polymerase Chain Reaction

RNA was isolated from 4 μ l \times 100 μ l samples of *E. coli* K-12 cultures incubated for 6-h with sub-MIC concentrations of each respective antisense (KFF)₃K-PNA oligomer (8 μ M for anti-*mazE*, 4 μ M for anti-*hipB*, 16 μ M for anti-*thyA*, and 1 μ M for anti-*gltX*). The cells were collected by centrifugation, and total bacterial RNA was isolated using a High Pure RNA Isolation

Kit (Roche Molecular Systems), following the protocol provided by the manufacturer. All qPCR procedures were performed according to the MIQE guidelines (Bustin et al., 2009). To detect the expression of the *mazE*, *mazF*, *thyA*, *hipB*, *hipA*, and *gltX* genes, 50 ng of the total RNA was reverse transcribed to generate cDNA using a Maxima First Strand cDNA Synthesis Kit for RT-qPCR with dsDNase (Thermo Scientific™), as outlined in the manufacturer's protocol. qPCR was performed using SYBR® Green Master Mix (Bio-Rad Laboratories Inc., United States) according to the supplied instructions. The level of the transcript of the essential *gyrA* gene was used for normalization (Rocha et al., 2015). The gene-specific primer pairs used for qPCR are listed in **Supplementary Table 3**. Amplification was performed in a Biorad CFX96 Touch™ Real-Time PCR Detection System (Bio-Rad Laboratories Inc., United States). Relative quantification of gene transcription was performed using the $\Delta\Delta$ CT method (Livak and Schmittgen, 2001). The presented data represent averages of triplicate determinations, performed at least two times. Statistical analyses were performed with one-way ANOVA with Fisher's test for multiple comparisons. Differences between treated and non-treated control samples were considered not significant ($P \geq 0.05$), marginally significant ($P < 0.05$)*, or significant ($P < 0.01$)**.

Synergy With Antibiotics – Fractional Inhibitory Concentrations

The interaction of (KFF)₃K-PNAs and antibiotics was examined using a standard checkerboard microdilution method (Figure 5B; Hsieh et al., 1993). Samples of *E. coli* O157:H7 culture grown in MHB were added to the wells of sterile 96-well plates containing combinations of two agents at various concentrations, and the plates were incubated at 37°C for 12 h. The OD₆₀₀ of the culture in each well was then determined using a plate reader. To define the nature of the interactions, the Fractional Inhibitory Concentration Indices (FIC_i) were calculated for each well with the equation $FIC_i = FIC_A + FIC_B = (C_A/MIC_A) + (C_B/MIC_B)$, where MIC_A and MIC_B are the MICs of compounds A and B alone, respectively, and C_A and C_B are the concentrations of the compounds in combination, respectively. The FIC_i values were interpreted using a conservative model restricting interpretation to the following interaction categories: synergy (FIC_i \leq 0.5), additive (FIC_i > 0.5–1.0), and indifference (1.0–4.0) (Doern, 2014).

Cytotoxicity Assay

HEK-293 cells were cultured in DMEM medium with high glucose (Lonza) supplemented with 10% FBS (Biowest) and Penicillin–Streptomycin (50 U/ml, Gibco) at 37°C in 5% CO₂. The cells were seeded at 5×10^4 or 10^5 per well in 96-well plates for incubations of 24 or 48 h, respectively. Wells contained the (KFF)₃K-PNAs at a final concentration of 32 μ M. Cell viability following incubation with the (KFF)₃K-PNAs was determined using the standard MTT [3-(4,5-dimethylthiazol-2-yl)-2,5-diphenyltetrazolium bromide] (Merck) assay (Mosmann, 1983) with absorbance at 590 nm measured using a plate reading spectrophotometer (Synergy H1MFDG, Biotek). Each

experiment was performed for three independent biological replicates. Statistical significance compared to untreated control samples was determined using the Mann-Whitney U test. All results were considered as statistically significant if $P < 0.05$.

DATA AVAILABILITY STATEMENT

The raw data supporting the conclusions of this manuscript will be made available by the authors, without undue reservation, to any qualified researcher.

AUTHOR CONTRIBUTIONS

MR designed the PNA sequences, performed the MIC, RT-qPCR, and FIC experiments, and analyzed the data. TP synthesized the PNA oligomers and PNA-peptides. JC, DB, and MR designed and prepared the *E. coli* K-12 MG1655 $\Delta mazF$ mutant. MK examined the cytotoxic effect of (KFF)₃K-PNAs on eukaryotic cells. JT and DB supervised the overall project. MR, TP, and JT wrote the manuscript. All authors discussed the results and revised the manuscript.

REFERENCES

- Abushahba, M. F. N., Mohammad, H., Thangamani, S., Hussein, A. A. A., and Seleem, M. N. (2016). Impact of different cell penetrating peptides on the efficacy of antisense therapeutics for targeting intracellular pathogens. *Sci. Rep.* 6:20832. doi: 10.1038/srep20832
- Amato, S. M., and Brynildsen, M. P. (2015). Persister heterogeneity arising from a single metabolic stress. *Curr. Biol.* 25, 2090–2098. doi: 10.1016/j.cub.2015.06.034
- Bai, H., You, Y., Yan, H., Meng, J., Xue, X., Hou, Z., et al. (2012). Antisense inhibition of gene expression and growth in gram-negative bacteria by cell-penetrating peptide conjugates of peptide nucleic acids targeted to rpoD gene. *Biomaterials* 33, 659–667. doi: 10.1016/j.biomaterials.2011.09.075
- Baraniak, A. (2002). Ceftazidime-hydrolysing CTX-M-15 extended-spectrum beta-lactamase (ESBL) in Poland. *J. Antimicrob. Chemother.* 50, 393–396. doi: 10.1093/jac/dkf151
- Bendifallah, N., Rasmussen, F. W., Zachar, V., Ebbesen, P., Nielsen, P. E., and Koppelhus, U. (2006). Evaluation of cell-penetrating peptides (CPPs) as vehicles for intracellular delivery of antisense peptide nucleic acid (PNA). *Bioconjug. Chem.* 17, 750–758. doi: 10.1021/bc050283q
- Bushby, S. R. M. (1975). Synergy of trimethoprim-sulfamethoxazole. *Can. Med. Assoc. J.* 112, 638–668.
- Bustin, S. A., Benes, V., Garson, J. A., Hellems, J., Huggett, J., Kubista, M., et al. (2009). The MIQE guidelines: minimum information for publication of quantitative real-time PCR experiments. *Clin. Chem.* 55, 611–622. doi: 10.1373/clinchem.2008.112797
- Cashel, M., Gentry, D. R., Hernandez, V. J., and Vinella, D. (1996). The stringent response. *Escherichia coli* and *Salmonella*. *Cell Mol. Biol.* 2, 913–931. doi: 10.1128/IAI.00193-11
- Chan, W. T., Balsa, D., and Espinosa, M. (2015). One cannot rule them all: are bacterial toxins-antitoxins druggable? *FEMS Microbiol. Rev.* 39, 522–540. doi: 10.1093/femsre/fuv002
- Chan, W. T., Espinosa, M., and Yeo, C. C. (2016). Keeping the wolves at bay: antitoxins of prokaryotic type II toxin-antitoxin systems. *Front. Mol. Biosci.* 3:9. doi: 10.3389/fmolb.2016.00009
- Chan, W. T., Moreno-Córdoba, I., Yeo, C. C., and Espinosa, M. (2012). Toxin-antitoxin genes of the Gram-positive pathogen *Streptococcus pneumoniae*: so

FUNDING

We acknowledge support from the National Science Centre, Poland (PRELUDIUM 2017/25/N/NZ1/01578 to MR; SYMFONIA 2014/12/W/ST5/00589 to JT, MR, TP, and MK), the Ministry of Science and Higher Education through the CeNT, University of Warsaw intramural grant DSM #501-D313-86-0117000-02, and Polish-U.S. Fulbright Commission (to JT and MR).

ACKNOWLEDGMENTS

We thank A. Szalewska-Pałasz and A. Krawczyk-Balska for providing the *E. coli* O157:H7 and WR3551/98 strains, respectively. JT would like to thank K. Jażdżewski for helpful discussions.

SUPPLEMENTARY MATERIAL

The Supplementary Material for this article can be found online at: <https://www.frontiersin.org/articles/10.3389/fmicb.2018.02870/full#supplementary-material>

- few and yet so many. *Microbiol. Mol. Biol. Rev.* 76, 773–791. doi: 10.1128/MMBR.00030-12
- Chowdhury, N., Kwan, B. W., and Wood, T. K. (2016). Persistence increases in the absence of the alarmone guanosine tetraphosphate by reducing cell growth. *Sci. Rep.* 6:20519. doi: 10.1038/srep20519
- CLSI (2015). *Methods for Dilution Antimicrobial Susceptibility Tests for Bacteria That Grow Aerobically. Approved Standard*, 9th Edn. Wayne, PA: CLSI,
- Coates, A. R. M., and Hu, Y. (2007). Novel approaches to developing new antibiotics for bacterial infections. *Br. J. Pharmacol.* 152, 1147–1154. doi: 10.1038/sj.bjp.0707432
- Deere, J., Iversen, P., and Geller, B. L. (2005). Antisense phosphorodiamidate morpholino oligomer length and target position effects on gene-specific inhibition in *Escherichia coli*. *Antimicrob. Agents Chemother.* 49, 249–255. doi: 10.1128/AAC.49.1.249-255.2005
- Dias, N., and Stein, C. A. (2002). Antisense oligonucleotides: basic concepts and mechanisms. *Mol. Cancer Ther.* 1, 347–355.
- Díaz-Orejón, R., Espinosa, M., and Yeo, C. C. (2017). The importance of the expendable: toxin-antitoxin genes in plasmids and chromosomes. *Front. Microbiol.* 8:1479. doi: 10.3389/fmicb.2017.01479
- Doern, C. D. (2014). When does 2 plus 2 equal 5? A review of antimicrobial synergy testing. *J. Clin. Microbiol.* 52, 4124–4128. doi: 10.1128/JCM.01121-14
- Dryselius, R., Aswasti, S. K., Rajarao, G. K., Nielsen, P. E., and Good, L. (2003). The translation start codon region is sensitive to antisense PNA inhibition in *Escherichia coli*. *Oligonucleotides* 13, 427–433. doi: 10.1089/154545703322860753
- Dryselius, R., Nekhotiaeva, N., and Good, L. (2005). Antimicrobial synergy between mRNA- and protein-level inhibitors. *J. Antimicrob. Chemother.* 56, 97–103. doi: 10.1093/jac/dki173
- Dryselius, R., Nikraves, A., Kulyté, A., Goh, S., and Good, L. (2006). Variable coordination of cotranscribed genes in *Escherichia coli* following antisense repression. *BMC Microbiol.* 6:97. doi: 10.1186/1471-2180-6-97
- Dziewit, L., Adamczuk, M., Szuplewska, M., and Bartosik, D. (2011). DIY series of genetic cassettes useful in construction of versatile vectors specific for Alphaproteobacteria. *J. Microbiol. Methods* 86, 166–174. doi: 10.1016/j.mimet.2011.04.016

- Engelberg-Kulka, H., Hazan, R., and Amitai, S. (2005). mazEF: a chromosomal toxin-antitoxin module that triggers programmed cell death in bacteria. *J. Cell Sci.* 118, 4327–4332. doi: 10.1242/jcs.02619
- Engelberg-Kulka, H., Sat, B., Reches, M., Amitai, S., and Hazan, R. (2004). Bacterial programmed cell death systems as targets for antibiotics. *Trends Microbiol.* 12, 66–71. doi: 10.1016/j.tim.2003.12.008
- Eriksson, M., Nielsen, P. E., and Good, L. (2002). Cell permeabilization and uptake of antisense peptide-peptide nucleic acid (PNA) into *Escherichia coli*. *J. Biol. Chem.* 277, 7144–7147. doi: 10.1074/jbc.M106624200
- Evers, M. M., Toonen, L. J. A., and van Roon-Mom, W. M. C. (2015). Antisense oligonucleotides in therapy for neurodegenerative disorders. *Adv. Drug Deliv. Rev.* 87, 90–103. doi: 10.1016/j.addr.2015.03.008
- Fair, R. J., and Tor, Y. (2014). Antibiotics and bacterial resistance in the 21st century. *Perspect. Med. Chem.* 6, 25–64. doi: 10.4137/PMC.S14459
- Fernandez-Garcia, L., Blasco, L., Lopez, M., Bou, G., Garcia-Contreras, R., Wood, T., et al. (2016). Toxin-antitoxin systems in clinical pathogens. *Toxins* 8, 1–23. doi: 10.3390/toxins8070227
- Fisher, R. A., Gollan, B., and Helaine, S. (2017). Persistent bacterial infections and persister cells. *Nat. Rev. Microbiol.* 15, 453–464. doi: 10.1038/nrmicro.2017.42
- Formation, A. P., Shan, Y., Gandt, A. B., Rowe, S. E., Deisinger, J. P., Conlon, B. P., et al. (2017). ATP-dependent persister formation in *Escherichia coli*. *mBio* 8:e2267-16. doi: 10.1128/mBio.02267-16
- Fu, Z., Tamber, S., Memmi, G., Donegan, N. P., and Cheung, A. L. (2009). Overexpression of MazF Sa in *Staphylococcus aureus* induces bacteriostasis by selectively targeting mRNAs for cleavage. *J. Bacteriol.* 191, 2051–2059. doi: 10.1128/JB.00907-08
- Germain, E., Castro-Roa, D., Zenkin, N., and Gerdes, K. (2013). Molecular mechanism of bacterial persistence by HipA. *Mol. Cell* 52, 248–254. doi: 10.1016/j.molcel.2013.08.045
- Gibson, D. G., Young, L., Chuang, R.-Y., Venter, J. C., Hutchison, C. A., and Smith, H. O. (2009). Enzymatic assembly of DNA molecules up to several hundred kilobases. *Nat. Methods* 6, 343–345. doi: 10.1038/nmeth.1318
- Goh, S., Boberek, J. M., Nakashima, N., Stach, J., and Good, L. (2009). Concurrent growth rate and transcript analyses reveal essential gene stringency in *Escherichia coli*. *PLoS One* 4:e6061. doi: 10.1371/journal.pone.0006061
- Good, L., Awasthi, S. K., Dryselius, R., Larsson, O., and Nielsen, P. E. (2001). Bactericidal antisense effects of peptide-PNA conjugates. *Nat. Biotechnol.* 19, 360–364. doi: 10.1038/86753
- Good, L., Sandberg, R., Larsson, O., Nielsen, P. E., and Wahlestedt, C. (2000). Antisense PNA effects in *Escherichia coli* are limited by the outer-membrane LPS layer. *Microbiology* 146, 2665–2670. doi: 10.1099/00221287-146-10-2665
- Górska, A., Markowska-Zagrajek, A., Równicki, M., and Trylska, J. (2016). Scanning of 16S ribosomal RNA for peptide nucleic acid targets. *J. Phys. Chem. B* 120, 8369–8378. doi: 10.1021/acs.jpcc.6b02081
- Harms, A., Brodersen, D. E., Mitarai, N., and Gerdes, K. (2018). Toxins, targets, and triggers: an overview of toxin-antitoxin biology. *Mol. Cell* 70, 768–784. doi: 10.1016/j.molcel.2018.01.003
- Harrison, J. J., Wade, W. D., Akerman, S., Vacchi-Suzzi, C., Stremick, C. A., Turner, R. J., et al. (2009). The chromosomal toxin gene yafQ is a determinant of multidrug tolerance for *Escherichia coli* growing in a biofilm. *Antimicrob. Agents Chemother.* 53, 2253–2258. doi: 10.1128/AAC.00043-09
- Harvey, R. J. (1982). Synergism in the folate pathway. *Rev. Infect. Dis.* 4, 255–260. doi: 10.1093/clinids/4.2.255
- Hatamoto, M., Nakai, K., Ohashi, A., and Imachi, H. (2009). Sequence-specific bacterial growth inhibition by peptide nucleic acid targeted to the mRNA binding site of 16S rRNA. *Appl. Microbiol. Biotechnol.* 84, 1161–1168. doi: 10.1007/s00253-009-2099-0
- Hayes, F., and Van Melder, L. (2011). Toxins-antitoxins: diversity, evolution and function. *Crit. Rev. Biochem. Mol. Biol.* 46, 386–408. doi: 10.3109/10409238.2011.600437
- Hazan, R., Sat, B., and Engelberg-kulka, H. (2004). *Escherichia coli* mazEF - mediated cell death is triggered by various stressful conditions. *Genet. Mol. Biol.* 186, 3663–3669. doi: 10.1128/JB.186.11.3663
- Hnedzko, D., Mcgee, D. W., Karamitas, Y. A., and Rozners, E. (2017). Sequence-selective recognition of double-stranded RNA and enhanced cellular uptake of cationic nucleobase and backbone-modified peptide nucleic acids. *RNA* 23:58. doi: 10.1261/rna.058362
- Hsieh, M. H., Yu, C. M., Yu, V. L., and Chow, J. W. (1993). Synergy assessed by checkerboard a critical analysis. *Diagn. Microbiol. Infect. Dis.* 16, 343–349. doi: 10.1016/0732-8893(93)90087-N
- Kaspy, I., Rotem, E., Weiss, N., Ronin, I., Balaban, N. Q., and Glaser, G. (2013). HipA-mediated antibiotic persistence via phosphorylation of the glutamyl-tRNA-synthetase. *Nat. Commun.* 4:3001. doi: 10.1038/ncomms4001
- Kędzierska, B., and Hayes, F. (2016). Emerging roles of toxin-antitoxin modules in bacterial pathogenesis. *Molecules* 21:E790. doi: 10.3390/molecules21060790
- Kim, D. H., Kang, S. M., Park, S. J., Jin, C., Yoon, H. J., and Lee, B. J. (2018). Functional insights into the *Streptococcus pneumoniae* HicBA toxin-antitoxin system based on a structural study. *Nucleic Acids Res.* 46, 6371–6386. doi: 10.1093/nar/gky469
- Kint, C. I., Verstraeten, N., Fauvart, M., and Michiels, J. (2012). New-found fundamentals of bacterial persistence. *Trends Microbiol.* 20, 577–585. doi: 10.1016/j.tim.2012.08.009
- Kirkpatrick, C. L., Martins, D., Redder, P., Frandi, A., Mignolet, J., Chapalay, J. B., et al. (2016). Growth control switch by a DNA-damage- inducible toxin-antitoxin system in *Caulobacter crescentus*. *Nat. Microbiol.* 1:16008. doi: 10.1038/nmicrobiol.2016.8
- Kulik, M., Markowska-Zagrajek, A., Wojciechowska, M., Grzela, R., Witula, T., and Trylska, J. (2017). Helix 69 of *Escherichia coli* 23S ribosomal RNA as a peptide nucleic acid target. *Biochimie* 138, 32–42. doi: 10.1016/j.biochi.2017.04.001
- Kurupati, P., Tan, K. S. W., Kumarasinghe, G., and Poh, C. L. (2007). Inhibition of gene expression and growth by antisense peptide nucleic acids in a multidrug-resistant beta-lactamase-producing *Klebsiella pneumoniae* strain. *Antimicrob. Agents Chemother.* 51, 805–811. doi: 10.1128/AAC.00709-06
- Lechat, P., Hummel, L., Rousseau, S., and Moszer, I. (2008). GenoList: an integrated environment for comparative analysis of microbial genomes. *Nucleic Acids Res.* 36, 469–474. doi: 10.1093/nar/gkm1042
- Lee, K. Y., and Lee, B. J. (2016). Structure, biology, and therapeutic application of toxin-antitoxin systems in pathogenic bacteria. *Toxins* 8:E305. doi: 10.3390/toxins8100305
- Lewis, K. (2007). Persister cells, dormancy and infectious disease. *Nat. Rev. Microbiol.* 5, 48–56. doi: 10.1038/nrmicro1557
- Lewis, K. (2008). Multidrug tolerance of biofilms and persister cells. *Curr. Top. Microbiol. Immunol.* 322, 107–131.
- Lioy, V. S., Rey, O., Balsa, D., Pellicer, T., and Alonso, J. C. (2010). A toxin-antitoxin module as a target for antimicrobial development. *Plasmid* 63, 31–39. doi: 10.1016/j.plasmid.2009.09.005
- Livak, K. J., and Schmittgen, T. D. (2001). Analysis of relative gene expression data using real-time quantitative PCR and the 2-DDCT method. *Methods* 25, 402–408. doi: 10.1006/meth.2001.1262
- Lobato-Márquez, D., Díaz-Orejas, R., and García-del Portillo, F. (2016). Toxin-antitoxins and bacterial virulence. *FEMS Microbiol. Rev.* 40, 592–609. doi: 10.1093/femsre/fuw022
- Łoś, J. M., Golec, P., Węgrzyn, G., Węgrzyn, A., and Łoś, M. (2008). Simple method for plating *Escherichia coli* bacteriophages forming very small plaques or no plaques under standard conditions. *Appl. Environ. Microbiol.* 74, 5113–5120. doi: 10.1128/AEM.00306-08
- Ma, Y., Zhu, Y., Li, W., Liu, F., Lv, N., Li, J., et al. (2015). Characteristics of persister cells and the diversity of type II toxin - antitoxin system in *Acinetobacter baumannii*. *Wei Sheng Wu Xue Bao Acta Microbiol. Sin.* 55, 949–958.
- Mosmann, T. (1983). Rapid colorimetric assay for cellular growth and survival: application to proliferation and cytotoxicity assays. *J. Immunol. Methods* 65, 55–63. doi: 10.1016/0022-1759(83)90303-4
- Mu, Y., Shen, Z., Jeon, B., Dai, L., and Zhang, Q. (2013). Synergistic effects of anti-CmeA and anti-CmeB peptide nucleic acids on sensitizing *Campylobacter jejuni* to antibiotics. *Antimicrob. Agents Chemother.* 57, 4575–4577. doi: 10.1128/AAC.00605-13
- Narenji, H., Gholizadeh, P., Aghazadeh, M., Rezaee, M. A., Asgharzadeh, M., and Kafil, H. S. (2017). Peptide nucleic acids (PNAs): currently potential bactericidal agents. *Biomed. Pharmacother.* 93, 580–588. doi: 10.1016/j.biopha.2017.06.092
- Nekhotiaeva, N., Awasthi, S. K., Nielsen, P. E., and Good, L. (2004). Inhibition of *Staphylococcus aureus* gene expression and growth using antisense peptide nucleic acids. *Mol. Ther.* 10, 652–659. doi: 10.1016/j.ymthe.2004.07.006
- Nielsen, P. E., Egholm, M., Berg, R. H., and Buchardt, O. (1991). Sequence-selective recognition of DNA by strand displacement with a thymine-substituted polyamide. *Science* 254, 1497–1500. doi: 10.1126/science.1962210

- Nikraves, A., Dryselius, R., Faridani, O. R., Goh, S., Sadeghizadeh, M., Behmanesh, M., et al. (2007). Antisense PNA accumulates in *Escherichia coli* and mediates a long post-antibiotic effect. *Mol. Ther.* 15, 1537–1542. doi: 10.1038/sj.mt.6300209
- Ogata, H., Goto, S., Sato, K., Fujibuchi, W., Bono, H., and Kanehisa, M. (1999). KEGG: kyoto encyclopedia of genes and genomes. *Nucleic Acids Res.* 27, 29–34. doi: 10.1093/nar/27.1.29
- Page, R., and Peti, W. (2016). Toxin-antitoxin systems in bacterial growth arrest and persistence. *Nat. Chem. Biol.* 12, 208–214. doi: 10.1038/nchembio.2044
- Pandey, V. N., Upadhyay, A., and Chaubey, B. (2009). Prospects for antisense peptide nucleic acid (PNA) therapies for HIV. *Expert Opin. Biol. Ther.* 9, 975–989. doi: 10.1517/14712590903052877
- Patenge, N., Pappesch, R., Krawack, F., Walda, C., Mraheil, M. A., Jacob, A., et al. (2013). Inhibition of growth and gene expression by PNA-peptide conjugates in *Streptococcus pyogenes*. *Mol. Ther. Nucleic Acids* 2:e132. doi: 10.1038/mtna.2013.62
- Pedersen, K., Christensen, S. K., and Gerdes, K. (2002). Rapid induction and reversal of a bacteriostatic condition by controlled expression of toxins and antitoxins. *Mol. Microbiol.* 45, 501–510. doi: 10.1111/j.1540-5915.2006.00123.x
- Philippe, N., Alcaraz, J. P., Coursange, E., Geiselmann, J., and Schneider, D. (2004). Improvement of pCVD442, a suicide plasmid for gene allele exchange in bacteria. *Plasmid* 51, 246–255. doi: 10.1016/j.plasmid.2004.02.003
- Popenda, M., Szachniuk, M., Antczak, M., Purzycka, K. J., Lukasiak, P., Bartol, N., et al. (2012). Automated 3D structure composition for large RNAs. *Nucleic Acids Res.* 40:e112. doi: 10.1093/nar/gks339
- Pósfai, G., Kolisnychenko, V., Bereczki, Z., and Blattner, F. R. (1999). Markerless gene replacement in *Escherichia coli* stimulated by a double-strand break in the chromosome. *Nucleic Acids Res.* 27, 4409–4415. doi: 10.1093/nar/27.22.4409
- Rasmussen, L. C. V., Sperling-Petersen, H. U., and Mortensen, K. K. (2007). Hitting bacteria at the heart of the central dogma: sequence-specific inhibition. *Microb. Cell Fact.* 6:24. doi: 10.1186/1475-2859-6-24
- Rocha, D. J. P., Santos, C. S., and Pacheco, L. G. C. (2015). Bacterial reference genes for gene expression studies by RT-qPCR: survey and analysis. *Antonie Van Leeuwenhoek* 108, 685–693. doi: 10.1007/s10482-015-0524-1
- Rocker, A., and Meinhart, A. (2016). Type II toxin: antitoxin systems. More than small selfish entities? *Curr. Genet.* 62, 287–290. doi: 10.1007/s00294-015-0541-7
- Rothenbacher, F. P., Suzuki, M., Hurley, J. M., Montville, T. J., Kirn, T. J., Ouyang, M., et al. (2012). Clostridium difficile MazF toxin exhibits selective, not global, mRNA cleavage. *J. Bacteriol.* 194, 3464–3474. doi: 10.1128/JB.00217-12
- Równicki, M., Wojciechowska, M., Wierzbą, A. J., Czarnecki, J., Bartosik, D., Gryko, D., et al. (2017). Vitamin B₁₂ as a carrier of peptide nucleic acid (PNA) into bacterial cells. *Sci. Rep.* 7:7644. doi: 10.1038/s41598-017-08032-8
- Rozners, E. (2012). Recent advances in chemical modification of peptide nucleic acids. *J. Nucleic Acids* 2012:518162. doi: 10.1155/2012/518162
- Schifano, J. M., Cruz, J. W., Vvedenskaya, I. O., Edifor, R., Ouyang, M., Husson, R. N., et al. (2016). tRNA is a new target for cleavage by a MazF toxin. *Nucleic Acids Res.* 44:gkv1370. doi: 10.1093/nar/gkv1370
- Schneider, E. K., Reyes-Ortega, F., Velkov, T., and Li, J. (2017). Antibiotic-non-antibiotic combinations for combating extremely drug-resistant Gram-negative ‘superbugs’. *Essays Biochem.* 61, 115–125. doi: 10.1042/EBC20160058
- Schumacher, M. A., Piro, K. M., Xu, W., Hansen, S., Lewis, K., and Brennan, R. G. (2009). Molecular mechanisms of HipA mediated multidrug tolerance and its neutralization by HipB. *Science* 323, 396–401. doi: 10.1126/science.1163806
- Schuster, C. F., Park, J. H., Prax, M., Herbig, A., Nieselt, K., Rosenstein, R., et al. (2013). Characterization of a MazEF toxin-antitoxin homologue from *Staphylococcus equorum*. *J. Bacteriol.* 195, 115–125. doi: 10.1128/JB.00400-12
- Shapiro, S. (2013). Speculative strategies for new antibacterials: all roads should not lead to Rome. *J. Antibiot.* 66, 371–386. doi: 10.1038/ja.2013.27
- Sharma, P., Teymournejad, O., and Rikihisa, Y. (2017). Peptide nucleic acid knockdown and intra-host cell complementation of ehrlichia type IV secretion system effector. *Front. Cell. Infect. Microbiol.* 7:228. doi: 10.3389/fcimb.2017.00228
- Tripathi, A., Dewan, P. C., Siddique, S. A., and Varadarajan, R. (2014). MazF-induced growth inhibition and persister generation in *escherichia coli*. *J. Biol. Chem.* 289, 4191–4205. doi: 10.1074/jbc.M113.510511
- Ventola, C. L. (2015a). The antibiotic resistance crisis. Part 1: causes and threats. *Pharm. Ther.* 40, 277–283.
- Ventola, C. L. (2015b). The antibiotic resistance crisis. Part 2: management strategies and new agents. *Pharm. Ther.* 40, 344–352.
- Verma, S., Kumar, S., Gupta, V. P., Gourinath, S., Bhatnagar, S., and Bhatnagar, R. (2015). Structural basis of *Bacillus anthracis* MoxXT disruption and the modulation of MoxT ribonuclease activity by rationally designed peptides. *J. Biomol. Struct. Dyn.* 33, 606–624. doi: 10.1080/07391102.2014.899924
- Wen, Y., Behiels, E., and Devreese, B. (2014). Toxin-antitoxin systems: their role in persistence, biofilm formation, and pathogenicity. *Pathog. Dis.* 70, 240–249. doi: 10.1111/2049-632X.12145
- Williams, J., and Hergenrother, P. (2014). Artificial activation of toxin-antitoxin systems as an antibacterial strategy. *Trends Microbiol.* 20, 291–298. doi: 10.1016/j.tim.2012.02.005
- Wood, T. K., Knabel, S. J., and Kwan, B. W. (2013). Bacterial persister cell formation and dormancy. *Appl. Environ. Microbiol.* 79, 7116–7121. doi: 10.1128/AEM.02636-13
- Yamaguchi, Y., and Inouye, M. (2009). Chapter 12 mRNA Interferases, Sequence-Specific Endoribonucleases from the Toxin-Antitoxin Systems, 1st Edn. Amsterdam: Elsevier Inc., doi: 10.1016/S0079-6603(08)00812-X
- Yamaguchi, Y., Nariya, H., Park, J. H., and Inouye, M. (2012). Inhibition of specific gene expressions by protein-mediated mRNA interference. *Nat. Commun.* 3, 606–607. doi: 10.1038/ncomms1621
- Zeng, Z., Han, S., Hong, W., Lang, Y., Li, F., Liu, Y., et al. (2016). A tat-conjugated peptide nucleic acid tat-PNA-DR inhibits hepatitis B virus replication in vitro and in vivo by targeting LTR direct repeats of HBV RNA. *Mol. Ther. Nucleic Acids* 5:e295. doi: 10.1038/mtna.2016.11
- Zuker, M. (2003). Mfold web server for nucleic acid folding and hybridization prediction. *Nucleic Acids Res.* 31, 3406–3415. doi: 10.1093/nar/gkg595

Conflict of Interest Statement: The authors declare that the research was conducted in the absence of any commercial or financial relationships that could be construed as a potential conflict of interest.

Copyright © 2018 Równicki, Pieńko, Czarnecki, Kolanowska, Bartosik and Trylska. This is an open-access article distributed under the terms of the Creative Commons Attribution License (CC BY). The use, distribution or reproduction in other forums is permitted, provided the original author(s) and the copyright owner(s) are credited and that the original publication in this journal is cited, in accordance with accepted academic practice. No use, distribution or reproduction is permitted which does not comply with these terms.



Improved Biodistribution and Extended Serum Half-Life of a Bacteriophage Endolysin by Albumin Binding Domain Fusion

Johan Seijsing^{1*†}, Anna M. Sobieraj^{1‡}, Nadia Keller², Yang Shen¹,
Annelies S. Zinkernagel², Martin J. Loessner¹ and Mathias Schmelcher¹

¹ Laboratory of Food Microbiology, Institute of Food, Nutrition and Health, ETH Zürich, Zürich, Switzerland, ² Division of Infectious Diseases and Hospital Epidemiology, University Hospital Zürich – University of Zürich, Zürich, Switzerland

OPEN ACCESS

Edited by:

You-Hee Cho,
CHA University, South Korea

Reviewed by:

Melinda J. Mayer,
Quadram Institute, United Kingdom
Pilar García,
Spanish National Research Council
(CSIC), Spain

*Correspondence:

Johan Seijsing
johan.seijsing@su.se

† Present address:

Johan Seijsing,
Department of Molecular Biosciences,
The Wenner-Gren Institute, Stockholm
University, Stockholm, Sweden

‡ These authors have contributed
equally to this work as co-first authors

Specialty section:

This article was submitted to
Antimicrobials, Resistance
and Chemotherapy,
a section of the journal
Frontiers in Microbiology

Received: 07 October 2018

Accepted: 14 November 2018

Published: 27 November 2018

Citation:

Seijsing J, Sobieraj AM, Keller N,
Shen Y, Zinkernagel AS, Loessner MJ
and Schmelcher M (2018) Improved
Biodistribution and Extended Serum
Half-Life of a Bacteriophage Endolysin
by Albumin Binding Domain Fusion.
Front. Microbiol. 9:2927.
doi: 10.3389/fmicb.2018.02927

The increasing number of multidrug-resistant bacteria intensifies the need to develop new antimicrobial agents. Endolysins are bacteriophage-derived enzymes that degrade the bacterial cell wall and hold promise as a new class of highly specific and versatile antimicrobials. One major limitation to the therapeutic use of endolysins is their often short serum circulation half-life, mostly due to kidney excretion and lysosomal degradation. One strategy to increase the half-life of protein drugs is fusion to the albumin-binding domain (ABD). By high-affinity binding to serum albumin, ABD creates a complex with large hydrodynamic volume, reducing kidney excretion and lysosomal degradation. The aim of this study was to investigate the *in vitro* antibacterial activity and *in vivo* biodistribution and half-life of an engineered variant of the *Staphylococcus aureus* phage endolysin LysK. The ABD sequence was introduced at different positions within the enzyme, and lytic activity of each variant was determined *in vitro* and *ex vivo* in human serum. Half-life and biodistribution were assessed *in vivo* by intravenous injection of europium-labeled proteins into C57BL/6 wild-type mice. Our data demonstrates that fusion of the endolysin to ABD improves its serum circulation half-life and reduces its deposition in the kidneys *in vivo*. The most active construct reduced *S. aureus* counts in human serum *ex vivo* by 3 logs within 60 min. We conclude that ABD fusions provide an effective strategy to extend the half-life of antibacterial enzymes, supporting their therapeutic potential for treatment of systemic bacterial infections.

Keywords: staphylococci, antibiotic alternatives, biodistribution, half-life, endolysin, albumin binding domain (ABD), LysK, bacteriophage

INTRODUCTION

The important human pathogen *Staphylococcus aureus* has acquired various antibiotic resistances over the years. Of particular importance are methicillin-resistant (MRSA) and vancomycin-resistant *S. aureus* (VRSA) (Chambers and Deleo, 2010).

In order to impede this development, new antimicrobials with alternative mechanisms of action and a reduced chance of resistance development are needed. Endolysins are bacteriophage-derived enzymes (peptidoglycan hydrolases, PGHs) with the ability to degrade the peptidoglycan of the bacterial cell wall, thereby causing cell death (Schmelcher et al., 2012).

The most important advantages of endolysins as antimicrobials compared to conventional antibiotics include their rapid killing kinetics, reduced risk of bacterial resistance (Spratt, 1994;

Schmelcher et al., 2012), and the high specificity for their target bacteria, leaving commensal and possibly beneficial microorganisms unaffected (Schmelcher et al., 2012).

LysK, the endolysin of the staphylococcal phage K, is an example of a well-characterized PGH active against staphylococci (O'Flaherty et al., 2005). The modular structure of LysK (O'Flaherty et al., 2004) consists of a C-terminal SH3b cell wall binding domain (CBD) (Whistock and James, 1999), and two enzymatically active domains (EADs): an N-terminal cysteine, histidine-dependent amidohydrolase/peptidase (CHAP) domain (Bateman and Rawlings, 2003), and a centrally located amidase-2 (N-acetylmuramoyl L-alanine amidase). It has been shown that LysK maintains its high activity even if lacking the amidase-2 domain (Becker et al., 2009), and the CHAP domain has been shown to have high activity on its own (Horgan et al., 2009).

The strong anti-staphylococcal activity of LysK and its engineered variants has been demonstrated both *in vitro* and *in vivo* (Kokai-Kun et al., 2007; Rashel et al., 2007; Daniel et al., 2010; Fenton et al., 2010; Gu et al., 2011; Jun et al., 2013; Schmelcher et al., 2014). However, despite some encouraging results with this and other endolysins (Haddad Kashani et al., 2017), systemic administration of most protein-based drugs, including endolysins, is currently hampered by their short serum circulation half-life (Loeffler et al., 2003; Walsh et al., 2003). The decline in drug concentration is characterized by alpha and beta phase decay. After intravenous administration, concentrations decline rapidly as the drug is distributed into the tissues and organs (Lobo et al., 2004). Subsequently, the residual concentration decreases due to inactivation by antibodies (Jawa et al., 2013), degradation by proteases, endocytosis by epithelial cells, and kidney excretion (Werle and Bernkop-Schnürch, 2006).

Various approaches may extend the half-life of proteins (Patel and Benfield, 1996; Matthews et al., 2008; Kontermann, 2011). A promising strategy is fusion of the albumin binding domain (ABD) to the protein of interest (Nygren et al., 1991). ABD binds to serum albumin with strong affinity and forms a complex with a large hydrodynamic volume, avoiding glomerular filtration (Jonsson et al., 2008). Moreover, proteins fused to ABD are indirectly recycled by the FcRn (Chaudhury et al., 2003). Human serum albumin (HSA) has a serum circulation half-life of 3 weeks in humans (Doweiko and Nompleggi, 1991), whereas murine serum albumin (MSA) has a half-life of 35 h in mice (Chaudhury et al., 2003). Proteins recruiting albumin through high-affinity ABDs have been reported to show similar half-lives (Seijsing et al., 2014).

In this study, we investigated the bacteriolytic activity, serum circulation half-life and biodistribution of engineered variants of the endolysin LysK, with and without ABD.

MATERIALS AND METHODS

Plasmid and DNA Construct Design

Gene synthesis and subcloning into the pET21a(+) vector (Novagen, Darmstadt, Germany) were performed by BioBasic Inc. (Markham, ON, Canada), and modifications resulting in LysK variants without Amidase-2 domain and Lys6-tag

were performed in-house using standard molecular cloning techniques (Green and Sambrook, 2012). Schematics of all created constructs, with the corresponding names and acronyms are presented in **Figure 1**. The ABD used in this study (ABD035) is an affinity-matured variant (Jonsson et al., 2008) from streptococcal protein G (Nygren et al., 1991; Johansson et al., 2002).

Recombinant Protein Expression and Purification

Vectors encoding target proteins were introduced into BL21 Gold (DE3) *E. coli* cells (Stratagene, La Jolla, CA, United States) (**Table 1**) by electroporation. Cells were grown at 37°C and 220 RPM in LB-PE medium (15 g/L Tryptone, 8 g/L Yeast extract, 5 g/L NaCl, pH 7.8) supplemented with 100 µg/mL ampicillin until OD₆₀₀ reached 0.5. Protein expression was induced by adding 0.5 mM IPTG, and cultivation was continued over night at 19°C and 120 RPM. Cells were pelleted using centrifugation and disrupted using both a Stansted Fluid Power Pressure Cell Homogenizer (100 MPa) and sonication on ice/ethanol slurry with a Bandelin Sonopuls HD 2076 (2 min, 1:1 pulses, 50% power). Proteins were purified from cleared crude extracts using nickel affinity chromatography. For the *in vivo* study, the following modifications were made to reduce endotoxin concentrations. Vectors were transformed into electrocompetent *E. coli* ClearColi BL21(DE3) (Lucigen, Middleton, WI, United States) (**Table 1**). LB-PES (15 g/L Tryptone, 8 g/L yeast extract, 10 g/L NaCl, pH 7.8) medium was used for all cultivations. Bacteria were lysed by sonication only. During purification, the columns were washed twice with 25 ml of ice cold lysis buffer supplemented with 0.1% Triton X-114 (Reichert et al., 2006), and subsequently 25 ml of lysis buffer. Proteins were tested for endotoxins using the EndoZyme kit (Hyglos, Regensburg, Germany) according to manufacturer's instructions.

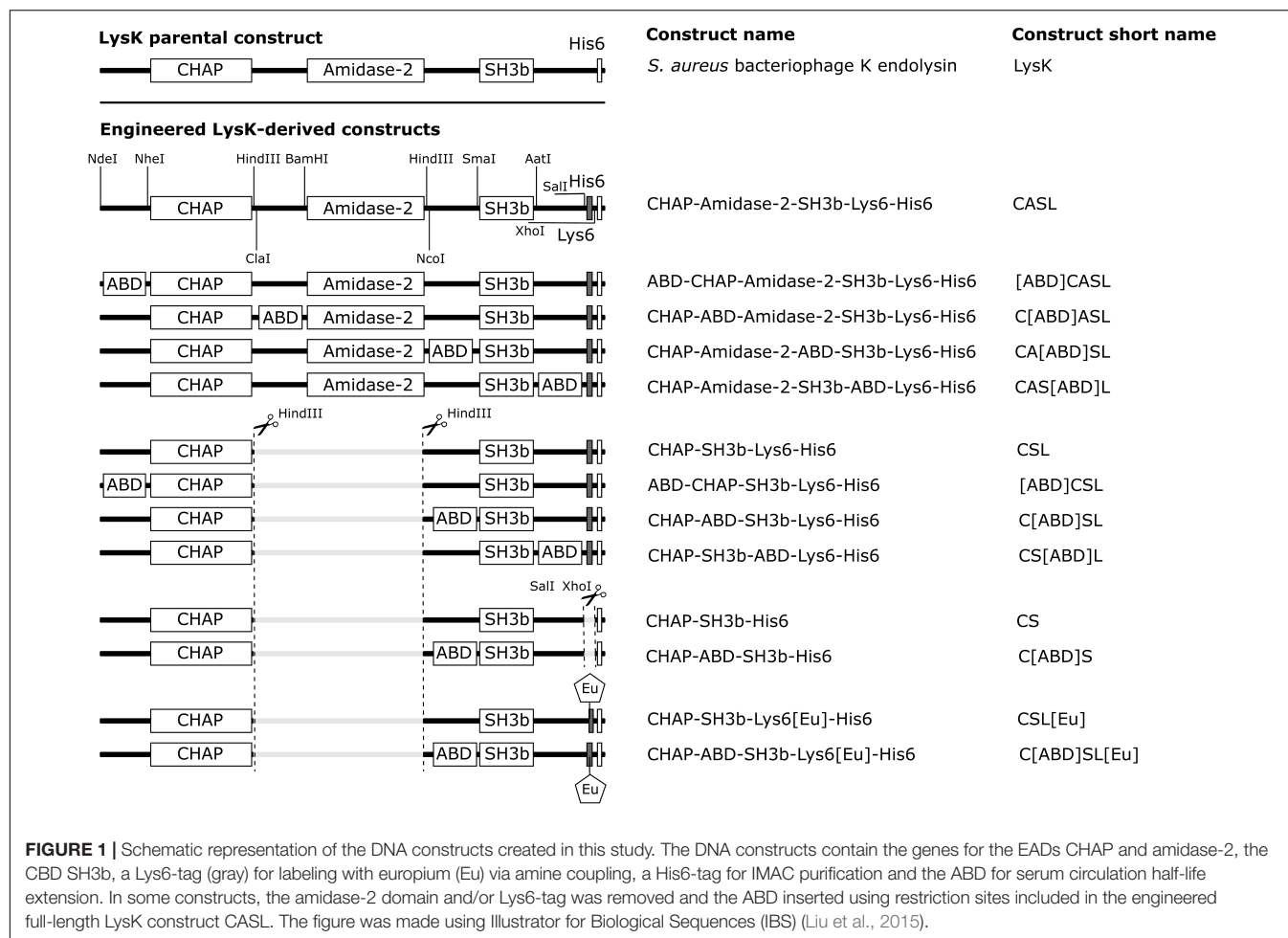
Europium Labeling

Europium labeling of proteins via the Eu-chelator complex (Sodium[4'-(4'-Amino-4-biphenyl)-2,2':6',2''-terpyridine-6,6''-diylbis(methyliminodiacetato)]europate(III)) was performed by BioTeZ (Berlin, Germany).

Surface Plasmon Resonance

For measuring binding of ABD-containing constructs to HSA by surface plasmon resonance (SPR), a Biacore X (GE Healthcare, Uppsala, Sweden) with a C1 sensor chip and HBS-T running buffer was used essentially as previously described (Jonsson et al., 2008).

Human serum albumin (HSA; 100 µg/ml) was immobilized in flow cell 2 using an Amine Coupling Kit (GE Healthcare, Uppsala, Sweden) according to the manufacturer's instructions. For interaction analysis, 30 µl of endolysin construct at a concentration of 50 nM was injected, with flow cell 1 serving as the reference. The chip surface was regenerated using 15 mM HCl.

**TABLE 1 |** Bacterial strains used in this study.

Strain	Source	Reference
<i>Staphylococcus aureus</i> SA113 (ATCC 35556)	Andreas Peschel, University of Tübingen, Germany	(Kristian et al., 2004)
<i>S. aureus</i> Newman D2C (ATCC 25904)	Brigitte Berger-Bächi, University of Zurich, Switzerland	(Bischoff et al., 2004)
<i>E. coli</i> BL21-Gold(DE3)	Stratagene, La Jolla, CA, United States	
<i>E. coli</i> ClearColi BL21(DE3)	Lucigen, Middleton, WI, United States	

Turbidity Reduction Assay

The assay was performed essentially as described before (Schmelcher et al., 2014), using *S. aureus* SA113 (Kristian et al., 2004) (Table 1) and PBS supplemented with 5 μ M HSA (PBS-HSA). Specific enzymatic activity was expressed as $\Delta OD_{600} \text{ min}^{-1} \mu\text{M}^{-1}$. For comparison of specific activities, one-way ANOVA was performed. The impact of Lys6-tags on activity was assessed by an unpaired *t*-test (GraphPad Prism, 7.02).

Time Kill Assay

For the time kill assay, *S. aureus* Newman (Bischoff et al., 2004) (Table 1) was grown in LB medium to an OD_{600} of 0.5, and the assay was performed essentially as previously described (Schuch et al., 1986). Target bacteria at a concentration of 10^6 CFU/ml were mixed with 200 nM of endolysin in human

serum (H4522, Sigma-Aldrich, St Louis, MO, United States). Human serum alone was used as negative control. For statistical analysis, two-way ANOVA on log-transformed data followed by Sidak's multiple comparisons test (GraphPad Prism, 7.02) was performed.

In vivo Half-Life and Biodistribution Study

Eight to ten weeks old female C57BL/6 wild-type mice (Janvier, Le Genest St. Isle, France) were separated into two groups of four mice each. Animals were injected intravenously into the tail vein with ~ 7 nmol/kg body weight (100 μ L, 1.4 μ M) of Eu-labeled C[ABD]SL[Eu] or the control CSL[Eu]. Blood was drawn from the tail vein after 0.25, 24, 72, 120, and 144 h. Heparinized blood was centrifuged and plasma was collected. Mice were

euthanized at 144 or 216 h, and organs were homogenized using a TissueLyser (Qiagen, Valencia, CA, United States) in PBS (1:1 weight/volume ratio). The Europium content in the blood and organ samples was determined using an Infinite M1000 PRO (Tecan, Durham, NC, United States) time-resolved fluorescence plate reader. Obtained values were correlated to a spiked standard dilution series of respective proteins in mouse serum or a homogenate of respective organs.

Serum concentrations were plotted against time, and the four last values were used to calculate the beta half-life of the protein using a one phase decay model in Prism (GraphPad Software, San Diego, CA, United States). Student's *t*-test was used to compare protein concentrations in the serum at the last time point at 144 h. For comparing protein concentrations in organ samples, a two-way ANOVA on log-transformed data followed by Sidak's multiple comparisons test was performed.

Results

Design and Production of Peptidoglycan Hydrolase Constructs

A high affinity variant of ABD [ABD035 (Jonsson et al., 2008)] was selected for fusion to full length and shortened versions of the LysK endolysin. The shortened versions feature a deletion of the centrally located amidase-2 domain, since this domain reportedly contributes little to the overall activity of the enzyme (Becker et al., 2009). Different variants of LysK-ABD fusion constructs were created, with the ABD inserted at various positions within the proteins (Figure 1), in an effort to identify the ABD-tagged version with the highest staphylolytic activity.

All constructs featured a C-terminally located His6-tag to allow purification by immobilized metal ion affinity chromatography (IMAC). In order to allow for directed europium (Eu) labeling, all constructs generated in the first round of cloning contained a Lys6-tag upstream of the His6-tag, thereby reducing the risk of compromising activity by the labeling process. Eu labeling was used to measure the concentration of the proteins in blood and organs using time-resolved fluorescence.

Protein identity and purity of protein preparations were controlled by SDS-PAGE (Supplementary Figure S1A). A prominent additional band of lower than expected molecular weight was observed for all engineered constructs containing the amidase-2 domain, whereas this band was not detected in the parental LysK-His6. Consequently, all constructs yielding the observed truncated protein product were excluded from further experiments.

High-Affinity Albumin Binding Domain (ABD) Mediates Binding of Peptidoglycan Hydrolase Constructs to Human Serum Albumin

The selected fusion constructs were investigated for their ability to bind to HSA using surface plasmon resonance analysis. HSA was immobilized on the surface of a sensor chip, and interaction of fusion proteins in solution with the immobilized HSA was

monitored in real-time. All three protein constructs containing an ABD showed strong binding to HSA, whereas the non-ABD containing control showed weak binding (Supplementary Figure S2). These results suggest that the ABD retains its functionality within the context of the fusion proteins.

ABD-Containing Constructs Retain Bacteriolytic Activity *in vitro*

The *in vitro* lytic activity of the selected protein constructs was determined by a turbidity reduction assay, which measures the reduction in optical density of a bacterial suspension over time in response to different concentrations of endolysin. The assay was performed in PBS-HSA in order to account for any possible inhibition caused by steric hindrance upon binding of the ABD-containing endolysin constructs to HSA. The most active ABD-containing construct, C[ABD]SL, displayed an activity of $0.54 \Delta OD_{600} \text{ min}^{-1} \mu\text{M}^{-1}$ (compared to $2.94 \Delta OD_{600} \text{ min}^{-1} \mu\text{M}^{-1}$ for the parental enzyme CSL; Figure 2A) and was selected for further evaluation *in vitro* and *in vivo*.

As a next step, Lys6-tag-free variants of C[ABD]SL and the control CSL were generated, yielding the constructs CHAP-ABD-SH3b-His6 (C[ABD]S) and CHAP-SH3b-His6 (CS), respectively (Figure 1). Lys6-tags had been added to all original constructs to facilitate Eu labeling for *in vivo* experiments. However, they would not be included in enzymes used therapeutically. The Lys6-free constructs showed higher activity in the turbidity reduction assay compared to their tagged counterparts (Figure 2B), for which reason they were chosen for further *in vitro* analysis.

To investigate the influence of HSA on the activity of the control CS and C[ABD]S, both enzymes were compared in turbidity reduction assays performed in PBS only and PBS-HSA. In the presence of HSA, the activity of CS increased slightly as compared to PBS alone (Figure 2C). The reason for this may be that an excess of HSA reduces unspecific binding of the enzyme to the polystyrene of the 96-well plate, increasing the effective concentration of the endolysin construct in the solution. In contrast, the activity of the C[ABD]S construct decreased upon addition of HSA (Figure 2D). It is likely that the HSA binding causes steric hindrance impeding the activity of the endolysin construct or affecting the diffusion rate through the increased size of the complex.

In order to determine the staphylolytic activity of C[ABD]S and CS in an environment mimicking bacteremia, a time-kill assay with the selected constructs in human serum and the clinical isolate *S. aureus* Newman was conducted. Although the ABD-containing construct was less effective than the control enzyme in this experiment, it reduced the number of CFUs by approximately 3 log units within 60 min at a concentration of 200 nM (compared to 4 log units for the control) (Figure 3).

An Intramolecular ABD Increases the Serum Circulation Half-Life of C[ABD]SL[Eu] in Mice

The Lys6-tagged constructs C[ABD]SL and CSL were selected for investigating the effect of an intramolecular ABD on the

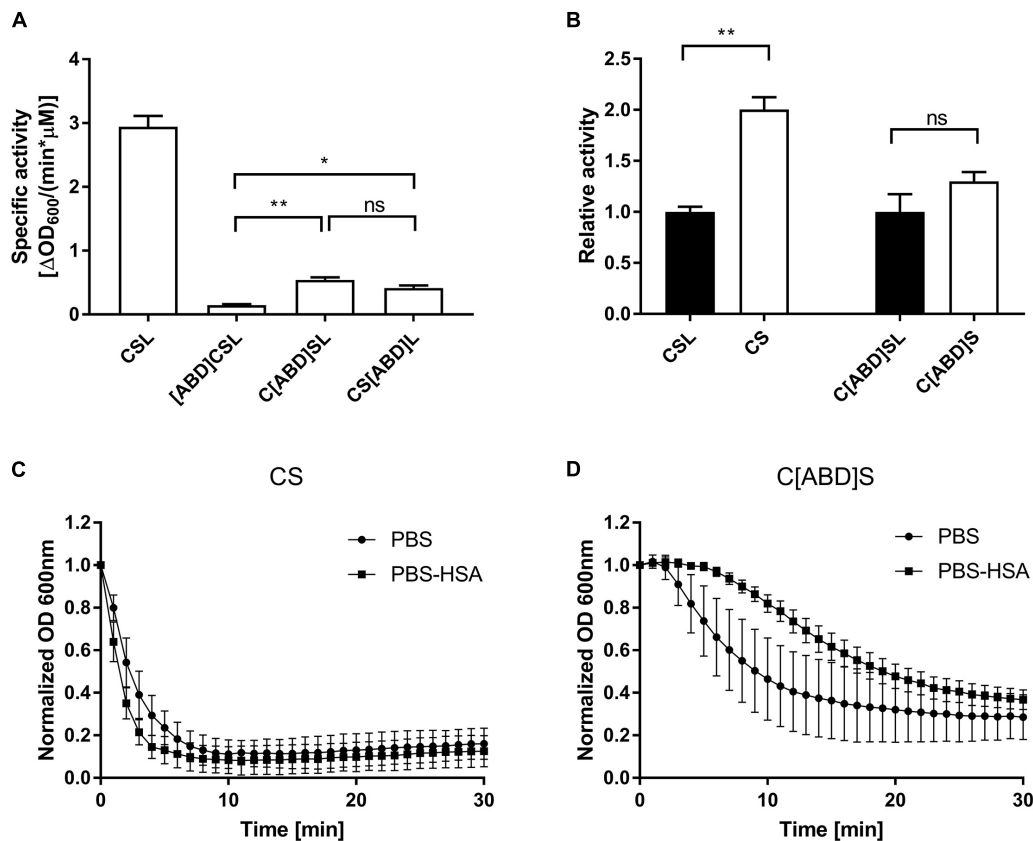


FIGURE 2 | *In vitro* analysis of PGH constructs with and without ABDs by turbidity reduction assays. *Staphylococcus aureus* SA113 substrate cells were mixed with indicated concentrations of endolysin constructs. The reduction in optical density over time was analyzed and the specific activity was calculated as $\Delta OD_{600}/(\text{min} \cdot \mu\text{M})$. **(A)** Comparison of the specific activities of the control PGH construct CSL and its ABD-containing derivatives. The experiment was performed in PBS-HSA. **(B)** Effect of the removal of Lys6-tags from CSL and its most active ABD-containing derivative. The experiment was performed in PBS-HSA. **(C,D)** Turbidity reduction assays comparing the activity of CS **(C)** and C[ABD]S **(D)** at 125 nM concentration in PBS and PBS-HSA. Data were control-corrected and normalized. Error bars represent the standard error of the mean from 3 **(A,B)** and 4 **(C,D)** individual experiments. * $p < 0.05$; ** $p < 0.01$; ns, non-significant.

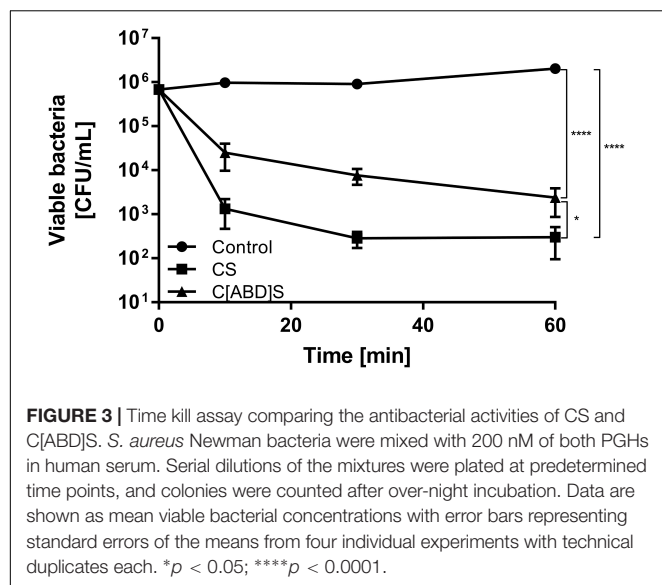
serum circulation half-life of these proteins in mice. To this end, preparations of both proteins of high purity (**Supplementary Figure S1B**) and with endotoxin concentrations <0.05 EU/ml were labeled with the lanthanide europium (Eu) in order to enable measurement of protein concentrations in murine blood and organs by time-resolved fluorescence.

The Eu-labeled ABD-containing protein CHAP-ABD-SH3b-Lys6[Eu]-His6 (C[ABD]SL[Eu]) and the control CHAP-SH3b-Lys6[Eu]-His6 (CSL[Eu]) were injected intravenously into C57BL/6 wild-type mice. The blood was sampled at predetermined time points and analyzed for target protein concentrations via time-resolved fluorescence. As previously described for other proteins (Wang et al., 2008; Seijsing et al., 2014), concentrations of both the ABD-containing construct and the control decreased over time following a biphasic process (**Figure 4A**). During the alpha phase, both concentrations decreased at approximately the same rate (approximately 2 log units within 24 h). However, during the beta phase, the ABD-containing protein showed a slower decrease in concentration than the control. After 144 h, the C[ABD]SL[Eu] concentration in the blood was 16-fold higher than that of the

control construct, which was statistically significant ($p < 0.05$). From these data, the serum circulation half-life was calculated to be 23 h for the control CSL[Eu] and 34 h for the ABD-containing C[ABD]SL[Eu].

ABD Prevents Endolysin Kidney Deposition

In addition to determining the half-life of both constructs in the blood, their biodistribution was investigated by measuring the concentrations of Eu-labeled proteins in various organs of the mice. Mice were euthanized and organs were harvested 144 or 216 h post-injection. Europium was found to accumulate in liver and kidneys over time, with the control CSL[Eu] yielding higher concentrations in both organs and at both time points than the ABD-containing C[ABD]SL[Eu]. This effect was statistically significant in the kidneys and was strongly pronounced at 216 h, where the difference between the constructs was more than 150-fold (**Figure 4B**). Protein concentrations in the spleen, lung, and heart were below the detection limit for both proteins.

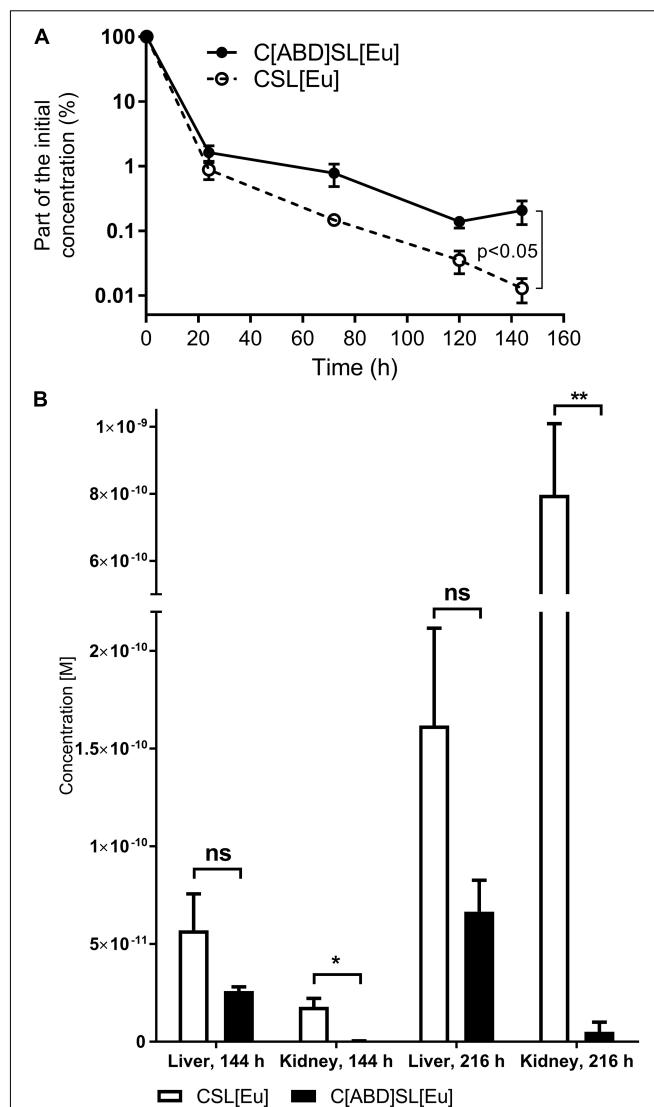


DISCUSSION

Therapeutic efficacy of a protein-based drug depends on several factors including activity *in vivo*, bioavailability at the site of infection, immunogenicity, and serum circulation half-life. Successful eradication of an infection can be achieved only if the local concentration of the therapeutic antimicrobial agent remains high enough over a sufficient period of time in order to kill the majority of bacteria. In this respect, an extended serum circulation half-life is considered advantageous, since it avoids the necessity of repeated or continuous administration (Walsh et al., 2003; Resch et al., 2011b).

The serum circulation half-lives of PGHs reported in the literature to date are short, ranging from 20.5 min to 1 h (Loeffler et al., 2003; Walsh et al., 2003; Jun et al., 2017). Efforts to extend the half-life of PGHs have been pursued, using PEGylation (Walsh et al., 2003; Resch et al., 2011b) or dimerization (Resch et al., 2011a). By conjugating a polyethylene glycol (PEG) polymer chain to a protein, its hydrodynamic volume increases, which reduces glomerular filtration in the kidneys. In addition, PEGylation can decrease immunogenicity if potential epitopes on the molecule are masked from the immune system (Veronese and Mero, 2008). Unfortunately, the introduction of bulky structures such as PEG has been found to severely affect and even inactivate enzymatic activity of endolysins (Resch et al., 2011b). Moreover, PEGylation is a cumbersome process that may result in multidisperse products, and anti-PEG antibodies have been observed in exposed patients, in addition to non-degraded PEG deposited in patients' livers (Knop et al., 2010).

An enzyme dimerization strategy has been used with the pneumococcal phage endolysin Cpl-1 (Resch et al., 2011a). In this case, monomeric endolysin molecules were dimerized by introduction of specific cysteine residues, which resulted in a 10-fold decrease in plasma clearance rate. However, this strategy may be successful only for endolysins which exhibit a natural tendency to dimerize, as suggested for Cpl-1 by the authors of the study.



Fusion of endolysins with ABD is a straightforward process that requires no posttranslational chemical modifications. The ABD can be iterated at different positions in the protein until a suitable construct is identified. Clearly, targeted modification represents a major advantage over biochemical approaches as compared to PEGylation, which always result in a heterogeneous mix of products. Not only does the ABD-HSA complex give

an increased hydrodynamic volume reducing kidney excretion but, as opposed to PEGylated proteins, it is also rescued from lysosomal degradation through recycling by the neonatal Fc receptor (FcRn) (Chaudhury et al., 2003). Furthermore, recombinant proteins are, unlike PEG, eventually degraded without leaving any chemical traces in the body.

Since endolysins are foreign to the body, they can be immunogenic, as previously reported (Loeffler et al., 2003; Fischetti, 2010; Schmelcher et al., 2012). It can be speculated that the ABD may indirectly dampen such a response. Since ABD fusion proteins form complexes with HSA in the blood, they are recycled back into the blood circulation by the FcRn when endocytosed by epithelial cells or antigen-presenting cells (Chaudhury et al., 2003). Thereby, fusion of ABD to the protein circumvents lysosomal degradation, which would otherwise lead to presentation of immunogenic epitopes by the major histocompatibility complex (MHC) and induce long-lasting B-cell mediated humoral immune response (Bryant and Ploegh, 2004).

In this study, we observed a relatively long half-life of 23 h in mice for the 35 kDa parental enzyme CSL[Eu], which was surprising given the previously published values.

A two- or multi-domain endolysin is likely to show a longer half-life than a globular protein with the same molecular weight due to its larger hydrodynamic volume. However, both Cpl-1 and lysostaphin are also two-domain modular proteins, with half-lives of 20.5 min (Loeffler et al., 2003) and less than 1 h (Walsh et al., 2003), respectively. In addition, the high pI of CSL (9.83) gives the protein a strong positive net charge, possibly resulting in attraction to negatively charged cells and tissues, thus delaying clearance. Such a hypothesis could be sustained considering the low pI of Cpl-1 (Loeffler et al., 2003). However, the pI of lysostaphin is similar, which suggests that the clearance mechanism also depends on other factors (Loeffler et al., 2003; Walsh et al., 2003). The difference in half-life between lysostaphin and the LysK-derivative CSL may also be explained by the different functions of these two enzymes. Lysostaphin is a bacteriocin acting from the outside, therefore relying on efficient diffusion. Thus, it can be reasoned that this protein has been optimized by evolution to minimize interactions with molecules in the environment, which may explain its rapid clearance. In contrast, LysK is a phage endolysin accessing the peptidoglycan from within. Free diffusion through the environment following bacterial lysis would be disadvantageous for the phage, due to the risk of harming not yet infected neighboring hosts (Verbree et al., 2017).

The SAL200 compound is a recombinant version of the staphylococcal endolysin SAL-1 highly similar to LysK. The *in vivo* serum circulation half-life of SAL200 was relatively long when tested in monkeys, ranging from 0.3 to 9.7 h (Jun et al., 2016). However, a recent clinical trial with SAL200 demonstrated a very short serum circulation half-life of only 0.04 to 0.38 h in humans (Jun et al., 2017). This indicates a large discrepancy in the drug's pharmacokinetics between different organisms, and suggests that the long *in vivo* serum circulation half-life of CSL[Eu] in mice may not be extrapolated to other systems. Here, introduction of an ABD into the CSL

protein resulted in a significant increase in serum circulation half-life in mice. The protein construct containing the high-affinity ABD035 showed a half-life of 34 h, which is in line with what has been reported for other ABD fusion proteins previously (Chaudhury et al., 2003; Orlova et al., 2013; Seijsing et al., 2014).

From the biodistribution data, it is evident that the ABD-containing construct C[ABD]SL[Eu] is superior to the non-ABD-containing control in avoiding kidney deposition. As discussed above, this is likely an effect of the differences in hydrodynamic volume and to a smaller extent FcRn recycling (Chaudhury et al., 2003; Roopenian and Akilesh, 2007; Akilesh et al., 2008). Likewise, the amount of C[ABD]SL[Eu] was lower than the non-ABD-containing control in the liver. Since proteins entering the liver are eliminated by specific receptors and unspecific phagocytic uptake (Solá and Griebenow, 2011), FcRn recycling is also here a likely explanation for the difference in deposition between the construct with and without ABD. While the difference in kidney deposition between C[ABD]SL[Eu] and the control became apparent already at the first investigated time point (144 h), it was surprising that the highest concentrations of both proteins were reached only after 216 h. This delay in clearance may be explained by the same reasons as for the unexpectedly long serum circulation half-life of the CSL[Eu], i.e., charge and other physicochemical properties.

Despite the potential benefits of half-life extension strategies regarding the *in vivo* efficacy of endolysin-based compounds, it should not be forgotten that any modification of these enzymes, be it through genetic engineering or biochemical approaches, can have a detrimental effect on their antimicrobial activity, which may outweigh the positive effect of an extended half-life on the overall efficacy. This may be due to reduced diffusion, steric hindrance, lower flexibility between individual domains or unpredictable changes affecting the folding of the molecule. Reduced enzymatic and antimicrobial activity was also observed for the C[ABD]S construct compared to the control in this study. The best way to improve the enzymatic activity is probably to work further in detail on the positioning of the ABD to avoid steric hindrance and allow for accurate flexibility between domains. However, it is encouraging to find that the ABD-containing construct was still very potent and reduced *S. aureus* by 3-logs in human serum within 60 min at the tested concentrations (compared to 4 logs for the control). Given this residual activity, our strategy compares favorably with other half-life extension approaches that lead to complete inactivation of the PGH (Walsh et al., 2003; Resch et al., 2011b). A strategy that likely would improve treatment, but possibly complicate the regulatory process, is to administer a mix of both highly active wild type endolysin to get high initial activity and the half-life extended variant to clear any persistent bacteria.

CONCLUSION

In conclusion, we have shown that fusion of an endolysin to the ABD represents a promising strategy to extend the

serum circulation half-life of a modular PGH, while retaining a considerable level of antimicrobial activity.

DATA AVAILABILITY STATEMENT

All datasets generated for this study are included in the manuscript and the **Supplementary Files**.

ETHICS STATEMENT

This study was carried out in accordance with the recommendations of the Guide for the Care and Use of Laboratory Animals of the National Institutes of Health. The protocol ZH251/14 was approved by the Institutional Animal Care and Use Committee of the University of Zurich.

AUTHOR CONTRIBUTIONS

JS, MS, AS, YS, and AS conceived and designed the experiments. JS, NK, and AS performed the experiments. JS, MS, NK, YS, and AS analyzed the data. ML and AZ contributed reagents, materials, and analysis tools. JS, MS, YS, and AS wrote the manuscript. JS, ML, and AZ provided funding.

REFERENCES

- Akilesh, S., Huber, T. B., Wu, H., Wang, G., Hartleben, B., Kopp, J. B., et al. (2008). Podocytes use FcRn to clear IgG from the glomerular basement membrane. *Proc. Natl. Acad. Sci. U.S.A.* 105, 967–972. doi: 10.1073/pnas.0711515105
- Bateman, A., and Rawlings, N. (2003). The CHAP domain: a large family of amidases including GSP amidase and peptidoglycan hydrolases. *Trends Biochem. Sci.* 28, 230–234. doi: 10.1016/S0968-0004(03)00062-68
- Becker, S. C., Dong, S., Baker, J. R., Foster-Frey, J., Pritchard, D. G., and Donovan, D. M. (2009). LysK CHAP endopeptidase domain is required for lysis of live staphylococcal cells. *FEMS Microbiol. Lett.* 294, 52–60. doi: 10.1111/j.1574-6968.2009.01541.x
- Bischoff, M., Dunman, P., Kormanec, J., Macapagal, D., Murphy, E., Mounts, W., et al. (2004). Microarray-based analysis of the *Staphylococcus aureus* B regulon. *Society* 186, 4085–4099. doi: 10.1128/JB.186.13.4085
- Bryant, P., and Ploegh, H. (2004). Class II MHC peptide loading by the professionals. *Curr. Opin. Immunol.* 16, 96–102. doi: 10.1016/j.coi.2003.11.011
- Chambers, H. F., and Deleo, F. R. (2010). Waves of resistance: *Staphylococcus aureus* in the antibiotic era. *Nat. Rev. Microbiol.* 7, 629–641. doi: 10.1038/nrmicro2200.Waves
- Chaudhury, C., Mehnaz, S., Robinson, J. M., Hayton, W. L., Pearl, D. K., Roopenian, D. C., et al. (2003). The major histocompatibility complex-related Fc receptor for IgG (FcRn) binds albumin and prolongs its lifespan. *J. Exp. Med.* 197, 315–322. doi: 10.1084/jem.20021829
- Daniel, A., Euler, C., Collin, M., Chahales, P., Gorelick, K. J., and Fischetti, V. A. (2010). Synergism between a novel chimeric lysin and oxacillin protects against infection by methicillin-resistant *Staphylococcus aureus*. *Antimicrob. Agents Chemother.* 54, 1603–1612. doi: 10.1128/AAC.01625-1629
- Doweiko, J., and Nompleggi, D. (1991). Role of albumin in human physiology and pathophysiology. *J. Parenter. Enter. Nutr.* 15, 207–211. doi: 10.1177/0148607191015002207
- Fenton, M., Casey, P. G., Hill, C., Gahan, C. G. M., Ross, R. P., McAuliffe, O., et al. (2010). The truncated phage lysin CHAPk eliminates *Staphylococcus aureus* in the nares of mice. *Bioeng. Bugs* 1, 404–407. doi: 10.4161/bbug.1.6.13422

FUNDING

This work was supported by Gållöstiftelsen (to JS); the Hans Werthén Foundation of the Royal Swedish Academy of Engineering Sciences (to JS); the Sven and Lilly Lawskis Foundation (to JS); the Olle Engkvist Byggmästare Foundation (to JS); the Swiss National Science Foundation (310030_146295/1 to AZ); and Micros (to ML).

ACKNOWLEDGMENTS

We would like to thank Samuel Zeeman, Kuan-Jen Lu, and George M. Gavin for providing access to the time-resolved fluorescence plate reader, and our funders below. Parts of this article were presented at the 5th EMBO Viruses of Microbes conference, Wroclaw, Poland, 2018 (Abstract ID: 241).

SUPPLEMENTARY MATERIAL

The Supplementary Material for this article can be found online at: <https://www.frontiersin.org/articles/10.3389/fmicb.2018.02927/full#supplementary-material>

- Fischetti, V. A. (2010). Bacteriophage endolysins: a novel anti-infective to control gram-positive pathogens. *Int. J. Med. Microbiol.* 300, 357–362. doi: 10.1016/j.ijmm.2010.04.002
- Green, M. R., and Sambrook, J. (2012). *Molecular Cloning: A Laboratory Manual. Fourth.* N.Y. Cold Spring Harbor, NY: Cold Spring Harbor Laboratory Press.
- Gu, J., Xu, W., Lei, L., Huang, J., Feng, X., Sun, C., et al. (2011). LysGH15, a novel bacteriophage lysin, protects a murine bacteremia model efficiently against lethal methicillin-resistant *Staphylococcus aureus* infection. *J. Clin. Microbiol.* 49, 111–117. doi: 10.1128/JCM.01144-1110
- Haddad Kashani, H., Schmelcher, M., Sabzalipoor, H., Seyed Hosseini, E., and Moniri, R. (2017). Recombinant endolysins as potential therapeutics against antibiotic-resistant *staphylococcus aureus*?: current status of research and novel delivery strategies. *Clin. Microbiol. Rev.* 31:e00071-17. doi: 10.1128/CMR.00071-17
- Horgan, M., O'Flynn, G., Garry, J., Cooney, J., Coffey, A., Fitzgerald, G. F., et al. (2009). Phage lysin LysK can be truncated to its CHAP domain and retain lytic activity against live antibiotic-resistant staphylococci. *Appl. Environ. Microbiol.* 75, 872–874. doi: 10.1128/AEM.01831-1838
- Jawa, V., Cousens, L. P., Awwad, M., Wakshull, E., Kropshofer, H., and De Groot, A. S. (2013). T-cell dependent immunogenicity of protein therapeutics: preclinical assessment and mitigation. *Clin. Immunol.* 149, 534–555. doi: 10.1016/j.clim.2013.09.006
- Johansson, M. U., Frick, I.-M., Nilsson, H., Kraulis, P. J., Hober, S., Jonasson, P., et al. (2002). Structure, specificity, and mode of interaction for bacterial albumin-binding modules. *J. Biol. Chem.* 277, 8114–8120. doi: 10.1074/jbc.M109943200
- Jonsson, A., Dogan, J., Herne, N., Abrahmsén, L., and Nygren, P.-A. (2008). Engineering of a femtomolar affinity binding protein to human serum albumin. *Protein Eng. Des. Sel.* 21, 515–527. doi: 10.1093/protein/gzn028
- Jun, S. Y., Jang, I. J., Yoon, S., Jang, K., Yu, K., Cho, J. Y., et al. (2017). Pharmacokinetics and tolerance of the phage endolysin-based candidate drug SAL200 after a single intravenous administration among healthy volunteers. *Antimicrob. Agents Chemother.* 61:e02629-16. doi: 10.1128/AAC.02629-2616
- Jun, S. Y., Jung, G. M., Yoon, S. J., Oh, M. D., Choi, Y. J., Lee, W. J., et al. (2013). Antibacterial properties of a pre-formulated recombinant phage endolysin,

- SAL-1. *Int. J. Antimicrob. Agents* 41, 156–161. doi: 10.1016/j.ijantimicag.2012.10.011
- Jun, S. Y., Jung, G. M., Yoon, S. J., Youm, S. Y., Han, H.-Y., Lee, J.-H., et al. (2016). Pharmacokinetics of the phage endolysin-based candidate drug SAL200 in monkeys and its appropriate intravenous dosing period. *Clin. Exp. Pharmacol. Physiol.* 43, 1013–1016. doi: 10.1111/1440-1681.12613
- Knop, K., Hoogenboom, R., Fischer, D., and Schubert, U. S. (2010). Poly(ethylene glycol) in drug delivery: pros and cons as well as potential alternatives. *Angew. Chem. Int. Ed. Engl.* 49, 6288–6308. doi: 10.1002/anie.200902672
- Kokai-Kun, J. F., Chanturiya, T., and Mond, J. J. (2007). Lysostaphin as a treatment for systemic *Staphylococcus aureus* infection in a mouse model. *J. Antimicrob. Chemother.* 60, 1051–1059. doi: 10.1093/jac/dkm347
- Kontermann, R. E. (2011). Strategies for extended serum half-life of protein therapeutics. *Curr. Opin. Biotechnol.* 22, 868–876. doi: 10.1016/j.copbio.2011.06.012
- Kristian, S. A., Golda, T., Ferracin, F., Cramton, S. E., Neumeister, B., Peschel, A., et al. (2004). The ability of biofilm formation does not influence virulence of *Staphylococcus aureus* and host response in a mouse tissue cage infection model. *Microb. Pathog.* 36, 237–245. doi: 10.1016/j.micpath.2003.12.004
- Liu, W., Xie, Y., Ma, J., Luo, X., Nie, P., Zuo, Z., et al. (2015). Sequence analysis IBS?: an illustrator for the presentation and visualization of biological sequences. *Bioinformatics* 31, 3359–3361. doi: 10.1093/bioinformatics/btv362
- Lobo, E. D., Hansen, R. J., and Balthasar, J. P. (2004). Antibody pharmacokinetics and pharmacodynamics. *J. Pharm. Sci.* 93, 2645–2668. doi: 10.1002/jps.20178
- Loeffler, J. M., Djurkovic, S., and Fischetti, V. A. (2003). Phage lytic enzyme Cpl-1 as a novel antimicrobial for pneumococcal bacteremia. *Infect. Immun.* 71, 6199–6204. doi: 10.1128/IAI.71.11.6199-6204.2003
- Matthews, J. E., Stewart, M. W., De Boever, E. H., Dobbins, R. L., Hodge, R. J., Walker, S. E., et al. (2008). Pharmacodynamics, pharmacokinetics, safety, and tolerability of albiglutide, a long-acting glucagon-like peptide-1 mimetic, in patients with type 2 diabetes. *J. Clin. Endocrinol. Metab.* 93, 4810–4817. doi: 10.1210/jc.2008-1518
- Nygren, P. A., Flodby, P., Andersson, R., Wigzell, H., and Uhlen, M. (1991). *In vivo* stabilization of a human recombinant CD4 derivative by fusion to a serum-albumin-binding receptor. *Vaccines* 91:363.
- O'Flaherty, S., Coffey, A., Edwards, R., Meaney, W., Fitzgerald, G. F., and Ross, R. P. (2004). Genome of staphylococcal phage κ : a new lineage of myoviridae infecting gram-positive bacteria with a low G+C content. *J. Bacteriol.* 186, 2862–2871. doi: 10.1128/JB.186.9.2862-2871.2004
- O'Flaherty, S., Coffey, A., Meaney, W., Fitzgerald, G. F., and Ross, R. P. (2005). The recombinant phage lysin LysK has a broad spectrum of lytic activity against clinically relevant staphylococci, including methicillin-resistant *Staphylococcus aureus*. *J. Bacteriol.* 187, 7161–7164. doi: 10.1128/JB.187.20.7161-7164.2005
- Orlova, A., Jonsson, A., Rosik, D., Lundqvist, H., Lindborg, M., Abrahmsen, L., et al. (2013). Site-specific radiometal labeling and improved biodistribution using ABY-027, a novel HER2-targeting affibody molecule-albumin-binding domain fusion protein. *J. Nucl. Med.* 54, 961–968. doi: 10.2967/jnumed.112.110700
- Patel, S. S., and Benfield, P. (1996). Pegaspargase (polyethylene Glycol-L-Asparaginase). *Clin. Immunother.* 5, 492–496. doi: 10.1007/BF03259345
- Rashel, M., Uchiyama, J., Ujihara, T., Uehara, Y., Kuramoto, S., Sugihara, S., et al. (2007). Efficient elimination of multidrug-resistant *Staphylococcus aureus* by cloned lysin derived from bacteriophage phi MR11. *J. Infect. Dis.* 196, 1237–1247. doi: 10.1086/521305
- Reichert, P., Schwarz, C., and Donzeau, M. (2006). Single step protocol to purify recombinant proteins with low endotoxin contents. *Protein Expr. Purif.* 46, 483–488. doi: 10.1016/j.pep.2005.09.027
- Resch, G., Moreillon, P., and Fischetti, V. A. (2011a). A stable phage lysin (Cpl-1) dimer with increased antipneumococcal activity and decreased plasma clearance. *Int. J. Antimicrob. Agents* 38, 516–521. doi: 10.1016/j.ijantimicag.2011.08.009
- Resch, G., Moreillon, P., and Fischetti, V. A. (2011b). PEGylating a bacteriophage endolysin inhibits its bactericidal activity. *AMB Express* 1:29. doi: 10.1186/2191-0855-1-29
- Roopenian, D. C., and Akilesh, S. (2007). FcRn: the neonatal Fc receptor comes of age. *Nat. Rev. Immunol.* 7, 715–725. doi: 10.1038/nri2155
- Schmelcher, M., Donovan, D. M., and Loessner, M. J. (2012). Bacteriophage endolysins as novel antimicrobials. *Future Microbiol.* 7, 1147–1171. doi: 10.2217/fmb.12.97
- Schmelcher, M., Shen, Y., Nelson, D. C., Eugster, M. R., Eichenseher, F., Hanke, D. C., et al. (2014). Evolutionarily distinct bacteriophage endolysins featuring conserved peptidoglycan cleavage sites protect mice from MRSA infection. *J. Antimicrob. Chemother.* 70, 1453–1465. doi: 10.1093/jac/dku552
- Schuch, R., Nelson, D., and Vincent, A. F. (1986). A bacteriolytic agent that detects and kills bacillus anthracis. *Exp. Biol. J. Gen. Physiol.* 124, 5–13. doi: 10.1038/nature01026
- Seijsing, J., Lindborg, M., Höiden-Guthenberg, I., Bönisch, H., Guneriusson, E., Frejd, F. Y., et al. (2014). An engineered affibody molecule with pH-dependent binding to FcRn mediates extended circulatory half-life of a fusion protein. *Proc. Natl. Acad. Sci. U.S.A.* 111, 17110–17115. doi: 10.1073/pnas.1417717111
- Solá, R. J., and Griebenow, K. (2011). Glycosylation of therapeutic proteins: an effective strategy to optimize efficacy. *BioDrugs* 24, 9–21. doi: 10.2165/11530550-000000000-00000.Glycosylation
- Spratt, B. G. (1994). Resistance to antibiotics mediated by target alterations. *Science* 264, 388–393. doi: 10.1126/science.8153626
- Verbree, C. T., Dätwyler, S. M., Meile, S., Eichenseher, F., Donovan, D. M., Loessner, M. J., et al. (2017). Identification of peptidoglycan hydrolase constructs with synergistic staphylolytic activity in cow's milk. *Appl. Environ. Microbiol.* 83, 1–15. doi: 10.1128/AEM.03445-3416
- Veronese, F. M., and Mero, A. (2008). The impact of PEGylation on biological therapies. *BioDrugs* 22, 315–329. doi: 10.2165/00063030-200822050-200822054
- Walsh, S., Shah, A., and Mond, J. (2003). Improved pharmacokinetics and reduced antibody reactivity of lysostaphin conjugated to polyethylene glycol. *Antimicrob. Agents Chemother.* 47, 554–558. doi: 10.1128/AAC.47.2.554-558.2003
- Wang, W., Wang, E. Q., and Balthasar, J. P. (2008). Monoclonal antibody pharmacokinetics and pharmacodynamics. *Clin. Pharmacol. Ther.* 84, 548–558. doi: 10.1038/clpt.2008.170
- Werle, M., and Bernkop-Schnürch, A. (2006). Strategies to improve plasma half life time of peptide and protein drugs. *Amino Acids* 30, 351–367. doi: 10.1007/s00726-005-0289-283
- Whisstock, J. C., and James, A. M. (1999). SH3 domains in prokaryotes. *Trends Biochem. Sci.* 24, 132–133. doi: 10.1016/S0968-0004(99)01366-1363

Conflict of Interest Statement: ML is an advisor for Microcos, a company producing phage-based antimicrobials.

The remaining authors declare no conflict of interest. The funders had no role in study design, data collection, data interpretation, or the decision to submit the work for publication.

Copyright © 2018 Seijsing, Sobieraj, Keller, Shen, Zinkernagel, Loessner and Schmelcher. This is an open-access article distributed under the terms of the Creative Commons Attribution License (CC BY). The use, distribution or reproduction in other forums is permitted, provided the original author(s) and the copyright owner(s) are credited and that the original publication in this journal is cited, in accordance with accepted academic practice. No use, distribution or reproduction is permitted which does not comply with these terms.



In vitro and *in vivo* Inhibitory Activity of NADPH Against the AmpC BER Class C β -Lactamase

Jung-Hyun Na^{1†}, Tae Hee Lee^{2,3†}, Soo-Bong Park^{1†}, Min-Kyu Kim^{4,5}, Bo-Gyeong Jeong¹, Kyung Min Chung^{2,3*} and Sun-Shin Cha^{1*}

¹ Department of Chemistry and Nanoscience, Ewha Womans University, Seoul, South Korea, ² Department of Microbiology and Immunology, Chonbuk National University Medical School, Jeonju, South Korea, ³ Institute for Medical Science, Chonbuk National University Medical School, Jeonju, South Korea, ⁴ Biotechnology Research Division, Korea Atomic Energy Research Institute, Jeongseup, South Korea, ⁵ Department of Radiation Biotechnology and Applied Radioisotope Science, University of Science and Technology, Daejeon, South Korea

OPEN ACCESS

Edited by:

You-Hee Cho,
CHA University, South Korea

Reviewed by:

Chang-Ro Lee,
Myongji University, South Korea
Krisztina M. Papp-Wallace,
Louis Stokes Cleveland VA Medical
Center, United States

*Correspondence:

Kyung Min Chung
kmin@jbnu.ac.kr
Sun-Shin Cha
chajung@ewha.ac.kr

[†]These authors have contributed
equally to this work

*Present Address:

Jung-Hyun Na,
Division of Discovery and
Optimization, New Drug Development
Center, KBIO HEALTH, Cheongju,
South Korea

Specialty section:

This article was submitted to
Clinical Microbiology,
a section of the journal
Frontiers in Cellular and Infection
Microbiology

Received: 09 October 2018

Accepted: 11 December 2018

Published: 21 December 2018

Citation:

Na J-H, Lee TH, Park S-B, Kim M-K,
Jeong B-G, Chung KM and Cha S-S
(2018) *In vitro* and *in vivo* Inhibitory
Activity of NADPH Against the AmpC
BER Class C β -Lactamase.
Front. Cell. Infect. Microbiol. 8:441.
doi: 10.3389/fcimb.2018.00441

β -Lactamase-mediated resistance to β -lactam antibiotics has been significantly threatening the efficacy of these clinically important antibacterial drugs. Although some β -lactamase inhibitors are prescribed in combination with β -lactam antibiotics to overcome this resistance, the emergence of enzymes resistant to current inhibitors necessitates the development of novel β -lactamase inhibitors. In this study, we evaluated the inhibitory effect of dinucleotides on an extended-spectrum class C β -lactamase, AmpC BER. Of the dinucleotides tested, NADPH, a cellular metabolite, decreased the nitrocefin-hydrolyzing activity of the enzyme with a K_i value of 103 μ M in a non-covalent competitive manner. In addition, the dissociation constant (K_D) between AmpC BER and NADPH was measured to be 40 μ M. According to our *in vitro* susceptibility study based on growth curves, NADPH restored the antibacterial activity of ceftazidime against a ceftazidime-resistant *Escherichia coli* BER strain producing AmpC BER. Remarkably, a single dose of combinatory treatment with NADPH and ceftazidime conferred marked therapeutic efficacy (100% survival rate) in a mouse model infected by the *E. coli* BER strain although NADPH or ceftazidime alone failed to prevent the lethal bacterial infection. These results may offer the potential of the dinucleotide scaffold for the development of novel β -lactamase inhibitors.

Keywords: antimicrobial resistance, class C β -lactamase, AmpC BER, NADPH, β -lactamase inhibitors, mouse infection model

INTRODUCTION

The β -lactam antibiotics are the mainstay in the treatment of serious bacterial infections in clinical use (Liu et al., 2015). However, the prevalence of β -lactamases produced by pathogenic bacteria has been the major obstacle to cure bacterial infections because these enzymes hydrolyze the essential β -lactam ring for antibiotic efficacy. In addition, the recent overuse of antibiotics in human medicine and agriculture has promoted alterations and mutations within β -lactamases (Fair and Tor, 2014), which extends their substrate spectrum and reduces the susceptibility of bacteria to the most clinically important antibiotics, including penicillin derivatives, cephalosporins, monobactams, and carbapenems (Bush and Jacoby, 2010).

In the past decades, a variety of β -lactamases have been identified, classified into four classes (Ambler classes A, B, C, and D) based on their amino acid sequences (Hall and Barlow, 2005), and investigated to overcome drawback of their drug resistances. One approach to preserve the utility of β -lactam antibiotics is to develop β -lactamase inhibitors that maintain the efficacy of β -lactam antibiotics by reducing the activity of β -lactamases (Davies, 1994). Several β -lactamase inhibitors, including β -lactam inhibitors (clavulanate, sulbactam, and tazobactam) and non- β -lactam inhibitors (avibactam and vaborbactam), have been developed and clinically used to treat bacterial infections in combination with β -lactam antibiotics (e.g., amoxicillin/clavulanate, ticarcillin/clavulanate, ampicillin/sulbactam, cefoperazone/sulbactam, piperacillin/tazobactam, ceftazidime/avibactam, and meropenem/vaborbactam) (Harris et al., 2015; Cho et al., 2018). However, clavulanate, sulbactam, and tazobactam display inhibitory activity only against class A β -lactamases with much less or no effect on class B, C, and D β -lactamases although avibactam is active against class A, C, and some D β -lactamases and vaborbactam inhibits class A and C β -lactamases. (Bush, 1988; Buynak, 2006; Drawz and Bonomo, 2010; Ehmann et al., 2013; Cho et al., 2018). Furthermore, the ongoing emergence and dissemination of novel β -lactamases that are resistant to currently available β -lactamase inhibitors and β -lactam antibiotic/ β -lactamase inhibitor combinations (Shields et al., 2017) highlights the need to develop new β -lactamase inhibitors.

Recently, it has been demonstrated that mononucleotides including adenosine 5'-(*P*-acetyl) monophosphate (acAMP), guanosine monophosphate (GMP), and inosine monophosphate (IMP) can exert inhibitory activities on class C β -lactamases (Kim et al., 2017; Na et al., 2017), which was inspired by the observation of the adenylated nucleophilic serine in the active sites of Fox-4 and AmpC BER (Lefurgy et al., 2015; Kim et al., 2017). Furthermore, the combination of acAMP and ceftazidime, a third-generation cephalosporin, significantly reduced the growth of antibiotic resistant bacteria (Kim et al., 2017). These results suggest that nucleotide scaffolds could be useful candidates to develop novel β -lactamase inhibitors. In this study, we describe the inhibitory activity of the reduced form of nicotinamide adenine dinucleotide 2'-phosphate (NADPH) against class C β -lactamases. Through *in vitro* assays and a mouse infection model, we characterized the inhibitory mechanism and effect of NADPH on an extended-spectrum class C β -lactamase, AmpC BER. Overall, these studies might facilitate the identification and design of new and high effective inhibitors targeting class C β -lactamases.

MATERIALS AND METHODS

Cloning, Expression, and Purification of Class C β -Lactamases

Cloning of class C β -lactamases (ACC-1, AmpC BER, AmpC EC2, CMY-2, and CMY-10) were performed as described previously (Kim et al., 2017). The constructs were transformed into the *E. coli* strain BL21 (DE3). Expression of

recombinant proteins was induced by 1 mM isopropyl β -D-1-thiogalactopyranoside for 18 h at 20°C when the optical density at 600 nm of the transformed cells reached ~0.5. After induction, the cells were harvested by centrifugation. The cell pellets were resuspended in Buffer A (50 mM Tris-HCl, pH 7.4) and disrupted by sonication. The insoluble fractions were removed by centrifugation and recombinant proteins in soluble fractions were successively purified by nickel-nitrilotriacetic acid agarose (GE healthcare, USA) and *m*-aminophenylboronic acid agarose (Sigma-Aldrich, USA) (Kim et al., 2017). The eluted fractions containing the proteins were finally loaded on to a Superdex 75 HR 16/60 columns (GE healthcare, USA) equilibrated with Buffer A.

Inhibition Assays

To evaluate inhibition activities of dinucleotides against class C β -lactamases, each enzyme (0.2 nM) was mixed with each dinucleotide (2 mM) in a 50 mM MES [2-(*N*-morpholino) ethanesulfonic acid] (pH 6.5) buffer. Then, nitrocefin (100 μ M) was added to each solution and the nitrocefin hydrolysis was monitored at 486 nm for 1 h (SpectraMAX Plus, Molecular Devices, USA). The enzyme activity was quantified based on a percentage equation of $[v_i/v_0 \times 100]$, where v_i and v_0 are the initial velocity of nitrocefin hydrolysis in the presence and absence of dinucleotides, respectively.

Four sets of rate experiments were carried out to determine the inhibition mechanism and the K_i value of NADPH. The double-reciprocal plots were generated by plotting the inverse initial velocity as a function of the inverse of the nitrocefin concentrations (10, 30, 40, 70, and 90 μ M) in the presence of various concentrations of NADPH (0, 20, 100, and 250 μ M). The plots were fitted to the competitive-inhibition equation.

$$v_0 = \frac{v_{\max}[S]}{K_m(1 + \frac{[I]}{K_i}) + [S]} \quad (1)$$

where v_{\max} is the maximum velocity of nitrocefin hydrolysis, $[S]$ is concentration of nitrocefin, and $[I]$ is the concentration of NADPH (Copeland, 2005). The reported value was calculated using the Origin software (OriginLab, USA).

Protein-Ligand Binding Affinity Determination

The auto isothermal titration calorimeter (Auto-ITC) assay was performed using MicroCal Auto-iTC200 at Korea Basic Science Institute. AmpC BER (167 μ M) and NADPH (2 mM) in the same buffer consisting of 20 mM HEPES pH 7.4 and 100 mM NaCl were loaded into the cell and the syringe, respectively. To detect thermo-changes during the enzyme-ligand interaction, 2 μ L of NADPH was injected to the cell containing AmpC BER 19 times with 150 s intervals at 25°C. The collected titration curve was fitted to the one-set-of-sites interaction model of Origin software (OriginLab, USA).

Reactivation Assays

The reactivation of inactivated AmpC BER was examined by a jump dilution method (Copeland et al., 2011). AmpC BER

(4 μ M) was completely inactivated by 10 mM NADPH or 500 μ M adenosine 5'-(*P*-acetyl) monophosphate (acAMP) for 2 h at room temperature. To remove excess inhibitors, the inactivated AmpC BER proteins were diluted 8,000-fold in a 50 mM MES buffer (pH 6.5) and 100 μ M nitrocefin without NADPH and acAMP. The reactivation of the diluted enzyme (0.5 nM) was monitored by measuring nitrocefin hydrolysis at 486 nm.

Molecular Modeling of the AmpC BER/NADPH Complex

To dock NADPH into the active site of AmpC BER, water, sulfate, and AMP molecules were removed from the structure of AmpC BER (PDB code 5F1G). Then, polar hydrogen atoms were added to AmpC BER. The coordinates of NADPH were generated with LibCheck (Vagin et al., 2004) which is a ligand builder in Coot. Docking of NADPH was performed with AutoDock Vina (Trott and Olson, 2010) in the active site of AmpC BER.

In vitro Antimicrobial Susceptibility Study

The *E. coli* clinical isolate BER (*E. coli* BER) producing AmpC BER was kindly provided by Dr. Patrice Nordmann. Ceftazidime (Sigma-Aldrich, St. Louis, MO) and NADPH (Sigma-Aldrich, St. Louis, MO) were dissolved in fresh distilled water for each experiment. *In vitro* antimicrobial susceptibility test was performed by using the microbial growth curve. For growth curve generation, 5×10^4 colony-forming units (CFU) of the *E. coli* BER isolate were inoculated to 100 mL of Luria-Bertani (LB) broth containing ceftazidime and/or NADPH by indicated concentration and cultured in a rotary shaker at 37°C. The growth based on optical density at 600 nm was measured with 2 h intervals for 20 h of the assay.

To evaluate the minimum inhibitory concentration (MIC) of ceftazidime against the *E. coli* BER strain in combination with NADPH, we used a modified broth microdilution method. Briefly, bacterial suspensions were diluted to a density of 1×10^3 CFU/mL in LB broth. The diluted bacteria (100 μ L) were then added to 96 well-microtiter plates containing 100 μ L of ceftazidime or ceftazidime with NADPH (417 μ g/mL) and incubated for 14–15 h at 35°C. MICs were determined as the lowest concentration of the antibiotic agent at which there was no visible bacterial growth. These MIC titrations were performed at three independent experiments in duplicate.

Ethics Statement for Animal Use

All mouse experiments were approved and performed according to the guidelines by the Institutional Animal Care and Use Committee at Chonbuk National University (Approved No. CBU 2014-0020 and CBU 2015-0040). All experiments were designed to reduce or minimize the numbers of animals used, and every effort was made to cause the minimum pain and distress to the animals.

Animal Study

All wild-type female CD1 mice were purchased from a commercial source (Orient Bio Inc., a branch of Charles River Laboratory, Seongnam, Korea) and housed in specific pathogen-free unit. Age-matched female CD1 mice (4–5 weeks old) were

intraperitoneally infected with 1×10^8 CFU of *E. coli* BER strain producing AmpC BER and then treated with a single dose of ceftazidime (460 μ g/mouse), and/or NADPH (15 mg/mouse) by intraperitoneal injection at 1 h after infection. The infected mice were followed by observation for more than 96 h.

Statistical Analysis

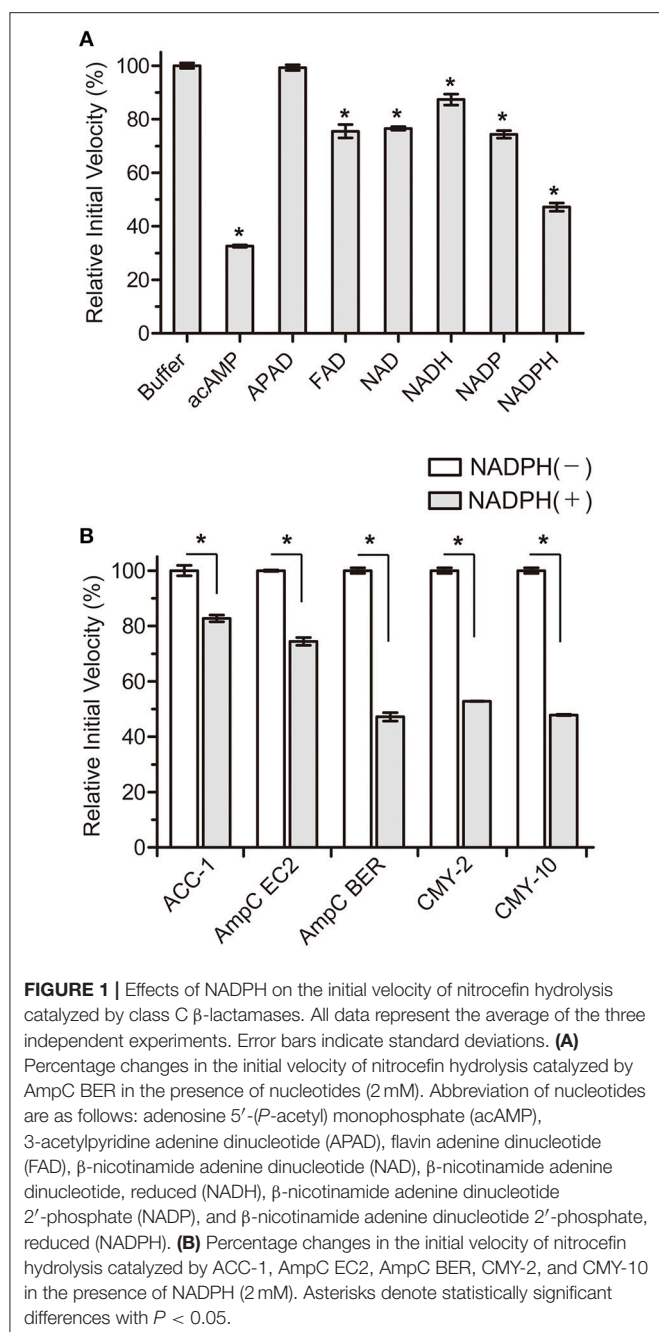
We used Prism software (GraphPad Software, Inc., CA, USA) to analyze all data. Briefly, statistical analyses of inhibitory effects of nucleotides on class C β -lactamases were performed using a two-tailed paired Student's *t*-test, and growth curves were compared using an ANOVA with a multiple comparisons test. Kaplan-Meier survival curves were analyzed by the long rank test. A *P* < 0.05 was considered statistically significant differences.

RESULTS AND DISCUSSION

NADPH Is a Competitive Inhibitor of AmpC BER

Recently, our studies demonstrated that GMP and IMP are non-covalent competitive inhibitors (Na et al., 2017) of class C β -lactamases and acAMP exerted its inhibitory effect through the covalent attachment of its AMP moiety to the nucleophilic serine residue of class C β -lactamases (Kim et al., 2017). Interestingly, the AMP moiety and GMP/IMP bind to R1 and R2 subsites in the active site of class C β -lactamases, respectively, although they have identical structures except for subtle differences in the purine base; the R1 and R2 subsites structurally refer to the distinct active site regions that accommodate the R1 side chain at the position C7 (or C6) and the R2 side chain at the position C3 (or C2) of β -lactam antibiotics on substrate binding, respectively (Kim et al., 2006). This observation suggested that the active site of class C β -lactamases composed of R1 and R2 subsites is probably large enough to accommodate two nucleotides.

Based on these perspectives and β -lactamase structures, our strategy focused on adenosine dinucleotides and investigated the inhibitory efficiency of these dinucleotides against the AmpC BER β -lactamase from an *E. coli* clinical isolate (*E. coli* BER); AmpC BER is an extended-spectrum class C enzyme that can hydrolyze ceftazidime and other oxymino cephalosporins (cefotaxime and cefepime) (Kim et al., 2006). Except for 3-acetylpyridine adenine dinucleotide (APAD), all tested adenosine dinucleotides including FAD, NAD, NADP, and NADPH reduced the initial velocity of nitrocefin hydrolysis catalyzed by AmpC BER (~15–55% inhibition, *P* \leq 0.0184) when compared to a negative buffer control (**Figure 1A**). Notably, NADPH induced ~55% reduction in the initial velocity of nitrocefin hydrolysis, which is comparable to the initial velocity of nitrocefin hydrolysis in the presence of acAMP as a positive control. NADPH also reduced the initial velocity of nitrocefin hydrolysis catalyzed by other class C β -lactamases including ACC-1, AmpC EC2, CMY-2, and CMY-10 (**Figure 1B**). These results demonstrate that NADPH could confer inhibitory effect on various class C β -lactamases. In line with this result, the compatible activity of NADP dinucleotide has also been observed for another β -lactamase. Ogawara and Horikawa showed that NADP decreased the benzylpenicillin-hydrolyzing activity of β -lactamase from



Streptomyces cellulosae although they did not evaluate the inhibition activity of NADPH (Ogawara and Horikawa, 1979).

In a further study, we subsequently investigated the inhibition mode of NADPH against AmpC BER. According to a previous study (Kim et al., 2017), the AMP moiety of acAMP was covalently attached to the nucleophilic serine of AmpC BER in an irreversible manner. Since the 2'-phospho-AMP and nicotinamide mononucleotide (NMN) in NADPH were connected through the phosphoanhydride bond (Figure 2A), we speculated that the nucleophilic serine would attack one of the phosphorous atoms of the phosphoanhydride and

the 2'-phospho-AMP or NMN moiety of NADPH might be covalently linked to the nucleophilic serine of AmpC BER with the NMN or 2'-phospho-AMP moiety as a leaving group, respectively. To test this possibility, we examine whether NADPH is an irreversible covalent inhibitor. Interestingly, AmpC BER inactivated by NADPH was reactivated in a time-dependent manner after the jump dilution (Figure 2B) whereas the reactivation of AmpC BER inactivated by acAMP was not detected as previously observed (Kim et al., 2017). Although more studies are required, it appears that the nucleophilic serine of AmpC BER couldn't attack the phosphorous atom of NADPH. As expected, the nucleophilic serine was revealed to be intact when AmpC BER inactivated by excess NADPH was analyzed by mass spectrometry (data not shown). Consequently, it is reasonable to assume that NADPH could inhibit class C β -lactamases in a non-covalent manner. We also performed steady-state kinetic analyses (Na et al., 2017) to determine the detailed inhibition mechanism of NADPH against AmpC BER. For these analyses, the double-reciprocal plots were generated by plotting the inverse initial velocity as a function of the inverse of the nitrocefin concentration in the presence of various concentrations of NADPH. Interestingly, v_{\max} remained constant but the apparent value of K_m increased along with increasing NADPH concentration (Figure 3A), which indicates that NADPH acted as a competitive inhibitor of AmpC BER. The K_i value of NADPH toward AmpC BER was determined to be 103 μ M. Furthermore, the dissociation constant (K_D) of NADPH toward AmpC BER measured by isothermal titration calorimeter (Figure 3B) was 40 μ M. Taken together, our data suggests that NADPH is a non-covalent competitive inhibitor of class C β -lactamases.

Molecular Docking Simulation of the AmpC BER/NADPH Complex

To get insights into the binding mode of NADPH in the active site of AmpC BER, we tried to solve the crystal structure of the AmpC BER/NADPH complex. However, our efforts to grow crystals of the complex has not been successful so far. In parallel with crystallization experiments, the *in silico* complex model was generated by docking NADPH into the active site of AmpC BER by using the AutoDock Vina program (Trott and Olson, 2010). According to the complex model, the 2'-phospho-AMP moiety exclusively interacts with residues in R1 subsite (Figure 4A). The pyrimidine ring and the imidazole ring in the adenine base make hydrogen bonds with Asp123 and Tyr221, respectively. The ribose is packed against Tyr221 with its 2'-phosphate group interacting with the backbone -NH groups of Ser212 and Gly322. The 5'-phosphate group of the ribose ring interacts with Asn152. However, the NMN moiety forms fewer interactions with residues in R2 subsite (Figure 4A). The nicotinamide ring stacks against Tyr150, the 2'-OH of the ribose is hydrogen bonded to Asn348, and the 5'-phosphate group interacts with the nucleophilic Ser64, Tyr150, and Asn152.

The *in silico* AmpC BER/NADPH complex model provides structural explanation why NADPH displayed a stronger inhibition activity than NADH and its oxidized form, NADP.

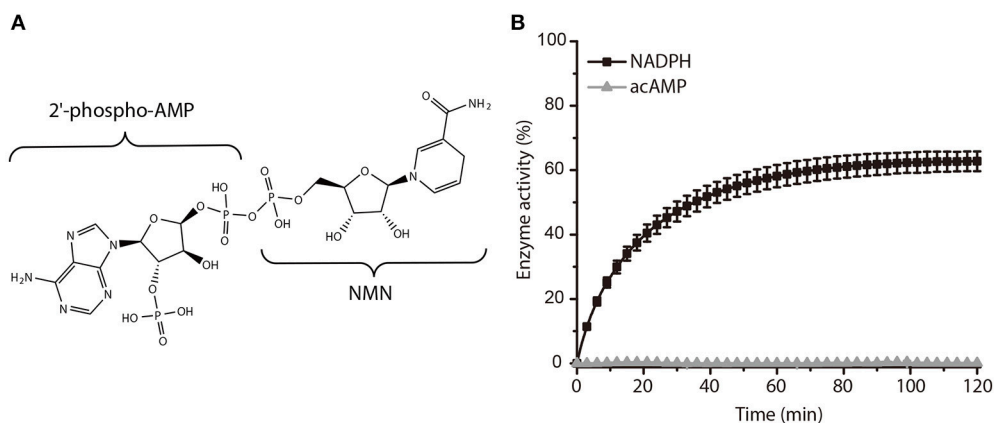


FIGURE 2 | Activity recovery of AmpC BER inactivated by NADPH. **(A)** Chemical structure of NADPH. **(B)** Time course of AmpC BER reactivation. Error bars indicate standard deviations for triplicate experiments.

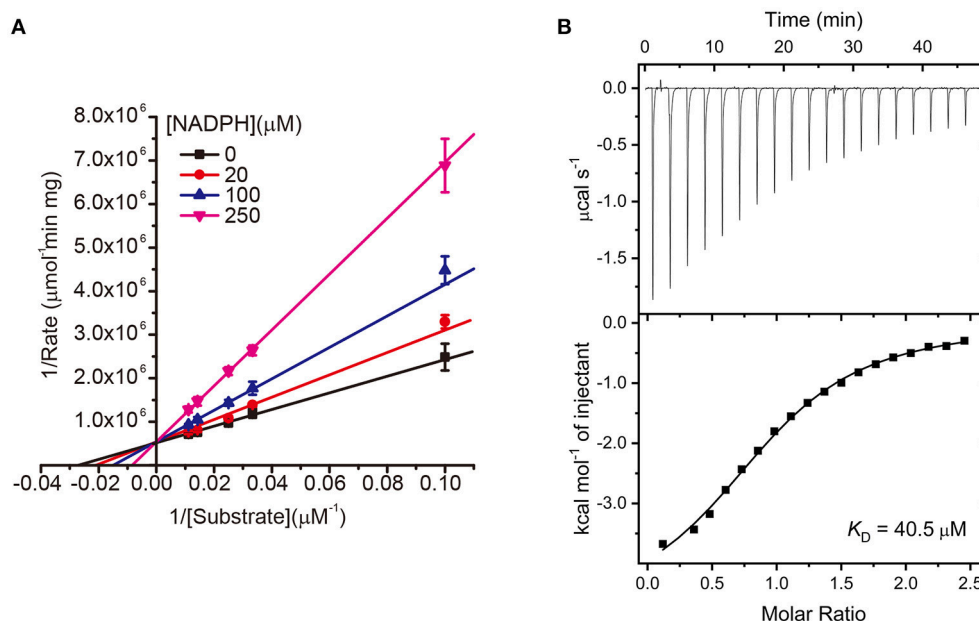
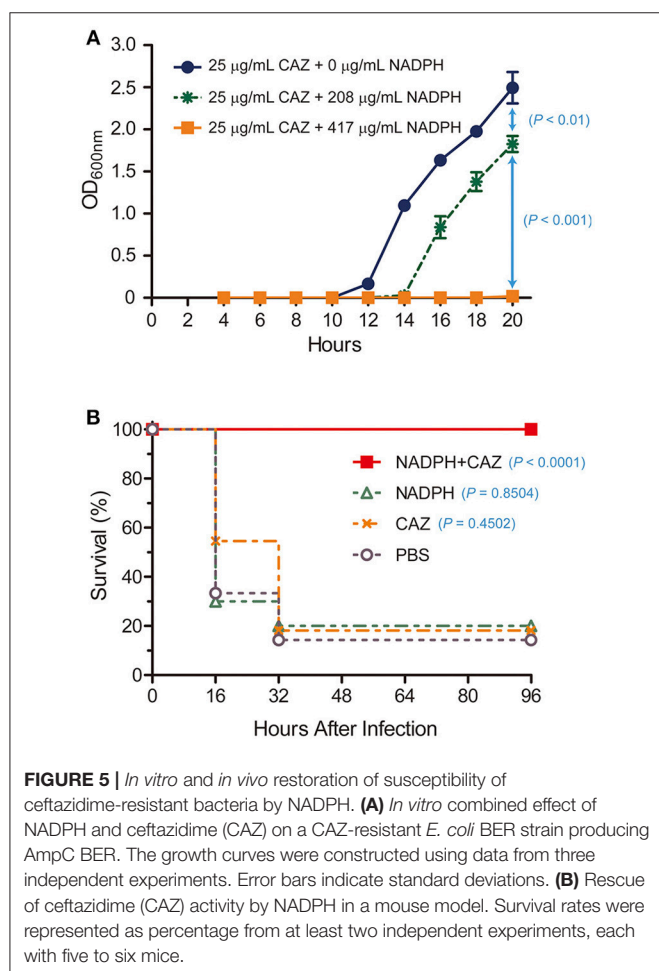
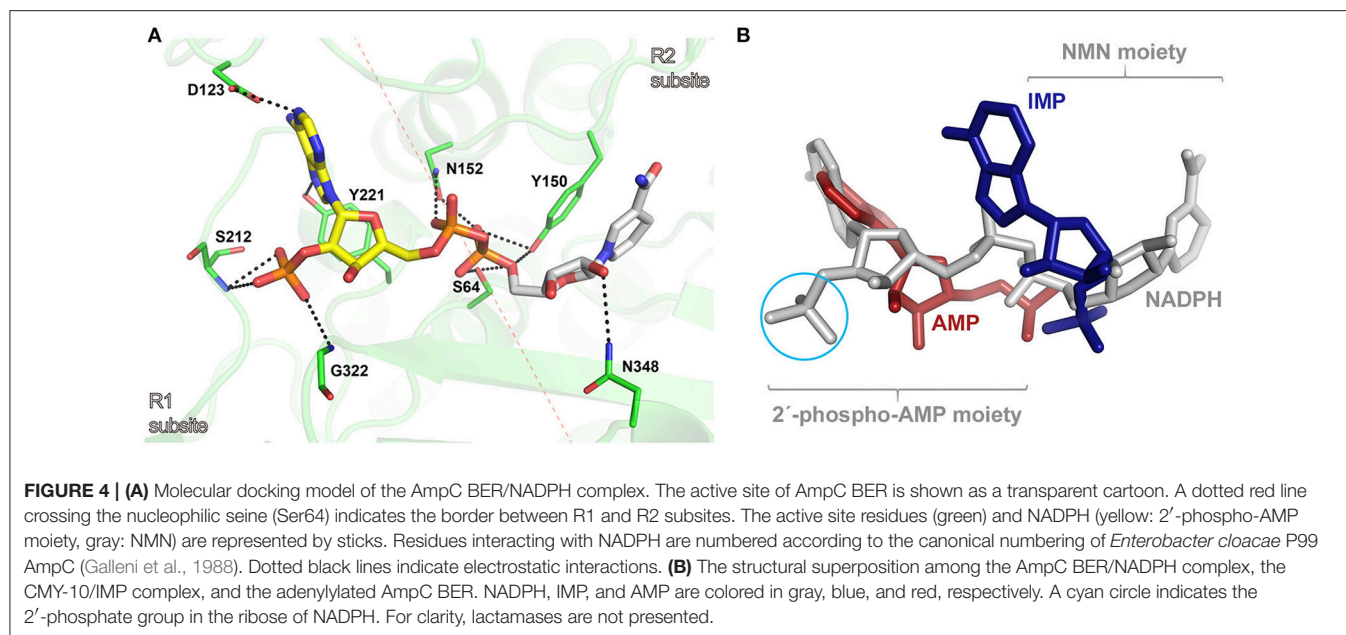


FIGURE 3 | **(A)** Lineweaver-Burk plots of AmpC BER inhibited by NADPH. All data represent the average of the three independent experiments. Error bars indicate standard deviations. **(B)** ITC experiment to measure the binding affinity of NADPH toward AmpC BER. The graph placed on the top is the raw titration curve and the bottom one is the fitted data utilized to calculate the K_D value.

The lower inhibition activity of NADH can be attributed to the absence of 2'-phosphate in the ribose considering multiple interactions between the phosphate group in NADPH and active site residues (**Figure 4A**). The structural differences between NADP and NADPH are the aromaticity and the number of hydrogen atoms in the nicotinamide ring. Some proteins can discriminate between NADP and NADPH. For example, in *Aspergillus nidulans* NmrA, a transcription repressor involved in the regulation of nitrogen metabolism, those subtle differences in the nicotinamide ring were suggested to affect ring stacking interactions with the side chain of a tyrosine residue, contributing

to the discrimination between NADP and NADPH (Lamb et al., 2003). It is notable that the nicotinamide ring of NADPH forms stacking interactions with the side chain of Tyr150 in our AmpC BER/NADPH complex model. The different inhibition activity of NADP and NADPH might be related to their different stacking interactions with Tyr150.

The *in silico* AmpC BER/NADPH complex model was superposed onto crystal structures of the adenylylated AmpC BER and the CMY-10/IMP complex. As shown in **Figure 4B**, the binding mode of NADPH is different from those of the adenylylate covalently linked to the nucleophilic serine of AmpC



BER and IMP. The 2'-phospho-AMP moiety of NADPH has an additional phosphate group compared to the adenylate and the single ring structure of the NMN moiety of NADPH is different from the double ring structure of IMP. The covalent linkage between the two moieties, together with structural disparity, is likely to affect interactions of NADPH with active site residues.

In vitro and *in vivo* Activity of NADPH in Combination With Ceftazidime Against the *E. coli* BER Strain

Based on our observation that NADPH was a competitive inhibitor of AmpC BER and nicely fit into the active site of AmpC BER in the modeled structure, we postulated that NADPH could be exploited to restore the antibiotic activity of ceftazidime toward the *E. coli* BER strain by inhibiting AmpC BER. To perform the *in vitro* antimicrobial susceptibility test based on growth rate, we determined whether ceftazidime in combination with NADPH could inhibit the growth of the ceftazidime-resistant *E. coli* BER strain (Figure 5A). Interestingly, the *E. coli* BER strain in the media containing both NADPH (208 μ g/mL and 417 μ g/mL) and ceftazidime (25 μ g/mL) displayed significantly lower growth rates than the bacteria in the media only containing ceftazidime (25 μ g/mL) ($P < 0.01$). The growth inhibitory effect of NADPH in combination with ceftazidime was dose dependent and the combination of 417 μ g/mL NADPH and 25 μ g/mL ceftazidime completely inhibited the growth ($P < 0.001$) until 20 h after seeding with 5×10^4 CFU of the *E. coli* BER strain. However, NADPH alone did not show any effect on the growth rate of the *E. coli* BER strain (data not shown). Supportively, the MIC of ceftazidime against

the *E. coli* BER strain was reduced from 32 $\mu\text{g/mL}$ in the absence of NADPH to 8 $\mu\text{g/mL}$ in the presence of 417 $\mu\text{g/mL}$ NADPH.

As the ceftazidime/NADPH combination effectively reduced the growth of the *E. coli* BER strain *in vitro*, we further investigated whether NADPH would provide therapeutic benefit *in vivo* against the ceftazidime-resistant bacteria through reversing AmpC BER-mediated resistance to this antibiotic. To evaluate this potential, post-exposure treatment experiments were performed in a mouse infection model (Figure 5B). Age-matched female CD1 mice, 4–5 weeks old, were intraperitoneally inoculated with a lethal dose (1×10^8 CFU) of the *E. coli* BER strain. At 1 h after infection, a single dose of ceftazidime (460 $\mu\text{g}/\text{mouse}$), NADPH (15 mg/mouse), or ceftazidime (460 $\mu\text{g}/\text{mouse}$) in combination with NADPH (15 mg/mouse) was treated into the infected mice through intraperitoneal injection. Notably, ceftazidime in combination with NADPH demonstrated the marked protective efficacy against the ceftazidime-resistant bacteria (100% survival rate, $P < 0.0001$) compared to the saline (PBS)-treated control ($\sim 14\%$ survival). In contrast, a single dose of either ceftazidime or NADPH did not provide significant benefit on survival (ceftazidime, $\sim 18\%$ survival rate, $P = 0.4502$; NADPH, 20% survival rate, $P = 0.8504$). Furthermore, when non-infected CD1 mice were intraperitoneally administrated with ceftazidime alone or NADPH alone, no detectable effects were observed on survival rate (100% survival rate; data not shown). Taken together, these findings suggest that the combinatorial treatment of ceftazidime with NADPH could resensitize the ceftazidime-resistant *E. coli* BER strain to ceftazidime through inhibiting the activity of AmpC BER β -lactamase, thereby preventing mice from lethal infection caused by the AmpC BER-producing *E. coli* strain. However, we acknowledge that the effective dose of NADPH observed in our primary study might be high but could be reduced through the chemical optimization to enhance the binding

affinity toward β -lactamases. In summary, although NADPH is metabolic dinucleotides that are widely used as cofactors or substrates in living organisms for redox reactions, anabolic pathways, mitochondrial functions, calcium homeostasis, and aging (Sohal et al., 1990; Krause, 2007; Spaans et al., 2015), we demonstrated that NADPH could be a competitive inhibitor of a class C β -lactamase, AmpC BER, and the combinatorial treatment with ceftazidime and NADPH provided significant antibacterial efficacy against the ceftazidime-resistant *E. coli* BER strain producing AmpC BER. Taken together, our findings suggest that dinucleotide scaffolds could lead to novel β -lactamase inhibitors that may have clinical potential as non-toxic inhibitors.

AUTHOR CONTRIBUTIONS

KC and S-SC designed experiments, analyzed data, and wrote the manuscript. J-HN, TL, S-BP, M-KK, and B-GJ performed experiments.

FUNDING

This study was supported by the National Research Foundation of Korea Grants (NRF-2015M1A5A1037480, NRF-2015R1D1A1A01056671, and NRF-2018R1D1A1B07050846) and a grant from the Collaborative Genome Program (20180430) funded by the Ministry of Oceans and Fisheries, Korea.

ACKNOWLEDGMENTS

We thank Dr. Eunha Hwang at the Korea Basic Science Institute for support with the use of the MicroCal Auto-iTC200 and Jung Hyun Lee for technical suggestions, and help with some of the experiments.

REFERENCES

- Bush, K. (1988). β -lactamase inhibitors from laboratory to clinic. *Clin. Microbiol. Rev.* 1, 109–123. doi: 10.1128/CMR.1.1.109
- Bush, K., and Jacoby, G. A. (2010). Updated functional classification of β -lactamases. *Antimicrob. Agents Chemother.* 54, 969–976. doi: 10.1128/AAC.01009-09
- Buynak, J. D. (2006). Understanding the longevity of the β -lactam antibiotics and of antibiotic/ β -lactamase inhibitor combinations. *Biochem. Pharmacol.* 71, 930–940. doi: 10.1016/j.bcp.2005.11.012
- Cho, J. C., Zmarlicka, M. T., Shaer, K. M., and Pardo, J. (2018). Meropenem/Vaborbactam, the first carbapenem/ β -lactamase inhibitor combination. *Ann. Pharmacother.* 52, 769–779. doi: 10.1177/1060028018763288
- Copeland, R. A. (2005). Evaluation of enzyme inhibitors in drug discovery. A guide for medicinal chemists and pharmacologists. *Methods Biochem. Anal.* 46, 1–265. doi: 10.1002/9781118540398
- Copeland, R. A., Basavapathruni, A., Moyer, M., and Scott, M. P. (2011). Impact of enzyme concentration and residence time on apparent activity recovery in jump dilution analysis. *Anal. Biochem.* 416, 206–210. doi: 10.1016/j.ab.2011.05.029
- Davies, J. (1994). Inactivation of antibiotics and the dissemination of resistance genes. *Science* 264, 375–382. doi: 10.1126/science.8153624
- Drawz, S. M., and Bonomo, R. A. (2010). Three decades of β -lactamase inhibitors. *Clin. Microbiol. Rev.* 23, 160–201. doi: 10.1128/CMR.00037-09
- Ehmann, D. E., Jahic, H., Ross, P. L., Gu, R. F., Hu, J., Durand-Reville, T. F., et al. (2013). Kinetics of avibactam inhibition against Class A, C, and D β -lactamases. *J. Biol. Chem.* 288, 27960–27971. doi: 10.1074/jbc.M113.485979
- Fair, R. J., and Tor, Y. (2014). Antibiotics and bacterial resistance in the 21st century. *Perspect. Medicin. Chem.* 6, 25–64. doi: 10.4137/PMC.S14459
- Galleni, M., Lindberg, F., Normark, S., Cole, S., Honore, N., Joris, B., et al. (1988). Sequence and comparative analysis of three *Enterobacter cloacae* ampC β -lactamase genes and their products. *Biochem. J.* 250, 753–760. doi: 10.1042/bj2500753
- Hall, B. G., and Barlow, M. (2005). Revised ambler classification of β -lactamases. *J. Antimicrob. Chemother.* 55, 1050–1051. doi: 10.1093/jac/dki130
- Harris, P. N., Tambyah, P. A., and Paterson, D. L. (2015). β -lactam and β -lactamase inhibitor combinations in the treatment of extended-spectrum β -lactamase producing Enterobacteriaceae: time for a reappraisal in the era of few antibiotic options? *Lancet Infect. Dis.* 15, 475–485. doi: 10.1016/S1473-3099(14)70950-8
- Kim, J. Y., Jung, H. I., An, Y. J., Lee, J. H., Kim, S. J., Jeong, S. H., et al. (2006). Structural basis for the extended substrate spectrum of CMY-10, a plasmid-encoded class C β -lactamase. *Mol. Microbiol.* 60, 907–916. doi: 10.1111/j.1365-2958.2006.05146.x
- Kim, M.-K., An, Y. J., Na, J.-H., Seol, J.-H., Ryu, J. Y., Lee, J., et al. (2017). Structural and mechanistic insights into the inhibition of class C β -lactamases through the

- adenylation of the nucleophilic serine. *J. Antimicrob. Chemother.* 72, 735–743. doi: 10.1093/jac/dkw491
- Krause, K. (2007). Aging: a revisited theory based on free radicals generated by NOX family NADPH oxidases. *Exp. Gerontol.* 42, 256–262. doi: 10.1016/j.exger.2006.10.011
- Lamb, H. K., Leslie, K., Dodds, A. L., Nutley, M., Cooper, A., Johnson, C., et al. (2003). The negative transcriptional regulator NmrA discriminates between oxidized and reduced dinucleotides. *J. Biol. Chem.* 278, 32107–32114. doi: 10.1074/jbc.M304104200
- Lefurgy, S. T., Malashkevich, V. N., Aguilan, J. T., Nieves, E., Mundorff, E. C., Biju, B., et al. (2015). Analysis of the structure and function of FOX-4 cephamycinase. *Antimicrob. Agents Chemother.* 60, 717–728. doi: 10.1128/AAC.01887-15
- Liu, X., Shi, Y., Kang, J. S., Oelschlaeger, P., and Yang, K. (2015). Amino acid thioester derivatives: a highly promising scaffold for the development of metallo- β -lactamase L1 inhibitors. *ACS Med. Chem. Lett.* 6, 660–664. doi: 10.1021/acsmedchemlett.5b00098
- Na, J.-H., An, Y. J., and Cha, S.-S. (2017). GMP and IMP are competitive inhibitors of CMY-10, an extended-spectrum class C β -lactamase. *Antimicrob. Agents Chemother.* 61:e00098-17. doi: 10.1128/AAC.0098-17
- Ogawara, H., and Horikawa, S. (1979). Purification of β -lactamase from streptomyces cellulosa by affinity chromatography on Blue Sepharose. *J. Antibiot.* 32, 1328–1335. doi: 10.7164/antibiotics.32.1328
- Shields, R. K., Chen, L., Cheng, S., Chavda, K. D., Press, E. G., Snyder, A., et al. (2017). Emergence of ceftazidime-avibactam resistance due to plasmid-borne bla_{KPC-3} mutations during treatment of carbapenem-resistant *Klebsiella pneumoniae* infections. *Antimicrob. Agents Chemother.* 61, e02097–e02016. doi: 10.1128/AAC.02097-16
- Sohal, R. S., Arnold, L., and Orr, W. C. (1990). Effect of age on superoxide dismutase, catalase, glutathione reductase, inorganic peroxides, TBA-reactive material, GSH/GSSG, NADPH/NADP and NADH/NAD in *Drosophila melanogaster*. *Mech. Ageing Dev.* 56, 223–235. doi: 10.1016/0047-6374(90)90084-S
- Spaans, S. K., Weusthuis, R. A., Van Der Oost, J., and Kengen, S. W. (2015). NADPH-generating systems in bacteria and archaea. *Front. Microbiol.* 6:742. doi: 10.3389/fmicb.2015.00742
- Trott, O., and Olson, A. J. (2010). AutoDock Vina: improving the speed and accuracy of docking with a new scoring function, efficient optimization, and multithreading. *J. Comput. Chem.* 31, 455–461. doi: 10.1002/jcc.21334
- Vagin, A. A., Steiner, R. A., Lebedev, A. A., Potterton, L., McNicholas, S., Long, F., et al. (2004). REFMAC5 dictionary: organization of prior chemical knowledge and guidelines for its use. *Acta Crystallogr. D Biol. Crystallogr.* 60, 2184–2195. doi: 10.1107/S0907444904023510

Conflict of Interest Statement: S-SC, J-HN, KC, TL are named inventors on patents for the use of NADPH and its derivatives as β -lactamase inhibitors.

The remaining authors declare that the research was conducted in the absence of any commercial or financial relationships that could be construed as a potential conflict of interest.

Copyright © 2018 Na, Lee, Park, Kim, Jeong, Chung and Cha. This is an open-access article distributed under the terms of the Creative Commons Attribution License (CC BY). The use, distribution or reproduction in other forums is permitted, provided the original author(s) and the copyright owner(s) are credited and that the original publication in this journal is cited, in accordance with accepted academic practice. No use, distribution or reproduction is permitted which does not comply with these terms.



Itaconimides as Novel Quorum Sensing Inhibitors of *Pseudomonas aeruginosa*

July Fong^{1†}, Kim T. Mortensen^{2†}, Amalie Nørskov², Katrine Qvortrup², Liang Yang^{1,3*}, Choon Hong Tan^{1,4}, Thomas E. Nielsen^{1,5} and Michael Givskov^{1,5*}

¹ Singapore Centre for Environmental Life Sciences Engineering, Nanyang Technological University, Singapore, Singapore, ² Department of Chemistry, Technical University of Denmark, Lyngby, Denmark, ³ Southern University of Science and Technology, Shenzhen, China, ⁴ Division of Chemistry and Biological Chemistry, School of Physical and Mathematical Sciences, Nanyang Technological University, Singapore, Singapore, ⁵ Department of Immunology and Microbiology, Costerton Biofilm Center, University of Copenhagen, Copenhagen, Denmark

OPEN ACCESS

Edited by:

You-Hee Cho,
CHA University, South Korea

Reviewed by:

Eric Déziel,
Institut National de la Recherche
Scientifique (INRS), Canada
Daniel Angel Ortiz,
Laboratory Corporation of America
Holdings (LabCorp), United States

*Correspondence:

Liang Yang
yangl@sustc.edu.cn
Michael Givskov
mgivskov@sund.ku.dk

[†]These authors have contributed
equally to this work

Specialty section:

This article was submitted to
Clinical Microbiology,
a section of the journal
Frontiers in Cellular and Infection
Microbiology

Received: 06 October 2018

Accepted: 11 December 2018

Published: 07 January 2019

Citation:

Fong J, Mortensen KT, Nørskov A,
Qvortrup K, Yang L, Tan CH,
Nielsen TE and Givskov M (2019)
Itaconimides as Novel Quorum
Sensing Inhibitors of *Pseudomonas*
aeruginosa.
Front. Cell. Infect. Microbiol. 8:443.
doi: 10.3389/fcimb.2018.00443

Pseudomonas aeruginosa is known as an opportunistic pathogen that often causes persistent infections associated with high level of antibiotic-resistance and biofilms formation. Chemical interference with bacterial cell-to-cell communication, termed quorum sensing (QS), has been recognized as an attractive approach to control infections and address the drug resistance problems currently observed worldwide. Instead of imposing direct selective pressure on bacterial growth, the right bioactive compounds can preferentially block QS-based communication and attenuate cascades of bacterial gene expression and production of virulence factors, thus leading to reduced pathogenicity. Herein, we report on the potential of itaconimides as quorum sensing inhibitors (QSI) of *P. aeruginosa*. An initial hit was discovered in a screening program of an in-house compound collection, and subsequent structure-activity relationship (SAR) studies provided analogs that could reduce expression of central QS-regulated virulence factors (elastase, rhamnolipid, and pyocyanin), and also successfully lead to the eradication of *P. aeruginosa* biofilms in combination with tobramycin. Further studies on the cytotoxicity of compounds using murine macrophages indicated no toxicity at common working concentrations, thereby pointing to the potential of these small molecules as promising entities for antimicrobial drug development.

Keywords: quorum sensing, biofilm, itaconimides, antivirulence, chemical biology

INTRODUCTION

Pseudomonas aeruginosa is an opportunistic pathogen and a major cause of nosocomial infections in patients with pneumonia, chronic wounds, urinary tract infections, and intensive care units (ICUs) (Vincent et al., 1995). As an opportunistic pathogen, this organism is highly adaptive, versatile and exhibits remarkable resistance toward many antimicrobial agents. Resistance is a distinctive characteristic of *P. aeruginosa*, due to its ability to express multiple resistance mechanisms, including enzymes and efflux pumps (Poole, 2001; Lister et al., 2009). U.S. Centers for Disease Control and Prevention (CDC) (2013) estimated that more than 20,000 deaths per year are attributed to antibiotic resistance cases. It has become a global issue, and we are threatened with the slow progress of new antibiotics development and lack of preventive measure for the spread of resistance.

In addition, *P. aeruginosa* is well-known to form biofilms, which have been identified as a major underlying cause of persistent infections in immunocompromised patients, chronic wounds as well as on medical devices like implants, catheters, tubes, artificial hip, and many more (Costerton et al., 1999). Biofilms infections are often characterized by their broad range resistance toward host defense mechanisms and antibiotic therapy. This results in prolonged treatment, complications in clinical outcomes, and additional socio-economic burdens. In cystic fibrosis patients, chronic biofilm infections of *P. aeruginosa* can cause premature death despite intensive antibiotic therapy care (Bjarnsholt et al., 2009).

The bacteria in biofilms often exhibit different phenotypic and genetic variants as compared to their planktonic counterparts. In the biofilm mode of life, bacterial cells are enclosed within a matrix of extracellular polymeric substances (EPS) comprises of exopolysaccharides, proteins, deoxyribonucleic acid (DNA), lipids or surfactants, and macromolecules that are self-produced by the cells (Flemming and Wingender, 2010). All of these could render antibiotics impenetrable, chelated or sequestered, and diminish the efficacy of the treatment. The presence of persister cells in biofilms also contributes to multidrug resistance property of biofilms (Lewis, 2007). Overall, the complex biology of biofilms represents a tremendous challenge to develop therapeutic agents that could successfully prevent or eradicate biofilms-associated infections.

The cell-to-cell communication system called quorum sensing (QS) has been reported to play major roles for establishing persistent, biofilm based infections (Hentzer et al., 2003; Alhede et al., 2009; Van Gennip et al., 2009; Chiang et al., 2013). The QS system in *P. aeruginosa* utilizes acyl homoserine lactones (AHLs) as signal molecules and comprises the Lux homologs LasRI and RhlRI. LasI synthase is responsible for the synthesis of *N*-(3-oxododecanoyl) homoserine lactone (3-oxo-C12-HSL), which will bind to its receptor LasR and activate transcription of genes responsible for virulence such as *lasB*, *apr*, and *toxA* (Gambello et al., 1993; Passador et al., 1993). The *las* system also positively regulates *rhl* system, where RhlI directs the synthesis of *N*-butanoylhomoserine lactone (C4-HSL) that would bind to its receptor RhlR and subsequently activate gene expression of QS target genes (Brint and Ohman, 1995; Pearson et al., 1995; Pesci et al., 1997). In addition, there is also a third signaling molecule “pseudomonas quinolone signal” (PQS) which is intertwined between the *las* and *rhl* systems (Schertzer et al., 2009). Recently, a fourth signal molecules called Integrative Quorum Sensing Signal (IQS) has been reported, which could overtake the central *las* system under phosphate depletion condition (Lee et al., 2013). QS defective *P. aeruginosa* mutants are attenuated as compared to the wild-type strain, and their biofilms are more susceptible toward antibiotics treatment and host immune system as compared to the wild-type (Pearson et al., 2000; Hentzer et al., 2002, 2003).

As QS governs various patterns of genes expression to control virulence and biofilm formation, it has been proposed that interfering with the communication system could be a promising strategy for the control and prevention of bacterial infections (Hentzer et al., 2003). Quorum sensing inhibitors (QSI) are

compounds that interfere with QS pathways, reduce expression of QS-controlled genes and attenuate infecting bacteria. As such compounds do not affect the growth of bacteria, these molecular entities pose lower selective pressure on bacteria and lower the risk of resistance development. Recent exploration of new classes of QSI comprises natural products, synthetic molecules, and enzymes that may quench or inactivate QS signals (Dong et al., 2001; Hentzer et al., 2002; Jakobsen et al., 2012; Fong et al., 2017). Unfortunately, no clinical candidates have yet been developed for therapy.

In the present study, we report a new class of small molecules that disrupt QS pathways in *P. aeruginosa*. The structurally related itaconimides and citraconimides have previously been reported to inhibit growth of mycobacteria (Balganesh et al., 1999). We synthesized a range of small molecules by an iterative structure-activity relationship (SAR) study and found two promising candidates for further biological investigation. The efficacies of these compounds were tested on *P. aeruginosa* QS bioreporter strains (*lasB-gfp*; *rhlA-gfp*; *pqsA-gfp*) and also on QS-controlled virulence phenotypes, such as elastase, pyocyanin, and rhamnolipid production.

MATERIALS AND METHODS

General Information

All chemicals were purchased from Sigma Aldrich and used without further purification. For biological studies, synthesized compounds were prepared in DMSO as 10 mM stock solution and stored at -20°C until further usage. Overnight culture of bacteria was grown in Lysogeny broth (LB) which consisted of 1% tryptone, 0.5% yeast extract, 0.5% NaCl. For bioreporter assay, strains were grown in ABTGC (AB minimal medium supplemented with 0.2% glucose and 0.2% casamino acids) (Clark and Maaloe, 1967) to minimize fluorescence interference. ABTG (with no casamino acid) medium was used for biofilms study in flow chambers. Strains used in this study can be found in **Table 1**. Summary of chemical synthesis and spectroscopy data can be found in **Supplementary Material**.

QS Inhibition Assay

From its frozen stock, compounds were diluted appropriately to their working concentration in ABTGC medium. Experiments were done as previously reported (Fong et al., 2017). Briefly, 200 μL of compounds was pipetted into the first rows of 96-well plates (Nunc, Denmark), followed by two-fold serial dilution to the rest of the rows. The last two rows were allocated to solvent control (DMSO 0.1%) and blank (media control). Overnight cultures of *P. aeruginosa* bioreporter strains were diluted to optical density at 600 nm (OD_{600}) of 0.02 ($\sim 2.5 \times 10^8$ CFU/mL). Next, 100 μL of the bacteria culture was added into each well to make final OD_{600} of 0.01. The plate was incubated at 37°C for 16 h, with time-point measurement of GFP fluorescence (excitation 485 nm, emission 535 nm) and OD_{600} recorded at every 15 min using Tecan Infinite 200 Pro plate reader (Tecan Group Ltd, Männedorf, Switzerland). The data were exported into excel files, and IC_{50} value calculation was determined using GraphPad Prism 6 software. For IC_{50} values determination, the

TABLE 1 | Bacterial strains used in this study.

Strains or plasmids	Relevant genotype and/or characteristics ^a
Strains	
PAO1	ATCC <i>Pseudomonas aeruginosa</i> (Hentzer et al., 2002)
PAO1- <i>gfp</i>	GFP-tagged wild-type <i>Pseudomonas aeruginosa</i> (Yang et al., 2007)
PAO1- <i>lasB-gfp</i>	PAO1 containing <i>lasB-gfp</i> (ASV) reporter fusion (Hentzer et al., 2002)
PAO1- <i>rhlA-gfp</i>	PAO1 containing <i>rhlA-gfp</i> (ASV) reporter fusion (Yang et al., 2007)
PAO1- <i>pqsA-gfp</i>	PAO1 containing <i>pqsA-gfp</i> (ASV) reporter fusion (Yang et al., 2009)
PAO1 Δ <i>las</i> / Δ <i>rhl</i>	Gm ^a ; PAO1 <i>lasI</i> and <i>rhlI</i> mutant (Hentzer et al., 2003)
PAO1 Δ <i>lasR</i>	PAO1 <i>lasR</i> mutant (Hentzer et al., 2003)
Δ <i>lasR-rhlA-gfp</i>	PAO1 <i>lasR</i> mutant containing <i>rhlA-gfp</i> (ASV) reporter fusion (Tan et al., 2013)
Δ <i>lasR-pqsA-gfp</i>	PAO1 <i>lasR</i> mutant containing <i>pqsA-gfp</i> (ASV) reporter fusion (Tan et al., 2013)

^aDescription of the strains' antibiotic resistance. Gm, gentamicin.

GFP/OD₆₀₀ values were taken at the time point between 4 and 6 h, where inhibition started to occur. All experiments were done in triplicate manner and repeated at least twice to confirm the results.

QS-Regulated Virulence Factor Assays

Elastase activity was measured using EnzChekElastase kit (Invitrogen, USA), following the manufacturer's instruction. Rhamnolipid was extracted and quantified using method reported by Koch et al. with modifications (Koch et al., 1991). Briefly, overnight cultures of *P. aeruginosa* were diluted into ABTGC medium (OD₆₀₀ = 0.01), with and without the presence of compounds (DMSO as control). Cultures were grown overnight at 37°C, 200 rpm. Rhamnolipid was extracted from the supernatant with diethyl ether (twice), and organic fractions were concentrated to yield yellowish-white solids. The solids were re-suspended in deionized water and added with 0.19% (w/v) orcinol in 50% H₂SO₄. It was then heated at 80°C for 20–30 min to give dark orange color. Absorbance was measured at 421 nm and the values were normalized with cell density at OD₆₀₀. Pyocyanin was extracted from overnight culture of *P. aeruginosa* grown in Kings Medium A Base [MilliQ water supplemented with proteose peptone (20 g/L), potassium sulfate (10 g/L), magnesium chloride, anhydrous (1.640 g/L), and glycerol (10% v/v)]. Supernatants were collected and extracted with chloroform and 0.2 M HCl. The presence of pyocyanin would turn the HCl solution into pinkish color. Absorbance was measured at 520 nm and normalized with cell density OD₆₀₀ values. Experiments were done in triplicate manner and repeated at least twice to confirm the results.

Biofilm Experiments

GFP-tagged *P. aeruginosa* were grown in ABTG medium and flowed through flow chambers as previously described (Sternberg and Tolker-Nielsen, 2006). Each flow chamber is

consisted of three-channel flow cells that were supplied with a flow of medium and oxygen, while waste medium would be directed into a waste flask. Briefly, overnight cultures were diluted 1,000 times in ABTG medium and injected into each channel for 1 h incubation time without flow. Next, the medium was allowed to flow into the flow cells and the velocity was maintained at 0.2 mm/s using Cole-Palmer peristaltic pump. Biofilms were grown for 72 h before treatment with compounds for further 48 h. To visualize dead cells, 300 μ L of propidium iodide (PI) stain was injected into each flow cells. Biofilm images were taken with LSM confocal laser scanning microscope (Carl Zeiss, Germany) at 20x objective lens. Microscopy images were processed with IMARIS software (Bitplane AG, Zurich, Switzerland). Experiments were done in triplicate manner and repeated at least twice to confirm the results.

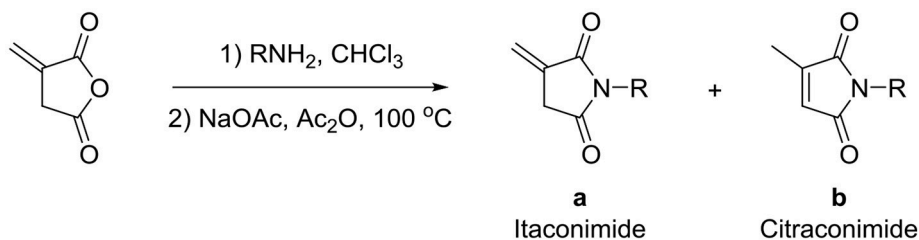
Cytotoxicity Assay

Toxicity assay was done as previously reported (Fong et al., 2017). Murine macrophage RAW264.7 cell lines were grown in Dulbecco's Modified Eagle's Medium (DMEM, Life Technologies), supplemented with 10% fetal bovine serum (Gibco) at 37°C and 5% CO₂. The cells were passaged into 96-well microplates, with each well containing 1×10^4 macrophages. After 16 h, the cells were washed with phosphate-buffered saline (PBS) and treated with compounds at varying concentration in 100 μ L DMEM. The plate was incubated at 37°C and 5% CO₂ for further 16 h. Resazurin was then added into each well to reach final concentration of 10 μ M for cell viability measurement. The live cells would be able to convert the dye to red color, whereby dead cells would remain as blue color. Absorbance was taken at 595 nm using Tecan Infinite 200 Pro plate reader (Tecan Group Ltd, Männedorf, Switzerland). Experiments were done in triplicate manner and repeated at least twice to confirm the results.

RESULTS

Synthesis and SAR Study

Recently, we discovered that 3-methylene-1-tetradecylpyrrolidine-2,5-dione (**Table 2, 1a**) displayed QSI activity against *P. aeruginosa* QS reporter strain (carrying a *lasB-gfp* fusion). Different variation on the left-hand side of **1a** proved that the exo-cyclic double bond was essential for its biological activity. This led us to focus on the synthesis and biological evaluation of *N*-substituted itaconimide analogs against *P. aeruginosa* (**Scheme 1**). The procedure for the synthesis of the itaconimides have been described by Cava et al. (1961) and Leow et al. (2008). The commercially available itaconic anhydride was treated with anilines (1.0 equiv.) in CHCl₃ to afford the corresponding α -itaconamic acids (Kyung et al., 1974). The resulting acids were subsequently treated with Ac₂O (3.5 equiv.) and NaOAc (0.5 equiv.) at elevated temperature to afford a mixture of itaconimide and the isomerized product citraconimide. Generally, the yield for the aniline derivatives was higher than that of the aliphatic amines. An overview of the synthesized compounds is provided below (**Table 2**).



SCHEME 1 | Synthesis of itaconimides and citraconimides.

QSI Activities of Itaconimides

The synthesized compounds were tested for their QS inhibitory activity against the *P. aeruginosa lasB-gfp* reporter strain. None of our synthesized compounds showed antibiotic properties (Supplementary Figures 1, 2). We found that both the *p*-bromophenyl and tetradecyl-substituted itaconimide (**12a** and **18a**) showed strong QS inhibition activity against the *lasB-gfp* reporter strain (Figure 1A). Both compounds inhibit the expression of *lasB-gfp* in a dose-dependent manner (Figure 1B). **18a** was proved to be the most active compound synthesized in this series, with almost 25-fold higher activity (IC_{50}) compared to our hit compound (Figures 1C,D).

To address the specificity of our compounds, we also tested our compounds against PAO1 wild-type (WT) and $\Delta lasR$ harboring either *rhlA-gfp* or *pqsA-gfp* fusions. In this case, we would be able to determine if the compounds could affect other QS pathways in *las*-dependent or independent manner. Both *rhlA* and *pqsA* are the first genes of *rhl* operon and *pqs* operon that code for the production of the rhamnolipid and PQS precursor molecules (Ochsner et al., 1994; Gallagher et al., 2002). To eliminate false positive, we also tested both compounds with a *gfp*-tagged *P. aeruginosa* (expresses GFP constitutively) as control and did not observe any reduction in the fluorescence signals (Supplementary Figure 3).

Compounds **12a** and **18a** were found to inhibit expression of *rhlA-gfp* and *pqsA-gfp* in PAO1 WT. IC_{50} values calculated for **12a** are $6.67 \pm 0.27 \mu\text{M}$ for *rhlA-gfp* and $2.51 \pm 0.19 \mu\text{M}$ for *pqsA-gfp*, whereby compound **18a** provides IC_{50} values of $0.61 \pm 0.04 \mu\text{M}$ for *rhlA-gfp* and 0.143 ± 0.13 for *pqsA-gfp* (Figure 2). At $10 \mu\text{M}$, compound **12a** was observed to inhibit *rhlA-gfp* more strongly in $\Delta lasR$ (78% inhibition) as compared to the wild-type (58% inhibition). In $\Delta lasR$ *pqsA-gfp* reporter strain, the inhibition only happened in the later stage. Meanwhile, compound **18a** was found to inhibit both *rhlA-gfp* and *pqsA-gfp* efficiently in $\Delta lasR$ (Figure 3). Therefore, it is likely that two compounds have different mechanisms, and compound **18a** affect multiple QS pathways in *las*-independent pathway.

Effects of Itaconimides on Virulence Production

Next, we investigated the effects of synthesized compounds on virulence factors produced by *P. aeruginosa*, notably elastase, rhamnolipid, and pyocyanin. The three virulence factors are under QS-regulation, therefore they could be a good indicator for evaluating antivirulence activities of our compounds. We

also included QS mutants as control strains, where they are defective in producing quorum sensing signals hence lower level of virulence production. At $10 \mu\text{M}$, both compounds were able to reduce all three virulence factors production. Elastase level was reduced almost half, and rhamnolipid and pyocyanin productions were abolished almost to the same level as mutant strains (Figure 4). The results showed that both compounds could indeed lower the production of virulence factors.

Effects of Itaconimides on *P. aeruginosa* Biofilms

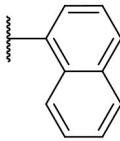
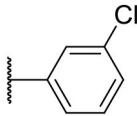
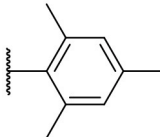
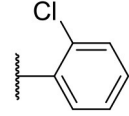
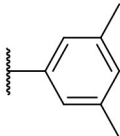
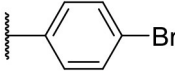
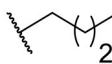
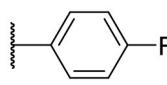
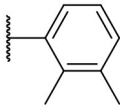
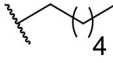
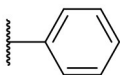
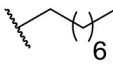
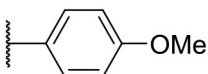
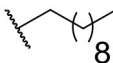
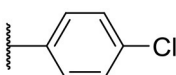
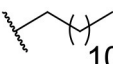
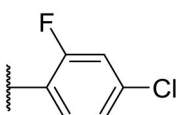
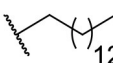
QS has been shown to play important roles in biofilms matrix formation (Davey et al., 2003; Sakuragi and Kolter, 2007). Mutants lacking QS often form flat and undifferentiated biofilms that could be easily cleared by antimicrobial agents and host immune system (Wu et al., 2001; Christensen et al., 2007). Here, we investigated if the itaconimides could eradicate biofilms formation when used in combination with tobramycin antibiotic.

From Figure 5, it can be seen that treatment with tobramycin alone ($10 \mu\text{g/ml}$) couldn't clear the whole population of *P. aeruginosa* biofilms. The dead cells only appeared on the surface of the biofilms, which indicated that the antibiotic could not penetrate into the biofilms. In addition, biofilms often contain extracellular DNA (eDNA) which could chelate aminoglycoside antibiotics and render it inactive (Chiang et al., 2013). At $10 \mu\text{M}$, itaconimide **12a** could remarkably kill the base population of the biofilms, but not the surface. When added together with tobramycin, the combination treatment successfully eradicated the whole population of biofilms, which appeared red. Compound **18a** did not show any synergistic effect when used together with tobramycin, which could be due to poor solubility in the aqueous media.

Cytotoxic Effects of Itaconimides on Macrophages

We next evaluated the potential application of compounds **12a** and **18a** for therapeutic application. To test the cytotoxic effects, both compounds were added into murine macrophage RAW2647 cell lines, and the cell viability was measured after 16h incubation time. Both compounds were observed to be toxic at $40 \mu\text{M}$, but not cytotoxic at their working concentration ($10 \mu\text{M}$ and lower, Figure 6). This indicates that they could be further used for subsequent *in vivo* experiments at their relevant concentration.

TABLE 2 | Summary of the synthesized compounds and the corresponding yields.

Compound	R	a (%) ^a	b (%) ^a	Compound	R	a (%) ^a	b (%) ^a
1		50	14	10		35	15
2		37	— ^b	11		61	9
3		17	— ^b	12		37	20
4		10	— ^b	13		40	19
5		47	— ^b	14		8	14
6		49	29	15		16	— ^b
7		— ^c		16		13	10
8		31	40	17		4	12
9		24	14	18		2	11

^aYields based on starting itaconic anhydride and purified after cyclization by flash column chromatography.

^bNot isolated.

^cCommercial sample.

DISCUSSION

In this study, we present the investigation of itaconimides as a novel QSI against *P. aeruginosa*. The approach of using QSI molecules to attenuate the virulence of pathogenic bacteria has advantages over conventional antibiotics

therapy. Instead of targeting the growth of bacteria (bactericidal or bacteriostatic strategies), QSI compounds pose lesser selective pressure for the development of resistant mutants. In several studies, it has been shown that mice treated with QSI afford better survival profile and lower bacteria count loads when compared to the

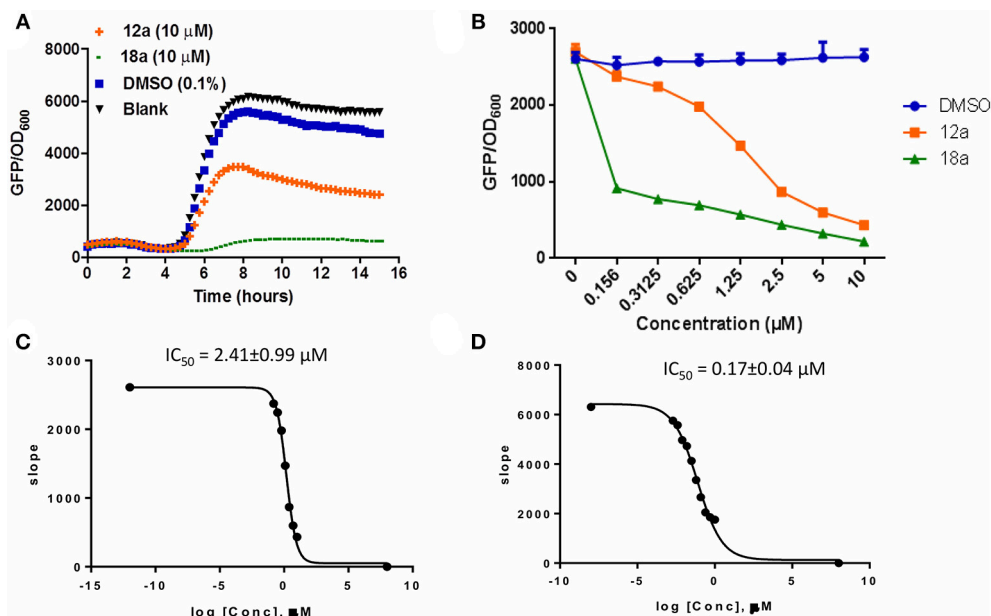


FIGURE 1 | (A) Effects of compounds **12a** and **18a** on PAO1-*lasB-gfp* reporter strain. DMSO 0.1% was used as solvent control. **(B)** Dose-response effects of compounds on *P. aeruginosa lasB-gfp*. **(C)** IC₅₀ values of **12a** and **18a** **(D)** on *lasB-gfp*. Calculation was done using GraphPad Prism 6 software, taken at time point between 4 and 6 h when QS inhibition started to occur. All experiments were done in triplicate manner (technical and biological replicates), only representative data are shown.

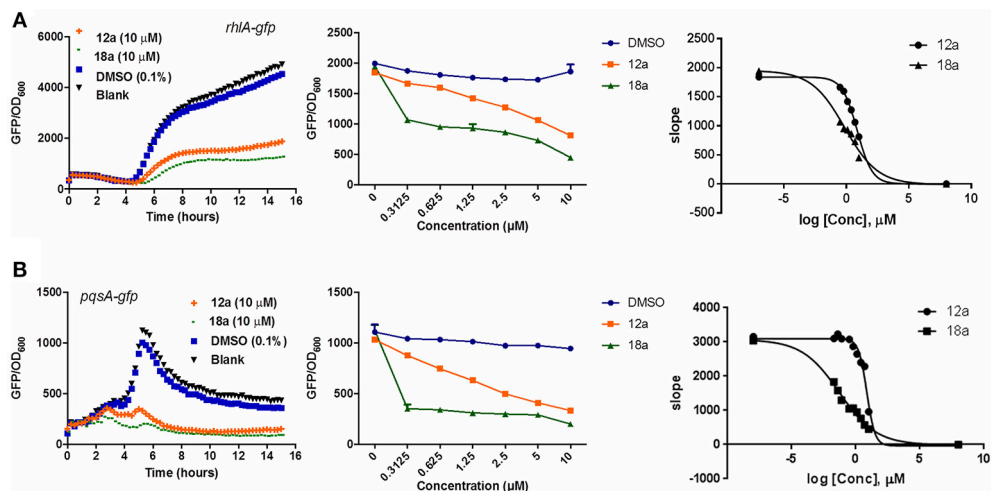


FIGURE 2 | QSI inhibition, dose-response and IC₅₀ values of compounds **12a** and **18a** on *P. aeruginosa rhlA-gfp* **(A)** and *pqsA-gfp* **(B)**. DMSO 0.1% was used as solvent control. For the IC₅₀ values, calculation was done using GraphPad Prism 6 software, taken at time point between 4 and 6 h when QS inhibition started to occur. All experiments were done in triplicate manner (technical and biological replicates), only representative data are shown.

control group (Hentzer et al., 2002, 2003; Jakobsen et al., 2013; Fong et al., 2017). With limited options of treatment available, antivirulence therapy could be a viable approach to mitigate the future crisis of antibiotic resistance.

In this study, a structure-activity relationship (SAR) study was performed to investigate the QSI activities of itaconimides and citraconimide analogs. We screened the compounds against

QS reporter strain *lasB-gfp*, where gene expression is under control of the QS *las* system. We first investigated the inhibitory properties of the two isomers with respect to *lasB-gfp* expression. Interestingly, the itaconimide scaffold was found to be more active than the citraconimide. Next, we investigated the influence of electron donating groups (EDGs) and electron withdrawing groups (EWGs) on the phenyl group. Whereas, *p*-anisidine moiety failed to improve activity, the more electron-withdrawing

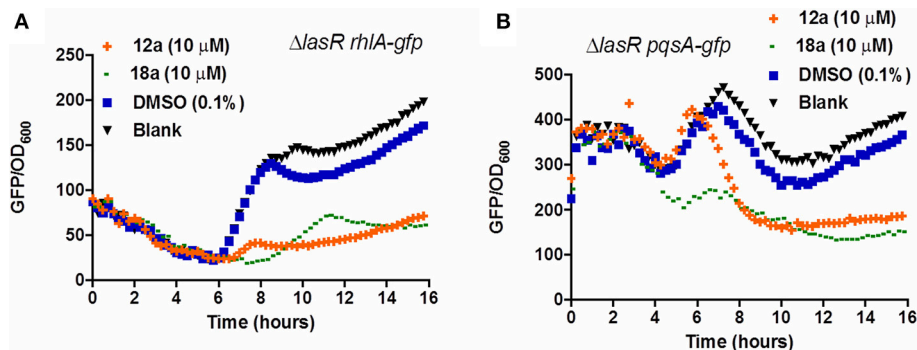


FIGURE 3 | QSI inhibition of compounds **12a** and **18a** on PAO1 $\Delta lasR rhIA-gfp$ (A) and $pqsA-gfp$ (B). DMSO 0.1% was used as solvent control. All experiments were done in triplicate manner (technical and biological replicates), only representative data are shown.

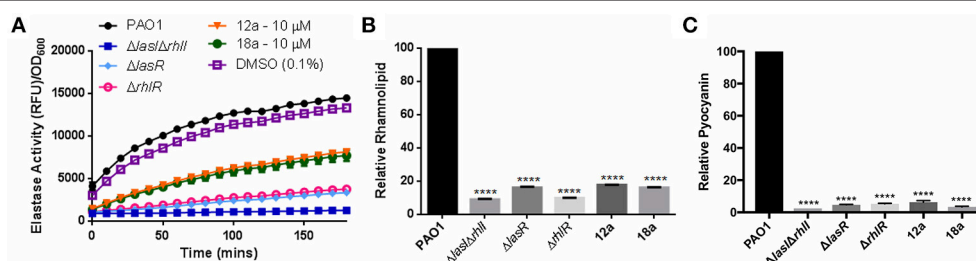


FIGURE 4 | Effects of compounds **12a** and **18a** on elastase (A), rhamnolipid (B), and pyocyanin production (C). Compounds were tested at final concentration of 10 μ M. All experiments were done in triplicate manner (technical and biological replicates). Error bars are means \pm SDs. **** p < 0.0001, Student's t -test.

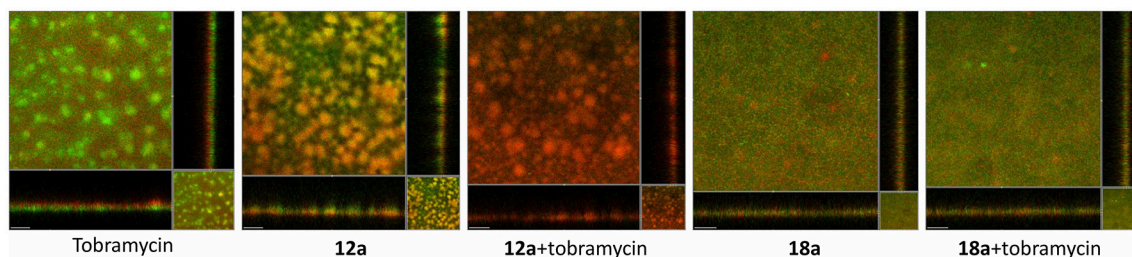


FIGURE 5 | *P. aeruginosa* biofilms formed on flow cells for 72 h, followed by treatment with medium containing antibiotic (tobramycin 10 μ g/ml) and compounds (10 μ M) for further 48 h. Live cells are *P. aeruginosa* tagged with GFP which appeared as green, and dead cells appeared as red. Scale bars, 50 μ m. Experiments were done in triplicate manner (technical and biological replicates), only representative images were shown.

4-chloro derivative induced a 1.4-fold inhibition of PAO1-*lasB-gfp*. This guided us to explore anilines with different EWGs. The most potent compound in this series was **12a** from 4-bromoaniline that results in a 4.4-fold increase over the parent aniline analog. To our surprise, the 4-fluoroaniline analog **13a** did not afford a more potent inhibitor. Alongside the findings that 4-bromoaniline provided a more potent analog, we also found that the octylamine analog **14a** was more active than our hit compound **1a**. Lastly, we also included aliphatic chains to mimic the long alkyl chain of C4-HSL and 3-oxo-C12-HSL. On this note, a second series

was synthesized from commercially available aliphatic amines with varying carbon lengths ($n = 4, 6, 8, 10, 12, 14$). A clear trend was observed, where longer alkyl chain resulted in lower IC₅₀ values. The outcome was quite interesting, as IC₅₀ values of the citraconimide substituents of these analogs (**16b**, **17b**, and **18b**) were significantly lowered. The most potent compound was found to be the tetradecylamine analog, **18a**, being the most active of both series. By substituting the naphthalene group with either 4-bromoaniline or long chain alkyl amines, IC₅₀ values against PAO1-*lasB-gfp* were significantly reduced to the low micromolar range ($2.41 \pm$

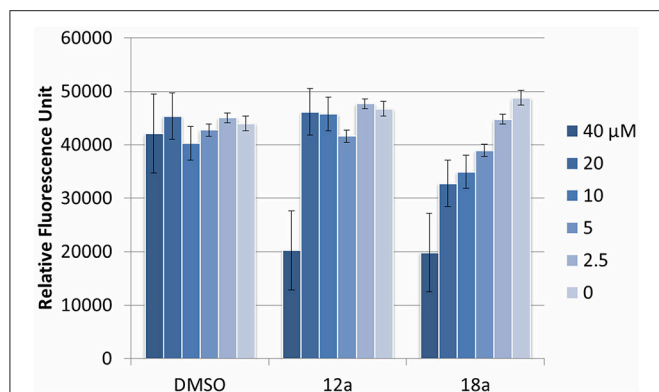


FIGURE 6 | Cytotoxic effect of compounds **12a** and **18a** on murine macrophages. DMSO was used as vehicle control. Compounds were tested at various concentrations (40 μ M and subsequent 2x dilution). Experiments were done in triplicate manner (technical and biological replicates). Error bars are means \pm SDs.

0.99 μ M for **12a** and $0.17 \pm 0.04 \mu$ M for **18a**). In summary, our SAR studies revealed two structurally important variations for the itaconimides that are highly important for QSI activity (Table 3).

Previous studies have emphasized the advantage of therapeutics that suppress multiple QS pathways (Fong et al., 2018). Indeed, *lasR* mutants are commonly found in patients suffering from cystic fibrosis and other clinical setting (Hamood et al., 1996; Cabrol et al., 2003; Marvig et al., 2014). Nevertheless, the loss-of-function *lasR* mutants continuously express virulence traits so *P. aeruginosa* could use other pathways to bypass LasR in controlling pathogenicity (Dekimpe and Déziel, 2009; Lee et al., 2013). Using different QS reporter strains in both PAO1 WT and Δ *lasR*, it can be deduced that our compounds do not specifically inhibit one QS pathway. Both compounds could inhibit expression of *rhIA-gfp* and *pqsA-gfp* in *lasR* mutant. The inhibition of *pqsA-gfp* in Δ *lasR* was less apparent for compound **12a**, which could indicate that the compound inhibits PQS system through *las*-dependent manner. The itaconimide analogs presented here hold unique potential as broad target QSIs to control infections via an anti-virulence strategy. Future work will aim to elucidate the mechanism on how both compounds inhibit QS in *P. aeruginosa*.

Next, we also tested the effects of our compounds on the production of various virulence factors, such as elastase, rhamnolipid, and pyocyanin production. Elastase is one of the major proteases produced by *P. aeruginosa*, involved in host tissue damage and host immune responses (Kamath et al., 2002). Rhamnolipid is also an essential virulence factor and plays several key roles in biofilms formation, swarming, and in particular host immune evasion. It promotes rapid necrotic killing of polymorphonuclear (PMNs) leukocytes and also infiltration of respiratory epithelial cells (Zulianello et al., 2006; Jensen et al., 2007). *P. aeruginosa* also secretes pyocyanin, blue redox-active secondary metabolite that has several deleterious effects on mammalian cells (Lau et al., 2004), which is also regulated by QS under *pqs* system. When tested at 10 μ M, the compounds could

TABLE 3 | Summary of IC₅₀ values of itaconimide (a) and citraconimide (b) analogs against PAO1-*lasB-gfp*.

Compound	a	b
1	7.37 \pm 0.71	–
2	23.52 \pm 0.81	–
3	10.27 \pm 0.05	–
4	–	–
5	17.95 \pm 0.49	–
6	10.67 \pm 0.49	–
7	–	NA
8	7.45 \pm 0.65	–
9	7.65 \pm 0.37	–
10	6.53 \pm 0.61	–
11	17.68 \pm 0.16	–
12	2.41 \pm 0.99	–
13	11.89 \pm 0.34	–
14	26.66 \pm 0.98	–
15	1.71 \pm 0.34	–
16	0.30 \pm 0.05	2.01 \pm 0.39
17	0.30 \pm 0.17	0.91 \pm 0.20
18	0.17 \pm 0.04	0.53 \pm 0.12

All IC₅₀ values were reported as μ M. Experiments were done in triplicate manner and repeated at least twice to confirm the results. NA, Not available.

reduce production of various virulence factors controlled by QS. This shows potential of our compounds as antivirulence agent of *P. aeruginosa*.

P. aeruginosa biofilms are highly resistant to most antibiotics, including the last-resort polymyxin antibiotic available, colistin (Chua et al., 2016). As QS has definite role in biofilms development, it has been proposed that QSI compounds could be used as prophylactic treatment for biofilms infections. One such case is using azithromycin, which inhibits QS and biofilm formation at sub-MIC concentration. Promising results were observed in pulmonary infections and CF patients in many clinical trials data upon treatment of low-dose of AZM (2 μ g/ml) (Hansen et al., 2005; Fleet et al., 2013). In this study, we utilized a combination of our compounds with the aminoglycoside tobramycin to treat *P. aeruginosa* biofilms grown on flow chambers for 3 days. We chose to study tobramycin because of its clinical relevance to cystic fibrosis (CF) patients. The clinical isolates from lung patients often confer resistance to aminoglycoside antibiotics (Hurley et al., 1995; Saiman et al., 1996). Our data also shows that treatment with tobramycin alone only kills the upper layer of biofilms. Combined with **12a**, we observed that the whole population of biofilms was eradicated. The results offer promising application of QSI in combination with antibiotics as a control for biofilm-associated infections.

It has been reported that stringent response, which provides rapid adaptation to environmental stresses, regulates QS network and also bacteria's survival in biofilms of *P. aeruginosa* (van Delden et al., 2001; Nguyen et al., 2011; Schafhauser et al., 2014). QS-deficient mutants also have lower catalase and superoxide dismutase activities, and therefore more sensitive to oxidative stress (Hassett et al., 1999). Through our biofilms experiment, we

could observe some cells death upon treatment with compound **12a** in the base of the biofilms. This raises the possibility that our compound could also target stringent response and other stress-response genes, which resulted in the observed killing effect. For compound **18a**, it contains long alkyl chain, which may render its solubility and penetration into the biofilms matrix. Future study will investigate how our compounds could synergize with other antibiotics to treat biofilms from other clinical isolates.

Lastly, we investigated the cytotoxic profile of our compounds on macrophages. The cytotoxicity of the compounds is important if they are to be used in animal studies for subsequent drug development. Results indicated that compound **12a** and **18a** are not toxic up to 40 μ M concentration. Still, further studies are needed to qualify the efficacy of the compounds in mice models for their potential as anti-biofilm agents, as well as their pharmacodynamic and pharmacokinetic profiles.

In conclusion, we report the novel use of itaconimides as antivirulence compounds for *P. aeruginosa*. These compounds suppress the *las*, *rhl*, and *pqs* QS systems of *P. aeruginosa*, and effectively abolish virulence expression activities. Compounds **12a** and **18a** showed low micromolar IC₅₀ values against all three QS reporter strains with only little toxicity against macrophages at the administrated concentration. Moreover, a synergistic effect with tobramycin was observed for the killing of *P. aeruginosa* biofilms, including otherwise the tolerant and hard to target sub-population cells. Overall, our findings point to a new class of hit

compounds of relevance to the development of new drugs against the superbug *P. aeruginosa*.

AUTHOR CONTRIBUTIONS

LY, TN, and MG designed methods and experiments. JF and KM performed the experiments and analyzed the data. AN, KQ, CT, and TN were in charge of the chemical synthesis. JF and KM wrote the paper and carefully revised by LY, TN, and MG. All authors have contributed to read and approved the manuscript.

FUNDING

This research was supported by the National Research Foundation and Ministry of Education Singapore under its Research Centre of Excellence Program and AcRF Tier 2 (MOE2016-T2-1-010) from Ministry of Education, Singapore. KM, KQ, and TN are grateful to The Danish Council for Independent Research (FTP grant 40616) for supporting this research.

SUPPLEMENTARY MATERIAL

The Supplementary Material for this article can be found online at: <https://www.frontiersin.org/articles/10.3389/fcimb.2018.00443/full#supplementary-material>

REFERENCES

- Alhede, M., Bjarnsholt, T., Jensen, P. Ø., Phipps, R. K., Moser, C., Christophersen, L., et al. (2009). *Pseudomonas aeruginosa* recognizes and responds aggressively to the presence of polymorphonuclear leukocytes. *Microbiology* 155, 3500–3508. doi: 10.1099/mic.0.031443-0
- Balganesh, M., Ethirajulu, K., Ganguly, B. S., Janakiraman, R., Kaur, P., Kajipalya, R., et al. (1999). Mycobacterial inhibitors. WO1999065483A1. Available online at: <https://patentscope.wipo.int/search/en/detail.jsf?docId=WO1999065483&tab=PCTBIBLIO&maxRec=1000>
- Bjarnsholt, T., Jensen, P. Ø., Fiandaca, M. J., Pedersen, J., Hansen, C. R., Andersen, C. B., et al. (2009). *Pseudomonas aeruginosa* biofilms in the respiratory tract of cystic fibrosis patients. *Pediatr. Pulmonol.* 44, 547–558. doi: 10.1002/ppul.21011
- Brint, J. M., and Ohman, D. E. (1995). Synthesis of multiple exoproducts in *Pseudomonas aeruginosa* is under the control of RhlR-RhlI, another set of regulators in strain PAO1 with homology to the autoinducer-responsive LuxR-LuxI family. *J. Bacteriol.* 177, 7155–7163. doi: 10.1128/jb.177.24.7155-7163.1995
- Cabrol, S., Olliver, A., Pier, G. B., Andremont, A., and Ruimy, R. (2003). Transcription of quorum-sensing system genes in clinical and environmental isolates of *Pseudomonas aeruginosa*. *J. Bacteriol.* 185, 7222–7230. doi: 10.1128/JB.185.24.7222-7230.2003
- Cava, M. P., Deana, A. A., Muth, K., and Mitchell, M. J. (1961). N-Phenylmaleimide. *Org. Synth.* 41:93. doi: 10.1522/orgsyn.041.0093
- Chiang, W.-C., Nilsson, M., Jensen, P. Ø., Høiby, N., Nielsen, T. E., Givskov, M., et al. (2013). Extracellular DNA shields against aminoglycosides in *Pseudomonas aeruginosa* biofilms. *Antimicrob. Agents Chemother.* 57, 2352–2361. doi: 10.1128/AAC.00001-13
- Christensen, L. D., Moser, C., Jensen, P. Ø., Rasmussen, T. B., Christophersen, L., Kjelleberg, S., et al. (2007). Impact of *Pseudomonas aeruginosa* quorum sensing on biofilm persistence in an *in vivo* intraperitoneal foreign-body infection model. *Microbiology* 153, 2312–2320. doi: 10.1099/mic.0.2007/006122-0
- Chua, S. L., Yam, J. K. H., Hao, P., Adav, S. S., Salido, M. M., Liu, Y., et al. (2016). Selective labelling and eradication of antibiotic-tolerant bacterial populations in *Pseudomonas aeruginosa* biofilms. *Nat. Commun.* 7:10750. doi: 10.1038/ncomms10750
- Clark, D. J., and Maaloe, O. (1967). DNA replication and the division cycle in *Escherichia coli*. *J. Mol. Biol.* 23, 99–112. doi: 10.1016/S0022-2836(67)80070-6
- Costerton, J. W., Stewart, P. S., and Greenberg, E. P. (1999). Bacterial biofilms: a common cause of persistent infections. *Science* 284, 1318–1322. doi: 10.1126/science.284.5418.1318
- Davey, M. E., Caiazza, N. C., and O'toole, G. A. (2003). Rhamnolipid surfactant production affects biofilm architecture in *Pseudomonas aeruginosa* PAO1. *J. Bacteriol.* 185, 1027–1036. doi: 10.1128/JB.185.3.1027-1036.2003
- Dekimpe, V., and Déziel, E. (2009). Revisiting the quorum-sensing hierarchy in *Pseudomonas aeruginosa*: the transcriptional regulator RhlR regulates LasR-specific factors. *Microbiology* 155, 712–723. doi: 10.1099/mic.0.022764-0
- Dong, Y.-H., Wang, L.-H., Xu, J.-L., Zhang, H.-B., Zhang, X.-F., and Zhang, L.-H. (2001). Quenching quorum-sensing-dependent bacterial infection by an N-acyl homoserine lactonase. *Nature* 414, 813–817. doi: 10.1038/35081101
- Fleet, J. E., Guha, K., Piper, S., Banya, W., Bilton, D., and Hodson, M. E. (2013). A retrospective analysis of the impact of azithromycin maintenance therapy on adults attending a UK cystic fibrosis clinic. *J. Cyst. Fibros.* 2013, 49–53. doi: 10.1016/j.jcf.2012.05.010
- Flemming, H.-C., and Wingender, J. (2010). The biofilm matrix. *Nat. Rev. Microbiol.* 8, 623–633. doi: 10.1038/nrmicro2415
- Fong, J., Yuan, M., Jakobsen, T. H., Mortensen, K. T., Santos, M. M. S. D., Chua, S. L., et al. (2017). Disulfide bond-containing ajoene analogues as novel quorum sensing inhibitors of *Pseudomonas aeruginosa*. *J. Med. Chem.* 60, 215–227. doi: 10.1021/acs.jmedchem.6b01025

- Fong, J., Zhang, C., Yang, R., Boo, Z. Z., Tan, S. K., Nielsen, T. E., et al. (2018). Combination therapy strategy of quorum quenching enzyme and quorum sensing inhibitor in suppressing multiple quorum sensing pathways of *P. aeruginosa*. *Sci. Rep.* 8:1155. doi: 10.1038/s41598-018-19504-w
- Gallagher, L. A., Mcknight, S. L., Kuznetsova, M. S., Pesci, E. C., and Manoil, C. (2002). Functions required for extracellular quinolone signaling by *Pseudomonas aeruginosa*. *J. Bacteriol.* 184, 6472–6480. doi: 10.1128/JB.184.23.6472-6480.2002
- Gambello, M. J., Kaye, S., and Iglewski, B. H. (1993). LasR of *Pseudomonas aeruginosa* is a transcriptional activator of the alkaline protease gene (*apr*) and an enhancer of exotoxin A expression. *Infect. Immun.* 61, 1180–1184.
- Hamood, A. N., Griswold, J., and Colmer, J. (1996). Characterization of elastase-deficient clinical isolates of *Pseudomonas aeruginosa*. *Infect. Immun.* 64, 3154–3160.
- Hansen, C. R., Pressler, T., Koch, C., and Høiby, N. (2005). Long-term azitromycin treatment of cystic fibrosis patients with chronic *Pseudomonas aeruginosa* infection; an observational cohort study. *J. Cyst. Fibros* 4, 35–40. doi: 10.1016/j.jcf.2004.09.001
- Hassett, D. J., Ma, J. F., Elkins, J. G., McDermott, T. R., Ochsner, U. A., West, S. E. H., et al. (1999). Quorum sensing in *Pseudomonas aeruginosa* controls expression of catalase and superoxide dismutase genes and mediates biofilm susceptibility to hydrogen peroxide. *Mol. Microbiol.* 34, 1082–1093. doi: 10.1046/j.1365-2958.1999.01672.x
- Hentzer, M., Riedel, K., Rasmussen, T. B., Heydorn, A., Andersen, J. B., Parsek, M. R., et al. (2002). Inhibition of quorum sensing in *Pseudomonas aeruginosa* biofilm bacteria by a halogenated furanone compound. *Microbiology* 148, 87–102. doi: 10.1099/00221287-148-1-87
- Hentzer, M., Wu, H., Andersen, J. B., Riedel, K., Rasmussen, T. B., Bagge, N., et al. (2003). Attenuation of *Pseudomonas aeruginosa* virulence by quorum sensing inhibitors. *EMBO J.* 22, 3803–3815. doi: 10.1093/emboj/cdg366
- Hurley, J. C., Miller, G. H., and Smith, A. L. (1995). Mechanism of amikacin resistance in *Pseudomonas aeruginosa* isolates from patients with cystic fibrosis. *Diagn. Microbiol. Infect. Dis.* 22, 331–336. doi: 10.1016/0732-8893(95)00138-6
- Jakobsen, T. H., Bjarnsholt, T., Jensen, P. Ø., Givskov, M., and Høiby, N. (2013). Targeting quorum sensing in *Pseudomonas aeruginosa* biofilms: current and emerging inhibitors. *Future Microbiol.* 8, 901–921. doi: 10.2217/fmb.13.57
- Jakobsen, T. H., Gennip, M. V., Phipps, R. K., Shanmugham, M. S., Christensen, L. D., Alhede, M., et al. (2012). Ajoene, a sulfur-rich molecule from garlic, inhibits genes controlled by quorum sensing. *Antimicrob. Agents Chemother.* 56:2314. doi: 10.1128/AAC.05919-11
- Jensen, P. Ø., Bjarnsholt, T., Phipps, R., Rasmussen, T. B., Calum, H., Christoffersen, L., et al. (2007). Rapid necrotic killing of polymorphonuclear leukocytes is caused by quorum-sensing-controlled production of rhamnolipid by *Pseudomonas aeruginosa*. *Microbiology* 153, 1329–1338. doi: 10.1099/mic.0.2006/003863-0
- Kamath, S., Kapatral, V., and Chakrabarty, A. M. (2002). Cellular function of elastase in *Pseudomonas aeruginosa*: role in the cleavage of nucleoside diphosphate kinase and in alginate synthesis. *Mol. Microbiol.* 30, 933–941. doi: 10.1046/j.1365-2958.1998.01121.x
- Koch, A. K., Kappeli, O., Fiechter, A., and Reiser, J. (1991). Hydrocarbon assimilation and biosurfactant production in *Pseudomonas aeruginosa* mutants. *J. Bacteriol.* 173, 4212–4219. doi: 10.1128/jb.173.13.4212-4219.1991
- Kyung, J. H., Cha, S., and Clapp, L. B. (1974). Identification of isomeric amides of itaconic acid by proton magnetic resonance spectroscopy. *Organ. Magn. Res.* 6, 466–468. doi: 10.1002/mrc.1270060816
- Lau, G. W., Hassett, D. J., Ran, H., and Kong, F. (2004). The role of pyocyanin in *Pseudomonas aeruginosa* infection. *Trends Mol. Med.* 10, 599–606. doi: 10.1016/j.molmed.2004.10.002
- Lee, J., Wu, J., Deng, Y., Wang, J., Wang, C., Wang, J., et al. (2013). A cell-cell communication signal integrates quorum sensing and stress response. *Nat. Chem. Biol.* 9, 339–343. doi: 10.1038/nchembio.1225
- Leow, D., Lin, S., Chittimalla, S. K., Fu, X., and Tan, C. H. (2008). Enantioselective protonation catalyzed by a chiral bicyclic guanidine derivative. *Angew. Chem. Int. Ed.* 47, 5641–5645. doi: 10.1002/anie.200801378
- Lewis, K. (2007). Persister cells, dormancy and infectious disease. *Nat. Rev. Microbiol.* 5, 48–56. doi: 10.1038/nrmicro1557
- Lister, P. D., Wolter, D. J., and Hanson, N. D. (2009). Antibacterial-resistant *Pseudomonas aeruginosa*: clinical impact and complex regulation of chromosomally encoded resistance mechanisms. *Clin. Microbiol. Rev.* 22, 582–610. doi: 10.1128/CMR.00040-09
- Marvig, R. L., Sommer, L. M., Molin, S., and Johansen, H. K. (2014). Convergent evolution and adaptation of *Pseudomonas aeruginosa* within patients with cystic fibrosis. *Nat. Genet.* 47, 1–9. doi: 10.1038/ng.3148
- Nguyen, D., Joshi-Datar, A., Lepine, F., Bauerle, E., Olakanmi, O., Beer, K., et al. (2011). Active starvation responses mediate antibiotic tolerance in biofilms and nutrient-limited bacteria. *Science* 334, 982–986. doi: 10.1126/science.1211037
- Ochsner, U. A., Fiechter, A., and Reiser, J. (1994). Isolation, characterization, and expression in *Escherichia coli* of the *Pseudomonas aeruginosa* *rhlAB* genes encoding a rhamnosyltransferase involved in rhamnolipid biosurfactant synthesis. *J. Biol. Chem.* 269, 19787–19795.
- Passadori, L., Cook, J. M., Gambello, M. J., Rust, L., and Iglewski, B. H. (1993). Expression of *Pseudomonas aeruginosa* virulence genes requires cell-to-cell communication. *Science* 260, 1127–1130. doi: 10.1126/science.8493556
- Pearson, J. P., Feldman, M., Iglewski, B. H., and Prince, A. (2000). *Pseudomonas aeruginosa* cell-to-cell signaling is required for virulence in a model of acute pulmonary infection. *Infect. Immun.* 68, 4331–4334. doi: 10.1128/IAI.68.7.4331-4334.2000
- Pearson, J. P., Passadori, L., Iglewski, B. H., and Greenberg, E. P. (1995). A second N-acylhomoserine lactone signal produced by *Pseudomonas aeruginosa*. *Proc. Natl. Acad. Sci. U.S.A.* 92, 1490–1494. doi: 10.1073/pnas.92.5.1490
- Pesci, E. C., Pearson, J. P., Seed, P. C., and Iglewski, B. H. (1997). Regulation of *las* and *rhl* quorum sensing in *Pseudomonas aeruginosa*. *J. Bacteriol.* 179, 3127–3132. doi: 10.1128/jb.179.10.3127-3132.1997
- Poole, K. (2001). Multidrug efflux pumps and antimicrobial resistance in *Pseudomonas aeruginosa* and related organisms. *J. Mol. Microbiol. Biotechnol.* 3, 255–264. Available online at: <https://www.karger.com/Journal/Home/22839>
- Saiman, L., Mehar, F., Niu, W. W., Neu, H. C., Shaw, K. J., Miller, G., et al. (1996). Antibiotic susceptibility of multiply resistant *Pseudomonas aeruginosa* isolated from patients with cystic fibrosis, including candidates for transplantation. *Clin. Infect. Dis.* 23, 532–537. doi: 10.1093/clinids/23.3.532
- Sakuragi, Y., and Kolter, R. (2007). Quorum-sensing regulation of the biofilm matrix genes (*pel*) of *Pseudomonas aeruginosa*. *J. Bacteriol.* 189, 5383–5386. doi: 10.1128/JB.00137-07
- Schafhauser, J., Lepine, F., McKay, G., Ahlgren, H. G., Khakimova, M., and Nguyen, D. (2014). The stringent response modulates 4-hydroxy-2-alkylquinoline biosynthesis and quorum-sensing hierarchy in *Pseudomonas aeruginosa*. *J. Bacteriol.* 196, 1641–1650. doi: 10.1128/JB.01086-13
- Schertzer, J. W., Boulette, M. L., and Whiteley, M. (2009). More than a signal: non-signaling properties of quorum sensing molecules. *Trends Microbiol.* 17, 189–195. doi: 10.1016/j.tim.2009.02.001
- Sternberg, C., and Tolker-Nielsen, T. (2006). Growing and analyzing biofilms in flow cells. *Curr. Protoc. Microbiol.* Chapter 1, Unit 1B 2. doi: 10.1002/9780471729259.mc01b02s00
- Tan, S. Y., Chua, S.-L., Chen, Y., Rice, S. A., Kjelleberg, S., Nielsen, T. E., et al. (2013). Identification of five structurally unrelated quorum-sensing inhibitors of *Pseudomonas aeruginosa* from a natural-derivative database. *Antimicrob. Agents Chemother.* 57, 5629–5641. doi: 10.1128/AAC.00955-13
- U.S. Centers for Disease Control and Prevention (CDC) (2013). *Antibiotic Resistance Threats in the United States*.
- van Delden, C., Comte, R., and Bally, M. (2001). Stringent response activates quorum sensing and modulates cell density-dependent gene expression in *Pseudomonas aeruginosa*. *J. Bacteriol.* 183, 5376–5384. doi: 10.1128/JB.183.18.5376-5384.2001
- Van Gennip, M., Christensen, L. D., Alhede, M., Phipps, R., Jensen, P. Ø., Christophersen, L., et al. (2009). Inactivation of the *rhlA* gene in *Pseudomonas aeruginosa* prevents rhamnolipid production, disabling the protection against polymorphonuclear leukocytes. *APMIS* 117, 537–546. doi: 10.1111/j.1600-0463.2009.02466.x
- Vincent, J.-L., Bihari, D. J., Suter, P. M., Bruining, H. A., White, J., Nicolas-Chanoine, M. H., et al. (1995). The prevalence of nosocomial infection in

- intensive care units in Europe. results of the european prevalence of infection in intensive care (epic) study. epic international advisory committee. *J. Am. Med. Assoc.* 274, 639–644. doi: 10.1001/jama.1995.03530080055041
- Wu, H., Song, Z., Givskov, M., Doring, G., Worlitzsch, D., Mathee, K., et al. (2001). *Pseudomonas aeruginosa* mutations in *lasI* and *rhlI* quorum sensing systems result in milder chronic lung infection. *Microbiology* 147, 1105–1113. doi: 10.1099/00221287-147-5-1105
- Yang, L., Barken, K. B., Skindersoe, M. E., Christensen, A. B., Givskov, M., and Tolker-Nielsen, T. (2007). Effects of iron on DNA release and biofilm development by *Pseudomonas aeruginosa*. *Microbiology* 153, 1318–1328. doi: 10.1099/mic.0.2006/004911-0
- Yang, L., Rybtke, M. T., Jakobsen, T. H., Hentzer, M., Bjarnsholt, T., Givskov, M., et al. (2009). Computer-aided identification of recognized drugs as *Pseudomonas aeruginosa* quorum-sensing inhibitors. *Antimicrob. Agents Chemother.* 53, 2432–2443. doi: 10.1128/AAC.01283-08
- Zulianello, L., Canard, C., Kohler, T., Caille, D., Lacroix, J.-S., and Meda, P. (2006). Rhamnolipids are virulence factors that promote early infiltration of primary human airway epithelia by *Pseudomonas aeruginosa*. *Infect. Immun.* 74, 3134–3147. doi: 10.1128/IAI.01772-05

Conflict of Interest Statement: The authors declare that the research was conducted in the absence of any commercial or financial relationships that could be construed as a potential conflict of interest.

Copyright © 2019 Fong, Mortensen, Nørskov, Qvortrup, Yang, Tan, Nielsen and Givskov. This is an open-access article distributed under the terms of the Creative Commons Attribution License (CC BY). The use, distribution or reproduction in other forums is permitted, provided the original author(s) and the copyright owner(s) are credited and that the original publication in this journal is cited, in accordance with accepted academic practice. No use, distribution or reproduction is permitted which does not comply with these terms.



A Novel Phage PD-6A3, and Its Endolysin Ply6A3, With Extended Lytic Activity Against *Acinetobacter baumannii*

Minle Wu^{1†}, Kongying Hu^{2†}, Youhua Xie², Yili Liu³, Di Mu⁴, Huimin Guo², Zhifan Zhang⁴, Yingcong Zhang¹, Dong Chang^{1*} and Yi Shi^{4*}

¹ Department of Clinical Laboratory, Shanghai Pudong Hospital, Fudan University, Shanghai, China, ² Key Laboratory of Medical Molecular Virology, School of Basic Medical Sciences, Fudan University, Shanghai, China, ³ Department of Clinical Laboratory, Shanghai Public Health Clinical Center, Shanghai, China, ⁴ Department of Clinical Laboratory, Shanghai Fourth People's Hospital Affiliated to Tongji University School of Medicine, Shanghai, China

OPEN ACCESS

Edited by:

Natalia V. Kirienko,
Rice University, United States

Reviewed by:

Andrei A. Zimin,
Institute of Biochemistry
and Physiology of Microorganisms
(RAS), Russia
Maria Tomas,
Complejo Hospitalario Universitario
A Coruña, Spain

*Correspondence:

Yi Shi
yishi750@163.com
Dong Chang
dongchang1969@163.com

[†] These authors have contributed
equally to this work

Specialty section:

This article was submitted to
Antimicrobials, Resistance
and Chemotherapy,
a section of the journal
Frontiers in Microbiology

Received: 22 September 2018

Accepted: 18 December 2018

Published: 09 January 2019

Citation:

Wu M, Hu K, Xie Y, Liu Y, Mu D,
Guo H, Zhang Z, Zhang Y, Chang D
and Shi Y (2019) A Novel Phage
PD-6A3, and Its Endolysin Ply6A3,
With Extended Lytic Activity Against
Acinetobacter baumannii.
Front. Microbiol. 9:3302.
doi: 10.3389/fmicb.2018.03302

With widespread abuse of antibiotics, bacterial resistance has increasingly become a serious threat. *Acinetobacter baumannii* has emerged as one of the most important hospital-acquired pathogens worldwide. Bacteriophages (also called “phages”) could be used as a potential alternative therapy to meet the challenges posed by such pathogens. Endolysins from phages have also been attracting increasing interest as potential antimicrobial agents. Here, we isolated 14 phages against *A. baumannii*, determined the lytic spectrum of each phage, and selected one with a relatively broad host range, named vB_AbaP_PD-6A3 (PD-6A3 for short), for its biological characteristics. We over-expressed and purified the endolysin (Ply6A3) from this phage and tested its biological characteristics. The PD-6A3 is a novel phage, which can kill 32.4% (179/552) of clinical multidrug resistant *A. baumannii* (MDRAB) isolates. Interestingly, *in vitro*, this endolysin could not only inhibit *A. baumannii*, but also that of other strains, such as *Escherichia coli* and methicillin-resistant *Staphylococcus aureus* (MRSA). We found that lethal *A. baumannii* sepsis mice could be effectively rescued *in vivo* by phage PD-6A3 and endolysin Ply6A3 intraperitoneal injection. These characteristics reveal the promising potential of phage PD-6A3 and endolysin Ply6A3 as attractive candidates for the control of *A. baumannii*-associated nosocomial infections.

Keywords: multidrug resistance *Acinetobacter baumannii*, endolysin, ESKAPE, sepsis, phage therapy, mice model

INTRODUCTION

Acinetobacter baumannii is a non-fermentative, Gram-negative bacillus that can be universally found in nature. It is a conditional pathogen that has been proven to be one of the major pathogens causing hospital-acquired infections, such as bacteremia, urinary tract infections, and ventilator-associated pneumonia (Doi et al., 2015).

An increasing number of *A. baumannii* strains have now been clinically proven to be multi-drug, and even pan-drug resistant (Lin, 2014; Shivaswamy et al., 2015; Khakhum et al., 2016). According to CHINET surveillance in China, *A. baumannii* accounts for 10.77% of all clinical isolates, and

is ranked the third most prevalent (Hu et al., 2016). The majority of these isolates are multidrug resistant *A. baumannii* (MDRAB), which is resistant to nearly all accessible antimicrobials. Therefore, the development of new tools to effectively manage *A. baumannii* infections is of great importance.

Bacteriophages (also called phages), as natural enemies of bacteria, exist abundantly in environments shared by their hosts. Phages were first discovered by Felix d'Hérelle in 1917 (Billiau, 2016; El-Shibiny and El-Sahhar, 2017). The lytic phages can specifically lyse pathogenic bacteria within their host range. In recent years, a huge importance has been given to the phage therapy and phage have been proposed as a valuable approach to control multiple pathogens (Melo et al., 2018).

In addition, phage endolysins, which phages use to digest the host bacterial cell wall to release progeny phages, have been suggested to be potent antibacterial agents in the treatment of Gram-positive pathogens both *in vitro* and in animal models (Yang et al., 2015; Zhang et al., 2016). However, the Gram-negative bacteria prevent the access of natural endolysins to peptidoglycan layer because of their outer membranes, thus making the exogenously added endolysins limited (Lim et al., 2014). Therefore, endolysins with strong lytic ability for the treatment of Gram-negative bacteria especially *A. baumannii* are urgently required.

We isolated and characterized a novel *A. baumannii* phage, PD6A3, and over-expressed its endolysin Ply6A3. Furthermore, the characteristics of the novel endolysin were evaluated. We then applied phage PD6A3 and endolysin Ply6A3 to the treatment of septic infections in mice. The present results support the potential use of phage PD6A3 and endolysin Ply6A3 as alternative antibacterial agents against drug-resistant *A. baumannii* infections.

MATERIALS AND METHODS

Bacterial Strains and Culture Conditions

The clinical bacterial strains, human cells, plasmids, and primers used in the present study are listed in Table 1. Altogether, 552 clinical MDRAB isolates (Supplementary Table 1), and *Pseudomonas aeruginosa*, *Escherichia coli*, *Klebsiella pneumoniae*, *Staphylococcus aureus*, and *Enterococcus faecium*, each comprising 40 isolates were collected between 2014 and 2017. These isolates were all collected from different patients at seven different hospitals in Shanghai, China and we have gotten written informed consents from these patients. Isolates were identified using the Vitek 2 compact system (Biomérieux, France). Antimicrobial susceptibility testing was performed using the broth microdilution method, recommended by the Clinical and Laboratory Standards Institute (CLSI, 2017). All isolates were identified by 16S rDNA sequencing analysis. The *E. coli* DH5 α and *E. coli* BL21 (DE3) cells were purchased from TransGen Biotech, China. The overnight bacterial culture was 1:100 inoculated to fresh Luria-Bertani (LB) broth and cells

were grown at 37°C with shaking at 220 rpm (Yang et al., 2015).

Phage Isolation and Lytic Spectrum of Single Phages and Phage Cocktail

In this study, 27 non-duplicate clinical strains of extensively drug-resistant (XDR) *A. baumannii* were used as indicators of phage isolation. All phages were isolated from sewage (Yele et al., 2012). The supernatant (20 mL) from the sewage was added to 10 mL 3 \times LB broth and 5 mL of mixed *A. baumannii*

TABLE 1 | Primers, phage, bacterial strains, and plasmids used in this study.

Name	Characteristics	Source
Forward primer	CGCTCGAGATGATTCT GACTAAGACGGATTAG	Sangon Biotech
Reverse primer	GCGAAGCTTCTATA AGTCCGCTAGAGCG	Sangon Biotech
pCold-SUMO	Expression vector (kanamycin resistant)	Our Laboratory Collection
pCold-SUMO-Ply6A3	Recombinant vector (kanamycin resistant)	This study
DH5 α <i>E. coli</i>	Amplification host for plasmid	Transgen Biotech
BL21(DE3) <i>E. coli</i>	Expression host for recombinant plasmid	Transgen Biotech
PD6A3	<i>A. baumannii</i> phage	Our Laboratory Collection
Ply6A3	The protein expressed by the endolysin gene	This study
AB1-AB200	MDR- <i>A. baumannii</i> , 200 clinical strains	Our Laboratory Collection
AB32	One of the host bacteria of Phage PD6A3	Our Laboratory Collection
AB01-AB040	PDR- <i>A. baumannii</i> , 40 clinical strains	Our Laboratory Collection
<i>Enterococcus faecium</i>	Vancomycin resistant, 40 clinical strains	Our Laboratory Collection
<i>Staphylococcus aureus</i>	Methicillin resistant, 40 clinical strains	Our Laboratory Collection
MRSA6	One of the host bacteria of Phage PD6A3	Our Laboratory Collection
<i>Klebsiella pneumoniae</i>	Extended spectrum β lactamases, 40 clinical strains	Our Laboratory Collection
<i>Pseudomonas aeruginosa</i>	Multi-drug Resistance, 40 clinical strains	Our Laboratory Collection
<i>Escherichia coli</i>	Extended spectrum β lactamases, 40 clinical strains	Our Laboratory Collection
HEK293T cells	Human renal epithelial cells	Our Laboratory Collection
THP-1 cells	Human mononuclear macrophage	Our Laboratory Collection

PD6A3, a novel *Acinetobacter baumannii* Phage. Ply6A3, the endolysin encoded by a novel *Acinetobacter baumannii* Phage PD6A3 gene. AB32, the No. 32 strains of multi-drug resistant *Acinetobacter baumannii*. MRSA6, the No. 6 strains of methicillin-resistant *Staphylococcus aureus*. HEK293T cells, human embryonic kidney cells 293. THP-1 cells, a human monocytic cell line derived from an acute monocytic leukemia patient.

culture, then incubated at 37°C and 100 rpm/min overnight. We used the double-layer agar method to incubate and purify the supernatants which including the phages. Each individual phage was purified using several consecutive rounds of plaque picking until single-plaque morphology was observed. Eventually, 14 virulent phages were obtained. To enrich the phages, each phage was mixed with its host cells by certain proportion then grown in LB soft agar overlays (0.75% agar) overnight. Then the lysate was collected in SM buffer, enriched at 4°C overnight using polyethylene glycol (PEG) 8000, further purified with CsCl density gradient ultracentrifugation and stored at 4°C (Hua et al., 2018).

Then, one drop of phage PD6A3 solution was added onto a copper mesh grid, after natural precipitation about 10 min, 50 µl 2% phosphotungstic acid was added to the grid. After drying, we used a Hitachi transmission electron microscope H-9500 (Japan) to examine the morphology of the phage (Huang et al., 2013).

Phage titers were assessed using double-layer agar method and represented by plaque-forming unit. The lytic spectrum of each phage was tested using the spot assay (Huang et al., 2013; Kitti et al., 2014). We also tested the lytic spectrum of a phage cocktail, which contained all 14 phages.

Biological Characterization and Lytic Effect of Phage PD-6A3

Thermal and pH stability tests were carried out using the double-layer technique (Capra et al., 2004). In the thermal stability tests, aliquots of phage PD6A3 preparations (10^9 CFU/ml) were treated at pH 7 and at different temperatures (4, 37, 40, 50, 60, and 70°C) in SM Buffer for 1 h. As for the pH stability experiments, phage preparations were treated with various pH buffers at (from pH 2 to pH 11) at 37°C in SM Buffer for 1 h and the phage titers were assessed. An adsorption experiment was performed according to Adams (Adams, 1959). Briefly, exponentially grown AB32 (a clinical pan-drug resistant *A. baumannii*) were infected with the phage at the MOI of 0.1. Aliquots of 1 ml were taken every minute (from 1 to 10 min) and then the supernatant containing the non-adsorbed phages were titrated using the double-layer method. A one-step growth experiment was determined using the method described by Pajunen et al. (2000). The AB32 was infected by Phage PD6A3 at a MOI of 0.01 and adsorbed for 5 min. During the incubation, samples were taken periodically (10-min intervals, over a period of 50 min) and immediately assayed for plaque titer. In the assay of phage infection curve, AB32 were mixed with the phage PD6A3 at different MOIs (from 0.00001 to 1) at 37°C. The control experiments were performed using equal volume of SM buffer. The OD600 values were measured at 30-min intervals until 7 h post-infection.

Extraction, Sequencing, and Bioinformatics of Phage Genomic DNA

The phage PD6A3 was purified by CsCl gradient ultracentrifugation method as described before. Genome sequence of the phage was obtained using the Illumina HiSeq 3000 Sequencing platform (Illumina, San Diego, CA,

United States) and the SOAPdenovo2 software for sequence assembly. Prediction and annotation between genes from phage PD6A3 and other phages were performed using GeneMarkS and Blast¹ (Jin et al., 2012). Functional annotation of ORFs and homology assignments between genes from phage PD6A3 and other phages were performed by the BLASTp¹. Expasy compute PI/MV tool² was used to determine isoelectric pH and molecular weight of the predicted ORFs. The Easyfig software was used to conducted the alignment of functional proteins of phage PD6A3 (Hua et al., 2018). An alignment of amino acid sequences between endolysin Ply6A3 and other endolysin gene was created using the Clustal X2 program (Kong and Ryu, 2015). The whole genome of phage PD6A3 was deposited at GenBank under accession number KY388102.1.

Identification and Cloning of the Putative Endolysin From Phage PD-6A3

Gene prediction was performed as described above. The phage PD-6A3 endolysin encoding gene was amplified with P1 and P2 primers (Table 1) and PrimeSTAR HS DNA polymerase kits (TaKaRa, China). The PCR products were purified using a Rapid Mini Plasmid Kit (TIANGEN, China). Furthermore, PCR products were resolved in a 1% agarose gel before purified. The gene was then linked to an expression vector named pCold-SUMO, which comprised a 6× His tag and SUMO tag (Guo et al., 2016). The recombinant vector was transformed into *E. coli* DH5α cells. After confirmation by restriction enzyme digestion and sequence analysis, the correct plasmids were transformed into the BL21(DE3) cells for over-expression.

Over-Expression and Purification of Endolysin Ply6A3

The BL21(DE3) cells were grown in LB medium containing kanamycin (50 µg/mL, Sangon Biotech, China) at 37°C overnight, diluted 1:100 in 0.5 L LB medium, then incubated until the OD 600 reached 0.6~0.8. Isopropyl β-D-thiogalactoside (IPTG) (TIANGEN, China) was added until the final concentration was 1 mM, then the mixture was incubated at 16°C for 18 h at 120 rpm. The following procedures were all performed in an ice-cold water bath (Diez-Martinez et al., 2015). The precipitate was resuspended in 25 mL PBS buffer (pH 7.4). The cell lysate was disrupted by sonication (Cole-Parmer, Ultrasonic Processors) (10 s pulse, 20 s rest over 30 min) before centrifuged at $12,000 \times g$ 4°C (Lai et al., 2011). The His-SUMO-Ply6A3 was purified using a Ni-nitrilotriacetic acid column (Novagen, United States), and equilibrated with a binding buffer (20 mM Tris-HCl, 300 mM NaCl, 10 mM imidazole; pH 8.0) at room temperature. The supernatant was filtered using a 0.22-mm membrane, after it was passed through the column at least three times. The His-SUMO- ply6A3 in the supernatant was washed with binding buffer (20 mM

¹<http://blast.ncbi.nlm.nih.gov/Blast.cgi>

²https://web.expasy.org/compute_pi/

Tris-HCl, 300 mM NaCl, 10 mM imidazole; pH 8.0) three times, and the same washing buffer was then eluted with elution buffer (20 mM Tris-HCl, 300 mM NaCl, 50 mM imidazole; pH 8.0). All samples were stored for SDS-PAGE and western blot analyses.

Cleavage of the SUMO Tag and Protein Concentration

The reaction assay was performed in a dialysis bag in a 4°C-refrigerator overnight. The SUMO protease and purified His-SUMO-ply6A3 were placed in dialysis at a ratio of 50:1 (vol/vol). The His-SUMO protein was cleaved with continuous stirring overnight, and the dialysis bag was placed in PBS buffer (pH 7.0) (Guo et al., 2016). The enzyme digested product was then purified using an affinity chromatography column (Novagen, United States). The protein solution was collected into a protein concentration tube with a molecular diameter of 10 kD (Amicon Ultra), and centrifuged at $4,000 \times g$ at 4°C for 30 min. The concentration of the purified protein was then measured using a Micro BCATM protein assay kit (Tiangen, China).

SDS-PAGE and Western Blot Analysis

The samples collected during expression, purification, and cleavage were subjected to 12% SDS-PAGE, and then transferred to polyvinylidene fluoride (PVDF) membranes (Kong and Ryu, 2015). The PVDF membranes were blocked with 5% bovine serum albumin in phosphate buffered saline with Tween 20 (PBST) for 3 h and then incubated with anti-His antibody (1:3000) (Sangon Biotech, China) overnight, followed by peroxidase-affiniPure goat anti-mouse IgG (1:10000) (Sangon Biotech, China) for 1 h.

Detection of Peptidoglycan Degradation by PlyAB3 Using the Diffusion Method

According to the enrichment technique recommended by Sun et al. (2005). The AB32 was incubated in 0.5 L LB medium at 37°C for 24 h then harvested by centrifugation, before washed several times with ddH₂O. Then placed in a boiling water bath for 45 min and broken by sonication. Next, centrifuged at 1000 r/min for 10 min, the supernatant was decanted. Centrifuged the supernatant again, the precipitate was incubated in 4% SDS before washed with ddH₂O and dehydrated alcohol, digested with 0.02% trypsin in PBS (pH 7.5) for 24 h. The walls were resuspended in 10% trichloroacetic acid at 70°C for 30 min. Then harvested by centrifugation and washed by ddH₂O, the peptidoglycan was then mixed in proportion (0.5%) with 15% SDS-polyacrylamide gel. After solidification, the gel was perforated with a sterilizing puncher. A volume of 20 µL endolysin Ply6A3 (2 mg/mL) was added to the hole formed. The negative control was PBS, and the positive control was lysozyme (2 mg/mL). The mixtures were sealed in a wet box and cultured at 37°C overnight, following which the samples were dyed with methylene blue stain for 2 h, and

bleached to transparent strips with ddH₂O (Blázquez et al., 2016).

Cytotoxicity of Phage PD-6A3 and Endolysin Ply6A3 to HEK293T and THP-1 Cells

The human embryonic kidney cells 293 (HEK293T) and a human monocytic cell THP-1 cells were both supplemented with fetal bovine serum (10%) and incubated in 5% CO₂ at 37°C (Shen et al., 2018). Cells were seeded into 96-well plates (10⁴ cells/well), then incubated for 24 h. They were then incubated with different concentrations of phage PD-6A3 or endolysin Ply6A3 for an additional 8 and 24 h (Yin et al., 2018). Cell viability was measured using the Cell Counting Kit-8 (CCK-8; Dojindo, Kumamoto, Japan) and absorbance was measured at 450 nm.

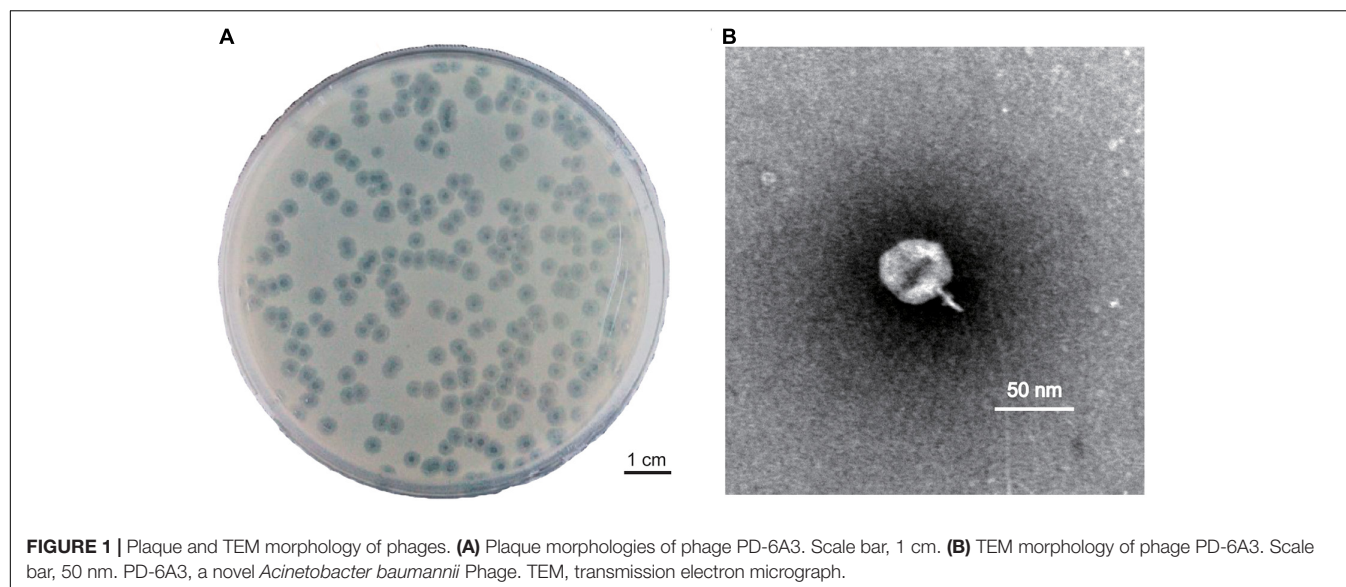
Biological Characterization and Enzyme Activity of Endolysin Ply6A3

To test the thermal and pH stability of endolysin Ply6A3, host bacteria Ab32, which grew to log phase, was repeatedly suspended three times with PBS. A volume of 100 µL endolysin (1 mg/mL, dissolved in PBS) was combined with 100 µL Ab32 (1 × 10⁹ cfu/mL), and added to a 96-well plate incubated at temperatures of 22, 27, 32, 37, and 42°C, at pH 7 for 0.5 h. For the pH assay, the mixture was incubated at pH 5.5, 6.0, 6.5, 7.0, 7.5, 8.0, and 8.5, at 37°C for 0.5 h (Kong and Ryu, 2015). A mixture of bacteria and PBS was used as the blank control group. Absorbance was measured before and after incubation. Based on the two readings, the percentage drop in bacterial turbidity was calculated.

The enzyme activity unit was defined as the reciprocal of the dilution at 37°C, after 30 min, which could have reduced the turbidity of the bacterium by 50%. The Ab32 was removed the bacterial outer membrane by 10% trichloromethane. The OD₆₀₀ of Ab32 which suspended in PBS was 1. The enzyme activity unit was determined by turbidimetric regression. The bacterial suspension was added to the 96-well plate, 100 µL per well. A volume of 100 µL of a double dilution of endolysin Ply6A3, with an initial concentration of 3.9 mg/mL, was added to each well. Absorbance was measured at 600 nm before and after incubation. Based on the two readings, the percentage drop in bacterial turbidity was calculated (Oliveira et al., 2016).

Lytic Spectrum of Endolysin Ply6A3 Against Clinical ESKAPE Isolates

The acronym ESKAPE stands for bacterial pathogens and include *E. faecium*, *S. aureus*, *K. pneumoniae*, *A. baumannii*, *P. aeruginosa*, and *Enterobacter*. The lytic spectrum of endolysin Ply6A3 against the 440 clinical isolates were determined by the plate method (Zhang et al., 2016). The clinical strains were suspended in 300 µL PBS (pH 7.4), to yield a final concentration of 1 × 10⁹ cfu/mL. The cells were plated with 4 mL agar (Lood et al., 2015). After solidification, the gel was perforate with a sterilizing puncher. A volume of 20 µL endolysin



Ply6A3 (1 mg/mL) was added into a hole. The phage PD-6A3 (1×10^8 PFU/mL), cocktail (1×10^8 PFU/mL) which contain the 14 phages and the PBS were added into three other holes as comparison. The mixtures were cultured at 37°C overnight.

Phage Therapy in the Mouse Sepsis Model

We investigated the ability of the phage PD6A3, phage cocktail (contain all the 14 phages) and endolysin Ply6A3, after removed endotoxin by the EndotoxinOUT kit (G-bioscience, United States), to work systemically to rescue sepsis in mice. Briefly, 80 6~8 weeks-old female BALB/c mice (Shanghai Laboratory Animal Company, China) were randomly assigned to eight groups ($n = 10$ per group) (Jun et al., 2014). The first three groups were inoculated intraperitoneally with 1 mL 1×10^9 CFU/mL of AB32 (minimum lethal dose, **Supplementary Figure 2**) and intraperitoneal administration with either 1 mL of endolysin Ply6A3 at 2 mg/mL (10 mice), 1 mL of phage PD6A3 (10^9 PFU/mL), or 1 mL of PBS (10 mice), 1 h later. The remaining five groups were only inoculated intraperitoneally with 1 mL PBS, 1 mL of endolysin Ply6A3 at 2 mg/mL, 1 mL of phage PD6A3 (10^9 PFU/mL), 1 mL of phage Cocktail (10^9 PFU/mL) or 1 mL of the mixture [0.5 mL of endolysin Ply6A3 at 2 mg/mL + 0.5 mL of phage PD6A3 (10^9 PFU/mL)] respectively. The animals were monitored for 7 days and the survival rate of each group was calculated. The white blood cell (WBC) count, levels of IL-10 (interleukin-10) and PCT (procalcitonin) were evaluated to assess the immune status (Henein et al., 2016). At 2 days post-infection, three mice were selected from each group and subjected to 0.1 mL pentobarbital sodium (10 g/mL) anesthesia by intraperitoneal injection. Blood was collected from each anesthetized mouse then was sent to the clinical laboratory for examination of the WBC. The serum for

measurement of IL-10 and PCT (Entenza et al., 2005) were used DuoSet enzyme-linked immunosorbent assay kits (R&D Systems). All the mice were sacrificed by cervical dislocation after experiment.

Statistical Analysis

Statistical calculations for mice survival rate were performed by Kaplan–Meier survival analysis with log-rank test (GraphPad Prism 7.0 software), and the comparison of cytokine levels between groups were analyzed statistically by Student's *t*-test (SPSS Statistics 21.0 software). *P*-values < 0.05 were considered statistically significant.

Ethics Statement

This study was carried out in accordance with the recommendations of “Animal experiment guidelines, the Animal Care Committee of Fudan University.” The protocol

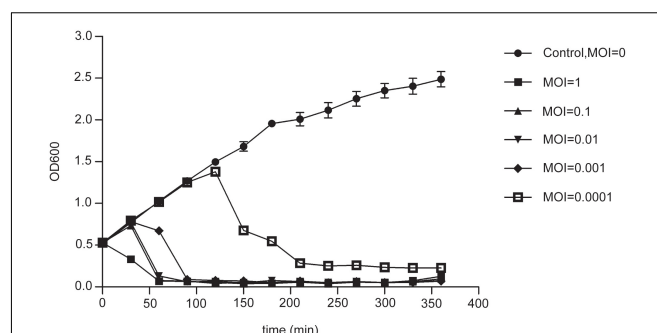


FIGURE 2 | The infection assay of phage PD-6A3 against *A. baumannii* *in vitro*. AB32 was infected by phage PD6A3 at MOI of 0, 1, 0.1, 0.01, 0.001 or 0.0001 and cultured for 7 h. The control experiments were performed using equal volume of SM buffer. This experiment was repeated three times, and the data were shown in the mean \pm SD. PD-6A3, a novel *Acinetobacter baumannii* Phage.

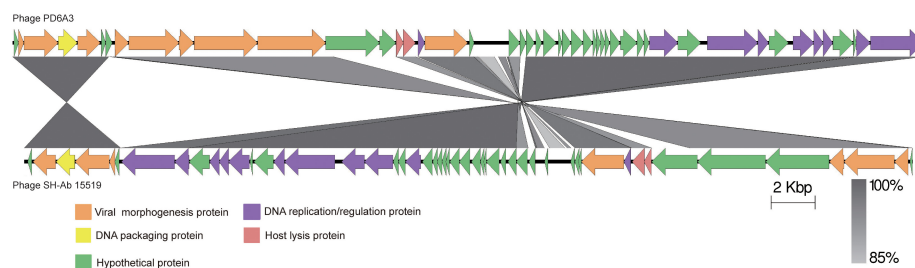


FIGURE 3 | The comparison of the complete genome sequence of the Phage PD6A3 using Easy fig against the closet homolog phage SH-AB15519. The colored arrows indicate ORFs according to their predicted function. The homologous regions between phages are indicated by gray shading.

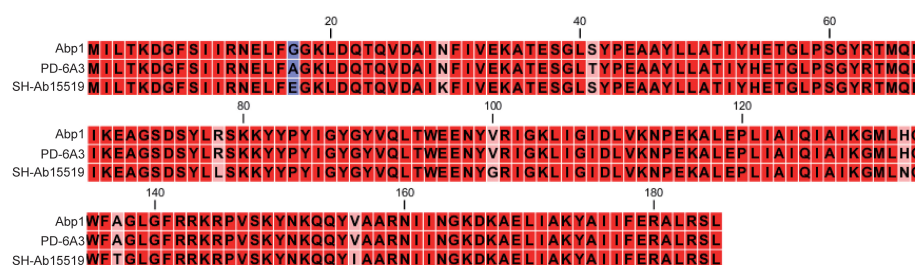


FIGURE 4 | Amino acid sequence alignment of the endolysin of Phage PD6A3. The sequences used for alignment analysis were the endolysin gene of Phage 6A3, Phage SH-Ab15519 and Phage Abp1. Eight mutation residues are indicated by different color.

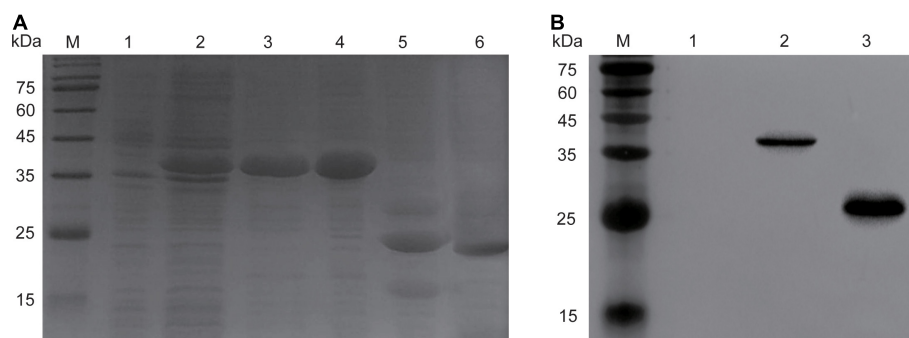


FIGURE 5 | Over expression and purification of endolysin Ply6A3. **(A)** Lane M, molecular weight marker; Lane 1, un-induced bacterial lysate; Lane 2, IPTG-induced bacterial lysate; Lane 3, purified His-SUMO-Ply6A3 protein; Lane 4, dialyzed His-SUMO-Ply6A3 protein; Lane 5, Ply6A3 protein after cleavage of the His-SUMO tag; Lane 6, purified endolysin Ply6A3 protein after cleavage and dialyze of the His-SUMO tag. **(B)** Lane M, molecular weight marker; Lane 1 un-induced bacterial lysate; Lane 2-4, IPTG-induced bacterial lysate; Lane 5, the His-SUMO tag cleaved from endolysin Ply6A3. Ply6A3, the endolysin encoded by a novel *Acinetobacter baumannii* Phage PD6A3 gene. IPTG, Isopropyl β -D-Thiogalactoside.

was approved by the 'the Animal Care Committee of Fudan University.'

RESULTS

Isolation and Lytic Spectrum of *A. baumannii* Phages

About 40 different virulent phages were isolated, and 14 of those were additionally tested host spectra. The 14 phages were designated as PD-Ab1, PD-Ab8, PD-Ab9, PD-Ab11, PD-Ab 15,

PD-Ab16, PD-Ab17, PD-Ab18, PD-6A1, PD-6A2, PD-6A3, PD-6A4, PD-7A1, and PD-7Ab3 (**Supplementary Table 2**). The results showed that all the phages have completely different lytic spectrum. Compared with the other 13 phages, phage PD-6A3 had a broader host range 32.4% (179/552) of the isolates. The cocktail which contains all the 14 phages was capable of lysing 54.0% (298/552) of the isolates. Thus, we chose phage PD-6A3 for further study.

Phage PD-6A3 formed clear, round, significant halos, 2–3 mm in diameter (**Figure 1A**). TEM showed that phage PD-6A3 possessed an isometric head (50 ± 10 nm in diameter) and a very short tail (9 ± 2 nm in length), which was nearly invisible

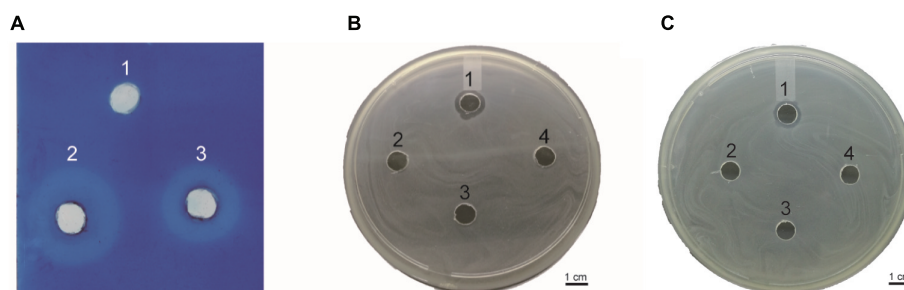


FIGURE 6 | (A) Detection of peptidoglycan degradation by endolysin Ply6A3 by diffusion method. Hole 1: 20 μ l PBS, Hole 2: 20 μ l Lysozyme (2 mg/ml), Hole 3: 20 μ l endolysin (2 mg/ml). **(B)** Lytic activity of endolysin against clinical AB32 isolates. **(C)** Lytic activity of endolysin Ply6A3 against clinical MRSA6 isolates. Hole 1: 20 μ l endolysin (2 mg/ml), Hole 2: 20 μ l Phage PD6A3 (10^8 cuf/ml), Hole 3: 20 μ l Phage Cocktail (10^8 cuf/ml) Hole 4: 20 μ l PBS. Scale bar, 1 cm. CFU, colony-forming units. PD6A3, a novel *Acinetobacter baumannii* Phage. Ply6A3, the endolysin encoded by a novel *Acinetobacter baumannii* Phage PD6A3 gene. AB32, the No. 32 strains of Multidrug Resistance *Acinetobacter baumannii*. MRSA6, the No. 6 strains of methicillin-resistant *Staphylococcus aureus*.

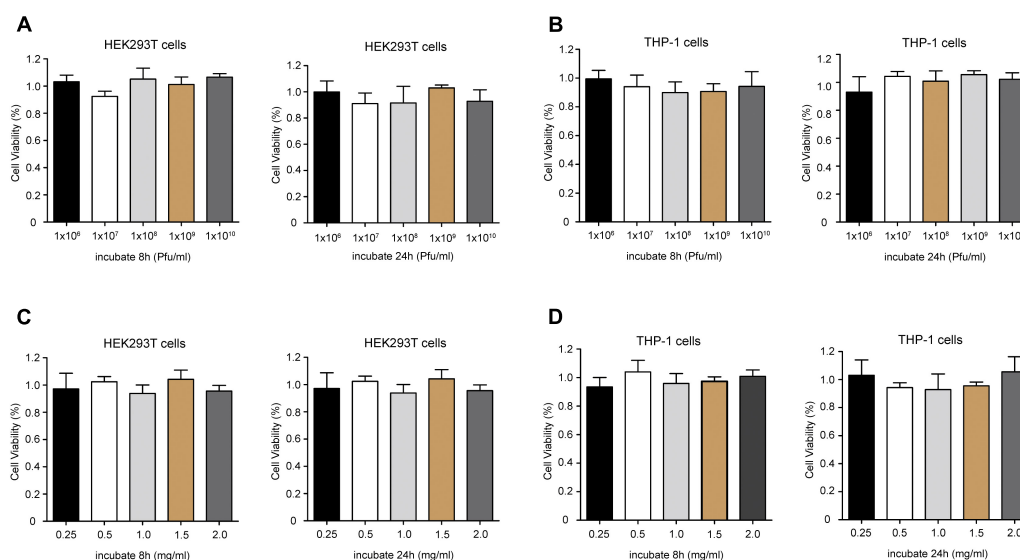


FIGURE 7 | Cell viability of HEK293T and THP-1 cells after incubation with different concentrations of Phage PD6A3 (A,B) and endolysin Ply6A3 (C,D). Cells were incubated with different concentrations of phage PD-6A3 (10^6 – 10^{10} PFU/mL) and endolysin Ply6A3 (0.25–2 mg/mL) for 8 h then followed by fresh complete media for 16 h. Or only incubated with different concentrations of phage PD-6A3 (10^6 – 10^{10} PFU/mL) and endolysin Ply6A3 (0.25–2 mg/mL) for 24 h. Cell viability was measured using the CCK-8. Data are mean \pm SD ($n = 6$). All the result shows that cell lines remained highly viable after incubation with endolysin Ply6A3. Ply6A3, the endolysin encoded by a novel *Acinetobacter baumannii* Phage PD6A3 gene. HEK293T cells, human embryonic kidney cells 293. THP-1 cells, a human monocytic cell line derived from an acute monocytic leukemia patient. CCK-8, Cell Counting Kit-8.

(Figure 1B). The phage was assigned to the order Caudovirales and family Podoviridae.

Biological Characterization and Lytic Effect of Phage PD-6A3

The stability of phage PD-6A3 was investigated at different temperatures and pH conditions. No significant loss in phage activity was observed after heating to temperatures between 4 and 50°C. In addition, it remained relatively stable after incubation at pH levels ranging from 5 to 10 (Supplementary Figures 1A,B). The adsorption experiment showed that more than 90% of the phage particles were adsorbed within 5 min incubation (Supplementary Figure 1C).

One-step growth experiments showed that the latent and eclipse periods were both 20 min and the burst size was 129 PFU per infected cell (Supplementary Figure 1D). The infection assay of phage PD-6A3 against AB32 was evaluated *in vitro*. The results showed that phage PD-6A3 could effectively reduce growth of the host bacteria, with OD values declining more quickly at MOI 1 than at MOI 0.1, 0.01, or 0.001 (Figure 2).

Sequencing and Bioinformatics Analysis of Phage PD-6A3 Genomic DNA

The phage PD-6A3 is a linear double-stranded DNA with a length of 41,563 bp and GC content of 39.48% (GenBank accession

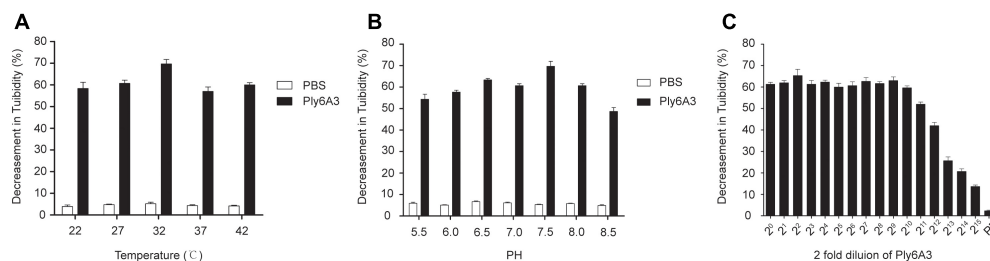


FIGURE 8 | (A) The thermal stability of endolysin Ply6A3. Endolysin was incubated at various temperatures for 30 min. **(B)** The pH stability of endolysin Ply6A3. Endolysin was incubated at the indicated pH conditions for 30 min. **(C)** Activity unit of endolysin Ply6A3. The initial concentration was 3.9 mg/mL, then double dilution. Data were obtained from three independent experiments and are shown as mean \pm SD. Ply6A3, the endolysin encoded by a novel *Acinetobacter baumannii* Phage PD6A3 gene. pH, hydrogen ion concentration. AB32, the No. 32 strains of Multidrug Resistance *Acinetobacter baumannii*.

No. KT388102.1). A total of 48 putative genes were identified by GeneMarks, on the positive strand (**Supplementary Table 3**). The average length of a gene was 776 bp. Genome analysis also reviewed that this phage carried no virulence and antibiotic resistance genes which assure its safety to be applied for phage therapy in the future.

The proteins encoded by phage PD-6A3 could be divided into five categories morphogenesis, DNA packing protein, host lysis, DNA replication/regulation, and hypothetical proteins (**Figure 3**). According to the NCBI database, phage PD-6A3 has similarities with *Acinetobacter* phage SH-Ab15519 (GenBank accession number: KY082667.1; 99% identity, 93% coverage). The relatedness of these two phages was also determined using the Easy fig software show that phage PD-6A3 shares only 22 completely identical proteins with *Acinetobacter* phage SH-Ab15519, which is relatively limited (**Figure 3**). These all showed that Phage PD6A3 is a novel phiKMV-like phage.

The endolysin gene of the phage PD6A3 is 558 bp and contains 185 amino acid residues (22.4 kDa protein), which belongs to glycoside hydrolase family 19. Conserved domain analysis has revealed the presence of a lysozyme-like (*N*-acetyl-*b*-D-muramidase) catalytic domain between residues 75 and 128. A ClustalX2 alignment of endolysin Ply6A3 with two phage endolysins showed similarity in the domain region, however, 8 amino acid mutations were found (**Figure 4**).

Cloning, Expression, Purification, and Assembly of Endolysin Ply6A3

The molecular weight of recombinant endolysin Ply6A3 is approximately 40 kDa (**Figure 5A**). A specific band (His-SUMO tag) of approximately 23 kDa was identified using specific His-tag antibodies (**Figure 5B**). The concentration of purified endolysin reached about 3.9 mg/mL.

Detection of Peptidoglycan Degradation by Endolysin PlyAB3 Using the Diffusion Method

This assay was performed to determine whether the endolysin Ply6A3 indeed with lytic activities toward cell walls (Lai et al., 2013). According to the principle of methylene blue staining, peptidoglycan stains blue (**Figure 6A**). Endolysin Ply6A3

(2 mg/mL) and lysozyme (2 mg/mL) can degrade peptidoglycan to form a transparent ring; whereas the negative control, PBS, showed no degradation and formed no transparent rings.

Cytotoxicity of Phage PD6A3 and Endolysin Ply6A3 to HEK293T and THP-1 Cells

The potential cytotoxicity of phage PD6A3 were evaluated using the HEK293T and THP-1 cells by the CCK-8 assay. The results showed that the percentage of viable HEK293T cells were around 100%, treated with Phage PD6A3 in 8 h and 24 h. We changed the cells to THP-1, and the result is the same (**Figures 7A,B**). And no significant cytotoxicity was observed in either HEK293T or THP-1 cells, treated with endolysin Ply6A3 (**Figures 7C,D**) (Shen et al., 2018; Yin et al., 2018).

Biological Characterization and Lytic Effect of Endolysin Ply6A3

The temperature and pH stability test revealed that endolysin Ply6A3 remained high activity at temperature between 22 and 42°C and at pH range from 5.5 to 8.5; however, its activity was significantly reduced at pH levels above 7.5 (**Figures 8A,B**). The broad range of thermal and pH stability facilitates the application of endolysin in phage therapy.

The lytic effect shown that, when the original concentration of endolysin Ply6A3 was 3.9 mg/mL, its dilution ratio

TABLE 2 | Lysis spectrum of endolysin Ply-6A3.

Bacteria	Positive	Total	Positive rate (%)
<i>Enterococcus faecium</i>	5	40	12.5
<i>Staphylococcus aureus</i>	9	40	22.5
<i>Klebsiella pneumonia</i>	3	40	7.5
<i>Pseudomonas aeruginosa</i>	0	40	0
<i>Escherichia coli</i>	8	40	20.0
MDR-A. <i>baumannii</i>	141	200	70.5
PDR-A. <i>baumannii</i>	21	40	52.5

MDR-A. *baumannii*, multi-drug resistant *Acinetobacter baumannii*. PDR-A. *baumannii*, pan-drug resistant *Acinetobacter baumannii*.

TABLE 3 | Lysis spectrum of endolysin Ply-6A3 and Phage PD6A3 toward 200 MDR-AB strains.

	Positive	Total	Positive rate (%)
Ply6A3	141	200	70.5
Phage PD6A3	58	200	29.0
Cocktail	90	200	45.0

PD6A3, a novel *Acinetobacter baumannii* Phage. Ply6A3, the endolysin encoded by a novel *Acinetobacter baumannii* Phage PD6A3 gene. Cocktail, the cocktail which contain all the 14 phages mentioned in this article.

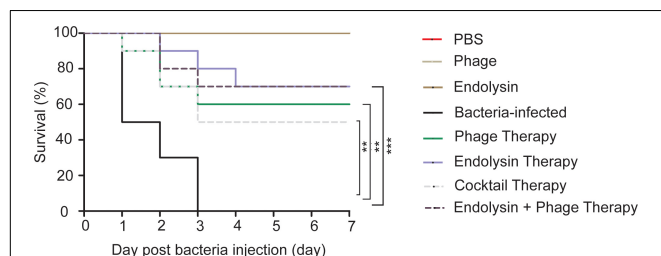


FIGURE 9 | Therapeutic efficacy of Phage PD6A3 and endolysin Ply6A3 against mice *A. baumannii* sepsis infections. Survival of mice that were sepsis infected with AB32 and then treated with endolysin Ply6A3, phage PD6A3; or only intraperitoneal injected with PBS, Phage, endolysin. Using log-rank (Mantel-Cox) test. Each group harbors 10 mice. $**P < 0.01$, $***P < 0.001$ compared with the Bacteria group. PD6A3, a novel *Acinetobacter baumannii* Phage. Ply6A3, the endolysin encoded by a novel *Acinetobacter baumannii* Phage PD6A3 gene. AB32, the No. 32 strains of Multidrug Resistance *Acinetobacter baumannii*.

was $1:2^{11}$, and the turbidity of AB32 could have been reduced by nearly 50% (Figure 8C). The results showed that the activity unit of endolysin Ply6A3 was 2048 unit/mL or 525 unit/mg. The amount of endolysin protein contained in each active unit was 1.9 μ g. After fitting to a function curve, the IC₅₀ of endolysin was calculated to be 1.6 μ g.

Lytic Spectrum of Endolysin Ply6A3

Lytic spectrum was determined by spot test, the results show that 141 of the 200 MDRAB strains could have been lysed by endolysin Ply6A3 (Table 2). Moreover,

21 of the 40 PDR-AB strains could have been lysed. In addition, the protein also showed lytic activity for other septic bacterial strains as follows: *E. faecium*, *S. aureus*, *K. pneumonia*, and *E. coli* strains. The lytic spectrum of endolysin Ply6A3 is broader than that of phage PD6A3 and phage Cocktail which contain 14 phages (Table 3). None of the 40 *P. aeruginosa* strains could have been lysed. Only one hole (added endolysin Ply6A3) formed a bright, clear inhibition zone (Figures 6B,C).

Phage Therapy in the Mouse Sepsis Model

To ascertain the effect of phage and endolysin against the sepsis mouse model, mouse was developed by intraperitoneal administration of *A. baumannii*. The survival rate of endolysin therapy group, endolysin + phage therapy group, phage therapy group and phage cocktail therapy group were 70, 70, 60, and 50%, respectively, higher than the bacterial group (Figure 9). Mice in the endolysin therapy group had milder clinical signs (slow reactions, lethargy, and activity reduction) than the mice in other three therapy groups. Furthermore, all mice in the negative control group (injected with PBS, phage or endolysin respectively) remained alive after 7 days.

On the second day of the experiment, WBC counts in all the 4 therapy groups were significantly lower than those in the sepsis control group ($P < 0.05$). Furthermore, WBC counts in the endolysin therapy group and endolysin + phage therapy group were significantly lower than those in the phage therapy group and phage cocktail group ($P < 0.05$). The levels of IL-10 and PCT were significantly elevated in sepsis group, while all the 4 therapy groups effectively reduced the level. The expression of WBC, IL-10 and PCT remained at basal levels in the mice from control, phage group and endolysin group (Figure 10).

DISCUSSION

Acinetobacter baumannii is an important nosocomial pathogen worldwide. This bacterium can be easily spread throughout

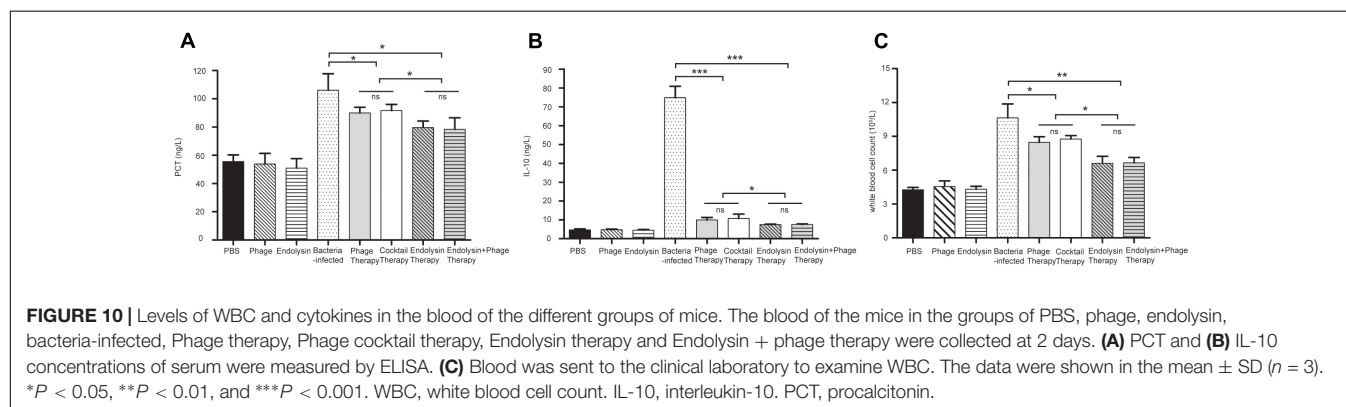


FIGURE 10 | Levels of WBC and cytokines in the blood of the different groups of mice. The blood of the mice in the groups of PBS, phage, endolysin, bacteria-infected, Phage therapy, Phage cocktail therapy, Endolysin therapy and Endolysin + phage therapy were collected at 2 days. (A) PCT and (B) IL-10 concentrations of serum were measured by ELISA. (C) Blood was sent to the clinical laboratory to examine WBC. The data were shown in the mean \pm SD ($n = 3$). $*P < 0.05$, $**P < 0.01$, and $***P < 0.001$. WBC, white blood cell count. IL-10, interleukin-10. PCT, procalcitonin.

healthcare facilities (Kusradze et al., 2016). The treatment of *A. baumannii* infection becomes increasingly difficult because of its resistance to many antimicrobial agents. Moreover, phages and their endolysins have drawn the attention of researchers to explore their potential as antimicrobial agents, because of the low probability of developing resistance, effectiveness against bacteria both *in vitro* and *vivo*, and ease of access (Oliveira et al., 2016).

The use of phages in animals has been reported in various applications, such as in the treatment of lung infections and skin wounds, and the results of such therapy have been significant (Lood et al., 2015; Shivaswamy et al., 2015; Henein et al., 2016). Hua and colleagues used an *A. baumannii* phage to rescue carbapenem-resistant *A. baumannii* (CRAB) lung infections (Hua et al., 2018). The use of endolysin treatments in animals is less common than that of phages. Zhang et al. (2016) proved the safety and efficacy of *Streptococcus suis* phage endolysin against *Streptococcus suis* infection in mice (Zhang et al., 2016). These experiments demonstrate that the phage and its endolysin could provide a promising future in the quest for treatments against bacterial infections. However, these studies have some limitations as follows: only a few resistant strains were used to test the lytic spectrum; all strains were collected from one hospital; the lack of a specific, effective concentration of the endolysin; and the lack of quantitative analysis with reliance on qualitative analysis. These limitations all render the reported lytic rates less convincing (Huang et al., 2014; Defraigne et al., 2016; Larpin et al., 2018).

We isolated 40 *A. baumannii* phages, among which phage PD-6A3 had a relatively broad host range of 32.4% (179/552) among clinical MDR *A. baumannii* isolates, and was selected for further study. Phage PD-6A3 showed outstanding characteristics compared to the other phages such as remained stable over a wide range of temperatures and pH conditions. Genome analysis also reviewed that this phage carried no virulence and antibiotic resistance genes. Considering these advantages, phage PD-6A3 proves to be promising for potential applications in *A. baumannii* infections.

We over-expressed and purified the endolysin. The final concentration of endolysin Ply6A3 was 3.9 mg/mL. Previous studies have rarely included quantitative descriptions. The endolysin remained stable over a wide range of temperatures and pH conditions. Our results demonstrate that as a murein hydrolase, endolysin Ply6A3 was able to degrade 141/200 clinical MDRAB isolates and 21/40 PDR-AB isolates. In addition, it was also able to degrade Enterococci, MRSA, *K. pneumoniae*, MDR- *P. aeruginosa*, and ESBL-*E. coli*, but Phage PD6A3 could not lyse any of them. Interestingly, we also over-expressed the endolysin of Phage Ab9 (GenBank accession number KY388103.), but it only could degrade 18/200 clinical MDRAB isolates which was very narrow compared to endolysin Ply6A3. In our future study, we will analysis this phenomenon in depth. Compared with previous articles, our research group tested the greatest number of bacterial strains, including *A. baumannii* and

other common pathogens (Lai et al., 2013). Interestingly, when endolysin Ply6A3, phage PD6A3 and phage cocktail acted on 200 MDRAB strains, the lytic spectrum of the endolysin was much broader than the other groups. This might be attributed to different features of the outer membrane structure, like a different composition in the lipopolysaccharides, which may prevent or facilitate the access to exogenous lysins (Huang et al., 2014). We are further studying this phenomenon.

We extracted the cell wall of *A. baumannii* (Endersen et al., 2015). The results demonstrated that the peptidoglycan can be degraded by endolysin Ply6A3 and lysozyme. However, only endolysin could lyse *A. baumannii* strains, whereas lysozyme could not. These findings indicate that endolysin Ply6A3 is exceptional in its ability to directly destroy the cell wall of Gram-positive bacteria. These findings are also consistent with previous reports of the ability of endolysins from Gram-negative phages to lyse bacterial cells through enzymatic activity.

Our research also indicated the safety of phage PD6A3 and endolysin Ply6A3 applied intraperitoneal injection for mice. No obvious side effect was observed after injection during the observation period. And no statistical significance was observed when compared cytokine levels in serum, WBC in blood of the phage group and endolysin group to the PBS group, which provided a further safety evidence for the phage therapy and endolysin therapy by intraperitoneal injection. If in combination, phage PD-6A3 and endolysin Ply6A3 had more activity than the cocktail of 14 phages.

Compared to the sepsis group, all the therapy groups showed significantly higher survival rates and with evident reductions in the WBC count, serum PCT, and serum IL-10. However, the difference in survival between the 4 therapy groups were not statistically significant ($P > 0.05$). This might because the relatively small sample size could have affected the accuracy of statistical analysis. On the second day of the experiment showed that the WBC count, serum IL-10 and PCT of the endolysin therapy group and endolysin + phage therapy group were lower than that of the phage therapy group and cocktail therapy group ($P < 0.05$), which implies that endolysins work faster than phages. However, these are just experimental proofs that not very close to clinical situation (such short an interval time in clinical practice is unlikely). And the outcome of endolysin Ply6A3, as a class of enzymes, after entering the body is not clear. These conclusions need to be verified through further studies especially supported by clinical trials (Takemura-Uchiyama et al., 2014; Regeimbal et al., 2016).

Taken together, phage PD-6A3 is a novel phiKMV-like phage with strong lytic activity. Its endolysin Ply6A3 is an effective antibiotic against Gram-negative and Gram-positive bacteria. In addition, we evaluated the safety, effectiveness, and routes of administration for phage PD6A3 and its endolysin Ply6A3, in the treatment of *A. baumannii* infections, both *in vivo* and *in vitro*.

Both agents have potentially therapeutic against infections caused by MDRAB strains in the future.

AUTHOR CONTRIBUTIONS

YS and DC designed and supervised the study. MW, YL, DM, HG, and ZZ performed the experiments, analyzed the data, and drafted the manuscript. KH and YZ performed the experiments and analyzed the data. YX provided advice and suggestions.

FUNDING

This study was funded by construction of important weak subjects of Shanghai Pudong New Area (Grant No. PWZbr2017-02) and supported by Shanghai Municipal Commission of

Health and Family Planning research project (Grant No. 201840261).

ACKNOWLEDGMENTS

The authors thank Yinxin Shen, Lijun Ming, and Shuai Tao for their efforts in support of this work and Yanfeng Liu for helpful discussions.

SUPPLEMENTARY MATERIAL

The Supplementary Material for this article can be found online at: <https://www.frontiersin.org/articles/10.3389/fmicb.2018.03302/full#supplementary-material>

REFERENCES

- Adams, M. H. (1959). *Bacteriophages*. New York, NY: Interscience Publishers.
- Billiau, A. (2016). At the centennial of the Bacteriophage: reviving the overlooked contribution of a forgotten pioneer. Richard Bruynoghe (1881–1957). *J. Hist. Biol.* 49, 559–580. doi: 10.1007/s10739-015-9429-0
- Blázquez, B., Fresco-Taboada, A., Iglesias-Bexiga, M., Menéndez, M., and García, P. (2016). PL3 amidase, a tailor-made lysin constructed by domain shuffling with potent killing activity against *Pneumococci* and related species. *Front. Microbiol.* 7:1156. doi: 10.3389/fmicb.2016.01156
- Capra, M. L., Quiberoni, A., and Reinheimer, J. A. (2004). Thermal and chemical resistance of *Lactobacillus casei* and *Lactobacillus paracasei* bacteriophages. *Lett. Appl. Microbiol.* 38, 499–504. doi: 10.1111/j.1472-765X.2004.01525.x
- CLSI (2017). “Performance standards for antimicrobial susceptibility testing,” in *Proceedings of the 27th Informational Supplement M100-S20* (Wayne, PA: Clinical and Laboratory Standards Institute).
- Defraigne, V., Schuermans, J., Grymonprez, B., Govers, S. K., Aertsen, A., Fauvart, M., et al. (2016). Efficacy of artilysin Art-175 against resistant and persistent *Acinetobacter baumannii*. *Antimicrob. Agents Chemother.* 60, 3480–3488. doi: 10.1128/AAC.00285-16
- Díez-Martínez, R., De Paz, H. D., García-Fernández, E., Bustamante, N., Euler, C. W., Fischetti, V. A., et al. (2015). A novel chimeric phage lysin with high in vitro and in vivo bactericidal activity against *Streptococcus pneumoniae*. *J. Antimicrob. Chemother.* 70, 1763–1773. doi: 10.1093/jac/dkv038
- Doi, Y., Murray, G., and Peleg, A. (2015). *Acinetobacter baumannii*: evolution of antimicrobial resistance—treatment options. *Semin. Res. Crit. Care* 36, 085–098. doi: 10.1055/s-0034-1398388
- El-Shibiny, A., and El-Sahhar, S. (2017). Bacteriophages: the possible solution to treat infections caused by pathogenic bacteria. *Can. J. Microbiol.* 63, 865–879. doi: 10.1139/cjm-2017-0030
- Endersen, L., Coffey, A., Ross, R. P., McAuliffe, O., Hill, C., and O’Mahony, J. (2015). Characterisation of the antibacterial properties of a bacterial derived peptidoglycan hydrolase (LysCs4), active against *C. sakazakii* and other Gram-negative food-related pathogens. *Int. J. Food Microbiol.* 215, 79–85. doi: 10.1016/j.jfoodmicro.2015.08.007
- Entenza, J. M., Loeffler, J. M., Grandgirard, D., Fischetti, V. A., and Moreillon, P. (2005). Therapeutic effects of bacteriophage Cpl-1 lysin against *Streptococcus pneumoniae* endocarditis in rats. *Antimicrob. Agents Chemother.* 49, 4789–4792. doi: 10.1128/AAC.49.11.4789-4792.2005
- Guo, H., Zhu, J., Tan, Y., Li, C., Chen, Z., Sun, S., et al. (2016). Self-assembly of virus-like particles of rabbit hemorrhagic disease virus capsid protein expressed in *Escherichia coli* and their immunogenicity in rabbits. *Antiviral Res.* 131, 85–91. doi: 10.1016/j.antiviral.2016.04.011
- Henein, A. E., Hanlon, G. W., Cooper, C. J., Denyer, S. P., and Maillard, J. (2016). A partially purified *Acinetobacter baumannii* phage preparation exhibits no cytotoxicity in 3T3 mouse fibroblast cells. *Front. Microbiol.* 7:1198. doi: 10.3389/fmicb.2016.01198
- Hu, F. P., Guo, Y., Zhu, D. M., Wang, F., Jiang, X. F., Xu, Y. C., et al. (2016). Resistance trends among clinical isolates in China reported from CHINET surveillance of bacterial resistance, 2005–2014. *Clin. Microbiol. Infect.* 22, S9–S14. doi: 10.1016/j.cmi.2016.01.001
- Hua, Y., Luo, T., Yang, Y., Dong, D., Wang, R., Wang, Y., et al. (2018). Phage therapy as a promising new treatment for lung infection caused by carbapenem-resistant *Acinetobacter baumannii* in mice. *Front. Microbiol.* 8:2659. doi: 10.3389/fmicb.2017.02659
- Huang, G., Le, S., Peng, Y., Zhao, Y., Yin, S., Zhang, L., et al. (2013). Characterization and genome sequencing of phage Abp1, a new phiKMV-like virus infecting multidrug-resistant *Acinetobacter baumannii*. *Curr. Microbiol.* 66, 535–543. doi: 10.1007/s00284-013-0308-7
- Huang, G., Shen, X., Gong, Y., Dong, Z., Zhao, X., Shen, W., et al. (2014). Antibacterial properties of *Acinetobacter baumannii* phage Abp1 endolysin (PlyAB1). *BMC Infect. Dis.* 14:681. doi: 10.1186/s12879-014-0681-2
- Jin, J., Li, Z. J., Wang, S. W., Wang, S. M., Huang, D. H., Li, Y. H., et al. (2012). Isolation and characterization of ZZ1, a novel lytic phage that infects *Acinetobacter baumannii* clinical isolates. *BMC Microbiol.* 12:156. doi: 10.1186/1471-2180-12-156
- Jun, S. Y., Jung, G. M., Yoon, S. J., Choi, Y., Koh, W. S., Moon, K. S., et al. (2014). Preclinical safety evaluation of intravenously administered SAL200 containing the recombinant phage endolysin SAL-1 as a pharmaceutical ingredient. *Antimicrob. Agents Chemother.* 58, 2084–2088. doi: 10.1128/AAC.02232-13
- Khakhum, N., Yordpratum, U., Boonmee, A., Tattawasart, U., Rodrigues, J. L. M., and Sermswan, R. W. (2016). Cloning, expression, and characterization of a peptidoglycan hydrolase from the *Burkholderia pseudomallei* phage ST79. *AMB Express* 6:77. doi: 10.1186/s13568-016-0251-7
- Kitti, T., Thummeepak, R., Thanwisai, A., Boonyodying, K., Kunthaler, D., Ritvirol, P., et al. (2014). Characterization and detection of endolysin gene from three *Acinetobacter baumannii* bacteriophages isolated from sewage water. *Indian J. Microbiol.* 54, 383–388. doi: 10.1007/s12088-014-0472-x
- Kong, M., and Ryu, S. (2015). Bacteriophage PBC1 and its endolysin as an antimicrobial agent against *Bacillus cereus*. *Appl. Environ. Microbiol.* 81, 2274–2283. doi: 10.1128/AEM.03485-14
- Kusradze, I., Karumidze, N., Rigvava, S., Dvalidze, T., Katsitadze, M., Amiranashvili, I., et al. (2016). Characterization and testing the efficiency of *Acinetobacter baumannii* phage vB-GEC_Ab-M-G7 as an antibacterial agent. *Front. Microbiol.* 7:1590. doi: 10.3389/fmicb.2016.01590
- Lai, M., Lin, N., Hu, A., Soo, P., Chen, L., Chen, L., et al. (2011). Antibacterial activity of *Acinetobacter baumannii* phage φAB2 endolysin (LysAB2) against both Gram-positive and Gram-negative bacteria. *Appl. Microbiol. Biotechnol.* 90, 529–539. doi: 10.1007/s00253-011-3104-y
- Lai, M., Soo, P., Lin, N., Hu, A., Chen, Y., Chen, L., et al. (2013). Identification and characterisation of the putative phage-related endolysins through full genome

- sequence analysis in *Acinetobacter baumannii* ATCC 17978. *Int. J. Antimicrob. Agents* 42, 141–148. doi: 10.1016/j.ijantimicag.2013.04.022
- Larpin, Y., Oechslin, F., Moreillon, P., Resch, G., Entenza, J. M., and Mancini, S. (2018). In vitro characterization of PlyE146, a novel phage lysin that targets Gram-negative bacteria. *PLoS One* 13:e0192507. doi: 10.1371/journal.pone.0192507
- Lim, J., Shin, H., Heu, S., and Ryu, S. (2014). Exogenous lytic activity of SPN9CC endolysin against gram-negative bacteria. *J. Microbiol. Biotechnol.* 24, 803–811. doi: 10.4014/jmb.1403.03035
- Lin, M. (2014). Antimicrobial resistance in *Acinetobacter baumannii*: from bench to bedside. *World J. Clin. Cases* 2:787. doi: 10.12998/wjcc.v2.i12.787
- Lood, R., Winer, B. Y., Pelzek, A. J., Diez-Martinez, R., Thandar, M., Euler, C. W., et al. (2015). Novel phage lysin capable of killing the multidrug-resistant gram-negative bacterium *Acinetobacter baumannii* in a mouse Bacteremia model. *Antimicrob. Agents Chemother.* 59, 1983–1991. doi: 10.1128/AAC.04641-14
- Melo, L. D. R., Brandao, A., Akturk, E., Santos, S. B., and Azeredo, J. (2018). Characterization of a new *Staphylococcus aureus* kayvirus harboring a lysin active against biofilms. *Viruses* 10:182. doi: 10.3390/v10040182
- Oliveira, H., Vilas Boas, D., Mesnage, S., Kluskens, L. D., Lavigne, R., Sillankorva, S., et al. (2016). Structural and enzymatic characterization of ABgp46, a novel phage endolysin with broad anti-gram-negative bacterial activity. *Front. Microbiol.* 7:208. doi: 10.3389/fmicb.2016.00208
- Pajunen, M., Kiljunen, S., and Skurnik, M. (2000). Bacteriophage phiYeO3-12, specific for *Yersinia enterocolitica* serotype O:3, is related to coliphages T3 and T7. *J. Bacteriol.* 182, 5114–5120. doi: 10.1128/JB.182.18.5114-5120.2000
- Regeimbal, J. M., Jacobs, A. C., Corey, B. W., Henry, M. S., Thompson, M. G., Pavlicek, R. L., et al. (2016). Personalized therapeutic cocktail of wild environmental phages rescues mice from *Acinetobacter baumannii* wound infections. *Antimicrob. Agents Chemother.* 60, 5806–5816. doi: 10.1128/AAC.02877-15
- Shen, Y., Zhang, J., Hao, W., Wang, T., Liu, J., Xie, Y., et al. (2018). Copolymer micelles function as pH-responsive nanocarriers to enhance the cytotoxicity of a HER2 aptamer in HER2-positive breast cancer cells. *Int. J. Nanomed.* 13, 537–553. doi: 10.2147/IJN.S149942
- Shivaswamy, V. C., Kalasuramath, S. B., Sadanand, C. K., Basavaraju, A. K., Ginnavaram, V., Bille, S., et al. (2015). Ability of bacteriophage in resolving wound infection caused by multidrug-resistant *Acinetobacter baumannii* in uncontrolled diabetic rats. *Microb. Drug Resist.* 21, 171–177. doi: 10.1089/mdr.2014.0120
- Sun, J., Shi, Y., Le, G., and Ma, X. (2005). Distinct immune response induced by peptidoglycan derived from *Lactobacillus* sp. *World J. Gastroenterol.* 11, 6330–6337. doi: 10.3748/wjg.v11.i40.6330
- Takemura-Uchiyama, I., Uchiyama, J., Osanai, M., Morimoto, N., Asagiri, T., Ujihara, T., et al. (2014). Experimental phage therapy against lethal lung-derived septicemia caused by *Staphylococcus aureus* in mice. *Microbes Infect.* 16, 512–517. doi: 10.1016/j.micinf.2014.02.011
- Yang, H., Wang, M., Yu, J., and Wei, H. (2015). Antibacterial activity of a novel peptide-modified lysin against *Acinetobacter baumannii* and *Pseudomonas aeruginosa*. *Front. Microbiol.* 6:1471. doi: 10.3389/fmicb.2015.01471
- Yele, A. B., Thawal, N. D., Sahu, P. K., and Chopade, B. A. (2012). Novel lytic bacteriophage AB7-IBB1 of *Acinetobacter baumannii*: isolation, characterization and its effect on biofilm. *Arch. Virol.* 157, 1441–1450. doi: 10.1007/s00705-012-1320-0
- Yin, S., Huang, G., Zhang, Y., Jiang, B., Yang, Z., Dong, Z., et al. (2018). Phage abp1 rescues human cells and mice from infection by pan-drug resistant *Acinetobacter Baumannii*. *Cell. Physiol. Biochem.* 44, 2337–2345. doi: 10.1159/000486117
- Zhang, H., Zhang, C., Wang, H., Yan, Y. X., and Sun, J. (2016). A novel prophage lysin Ply5218 with extended lytic activity and stability against *Streptococcus suis* infection. *FEMS Microbiol. Lett.* 363:fnw186. doi: 10.1093/femsle/fnw186

Conflict of Interest Statement: The authors declare that the research was conducted in the absence of any commercial or financial relationships that could be construed as a potential conflict of interest.

Copyright © 2019 Wu, Hu, Xie, Liu, Mu, Guo, Zhang, Zhang, Chang and Shi. This is an open-access article distributed under the terms of the Creative Commons Attribution License (CC BY). The use, distribution or reproduction in other forums is permitted, provided the original author(s) and the copyright owner(s) are credited and that the original publication in this journal is cited, in accordance with accepted academic practice. No use, distribution or reproduction is permitted which does not comply with these terms.



Corrigendum: A Novel Phage PD-6A3, and Its Endolysin Ply6A3, With Extended Lytic Activity Against *Acinetobacter baumannii*

Minle Wu^{1†}, Kongying Hu^{2†}, Youhua Xie², Yili Liu³, Di Mu⁴, Huimin Guo², Zhifan Zhang⁴, Yingcong Zhang¹, Dong Chang^{1*} and Yi Shi^{4*}

OPEN ACCESS

Approved by:

Frontiers in Microbiology Editorial
Office,
Frontiers Media SA, Switzerland

*Correspondence:

Yi Shi
yishi750@163.com
Dong Chang
dongchang1969@163.com

[†]These authors have contributed
equally to this work

Specialty section:

This article was submitted to
Antimicrobials, Resistance and
Chemotherapy,
a section of the journal
Frontiers in Microbiology

Received: 13 January 2019

Accepted: 23 January 2019

Published: 12 February 2019

Citation:

Wu M, Hu K, Xie Y, Liu Y, Mu D,
Guo H, Zhang Z, Zhang Y, Chang D
and Shi Y (2019) Corrigendum: A
Novel Phage PD-6A3, and Its
Endolysin Ply6A3, With Extended Lytic
Activity Against *Acinetobacter*
baumannii. *Front. Microbiol.* 10:196.
doi: 10.3389/fmicb.2019.00196

¹ Department of Clinical Laboratory, Shanghai Pudong Hospital, Fudan University, Shanghai, China, ² Key Laboratory of Medical Molecular Virology, School of Basic Medical Sciences, Fudan University, Shanghai, China, ³ Department of Clinical Laboratory, Shanghai Public Health Clinical Center, Shanghai, China, ⁴ Department of Clinical Laboratory, Shanghai Fourth People's Hospital affiliated to Tongji University School of Medicine, Shanghai, China

Keywords: multidrug resistance *Acinetobacter baumannii*, endolysin, ESKAPE, sepsis, phage therapy, mice model

A Corrigendum on

A Novel Phage PD-6A3, and Its Endolysin Ply6A3, With Extended Lytic Activity Against *Acinetobacter baumannii*

by Wu, M., Hu, K., Xie, Y., Liu, Y., Mu, D., Guo, H., et al. (2019). *Front. Microbiol.* 9:3302.
doi: 10.3389/fmicb.2018.03302

There is an error in the Funding statement. The correct name for the Funder is “Shanghai Municipal Commission of Health and Family Planning.”

Additionally, in the published article, there were errors in affiliations 1 and 4. Instead of “Department of Clinical Laboratory, Pudong Hospital Affiliated to Fudan University, Shanghai, China,” it should be “Department of Clinical Laboratory, Shanghai Pudong Hospital, Fudan University, Shanghai, China,” and in affiliation 4, instead of “Department of Clinical Laboratory, The Fourth People's Hospital of Shanghai, Shanghai, China,” it should be “Department of Clinical Laboratory, Shanghai Fourth People's Hospital affiliated to Tongji University School of Medicine, Shanghai, China.”

The authors apologize for these errors and state that this does not change the scientific conclusions of the article in any way. The original article has been updated.

Copyright © 2019 Wu, Hu, Xie, Liu, Mu, Guo, Zhang, Zhang, Chang and Shi. This is an open-access article distributed under the terms of the Creative Commons Attribution License (CC BY). The use, distribution or reproduction in other forums is permitted, provided the original author(s) and the copyright owner(s) are credited and that the original publication in this journal is cited, in accordance with accepted academic practice. No use, distribution or reproduction is permitted which does not comply with these terms.



Novel Pyoverdine Inhibitors Mitigate *Pseudomonas aeruginosa* Pathogenesis

Daniel R. Kirienko, Donghoon Kang and Natalia V. Kirienko*

Department of BioSciences, Rice University, Houston, TX, United States

OPEN ACCESS

Edited by:

Paolo Visca,
Università degli Studi Roma Tre, Italy

Reviewed by:

Pierre Cornelis,
Vrije Universiteit Brussel, Belgium
Rolf Kümmerli,
University of Zurich, Switzerland

*Correspondence:

Natalia V. Kirienko
kirienko@rice.edu

Specialty section:

This article was submitted to
Antimicrobials, Resistance
and Chemotherapy,
a section of the journal
Frontiers in Microbiology

Received: 09 October 2018

Accepted: 20 December 2018

Published: 09 January 2019

Citation:

Kirienko DR, Kang D and
Kirienko NV (2019) Novel Pyoverdine
Inhibitors Mitigate *Pseudomonas*
aeruginosa Pathogenesis.
Front. Microbiol. 9:3317.
doi: 10.3389/fmicb.2018.03317

Pseudomonas aeruginosa is a clinically important pathogen that causes a variety of infections, including urinary, respiratory, and other soft-tissue infections, particularly in hospitalized patients with immune defects, cystic fibrosis, or significant burns. Antimicrobial resistance is a substantial problem in *P. aeruginosa* treatment due to the inherent insensitivity of the pathogen to a wide variety of antimicrobial drugs and its rapid acquisition of additional resistance mechanisms. One strategy to circumvent this problem is the use of anti-virulent compounds to disrupt pathogenesis without directly compromising bacterial growth. One of the principle regulatory mechanisms for *P. aeruginosa*'s virulence is the iron-scavenging siderophore pyoverdine, as it governs in-host acquisition of iron, promotes expression of multiple virulence factors, and is directly toxic. Some combination of these activities renders pyoverdine indispensable for pathogenesis in mammalian models. Here we report identification of a panel of novel small molecules that disrupt pyoverdine function. These molecules directly act on pyoverdine, rather than affecting its biosynthesis. The compounds reduce the pathogenic effect of pyoverdine and improve the survival of *Caenorhabditis elegans* when challenged with *P. aeruginosa* by disrupting only this single virulence factor. Finally, these compounds can synergize with conventional antimicrobials, forming a more effective treatment. These compounds may help to identify, or be modified to become, viable drug leads in their own right. Finally, they also serve as useful tool compounds to probe pyoverdine activity.

Keywords: *Pseudomonas aeruginosa*, antivirulence, siderophore, pyoverdine, *Caenorhabditis elegans*

INTRODUCTION

Despite advances in antimicrobial chemotherapy, multidrug resistant bacteria continue to cause life-threatening infections, especially in hospitals and with immunocompromised patients. *Pseudomonas aeruginosa* is a particularly pernicious pathogen as it possesses several innate defense mechanisms against antibiotics. For example, *P. aeruginosa* expresses four major efflux pumps (MexAB-OprM, MexCD-OprJ, MexEF-OprN, and MexXY-OprM) that effectively reduce intracellular drug concentrations, preventing the compounds from reaching intracellular doses required for effect (Lomovskaya et al., 2001). These pumps confer resistance to several classes of commonly used drugs, including β -lactams, fluoroquinolones, and aminoglycosides (Poole et al., 1993, 1996; Köhler et al., 1997; Aires et al., 1999). Chemically inhibiting these pumps significantly

reduces the concentration of antimicrobial required for treatment (Lomovskaya et al., 2001). Unfortunately, *P. aeruginosa* also has several other mechanisms of resistance, including decreased membrane permeability and enzymes that modify or degrade antimicrobials (Kon and Rai, 2016). Drug targets are also prone to mutate to avoid antimicrobial sensitivity. In addition, *P. aeruginosa* produces robust biofilms that form a physical barrier between the pathogen and antimicrobial therapies (Mah and O'Toole, 2001; Anderson and O'Toole, 2008). *P. aeruginosa* readily acquires genetically encoded resistance determinants from other pathogens, further increasing resistance. The development and approval of new antimicrobials (especially new classes of antimicrobials) is typically a slower process than the development of resistance by the pathogen which also contributes to the increasing demand to at least supplement drug development efforts with novel treatment avenues for *P. aeruginosa* infections.

Perhaps the most promising route toward this goal is to target the virulence factors instead. Often, compromising these factors does not directly impinge on bacterial viability, which is predicted to reduce the pressure to evolve resistance. Virulence determinants come in a staggering array of forms, including toxins that directly damage the host (e.g., type III secretion effectors, pyocyanin, hemolysins, etc.) (Saliba et al., 2002; Cezairliyan et al., 2013; Managò et al., 2015; Dortet et al., 2018), proteins or co-factors that provide nutritional support for the pathogen (e.g., siderophores, carbohydrate permeases, etc.) (Minandri et al., 2016), or promote colonization (e.g., adhesins, quorum-sensing, and biofilm formation). Small-molecule inhibitors that target these systems mitigate bacterial pathogenicity, facilitating bacterial clearance by the host. Based on this idea, a number of antivirulence compounds have been proposed for *P. aeruginosa*, mostly targeting the pathogen's quorum-sensing systems and biofilm-forming capacity (Vandeputte et al., 2011; Tan et al., 2013; Imperi et al., 2014; Kang and Kirienko, 2017; Paczkowski et al., 2017; van Tilburg Bernardes et al., 2017; D'Angelo et al., 2018).

Although acute virulence determinants have generally received less attention in recent studies, the siderophore pyoverdine makes an attractive therapeutic target for several reasons. First, pyoverdine is essential for *P. aeruginosa* pathogenesis in various mammalian and invertebrate host models (Meyer et al., 1996; Takase et al., 2000; Imperi et al., 2013; Kirienko et al., 2013; Lopez-Medina et al., 2015; Minandri et al., 2016). Pyoverdine's exceptionally high affinity for ferric iron allows it to scavenge trace iron from the environment and also to abstract it from host iron-sequestering proteins such as transferrin and lactoferrin (Meyer et al., 1996; Xiao and Kisaalita, 1997). Second, pyoverdine can also hijack iron from other host sources, including mitochondria, which inflicts considerable damage on the host (Kirienko et al., 2013, 2015; Kang et al., 2018). Third, iron-bound pyoverdine (known as ferripyoverdine) functions as a signaling molecule that triggers the release of the alternate sigma factor PvdS from sequestration by the intermembrane FpvA/FpvR complex (Beare et al., 2003). Once released, PvdS promotes the expression of at least two secreted toxins (the translational inhibitor ToxA and the protease PrpL)

and also its own biosynthetic machinery (Ochsner et al., 1996; Wilderman et al., 2001; Lamont et al., 2002). Fourth, the iron provided by pyoverdine is required for biofilm formation (Banin et al., 2005). Finally, and perhaps most importantly, fluoropyrimidines have been successfully used in several hosts to target pyoverdine, which has substantially reduced host mortality (Imperi et al., 2013; Costabile et al., 2016; Kirienko et al., 2016).

In this study, we describe the identification of a group of novel small molecules that compromise pyoverdine function without acting as conventional antimicrobials. We show that these compounds ameliorate pyoverdine-mediated damage, and that their effect is specifically due to their inhibition of pyoverdine function. These drugs rescue *Caenorhabditis elegans* at mid-micromolar concentrations and exhibit drug-like profiles. Promisingly, these compounds demonstrate synergy when combined with a conventional anti-*Pseudomonas* antibiotic. These compounds may serve as drug leads themselves or tool compounds for the identification of a future class of virulence inhibitors with clinical utility.

MATERIALS AND METHODS

Bacterial and *C. elegans* Strains and Maintenance

The strains used in this study can be found in Table 1. *C. elegans* strain SS104 [*glp-4(bn2)*] was maintained on nematode growth medium (NGM) seeded with *Escherichia coli* strain OP50 at 15°C (Stiernagle, 2006). *P. fluorescens* WCS365 (Geels and Schippers, 1983) was a gift from Dr. Cara Haney, and was selected as a high pyoverdine producer. The *P. aeruginosa* PA14*pvdF* mutant has a Mariner transposon inserted into the *pvdF* locus, as verified by Sanger sequencing (Liberati et al., 2006). *Enterococcus faecalis* was a gift from Dr. Danielle Garsin.

Caenorhabditis elegans – *P. aeruginosa* Assay

The Liquid Killing assay was performed essentially as described (Anderson et al., 2018). In brief, *glp-4(bn2ts)* worms were synchronized by bleaching gravid adults and hatching in the absence of food at 15°C. L1 larvae were dropped onto plates

TABLE 1 | Strains used in this study.

Species	Strain	Reference
<i>C. elegans</i>	<i>glp-4(bn2)</i>	Beanan and Strome, 1992
<i>E. coli</i>	OP50	Stiernagle, 2006
<i>P. aeruginosa</i>	PA14	Rahme et al., 1995
<i>P. aeruginosa</i>	PA14Δ <i>pvdA</i>	Shanks et al., 2006; Kuchma et al., 2007
<i>P. aeruginosa</i>	PAO1	Holloway et al., 1994
<i>P. aeruginosa</i>	Boston 41501	ATCC 27853 (Medeiros et al., 1971)
<i>P. aeruginosa</i>	KM 306	ATCC 25010 (Yabuuchi and Ohya, 1972)
<i>P. aeruginosa</i>	6092	ATCC 33360 (Liu et al., 1983)
<i>P. fluorescens</i>	WCS365	Geels and Schippers, 1983
<i>E. faecalis</i>	OG1RF	Garsin et al., 2001

containing standard *E. coli* OP50, and then transferred to the non-permissive temperature to induce sterility. At the young adult stage, they were washed from plates, and sorted into 384-well plates containing *P. aeruginosa*. The bacteria were prepared by spreading a small amount of an overnight inoculum onto an SK media plate (Kirienko et al., 2014), and incubating the plate at 37°C for 1 day. Bacteria were then scraped from the plate and inoculated into LK media at a final OD₆₀₀ of 0.03.

For the assessment of potential synergistic interaction between antimicrobials and anti-virulents, *C. elegans* were incubated with *P. aeruginosa* strain PA14 for 24 h. After that 200 µg/mL (final) of gentamicin with or without pyoverdine inhibitors (100 µM) was added. Host survival was examined 24 h later using Sytox Orange staining as per standard Liquid Killing protocol.

High-Throughput Screening Hits

A high-content, high-throughput screen using the Liquid Killing assay was previously performed as described (Kirienko et al., 2016). Libraries with >1000 compounds screened are listed in **Supplementary Table S1**. Screening hits were purchased from varying companies through the chemical marketplace MolPort (Riga, Latvia). Small molecule purity (by HPLC) and identity (by mass spectrometry) was confirmed by vendors. When possible, compounds were sourced from more than one company to limit the possibility of misidentification. Analogous compounds were identified by searching chemical landscape using the Structure Search tools at MolPort.

Production of Cell-Free, Pyoverdine-Rich Filtrate

To produce pyoverdine-rich filtrate, *P. aeruginosa* or *P. fluorescens* strains were grown in modified M9 medium [1% (w/v) Difco 5× M9 salts, 11.3 g/L casamino acids, 0.4% glucose, 1 mM CaCl₂, 1 mM MgSO₄] for 20–22 h at 28°C (*P. fluorescens*) or 37°C (*P. aeruginosa*) with agitation. Subsequently, bacteria were pelleted by centrifugation at 10,000 g for 30 min. Supernatants were sequentially filtered through 0.45, 0.20, and 0.20 µm filters to remove residual bacteria. The resultant cell-free, pyoverdine-rich material was referred to as filtrate throughout the manuscript. All steps were performed using plastic containers.

Pyoverdine Measurements

A Cytation 5 multimode plate reader (BioTek Instruments, VT, United States) was used to assess quenching of pyoverdine by small molecules. To test pyoverdine fluorescence, *P. aeruginosa* strain PA14 was grown overnight in the presence of compounds, a single colony of *P. aeruginosa* strain PA14 was used to inoculate an overnight culture in LB, which was grown with agitation for 16 h at 37°C. The resulting culture was diluted 1000-fold and inoculated into modified M9 medium (see below) containing compound, DMSO, or FeCl₃ at 100 µM. Cultures were incubated at 37°C with shaking for 24 h. The resulting cultures were centrifuged, and pyoverdine fluorescence in the

media was determined spectrophotometrically with excitation 405 nm and emission 460 nm. Similarly, the ability of the compounds to quench pyoverdine fluorescence in bacteria-free pyoverdine-rich filtrate was assayed by adding equal amounts of bacteria-free, pyoverdine-rich filtrate and modified M9 medium containing 100 µM compound, DMSO, or FeCl₃. Quenching was measured after a 5 min incubation at room temperature. All pyoverdine measurements were performed within the linear range of the Cytation 5, which was empirically determined to be between 1,000 and 20,000 arbitrary fluorescence units using serial dilutions of pyoverdine-rich cell-free filtrate.

RNA Purification, NanoString, and qRT-PCR

For NanoString (NanoString Technologies, WA, United States) studies, 2,000 worms were exposed to 100 µM of LK11, LK31, LK31a, or ciclopirox olamine in S Basal media for 16 h in 6-well plates. Worms incubated in corresponding amount of DMSO for 16 h served as a normalization control. Afterward, worms were transferred into 15 mL conicals and washed twice with S Basal. Two biological replicates were tested for each condition. Gene expression was analyzed according to NanoString guidelines. For experiments involving quantification of expression of pyoverdine-dependent genes in the host, *glp-4(bn2)* worms were exposed to pyoverdine for 16 h in the presence or absence of small molecules at 50 µM. RNA collection and qRT-PCR were performed as previously described (Kirienko et al., 2008). Fold-changes were calculated using a $\Delta\Delta C_t$ method. Primer sequences are available upon request.

For assessing the effect of LK31 and LK31a on the expression of pyoverdine-dependent genes in *P. aeruginosa*, experiments were performed as follows: after 14 h growth in 6 mL of SK media supplemented with either DMSO or 100 µM inhibitor, cells were collected via centrifugation. RNA was extracted and purified using TRIzol reagent (Invitrogen, CA, United States) according to the manufacturer's protocols with minor adjustments. To ensure cell lysis, cells resuspended in TRIzol reagent were freeze-cracked and vortexed prior to phase separation. Purified RNA was treated with DNase I (Thermo Fisher Scientific, MA, United States) to eliminate genomic DNA contamination. Reverse transcription was performed using random decamers and Retroscript Kit (Thermo Fisher Scientific, MA, United States). qRT-PCR was conducted using SYBR green AzuraQuant Fast Green Fastmix (Azura, MA, United States) in a CFX-96 real-time thermocycler (Bio-Rad, CA, United States). Fold-changes were calculated using a $\Delta\Delta C_t$ method. Primer sequences are available upon request.

Compounds' Effect Under Iron-Limiting Conditions

WT *P. aeruginosa* PA14 or the PA14 $\Delta pvdA$ mutant were grown in 96-well plate in M9 media supplemented with casamino acids (BD Bacto, CA, United States) and with or without 6.25 µM ciclopirox olamine (CPX). PA14 CPX samples were supplemented with either DMSO or pyoverdine

inhibitors LK11, LK31, and LK31a at 100 μ M. The 96-well plate was incubated in Cytation 5 multimode plate reader (BioTek, VT, United States) at 37°C. OD₆₀₀ readings were recorded every 30 min for 22.5 h. Three biological replicates were performed.

MIC, CFU, and Microscopy Assays

To determine the minimum inhibitory concentration (MIC) of compounds for preventing bacterial growth, *P. aeruginosa* strain PA14 was grown in standard LB overnight and diluted 100,000-fold in SK media. Compounds were two-fold serially diluted and mixed with equal volumes of diluted bacteria in 96-well plates. Plates were incubated at 37°C for 24 h. Growth inhibition was visually scored on the basis of turbidity. Two wells were used per condition, and at least three biological replicates were performed. For quantification of colony-forming units (CFU), shaking cultures of *E. coli* strain OP50, *P. aeruginosa* strain PA14, or *E. faecalis* strain OG1RF were grown at 37°C. At appropriate time points, aliquots were taken from each culture, serially diluted five-fold in S Basal, and plated onto LB agar. Colonies were counted under a dissecting microscope.

For assessing the impact of LK12 treatment on *P. aeruginosa* strain PA14, a strain carrying a plasmid encoding GFP was inoculated at an initial concentration of OD₆₀₀ = 0.0001 in the presence of either 250 μ M NK12 or DMSO alone (1% v/v). All cultures included propidium iodide at a final concentration of 40 μ g/mL. At 4 or 8 h after inoculation, bacteria were removed and imaged using a Zeiss M2 upright fluorescent microscope (Carl Zeiss, Germany). Experiments with *Escherichia coli* strain OP50 transformed with a GFP-encoding plasmid were performed in the same fashion.

RESULTS

Selected Hits That Rescue *C. elegans* From *P. aeruginosa* Interfere With Pyoverdine Fluorescence

We previously carried out a fragment-based, high-content, high-throughput phenotypic screen comprising over 86,000 wells (Kirienko et al., 2016). The goal was to identify compounds that increase *C. elegans* survival during exposure to *P. aeruginosa* strain PA14. This assay identified approximately 70 novel small molecules that passed initial and second-pass retesting that showed statistically significant rescue. Apparent pan-assay interfering compounds (Baell and Holloway, 2010; Baell and Walters, 2014) were removed, leaving 61 compounds, 54 of which were commercially available at the time of our initial retesting (Figure 1A). We have previously demonstrated that some of the hits acted by interfering with bacterial iron metabolism (Kirienko et al., 2013) or by inhibiting the production of pyoverdine (Kirienko et al., 2016). Since pyoverdine toxicity is the principal factor underlying host killing, we hypothesized that at least some of the remaining hits may act by blocking pyoverdine function.

In the past, we have observed a strong positive correlation between pyoverdine fluorescence and toxicity

(Kirienko et al., 2013; Kang et al., 2018). On this basis, we predicted that we would be able to identify compounds that compromise pyoverdine toxicity by measuring fluorescence in the presence of the compound. We tested the ability of each of the 54 commercially available hits to reduce pyoverdine fluorescence in growing cultures of *P. aeruginosa* PA14 (Figure 1B). We also added each of the commercially available compounds to pyoverdine-enriched, cell-free filtrates to verify that a reduction in fluorescence would be observed there as well, to rule out the possibility that the compounds were merely preventing pyoverdine production or were non-specifically compromising bacterial growth. Using these assays we identified four hits (LK10, LK11, LK12, and LK31) that quenched more than half of pyoverdine fluorescence (Figure 1C). These compounds also dramatically reduced pyoverdine fluorescence in *P. aeruginosa* PAO1, another clinically derived strain (Figure 1D).

Consistent with our predictions, the ability of the compounds to both rescue *C. elegans* (example shown in Figures 2A,B) and quench pyoverdine (Figure 2C) were dosage dependent. Interestingly, the four pyoverdine inhibitors represented diverse structural classes (Figure 2D). In an effort to better relate the structures and the activities of the compounds, we searched for commercially available analogs. We used a structure-based search tool to identify the closest commercially available compounds, and acquired up to three analogs for each (see Supplementary Figure S1 for structures). Each analog was solubilized in DMSO and tested for the ability to reduce pyoverdine fluorescence (Figures 3A,B). LK31a, which differs from its parent compound LK31 by the addition of a carbonitrile group (Figure 3C), showed significantly greater efficacy in this assay than its parent molecule. In contrast, LK31b had no discernible activity. None of the analogs selected for LK10, LK11, or LK12 exhibited anti-pyoverdine activity greater than their parent compounds.

Structurally, pyoverdine is comprised of two disparate parts. The chromophore, which is shared by all fluorescent *Pseudomonads*, consists of a relatively compact, heavily modified dihydroxyquinoline moiety. Attached to this is an oligopeptide chain that is produced by non-ribosomal protein synthesis machinery and introduces a variety of non-standard and *D*-conformation amino acids into the chain. The genes involved in biosynthesis of the oligopeptide side chain exhibit greater sequence variation than most regions of the *P. aeruginosa* genome. As a consequence, *Pseudomonads* produce pyoverdines that are sufficiently variable for use as a tool for taxonomic differentiation, a process called siderotyping (Meyer et al., 1998; Fuchs et al., 2001; Meyer et al., 2002). Early in the molecular study of pyoverdine, when it became apparent that pyoverdines had heterogeneous amino acid chains, they were designated as type I, type II, and type III (Meyer et al., 1997; De Vos et al., 2001). Since clinically relevant strains of *P. aeruginosa* are known to produce each of these types of pyoverdine, we obtained relevant strains of *P. aeruginosa* from the ATCC. We also tested compound efficacy against pyoverdine produced by *P. fluorescens*, which is likely to be even more variant from the type I producing strains we already tested (PAO1 and PA14). In each case, the compounds quenched pyoverdine fluorescence (Figure 4).

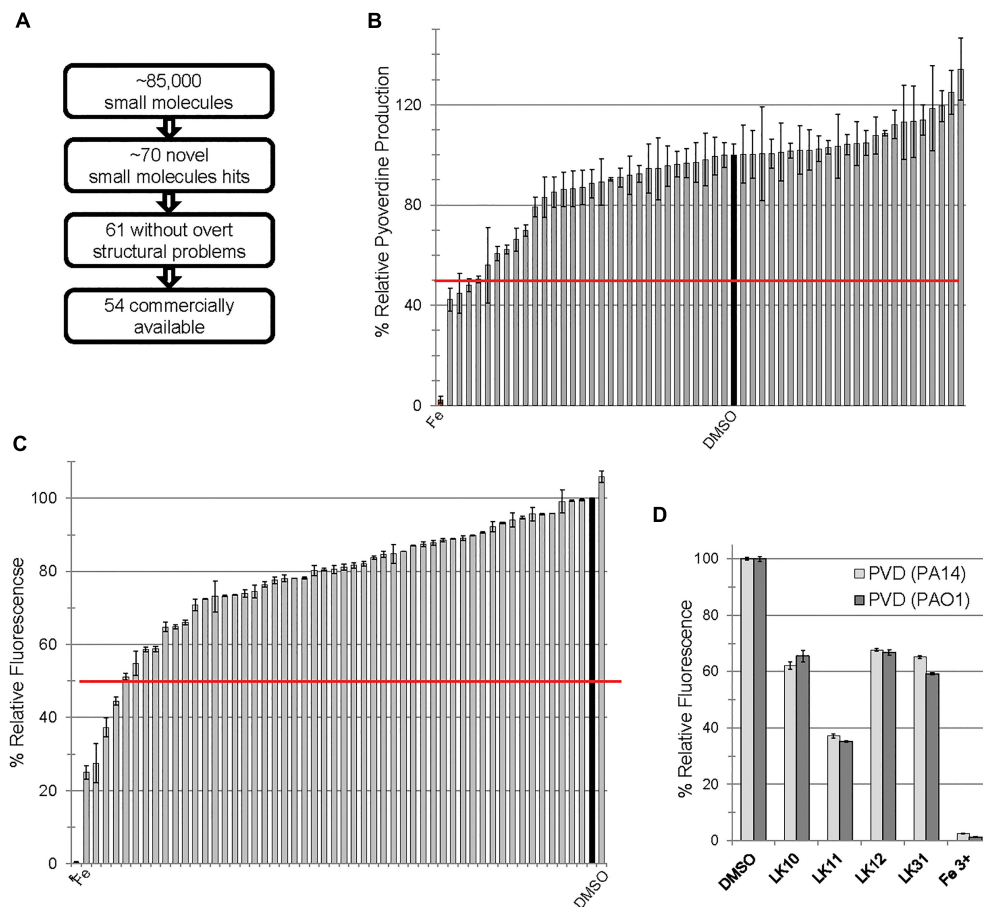


FIGURE 1 | Small molecules interfere with pyoverdine function. **(A)** Flow chart of screening summary for novel small molecules that rescue *Caenorhabditis elegans* from *Pseudomonas aeruginosa*. **(B)** Effect of small molecule hits on fluorescence of pyoverdine when bacteria were cultured 24 h in the presence of the compounds (250 μ M) or DMSO. **(C)** Fluorescence of pyoverdine in bacteria-free filtrate after a 5 min incubation with compound (250 μ M). **(D)** Selected small molecules are capable of quenching pyoverdine fluorescence from pyoverdine-rich filtrates produced by *P. aeruginosa* strain PA14 or PAO1. At least three biological replicates were performed for **B–D**. The red lines in **B,C** correspond to 50% decrease in fluorescence.

LK10 and LK12 Are Multifunctional Compounds

Although LK10, LK11, LK12, and LK31 reduce pyoverdine fluorescence, we tested whether the compounds also act as antimicrobials by examining their ability to prevent bacterial growth. Compounds were serially diluted in 96-well plates and *P. aeruginosa* was added and grown overnight. We also tested several standard antimicrobials with efficacy against *P. aeruginosa* as controls. Compounds with MIC values similar to their effective rescuing concentrations (defined as the concentration required for statistically significant rescue in Liquid Killing) were considered to have antimicrobial activity. For comparison, the known antimicrobials we tested showed MIC/EC ratios between 0.5 and 3 (**Figure 5A**). LK10 and LK12 also had MIC/EC ratios close to this range. On this basis, we have reclassified them as hybrid molecules, as they both inhibit *P. aeruginosa* growth and also quench pyoverdine fluorescence.

Since LK12 demonstrated the lowest MIC (suggesting the strongest antimicrobial effect), we further examined its

antibacterial properties. We grew *P. aeruginosa* in the presence of varying concentrations of LK12 and observed a concentration-dependent bactericidal effect (**Supplementary Figure S2A**). Interestingly, this effect appeared transient, as bacterial growth quickly recovered and the titer of viable bacteria was high by 16 h. We tested whether the compound also affected *E. coli* or *E. faecalis*. We noted that, although the compound had a more pronounced effect on *E. coli*, it was still transient (**Supplementary Figure S2B**). We hypothesize that the difference in efficacy is related to the difference in efflux pump efficiency and expression between *P. aeruginosa* and *E. coli*. Compound treatment slowed *E. faecalis* growth, but there were no overt signs that it was bactericidal, even at twice the concentration used for the gram-negative bacteria. This may suggest that LK12 is more effective in blocking the growth and development of gram-negative bacteria.

To verify that the bacteria were dead, we also tested *P. aeruginosa* PA14 that constitutively express GFP. Bacteria were grown in the presence of the compound for 8 h, and then washed and stained with propidium iodide. Propidium iodide is

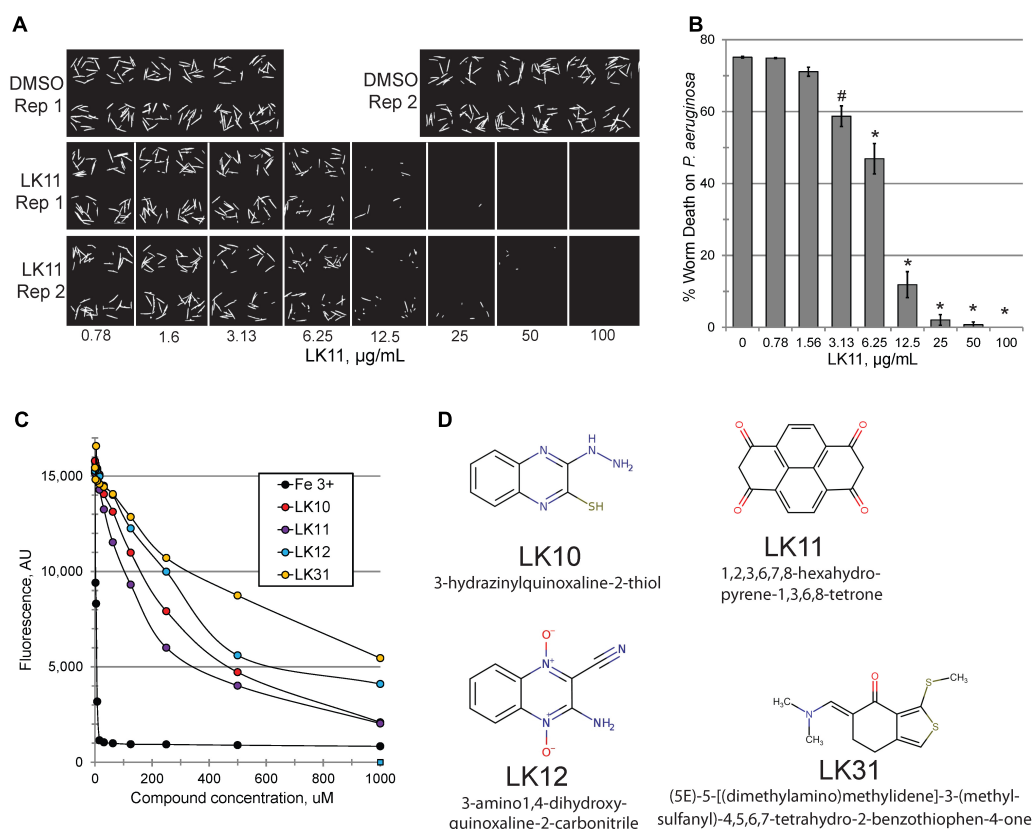


FIGURE 2 | LK11 demonstrates dosage-dependent rescue. Representative images **(A)** and quantification **(B)** of *C. elegans* death after incubation with *P. aeruginosa* in the presence of varying concentrations of LK11. The cell-impermeable dye Sytox Orange was used to stain dead worms. Each well contains ~ 18 worms. At least three biological replicates were performed. **(C)** Pyoverdine-rich filtrate was incubated with various concentrations of pyoverdine inhibitors or iron (III) and fluorescence was measured after 5 minutes. **(D)** The structures and IUPAC names of LK10, LK11, LK12, and LK31. p -values were calculated using Student's t -test, $*p < 0.01$, $^{\#}p < 0.05$.

a cell-impermeant dye, and will stain only dead bacterial cells (**Supplementary Figures S2C,D**). After 8 h, a large proportion of bacteria showed staining. Interestingly, we observed a very different phenomenon when we tried an analogous experiment using *E. coli* strain OP50. Instead of dividing properly, the morphology of *E. coli* cells changed to a longer, more filamentous state (**Supplementary Figures S2E,F**). This is consistent with a bacterial stress response to DNA damage (Suzuki et al., 1967; Walker and Pardee, 1968; Cushnie et al., 2016). Our findings are consistent with earlier reports about the capacity of LK12 to generate ROS and induce DNA damage (Ismail et al., 2010; Cheng et al., 2016).

Anti-pyoverdines Have Drug-Like Properties

We used the ability of LK11, LK31, and LK31a to quench pyoverdine fluorescence to determine their affinity for pyoverdine (**Supplementary Table S2**). Although the affinity of the compounds is relatively low, in the hundred micromolar range, this is common for 'very promising' hits from fragment-based drug discovery methods (Murray and Rees, 2009). It is worth noting that no overt toxicity was seen when *C. elegans*

was exposed to 128 μM LK11, LK31, or LK31a (**Supplementary Figure S3**). The other traits of the compounds generally conform to common drug design guidelines, such as Lipinski's Rule of Five (Lipinski et al., 2001) or The Rule of Three (Congreve et al., 2003; **Table 2**). These 'rules' have been empirically derived from successful drugs with known oral bioavailability and typically discriminate toward smaller, less reactive molecules. Consistent with this, all three have relatively low molecular weight (approximately 150–250 Da, **Table 2**). While not essential, low initial mass for leads is useful; drug development frequently involves adding functional groups that increase both affinity and mass. Based on these characteristics, LK11 and LK31/LK31a may serve as promising compounds for optimization. One intriguing possibility is that LK11 and LK31/LK31a could be combined into a single molecule with an even higher affinity if their binding sites are different and proximal to one another (Doak et al., 2016).

Pyoverdine Inhibitors Behave as *Bona Fide* Anti-virulents

Two factors suggested that LK11 and LK31 were acting as antivirulents. First, we were unable to use the compounds alone

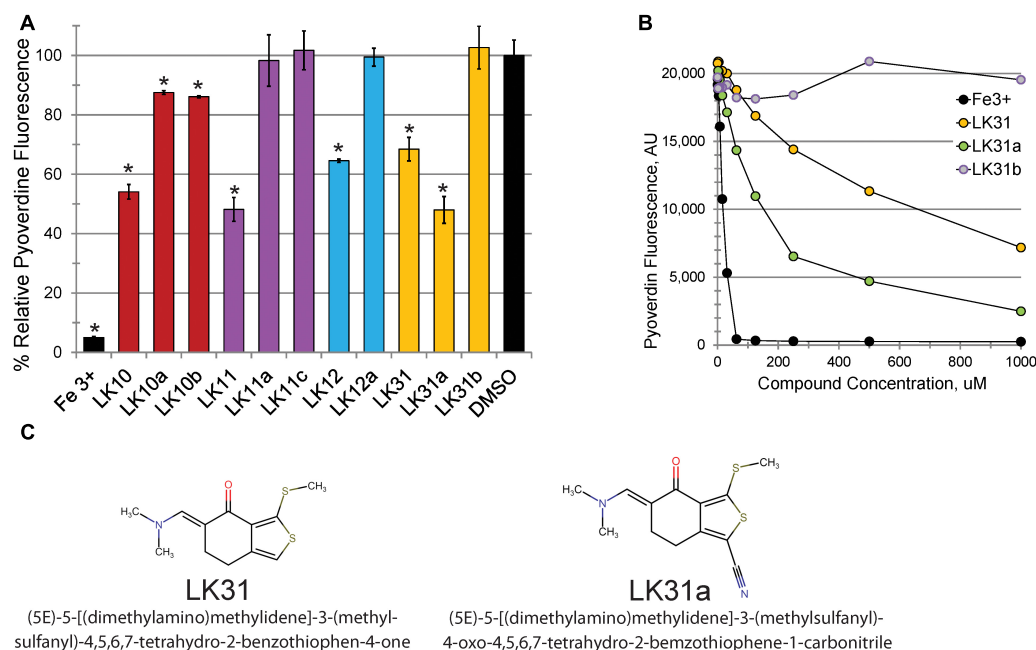


FIGURE 3 | Selected hits show dosage-dependent pyoverdine fluorescence quenching. **(A,B)** Fluorescence of bacteria-free, pyoverdine-rich filtrate after 5 min incubation with the compounds indicated at either fixed (250 μ M, **A**) or varying (**B**) concentrations. DMSO. **(C)** Structural comparison of a parent compound (LK31) and an analog with improved efficiency (LK31a). At least three biological replicates were performed for **A,B**. *p*-values were calculated using Student's *t*-test, **p* < 0.01.

to inhibit bacterial growth in standard MIC assays. Second, the MIC/EC ratios of LK11 and LK31 were at least an order of magnitude higher than the ratios for known antimicrobials. As pyoverdine is a large molecule requiring substantial cellular investment, disrupting or delaying bacterial growth significantly will delay pyoverdine biosynthesis. To rule out this potentially confounding issue, we carefully compared bacterial growth for cultures with various concentrations of LK11, LK31, LK31a, or DMSO alone. Rather than rely on spectroscopic measurements, which can be misleading, we serially diluted bacterial inocula and counted the number of viable bacterial colonies. Bacterial growth kinetics were unaffected by the presence of LK11, LK31, or LK31a in two different growth media (**Figures 5B,C**).

Under iron-limiting conditions pyoverdine becomes essential for bacterial survival and growth. For this reason, we anticipated that the compounds may compromise bacterial growth under these conditions. First, we compared the growth of wild-type *P. aeruginosa* PA14 and Δ *pvdA* pyoverdine production mutant in M9 media supplemented with casamino acids. In the absence of an exogenous iron chelator, growth of the strains was indistinguishable (**Figure 6**). In contrast, the addition of 6.25 μ M ciclopirox olamine (CPX) caused a small lag in wild-type development but compromised the growth of the Δ *pvdA* mutant, indicating that these conditions require pyoverdine for growth. Adding LK11, LK31, or LK31a to wild-type *P. aeruginosa* growing in the presence of CPX phenocopied the Δ *pvdA* defect, providing another piece of evidence to support that the compounds are compromising pyoverdine function.

Although these data substantially demonstrated that the pyoverdine inhibitors were compromising pyoverdine fluorescence and that they were not functioning by preventing bacterial growth under iron replete conditions, we also wanted to eliminate the possibility that their effect was due to the compounds exerting some uncharacterized effect on the host. For example, previous reports have shown that small molecules can trigger host defenses and extend *C. elegans* survival, even if they are toxic and will eventually kill the host as well (Pukkila-Worley et al., 2012). To test this, we used NanoString technology to assess the mRNA levels of 115 genes involved in *C. elegans* immune and stress response pathways. Gene expression was normalized to three housekeeping genes; (see **Supplementary Table S3** for the list of genes and fold-changes). mRNA was purified from *C. elegans* treated with either LK11, LK31, LK31a, or DMSO (as a control) in the absence of *P. aeruginosa* or pyoverdine. LK11 had minimal effect on the host, with only 4 genes (3.5%) showing upregulation between 3- and 10-fold. LK31 and LK31a each upregulated less than 10% of the genes surveilled (and generally upregulated the same genes, which is consistent with their structural similarity) (**Table 3**). In contrast, ~34% of the genes were upregulated in *C. elegans* exposed to the iron chelator ciclopirox olamine.

The screening assay used automatic scoring, and host death was inferred on the basis of staining with the cell impermeant dye Sytox Orange. Therefore, we also ruled out the possibility that the compounds were somehow preventing the dye from staining dead worms (or that the anti-pyoverdine compounds were

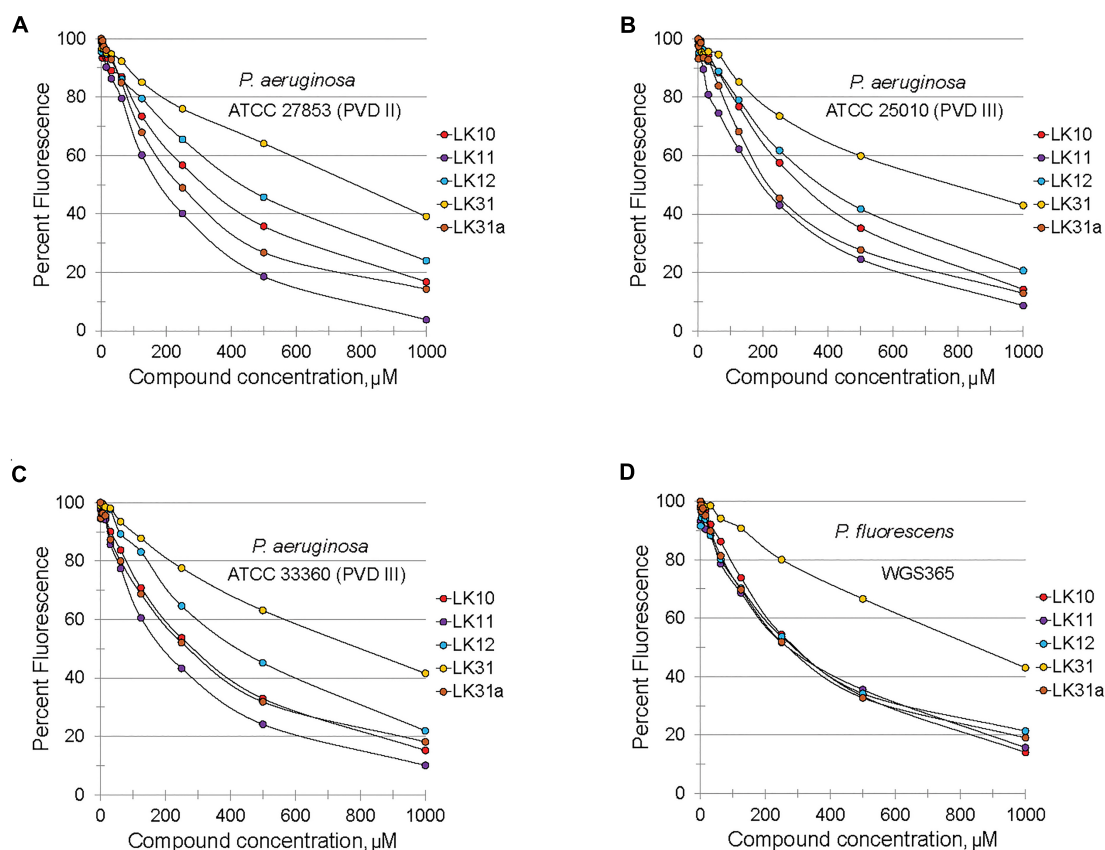


FIGURE 4 | Selected hits inhibit fluorescence of structurally diverse pyoverdines. (A–D) Fluorescence of bacteria-free, pyoverdine-rich filtrate after 5 min incubation with compounds at varying concentrations or DMSO. Filtrates were produced from the indicated strains. At least two biological replicates were performed.

interfering with the fluorescence of the dye) by staining heat-killed worms in the presence of the compounds (**Supplementary Figure S4**). As expected, staining was unaffected.

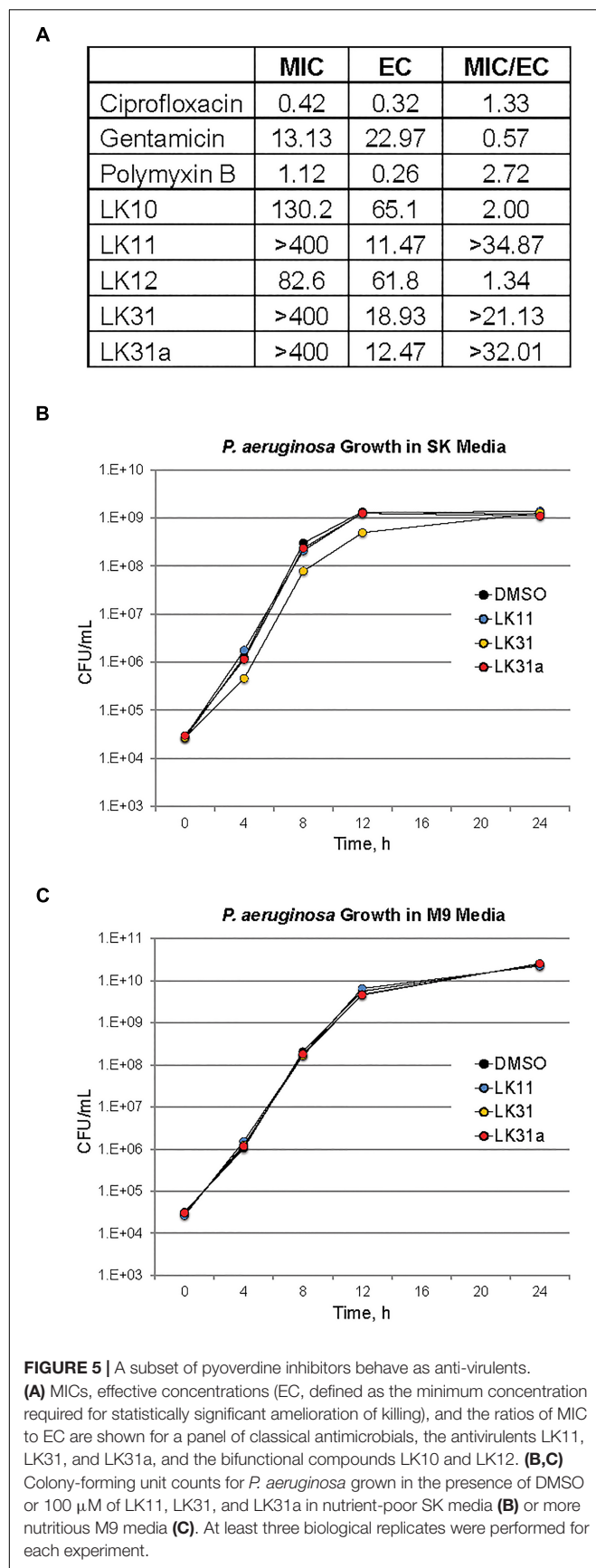
Anti-pyoverdine Compounds Specifically Minimize Pyoverdine Toxicity

We confirmed that LK11, LK31, and LK31a reduced bacterial virulence in *C. elegans*. As expected, all three compounds showed a strong, dose-dependent impact, limiting pathogenesis in the mid-micromolar range (**Figure 7A**). Based on our observations, these compounds are most likely functioning largely or entirely by limiting pyoverdine-mediated virulence. To further test this assertion, we measured the expression of pyoverdine-responsive genes (Kang et al., 2018) in *C. elegans* exposed to *P. aeruginosa* in the presence of LK11, LK31, LK31a, or DMSO. Upregulation of these genes was significantly diminished (**Figure 7B**) indicating that the toxicity of pyoverdine has been substantially blunted.

As noted above, iron-bound pyoverdine releases the alternative sigma factor PvdS from its sequestration at the plasma membrane, promoting the expression of several products, including itself, ToxA, and the protease PrpL (Ochsner et al., 1996; Wilderman et al., 2001; Lamont et al., 2002). If the compounds in question are compromising

pyoverdine function, we would expect transcription of these genes to be repressed in their presence. To test this, we assessed expression of PvdS-dependent genes (including *pvdS*, *pvdA*, *pvdE*, *pvdF*, *toxA*, and *prpL*) in *P. aeruginosa* PA14 grown in the presence of either DMSO, LK31, or LK31a, and observed that the compounds reduced their expression (**Supplementary Figure S5**). We also examined the expression of genes involved in pyochelin biosynthesis as a control. These genes were unaffected by treatment, as would be expected.

Although the anti-pyoverdine compounds LK11, LK31, and LK31a clearly quench pyoverdine fluorescence, reduce pyoverdine toxicity, and significantly decrease the pathogenesis of *P. aeruginosa*, it is formally possible that these phenomena are unrelated and that virulence attenuation is due to some other mechanism. The most straightforward way to test this is to assay whether the compounds mitigate *P. aeruginosa*-mediated virulence caused by a pyoverdine biosynthesis mutant. Pyoverdine mutants produce little to no pyoverdine and exhibit substantially reduced rates of killing *C. elegans* (Kirienko et al., 2013). We evaluated the ability of the *P. aeruginosa* PA14*pvdF* mutant strain to kill *C. elegans* when LK11, LK31, or LK31a are added. With the exception of the highest concentration tested (7- to 10-fold higher than the calculated EC), the compounds

**TABLE 2** | Chemical properties of pyoverdine inhibitors.

Molecule	MW, Da	LogP	Polar area	H Bond donor	H Bond acceptor	Rotatable bonds
LK11	264.2	2.1	68.3	0	4	0
LK31	253.4	2.9	73.8	0	4	2
LK31a	278.4	2.9	97.6	0	5	2
Goal	<500	-0.4...5.6	<1	<5	<10	<10

had little to no effect on the ability of the mutant strain to kill *C. elegans* (Figure 7C).

Anti-pyoverdine Compounds Synergize With Antibacterial Agents

In addition to serving as monotherapies, antivirulent drugs also have the potential to be included in therapeutic “cocktails” of multiple drugs that have synergistic activities. For example, the combination of pyoverdine inhibitors (to mitigate siderophore toxicity) and bacteriostatic or bactericidal drugs (to limit bacterial growth) is likely to be more effective than either drug alone. This is particularly due to pyoverdine’s ability to support other virulence factors, such as biofilms (reviewed in Kang and Kirienko, 2018). We predicted that the combination of an anti-pyoverdine like LK11, LK31, or LK31a with gentamicin would result in increased treatment efficiency in Liquid Killing when compared to antibiotic alone. To test this, we exposed worms to *P. aeruginosa* for 24 h and then added either antibiotic alone or antibiotic and an anti-pyoverdine compound. All three hit compounds showed a synergistic effect compared to antibiotic alone (Figure 8).

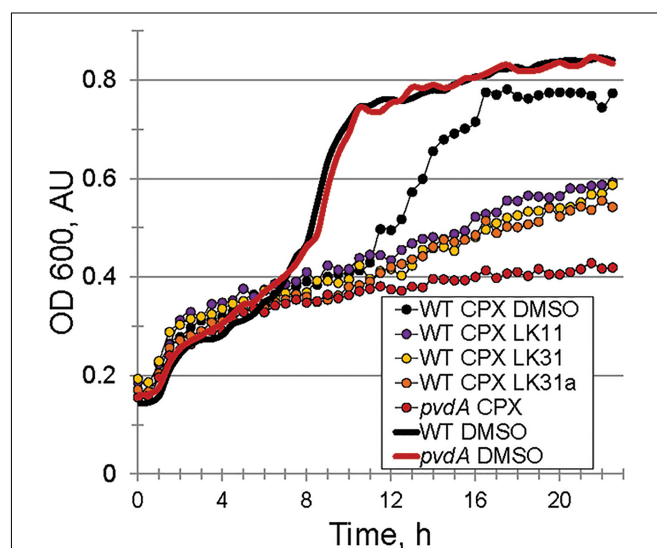


FIGURE 6 | Pyoverdine inhibitors disrupt bacterial growth under iron-limiting condition. Growth curves of WT *P. aeruginosa* PA14 and PA14pvdA. Iron limitation was induced by the presence of 6.5 μ M ciprofloxacin (CPX), an iron (III) chelator. DMSO or compounds were added at 100 μ M. Three biological replicates were performed.

TABLE 3 | Pyoverdine inhibitors do not trigger overt host defense response.

	LK11	LK31	LK31a	CPX
>3, <10	4	8	8	24
>10, <50	0	2	2	10
>50	0	0	0	5
Sum up	4	10	10	39
% Up	3.5	8.7	8.7	33.9

CPX – ciclopirox olamine, iron chelator. The number shown represents the number of genes in each category. Sum up – total number of upregulated genes. % Up – percentage of upregulated genes (out of 115 total).

DISCUSSION

Possible Mechanisms for Anti-pyoverdine Compounds

We observed that anti-pyoverdine compounds can quench the fluorescence of pyoverdine in cell-free filtrates, limit the expression of pyoverdine-dependent genes, and improve *C. elegans* survival after exposure to *P. aeruginosa* strain PA14. It is worth noting that, although they are effective at conferring resistance to pyoverdine, they do not completely abolish its activity, and are unlikely to compromise pyoverdine biosynthesis. This distinction is important for two reasons. First, non-vaccine treatments for bacterial pathogens need to be effective when used after infection. Second, *P. aeruginosa* recycles and reuses pyoverdine (Greenwald et al., 2007; Imperi et al., 2009). After import, oxidoreductases act upon ferripyoverdine to reduce iron (III) to iron (II), lowering the siderophore's affinity for the metal. This facilitates the non-destructive removal of iron. Afterward, iron-free pyoverdine is exported to continue its activities, including inflicting additional damage and promoting toxin expression. For these reasons, preventing the biosynthesis of pyoverdine is less desirable than compromising its activity.

It remains an open question how LK11, LK31, and LK31a interact with pyoverdine. The simplest explanation for our observations is that these compounds bind to the conserved dihydroxyquinoline chromophore. This would explain the ability of the molecules to quench pyoverdine fluorescence, which is dependent upon this region of the molecule. It would also explain how the compounds can effectively quench the fluorescence of such disparate pyoverdines. Unfortunately, it is difficult to rule out the possibility that the compounds are binding the peptide sidechains. The short length of these chains (generally between 8 and 15 amino acids) may limit the biophysical interactions that generally drive protein folding. As such, these peptide sequences could exhibit conformational similarities despite differences in primary sequence.

These compounds also restrict the production of pyoverdine-dependent virulence factors, including exotoxin A, the protease PrpL, and pyoverdine itself. Although we have not formally demonstrated that the pyoverdine-compound complex is incapable of binding to the FpvA receptor or that it prevents the release of PvdS from subcellular sequestration, the qRT-PCR data indicate that PvdS-mediated transcription is significantly reduced after compound treatment (**Supplementary Figure S5**).

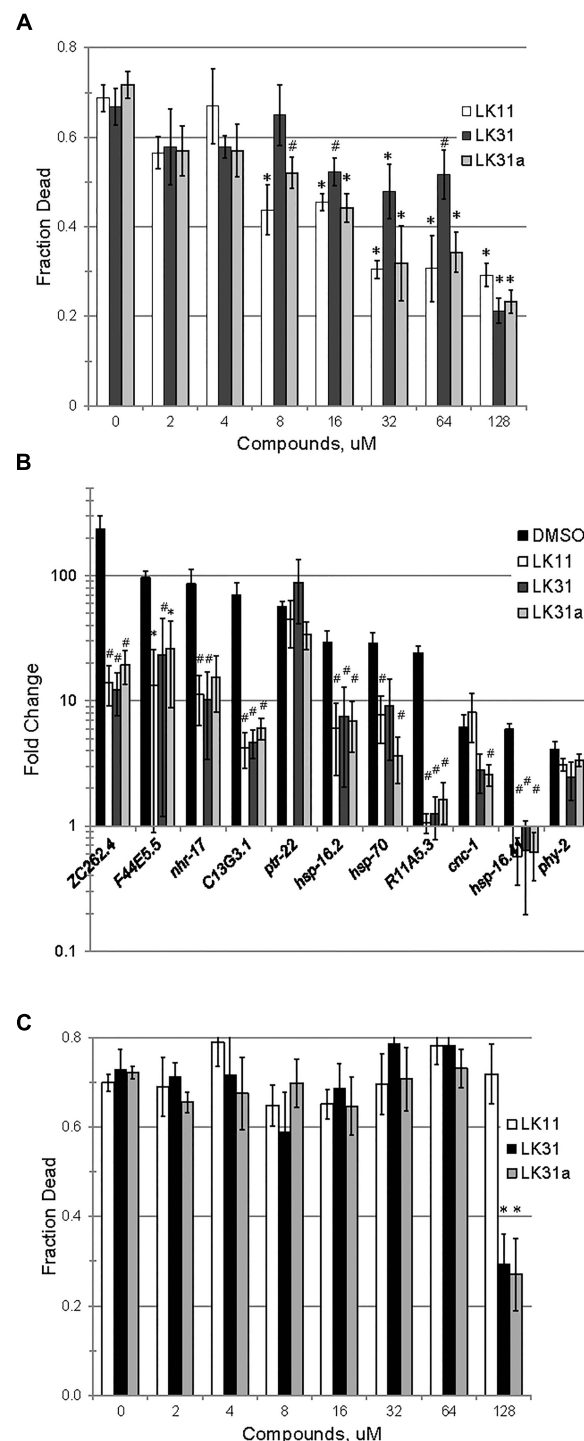
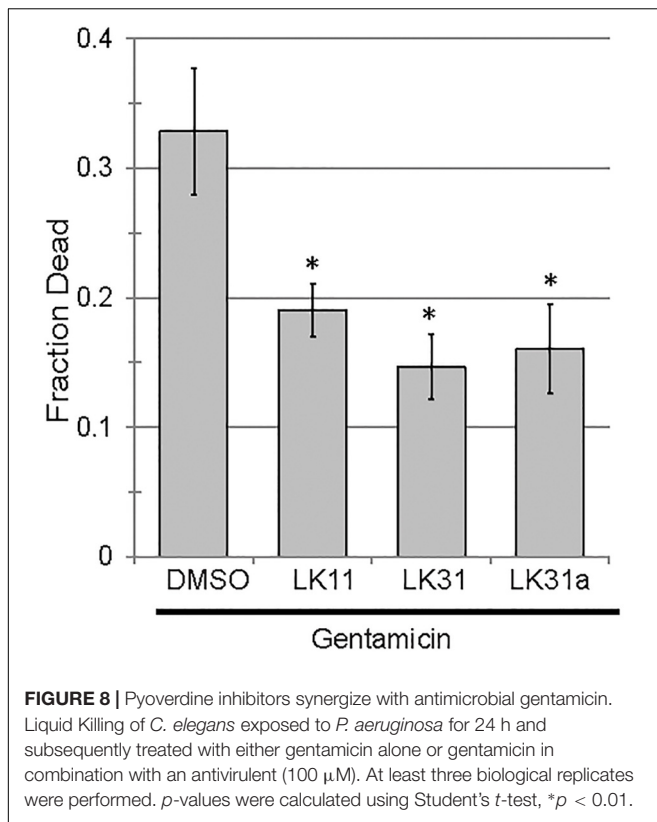


FIGURE 7 | LK11, LK31, and LK31a inhibit pyoverdine-mediated pathology. **(A)** Liquid Killing of *C. elegans* was assayed in the presence of varying doses of LK11, LK31, and LK31a. **(B)** qRT-PCR showing expression of a panel of genes upregulated by pyoverdine exposure during Liquid Killing of *C. elegans* treated with LK11, LK31, or LK31a (100 μ M). **(C)** Liquid Killing of *C. elegans* exposed to *P. aeruginosa* strain PA14pvdF, which is defective in pyoverdine biosynthesis, and treated with LK11, LK31, or LK31a at the concentrations indicated. At least three biological replicates were performed for **A–C**. *p*-values were calculated using Student's *t*-test, **p* < 0.01, #*p* < 0.05.



The most parsimonious explanation for this is that the compounds have prevented one or more of these feed-forward steps. This demonstrates the power of anti-virulents and validates pyoverdine as a target, since even these non-optimized hits show considerable potential to alleviate virulence in this model. The next step will be to test their ability to limit pathogenesis in a more complex host.

The other matter that remains to be resolved is whether the compounds preclude pyoverdine from binding iron. As demonstrated with ciclopirox olamine, these compounds are likely to transition from anti-virulents to antimicrobials under strict iron limitation, which is likely to be the case in most hosts, including humans. Anti-virulents are very desirable because they are anticipated to reduce the evolutionary pressure to acquire resistance. As such, it is undesirable for the pathogen to transition to a state where they act as antimicrobials. Ultimately, however, this difference may be somewhat academic. Virulence is a complex trait, associated with the expression of a wide variety of genes and the establishment of a specific homeostatic state in the pathogen. Using small molecules to meddle with this state could easily disrupt the pathogen's ability to survive or reproduce, with unpredictable consequences that are likely to depend upon the nature of the resistance that arises (Allen et al., 2014; Rezzoagli et al., 2018).

One possible outcome is that disrupting pyoverdine would stimulate increased production of alternative iron acquisition systems, like pyochelin. It is difficult to predict what effect this would have on virulence; typically, pyochelin is generally

reported to be dispensable for virulence in mammalian systems, especially when pyoverdine biosynthesis is intact (Takase et al., 2000; Minandri et al., 2016).

A less likely, but not disproven, possibility is that the compounds are preventing pyoverdine from carrying out its other activities without compromising its ability to bind iron. For example, previous reports have shown that pyoverdine inflicts considerable damage on mitochondria and activates mitochondrial surveillance pathways (Kirienko et al., 2015; Tjahjono and Kirienko, 2017; Kang et al., 2018). This almost certainly requires that the siderophore traverses the plasma membrane, both to directly acquire the iron that it removes as well as to bring it back to the pathogen. This is consistent with prior data from our lab that showed the pyoverdine removed iron from the host (Kang et al., 2018). This directly contrasts with another iron chelator, phenanthroline, which caused similar damage by chelating iron, but did not leave *C. elegans*. If the compounds are interfering with the ability of the siderophore to enter or exit host cells, virulence would be compromised in Liquid Killing, but iron acquisition in normal media would probably be unaffected.

Other Methods to Target Pyoverdine

The contributions of pyoverdine cytotoxicity to mammalian pathology remain important and unresolved, but pyoverdine clearly represents a valuable therapeutic target. To date, several approaches have been taken to target the pyoverdine siderophore system. Based on work by the Quax Lab (Nadal Jimenez et al., 2010), several groups have targeted PvdQ, which is required for pyoverdine maturation. The Gulick Lab carried out a high-throughput screen to identify small molecule inhibitors, and found a biaryl nitrile inhibitor of PvdQ (Drake and Gulick, 2011; Wurst et al., 2014). Other hits were identified by the Schreiber labs (Theriault et al., 2010) and a boronated alkyl chain by the Fast lab (Clevenger et al., 2013).

Interestingly, the biaryl nitrile inhibitor appears to synergize with a second class of pyoverdine inhibitors, fluoropyrimidines (Wurst et al., 2014). These compounds, including 5-fluorocytosine (5-FC) and 5-fluorouridine (5-FU) have been shown to compromise pyoverdine biosynthesis (Imperi et al., 2013; Costabile et al., 2016; Kirienko et al., 2016). Normally used as an antifungal, 5-FC has proven to be an effective method to inhibit *pvdS* expression (Imperi et al., 2013). This sigma factor is necessary for expression of the biosynthetic machinery that produces pyoverdine (Lamont et al., 2002). Suppression of *pvdS* in this fashion is sufficient to mediate rescue in *C. elegans* and in mice (Imperi et al., 2013; Kirienko et al., 2016). Interestingly, the mechanism of action remains unknown, but appears to require conversion of 5-FC to the well-known chemotherapeutic 5-fluorouracil (Imperi et al., 2013). From there, the drug is further metabolized to 5-fluorouridine (Kirienko et al., 2016). It remains unclear how this latter disrupts pyoverdine biosynthesis. Nevertheless, while fluoropyrimidines may serve as drugs of last resort for patients infected with pandrug-resistant *P. aeruginosa*, their profound cytotoxicity would appear to limit the potential of these therapies.

Another widely explored approach is to directly target pyoverdine by adding gallium (III) to the system to compete with Fe^{3+} . Although the ionic radii of Ga^{3+} and Fe^{3+} are nearly identical, and most proteins that use Fe^{3+} as a cofactor can incorporate Ga^{3+} , gallium is redox inactive under biological conditions. Since the removal of Fe^{3+} from pyoverdine requires its reduction to Fe^{2+} , Ga^{3+} becomes irreversibly bound to pyoverdine. Tests in animal models show that gallium can disrupt *P. aeruginosa* growth and inhibit biofilm formation (Kaneko et al., 2007; Banin et al., 2008; DeLeon et al., 2009). Unfortunately, Ga^{3+} has proven less effective in human serum, as elegant work by Paolo Visca's group demonstrated that the combination of *P. aeruginosa* proteases and pyoverdine's capacity for removing iron from host proteins facilitated pathogen growth, even in the presence of maximally achievable concentrations of Ga^{3+} (Bonchi et al., 2015). Although it remains an open question whether gallium will be more effective in human pulmonary environments, the promise of the early results is tempered by these findings. Some available evidence also suggests that gallium-bound pyoverdine still triggers the production of most pyoverdine-dependent virulence factors (Garcia-Contreras et al., 2014), although others have not seen this effect (Rezzoagli et al., 2018). Several other concerns, such as the immunosuppressive effect of Ga^{3+} and the difficulty of effectively using gallium as a treatment after the establishment of an infection (as opposed to pre-treatment or simultaneous treatment, as was used in most model assays) have also been expressed (Minandri et al., 2014).

Although none of the antivirulents described for *P. aeruginosa* are ready for clinical use, it is quite clear that new treatments, especially those that are not conventional antimicrobials, are urgently needed. Pyoverdine represents an invaluable target, due to its direct toxicity, position at the crux of nutrient acquisition, and regulation of virulence factors. Accordingly, it is likely that it will be an important target for chemical intervention. The antivirulents in this paper demonstrate proof of principle for

targeting pyoverdine's function, rather than its synthesis. They also represent promising fragments for lead generation and will serve as useful tool compounds for new *P. aeruginosa* discovery.

AUTHOR CONTRIBUTIONS

All authors designed and performed the experiments, analyzed the results, edited the manuscript, and were aware of this submission. NK supervised the project. DKi wrote the first draft. NK acquired funding.

FUNDING

This study was supported by the National Institute of Health grants K22AI110552 and R35GM129294, by the Welch Foundation grant C-1930, and the Cancer Prevention and Research Institute of Texas grant RR150044 awarded to NK. The funders had no role in study design, data collection and analysis, decision to publish, or preparation of the manuscript.

ACKNOWLEDGMENTS

Pseudomonas fluorescens strain WGS365 was a gift of Dr. Cara Haney, University of British Columbia. *E. faecalis* OG1RF was a gift of Dr. Danielle Garsin, University of Texas, McGovern Medical School.

SUPPLEMENTARY MATERIAL

The Supplementary Material for this article can be found online at: <https://www.frontiersin.org/articles/10.3389/fmicb.2018.03317/full#supplementary-material>

REFERENCES

- Aires, J. R., Köhler, T., Nikaido, H., and Plésiat, P. (1999). Involvement of an active efflux system in the natural resistance of *Pseudomonas aeruginosa* to aminoglycosides. *Antimicrob. Agents Chemother.* 43, 2624–2628. doi: 10.1128/AAC.43.11.2624
- Allen, R. C., Popat, R., Diggle, S. P., and Brown, S. P. (2014). Targeting virulence: can we make evolution-proof drugs? *Nat. Rev. Microbiol.* 12, 300–308. doi: 10.1038/nrmicro3232
- Anderson, G. G., and O'Toole, G. A. (2008). Innate and induced resistance mechanisms of bacterial biofilms. *Curr. Top. Microbiol. Immunol.* 322, 85–105. doi: 10.1007/978-3-540-75418-3_5
- Anderson, Q. L., Revtovich, A. V., and Kirienko, N. V. (2018). A high-throughput, high-content, liquid-based *C. elegans* pathosystem. *J. Vis. Exp.* 137:e58068. doi: 10.3791/58068
- Baell, J., and Walters, M. A. (2014). Chemistry: chemical con artists foil drug discovery. *Nature* 513, 481–483. doi: 10.1038/513481a
- Baell, J. B., and Holloway, G. A. (2010). New substructure filters for removal of pan assay interference compounds (PAINS) from screening libraries and for their exclusion in bioassays. *J. Med. Chem.* 53, 2719–2740. doi: 10.1021/jm901137j
- Banin, E., Lozinski, A., Brady, K. M., Berenshtein, E., Butterfield, P. W., Moshe, M., et al. (2008). The potential of desferrioxamine-gallium as an anti-*Pseudomonas* therapeutic agent. *Proc. Natl. Acad. Sci. U.S.A.* 105, 16761–16766. doi: 10.1073/pnas.0808608105
- Banin, E., Vasil, M. L., and Greenberg, E. P. (2005). Iron and *Pseudomonas aeruginosa* biofilm formation. *Proc. Natl. Acad. Sci. U.S.A.* 102, 11076–11081. doi: 10.1073/pnas.0504266102
- Beanan, M. J., and Strome, S. (1992). Characterization of a germ-line proliferation mutation in *C. elegans*. *Development* 116, 755–766.
- Beare, P. A., For, R. J., Martin, L. W., and Lamont, I. L. (2003). Siderophore-mediated cell signalling in *Pseudomonas aeruginosa*: divergent pathways regulate virulence factor production and siderophore receptor synthesis. *Mol. Microbiol.* 47, 195–207. doi: 10.1046/j.1365-2958.2003.03288.x
- Bonchi, C., Frangipani, E., Imperi, F., and Visca, P. (2015). Pyoverdine and proteases affect the response of *Pseudomonas aeruginosa* to gallium in human serum. *Antimicrob. Agents Chemother.* 59, 5641–5646. doi: 10.1128/AAC.01097-15
- Cezairliyan, B., Vinayavekhin, N., Grenfell-Lee, D., Yuen, G. J., Saghatelian, A., and Ausubel, F. M. (2013). Identification of *Pseudomonas aeruginosa* phenazines that kill *Caenorhabditis elegans*. *PLoS Pathog.* 9:e1003101. doi: 10.1371/journal.ppat.1003101
- Cheng, G., Sa, W., Cao, C., Guo, L., Hao, H., Liu, Z., et al. (2016). Quinoxaline 1,4-di-N-Oxides: biological activities and mechanisms of actions. *Front. Pharmacol.* 7:64. doi: 10.3389/fphar.2016.00064

- Clevenger, K. D., Wu, R., Er, J. A., Liu, D., and Fast, W. (2013). Rational design of a transition state analogue with picomolar affinity for *Pseudomonas aeruginosa* PvdQ, a siderophore biosynthetic enzyme. *ACS Chemical Biol.* 8, 2192–2200. doi: 10.1021/cb400345h
- Congreve, M., Carr, R., Murray, C., and Jhoti, H. (2003). A 'rule of three' for fragment-based lead discovery? *Drug Discov. Today* 8, 876–877. doi: 10.1016/S1359-6446(03)02831-9
- Costabile, G., d'Angelo, I., d'Emmanuele, di Villa, Bianca, R., Mitidieri, E., et al. (2016). Development of inhalable hyaluronan/mannitol composite dry powders for flucytosine repositioning in local therapy of lung infections. *J. Control Release* 238, 80–91. doi: 10.1016/j.jconrel.2016.07.029
- Cushnie, T. P., O'Driscoll, N. H., and Lamb, A. J. (2016). Morphological and ultrastructural changes in bacterial cells as an indicator of antibacterial mechanism of action. *Cell. Mol. Life Sci.* 73, 4471–4492. doi: 10.1007/s00018-016-2302-2
- D'Angelo, F., Baldelli, V., Halliday, N., Pantalone, P., Politicelli, F., Fiscarelli, E., et al. (2018). Identification of FDA-approved drugs as antivirulence agents targeting the pqs quorum-sensing system of *Pseudomonas aeruginosa*. *Antimicrob. Agents Chemother.* 62:e1296–18. doi: 10.1128/AAC.01296-18
- De Vos, D., De Chial, M., Cochez, C., Jansen, S., Tummeler, B., Meyer, J. M., et al. (2001). Study of pyoverdine type and production by *Pseudomonas aeruginosa* isolated from cystic fibrosis patients: prevalence of type II pyoverdine isolates and accumulation of pyoverdine-negative mutations. *Arch. Microbiol.* 175, 384–388. doi: 10.1007/s002030100278
- DeLeon, K., Balldin, F., Watters, C., Hamood, A., Griswold, J., Sreedharan, S., et al. (2009). Gallium maltolate treatment eradicates *Pseudomonas aeruginosa* infection in thermally injured mice. *Antimicrob. Agents Chemother.* 53, 1331–1337. doi: 10.1128/AAC.01330-08
- Doak, B. C., Norton, R. S., and Scanlon, M. J. (2016). The ways and means of fragment-based drug design. *Pharmacol. Ther.* 167, 28–37. doi: 10.1016/j.pharmthera.2016.07.003
- Dortet, L., Lombardi, C., Cretin, F., Dessen, A., and Filloux, A. (2018). Pore-forming activity of the *Pseudomonas aeruginosa* type III secretion system translocon alters the host epigenome. *Nat. Microbiol.* 3, 378–386. doi: 10.1038/s41564-018-0109-7
- Drake, E. J., and Gulick, A. M. (2011). Structural characterization and high-throughput screening of inhibitors of PvdQ, an NTN hydrolase involved in pyoverdine synthesis. *ACS Chem. Biol.* 6, 1277–1286. doi: 10.1021/cb2002973
- Fuchs, R., Schafer, M., Geoffroy, V., and Meyer, J. M. (2001). Siderotyping—a powerful tool for the characterization of pyoverdines. *Curr. Top. Med. Chem.* 1, 31–57. doi: 10.2174/1568026013395542
- Garcia-Contreras, R., Perez-Eretza, B., Lira-Silva, E., Jasso-Chavez, R., Coria-Jimenez, R., Rangel-Vega, A., et al. (2014). Gallium induces the production of virulence factors in *Pseudomonas aeruginosa*. *Pathog. Dis.* 70, 95–98. doi: 10.1111/2049-632X.12105
- Garsin, D. A., Sifri, C. D., Mylonakis, E., Qin, X., Singh, K. V., Murray, B. E., et al. (2001). A simple model host for identifying Gram-positive virulence factors. *Proc. Natl. Acad. Sci. U.S.A.* 98, 10892–10897. doi: 10.1073/pnas.191378698
- Geels, F. P., and Schippers, B. (1983). Reduction of yield depressions in high frequency potato cropping soil after seed tuber treatments with antagonistic fluorescent *Pseudomonas* spp. *J. Phytopathol.* 108, 207–214. doi: 10.1111/j.1439-0434.1983.tb00580.x
- Greenwald, J., Hoegy, F., Nader, M., Journet, L., Mislin, G. L., Graumann, P. L., et al. (2007). Real time fluorescent resonance energy transfer visualization of ferric pyoverdine uptake in *Pseudomonas aeruginosa*. A role for ferrous iron. *J. Biol. Chem.* 282, 2987–2995. doi: 10.1074/jbc.M609238200
- Holloway, B. W., Romling, U., and Tummeler, B. (1994). Genomic mapping of *Pseudomonas aeruginosa* PAO. *Microbiology* 140(Pt 11), 2907–2929. doi: 10.1099/13500872-140-11-2907
- Imperi, F., Leoni, L., and Visca, P. (2014). Antivirulence activity of azithromycin in *Pseudomonas aeruginosa*. *Front. Microbiol.* 5:178. doi: 10.3389/fmicb.2014.00178
- Imperi, F., Massai, F., Facchini, M., Frangipani, E., Visaggio, D., Leoni, L., et al. (2013). Repurposing the antimycotic drug flucytosine for suppression of *Pseudomonas aeruginosa* pathogenicity. *Proc. Natl. Acad. Sci. U.S.A.* 110, 7458–7463. doi: 10.1073/pnas.1222706110
- Imperi, F., Tiburzi, F., and Visca, P. (2009). Molecular basis of pyoverdine siderophore recycling in *Pseudomonas aeruginosa*. *Proc. Natl. Acad. Sci. U.S.A.* 106, 20440–20445. doi: 10.1073/pnas.0908760106
- Ismail, M. M., Amin, K. M., Noaman, E., Soliman, D. H., and Ammar, Y. A. (2010). New quinoxaline 1, 4-di-N-oxides: anticancer and hypoxia-selective therapeutic agents. *Eur. J. Med. Chem.* 45, 2733–2738. doi: 10.1016/j.ejmech.2010.02.052
- Kaneko, Y., Thoendel, M., Olakanmi, O., Britigan, B. E., and Singh, P. K. (2007). The transition metal gallium disrupts *Pseudomonas aeruginosa* iron metabolism and has antimicrobial and antibiofilm activity. *J. Clin. Invest.* 117, 877–888. doi: 10.1172/JCI30783
- Kang, D., Kirienko, D. R., Webster, P., Fisher, A. L., and Kirienko, N. V. (2018). Pyoverdine, a siderophore from *Pseudomonas aeruginosa*, translocates into *C. elegans*, removes iron, and activates a distinct host response. *Virulence* 9, 804–817. doi: 10.1080/21505594.2018.1449508
- Kang, D., and Kirienko, N. V. (2017). High-Throughput genetic screen reveals that early attachment and biofilm formation are necessary for full pyoverdine production by *Pseudomonas aeruginosa*. *Front. Microbiol.* 8:1707. doi: 10.3389/fmicb.2017.01707
- Kang, D., and Kirienko, N. V. (2018). Interdependence between iron acquisition and biofilm formation in *Pseudomonas aeruginosa*. *J. Microbiol.* 56, 449–457. doi: 10.1007/s12275-018-8114-3
- Kirienko, D. R., Revtovich, A. V., and Kirienko, N. V. (2016). A high-content, phenotypic screen identifies fluorouridine as an inhibitor of pyoverdine biosynthesis and *Pseudomonas aeruginosa* virulence. *mSphere* 1:e217–16. doi: 10.1128/mSphere.00217-16
- Kirienko, N. V., Ausubel, F. M., and Ruvkun, G. (2015). Mitophagy confers resistance to siderophore-mediated killing by *Pseudomonas aeruginosa*. *Proc. Natl. Acad. Sci. U.S.A.* 112, 1821–1826. doi: 10.1073/pnas.1424954112
- Kirienko, N. V., Cezairliyan, B. O., Ausubel, F. M., and Powell, J. R. (2014). *Pseudomonas aeruginosa* PA14 pathogenesis in caenorhabditis elegans. *Methods Mol. Biol.* 1149, 653–669. doi: 10.1007/978-1-4939-0473-0_50
- Kirienko, N. V., Kirienko, D. R., Larkins-Ford, J., Wählby, C., Ruvkun, G., and Ausubel, F. M. (2013). *Pseudomonas aeruginosa* disrupts caenorhabditis elegans iron homeostasis, causing a hypoxic response and death. *Cell Host Microbe* 13, 406–416. doi: 10.1016/j.chom.2013.03.003
- Kirienko, N. V., McEnerney, J. D., and Fay, D. S. (2008). Coordinated regulation of intestinal functions in *C. elegans* by LIN-35/Rb and SLR-2. *PLoS Genet.* 4:e1000059. doi: 10.1371/journal.pgen.1000059
- Köhler, T., Michéa-Hamzehpour, M., Henze, U., Gotoh, N., Curty, L. K., and Pechère, J. C. (1997). Characterization of MexE-MexF-OprN, a positively regulated multidrug efflux system of *Pseudomonas aeruginosa*. *Mol. Microbiol.* 23, 345–354. doi: 10.1046/j.1365-2958.1997.2281594.x
- Kon, K., and Rai, M. (2016). *Antibiotic Resistance: Mechanisms and New Antimicrobial Approaches*. Cambridge: Academic Press.
- Kuchma, S. L., Brothers, K. M., Merritt, J. H., Liberati, N. T., Ausubel, F. M., and O'Toole, G. A. (2007). BifA, a cyclic-Di-GMP phosphodiesterase, inversely regulates biofilm formation and swarming motility by *Pseudomonas aeruginosa* PA14. *J. Bacteriol.* 189, 8165–8178. doi: 10.1128/JB.00586-07
- Lamont, I. L., Beare, P. A., Ochsner, U., Vasil, A. I., and Vasil, M. L. (2002). Siderophore-mediated signaling regulates virulence factor production in *Pseudomonas aeruginosa*. *Proc. Natl. Acad. Sci. U.S.A.* 99, 7072–7077. doi: 10.1073/pnas.092016999
- Liberati, N. T., Urbach, J. M., Miyata, S., Lee, D. G., Drenkard, E., Wu, G., et al. (2006). An ordered, nonredundant library of *Pseudomonas aeruginosa* strain PA14 transposon insertion mutants. *Proc. Natl. Acad. Sci. U.S.A.* 103, 2833–2838. doi: 10.1073/pnas.0511100103
- Lipinski, C. A., Lombardo, F., Dominy, B. W., and Feeney, P. J. (2001). Experimental and computational approaches to estimate solubility and permeability in drug discovery and development settings. *Adv. Drug Deliv. Rev.* 46, 3–26. doi: 10.1016/S0169-409X(00)00129-0
- Liu, P. V., Matsumoto, H., Kusama, H., and Bergan, T. (1983). Survey of heat-stable, major somatic antigens of *Pseudomonas aeruginosa*. *Int. J. Syst. Bacteriol.* 33, 256–264. doi: 10.1099/00207713-33-2-256
- Lomovskaya, O., Warren, M. S., Lee, A., Galazzo, J., Fronko, R., Lee, M., et al. (2001). Identification and characterization of inhibitors of multidrug resistance efflux pumps in *Pseudomonas aeruginosa*: novel agents for combination therapy. *Antimicrob. Agents Chemother.* 45, 105–116. doi: 10.1128/AAC.45.1.105-116.2001

- Lopez-Medina, E., Fan, D., Coughlin, L. A., Ho, E. X., Lamont, I. L., Reimmann, C., et al. (2015). *Candida albicans* inhibits *Pseudomonas aeruginosa* virulence through suppression of pyochelin and pyoverdine biosynthesis. *PLoS Pathog.* 11:e1005129. doi: 10.1371/journal.ppat.1005129
- Mah, T. F., and O'Toole, G. A. (2001). Mechanisms of biofilm resistance to antimicrobial agents. *Trends Microbiol.* 9, 34–39. doi: 10.1016/S0966-842X(00)01913-2
- Managò, A., Becker, K. A., Carpinteiro, A., Wilker, B., Soddemann, M., Seitz, A. P., et al. (2015). *Pseudomonas aeruginosa* pyocyanin induces neutrophil death via mitochondrial reactive oxygen species and mitochondrial acid sphingomyelinase. *Antioxid. Redox Signal.* 22, 1097–1110. doi: 10.1089/ars.2014.5979
- Medeiros, A. A., O'Brien, T. F., Wacker, W. E., and Yulug, N. F. (1971). Effect of salt concentration on the apparent in-vitro susceptibility of *Pseudomonas* and other gram-negative bacilli to gentamicin. *J. Infect. Dis.* 124(Suppl.), S59–S64. doi: 10.1093/infdis/124.Supplement_1.S59
- Meyer, J. M., Geoffroy, V. A., Baida, N., Gardan, L., Izard, D., Lemanceau, P., et al. (2002). Siderophore typing, a powerful tool for the identification of fluorescent and nonfluorescent pseudomonads. *Appl. Environ. Microbiol.* 68, 2745–2753. doi: 10.1128/AEM.68.6.2745-2753.2002
- Meyer, J. M., Neely, A., Stintzi, A., Georges, C., and Holder, I. A. (1996). Pyoverdine is essential for virulence of *Pseudomonas aeruginosa*. *Infect. Immun.* 64, 518–523.
- Meyer, J. M., Stintzi, A., Coulanges, V., Shivaji, S., Voss, J. A., Taraz, K., et al. (1998). Siderotyping of fluorescent pseudomonads: characterization of pyoverdines of *Pseudomonas fluorescens* and *Pseudomonas putida* strains from Antarctica. *Microbiology* 144(Pt 11), 3119–3126.
- Meyer, J. M., Stintzi, A., De Vos, D., Cornelis, P., Tappe, R., Taraz, K., et al. (1997). Use of siderophores to type pseudomonads: the three *Pseudomonas aeruginosa* pyoverdine systems. *Microbiology* 143(Pt 1), 35–43. doi: 10.1099/00221287-143-1-35
- Minandri, F., Bonchi, C., Frangipani, E., Imperi, F., and Visca, P. (2014). Promises and failures of gallium as an antibacterial agent. *Future Microbiol.* 9, 379–397. doi: 10.2217/fmb.14.3
- Minandri, F., Imperi, F., Frangipani, E., Bonchi, C., Visaggio, D., Facchini, M., et al. (2016). Role of iron uptake systems in *Pseudomonas aeruginosa* virulence and airway infection. *Infect. Immun.* 84, 2324–2335. doi: 10.1128/IAI.00098-16
- Murray, C. W., and Rees, D. C. (2009). The rise of fragment-based drug discovery. *Nat. Chem.* 1, 187–192. doi: 10.1038/nchem.217
- Nadal Jimenez, P., Koch, G., Papaioannou, E., Wahjudi, M., Krzeslak, J., Coenye, T., et al. (2010). Role of PvdQ in *Pseudomonas aeruginosa* virulence under iron-limiting conditions. *Microbiology* 156, 49–59. doi: 10.1099/mic.0.030973-0
- Ochsner, U. A., Johnson, Z., Lamont, I. L., Cunliffe, H. E., and Vasil, M. L. (1996). Exotoxin A production in *Pseudomonas aeruginosa* requires the iron-regulated pvdS gene encoding an alternative sigma factor. *Mol. Microbiol.* 21, 1019–1028. doi: 10.1046/j.1365-2958.1996.481425.x
- Paczkowski, J. E., Mukherjee, S., McCready, A. R., Cong, J. P., Aquino, C. J., Kim, H., et al. (2017). Flavonoids suppress *Pseudomonas aeruginosa* virulence through allosteric inhibition of quorum-sensing receptors. *J. Biol. Chem.* 292, 4064–4076. doi: 10.1074/jbc.M116.770552
- Poole, K., Gotoh, N., Tsujimoto, H., Zhao, Q., Wada, A., Yamasaki, T., et al. (1996). Overexpression of the mexC-mexD-opr efflux operon in nfxB-type multidrug-resistant strains of *Pseudomonas aeruginosa*. *Mol. Microbiol.* 21, 713–724. doi: 10.1046/j.1365-2958.1996.281397.x
- Poole, K., Krebs, K., McNally, C., and Neshat, S. (1993). Multiple antibiotic resistance in *Pseudomonas aeruginosa*: evidence for involvement of an efflux operon. *J. Bacteriol.* 175, 7363–7372. doi: 10.1128/jb.175.22.7363-7372.1993
- Pukkila-Worley, R., Feinbaum, R., Kirienko, N. V., Larkins-Ford, J., Conery, A. L., and Ausubel, F. M. (2012). Stimulation of host immune defenses by a small molecule protects *C. elegans* from bacterial infection. *PLoS Genet.* 8:e1002733. doi: 10.1371/journal.pgen.1002733
- Rahme, L. G., Stevens, E. J., Wolford, S. F., Shao, J., Tompkins, R. G., and Ausubel, F. M. (1995). Common virulence factors for bacterial pathogenicity in plants and animals. *Science* 268, 1899–1902. doi: 10.1126/science.7604262
- Rezzoagli, C., Wilson, D., Weigert, M., Wyder, S., and Kummerli, R. (2018). Probing the evolutionary robustness of two repurposed drugs targeting iron uptake in *Pseudomonas aeruginosa*. *Evol. Med. Public Health* 2018, 246–259. doi: 10.1093/emph/eoy026
- Saliba, A. M., Filloux, A., Ball, G., Silva, A. S., Assis, M. C., and Plotkowski, M. C. (2002). Type III secretion-mediated killing of endothelial cells by *Pseudomonas aeruginosa*. *Microb. Pathog.* 33, 153–166. doi: 10.1016/S0882-4010(02)90522-X
- Shanks, R. M., Caiazza, N. C., Hinsa, S. M., Toutain, C. M., and O'Toole, G. A. (2006). Saccharomyces cerevisiae-based molecular tool kit for manipulation of genes from gram-negative bacteria. *Appl. Environ. Microbiol.* 72, 5027–5036. doi: 10.1128/AEM.00682-06
- Stiernagle, T. (2006). *Maintenance of C. elegans*. *WormBook: the online review of C. elegans biology*. Minneapolis, MN: University of Minnesota.
- Suzuki, H., Pangborn, J., and Kilgore, W. W. (1967). Filamentous cells of *Escherichia coli* formed in the presence of mitomycin. *J. Bacteriol.* 93, 683–688.
- Takase, H., Nitanai, H., Hoshino, K., and Otani, T. (2000). Impact of siderophore production on *Pseudomonas aeruginosa* infections in immunosuppressed mice. *Infect. Immun.* 68, 1834–1839. doi: 10.1128/IAI.68.4.1834-1839.2000
- Tan, S. Y., Chua, S. L., Chen, Y., Rice, S. A., Kjelleberg, S., Nielsen, T. E., et al. (2013). Identification of five structurally unrelated quorum-sensing inhibitors of *Pseudomonas aeruginosa* from a natural-derivative database. *Antimicrob. Agents Chemother.* 57, 5629–5641. doi: 10.1128/AAC.00955-13
- Theriat, J. R., Wurst, J., Jewett, I., Verplank, L., Perez, J. R., Gulick, A. M., et al. (2010). "Identification of a small molecule inhibitor of *Pseudomonas aeruginosa* PvdQ acylase, an enzyme involved in siderophore pyoverdine synthesis," in *Probe Reports from the NIH Molecular Libraries Program*, (Bethesda MD: National Center for Biotechnology Information).
- Tjahjono, E., and Kirienko, N. V. (2017). A conserved mitochondrial surveillance pathway is required for defense against *Pseudomonas aeruginosa*. *PLoS Genet.* 13:e1006876. doi: 10.1371/journal.pgen.1006876
- van Tilburg Bernardes, E., Charron-Mazenod, L., Reading, D. J., Reckseidler-Zenteno, S. L., and Lewenza, S. (2017). Exopolysaccharide-repressing small molecules with antibiofilm and antivirulence activity against *Pseudomonas aeruginosa*. *Antimicrob. Agents Chemother.* 61:e1997–16. doi: 10.1128/AAC.01997-16
- Vandeputte, O. M., Kiendrebego, M., Rasamiravaka, T., Stévigny, C., Duez, P., Rajaonson, S., et al. (2011). The flavanone naringenin reduces the production of quorum sensing-controlled virulence factors in *Pseudomonas aeruginosa* PAO1. *Microbiology* 157, 2120–2132. doi: 10.1099/mic.0.049338-0
- Walker, J. R., and Pardee, A. B. (1968). Evidence for a relationship between deoxyribonucleic acid metabolism and septum formation in *Escherichia coli*. *J. Bacteriol.* 95, 123–131.
- Wilderman, P. J., Vasil, A. I., Johnson, Z., Wilson, M. J., Cunliffe, H. E., Lamont, I. L., et al. (2001). Characterization of an endoprotease (PrpL) encoded by a PvdS-regulated gene in *Pseudomonas aeruginosa*. *Infect. Immun.* 69, 5385–5394. doi: 10.1128/IAI.69.9.5385-5394.2001
- Wurst, J. M., Drake, E. J., Theriat, J. R., Jewett, I. T., VerPlank, L., Perez, J. R., et al. (2014). Identification of inhibitors of PvdQ, an enzyme involved in the synthesis of the siderophore pyoverdine. *ACS Chem. Biol.* 9, 1536–1544. doi: 10.1021/cb5001586
- Xiao, R., and Kisaalita, W. S. (1997). Iron acquisition from transferrin and lactoferrin by *Pseudomonas aeruginosa* pyoverdine. *Microbiology* 143(Pt 7), 2509–2515. doi: 10.1099/00221287-143-7-2509
- Yabuuchi, E., and Ohya, A. (1972). Characterization of "Pyomelanin"-Producing Strains of *Pseudomonas aeruginosa*. *Int. J. Syst. Bacteriol.* 22, 53–64. doi: 10.1099/00207713-22-2-53

Conflict of Interest Statement: The authors declare that the research was conducted in the absence of any commercial or financial relationships that could be construed as a potential conflict of interest.

Copyright © 2019 Kirienko, Kang and Kirienko. This is an open-access article distributed under the terms of the Creative Commons Attribution License (CC BY). The use, distribution or reproduction in other forums is permitted, provided the original author(s) and the copyright owner(s) are credited and that the original publication in this journal is cited, in accordance with accepted academic practice. No use, distribution or reproduction is permitted which does not comply with these terms.



Exploiting the Richness of Environmental Waterborne Bacterial Species to Find Natural *Legionella pneumophila* Competitors

Marie-Hélène Corre, Vincent Delafont, Anasthasia Legrand, Jean-Marc Berjeaud and Julien Verdon*

Laboratoire Ecologie et Biologie des Interactions, UMR CNRS 7267, Université de Poitiers, Poitiers, France

OPEN ACCESS

Edited by:

Natalia V. Kiriienko,
Rice University, United States

Reviewed by:

Sebastien P. Faucher,
McGill University, Canada
Marina Santic',
University of Rijeka, Croatia

*Correspondence:

Julien Verdon
julien.verdon@univ-poitiers.fr

Specialty section:

This article was submitted to
Antimicrobials, Resistance
and Chemotherapy,
a section of the journal
Frontiers in Microbiology

Received: 26 October 2018

Accepted: 31 December 2018

Published: 15 January 2019

Citation:

Corre M-H, Delafont V, Legrand A,
Berjeaud J-M and Verdon J (2019)
Exploiting the Richness
of Environmental Waterborne
Bacterial Species to Find Natural
Legionella pneumophila Competitors.
Front. Microbiol. 9:3360.
doi: 10.3389/fmicb.2018.03360

Legionella pneumophila is one of the most tracked waterborne pathogens and remains an important threat to human health. Despite the use of biocides, *L. pneumophila* is able to persist in engineered water systems with the help of multispecies biofilms and phagocytic protists. For few years now, high-throughput sequencing methods have enabled a better understanding of microbial communities in freshwater environments. Those unexplored and complex communities compete for nutrients using antagonistic molecules as war weapons. Up to now, few of these molecules were characterized in regards of *L. pneumophila* sensitivity. In this context, we established, from five freshwater environments, a vast collection of culturable bacteria and investigated their ability to inhibit the growth of *L. pneumophila*. All bacterial isolates were classified within 4 phyla, namely Proteobacteria (179/273), Bacteroidetes (48/273), Firmicutes (43/273), and Actinobacteria (3/273) according to 16S rRNA coding sequences. *Aeromonas*, *Bacillus*, *Flavobacterium*, and *Pseudomonas* were the most abundant genera (154/273). Among the 273 isolates, 178 (65.2%) were shown to be active against *L. pneumophila* including 137 isolates of the four previously cited main genera. Additionally, other less represented genera depicted anti-*Legionella* activity such as *Acinetobacter*, *Kluyvera*, *Rahnella*, or *Sphingobacterium*. Furthermore, various inhibition diameters were observed among active isolates, ranging from 0.4 to 9 cm. Such variability suggests the presence of numerous and diverse natural compounds in the microenvironment of *L. pneumophila*. These molecules include both diffusible secreted compounds and volatile organic compounds, the latter being mainly produced by *Pseudomonas* strains. Altogether, this work sheds light on unexplored freshwater bacterial communities that could be relevant for the biological control of *L. pneumophila* in manmade water systems.

Keywords: *Legionella*, freshwater environments, *Pseudomonas*, bacterial community, inhibition profile, volatile organic compound, antimicrobials

INTRODUCTION

Water is essential to sustain life and granting free access to drinking-water is considered a basic human right. Therefore, water sources used for human consumption must be biologically safe, to avoid any risk for health. Indeed, the most common and widespread health risk associated with drinking water is represented by infectious diseases caused by pathogenic bacteria, viruses

and parasites (World Health Organization, 2011). Most waterborne pathogens are introduced into drinking water supplies by the classic fecal-water-oral route of transmission (Ashbolt, 2015). However, other non-fecal but potentially pathogenic microorganisms like *Legionella* sp., non-tuberculous mycobacteria, *Pseudomonas aeruginosa* or free-living amoebae, may colonize engineered water systems (Falkinham et al., 2015b; Wang et al., 2017). In hot water systems and cooling towers, bacteria of the genus *Legionella* represent a particular concern and remain one of the most tracked agents, being considered as opportunistic premise plumbing pathogens (Falkinham et al., 2015a). They are part of the natural flora in many freshwater environments (i.e., rivers, streams) where they occur in relatively low numbers (Declerck et al., 2009; Declerck, 2010). *L. pneumophila* is recognized as responsible for Legionnaires' disease (LD), a life-threatening pneumonia, and a mild form of illness named Pontiac fever (Diederer, 2008). Furthermore, the serogroup 1 is responsible for 82.9% of the LD cases in Europe (Beauté, 2017; Hamilton et al., 2018) and for over 80% of the cases worldwide (Yu et al., 2002; Newton et al., 2010). Species other than *pneumophila* account usually for less than 10% of human infections, and mostly involve *L. micdadei*, *L. bozemanii*, and *L. longbeachae* (Beauté, 2017). Some water safety plans in distribution systems, recommended by the World Health Organization, were implemented (Parr et al., 2015) such as the one published by the ASHRAE (American Society of Heating, Refrigerating, and Air-Conditioning Engineers) in 2015. This plan focuses on hazards and hazardous events for implementing control measures which aim at avoiding *Legionella* transmission and limiting its proliferation (American Society of Heating Refrigerating and Air-Conditioning Engineers, 2015).

Persistence and colonization of *Legionella* sp. in engineered water systems is mediated by the presence of multispecies biofilms and protists like free-living amoebae (Abu Khweek and Amer, 2018). Moreover, protists serve as a natural playground for *L. pneumophila*, "training" bacteria to resist phagocytic destruction (Boamah et al., 2017). The cozy intracellular microenvironment provided by protists host cells also protects *L. pneumophila* from adverse environmental conditions representing as well a nutrient-rich replicative niche. Indeed, this intracellular lifestyle protects bacteria from being efficiently killed by water disinfection procedures (Dupuy et al., 2011). However, as mentioned by the French law n° 2009-967 (2009/08/03) adopted from discussions of the "Grenelle de l'environnement," the control of disinfection by-products must be improved in order to avoid or limit exposure to potentially undesirable chemicals while maintaining a safe water sanitation process. In line with this aim, the description of new natural antibacterial agents active against *L. pneumophila* is a promising strategy.

To date, few studies have shown that various natural compounds efficiently inhibit *L. pneumophila* growth (for recent review, see Berjeaud et al., 2016). However, those compounds, mainly antimicrobial peptides and components of essential oils, don't originate from the microenvironment of *L. pneumophila*. The survival of *L. pneumophila* in water

environments, aside from being sheltered within protists, is also driven by interactions with bacterial inhabitants found as planktonic cells or cells engulfed in mixed community biofilms (Abdel-Nour et al., 2013). *L. pneumophila* can acquire nutrients through synergistic relationships with members of biofilm communities (Tison et al., 1980; Wadowsky and Yee, 1983; Stout et al., 1985; Stewart et al., 2012; Koide et al., 2014; Boamah et al., 2017). Moreover, *L. pneumophila* is capable of surviving by necrotrophic growth on dead cell masses (Temmerman et al., 2006). While interactions promoting *L. pneumophila* survival in oligotrophic water environments are described, competition for nutrients is raging (Abu Khweek and Amer, 2018). Thus, it is reasonable to hypothesize that active molecules are locally produced by biological challengers. Surprisingly, very few papers have described such compounds. In 2008, a study tested 80 aquatic bacterial isolates and showed that 55 displayed antagonistic activity against *L. pneumophila* (Guerrieri et al., 2008). Interestingly, 60 of all tested isolates (75%) were *Pseudomonas* and 43 of them were active against *L. pneumophila* as determined by spot-on-lawn assay. Other species were also described to antagonize the persistence of *L. pneumophila* within biofilms, e.g., *Acidovorax* sp., *Aeromonas hydrophila*, *Burkholderia cepacia*, or *Sphingomonas* sp. (Guerrieri et al., 2008). However, to date, molecules of interest remain uncharacterized. Concomitantly, high-throughput sequencing technologies have enabled a fine characterization of environmental microbiomes such as those dwelling in drinking water distribution systems (Ji et al., 2015; Proctor and Hammes, 2015), shedding light on unexplored and complex microbial communities, potentially hiding new potent antibacterial compounds.

Thus, the aim of the present study was to unravel the potential of those unexplored waterborne bacteria to inhibit the growth of *L. pneumophila*, in order to find new active compounds from natural origin. Environmental aquatic bacteria were thus sampled from five freshwater environments in order to establish a large culturable bacterial collection. Species belonging to various genera and species were then screened for their antagonistic activity toward *L. pneumophila* and identified.

MATERIALS AND METHODS

Water Sampling

Five different water sources were sampled: pond water, swimming pool water, river water, tap water and well water. Each sample was collected in January 2016 in the Vienne department (Nouvelle-Aquitaine, France). Both water samples from a private pond and a private well were collected at Chatellerault (46°49'04" N, 0°32'46" E). The river water was sampled from the Vienne River in Bonneuil-Matours (46°40'57" N, 0°34'17" E). A sample of an untreated private swimming pool water was collected at Sèvres-Anxaumont (46°34'14" N, 0°27'57" E). Finally, tap water was sampled from the drinking water network of Poitiers (46°34'55" N, 0°20'10" E).

Environmental Bacterial Strains Collection

A volume of 1 mL from each water sample was spread onto R2A agar plates within a maximum of 5 h after the original sampling. All plates were incubated for 72 h at 22, 30, or 37°C. After 72 h, isolated colonies were collected and re-isolated on new R2A agar plates to assure the purity of aquatic isolates. In total, 273 purified isolates were obtained and kept frozen at −80°C until use.

16S rRNA Gene Sequencing

Aquatic bacterial isolates were identified by 16S rRNA gene sequencing. For DNA extraction, a colony was suspended in 200 µL of sterile water and the sample was boiled 10 min. Samples were then centrifuged (8000 × g, 15 min) and supernatants containing DNA were kept at −20°C. The 16S rRNA coding gene of bacterial isolates was amplified by PCR with the universal primer set 27F (5′-AGA GTT TGA TCM TGG CTC AG-3′)/786R (5′-CTA CCA GGG TAT CTA ATC-3′), targeting the V1-V4 region of the gene. Amplification was carried out as follows: denaturation at 94°C for 30 s, annealing at 50°C for 30 s, and extension at 72°C for 1 min, for a total of 30 cycles, followed by a final elongation at 72°C for 5 min. Then, PCR products were subjected to 1% agarose gel electrophoresis. For PCR-products clean-up, 1 U/µL of Shrimp Alkaline Phosphatase (M0371S, New England Biolabs) and 10 U/µL of Exonuclease I (M0293S, New England Biolabs) were added to 6 µL of PCR products. DNA sequencing was completed with the ABI Prism BigDye terminator v3.1 sequencing kit (Applied Biosystems, Carlsbad, CA, United States) and then analyzed by an automatic ABI Prism 3730 genetic analyzer (Applied Biosystems, Carlsbad, CA, United States). Sequences were assembled with SerialCloner software and confronted against the nr/nt sequence database using BLASTn (Altschul et al., 1990). All sequences have been deposited in the GenBank database under accession numbers MH591484 to MH591754. Full list of accession numbers is given in **Supplementary Table 1**.

Phylogenetic Analysis

Consensus from 16S rRNA gene coding sequences of the 273 isolates were aligned using MUSCLE algorithm (Edgar, 2004a,b). The phylogenetic analysis of 480 bp aligned sequences from the V2–V4 16S gene regions (Position: 201–681) was performed using MEGA V7 software (Kumar et al., 2016). Phylogeny was inferred by maximum likelihood, with 1000 bootstrap iterations to test the robustness of the nodes. The resulting tree was uploaded and formatted using iTOL (Letunic and Bork, 2016).

Screening for Anti-*Legionella* Activity

Legionella pneumophila serogroup 1 Lens CIP 108286 (Cazalet et al., 2008) was used as the reference strain for anti-*Legionella* experiments. All strains were screened for anti-*Legionella* activity by spot-on-lawn assay as described previously (Loiseau et al., 2015). Briefly, *L. pneumophila* was cultured at 37°C in buffered yeast extract (BYE) liquid medium for 72 h under shaking (150 rpm). The pre-culture was then diluted with fresh BYE to a concentration of 10⁸ CFU/mL and a volume of 100 µL

was spread onto a buffered charcoal yeast extract (BCYE) agar plate with a cotton swab. Then, 10 µL of suspension of each isolate (obtained from a fresh pre-culture on agar plates) were spotted onto the center of the agar plate. Each plate was then incubated for 48 h at 22, 30, or 37°C. A second incubation step was done at 37°C for 48 h to allow *L. pneumophila* growth. Anti-*Legionella* compounds production was revealed by an inhibition zone around the producer strain. For each tested strain, the diameter of the inhibition area was measured.

L. pneumophila Long-Range Inhibition Assay

This assay was used for environmental bacterial isolates which totally inhibit the growth of *L. pneumophila* on agar plate. A 6-well plate assay was thus designed to physically separate environmental isolates from *L. pneumophila* Lens in order to determine whether emitted volatiles organic compounds (VOCs) could inhibit or not the growth of *L. pneumophila*. Each well was filled with 5 mL of BCYE. Then, 10 µL of a suspension of GFP-expressing *L. pneumophila* Lens (Bigot et al., 2013) (OD_{600 nm} adjusted to 0.1) were spotted onto both upper sides of the plate. Finally, 40 µL of a suspension of selected isolate (OD_{600 nm} adjusted to 1) were spotted onto the upper center of the plate. Depending of the tested isolate, plates were incubated for 48 h at 22, 30, or 37°C. A second step of incubation was done for 48 h at 37°C. Anti-*Legionella* activity mediated by VOCs production was quantified by measuring the fluorescence of GFP with a TriStar² LB 942 Microplate Reader (Berthold Technologies, Bad Wildbad, Germany).

Data Analysis

For analyzing the distribution of diameters among the five water sub-collections, violin plots were constructed using R environment with the package “ggplot2” (Wickham, 2009). To assess the alpha-diversity within each water collection, the Shannon diversity index (H) was calculated based on relative abundance for assigned genera. To evaluate the evenness of each community, Pielou’s index (J) was computed. Both indexes were calculated in R environment using the package “Vegan” (Oksanen et al., 2018). Finally, a heatmap representing inhibition diameters distribution among bacterial genera was constructed using Plotly online software¹.

RESULTS

Waterborne Bacteria Exhibit a High Proportion of Anti-*Legionella* Compounds Producers

Firstly, a total of 273 bacterial isolates were recovered and purified from the five different freshwater sources (Pond, Pool, River, Tap, and Well) used in this study. For each water sample, between 51 and 67 isolates were obtained per mL of a given water sample except for the tap water sample for which the

¹<https://plot.ly/>

cultivable bacterial biomass was lower (29 strains) (**Figure 1A**). Secondly, the collection of aquatic bacterial isolates was screened for the ability to produce anti-*Legionella* compounds using an agar plate assay (repeated at least three times per isolate). Among the 273 isolates, 178 (65.2%) were shown to be active against *L. pneumophila* Lens CIP 108286 (**Figure 1A**). Furthermore, those active isolates were not equally distributed among the five water sub-collections: 52/67 from the pond sub-collection (77.7% of isolates), 40/51 from the pool sub-collection (78.4% of isolates), 61/66 from the river sub-collection (92.4% of isolates), 25/62 from the well sub-collection (39.7% of isolates) and 0/29 for the tap sub-collection (**Figure 1A**). Interestingly, various inhibition diameters were observed among active isolates, ranging from 0.4 to 9 cm (**Figure 1B**). However, for each water sub-collection, most of inhibition diameters values were comprised between 0.4 and 2 cm. This inhibition profile was mainly observed for the well water and the river water sub-collections representing 68 and 60.6% of the total active isolates, respectively. Another point of interest is the full inhibition profile (diameter of 9 cm) displayed by several isolates from the collection (**Figure 1B**). Surprisingly, those isolates were not evenly distributed but were mostly found in the pond water sub-collection (38.4% of total active isolates). In all other water sub-collections, the proportion of isolates displaying a total inhibition profile was lower (7.5, 6.6, and 4% of total active isolates in the pool, the river and the well water sub-collections respectively).

Gammaproteobacteria and Firmicutes Are the Major Clades of Anti-*Legionella* Bacteria

In order to explore taxonomic affiliations of bacterial isolates, a systematic sequencing of the 16S rRNA coding gene sequence was performed. Resulting sequences were used to reconstruct a phylogenetic tree presented in **Figure 2**. All bacterial isolates were classified within 4 phyla, namely Proteobacteria (179/273), Bacteroidetes (48/273), Firmicutes (43/273), and Actinobacteria (3/273). In regards to the anti-*Legionella* activity, the Firmicutes phylum and the Gammaproteobacteria class stood out as clades containing the highest proportion of active isolates, as 89.8% of Gammaproteobacteria and 88.4% of Firmicutes showed inhibition of *Legionella* growth. Conversely, the Alphaproteobacteria class, for which most isolates originated from the tap water sub-collection, harbored the lowest proportion of active isolates (9.1%) (**Figure 2**). Genera such as *Bradyrhizobium* and *Novosphingobium*, which were exclusively isolated from the tap water, did not show any anti-*Legionella* activity. Overall, members of the Gammaproteobacteria class were the most frequently isolated bacteria, regardless of the environmental water source. Within this class, *Aeromonas* and *Pseudomonas* were the most represented genera, which were found in all samples except in the tap water sub-collection. Together with *Flavobacterium* (Bacteroidetes) and *Bacillus* (Firmicutes), these four genera dominated the collected bacterial community as they represented 56.4% (154/273) of all isolates of the collection (**Figure 2**). Within those 154 isolates, 89% (137/154) were found active thus representing

100% of *Aeromonas* isolates, 94.7% of *Bacillus* isolates, 51.8% of *Flavobacterium* isolates and 97.1% of *Pseudomonas* isolates (**Figure 2**).

The Well Water Sub-collection Harbors the Most Diverse Cultivable Bacterial Flora

With the aim to estimate the bacterial diversity and species evenness within water sub-collections, Shannon H diversity and Pielou's evenness indexes were calculated (**Figure 3A**). Concerning the bacterial richness, the well water contains the most diverse community ($H = 2.52$; 12 equally common species) while the tap water is the lowest ($H = 1.09$) which is not surprising because this sub-collection contains only three genera. The pool water and the river water richness were similar (H ranging from 2.02 to 2.2) whereas the pond water is poorly diverse with a H index = 1.6 (**Figure 3A**). Furthermore, the less even community identified corresponds to the pond water ($J = 0.63$), suggesting the dominance of few genera, in addition to a more distinct bacterial community assemblage when compared to others water samples. In the tap water, no dominant species could be identified as the community was very even ($J = 0.99$), which is likely to be linked with the low richness of this sub-collection (**Figure 3A**). The well water and the pool water showed similar J index (0.84 and 0.83, respectively), suggesting the absence of highly dominant species based on the presented dataset (**Supplementary Table 1**). Those pieces of data indicate that both communities differ in bacterial diversity but do not contain much specific genera. To complete this analysis and further identify potential dominant taxa, relative abundances of the four main bacterial genera (*Aeromonas*, *Bacillus*, *Flavobacterium*, and *Pseudomonas*) present in the water sub-collections were determined (**Figure 3B**). Altogether, those genera represented up to 70% of the total bacterial community. Both their distribution and abundance show a high amount of *Pseudomonas* isolates in the pond water sub-collection (58% of all isolates), *Bacillus* isolates in the river water sub-collection (41% of all isolates) and *Flavobacterium* isolates in the well water sub-collection (31% of all isolates) (**Figure 3B**). *Aeromonas* isolates were present in all sub-collections, although less abundantly than the three others genera.

Diffusible Molecules and/or Volatile Compounds Are the Cause of the Anti-*Legionella* Activity

To decipher the underlying variety of anti-*Legionella* activity displayed by active strains, a heatmap was drawn, highlighting clusters according to the diameter of inhibition. Overall three clusters were identified, showing diameters of inhibition (i) inferior to 2 cm, (ii) between 2 and 6 cm, and (iii) equal to 9 cm (total inhibition), in addition to strains devoid of anti-*Legionella* activity (**Figure 4** and **Table 1**). Among 25 active genera, 17 showed a specific inhibition profile with a constant diameter of inhibition (i.e., induced by more than 70% of all strains within the genus). A total absence of inhibition could be consistently observed for *Flectobacter*, *Pedobacter* (Bacteroidetes), *Exiguobacterium* (Firmicutes), *Sphingobium*, *Starkeya*,

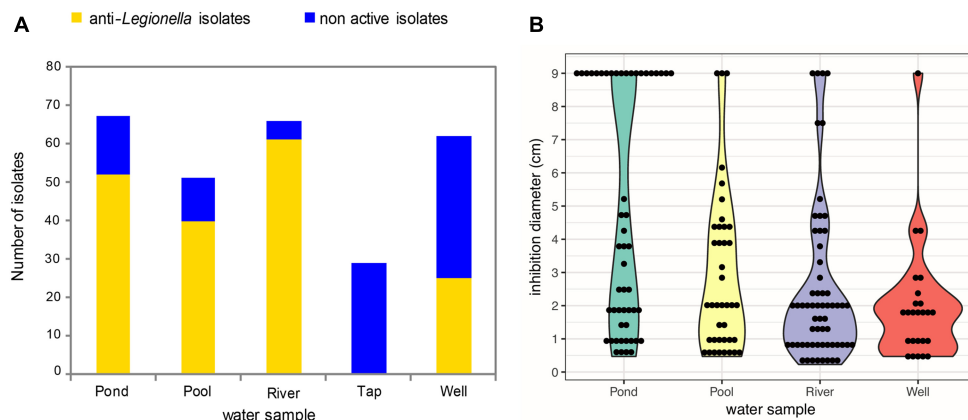


FIGURE 1 | Abundance and distribution of active anti-*Legionella* bacterial isolates and their inhibition diameters among the five water sub-collections. **(A)** Active isolates are colored in yellow while non-active isolates are colored in blue. The screening was realized by using spot and lawn assay method. **(B)** Violin Plot distribution of inhibition diameters among anti-*Legionella* isolates. Since there is no active isolate within the tap water, the corresponding sub-collection was not represented.

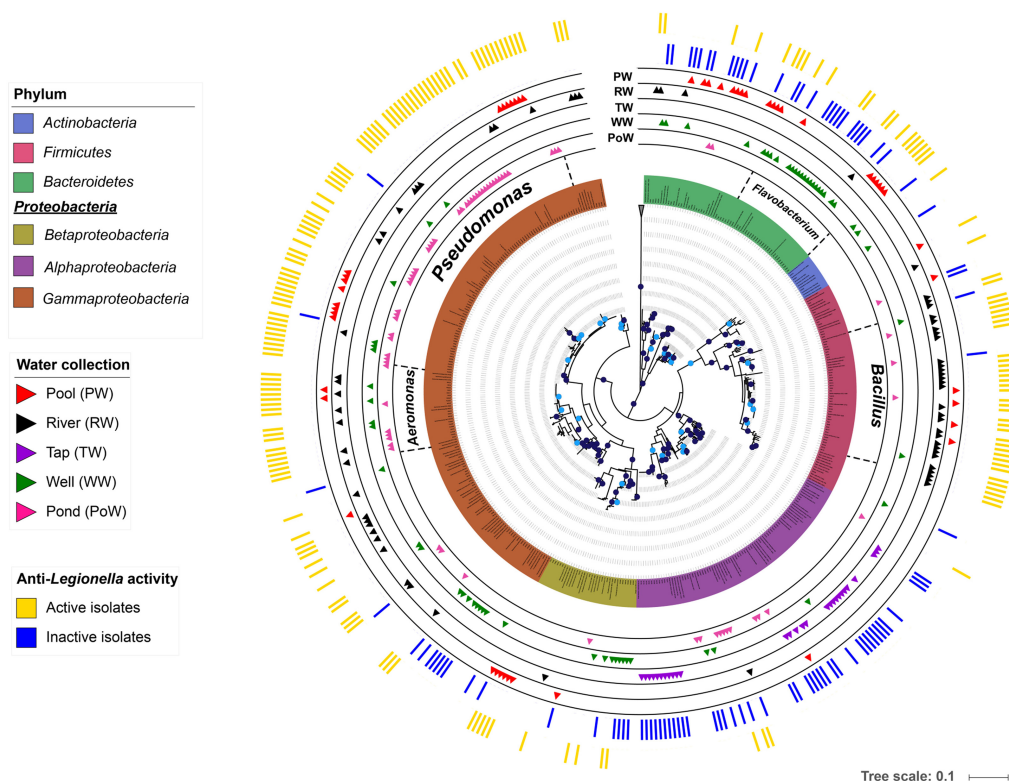
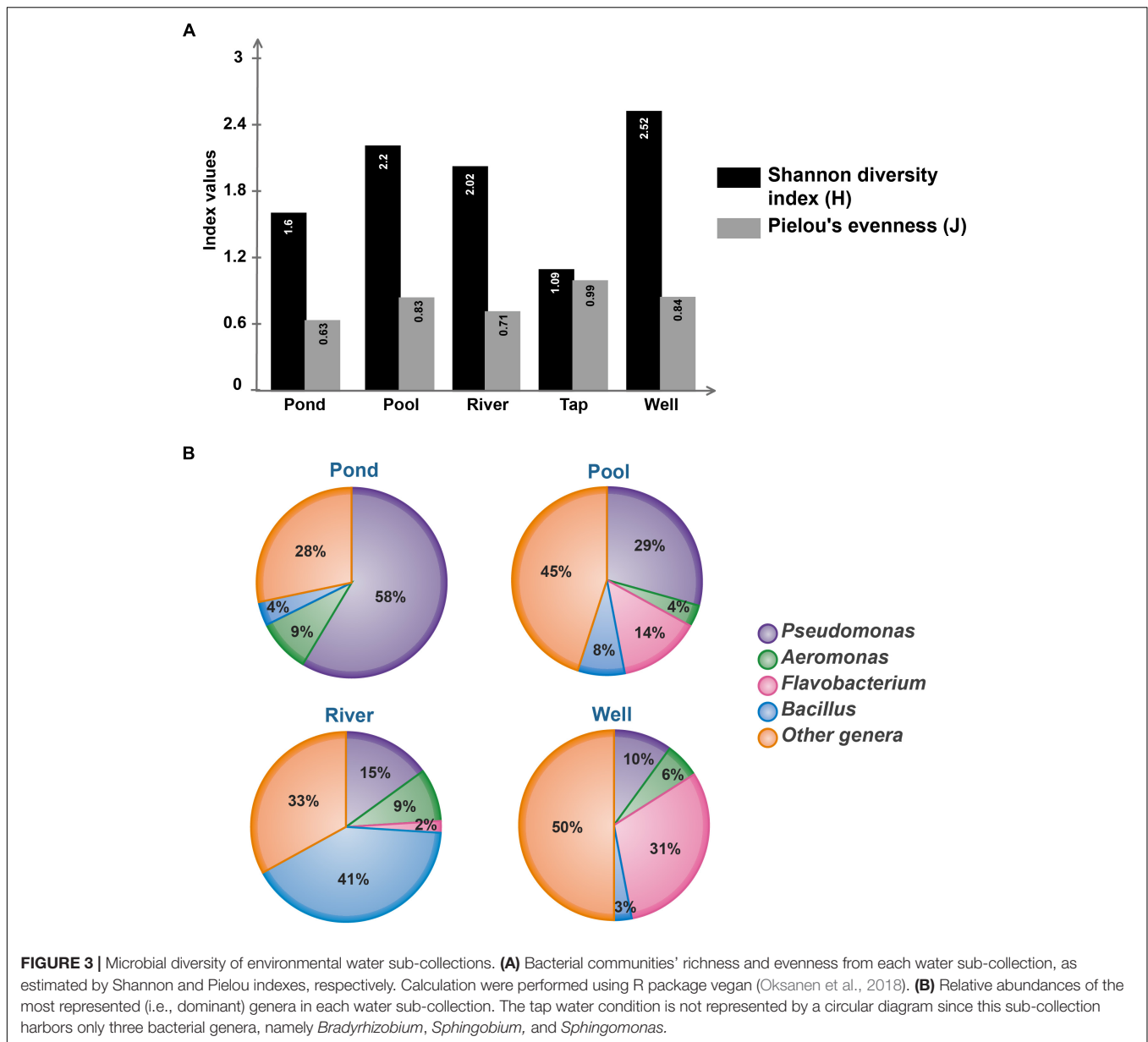


FIGURE 2 | Phylogenetic tree of anti-*Legionella*-associated environmental bacteria. The phylogenetic analysis was performed using the maximum likelihood phylogenetic method on MEGA v7 and the tree was viewed with iTOL (Letunic and Bork, 2016). Branches with bootstrap values (1000 replicates) higher than 70% are marked with dark blue dots, and those between 60 and 70% with light blue dots (The tree did not have branches with bootstrap value less than 60%). Environmental bacterial strains are color-coded by phyla, except for the Alphaproteobacteria, Betaproteobacteria, and Gammaproteobacteria which are depicted at the class level. The outer colored bands show the anti-*Legionella* profile with active isolates in yellow and inactive isolates in blue. The five internal bands show the distribution of each isolate among the five environmental water sub-collections (pond, pool, river, tap, and well).

Bradyrhizobium, *Brevundimonas* (Alphaproteobacteria), *Deefgea* (Betaproteobacteria) and *Lysobacter* (Gammaproteobacteria). Profiles corresponding to diameters of inhibition inferior

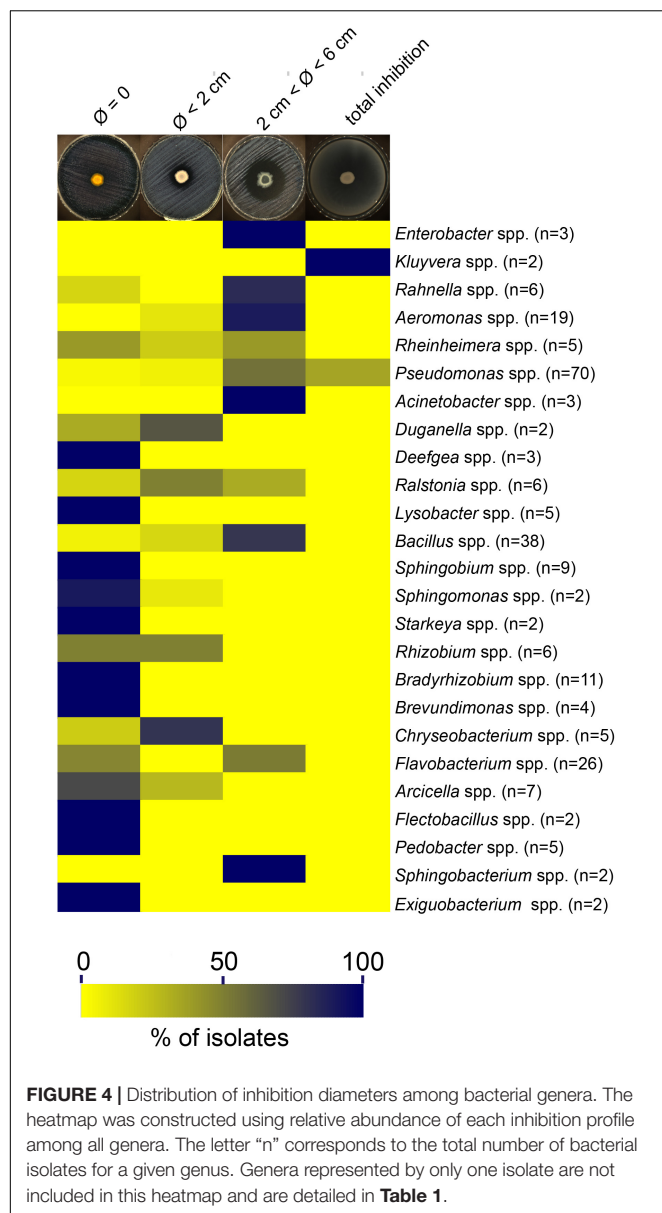
to 2 cm were observed for *Arthrobacter* (Actinobacteria), *Chryseobacterium* (Bacteroidetes), *Brevibacillus* (Firmicutes), *Achromobacter*, *Acidovorax*, *Duganella*, and *Rhodospirillum*



(Betaproteobacteria). Profiles resulting in diameter of inhibition between 2 and 6 cm were observed for a large variety of Gammaproteobacteria isolates, affiliated to *Acinetobacter*, *Aeromonas*, *Enterobacter*, *Escherichia*, *Erwinia*, *Klebsiella*, and *Rahnella* genera; other clades were less diversely represented with *Lysinibacter* (Actinobacteria), *Sphingobacterium* (Bacteroidetes) and *Bacillus* (Firmicutes). Other genera could not be classified in such clusters, as large intra genus variability could be observed (e.g., *Rheinheimera*, *Ralstonia*) (Figure 4).

Unexpectedly, isolates belonging from two genera were found to totally inhibit the growth of *L. pneumophila* since no colony was detected on entire Petri-dishes when compared with *L. pneumophila* grown alone: *Kluyvera* and *Pseudomonas* (Figure 4). Among the 70 isolates of *Pseudomonas*, only 26 (37.1%) were concerned while the two isolates of *Kluyvera*

(100%) available in the collection exhibited this capacity. Those results suggest that at least one highly diffusible and/or a volatile antagonistic molecule could be produced. To further investigate this possibility, we designed a 6-well antagonistic assay enabling the quantification of long-range aerial interference between *Kluyvera*/*Pseudomonas* and physically separated GFP-expressing *L. pneumophila* Lens. Thus, the volatile activity could be visually estimated as a function of *L. pneumophila* growth (Figure 5A). The use of a GFP-expressing *L. pneumophila* strain also allowed for a quantitative estimate of growth inhibition through fluorescence intensity measurements. This experimental design allowed us to verify simultaneously both hypotheses and an example is given in Figure 5B for the strain RW332. While no *Kluyvera* isolates were shown to produce volatile compounds capable of inhibiting *L. pneumophila* growth, 6 out of



26 *Pseudomonas* isolates displayed this capacity and may produce at least one anti-*L. pneumophila* volatile compound. In contrast, the 20 others *Pseudomonas* as well as the 2 *Kluyvera* isolates may have produced one or more highly active diffusible antagonistic molecules.

DISCUSSION

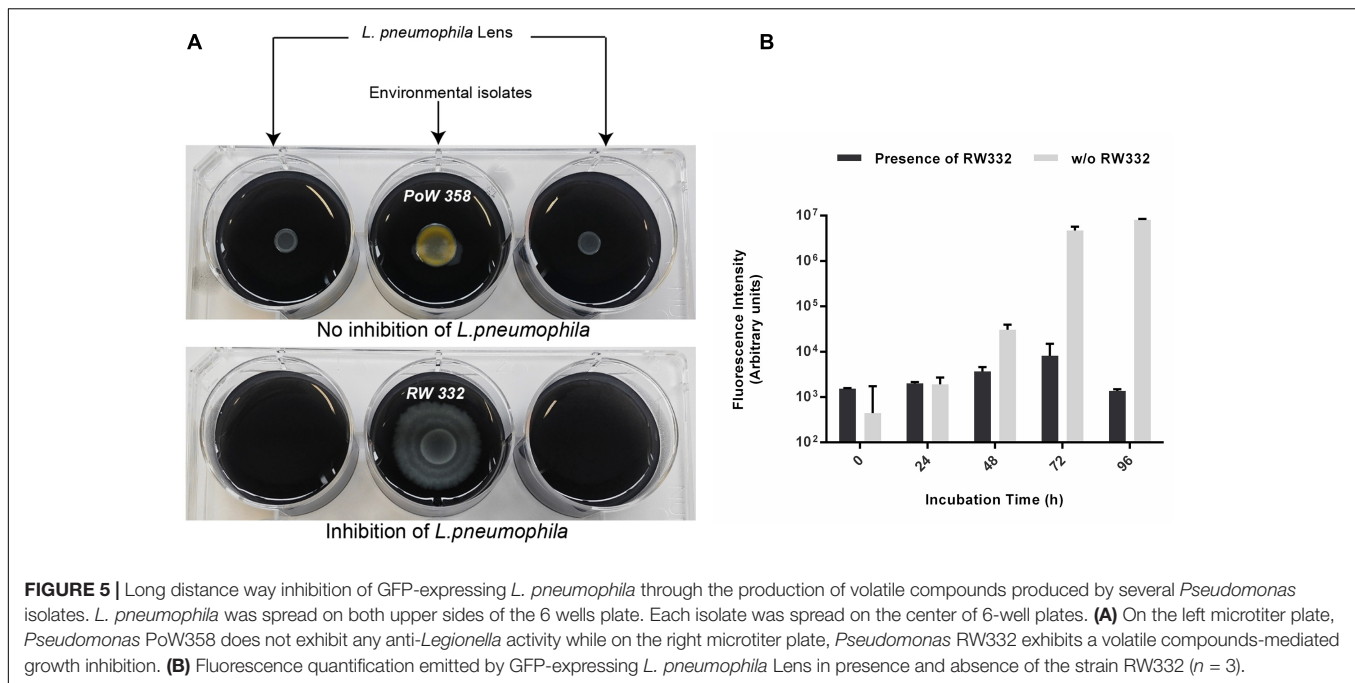
Artificial water systems provide suitable conditions for growth and multiplication of waterborne pathogens including *L. pneumophila*, the causative agent of LD (Van Heijnsbergen et al., 2015). Characteristics shared by some waterborne pathogens include proliferation in biofilms, uptake, survival, and proliferation within an amoeba host and disinfectant resistance (e.g., chlorine, chloramine). The survey and the control of

TABLE 1 | Inhibition diameters for genera with only one representing isolate in the collection.

Genus	Diameter (cm)
<i>Azospirillum</i>	Ø = 0
<i>Curtobacterium</i>	Ø = 0
<i>Novosphingobium</i>	Ø = 0
<i>Pseudacidovorax</i>	Ø = 0
<i>Pseudoxanthomonas</i>	Ø = 0
<i>Rhodococcus</i>	Ø = 0
<i>Shewanella</i>	Ø = 0
<i>Staphylococcus</i>	Ø = 0
<i>Achromobacter</i>	Ø < 2
<i>Acidovorax</i>	Ø < 2
<i>Arthrobacter</i>	Ø < 2
<i>Brevibacillus</i>	Ø < 2
<i>Rhodiferax</i>	Ø < 2
<i>Escherichia</i>	2 < Ø < 6
<i>Erwinia</i>	2 < Ø < 6
<i>Klebsiella</i>	2 < Ø < 6
<i>Lysinibacillus</i>	2 < Ø < 6

disinfection by-products are key factors for minimizing people exposure while maintaining satisfactory disinfection processes. However, the array of investigated compounds displaying anti-*Legionella* activity remains limited (Berjeaud et al., 2016). When available, those compounds were purified from organisms not found in the microenvironment of *L. pneumophila*. Thus, in this study, we established a vast freshwater bacterial collection in order to investigate the presence of *L. pneumophila*-inhibiting bacterial strains sharing the same ecological niches.

Five freshwater sources were sampled (bulk water) to increase the biodiversity of harvested bacteria and potentially active isolates. Among the 273 isolates, 178 (65.2%) were shown to be active against *L. pneumophila* as revealed by the presence of an inhibition area on Petri dishes. The diversity of inhibition diameters obtained could be linked to many factors such as the physical and chemical properties of active compounds, the physiological state of the target, the metabolic activity of the producing strain or the number of compounds that are produced. Nevertheless, those pieces of data are in agreement with those obtained by Guerrieri and coworkers who isolated 51 strains (51/75; 68%) active against *L. pneumophila* from different tap water samples (Guerrieri et al., 2008). It is, however, important to stress that 75% of tested strains in the above-mentioned study belonged to the *Pseudomonas* genus and the biodiversity of their collection was somewhat restrained. Nonetheless, they showed that among their 20 non-*Pseudomonas* remaining strains (9 *Acinetobacter* spp., 2 *A. faecalis* odorans, 2 *A. hydrophila*, 2 *B. cepacia*, and 1 *Flavobacterium* spp.), 12 (60%) were active against *L. pneumophila*. In our study 70 strains (25.6%) belong to the *Pseudomonas* genus and, as expected, all but 2 displayed antagonistic activity. Among active genera in the collection, 20 are newly described as anti-*Legionella* to the best of our knowledge. Only *Aeromonas* (Cotuk and Dogruoz, 2005; Guerrieri et al., 2008), *Bacillus* (Loiseau et al., 2015), *Acinetobacter*, *Flavobacterium*, and



Pseudomonas (Guerrieri et al., 2008) have been previously reported. Moreover, for many of them, such as *Chryseobacterium*, *Ralstonia*, or *Rheinheimera*, we have collected more than one active isolate, hence reinforcing the conservation of such antagonistic aspect across isolates from the same genus. However, it has to be noted that because R2A was used to recovered water bacteria, other genera that cannot grow on this medium and that might produce anti-*Legionella* compounds could not be detected in this study.

The diversity of bacteria isolated in this study was shown to be modulated by the water source that was sampled. The well water corresponded to the most diverse source, whereas the tap water showed the lowest diversity. Apart from the pond water where *Pseudomonas* spp. accounted for more than half of the isolates, no highly dominant taxa were found in other samples. Indeed, the source-specific diversity contributed to gather a large and diversified collection of bacterial isolates, affiliated to four phyla, namely Actinobacteria, Bacteroidetes, Firmicutes and Proteobacteria. Most active isolates, 153/178 (86%) were recovered from pond, pool and river water samples accounting for 77.4–92.4% of all strains. Surprisingly, no active strain was isolated from the tap water sample, which is also the less diverse bacterial sub-collection with only three genera (*Bradyrhizobium*, *Sphingobium*, and *Sphingomonas*) maybe because it is the only one sample coming from a treated water system. This result may suggest that water treatment remove anti-*Legionella* bacterial species from the bulk water. However, further investigations are required to elucidate whether such treatments could indirectly favor *Legionella* sp. persistence by eliminating natural competitors. The three most represented genera, i.e., *Bacillus*, *Pseudomonas*, and *Flavobacterium*, all displayed anti-*Legionella* activity, at least for 50% of isolates. As suggested by the sequence comparisons and phylogeny, isolates affiliated to these

three genera are highly likely to represent a various set of distinct species and strains. However, because of the underlying limitations of 16S rRNA-based bacterial identification, this diversity is surely underestimated. Other methods such as multi-locus sequence typing or whole genome sequencing would indubitably give more information in this regard.

The literature concerning the chemical nature of diffusible molecules responsible for anti-*Legionella* activity still remains scarce to this day. Recently, surfactin, the most known and well-studied biosurfactant from *Bacillus subtilis*, has been shown to exhibit a potent activity toward many *Legionella* species including the Lens strain (CIP 108286) (Loiseau et al., 2015). Moreover, *Legionella* bacteria appeared highly sensitive to this lipopeptide (MICs of 1–4 $\mu\text{g/mL}$) in comparison with the few susceptible species reported so far (Berjeaud et al., 2016). Biosurfactants, which are well-studied microbial metabolites, are often classified according to their chemical composition and their molecular weight. These low (i.e., glycolipids, phospholipids, and lipopeptides) and high-molecular weight (i.e., polysaccharides, proteins, lipoproteins, and LPS) compounds are produced by many bacterial genera including *Acinetobacter*, *Bacillus* and *Pseudomonas* (Płociniczak et al., 2011). As *L. pneumophila* was previously described to be sensitive to various membrane-active biomolecules (Berjeaud et al., 2016), lipopeptides from *Bacillus* and rhamnolipids from *Pseudomonas* might be potent anti-*Legionella* weapons. Additionally, many antimicrobial peptides (AMPs) were found capable of killing *Legionella* sp. (Berjeaud et al., 2016). Those AMPs were characterized from various organisms like warnericin RK and PSM from *Staphylococci* (Marchand et al., 2011; Verdon et al., 2008), Ci-PAP-A22 and Ci-MAM-A24 from marine *Ciona intestinalis* (Schlüsselhuber et al., 2015), Armadillidin H from the woodlouse *Armadillidium vulgare* (Verdon et al., 2016) and a defensin from the greater wax

moth *Galleria mellonella* (Palusińska-Szys et al., 2012). However, very few bacterial genera identified in our study were described to produce AMPs. To our knowledge, only *Aeromonas* (Tasiemski et al., 2015), *Escherichia* (Rebuffat, 2012), and *Klebsiella* (de Lorenzo and Pugsley, 1985) were reported so far. As those AMPs have never been tested against *L. pneumophila*, we hypothesize that they might eventually be involved in the antagonism ability of such isolates. However, further biochemical investigations would be necessary to purify and characterize such AMPs and to explore their potential use as biocontrol agents against *L. pneumophila*. Ultimately, many biomolecules are active against *L. pneumophila*, including molecules that are described to exhibit a poor antibacterial potency (e.g., warnericin RK or surfactin) (Berjeaud et al., 2016). *L. pneumophila* might have some particularities that could explain this sensitivity and part of the answer definitely lies in the composition of its envelope. For example, this bacterium contains an elevated amount of branched chain fatty acids and this characteristic was linked to its sensitivity to an antimicrobial peptide (Verdon et al., 2011). In the same way, detergents are very effective as anti-*Legionella* agents (Verdon et al., 2009) highlighting the crucial role played by some cell surface components. As underlined by those studies, the sensitivity *L. pneumophila* to various biomolecules is poorly understood because there is a current lack of mechanistic data (Berjeaud et al., 2016).

The well antagonistic assay used to physically separate *Kluyvera/Pseudomonas* isolates from GFP-expressing *L. pneumophila* Lens, allowed us to detect the production of at least one anti-*Legionella* volatile organic compound (VOC) from 6 *Pseudomonas* strains since aerial exposure to volatile molecule(s) released from those strains inhibited the growth of *L. pneumophila*. It is the first report published so far of such a long-range aerial interference between *Pseudomonas* and *Legionella*. VOCs and volatiles have been studied primarily in a context of inter-kingdom responses and their roles in bacterium-to-bacterium interactions are largely unexplored (Schulz and Dickschat, 2007). However, several studies suggested that bacterial VOCs could influence some phenotypes such as colony morphogenesis, biofilm formation, pigment production or antibiotic resistance (Bernier et al., 2011; Létoffé et al., 2014). The reasons why microorganisms produce volatiles remain unclear even if numerous functions such as communication, quorum sensing mechanisms and defense have been suggested (Kai et al., 2009). Nevertheless, these assumptions are difficult to demonstrate. Indeed, some bacterial volatiles have antifungal activity (Popova et al., 2014; Lo Cantore et al., 2015) while others can also serve as signals, attracting or repelling different

organisms. Furthermore, they can also induce resistance mechanism toward bacterial pathogens in plants or promote their growth (Farag et al., 2013). To date, none of these molecules was described as being anti-*Legionella*. Further investigations are needed to extract and analyze these molecules in order to decipher their mechanism of action. However, the role played by those volatiles compounds in an aquatic environment remains completely unknown.

In summary, the high proportion of anti-*Legionella* isolates recovered emphasizes that freshwater environments are not favorable to *L. pneumophila* in contrast to treated manmade water settings and highlights the key role played by biofilms and protists that shelter this human pathogen from competitors and harsh conditions (e.g., low temperature, presence of biocides). Thus, by collecting a vast array of *L. pneumophila* competitors, this study represents a first step and a prerequisite for further identification of potentially novel and active biomolecules.

AUTHOR CONTRIBUTIONS

M-HC, JM-B, and JV conceived and designed the study. M-HC performed experiments with the help of AL for antagonism experiments. M-HC and VD analyzed the data. J-MB and JV supervised the work. All authors edited the final manuscript.

FUNDING

This work received financial support from the French National Research Program for Environmental and Occupational Health of ANSES, grant EST-2015/1/111.

ACKNOWLEDGMENTS

We thank Daniel Guyonnet and Willy Aucher for their support around 16S rRNA coding gene sequencing experiments. We also thank Yoann Perrin, Cyril Noel, and Didier Bouchon for their help on data analysis.

SUPPLEMENTARY MATERIAL

The Supplementary Material for this article can be found online at: <https://www.frontiersin.org/articles/10.3389/fmicb.2018.03360/full#supplementary-material>

REFERENCES

- Abdel-Nour, M., Duncan, C., Low, D. E., and Guyard, C. (2013). Biofilms: the stronghold of *Legionella pneumophila*. *Int. J. Mol. Sci.* 14, 21660–21675. doi: 10.3390/ijms141121660
- Abu Khweek, A., and Amer, A. O. (2018). Factors mediating environmental biofilm formation by *Legionella pneumophila*. *Front. Cell. Infect. Microbiol.* 8:38. doi: 10.3389/fcimb.2018.00038
- Altschul, S. F., Gish, W., Miller, W., Myers, E. W., and Lipman, D. J. (1990). Basic local alignment search tool. *J. Mol. Biol.* 215, 403–410. doi: 10.1016/S0022-2836(05)80360-2
- American Society of Heating Refrigerating and Air-Conditioning Engineers (2015). *BSR/ASHRAE Standard 188P: Public Review Draft Prevention of Legionellosis Associated With Building Water Systems*. Available at: <http://www.weasengineering.com/assets/ashrae-188p-fourth-public-review-9-2014.pdf>

- Ashbolt, N. (2015). Environmental (Saprozoic) pathogens of engineered water systems: understanding their ecology for risk assessment and management. *Pathogens* 4, 390–405. doi: 10.3390/pathogens4020390
- Beauté, J. (2017). Legionnaires' disease in Europe, 2011 to 2015. *Euro Surveill.* 22:30566. doi: 10.2807/1560-7917.ES.2017.22.27.30566
- Berjeaud, J. M., Chevalier, S., Schlusshuber, M., Portier, E., Loiseau, C., Aucher, W., et al. (2016). *Legionella pneumophila*: the paradox of a highly sensitive opportunistic waterborne pathogen able to persist in the environment. *Front. Microbiol.* 7:486. doi: 10.3389/fmicb.2016.00486
- Bernier, S. P., Létoffé, S., Delepierre, M., and Ghigo, J. M. (2011). Biogenic ammonia modifies antibiotic resistance at a distance in physically separated bacteria. *Mol. Microbiol.* 81, 705–716. doi: 10.1111/j.1365-2958.2011.07724.x
- Bigot, R., Bertaux, J., Frere, J., and Berjeaud, J. (2013). Intra-amoeba multiplication induces chemotaxis and biofilm colonization and formation for *Legionella*. *PLoS One* 8:e77875. doi: 10.1371/journal.pone.0077875
- Boamah, D. K., Zhou, G., Ensminger, A. W., and O'Connor, T. J. (2017). From many hosts, one accidental pathogen: the diverse protozoan hosts of *Legionella*. *Front. Cell. Infect. Microbiol.* 7:477. doi: 10.3389/fcimb.2017.00477
- Cazalet, C., Jarraud, S., Ghavi-Helm, Y., Kunst, F., Glaser, P., Etienne, J., et al. (2008). Multigenome analysis identifies a worldwide distributed epidemic *Legionella pneumophila* clone that emerged within a highly diverse species. *Genome Res.* 18, 431–441. doi: 10.1101/gr.7229808
- Cotuk, A., and Dogruoz, N. (2005). The effects of *Pseudomonas* and *Aeromonas* strains on *Legionella pneumophila* growth. *Ann. Microbiol.* 55, 219–224.
- de Lorenzo, V., and Pugsley, A. P. (1985). Microcin E492, a low-molecular-weight peptide antibiotic which causes depolarization of the *Escherichia coli* cytoplasmic membrane. *Antimicrob. Agents Chemother.* 27, 666–669. doi: 10.1128/AAC.27.4.666
- Declerck, P. (2010). Biofilms: the environmental playground of *Legionella pneumophila*. *Environ. Microbiol.* 12, 557–566. doi: 10.1111/j.1462-2920.2009.02025.x
- Declerck, P., Behets, J., Margineanu, A., van Hoef, V., De Keersmaecker, B., and Olivier, F. (2009). Replication of *Legionella pneumophila* in biofilms of water distribution pipes. *Microbiol. Res.* 164, 593–603. doi: 10.1016/j.micres.2007.06.001
- Diederer, B. M. W. (2008). *Legionella* spp. and legionnaires' disease. *J. Infect.* 56, 1–12. doi: 10.1016/j.jinf.2007.09.010
- Dupuy, M., Mazoua, S., Berne, F., Bodet, C., Garrec, N., Herbelin, P., et al. (2011). Efficiency of water disinfectants against *Legionella pneumophila* and *Acanthamoeba*. *Water Res.* 45, 1087–1094. doi: 10.1016/j.watres.2010.10.025
- Edgar, R. C. (2004a). MUSCLE: a multiple sequence alignment method with reduced time and space complexity. *BMC Bioinformatics* 5:133. doi: 10.1186/1471-2105-5-113
- Edgar, R. C. (2004b). MUSCLE: multiple sequence alignment with high accuracy and high throughput. *Nucleic Acids Res.* 32, 1792–1797. doi: 10.1093/nar/gkh340
- Falkinham, J. O., Hilborn, E. D., Arduino, M. J., Pruden, A., and Edwards, M. A. (2015a). Epidemiology and ecology of opportunistic premise plumbing pathogens: *Legionella pneumophila*, *Mycobacterium avium*, and *Pseudomonas aeruginosa*. *Environ. Health Perspect.* 123, 749–758. doi: 10.1289/ehp.1408692
- Falkinham, J. O., Pruden, A., and Edwards, M. (2015b). Opportunistic premise plumbing pathogens: increasingly important pathogens in drinking water. *Pathogens* 4, 373–386. doi: 10.3390/pathogens4020373
- Farag, M. A., Zhang, H., and Ryu, C. M. (2013). Dynamic chemical communication between plants and bacteria through airborne signals: induced resistance by bacterial volatiles. *J. Chem. Ecol.* 39, 1007–1018. doi: 10.1007/s10886-013-0317-9
- Guerrieri, E., Bondi, M., Sabia, C., De Niederhäusern, S., Borella, P., and Messi, P. (2008). Effect of bacterial interference on biofilm development by *Legionella pneumophila*. *Curr. Microbiol.* 57, 532–536. doi: 10.1007/s00284-008-9237-2
- Hamilton, K. A., Prussin, A. J., Ahmed, W., and Haas, C. N. (2018). Outbreaks of legionnaires' disease and pontiac fever 2006–2017. *Curr. Environ. Health Rep.* 5, 263–271. doi: 10.1007/s40572-018-0201-4
- Ji, P., Parks, J., Edwards, M. A., and Pruden, A. (2015). Impact of water chemistry, pipe material and stagnation on the building plumbing microbiome. *PLoS One* 10:e0141087. doi: 10.1371/journal.pone.0141087
- Kai, M., Hausteine, M., Molina, F., Petri, A., Scholz, B., and Piechulla, B. (2009). Bacterial volatiles and their action potential. *Appl. Microbiol. Biotechnol.* 81, 1001–1012. doi: 10.1007/s00253-008-1760-3
- Koide, M., Higa, F., Tateyama, M., Cash, H. L., Hokama, A., and Fujita, J. (2014). Role of *Brevundimonas vesicularis* in supporting the growth of *Legionella* in nutrient-poor environments. *New Microbiol.* 37, 33–39.
- Kumar, S., Stecher, G., and Tamura, K. (2016). MEGA7: molecular evolutionary genetics analysis version 7.0 for bigger datasets. *Mol. Biol. Evol.* 33, 1870–1874. doi: 10.1093/molbev/msw054
- Létoffé, S., Audrain, B., Bernier, S. P., Delepierre, M., and Ghigo, J. M. (2014). Aerial exposure to the bacterial volatile compound trimethylamine modifies antibiotic resistance of physically separated bacteria by raising culture medium pH. *mBio* 5, 1–12. doi: 10.1128/mBio.00944-13
- Letunic, I., and Bork, P. (2016). Interactive tree of life (iTOL) v3: an online tool for the display and annotation of phylogenetic and other trees. *Nucleic Acids Res.* 44, W242–W245. doi: 10.1093/nar/gkw290
- Lo Cantore, P., Giorgio, A., and Iacobellis, N. S. (2015). Bioactivity of volatile organic compounds produced by *Pseudomonas tolaasii*. *Front. Microbiol.* 6:1082. doi: 10.3389/fmicb.2015.01082
- Loiseau, C., Schlusshuber, M., Bigot, R., Bertaux, J., Berjeaud, J. M., and Verdon, J. (2015). Surfactin from *Bacillus subtilis* displays an unexpected anti-*Legionella* activity. *Appl. Microbiol. Biotechnol.* 99, 5083–5093. doi: 10.1007/s00253-014-6317-z
- Marchand, A., Verdon, J., Lacombe, C., Crapart, S., Héchard, Y., and Berjeaud, J. M. (2011). Anti-*Legionella* activity of staphylococcal hemolytic peptides. *Peptides* 32, 845–851. doi: 10.1016/j.peptides.2011.01.025
- Newton, H. J., Ang, D. K. Y., Van Driel, I. R., and Hartland, E. L. (2010). Molecular pathogenesis of infections caused by *Legionella pneumophila*. *Clin. Microbiol. Rev.* 23, 274–298. doi: 10.1128/CMR.00052-09
- Oksanen, J., Blanchet, F. G., Friendly, M., Kindt, R., Legendre, P., McGlinn, D., et al. (2018). *Package "vegan": Community Ecology Package*. Available at: <https://cran.r-project.org/web/packages/vegan/vegan.pdf>.
- Palusińska-Szyszk, M., Zdybicka-Barabas, A., Pawlikowska-Pawlęga, B., Mak, P., and Cytryńska, M. (2012). Anti-*Legionella pneumophila* activity of *Galleria mellonella* defensin and apolipoprotein III. *Int. J. Mol. Sci.* 13, 17048–17064. doi: 10.3390/ijms131217048
- Parr, A., Whitney, E. A., and Berkelman, R. L. (2015). Legionellosis on the rise: a review of guidelines for prevention in the united states. *J. Public Health Manag. Pract.* 21, E17–E26. doi: 10.1097/PHH.0000000000000123
- Płociniczak, M. P., Plaza, G. A., and Piotrowska-seget, Z. (2011). Environmental applications of biosurfactants: recent advances. *Int. J. Mol. Sci.* 12, 633–654. doi: 10.3390/ijms12010633
- Popova, A. A., Koksharova, O. A., Lipasova, V. A., Zaitseva, J. V., Katkova-Zhukotskaya, O. A., Eremina, S. I., et al. (2014). Inhibitory and toxic effects of volatiles emitted by strains of *Pseudomonas* and *Serratia* on growth and survival of selected microorganisms, *Caenorhabditis elegans*, and *Drosophila melanogaster*. *Biomed. Res. Int.* 2014:125704. doi: 10.1155/2014/125704
- Proctor, C. R., and Hammes, F. (2015). Drinking water microbiology-from measurement to management. *Curr. Opin. Biotechnol.* 33, 87–94. doi: 10.1016/j.copbio.2014.12.014
- Rebuffat, S. (2012). Microcins in action: amazing defence strategies of enterobacteria. *Biochem. Soc. Trans.* 40, 1456–1462. doi: 10.1042/BST20120183
- Schlusshuber, M., Humblot, V., Casale, S., Méthivier, C., Verdon, J., Leippe, M., et al. (2015). Potent antimicrobial peptides against *Legionella pneumophila* and its environmental host, *Acanthamoeba castellanii*. *Appl. Microbiol. Biotechnol.* 99, 4879–4891. doi: 10.1007/s00253-015-6381-z
- Schulz, S., and Dickschat, J. S. (2007). Bacterial volatiles: the smell of small organisms. *Nat. Prod. Rep.* 24, 814–842. doi: 10.1039/b507392h
- Stewart, C. R., Muthye, V., and Cianciotto, N. P. (2012). *Legionella pneumophila* persists within biofilms formed by *Klebsiella pneumoniae*, *Flavobacterium* sp., and *Pseudomonas fluorescens* under dynamic flow conditions. *PLoS One* 7:e50560. doi: 10.1371/journal.pone.0050560
- Stout, J. E., Yu, V. L., and Best, M. G. (1985). Ecology of *Legionella pneumophila* within water distribution systems. *Appl. Environ. Microbiol.* 49, 221–228.
- Tasiemski, A., Massol, F., Cuvillier-hot, V., Boidin-wichlacz, C., Roger, E., Rodet, F., et al. (2015). Reciprocal immune benefit based on complementary production

- of antibiotics by the leech *Hirudo verbana* and its gut symbiont *Aeromonas veronii*. *Sci. Rep.* 5:17498. doi: 10.1038/srep17498
- Temmerman, R., Vervaeeren, H., Noseda, B., Boon, N., and Verstraete, W. (2006). Necrotrophic growth of *Legionella pneumophila*. *Appl. Environ. Microbiol.* 72, 4323–4328. doi: 10.1128/AEM.00070-06
- Tison, D. L., Pope, I. D. H., Cherry, W. B., and Fliermans, C. B. (1980). Growth of *Legionella pneumophila* in association with growth of *Legionella pneumophila* in association with blue-green algae (Cyanobacteria). *Appl. Environ. Microbiol.* 39, 456–459.
- Van Heijnsbergen, E., Schalk, J. A. C., Euser, S. M., Brandsema, P. S., Den Boer, J. W., and De Roda Husman, A. M. (2015). Confirmed and potential sources of *Legionella* reviewed. *Environ. Sci. Technol.* 49, 4797–4815. doi: 10.1021/acs.est.5b00142
- Verdon, J., Berjeaud, J. M., Lacombe, C., and Héchard, Y. (2008). Characterization of anti-*Legionella* activity of warnericin RK and delta-lysine I from *Staphylococcus warneri*. *Peptides* 29, 978–984. doi: 10.1016/j.peptides.2008.01.017
- Verdon, J., Coutos-Thevenot, P., Rodier, M. H., Landon, C., Depayras, S., Noel, C., et al. (2016). Armadillidin H, a glycine-rich peptide from the terrestrial crustacean *Armadillidium vulgare*, displays an unexpected wide antimicrobial spectrum with membranolytic activity. *Front. Microbiol.* 7:1484. doi: 10.3389/fmicb.2016.01484
- Verdon, J., Falge, M., Maier, E., Bruhn, H., Steinert, M., Faber, C., et al. (2009). Detergent-like activity and α -helical structure of warnericin RK, an anti-*Legionella* peptide. *Biophys. J.* 97, 1933–1940. doi: 10.1016/j.bpj.2009.06.053
- Verdon, J., Labanowski, J., Sahr, T., Ferreira, T., Lacombe, C., Buchrieser, C., et al. (2011). Fatty acid composition modulates sensitivity of *Legionella pneumophila* to warnericin RK, an antimicrobial peptide. *Biochim. Biophys. Acta* 1808, 1146–1153. doi: 10.1016/j.bbame.2010.12.011
- Wadowsky, R. M., and Yee, R. B. (1983). Satellite growth of *Legionella pneumophila* with an environmental isolate of *Flavobacterium breve*. *Appl. Environ. Microbiol.* 46, 1447–1449.
- Wang, H., Bedard, E., Prevost, M., Camper, A. K., Hill, V. R., and Pruden, A. (2017). Methodological approaches for monitoring opportunistic pathogens in premise plumbing: a review. *Water Res.* 117, 68–86. doi: 10.1016/j.watres.2017.03.046
- Wickham, H. (2009). *Ggplot2: Elegant Graphics for Data Analysis*. New York: Springer.
- World Health Organization. (2011). *Guidelines for Drinking-Water Quality*. Geneva: World Health Organization.
- Yu, V. L., Plouffe, J. F., Pastoris, M. C., Stout, J. E., Schousboe, M., Widmer, A., et al. (2002). Distribution of legionella species and serogroups isolated by culture in patients with sporadic community acquired legionellosis: an international collaborative survey. *J. Infect. Dis.* 186, 127–128. doi: 10.1086/341087

Conflict of Interest Statement: The authors declare that the research was conducted in the absence of any commercial or financial relationships that could be construed as a potential conflict of interest.

Copyright © 2019 Corre, Delafont, Legrand, Berjeaud and Verdon. This is an open-access article distributed under the terms of the Creative Commons Attribution License (CC BY). The use, distribution or reproduction in other forums is permitted, provided the original author(s) and the copyright owner(s) are credited and that the original publication in this journal is cited, in accordance with accepted academic practice. No use, distribution or reproduction is permitted which does not comply with these terms.



Drug Repurposing for the Treatment of Bacterial and Fungal Infections

Andrea Miró-Canturri[†], Rafael Ayerbe-Algaba[†] and Younes Smani^{*}

Clinical Unit of Infectious Diseases, Microbiology and Preventive Medicine, Institute of Biomedicine of Seville (IBiS), University Hospital Virgen del Rocío, CSIC, University of Seville, Seville, Spain

OPEN ACCESS

Edited by:

Natalia V. Kirienko,
Rice University, United States

Reviewed by:

Eleftherios Mylonakis,
Alpert Medical School, United States
Giordano Rampioni,
Università degli Studi Roma Tre, Italy
Read Pukkila-Worley,
University of Massachusetts Medical
School, United States

*Correspondence:

Younes Smani
ysmani-ibis@us.es;
y_smani@hotmail.com

[†]These authors have contributed
equally to this work

Specialty section:

This article was submitted to
Antimicrobials, Resistance
and Chemotherapy,
a section of the journal
Frontiers in Microbiology

Received: 02 October 2018

Accepted: 11 January 2019

Published: 28 January 2019

Citation:

Miró-Canturri A, Ayerbe-Algaba R
and Smani Y (2019) Drug
Repurposing for the Treatment
of Bacterial and Fungal Infections.
Front. Microbiol. 10:41.
doi: 10.3389/fmicb.2019.00041

Multidrug-resistant (MDR) pathogens pose a well-recognized global health threat that demands effective solutions; the situation is deemed a global priority by the World Health Organization and the European Centre for Disease Prevention and Control. Therefore, the development of new antimicrobial therapeutic strategies requires immediate attention to avoid the ten million deaths predicted to occur by 2050 as a result of MDR bacteria. The repurposing of drugs as therapeutic alternatives for infections has recently gained renewed interest. As drugs approved by the United States Food and Drug Administration, information about their pharmacological characteristics in preclinical and clinical trials is available. Therefore, the time and economic costs required to evaluate these drugs for other therapeutic applications, such as the treatment of bacterial and fungal infections, are mitigated. The goal of this review is to provide an overview of the scientific evidence on potential non-antimicrobial drugs targeting bacteria and fungi. In particular, we aim to: (i) list the approved drugs identified in drug screens as potential alternative treatments for infections caused by MDR pathogens; (ii) review their mechanisms of action against bacteria and fungi; and (iii) summarize the outcome of preclinical and clinical trials investigating approved drugs that target these pathogens.

Keywords: repurposing drug, bacteria, fungi, antimicrobial resistance, infection

INTRODUCTION

Bacteria and fungi are highly efficient in acquiring antimicrobial resistance encoded by genomic changes ranging in scale from point mutations, through the assembly of preexisting genetic elements, to the horizontal import of genes from the environment (Kung et al., 2010; Cowen et al., 2015; Yelin and Kishony, 2018). Compounding the problem of antimicrobial resistance is the immediate threat of a reduction in the discovery and development of new antibiotics, the dangers of which have recently been made clear by the World Health Organization (WHO) (Tacconelli et al., 2018) and other European institutions (O'Neill, 2016; Årdal et al., 2018). Consequently, a perfect storm is converging with regard to these infections: increasing antimicrobial resistance with a decreased new drug development (O'Neill, 2016). This context

is likely the best example of the purported “Post-Antibiotic Era,” with relevance even in non-specialized media (Bagley and Outtersen, 2017). It is clear that effective solutions are urgently needed as stressed by various institutions.

New policies and actions are necessary to avoid the figures predicted for 2050 that attribute ten million deaths worldwide to antimicrobial resistance (O’Neill, 2016). Such efforts might include: a massive global public awareness campaign; improvements in hygiene and prevention of the spread of infection; increase global surveillance of drug resistance and the appropriate antimicrobial consumption in humans and animals; the promotion of novel rapid diagnostics to curtail the unnecessary use of antimicrobial agents; and the promotion, development, and use of vaccines and other alternatives to both prevent and treat bacterial infections (O’Neill, 2016). Therefore, the development of new antimicrobial therapeutic strategies for use alone or together with one of the scarce but clinically relevant antibiotics has become exigent. In this environment, “repurposing” (defined as investigating new uses for existing drugs) has gained renewed interest, as reflected by several recent studies (Fischbach and Walsh, 2009; Brown, 2015; Rampioni et al., 2017). The combination of these existing drugs with antimicrobial agents currently in clinical use is also under consideration.

A literature review was conducted to search for potential non-antimicrobial candidate drugs that are not intentionally used as antimicrobial agents but have one or more antimicrobial properties. A variety of drug families have been considered including: anthelmintics (Lim et al., 2013; Rajamuthiah et al., 2015; Gooyit and Janda, 2016; Joffe et al., 2017); anticancer drugs (Ueda et al., 2009; Butts et al., 2014; Yeo et al., 2018); anti-inflammatory/immunomodulatory drugs (Artini et al., 2014; Thangamani et al., 2015b; Ogundeji et al., 2016); antipsychotic and antidepressant drugs (Lieberman and Higgins, 2009; Andersson et al., 2016; Holbrook et al., 2017); statins (Parihar et al., 2014; Thangamani et al., 2015a; Ribeiro et al., 2017); and iron-storage drugs (Gi et al., 2014). While these drugs are approved for their clinical indications, promising antibacterial and antifungal activities have been reported in preclinical and clinical studies. It is noteworthy that repurposing drugs is a very promising approach with several advantages. As drugs approved by the Federal Drug Administration (FDA), information about their pharmacological characteristics (both safety and pharmacokinetic) in preclinical and clinical trials is widely available. Therefore, the time and economic costs associated with the repurposing of these drugs for other therapeutic applications such as the treatment of bacterial and fungal infections will be minimized.

In this review, we focus on the current state of knowledge regarding the repurposing of drugs in terms of their modes of action, antimicrobial efficacy and breadth of spectrum against bacteria and fungi, as well as the advances to-date in their development as antimicrobial agents for clinical use. To this end, we introduce in Pubmed database different key words such as repurposing drugs, antibacterial and/or antifungal in order to find published literature about the

repurposing drugs for treatment of bacterial and fungal infections.

POTENTIAL DRUGS FOR REPURPOSING AGAINST INFECTIOUS AGENTS

The antibacterial and antifungal activities of repurposing drugs and their modes of action are summarized in **Table 1** and **Figure 1**.

Anthelmintic Drugs Repurposed Against Bacteria and Fungi

Anthelmintic drugs constitute a large class of medications used for the treatment of helminthiasis. Their activities aside from their use against parasitic infections are being investigated in other areas such as oncology (Dogra et al., 2018; Wang et al., 2018). The activity of these drugs against Gram-positive and Gram-negative bacteria, and fungi has been reported. The salicylanilide family contains a number of the anthelmintic drugs approved for the treatment of parasitic infections. The most widely used members of this family include niclosamide for humans (Chen et al., 2018) and oxiclozanide, rafoxanide, and closantel for animals (Martin, 1997).

The mode of action of salicylanilides is not completely understood, but they are thought to act as uncouplers of oxidative phosphorylation, thereby impairing the motility of parasites. Rajamuthiah et al. (2015) described the efficacy of niclosamide and oxiclozanide against methicillin-, vancomycin-, linezolid-, or daptomycin-resistant *Staphylococcus aureus* isolates. They reported that niclosamide presented bacteriostatic activity whereas oxiclozanide exhibited antibacterial action, likely due to damage in the bacterial membrane. Together with niclosamide and oxiclozanide, other members of the salicylanilides family such as rafoxanide and closantel have presented greater bactericidal activity against the logarithmic and stationary phases of *Clostridium difficile* than vancomycin (Gooyit and Janda, 2016). Avermectins, a broad-spectrum class of anthelmintic drugs which include ivermectin, selamectin, and moxidectin, demonstrated efficacy *in vitro* against *Mycobacterium tuberculosis* and *Mycobacterium ulcerans* with minimum inhibitory concentration (MIC) values ranging from 1 to 8 mg/L and 4 to 8 mg/L, respectively (Lim et al., 2013; Omansen et al., 2015). Moreover, ivermectin showed efficacy against *S. aureus* clinical isolates including methicillin-resistant strains (MRSA) (Ashraf et al., 2018). *In vivo*, ivermectin improves LPS-induced survival in mice by reducing serum and murine macrophage levels of TNF- α , IL-1 β , and IL-6 and blocking the NF- κ B pathway (Zhang et al., 2008).

In Gram-negative bacteria, only niclosamide exhibited antibacterial activity. This drug showed an anti-virulent effect against *Pseudomonas aeruginosa* via the inhibition of quorum sensing and virulence genes, reducing elastase and pyocyanin levels (Imperi et al., 2013b). In *Acinetobacter baumannii* and *Klebsiella pneumoniae*, niclosamide is able to increase the proportion of negative charges on their cell walls, and to potentiate the activity of colistin against colistin-resistant

TABLE 1 | Direct antibacterial and antifungal activity of repurposed drugs.

Drugs	Clinical indication	Target bacteria	Mechanisms of action	Reference
Nicosamide*	Helminthiasis	<i>P. aeruginosa</i>	Inhibition of quorum sensing and various virulence genes, and reduction of elastase and pyocyanin levels	Imperi et al., 2013b
Oxytocanide	Helminthiasis	<i>S. aureus</i>	Bacterial membrane damage	Rajamuthiah et al., 2015
Mebendazole	Helminthiasis	<i>C. neoformans</i>	Morphological alterations by reducing capsular dimensions	Joffe et al., 2017
Quinacrine	Helminthiasis	<i>C. albicans</i>	Inhibition of filamentation	Kulkarny et al., 2014
Floxuridine	Colorectal cancer	<i>S. aureus</i>	Inhibition of the SaeRS two-component system, and inhibition of the transcription of other virulence regulatory systems	Yeo et al., 2018
Streptozotocin	Pancreatic islet cell cancer	<i>S. aureus</i>	Inhibition of the SaeRS two-component system, and inhibition of the transcription of other virulence regulatory systems	Yeo et al., 2018
Toremifene	Breast cancer	<i>S. mutans</i> and <i>P. gingivallis</i>	Membrane permeabilization and damage	Gerits et al., 2017
Tamoxifen	Breast cancer	<i>C. neoformans</i>	Binding to the two essential EF-hand proteins calmodulin 1 (Cam1) and calmodulin-like protein (Cml) and prevention of Cam1 from binding to its well-characterized substrate calcineurin	Butts et al., 2014
Raloxifene	Breast cancer	<i>C. neoformans</i>	Binding to the two essential EF-hand proteins calmodulin (Cam1) and calmodulin-like protein (Cml) and prevention of Cam1 from binding to its well-characterized substrate calcineurin	Butts et al., 2014
Clomiphene	Fertility	<i>P. aeruginosa</i>	Binding to PhzB2 which is involved in the production of pyocyanin, a pigment related with the virulence of <i>P. aeruginosa</i>	Ho Sui et al., 2012
Finasteride	Benign prostatic hyperplasia	<i>S. aureus</i>	Inhibition of undecaprenyl diphosphate synthase involved in the synthesis of teichoic acid wall	Farha et al., 2015
5-fluorouracil	Solid tumors	<i>C. albicans</i>	Inhibition of filamentation	Routh et al., 2013
Doxorubicin	Bladder, breast, stomach, lung, ovarian, and thyroid cancers	<i>P. aeruginosa</i>	Inhibition of biofilm formation and quorum sensing	Ueda et al., 2009
		<i>C. albicans</i>	Inhibition of filamentation	Chavez-Dozal et al., 2014
Daurorubicin	Acute myeloid leukemia, acute lymphocytic leukemia, chronic myelogenous leukemia, and Kaposi's sarcoma	<i>C. albicans</i>	Inhibition of filamentation	Chavez-Dozal et al., 2014
Clofoctol	Bacterial infection	<i>P. aeruginosa</i>	Inhibition of the pqs system, probably by targeting the transcriptional regulator PqsR	D'Angelo et al., 2018
Azithromycin	Bacterial infection	<i>P. aeruginosa</i>	Interaction with the ribosome, resulting in direct and/or indirect repression of specific subsets of genes involved in virulence, quorum sensing, biofilm formation,	Imperi et al., 2014
5-fluorocytosine	Fungal infection	<i>P. aeruginosa</i>	Inhibition of the production of pyoverdine, P1p protease, and exotoxin A by downregulation of the <i>pvdS</i> gene.	Imperi et al., 2013a
Clotrimazole and miconazole	Fungal infection	<i>P. aeruginosa</i>	Inhibition of the <i>pqs</i> activity through the possible inactivation of 2-alkyl-4-quinolones (AQ) production or reception	D'Angelo et al., 2018
Gallium nitrate*	Lymphoma and bladder cancer	<i>P. aeruginosa</i>	Effects on iron metabolism	Antunes et al., 2012
Celecoxib	Inflammation	<i>S. aureus</i> , <i>B. anthracis</i> , <i>B. subtilis</i> , and <i>M. smegmatis</i>	Inhibition of bacterial DNA, RNA, protein synthesis, and cell wall	Thangamani et al., 2015b
Diflunisal	Inflammation	<i>S. aureus</i>	Inhibition of ArgA, a regulator protein which inhibits alpha-type phenol soluble modulins toxins	Hendrix et al., 2016
Glatiramer acetate	Inflammation	<i>P. aeruginosa</i>	Disruption of biofilm formation	Christiansen et al., 2017

(Continued)

TABLE 1 | Continued

Drugs	Clinical indication	Target bacteria	Mechanisms of action	Reference
Aspirin and ibuprofen	Inflammation	<i>C. neoformans</i> and <i>C. gattii</i>	Stress induction via activation of the high-osmolarity glycerol (HOG) pathway, and activation of reactive oxygen species (ROS)-mediated membrane damage	Ogundejí et al., 2016
Pimozide	Severe Tourette's syndrome and schizophrenia	<i>L. monocytogenes</i>	Reduction of <i>L. monocytogenes</i> internalization by phagocytic cells by decreasing vacuolar escape and diminishing cell-to-cell spread	Lieberman and Higgins, 2009
Azathioprine	Crohn's disease	<i>P. aeruginosa</i> and <i>E. coli</i>	Inhibition of WspR. WspR is a diguanylate cyclase involved in the regulation of a signal molecule called cyclic-di-GMP (c-di-GMP) known as a regulated of the bacterial biofilm formation	Antoniani et al., 2013
Simvastatin	Hypercholesterolemia	<i>M. tuberculosis</i>	Reduction of cholesterol within phagosomal membrane	Parthar et al., 2014
Atorvastatin	Hypercholesterolemia	<i>C. gattii</i>	Reduction of the ergosterol content in the cell membrane and alteration of the properties of the polysaccharide capsule; increase in the production of ROS by macrophages; and reduction of yeast phagocytosis and the intracellular proliferation rate	Ribeiro et al., 2017
Ebselen*	Bipolar disorder and ischemic stroke	<i>S. aureus</i> , <i>C. difficile</i>	Reduction of biofilm formation and targeting of the glucosyltransferase domain toxins	Gi et al., 2014; Peng et al., 2018
Pentetic acid	Hypocalcemia	<i>P. aeruginosa</i>	Reduction of biofilm formation and inhibition of elastase	Gi et al., 2014
Auranofin	Rheumatoid arthritis	<i>S. aureus</i>	DNA inhibition and protein synthesis, and downregulation of toxin production	Thangamani et al., 2016a

* Some of the drugs listed in this table displayed multiple effects against different pathogens, and that only the findings of an exemplifying study are reported in the table. Other studies on the same drugs are discussed in the text.

A. baumannii and *K. pneumoniae* (Ayerbe-Algaba et al., 2018). Recently, the effectiveness of niclosamide against *Helicobacter pylori* has been described, showing an MIC of 0.25 mg/L against the ATCC 49503 strain (Tharmalingam et al., 2018). Furthermore, niclosamide has demonstrated an immunomodulatory role by decreasing the secretion of IL-8 in a gastric cancer cell line after *H. pylori* infection (Tharmalingam et al., 2018). Niclosamide also showed therapeutic efficacy in an experimental infection model of *Galleria mellonella* larvae infected with *P. aeruginosa* and *H. pylori* (Imperi et al., 2013b; Tharmalingam et al., 2018). The formulation of niclosamide under nanosuspension showed lower toxicity in a rat lung infection model involving *P. aeruginosa*; the results of this study are potentially favorable for the further study of this formulation (Costabile et al., 2015).

In the case of fungi, mebendazole inhibited the growth of *Cryptococcus neoformans* and *Cryptococcus gattii* and affected the formation of biofilm by *C. neoformans* (Joffe et al., 2017). The combination of mebendazole with amphotericin B increased the fungicidal activity of amphotericin B against *C. neoformans* twofold (Joffe et al., 2017). Moreover, quinacrine, in monotherapy, has been shown *in vitro* to be effective for the prevention and treatment of *Candida albicans* biofilms, accumulating in vacuoles and causing defects in endocytosis (Kulkarny et al., 2014). In combination with caspofungin or amphotericin B, quinacrine has demonstrated synergy against *C. albicans* (Kulkarny et al., 2014).

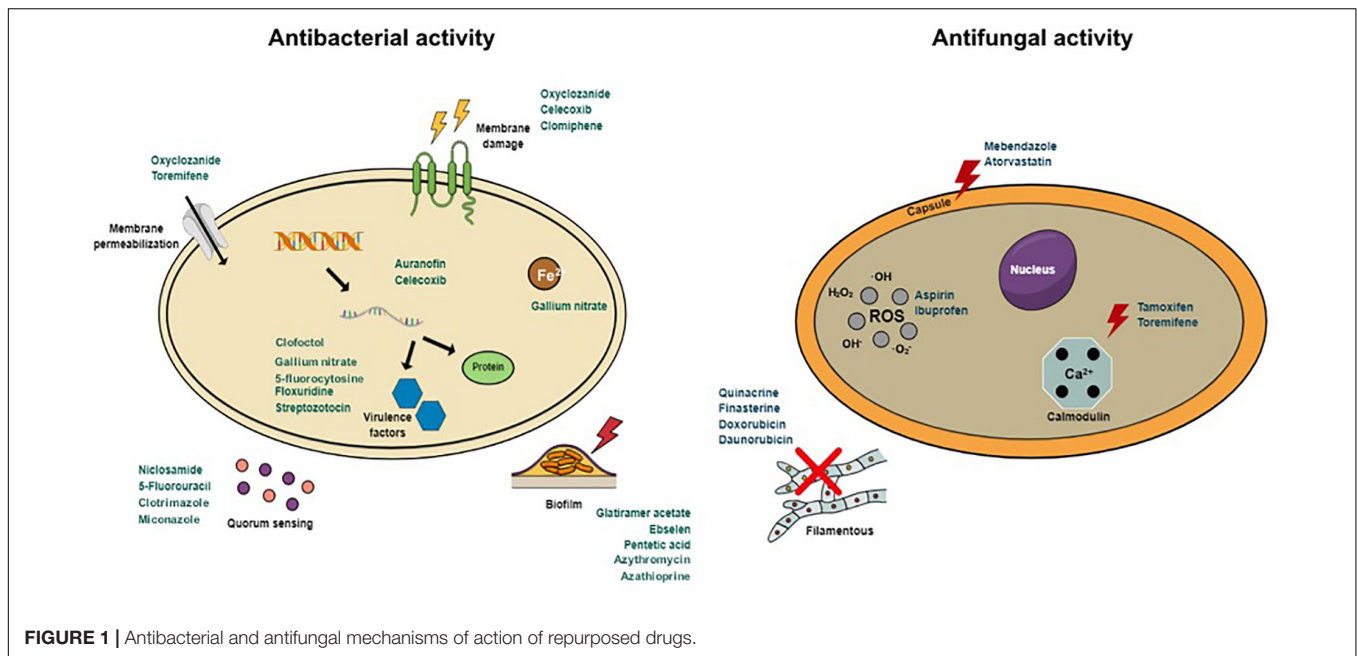
These studies highlight the potential use of the anthelmintic drugs as antimicrobial agents as monotherapy for infections caused by Gram-positive and Gram-negative bacteria and fungi; although *in vivo* studies in vertebrate experimental models should be conducted.

Anticancer Drugs Repurposed Against Bacteria and Fungi

The antibacterial activity of anticancer drugs has also been reported (Soo et al., 2017). Most of them act against Gram-positive pathogens.

The FDA-approved anticancer drugs floxuridine (mostly used in colorectal cancer) and streptozotocin (used for pancreatic islet cell cancer) have exhibited activity against *S. aureus* by inhibiting the SaeRS two-component system (TCS) (Yeo et al., 2018). SaeRS TCS is an important transcriptional regulator of different virulence factors of *S. aureus* including adhesins, toxins, and enzymes (Yeo et al., 2018). Floxuridine showed direct antibacterial activity by inhibiting the growth of *S. aureus* USA300 at a concentration of 0.0625 mg/L *in vitro* and increasing the survival of mice by 60% in a murine model of blood infection *in vivo* (Yeo et al., 2018). On the other hand, streptozotocin did not affect staphylococcal growth *in vitro* but reduced the mortality of mice to 10% *in vivo* (Yeo et al., 2018). Both drugs not only cause significant changes in the transcription of *S. aureus* genes, but also inhibit the transcription of other virulence regulatory systems of *S. aureus* (Yeo et al., 2018).

Another group of anticancer drugs developed to combat breast cancer is the selective estrogen receptor modulators



(SERMs). Tamoxifen has been reported to exhibit activity against *S. aureus* (Corriden et al., 2015) and its analog toremifene showed efficacy against oral infection caused by *Streptococcus mutans* (Gerits et al., 2017). Toremifene also has been shown to reduce biofilm formation by *S. mutans* due to a possible increase in membrane permeabilization and therefore, membrane damage (Gerits et al., 2017). Clomiphene, another SERM in preclinical development for the treatment of fertility, has demonstrated efficacy against *S. aureus* and *Bacillus subtilis* *in vitro*, with an MIC value of 8 mg/L, and incubation of *B. subtilis* with this concentration of clomiphene changed its morphology (Farha et al., 2015). The mode of action of clomiphene is through the inhibition of undecaprenyl diphosphate synthase (UPPS), an enzyme involved in the synthesis of the teichoic acid wall of *S. aureus* (Farha et al., 2015). Due to this action on the bacterial wall, clomiphene exhibits synergy with β -lactams in restoring MRSA susceptibility (Farha et al., 2015).

Other anticancer drugs were tested as adjunctive therapies against *M. tuberculosis* infection. One such drug, denileukin diftitox, is currently used for the treatment of cutaneous T-cell lymphoma (Gupta et al., 2017). Treatment with denileukin diftitox slightly reduced the lung bacterial count in mice aerosol-infected with *M. tuberculosis* (Gupta et al., 2017). The addition of this drug to standard tuberculosis treatments, composed of rifampin, isoniazid, and pyrazinamide, similarly reduced the bacterial burden (Gupta et al., 2017).

Different studies have been also performed on Gram-negative bacteria to evaluate the antibacterial effect of anticancer drugs. A potent anticancer drug indicated for the treatment of different types of solid tumors called 5-fluorouracil, as well as gallium nitrate, an anticancer drug for the treatment of lymphoma and bladder cancer, have been extensively studied (Banin et al., 2008; Bonchi et al., 2014; Minandri et al., 2014; Rangel-Vega et al.,

2015). 5-fluorouracil has been used against a collection of 5,850 mutants of the *P. aeruginosa* PA14 strain, revealing positive activity via the regulation of a large number of genes involved in quorum sensing and biofilm formation (Ueda et al., 2009; Rangel-Vega et al., 2015). Also, gallium nitrate has demonstrated *in vitro* an inhibitory effect on bacterial growth in a collection of 58 multidrug-resistant (MDR) *A. baumannii* strains, and in *P. aeruginosa* at concentrations $>3.13 \mu\text{M}$ (Kaneko et al., 2007; Antunes et al., 2012; Frangipani et al., 2014); although the presence of pyoverdine and proteases in human serum reduce the efficacy of gallium nitrate against *P. aeruginosa* by increasing its MIC (Bonchi et al., 2015). At non-bactericidal concentrations, gallium nitrate can affect the production of virulence factors of *P. aeruginosa* (Kaneko et al., 2007; García-Contreras et al., 2014). In *G. mellonella*, the administration of this drug alone or in combination with colistin, at concentrations mimicking the human therapeutic dose of gallium nitrate used for cancer patients (28 μM), significantly increased the survival of larvae after infection by *A. baumannii* (Antunes et al., 2012). Moreover, in murine models of acute and chronic lung infections by *P. aeruginosa* and *A. baumannii*, gallium nitrate has reduced lung injury and bacterial loads in tissues (Kaneko et al., 2007; de Léséleuc et al., 2012). Regarding SERM drugs, toremifene has shown efficacy against oral infection caused by *Porphyromonas gingivalis* (Gerits et al., 2017), and raloxifene attenuated *in vitro* and in *Caenorhabditis elegans* model the virulence of *P. aeruginosa* by binding to PhzB2 which is involved in the production of pyocyanin, a pigment related with the virulence of this pathogen (Ho Sui et al., 2012).

In the case of fungi, the activity of anticancer drugs has also been investigated. Floxuridine, at twice its half maximal inhibitory concentration (IC₅₀) value, has exhibited fungicidal

activity against *Exserohilum rostratum* reducing the hyphae-derived CFU (colony-forming unit) of this fungus (Sun et al., 2013). The SERM compounds such as tamoxifen and toremifene have also shown fungicidal activity against *C. neoformans*. They also display a number of pharmacological properties desirable for anticryptococcal drugs, including synergistic fungicidal activity with fluconazole and/or amphotericin B *in vitro* and *in vivo*, oral bioavailability, and activity within macrophages (Butts et al., 2014). They bind directly to the two essential EF-hand proteins calmodulin 1 (Cam1) and calmodulin-like protein 1 (Cml1) of *C. neoformans*, preventing Cam1 from binding to its well-characterized substrate calcineurin (Cna1), thereby blocking Cna1 activation (Butts et al., 2014). In whole cells, toremifene and tamoxifen are known to block the calcineurin-dependent nuclear localization of the transcription factor Crz1 (Butts et al., 2014). Together, both drugs have inhibited the growth of *C. neoformans* within macrophages, a niche not accessible to current antifungal drugs (Butts et al., 2014). In murine-disseminated cryptococcosis, tamoxifen in combination with fluconazole decreased the brain burden by $\sim 1 \log_{10}$ CFU/g (Butts et al., 2014). Against *C. albicans* and *Candida glabrata*, toremifene has enhanced the antibiofilm activity of amphotericin B and caspofungin [fractional inhibitory concentration index (FICI) < 0.5 both *in vitro* and *in vivo* worm infection models (Delattin et al., 2014)].

Other anticancer drug such as finasteride, a 5- α -reductase inhibitor commonly used for the treatment of benign prostatic hyperplasia, was highly effective in both the prevention and destruction of *C. albicans* biofilm formation at doses greater than 16 and 128 mg/L, respectively (Chavez-Dozal et al., 2014). In combination with 2 mg/L fluconazole, 2 mg/L, finasteride exhibited synergistic activity in the prevention of biofilm formation by *C. albicans* (Chavez-Dozal et al., 2014). Similar effects were observed in the presence of doxorubicin and daunorubicin that inhibited the morphogenesis of *C. albicans* (Routh et al., 2013).

Anticancer drugs not only target bacteria and fungi but can also regulate the host response. Floxuridine and streptozotocin have presented a protective effect on the host by reducing *S. aureus*-mediated killing in human neutrophils (Yeo et al., 2018). Moreover, tamoxifen can stimulate chemotaxis, phagocytosis, and neutrophil extracellular trap (NET) formation through the modulation of the ceramide pathway upon infection with *S. aureus* (Corriden et al., 2015). Unlike tamoxifen, its analog raloxifene has been shown to reduce NET formation in human neutrophils, thus resulting in cell death of *S. aureus* (Flores et al., 2016). In addition, denileukin diftitox has been reported to bind to the IL-2 receptor in T lymphocytes, thereby introducing diphtheria toxin inside these cells to suppress them. The decrease in this type of T cell hinders the replication of *M. tuberculosis* (Gupta et al., 2017). It is noteworthy to mention that toxicity of anticancer drugs is important in terms of their establishment as antibacterial drugs. Tamoxifen has been used for over 30 years to treat breast cancer. The doses of tamoxifen used in animals (250 mg/kg) (Corriden et al., 2015) and in humans (20–40 mg) are generally tolerated. For clomiphene, acute oral LD₅₀ in mice and rats were 1,700 and 5,750 mg/kg, respectively (Drug Bank, 2018). The toxic dose of clomiphene

in humans is unknown but toxic effects accompanying acute overdosage were not observed (Drug Bank, 2018). In the case of gallium nitrate, the treatment of hypercalcemia was performed with continuous intravenous infusion (200 mg/m²/day during 5 days) being generally well tolerated (Warrell et al., 1988). On the other hand, higher doses (300 mg/m²/day during 5–7 days) were used in cancer and side effects such as diarrhea and renal toxicity were observed (Chitambar, 2010).

Anti-inflammatory and Immunomodulatory Drugs Repurposed Against Bacteria and Fungi

As is the case with anticancer drugs, anti-inflammatory and immunomodulatory drugs have demonstrated more antibacterial activity against Gram-positive than Gram-negative bacteria and fungi.

Celecoxib, a non-steroidal anti-inflammatory drug (NSAID), showed antibacterial activity against several pathogens including *S. aureus*, *Bacillus anthracis*, *B. subtilis*, and *M. smegmatis* (Thangamani et al., 2015b). Celecoxib has demonstrated non-specific targeting by inhibiting bacterial DNA and RNA replication, protein synthesis, and cell wall formation (Thangamani et al., 2015b), as well as reducing the levels of IL-6, TNF- α , IL-1 β , and MCP-1 (monocyte-chemoattractant protein-1) in skin lesions caused by *S. aureus* infection (Thangamani et al., 2015b). Moreover, this drug has exhibited synergy with several topical and systemic antimicrobials used against *S. aureus*, with the exception of linezolid (Thangamani et al., 2015b).

Other NSAIDs, such as diflunisal in combination with diclofenac, ibuprofen and verapamil have shown antibacterial activity against *S. aureus* and *M. tuberculosis* (Dutta et al., 2007; Vilaplana et al., 2013; Gupta et al., 2015; Hendrix et al., 2016). It was reported that diflunisal did not affect the bacterial growth of *S. aureus in vitro*, but did inhibit their toxicity in murine and human osteoblasts *in vivo* (Hendrix et al., 2016). Confirmed data have been observed in mice treated with diflunisal, which have presented less cortical bone marrow destruction, although a reduction in the bacterial load was not observed (Hendrix et al., 2016). Even though bacterial growth was not compromised, diflunisal inhibited accessory gene regulator A (AgrA), a regulator protein which inhibits alpha-type phenol soluble modulins (PSMs) and may contribute to a reduction in *S. aureus* virulence (Hendrix et al., 2016). In the case of verapamil, it has potentiated the activity of bedaquiline, a novel drug used to treat MDR tuberculosis, against *M. tuberculosis* (Dutta et al., 2007; Gupta et al., 2015). Moreover, treatment with ibuprofen significantly decreased the bacterial load and increased mice survival in an experimental model of active tuberculosis (Vilaplana et al., 2013).

For Gram-negative bacteria, celecoxib and betamethasone in combination with antibiotics have demonstrated activity against different bacterial species (Artini et al., 2014; Thangamani et al., 2015b). Celecoxib has presented synergy with colistin against *A. baumannii*, *P. aeruginosa*, *Escherichia coli*, *K. pneumoniae* and *Salmonella enterica* serovar

Typhimurium (Thangamani et al., 2015b), and betamethasone has demonstrated synergy with ceftazidime, erythromycin, and ofloxacin against *P. aeruginosa* and some strains of *E. coli* (Artini et al., 2014). Diclofenac, in turn, was found to exhibit efficacy both *in vitro* and *in vivo* against *S. enterica* serovar Typhimurium (Dutta et al., 2007). In the case of glatiramer acetate, a drug used in the treatment of multiple sclerosis, activity against *A. baumannii*, *P. aeruginosa*, and *E. coli* reference strains, and against *A. baumannii* and *P. aeruginosa* clinical isolates from bacteremia and chronic respiratory infections in cystic fibrosis patients has been observed by disruption of the biofilm formation (Christiansen et al., 2017).

Like anticancer drugs, some anti-inflammatory and immunosuppressive drugs such as aspirin, ibuprofen, and tacrolimus have shown antifungal activity against *C. neoformans*, *C. gattii*, and *E. rostratum*, respectively (Sun et al., 2013; Ogundeji et al., 2016). The treatment of cryptococcal cells with aspirin and ibuprofen has led to the induction of stress via activation of the high-osmolarity glycerol (HOG) pathway in *C. neoformans* and *C. gattii*, and to their death through the activation of reactive oxygen species (ROS)-mediated membrane damage (Ogundeji et al., 2016). The MICs of these drugs did not negatively affect growth or impair macrophage function; rather, they enhanced the ability of these immune cells to phagocytose cryptococcal cells (Ogundeji et al., 2016). Moreover, treatment with tacrolimus at twice its IC₅₀ value significantly reduced the hyphae-derived CFU of *E. rostratum* (Sun et al., 2013).

Antipsychotic and Antidepressant Drugs Repurposed Against Bacteria and Fungi

Trifluoperazine, an antipsychotic drug, has showed therapeutic efficacy in a murine model of *C. difficile* infection, presenting higher survival rates than those treated with vancomycin; a decrease in inflammation and edema was also observed compared with the infected group (Andersson et al., 2016). Furthermore, together with amoxapine, trifluoperazine in combination with vancomycin protected 80% and 100% of mice, respectively, from severe oral infection caused by *C. difficile* (Andersson et al., 2016). Rani Basu et al. (2005) reported that the combination of two different non-antimicrobial drugs, prochlorperazine and methdilazine, may present antibacterial activity against *S. aureus*.

For Gram-negative bacteria, pimozide, used for the treatment of severe Tourette's syndrome and schizophrenia, has reduced *in vitro* the internalization of *S. enterica* serovar Typhimurium and *E. coli* by phagocytic cells (Lieberman and Higgins, 2009). Moreover, pimozide reduced the bacterial uptake and vacuolar escape of *Listeria monocytogenes* in bone marrow-derived macrophages, as well as the invasion and cell-to-cell spread of the bacteria during the infection of non-phagocytic cells (Lieberman and Higgins, 2009). In addition, the drugs trifluoperazine and amoxapine were shown to be active against *Yersinia pestis* after screening of a library of 780 FDA-approved drugs to identify molecules which reduce *Y. pestis* cytotoxicity in murine macrophages (Andersson et al., 2016). These two compounds exhibited therapeutic efficacy in a murine model of pneumonic

plague by *Y. pestis*; although the treatment was less effective when administration of the drug was delayed (Andersson et al., 2017). However, their efficacy was improved when both compounds were administered in combination with levofloxacin (Andersson et al., 2017). In addition to this study, amoxapine was reported to present therapeutic efficacy in an experimental murine model of respiratory infection caused by *K. pneumoniae* (Andersson et al., 2017). Finally, azathioprine, an antidepressant drug used for the treatment of Crohn's disease, has exhibited anti-biofilm activity against *P. aeruginosa* and *E. coli* through the inhibition of WspR (Antoniani et al., 2013). WspR is a diguanylate cyclase involved in the regulation of a signal molecule called cyclic-di-GMP (c-di-GMP) known as a regulator of the bacterial biofilm formation (Antoniani et al., 2013).

In the case of fungi, the antipsychotic drug bromperidol has exhibited synergy with various azoles against *C. albicans*, *C. glabrata*, and *Aspergillus terreus* (Holbrook et al., 2017). Bromperidol has demonstrated synergy with posaconazole and voriconazole, and partial synergy with itraconazole and ketoconazole against *C. albicans*, *C. glabrata*, and *A. terreus*, as demonstrated by checkerboard and time-kill assays (Holbrook et al., 2017). Moreover, bromperidol in combination with posaconazole and voriconazole, increased the disruption of biofilm formation by sessile cells of *C. albicans* induced by both azoles. Their sessile MICs were reduced from >32 to 0.5 mg/L (Holbrook et al., 2017).

Other Drugs Repurposed Against Bacteria and Fungi

Other drugs with different modes of action and clinical indications have been evaluated as antibacterial agents. Auranofin, which is used for the treatment of rheumatoid arthritis, has shown in monotherapy greater activity against a wide range of Gram-positive bacteria including *S. pneumoniae*, *S. aureus*, *Enterococcus faecium*, *E. faecalis*, and *Streptococcus agalactiae* when compared with vancomycin or linezolid (Aguinagale et al., 2015; Thangamani et al., 2016a,b). *In vivo*, auranofin and its analogs have demonstrated therapeutic efficacy in different experimental models such as MRSA septicemic infection, MRSA skin infection, MRSA implant infection model (a model involving mesh-associated biofilm), and MRSA intramuscular infection model (Aguinagale et al., 2015; Thangamani et al., 2016a,b). Interestingly, auranofin has demonstrated synergy with the commonly used antibiotics such as ciprofloxacin, linezolid, and gentamicin against MRSA (Thangamani et al., 2016b). In order to improve the activity of auranofin, different analogs were synthesized and display improved antibacterial activity against *S. aureus* and *S. pneumoniae* causing bacteremia in murine model (Aguinagale et al., 2015). The mode of action of auranofin against *S. aureus* has been deciphered using the macromolecular biosynthesis assay which showed that auranofin acts on the inhibition of DNA replication and protein synthesis, downregulating the toxin production (Thangamani et al., 2016a).

Ebselen; despite the fact that it is not an FDA-approved drug, it is being investigated in clinical trials for the treatment of

bipolar disorder and ischemic stroke, has also been evaluated. Two studies have suggested that this compound exhibited antibacterial activity against *C. difficile* *in vitro* and *in vivo* by targeting glucosyltransferase domain (GTD) of *C. difficile* toxins (Peng et al., 2018), and against MRSA and vancomycin-resistant *S. aureus* (VRSA) with MIC values <1 mg/L (Thangamani et al., 2015c). Moreover, ebselen has also reduced the biofilm formation by *S. aureus* (Gi et al., 2014). Synergy between this drug and fusidic acid, retapamulin, mupirocin, and daptomycin against *S. aureus* strains was confirmed using a Bliss model (Thangamani et al., 2015c).

Besides these two drugs, the antihistaminic compounds terfenadine and its analogs were also investigated as potential antibacterial drugs. Terfenadine has showed reasonable activity against *S. aureus* (Perlmutter et al., 2014). In order to improve their activity, 84 derivatives were synthesized that have presented greater MIC values against *S. aureus* (1 mg/L) as well as activity against *E. faecium*, *E. faecalis*, and *M. tuberculosis* (Perlmutter et al., 2014).

In the case of statins, simvastatin, used in the treatment of atherosclerotic cardiovascular disease and hypercholesterolemia, has exhibited antibacterial activity in monotherapy against *M. tuberculosis* (Parihar et al., 2014; Skerry et al., 2014). It marginally reduced the bacterial load 4 and 8 weeks after infection with *M. tuberculosis* by aerosol exposure; presumably by reducing cholesterol synthesis due to the inhibition of HMG-CoA reductase within the phagosomal membrane. This process has consequently enhanced the maturation of phagosomes, known to provide better defense against *M. tuberculosis*, and by inducing the autophagy of *M. tuberculosis*-infected macrophages (Parihar et al., 2014). The addition of simvastatin to the first-line tuberculosis therapy (rifampicin + isoniazid + pyrazinamide) may help to reduce mycobacterial infection and tissue damage in *M. tuberculosis*-infected mice (Skerry et al., 2014). Similarly, atorvastatin, another statin drug, has also demonstrated synergistic activity with rifampin *in vitro* against *M. tuberculosis* and in a murine model of *Mycobacterium leprae* infection (Lobato et al., 2014).

Regarding Gram-negative bacteria, auranofin exhibited synergy with polymyxin B against *A. baumannii*, *P. aeruginosa*, *K. pneumoniae* and *S. enterica* serovar Typhimurium (Thangamani et al., 2016a).

Ebselen has also presented antibacterial effect against *A. baumannii* and *E. coli* by reducing their bacterial growth at MICs of 32 μ M and <128 μ M, respectively. This bacterial reduction growth was due to the inhibition of TonB-mediated physiology, which is involved in iron acquisition from host sources (Nairn et al., 2017). Furthermore, ebselen exhibited anti-virulence activity against *P. aeruginosa* by targeting c-di-GMP signaling pathway, which regulates motility and biofilm formation (Gi et al., 2014; Lieberman et al., 2014).

In the case of statins, the combination of simvastatin with sub-inhibitory concentrations of colistin presented synergistic effect against a collection of *A. baumannii*, *E. coli*, *K. pneumoniae*, *P. aeruginosa*, and *S. enterica* serovar Typhimurium reducing the MIC of simvastatin from >256 mg/L to a range between 8 and 32 mg/L (Thangamani et al., 2015a). In addition, screening of an

FDA-approved drug library has identified pentetic acid, an iron chelator, as an inhibitor of elastase, an important exoprotease as well as a reducer of biofilm formation by *P. aeruginosa* (Gi et al., 2014). When applied to *P. aeruginosa* infections in human lung tissue, pentetic acid increased the viability of human lung epithelial A549 cells post-infection (Gi et al., 2014). Interestingly, pentetic acid has also demonstrated therapeutic efficacy in a murine experimental model of respiratory infection by *P. aeruginosa* by increasing 42% the mice survival 5 days post-infection (Gi et al., 2014).

Moreover, calcitriol, a bioactive form of vitamin D3 used to treat hypocalcemic conditions and renal osteodystrophy, has been described as an enhancer of bactericidal activity against *P. aeruginosa*, due to its capacity to modulate the activity of monocytes and macrophages by increasing their bacterial killing (Nouari et al., 2015).

Other drugs that have presented anti-virulence effect against *P. aeruginosa* have been reported. For example 5-fluorocytosine, an antifungal drug, has been shown to reduce *in vitro* the production of virulence factors by *P. aeruginosa* such as pyoverdine, PrpL protease, and exotoxin A by downregulating *pvdS* gene expression (Imperi et al., 2013a), and to suppress *in vivo* the pathogenicity of *P. aeruginosa* in a murine model of lung infection (Imperi et al., 2013a). Other antifungal drugs such as clotrimazole and miconazole were identified as inhibitors of 2-heptyl-3-hydroxy-4 quinolone (PQS) quorum sensing (QS) system. This system is based on signal 2-alkyl-4-quinolones (AQ): PQS and 2-heptyl-4-hydroxyquinolone (HHQ) which can bind and activate the regulator PqsR and controls the expression of *P. aeruginosa* virulence factors. D'Angelo et al. (2018) have shown that probably both drugs modify PqsR function by competing with PQS and HHQ for the PqsR ligand-binding site. Finally, clofocetol and azithromycin, drugs originally developed as antibiotics against Gram-positive and Gram-negative bacteria, respectively, were found to have also anti-virulence properties against *P. aeruginosa* (Imperi et al., 2014; D'Angelo et al., 2018).

In the case of fungi, atorvastatin has demonstrated different effects on the host and the yeast by: (i) reducing the ergosterol content in the cell membrane and altering the properties of the polysaccharide capsule of *C. gattii*; (ii) increasing the production of ROS by macrophages; and (iii) reducing yeast phagocytosis and the intracellular proliferation rate (Ribeiro et al., 2017). Atorvastatin in combination with fluconazole was also tested as an adjuvant to control fungal infections. This combination demonstrated synergy *in vitro* against one strain of *C. gattii*. *In vivo*, atorvastatin plus fluconazole increased the survival of mice and reduced the burden of *C. gattii* in the lungs and brain (Ribeiro et al., 2017). Moreover, preclinical antimalarial drugs such as MMV665943 have been shown to inhibit and delay growth at submicromolar concentrations and exhibit fungicidal activity at concentrations greater than 1.56 μ M against *C. albicans*, *C. neoformans*, *C. gattii* and *Lomentospora prolificans*. More specifically, this compound at concentrations greater than 1.56 μ M affects the polysaccharide capsule thickness of *C. neoformans* (Jung et al., 2018).

Regarding the immune response modulation, ebselen and auranofin reduced the production of inflammatory cytokines

such as TNF- α , IL-6, IL-1 β , and MCP-1 in skin lesions infected by *S. aureus* (Thangamani et al., 2016a, 2015c). Similarly, calcitriol has shown a modulatory effect on monocytes and macrophages against *P. aeruginosa* infection by increasing their bacterial killing (Nouari et al., 2015). The mechanism of action of calcitriol on the immune system is unknown; although its downregulating effect on IL-1 β , IL-6, and IL-8 has been observed (Xue et al., 2002). In the case of statin, simvastatin has been reported to modulate the production of proinflammatory cytokines (IL-8 and CCL20) and Kruppel-like factors (an emerging group of immune system regulators) in *P. aeruginosa* respiratory infections (Hennessy et al., 2014).

CLINICAL APPLICATION OF REPURPOSED DRUGS AGAINST INFECTIOUS AGENTS

Even though repurposed drugs showed promising preclinical data, to our knowledge only three clinical studies have been performed or are currently underway.

A randomized study on the role of aspirin in tuberculous meningitis suggested that aspirin in combination with corticosteroids reduced the incidence of strokes and mortality (Misra et al., 2010). A similar study on the role of aspirin as an adjunct with steroids for the treatment of HIV-negative adults with tuberculous meningitis in Vietnam is still ongoing, now in Phase II trial (clinical trials identifier: NCT02237365). Another Phase III trial (ClinicalTrials.gov Identifier: NCT02060006) is being conducted to evaluate the feasibility and efficacy of using meloxicam, a cheap and widely available NSAID, as a preventive intervention for tuberculous-immune reconstituted inflammatory syndrome; results from this study have yet to be published (Maitra et al., 2016).

REFERENCES

- Aguinalde, L., Díez-Martínez, R., Yuste, J., Royo, I., Gil, C., Lasa, I., et al. (2015). Aurafinofin efficacy against MDR *Streptococcus pneumoniae* and *Staphylococcus aureus* infections. *J. Antimicrob. Chemother.* 70, 2608–2617. doi: 10.1093/jac/dkv163
- Andersson, J. A., Fitts, E. C., Kirtley, M. L., Ponnusamy, D., Peniche, A. G., Dann, S. M., et al. (2016). New role for FDA-approved drugs in combating antibiotic-resistant bacteria. *Antimicrob. Agents Chemother.* 60, 3717–3729. doi: 10.1128/AAC.00326-16
- Andersson, J. A., Sha, J., Kirtley, M. L., Reyes, E., Fitts, E. C., Dann, S. M., et al. (2017). Combating multidrug-resistant pathogens with host-directed nonantibiotic therapeutics. *Antimicrob. Agents Chemother.* 62, e1943–e1917. doi: 10.1128/AAC.01943-17
- Antoniani, D., Rossi, E., Rinaldo, S., Bocci, P., Lolicato, M., Paiardini, A., et al. (2013). The immunosuppressive drug azathioprine inhibits biosynthesis of the bacterial signal molecule cyclic-di-GMP by interfering with intracellular nucleotide pool availability. *Appl. Microbiol. Biotechnol.* 97, 7325–7336. doi: 10.1007/s00253-013-4875-0
- Antunes, L. C. S., Imperi, F., Minandri, F., and Visca, P. (2012). In vitro and in vivo antimicrobial activities of gallium nitrate against multidrug-resistant *Acinetobacter baumannii*. *Antimicrob. Agents Chemother.* 56, 5961–5970. doi: 10.1128/AAC.01519-12
- Årdal, C., Baraldi E., Theuretzbacher, U., Outtersson, K., Plahte, J., Ciabuschi, F., et al. (2018). Insights into early stage of antibiotic development in small- and medium-sized enterprises: a survey of targets, costs, and durations. *J. Pharm. Policy Pract.* 11:8. doi: 10.1186/s40545-018-0135-0
- Artini, M., Cellini, R., Tilota, A., Barbato, M., Koverech, A., Selan, L., et al. (2014). Effect of betamethasone in combination with antibiotics on gram positive and gram negative bacteria. *Int. J. Immunopathol. Pharmacol.* 27, 675–682. doi: 10.1177/039463201402700426
- Ashraf, S., Chaudhry, U., Raza, A., Ghosh, D., and Zhao, X. (2018). In vitro activity of ivermectin against *Staphylococcus aureus* clinical isolates. *Antimicrob. Resist. Infect. Control* 7:27. doi: 10.1186/s13756-018-0314-4
- Ayerbe-Algaba, R., Gil-Marqués, M. L., Jiménez-Mejías, M. E., Sánchez-Encinales, V., Parra-Millán, R., Pachón Ibáñez, M. E., et al. (2018). Synergistic activity of niclosamide in combination with colistin against colistin-susceptible and colistin-resistant *Acinetobacter baumannii* and *Klebsiella pneumoniae*. *Front. Cell. Infect. Microbiol.* 8:348. doi: 10.3389/fcimb.2018.00348
- Bagley, N., and Outtersson, K. (2017). *We Will Miss Antibiotics When They're Gone* Available at: www.nytimes.com/2017/01/18/opinion/how-to-avoid-a-post-antibiotic-world.html
- Banin, E., Lozinski, A., Brady, K. M., Berenshtein, E., Butterfield, P. W., Moshe, M., et al. (2008). The potential of desferrioxamine-gallium as an anti-*Pseudomonas* therapeutic agent. *Proc. Natl. Acad. Sci. U.S.A.* 105, 16761–16766. doi: 10.1073/pnas.0808608105
- Bonchi, C., Frangipani, E., Imperi, F., and Visca, P. (2015). Pyoverdine and proteases affect the response of *Pseudomonas aeruginosa* to gallium in human

CONCLUSION AND PERSPECTIVES

In the last decade, substantial progress has been made in the development of repurposed drugs for the treatment of bacterial and fungal infections. Several compounds have yielded promising data but developmental efforts remain in the preclinical stage. Additional relevant issues should be taken into account in the preclinical development of repurposing drugs including possible need for new formulations to increase their bioavailability and ADMET tests if the administration route is changed, possible negative effect of the primary drug activity (especially for anticancer and antipsychotic drugs), and challenges for intellectual property rights. Moreover, further clinical studies are needed to address the urgent demand for new treatments targeting infections caused by bacteria and fungi.

AUTHOR CONTRIBUTIONS

AM-C, RA-A, and YS wrote the manuscript. All authors read and approved the final manuscript.

FUNDING

This study was supported by Miguel Servet Tipo I Project grant, Instituto de Salud Carlos III, Subdirección General de Redes y Centros de Investigación Cooperativa, Ministerio de Economía, Industria y Competitividad (CP15/00132), the Instituto de Salud Carlos III, Proyectos de Investigación en Salud (Grant No. PI16/01378). YS is supported by the Subprograma Miguel Servet Tipo I from the Ministerio de Economía y Competitividad of Spain (CP15/00132).

- serum. *Antimicrob. Agents Chemother.* 59, 5641–5646. doi: 10.1128/AAC.01097-15
- Bonchi, C., Imperi, F., Minandri, F., Visca, P., and Frangipani, E. (2014). Repurposing of gallium-based drugs for antibacterial therapy. *Biofactors* 40, 303–312. doi: 10.1002/biof.1159
- Brown, D. (2015). Antibiotic resistance breakers: can repurposed drugs fill the antibiotic discovery void? *Nat. Rev. Drug Discov.* 4, 821–832. doi: 10.1038/nrd4675
- Butts, A., Koselny, K., Chabrier-Roselló, Y., Semighini, C. P., Brown, J. C. S., Wang, X., et al. (2014). Estrogen receptor antagonists are anti-cryptococcal agents that directly bind EF hand proteins and synergize with fluconazole in vivo. *mBio* 5:e765-13. doi: 10.1128/mBio.00765-13
- Chavez-Dozal, A. A., Lown, L., Jahng, M., Walraven, C. J., and Lee, S. A. (2014). *In vitro* analysis of finasteride activity against *Candida albicans* urinary biofilm formation and filamentation. *Antimicrob. Agents Chemother.* 58, 5855–5862. doi: 10.1128/AAC.03137-14
- Chen, W., Mook, R. A. Jr., Premont, R. T., and Wang, J. (2018). Niclosamide: beyond an antihelminthic drug. *Cell Signal.* 41, 89–96. doi: 10.1016/j.cellsig.2017.04.001
- Chitambar, C. R. (2010). Medical applications and toxicities of gallium compounds. *Int. J. Environ. Res. Public Health* 7, 2337–2361. doi: 10.3390/ijerph7052337
- Christiansen, S. H., Murphy, R. A., Juul-Madsen, K., Fredborg, M., Hvam, M. L., Axelgaard, E., et al. (2017). The immunomodulatory drug glatiramer acetate is also an effective antimicrobial agent that kills Gram-negative bacteria. *Sci. Rep.* 7:15653. doi: 10.1038/s41598-017-15969-3
- Corriden, R., Hollands, A., Olson, J., Derieux, J., Lopez, J., Chang, J. T., et al. (2015). Tamoxifen augments the innate immune function of neutrophils through modulation of intracellular ceramide. *Nat. Commun.* 6:8369. doi: 10.1038/ncomms9369
- Costabile, G., d'Angelo, I., Rampioni, G., Bondi, R., Pompili, B., Ascenzioni, F., et al. (2015). Towards repositioning niclosamide for anti-virulence therapy of *Pseudomonas aeruginosa* lung infections: development of inhalable formulations through nanosuspension technology. *Mol. Pharm.* 12, 2604–2617. doi: 10.1021/acs.molpharmaceut.5b00098
- Cowen, L. E., Sanglard, D., Howard, S. J., Rojers, P. D., and Perlin, D. S. (2015). Mechanisms of antifungal drug resistance. *Cold Spring Harb. Perspect. Med.* 5:a019752. doi: 10.1101/cshperspect.a019752
- D'Angelo, F., Baldelli, V., Halliday, N., Pantalone, P., Polticelli, F., Fiscarelli, E., et al. (2018). Identification of FDA-approved drugs as antivirulence agents targeting the pqs quorum sensing system of *Pseudomonas aeruginosa*. *Antimicrob. Agents Chemother.* 62, e1296–e1218. doi: 10.1128/AAC.01296-18
- de Léséleuc, L., Harris, G., KuoLee, R., and Chen, W. (2012). *In vitro* and *in vivo* biological activities of iron chelators and gallium nitrate against *Acinetobacter baumannii*. *Antimicrob. Agents Chemother.* 56, 5397–5400. doi: 10.1128/AAC.00778-12
- Delattin, N., De Brucker, K., Vandamme, K., Meert, E., Marchand, A., Chaltin, P., et al. (2014). Repurposing as a means to increase the activity of amphotericin B and caspofungin against *Candida albicans* biofilms. *J. Antimicrob. Chemother.* 69, 1035–1044. doi: 10.1093/jac/dkt449
- Dogra, N., Kumar, A., and Mukhopadhyay, T. (2018). Fenbendazole acts as a moderate microtubule destabilizing agent and causes cancer cell death by modulating multiple cellular pathways. *Sci. Rep.* 8:11926. doi: 10.1038/s41598-018-30158-6
- Drug Bank. (2018). *Clomiphene*. Available at: <https://www.drugbank.ca/drugs/DB00882>
- Dutta, N. K., Annadurai, S., Mazumdar, K., Dastidar, S. G., Kristiansen, J. E., Molnar, J., et al. (2007). Potential management of resistant microbial infections with a novel non-antibiotic: the anti-inflammatory drug diclofenac sodium. *Int. J. Antimicrob. Agents* 30, 242–249. doi: 10.1016/j.ijantimicag.2007.04.018
- Farha, M. A., Czarny, T. L., Myers, C. L., Worrall, L. J., French, S., Conrady, D. G., et al. (2015). Antagonism screen for inhibitors of bacterial cell wall biogenesis uncovers an inhibitor of undecaprenyl diphosphate synthase. *Proc. Natl. Acad. Sci. U.S.A.* 112, 11048–11053. doi: 10.1073/pnas.1511751112
- Fischbach, M. A., and Walsh, C. T. (2009). Antibiotics for emerging pathogens. *Science* 325, 1089–1093. doi: 10.1126/science.1176667
- Flores, R., Döhrmann, S., Schaal, C., Hakkim, A., Nizet, V., and Corriden, R. (2016). The selective estrogen receptor modulator raloxifene inhibits neutrophil extracellular trap formation. *Front. Immunol.* 7:566. doi: 10.3389/fimmu.2016.00566
- Frangipani, E., Bonchi, C., Minandri, F., Imperi, F., and Visca, P. (2014). Pyochelin potentiates the inhibitory activity of gallium on *Pseudomonas aeruginosa*. *Antimicrob. Agents Chemother.* 58, 5572–5575. doi: 10.1128/AAC.03154-14
- García-Contreras, R., Pérez-Eretza, B., Lira-Silva, E., Jasso-Chávez, R., Coria-Jiménez, R., Rangel-Vega, A., et al. (2014). Gallium induces the production of virulence factors in *Pseudomonas aeruginosa*. *Pathog. Dis.* 70, 95–98. doi: 10.1111/2049-632X.12105
- Gerits, E., Defraigne, V., Vandamme, K., De Cremer, K., De Brucker, K., Thevissen, K., et al. (2017). Repurposing toremifene for treatment of oral bacterial infections. *Antimicrob. Agents Chemother.* 61, e1846–e1816. doi: 10.1128/AAC.01846-16
- Gi, M., Jeong, J., Lee, K., Lee, K. M., Toyofuku, M., Yong, D. E., et al. (2014). A drug-repositioning screening identifies pentetic acid as a potential therapeutic agent for suppressing the elastase-mediated virulence of *Pseudomonas aeruginosa*. *Antimicrob. Agents Chemother.* 58, 7205–7214. doi: 10.1128/AAC.03063-14
- Gooyit, M., and Janda, K. D. (2016). Reprofiled anthelmintics abate hypervirulent stationary-phase *Clostridium difficile*. *Sci. Rep.* 6:33642. doi: 10.1038/srep33642
- Gupta, S., Cheung, L., Pokkali, S., Winglee, K., Guo, H., Murphy, J. R., et al. (2017). Suppressor cell-depleting immunotherapy with denileukin difitox is an effective host-directed therapy for tuberculosis. *J. Infect. Dis.* 215, 1883–1887. doi: 10.1093/infdis/jix208
- Gupta, S., Tyagi, S., and Bishai, W. R. (2015). Verapamil increases the bactericidal activity of bedaquiline against *Mycobacterium tuberculosis* in a mouse model. *Antimicrob. Agents Chemother.* 59, 673–676. doi: 10.1128/AAC.04019-14
- Hendrix, A. S., Spoonmore, T. J., Wilde, A. D., Putnam, N. E., Hammer, N. D., Snyder, D. J., et al. (2016). Repurposing the nonsteroidal anti-inflammatory drug diflunisal as an osteoprotective, antivirulence therapy for *Staphylococcus aureus* osteomyelitis. *Antimicrob. Agents Chemother.* 60, 5322–5330. doi: 10.1128/AAC.00834-16
- Hennessy, E., O'Callaghan, J., Mooij, M. J., Legendre, C., Camacho-Vanegas, O., Camacho, S. C., et al. (2014). The impact of simvastatin on pulmonary effectors of *Pseudomonas aeruginosa* infection. *PLoS One* 9:e102200. doi: 10.1371/journal.pone.0102200
- Ho Sui, S. J., Lo, R., Fernandes, A. R., Caulfield, M. D., Lerman, J. A., Xie, L., et al. (2012). Raloxifene attenuates *Pseudomonas aeruginosa* pyocyanin production and virulence. *Int. J. Antimicrob. Agents* 40, 246–251. doi: 10.1016/j.ijantimicag.2012.05.009
- Holbrook, S. Y. L., Garzan, A., Dennis, E. K., Shrestha, S. K., and Tsodikova, S. G. (2017). Repurposing antipsychotic drugs into antifungal agents: synergistic combinations of azoles and bromperidol derivatives in the treatment of various fungal infections. *Eur. J. Med. Chem.* 139, 12–21. doi: 10.1016/j.ejmech.2017.07.030
- Imperi, F., Leoni, L., and Visca, P. (2014). Antivirulence activity of azithromycin in *Pseudomonas aeruginosa*. *Front. Microbiol.* 5:178. doi: 10.3389/fmicb.2014.00178
- Imperi, F., Massai, F., Facchini, M., Frangipani, E., Visaggio, D., Leoni, L., et al. (2013a). Repurposing the antimycotic drug flucytosine for suppression of *Pseudomonas aeruginosa* pathogenicity. *Proc. Natl. Acad. Sci. U.S.A.* 110, 7458–7463. doi: 10.1073/pnas.1222706110
- Imperi, F., Massai, F., Ramachandran Pillai, C., Longo, F., Zennaro, E., Rampioni, G., et al. (2013b). New life for an old drug: the anthelmintic drug niclosamide inhibits *Pseudomonas aeruginosa* quorum sensing. *Antimicrob. Agents Chemother.* 57, 996–1005. doi: 10.1128/AAC.01952-12
- Joffe, L. S., Schneider, R., Lopes, W., Azvedo, R., Staats, C. C., Kmetzsch, L., et al. (2017). The anti-helminthic compound mebendazole has multiple antifungal effects against *Cryptococcus neoformans*. *Front. Microbiol.* 8:535. doi: 10.3389/fmicb.2017.00535
- Jung, E. H., Meyers, D. J., Bosch, J., and Casadevall, A. (2018). Novel antifungal compounds discovered in medicines for malaria venture's malaria box. *mSphere* 3:e537-17. doi: 10.1128/mSphere.00537-17

- Kaneko, Y., Thoendel, M., Olakanmi, O., Britigan, B. E., and Singh, P. K. (2007). The transition metal gallium disrupts *Pseudomonas aeruginosa* iron metabolism and has antimicrobial and antibiofilm activity. *J. Clin. Invest.* 117, 877–888. doi: 10.1172/JCI30783
- Kulkarny, V. V., Chavez-Dozal, A., Rane, H. S., Jahng, M., Bernardo, S. M., Parra, K. J., et al. (2014). Quinacrine inhibits *Candida albicans* growth and filamentation at neutral pH. *Antimicrob. Agents Chemother.* 58, 7501–7509. doi: 10.1128/AAC.03083-14
- Kung, V. L., Ozea, E. A., and Hauser, A. S. (2010). The accessory genome of *Pseudomonas aeruginosa*. *Microbiol. Mol. Biol. Rev.* 74, 621–641. doi: 10.1128/MMBR.00027-10
- Lieberman, L. A., and Higgins, D. E. (2009). A small-molecule screen identifies the antipsychotic drug pimozide as an inhibitor of *Listeria monocytogenes* infection. *Antimicrob. Agents Chemother.* 53, 756–764. doi: 10.1128/AAC.00607-08
- Lieberman, O. J., Orr, M. W., Wang, Y., and Lee, V. T. (2014). High-throughput screening using the differential radial capillary action of ligand assay identifies ebselen as an inhibitor of diguanylate cyclases. *ACS Chem. Biol.* 9, 183–192. doi: 10.1021/cb400485k
- Lim, L. E., Vilchèze, C., Ng, C., Jacobs, W. R. Jr., Ramón-García, S., and Thompson, C. J. (2013). Anthelmintic avermectins kill *Mycobacterium tuberculosis*, including multidrug-resistant clinical strains. *Antimicrob. Agents Chemother.* 57, 1040–1046. doi: 10.1128/AAC.01696-12
- Lobato, L. S., Rosa, P. S., Ferreira Jda, S., Neumann Ada, S., da Silva, M. G., do Nascimento, D. C., et al. (2014). Statins increase rifampin mycobactericidal effect. *Antimicrob. Agents Chemother.* 58, 5766–5774. doi: 10.1128/AAC.01826-13
- Maitra, A., Bates, S., Shaik, M., Evangelopoulos, D., Abubakar, I., McHugh, T. D., et al. (2016). Repurposing drugs for treatment of tuberculosis: a role for non-steroidal anti-inflammatory drugs. *Br. Med. Bull.* 118, 138–148. doi: 10.1093/bmb/ldw019
- Martin, R. J. (1997). Modes of action of anthelmintic drugs. *Vet. J.* 154, 11–34. doi: 10.1016/S1090-0233(05)80005-X
- Minandri, F., Bonchi, C., Frangipani, E., Imperi, F., and Visca, P. (2014). Promises and failures of gallium as an antibacterial agent. *Future Microbiol.* 9, 379–397. doi: 10.2217/fmb.14.3
- Misra, U. K., Kalita, J., and Nair, P. P. (2010). Role of aspirin in tuberculous meningitis: a randomized open label placebo controlled trial. *J. Neurol. Sci.* 293, 12–17. doi: 10.1016/j.jns.2010.03.025
- Nairn, B. L., Eliasson, O. S., Hyder, D. R., Long, N. J., Majumdar, A., Chakravorty, S., et al. (2017). Fluorescence high-throughput screening for inhibitors of TonB action. *J. Bacteriol.* 199, e889–e816. doi: 10.1128/JB.00889-16
- Nouari, W., Ysmail-Dahlouk, L., and Aribi, M. (2015). Vitamin D3 enhances bactericidal activity of macrophage against *Pseudomonas aeruginosa*. *Int. Immunopharmacol.* 30, 94–101. doi: 10.1016/j.intimp.2015.11.033
- Ogundej, A. O., Pohl, C. H., and Sebolai, O. M. (2016). Repurposing of aspirin and ibuprofen as candidate anti-cryptococcus drugs. *Antimicrob. Agents Chemother.* 60, 4799–4808. doi: 10.1128/AAC.02810-15
- Omansen, T. F., Porter, J. L., Johnson, P. D., van der Werf, T. S., Stienstra, Y., and Stinear, T. P. (2015). *In-vitro* activity of avermectins against *Mycobacterium ulcerans*. *PLoS Negl. Trop. Dis.* 9:e0003549. doi: 10.1371/journal.pntd.0003549
- O'Neill, J. (2016). *Tackling Drug-Resistant Infections Globally: Final Report, and Recommendations The Review on Antimicrobial Resistance*. Available at: https://amr-review.org/sites/default/files/160525_Final%20paper_with%20cover.pdf
- Parihar, S. P., Guler, R., Khutlang, R., Lang, D. M., Hurdal, R., Mhlanga, M. M., et al. (2014). Statin therapy reduces the *Mycobacterium tuberculosis* burden in human macrophages and in mice by enhancing autophagy and phagosome maturation. *J. Infect. Dis.* 209, 754–763. doi: 10.1093/infdis/jit550
- Peng, Z., Ling, L., Stratton, C. W., Li, C., Polage, C. R., Wu, B., et al. (2018). Advances in the diagnosis and treatment of *Clostridium difficile* infections. *Emerg. Microbes Infect.* 7:15. doi: 10.1038/s41426-017-0019-4
- Perlmutter, J. I., Forbes, L. T., Krysan, D. J., Ebsworth-Mojica, K., Colquhoun, J. M., Wang, J. L., et al. (2014). Repurposing the antihistamine terfenadine for antimicrobial activity against *Staphylococcus aureus*. *J. Med. Chem.* 57, 8540–8562. doi: 10.1021/jm5010682
- Rajamuthiah, R., Fuchs, B. B., Conery, A. L., Kim, W., Jayamani, E., Kwon, B., et al. (2015). Repurposing salicylanilide anthelmintic drugs to combat drug resistant *Staphylococcus aureus*. *PLoS One* 10:e0124595. doi: 10.1371/journal.pone.0124595
- Rampioni, G., Visca, P., Leoni, L., and Imperi, F. (2017). Drug repurposing for antivirulence therapy against opportunistic bacterial pathogens. *Emerg. Top. Life Sci.* 1, 13–23. doi: 10.1042/ETLS20160018
- Rangel-Vega, A., Bernstein, L. R., Mandujano-Tinoco, E. A., García-Contreras, S. J., and García-Contreras, R. (2015). Drug repurposing as an alternative for the treatment of recalcitrant bacterial infections. *Front. Microbiol.* 6:282. doi: 10.3389/fmicb.2015.00282
- Rani Basu, L., Mazumdar, K., Dutta, N. K., Karak, P., and Dastidar, S. G. (2005). Antibacterial property of the antipsychotic agent prochlorperazine, and its synergism with methdilazine. *Microbiol. Res.* 60, 95–100. doi: 10.1016/j.micres.2004.10.002
- Ribeiro, N. Q., Costa, M. C., Magalhães, T. F. F., Carneiro, H. C. S., Oliveira, L. V., Fontes, A. C. L., et al. (2017). Atorvastatin as a promising anticryptococcal agent. *Int. J. Antimicrob. Agents* 49, 695–702. doi: 10.1016/j.ijantimicag.2017.04.005
- Routh, M. M., Chauhan, M. N., and Karuppayil, S. M. (2013). Cancer drugs inhibit morphogenesis in the human fungal pathogen *Candida albicans*. *Braz. J. Microbiol.* 44, 855–859. doi: 10.1590/S1517-83822013000300029
- Skerry, C., Pinn, M. L., Bruiners, N., Pine, R., Gennaro, M. L., and Karakousis, P. C. (2014). Simvastatin increases the in vivo activity of the first-line tuberculosis regimen. *J. Antimicrob. Chemother.* 69, 2453–2457. doi: 10.1093/jac/dku166
- Soo, V. W., Kwan, B. W., Quezada, H., Castillo-Juárez, I., Pérez-Eretza, B., García-Contreras, S. J., et al. (2017). Repurposing of anticancer drugs for the treatment of bacterial infections. *Curr. Top. Med. Chem.* 7, 1157–1176. doi: 10.2174/1568026616666160930131737
- Sun, W., Park, Y. D., Sugui, J. A., Fothergill, A., Southall, N., Shinn, P., et al. (2013). Rapid identification of antifungal compounds against *Exserohilum rostratum* using high throughput drug repurposing Screens. *PLoS One* 8:e70506. doi: 10.1371/journal.pone.0070506
- Tacconelli, E., Carrara, E., Savoldi, A., Harbarth, S., Mendelson, M., Monnet, D. L., et al. (2018). Discovery, research, and development of new antibiotics: the WHO priority list of antibiotic-resistant bacteria and tuberculosis. *Lancet Infect. Dis.* 18, 318–327. doi: 10.1016/S1473-3099(17)30753-3
- Thangamani, S., Mohammad, H., Abushahba, M. F., Sobreira, T. J., Hedrick, V. E., Paul, L. N., et al. (2016a). Antibacterial activity and mechanism of action of auranofin against multi-drug resistant bacterial pathogens. *Sci. Rep.* 6:22571. doi: 10.1038/srep22571
- Thangamani, S., Mohammad, H., Abushahba, M. F., Sobreira, T. J., and Seleem, M. N. (2016b). Repurposing auranofin for the treatment of cutaneous staphylococcal infections. *Int. J. Antimicrob. Agents* 47, 195–201. doi: 10.1016/j.ijantimicag.2015.12.016
- Thangamani, S., Mohammad, H., Abushahba, M. F. N., Hamed, M. I., Sobreira, T. J. P., Hedrick, V. E., et al. (2015a). Exploring simvastatin, an antihyperlipidemic drug, as a potential topical antibacterial agent. *Sci. Rep.* 5:16407. doi: 10.1038/srep16407
- Thangamani, S., Younis, W., and Seleem, M. N. (2015b). Repurposing celecoxib as a topical antimicrobial agent. *Front. Microbiol.* 6:750. doi: 10.3389/fmicb.2015.00750
- Thangamani, S., Younis, W., and Seleem, M. N. (2015c). Repurposing ebselen for treatment of multidrug-resistant staphylococcal infections. *Sci. Rep.* 5:11596. doi: 10.1038/srep11596
- Tharmalingam, N., Port, J., Castillo, D., and Mylonakis, E. (2018). Repurposing the anthelmintic drug niclosamide to combat *Helicobacter pylori*. *Sci. Rep.* 8:3701. doi: 10.1038/s41598-018-22037-x
- Ueda, A., Attila, C., Whiteley, M., and Wood, T. K. (2009). Uracil influences quorum sensing and biofilm formation in *Pseudomonas aeruginosa* and fluorouracil is an antagonist. *Microb. Biotechnol.* 2, 62–74. doi: 10.1111/j.1751-7915.2008.00060.x
- Vilaplana, C., Marzo, E., Tapia, G., Diaz, J., Garcia, V., and Cardona, P. J. (2013). Ibuprofen therapy resulted in significantly decreased tissue bacillary loads and increased survival in a new murine experimental model of active tuberculosis. *J. Infect. Dis.* 208, 199–202. doi: 10.1093/infdis/jit152
- Wang, L. H., Xu, M., Fu, L. Q., Chen, X. Y., and Yang, F. (2018). The antihelmintic niclosamide inhibits cancer stemness, extracellular matrix remodeling, and

- metastasis through dysregulation of the nuclear β -catenin/c-Myc axis in OSCC. *Sci. Rep.* 8:12776. doi: 10.1038/s41598-018-30692-3
- Warrell, R. P. Jr., Israek, R., Frisone, M., Snyder, T., Gaynor, J. J., and Bockman, R. S. (1988). Gallium nitrate for acute treatment of cancer-related hypercalcemia. A randomized, double-blind comparison to calcitonin. *Ann. Intern. Med.* 108, 669–674. doi: 10.7326/0003-4819-108-5-669
- Xue, M. L., Zhu, H., Thacur, A., and Willcox, M. (2002). $1\alpha,25$ -Dihydroxyvitamin D3 inhibits pro-inflammatory cytokine and chemokine expression in human corneal epithelial cells colonized with *Pseudomonas aeruginosa*. *Immunol. Cell Biol.* 80, 340–345. doi: 10.1046/j.1440-1711.80.4august.1.x
- Yelin, I., and Kishony, R. (2018). SnapShot: antibiotic resistance. *Cell* 172, 1136–1136. doi: 10.1016/j.cell.2018.02.018
- Yeo, W. S., Arya, R., Kim, K. K., Jeong, H., Cho, K. H., and Bae, T. (2018). The FDA-approved anti-cancer drugs, streptozotocin and floxuridine, reduce the virulence of *Staphylococcus aureus*. *Sci. Rep.* 8:2521. doi: 10.1038/s41598-018-20617-5
- Zhang, X., Song, Y., Ci, X., An, N., Ju, Y., Li, H., et al. (2008). Ivermectin inhibits LPS-induced production of inflammatory cytokines and improves LPS-induced survival in mice. *Inflamm. Res.* 57, 524–529. doi: 10.1007/s00011-008-8007-8

Conflict of Interest Statement: The authors declare that the research was conducted in the absence of any commercial or financial relationships that could be construed as a potential conflict of interest.

Copyright © 2019 Miró-Canturri, Ayerbe-Algaba and Smani. This is an open-access article distributed under the terms of the Creative Commons Attribution License (CC BY). The use, distribution or reproduction in other forums is permitted, provided the original author(s) and the copyright owner(s) are credited and that the original publication in this journal is cited, in accordance with accepted academic practice. No use, distribution or reproduction is permitted which does not comply with these terms.



Redirecting an Anticancer to an Antibacterial Hit Against Methicillin-Resistant *Staphylococcus aureus*

Hye-Jeong Jang[†], In-Young Chung[†], Changjin Lim, Sungkyun Chung, Bi-o Kim, Eun Sook Kim, Seok-Ho Kim* and You-Hee Cho*

Department of Pharmacy, College of Pharmacy and Institute of Pharmaceutical Sciences, CHA University, Seongnam, South Korea

OPEN ACCESS

Edited by:

Raffaele Zarilli,
University of Naples Federico II, Italy

Reviewed by:

Rita Berisio,
Italian National Research Council
(CNR), Italy
Maria Bagattini,
University of Naples Federico II, Italy
Eliana De Gregorio,
University of Naples Federico II, Italy

*Correspondence:

Seok-Ho Kim
ksh3410@cha.ac.kr
You-Hee Cho
youhee@cha.ac.kr

[†] These authors have contributed
equally to this work

Specialty section:

This article was submitted to
Antimicrobials, Resistance
and Chemotherapy,
a section of the journal
Frontiers in Microbiology

Received: 10 November 2018

Accepted: 11 February 2019

Published: 25 February 2019

Citation:

Jang H-J, Chung I-Y, Lim C,
Chung S, Kim B-o, Kim ES, Kim S-H
and Cho Y-H (2019) Redirecting an
Anticancer to an Antibacterial Hit
Against Methicillin-Resistant
Staphylococcus aureus.
Front. Microbiol. 10:350.
doi: 10.3389/fmicb.2019.00350

YM155 is a clinically evaluated anticancer with a fused naphthoquinone-imidazolium scaffold. In this study, we demonstrated that based on weak or cryptic antibacterial activity of YM155 against methicillin-resistant *Staphylococcus aureus* (MRSA) (MIC of 50 μ g/ml), some congeneric compounds with short alkyl chains (e.g., c5 with a hexyl chain) at the N3 position of the scaffold, displayed more potent antibacterial activity against MRSA (MIC of 3.13 μ g/ml), which is in a clinically achievable range. Their antibacterial activity was evident against Gram-negative bacteria, only in the presence of the outer membrane-permeabilizing agent, polymyxin B. The antibacterial efficacy of c5 was confirmed using the *Drosophila* systemic infection model. We also characterized five spontaneous c5-resistant MRSA mutants that carry mutations in the *ubiE* gene, for quinone metabolism and respiratory electron transfer, and subsequently exhibited reduced respiration activity. The antibacterial activity of c5 was compromised either by an antioxidant, *N*-acetylcysteine, or in an anaerobic condition. These suggest that the antibacterial mechanism of c5 involves the generation of reactive oxygen species (ROS), presumably during respiratory electron transport. This study provides an insight into “drug redirecting,” through a chemical modification, based on an ROS-generating pharmacophore.

Keywords: MRSA, gram-positive, antibacterials, drug repurposing, drug redirecting

INTRODUCTION

Since antibiotic therapy was introduced into clinical practice, bacterial pathogens have been developing antibiotic resistance more rapidly. This resistance reduces or eliminates the effectiveness of the antibiotic regimen. In addition, opportunistic pathogens with intrinsic resistance to multiple antibiotics have become emerging problems in public health. In developed countries, a group of bacterial species that have acquired multiple drug resistances are often referred to as the ESKAPE pathogens, aptly named for their ability to “escape” the effects of currently available antibacterial drugs (Rice, 2008). *Staphylococcus aureus* is noteworthy among those pathogens as it is a very versatile Gram-positive bacterium, whose antibiotic resistance has been of great concern, particularly in hospital environments where it is often the cause of post-surgical wound

infections (Cohen, 1992; Tomasz, 1994; Engemann et al., 2003). Infections with *S. aureus* have become increasingly difficult to treat due to the emergence and rapid spread of methicillin-resistant *S. aureus* (MRSA), which are important nosocomial pathogens associated with increased morbidity and mortality worldwide (Lowy, 1998; Diekema et al., 2001). MRSA has become increasingly resistant to multiple classes of antibiotics including not only β -lactams, but also macrolides, quinolones, and even vancomycin (Leclercq, 2002; Lowy, 2003). Because community-associated MRSA infections are becoming more and more common (Mediavilla et al., 2012), there is an urgent need to develop antibacterial agents with features aimed to effectively target MRSA infections.

Although the search for antibacterials with novel scaffolds is of utmost importance at this juncture, mining and/or repurposing based on chemically modified bioactive compounds is considered an attractive proposition. Fused imidazolium analogs are known as anticancer agents, in large part due to their involvement in the reactive oxygen species (ROS)-mediated enhancement of apoptotic functions, although the additional and detailed mode of action remains elusive (Ho et al., 2015). Among them, YM155 (sepantronium bromide) [1-(2-methoxyethyl)-2-methyl-3-(pyrazin-2-ylmethyl)-4,9-dioxo-4,9-dihydro-1*H*-naphtho(2,3-*d*)imidazolium bromide] was identified by a high-throughput screening of chemical libraries, to screen for inhibitors of the expression of an anti-apoptotic protein, survivin, whose expression is increased in most solid tumors (Nakahara et al., 2007). Preclinical studies using YM155 showed inhibition of survivin at both the mRNA and protein levels and exhibited anticancer activity in mouse models (Nakahara et al., 2007).

In this study, we have identified cryptic or weak antibacterial activity of an anticancer, YM155, against MRSA and enhanced the activity through chemical modification at its N3 position. Its congeners with short alkyl chains, instead of the pyrazin-2-ylmethyl moiety, displayed more potent antibacterial activity. Their inhibitory activity is selective toward Gram-positive bacteria, due to the permeability barrier in Gram-negative bacteria and presumably in mammalian cells. This strategy conceptualizes “drug redirecting,” which may be distinct from “drug repurposing” in that it involves drug modification to change/redirect the cellular targets and the subsequent indications.

MATERIALS AND METHODS

Bacterial Strains and Culture Conditions

The bacterial strains used in this study are listed in (Supplementary Table S1). *Pseudomonas aeruginosa*, *Escherichia coli*, *Klebsiella pneumoniae*, *Bacillus subtilis*, *S. aureus* strains were grown at 37°C using Luria-Bertani (LB) (1% tryptone, 0.5% yeast extract, and 1% NaCl) broth, Mueller-Hinton (MH) broth, and M9-glucose minimal medium (1.2% Na₂HPO₄, 0.3% KH₂PO₄, 0.05% NaCl, 0.1% NH₄Cl, 2 mM MgSO₄, 0.1 mM CaCl₂, and 0.4% glucose) or on 2% Bacto-agar solidified LB plates. Overnight-grown cultures were used as inoculum (1.6×10^7 CFU/ml) into fresh LB broth and grown at 37°C in a

shaking incubator until the logarithmic (OD₆₀₀ = 1.0) phase, and then the cell cultures were used for the experiments described herein. For anaerobic growth, bacteria were grown in an LB medium in an anaerobic jar with AnaeroPack (MGC).

Synthesis of YM155 and Its Congeners

The fused imidazolium analogs were synthesized and purified as described previously (Kuo et al., 1996; Ho et al., 2015). All reagents and chemicals were obtained from Sigma-Aldrich and Merck, unless otherwise specified. YM155 was purchased from Aladdin Industrial Corporation. UV spectra were recorded on a Jasco spectrophotometer equipped with a Peltier temperature control unit. The synthesized compounds were dissolved in dimethyl sulfoxide (DMSO).

Determination of Minimal Inhibitory Concentration (MIC)

Minimal inhibitory concentrations for YM155 congeners were determined in MH broth by the broth microdilution method, using standard microbiological procedures according to NCCLS guidelines, as per document no. M07-A8 (2012). The medium, with a 2-fold serial dilution of each compound in the MH broth, was subjected to inoculation with the indicated bacterial strains (5×10^5 CFU/ml) that had been grown at 37°C to the logarithmic growth phase (OD₆₀₀ = 1.0) and then incubated at 37°C on a rotatory shaker. The MIC values were recorded as the lowest concentration of the compound at which no signs of growth were observed, based on the OD₆₀₀ value of less than 0.05 after 18 h of incubation. The MIC values were confirmed by three independent experiments. Methicillin and gentamicin were used as the control antibiotics.

Measurement of Antibacterial Activity

The sensitivity of bacterial cells was evaluated by a spotting assay. The 10-fold serial dilutions (3 μ l) of the cell cultures in the LB broth were spotted onto an LB agar plate containing chemicals

TABLE 1 | MICs of YM155 and its analogs against MRSA, SA3^a.

Compound	MIC (μ g/ml)	MIC (μ M)	MW
YM155	50	112.79	443.29
a1	3.13	7.09	441.32
a2	100	231.87	431.28
a3	6.25	13.97	447.35
b1	12.5	31.63	395.25
b2	25	61.09	409.27
b3	50	118.12	423.3
b4	25	57.17	437.33
c1	25	65.91	379.3
c2	12.5	31.78	393.3
c3	12.5	30.69	407.3
c4	6.25	14.84	421.3
c5	3.13	7.19	435.3

a: the MIC values of these compounds against *Escherichia coli* (MG1655) and *Pseudomonas aeruginosa* (PA14) have been determined as >500 μ g/ml.

such as YM155 and its analogs or antibiotics (methicillin or gentamicin), at the indicated concentrations, to enumerate the survivor bacteria. The plates were incubated overnight at 37°C. For an ROS-scavenging agent, 10 mM *N*-acetyl cysteine (NAC) was amended.

Time-to-Kill Experiment

The MRSA bacteria were cultured to OD₆₀₀ of 1.0 in an MH broth and then diluted to approximately 5×10^5 CFU/ml. The cell cultures were treated with 0.78, 1.56, 3.13, 6.25, and 12.5 µg/ml of the hit (c5) with more potent antibacterial activity and incubated for 10 h at 37°C. At 1 or 2-h time intervals, the aliquots (1 ml) were taken from the samples and then plated onto LB agar plates to enumerate the viable bacteria. The experiments were performed four times.

Cell Permeabilization Using Polymyxin B (PMB)

Escherichia coli and *P. aeruginosa* cells were grown until the logarithmic phase in LB medium and then diluted to 5×10^5 CFU/ml. To increase the membrane permeability, the cells were treated with 0.05, 0.1, or 0.2 µg/ml of PMB. The samples were collected at various time intervals and then plated onto LB agar plates to enumerate the viable bacteria. The experiments were performed four times.

Measurement of Antibacterial Efficacy

In order to determine the antibacterial efficacy of c5, *Drosophila* systemic infection was performed as previously described (Lau et al., 2003; Kim et al., 2008). *Drosophila melanogaster* strain Oregon R, was grown and maintained at 25°C using the corn

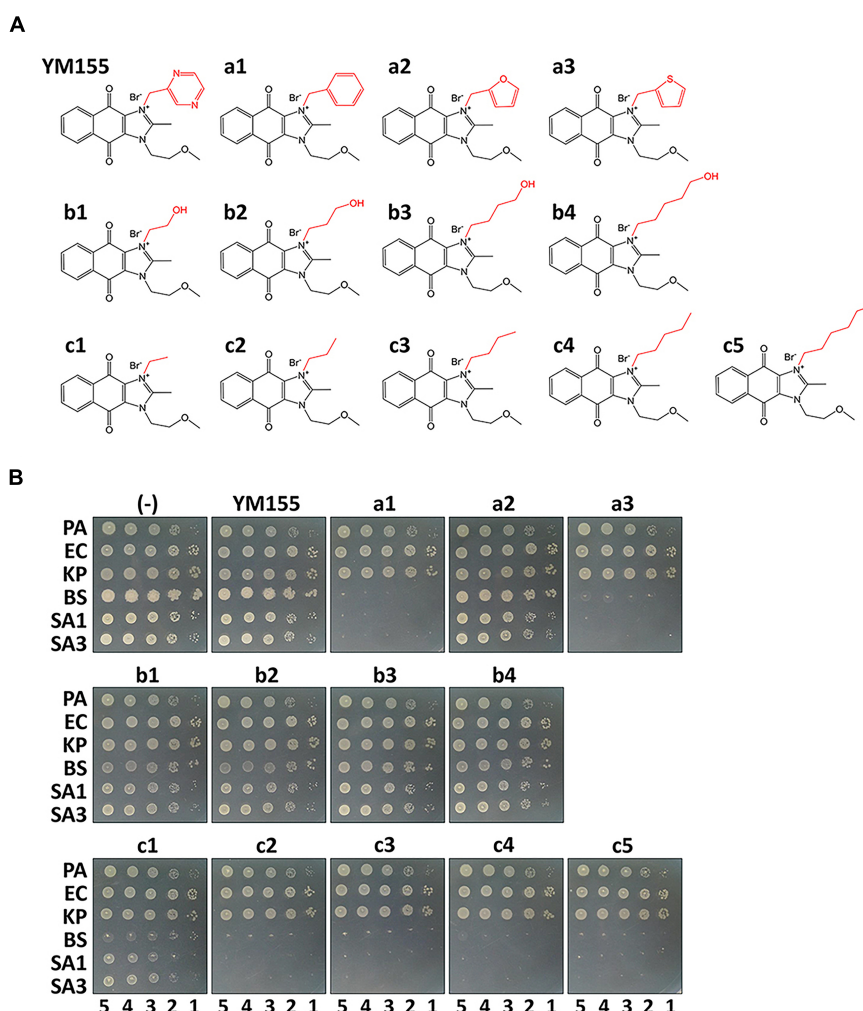


FIGURE 1 | Antibacterial activity *in vitro*. **(A)** Structure of YM155 and its analogs: Group a (a1~a3), b (b1~b4) and c (c1~c5) are analogs at N3 position of YM155. Group a has a ring structure, group b has a terminally hydroxylated alkyl chain, and group c has an alkyl chain. **(B)** Susceptibility of various bacterial strains to YM155 and its analogs: The Gram-negative (*Pseudomonas aeruginosa*, PA; *Escherichia coli*, EC; and *Klebsiella pneumoniae*, KP) and Gram-positive (*Bacillus subtilis*, BS; *Staphylococcus aureus* MSSA, SA1; and *S. aureus* MRSA, SA3) cells were grown to the logarithmic growth phase. Ten-fold serial dilutions of the cell cultures were spotted onto an LB agar plate (-), and LB agar plate containing YM155 (7.5 µg/ml), or its analogs (7.5 µg/ml). The numbers indicate the log(CFU) of the applied bacterial spots.

meal-dextrose medium [0.93% agar, 6.24% dry yeast, 4.08% corn meal, 8.62% dextrose, 0.1% methyl paraben, and 0.45% (v/v) propionic acid]. For systemic infection, 4- to 5-day-old adult female flies were infected by pricking the dorsal thorax with a 0.4 mm needle (Ernest F. Fullam, Inc.). The needle was dipped into PBS-diluted bacterial suspension containing PA14 (10^7 CFU/ml) and/or SA3 (10^8 CFU/ml) grown to the OD₆₀₀ of 3.0 (Lee et al., 2018). Infected flies were transferred to a new medium overlaid with 80 μ l of c5 compound (1 mg/ml). Survival rates of the infected flies were monitored for up to 72 h post-infection. Flies that died within 12 h were excluded in mortality determination. Mortality assay was repeated at least four times.

Spontaneous Mutagenesis and Whole-Genome Sequencing (WGS)

Staphylococcus aureus SA3 was grown at 37°C using LB broth. Overnight-grown cultures were used as inoculum (1.6×10^7 CFU/ml) into fresh LB broth and grown at 37°C in a shaking incubator to OD₆₀₀ of 1.0. The cell culture was plated onto LB agar plates with 40 μ g/ml of c5 and incubated at 37°C for approximately 36 h. The well-growing colonies were isolated and analyzed by WGS.

Respiration Activity Assay Using 2,3,5-Triphenyl Tetrazolium (TTC)

The bacterial cells were grown to the logarithmic growth phase (OD₆₀₀ of 1.0) at 37°C. Three microliters of cell cultures were spotted onto an LB agar plate containing either TTC (0.015%) or TTC (0.015%) and glucose (0.2%).

Measurement of ROS Generation

Reactive oxygen species generation was measured using hydroxyphenyl fluorescein (HPF), which is known to react with hydroxyl radicals and peroxynitrite (Setsukinai et al., 2003). The bacteria were cultured to OD₆₀₀ of 0.5 in M9 minimal medium and incubated with HPF (5 μ M) for 30 min. The cells were then washed and resuspended in 1 ml of M9 minimal medium containing 0.75 and 1.5 μ g/ml of c5 or b4. The samples were incubated for 3 h at 37°C and the fluorescence was measured at a 1-h time interval at 490-nm excitation and 525-nm emission. ROS measurement was repeated three times.

Statistics

Statistical analysis was performed using the GraphPad Prism version 6.0 (GraphPad Software, La Jolla, CA, United States). Data for each analysis represents a set of five repetitions. Statistical significance between the groups is indicated, based on a *p*-value of less than 0.01 (**p* < 0.01; ***p* < 0.001) by using the Kaplan-Meier log-rank test and the Student's *t*-test. Error bars represent the standard deviations.

RESULTS

YM155 and Its Congeners Display Antibacterial Activity

During our endeavors to find potential antibacterial against the major nosocomial bacterial pathogens, we identified the weak antibacterial activity of YM155 against a methicillin-resistant

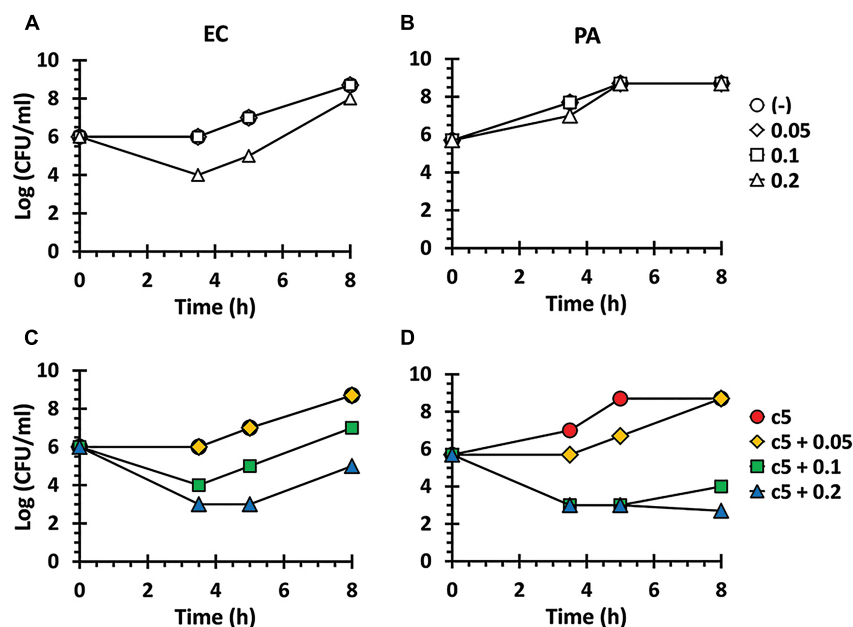
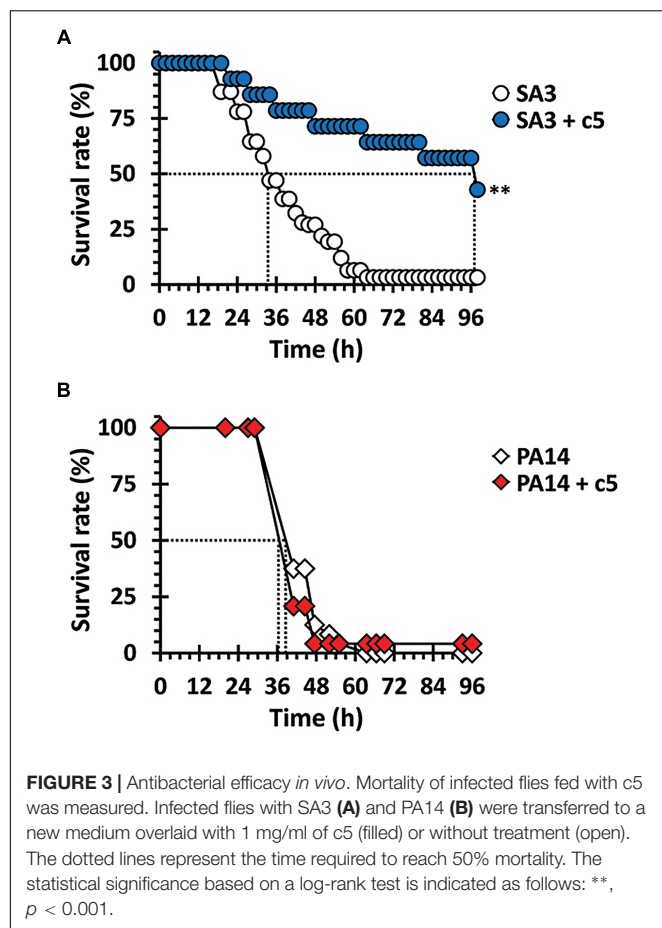


FIGURE 2 | Antibacterial activity in the presence of polymyxin B (PMB). Antibacterial activity against *E. coli* (EC) (A,C) and *P. aeruginosa* (PA) (B,D) in the presence of PMB. The EC and PA culture suspensions (5×10^5 CFU/ml) were incubated in LB broth with nothing (open circle), with c5 (12.5 μ g/ml) only (filled circle), with PMB (0.05, 0.1, or 0.2 μ g/ml) only (A,B), or with both c5 (12.5 μ g/ml) and PMB (0.05, 0.1, or 0.2 μ g/ml) (C,D). The viable cells were counted by plating onto LB agar plates at the designated time points.



S. aureus strain, SA3 (Table 1). We designed its analogs at the N3 position, and a series of compounds depicted in Figure 1A were tested for antibacterial activity in comparison with YM155. Group a (a1~a3) has an aromatic or heteroaromatic ring structure and group b (b1~b4) with a terminal hydroxyl residue, includes b1 and b2, both of which have a similar structure of half of the pyrazine ring of YM155. Group c (c1~c5) was similar to group b, but without the hydroxyl residue. We excluded group a compounds due to the lack of aqueous solubility. Among the group b compounds, b1 showed the highest antibacterial activity, whereas b3 displayed weaker activity than YM155 did (Figure 1B and Table 1). It is of marked interest that group c compounds exhibited the strongest antibacterial activity, depending on the length of the chains. The time-dependent bactericidal activity of c5 was also determined (Supplementary Figure S1). These results suggest that the substitution at the N3 position is critical to modulate the activity of the YM155 scaffold in regards to the antibacterial activity against Gram-positive bacteria including MRSA.

Bioactivity of c5, a Representative YM155 Congener, Is Selective

As shown in Figure 1B, these compounds were not sufficiently antibacterial against Gram-negative bacteria, suggesting that the

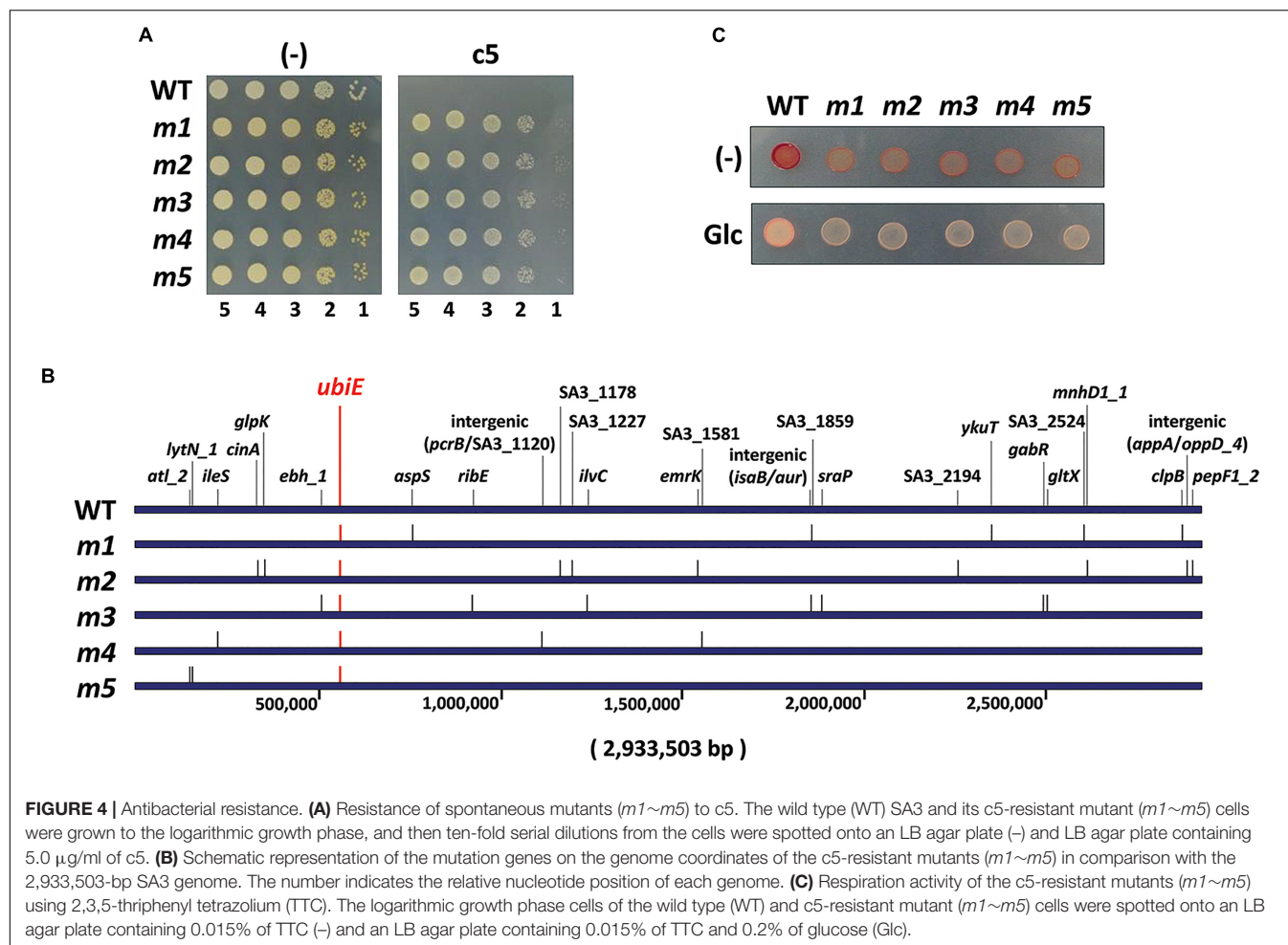
outer membrane might prevent these compounds from entering the bacterial cells as observed with other antibacterials such as erythromycin and fusidic acid (Saha et al., 2008; Delcour, 2009). Thus, we have examined whether the permeabilizing agent, polymyxin B (PMB), at a sub-inhibitory concentration, could affect the growth of the Gram-negative bacteria in the presence of c5 (Figure 1A), as the representative compound with the lowest MIC and good aqueous solubility (Table 1). As shown in Figure 2, PMB did not affect the growth of *E. coli* (MG1655) and *P. aeruginosa* (PA14) below 0.1 and 0.2 $\mu\text{g/ml}$, respectively. At the sub-lethal concentrations of PMB, c5 (12.5 $\mu\text{g/ml}$) was able to kill both Gram-negative species in a dose-dependent manner of PMB, whereas their growth was not affected at all in the absence of PMB (Figures 2C,D). Interestingly, we have observed the similar but slightly different killing patterns using the PMB nonapeptide (PMBN), a non-toxic derivative of PMB (Supplementary Figure S2), suggesting the presumable synergy between PMB and c5 in ROS generation in Gram-negative bacteria (see below). These results suggest that the selective antibacterial activity of c5, and presumably the aforementioned congeneric compounds, against the Gram-positive bacteria, is most likely associated with the permeability to the target bacterial cells.

c5 Rescues *Drosophila* Specifically From Infection Caused by MRSA

The antibacterial efficacy of c5 was evaluated in the *Drosophila* systemic infection model. The MRSA, SA3 with multiple antibiotic resistance was more virulent than the methicillin-sensitive *S. aureus* (MSSA), SA1 in the fly systemic infection model (Supplementary Figure S3). Based on the antibacterial activity of c5 toward SA3, flies were pricked with SA3 or *P. aeruginosa* PA14 as described in Materials and Methods. Figure 3 shows that a significant protection from mortality, caused by SA3, was observed by adding the c5 compound to the fly media (up to 1 mg/ml), whereas c5 did not reduce the mortality caused by PA14. This is also important with regards to the toxicity of this compound, in that c5 is not apparently toxic to the flies. This needs to be further verified using mammalian acute and chronic toxicity models. Altogether, we suggest that the potent *in vitro* activity of c5 translates *in vivo* into a selective antibacterial activity that rescues flies from the systemic infection caused by MRSA, but not by *P. aeruginosa*.

The Mutants in Quinone Biosynthesis Are Resistant to c5

In order to assess the mode of action of the antibacterial activity of c5, we have isolated 11 spontaneous mutants ($m1\sim m11$) whose growth was not inhibited by c5 (Figure 4A). The frequency of the spontaneous mutation was about 10^9 , within the normal range of spontaneous mutations due to base transition. Whole genome sequencing of the randomly selected five c5-resistant mutants ($m1\sim m5$) revealed multiple mutations in each mutant (6 for $m1$, 10 for $m2$, 8 for $m3$, 4 for $m4$, and 3 for $m5$) (Figure 4B). It is remarkable that they had nonsense mutations in common for a gene, *ubiE*: TTA to TAA at the 54th leucine codon for

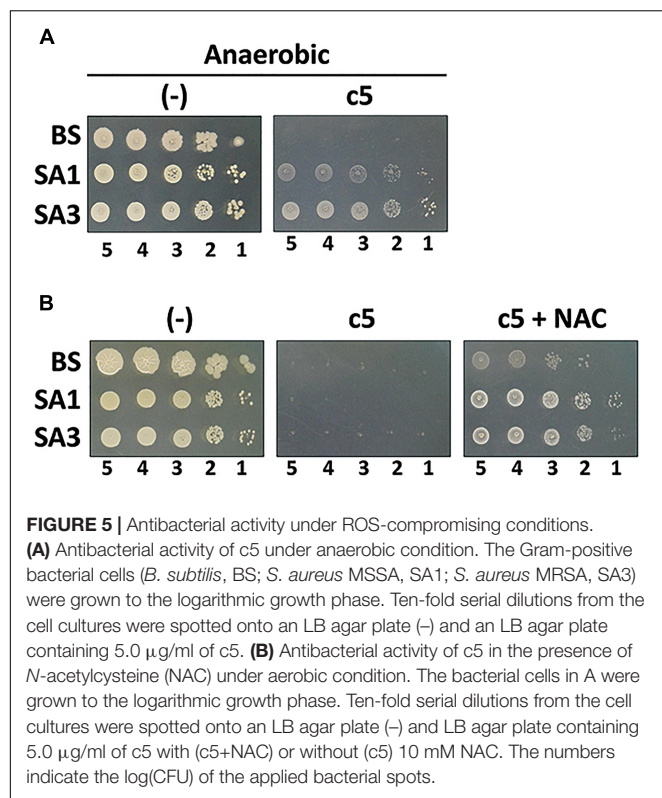


m1~*m4* and AAA to TAA at the 52nd lysine codon for *m5*. This gene encodes a methyltransferase crucial for biosynthesis of ubiquinone and menaquinone (MQ), which are the widespread respiratory quinones in bacterial species. This result suggests that a certain change caused by the *ubiE* mutations in the respiratory chain might be able to render MRSA resistant to *c5*. Because nonsense mutations normally result in a loss-of-function, it is highly likely that UbiE is not the direct target for *c5* and that the change in respiratory chain(s) due to the UbiE loss may affect the electron flow during the respiration, resulting in the reduction of the *c5* bioactivity. This result suggests that the *ubiE* mutations of the aforementioned mutants might most likely be responsible for the *c5*-resistance phenotype. Alternatively, it is also probable that a change, due to the mutations in quinone biosynthesis, may enable the cells to bypass the *c5*-inhibited pathway for growth, which needs to be further elucidated.

Antibacterial Activity of *c5* Involves Reactive Oxygen Species (ROS)

c5, as well as the other compounds in this study, contain the naphthoquinone scaffold of vitamin K-family compounds

such as MQ (vitamin K₂) and menadione (MD, vitamin K₃). MQ is the major or sole isoprenoid quinone in most Gram-positive and anaerobic Gram-negative bacteria, which transfer electrons in the respiratory chain (Collins and Jones, 1981), while MD is a synthetic chemical well-known for its reactive oxygen species (ROS)-generating activity (Criddle et al., 2006). More importantly, the *ubiE* mutations that may affect the electron flow in the respiratory chain, are involved in *c5*-resistance (Figure 4). We hypothesized that ROS generation during aerobic respiration might be facilitated and/or augmented by *c5*. In order to verify this, we first assessed the antibacterial activity under anaerobic conditions (Figure 5A). The antibacterial activity against *S. aureus* strains was compromised under anaerobic conditions. To further verify the involvement of ROS generation in the *c5* bioactivity, an antioxidant compound, *N*-acetylcysteine (NAC) was exploited. As shown in Figure 5B, the antibacterial activity of *c5* was also impaired in the presence of NAC under aerobic conditions. We next investigated whether ROS generation was indeed observed by *c5* treatment in SA3, using the hydroxyl radical sensor, hydroxyphenyl fluorescein (HPF). As shown in Figure 6, ROS generation was clearly observed in the Gram-positive bacteria (SA3 and BS). It is noteworthy that the *c5*-mediated ROS generation was impaired



in a c5-resistant mutant as well as in *P. aeruginosa*. Unlike c5, b4, as a representative with a similar-length side chain but without antibacterial activity (Figure 1), was clearly unable to generate ROS at similar concentrations (Figure 6E). These results suggest that the antibacterial activity of c5 is most likely associated with ROS generation that would be enhanced by this compound in MRSA.

DISCUSSION

Methicillin-resistant *Staphylococcus aureus* infections continue to pose a new threat and is a significant public health challenge, due to over 50% failure rates in the conventional antibiotic treatment of infected patients (Soriano et al., 2008; Gould et al., 2012). Despite the urgent need for new effective antibacterials to treat MRSA infections, the traditional approach in drug development is consuming tremendous amounts of time and resources, as bacterial resistance continues to rapidly develop. This has led researchers to explore alternative approaches such as drug repurposing, which utilizes approved drugs used primarily for other purposes to treat bacterial infections. Auranofin is such an example, as it was initially approved as an anti-rheumatic agent. It is known that auranofin displays antiviral, antiprotozoal, and anticancer activities (Chirullo et al., 2013; Chen et al., 2014). It also showed potent antibacterial activity against replicating and non-replicating *Mycobacterium tuberculosis* as well as other Gram-positive bacteria including MRSA (Cassetta et al., 2014; Harbut et al., 2015).

As an independent approach, we started with a different compound, YM155, which is an anticancer drug candidate. YM155 is currently under clinical trials for combination therapy with approved anticancer drugs such as carboplatin and paclitaxel (Kelly et al., 2013). The fused imidazolium compound possesses the naphthoquinone scaffold that might act as the pharmacophore which presumably provokes ROS formation. These result in mitochondrial dysfunction and subsequent apoptosis, the major contributor of bioactivity in this compound (Ho et al., 2015). This YM155 property has led us to the idea that YM155 may exhibit bactericidal activity upon entry into the bacterial cells. In the present study, we observed weak or cryptic antibacterial activity of YM155 against Gram-positive bacteria including MRSA. To witness this observation, we sought to enhance its antibacterial activity and solubility through chemical modification at the N3 position of the scaffold. This position is relatively easy to introduce several modifications at a reasonable efficiency, in a late stage of chemical synthesis. More importantly for this study, pyrazine moiety that is not easy to deal with in chemical synthesis, was required for anticancer activity, but not for antibacterial activity. Among the chemically modified congeners, those with alkyl chains displayed better activity and solubility, and the c5 compound with a hexyl chain was selected for further analyses as the antibacterial hit compound for anti-MRSA candidates. Based on these considerations, our approach clearly differs from drug repurposing studies, since included chemical modification(s) to change (i.e., redirect) the target indications. This new approach in drug discovery would be “drug redirecting.” The redirected drugs literally belong to the incrementally modified drugs (IMDs).

Another key implication of this study was that our drug redirecting strategy was validated by using the naphthoquinone scaffold as the pharmacophore, fused with the imidazolium ring, as the moiety for chemical modification affordable to modulate its target-specific permeability. Currently, we have been more comprehensively investigating whether the N3 position of this scaffold is necessary and sufficient to affect the target-specificity. This investigation is necessary in order to identify the molecular and submolecular determinants of the target cells, primarily by massively modulating the permeability. This knowledge will be exploited for application of the naphthoquinone imidazolium scaffold and its ROS-generating activity, to inhibit various cell types associated with human diseases including mammals, protozoa, fungi, and Gram-negative bacteria. With the recent discovery of the key traits required for the permeability to Gram-negative bacteria (Richter et al., 2017), more comprehensive structure-activity-relationship (SAR) studies on this scaffold will further strengthen the utility of the drug platform, for more suitable exploitation by rewiring or broadening the target-specificity. In a broader context, however, we believe we are now in the beginning stage of reincarnating the approved drugs or known compounds based on chemical modifications beyond just repurposing them as they are. This drug redirecting can be done primarily by structural modifications to revise their target cell types. In this case, their pharmacophores essentially need to work irrespective of cell types, once they enter the subcellular localizations such as the cytosol and

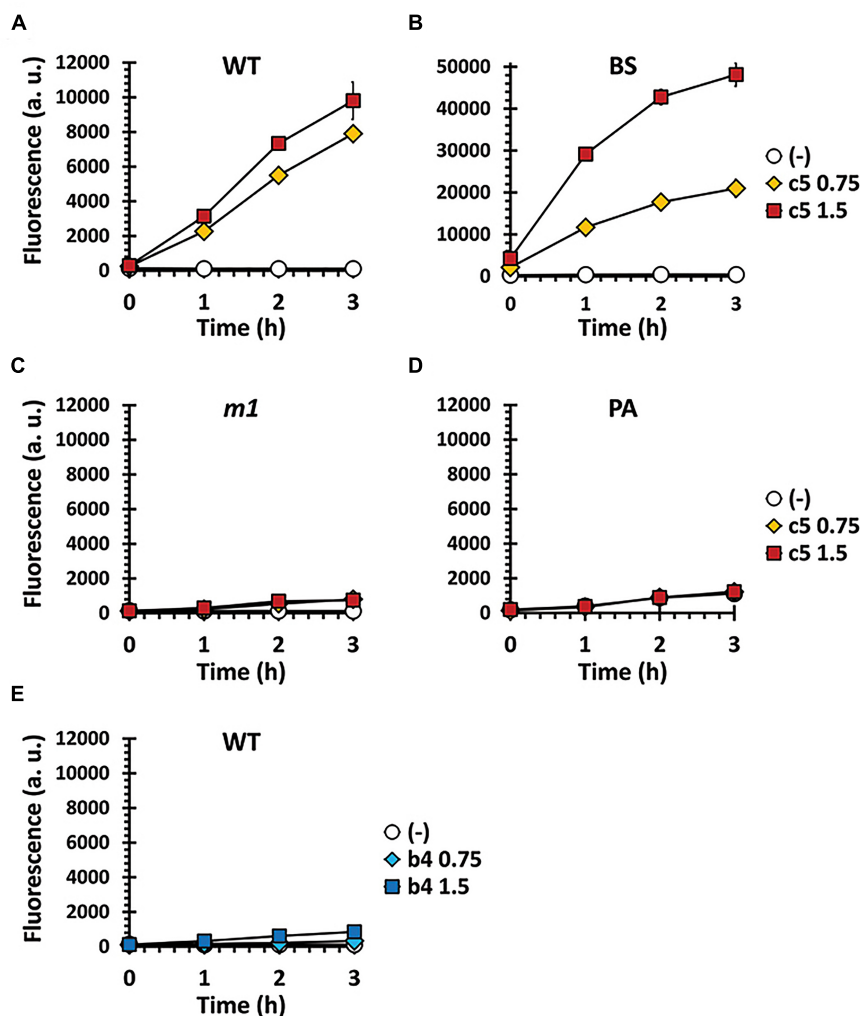


FIGURE 6 | ROS formation by c5 under aerobic condition. ROS generation was measured in SA3 (WT) (A,E) and its mutant (*m1*) (C) as well as in *B. subtilis* (BS) (B) and *P. aeruginosa* (PA) (D), which had been grown to the logarithmic growth phase in M9 minimal medium containing 0.75 (diamond) or 1.5 $\mu\text{g/ml}$ (square) of either c5 (A–D) or b4 (E). No-compound controls (empty circle) were included to investigate the endogenous ROS generation. The data of three independent experiments were pooled and means are shown. Error bars represent standard deviations of the means.

cytoplasmic membrane. While we have demonstrated that the fused naphthoquinone imidazolium bromide works well for drug redirecting strategies in antibacterials, further research is required to reveal additional pharmacophores appropriate for drug redirecting strategies and to improve the utility of this new approach. All these endeavors will be valuable in the era of target-specific and/or side effect-free therapy, as well as in new antibacterial discovery, since we need to target the specific sets of harmfully outgrowing microbes among the complex microbial communities in our bodies.

AUTHOR CONTRIBUTIONS

Y-HC and I-YC conceived and designed the study. H-JJ, I-YC, CL, and SC designed and performed the experiments, and collected and analyzed the experimental data. CL, SC, and S-HK

synthesized and identified the chemical compounds. B-oK and EK provided reagents. H-JJ, I-YC, S-HK, and Y-HC wrote the manuscript. All authors reviewed the manuscript.

FUNDING

This work was supported by the National Research Foundation of Korea (NRF) Grants (NRF-2015R1C1A1A02037359, NRF-2014R1A1A1006317, and NRF-2017M3A9E4077204).

SUPPLEMENTARY MATERIAL

The Supplementary Material for this article can be found online at: <https://www.frontiersin.org/articles/10.3389/fmicb.2019.00350/full#supplementary-material>

REFERENCES

- Cassetta, M. I., Marzo, T., Fallani, S., Novelli, A., and Messori, L. (2014). Drug repositioning: auranofin as a prospective antimicrobial agent for the treatment of severe *staphylococcal* infections. *Biometals* 27, 787–791. doi: 10.1007/s10534-014-9743-6
- Chen, X., Shi, X., Zhao, C., Li, X., Lan, X., Liu, S., et al. (2014). Anti-rheumatic agent auranofin induced apoptosis in chronic myeloid leukemia cells resistant to imatinib through both Bcr/Abl-dependent and -independent mechanisms. *Oncotarget* 5, 9118–9132. doi: 10.18632/oncotarget.2361
- Chirullo, B., Sgarbanti, R., Limongi, D., Shytaj, I. L., Alvarez, D., Das, B., et al. (2013). A candidate anti-HIV reservoir compound, auranofin, exerts a selective 'anti-memory' effect by exploiting the baseline oxidative status of lymphocytes. *Cell Death Dis.* 4:e944. doi: 10.1038/cddis.2013.473
- Cohen, M. L. (1992). Epidemiology of drug resistance: implications for a post-antimicrobial era. *Science* 257, 1050–1055.
- Collins, M. D., and Jones, D. (1981). Distribution of isoprenoid quinone structural types in bacteria and their taxonomic implication. *Microbiol. Rev.* 45, 316–354.
- Cridde, D. N., Gillies, S., Baumgartner-Wilson, H. K., Jaffar, M., Chinje, E. C., Passmore, S., et al. (2006). Menadione-induced reactive oxygen species generation via redox cycling promotes apoptosis of murine pancreatic acinar cells. *J. Biol. Chem.* 281, 40485–40492. doi: 10.1074/jbc.M607704200
- Delcour, A. H. (2009). Outer membrane permeability and antibiotic resistance. *Biochim. Biophys. Acta* 1794, 808–816. doi: 10.1016/j.bbapap.2008.11.005
- Diekema, D. J., Pfaller, M. A., Schmitz, F. J., Smayevsky, J., Bell, J., Jones, R. N., et al. (2001). Survey of infections due to *Staphylococcus* species: frequency of occurrence and antimicrobial susceptibility of isolates collected in the United States, Canada, Latin America, Europe, and the Western Pacific region for the SENTRY Antimicrobial Surveillance Program, 1997–1999. *Clin. Infect. Dis.* 32(Suppl. 2), S114–S132. doi: 10.1086/320184
- Engemann, J. J., Carmeli, Y., Cosgrove, S. E., Fowler, V. G., Bronstein, M. Z., Trivette, S. L., et al. (2003). Adverse clinical and economic outcomes attributable to methicillin resistance among patients with *Staphylococcus aureus* surgical site infection. *Clin. Infect. Dis.* 36, 592–598. doi: 10.1086/367653
- Gould, I. M., David, M. Z., Esposito, S., Garau, J., Lina, G., Mazzei, T., et al. (2012). New insights into methicillin-resistant *Staphylococcus aureus* (MRSA) pathogenesis, treatment and resistance. *Int. J. Antimicrob. Agents* 39, 96–104. doi: 10.1016/j.ijantimicag.2011.09.028
- Harbut, M. B., Vilcheze, C., Luo, X., Hensler, M. E., Guo, H., Yang, B., et al. (2015). Auranofin exerts broad-spectrum bactericidal activities by targeting thiol-redox homeostasis. *Proc. Natl. Acad. Sci. U.S.A.* 112, 4453–4458. doi: 10.1073/pnas.1504022112
- Ho, S. H., Sim, M. Y., Yee, W. L., Yang, T., Yuen, S. P., and Go, M. L. (2015). Antiproliferative, DNA intercalation and redox cycling activities of dioxonaphtho[2,3-d]imidazolium analogs of YM155: a structure-activity relationship study. *Eur. J. Med. Chem.* 104, 42–56. doi: 10.1016/j.ejmech.2015.09.026
- Kelly, R. J., Thomas, A., Rajan, A., Chun, G., Lopez-Chavez, A., Szabo, E., et al. (2013). A phase I/II study of sepantronium bromide (YM155, survivin suppressor) with paclitaxel and carboplatin in patients with advanced non-small-cell lung cancer. *Ann. Oncol.* 24, 2601–2606. doi: 10.1093/annonc/mdt249
- Kim, S.-H., Park, S.-Y., Heo, Y.-J., and Cho, Y.-H. (2008). *Drosophila melanogaster*-based screening for multihost virulence factors of *Pseudomonas aeruginosa* PA14 and identification of a virulence-attenuating factor. *HudA. Infect. Immun.* 76, 4152–4162. doi: 10.1128/IAI.01637-07
- Kuo, S. C., Ibuka, T., Huang, L. J., Lien, J. C., Yean, S. R., Huang, S. C., et al. (1996). Synthesis and cytotoxicity of 1,2-disubstituted naphth[2,3-d]imidazole-4,9-diones and related compounds. *J. Med. Chem.* 39, 1447–1451. doi: 10.1021/jm950247k
- Lau, G. W., Goumnerov, B. C., Walendziewicz, C. L., Hewitson, J., Xiao, W., Mahajan-Miklos, S., et al. (2003). The *Drosophila melanogaster* Toll pathway participates in resistance to infection by the gram-negative human pathogen *Pseudomonas aeruginosa*. *Infect. Immun.* 71, 4059–4066.
- Leclercq, R. (2002). Mechanisms of resistance to macrolides and lincosamides: nature of the resistance elements and their clinical implications. *Clin. Infect. Dis.* 34, 482–492. doi: 10.1086/324626
- Lee, Y.-J., Jang, H.-J., Chung, I.-Y., and Cho, Y.-H. (2018). *Drosophila melanogaster* as a polymicrobial infection model for *Pseudomonas aeruginosa* and *Staphylococcus aureus*. *J. Microbiol.* 56, 534–541. doi: 10.1007/s12275-018-8331-9
- Lowy, F. D. (1998). *Staphylococcus aureus* infections. *N. Engl. J. Med.* 339, 520–532. doi: 10.1056/NEJM199808203390806
- Lowy, F. D. (2003). Antimicrobial resistance: the example of *Staphylococcus aureus*. *J. Clin. Invest.* 111, 1265–1273. doi: 10.1172/JCI18535
- Mediavilla, J. R., Chen, L., Mathema, B., and Kreiswirth, B. N. (2012). Global epidemiology of community-associated methicillin resistant *Staphylococcus aureus* (CA-MRSA). *Curr. Opin. Microbiol.* 15, 588–595. doi: 10.1016/j.mib.2012.08.003
- Nakahara, T., Kita, A., Yamanaka, K., Mori, M., Amino, N., Takeuchi, M., et al. (2007). YM155, a novel small-molecule survivin suppressant, induces regression of established human hormone-refractory prostate tumor xenografts. *Cancer Res.* 67, 8014–8021. doi: 10.1158/0008-5472.CAN-07-1343
- Rice, L. B. (2008). Federal funding for the study of antimicrobial resistance in nosocomial pathogens: no ESKAPE. *J. Infect. Dis.* 197, 1079–1081. doi: 10.1086/533452
- Richter, M. F., Drown, B. S., Riley, A. P., Garcia, A., Shirai, T., Svec, R. L., et al. (2017). Predictive compound accumulation rules yield a broad-spectrum antibiotic. *Nature* 545, 299–304. doi: 10.1038/nature22308
- Saha, S., Savage, P. B., and Bal, M. (2008). Enhancement of the efficacy of erythromycin in multiple antibiotic-resistant gram-negative bacterial pathogens. *J. Appl. Microbiol.* 105, 822–828. doi: 10.1111/j.1365-2672.2008.03820.x
- Setsukinai, K., Urano, Y., Kakinuma, K., Majima, H. J., and Nagano, T. (2003). Development of novel fluorescence probes that can reliably detect reactive oxygen species and distinguish specific species. *J. Biol. Chem.* 278, 3170–3175. doi: 10.1074/jbc.M209264200
- Soriano, A., Marco, F., Martinez, J. A., Pisos, E., Almela, M., Dimova, V. P., et al. (2008). Influence of vancomycin minimum inhibitory concentration on the treatment of methicillin-resistant *Staphylococcus aureus* bacteremia. *Clin. Infect. Dis.* 46, 193–200. doi: 10.1086/524667
- Tomasz, A. (1994). Benefit and risk in the beta-lactam antibiotic-resistance strategies of *Streptococcus pneumoniae* and *Staphylococcus aureus*. *Trends Microbiol.* 2, 380–385.

Conflict of Interest Statement: The authors declare that the research was conducted in the absence of any commercial or financial relationships that could be construed as a potential conflict of interest.

Copyright © 2019 Jang, Chung, Lim, Chung, Kim, Kim, Kim and Cho. This is an open-access article distributed under the terms of the Creative Commons Attribution License (CC BY). The use, distribution or reproduction in other forums is permitted, provided the original author(s) and the copyright owner(s) are credited and that the original publication in this journal is cited, in accordance with accepted academic practice. No use, distribution or reproduction is permitted which does not comply with these terms.



Activity and Impact on Resistance Development of Two Antivirulence Fluoropyrimidine Drugs in *Pseudomonas aeruginosa*

Francesco Imperi^{1,2*}, Ersilia V. Fiscarelli³, Daniela Visaggio¹, Livia Leoni¹ and Paolo Visca¹

¹ Department of Science, Roma Tre University, Rome, Italy, ² Laboratory affiliated to Istituto Pasteur Italia-Fondazione Cenci Bolognietti, Department of Biology and Biotechnology Charles Darwin, Sapienza University of Rome, Rome, Italy, ³ Laboratory of Cystic Fibrosis Microbiology, Bambino Gesù Hospital, Rome, Italy

OPEN ACCESS

Edited by:

Natalia V. Kirienko,
Rice University, United States

Reviewed by:

Carlos Juan,
Instituto de Investigación Sanitaria de
Palma (IdISPa), Spain

Pierre Cornelis,
Vrije University Brussel, Belgium

Michael L. Vasil,
University of Colorado School of
Medicine, United States

*Correspondence:

Francesco Imperi
francesco.imperi@uniroma3.it

Specialty section:

This article was submitted to
Clinical Microbiology,
a section of the journal
Frontiers in Cellular and Infection
Microbiology

Received: 10 December 2018

Accepted: 15 February 2019

Published: 11 March 2019

Citation:

Imperi F, Fiscarelli EV, Visaggio D,
Leoni L and Visca P (2019) Activity
and Impact on Resistance
Development of Two Antivirulence
Fluoropyrimidine Drugs in
Pseudomonas aeruginosa.
Front. Cell. Infect. Microbiol. 9:49.
doi: 10.3389/fcimb.2019.00049

The rise in antibiotic resistance among bacterial pathogens has prompted the exploitation of alternative antibacterial strategies, such as antivirulence therapy. By inhibiting virulence traits, antivirulence drugs are expected to lessen pathogenicity without affecting bacterial growth, therefore avoiding the spread of resistance. However, some studies argued against this assumption, and the lack of antivirulence drugs in clinical use hampers the empirical assessment of this concept. Here we compared the mode of action and range of activity of two drugs which have been proposed for repurposing as quorum sensing and pyoverdine inhibitors in the human pathogen *Pseudomonas aeruginosa*: the anticancer drug 5-fluorouracil (5-FU) and the antimycotic drug 5-fluorocytosine (5-FC), respectively. The effect on bacterial growth, emergence and spread of resistance, and activity against clinical isolates were assessed. Our results confirm that 5-FU has growth inhibitory activity on reference strains and can rapidly select for spontaneous resistant mutants with loss-of-function mutations in the *upp* gene, responsible for uracil conversion into UMP. These mutants were also insensitive to the anti-pyoverdine effect of 5-FC. Conversely, 5-FC did not cause relevant growth inhibition, likely because of poor enzymatic conversion into 5-FU by cytosine deaminase. However, coculturing experiments showed that 5-FU resistant mutants can outcompete sensitive cells in mixed populations, in the presence of not only 5-FU but also 5-FC. Moreover, we observed that serial passages of wild-type cells in 5-FC-containing medium leads to the appearance and spread of 5-FC insensitive sub-populations of 5-FU resistant cells. The different effect on growth of 5-FU and 5-FC was overall conserved in a large collection of cystic fibrosis (CF) isolates, corresponding to different infection stages and antibiotic resistance profiles, although high variability was observed among strains. Notably, this analysis also revealed a significant number of pyoverdine-deficient isolates, whose proportion apparently increases over the course of the CF infection. This study demonstrates that the efficacy of an antivirulence drug with no apparent effect on growth can be significantly influenced by the emergence of insensitive mutants, and highlights the importance of the assessment of resistance-associated fitness cost and activity on clinical isolates for the development of “resistance-proof” antivirulence drugs.

Keywords: acquired resistance, antimetabolite, antivirulence drug, cystic fibrosis, *Pseudomonas aeruginosa*, siderophore, virulence

INTRODUCTION

Antibiotic resistance is a serious public health concern at the global level, as an alarmingly high level of drug resistance has been reported in most common bacterial pathogens (Tommasi et al., 2015), calling for the investigation of alternative therapeutic options. In the last decades, researchers started looking at virulence factors as targets for the development of novel anti-infective drugs aimed at inhibiting pathogen-dependent host damage rather than bacterial growth (Finlay and Falkow, 1997). Such molecules are referred to as antivirulence drugs (Rasko and Sperandio, 2010).

Traditional antibiotics hit essential cellular processes that are widely conserved among bacteria (Lange et al., 2007), imposing a strong selective pressure for resistant mutants and often causing damage and/or dysbiosis in the normal microbiota. Conversely, antivirulence drugs should target virulence-related traits which are typically pathogen-specific and not strictly required for bacterial growth. Hence, they are expected to exert negligible effects on commensal bacteria and to decrease the evolution rates toward resistance (Rasko and Sperandio, 2010). However, since antivirulence drugs still have to enter the cell and/or interact with specific molecular targets to exert their inhibitory activity, the existence of mechanisms conferring resistance to antivirulence compounds is predictable and, indeed, some of them have already been documented, such as modification of the target or extrusion of the antivirulence drug by efflux pumps (Shakhnovich et al., 2007; Maeda et al., 2012). Whether these mechanisms of resistance would be positively selected during the infection remains a matter of debate (García-Contreras et al., 2016; Russo et al., 2016). It has been proposed that the spread of mutant clones resistant to antivirulence drugs could depend on the “public availability” of the targeted virulence factor in the bacterial population. While shared (secreted) virulence factors are public goods that can be used by both sensitive and resistant subpopulations, individualized (cell-associated) virulence factors are private goods that benefit only the resistant producers, thus providing a selective advantage to the resistant subpopulation (reviewed in Allen et al., 2014; Ruer et al., 2015; Maura et al., 2016). Irrespective of the specific conditions, it is however commonly accepted that the selective pressure for resistance to antivirulence agents is likely much weaker than that for resistance to antibiotics (Maura et al., 2016). Unfortunately, the lack of antivirulence drugs in human or animal therapy does not allow the verification of these theories in a clinical or veterinary setting.

The present study was aimed at gaining further insights in the field of antivirulence drug discovery by comparing the mode of action, selective pressure toward resistance and range of activity of two fluorinated pyrimidine drugs, the anticancer drug 5-fluorouracil (5-FU) and the antimycotic drug 5-fluorocytosine (5-FC), which have been proposed for repurposing as quorum sensing and pyoverdine inhibitors in the opportunistic human pathogen *Pseudomonas aeruginosa*, respectively. The antivirulence activity of 5-FU against *P. aeruginosa* was identified when it was found to counteract uracil-mediated activation of the quorum sensing response and to repress the expression of several virulence traits, including

biofilm formation (Ueda et al., 2009). The antivirulence potential of fluorinated pyrimidines was later expanded by a drug repurposing screening campaign, which identified 5-FC as a potent inhibitor of pyoverdine siderophore production, and showed that this antimycotic drug can also suppress *P. aeruginosa* lethality in a mouse model of acute lung infection (Imperi et al., 2013), in line with the crucial role of pyoverdine-mediated iron uptake and virulence in this infection model (Minandri et al., 2016). The anti-*P. aeruginosa* efficacy of fluorinated pyrimidines was also supported by an *in vivo* screening in the *Caenorhabditis elegans* infection model, that revealed anti-pathogenic and anti-pyoverdine activities in 5-FU, 5-FC, and 5-fluorouridine (Kirienko et al., 2016). Notably, 5-FU had a broad inhibitory effect on several virulence phenotypes (Ueda et al., 2009), while 5-FC appeared to exert its antivirulence activity by targeting mainly the production of the pyoverdine siderophore and of pyoverdine-regulated virulence factors (Imperi et al., 2013; Kirienko et al., 2016). These works also reported that, while 5-FC does not affect *P. aeruginosa* growth even at high concentrations, 5-FU has a strong bacteriostatic effect on *P. aeruginosa*, in agreement with an older report describing the growth inhibitory activity of 5-FU, but not of 5-FC, against this bacterium (West, 1986).

Here we provide evidence that 5-FC and 5-FU likely share the same mechanism of action, and that the modest growth inhibitory activity of 5-FC is due to poor uptake and/or limited conversion into 5-FU by *P. aeruginosa* cytosine deaminase. By using co-culturing approaches and *in vitro* evolution experiments, we also demonstrated that 5-FC/5-FU insensitive spontaneous mutants with a defective pyrimidine salvage pathway readily emerge and spread in 5-FU treated populations and that, unexpectedly, these resistant mutants are also selected by 5-FC treatment, though at lower frequency. Finally, we found that the growth inhibitory and/or anti-pyoverdine activities of these two drugs are overall conserved in a large collection of cystic fibrosis (CF) isolates, although some inter-strain variability was observed.

MATERIALS AND METHODS

Bacterial Strains, Growth Conditions, And Plasmids

Laboratory bacterial strains and plasmids used in this study are listed in **Supplementary Table 1**, while the 100 *P. aeruginosa* CF isolates analyzed in this work are described in **Supplementary Table 2**. The CF isolates belong to the collection of bacterial strains isolated from respiratory secretions (sputum, hypopharyngeal aspirate, bronchoalveolar lavage) of CF patients in follow-up at the Cystic Fibrosis Center of the Bambino Gesù Children's Hospital (Rome, Italy). Strain isolation and characterization were performed with the informed consent of the patients or of their parents/legal guardians for minors. Strains were grown in Lysogeny Broth, Lennox formulation (LB), or Mueller-Hinton (MH) as iron-rich media (Acumedia). The iron-depleted complex medium TSBD (Ohman et al., 1980) or the M9 minimal medium supplemented with 20 mM sodium

succinate (SM9, Sambrook et al., 1989) were used as iron-poor media, to which FeCl_3 was added at the indicated concentrations when required. Growth and pyoverdine assays were performed on bacteria cultured at 37°C in 96-well microtiter plates (200 μl of medium in each well) under static conditions, unless otherwise stated.

Plasmid Construction

The plasmid pUCP_{upp} was generated by cloning the coding sequence and the promoter region of the *upp* gene, previously amplified using the PAO1 genomic DNA as the template, into pUCP18. Primers and restriction sites used for PCR and gene cloning are listed in **Supplementary Table 1**.

The plasmid pUCP_{codA} was generated by extracting the coding sequence of *codA* from plasmid pUCP_{codA} by BamHI-HindIII restriction. The fragment was blunt subcloned into pUCP18_{codB} previously digested by SmaI. The correct fragment orientation was verified by restriction analysis. All constructs were verified by DNA sequencing.

Growth and Pyoverdine Measurements

Growth was measured as the OD₆₀₀ of bacterial cultures or of appropriate dilutions in sterile growth medium in a spectrophotometer or, when indicated, in a microtiter plate reader (Victor²V, Wallac). Unless otherwise stated, for growth and compound sensitivity assays bacteria were inoculated at $\sim 10^6$ cells/ml from late exponential or early stationary phase cultures. In long-term resistance development assays, at each passage bacterial cultures were diluted 1:100 in fresh medium.

Pyoverdine production was measured as the OD₄₀₅ of culture supernatants appropriately diluted in 0.1 M Tris-HCl (pH 8), using the supernatant of a pyoverdine-deficient mutant (PAO1 Δ *pvdA*) as blank, and normalized to the OD₆₀₀ of the corresponding culture (Imperi et al., 2010). Pyoverdine production by CF isolates was assessed fluorimetrically by recording the emission at 450 nm upon excitation at 400 nm (Imperi et al., 2009) of culture supernatants appropriately diluted in sterile growth medium, and normalized to the OD₆₀₀ of the corresponding culture.

Selection and Characterization of Spontaneous 5-FU Resistant Isolates

To obtain spontaneous 5-FU resistant isolates, *P. aeruginosa* PAO1 was cultured in LB until the late-exponential phase, normalized at ca. 2×10^9 cells/ml in saline and 100- μl aliquots were plated onto SM9 agar plates containing 120 $\mu\text{g}/\text{ml}$ 5-FU. Five microliters of serial 10-fold dilutions of the stock bacterial suspension were also spotted onto SM9 agar in the absence of 5-FU. Frequency of spontaneous 5-FU resistant mutants was calculated as the ratio between colony forming units (CFU)/ml obtained on 5-FU-containing plates and CFU/ml obtained on plates without 5-FU after 48 h of incubation at 37°C.

To check the DNA sequence of the *upp* gene in selected 5-FU-resistant mutants, their genomic DNA was extracted using GenElute Bacterial Genomic DNA kit (Sigma-Aldrich) and used as the template for a PCR with primers external to the *upp* gene

(**Supplementary Table 1**), which were also used for sequencing of both DNA strands.

Statistical Analyses

Statistical analysis was performed with the software GraphPad Instat, using either using One-Way Analysis of Variance (ANOVA) followed by Tukey-Kramer multiple comparison tests or the Kruskal-Wallis test followed by uncorrected Dunn's multiple comparison test.

RESULTS

Both 5-FC and 5-FU Reduce Pyoverdine Production but Only 5-FU Causes Relevant Growth Inhibition

As a first attempt to compare the activity of the two antimetabolite drugs 5-FC and 5-FU we assessed their effect on growth and pyoverdine production of the reference strain *P. aeruginosa* PAO1 in the iron-poor complex medium TSBD which was originally used by our group in the screening of anti-pyoverdine activity among FDA-approved drugs (Imperi et al., 2013). In line with the results recently obtained by the Kirienko's group using NGM (nematode growth medium) (Kirienko et al., 2016), we confirmed that 5-FC has poor growth inhibitory activity at concentrations up to 1 mM, while 5-FU strongly inhibits *P. aeruginosa* PAO1 growth between 100 and 1,000 μM (**Figure 1**). Both compounds caused strong reduction of pyoverdine production at all concentrations tested ($\geq 10 \mu\text{M}$; **Figure 1**).

To confirm that the differential effect of 5-FC and 5-FU on *P. aeruginosa* PAO1 growth was not specific to the iron-poor culture medium used to monitor pyoverdine production, we also performed growth inhibition assays in different media, including complex iron-rich media (MH and LB), the minimal medium SM9 and, as control, TSBD. Growth was measured in a microtiter plate reader after 20 h at 37°C under static conditions, in order to determine IC₉₀ values (compound concentrations needed to cause 90% growth inhibition). As shown in **Supplementary Figure 1**, 5-FC did not cause relevant alteration of *P. aeruginosa* PAO1 growth in any tested medium. In contrast, 5-FU inhibited growth in all media, although the inhibitory effect varied depending on the medium, with IC₉₀ values ranging from 20 μM in the minimal medium SM9 to 625–2,500 μM in complex media (**Supplementary Figure 1**).

Poor Conversion of 5-FC Into 5-FU Is Responsible for the Lack of Growth-Inhibitory Activity Of 5-FC

We have previously demonstrated that the anti-pyoverdine activity of 5-FC relies on its metabolic conversion into 5-FU in the cytoplasm of *P. aeruginosa* cells, which requires the concomitant activity of cytosine permease CodB and cytosine deaminase CodA, involved in 5-FC transport and conversion into 5-FU, respectively (Imperi et al., 2013). The finding that, differently from 5-FU, 5-FC has marginal (if any) activity on growth (**Figure 1**; Kirienko et al., 2016) suggests that the uptake

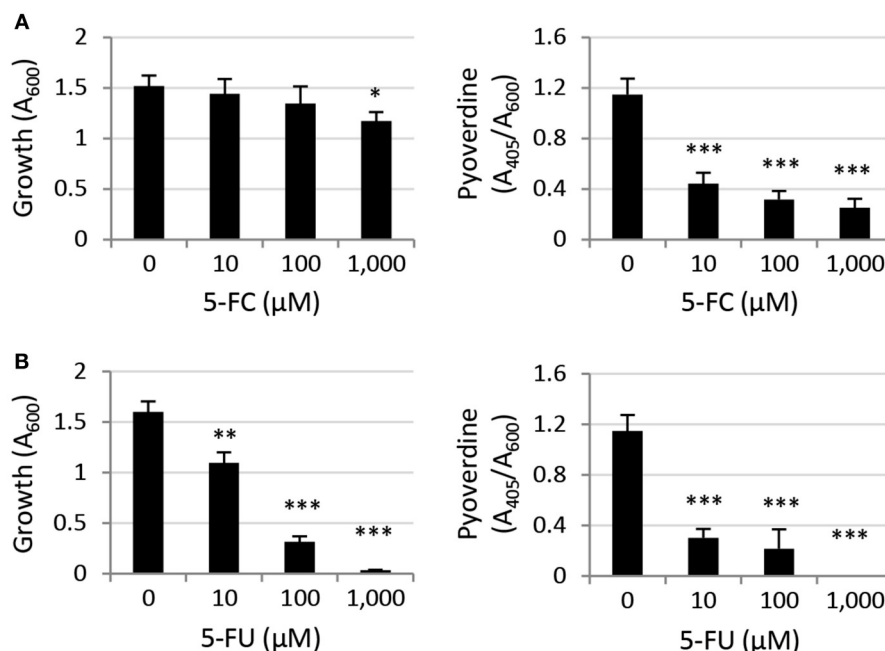


FIGURE 1 | Effect of (A) 5-fluorocytosine (5-FC) and (B) 5-fluorouracil (5-FU) (0–1,000 μM) on *P. aeruginosa* PAO1 growth (left panels) and relative pyoverdine production (right panels) after 14-h growth at 37°C in the iron-poor complex medium TSD. Values represent the mean (±SD) of six independent assays. Asterisks indicate statistically significant differences with respect to the untreated control (**P* < 0.05, ***P* < 0.01, ****P* < 0.001; ANOVA).

of 5-FC and/or its conversion into 5-FU could represent the limiting step(s) for its antibacterial activity. To explore this hypothesis, we investigated the effect of CodAB overexpression on 5-FC sensitivity in the wild type PAO1. As reported in **Figure 2A**, CodAB-overexpressing cells showed a marked sensitivity to 5-FC, which completely inhibited bacterial growth in SM9 minimal medium at low μM concentrations. As expected, CodAB overexpression did not influence the activity of 5-FU (**Figure 2A**), indicating that the observed increase in the growth inhibitory effect of 5-FC was not related to a general increase in sensitivity to fluorinated pyrimidine analogs. Notably, individual overexpression of CodA and, to a lesser extent, of CodB also increased *P. aeruginosa* sensitivity to 5-FC, even if the effect was much lower than that caused by CodAB overexpression (**Figure 2B**). These results indirectly imply that exogenously provided 5-FC is poorly converted into 5-FU by *P. aeruginosa* PAO1 cells, hence suggesting that the differential antivirulence and growth inhibitory effect of 5-FU is likely dependent on the intracellular concentration of this antimetabolite.

Spontaneous 5-FU Resistant Mutants Acquire Mutations in the *upp* Gene and Are Also Insensitive to the Anti-pyoverdine Activity Of 5-FC

Taking advantage of the strong inhibitory effect of 5-FU on *P. aeruginosa* PAO1 growth in the minimal medium SM9 (**Supplementary Figure 1**), we used SM9 agar plates supplemented with 120 μM 5-FU (6 × IC₉₀) to select for

spontaneous mutants resistant to this drug. In five independent experiments, we obtained 5-FU resistant isolates with an average frequency of $1.3 (\pm 0.7) \times 10^{-7}$. When streaked on SM9 agar plates containing either 100 μM 5-FC or 100 μM 5-FU, all colonies appeared to be not only resistant to 5-FU but also insensitive to the inhibitory activity of 5-FC on pyoverdine production, which was visually assessed as fluorescence under the UV light (data not shown; Visaggio et al., 2015). To confirm this qualitative observation, we selected five spontaneous mutants (obtained in independent assays) and quantitatively assessed their growth and pyoverdine production profile in the presence of high concentrations of 5-FU or 5-FC (100 and 1,000 μM) (**Figure 3**). All mutants were found to be resistant to the growth inhibitory effect of 5-FU as well as to the anti-pyoverdine activity of both drugs, although pyoverdine production was still partly repressed by 5-FU in the spontaneous mutants R2 and R4 (**Figure 3**).

Very recently it has been shown that *P. aeruginosa* mutants resistant to 5-FC spontaneously arise after long-term treatment with 5-FC in human serum, and whole genome sequencing revealed that these mutants invariably carried mutations in the *upp* gene (Rezzoagli et al., 2018), which encodes the uracil phosphoribosyltransferase responsible for conversion of uracil into the nucleotide precursor UMP in the pyrimidine salvage pathway (Beck and O'Donovan, 2008). To verify whether *upp* mutations were also present in our spontaneous 5-FU resistant mutants, we sequenced the entire *upp* gene, including its promoter. A nonsense point mutation was identified in the isolate R5, causing premature translation termination at

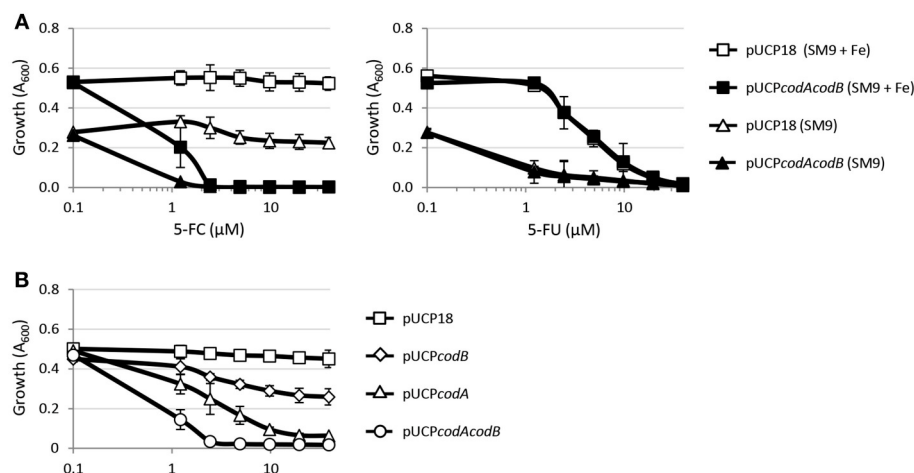


FIGURE 2 | (A) Effect of 5-fluorocytosine (5-FC, left panel) or 5-fluorouracil (5-FU, right panel) at the indicated concentrations on the growth of *P. aeruginosa* PAO1 pUCP18 or *P. aeruginosa* PAO1 pUCPcodAcodB in SM9 minimal medium, supplemented or not with 100 μM FeCl₃ (+ Fe), after 18-h incubation in microtiter plates at 37°C. **(B)** Effect of 5-FC on the growth of *P. aeruginosa* PAO1 harboring pUCP18, pUCPcodA, pUCPcodB, or pUCPcodAcodB in SM9 with 100 μM FeCl₃ after 18-h incubation in microtiter plates at 37°C. Growth (OD₆₀₀) was measured in a microtiter plate reader, and values represent the mean (±SD) of three independent assays.

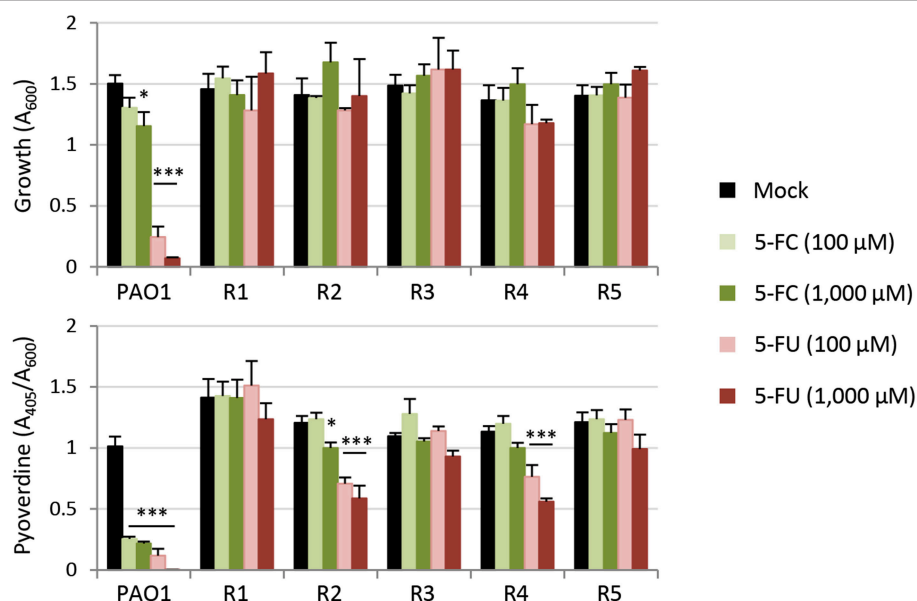


FIGURE 3 | Effect of 5-fluorocytosine (5-FC) and 5-fluorouracil (5-FU) (0–1,000 μM) on growth and relative pyoverdine production (upper and lower panel, respectively) of *P. aeruginosa* PAO1 and five isogenic spontaneous mutants resistant to 5-FU (R1–R5) cultured in TSD for 14 h in microtiter plates at 37°C. Values represent the mean (±SD) of three independent experiments. Asterisks indicate statistically significant differences with respect to the corresponding untreated control (**P* < 0.05, ****P* < 0.001; ANOVA).

codon 57 (of 213). Missense point mutations were identified in isolates R1, R2, and R4, leading to the amino acid substitution H173P (R1) or H8P (R2 and R4, carrying an identical mutation although they were selected in independent assays) (Supplementary Table 1). For the remaining clone (R3), several attempts to amplify the *upp* gene with different primer pairs failed, and amplification and sequencing of the *upp* genomic locus revealed a ca. 5-kb deletion event involving the *upp*

gene and the neighboring genes PA4642–PA4645, *uraA*, *cupE1*, and part of *cupE2* (Supplementary Figure 2). Notably, codons 8 and 173 correspond to hotspot mutation sites that were identified in the *Salmonella enterica upp* gene of *in vitro*-selected 5-FU resistant mutants (Glaab et al., 2005), and encode for histidine residues that are highly conserved in Upp proteins from eubacterial species (Supplementary Figure 3), arguing for an important role of such residues in the functionality of the

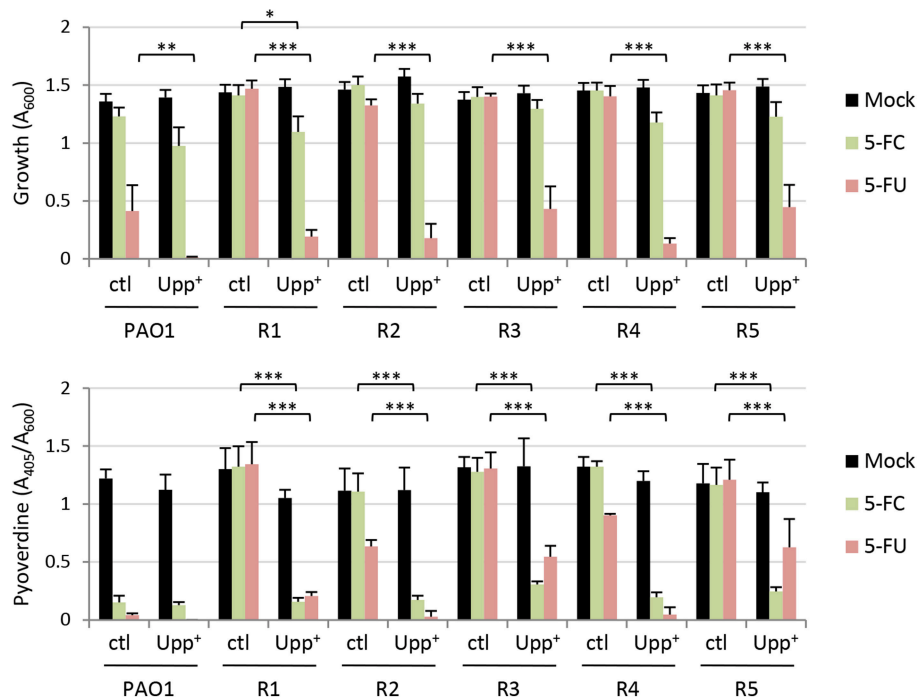


FIGURE 4 | Effect of 5-fluorocytosine (5-FC) and 5-fluorouracil (5-FU) supplemented at 100 μ M on growth and relative pyoverdine production (upper and lower panel, respectively) of *P. aeruginosa* PAO1 and five isogenic spontaneous mutants resistant to 5-FU (R1–R5), containing the empty plasmid pUCP18 (ctl) or the Upp-expressing construct pUCP_{Upp} (Upp⁺). Measurements were taken after 14-h growth in TSBD in microtiter plates at 37°C. Values represent the mean (\pm SD) of three independent experiments. Asterisks indicate statistically significant differences with respect to the corresponding control carrying the empty plasmid and cultured under the same condition (* P < 0.05, ** P < 0.01, *** P < 0.001; ANOVA).

enzyme. To verify this hypothesis and, thus, to tentatively correlate 5-FU resistance with the loss of function of Upp, we complemented the 5-FU resistant mutants with a plasmid expressing the wild type copy of the *upp* gene, and determined the effect on 5-FU and 5-FC sensitivity. Overall, the expression of a functional Upp protein in 5-FU resistant mutants almost completely restored their sensitivity to 5-FU and also rescued the anti-pyoverdine activity of 5-FC, indirectly confirming that the mutations identified in the *upp* gene of these isolates likely result in the loss of Upp function (Figure 4).

5-FU Resistant Mutants Are Positively Selected in the Presence of Clinically-Relevant Concentrations of Both 5-FU And 5-FC

The availability of spontaneous 5-FU resistant isolates that were also insensitive to the anti-pyoverdine effect of 5-FC gave us the opportunity to assess whether the genetic events leading to 5-FC insensitivity could be selected for during 5-FC treatment. As a first attempt to investigate this issue, we co-cultured the wild type PAO1 and each spontaneous resistant isolate (R1–R5) in a 100:1 ratio in the iron-poor medium TSBD in the presence or absence of 5-FC at 400 μ M, corresponding to the maximum serum concentration of 5-FC that is well-tolerated in humans (50 μ g/mL, ca. 390 μ M; Vermes et al., 2000), and a 10-fold lower

concentration (40 μ M). When the cultures reached the stationary phase (after \sim 10 generations), the percentage of 5-FU resistant cells with respect to 5-FU sensitive cells was determined through serial dilution plating on SM9 agar plates containing or not 120 μ M 5-FU. Notably, 5-FU resistant cells rose from 1% to about 10 and 15% in the presence of 40 and 400 μ M 5-FC, respectively (Figure 5). As control, the same experiment was also performed with equivalent concentrations of 5-FU. In line with the strong growth inhibitory activity of 5-FU (Figures 1, 2; Kirienko et al., 2016), 5-FU resistant cells completely outcompeted wild type ones in the presence of both 5-FU concentrations (Figure 5). The percentage of 5-FU resistant cells remained nearly constant (ca. 1.4%) in the absence of drugs (Figure 5), indicating that the increased fitness of 5-FU resistant cells observed in the presence of 5-FC was actually due to their competitive advantage over wild type (sensitive) cells.

The above experiment indicates that, when a relatively abundant number of 5-FC insensitive cells (1%) are artificially introduced in the population, they are positively selected by 5-FC treatments. To corroborate this finding in a more natural setting, a long-term experiment was performed by sequentially culturing the wild type PAO1 in TSBD containing 40 or 400 μ M 5-FC or 5-FU for 7 passages (each involving almost 7 generations, for a total of ca. 46 generations). Growth and pyoverdine production were monitored over passages, while the percentage of 5-FU resistant cells was determined at the end of the experiment

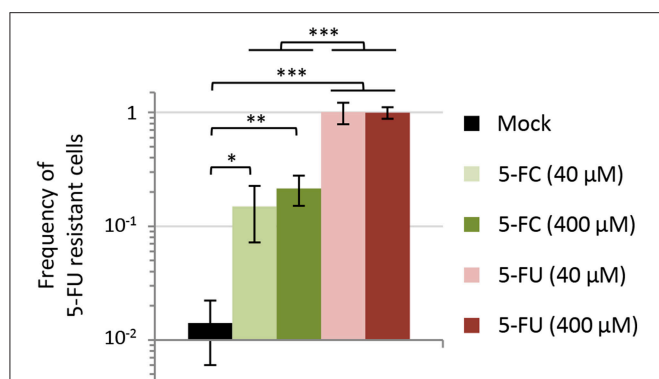


FIGURE 5 | Effect of 5-fluorocytosine (5-FC) and 5-fluorouracil (5-FU) at 40 or 400 μM on the competitive fitness of spontaneous 5-FU resistant mutants of *P. aeruginosa* PAO1. Each 5-FU resistant isolate (R1, R2, R3, R4, or R5) and the parental strain PAO1 were precultured in TSBD with 50 μM FeCl_3 and then inoculated at 1:1,000 final dilution in TSBD in a 1:100 ratio (5-FU R:WT). Percentage of 5-FU resistant cells with respect to 5-FU sensitive ones was evaluated after 16-h incubation at 37°C by plating on SM9 agar plates with or without 120 μM 5-FU. Values represent the mean (\pm SD) of ten independent experiments (two for each 5-FU resistant isolate). Asterisks indicate statistically significant differences (* P < 0.05, ** P < 0.01, *** P < 0.001; ANOVA).

(Figure 6). This assay was aimed at verifying whether the 5-FU insensitive cells emerging in the population are positively selected by the drug treatment. As expected, over the passages the cultures treated with 5-FU became progressively more resistant to this drug. After 7 passages, the cultures exposed to 5-FU showed growth and pyoverdine levels comparable to untreated cultures, irrespective of the 5-FU concentration used in subcultures (Figure 6A), and accordingly they contained only 5-FU resistant cells (Figure 6B). Conversely, sensitivity to the anti-pyoverdine effect of 5-FC remained overall constant over the course of the experiment for cultures treated with this drug, irrespective of the concentration used (Figure 6A). However, long-term exposure to 5-FC led to an 80-fold or a 1,500-fold increase in the frequency of 5-FU resistant cells in the bacterial populations as compared to untreated cultures (Figure 6B). At the end of our assay, 5-FU resistant cells still represented $\leq 0.1\%$ of the whole population, and for this reason they did not (yet) affect the efficacy of 5-FC in inhibiting pyoverdine production by the bacterial culture. Nevertheless, overall these results clearly indicate that, at clinically meaningful concentrations, 5-FC can exert a selective pressure in the TSBD medium which is much lower than that exerted by 5-FU, but still enough to promote the emergence of 5-FC insensitive subpopulations.

The Differential Activity of 5-FC and 5-FU Is Overall Conserved in a Collection of *P. aeruginosa* CF Isolates

An important step in the development of any antibacterial drug is the evaluation of its activity on large panels of clinical strains. Since fluoropyrimidines have potential application as antivirulence adjuvants in treatment of *P. aeruginosa* infection in CF patients (Costabile et al., 2016), we compared the

growth inhibitory and anti-pyoverdine effects of 5-FC and 5-FU at two different concentrations (10 and 100 μM) on 100 *P. aeruginosa* clinical strains isolated from the lung of CF patients. The collection included sequential isolates obtained during several years after establishment of the lung infection and showing different antibiotic resistance profiles (Supplementary Table 2), in order to verify whether the long-lasting *in vivo* adaption of *P. aeruginosa* to the CF lung and/or the acquisition of resistance to conventional antibiotics could affect the efficacy of the antivirulence drugs 5-FC and 5-FU.

Three isolates did not grow in the iron-depleted medium used to assess pyoverdine production (TSBD) (Supplementary Table 2) and, for this reason, were not included in the analysis. Moreover, a relevant percentage of CF isolates (17.5%) did not produce detectable amounts of pyoverdine under the conditions tested, and were therefore considered as pyoverdine-deficient strains in this work (Supplementary Table 2). Notably, the percentage of these pyoverdine-deficient isolates appeared to increase over years of CF lung colonization (Supplementary Figure 4).

Although high variability in both antivirulence and growth inhibitory activities was observed among strains, CF isolates were found to be overall sensitive to the anti-pyoverdine activity of both 5-FC and 5-FU (Figure 7). However, while 5-FC had moderate effect on the growth ($<30\%$ reduction) of most ($\geq 70\%$) isolates, and no significant differences were observed between 10 and 100 μM 5-FC treatments, 5-FU caused a strong inhibition of growth in a dose-dependent manner, with $>50\%$ growth reduction for the majority (80%) of isolates at 100 μM concentration (Figure 7, Supplementary Table 2), in accordance with the results obtained for the reference strain PAO1 (Figure 1). For the great majority of isolates, a good correlation was observed between susceptibility to the growth inhibitory effect of 5-FU and susceptibility to the anti-pyoverdine activity of 5-FC (Supplementary Table 2), further confirming that the modes of action of these drugs are intimately linked in *P. aeruginosa*. However, some exceptions were noted, such as isolates that were highly sensitive to the anti-pyoverdine activity of 5-FC but less susceptible to growth inhibition by 5-FU (e.g., isolates BG17, BG79, and BG84), and isolates showing high growth inhibition but low pyoverdine reduction in the presence of 5-FU and/or 5-FC (e.g., isolates BG49 and BG55) (Supplementary Table 2).

When CF isolates were grouped according to the duration of CF lung colonization or of their antibiotic resistance profile no statistically-significant differences were observed among groups for 5-FC treatments (Supplementary Figure 5), suggesting that the adaptation of *P. aeruginosa* to the CF lung and the expression of antibiotic resistance determinants have no impact on 5-FC sensitivity. Similar results were overall obtained for 5-FU, although isolates from early stages of chronic colonization showed slightly higher sensitivity to 5-FU (Supplementary Figure 5).

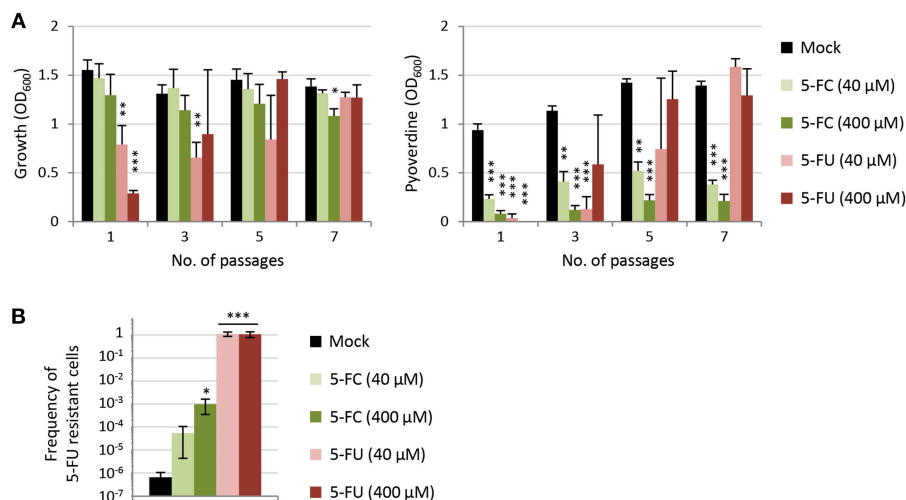


FIGURE 6 | (A) Effect of 5-fluorocytosine (5-FC) and 5-fluorouracil (5-FU) on growth and relative pyoverdine production (left and right panel, respectively) of *P. aeruginosa* PAO1 cultured for 7 subsequent passages (1:100 dilution each) in TSBD in the presence or absence of 5-FC or 5-FU at 40 or 400 μM. **(B)** Frequency of 5-FU resistant cells after 7 passages in TSBD in the presence or in the absence of 5-FC or 5-FU at 40 or 400 μM. Values represent the mean (±SD) of three independent experiments. Asterisks indicate statistically significant differences with respect to the corresponding untreated control (* $P < 0.05$, ** $P < 0.01$, *** $P < 0.001$; ANOVA).

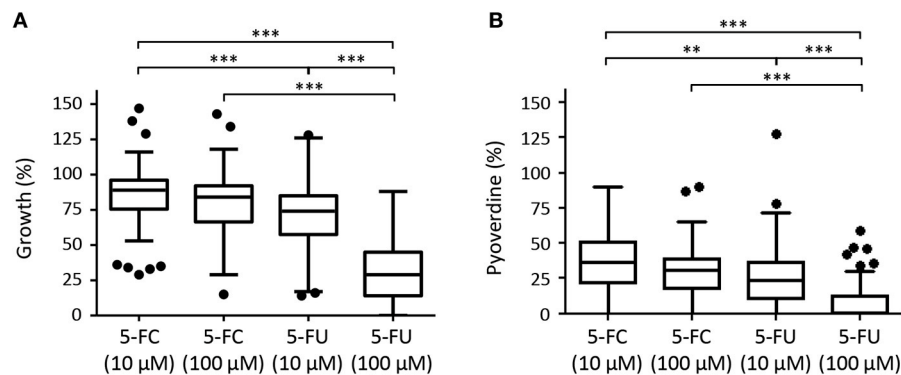


FIGURE 7 | Box plots with Turkey whiskers showing the effect of 5-fluorocytosine (5-FC) and 5-fluorouracil (5-FU) at 10 or 100 μM on growth **(A)** and pyoverdine production **(B)** in a collection of 97 **(A)** or 80 **(B)** *P. aeruginosa* CF isolates cultured in TSBD until the late-exponential growth phase. Data are expressed as percentage with respect to untreated cultures (100%). For each isolates, values are the mean of two or three independent assays. Of the 100 isolates originally included in the collection, 3 did not grow and 17 did not produce detectable amounts of pyoverdine under the conditions tested, and were not included in the plots shown in **(A,B)**, respectively. Black dots represent the outliers. Asterisks indicate statistically significant differences (** $P < 0.01$, *** $P < 0.001$; Kruskal-Wallis).

DISCUSSION

By definition, antivirulence drugs are compounds that should suppress virulence phenotypes without affecting bacterial growth. This paradigm has been used in the last 15 years to search for antivirulence activities in natural or synthetic compounds, as well as in drugs already used for other clinical purposes, for their repositioning as antivirulence agents (Rangel-Vega et al., 2015; Mühlen and Dersch, 2016; Silva et al., 2016; Dickey et al., 2017; Johnson and Abramovitch, 2017; Rampioni et al., 2017a). Hundreds of antivirulence compounds have been proposed so far, and for most of them it has been demonstrated that they actually inhibit pathogenic traits at concentrations that

have no impact on bacterial growth and cell viability, at least *in vitro*. The selectivity toward virulence is indispensable to ensure that antivirulence drugs provide an important advantage over traditional antibiotics, i.e., the lower selective pressure toward the emergence and spread of drug resistance. However, relatively few studies have actually explored the possible acquisition of resistance to antivirulence drugs and/or the effect of such resistance on the efficacy of antivirulence treatments.

To investigate this aspect, in this work we analyzed two highly-related antivirulence drugs endowed with significant antivirulence activity and different impact on *P. aeruginosa* growth, namely the fluorinated pyrimidine analogs 5-FU and 5-FC (Figure 1, Supplementary Figure 1; Kirienko et al.,

2016). The growth inhibitory activity of 5-FU allowed us to easily select spontaneous 5-FU-resistant mutants, which were characterized by loss-of-function mutations in the *upp* gene, responsible for conversion of uracil into the nucleotide precursor UMP in the pyrimidine salvage pathway (Figures 3, 4, Supplementary Table 1; Beck and O'Donovan, 2008). This implies that the growth inhibitory activity of 5-FU is mainly related to inhibition of nucleic acid synthesis, as it has been proposed to occur in yeasts and cancer cells (Vermees et al., 2000; Longley et al., 2003). Interestingly, 5-FU-resistant mutants also became resistant to the anti-pyoverdine activity of 5-FC (Figure 3). This finding is not new, as mutations in the *upp* gene were recently identified through whole genome sequencing in 5-FC insensitive clones of *P. aeruginosa* selected during 5-FC treatment after subsequent passages in human serum (Rezzoagli et al., 2018), a medium in which iron uptake mediated by pyoverdine is important for growth (Bonchi et al., 2015). The evidence that Upp dysfunction confers resistance to both 5-FU and 5-FC strongly suggests that these two drugs likely share the same mechanism(s) of action. Accordingly, we found that 5-FC becomes highly toxic to *P. aeruginosa* cells which ectopically over-express both CodB and CodA or CodA alone (Figure 2), implying that poor cytoplasmic conversion of 5-FC into 5-FU is responsible for the modest growth inhibitory effect of 5-FC.

To date, the molecular target(s) and mechanism(s) of action allowing 5-FU metabolic derivatives to exert their antibacterial or anti-pyoverdine activity are still unknown. It could be hypothesized that fluorinated ribonucleotides have a different impact on the transcription and/or translation of different subsets of genes, with some virulence genes (e.g., pyoverdine genes) being more sensitive to inhibition of gene expression than housekeeping genes, thus explaining the antivirulence activity of these compounds at intracellular concentrations that do not affect growth. Such kind of effect has been proposed to explain the selective inhibition of some virulence genes by azithromycin at sub-MIC concentrations in *P. aeruginosa* (reviewed in Imperi et al., 2014). An alternative hypothesis is that fluorinated ribonucleotides could cause a general imbalance in the metabolic fluxes of the cell, which would be proportional to the intracellular concentration of the toxic compounds. At sub-inhibitory concentrations, this could result in the redistribution of cell energy and metabolites toward essential functions at the expense of non-essential processes, such as the energy-demanding biosynthesis of the pyoverdine siderophore (Visca et al., 2007), in order to ensure cell viability and reproduction. Although some reports have indeed highlighted some direct or indirect effects of catabolism and/or nutrient availability on virulence gene expression in *P. aeruginosa* (Linares et al., 2010; Yeung and Hancock, 2011; Raneri et al., 2018), further studies are still needed to verify and characterize the possible link between the metabolic state of the cell and its virulence potential.

What was unexpected is the finding that, when 5-FU/5-FC resistant mutants were artificially mixed with a population of sensitive cells in a culture medium (TSBD) in which 5-FC has basically no growth inhibitory effect and pyoverdine is dispensable for growth (Figure 1, Supplementary Figure 1;

Imperi et al., 2013), these mutants were positively selected in the presence of 5-FC (Figure 5). Such evidence was corroborated by subsequent passages of the wild type strain PAO1 in the presence of 5-FC, which led to the emergence and spread of small sub-populations of 5-FC insensitive cells (Figure 6). This result clearly indicates that 5-FC may exert some selective pressure for resistance, even under conditions where it has no apparent effect on growth. Whether this might be due to subtle effects of 5-FC on metabolism or to a competitive advantage of cells with an impaired pyrimidine salvage pathway (*upp* mutants) over parental cells under the specific conditions tested remains to be determined. It must be remarked, however, that 5-FC/5-FU resistant mutants are much more readily selected by 5-FU treatments than by 5-FC treatments (Figures 5, 6), in line with the relevant growth inhibition caused by 5-FU (Figure 1 and Supplementary Figure 1). This provides a direct evidence that the emergence and spread of drug insensitive populations are proportional to the growth inhibitory activity of the drug (Maura et al., 2016).

With respect to the highly-conserved and constitutively-expressed antibiotic targets, the presence, expression levels and relevance to infection of virulence factors are often strain-dependent. This is especially true for opportunistic pathogens, such as *P. aeruginosa*, in which the virulence potential is multifactorial and combinatorial, implying that different combinations of pathogenic traits are important for virulence in different strains and/or in different infection models (Lee et al., 2006; Dubern et al., 2015). Thus, an important aspect of antivirulence drug development should be the evaluation of the range of antivirulence activity on large panels of clinical isolates (García-Contreras et al., 2013; Rampioni et al., 2017a,b). As demonstrated in this work using a large collection of CF isolates, the growth and pyoverdine inhibitory effects of 5-FC and 5-FU is overall conserved for clinical isolates (Figure 7), even if few strains revealed peculiar behaviors, such as low responsiveness to one drug and high sensitivity to the other (Supplementary Table 2). Even though these exceptions were not further investigated in this work, they suggest that the activity of 5-FC and 5-FU could be at least partly decoupled in some genetic backgrounds. Finally, it should be noted that a relatively high percentage of the CF isolates (17.5%) were found to be defective in pyoverdine production. As expected, pyoverdine deficiency was more prevalent among isolates obtained at late stages of chronic infection (Supplementary Figure 4), in accordance with previous reports showing that *P. aeruginosa* evolves in the CF lung toward less virulent phenotypes and/or the use of iron sources alternative to pyoverdine (De Vos et al., 2001; Marvig et al., 2014, 2015). However, pyoverdine-deficient strains also represented almost 10% of CF isolates from early stages of infection (Supplementary Figure 4). Given that these isolates are likely to be insensitive to the antivirulence activity of 5-FC, this evidence suggests that the treatment with 5-FC could have no (or poor) efficacy in a relevant number of CF patients.

In conclusion, this work clearly demonstrates that the lack of evident growth inhibitory activity in a putative antivirulence

drug is not sufficient to rule out that resistance mechanisms can emerge and spread in the bacterial population, even under *in vitro* conditions in which the targeted virulence factor(s) is not required for growth. Although it might be argued that our results could represent a specific case related to the drugs (i.e., fluorinated pyrimidines) used in the present work, it is important to note that the number of studies proposing antimetabolites or even antibiotics at sub-MIC concentrations as potential antivirulence compounds is constantly increasing (Rangel-Vega et al., 2015; Mühlen and Dersch, 2016; Silva et al., 2016; Johnson and Abramovitch, 2017; Rampioni et al., 2017a; Soo et al., 2017; D'Angelo et al., 2018). In our opinion, the isolation of drug-insensitive spontaneous mutants, either by direct selection in the presence of high (inhibitory) drug concentrations or by means of more sophisticated culturing approaches to mimic conditions in which the targeted virulence factor(s) is important for growth (Maeda et al., 2012; Rezzoagli et al., 2018), and the assessment of the fitness of these resistant mutants during drug exposure should be mandatory tests in the antivirulence research field. This would ultimately increase the chance to identify and develop antivirulence drugs that are nearly “resistance-proof.”

DATA AVAILABILITY

All datasets generated for this study are included in the manuscript and/or the supplementary files.

REFERENCES

- Allen, R. C., Popat, R., Diggle, S. P., and Brown, S. P. (2014). Targeting virulence: can we make evolution-proof drugs? *Nat. Rev. Microbiol.* 12, 300–308. doi: 10.1038/nrmicro3232
- Beck, D. A., and O'Donovan, G. A. (2008). Pathways of pyrimidine salvage in *Pseudomonas* and former *Pseudomonas*: detection of recycling enzymes using high-performance liquid chromatography. *Curr. Microbiol.* 56, 162–167. doi: 10.1007/s00284-007-9050-3
- Bonchi, C., Frangipani, E., Imperi, F., and Visca, P. (2015). Pyoverdine and proteases affect the response of *Pseudomonas aeruginosa* to gallium in human serum. *Antimicrob. Agents Chemother.* 59, 5641–5646. doi: 10.1128/AAC.01097-15
- Costabile, G., d'Angelo, I., d'Emmanuele di Villa Bianca, R., Mitidieri, E., Pompili, B., Del Porto, P., et al. (2016). Development of inhalable hyaluronan/mannitol composite dry powders for flucytosine repositioning in local therapy of lung infections. *J. Control. Release* 238, 80–91. doi: 10.1016/j.jconrel.2016.07.029
- D'Angelo, F., Baldelli, V., Halliday, N., Pantalone, P., Politicelli, F., Fiscarelli, E., et al. (2018). Identification of FDA-approved drugs as antivirulence agents targeting the pqs quorum-sensing system of *Pseudomonas aeruginosa*. *Antimicrob. Agents Chemother.* 62, e01296–e01218. doi: 10.1128/AAC.01296-18
- De Vos, D., De Chial, M., Cochez, C., Jansen, S., Tümmeler, B., Meyer, J. M., et al. (2001). Study of pyoverdine type and production by *Pseudomonas aeruginosa* isolated from cystic fibrosis patients: prevalence of type II pyoverdine isolates and accumulation of pyoverdine-negative mutations. *Arch. Microbiol.* 175, 384–388. doi: 10.1007/s002030100278
- Dickey, S. W., Cheung, G. Y. C., and Otto, M. (2017). Different drugs for bad bugs: antivirulence strategies in the age of antibiotic resistance. *Nat. Rev. Drug Discov.* 16, 457–471. doi: 10.1038/nrd.2017.23

AUTHOR CONTRIBUTIONS

FI and PV conceived and designed experiments and wrote the paper. FI and DV performed the experiments. FI, EF, LL, and PV analyzed the data and contributed reagents, materials, and analysis tools. All authors read and approved the final manuscript.

FUNDING

This work was supported by the Italian Cystic Fibrosis Research Foundation (grants FFC#10/2013 and FFC# 17/2018), the Sapienza University of Rome (grant Ateneo 2015), the Regione Lazio (prot. 85-2017-13763) and the Grant of Excellence Departments, MIUR-Italy.

ACKNOWLEDGMENTS

We are grateful to Chiara Benvenuto for technical assistance in the screening of the CF strain collection during the preparation of her bachelor thesis.

SUPPLEMENTARY MATERIAL

The Supplementary Material for this article can be found online at: <https://www.frontiersin.org/articles/10.3389/fcimb.2019.00049/full#supplementary-material>

- Dubern, J. F., Cigana, C., De Simone, M., Lazenby, J., Juhas, M., Schwager, S., et al. (2015). Integrated whole-genome screening for *Pseudomonas aeruginosa* virulence genes using multiple disease models reveals that pathogenicity is host specific. *Environ. Microbiol.* 17, 4379–4393. doi: 10.1111/1462-2920.12863
- Finlay, B. B., and Falkow, S. (1997). Common themes in microbial pathogenicity revisited. *Microbiol. Mol. Biol. Rev.* 61, 136–169.
- García-Contreras, R., Maeda, T., and Wood, T. K. (2016). Can resistance against quorum-sensing interference be selected? *ISME J.* 10, 4–10. doi: 10.1038/ismej.2015.84
- García-Contreras, R., Martínez-Vázquez, M., Velázquez Guadarrama, N., Villegas Pañeda, A. G., Hashimoto, T., Maeda, T., et al. (2013). Resistance to the quorum-quenching compounds brominated furanone C-30 and 5-fluorouracil in *Pseudomonas aeruginosa* clinical isolates. *Pathog. Dis.* 68, 8–11. doi: 10.1111/2049-632X.12039
- Glaab, W. E., Mitchell, L. S., Miller, J. E., Vlasakova, K., and Skopek, T. R. (2005). 5-fluorouracil forward mutation assay in *Salmonella*: determination of mutational target and spontaneous mutational spectra. *Mutat. Res.* 578, 238–246. doi: 10.1016/j.mrfmmm.2005.05.021
- Imperi, F., Leoni, L., and Visca, P. (2014). Antivirulence activity of azithromycin in *Pseudomonas aeruginosa*. *Front. Microbiol.* 5:178. doi: 10.3389/fmicb.2014.00178
- Imperi, F., Massai, F., Facchini, M., Frangipani, E., Visaggio, D., Leoni, L., et al. (2013). Repurposing the antimycotic drug flucytosine for suppression of *Pseudomonas aeruginosa* pathogenicity. *Proc. Natl. Acad. Sci. U.S.A.* 110, 7458–7463. doi: 10.1073/pnas.1222706110
- Imperi, F., Tiburzi, F., Fimia, G. M., and Visca, P. (2010). Transcriptional control of the *pvdS* iron starvation sigma factor gene by the master regulator of sulfur metabolism CysB in *Pseudomonas aeruginosa*. *Environ. Microbiol.* 12, 1630–1642. doi: 10.1111/j.1462-2920.2010.02210.x
- Imperi, F., Tiburzi, F., and Visca, P. (2009). Molecular basis of pyoverdine siderophore recycling in *Pseudomonas aeruginosa*. *Proc. Natl. Acad. Sci. U.S.A.* 106, 20440–20445. doi: 10.1073/pnas.0908760106

- Johnson, B. K., and Abramovitch, R. B. (2017). Small molecules that sabotage bacterial virulence. *Trends Pharmacol. Sci.* 38, 339–362. doi: 10.1016/j.tips.2017.01.004
- Kirienko, D. R., Revtovich, A. V., and Kirienko, N. V. (2016). A high-content, phenotypic screen identifies fluorouridine as an inhibitor of pyoverdine biosynthesis and *Pseudomonas aeruginosa* Virulence. *mSphere* 1, e00217–e00216. doi: 10.1128/mSphere.00217-16
- Lange, R. P., Locher, H. H., Wyss, P. C., and Then, R. L. (2007). The targets of currently used antibacterial agents: lessons for drug discovery. *Curr. Pharm. Des.* 13, 3140–3154. doi: 10.2174/138161207782110408
- Lee, D. G., Urbach, J. M., Wu, G., Liberati, N. T., Feinbaum, R. L., Miyata, S., et al. (2006). Genomic analysis reveals that *Pseudomonas aeruginosa* virulence is combinatorial. *Genome Biol.* 7:R90. doi: 10.1186/gb-2006-7-10-r90
- Linares, J. F., Moreno, R., Fajardo, A., Martínez-Solano, L., Escalante, R., Rojo, F., et al. (2010). The global regulator Crc modulates metabolism, susceptibility to antibiotics and virulence in *Pseudomonas aeruginosa*. *Environ. Microbiol.* 12, 3196–3212. doi: 10.1111/j.1462-2920.2010.02292.x
- Longley, D. B., Harkin, D. P., and Johnston, P. G. (2003). 5-fluorouracil: mechanisms of action and clinical strategies. *Nat. Rev. Cancer.* 3, 330–338. doi: 10.1038/nrc1074
- Maeda, T., García-Contreras, R., Pu, M., Sheng, L., García, L. R., Tomás, M., et al. (2012). Quorum quenching quandary: resistance to antivirulence compounds. *ISME J.* 6, 493–501. doi: 10.1038/ismej.2011.122
- Marvig, R. L., Damkier, S., Khademi, S. M., Markussen, T. M., Molin, S., and Jelsbak, L. (2014). Within-host evolution of *Pseudomonas aeruginosa* reveals adaptation toward iron acquisition from hemoglobin. *MBio* 5, e00966–e00914. doi: 10.1128/mBio.00966-14
- Marvig, R. L., Sommer, L. M., Molin, S., and Johansen, H. K. (2015). Convergent evolution and adaptation of *Pseudomonas aeruginosa* within patients with cystic fibrosis. *Nat. Genet.* 47, 57–64. doi: 10.1038/ng.3148
- Maura, D., Ballok, A. E., and Rahme, L. G. (2016). Considerations and caveats in anti-virulence drug development. *Curr. Opin. Microbiol.* 33, 41–46. doi: 10.1016/j.mib.2016.06.001
- Minandri, F., Imperi, F., Frangipani, E., Bonchi, C., Visaggio, D., Facchini, M., et al. (2016). Role of iron uptake systems in *Pseudomonas aeruginosa* virulence and airway infection. *Infect. Immun.* 84, 2324–2335. doi: 10.1128/IAI.00098-16
- Mühlen, S., and Dersch, P. (2016). Anti-virulence strategies to target bacterial infections. *Curr. Top. Microbiol. Immunol.* 398, 147–183. doi: 10.1007/82_2015_490
- Ohman, D. E., Sadoff, J. C., and Iglewski, B. H. (1980). Toxin A-deficient mutants of *Pseudomonas aeruginosa* PA103: isolation and characterization. *Infect. Immun.* 28, 899–908.
- Rampioni, G., Pillai, C. R., Longo, F., Bondi, R., Baldelli, V., Messina, M., et al. (2017b). Effect of efflux pump inhibition on *Pseudomonas aeruginosa* transcriptome and virulence. *Sci. Rep.* 7:11392. doi: 10.1038/s41598-017-11892-9
- Rampioni, G., Visca, P., Leoni, L., and Imperi, F. (2017a). Drug repurposing for antivirulence therapy against opportunistic bacterial pathogens. *Emerg. Top. Life Sci.* 1, 13–22. doi: 10.1042/ETLS20160018
- Raneri, M., Pinatol, E., Peano, C., Rampioni, G., Leoni, L., Bianconi, I., et al. (2018). *Pseudomonas aeruginosa* mutants defective in glucose uptake have pleiotropic phenotype and altered virulence in non-mammal infection models. *Sci. Rep.* 8:16912. doi: 10.1038/s41598-018-35087-y
- Rangel-Vega, A., Bernstein, L. R., Mandujano-Tinoco, E. A., García-Contreras, S. J., and García-Contreras, R. (2015). Drug repurposing as an alternative for the treatment of recalcitrant bacterial infections. *Front. Microbiol.* 6:282. doi: 10.3389/fmicb.2015.00282
- Rasko, D. A., and Sperandio, V. (2010). Anti-virulence strategies to combat bacteria-mediated disease. *Nat. Rev. Drug Discov.* 9, 117–128. doi: 10.1038/nrd3013
- Rezzoagli, C., Wilson, D., Weigert, M., Wyder, S., and Kümmerli, R. (2018). Probing the evolutionary robustness of two repurposed drugs targeting iron uptake in *Pseudomonas aeruginosa*. *Evol. Med. Public Health* 2018, 246–259. doi: 10.1093/emph/eoy026
- Ruer, S., Pinotsis, N., Steadman, D., Waksman, G., and Remaut, H. (2015). Virulence-targeted antibacterials: concept, promise, and susceptibility to resistance mechanisms. *Chem. Biol. Drug. Des.* 86, 379–399. doi: 10.1111/cbdd.12517
- Russo, T. A., Spellberg, B., and Johnson, J. R. (2016). Important complexities of the antivirulence target paradigm: a novel ostensibly resistance-avoiding approach for treating infections. *J. Infect. Dis.* 213, 901–903. doi: 10.1093/infdis/jiv533
- Sambrook, J., Fritsch, E. F., and Maniatis, T. (1989). *Molecular Cloning: a Laboratory Manual, 2nd Edn.* Cold Spring Harbor, NY: Cold Spring Harbor Laboratory.
- Shakhnovich, E. A., Sturtevant, D., and Mekalanos, J. J. (2007). Molecular mechanisms of virastatin resistance by non-O1/non-O139 strains of *Vibrio cholerae*. *Mol. Microbiol.* 66, 1331–1341. doi: 10.1111/j.1365-2958.2007.05984.x
- Silva, L. N., Zimmer, K. R., Macedo, A. J., and Trentin, D. S. (2016). Plant natural products targeting bacterial virulence factors. *Chem. Rev.* 116, 9162–9236. doi: 10.1021/acs.chemrev.6b00184
- Soo, V. W., Kwan, B. W., Quezada, H., Castillo-Juárez, I., Pérez-Eretza, B., García-Contreras, S. J., et al. (2017). Repurposing of anticancer drugs for the treatment of bacterial infections. *Curr. Top. Med. Chem.* 17, 1157–1176. doi: 10.2174/1568026616666160930131737
- Tommasi, R., Brown, D. G., Walkup, G. K., Manchester, J. I., and Miller, A. A. (2015). ESKAPEing the labyrinth of antibacterial discovery. *Nat. Rev. Drug Discov.* 14, 529–542. doi: 10.1038/nrd4572
- Ueda, A., Attila, C., Whiteley, M., and Wood, T. K. (2009). Uracil influences quorum sensing and biofilm formation in *Pseudomonas aeruginosa* and fluorouracil is an antagonist. *Microb. Biotechnol.* 2, 62–74. doi: 10.1111/j.1751-7915.2008.00060.x
- Vermes, A., Guchelaar, H. J., and Dankert, J. (2000). Flucytosine: a review of its pharmacology, clinical indications, pharmacokinetics, toxicity and drug interactions. *J. Antimicrob. Chemother.* 46, 171–179. doi: 10.1093/jac/46.2.171
- Visaggio, D., Pasqua, M., Bonchi, C., Kaever, V., Visca, P., and Imperi, F. (2015). Cell aggregation promotes pyoverdine-dependent iron uptake and virulence in *Pseudomonas aeruginosa*. *Front. Microbiol.* 6:902. doi: 10.3389/fmicb.2015.00902
- Visca, P., Imperi, F., and Lamont, I. L. (2007). Pyoverdine siderophores: from biogenesis to biosignificance. *Trends Microbiol.* 15, 22–30. doi: 10.1016/j.tim.2006.11.004
- West, T. P. and Chu, C. P. (1986). Utilization of pyrimidines and pyrimidine analogues by fluorescent pseudomonads. *Microbios* 47, 149–157.
- Yeung, A. T., Bains, M., and Hancock, R. E. (2011). The sensor kinase CbrA is a global regulator that modulates metabolism, virulence, and antibiotic resistance in *Pseudomonas aeruginosa*. *J. Bacteriol.* 193, 918–931. doi: 10.1128/JB.00911-10

Conflict of Interest Statement: The authors declare that the research was conducted in the absence of any commercial or financial relationships that could be construed as a potential conflict of interest.

Copyright © 2019 Imperi, Fiscarelli, Visaggio, Leoni and Visca. This is an open-access article distributed under the terms of the Creative Commons Attribution License (CC BY). The use, distribution or reproduction in other forums is permitted, provided the original author(s) and the copyright owner(s) are credited and that the original publication in this journal is cited, in accordance with accepted academic practice. No use, distribution or reproduction is permitted which does not comply with these terms.



Recent Advances in Anti-virulence Therapeutic Strategies With a Focus on Dismantling Bacterial Membrane Microdomains, Toxin Neutralization, Quorum-Sensing Interference and Biofilm Inhibition

OPEN ACCESS

Edited by:

Natalia V. Kirienko,
Rice University, United States

Reviewed by:

Michael L. Vasil,
School of Medicine, University of
Colorado Denver, United States

Michael Otto,
National Institute of Allergy and
Infectious Diseases (NIAID),
United States

*Correspondence:

Octavio Luiz Franco
ocfranco@gmail.com

Specialty section:

This article was submitted to
Clinical Microbiology,
a section of the journal
Frontiers in Cellular and Infection
Microbiology

Received: 11 October 2018

Accepted: 05 March 2019

Published: 02 April 2019

Citation:

Fleitas Martínez O, Cardoso MH,
Ribeiro SM and Franco OL (2019)
Recent Advances in Anti-virulence
Therapeutic Strategies With a Focus
on Dismantling Bacterial Membrane
Microdomains, Toxin Neutralization,
Quorum-Sensing Interference and
Biofilm Inhibition.
Front. Cell. Infect. Microbiol. 9:74.
doi: 10.3389/fcimb.2019.00074

Osmel Fleitas Martínez^{1,2}, Marlon Henrique Cardoso^{1,2,3}, Suzana Meira Ribeiro⁴ and Octavio Luiz Franco^{1,2,3*}

¹ Programa de Pós-Graduação em Patologia Molecular, Faculdade de Medicina, Universidade de Brasília, Brasília, Brazil,

² Programa de Pós-Graduação em Ciências Genômicas e Biotecnologia, Centro de Análises Proteômicas e Bioquímicas, Universidade Católica de Brasília, Brasília, Brazil, ³ S-inova Biotech, Programa de Pós-Graduação em Biotecnologia, Universidade Católica Dom Bosco, Campo Grande, Brazil, ⁴ Programa de Pós-Graduação em Ciências da Saúde, Universidade Federal da Grande Dourados, Dourados, Brazil

Antimicrobial resistance constitutes one of the major challenges facing humanity in the Twenty-First century. The spread of resistant pathogens has been such that the possibility of returning to a pre-antibiotic era is real. In this scenario, innovative therapeutic strategies must be employed to restrict resistance. Among the innovative proposed strategies, anti-virulence therapy has been envisioned as a promising alternative for effective control of the emergence and spread of resistant pathogens. This review presents some of the anti-virulence strategies that are currently being developed, it will cover strategies focused on quench pathogen quorum sensing (QS) systems, disassemble of bacterial functional membrane microdomains (FMMs), disruption of biofilm formation and bacterial toxin neutralization.

Keywords: anti-virulence therapy, antibiotic resistance, bacterial membrane microdomains, quorum sensing, biofilms, bacterial toxins

INTRODUCTION

Antimicrobial resistance has turned a serious concern to the human health, because in addition to the death caused by drug-resistant pathogens (~700,000 death annually and it is estimated ~10 million for the year 2050), important medical procedures such as organ transplantation, cancer chemotherapy and surgery are also compromised (O'Neill, 2016). Antimicrobial resistance is a multifactorial phenomenon. Therefore, to circumvent it, a range of actions are needed (WHO, 2018). According that, the innovative antimicrobial compounds development that operate under different principles to those of conventional antibiotics constitutes an important element in the

battle against resistance (Munguia and Nizet, 2017). Among the new therapeutic strategies, anti-virulence therapy has emerged as a promising alternative since instead of killing the pathogens; it tries to deprive them from their virulence factors. Accordingly, the selective pressure exerted over pathogens should be lower than that exerted by conventional antibiotics and the emergence and spread of resistant mutants could be less frequent (Sully et al., 2014; Daly et al., 2015; Quave et al., 2015; Vale et al., 2016; Munguia and Nizet, 2017). However, *Pseudomonas aeruginosa* has developed resistance to anti-virulence drugs (Maeda et al., 2012; García-Contreras et al., 2013, 2015).

Virulence factors are microbial components (biomolecules and structures) used by pathogens to colonize, invade and persist in a susceptible host (Peterson, 1996; Defoirdt, 2017). The production of these factors is under the control of regulatory mechanisms; therefore, in principle interference with these regulatory mechanisms could affect the production of several virulence factors (Defoirdt, 2017). In this regard, quorum-sensing systems (QS) are involved in the regulation of the production of several virulence factors and consequently constitute one of the most exploited targets for the development of anti-virulence drugs (Defoirdt, 2017; Schütz and Empting, 2018). Moreover, the proper folding and/or oligomerization of virulence factors are pivotal for their biological activities. Therefore, the bacterial machinery involved in the virulence factors assembly is also a suitable target for disturbing pathogen virulence via anti-virulence drugs (Heras et al., 2015; Kahler et al., 2018). Recently, it has been described that bacterial functional membrane microdomains (FMMs) play a significant role in the assembly of several virulence factors, hence turning FMMs in an attractive target for drug development (García-Fernández et al., 2017; Koch et al., 2017; Mielich-Süss et al., 2017). In addition to disrupting the production and assembly of virulence factors; anti-virulence drugs have also been focused on interfering with the virulence factor functions (Mühlen and Dersch, 2016; Dickey et al., 2017). In that view, toxin neutralization constitutes a useful strategy to diminish the virulence of pathogens, as secretion of toxins is used by pathogens to colonize the host as well as to evade host immune system response (Heras et al., 2015; Kong et al., 2016; Rudkin et al., 2017). In addition, biofilm growing is a strategy used by pathogens to overcome the host immune system response (Gunn et al., 2016; Watters et al., 2016). Several anti-virulence strategies have been directed to disturb biofilm via interference with bacterial adhesion, extracellular matrix production or disintegration of existing biofilm (Feng et al., 2018; Liu et al., 2018; Puga et al., 2018).

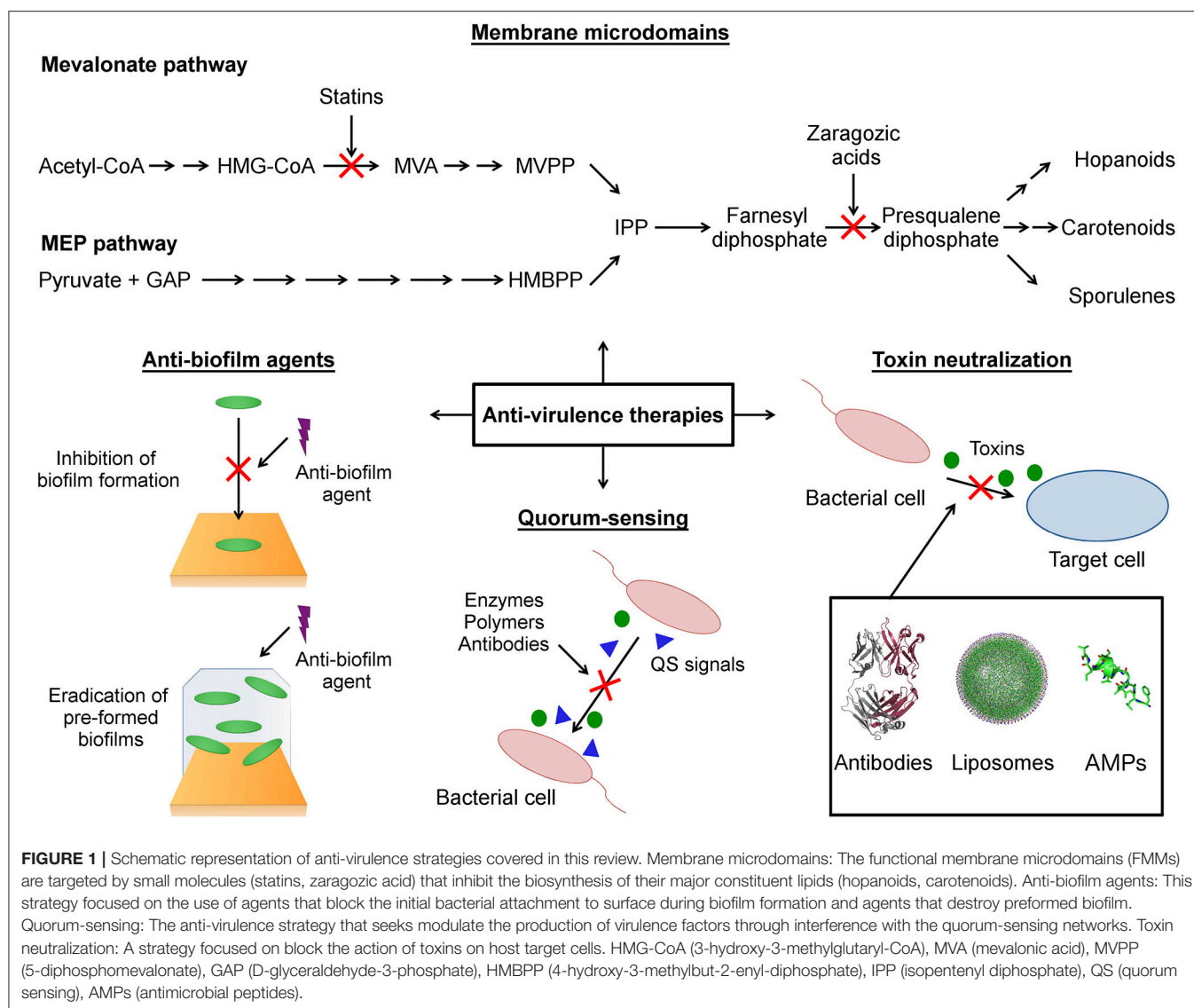
Given the significance attributed to anti-virulence therapy in the scientific community, and especially regarding antimicrobial resistance, this review is directed toward some recent findings in this area. It will uncover innovative strategies that are being implemented to quench pathogen quorum sensing (QS) systems, disassemble functional membrane microdomains (FMMs), disrupt biofilm formation and neutralize toxins (**Figure 1** and **Table 1**). Some of the challenges that anti-virulence therapy faces as an emerging treatment in overcoming multidrug resistant pathogens will also be highlighted.

DISMANTLING BACTERIAL MEMBRANE MICRODOMAINS

To develop new therapeutic strategies against multidrug-resistant pathogens, a suitable approach could be designing antimicrobial compounds that target bacterial structures other than the targets of the major conventional antibiotics. In this respect, the bacterial cytoplasmic membrane constitutes an attractive target as it functions as a barrier that maintains favorable intracellular physicochemical conditions for the correct development of bacterial metabolism. In addition, the cytoplasmic membrane regulates the exchange of information and substances with the extracellular medium (Poolman et al., 2004; Strahl and Errington, 2017). Structural changes in membranes to resist antimicrobial compounds could involve an elevate fitness cost and consequently could be less likely to occur (Zaslhoff, 2002). However, it has been reported membrane modifications linked to resistance toward antimicrobial compounds (Nuri et al., 2015; Joo et al., 2016). Therefore, compounds that interfere with structural organization and/or functions associated with membranes without affecting bacterial growth could be desirable.

In particular, bacterial membranes contain FMMs which are eukaryotic lipid-raft-like domains that enclose a characteristic lipid and protein composition. Specifically, they appear be rich in polyisoprenoid lipids like hopanoids and carotenoids, conferring compact, rigid, and hydrophobic features that could limit the diffusion of FMM-associated proteins away from them (Bramkamp and Lopez, 2015). As regards FMM-associated protein composition, bacterial protein flotillins are essential FMM components. These proteins are closely associated with microdomains and are involved in the membrane fluidity regulation as well as promoting and stabilizing the assembly of specific protein complexes via their scaffold activity (Lopez and Koch, 2017). Other FMM-associated proteins are involved in signaling networks (e.g., sensor kinase KinC), protein secretion machinery (e.g., Sec Y and Sec A) and proteolytic complexes (e.g., FtsH protease complex) (Bramkamp and Lopez, 2015; Lopez and Koch, 2017). Most of these FMM-associated proteins are functionally active when they form multimeric complexes. Therefore, FMMs could be seen as protein complexes assembly platforms with punctuating distribution along bacterial cytoplasmic membrane, where the recruited proteins undergo efficient oligomerization and consequently become functionally active (Bramkamp and Lopez, 2015; Lopez and Koch, 2017).

Experimental evidence has shown that mutant strains in genes involved in the production of FMM structural components could be hampered in establishing virulence determinants. A *Bacillus subtilis* mutant in the *yisP* gene was ineffective in biofilm formation. The gene *yisP* encodes for phosphatase YisP, which produces farnesol from farnesyl diphosphate (López and Kolter, 2010; Feng et al., 2014). Moreover, *B. subtilis* double mutant ($\Delta floT \Delta yqfA$) in genes that encode for the flotillin-like proteins FloT and YqfA (FloA) was defective in the formation of biofilms and sporulation (López and Kolter, 2010; Yepes et al., 2012). *Bacillus subtilis* mutants $\Delta yisP$, Δ



yuaG, $\Delta yqfA$, and $\Delta yuaG \Delta yqfA$ showed diminished Sec-dependent secretion efficiency (Bach and Bramkamp, 2013). Furthermore, a *Campylobacter jejuni* mutant in the gene *cj0268c* displayed reduced adherence to Caco2 cells. The gene *cj0268c* encodes for a protein that contains a SPFH domain, which is typical for flotillin-like proteins (Tareen et al., 2013). In addition, gnotobiotic IL-10^{-/-} mice infected with *C. jejuni* *cj0268c* mutant developed reduced intestinal immunopathology in comparison with ones infected with parental strain and complemented strain (Heimesaat et al., 2014). Recently, it was observed that lack of the gene *floA* in *Staphylococcus aureus* may impact the function of the type VII secretion system (T7SS). Consequently, the $\Delta floA$ mutant exhibited a reduced virulence in a murine model (Mielich-Süss et al., 2017). Similarly, another study showed that the *S. aureus* $\Delta floA$ mutant exhibited diminished virulence in both an invertebrate infection model (*Galleria mellonella*) and a

murine infection model. Specifically, a perturbed degradosome activity was observed; probably by the defective FloA-assisted oligomerization of RNase Rny in the $\Delta floA$ mutant (Koch et al., 2017). All these experimental items of evidence suggest that FMMs could be an attractive target to develop anti-virulence therapy.

In accordance with the above described experimental evidence, several studies have demonstrated that small molecules, which interfere with polyisoprenoid lipid biosynthesis metabolic pathways and with FMM' physicochemical properties, attenuated the virulence of pathogens *in vitro* and *in vivo* (Table 1) (García-Fernández et al., 2017; Koch et al., 2017; Mielich-Süss et al., 2017). Isoprenoids are organic molecules that involve significant diversity of chemical structures and functions; however, they all derive from isopentenyl diphosphate (IPP) or its isomer dimethylallyl diphosphate (DMAPP) (Heuston et al., 2012; Pérez-Gil and Rodríguez-Concepción,

2013). These precursor molecules are synthesized in bacteria through two metabolic pathways including the mevalonate pathway and the 2C-methyl-D-erythritol 4-phosphate (MEP) pathway. The MEP pathway is used by most bacteria. However, the mevalonate pathway is used exclusively by pathogens like *Borrelia burgdorferi*, *S. aureus*, *Streptococcus pneumoniae*, *Enterococcus faecalis*, and is also present in animals (Wilding et al., 2000a; Pérez-Gil and Rodríguez-Concepción, 2013). Moreover, *Listeria monocytogenes* and some *Streptomyces* strains contain both pathways. Bacteria such as *Rickettsia* and *Mycoplasma* do not contain genes that encode for the enzymes involved in the mevalonate and MEP pathways, and therefore they lack both isoprenoid pathways (Pérez-Gil and Rodríguez-Concepción, 2013).

Because the mevalonate pathway is shared between humans and bacteria, in principle, hypercholesterolemia-treating drugs in humans could exert an inhibitory effect on the bacterial mevalonate pathway (Bramkamp and Lopez, 2015). Statins are a class of drugs that target the enzyme class I HMG-CoA reductase (3-hydroxy-3-methylglutaryl-Coenzyme A reductase), which catalyzes the conversion of 3-hydroxy-3-methylglutaryl-Coenzyme A (HMG-CoA) to coenzyme A (CoA) and mevalonate via reductive deacylation, in the human mevalonate pathway (Istvan and Deisenhofer, 2001; Tobert, 2003). Statins bind to the class I HMG-CoA reductase active site, affecting the binding of biological substrate HMG-CoA, and therefore act as competitive inhibitors (Istvan and Deisenhofer, 2001). Similarly, as takes place for human HMG-CoA reductase, statins are also class II HMG-CoA reductase (bacteria and archaea) inhibitors. However, statins exert a diminished inhibitory activity toward class II HMG-CoA reductases [inhibition constant (K_i) in the micro and millimolar range] than class I (K_i in the nanomolar range), which appear to be associated with structural differences between these enzyme classes (Alberts et al., 1980; Kim et al., 2000; Wilding et al., 2000b; Tabernero et al., 2003; Hedl and Rodwell, 2004; Haines et al., 2013). It is important to highlight that some statins with antibacterial activity against Gram-positive and Gram-negative bacteria have been reported. Such capability matched to their wide clinical use, potentially favoring the statins resistance emergence (Ko et al., 2017).

In addition to statins, another inhibitors of bacterial HMG-CoA reductase are the plant-derived compounds annonaceous acetogenins. Feng et al. (2011) showed that squamostating A, squamostating B, squamocin C, and asimicin A were more potent *S. pneumoniae* HMG-CoA reductase inhibitors than lovastatin (Feng et al., 2011). Moreover, Li et al. (2012) using a structure-based screening approach identified several potential *S. pneumoniae* HMG-CoA reductase inhibitors with IC_{50} values in the μ M range (Li et al., 2012).

Other enzymes that have been targeted to disrupt the production of polyisoprenoids are the bacterial “head-to-head” terpene synthases. This class of enzymes catalyzes the formation of a cyclopropylcarbinyl diphosphate intermediate (e.g., presqualene diphosphate) via C1'-2, 3 condensation of two isoprenoid diphosphate molecules (e.g., farnesyl diphosphate) (Lin et al., 2010). Subsequently, the presqualene diphosphate undergoes rearrangement that involves ring opening catalyzed

by the same “head-to-head” terpene synthase [e.g., *S. aureus* dehydrosqualene synthase (CrtM)] or by partner enzymes (e.g., *Zymomonas mobilis* HpnC) rendering dehydrosqualene or hydroxysqualene (Lin et al., 2010; Pan et al., 2015a; Schwalen et al., 2017). Because the “head-to-head” terpene synthases act on IPP synthesis downstream, inhibitors as zaragozic acid family compounds, which are potent inhibitors of “head-to-head” terpene synthases, could hinder the production of polyisoprenoid lipids in many bacterial species and, therefore, disturb the structural assembly and function of the FMMs (Bramkamp and Lopez, 2015).

Supporting the potential use of these sterol synthesis inhibitory drugs as effective anti-FMM drugs, García-Fernández et al. (2017) showed that the penicillin-binding protein PBP2a, which mediates resistance to β -lactam antibiotics in the pathogen methicillin-resistant *Staphylococcus aureus* (MRSA), was associated with FMMs. The treatment of the MRSA culture with 50 μ M of zaragozic acid did not affect the bacterial growth but affected FMMs formation with the consequent disturbance of PBP2a oligomerization, which could imply a non-optimal functionality of PBP2a. In support of this, zaragozic acid-treated MRSA showed a β -lactam-sensitive phenotype in comparison with the non-treated MRSA. Likewise, MRSA treatment with simvastatin, lovastatin, mevastatin and pravastatin enhanced the antimicrobial activity of oxacillin toward the resistant pathogen. Moreover, oxacillin-treated MRSA-infected mice showed a significantly lower survival rate than oxacillin/zaragozic acid-treated MRSA-infected mice. Mice infected with a MRSA strain isolated from a pneumonia patient and treated with oxacillin exhibited a significantly higher bacterial load in lungs than oxacillin/zaragozic acid-treated mice (García-Fernández et al., 2017). This study show the potential of anti-FMM drugs to revert an antibiotic-resistant phenotype into an antibiotic-sensitive phenotype. Besides, it has been demonstrated that treatment of *S. aureus* with zaragozic acid, miltefosine and 5-doxyl-stearic acid (5-DSA) (miltefosine and 5-DSA alter physicochemical properties of lipid-rafts) disturbed FMMs assembly and consequently inhibited FloA oligomerization and scaffold activity. Impaired functional FloA could yield non-proper oligomerization of the RNase Rny, therefore affecting the *S. aureus* degradosome machinery, which is important for the regulation of virulence factors-coding genes expression (Koch et al., 2017). Using a murine infection model it was observed that *S. aureus*-infected mice treated with zaragozic acid, miltefosine, or 5-DSA displayed a significantly higher survival rate than non-treated infected mice. Additionally, in another infection experiment, it was demonstrated that in the treated animals' lungs, small RNAs *rsaA* and *sau63* had significantly higher expression in comparison to untreated controls. This suggested defective degradosome function mediated by the inhibition of FloA oligomerization *in vivo* (Koch et al., 2017). Other evidence of anti-FMM drugs' potential in anti-virulence therapy was recently revealed. It was observed that *S. aureus* treatment with zaragozic acid, simvastatin, or 5-DSA disturbed the correct assembly of T7SS and consequently affected the secretion of T7SS-associated virulence factors. It was suggested that this effect of the anti-FMM compounds on T7SS functionality could involve

TABLE 1 | Inhibitors of functional membrane microdomains assembly, quorum-sensing systems, biofilm formation, and toxin production and function.

Inhibitor	Inhibitory activity	Bacteria	Virulence factors affected	References
Zaragozic acid	Anti-FMM	<i>S. aureus</i>	<ul style="list-style-type: none"> PBP2a oligomerization Rny oligomerization T7SS system assembly 	García-Fernández et al., 2017; Koch et al., 2017; Mielich-Süss et al., 2017
Miltefosine	Anti-FMM	<i>S. aureus</i>	<ul style="list-style-type: none"> Rny oligomerization 	Koch et al., 2017
5-DSA	Anti-FMM	<i>S. aureus</i>	<ul style="list-style-type: none"> Rny oligomerization T7SS system assembly 	Koch et al., 2017; Mielich-Süss et al., 2017
Simvastatin	Anti-FMM	<i>S. aureus</i>	<ul style="list-style-type: none"> T7SS system assembly 	Mielich-Süss et al., 2017
CRISPR-Cas9	Anti-QS Anti-biofilm	<i>E. coli</i> SE15	<ul style="list-style-type: none"> Reduced biofilm formation Down-regulation of <i>mqsR</i>, <i>pgaB</i>, <i>pgaC</i>, <i>csgE</i>, and <i>csgF</i> 	Kang et al., 2017
CRISPR interference	Anti-QS Anti-biofilm	<i>E. coli</i> AK-117	<ul style="list-style-type: none"> Reduced biofilm formation 	Zuberi et al., 2017
2-(methylsulfonyl)-4-(1H-tetrazol-1-yl)pyrimidine	Anti-QS Anti-biofilm	<i>P. aeruginosa</i>	<ul style="list-style-type: none"> Reduced biofilm formation Reduced production of pyocyanin and pyoverdine 	Thomann et al., 2016
(z)-5-octyldenethiazolidine-2,4-dione (TZD-C8)	Anti-QS Anti-biofilm	<i>P. aeruginosa</i>	<ul style="list-style-type: none"> Reduced biofilm formation Reduced swarming motility 	Lidor et al., 2015
Diketopiperazine	Anti-QS Anti-biofilm	<i>Burkholderia cenocepacia</i>	<ul style="list-style-type: none"> Reduced biofilm formation Reduced protease and siderophore production 	Scoffone et al., 2016
ω -Hydroxyemodin	Anti-QS Anti-toxin	<i>S. aureus</i>	<ul style="list-style-type: none"> Reduced RNAlII, <i>psmA</i> and <i>hla</i> transcription 	Daly et al., 2015
Biaryl hydroxyketones	Anti-QS Anti-toxin	<i>S. aureus</i>	<ul style="list-style-type: none"> Reduced RNAlII, <i>psmA</i> and <i>hla</i> transcription 	Greenberg et al., 2018
(KFF)3 K peptide-conjugated locked nucleic acids	Anti-QS Anti-toxin	<i>S. aureus</i>	<ul style="list-style-type: none"> Reduced expression of RNAlII, <i>psmA</i>, <i>psmβ</i>, <i>hla</i>, and <i>pvl</i> 	Da et al., 2017
3-(2,4-dichlorophenyl)-1-(1H-pyrrol-2-yl)-2-propen-1-one	Anti-QS Anti-biofilm	<i>V. harveyi</i>	<ul style="list-style-type: none"> Reduced biofilm production Biofilm disintegration Swimming and swarming motility reduction. 	Rajamanikandan et al., 2017a
Zingerone	Anti-QS Anti-biofilm	<i>P. aeruginosa</i> PAO1 <i>P. aeruginosa</i> clinical isolates.	<ul style="list-style-type: none"> Reduced biofilm, pyocyanin, hemolysin, elastase, proteases, rhamnolipid production Reduced swarming, swimming, and twitching motility 	Kumar et al., 2015
AHL-nitric oxide hybrids	Anti-QS	<i>P. aeruginosa</i> PA14 <i>P. aeruginosa</i> PAO1	<ul style="list-style-type: none"> Reduced pyocyanin and elastase production 	Kutty et al., 2015
Flavonoids	Anti-QS	<i>P. aeruginosa</i> PA14	<ul style="list-style-type: none"> Reduced pyocyanin production and swarming motility <i>rhlA</i> transcription inhibition 	Paczkowski et al., 2017
Terrein	Anti-QS Anti-biofilm	<i>P. aeruginosa</i> PAO1	<ul style="list-style-type: none"> Reduced elastase, pyocyanin, rhamnolipid, and biofilm production Attenuated <i>in vivo</i> virulence of <i>P. aeruginosa</i> PAO1 toward <i>C. elegans</i> and mice 	Kim et al., 2018
Parthenolide	Anti-QS Anti-biofilm	<i>P. aeruginosa</i> PAO1	<ul style="list-style-type: none"> Reduced pyocyanin, proteases, and biofilm production Reduced swarming motility 	Kalia et al., 2018
N-(4-(fluoroanilino)-butanoyl)-L-homoserine lactone N-(4-(chloroanilino)-butanoyl)-L-homoserine lactone	Anti-QS Anti-biofilm	<i>P. aeruginosa</i> PA330 <i>P. aeruginosa</i> PA282	<ul style="list-style-type: none"> Reduced biofilm production 	Kalaiaarasan et al., 2017

(Continued)

TABLE 1 | Continued

Inhibitor	Inhibitory activity	Bacteria	Virulence factors affected	References
Pyrone analogs	Anti-QS Anti-biofilm	<i>P. aeruginosa</i>	<ul style="list-style-type: none"> Down-regulation of <i>lasA</i>, <i>lasB</i>, <i>rhlA</i>, <i>rhlB</i> <i>phzC1</i>, and <i>phzE1</i> Reduced biofilm production 	Park et al., 2015
Pyridoxal lactohydrazone	Anti-QS Anti-biofilm	<i>P. aeruginosa</i> PAO1	<ul style="list-style-type: none"> Reduced biofilm, alginate and pyocyanin production Reduced swarming and twitching motility 	Heidari et al., 2017
1,5-dihydropyrrol-2-ones analogs	Anti-QS	<i>E. coli</i> JB357 <i>gfp</i> reporter strain	<ul style="list-style-type: none"> QS inhibition 	Goh et al., 2015
Triaryl derivatives	Anti-QS	<i>E. coli</i> BL21 DE3 Gold reporter strain		Capilato et al., 2017
Triphenyl scaffold-based hybrid compounds	Anti-QS	<i>E. coli</i> JLD 271 reporter strain		O'Reilly and Blackwell, 2015
Non-native AHL	Anti-QS	<i>E. coli</i> JLD 271 and <i>P. aeruginosa</i> PAO-JP2 reporter strains		Eibergen et al., 2015
Fluoro-substituted Isothiocyanates	Anti-QS	<i>P. aeruginosa</i>	<ul style="list-style-type: none"> Reduced pyocyanin production Reduced swarming motility Attenuated <i>in vivo</i> virulence of <i>P. aeruginosa</i> PAO1-UW toward <i>C. elegans</i> Attenuated <i>P. aeruginosa</i> PA14 virulence in an <i>ex-vivo</i> human skin burn wound model 	Amara et al., 2016
Zeaxanthin	Anti-QS Anti-biofilm	<i>P. aeruginosa</i> PAO1	<ul style="list-style-type: none"> Reduced biofilm formation Downregulated <i>rhlA</i> and <i>lasB</i> expression 	Gökalsin et al., 2017
Phenyllactic acid	Anti-QS Anti-biofilm Anti-toxin	<i>P. aeruginosa</i> PAO1 and clinical isolates	<ul style="list-style-type: none"> Reduced pyocyanin, proteases, rhamnolipid, and hemolysin production Reduced swarming motility Reduced biofilm production 	Chatterjee et al., 2017
Metformin	Anti-QS Anti-biofilm Anti-toxin	<i>P. aeruginosa</i> PAO1	<ul style="list-style-type: none"> Reduced biofilm, pyocyanin, proteases, hemolysin and elastase production Reduced swimming and twitching motility 	Abbas et al., 2017
Glyceryl trinitrate	Anti-QS Anti-biofilm	<i>P. aeruginosa</i> PAO1 and clinical isolates	<ul style="list-style-type: none"> Reduced biofilm, pyocyanin and proteases production 	Abbas and Shaldam, 2016
4-amino-quinolone-based compounds	Anti-QS Anti-biofilm	<i>P. aeruginosa</i> PAO1-L <i>P. aeruginosa</i> PA14	<ul style="list-style-type: none"> Reduced biofilm and pyocyanin production 	Soukariah et al., 2018
Lactam-bridged AIP analogs	Anti-QS	<i>S. aureus</i> reporter strains		Tal-Gan et al., 2016
Solonamides analogs	Anti-QS Anti-toxin	<i>S. aureus</i>	<ul style="list-style-type: none"> Reduced <i>RNAIII</i> and <i>hla</i> expression Marginally enhanced biofilm formation 	Baldry et al., 2016
AIP-II peptidomimetics	Anti-QS	<i>S. aureus</i> reporter strains		Vasquez et al., 2017
Lactam hybrids of solonamide B and AIP	Anti-QS	<i>S. aureus</i> RN10829 reporter strain		Hansen et al., 2018
Truncated AIP	Anti-QS	<i>S. lugdunensis</i> AH4031 reporter strain		Gordon et al., 2016
AIP analogs	Anti-QS Anti-biofilm	<i>S. epidermidis</i> RP62A	<ul style="list-style-type: none"> Reduced biofilm formation (using non-native agonist of AgrC-type I) 	Yang et al., 2016
Linear peptidomimetics	Anti-QS Anti-toxin	<i>S. aureus</i> 8325-4 <i>S. aureus</i> reporter strains	<ul style="list-style-type: none"> Reduced expression of <i>RNAIII</i> Reduced <i>hla</i> expression 	Karathanasi et al., 2018
Bicyclo [2.2.1] hept-5-ene-2,3-dicarboxylic acid 2,6-dimethylpyridine 1-oxide	Anti-QS Anti-biofilm	<i>V. harveyi</i>	<ul style="list-style-type: none"> Reduced biofilm production Disintegrated mature biofilm Reduced swarming and swimming 	Rajamanikandan et al., 2017b

(Continued)

TABLE 1 | Continued

Inhibitor	Inhibitory activity	Bacteria	Virulence factors affected	References
Coumarin	Anti-QS Anti-biofilm	<i>P. aeruginosa</i> PAO1 and clinical isolates	<ul style="list-style-type: none"> • Reduced biofilm production • Down-regulation of <i>lasI</i>, <i>rhlI</i>, <i>rhlR</i>, <i>pqsB</i>, <i>pqsC</i>, <i>pqsH</i>, <i>ambBCDE</i> • Reduced protease and pyocyanin production • Reduced expression of T3SS secretion system-associated genes 	Zhang et al., 2018
T315 compound	Anti-biofilm	<i>S. enterica</i> serovar Typhimurium <i>S. enterica</i> serovar Typhi <i>A. baumannii</i>	<ul style="list-style-type: none"> • Reduced biofilm production 	Moshiri et al., 2018
2-aminobenzimidazole derivatives	Anti-biofilm	<i>S. enterica</i> serovar Typhimurium	<ul style="list-style-type: none"> • Reduced biofilm production 	Huggins et al., 2018
[3-(2-furylmethyl)-2-[[[5-hydroxy-1H-pyrazol-3-yl)methyl]thio]-3,5,6,7-tetrahydro-4H-cyclopenta [4,5]thieno[2,3- <i>d</i>]pyrimidin-4-on]	Anti-biofilm	<i>S. enterica</i> serovar Typhi <i>S. enterica</i> serovar Typhimurium <i>A. baumannii</i>	<ul style="list-style-type: none"> • Reduced biofilm production 	Koopman et al., 2015
3F1 compound	Anti-biofilm	<i>S. mutans</i>	<ul style="list-style-type: none"> • Biofilm dispersion 	Garcia et al., 2017
2-amino-imidazole/triazole conjugate	Anti-biofilm	<i>S. mutans</i>	<ul style="list-style-type: none"> • Reduced biofilm production 	Pan et al., 2015b
Peptidomimetic compounds	Anti-biofilm	<i>Porphyromonas gingivalis</i>	<ul style="list-style-type: none"> • Three-species biofilm inhibition 	Tan et al., 2018
1,2,3-triazole-based peptidomimetics	Anti-biofilm	<i>P. gingivalis</i>	<ul style="list-style-type: none"> • Reduced two-species biofilm formation (inhibition of adherence of <i>P. gingivalis</i> to <i>S. gordonii</i>) 	Patil et al., 2016
Kaempferol	Anti-biofilm	<i>S. aureus</i>	<ul style="list-style-type: none"> • Reduced biofilm production (inhibition of initial attachment) • Inhibition of sortase A activity • Downregulation of <i>clfA</i>, <i>clfB</i>, <i>fnbA</i> and <i>fnbB</i> expression 	Ming et al., 2017
5-benzylidene-4-oxazolidinones	Anti-biofilm	<i>S. aureus</i>	<ul style="list-style-type: none"> • Reduced biofilm production • Biofilm dispersion 	Edwards et al., 2017
p-tolyl(3-phenylpropyl)carbamate	Anti-biofilm	<i>S. aureus</i>	<ul style="list-style-type: none"> • Reduced biofilm production 	Stephens et al., 2016
Antibiofilm compound 1 (ABC-1)	Anti-biofilm	<i>S. aureus</i>	<ul style="list-style-type: none"> • Reduced biofilm production • Reduced polysaccharide intercellular adhesin (PIA) production and eDNA release • Downregulation of <i>spa</i> expression 	Shrestha et al., 2016
Zosteric acid derivatives	Anti-biofilm	<i>E. coli</i>	<ul style="list-style-type: none"> • Reduced biofilm production 	Cattò et al., 2015
Pyrimidinedione	Anti-biofilm	<i>S. pneumoniae</i> <i>S. aureus</i> <i>S. epidermidis</i>	<ul style="list-style-type: none"> • Reduced biofilm production 	Yadav et al., 2015
Resveratrol	Anti-toxin Anti-QS	<i>S. aureus</i>	<ul style="list-style-type: none"> • Downregulation of <i>hla</i>, <i>RNAIII</i> and <i>saeRS</i> expression • Reduced α-hemolysin production 	Duan et al., 2018; Tang et al., 2018
Lysionotin	Anti-toxin Anti-QS	<i>S. aureus</i>	<ul style="list-style-type: none"> • Downregulation of <i>hla</i>, and <i>agr</i> expression • Reduced α-hemolysin production 	Teng et al., 2017
Eriodictyol	Anti-toxin Anti-QS	<i>S. aureus</i>	<ul style="list-style-type: none"> • Downregulation of <i>hla</i> and <i>RNAIII</i> expression • Reduced α-hemolysin production • Reduced hemolysis 	Xuewen et al., 2018
Chalcone	Anti-toxin Anti-QS Anti-biofilm	<i>S. aureus</i>	<ul style="list-style-type: none"> • Downregulation of <i>hla</i> and <i>agrA</i> expression • Reduced α-hemolysin production • Inhibition of Sortase A activity • Reduced adherence to fibronectin • Reduced hemolysis • Reduced biofilm formation 	Zhang et al., 2017a

(Continued)

TABLE 1 | Continued

Inhibitor	Inhibitory activity	Bacteria	Virulence factors affected	References
Prim-O-Glucosylcimifugin	Anti-toxin Anti-QS	<i>S. aureus</i>	<ul style="list-style-type: none"> • Reduced α-hemolysin production • Downregulation of <i>hla</i> and <i>RNAIII</i> expression • Reduced hemolysis 	Ping et al., 2018
Dracorhodin perchlorate	Anti-toxin Anti-QS	<i>S. aureus</i>	<ul style="list-style-type: none"> • Reduced α-hemolysin production • Downregulation of <i>hla</i> and <i>RNAIII</i> expression • Reduced hemolysis 	Liu et al., 2017
Sclareol	Anti-toxin Anti-QS	<i>S. aureus</i>	<ul style="list-style-type: none"> • Reduced α-hemolysin production • Downregulation of <i>hla</i> and <i>RNAIII</i> expression • Reduced hemolysis 	Ping et al., 2017
2-aminoimidazole derivatives	Anti-toxin	<i>Clostridium difficile</i>	<ul style="list-style-type: none"> • Reduced toxin activity 	Thanissery et al., 2018
Peptides	Anti-toxin	<i>Aggregatibacter actinomycetemcomitans</i>	<ul style="list-style-type: none"> • Inhibition of LtxA-mediated cytotoxicity 	Krueger et al., 2018
Galloylated catechins	Anti-toxin	<i>A. actinomycetemcomitans</i>	<ul style="list-style-type: none"> • Inhibition of LtxA-mediated cytotoxicity 	Chang et al., 2019

impaired FloA scaffold activity, since FloA interacted with the component EssB of T7SS and assisted in the complex assembly. Additionally, it was verified that in BALB/c mice infected with *S. aureus* and treated with zaragozic acid the levels of IgM antibodies against T7SS substrates such as Esx A, Esx B, Esx C, and Esx D were inferior to those in non-treated controls (Mielich-Süss et al., 2017).

MANIPULATING BACTERIAL QUORUM SENSING SYSTEMS

For the establishment of successful host infection by pathogenic bacteria it is necessary to have coordinated actions among the population members of the infecting pathogen. These synchronized actions may be achieved through communication systems between bacteria. Therefore, bacterial communication systems are important players in the establishment of a successful host-infection process and consequently are attractive targets for developing anti-virulence therapeutic strategies (Defoirdt, 2017; Munguia and Nizet, 2017). One of the bacterial communication systems that is most studied and distributed among bacteria is the quorum-sensing (QS) network. Independently of the diversity of bacterial QS systems' architecture and functional components, these communication systems are commonly based on a sequence of events that consist of the production of chemical signaling molecules (autoinducers), which are secreted to the external medium and accumulate until reaching a threshold of concentration that is detected by bacteria. Subsequently, a change in the gene-expression patterns take place in response to the detected signaling molecules (Waters and Bassler, 2005; Papenfort and Bassler, 2016). The strategies for disturbing and manipulating QS networks aim to interfere with these basic events (Table 1).

However, these quorum quenching strategies have to face several challenges to become feasible therapeutic options. The

expression of certain virulence factor could be subjected to the control of several regulatory mechanisms other than the targeted QS system (Arya and Princy, 2016). Depending on the environment factors find by the pathogen; some of these regulatory mechanisms could influence the virulence factor expression more predominantly than others (Goerke et al., 2001; Xiong et al., 2006; Zurek et al., 2014; Liu et al., 2016). Another element that could represent a challenge is the diversity of QS systems that could be present in a pathogen; and that these could form complex interconnected networks (Lee and Zhang, 2015; Koul et al., 2016). Furthermore, in some cases, the interference with the QS systems could promote the virulence instead of attenuated it (Köhler et al., 2010; García-Contreras, 2016). In addition, interference with QS systems could affect the pathogen growth, which could exert selective pressure and facilitate the emergence of resistant pathogens (García-Contreras, 2016). Moreover, in a polymicrobial infection, because the interaction between pathogens could be mediated by QS-controlled factors, the interference with QS systems in a pathogen potentially could facilitate the pathogenicity and antibiotic resistance of the co-infecting pathogens (O'Brien and Fothergill, 2017; Radlinski et al., 2017). Also, it is important to have diagnostic tools sensitive enough that allow the detection of the infecting pathogen at low cellular densities; so that quorum quenching strategies could be implemented before the pathogen reach the quorum necessary to trigger their pathogenic potential (Kalia et al., 2019).

Interference With Quorum-Sensing Signal Biosynthesis

One of the approaches to disrupting QS systems is based on the interference in signal production. This strategy is centered on inhibiting the activity of the autoinducer-producing enzymes via small inhibitory molecules, which are mainly substrate structural analogs or transition state analogs and do not affect bacterial growth (LaSarre and Federle, 2013). The advantages of this strategy are that enzymes involved in the production

of autoinducers are not present in mammalian cells and are encoded in the genome of several bacterial species (LaSarre and Federle, 2013; Pereira et al., 2013). Moreover, it is possible that an effect on the activity of a particular enzyme [e.g., 5'-methylthioadenosine/S adenosylhomocysteine nucleosidase (MTAN nucleosidase)] could in turn affect the production of more than one type of autoinducer (Gutierrez et al., 2009). However, the fact that target enzymes have intracellular localization raises several challenges for the implementation of this strategy. Primarily, the inhibitory compounds should overcome the diffusion barriers imposed by bacterial surface structures, particularly difficult in Gram-negative bacteria, which contain a double membrane system. Furthermore, once inside the cell, the inhibitors could be expelled to extracellular space by efflux pumps. In addition, the inhibitor compounds could inhibit enzymes involved in important metabolic processes, compromising the cellular viability, and therefore creating selective pressure on the bacteria (Hinsberger et al., 2014; Sahner et al., 2015; Ji et al., 2016).

Despite all these possible limitations, several studies using *in cellulo* and *in vivo* approaches suggested the feasibility of the use of autoinducer-producing enzyme inhibitors. Gutierrez et al. (2009) showed that transition state analogs of the enzyme MTAN nucleosidase suppressed the production of autoinducers by *Vibrio cholerae* and enterohemorrhagic *Escherichia coli* O157:H7. Specifically, the inhibitors 5'-methylthio-DADMe-Immucillin-A, 5'-ethylthio-DADMe-Immucillin-A, and 5'-butylthio-DADMe-Immucillin-A inhibited the MTAN activity in a dose-dependent fashion, and consequently the production of autoinducers, without disturbing bacterial growth in *V. cholerae* N1696 culture. Similar behavior was observed in *Escherichia coli* O157:H7 culture, where 5'-methylthio-DADMe-Immucillin-A and 5'-butylthio-DADMe-Immucillin-A inhibited the production of AI-2 in a dose-dependent mode, without affecting bacterial growth. Importantly, both bacterial strains maintained the 5'-butylthio-DADMe-Immucillin-A sensitive phenotype after growth for several generations when challenged with the inhibitor, suggesting that there was no emergence of resistance. In agreement with the reduction of AI-2 production, reduced biofilm-forming capacity was observed in both bacterial species when they were treated with the 5'-butylthio-DADMe-Immucillin-A inhibitor (Gutierrez et al., 2009).

Another bacterial pathogen for which QS signal-producing enzyme inhibitors have been developed is *Pseudomonas aeruginosa*. This pathogen contains a particular QS system [*Pseudomonas* quinolone system (*pqs*)] which uses PQS (3,4-dihydroxy-2-heptylquinoline, *Pseudomonas* quinolone signal) and HHQ (2-heptyl-4-hydroxyquinoline) as QS signal molecules (LaSarre and Federle, 2013; Papenfort and Bassler, 2016). The production of HHQ and PQS starts with activity of the enzyme anthranilyl-CoA ligase (PqsA) which catalyzes the activation of anthranilate to anthraniloyl-coenzyme A via an anthranilyl-AMP reaction intermediate. Sulfonyl-adenosine compounds (anthranilyl-MAS and anthranilyl-AMSN) that mimic the anthranilyl-AMP intermediate were PqsA inhibitors that reduced the production of HHQ and PQS by *P. aeruginosa* PA14 strain (Ji et al., 2016). In addition

to intermediate-mimic compounds, other PqsA inhibitors are substrate structural analogs. *P. aeruginosa* PAO1 strain challenged with the anthranilate analog methyl-anthranilate reduced in a dose-dependent fashion PQS production as well as elastase activity. Elastase is a virulence factor that is under the control of the *pqs* QS system (Calfee et al., 2001). However, in other study, the effect of methyl-anthranilate in reducing *P. aeruginosa* PA14-produced PQS and HHQ levels was less potent, and the most powerful compounds were halogenated anthranilate analogs. In addition, some of these halogenated analogs showed effectivity *in vivo* in reducing the virulence and limiting *P. aeruginosa* systemic dissemination in infected mice (Lesic et al., 2007). In addition to PqsA, another enzyme linked to the PQS biosynthesis pathway that has been targeted is PqsD. This enzyme catalyzes the formation of the 2-aminobenzoyl-CoA by the condensation of anthraniloyl-CoA with malonyl-CoA via a tetrahedral transition state. The treatment of *P. aeruginosa* PA14 with the potent PqsD inhibitor (2-nitrophenyl) phenyl methanol disturbed the production of HHQ and PQS as well as reducing the biofilm volume (Storz et al., 2012). Moreover, some catechol-derivative compounds that act as PqsD inhibitors by blocking the access of the natural substrate to the active site of PqsD reduced the production of HHQ by *P. aeruginosa* (Allegretta et al., 2015).

Furthermore, the enzyme PqsBC, which catalyzes the condensation of octanoyl-CoA and 2-aminobenzoylacetate rendering HHQ is also a QS inhibitor target. In this regard, it was observed that the PqsBC competitive inhibitor 2-aminoacetophenone (2-AA) affected HHQ production by the recombinant *P. putida* KT2440 strain (Drees et al., 2016). However, strategies focused on PqsBC inhibition could carry unwanted effects. The PqsBC substrate 2-aminobenzoylacetate could transform in 2-AA or 2,4-dihydroxyquinoline (DHQ) (Dulcey et al., 2013). The 2-AA promoted the emergence of persister cells in pathogens as *P. aeruginosa*, *A. baumannii* and *Burkholderia thailandensis*, whereas DHQ has been linked to *P. aeruginosa* pathogenicity (Que et al., 2013; Gruber et al., 2016). In principle, the inhibition PqsBC could provoke the accumulation of 2-aminobenzoylacetate, favoring the formation of 2-AA and DHQ, which could promote the emergence of antibiotic tolerant pathogens and/or increase in the pathogenicity (Allegretta et al., 2017; Maura et al., 2017). In this regard, it has been demonstrated that the treatment of a *P. aeruginosa* *mvfR* mutant (constitutively expressed the *pqs ABCDE* operon) with some benzamide-benzimidazole compounds (PqsBC inhibitors) may provoked the accumulation of 2-AA and DHQ (Maura et al., 2017). In addition, in the *P. aeruginosa* PA14 parental strain, the treatment with some of these PqsBC inhibitors (specifically those also contain a low anti-MvfR (PqsR) activity) did affect only partially the production of 2-AA and DHQ and did not inhibit the tolerance to meropenem (Maura et al., 2017). In another study performed by Allegretta et al. (2017), the treatment of *P. aeruginosa* PA14 and a PA 14 *pqsH* mutant with PqsBC inhibitors, produced an increase at 2-AA and DHQ levels. One of these PqsBC inhibitors increased the subpopulation of persister *P. aeruginosa* PA14 cells to levels similar to a *pqsBC* mutant strain

(Allegretta et al., 2017). Interestingly, in this study it was observed that treatment with PqsBC inhibitors increased the 4-hydroxy-2-heptylquinoline-N-oxide (HQNO) levels. This molecular specie has been also linked to the emergence of antibiotic tolerance in *P. aeruginosa* (Hazan et al., 2016; Allegretta et al., 2017). HQNO appears to boost bacterial autolysis with the subsequent DNA release, which facilitates biofilm formation making the pathogen more tolerant to antibiotics (Hazan et al., 2016). Moreover, the HQNO produced by *P. aeruginosa* also influence the *S. aureus* susceptibility to antibiotics (Orazi and O'Toole, 2017; Radlinski et al., 2017). In another study, it was shown that *P. aeruginosa* $\Delta pqsB$ and $\Delta pqsC$ mutants that only produce DHQ, were more virulent in *C. elegans* than a quinolone-null mutant $\Delta pqsAB$. An increased colonization capacity of *C. elegans* was observed for the $\Delta pqsB$ mutant in comparison with the $\Delta pqsAB$ mutant (Gruber et al., 2016).

Additional support for the feasibility of using QS signal biosynthesis inhibitors *in vivo* was demonstrated by the use of ambuic acid as an anti-virulence compound in a murine model of intradermal MRSA challenge. The treatment with ambuic acid impaired the virulence exerted by *S. aureus* in the infected animals, as it attenuated skin ulcer formation and the signs of infection-induced morbidity. The anti-virulence effect of ambuic acid was mediated by inhibition of the *agr* quorum sensing system (Todd et al., 2017).

Inactivation of Quorum-Sensing Signal

Among the quorum quenching strategies one of the most exploited is the inactivation of QS signals (LaSarre and Federle, 2013). This is a strategy that exists in the natural interactions between microbial populations, and it has been extrapolated as an approach to modulating the virulence of bacterial pathogens. This virulence modulation through interference with QS signal is centered mainly on the use of QS signal-degrading enzymes (LaSarre and Federle, 2013; Fetzner, 2015). The advantage of this strategy is that it targets the QS signal after it is secreted to extracellular medium. Therefore, there is greater access to the target and challenges associated with penetrating bacterial cells are avoided. Moreover, as an extracellular factor is targeted, the emergence and spread of resistance could be less probable, but potential resistance mechanisms have been envisioned (Defoirdt et al., 2010; Fetzner, 2015; Vale et al., 2016).

The most thoroughly characterized quorum quenching enzymes are acyl-homoserine lactone (acyl-HSL) lactonases, acyl-HSL acylases, and acyl-HSL oxidoreductases, which target the QS signal acyl-homoserine lactones (acyl-HSLs) (Fetzner, 2015). The acyl-HSL lactonases and acyl-HSL acylases destroy acyl-HSL molecules via homoserine lactone ring hydrolysis (specifically the ester bond) or amide bond hydrolysis between the acyl tail and the homoserine lactone ring, respectively. Otherwise, the acyl-HSL oxidoreductases modify acyl-HSLs molecules chemically via oxidation or reduction of the acyl chain instead of degrading them (LaSarre and Federle, 2013; Fetzner, 2015). Other types of quorum quenching enzymes that have been characterized include *E. coli* LsrK kinase that targets the AI-2, and dioxygenases Hod from *Arthrobacter* sp. Rue61a, Aqdc1 and Aqdc2 from

Mycobacterium abscessus subsp. *abscessus* and *Rhodococcus erythropolis* BG43 that target alkylquinolone-type molecules (Pustelny et al., 2009; Roy et al., 2010; Müller et al., 2015; Birmes et al., 2017). LsrK catalyzes the phosphorylation of AI-2 molecules, rendering phospho-AI-2, whereas dioxygenases mediate a dioxygenolytic cleavage of PQS, rendering N-octanoylanthranilic acid and carbon monoxide (Pustelny et al., 2009; Roy et al., 2010).

The potential for using quorum quenching enzymes in clinical infection treatment is supported by several studies. Recently, Utari et al. (2018) used mouse models of pulmonary *P. aeruginosa* infection and showed the efficacy of intranasally administered PvdQ acylase in hindering *P. aeruginosa* virulence. In a lethal infection model, PvdQ-treated animals presented a 5-fold lower bacterial load than non-treated animals, as well as a longer survival time. Moreover, PvdQ-treated mice showed lower lung inflammation, CXCL2 and TNF- α levels than non-treated animals in a sub-lethal infection model. It is noteworthy that intranasally supplied PvdQ acylase was shown to be safe as it was well tolerated by animals (Utari et al., 2018). Previously, using a *Caenorhabditis elegans* infection model, the potential of PvdQ acylase as an anti-virulence agent had been shown (Papaioannou et al., 2009). Penicillin V acylases PaPVA and AtPVA from the Gram-negative bacteria *Pectobacterium atrosepticum* and *Agrobacterium tumefaciens* also exerted quorum quenching activity on *P. aeruginosa*. The supplementation of these two acylases to *P. aeruginosa* PAO1 provoked a reduction in 3-oxo-C₁₂-HSL levels, elastase activity, pyocyanin and biofilm production. In addition, the survival rates of *G. mellonella* infected with *P. aeruginosa* PAO1 pre-treated with acylases were higher than *G. mellonella* larvae infected with *P. aeruginosa* PAO1 without acylases pre-treatment (Sunder et al., 2017).

Another quorum quenching enzyme that has been tested *in vivo* is the engineered lactonase SsoPox-W263I. Using an acute lethal model of *P. aeruginosa* pneumonia in rats, Hraiech et al. (2014) demonstrated that intra-tracheally delivered SsoPox-W263I immediately after infection with *P. aeruginosa* PAO1 significantly reduced the mortality rate and the lung damage. SsoPox-W263I was well tolerated by rats (Hraiech et al., 2014). Recently, SsoPox-W263I showed anti-virulence activity against clinical *P. aeruginosa* isolates. Interestingly, SsoPox-W263I immobilization did not affect the anti-virulence activity against *P. aeruginosa* PAO1 (Guendouze et al., 2017). Moreover, AiiM lactonase attenuated *P. aeruginosa* PAO1 virulence in an acute pneumonia murine model. Mice infected via intratracheal with an AiiM-expressing *P. aeruginosa* PAO1 strain showed less lung injury, lower pro-inflammatory cytokines levels, and lower mortality than animals infected with an AiiM-nonexpressing *P. aeruginosa* PAO1 strain. In addition, in AiiM-expressing *P. aeruginosa* PAO1 infected mice there was a reduced systemic dissemination of the infection in comparison with the AiiM-nonexpressing *P. aeruginosa* PAO1 infected ones (Migiyama et al., 2013). Based on a *C. elegans* infection model it was demonstrated that lactonase MomL from *Muricauda olearia* increased the survival of *P. aeruginosa* PAO1-infected nematodes without showing toxic effects. However, a protective

effect was not observed in *A. baumannii*-infected nematodes (Tang et al., 2015; Zhang et al., 2017b).

Furthermore, recently discovered quorum-quenching enzymes show potential as anti-virulence agents. Lactonases AaL isolated from *Alicyclobacillus acidoterrestris*, AiiK from *Kurtzia huakui* LAM0618^T and Aii810 from Mao-tofu metagenome, inhibited virulence factors production and biofilm formation by *A. baumannii* and *P. aeruginosa* PAO1 without affecting bacterial growth (Fan et al., 2017; Bergonzi et al., 2018; Dong et al., 2018). Another newly described quorum-quenching enzyme is AidA, which was identified in *A. baumannii* clinical isolates (López et al., 2017).

In addition to quorum-quenching enzymes, QS signal inactivation is also reached by the action of anti-QS signal antibodies and synthetic polymers that sequester it (Piletska et al., 2010; LaSarre and Federle, 2013). The use of antibodies with therapeutic aims offers desirable effects, such as high specificity to the target coupled with low off-target cytotoxicity (Palliyil et al., 2014). However, developing anti-QS signal antibodies is a challenging task, because these signals are small size molecules and generally not structurally complex, making them poor antigens (Palliyil et al., 2014). Despite this, several studies support the potential of antibodies in disturbing quorum-sensing networks. Recently, centered on the *agr* type I quorum-sensing system of *S. aureus*, a virus-like particle (VLP)-based *agr* type I vaccine was developed using a *P. aeruginosa* RNA bacteriophage PP7 coat protein inserted with a *S. aureus* sequence-modified autoinducer peptide-1 (AIP1S, cysteine was substituted by serine, YSTSDIFIM). In this vaccinal candidate (PP7-AIP1S) the AIP1S peptide was exposed on the surface of the VLP, and immunized mice with PP7-AIP1S developed antibodies that specifically recognized the original *S. aureus* AIP1 *in vitro*. In addition, using a murine model of *S. aureus* SSTI (skin and soft tissue infection), it was observed that after a challenge with a virulent *S. aureus* USA300 isolate LAC (*agr*-type I), in PP7-AIP1S immunized mice reduced *agr*-type I-mediated pathogenesis was developed, compared to the non-immunized animals. Reduced alpha-hemolysin levels, as well as RNAPIII transcription at the infection site in the immunized animals, together with the *in vitro* antibodies binding (from immunized animals) to AIP1 suggested the occurrence of immune suppression of *agr*-signaling during the infection (Daly et al., 2017). Using a peptide library displayed on VLP, O'Rourke et al. (2014) identified eight peptides (VLP-peptides) that bind specifically to the antigen-binding site of the monoclonal antibody AP4-24H11. This monoclonal antibody specifically bound and neutralized the autoinducer peptide-4 (AIP4) from *S. aureus* and protected animals from *S. aureus* pathogenicity, as was shown previously by Park et al. (2007). From the eight AP4-24H11-bonding VLP-peptides, two of them, when administered alone, apparently induced a protective response (reduced abscess and dermonecrosis) against *S. aureus* *agr*-type IV isolate AH1872 infection in immunized mice. Additionally, the immunization of mice with a combination of these two VLP-peptides protected those from *S. aureus* AH1872 infection via inhibition of *agr*-signaling (O'Rourke et al., 2014). Furthermore, it was observed that sheep-mouse chimeric monoclonal antibodies with affinity in the

nanomolar range against HSL molecules protected *C. elegans* nematodes and mice infected with *P. aeruginosa* PA058. In infected mice, this protection appears to be associated with the antibody-mediated scavenging of HSL molecules and not by effects on the bacterial load (Palliyil et al., 2014). Moreover, immunized mice with 3-oxo- dodecanoyl homoserine lactone conjugated to BSA (3-oxo-c12-HSL-BSA) developed specific antibodies against the HSL and intermediate protection was observed after intranasal infection with *P. aeruginosa* PAO1. Interestingly, the lung bacterial burden was not affected in the immunized mice, and the levels of TNF- α (lung) and 3-oxo-c12-HSL (lung and serum) were lower than in non-immunized animals (Miyairi et al., 2006).

In addition to interference with QS signaling, monoclonal antibodies against QS signal molecules also protect from cytotoxic effects exerted by these molecules on host cells. Kaufmann et al. (2008) observed *in vitro* that the monoclonal antibody RS2-1G9 protected murine bone marrow-derived macrophages in a concentration-dependent fashion from the cytotoxicity associated with 3-oxo-C12-HSL (Kaufmann et al., 2008). Previously, it was demonstrated that serum from immunized animals with 3-oxo-C12-HSL-BSA inhibited the autoinducer-dependent apoptosis of the macrophage cell line P388D1 (Miyairi et al., 2006).

Synthetic polymers constitute another alternative for interference with QS signal. These polymers bind and sequester the QS signal without affecting bacterial growth; therefore, they should not exert selective pressure. A pioneering work by Piletska et al. (2010) demonstrated that signal-sequestering polymers interfered with the *Vibrio fischeri* QS network-based on 3-oxo-C6-HSL. The sequestering of 3-oxo-C6-HSL by the polymers impaired the bioluminescence production as well as biofilm formation (Piletska et al., 2010). In a subsequent work by this group, it was showed that an itaconic acid (IA)-based-molecular imprinted polymer (MIP) impaired *P. aeruginosa* biofilm formation by sequestering the 3-oxo-C12-HSL QS signal (Piletska et al., 2011). Moreover, linear polymers (IA-based polymers and methacrylic acid-based polymers) reduced *V. fischeri* bioluminescence and *Aeromonas hydrophila* biofilm production through lactones sequestering. The IA-based polymers were more effective than methacrylic acid-based polymers regarding the quorum-quenching activity. Importantly, the polymers did not show cytotoxic effects on mammalian cells and did not affect bacterial growth (Cavaleiro et al., 2015). Recently, it was observed that 2-hydroxyethyl methacrylate (HEMA)-based MIPs suppressed the biofilm formation by *P. aeruginosa*; however, IA-based MIPs were not effective in the biofilm attenuation (Ma et al., 2018).

Interference With Quorum Sensing Signal Detection

Interference with signal detection is another of the most exploited strategies for disrupting QS systems. Some of these QS signal detection inhibitors are signal structural analogs that compete with the signal molecule by binding at the ligand-binding site in the receptor (Stevens et al., 2010). Moreover,

other inhibitors could act in a non-competitive fashion (e.g., halogenate furanones, isothiocyanate-based covalent inhibitors, and flavonoids) (Koch et al., 2005; Amara et al., 2016; Paczkowski et al., 2017). The inhibitors binding to the receptors directly affect the signaling cascade by different pathways, including block signal binding, structural destabilization of the receptor, impaired receptor dimerization, impaired DNA binding, or impaired interaction with RNA polymerase (Stevens et al., 2010; Paczkowski et al., 2017; Suneby et al., 2017). Moreover, it has been shown that agonists of the QS signal can also exert inhibitory activity on QS systems. Some QS circuits are arranged in hierarchically cross-regulated networks, e.g., in *P. aeruginosa* the *las*-QS system positively regulates *rhl*- and *pqs*-QS systems, in addition the activated *pqs*-QS system also positively regulates the *rhl*-QS system, whereas this exerts negative regulation on the *pqs*-QS system (Lee and Zhang, 2015). Therefore, by modulating the activity of one QS system, it is possible to influence the activity of the other QS systems. In this respect, Welsh et al. (2015) observed that some agonists of RhlR attenuated the expression of virulence factors controlled by the *pqs*-QS system in *P. aeruginosa*. Disruption of cross-regulation of *rhl*-*pqs* systems was proposed as a novel mechanism of QS inhibition (Welsh et al., 2015).

The use of small molecules to disturb QS signal detection has to face several challenges. In this respect, structural stability of the inhibitors is a very important issue; some structural analogs of HSLs and AIPs are prone to hydrolysis, depending on the characteristics of the media (Glansdorp et al., 2004; Vasquez et al., 2017). In addition, inhibitors could be potentially degraded by enzymes as well as targeted by efflux pumps (Maeda et al., 2012; Grandclément et al., 2015). Moreover, the inhibitory effect observed could be strain-dependent, and it is therefore important to include several strains in the studies (García-Contreras et al., 2015). Despite the challenges, the feasibility of QS signal detection inhibition as a quorum-quenching strategy is supported by several *in vivo* studies.

Meta-bromo-thiolactone (mBTL) is a partial agonist/ partial antagonist of both RhlR and LasR receptors in the HSL-guided QS systems of *P. aeruginosa*, and RhlR inhibition is its main mechanism of action *in vivo*. This compound potently inhibited *P. aeruginosa* PA14 pyocyanin and biofilm production without affecting bacterial growth. In addition, the treatment of *P. aeruginosa* PA14 with mBTL down-regulated the expression of several LasR- and RhlR-controlled virulence factor genes. The treatment of wild-type and *P. aeruginosa* PA14 *lasR* mutant strains with mBTL reduced the pathogenesis exerted by these strains in *C. elegans* and human lung carcinoma cell line A549 (O'Loughlin et al., 2013). Another inhibitor of *P. aeruginosa* HSL-based QS systems that has been tested *in vivo* is the fungal metabolite terrein. The treatment of *P. aeruginosa* PAO1 with terrein provoked a reduction in a dose-dependent manner in the production of virulence factors elastase, pyocyanin, and rhamnolipid as well as in biofilm formation without affecting bacterial growth. In addition, terrein showed to be more stable than the QS inhibitor furanone C-30 and enhanced the anti-biofilm activity of ciprofloxacin when used in combination. Importantly, terrein mediated protection of *C. elegans* and

mice against *P. aeruginosa* PAO1 infection in a fast killing infection assay and murine airway infection model, respectively. Interestingly, it was observed that the QS system and c-di-GMP signaling pathway could be interconnected, and that terrein could act as a dual inhibitor of these systems (Kim et al., 2018). Moreover, HSL analogs that act as covalent inhibitors of LasR receptor were seen to be promising *in vivo* tests. Specifically, the isothiocyanate- and fluoroisothiocyanate-based covalent inhibitors (ITC-12 and ITC-F, respectively) attenuated the virulence of *P. aeruginosa* PAO1-UW and consequently increased the survival of *C. elegans* worms during an infection assay with this pathogen. The ITC-F treated group showed a significant survival rate in comparison with the control group. Moreover, using an *ex-vivo* human skin burn wound model it was observed that ITC-F and ITC-12 treatment impaired the establishment of infection by *P. aeruginosa* PA14 (Amara et al., 2016). In addition to HSL-based QS systems in *P. aeruginosa*, the PQS-based QS system is also involved in the regulation of virulence factor production. In this regard, maybe inhibitors that could affect these two QS system types would be desirable. Among them, 3-Phenyllactic acid (PLA) is an organic compound produced by *Lactobacillus* spp that acts as a QS sensing inhibitor that potentially could bind to RhlR and PqsR receptors with high affinity (Chatterjee et al., 2017). Recently, Chatterjee et al. (2017) showed that PLA impaired the attachment of *P. aeruginosa* PAO1 on a catheter tube, using a Medaka fish intraperitoneal catheter-associated infection models (Chatterjee et al., 2017).

Furthermore, *agr*-QS system inhibition has been shown to be an achievable strategy for controlling the virulence of pathogens like *S. aureus*. In this regard, atopic dermatitis is a chronic inflammatory skin disease where *S. aureus* triggers an immunopathology response through mast cell degranulation. This mast cell degranulation could be induced by the bacterial δ -toxin, which is encoded by the *hld* gene that is under control of the *agr*-QS system (Baldry et al., 2018; Geoghegan et al., 2018). Recently, the effectiveness of the *agr*-QS inhibitor solonamide B in suppressing the *S. aureus* δ -toxin-induced-inflammatory response was tested using a modified epicutaneous colonization mouse model. Animals infected with *S. aureus* and treated with solonamide B showed a reduced skin inflammatory cell infiltrate, less skin damage, reduced RNAPIII expression and production of pro-inflammatory cytokines in comparison to non-treated animals, suggesting that *agr*-QS inhibitors could effectively attenuate *S. aureus* pathogenesis *in vivo* (Baldry et al., 2018).

Innovative Quorum Quenching Strategies

In addition to the use of quorum quenching enzymes and quorum sensing inhibitors, some innovative therapeutic strategies to interfere with quorum sensing networks are being developed. One of the challenges in disrupting quorum sensing networks is the fact that a pathogen may possess several QS systems of the same class, for example *P. aeruginosa* contains the AHL-based systems LasRI and RhlRI (Lee and Zhang, 2015). Therefore, acquiring complete inhibition of the QS systems using quorum-quenching enzymes or quorum-quenching inhibitors in a monotherapy-based scheme could be difficult (Fong et al., 2018). Based on this challenge, Fong et al. (2018) tested the

capacity of a combinatory therapy using the quorum-quenching enzyme AiiA and the quorum-sensing inhibitor G1 (LuxR-type receptor inhibitor) to suppress the QS systems in *P. aeruginosa*. It was observed that combinatory therapy inhibited the expression of *lasB-gfp*, *pqsA-gfp*, and *rhlA-gfp* in *P. aeruginosa* PAO1 bioreporter strains more potently than single treatments. The *rhlA* gene is involved in the biosynthesis of rhamnolipid and is under RhlR-transcriptional regulation. In accordance with this, the inhibitory effect on rhamnolipid biosynthesis was verified in a *P. aeruginosa* PAO1 strain. The level of synthesized rhamnolipid in the combinatory therapy-treated bacteria was nearly to the rhamnolipid level in a $\Delta lasI \Delta rhlI$ mutant strain (Fong et al., 2018). All this evidence suggests that using combinatory therapy with different types of quorum-quenching agents it is possible to disturb diverse quorum-sensing systems existing in pathogens.

In the combinatory therapy described above, a multi-target effect is achieved by joining two therapeutic agents that target different components in the QS networks. However, it is possible to get the same multi-target effect using a single compound (Thomann et al., 2016; Maura et al., 2017). Recently a drug with dual inhibitory activity toward the PqsR and PqsD components of the *P. aeruginosa* *pqs* QS system was developed. This dual inhibitor [2-(methylsulfonyl)-4-(1H-tetrazol-1-yl)pyrimidine] was developed from a common molecular scaffold existing in single PqsR- antagonist and PqsD-inhibitor. *In vitro* analysis showed that the dual inhibitor disturbed the production of the virulence factors pyocyanin and pyoverdine as well as the biofilm production by *P. aeruginosa* PA14. In addition, the dual inhibitory compound increased the survival rate of *G. mellonella* larvae infected with *P. aeruginosa* PA14 (Thomann et al., 2016). Moreover, Maura et al. (2017) observed that some benzamide-benzimidazole-based compounds also act as dual inhibitors of the *pqs*-QS system in *P. aeruginosa*. These dual inhibitory compounds targeted the proteins PqsR (MvfR) and PqsBC and could be grouped depending on their inhibition patterns in: PqsR-PqsBC dual inhibitors with high anti-PqsR and high anti-PqsBC activity or PqsR-PqsBC dual inhibitors with low anti-PqsR activity and high anti-PqsBC activity. The treatment with some of these dual inhibitors increased the survival rate of human lung epithelial cells and RAW264.7 macrophages when infected with *P. aeruginosa* PA14 (Maura et al., 2017). Among the dual inhibitors, those exert a high anti-PqsR activity constitute an attractive therapeutic option because interfere with the production of 2-AA and consequently limit the emergence of antibiotic-tolerant bacteria as was previously discussed.

Recently it has been demonstrated that it is possible to manipulate the AI-2 levels through “controller cells” (Quan et al., 2017). These “controller cells” are based on a subset of “consumer cells” and another of “supplier cells.” The “consumer cells” were engineered to overexpress genes involved in the uptake and processing of AI-2 in *E. coli* (e.g., *lsrACDBK* and *lsrACDBFGK*) while the “supplier cells” in genes involved in the biosynthesis of AI-2 (*luxS* and *mtn*). Because these “controller cells” influence the environmental AI-2 levels they will have a direct impact on biofilm formation. In line with this, it was observed that “consumer cells” decreased biofilm

formation by *E. coli* reporter strain, whereas “supplier cells” enhanced biofilm formation (Quan et al., 2017). This suggests a route toward future therapeutic strategies based on engineered cells that act as “controller cells.” In addition, it is possible to modulate microbial behavior through AI-2 levels via a synthetic mammalian cell-based microbial-control device, as was demonstrated by Sedlmayer et al. (2018). This microbial-control device consisted of engineered mammalian cells with a formyl peptide sensor module coupled to AI-2 production and release module. Essentially, the engineered mammalian cells detect formyl peptides released by pathogens (peptides produced by a broad range of bacterial species) and trigger the production and release of AI-2. It was showed that biofilm formation by *Candida albicans* was reduced when this pathogen was co-cultured with microbial-control-engineered cells. This system appears to be a promising anti-virulence strategy, as ubiquitous pathogen signals are detected with high sensitivity (nM range), and robust production of the autoinducer takes place (without being toxic for the host) influencing bacterial communication without exerting selective pressure. In addition, the fact that autoinducer production is coupled to signal detection allows a synchronized response in accordance with the infection dynamic (Sedlmayer et al., 2018). Moreover, it possible to engineer bacteria that will sense the presence of pathogenic bacteria via the quorum sensing system and, once detected, will release anti-pathogens agents. Hwang et al. (2017) engineered a probiotic *E. coli* Nissle 1917 strain for sense 3-oxo-C12 HSL from *P. aeruginosa* and respond by autolysing itself via lysin E7 with the consequent release of the bacteriocin pyocin S5 and the anti-biofilm enzyme DspB, which exerted an anti-*P. aeruginosa* activity. The feasibility of this approach was demonstrated *in vivo* using *C. elegans* and murine infection models, where the engineered strain showed prophylactic and therapeutic effects (Hwang et al., 2017).

Although the strategy of interference with autoinducer biosynthesis has been based on the discovery and design of small molecules that inhibit the enzymatic activity, it has been envisioned that engineered bacterial strains could be an alternative. Recently, it was showed that it is possible to disrupt biofilm production in clinical isolates through the manipulation of the expression levels of the enzyme LuxS. Specifically, using the Clustered Regularly Interspaced Short Palindromic Repeats-Cas 9 interference (CRISPRi) system, the expression of LuxS enzyme was suppressed in clinical *E. coli* isolates. It was suggested that CRISPRi edited cells could be an alternative strategy for controlling biofilm production in nosocomial settings through CRISPRi system delivery via nucleic acid conjugation (Zuberi et al., 2017). However, delivery of CRISPRi system in nosocomial setting via nucleic acid conjugation could be a very challenging task. Given the fact that nucleic acid conjugation could occur between different bacterial species (Musovic et al., 2006; Goren et al., 2010; Crémet et al., 2012; Van Meervenne et al., 2012); could be possible the transfer of the CRISPRi system from the edited cells to co-existing bacteria other than target bacteria. In this regard, maybe the utilization of narrow host range plasmids as vectors for CRISPRi delivery could limit such potential off-target effect. In addition, the nucleic acid conjugation effectivity in established biofilms could be compromised (Merkey et al.,

2011; Stalder and Top, 2016). This could limit the use of CRISPRi edited cells for the treatment of formed biofilms. In this sense, maybe the utilization of engineered phages as vehicles for CRISPRi system delivery could be an attractive alternative. Phages have shown to be a CRISPR delivery system with specificity to pathogenic bacteria as well as with capacity to removing established biofilms (Lu and Collins, 2007; Bikard et al., 2014; Citorik et al., 2014; Alves et al., 2016; Fong et al., 2017).

PREVENTING BIOFILM FORMATION AND AFFECTING THE BIOFILM STRUCTURE WITHOUT KILLING BACTERIA

Bacteria can live in a community called biofilm, a structure that can be formed by extracellular polymeric substances, such as DNA, protein, and polysaccharides (Flemming et al., 2016). After forming biofilms, bacteria can disperse and colonize other environments (Fleming and Rumbaugh, 2017). This lifestyle can protect bacteria against potential environmental stress, such as antibiotics and host defense components (Hall and Mah, 2017; Tseng et al., 2018). In the clinical situation, biofilm formed by pathogenic bacteria can establish themselves on human surfaces or medical devices, including implants, catheter, endotracheal tubes and others (Rieger et al., 2016; Konstantinović et al., 2017; Kenaley et al., 2018; Silva et al., 2018). Biofilm formation on these surfaces can serve as a source of infection. The successful establishment of pathogenic biofilm on human surfaces can cause chronic infections and limit the success of antibiotic therapy (Rytke et al., 2015; Li et al., 2017). In general, combating biofilms may require high antibiotic doses and a combination of strategies (Ribeiro et al., 2016). Unfortunately, many of the marketed antibiotics fail to affect biofilm, especially if they are formed by resistant bacteria. To overcome this problem, researchers have prospected compounds from the natural world (from animals, plants, fungi, viruses, and even bacteria) or synthetics (synthesized through the chemical process and/or screened from chemical libraries) (Rajput et al., 2017). In both situations, anti-biofilm agents can be represented by a variety of organic and inorganic chemical compounds (Rajput et al., 2017).

Anti-virulence compounds against biofilms could be used to limit bacterial adhesion on surfaces (Liu et al., 2018; Ranfaing et al., 2018) to affect the production of an extracellular matrix (Feng et al., 2018) and to disturb the existing biofilm (Puga et al., 2018; Table 1). Some examples of anti-virulence compounds cited here work against non-pathogenic bacteria to humans and animals. However, the approaches using these bacteria may serve as proof of principle to study anti-virulence compounds against biofilms in a general way.

In the prevention scenario, one possibility consists of interfering with structures associated with the successful establishment of biofilms such as flagella (that favor the bacterial motility and interaction with surfaces) and fimbriae (with structures that facilitate bacterial adhesion). Higrocin C (a compound isolated from marine-derived *Streptomyces* sp. SCSGAA 0027) for example, suppressed swimming motility of *Bacillus amyloliquefaciens* SCSGAB0082, which could explain the

biofilm inhibition (Wang et al., 2018a). Transcriptome studies showed downregulation (more than twofold) of genes associated with bacterial chemotaxis and flagellar motor (Wang et al., 2018a). Coumarin, for example, presents the ability to prevent bacteria biofilm without affecting bacterial growth (Lee et al., 2014). This compound repressed curli genes and motility genes in *E. coli* O157:H7 and reduced fimbriae production, swarming motility, and biofilm formation (Lee et al., 2014).

Another way to prevent biofilm formation consists of affecting the extracellular matrix production. A chemical compound named TCC (3, 3', 4', 5-tetrachlorosalicylanilide) for example, inhibited *B. subtilis* biofilm formation by reducing extracellular matrix production. This was associated with the repression of SinR protein negative regulated genes (involved in extracellular matrix production) (Feng et al., 2018). Other studies have shown that compounds that prevent biofilm formation can potentially affect bacterial cell communication by degrading quorum-sensing molecules (Ivanova et al., 2015; Passos da Silva et al., 2017).

In the context of combating existing biofilms, compounds can be used to destroy components of extracellular matrix, such as DNA, proteins and carbohydrates (Puga et al., 2018). In this context, enzymes have been used as potential agents to disrupt mono and polymicrobial biofilm (Puga et al., 2018). DNase I, for example, presents the ability to degrade extracellular DNA of *Campylobacter jejuni*, promoting biofilm removal without affecting bacterial viability (Brown et al., 2015).

The understanding of mechanisms involved in the formation of bacterial biofilm, as well as the understanding of their cells and biofilm structures, could indicate possible targets to develop compounds that affect biofilm without killing bacteria. In addition to potential anti-biofilm therapy, agents that can prevent or disperse biofilm could potentially combine with anti-virulence compounds. For example, anti-virulence agents could be used to neutralize endotoxins from bacterial cells that disperse from biofilms and thus prevent or minimize the harmful effects of the host inflammatory response against bacterial infection.

BACTERIAL TOXIN NEUTRALIZATION

It is known that pathogenic bacteria may produce diverse virulence determinants in order to successfully survive host system responses, as well as colonizing a host (Kong et al., 2016). Among them, toxins comprise proteins expressed by bacteria during post-exponential and early stationary phases that have been divided into different classes, including hemolysin (Powers et al., 2015), leukotoxin (Zivkovic et al., 2011), exfoliative toxins (Bukowski et al., 2010), endotoxin (Heinbockel et al., 2018), among others. These protein-based toxins are intrinsically related to physical damage, biochemical degradation and signaling interruption in the host cells, resulting in immune system evasion and characterizing pathogen-to-host interactions (Wei et al., 2017). Bacterial toxin neutralization, for instance, has been shown to compromise bacterial proliferation and survival in the host (Ortines et al., 2018). More importantly, unlike antibiotic-based treatments, anti-toxin or anti-virulence

therapies do not affect bacterial viability directly and, as a consequence, could impose reduced selective pressure, probably decreasing the frequency of resistance events (Rasko and Sperandio, 2010). In addition, anti-virulence compounds are also known to preserve the host's endogenous microbiome as they target virulent factors secreted exclusively by pathogenic bacteria (Clatworthy et al., 2007). In this context, here we described compounds, including antibodies, nanoparticles, small molecules, and bioactive peptides (**Figure 1** and **Table 1**), which have been studied recently as promising candidates for anti-virulence therapies that aim to treat and prevent bacterial infections.

The α -toxin (AT), also known as α -hemolysin, is a key virulence factor expressed by *S. aureus* that has been investigated in different animal infection models, including bacteremia, pneumonia and skin/soft tissue infections (Surewaard et al., 2018). This toxin is capable of lysing red blood cells, and also targets monocytes, macrophages and neutrophils (Bubeck Wardenburg et al., 2007). Moreover, in the clinic, AT levels in patients are often correlated with disease severity (Jenkins et al., 2015). Studies have shown that rabbits with acute bacterial skin and skin structure infections (ABSSSI) caused by AT-expressing methicillin-resistant *S. aureus* (MRSA) develop severe infections similar to those observed in humans, including the presence of large dermonecrotic lesions. In contrast, rabbits infected with a mutant deficient AT strain developed only small dermonecrotic lesions (Le et al., 2016). One major anti-virulence strategy to neutralize AT consists of using antibodies. The study cited above also reported a significant decrease in the disease severity thought AT neutralization by treating the rabbits with an anti-AT human monoclonal antibody (mAb) (MEDI4893*) (Le et al., 2016). Similarly, Ortines et al. (2018) observed in non-diabetic and diabetic mice that *S. aureus*-infected animals passively immunized with anti-AT mAb (MEDI4893*) showed decreased wound size and bacterial counts when compared to the untreated controls. Moreover, those authors also showed the differential host immune response effects, revealing different patterns of macrophage, monocyte and neutrophil infiltrates, as well as neutrophil extracellular traps (NETs) in non-diabetic and diabetic mice (Ortines et al., 2018).

In addition to skin infections, *S. aureus* strains are often associated with respiratory mono-infections and co-infections with Gram-negative strains, including *P. aeruginosa* and *Klebsiella pneumoniae*. In a study by Cohen et al. (2016), it was shown that *S. aureus* AT, in a mixed pathogen-lung infection model, could potentiate Gram-negative bacterial dissemination and lethality. This situation, however, could be circumvented by the passive immunization of mice with an anti-AT mAb, leading to *S. aureus* and co-pathogens (Gram-negative bacteria) clearance in the lungs (Cohen et al., 2016). Additionally to mAb, the intravenous immunoglobulin (IVIG), which consists of a polyclonal human antibody pool, has been investigated regarding its protective effects against necrotizing pneumonia caused by different epidemic community-associated and hospital-associated MRSA strains (Diep et al., 2016). As reported by Diep et al. (2016), two IVIG antibodies specific to an AT (α -hemolysin, HTa) and a Panton-Valentine leukocidin

(PVL) conferred protection on immunized rabbits against MRSA, leading to improved survival outcomes (Diep et al., 2016).

In the clinic, patients affected by bacteremia, including *S. aureus*, may present occlusion of small blood vessels by the formation of large platelet aggregates (van der Poll and Opal, 2008). In a recent study, it was reported that AT induces rapid platelet aggregation and liver injury, causing multi-organ dysfunction during *S. aureus* sepsis (Surewaard et al., 2018). Interestingly, however, all these damaging effects could be prevented in mice treated with the anti-AT mAb (MEDI4893*) (Surewaard et al., 2018), thus reinforcing the importance of monoclonal antibodies as bacterial toxin neutralizing agents in anti-virulence therapies. More recently, Wang et al. (2018b), reported a novel vaccine platform based on extracellular vesicles (EVs) from *S. aureus*. In that work, the authors purified EVs from a genetically engineered *S. aureus* capable of overexpressing detoxified cytolysins (HlaH35L and LuKE), which were non-toxic, immunogenic and protected mice from lethal sepsis caused by *S. aureus* (Wang et al., 2018b). Also in the field of *S. aureus* toxin neutralization, the monoclonal antibody, ASN100 (Arsanis Inc.), which consists of the combination of two human IgG1k monoclonal antibodies, ASN1 and ASN2, has shown promising results in the neutralization of six *S. aureus* toxins (Rouha et al., 2015; Badarau et al., 2016). Despite the advances in the usage ASN100 in the clinic, the company Arsanis Inc. has discontinued a phase II clinical trial for ASN100 as it failed to prove its effectiveness in high-risk, mechanically ventilated patients with *S. aureus* pneumonia.

Antibodies have also been applied as anti-virulent therapies involving *Clostridium difficile*, which represents a primary cause of nosocomial antibiotic-related diarrhea. This bacterium produces two main virulence factors, toxin A (TcdA) and toxin B (TcdB), responsible for gastrointestinal epithelial damage and colonic inflammation. In this matter, the engineering and use of TcdA/B-neutralizing antibodies appears as a promising approach to counter diarrhea episodes caused by *C. difficile* infections. With that in mind, Andersen et al. (2016) developed an antitoxin strategy to express TcdB-neutralizing antibody fragments in *Lactobacillus* strains in the gastrointestinal tract of hamsters infected with a TcdA⁻/TcdB⁺ *C. difficile* strain. Initially, *in vitro* studies were carried out to confirm the ability of the expressed fragments in neutralizing the cytotoxic effect of TcdB. Moreover, *in vivo* assays revealed that *Lactobacillus* strains expressing two TcdB-neutralizing antibodies led to improved survival rates in the treated group. Furthermore, the protection with TcdB-neutralizing antibodies also preserved the gastrointestinal tract of the animals as no damages or limited inflammation were observed (Andersen et al., 2016). In addition to antibody-based therapies, studies have also explored the potential of small molecules as inhibitors of *C. difficile* TcdB. Tam et al. (2015) reported a high-throughput phenotypic method for screening small molecules capable of protecting human cells from TcdB. As a result, the authors reported a series of small molecules with diverse mechanisms of action on TcdB, including direct binding, sequestration of TcdB, non-competitive inhibition of the glucosyl-transferase activity of TcdB, as well as endosomal maturation inhibition (Tam et al., 2015). However, *in vivo* studies

are still underway to confirm the effectiveness of these small molecules in *C. difficile* infections.

Apart from the application of anti-toxin antibodies and small molecules in anti-virulence therapies, studies have also highlighted the importance of engineered nanoparticle mimicking cell membranes (e.g., liposomes) in sequestering cytotoxic bacterial toxins both *in vitro* and *in vivo* (Fang et al., 2015). Artificial liposomes are constituted exclusively of natural lipids and therefore are not active against bacteria, thus allowing their usage in combination with antibiotics for bacterial infection treatment. Henry et al. (2015), for instance, showed the potential of artificial liposomes in sequestering bacterial toxins *in vitro*, along with the preservation of the integrity of mammalian cells. The authors also observed that, during *in vivo* experiments, the administration of artificial liposomes resulted in mice recovering from septicemia caused by *S. aureus* and *Streptococcus pneumoniae*, as well as mice being protected against pneumonia (Henry et al., 2015). Moreover, combining the artificial liposomes with conventional antibiotics, including vancomycin and penicillin, improved survival rates were observed when compared to mono-therapies (Henry et al., 2015).

Bacteria secrete a wide variety of toxins during host colonization and infection, which represents a bottleneck when it comes to vaccine development aiming at anti-virulence therapies. Indeed, vaccine strategies based on multiple targets (bacterial toxins) have already been reported; however, the identification and further confirmation of virulence factors secreted by bacteria is considered a costly and time-consuming method (Fujita and Taguchi, 2011). As an alternative, studies have proposed the use of multiantigenic nanotoxoids based on naturally occurring bacterial proteins to develop vaccines against pathogenic bacteria. Wei et al. (2017) reported a feasible approach for entrapping diverse toxins from bacterial protein preparations using a membrane-coated nanosponge construct capable of delivering these virulence factors in the organism and, consequently, combating bacterial infections. As for the other anti-virulence therapies here described, the nanoparticle-based neutralization and delivery not only usefully prevent severe bacterial infections but also decrease the risk of antibiotic resistance events (Wei et al., 2017).

Besides the secretion of protein-based toxins, the bacterial LPS in the host's blood stream is known to cause severe immune system stimulation, resulting in septic shock and sepsis (Rietschel et al., 1996). Among the strategies to neutralize LPS, the application of antimicrobial peptides (AMPs) has shown promising results. Moreover, the mechanisms of action and structural arrangements of some AMPs in contact with LPS have already been investigated, including polymyxins (Pristovsek and Kidric, 1999), temporins (Bhunia et al., 2011), and melittins (Bhunia et al., 2007). This class of antimicrobials is well known for its multifunctionality and structural diversity. Studies have shown that AMPs with extended activities, including immunomodulatory, are capable of binding to LPS and, consequently, decreasing the production of nitric oxide and tumor necrosis factor- α (TNF- α), which are commonly related to tissue damage (Pulido et al., 2012). Chih et al. (2015), for instance, have reported the antiendotoxin effects of two

antimicrobial peptides, S1 and KWWK. Interestingly, the authors observed that LPS-neutralizing activities were directly related to the addition of β -naphthylalanine end-tags in both peptides, which was also reflected in the dose-dependent inhibition of nitrite oxide production and TNF- α release *in vitro* and *in vivo* (Chih et al., 2015). In addition, other AMPs, including members from the Pep19-2.5 family (Heinbockel et al., 2018) and retrocyclins (Kudryashova et al., 2015), have revealed the ability to unfold bacterial toxins, as well as causing conformational changes such as toxin aggregation and fluidity (Heinbockel et al., 2018).

FUTURE DIRECTIONS

The antimicrobial resistance threat has driven the global scientific community to search for effective solutions. Given the fact that antimicrobial resistance is a multifactorial phenomenon, the solution for this problem involves a range of approaches focused on controlling the factors that facilitate the emergence and spread of resistance. One of these approaches consists of developing new therapeutic agents that operate under different principles to the currently available antibiotics. In this respect, anti-virulence therapy has been envisioned as a promising alternative with the aim of controlling pathogen virulence in a pathogen-specific fashion, without exerting strong selective pressure on the pathogens.

However, as an emerging therapeutic strategy, anti-virulence therapy has to face several challenges. The selection of the targeted virulence factor(s) is of critical importance for the effectiveness of the strategy in terms of evolutionary robustness. In line with this, a suitable target should be a virulence factor whose disruption does not imply (or imply minimal) fitness consequences for the pathogen (Vale et al., 2016). Moreover, a virulence factor that is conserved between different pathogens could be ideal, because in principle it would be possible to treat polymicrobial infections with a single anti-virulence drug (Maura et al., 2016). It is necessary to understand the detailed dynamics of action of the targeted virulence factor as well as the dynamics of production (Dickey et al., 2017). For example, during *P. aeruginosa* infection of cystic fibrosis patients take place an acute to chronic infection transition. This shift involves down-regulation of virulence factors as the flagellum, T3SS secretion system, proteases, and others; while virulence factors as exopolysaccharides are up-regulated (Hogardt and Heesemann, 2013; Sousa and Pereira, 2014). Therefore, the anti-virulence agent that target some of these virulence factors should be supplemented in accordance with this dynamic of expression. In addition to knowing the targeted virulence factor production dynamics, it is important to know if this virulence factor undergoes chemical modifications that modulate its activity. Furthermore, as anti-virulence therapy works in a pathogen-specific fashion, it is important to have diagnostic methods like matrix-assisted laser desorption ionization-time of flight mass spectrometry (MALDI-TOF), microarray-based nucleic acid test, magnetic resonance-based diagnostic, fluorescence *in situ* hybridization (FISH) test, next generation sequencing (NGS)

and multiplex PCR-based diagnostic test, which permit rapid and precise identification of the infection-causing pathogen (Dickey et al., 2017; Messacar et al., 2017). It is also mandatory to define which parameters will be taken into account for measuring the effectivity of the anti-virulence therapy and for which type of infection the therapy is most suitable (Maura et al., 2016; Dickey et al., 2017). For example, in certain types of *S. aureus* infections (e.g., chronic and bacteremia), a dysfunctional *agr*-QS system appears to be beneficial for the pathogen (Khan et al., 2015). Moreover, recently it has been reported that defective *agr*-QS system could mediate the tolerance to certain antibiotics (gentamicin and ciprofloxacin; Kumar et al., 2017). In addition, it has been suggested that phenol-soluble modulins (PSMs) are involved in the control of *S. aureus* persister cells population (Bojer et al., 2018). Because the PSMs production is under the control of the *agr*-QS system, it is probably that a defective *agr*-QS system down-regulate the expression of PSMs which could favor the emergence of persister cells to certain antibiotics. Therefore, in the above-pointed situations maybe

anti-virulence therapies based on *agr*-QS system inhibition could be not a feasible strategy. Although anti-virulence therapy is an emerging field, several potential anti-virulence drugs have already been identified, and existing chemical libraries for antibiotic discovery could be a valuable source for rapid identification of novel anti-virulence drugs (Maura et al., 2016; Dickey et al., 2017). At this point, it is necessary to direct these potential anti-virulence candidates toward pre-clinical and clinical trials.

AUTHOR CONTRIBUTIONS

OF, MC, and SR wrote the manuscript. MC performed the figures. OLF designed and revised the manuscript.

ACKNOWLEDGMENTS

This work was supported by CAPES, CNPq, FAPDF, FUNDECT, UCB, and UCDB.

REFERENCES

- Abbas, H. A., Elsherbini, A. M., and Shaldam, M. A. (2017). Repurposing metformin as a quorum sensing inhibitor in *Pseudomonas aeruginosa*. *Afr. Health Sci.* 17, 808–819. doi: 10.4314/ahs.v17i3.24
- Abbas, H. A., and Shaldam, M. A. (2016). Glyceryl trinitrate is a novel inhibitor of quorum sensing in *Pseudomonas aeruginosa*. *Afr. Health Sci.* 16, 1109–1117. doi: 10.4314/ahs.v16i4.29
- Alberts, A., Chen, J., Kuron, G., Hunt, V., Huff, J., Hoffman, C., et al. (1980). Mevinolin: a highly potent competitive inhibitor of hydroxymethylglutaryl-coenzyme A reductase and a cholesterol-lowering agent. *Proc. Natl. Acad. Sci. U.S.A.* 77, 3957–3961. doi: 10.1073/pnas.77.7.3957
- Allegretta, G., Maurer, C. K., Eberhard, J., Maura, D., Hartmann, R. W., Rahme, L., et al. (2017). In-depth profiling of MvfR-regulated small molecules in *Pseudomonas aeruginosa* after quorum sensing inhibitor treatment. *Front. Microbiol.* 8:924. doi: 10.3389/fmicb.2017.00924
- Allegretta, G., Weidel, E., Empting, M., and Hartmann, R. W. (2015). Catechol-based substrates of chalcone synthase as a scaffold for novel inhibitors of PqsD. *Eur. J. Med. Chem.* 90, 351–359. doi: 10.1016/j.ejmech.2014.11.055
- Alves, D. R., Perez-Esteban, P., Kot, W., Bean, J., Arnot, T., Hansen, L. H., et al. (2016). A novel bacteriophage cocktail reduces and disperses *Pseudomonas aeruginosa* biofilms under static and flow conditions. *Microb. Biotechnol.* 9, 61–74. doi: 10.1111/1751-7915.12316
- Amara, N., Gregor, R., Rayo, J., Dandela, R., Daniel, E., Liubin, N., et al. (2016). Fine-tuning covalent inhibition of bacterial quorum sensing. *Chembiochem* 17, 825–835. doi: 10.1002/cbic.201500676
- Andersen, K. K., Strokappe, N. M., Hultberg, A., Truusalu, K., Smidt, I., Mikelsaar, R. H., et al. (2016). Neutralization of clostridium difficile toxin B mediated by engineered lactobacilli that produce single-domain antibodies. *Infect. Immun.* 84, 395–406. doi: 10.1128/IAI.00870-15
- Arya, R., and Princy, S. A. (2016). Exploration of modulated genetic circuits governing virulence determinants in *Staphylococcus aureus*. *Indian J. Microbiol.* 56, 19–27. doi: 10.1007/s12088-015-0555-3
- Bach, J. N., and Bramkamp, M. (2013). Flotillins functionally organize the bacterial membrane. *Mol. Microbiol.* 88, 1205–1217. doi: 10.1111/mmi.12252
- Badarau, A., Rouha, H., Malafa, S., Battles, M. B., Walker, L., Nielson, N., et al. (2016). Context matters: The importance of dimerization-induced conformation of the LukGH leukocidin of *Staphylococcus aureus* for the generation of neutralizing antibodies. *MABS* 8, 1347–1360. doi: 10.1080/19420862.2016.1215791
- Baldry, M., Kitir, B., Frøkiær, H., Christensen, S. B., Taverne, N., Meijerink, M., et al. (2016). The *agr* inhibitors solonamide B and analogues alter immune responses to *Staphylococcus aureus* but do not exhibit adverse effects on immune cell functions. *PLoS ONE* 11:e0145618. doi: 10.1371/journal.pone.0145618
- Baldry, M., Nakamura, Y., Nakagawa, S., Frees, D., Matsue, H., Núñez, G., et al. (2018). Application of an *agr*-specific anti-virulence compound as therapy for *Staphylococcus aureus*-induced inflammatory skin disease. *J. Infect. Dis.* 218, 1009–1013. doi: 10.1093/infdis/jiy259
- Bergonzi, C., Schwab, M., Naik, T., Daudé, D., Chabrière, E., and Elias, M. (2018). Structural and biochemical characterization of AaL, a quorum quenching lactonase with unusual kinetic properties. *Sci. Rep.* 8:11262. doi: 10.1038/s41598-018-28988-5
- Bhunia, A., Domadia, P. N., and Bhattacharjya, S. (2007). Structural and thermodynamic analyses of the interaction between melittin and lipopolysaccharide. *Biochim. Biophys. Acta* 1768, 3282–3291. doi: 10.1016/j.bbame.2007.07.017
- Bhunia, A., Saravanan, R., Mohanram, H., Mangoni, M. L., and Bhattacharjya, S. (2011). NMR structures and interactions of temporin-1Tl and temporin-1Tb with lipopolysaccharide micelles: mechanistic insights into outer membrane permeabilization and synergistic activity. *J. Biol. Chem.* 286, 24394–24406. doi: 10.1074/jbc.M110.189662
- Bikard, D., Euler, C. W., Jiang, W., Nussenzweig, P. M., Goldberg, G. W., Duportet, X., et al. (2014). Exploiting CRISPR-Cas nucleases to produce sequence-specific antimicrobials. *Nat. Biotechnol.* 32:1146. doi: 10.1038/nbt.3043
- Birmes, F. S., Wolf, T., Kohl, T. A., Rüger, K., Bange, F., Kalinowski, J., et al. (2017). *Mycobacterium abscessus* subsp. *abscessus* is capable of degrading *Pseudomonas aeruginosa* quinolone signals. *Front. Microbiol.* 8:339. doi: 10.3389/fmicb.2017.00339
- Bojer, M. S., Lindemose, S., Vestergaard, M., and Ingmer, H. (2018). Quorum sensing-regulated phenol-soluble modulins limit persister cell populations in *Staphylococcus aureus*. *Front. Microbiol.* 9:255. doi: 10.3389/fmicb.2018.00255
- Bramkamp, M., and Lopez, D. (2015). Exploring the existence of lipid rafts in bacteria. *Microbiol. Mol. Biol. Rev.* 79, 81–100. doi: 10.1128/MMBR.00036-14
- Brown, H. L., Hanman, K., Reuter, M., Betts, R. P., and Van Vliet, A. H. (2015). *Campylobacter jejuni* biofilms contain extracellular DNA and are sensitive to DNase I treatment. *Front. Microbiol.* 6:699. doi: 10.3389/fmicb.2015.00699
- Bubeck Wardenburg, J., Bae, T., Otto, M., Deleo, F. R., and Schneewind, O. (2007). Poring over pores: alpha-hemolysin and Panton-Valentine leukocidin in *Staphylococcus aureus* pneumonia. *Nat. Med.* 13, 1405–1406. doi: 10.1038/nm1207-1405
- Bukowski, M., Wladyka, B., and Dubin, G. (2010). Exfoliative toxins of *Staphylococcus aureus*. *Toxins* 2, 1148–1165. doi: 10.3390/toxins2051148

- Calfee, M. W., Coleman, J. P., and Pesci, E. C. (2001). Interference with *Pseudomonas* quinolone signal synthesis inhibits virulence factor expression by *Pseudomonas aeruginosa*. *Proc. Natl. Acad. Sci. U.S.A.* 98, 11633–11637. doi: 10.1073/pnas.201328498
- Capitato, J. N., Philipp, S. V., Reardon, T., McConnell, A., Oliver, D. C., Warren, A., et al. (2017). Development of a novel series of non-natural triaryl agonists and antagonists of the *Pseudomonas aeruginosa* LasR quorum sensing receptor. *Bioorg. Med. Chem.* 25, 153–165. doi: 10.1016/j.bmc.2016.10.021
- Cattò, C., Dell'Orto, S., Villa, F., Villa, S., Gelain, A., Vitali, A., et al. (2015). Unravelling the structural and molecular basis responsible for the anti-biofilm activity of zosteric acid. *PLoS ONE* 10:e0131519. doi: 10.1371/journal.pone.0131519
- Cavaleiro, E., Duarte, A. S., Esteves, A. C., Correia, A., Whitcombe, M. J., Piletska, E. V., et al. (2015). Novel linear polymers able to inhibit bacterial quorum sensing. *Macromol. Biosci.* 15, 647–656. doi: 10.1002/mabi.201400447
- Chang, E. H., Huang, J., Lin, Z., and Brown, A. C. (2019). Catechin-mediated restructuring of a bacterial toxin inhibits activity. *Biochim. Biophys. Acta General Subjects* 1863, 191–198. doi: 10.1016/j.bbagen.2018.10.011
- Chatterjee, M., D'Morris, S., Paul, V., Warrior, S., Vasudevan, A. K., Vanuopadath, M., et al. (2017). Mechanistic understanding of Phenyllactic acid mediated inhibition of quorum sensing and biofilm development in *Pseudomonas aeruginosa*. *Appl. Microbiol. Biotechnol.* 101, 8223–8236. doi: 10.1007/s00253-017-8546-4
- Chih, Y. H., Lin, Y. S., Yip, B. S., Wei, H. J., Chu, H. L., Yu, H. Y., et al. (2015). Ultrashort antimicrobial peptides with antiendotoxin properties. *Antimicrob. Agents Chemother.* 59, 5052–5056. doi: 10.1128/AAC.00519-15
- Citorik, R. J., Mimeo, M., and Lu, T. K. (2014). Sequence-specific antimicrobials using efficiently delivered RNA-guided nucleases. *Nat. Biotechnol.* 32, 1141–1145. doi: 10.1038/nbt.3011
- Clatworthy, A. E., Pierson, E., and Hung, D. T. (2007). Targeting virulence: a new paradigm for antimicrobial therapy. *Nat. Chem. Biol.* 3, 541–548. doi: 10.1038/nchembio.2007.24
- Cohen, T. S., Hilliard, J. J., Jones-Nelson, O., Keller, A. E., O'Day, T., Tkaczyk, C., et al. (2016). *Staphylococcus aureus* alpha toxin potentiates opportunistic bacterial lung infections. *Sci. Transl. Med.* 8:329ra331. doi: 10.1126/scitranslmed.aad9922
- Crémet, L., Bourigault, C., Lepelletier, D., Guillozeuic, A., Juvin, M.-E., Reynaud, A., et al. (2012). Nosocomial outbreak of carbapenem-resistant *Enterobacter cloacae* highlighting the interspecies transferability of the bla OXA-48 gene in the gut flora. *J. Antimicrob. Chemother.* 67, 1041–1043. doi: 10.1093/jac/dkr547
- Da, F., Yao, L., Su, Z., Hou, Z., Li, Z., Xue, X., et al. (2017). Antisense locked nucleic acids targeting agrA inhibit quorum sensing and pathogenesis of community-associated methicillin-resistant *Staphylococcus aureus*. *J. Appl. Microbiol.* 122, 257–267. doi: 10.1111/jam.13321
- Daly, S. M., Elmore, B. O., Kavanaugh, J. S., Triplett, K. D., Figueroa, M., Raja, H. A., et al. (2015). ω -Hydroxyemodin limits *Staphylococcus aureus* quorum sensing-mediated pathogenesis and inflammation. *Antimicrob. Agents Chemother.* 59, 2223–2235. doi: 10.1128/AAC.04564-14
- Daly, S. M., Joyner, J. A., Triplett, K. D., Elmore, B. O., Pokhrel, S., Fietze, K. M., et al. (2017). VLP-based vaccine induces immune control of *Staphylococcus aureus* virulence regulation. *Sci. Rep.* 7:637. doi: 10.1038/s41598-017-00753-0
- Defoirdt, T. (2017). Quorum-sensing systems as targets for antivirulence therapy. *Trends Microbiol.* 26, 313–328. doi: 10.1016/j.tim.2017.10.005
- Defoirdt, T., Boon, N., and Bossier, P. (2010). Can bacteria evolve resistance to quorum sensing disruption? *PLoS Pathog.* 6:e1000989. doi: 10.1371/journal.ppat.1000989
- Dickey, S. W., Cheung, G. Y., and Otto, M. (2017). Different drugs for bad bugs: antivirulence strategies in the age of antibiotic resistance. *Nat. Rev. Drug Discovery* 16:457. doi: 10.1038/nrd.2017.23
- Diep, B. A., Le, V. T., Badiou, C., Le, H. N., Pinheiro, M. G., Duong, A. H., et al. (2016). IVIG-mediated protection against necrotizing pneumonia caused by MRSA. *Sci. Transl. Med.* 8:357ra124. doi: 10.1126/scitranslmed.aag1153
- Dong, W., Zhu, J., Guo, X., Kong, D., Zhang, Q., Zhou, Y., et al. (2018). Characterization of AiiK, an AHL lactonase, from *Kurthia huakuii* LAM0618 T and its application in quorum quenching on *Pseudomonas aeruginosa* PAO1. *Sci. Rep.* 8:6013. doi: 10.1038/s41598-018-24507-8
- Drees, S. L., Li, C., Prasetya, F., Saleem, M., Dreveny, I., Williams, P., et al. (2016). PqsBC, a condensing enzyme in the biosynthesis of the *Pseudomonas aeruginosa* quinolone signal crystal structure, inhibition, and reaction mechanism. *J. Biol. Chem.* 291, 6610–6624. doi: 10.1074/jbc.M115.708453
- Duan, J., Li, M., Hao, Z., Shen, X., Liu, L., Jin, Y., et al. (2018). Subinhibitory concentrations of resveratrol reduce alpha-hemolysin production in *Staphylococcus aureus* isolates by downregulating saeRS. *Emerg. Microb. Infect.* 7:136. doi: 10.1038/s41426-018-0142-x
- Dulcey, C. E., Dekimpe, V., Fauvel, D.-A., Milot, S., Groleau, M.-C., Doucet, N., et al. (2013). The end of an old hypothesis: the *Pseudomonas* signaling molecules 4-hydroxy-2-alkylquinolones derive from fatty acids, not 3-ketofatty acids. *Chem. Biol.* 20, 1481–1491. doi: 10.1016/j.chembiol.2013.09.021
- Edwards, G. A., Shymanska, N. V., and Pierce, J. G. (2017). 5-Benzylidene-4-oxazolidinones potently inhibit biofilm formation in Methicillin-resistant *Staphylococcus aureus*. *Chem. Commun.* 53, 7353–7356. doi: 10.1039/C7CC03626D
- Eibergen, N. R., Moore, J. D., Mattmann, M. E., and Blackwell, H. E. (2015). Potent and selective modulation of the RhlR quorum sensing receptor by using non-native ligands: an emerging target for virulence control in *Pseudomonas aeruginosa*. *Chembiochem* 16, 2348–2356. doi: 10.1002/cbic.2015.00357
- Fan, X., Liang, M., Wang, L., Chen, R., Li, H., and Liu, X. (2017). Aii810, a novel cold-adapted N-acylhomoserine lactonase discovered in a metagenome, can strongly attenuate *Pseudomonas aeruginosa* virulence factors and biofilm formation. *Front. Microbiol.* 8:1950. doi: 10.3389/fmicb.2017.01950
- Fang, R. H., Luk, B. T., Hu, C. M., and Zhang, L. (2015). Engineered nanoparticles mimicking cell membranes for toxin neutralization. *Adv. Drug Deliv. Rev.* 90, 69–80. doi: 10.1016/j.addr.2015.04.001
- Feng, L., Zhou, L., Sun, Y., Gui, J., Wang, X., Wu, P., et al. (2011). Specific inhibitions of annonaceous acetogenins on class II 3-hydroxy-3-methylglutaryl coenzyme A reductase from *Streptococcus pneumoniae*. *Bioorg. Med. Chem.* 19, 3512–3519. doi: 10.1016/j.bmc.2011.04.019
- Feng, X., Guo, W., Zheng, H., Du, J., Luo, H., Wu, Q., et al. (2018). Inhibition of biofilm formation by chemical uncoupler, 3', 4', 5-tetrachlorosalicylanilide (TCS): from the perspective of quorum sensing and biofilm related genes. *Biochem. Eng. J.* 137, 95–99. doi: 10.1016/j.bej.2018.05.010
- Feng, X., Hu, Y., Zheng, Y., Zhu, W., Li, K., Huang, C.-H., et al. (2014). Structural and functional analysis of *Bacillus subtilis* YisP reveals a role of its product in biofilm production. *Chem. Biol.* 21, 1557–1563. doi: 10.1016/j.chembiol.2014.08.018
- Fetzner, S. (2015). Quorum quenching enzymes. *J. Biotechnol.* 201, 2–14. doi: 10.1016/j.jbiotec.2014.09.001
- Fleming, D., and Rumbaugh, K. P. (2017). Approaches to dispersing medical biofilms. *Microorganisms* 5:15. doi: 10.3390/microorganisms5020015
- Flemming, H.-C., Wingender, J., Szewzyk, U., Steinberg, P., Rice, S. A., and Kjelleberg, S. (2016). Biofilms: an emergent form of bacterial life. *Nat. Rev. Microbiol.* 14:563. doi: 10.1038/nrmicro.2016.94
- Fong, J., Zhang, C., Yang, R., Boo, Z. Z., Tan, S. K., Nielsen, T. E., et al. (2018). Combination therapy strategy of quorum quenching enzyme and quorum sensing inhibitor in suppressing multiple quorum sensing pathways of *P. aeruginosa*. *Sci. Rep.* 8:1155. doi: 10.1038/s41598-018-19504-w
- Fong, S. A., Drilling, A., Morales, S., Cornet, M. E., Woodworth, B. A., Fokkens, W. J., et al. (2017). Activity of bacteriophages in removing biofilms of *Pseudomonas aeruginosa* isolates from chronic rhinosinusitis patients. *Front. Cell. Infect. Microbiol.* 7:418. doi: 10.3389/fcimb.2017.00418
- Fujita, Y., and Taguchi, H. (2011). Current status of multiple antigen-presenting peptide vaccine systems: application of organic and inorganic nanoparticles. *Chem. Cent. J.* 5: 48. doi: 10.1186/1752-153X-5-48
- García, S., Blackledge, M., Michalek, S., Su, L., Ptacek, T., Eipers, P., et al. (2017). Targeting of *Streptococcus mutans* biofilms by a novel small molecule prevents dental caries and preserves the oral microbiome. *J. Dent. Res.* 96, 807–814. doi: 10.1177/0022034517698096
- García-Contreras, R. (2016). Is quorum sensing interference a viable alternative to treat *Pseudomonas aeruginosa* infections? *Front. Microbiol.* 7:1454. doi: 10.3389/fmicb.2016.01454
- García-Contreras, R., Martínez-Vázquez, M., Velázquez Guadarrama, N., Villegas Pañeda, A. G., Hashimoto, T., Maeda, T., et al. (2013). Resistance to the quorum-quenching compounds brominated furanone C-30 and 5-fluorouracil in *Pseudomonas aeruginosa* clinical isolates. *Pathog. Dis.* 68, 8–11. doi: 10.1111/2049-632X.12039

- García-Contreras, R., Pérez-Eretza, B., Jasso-Chávez, R., Lira-Silva, E., Roldán-Sánchez, J. A., González-Valdez, A., et al. (2015). High variability in quorum quenching and growth inhibition by furanone C-30 in *Pseudomonas aeruginosa* clinical isolates from cystic fibrosis patients. *Pathog. Dis.* 73:ftv040. doi: 10.1093/femspd/ftv040
- García-Fernández, E., Koch, G., Wagner, R. M., Fekete, A., Stengel, S. T., Schneider, J., et al. (2017). Membrane microdomain disassembly inhibits MRSA antibiotic resistance. *Cell* 171, 1354–1367.e20. doi: 10.1016/j.cell.2017.10.012
- Geoghegan, J. A., Irvine, A. D., and Foster, T. J. (2018). *Staphylococcus aureus* and atopic dermatitis: a complex and evolving relationship. *Trends Microbiol.* 26, 484–497. doi: 10.1016/j.tim.2017.11.008
- Glansdorp, F. G., Thomas, G. L., Lee, J. K., Dutton, J. M., Salmond, G. P., Welch, M., et al. (2004). Synthesis and stability of small molecule probes for *Pseudomonas aeruginosa* quorum sensing modulation. *Org. Biomol. Chem.* 2, 3329–3336. doi: 10.1039/b412802h
- Goerke, C., Fluckiger, U., Steinhuber, A., Zimmerli, W., and Wolz, C. (2001). Impact of the regulatory loci agr, sarA and sae of *Staphylococcus aureus* on the induction of α -toxin during device-related infection resolved by direct quantitative transcript analysis. *Mol. Microbiol.* 40, 1439–1447. doi: 10.1046/j.1365-2958.2001.02494.x
- Goh, W.-K., Gardner, C. R., Sekhar, K. V. C., Biswas, N. N., Nizalapur, S., Rice, S. A., et al. (2015). Synthesis, quorum sensing inhibition and docking studies of 1, 5-dihydropyrrol-2-ones. *Bioorg. Med. Chem.* 23, 7366–7377. doi: 10.1016/j.bmc.2015.10.025
- Gökalsin, B., Aksoydan, B., Erman, B., and Sesal, N. C. (2017). Reducing virulence and biofilm of *Pseudomonas aeruginosa* by potential quorum sensing inhibitor carotenoid: zeaxanthin. *Microb. Ecol.* 74, 466–473. doi: 10.1007/s00248-017-0949-3
- Gordon, C. P., Olson, S. D., Lister, J. L., Kavanaugh, J. S., and Horswill, A. R. (2016). Truncated autoinducing peptides as antagonists of *Staphylococcus lugdunensis* quorum sensing. *J. Med. Chem.* 59, 8879–8888. doi: 10.1021/acs.jmedchem.6b00727
- Goren, M. G., Carmeli, Y., Schwaber, M. J., Chmelnitsky, I., Schechner, V., and Navon-Venezia, S. (2010). Transfer of carbapenem-resistant plasmid from *Klebsiella pneumoniae* ST258 to *Escherichia coli* in patient. *Emerging Infect. Dis.* 16, 1014–1017. doi: 10.3201/eid1606.091671
- Grandclément, C., Tannières, M., Moréra, S., Dessaux, Y., and Faure, D. (2015). Quorum quenching: role in nature and applied developments. *FEMS Microbiol. Rev.* 40, 86–116. doi: 10.1093/femsre/fuv038
- Greenberg, M., Kuo, D., Jankowsky, E., Long, L., Hager, C., Bandi, K., et al. (2018). Small-molecule AgrA inhibitors F12 and F19 act as antivirulence agents against Gram-positive pathogens. *Sci. Rep.* 8:14578. doi: 10.1038/s41598-018-32829-w
- Gruber, J. D., Chen, W., Parnham, S., Beauchesne, K., Moeller, P., Flume, P. A., et al. (2016). The role of 2, 4-dihydroxyquinoline (DHQ) in *Pseudomonas aeruginosa* pathogenicity. *PeerJ* 4:e1495. doi: 10.7717/peerj.1495
- Guendouze, A., Plener, L., Bzdrenga, J., Jacquet, P., Rémy, B., Elias, M., et al. (2017). Effect of quorum quenching lactonase in clinical isolates of *Pseudomonas aeruginosa* and comparison with quorum sensing inhibitors. *Front. Microbiol.* 8:227. doi: 10.3389/fmicb.2017.00227
- Gunn, J. S., Bakaletz, L. O., and Wozniak, D. J. (2016). What is on the outside matters: the role of the extracellular polymeric substance of gram-negative biofilms in evading host immunity and as a target for therapeutic intervention. *J. Biol. Chem.* 291, 12538–12546. doi: 10.1074/jbc.R115.707547
- Gutierrez, J. A., Crowder, T., Rinaldo-Matthis, A., Ho, M.-C., Almo, S. C., and Schramm, V. L. (2009). Transition state analogs of 5'-methylthioadenosine nucleosidase disrupt quorum sensing. *Nat. Chem. Biol.* 5:251. doi: 10.1038/nchembio.153
- Haines, B. E., Wiest, O., and Stauffacher, C. V. (2013). The increasingly complex mechanism of HMG-CoA reductase. *Acc. Chem. Res.* 46, 2416–2426. doi: 10.1021/ar3003267
- Hall, C. W., and Mah, T.-F. (2017). Molecular mechanisms of biofilm-based antibiotic resistance and tolerance in pathogenic bacteria. *FEMS Microbiol. Rev.* 41, 276–301. doi: 10.1093/femsre/fux010
- Hansen, A. M., Peng, P., Baldry, M., Perez-Gassol, I., Christensen, S. B., Vinther, J. M. O., et al. (2018). Lactam hybrid analogues of solonomide B and autoinducing peptides as potent *S. aureus* AgrC antagonists. *Eur. J. Med. Chem.* 152, 370–376. doi: 10.1016/j.ejmech.2018.04.053
- Hazan, R., Que, Y. A., Maura, D., Strobel, B., Majcherczyk, P. A., Hopper, L. R., et al. (2016). Auto poisoning of the respiratory chain by a quorum-sensing-regulated molecule favors biofilm formation and antibiotic tolerance. *Curr. Biol.* 26, 195–206. doi: 10.1016/j.cub.2015.11.056
- Hedl, M., and Rodwell, V. W. (2004). Inhibition of the Class II HMG-CoA reductase of *Pseudomonas mevalonii*. *Protein Sci.* 13, 1693–1697. doi: 10.1110/ps.03597504
- Heidari, A., Noshiranzadeh, N., Haghi, F., and Bikas, R. (2017). Inhibition of quorum sensing related virulence factors of *Pseudomonas aeruginosa* by pyridoxal lactohydrazone. *Microb. Pathog.* 112, 103–110. doi: 10.1016/j.micpath.2017.09.043
- Heimesaat, M. M., Lugert, R., Fischer, A., Alutis, M., Kühl, A. A., Zautner, A. E., et al. (2014). Impact of *Campylobacter jejuni* cJ0268c knockout mutation on intestinal colonization, translocation, and induction of immunopathology in gnotobiotic IL-10 deficient mice. *PLoS ONE* 9:e90148. doi: 10.1371/journal.pone.0090148
- Heinbockel, L., Weindl, G., Martinez-de-Tejada, G., Correa, W., Sanchez-Gomez, S., Barcena-Varela, S., et al. (2018). Inhibition of lipopolysaccharide- and lipoprotein-induced inflammation by antitoxin peptide Pep19-2.5. *Front. Immunol.* 9:1704. doi: 10.3389/fimmu.2018.01704
- Henry, B. D., Neill, D. R., Becker, K. A., Gore, S., Bricio-Moreno, L., Ziobro, R., et al. (2015). Engineered liposomes sequester bacterial exotoxins and protect from severe invasive infections in mice. *Nat. Biotechnol.* 33, 81–88. doi: 10.1038/nbt.3037
- Heras, B., Scanlon, M. J., and Martin, J. L. (2015). Targeting virulence not viability in the search for future antibacterials. *Br. J. Clin. Pharmacol.* 79, 208–215. doi: 10.1111/bcp.12356
- Heuston, S., Begley, M., Gahan, C. G., and Hill, C. (2012). Isoprenoid biosynthesis in bacterial pathogens. *Microbiology* 158, 1389–1401. doi: 10.1099/mic.0.051599-0
- Hinsberger, S., de Jong, J. C., Groh, M., Haupenthal, J., and Hartmann, R. W. (2014). Benzamidobenzoic acids as potent PqsD inhibitors for the treatment of *Pseudomonas aeruginosa* infections. *Eur. J. Med. Chem.* 76, 343–351. doi: 10.1016/j.ejmech.2014.02.014
- Hogardt, M., and Heesemann, J. (2013). Microevolution of *Pseudomonas aeruginosa* to a chronic pathogen of the cystic fibrosis lung. *Curr Top Microbiol Immunol.* 358, 91–118. doi: 10.1007/82_2011_199
- Hraiech, S., Hiblot, J., Lafleur, J., Lepidi, H., Papazian, L., Rolain, J.-M., et al. (2014). Inhaled lactonase reduces *Pseudomonas aeruginosa* quorum sensing and mortality in rat pneumonia. *PLoS ONE* 9:e107125. doi: 10.1371/journal.pone.0107125
- Huggins, W. M., Nguyen, T. V., Hahn, N. A., Baker, J. T., Kuo, L. G., Kaur, D., et al. (2018). 2-Aminobenzimidazoles as antibiofilm agents against *Salmonella enterica* serovar typhimurium. *Medchemcomm* 9, 1547–1552. doi: 10.1039/C8MD00298C
- Hwang, I. Y., Koh, E., Wong, A., March, J. C., Bentley, W. E., Lee, Y. S., et al. (2017). Engineered probiotic *Escherichia coli* can eliminate and prevent *Pseudomonas aeruginosa* gut infection in animal models. *Nat. Commun.* 8:15028. doi: 10.1038/ncomms15028
- Istvan, E. S., and Deisenhofer, J. (2001). Structural mechanism for statin inhibition of HMG-CoA reductase. *Science* 292, 1160–1164. doi: 10.1126/science.1059344
- Ivanova, K., Fernandes, M. M., Francesko, A., Mendoza, E., Guezguez, J., Burnet, M., et al. (2015). Quorum-quenching and matrix-degrading enzymes in multilayer coatings synergistically prevent bacterial biofilm formation on urinary catheters. *ACS Appl. Mater. Interfaces* 7, 27066–27077. doi: 10.1021/acsami.5b09489
- Jenkins, A., Diep, B. A., Mai, T. T., Vo, N. H., Warrenner, P., Suzich, J., et al. (2015). Differential expression and roles of *Staphylococcus aureus* virulence determinants during colonization and disease. *MBio.* 6, e02272–e02214. doi: 10.1128/mBio.02272-14
- Ji, C., Sharma, I., Pratihari, D., Hudson, L. L., Maura, D., Guney, T., et al. (2016). Designed small-molecule inhibitors of the anthranil-CoA synthetase PqsA block quinolone biosynthesis in *Pseudomonas aeruginosa*. *ACS Chem. Biol.* 11, 3061–3067. doi: 10.1021/acscmbio.6b00575
- Joo, H.-S., Fu, C.-I., and Otto, M. (2016). Bacterial strategies of resistance to antimicrobial peptides. *Phil. Trans. R. Soc. B* 371:20150292. doi: 10.1098/rstb.2015.0292

- Kahler, C. M., Sarkar-Tyson, M., Kibble, E. A., Stubbs, K. A., and Vrieling, A. (2018). Enzyme targets for drug design of new anti-virulence therapeutics. *Curr. Opin. Struct. Biol.* 53, 140–150. doi: 10.1016/j.sbi.2018.08.010
- Kalaivasan, E., Thirumalaswamy, K., Harish, B. N., Gnanasambandam, V., Sali, V. K., and John, J. (2017). Inhibition of quorum sensing-controlled biofilm formation in *Pseudomonas aeruginosa* by quorum-sensing inhibitors. *Microb. Pathog.* 111, 99–107. doi: 10.1016/j.micpath.2017.08.017
- Kalia, M., Yadav, V. K., Singh, P. K., Sharma, D., Narvi, S. S., and Agarwal, V. (2018). Exploring the impact of parthenolide as anti-quorum sensing and anti-biofilm agent against *Pseudomonas aeruginosa*. *Life Sci.* 199, 96–103. doi: 10.1016/j.lfs.2018.03.013
- Kalia, V. C., Patel, S. K., Kang, Y. C., and Lee, J.-K. (2019). Quorum sensing inhibitors as antipathogens: biotechnological applications. *Biotechnol. Adv.* 37, 68–90. doi: 10.1016/j.biotechadv.2018.11.006
- Kang, S., Kim, J., Hur, J. K., and Lee, S.-S. (2017). CRISPR-based genome editing of clinically important *Escherichia coli* SE15 isolated from indwelling urinary catheters of patients. *J. Med. Microbiol.* 66, 18–25. doi: 10.1099/jmm.0.000406
- Karathanasi, G., Bojer, M. S., Baldry, M., Johannessen, B. A., Wolff, S., Greco, I., et al. (2018). Linear peptidomimetics as potent antagonists of *Staphylococcus aureus* agr quorum sensing. *Sci. Rep.* 8:3562. doi: 10.1038/s41598-018-21951-4
- Kaufmann, G. F., Park, J., Mee, J. M., Ulevitch, R. J., and Janda, K. D. (2008). The quorum quenching antibody RS2-1G9 protects macrophages from the cytotoxic effects of the *Pseudomonas aeruginosa* quorum sensing signalling molecule N-3-oxo-dodecanoyl-homoserine lactone. *Mol. Immunol.* 45, 2710–2714. doi: 10.1016/j.molimm.2008.01.010
- Kenaley, K. M., Blackson, T., Boylan, L., Ciarlo, J., Antunes, M., Shaffer, T. H., et al. (2018). Impact of endotracheal tube biofilm and respiratory secretions on airway resistance and mechanics of breathing in a neonatal lung model. *J. Appl. Physiol.* 125, 1227–1231. doi: 10.1152/jappphysiol.00083.2018
- Khan, B. A., Yeh, A. J., Cheung, G. Y., and Otto, M. (2015). Investigational therapies targeting quorum-sensing for the treatment of *Staphylococcus aureus* infections. *Expert Opin. Investig. Drugs* 24, 689–704. doi: 10.1517/13543784.2015.1019062
- Kim, B., Park, J.-S., Choi, H.-Y., Yoon, S. S., and Kim, W.-G. (2018). Terrein is an inhibitor of quorum sensing and c-di-GMP in *Pseudomonas aeruginosa*: a connection between quorum sensing and c-di-GMP. *Sci. Rep.* 8:8617. doi: 10.1038/s41598-018-26974-5
- Kim, D.-Y., Stauffacher, C. V., and Rodwell, V. W. (2000). Dual coenzyme specificity of *Archaeoglobus fulgidus* HMG-CoA reductase. *Protein Sci.* 9, 1226–1234. doi: 10.1110/ps.9.6.1226
- Ko, H. H., Lareu, R. R., Dix, B. R., and Hughes, J. D. (2017). Statins: antimicrobial resistance breakers or makers? *PeerJ* 5:e3952. doi: 10.7717/peerj.3952
- Koch, B., Liljefors, T., Persson, T., Nielsen, J., Kjelleberg, S., and Givskov, M. (2005). The LuxR receptor: the sites of interaction with quorum-sensing signals and inhibitors. *Microbiology* 151, 3589–3602. doi: 10.1099/mic.0.27954-0
- Koch, G., Wermser, C., Acosta, I. C., Kricks, L., Stengel, S. T., Yepes, A., et al. (2017). Attenuating *Staphylococcus aureus* virulence by targeting flotillin protein scaffold activity. *Cell Chem. Biol.* 24, 845–857.e46. doi: 10.1016/j.chembiol.2017.05.027
- Köhler, T., Perron, G. G., Buckling, A., and Van Delden, C. (2010). Quorum sensing inhibition selects for virulence and cooperation in *Pseudomonas aeruginosa*. *PLoS Pathog.* 6:e1000883. doi: 10.1371/journal.ppat.1000883
- Kong, C., Neoh, H. M., and Nathan, S. (2016). Targeting *Staphylococcus aureus* toxins: a potential form of anti-virulence therapy. *Toxins* 8:72. doi: 10.3390/toxins8030072
- Konstantinović, N., Cirković, I., Đukić, S., Marić, V., and Božić, D. D. (2017). Biofilm formation of *Achromobacter xylosoxidans* on contact lens. *Acta Microbiol. Immunol. Hung.* 64, 293–300. doi: 10.1556/030.64.2017.005
- Koopman, J. A., Marshall, J. M., Bhatia, A., Eguale, T., Kwiek, J. J., and Gunn, J. S. (2015). Inhibition of *Salmonella enterica* biofilm formation using small molecule adenosine mimetics. *Antimicrob. Agents Chemother.* 59, 76–84. doi: 10.1128/AAC.03407-14
- Koul, S., Prakash, J., Mishra, A., and Kalia, V. C. (2016). Potential emergence of multi-quorum sensing inhibitor resistant (MQSIR) bacteria. *Indian J. Microbiol.* 56, 1–18. doi: 10.1007/s12088-015-0558-0
- Krueger, E., Hayes, S., Chang, E. H., Yutuc, S., and Brown, A. C. (2018). Receptor-based peptides for inhibition of RTX leukotoxin (LtxA) activity. *ACS Infect. Dis.* 4, 1073–1081. doi: 10.1021/acscinfecdis.7b00230
- Kudryashova, E., Seveau, S., Lu, W., and Kudryashov, D. S. (2015). Retrocyclins neutralize bacterial toxins by potentiating their unfolding. *Biochem. J.* 467, 311–320. doi: 10.1042/BJ20150049
- Kumar, K., Chen, J., Drlica, K., and Shopsin, B. (2017). Tuning of the lethal response to multiple stressors with a single-site mutation during clinical infection by *Staphylococcus aureus*. *MBio.* 8, e01476–e01417. doi: 10.1128/mBio.01476-17
- Kumar, L., Chhibber, S., Kumar, R., Kumar, M., and Harjai, K. (2015). Zingerone silences quorum sensing and attenuates virulence of *Pseudomonas aeruginosa*. *Fitoterapia* 102, 84–95. doi: 10.1016/j.fitote.2015.02.002
- Kutty, S. K., Barraud, N., Ho, K. K., Iskander, G. M., Griffith, R., Rice, S. A., et al. (2015). Hybrids of acylated homoserine lactone and nitric oxide donors as inhibitors of quorum sensing and virulence factors in *Pseudomonas aeruginosa*. *Org. Biomol. Chem.* 13, 9850–9861. doi: 10.1039/C5OB01373A
- LaSarre, B., and Federle, M. J. (2013). Exploiting quorum sensing to confuse bacterial pathogens. *Microbiol. Mol. Biol. Rev.* 77, 73–111. doi: 10.1128/MMBR.00046-12
- Le, V. T., Tkaczyk, C., Chau, S., Rao, R. L., Dip, E. C., Pereira-Franchi, E. P., et al. (2016). Critical role of alpha-toxin and protective effects of its neutralization by a human antibody in acute bacterial skin and skin structure infections. *Antimicrob. Agents Chemother.* 60, 5640–5648. doi: 10.1128/AAC.00710-16
- Lee, J., and Zhang, L. (2015). The hierarchy quorum sensing network in *Pseudomonas aeruginosa*. *Protein Cell* 6, 26–41. doi: 10.1007/s13238-014-0100-x
- Lee, J.-H., Kim, Y.-G., Cho, H. S., Ryu, S. Y., Cho, M. H., and Lee, J. (2014). Coumarins reduce biofilm formation and the virulence of *Escherichia coli* O157: H7. *Phytomedicine* 21, 1037–1042. doi: 10.1016/j.phymed.2014.04.008
- Lesic, B., Lépine, F., Déziel, E., Zhang, J., Zhang, Q., Padfield, K., et al. (2007). Inhibitors of pathogen intercellular signals as selective anti-infective compounds. *PLoS Pathog.* 3:e126. doi: 10.1371/journal.ppat.0030126
- Li, C., Wu, Y., Riehle, A., Ma, J., Kamler, M., Gulbins, E., et al. (2017). *Staphylococcus aureus* survives in cystic fibrosis macrophages forming a reservoir for chronic pneumonia. *Infect. Immun.* 85:e00883-16. doi: 10.1128/IAI.00883-16
- Li, D., Gui, J., Li, Y., Feng, L., Han, X., Sun, Y., et al. (2012). Structure-based design and screen of novel inhibitors for class II 3-hydroxy-3-methylglutaryl coenzyme A reductase from *Streptococcus pneumoniae*. *J. Chem. Inf. Model.* 52, 1833–1841. doi: 10.1021/ci300163v
- Lidor, O., Al-Quntar, A., Pesci, E., and Steinberg, D. (2015). Mechanistic analysis of a synthetic inhibitor of the *Pseudomonas aeruginosa* LasI quorum-sensing signal synthase. *Sci. Rep.* 5:16569. doi: 10.1038/srep16569
- Lin, F.-Y., Liu, C.-I., Liu, Y.-L., Zhang, Y., Wang, K., Jeng, W.-Y., et al. (2010). Mechanism of action and inhibition of dehydroquinate synthase. *Proc. Natl. Acad. Sci. U.S.A.* 107, 21337–21342. doi: 10.1073/pnas.1010907107
- Liu, Q., Yeo, W. S., and Bae, T. (2016). The SaeRS two-component system of *Staphylococcus aureus*. *Genes* 7:81. doi: 10.3390/genes7100081
- Liu, X., Peng, L., Meng, J., Zhu, Z., Han, B., and Wang, S. (2018). Protein-mediated anti-adhesion surface against oral bacteria. *Nanoscale* 10, 2711–2714. doi: 10.1039/C7NR08844B
- Liu, Y., Shi, D., Guo, Y., Li, M., Zha, Y., Wang, Q., et al. (2017). Dracorhodin perochlorate attenuates *Staphylococcus aureus* USA300 virulence by decreasing α -toxin expression. *World J. Microbiol. Biotechnol.* 33:17. doi: 10.1007/s11274-016-2129-x
- Lopez, D., and Koch, G. (2017). Exploring functional membrane microdomains in bacteria: an overview. *Curr. Opin. Microbiol.* 36, 76–84. doi: 10.1016/j.mib.2017.02.001
- López, D., and Kolter, R. (2010). Functional microdomains in bacterial membranes. *Genes Dev.* 24, 1893–1902. doi: 10.1101/gad.1945010
- López, M., Mayer, C., Fernández-García, L., Blasco, L., Muras, A., Ruiz, F. M., et al. (2017). Quorum sensing network in clinical strains of *A. baumannii*: AidA is a new quorum quenching enzyme. *PLoS ONE* 12:e0174454. doi: 10.1371/journal.pone.0174454
- Lu, T. K., and Collins, J. J. (2007). Dispersing biofilms with engineered enzymatic bacteriophage. *Proc. Natl. Acad. Sci. U.S.A.* 104, 11197–11202. doi: 10.1073/pnas.0704624104
- Ma, L., Feng, S., de la Fuente-Núñez, C., Hancock, R. E., and Lu, X. (2018). Development of molecularly imprinted polymers to block quorum sensing

- and inhibit bacterial biofilm formation. *ACS Appl. Mater. Interfaces*. 10, 18450–18457. doi: 10.1021/acsami.8b01584
- Maeda, T., García-Contreras, R., Pu, M., Sheng, L., García, L. R., Tomás, M., et al. (2012). Quorum quenching quandary: resistance to antivirulence compounds. *ISME J.* 6, 493–501. doi: 10.1038/ismej.2011.122
- Maura, D., Ballok, A. E., and Rahme, L. G. (2016). Considerations and caveats in anti-virulence drug development. *Curr. Opin. Microbiol.* 33, 41–46. doi: 10.1016/j.mib.2016.06.001
- Maura, D., Drees, S. L., Bandyopadhyaya, A., Kitao, T., Negri, M., Starkey, M., et al. (2017). Polypharmacology approaches against the *Pseudomonas aeruginosa* MvfR regulon and their application in blocking virulence and antibiotic tolerance. *ACS Chem. Biol.* 12, 1435–1443. doi: 10.1021/acscchembio.6b01139
- Merkey, B. V., Lardon, L. A., Seoane, J. M., Kreft, J. U., and Smets, B. F. (2011). Growth dependence of conjugation explains limited plasmid invasion in biofilms: an individual-based modelling study. *Environ. Microbiol.* 13, 2435–2452. doi: 10.1111/j.1462-2920.2011.02535.x
- Messacar, K., Parker, S. K., Todd, J. K., and Dominguez, S. R. (2017). Implementation of rapid molecular infectious disease diagnostics: the role of diagnostic and antimicrobial stewardship. *J. Clin. Microbiol.* 57, 715–723. doi: 10.1128/JCM.02264-16
- Mielich-Süss, B., Wagner, R. M., Mietrach, N., Hertlein, T., Marincola, G., Ohlsen, K., et al. (2017). Flotillin scaffold activity contributes to type VII secretion system assembly in *Staphylococcus aureus*. *PLoS Pathog.* 13:e1006728. doi: 10.1371/journal.ppat.1006728
- Migiyama, Y., Kaneko, Y., Yanagihara, K., Morohoshi, T., Morinaga, Y., Nakamura, S., et al. (2013). Efficacy of AiiM, an N-acylhomoserine lactonase, against *Pseudomonas aeruginosa* in a mouse model of acute pneumonia. *Antimicrob. Agents Chemother.* 57, 3653–3658. doi: 10.1128/AAC.00456-13
- Ming, D., Wang, D., Cao, F., Xiang, H., Mu, D., Cao, J., et al. (2017). Kaempferol inhibits the primary attachment phase of biofilm formation in *Staphylococcus aureus*. *Front. Microbiol.* 8:2263. doi: 10.3389/fmicb.2017.02263
- Miyairi, S., Tateda, K., Fuse, E. T., Ueda, C., Saito, H., Takabatake, T., et al. (2006). Immunization with 3-oxododecanoyl-L-homoserine lactone–protein conjugate protects mice from lethal *Pseudomonas aeruginosa* lung infection. *J. Med. Microbiol.* 55, 1381–1387. doi: 10.1099/jmm.0.46658-0
- Moshiri, J., Kaur, D., Hambira, C. M., Sandala, J. L., Koopman, J. A., Fuchs, J. R., et al. (2018). Identification of a small molecule anti-biofilm agent against *Salmonella enterica*. *Front. Microbiol.* 9:2804. doi: 10.3389/fmicb.2018.02804
- Mühlen, S., and Dersch, P. (2016). Anti-virulence strategies to target bacterial infections. *Curr. Top. Microbiol. Immunol.* 398, 147–183. doi: 10.1007/82_2015_490
- Müller, C., Birmes, F. S., Rückert, C., Kalinowski, J., and Fetzner, S. (2015). Rhodococcus erythropolis BG43 genes mediating *Pseudomonas aeruginosa* quinolone signal degradation and virulence factor attenuation. *Appl. Environ. Microbiol.* 22, 7720–7729. doi: 10.1128/AEM.02145-15
- Munguia, J., and Nizet, V. (2017). Pharmacological targeting of the host–pathogen interaction: alternatives to classical antibiotics to combat drug-resistant superbugs. *Trends Pharmacol. Sci.* 38, 473–488. doi: 10.1016/j.tips.2017.02.003
- Musovic, S., Oregaard, G., Kroer, N., and Sørensen, S. J. (2006). Cultivation-independent examination of horizontal transfer and host range of an IncP-1 plasmid among gram-positive and gram-negative bacteria indigenous to the barley rhizosphere. *Appl. Environ. Microbiol.* 72, 6687–6692. doi: 10.1128/AEM.00013-06
- Nuri, R., Shprung, T., and Shai, Y. (2015). Defensive remodeling: how bacterial surface properties and biofilm formation promote resistance to antimicrobial peptides. *Biochim. Biophys. Acta* 1848, 3089–3100. doi: 10.1016/j.bbmem.2015.05.022
- O'Brien, S., and Fothergill, J. L. (2017). The role of multispecies social interactions in shaping *Pseudomonas aeruginosa* pathogenicity in the cystic fibrosis lung. *FEMS Microbiol. Lett.* 364:fnx128. doi: 10.1093/femsle/fnx128
- O'Loughlin, C. T., Miller, L. C., Siryaporn, A., Drescher, K., Semmelhack, M. F., and Bassler, B. L. (2013). A quorum-sensing inhibitor blocks *Pseudomonas aeruginosa* virulence and biofilm formation. *Proc. Natl. Acad. Sci. U.S.A.* 110, 17981–17986. doi: 10.1073/pnas.1316981110
- O'Neill, J. (2016). *Tackling Drug-Resistant Infections Globally: Final Report and Recommendations*. HM Government and Wellcome Trust.
- Orazi, G., and O'Toole, G. A. (2017). *Pseudomonas aeruginosa* alters *Staphylococcus aureus* sensitivity to vancomycin in a biofilm model of cystic fibrosis infection. *MBio.* 8:e00873–17. doi: 10.1128/mBio.00873-17
- O'Reilly, M. C., and Blackwell, H. E. (2015). Structure-based design and biological evaluation of triphenyl scaffold-based hybrid compounds as hydrolytically stable modulators of a LuxR-Type quorum sensing receptor. *ACS Infect. Dis.* 2, 32–38. doi: 10.1021/acsinfectdis.5b00112
- O'Rourke, J. P., Daly, S. M., Triplett, K. D., Peabody, D., Chackerian, B., and Hall, P. R. (2014). Development of a mimotope vaccine targeting the *Staphylococcus aureus* quorum sensing pathway. *PLoS ONE* 9:e111198. doi: 10.1371/journal.pone.0111198
- Ortines, R. V., Liu, H., Cheng, L. L., Cohen, T. S., Lawlor, H., Gami, A., et al. (2018). Neutralizing alpha-toxin accelerates healing of *Staphylococcus aureus*-infected wounds in nondiabetic and diabetic mice. *Antimicrob. Agents Chemother.* 62:e02288–17. doi: 10.1128/AAC.02288-17
- Paczkowski, J. E., Mukherjee, S., McCready, A. R., Cong, J.-P., Aquino, C. J., Kim, H., et al. (2017). Flavonoids suppress *Pseudomonas aeruginosa* virulence through allosteric inhibition of quorum-sensing receptors. *J. Biol. Chem.* 292, 4064–4076. doi: 10.1074/jbc.M116.770552
- Palliyil, S., Downham, C., Broadbent, I., Charlton, K., and Porter, A. J. (2014). High-sensitivity monoclonal antibodies specific for homoserine lactones protect mice from lethal *Pseudomonas aeruginosa* infections. *Appl. Environ. Microbiol.* 80, 462–469. doi: 10.1128/AEM.02912-13
- Pan, J.-J., Solbiati, J. O., Ramamoorthy, G., Hillerich, B. S., Seidel, R. D., Cronan, J. E., et al. (2015a). Biosynthesis of squalene from farnesyl diphosphate in bacteria: three steps catalyzed by three enzymes. *ACS Central Sci.* 1, 77–82. doi: 10.1021/acscentsci.5b00115
- Pan, W., Fan, M., Wu, H., Melander, C., and Liu, C. (2015b). A new small molecule inhibits *Streptococcus mutans* biofilms *in vitro* and *in vivo*. *J. Appl. Microbiol.* 119, 1403–1411. doi: 10.1111/jam.12940
- Papaioannou, E., Wahjudi, M., Nadal-Jimenez, P., Koch, G., Sestroikromo, R., and Quax, W. J. (2009). Quorum-quenching acylase reduces the virulence of *Pseudomonas aeruginosa* in a *Caenorhabditis elegans* infection model. *Antimicrob. Agents Chemother.* 53, 4891–4897. doi: 10.1128/AAC.00380-09
- Papenfort, K., and Bassler, B. L. (2016). Quorum sensing signal–response systems in gram-negative bacteria. *Nat. Rev. Microbiol.* 14:576. doi: 10.1038/nrmicro.2016.89
- Park, J., Jagasia, R., Kaufmann, G. F., Mathison, J. C., Ruiz, D. I., Moss, J. A., et al. (2007). Infection control by antibody disruption of bacterial quorum sensing signaling. *Chem. Biol.* 14, 1119–1127. doi: 10.1016/j.chembiol.2007.08.013
- Park, S., Kim, H.-S., Ok, K., Kim, Y., Park, H.-D., and Byun, Y. (2015). Design, synthesis and biological evaluation of 4-(alkyloxy)-6-methyl-2H-pyran-2-one derivatives as quorum sensing inhibitors. *Bioorg. Med. Chem. Lett.* 25, 2913–2917. doi: 10.1016/j.bmcl.2015.05.054
- Passos da Silva, D., Schofield, M. C., Parsek, M. R., and Tseng, B. S. (2017). An update on the sociomicrobiology of quorum sensing in gram-negative biofilm development. *Pathogens* 6:51. doi: 10.3390/pathogens6040051
- Patil, P. C., Tan, J., Demuth, D. R., and Luzzio, F. A. (2016). 1, 2, 3-Triazole-based inhibitors of *Porphyromonas gingivalis* adherence to oral streptococci and biofilm formation. *Bioorg. Med. Chem.* 24, 5410–5417. doi: 10.1016/j.bmc.2016.08.059
- Pereira, C. S., Thompson, J. A., and Xavier, K. B. (2013). AI-2-mediated signalling in bacteria. *FEMS Microbiol. Rev.* 37, 156–181. doi: 10.1111/j.1574-6976.2012.00345.x
- Pérez-Gil, J., and Rodríguez-Concepción, M. (2013). Metabolic plasticity for isoprenoid biosynthesis in bacteria. *Biochem. J.* 452, 19–25. doi: 10.1042/BJ20121899
- Peterson, J. W. (1996). "Bacterial pathogenesis," in *Medical Microbiology*. 4th Edn. (University of Texas Medical Branch at Galveston).
- Piletska, E. V., Stavroulakis, G., Karim, K., Whitcombe, M. J., Chianella, I., Sharma, A., et al. (2010). Attenuation of *Vibrio fischeri* quorum sensing using rationally designed polymers. *Biomacromolecules* 11, 975–980. doi: 10.1021/bm901451j
- Piletska, E. V., Stavroulakis, G., Larcombe, L. D., Whitcombe, M. J., Sharma, A., Primrose, S., et al. (2011). Passive control of quorum sensing: prevention of *Pseudomonas aeruginosa* biofilm formation by imprinted polymers. *Biomacromolecules* 12, 1067–1071. doi: 10.1021/bm101410q
- Ping, O., Mao, S., Xuewen, H., Kaiyu, W., Zhongqiong, Y., Hualin, F., et al. (2017). Sclareol protects *Staphylococcus aureus*-induced lung cell injury via

- inhibiting alpha-hemolysin expression. *J. Microbiol. Biotechnol.* 27, 19–25. doi: 10.4014/jmb.1606.06039
- Ping, O., Ruixue, Y., Jiaqiang, D., Kaiyu, W., Jing, F., Yi, G., et al. (2018). Subinhibitory concentrations of prim-o-glucosylcimifugin decrease the expression of alpha-hemolysin in *Staphylococcus aureus* (USA300). *Evid. Based Complement. Alternat. Med.* 2018:7579808. doi: 10.1155/2018/7579808
- Poolman, B., Spitzer, J. J., and Wood, J. M. (2004). Bacterial osmosensing: roles of membrane structure and electrostatics in lipid-protein and protein-protein interactions. *Biochim. Biophys. Acta* 1666, 88–104. doi: 10.1016/j.bbame.2004.06.013
- Powers, M. E., Becker, R. E., Sailer, A., Turner, J. R., and Bubeck Wardenburg, J. (2015). Synergistic action of *Staphylococcus aureus* alpha-toxin on platelets and myeloid lineage cells contributes to lethal sepsis. *Cell Host Microbe* 17, 775–787. doi: 10.1016/j.chom.2015.05.011
- Pristovsek, P., and Kidric, J. (1999). Solution structure of polymyxins B and E and effect of binding to lipopolysaccharide: an NMR and molecular modeling study. *J. Med. Chem.* 42, 4604–4613. doi: 10.1021/jm991031b
- Puga, C., Rodríguez-López, P., Cabo, M., SanJose, C., and Orgaz, B. (2018). Enzymatic dispersal of dual-species biofilms carrying *Listeria monocytogenes* and other associated food industry bacteria. *Food Control* 94, 222–228. doi: 10.1016/j.foodcont.2018.07.017
- Pulido, D., Nogues, M. V., Boix, E., and Torrent, M. (2012). Lipopolysaccharide neutralization by antimicrobial peptides: a gambit in the innate host defense strategy. *J. Innate Immun.* 4, 327–336. doi: 10.1159/000336713
- Pustelny, C., Albers, A., Büldt-Karentzopoulos, K., Parschat, K., Chhabra, S. R., Cámara, M., et al. (2009). Dioxigenase-mediated quenching of quinolone-dependent quorum sensing in *Pseudomonas aeruginosa*. *Chem. Biol.* 16, 1259–1267. doi: 10.1016/j.chembiol.2009.11.013
- Quan, Y., Meng, F., Ma, X., Song, X., Liu, X., Gao, W., et al. (2017). Regulation of bacteria population behaviors by AI-2 “consumer cells” and “supplier cells”. *BMC Microbiol.* 17:198. doi: 10.1186/s12866-017-1107-2
- Quave, C. L., Lyles, J. T., Kavanaugh, J. S., Nelson, K., Parlet, C. P., Crosby, H. A., et al. (2015). *Castanea sativa* (European Chestnut) leaf extracts rich in ursene and oleanene derivatives block *Staphylococcus aureus* virulence and pathogenesis without detectable resistance. *PLoS ONE* 10:e0136486. doi: 10.1371/journal.pone.0136486
- Que, Y.-A., Hazan, R., Strobel, B., Maura, D., He, J., Kesarwani, M., et al. (2013). A quorum sensing small volatile molecule promotes antibiotic tolerance in bacteria. *PLoS ONE* 8:e80140. doi: 10.1371/journal.pone.0080140
- Radlinski, L., Rowe, S. E., Kartchner, L. B., Maile, R., Cairns, B. A., Vitko, N. P., et al. (2017). *Pseudomonas aeruginosa* exoproducts determine antibiotic efficacy against *Staphylococcus aureus*. *PLoS Biol.* 15:e2003981. doi: 10.1371/journal.pbio.2003981
- Rajamanikandan, S., Jeyakanthan, J., and Srinivasan, P. (2017a). Discovery of potent inhibitors targeting *Vibrio harveyi* LuxR through shape and e-pharmacophore based virtual screening and its biological evaluation. *Microb. Pathog.* 103, 40–56. doi: 10.1016/j.micpath.2016.12.003
- Rajamanikandan, S., Jeyakanthan, J., and Srinivasan, P. (2017b). Molecular docking, molecular dynamics simulations, computational screening to design quorum sensing inhibitors targeting LuxP of *Vibrio harveyi* and its biological evaluation. *Appl. Biochem. Biotechnol.* 181, 192–218. doi: 10.1007/s12010-016-2207-4
- Rajput, A., Thakur, A., Sharma, S., and Kumar, M. (2017). aBiofilm: a resource of anti-biofilm agents and their potential implications in targeting antibiotic drug resistance. *Nucleic Acids Res.* 46, D894–D900. doi: 10.1093/nar/gkx1157
- Ranfaing, J., Dunyach-Remy, C., Lavigne, J.-P., and Sotto, A. (2018). Propolis potentiates the effect of cranberry (*Vaccinium macrocarpon*) in reducing the motility and the biofilm formation of uropathogenic *Escherichia coli*. *PLoS ONE* 13:e0202609. doi: 10.1371/journal.pone.0202609
- Rasko, D. A., and Sperandio, V. (2010). Anti-virulence strategies to combat bacteria-mediated disease. *Nat. Rev. Drug Discov.* 9, 117–128. doi: 10.1038/nrd3013
- Ribeiro, S. M., Felício, M. R., Boas, E. V., Gonçalves, S., Costa, F. F., Samy, R. P., et al. (2016). New frontiers for anti-biofilm drug development. *Pharmacol. Ther.* 160, 133–144. doi: 10.1016/j.pharmthera.2016.02.006
- Rieger, U. M., Djedovic, G., Pattiss, A., Raschke, G. F., Frei, R., Pierer, G., et al. (2016). Presence of biofilms on polyurethane-coated breast implants: preliminary results. *J. Long Term Eff. Med. Implants* 26, 237–243. doi: 10.1615/JLongTermEffMedImplants.2016016851
- Rietschel, E. T., Brade, H., Holst, O., Brade, L., Müller-Loennies, S., Mamat, U., et al. (1996). Bacterial endotoxin: chemical constitution, biological recognition, host response, and immunological detoxification. *Curr. Top. Microbiol. Immunol.* 216, 39–81. doi: 10.1007/978-3-642-80186-0_3
- Rouha, H., Badarau, A., Visram, Z. C., Battles, M. B., Prinz, B., Magyarics, Z., et al. (2015). Five birds, one stone: neutralization of α -hemolysin and 4 bi-component leukocidins of *Staphylococcus aureus* with a single human monoclonal antibody. *MAbs* 7, 243–254. doi: 10.4161/19420862.2014.985132
- Roy, V., Fernandes, R., Tsao, C.-Y., and Bentley, W. E. (2010). Cross species quorum quenching using a native AI-2 processing enzyme. *ACS Chem. Biol.* 5, 223–232. doi: 10.1021/cb9002738
- Rudkin, J. K., McLoughlin, R. M., Preston, A., and Massey, R. C. (2017). Bacterial toxins: offensive, defensive, or something else altogether? *PLoS Pathog.* 13:e1006452. doi: 10.1371/journal.ppat.1006452
- Rybtke, M., Hultqvist, L. D., Givskov, M., and Tolker-Nielsen, T. (2015). *Pseudomonas aeruginosa* biofilm infections: community structure, antimicrobial tolerance and immune response. *J. Mol. Biol.* 427, 3628–3645. doi: 10.1016/j.jmb.2015.08.016
- Sahner, J. H., Empting, M., Kamal, A., Weidel, E., Groh, M., Börger, C., et al. (2015). Exploring the chemical space of ureidothiophene-2-carboxylic acids as inhibitors of the quorum sensing enzyme PqsD from *Pseudomonas aeruginosa*. *Eur. J. Med. Chem.* 96, 14–21. doi: 10.1016/j.ejmech.2015.04.007
- Schütz, C., and Empting, M. (2018). Targeting the *Pseudomonas* quinolone signal quorum sensing system for the discovery of novel anti-infective pathoblockers. *Beilstein J. Org. Chem.* 14, 2627–2645. doi: 10.3762/bjoc.14.241
- Schwalen, C. J., Feng, X., Liu, W., Bing, O., Ko, T. P., Shin, C. J., et al. (2017). Head-to-head prenyl synthases in pathogenic bacteria. *Chembiochem* 18, 985–991. doi: 10.1002/cbic.201700099
- Scoffone, V. C., Chiarelli, L. R., Makarov, V., Brackman, G., Israyilova, A., Azzalin, A., et al. (2016). Discovery of new diketopiperazines inhibiting Burkholderia cenocepacia quorum sensing *in vitro* and *in vivo*. *Sci. Rep.* 6:32487. doi: 10.1038/srep32487
- Sedlmayer, F., Hell, D., Müller, M., Ausländer, D., and Fussenegger, M. (2018). Designer cells programming quorum-sensing interference with microbes. *Nat. Commun.* 9:1822. doi: 10.1038/s41467-018-04223-7
- Shrestha, L., Kayama, S., Sasaki, M., Kato, F., Hisatsune, J., Tsuruda, K., et al. (2016). Inhibitory effects of antibiofilm compound 1 against *Staphylococcus aureus* biofilms. *Microbiol. Immunol.* 60, 148–159. doi: 10.1111/1348-0421.12359
- Silva, T., Freitas, A., Pinheiro, M., Watanabe, E., and Albuquerque, R. (2018). Oral biofilm formation on different materials for dental implants. *J. Visual. Exp.* 136:e57756. doi: 10.3791/57756
- Soukari, F., Vico Oton, E., Dubern, J.-F., Gomes, J., Halliday, N., de Pilar Crespo, M., et al. (2018). *In silico* and *in vitro*-guided identification of inhibitors of alkylquinolone-dependent quorum sensing in *pseudomonas aeruginosa*. *Molecules* 23:257. doi: 10.3390/molecules23020257
- Sousa, A. M., and Pereira, M. O. (2014). *Pseudomonas aeruginosa* diversification during infection development in cystic fibrosis lungs—a review. *Pathogens* 3, 680–703. doi: 10.3390/pathogens3030680
- Stalder, T., and Top, E. (2016). Plasmid transfer in biofilms: a perspective on limitations and opportunities. *NPJ Biofilms Microbiomes* 2:16022. doi: 10.1038/npjbiofilms.2016.22
- Stephens, M. D., Yodsanit, N., and Melander, C. (2016). Evaluation of ethyl N-(2-phenethyl) carbamate analogues as biofilm inhibitors of methicillin resistant *Staphylococcus aureus*. *Org. Biomol. Chem.* 14, 6853–6856. doi: 10.1039/C6OB00706F
- Stevens, A. M., Queneau, Y., Souler, L., Bodman, S. V., and Doutheau, A. (2010). Mechanisms and synthetic modulators of AHL-dependent gene regulation. *Chem. Rev.* 111, 4–27. doi: 10.1021/cr100064s
- Storz, M. P., Maurer, C. K., Zimmer, C., Wagner, N., Brengel, C., de Jong, J. C., et al. (2012). Validation of PqsD as an anti-biofilm target in *Pseudomonas aeruginosa* by development of small-molecule inhibitors. *J. Am. Chem. Soc.* 134, 16143–16146. doi: 10.1021/ja3072397
- Strahl, H., and Errington, J. (2017). Bacterial membranes: structure, domains, and function. *Annu. Rev. Microbiol.* 71, 519–538. doi: 10.1146/annurev-micro-102215-095630

- Sully, E. K., Malachowa, N., Elmore, B. O., Alexander, S. M., Femling, J. K., Gray, B. M., et al. (2014). Selective chemical inhibition of agr quorum sensing in *Staphylococcus aureus* promotes host defense with minimal impact on resistance. *PLoS Pathog.* 10:e1004174. doi: 10.1371/journal.ppat.1004174
- Sunder, A. V., Utari, P. D., Ramasamy, S., van Merkerk, R., Quax, W., and Pundel, A. (2017). Penicillin V acylases from gram-negative bacteria degrade N-acylhomoserine lactones and attenuate virulence in *Pseudomonas aeruginosa*. *Appl. Microbiol. Biotechnol.* 101, 2383–2395. doi: 10.1007/s00253-016-8031-5
- Suneby, E. G., Herndon, L. R., and Schneider, T. L. (2017). *Pseudomonas aeruginosa* LasR- DNA binding is directly inhibited by quorum sensing antagonists. *ACS Infect. Dis.* 3, 183–189. doi: 10.1021/acsinfecdis.6b00163
- Surewaard, B. G. J., Thanabalasuriar, A., Zeng, Z., Tkaczyk, C., Cohen, T. S., Bardoel, B. W., et al. (2018). alpha-toxin induces platelet aggregation and liver injury during *Staphylococcus aureus* sepsis. *Cell Host Microbe* 24, 271–284.e73. doi: 10.1016/j.chom.2018.06.017
- Taberner, L., Rodwell, V. W., and Stauffacher, C. V. (2003). Crystal structure of a statin bound to a class II HMG-CoA reductase. *J. Biol. Chem.* 278, 19933–19938. doi: 10.1074/jbc.M213006200
- Tal-Gan, Y., Ivancic, M., Cornilescu, G., Yang, T., and Blackwell, H. E. (2016). Highly stable, amide-bridged autoinducing peptide analogues that strongly inhibit the AgrC quorum sensing receptor in *Staphylococcus aureus*. *Angewandte Chem.* 128, 9059–9063. doi: 10.1002/ange.201602974
- Tam, J., Beilhart, G. L., Auger, A., Gupta, P., Therien, A. G., and Melnyk, R. A. (2015). Small molecule inhibitors of clostridium difficile toxin B-induced cellular damage. *Chem. Biol.* 22, 175–185. doi: 10.1016/j.chembiol.2014.12.010
- Tan, J., Patil, P. C., Luzzio, F. A., and Demuth, D. R. (2018). *In vitro* and *in vivo* activity of peptidomimetic compounds that target the periodontal pathogen *Porphyromonas gingivalis*. *Antimicrob. Agents Chemother.* 62:e00400-18. doi: 10.1128/AAC.00400-18
- Tang, F., Li, L., Meng, X., Li, B., Wang, C.-Q., Wang, S.-Q., et al. (2018). Inhibition of alpha-hemolysin expression by resveratrol attenuates *Staphylococcus aureus* virulence. *Microb. Pathog.* 127, 85–90. doi: 10.1016/j.micpath.2018.11.027
- Tang, K., Su, Y., Brackman, G., Cui, F., Zhang, Y., Shi, X., et al. (2015). MomL, a novel marine-derived N-acyl homoserine lactonase from *Muricauda olearia*. *Appl. Environ. Microbiol.* 81, 774–782. doi: 10.1128/AEM.02805-14
- Tareen, A. M., Lüder, C. G., Zautner, A. E., Groß, U., Heimesaat, M. M., Bereswill, S., et al. (2013). The *Campylobacter jejuni* Cj0268c protein is required for adhesion and invasion *in vitro*. *PLoS ONE* 8:e81069. doi: 10.1371/journal.pone.0081069
- Teng, Z., Shi, D., Liu, H., Shen, Z., Zha, Y., Li, W., et al. (2017). Lysionotin attenuates *Staphylococcus aureus* pathogenicity by inhibiting alpha-toxin expression. *Appl. Microbiol. Biotechnol.* 101, 6697–6703. doi: 10.1007/s00253-017-8417-z
- Thanissery, R., Zeng, D., Doyle, R. G., and Theriot, C. M. (2018). A small molecule-screening pipeline to evaluate the therapeutic potential of 2-aminoimidazole nucleobases against clostridium difficile. *Front. Microbiol.* 9:1206. doi: 10.3389/fmicb.2018.01206
- Thomann, A., de Mello Martins, A. G., Brengel, C., Empting, M., and Hartmann, R. W. (2016). Application of dual inhibition concept within looped autoregulatory systems toward antivirulence agents against *Pseudomonas aeruginosa* infections. *ACS Chem. Biol.* 11, 1279–1286. doi: 10.1021/acschembio.6b00117
- Tobert, J. A. (2003). Lovastatin and beyond: the history of the HMG-CoA reductase inhibitors. *Nat. Rev. Drug Discov.* 2:517. doi: 10.1038/nrd1112
- Todd, D. A., Parlet, C. P., Crosby, H. A., Malone, C. L., Heilmann, K. P., Horswill, A. R., et al. (2017). Signal biosynthesis inhibition with ambuic acid as a strategy to target antibiotic-resistant infections. *Antimicrob. Agents Chemother.* 61:e00263–17. doi: 10.1128/AAC.00263-17
- Tseng, B. S., Reichhardt, C., Merrihew, G. E., Araujo-Hernandez, S. A., Harrison, J. J., MacCoss, M. J., et al. (2018). A biofilm matrix-associated protease inhibitor protects *Pseudomonas aeruginosa* from proteolytic attack. *MBio.* 9:e00543–18. doi: 10.1128/mBio.00543-18
- Utari, P. D., Setroikromo, R., Melgert, B. N., and Quax, W. J. (2018). PvdQ quorum quenching acylase attenuates *Pseudomonas aeruginosa* virulence in a mouse model of pulmonary infection. *Front. Cell. Infection Microbiol.* 8:119. doi: 10.3389/fcimb.2018.00119
- Vale, P. F., McNally, L., Doeschl-Wilson, A., King, K. C., Popat, R., Domingo-Sananes, M. R., et al. (2016). Beyond killing can we find new ways to manage infection? *Evol. Med. Public Health* 2016, 148–157. doi: 10.1093/emph/eow012
- van der Poll, T., and Opal, S. M. (2008). Host-pathogen interactions in sepsis. *Lancet Infect. Dis.* 8, 32–43. doi: 10.1016/S1473-3099(07)70265-7
- Van Meervenne, E., Van Coillie, E., Kerckhof, F.-M., Devlieghere, F., Herman, L., De Gelder, L. S., et al. (2012). Strain-specific transfer of antibiotic resistance from an environmental plasmid to foodborne pathogens. *Biomed Res. Int.* 2012:834598. doi: 10.1155/2012/834598
- Vasquez, J. K., Tal-Gan, Y., Cornilescu, G., Tyler, K. A., and Blackwell, H. E. (2017). Simplified AIP-II peptidomimetics are potent inhibitors of *Staphylococcus aureus* AgrC quorum sensing receptors. *Chembiochem* 18, 413–423. doi: 10.1002/cbic.201600516
- Wang, J., Nong, X.-H., Amin, M., and Qi, S.-H. (2018a). Hygrocin C from marine-derived *Streptomyces* sp. SCSGAA 0027 inhibits biofilm formation in *Bacillus amyloliquefaciens* SCSGAB0082 isolated from South China Sea gorgonian. *Appl. Microbiol. Biotechnol.* 102, 1417–1427. doi: 10.1007/s00253-017-8672-z
- Wang, X., Thompson, C. D., Weidenmaier, C., and Lee, J. C. (2018b). Release of *Staphylococcus aureus* extracellular vesicles and their application as a vaccine platform. *Nat. Commun.* 9:1379. doi: 10.1038/s41467-018-03847-z
- Waters, C. M., and Bassler, B. L. (2005). Quorum sensing: cell-to-cell communication in bacteria. *Annu. Rev. Cell Dev. Biol.* 21, 319–346. doi: 10.1146/annurev.cellbio.21.012704.131001
- Watters, C., Fleming, D., Bishop, D., and Rumbaugh, K. (2016). “Host responses to biofilm,” in *Progress in Molecular Biology and Translational Science*, eds M. San Francisco, B. San Francisco (Elsevier), 193–239.
- Wei, X., Gao, J., Wang, F., Ying, M., Angsantikul, P., Kroll, A. V., et al. (2017). *In situ* capture of bacterial toxins for antivirulence vaccination. *Adv. Mater.* 29:1701644. doi: 10.1002/adma.201701644
- Welsh, M. A., Eibergen, N. R., Moore, J. D., and Blackwell, H. E. (2015). Small molecule disruption of quorum sensing cross-regulation in *Pseudomonas aeruginosa* causes major and unexpected alterations to virulence phenotypes. *J. Am. Chem. Soc.* 137, 1510–1519. doi: 10.1021/ja5110798
- WHO (2018). *Antibiotic Resistance [Online]*. Available: online at <http://www.who.int/news-room/fact-sheets/detail/antibiotic-resistance> (Accessed 16 september 2018).
- Wilding, E. I., Brown, J. R., Bryant, A. P., Chalker, A. F., Holmes, D. J., Ingraham, K. A., et al. (2000a). Identification, evolution, and essentiality of the mevalonate pathway for isopentenyl diphosphate biosynthesis in gram-positive cocci. *J. Bacteriol.* 182, 4319–4327. doi: 10.1128/JB.182.15.4319-4327.2000
- Wilding, E. I., Kim, D.-Y., Bryant, A. P., Gwynn, M. N., Lunsford, R. D., McDevitt, D., et al. (2000b). Essentiality, expression, and characterization of the class II 3-hydroxy-3-methylglutaryl coenzyme A reductase of *Staphylococcus aureus*. *J. Bacteriol.* 182, 5147–5152. doi: 10.1128/JB.182.18.5147-5152.2000
- Xiong, Y. Q., Willard, J., Yeaman, M. R., Cheung, A. L., and Bayer, A. S. (2006). Regulation of *Staphylococcus aureus* alpha-toxin gene (hla) expression by agr, sarA and sae *in vitro* and in experimental infective endocarditis. *J. Infect. Dis.* 194, 1267–1275. doi: 10.1086/508210
- Xu, W., Ping, O., Zhongwei, Y., Zhongqiong, Y., Hualin, F., Juchun, L., et al. (2018). Eriodictyol protects against *Staphylococcus aureus*-induced lung cell injury by inhibiting alpha-hemolysin expression. *World J. Microbiol. Biotechnol.* 34:64. doi: 10.1007/s11274-018-2446-3
- Yadav, M. K., Go, Y. Y., Chae, S.-W., and Song, J.-J. (2015). The small molecule dam inhibitor, pyrimidinedione, disrupts *Streptococcus pneumoniae* biofilm growth *in vitro*. *PLoS ONE* 10:e0139238. doi: 10.1371/journal.pone.0139238
- Yang, T., Tal-Gan, Y., Paharik, A. E., Horswill, A. R., and Blackwell, H. E. (2016). Structure-function analyses of a *Staphylococcus epidermidis* autoinducing peptide reveals motifs critical for AgrC-type receptor modulation. *ACS Chem. Biol.* 11, 1982–1991. doi: 10.1021/acschembio.6b00120
- Yepes, A., Schneider, J., Mielich, B., Koch, G., García-Betancur, J. C., Ramamurthi, K. S., et al. (2012). The biofilm formation defect of a *Bacillus subtilis* flotillin-defective mutant involves the protease FtsH. *Mol. Microbiol.* 86, 457–471. doi: 10.1111/j.1365-2958.2012.08205.x
- Zaslouff, M. (2002). Antimicrobial peptides of multicellular organisms. *Nature* 415, 389–395. doi: 10.1038/415389a
- Zhang, B., Teng, Z., Li, X., Lu, G., Deng, X., Niu, X., et al. (2017a). Chalcone attenuates *Staphylococcus aureus* virulence by targeting sortase A and alpha-hemolysin. *Front. Microbiol.* 8:1715. doi: 10.3389/fmicb.2017.01715
- Zhang, Y., Brackman, G., and Coenye, T. (2017b). Pitfalls associated with evaluating enzymatic quorum quenching activity: the case of MomL and its

- effect on *Pseudomonas aeruginosa* and *Acinetobacter baumannii* biofilms. *PeerJ* 5:e3251. doi: 10.7717/peerj.3251
- Zhang, Y., Sass, A., Van Acker, H., Wille, J., Verhasselt, B., Van Nieuwerburgh, F., et al. (2018). Coumarin reduces virulence and biofilm formation in *Pseudomonas aeruginosa* by affecting quorum sensing, type III secretion and c-di-GMP levels. *Front. Microbiol.* 9:1952. doi: 10.3389/fmicb.2018.01952
- Zivkovic, A., Sharif, O., Stich, K., Doninger, B., Biaggio, M., Colinge, J., et al. (2011). TLR 2 and CD14 mediate innate immunity and lung inflammation to staphylococcal Pantone-Valentine leukocidin *in vivo*. *J. Immunol.* 186, 1608–1617. doi: 10.4049/jimmunol.1001665
- Zuberi, A., Misba, L., and Khan, A. U. (2017). CRISPR interference (CRISPRi) inhibition of luxS gene expression in *E. coli*: an approach to inhibit biofilm. *Front. Cell. Infection Microbiol.* 7:214. doi: 10.3389/fcimb.2017.00214
- Zurek, O. W., Nygaard, T. K., Watkins, R. L., Pallister, K. B., Torres, V. J., Horswill, A. R., et al. (2014). The role of innate immunity in promoting SaeR/S-mediated virulence in *Staphylococcus aureus*. *J. Innate Immun.* 6, 21–30. doi: 10.1159/000351200
- Conflict of Interest Statement:** The authors declare that the research was conducted in the absence of any commercial or financial relationships that could be construed as a potential conflict of interest.

Copyright © 2019 Fleitas Martínez, Cardoso, Ribeiro and Franco. This is an open-access article distributed under the terms of the Creative Commons Attribution License (CC BY). The use, distribution or reproduction in other forums is permitted, provided the original author(s) and the copyright owner(s) are credited and that the original publication in this journal is cited, in accordance with accepted academic practice. No use, distribution or reproduction is permitted which does not comply with these terms.



Activity of a Synthetic Peptide Targeting MgtC on *Pseudomonas aeruginosa* Intramacrophage Survival and Biofilm Formation

Malika Moussouni^{1,2}, Pauline Nogaret^{1,2†}, Preeti Garai^{1,2†}, Bérengère Ize³, Eric Vivès⁴ and Anne-Béatrice Blanc-Potard^{1,2*}

¹ Laboratoire de Dynamique des Interactions Membranaires Normales et Pathologiques, Université Montpellier, Montpellier, France, ² CNRS, UMR5235, Montpellier, France, ³ Laboratoire d'Ingénierie des Systèmes Macromoléculaires, Institut de Microbiologie de la Méditerranée, CNRS & Aix-Marseille University of Marseille, Marseille, France, ⁴ Centre de Recherche en Biologie cellulaire de Montpellier, CNRS UMR 5237, Montpellier, France

OPEN ACCESS

Edited by:

Natalia V. Kirienco,
Rice University, United States

Reviewed by:

Ester Boix,
Autonomous University of Barcelona,
Spain
Olivier Lesouhaitier,
Université de Rouen, France
Cezar M. Khursigara,
University of Guelph, Canada

*Correspondence:

Anne-Béatrice Blanc-Potard
anne.blanc-potard@univ-montp2.fr

[†]These authors have contributed
equally to this work

Specialty section:

This article was submitted to
Clinical Microbiology,
a section of the journal
Frontiers in Cellular and Infection
Microbiology

Received: 20 December 2018

Accepted: 11 March 2019

Published: 02 April 2019

Citation:

Moussouni M, Nogaret P, Garai P, Ize B, Vivès E and Blanc-Potard A-B (2019) Activity of a Synthetic Peptide Targeting MgtC on *Pseudomonas aeruginosa* Intramacrophage Survival and Biofilm Formation. *Front. Cell. Infect. Microbiol.* 9:84. doi: 10.3389/fcimb.2019.00084

Antivirulence strategies aim to target pathogenicity factors while bypassing the pressure on the bacterium to develop resistance. The MgtC membrane protein has been proposed as an attractive target that is involved in the ability of several major bacterial pathogens, including *Pseudomonas aeruginosa*, to survive inside macrophages. In liquid culture, *P. aeruginosa* MgtC acts negatively on biofilm formation. However, a putative link between these two functions of MgtC in *P. aeruginosa* has not been experimentally addressed. In the present study, we first investigated the contribution of exopolysaccharides (EPS) in the intramacrophage survival defect and biofilm increase of *mgtC* mutant. Within infected macrophages, expression of EPS genes *psl* and *alg* was increased in a *P. aeruginosa* *mgtC* mutant strain comparatively to wild-type strain. However, the intramacrophage survival defect of *mgtC* mutant was not rescued upon introduction of *psl* or *alg* mutation, suggesting that MgtC intramacrophage role is unrelated to EPS production, whereas the increased biofilm formation of *mgtC* mutant was partially suppressed by introduction of *psl* mutation. We aimed to develop an antivirulence strategy targeting MgtC, by taking advantage of a natural antagonistic peptide, MgtR. Heterologous expression of *mgtR* in *P. aeruginosa* PAO1 was shown to reduce its ability to survive within macrophages. We investigated for the first time the biological effect of a synthetic MgtR peptide on *P. aeruginosa*. Exogenously added synthetic MgtR peptide lowered the intramacrophage survival of wild-type *P. aeruginosa* PAO1, thus mimicking the phenotype of an *mgtC* mutant as well as the effect of endogenously produced MgtR peptide. In correlation with this finding, addition of MgtR peptide to bacterial culture strongly reduced MgtC protein level, without reducing bacterial growth or viability, thus differing from classical antimicrobial peptides. On the other hand, the addition of exogenous MgtR peptide did not affect significantly biofilm formation, indicating an action toward EPS-independent phenotype rather than EPS-related phenotype. Cumulatively, our results show an antivirulence action of synthetic MgtR peptide, which may be more potent against acute infection, and provide a proof of concept for further exploitation of anti-*Pseudomonas* strategies.

Keywords: *Pseudomonas aeruginosa*, antivirulence strategy, MgtC, peptide, macrophage, EPS

INTRODUCTION

The increasing understanding of bacterial pathogenesis has revealed potential strategies to develop novel drugs against infectious bacteria (Heras et al., 2015; Hauser et al., 2016; Mühlen and Dersch, 2016; Dickey et al., 2017). Interference with bacterial virulence is a promising alternative approach or a complementary adjunct to traditional antimicrobial therapy. This approach does not mediate direct bacterial killing, at least *in vitro*, therefore it is thought to apply less selective pressure for resistance and better preserve microbiota. The MgtC membrane protein has been proposed as a suitable target for antivirulence strategies because it is a virulence factor conserved in several bacterial pathogens (Alix and Blanc-Potard, 2007; Belon and Blanc-Potard, 2016). MgtC, which was first described in *Salmonella enterica* serovar Typhimurium (*S. Typhimurium*), is a critical factor for the intramacrophage survival of various unrelated intracellular pathogens (*Salmonella* spp., *Mycobacterium tuberculosis*, *Brucella suis* and *Burkholderia cenocepacia*), as well as so-called extracellular pathogens that can transiently reside within cells (*Yersinia pestis*, *Pseudomonas aeruginosa*) (Blanc-Potard and Groisman, 1997; Buchmeier et al., 2000; Lavigne et al., 2005; Grabenstein et al., 2006; Maloney and Valvano, 2006; Belon et al., 2015).

The environmental bacterium and opportunistic human pathogen *P. aeruginosa* is responsible for a variety of acute infections and is a major cause of mortality in chronically infected cystic fibrosis (CF) patients. Due to the increasing number of antibiotic resistant clinical isolates, *P. aeruginosa* has been listed in the WHO top priority list for drug development (Tacconelli et al., 2018). The chronic infection of *P. aeruginosa* and its resistance to treatment is largely due to its ability to form biofilms, which relies on the production of exopolysaccharides (EPS), as reviewed by Klockgether and Tümmler (2017). Recent studies have highlighted the role of intracellular stages during *P. aeruginosa* infection, which may contribute to bacterial dissemination and *in vivo* resistance to antibiotics (Brannon et al., 2009; Buyck et al., 2013). In *P. aeruginosa*, *mgtC* expression is induced inside macrophages, which is consistent with its contribution to bacterial intramacrophage survival, and the *mgtC* mutant (in the PAO1 background) is attenuated in an acute model of infection in zebrafish embryos (Belon et al., 2015; Bernut et al., 2015). MgtC was also found to limit biofilm formation and EPS production in magnesium deprived medium, a condition known to activate *mgtC* transcription (Belon et al., 2015). Interestingly, MgtC has been shown to repress cellulose production in *S. Typhimurium*, which in turn promotes bacterial replication within macrophages (Pontes et al., 2015). Cellulose is not produced by *P. aeruginosa*, but these results suggested a potential link between the production of *P. aeruginosa* EPS and intramacrophage behavior (Belon et al., 2015; Bernut et al., 2015). Three polysaccharides, namely Psl, Pel and alginate, compose *P. aeruginosa* EPS (Wei and Ma, 2013), and contribute to the formation of biofilms (Ghafoor et al., 2011). Psl has a major contribution in biofilm formation, being required for adhesion of bacteria, which is critical for biofilm initiation, as well as maintenance of the biofilm structure. Pel is responsible for

pellicle formation on air-liquid interface and formation of solid surface-associated biofilms. Pel could function together with other EPS throughout biofilm development in *P. aeruginosa* PAO1, although in a less important way as compared to Psl (Yang et al., 2011). Alginate is the exopolysaccharide that is mainly produced by *P. aeruginosa* clinical isolates from the lungs of CF patients, where it plays important roles in structural stability and protection of biofilms. However, it is not absolutely required during the formation of non-mucoid biofilms *in vitro*, as shown for PAO1 strain (Wozniak et al., 2003).

Of interest in the context of an antivirulence approach, a natural peptide antagonistic to MgtC has been described. This peptide, called MgtR, is a very small membrane protein of 30 amino-acids (thus referred as peptide) identified in *S. Typhimurium*, where it promotes the degradation of the MgtC virulence factor by FtsH protease (Alix and Blanc-Potard, 2008; Lee and Groisman, 2010). MgtR is part of a novel class of regulatory molecules that can interact with membrane proteins and can subsequently act on the stability of these membrane proteins (Alix and Blanc-Potard, 2009; Lipka and Goulian, 2009; Wang et al., 2017). Overexpression of *mgtR* reduced intramacrophage survival of a wild-type *Salmonella* strain, thus indicating that MgtR can lower *Salmonella* virulence (Alix and Blanc-Potard, 2008). MgtR has been shown to directly interact with the *Salmonella* MgtC membrane protein (Alix and Blanc-Potard, 2008). Moreover, the *Salmonella* MgtR membrane peptide can also interact with MgtC protein from *M. tuberculosis* and *P. aeruginosa* (Belon et al., 2015, 2016). *M. tuberculosis* and all *P. aeruginosa* strains naturally lack *mgtR* gene, but ectopic expression of *Salmonella mgtR* in mycobacteria and *P. aeruginosa* mimicked the phenotypes reported for *mgtC* deletion mutants (Belon et al., 2015, 2016). Thus, these findings show an antivirulence action of MgtR upon endogenous production in several bacterial pathogens.

In the present study, we addressed the contribution of EPS to the phenotypes of *P. aeruginosa mgtC* mutant and investigated further an antivirulence strategy targeting MgtC on *P. aeruginosa*. We first investigated the contribution of individual EPS components (alginate, Psl and Pel) to the intramacrophage survival defect of *P. aeruginosa mgtC* mutant as well as biofilm formation. Then, studies with synthetic peptide added exogenously were carried out for the first time to further evaluate the efficiency of an antivirulence strategy based on MgtR. We investigated the biological effect of a synthetic MgtR peptide toward *P. aeruginosa* ability to survive inside macrophages and form biofilm.

MATERIALS AND METHODS

Bacterial Strains and Growth Conditions

Bacterial strains and plasmids are described in Table 1. *P. aeruginosa* strains are in the PAO1 background. *P. aeruginosa* was grown at 37°C in Luria broth (LB). Growth in magnesium-deprived medium was done in No-carbon essential (NCE)-minimal medium (28 mM KH₂PO₄, 28 mM K₂HPO₄·3H₂O, 16 mM NaNH₄HPO₄·4H₂O) supplemented with 0.1% casamino

TABLE 1 | Bacterial strains and plasmids used in the study.

Name	Description	References
PAO1	Wild-type	Laboratory collection
PAO1 Δ mgtC		Belon et al., 2015
PAO1 Δ alg8	alg8 deletion mutant	Periasamy et al., 2015
PAO1 Δ mgtC Δ psl	Δ mgtC Δ pslD	This study
PAO1 Δ mgtC Δ alg	Δ mgtC Δ alg8	This study
pRK2013	Tra ⁺ , Mob ⁺ , ColE1, KmR	Laboratory collection
pMF230	GFPmut2	Nivens et al., 2001
pKNG101	Suicide vector Sm ^R ; sacB ⁺	Kaniga et al., 1991
pKNGpslD	Δ pslD deletion in pKNG101	This study
pSBC44	Δ mgtC deletion in pKNG101	Belon et al., 2015

acids, 38 mM glycerol and 10 μ M MgSO₄ as described earlier (Rang et al., 2007). Plasmid pMF230 (constitutive GFP expression, obtained from Addgene) was introduced in *P. aeruginosa* by conjugation, using an *E. coli* strain containing pRK2013. Recombinant bacteria were selected on *Pseudomonas* isolation agar (PIA) containing carbenicillin at the concentration of 300 μ g/ml. Construction of *mgtC* *psl* and *mgtC* *alg* double mutant strains was done as described earlier (Belon et al., 2015) by allelic exchange of the *pslD* gene in *mgtC* mutant using a pKNG*pslD* suicide plasmid or allelic exchange of the *mgtC* gene in the *alg8* mutant (harboring a deletion of *alg* operon) using the pSBC44 suicide plasmid, respectively (Table 1).

Peptide Synthesis

MgtR peptide (MNRSPDKIIALIFLLISLLVLCLALWQIVF) was synthesized by a solid-phase method using the Fmoc methodology on an automated microwave peptide synthesizer (Liberty-1, CEM, Orsay, France) as previously described (Belon et al., 2016). H-Rink amide ChemMatrix resin (100 micromoles, substitution 0.37 mmol/g, Longjumeau, France) was used. The peptide was synthesized following a double-coupling step for each amino acid (400 micromoles) activated with TBTU (500 micromoles). Additionally an acetylation step was applied at the end of each amino-acid incorporation to prevent the formation of incomplete peptides. At the end of the assembly, the N-terminal Fmoc was kept on the peptide and the peptide/resin was stored at 4°C under inert atmosphere. When required, peptide/resin was treated to remove the Fmoc group, rinsed and dried under vacuum before the final deprotection procedure. The peptide/resin was then treated with 10 ml/g of cleavage cocktail (trifluoroacetic acid/triisopropylsilane/H₂O/1,2-ethanedithiol (94/1/2.5/2.5%: vol/vol) at room temperature for 90 min. The peptide was then precipitated with cold ether and centrifuged before resuspension in acetonitrile/water (30/70: vol/vol), freezing and freeze-drying. The final product was resuspended in isopropanol/water (50%/50%: vol/vol) without any purification and analyzed by MALDI-TOF mass spectrometry. The expected mass is 3,456.39 and the measured one was 3,456.78 ([MH]⁺). Circular dichroism spectra were recorded on a Jasco 810 (Japan) dichrograph in quartz suprasil cells (Hellma) with an optical path of 1 mm using 40 μ M peptide in 30% isopropanol with and

without SDS 4%. For experimentations, peptide was resuspended at a concentration of 3.2 mM in DMSO/water (50%/50%: vol/vol) and sonicated for 15 min before use. Using the same procedure, we also synthesized a scrambled peptide based on the amino-acid sequence of MgtR (permutation of the original peptide, ILFVADSLQMIPLCLRIWVVALKINILFSVL). The measured mass correlated with the expected one.

Infection of Macrophages and Quantification of Intracellular Bacteria

J774 cells (J774A.1) were maintained at 37°C in 5% CO₂ in Dulbecco's modified Eagle medium (DMEM) (Gibco) supplemented with 10% fetal bovine serum (FBS) (Gibco). The infection of J774 macrophages by *P. aeruginosa* was carried out essentially as described previously (Belon et al., 2015). Mid-log phase *P. aeruginosa* grown in LB broth was centrifuged and resuspended in PBS to infect J774 macrophages (5 × 10⁵ cells/well) at an MOI of 10. After 5 min centrifugation of the 24-well culture plate for synchronization of infection, bacterial phagocytosis was allowed to proceed for 25 min. Cells were washed three times with sterile PBS and fresh DMEM media supplemented with 400 μ g/ml gentamicin was added, which was retained throughout the infection. Macrophages were lysed after 20 min (T0) or 2 h (T1) of gentamicin treatment, by using 0.1% Triton X-100 and the number of viable bacteria was determined by subsequent plating onto LB agar plates. The percentage of survival was obtained by multiplying with 100 the ratio of the bacterial colony forming units (CFU) at T1 to that of T0.

RNA Extraction and Quantitative RT-PCR (qRT-PCR)

For bacterial RNA extraction from infected J774, 6.5 × 10⁶ macrophages were seeded into a 100 cm² tissue culture dish and infected at an MOI of 10 as described above. One hour after phagocytosis, cells were washed three times with PBS, lysed with 0.1% Triton X100 and pelleted by centrifugation at 13,000 rpm for 10 min at 15°C. Bacteria were resuspended in 500 μ l PBS and the non-resuspended cellular debris were discarded. 900 μ l of RNA protect reagent (Qiagen) was added and incubated for 5 min. The sample was centrifuged at 13,000 rpm for 10 min. Bacteria in the pellet were lysed with lysozyme and RNA was prepared with RNEasy kit (Qiagen). Superscript III reverse transcriptase (Invitrogen) was used for reverse transcription. Controls without reverse transcriptase were done on each RNA sample to rule out possible DNA contamination. Quantitative real-time PCR (Q-RT-PCR) was performed using a Light Cycler 480 SYBR Green I Master mix in a 480 Light Cycler instrument (Roche). PCR conditions were as follows: 3 min denaturation at 98°C, 45 cycles of 98°C for 5 s, 60°C for 10 s, and 72°C for 10 s. The sequences of primers used for RT-PCR are listed in Supplemental Table 1.

LDH Assay

The cytotoxicity of synthetic peptide was assessed by release of lactate dehydrogenase (LDH) using the Pierce LDH cytotoxicity assay kit (Thermo Scientific). Macrophages were seeded in a 96 well plate and treated with peptide (120 μ M) for 18 h. The assay

was performed on 50 μ l of the culture supernatant according to manufacturer's instructions. The percentage of LDH release was first normalized to that of the untreated control and then calculated relatively to that of untreated cells lysed with Triton X-100, which was set at 100% LDH release.

Biofilm Formation

Biofilm formation in LB medium was carried out in 96-well plate. Overnight culture of PAO1, grown in LB, was diluted 1:100 in LB and 200 μ l was aliquoted in 96-well plate in triplicates. Peptide was added at the concentration of 120 μ M and DMSO (2% final) was used as solvent control. The plate was incubated at 28°C for 48 h under static condition. After 48 h, culture was discarded and wells were washed with water. Biofilm appeared in the form of rings on the walls of the wells. Crystal Violet (CV) was added to each well to stain the biofilm for 15 min at room temperature. After staining, wells were washed with water to remove excess of CV and 70% ethanol was added to dissolve the stain. The dissolved stain was taken in a fresh plate to measure the absorbance at 570 nm.

Biofilm formation in low magnesium medium was carried out in glass tubes. Overnight culture of bacterial strains, grown in LB, was washed with NCE medium and diluted 1:20 into 500 μ l of NCE medium supplemented with 10 μ M Mg^{2+} in the glass tube. MgtR peptide was added at the concentration of 120 μ M and DMSO was used as solvent control. The glass tubes were incubated at 30°C for 24 h under static condition. Staining of biofilm ring with CV (0.1%) was quantified as described above. To measure bacterial viability, aliquots of bacterial culture and PBS-washed ring were diluted in PBS for CFU counting.

Preparation of Lysates From Bacterial Cultures Treated With Synthetic Peptide

Overnight culture of *P. aeruginosa* grown in LB medium was diluted 1:5 in LB and grown until OD_{600nm} of 0.8 to 1. Bacteria were washed in NCE medium (Blanc-Potard and Groisman, 1997) without magnesium and were resuspended in the same medium supplemented with 10 μ M Mg^{2+} and synthetic peptides (at the indicated concentration) or DMSO as control. Bacteria were harvested after 4–5 h of incubation at 37°C. To prepare whole-cell extracts, cultures were normalized to OD_{600nm}, centrifuged, re-suspended in Laemmli buffer and lysed by heating at 95°C for 10 min before performing Western Blot assay.

Preparation of Anti-PA4635 Antibodies

A DNA fragment encoding the C-terminal domain of MgtC (PA4635) was amplified using primers indicated in **Supplemental Table 1** and cloned into pQE30 vector (Qiagen). Recombinant plasmid was introduced into M15/pRep4 *E. coli* strain to express and purify the His-tagged recombinant protein as described (Alix and Blanc-Potard, 2008). Polyclonal antibodies were produced upon immunization of rabbit with the PA4635 C-ter domain (Eurogentec).

Western Blot Analysis

Total bacterial lysates were electrophoresed on 12.5% SDS-PAGE gels and transferred onto nitrocellulose membrane (Invitrogen) for immunoblotting. Rabbit anti-PA4635 were used at 1:2,000 dilution and Mouse anti-EF-Tu antibody (Ball et al., 2016) was used at 1:20,000 dilution. Anti-rabbit or anti-mouse antibodies (dilution 1:30,000) labeled with fluorescent dye DyLight 800 (Thermoscientific) were used for the detection of PA4635 and EF-Tu using LICOR Odyssey Fc Imaging System (excitation 783 nm and emission 797 nm) to quantify the amount of proteins.

RESULTS AND DISCUSSION

Contribution of EPS to the Intramacrophage Survival Defect and Biofilm Phenotype of *P. aeruginosa*

In vitro, *P. aeruginosa* PAO1 produces mainly Psl and Pel, whereas alginate synthesis is negatively regulated in this non-mucoidal strain by the anti-sigma factor of MucA (Schurr et al., 1996; Franklin et al., 2011). However, the expression of EPS genes has not been measured when PAO1 resides in macrophages. To address a putative link between the intramacrophage survival defect of *P. aeruginosa* *mgtC* mutant and EPS production, we first analyzed the level of expression of candidate individual EPS genes, *pelA*, *pslA*, and *algE*, in *P. aeruginosa* *mgtC* mutant and wild-type strain residing in J774 macrophages. Each of these genes is a part of the respective operons required for synthesis of Pel, Psl and alginate polysaccharides (Franklin et al., 2011). A significant increased expression of *pslA* and, to a lesser extent, *algE* was detected in *mgtC* mutant as compared to wild-type strain, whereas *pelA* expression remained unaltered (**Figure 1**), suggesting a higher production of Psl and alginate inside macrophages by *mgtC* mutant.

A *Salmonella* *mgtC* mutant has been reported to exhibit increased production of cellulose, another type of exopolysaccharide, inside macrophages, and the intramacrophage replication defect of the *Salmonella* *mgtC* mutant could be reversed by an additional mutation in the *bcsA* gene that prevented cellulose synthesis (Pontes et al., 2015). To investigate whether the intramacrophage survival defect of the *P. aeruginosa* *mgtC* mutant could be related to increased Psl or alginate production within macrophages, we constructed *mgtC pslD*, and *mgtC alg8* double mutants (see Materials and Methods), because *pslD* and *alg8* are essential for Psl and alginate synthesis, respectively (Remminghorst and Rehm, 2006; Byrd et al., 2009). No rescue in the survival inside macrophages was observed for *mgtC* mutant in the presence of *psl* or *alg* mutation (**Figure 2A**), indicating that the survival defect of *P. aeruginosa* *mgtC* mutant is not linked to increased production of Psl or alginate. Thus, despite the observed increased expression of *psl* and *alg* genes, EPS did not contribute to the intramacrophage phenotype of *P. aeruginosa* *mgtC* mutant. These findings differ from the results obtained in *S. Typhimurium* with *mgtC bcsA* double mutant (Pontes et al., 2015). In contrast to *P. aeruginosa*, *Salmonella* actively replicates inside macrophages, and increased

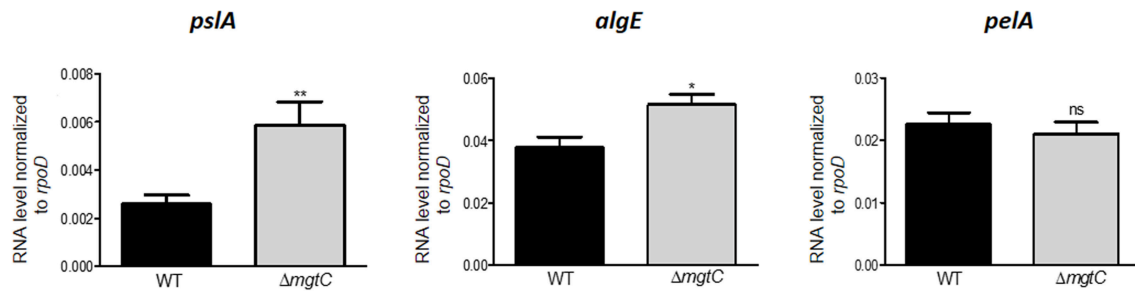


FIGURE 1 | Expression of EPS genes in *P. aeruginosa* strains residing in J774 macrophages. Expression of EPS genes in strains PAO1 wild-type (WT) and $\Delta mgtC$ mutant infecting J774 macrophages. RNA was extracted from bacteria isolated from infected macrophages 1 h after phagocytosis. The level of *pslA*, *algE*, and *pelA* transcripts relative to those of the house-keeping gene *rpoD* was measured by qRT-PCR and plotted on the Y-axis. Error bars correspond to standard errors from at least three independent experiments. The asterisks indicate *P*-values (Student's *t*-test **P* < 0.05, ***P* < 0.01), showing statistical significance with respect to WT.

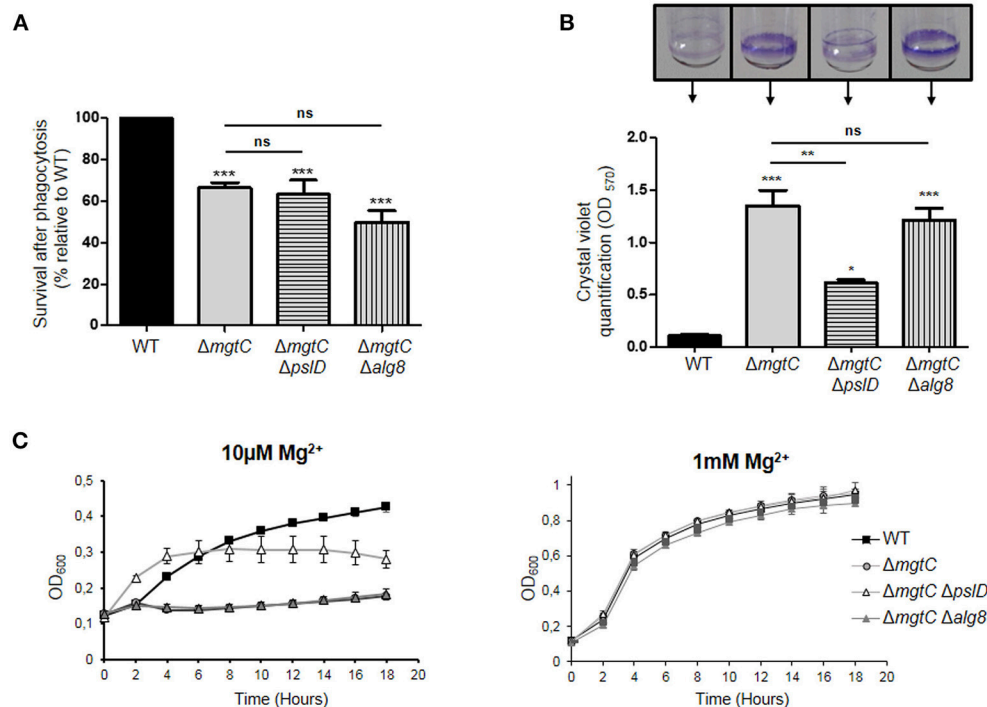


FIGURE 2 | Phenotypes of *mgtC pslD* and *mgtC alg8* double mutants. **(A)** Behavior of *mgtC pslD* and *mgtC alg8* double mutant within J774 macrophages. Survival of *P. aeruginosa* PAO1 WT, $\Delta mgtC$, $\Delta mgtC \Delta pslD$ and $\Delta mgtC \Delta alg8$ strains was assessed upon phagocytosis by J774 macrophages. Results are expressed as percentage of surviving bacteria 2 h after phagocytosis compared to the number of bacteria 20 min after phagocytosis and are normalized to 100% for WT strain. Error bars correspond to standard errors from four independent experiments. The asterisks indicate *P*-values (One-way ANOVA followed by a Bonferroni post-test. ****P* < 0.001). **(B)** Quantification of bacterial adherence to glass tubes to infer the ability of strains to form biofilm. *P. aeruginosa* strains PAO1 WT, $\Delta mgtC$, $\Delta mgtC \Delta pslD$, and $\Delta mgtC \Delta alg8$ were grown at 30°C for 24 h in NCE medium with 10 μ M $MgSO_4$. The biofilm quantification is visualized by CV ring on the glass tubes and CV is quantified at 570 nm. Error bars correspond to standard errors (+SE) from three independent experiments and the asterisks indicate *P*-values (One-way ANOVA followed by a Bonferroni post-test, **P* < 0.05, ***P* < 0.01, ****P* < 0.001). **(C)** Growth curve of *P. aeruginosa* strains PAO1, $\Delta mgtC$, $\Delta mgtC \Delta pslD$ and $\Delta mgtC \Delta alg8$ in NCE medium supplemented with 10 μ M (left panel) or 1 mM (right panel) $MgSO_4$. The results are expressed as the mean \pm SD of three independent experiments.

cellulose production may somehow contribute to the replication defect of *Salmonella mgtC* mutant within macrophages.

As reported earlier, the formation of biofilm was found to be significantly increased for *mgtC* mutant comparatively to wild-type strain in low magnesium medium (**Figure 2B**), a condition that induces expression of *mgtC* gene (Belon et al., 2015). The

formation of biofilm of *mgtC alg8* double mutant was identical to the one of *mgtC* mutant, whereas the biofilm formation was significantly reduced in *mgtC pslD* double mutant comparatively to *mgtC* mutant (**Figure 2B**). This finding correlated with the growth curves of the different strains in low magnesium (10 μ M) medium (**Figure 2C**), where growth of *mgtC* mutant

was impaired in low magnesium medium comparatively to wild-type strain, and presence of a *pslD* mutation, but not an *alg8* mutation, improved the growth of the *mgtC* mutant (Figure 2C). All strains grew similarly in medium supplemented with 1 mM magnesium (Figure 2C).

Non-mucoid *P. aeruginosa* strains, as PAO1, utilize primarily the Psl and Pel polysaccharides for biofilm formation, whereas alginate is the predominant extracellular polysaccharide of the matrix of mucoid strains (Wozniak et al., 2003). Our results indicate that Psl polysaccharide, which is known to be more important than Pel polysaccharide in *P. aeruginosa* PAO1 biofilm formation (Yang et al., 2011), contributes to the increased biofilm formation and impaired growth of *mgtC* mutant in magnesium deprived medium. The growth defect of the *mgtC* mutant in low magnesium medium is associated with the formation of bacterial aggregates both on the tube (at the air-liquid level) and within the culture, thus reminiscent of biofilm initiation. This is consistent with the contribution of Psl, which is known to be produced during planktonic growth, mediating attachment to surfaces and contributing to microcolony formation (Ghafoor et al., 2011).

Effect of Synthetic MgtR Peptide on Macrophage Survival of Wild-Type *P. aeruginosa* PAO1 Strain

P. aeruginosa naturally lacks *mgtR* gene, but ectopic expression of *Salmonella mgtR* in *P. aeruginosa* reduced intramacrophage survival, thus mimicking the phenotype reported for *mgtC* deletion mutant (Belon et al., 2015). To investigate the effect of exogenous addition of peptide, we added synthetic MgtR peptide to *P. aeruginosa*. The MgtR peptide, which harbors 73% of hydrophobic residues, is predicted to be organized in a single transmembrane helix (Figure 3A), which has been confirmed by an NMR structural analysis (Jean-Francois et al., 2014). MgtR was chemically synthesized using optimized protocol for hydrophobic peptides (see Materials and Methods) and the alpha-helical fold was verified by circular dichroism (Supplemental Figure S1). To address the effect of synthetic peptide on the ability of wild-type *P. aeruginosa* PAO1 strain to survive inside macrophages, bacteria were treated for 15 min, before phagocytosis, with 120 μ M of peptide solubilized in DMSO. Bacteria pretreated with DMSO were used as control. Phagocytosis by J774 macrophages was allowed for 30 min before removing extracellular bacteria with PBS washes and gentamicin treatment. The bacterial survival was then monitored for 2 h after phagocytosis. Bacteria treated with MgtR peptide had a significantly lower intramacrophage survival than bacteria treated with DMSO, which is in the same range as the one observed for *mgtC* mutant (Figure 3B). Interestingly, addition of MgtR peptide did not lower the survival of *mgtC* mutant, suggesting that the presence of MgtC plays a role in the biological activity of the synthetic peptide toward macrophage infection (Figure 3B). In the condition used, the MgtR peptide is not cytotoxic to J774 cells as shown by quantification of LDH release (Supplemental Figure S2). We designed and synthesized a scrambled peptide that contained the amino-acids of MgtR in a scrambled order, thus retaining the hydrophobicity, but

lacking a predicted membrane helix, as shown using the TMHMM program (Figure 3A). As expected, the scrambled peptide exhibited a circular dichroism spectra that differs from the one of MgtR, indicative of a loss of the alpha-helix structure (Supplemental Figure S1). Importantly, no significant decrease of intramacrophage survival was observed with this scrambled peptide used at 120 μ M (Figure 3C), suggesting that the biological effect of the synthetic MgtR peptide is somehow linked to sequence specificity and not only to overall hydrophobicity.

Intramacrophage survival assay with wild-type *P. aeruginosa* strain showed that addition of exogenous MgtR peptide mimics the phenotype of *mgtC* mutant as well as the effect previously reported upon endogenous expression of the peptide in PAO1, supporting a biological activity exhibited by this synthetic peptide. Moreover, this biological activity is linked to the presence of MgtC.

Effect of Synthetic MgtR Peptide on MgtC Protein Level, Bacterial Growth and Biofilm Formation With *P. aeruginosa* Wild-Type PAO1

To address the mechanism of action of MgtR peptide, we have conducted additional experiments upon addition of the peptide to *P. aeruginosa* bacterial cultures. Because endogenous MgtR peptide drives MgtC to degradation in *S. Typhimurium* (Alix and Blanc-Potard, 2008), we investigated the effect of synthetic MgtR peptide on the level of *P. aeruginosa* MgtC protein. Total lysates were prepared from bacteria grown in magnesium deprived medium, a condition that induces expression of *mgtC* gene (Belon et al., 2015), treated or not with peptide. Western blotting was carried out with anti-MgtC antibodies (see Materials and Methods). Hybridization with antibodies against EF-Tu were used as control (Ball et al., 2016). Addition of peptide to bacterial culture caused a decrease in the level of MgtC in a dose responsive manner, with the highest reduction at a final concentration of 120 μ M, whereas the level of EF-Tu control protein remained unchanged (Figure 4A). In contrast to MgtR, the scrambled peptide had only a minor effect on the level of MgtC protein (Figure 4B).

We also monitored the effect of MgtR on bacterial viability and growth, to determine whether MgtR behaves as the known antimicrobial peptides. The effect of MgtR on the level of MgtC protein is not related to an effect on bacterial viability in NCE medium (Figure 4C), which is consistent with the constant level of EF-Tu control protein. We have also shown that addition of MgtR peptide had no effect on bacterial growth in LB medium (Figure 4D), indicating that synthetic MgtR does not have a classical antibacterial effect.

We further investigated the effect of MgtR on the ability of *P. aeruginosa* to form biofilm. We first tested biofilm formation of PAO1 strain grown in LB medium. Addition of MgtR did not change significantly the ability of PAO1 to form biofilm (Figure 5A). Biofilm formation was also tested in magnesium deprived medium. As shown before, increased biofilm formation is seen with the *mgtC* mutant strain comparatively to wild-type strain, but no significant increase is detected upon

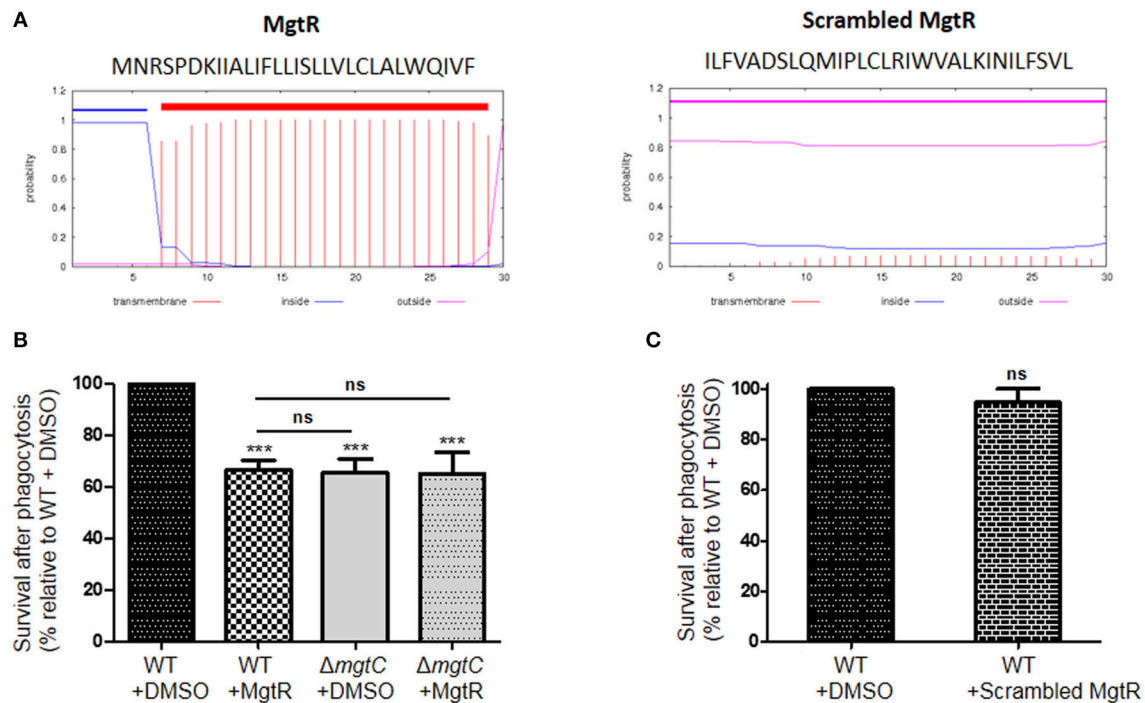


FIGURE 3 | Effect of synthetic MgtR peptide on *P. aeruginosa* intramacrophage survival. **(A)** Sequence and transmembrane helix prediction for MgtR and scrambled MgtR peptides, using TMHMM program (<http://www.cbs.dtu.dk/services/TMHMM/>). **(B)** To test the effect of synthetic MgtR peptide on *P. aeruginosa* intramacrophage survival, PAO1 WT strain was treated with 120 μ M of MgtR peptide or DMSO for 15 min before phagocytosis. A Δ mgtC mutant treated with DMSO or MgtR peptide (120 μ M) is used as control. Error bars correspond to standard errors (+SE) from at least four experiments. Statistical analysis was performed with one-way ANOVA followed by a Bonferroni post-test, *** $P < 0.001$. **(C)** To test the effect of synthetic scrambled MgtR peptide on *P. aeruginosa* intramacrophage survival, PAO1 WT strain was treated with 120 μ M of MgtR scrambled peptide or DMSO for 15 min before phagocytosis. Error bar corresponds to standard errors (+SE) from at least three experiments. Statistical analysis was performed with one-way ANOVA followed by a Bonferroni post-test.

addition of MgtR peptide to PAO1 strain in the condition tested (**Figure 5B**). Moreover, bacterial viability, in the ring or in the planktonic fraction, is not significantly modified in PAO1 treated with MgtR comparatively to non-treated bacteria (**Supplemental Figure S3**).

Cumulatively, we have shown that, in addition to reduce intramacrophage survival, the biological action of synthetic MgtR is associated with a decreased level of MgtC protein, without any effect on growth rate. Despite the decreased level of MgtC, the exogenous peptide had no effect on biofilm formation. A similar finding was found upon endogenous production of MgtR (**Supplemental Figure S4**). These results may indicate that the effect of MgtR is delayed upon long term phenotype, such as biofilm. We cannot exclude a deterioration of the peptide with time. In addition, or alternatively, MgtR may also act by preventing protein-protein interaction relevant for intramacrophage survival but not for biofilm formation.

CONCLUSION

Antivirulence strategies are being increasingly considered in the age of antibiotic resistance (Dickey et al., 2017) and we have previously proposed MgtC as a valuable target with a potent inhibitory peptide, MgtR. The function of MgtC has been mainly studied in *S. Typhimurium*, where it exhibits pleiotropic

roles, including inhibition of F_1F_o ATP synthase (Lee et al., 2013) and modulation of cellulose production (Pontes et al., 2015). Our results provide a link between *P. aeruginosa* MgtC and EPS production and show an implication of EPS, more specifically Psl, for the increased biofilm formation of *mgtC* mutant in magnesium deprived medium. However, EPS are not involved in the intramacrophage behavior of *P. aeruginosa mgtC* mutant, thus differing from the role reported for cellulose in the intracellular pathogen *S. Typhimurium*.

Our previous results indicated that endogenous production of MgtR lowered the intramacrophage survival of wild-type *P. aeruginosa* PAO1 strain (Belon et al., 2015). Using for the first time a synthetic MgtR peptide on PAO1 strain led to a similar effect, associated with a decrease of MgtC protein level, thus supporting the use of such peptide to target the MgtC virulence factor. MgtR did however not increase significantly biofilm formation, indicating an action towards EPS-independent phenotype rather than EPS-related phenotype. The lack of significant effect with a synthetic scrambled peptide derived from MgtR suggested that biological activity of synthetic MgtR peptide is somehow linked to sequence specificity and not to overall hydrophobicity. Hydrophobic compounds as MgtR remain difficult to handle and therefore improving peptide solubility, while keeping efficiency, will be valuable. The interest for peptides as new therapeutic molecules has recently increased

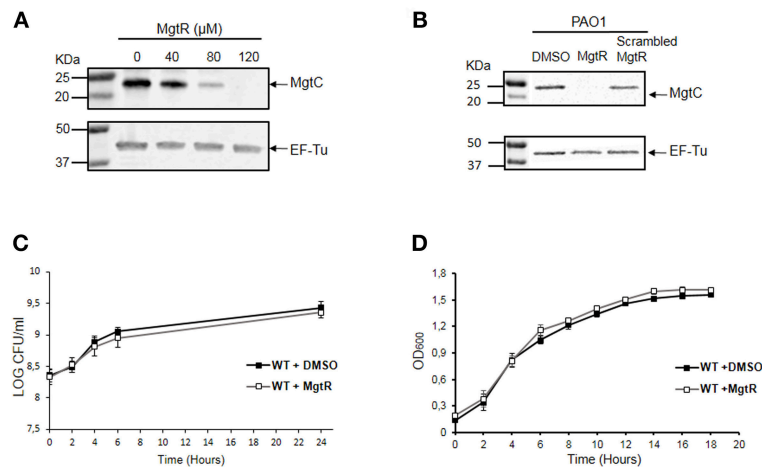


FIGURE 4 | Effect of synthetic MgtR peptide on the level of MgtC protein and on *P. aeruginosa* growth rate. **(A)** Effect of MgtR peptide on MgtC level is evaluated on total lysates of PAO1 WT bacteria incubated during 4 h with different concentrations of MgtR peptide in NCE medium supplemented with 10 μ M MgSO_4 . The membranes were probed with the anti-MgtC and anti-EF-Tu antibodies, as loading control. A representative experiment out of three independent experiments is shown. The quantified ratio PA4635/EF-Tu is 1, 0.95, 0.28, 0.01 for MgtR concentrations of 0, 40, 80, and 120 μ M, respectively. **(B)** Effect of a scrambled peptide derived from MgtR on the level of MgtC protein. PAO1 WT bacteria were grown for 1.5 h in NCE medium supplemented with 10 μ M MgSO_4 before addition of 120 μ M MgtR or 120 μ M scrambled MgtR and were incubated further for 5 h before harvesting total lysates for blotting. A representative experiment out of three independent experiments is shown. **(C)** Effect of MgtR peptide on bacterial viability in NCE medium. PAO1 WT strain was treated with 120 μ M MgtR and incubated in NCE medium supplemented with 10 μ M MgSO_4 for 24 h. At indicated time points, 10 μ l of the culture was collected and diluted on LB agar plate to quantify CFUs. The results are expressed as the mean \pm SD of three independent experiments. **(D)** Effect of MgtR peptide (120 μ M) on the bacterial growth of PAO1 WT in LB medium. The results are expressed as the mean \pm SD of three independent experiments.

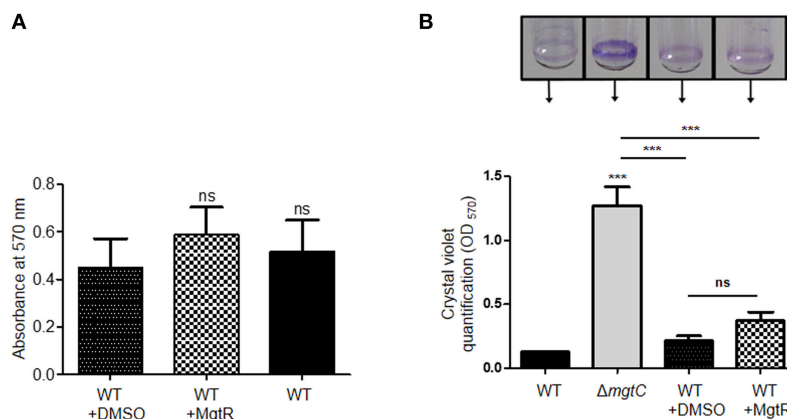


FIGURE 5 | Biofilm formation in the presence of synthetic MgtR peptide. **(A)** Quantification of bacterial adherence in LB medium. PAO1 WT strain was incubated with 120 μ M MgtR peptide or DMSO as control in LB and allowed to form biofilm at 28°C for 48 h in 96 well plate. Biofilm was stained with crystal violet and absorbance was measured at 570 nm. Statistical analysis was done on three independent experiments by one way ANOVA, where all samples were compared to DMSO using Dunnet's multiple comparison post-test, showing statistical significance with respect to DMSO control (ns > 0.05, non-significant). **(B)** Quantification of bacterial adherence to glass tubes in magnesium deprived medium. Adherence assay was carried out with PAO1 WT and Δ mgtC strains grown at 30°C for 24 h in NCE medium with 10 μ M MgSO_4 supplemented or not with 120 μ M MgtR peptide. The ring on the glass tube is visualized by crystal violet staining and quantified by measuring OD₅₇₀. Error bars correspond to standard errors (+SE) from three independent experiments and the asterisks indicate *P*-values (One-way ANOVA followed by a Bonferroni post-test, ****P* < 0.001).

(Kruger, 2017), and peptide modulators of protein-protein interaction in membranes are promising molecules (Stone and Deber, 2017). The present work thus identifies a synthetic hydrophobic peptide, issued from a natural bacterial peptide, which could limit bacterial pathogenesis and which differs from classical anti-microbial peptides (Mahlapuu et al., 2016) because of lack of effect on bacterial viability.

Further work will be required to decipher the mechanism of action of synthetic MgtR peptide. Our present results show that peptide addition is associated with a decreased level of MgtC protein but, as suggested earlier, MgtR may also prevent protein-protein interaction involving the MgtC protein (Belon et al., 2016). The lack of effect of MgtR peptide in the context of a *mgtC* mutant suggests that its biological effect is mainly related

to the presence of MgtC protein. Despite this finding and the absence of noticeable growth defect upon addition of MgtR, it would be of interest to test in a more general way the impact of synthetic MgtR on membrane fluidity and integrity. Interestingly, MgtR does not appear to modulate biofilm formation, suggesting that MgtR may act more specifically during acute infection than chronic infection. Given the proof of concept provided by our results on infected cells with PAO1 strain, further work will be required to test the efficiency of such peptide on *P. aeruginosa* clinical isolates and in an animal model of infection.

DATA AVAILABILITY

All datasets generated for this study are included in the manuscript and/or the **Supplementary Files**.

AUTHOR CONTRIBUTIONS

MM, PG, and A-BB-P conceived the project. MM, PN, PG, and A-BB-P designed and analyzed the experiments. MM, PN, and PG performed the experiments. BI performed construction of

double mutants and EV carried out peptide synthesis and circular dichroism analysis. MM, PG, and A-BB-P wrote the paper and all authors edited and approved the manuscript.

ACKNOWLEDGMENTS

We are grateful to Scott Rice (NTU, Singapore) and Sophie Bleves (Marseille, France) for providing strains. We are grateful to Pascal Verdié from the SynBio3 platform for providing peptide synthesis facilities, to Albert Meyer for performing MALDI spectrometry analysis, both from the Institut des Biomolécules Max Mousseron, Montpellier. This work is supported by Vaincre La Mucoviscidose (RIF20170502042) and Association Gregory Lemarchal. MM is supported by Vaincre La Mucoviscidose (RIF20170502042) and PG is supported by the Association Méditerranée Infection.

SUPPLEMENTARY MATERIAL

The Supplementary Material for this article can be found online at: <https://www.frontiersin.org/articles/10.3389/fcimb.2019.00084/full#supplementary-material>

REFERENCES

- Alix, E., and Blanc-Potard, A. B. (2007). MgtC: a key player in intramacrophage survival. *Trends Microbiol.* 15, 252–256. doi: 10.1016/j.tim.2007.03.007
- Alix, E., and Blanc-Potard, A. B. (2008). Peptide-assisted degradation of the *Salmonella* MgtC virulence factor. *EMBO J.* 27, 546–557. doi: 10.1038/sj.emboj.7601983
- Alix, E., and Blanc-Potard, A. B. (2009). Hydrophobic peptides: novel regulators within bacterial membrane. *Mol. Microbiol.* 72, 5–11. doi: 10.1111/j.1365-2958.2009.06626.x
- Ball, G., Antelmann, H., Imbert, P. R., Gimenez, M. R., Voulhoux, R., and Ize, B. (2016). Contribution of the twin arginine translocation system to the exoproteome of *Pseudomonas aeruginosa*. *Sci. Rep.* 6:27675. doi: 10.1038/srep27675
- Belon, C., and Blanc-Potard, A. B. (2016). Intramacrophage survival for extracellular bacterial pathogens: MgtC as a key adaptive factor. *Front. Cell. Infect. Microbiol.* 6:52. doi: 10.3389/fcimb.2016.00052
- Belon, C., Rosas Olvera, M., Vives, E., Kremer, L., Gannoun-Zaki, L., and Blanc-Potard, A. B. (2016). Use of the *Salmonella* MgtR peptide as an antagonist of the *Mycobacterium* MgtC virulence factor. *Future Microbiol.* 11, 215–225. doi: 10.2217/fmb.15.134
- Belon, C., Soscia, C., Bernut, A., Laubier, A., Bleves, S., and Blanc-Potard, A. B. (2015). A Macrophage subversion factor is shared by intracellular and extracellular pathogens. *PLoS Pathog.* 11:e1004969. doi: 10.1371/journal.ppat.1004969
- Bernut, A., Belon, C., Soscia, C., Bleves, S., and Blanc-Potard, A. B. (2015). Intracellular phase for an extracellular bacterial pathogen: MgtC shows the way. *Microb. Cell.* 2, 353–355. doi: 10.15698/mic2015.09.227
- Blanc-Potard, A. B., and Groisman, E. A. (1997). The *Salmonella* *selC* locus contains a pathogenicity island mediating intramacrophage survival. *EMBO J.* 16, 5376–5385. doi: 10.1093/emboj/16.17.5376
- Brannon, M. K., Davis, J. M., Mathias, J. R., Hall, C. J., Emerson, J. C., Crosier, P. S., et al. (2009). *Pseudomonas aeruginosa* type III secretion system interacts with phagocytes to modulate systemic infection of zebrafish embryos. *Cell. Microbiol.* 11, 755–768. doi: 10.1111/j.1462-5822.2009.01288.x
- Buchmeier, N., Blanc-Potard, A., Ehrh, S., Piddington, D., Riley, L., and Groisman, E. A. (2000). A parallel intraphagosomal survival strategy shared by *Mycobacterium tuberculosis* and *Salmonella enterica*. *Mol. Microbiol.* 35, 1375–1382. doi: 10.1046/j.1365-2958.2000.01797.x
- Buyck, J. M., Tulkens, P. M., and Van Bambeke, F. (2013). Pharmacodynamic evaluation of the intracellular activity of antibiotics towards *Pseudomonas aeruginosa* PAO1 in a model of THP-1 human monocytes. *Antimicrob. Agents Chemother.* 57, 2310–2318. doi: 10.1128/AAC.02609-12
- Byrd, M. S., Sadovskaya, I., Vinogradov, E., Lu, H., Sprinkle, A. B., Richardson, S. H., et al. (2009). Genetic and biochemical analyses of the *Pseudomonas aeruginosa* Psl exopolysaccharide reveal overlapping roles for polysaccharide synthesis enzymes in Psl and LPS production. *Mol. Microbiol.* 73, 622–638. doi: 10.1111/j.1365-2958.2009.06795.x
- Dickey, S. W., Cheung, G. Y. C., and Otto, M. (2017). Different drugs for bad bugs: antivirulence strategies in the age of antibiotic resistance. *Nat. Rev. Drug Discov.* 16, 457–471. doi: 10.1038/nrd.2017.23
- Franklin, M. J., Nivens, D. E., Weadge, J. T., and Howell, P. L. (2011). Biosynthesis of the *Pseudomonas aeruginosa* extracellular polysaccharides, Alginate, Pel, and Psl. *Front. Microbiol.* 2:167. doi: 10.3389/fmicb.2011.00167
- Ghafoor, A., Hay, I. D., and Rehm, B. H. (2011). Role of exopolysaccharides in *Pseudomonas aeruginosa* biofilm formation and architecture. *Appl. Environ. Microbiol.* 77, 5238–5246. doi: 10.1128/AEM.00637-11
- Grabenstein, J. P., Fukuto, H. S., Palmer, L. E., and Bliska, J. B. (2006). Characterization of phagosome trafficking and identification of PhoP-regulated genes important for survival of *Yersinia pestis* in macrophages. *Infect. Immun.* 74, 3727–3741. doi: 10.1128/IAI.00255-06
- Hauser, A. R., Meccas, J., and Moir, D. T. (2016). Beyond antibiotics: new therapeutic approaches for bacterial infections. *Clin. Infect. Dis.* 63, 89–95. doi: 10.1093/cid/ciw200
- Heras, B., Scanlon, M. J., and Martin, J. L. (2015). Targeting virulence not viability in the search for future antibacterials. *Br. J. Clin. Pharmacol.* 79, 208–215. doi: 10.1111/bcp.12356
- Jean-Francois, F. L., Dai, J., Yu, L., Myrick, A., Rubin, E., Fajer, P. G., et al. (2014). Binding of MgtR, a *Salmonella* transmembrane regulatory peptide, to MgtC, a *Mycobacterium tuberculosis* virulence factor: a structural study. *J. Mol. Biol.* 426, 436–446. doi: 10.1016/j.jmb.2013.10.014
- Kaniga, K., Delor, I., and Cornelis, G. R. (1991). A wide-host-range suicide vector for improving reverse genetics in gram-negative bacteria: inactivation of the *blaA* gene of *Yersinia enterocolitica*. *Gene.* 109, 137–141. doi: 10.1016/0378-1119(91)90599-7

- Klockgether, J., and Tümmler, B. (2017). Recent advances in understanding *Pseudomonas aeruginosa* as a pathogen. *F1000Res.* 6:1261. doi: 10.12688/f1000research.10506.1
- Kruger, R. P. (2017). The coming peptide tidal wave. *Cell.* 171:497. doi: 10.1016/j.cell.2017.10.010
- Lavigne, J. P., O'Callaghan, D., and Blanc-Potard, A. B. (2005). Requirement of MgtC for *Brucella suis* intramacrophage growth: a potential mechanism shared by *Salmonella enterica* and *Mycobacterium tuberculosis* for adaptation to a low-Mg²⁺ environment. *Infect. Immun.* 73, 3160–3163. doi: 10.1128/IAI.73.5.3160-3163.2005
- Lee, E. J., and Groisman, E. A. (2010). An antisense RNA that governs the expression kinetics of a multifunctional virulence gene. *Mol. Microbiol.* 76, 1020–1033. doi: 10.1111/j.1365-2958.2010.07161.x
- Lee, E. J., Pontes, M. H., and Groisman, E. A. (2013). A bacterial virulence protein promotes pathogenicity by inhibiting the bacterium's own F1Fo ATP synthase. *Cell.* 154, 146–156. doi: 10.1016/j.cell.2013.06.004
- Lippa, A. M., and Goulian, M. (2009). Feedback inhibition in the PhoQ/PhoP signaling system by a membrane peptide. *PLoS Genet.* 5:e1000788. doi: 10.1371/journal.pgen.1000788
- Mahlpuu, M., Håkansson, J., Ringstad, L., and Björn, C. (2016). Antimicrobial peptides: an emerging category of therapeutic agents. *Front. Cell. Infect. Microbiol.* 6:194. doi: 10.3389/fcimb.2016.00194
- Maloney, K. E., and Valvano, M. A. (2006). The *mgtC* gene of *Burkholderia cenocepacia* is required for growth under magnesium limitation conditions and intracellular survival in macrophages. *Infect. Immun.* 74, 5477–5486. doi: 10.1128/IAI.00798-06
- Mühlen, S., and Dersch, P. (2016). Anti-virulence strategies to target bacterial infections. *Curr. Top. Microbiol. Immunol.* 398, 147–183. doi: 10.1007/82_2015_490
- Nivens, D. E., Ohman, D. E., Williams, J., and Franklin, M. J. (2001). Role of alginate and its O acetylation in formation of *Pseudomonas aeruginosa* microcolonies and biofilms. *J. Bacteriol.* 183, 1047–1057. doi: 10.1128/JB.183.3.1047-1057.2001
- Periasamy, S., Nair, H. A., Lee, K. W., Ong, J., Goh, J. Q., Kjelleberg, S., et al. (2015). *Pseudomonas aeruginosa* PAO1 exopolysaccharides are important for mixed species biofilm community development and stress tolerance. *Front. Microbiol.* 6:851. doi: 10.3389/fmicb.2015.00851
- Pontes, M. H., Lee, E. J., Choi, J., and Groisman, E. A. (2015). *Salmonella* promotes virulence by repressing cellulose production. *Proc. Natl. Acad. Sci. U.S.A.* 112, 5183–5188. doi: 10.1073/pnas.1500989112
- Rang, C., Alix, E., Felix, C., Heitz, A., Tasse, L., and Blanc-Potard, A. B. (2007). Dual role of the MgtC virulence factor in host and non-host environments. *Mol. Microbiol.* 63, 605–622. doi: 10.1111/j.1365-2958.2006.05542.x
- Remminghorst, U., and Rehm, B. H. (2006). *In vitro* alginate polymerization and the functional role of Alg8 in alginate production by *Pseudomonas aeruginosa*. *Appl. Environ. Microbiol.* 72, 298–305. doi: 10.1128/AEM.72.1.298-305.2006
- Schurr, M. J., Yu, H., Martinez-Salazar, J. M., Boucher, J. C., and Deretic, V. (1996). Control of AlgU, a member of the sigma E-like family of stress sigma factors, by the negative regulators MucA and MucB and *Pseudomonas aeruginosa* conversion to mucoidy in cystic fibrosis. *J. Bacteriol.* 178, 4997–5004. doi: 10.1128/jb.178.16.4997-5004.1996
- Stone, T. A., and Deber, C. M. (2017). Therapeutic design of peptide modulators of protein-protein interactions in membranes. *Biochim. Biophys. Acta.* 1859, 577–585. doi: 10.1016/j.bbame.2016.08.013
- Tacconelli, E., Carrara, E., Savoldi, A., Harbarth, S., Mendelson, M., Monnet, D. L., et al. (2018). Discovery, research, and development of new antibiotics: the WHO priority list of antibiotic-resistant bacteria and tuberculosis. *Lancet Infect. Dis.* 18, 318–327. doi: 10.1016/S1473-3099(17)30753-3
- Wang, H., Yin, X., Wu Orr, M., Dambach, M., Curtis, R., and Storz, G. (2017). Increasing intracellular magnesium levels with the 31-amino acid MgtS protein. *Proc. Natl. Acad. Sci. U.S.A.* 114, 5689–5694. doi: 10.1073/pnas.1703415114
- Wei, Q., and Ma, L. Z. (2013). Biofilm matrix and its regulation in *Pseudomonas aeruginosa*. *Int. J. Mol. Sci.* 14, 20983–21005. doi: 10.3390/ijms141020983
- Wozniak, D. J., Wyckoff, T. J., Starkey, M., Keyser, R., Azadi, P., O'Toole, G. A., et al. (2003). Alginate is not a significant component of the extracellular polysaccharide matrix of PA14 and PAO1 *Pseudomonas aeruginosa* biofilms. *Proc. Natl. Acad. Sci. U.S.A.* 100, 7907–7912. doi: 10.1073/pnas.1231792100
- Yang, L., Hu, Y., Liu, Y., Zhang, J., Ulstrup, J., and Molin, S. (2011). Distinct roles of extracellular polymeric substances in *Pseudomonas aeruginosa* biofilm development. *Environ. Microbiol.* 13, 1705–1717. doi: 10.1111/j.1462-2920.2011.02503.x

Conflict of Interest Statement: The authors declare that the research was conducted in the absence of any commercial or financial relationships that could be construed as a potential conflict of interest.

Copyright © 2019 Moussouni, Nogaret, Garai, Ize, Vivès and Blanc-Potard. This is an open-access article distributed under the terms of the Creative Commons Attribution License (CC BY). The use, distribution or reproduction in other forums is permitted, provided the original author(s) and the copyright owner(s) are credited and that the original publication in this journal is cited, in accordance with accepted academic practice. No use, distribution or reproduction is permitted which does not comply with these terms.



Application of Antimicrobial Peptides of the Innate Immune System in Combination With Conventional Antibiotics—A Novel Way to Combat Antibiotic Resistance?

Maria S. Zharkova¹, Dmitriy S. Orlov¹, Olga Yu. Golubeva², Oleg B. Chakchir³, Igor E. Eliseev³, Tatyana M. Grinchuk⁴ and Olga V. Shamova^{1*}

¹ Laboratory of Design and Synthesis of Biologically Active Peptides, Department of General Pathology and Pathophysiology, FSBSI Institute of Experimental Medicine, Saint Petersburg, Russia, ² Laboratory of Nanostructures Research, Institute of Silicate Chemistry of the Russian Academy of Sciences, Saint Petersburg, Russia, ³ Nanobiotechnology Laboratory, Saint Petersburg National Research Academic University of the Russian Academy of Science, Saint Petersburg, Russia, ⁴ Laboratory of Intracellular Signaling, Institute of Cytology of the Russian Academy of Science, Saint Petersburg, Russia

OPEN ACCESS

Edited by:

Natalia V. Kirienko,
Rice University, United States

Reviewed by:

George Sakoulas,
University of California, San Diego,
United States
Wojciech Kamysz,
Medical University of Gdansk, Poland
Emilia Bagnicka,
Institute of Genetics and Animal
Breeding (PAS), Poland

*Correspondence:

Olga V. Shamova
oshamova@yandex.ru

Specialty section:

This article was submitted to
Clinical Microbiology,
a section of the journal
Frontiers in Cellular and Infection
Microbiology

Received: 10 November 2018

Accepted: 10 April 2019

Published: 30 April 2019

Citation:

Zharkova MS, Orlov DS, Golubeva OY, Chakchir OB, Eliseev IE, Grinchuk TM and Shamova OV (2019) Application of Antimicrobial Peptides of the Innate Immune System in Combination With Conventional Antibiotics—A Novel Way to Combat Antibiotic Resistance? *Front. Cell. Infect. Microbiol.* 9:128. doi: 10.3389/fcimb.2019.00128

Rapidly growing resistance of pathogenic bacteria to conventional antibiotics leads to inefficiency of traditional approaches of countering infections and determines the urgent need for a search of fundamentally new anti-infective drugs. Antimicrobial peptides (AMPs) of the innate immune system are promising candidates for a role of such novel antibiotics. However, some cytotoxicity of AMPs toward host cells limits their active implementation in medicine and forces attempts to design numerous structural analogs of the peptides with optimized properties. An alternative route for the successful AMPs introduction may be their usage in combination with conventional antibiotics. Synergistic antibacterial effects have been reported for a number of such combinations, however, the molecular mechanisms of the synergy remain poorly understood and little is known whether AMPs cytotoxicity for the host cells increases upon their application with antibiotics. Our study is directed to examination of a combined action of natural AMPs with different structure and mode of action (porcine protegrin 1, caprine bactenecin ChBac3.4, human alpha- and beta-defensins (HNP-1, HNP-4, hBD-2, hBD-3), human cathelicidin LL-37), and egg white lysozyme with varied antibiotic agents (gentamicin, ofloxacin, oxacillin, rifampicin, polymyxin B, silver nanoparticles) toward selected bacteria, including drug-sensitive and drug-resistant strains, as well as toward some mammalian cells (human erythrocytes, PBMC, neutrophils, murine peritoneal macrophages and Ehrlich ascites carcinoma cells). Using “checkerboard titrations” for fractional inhibitory concentration indexes evaluation, it was found that synergy in antibacterial action mainly occurs between highly membrane-active AMPs (e.g., protegrin 1, hBD-3) and antibiotics with intracellular targets (e.g., gentamicin, rifampicin), suggesting bioavailability increase as the main model of such interaction. In some combinations modulation of dynamics of AMP-bacterial membrane interaction in presence of the antibiotic was also shown. Cytotoxic effects of the same combinations toward normal eukaryotic cells were rarely synergistic. The obtained data approve that

combined application of antimicrobial peptides with antibiotics or other antimicrobials is a promising strategy for further development of new approach for combating antibiotic-resistant bacteria by usage of AMP-based therapeutics. Revealing the conventional antibiotics that increase the activity of human endogenous AMPs against particular pathogens is also important for cure strategies elaboration.

Keywords: antimicrobial peptides, synergy, antibiotics, drug-resistant bacteria, antibacterial activity

INTRODUCTION

The XX century was marked by the undeniable success in the field of treatment and prophylactics of the infectious diseases. However, the spread of the drug resistance amongst pathogenic microbes poses a serious threat to the existing medical doctrine founded on the effective use of antibiotics (Rossolini et al., 2014; Ventola, 2015a). Said phenomenon endangers not only the successful cure of the infections caused by the resistant pathogens *per se*, but the whole spectrum of therapeutic procedures associated with the risk of infectious complications, including surgery, chemotherapy, etc. (Ventola, 2015a). The gravity of the problem at hand is publicly acknowledged worldwide. Thus, in 2015 the Global Action Plan on antimicrobial resistance (World Health Organization, 2015) was endorsed at the Sixty-eighth World Health Assembly. Necessary measures which must be taken in the face of the growing danger of antimicrobial resistance include different scientific, social, and economic aspects, but the development of new compounds or non-traditional methods effective against multidrug-resistant microorganisms is still the cornerstone of the whole strategy (World Health Organization, 2015).

Antimicrobial peptides (AMPs), evolutionary ancient and conservative tools of the innate immune system providing immediate response to the large set of various pathogens (Wiesner and Vilcinskas, 2010), are seen as promising candidates for the development of novel antibiotics (Gordon et al., 2005; Guaní-Guerra et al., 2010; Mahlapuu et al., 2016). These peptides are stored in granules of phagocytic cells and exert their effects in phagolysosomes or being secreted extracellularly; they are also widely expressed and released at epithelial surfaces and in a site of inflammation (Zasloff, 2002; Tosi, 2005; Maróti et al., 2011; Gallo and Hooper, 2012). AMPs remarkably differ in amino acid sequence and structure, but most of them are cationic and they can adopt an amphipathic conformation, thus, they are able to easily interact with the negatively charged components on the surface of bacterial cells and integrate into the lipid bilayers (Phoenix et al., 2013; Haney et al., 2017). The main mechanism of antibacterial action of AMPs is related with their ability to alter membrane permeability and damage its structure (Hancock and Rozek, 2002; Teixeira et al., 2012). This process is accompanied by the leakage of vital components, ions, and metabolites. Membrane destabilization additionally affects functioning of membrane-associated protein complexes (Nguyen et al., 2011; Wilmes et al., 2011). Some AMPs are non-membranolytic and penetrate bacterial membranes without disturbing their integrity. They have intracellular targets and

interfere with the metabolic processes, including synthesis of the vitally important cell components (Brogden, 2005; Hale and Hancock, 2007; Le et al., 2017). Wide-scale multitargeted action is believed to be one of the reasons for the effectiveness of AMPs toward multidrug-resistant bacterial strains and an obstacle for the development of a high resistance level to such compounds (Wimley, 2010; Guilhelmelli et al., 2013; LaRock and Nizet, 2015). Overall, the beneficial features of AMPs are their broad spectrum of activity, swift, and effective bacterial killing that also complicates the resistance development, and possible additional effects such as immunomodulation (Mansour et al., 2014) and wound healing promotion (Ramanathan et al., 2002; Carretero et al., 2008; Pfalzgraff et al., 2018) demonstrated for certain peptides.

Combined use of antimicrobials, in particular those with different targets, is a known strategy to overcome multiple drug resistance (Pillai et al., 2005; Zimmerman et al., 2007; Turnidge, 2014; Ventola, 2015b). It also allows reducing the dosages, attenuating side effects and enhancing selectivity of compounds (Chou, 2006). The concept of combined use comes even more naturally concerning the AMPs, as in many tissues these compounds are expressed together in certain groups and are shown to possess synergy with each other (Chen et al., 2005; Dale and Fredericks, 2005; Lai and Gallo, 2009; Marxer et al., 2016). Such synergy is believed to be one of the keys to their successfulness in combating different resistance mechanisms invented by pathogenic bacteria during the long evolutionary coexistence with the immune system of the host (Guilhelmelli et al., 2013; LaRock and Nizet, 2015). So, the combined use of AMPs with other antimicrobials such as conventional antibiotics definitely has potential to increase the effectiveness of both groups of compounds.

It is also noted that the high efficacy of individual antimicrobial agent *in vivo* may be in fact caused by a synergistic interaction with the antimicrobial peptides of the organism (Knappe et al., 2016). And vice versa, it is of interest to identify drugs that can enhance the effects of the body's own defense system (Sakoulas et al., 2014). Revealing such dependencies for human AMPs and antibiotics used in clinics may be of help for the optimization of cure strategies in some cases.

One of the prominent examples of the AMPs with distinctly membranolytic mode of action is protegrin 1 (PG-1) (Steinberg et al., 1997; Bolintineanu and Kaznessis, 2011), isolated from pig leukocytes (Kokryakov et al., 1993). It possesses a β -hairpin conformation stabilized by two disulfide bonds (Aumelas et al., 1996). In contrast, proline-rich AMPs are known for their low damaging action on membranes. A peculiar representative of

this group is caprine batenecin with the molecular weight of 3.4 kDa (ChBac3.4) from the leukocytes of the domestic goat *Capra hircus*, which exhibits a pronounced effect not only on Gram-negative, but also on Gram-positive bacteria, unlike the majority of proline-rich peptides (Shamova et al., 2009). This linear AMP, supposedly, has a dual mechanism of action, similar to the one described for Bac7 (1–35) (Mattiuzzo et al., 2007; Shamova et al., 2009). It is suggested that in low concentrations it acts by a non-lytic mechanism via intracellular targets, possibly, binding to the aminoacyl site of bacterial ribosomes (Krizsan et al., 2015; Roy et al., 2015) or interfering with the chaperone-dependent protein folding (Otvos, 2002; Scocchi et al., 2009; Zahn et al., 2013), as described for other proline-rich peptides. In higher concentrations ChBac3.4 actively damage the bacterial membranes, although not as fast as PG-1 (Shamova et al., 2009).

The main groups of AMPs presented in humans include cathelicidins and α - and β -defensins. The only human cathelicidin LL-37, when it contact with the bacterial membrane, adopts the conformation of an amphipathic α -helix (Vandamme et al., 2012). Defensins are stabilized by three disulfide bonds and are folded into the three-stranded antiparallel β -sheet (Lehrer and Lu, 2012). β -Defensins have an additional α -helical region at the N-terminus, which presumably facilitates anchoring of the peptide into bacterial membrane (Taylor et al., 2008; Machado and Ottolini, 2015). Antimicrobial activity of LL-37 and defensins is associated with the damaging of bacterial membranes, but it is noted that disruptive action of α -defensins on them progresses rather slowly, but is accompanied by the decrease in the synthesis of bacterial DNA, RNA and proteins, and the bacterium also loses an ability to form colonies (Lehrer and Lu, 2012). Solid-state NMR spectroscopy data support a “dimer pore” topology for the pores formed by α -defensin HNP-1 in model membranes (Zhang et al., 2011). These pores do not cause a significant disorder in the membrane lipid packing (Lehrer and Lu, 2012). Recent findings shows, that hBD-3 and HNP-1 can also inhibit the bacterial cell wall synthesis by specifically binding lipid II (de Leeuw et al., 2010; Sass et al., 2010).

Some AMP-like properties are also found in antimicrobial proteins, for example in lysozyme, which is widely presented in animals. It is an important component of the secretions of many glands, including mammary, salivary, and lacrimal, and of the mucus of nasopharynx and gastrointestinal tract (Fleming, 1922; Fábíán et al., 2012). Lysozyme shows activity primarily against Gram-positive bacteria, catalyzing the lytic degradation of peptidoglycan, which is the major component of their cell wall (Masschalck and Michiels, 2003). However, there are reports suggesting that it can also act by a non-enzymatic mechanism probably similar to that of AMPs (Laible and Germaine, 1985; Ibrahim et al., 2001).

Unlike AMPs, clinically used antibiotics usually act via specific interactions with their molecular targets. Antibiotics can be classified on several groups depending on the vital process or structure of bacterial cell they affect. Due to the diversity of mechanisms of action they represent a perspective pool for searching synergistic interactions. In current study oxacillin, polymyxin B, gentamicin, amikacin, rifampicin, ofloxacin, erythromycin and meropenem were used. Oxacillin

is a penicillinase-resistant β -lactam, which inhibits bacterial cell wall biosynthesis (Kong et al., 2010). Polymyxin B is a peptide antibiotic of bacterial origin, which increases the permeability of the bacterial membranes, similarly to AMPs (Carmona-Ribeiro and de Melo Carrasco, 2014). Gentamicin and amikacin are aminoglycosides and inhibit protein biosynthesis by the covalent irreversible binding to the 30S subunit of bacterial ribosomes (Davis, 1987). Rifampicin creates obstacles to the process of transcription by inhibiting bacterial DNA-dependent RNA polymerase (Wehrli, 1983). Ofloxacin is a quinolone antibiotic. It inhibits DNA-gyrase essential for DNA replication, thus, interfering with the bacterial cell division (Aldred et al., 2014). Erythromycin is a macrolide antibiotic. It reversibly binds to the 50S subunit of the ribosome and has a bacteriostatic effect (Keskar and Jugade, 2015). Meropenem is one of the carbapenems, β -lactam antibiotics, resistant to the majority of the bacterial β -lactamases (Papp-Wallace et al., 2011). The spread of resistance to carbapenems in recent years is one of the most concerning tendencies. Carbapenem-resistant strains, especially Gram-negative ones, including *Acinetobacter baumannii*, *Pseudomonas aeruginosa*, and various species of the *Enterobacteriaceae* family (in particular, *Klebsiella*, *Escherichia coli*, *Serratia*, and *Proteus*), are topping the global priority list of antibiotic-resistant bacteria, composed by World Health Organization (2017).

Another class of antimicrobial substances, which attracts the attention of researchers as a promising and effective tool against drug-resistant pathogens, is nanoparticles of various metals, in particular, of silver (Rai et al., 2012; Markowska et al., 2013; Cavassin et al., 2015), which has been known for its bactericidal properties for thousands of years (Alexander, 2009; Yang et al., 2018). The mechanism of antimicrobial action of silver nanoparticles has not been completely deciphered yet, but it is associated with their ability to affect the proper functioning of membrane associated proteins, including those of respiratory chain, stimulate ROS production and induce oxidative stress (Durán et al., 2010; Lara et al., 2011). The toxicity of nanoparticles was found to be much lower than that of ionic silver, however the problem of their side effects has not been completely solved (Durán et al., 2010, 2015; Stensberg et al., 2011). Reducing their effective concentrations by combined use with other antimicrobials can be beneficial.

The present study is dedicated to examining a combined action of natural antimicrobial peptides of different structure and mode of action [porcine PG-1, caprine batenecin ChBac3.4, human α - and β -defensins (HNP-1, HNP-4; hBD-2, hBD-3), human cathelicidin LL-37] and egg white lysozyme with antibiotic agents, possessing varied targets in bacterial cells (selected antibiotics, silver nanoparticles), in a search of novel approaches of combined antimicrobial therapy for combating drug-resistant microbes. The tasks of the study included exploration of the activity of these combinations against a number of drug-sensitive strains, as well as several multi-resistant isolates. Combined hemolytic activity and cytotoxic action toward mammalian cells were also considered to assess the possibility of reducing toxic effects and increase selectivity.

MATERIALS AND METHODS

Materials

Antimicrobial Peptides and Proteins

Chemically synthesized bactenecin ChBac3.4 was kindly provided by Dr. A. Kolobov (State Research Institute of Highly Pure Biopreparations, Saint Petersburg, Russia). It has been produced by Fmoc/tBu-strategy on solid-phase using a Liberty microwave peptide synthesizer (CEM Corp., USA), according to a standard synthesis protocols. Peptide purification was carried out by RP-HPLC (Gilson; France) on a Waters Prep-NovaPak 6 μ m C18 (19 \times 300 mm) column. Purity, as assessed by reverse phase analytical chromatography on DeltaPak 5 μ m C18 100A (3.9 \times 150 mm) column, was about 99%. The molecular mass was confirmed by MALDI-TOF MS. Protegrin 1 (PG-1) was a gift from Prof. R. Lehrer (University of California, Los Angeles). This peptide was produced by SynPep Corporation (USA); purity of synthetic PG-1 was 99 %. LL-37, human α - and β -defensins were purchased at Peptide Institute, Inc., Japan. Egg white lysozyme was obtained from BioChemica, Germany. We prepared stock solutions of the peptides from Peptide Institute, Inc., Japan, according to the instruction provided by the manufacturer. For other peptides the concentration of stock solutions was spectrophotometrically verified based on their molar extinction coefficients at 280 nm (Pace et al., 1995).

Silver Nanoparticles

Silver nanoparticles were synthesized by the photo-reduction of AgNO₃ in presence of gelatin, which was used as an additional stabilizer. AgNO₃ (99.9%, Chimmedsynthesis, Russia) and gelatin (Acros, Russia) were used for synthesis. 0.05 g of gelatin was added to 4 ml of H₂O. Aqueous AgNO₃ (6 ml, 1 M) was added to gelatin solution by continuous stirring. The solution obtained was placed into UV-reactor for UV irradiation for 24 h at room temperature. Dialysis was performed to remove unbound gelatin and ionic silver, and the low level of the latter in the samples was confirmed by the ionometry. The nanoparticles diameter (including gelatin coating) determined by electron microscopy was approximately 50 nm.

Antibiotics, Culture Media, and Other Reagents

All antibiotic powders, as well as phosphate-buffered saline (PBS) tablets, bovine serum albumin (BSA), o-nitrophenyl- β -D-galactoside (ONPG), ethylenediaminetetraacetic acid (EDTA), and methylthiazolyldiphenyl-tetrazolium bromide (MTT) were bought from Sigma, USA. Müller-Hinton broth M391 was purchased from Oxoid, Germany. Other reagents and media were supplied from BioloT, Russia.

Bacterial Strains

Escherichia coli ML-35p and MRSA (methicillin-resistant *Staphylococcus aureus*) ATCC 33591 bacterial strains were kindly provided by Professor R. Lehrer, University of California, Los Angeles, USA. *Micrococcus luteus* CIP A270 was obtained from the collection of the Department of Molecular Microbiology of the Institute of Experimental Medicine, Saint Petersburg, Russia. Antibiotic-resistant Gram-negative bacteria *Escherichia coli* ESBL 521/17 (resistant to ampicillin, amoxicillin/clavulonic

acid, cefotaxime, ceftazidime, cefixime, aztreonam, netilmicin, ciprofloxacin, trimethoprim/sulfamethoxazole), *Pseudomonas aeruginosa* MDR 522/17 (resistant to meropenem, ceftazidime, cefixime, amikacin, gentamycin, netilmicin, ciprofloxacin, colistin), *Klebsiella pneumoniae* ESBL 344/17 (resistant to ampicillin), *Acinetobacter baumannii* 7226/16 (resistant to imipenem, gentamicin, tobramycin, ciprofloxacin, trimethoprim/sulfamethoxazole) and the susceptible strain of *Acinetobacter baumannii* were isolated from infected wounds, or from patient's urine in case of *E. coli* and generously provided by Prof. G.E. Afinogenov from Saint Petersburg State University and Dr. A. Afinogenova from the Research Institute of Epidemiology and Microbiology named after L. Pasteur, Saint Petersburg, Russia. Multidrug-resistant Gram-positive clinical isolate *Staphylococcus aureus* 1399/17 (resistant to ampicillin, oxacillin, gentamicin, amikacin, ofloxacin) originated from the same source.

Eukaryotic Cells

Human erythrocytes, mononuclear cells (PBMC) and neutrophils used in the study were isolated from peripheral blood of healthy donors.

To obtain erythrocytes, heparinized blood was centrifuged for 10 min at 300 g and 4°C. The supernatant liquid was removed, 10 ml of cooled PBS containing 4 mM of EDTA (pH 7.4) was added to the precipitate, and the mixture was centrifuged for 10 min under the same conditions. Then, red blood cells were washed three more times with cooled PBS. The sedimented red blood cells were used for the hemolytic test.

To obtain neutrophils and mononuclear cells, whole heparinized blood was diluted with sterile PBS in a 1:1 ratio and carefully inserted into the sterile polystyrene 50 ml tube upon the 5 ml of the sterile Ficoll-400 (Pharmacia, Sweden) with a density of 1.077. The tube was centrifuged at 600 g and 4°C for 40 min. After separation, the mononuclear "ring" located between the blood plasma and Ficoll was collected with a Pasteur pipette, transferred to another tube, and washed twice with 10 ml of sterile PBS by centrifugation for 10 min at 300 g and 4°C.

The pellet formed under the Ficoll-400 layer after separation contained both neutrophils and erythrocytes. It was also transferred into a separate tube, where the red blood cells were lysed with 0.83% ammonium chloride solution, which was added in a ratio of 1:4. After the thorough mixing, the suspension was incubated for 10 min at room temperature, and then centrifuged for 10 min at 300 g and 4°C. The resulting precipitate containing neutrophils was washed twice with the sterile PBS.

After washing, both mononuclear cells and neutrophils were resuspended in 1–2 ml of RPMI-1640 culture medium and immediately used in MTT test.

Peritoneal macrophages and Ehrlich ascites carcinoma (EAC) cells were obtained from (C57BL/6J \times CBA/J) F1 hybrid male mice, 3 months old (body weight of 18–22 g). The animals were maintained under the standard vivarium conditions at room temperature with a 12-h light/12-h dark cycle, free access to food and water, according to the standards of laboratory animal welfare.

Before the cells extraction, mice were sacrificed by cervical dislocation in accordance with the supplement to the Directive 86/609/EEC and its update Directive 2010/63/EU addressing the recommendations for euthanasia of experimental animals (Close et al., 1996). To obtain peritoneal macrophages, healthy mice were used. The abdominal cavity of each animal was washed with 3 ml of sterile PBS using a Pasteur pipette. The culture of EAC cells was kindly provided by Dr. E.P. Kiseleva (Immunology Department of the Institute of Experimental Medicine, Saint Petersburg, Russia). On the tenth day after the intraperitoneal tumor inoculation, 0.5–1.5 ml of ascitic fluid containing EAC cells was obtained from the abdominal cavity of the animals. Murine cells (normal or tumor) were washed twice with 10 ml of sterile PBS and resuspended in RPMI-1640 medium as described above for human neutrophils and PBMC.

The human erythromyeloid leukemia cell line K562 was obtained from the collection of the Institute of Cytology RAS (Saint Petersburg, Russia) and cultured in RPMI-1640 medium containing gentamicin (100 µg/ml) and 10% of fetal bovine serum at 37°C, 5% CO₂. Doxorubicin-resistant K562 cells were obtained from the parent line by continuous exposure of the cells to increasing concentrations of doxorubicin from 0.00016 to 2 µg/ml as described (Grinchuk et al., 1998), and their resistance to doxorubicin was 1–2 orders of magnitude higher than in the original K562 cells. Drug resistance was maintained by monthly selection with the antibiotic (2 µg/ml in the culturing medium). Doxorubicin was removed from the medium 3 days prior to beginning any experiments. Before the testing K562 cells were washed twice with PBS and resuspended in RPMI-1640 in the same way as the other cell types.

Antibacterial Assays

Broth Microdilution Assay

Prior to the “checkerboard” synergy test the minimal inhibitory concentrations (MIC) of individual substances were determined using broth microdilution assay. Testing was performed in 60-well polystyrene Terasaki microplates with V-shaped bottom generally according to the guidelines of the European Committee for Antimicrobial Susceptibility Testing with subtle modifications designed for AMP testing (Tossi et al., 1997; Wiegand et al., 2008). Cultivation of bacteria was carried out in 2.1% Müller-Hinton broth at 37°C with shaking. Two-fold serial dilutions of peptides, antibiotics and other antimicrobials were made with 10 mM sodium phosphate buffer, pH 7.4, containing 0.1% of BSA. The plates were preliminary incubated with 0.1% BSA for 1 h at 37°C to reduce a non-specific binding of peptides to the plates. After that BSA was removed, and serial dilutions were added into the plate wells in triplicates followed by the same volume of the suspension of bacterial cells in logarithmic phase of growth in concentration of 1×10^6 CFU/ml. After the 18 h overnight incubation at 37°C, the MIC value for each compound was determined as its lowest concentration completely inhibiting the visible growth of bacteria. The final results were calculated as median values based on 3–6 independent experiments.

Checkerboard Titration Method

The combined antimicrobial action of AMPs and other antimicrobial compounds was assessed using checkerboard titration approach under the conditions similar to that of the microdilution assay. According to checkerboard titration template, one component (A) of the combination was diluted along the rows of the plate, while the other (B) was diluted down the columns, thereby creating the variety of mixtures with different concentrations of tested compounds. 2.5 µl of corresponding solutions of the components A and B were added into each well of the plate. Into the first column and the last row the same amount of 10 mM sodium phosphate buffer, pH 7.4, containing 0.1% of BSA was introduced instead of the second component. Thus, all wells contained 5 µl of antimicrobial compounds solutions (solo or in combination). The same volume of bacterial suspension, prepared as described for microdilution assay, was added into each well. The results were recorded after the overnight incubation, visually indicating the presence or absence of the microbial growth in the corresponding wells. Based on the obtained data the isobolograms of combined action were plotted and/or Fractional Inhibitory Concentration Indices (FICI) were calculated. The latter was done as follows: $FICI = [A]/[MIC A] + [B]/[MIC B]$, where [A] and [B] are respective concentrations of substances A and B in their combination effectively inhibiting bacterial growth, and [MIC A] and [MIC B] are the individual MICs of A and B when they are used alone. Depending on the minimal value of the FICI the combined effect of the combination was classified as antagonism ($FICI > 2$), independent action ($1 < FICI \leq 2$), additivity ($0.5 < FICI \leq 1$) or synergy ($FICI \leq 0.5$), as is recommended in the literature and due to some drawbacks of the serial dilution method (Hsieh et al., 1993; Orhan et al., 2005; Fehri et al., 2007). FICIs were assessed in 3–6 independent experiments and median values were used to define the nature of interaction.

Bacterial Membrane Permeabilization Assay

The ability of antimicrobial peptides, alone and in combinations, to increase the permeability of the cytoplasmic membrane of Gram-negative bacteria was examined using a previously described procedure (Lehrer et al., 1988). The method is based on the certain features of the specifically designed *E. coli* ML-35p bacterial strain. As its parental strain *E. coli* ML-35, this bacterium constitutively expresses cytoplasmic β-galactosidase, but is unable to transport β-galactoside containing substrates through the inner membrane in normal circumstances due to the lack of lactose permease. In addition, *E. coli* ML-35p also possesses periplasmic β-lactamase. If the cytoplasmic membrane of the bacterium is damaged, the chromogenic marker o-nitrophenyl-β-D-galactoside (ONPG) penetrates into the cell and, when digested by bacterial β-galactosidase, produces a colored product o-nitrophenol. The accumulation of the latter can be spectrophotometrically detected at a wavelength of 420 nm.

Escherichia coli ML-35p was cultivated in the sterile 3% Trypticase soy broth (TSB) for 18 h at 37°C, then washed three times with 10 mM sodium phosphate buffer, pH 7.4 (10 min centrifugation at 600 g and 4°C), diluted up to the OD of 0.4 at

620 nm (1×10^8 CFU/ml concentration), and used immediately or kept on ice until the start of the test. The incubation wells for the testing contained antimicrobial components (alone or in combinations) in concentrations equal to $\frac{1}{4}$ of MIC, 10 mM sodium phosphate buffer with 100 mM NaCl (pH 7.4), 2.5 mM ONPG, and 2.5×10^7 CFU/ml of bacteria in a stationary growth phase washed out of the culture medium. Controls contained equivalent volume of acidified water instead of antimicrobial agent(s). The assay was started by adding the bacteria and was run at 37°C, with periodical shaking. Optical density (OD) measurement at 420 nm was performed every minute for 1–2 h using SpectraMax 250 Microplate Spectrophotometer (Molecular Devices, USA) and its SoftMax PRO software.

Cytotoxicity Assays

Combined Hemolytic or Cytotoxic Action

Examining the combined cytotoxic effects of various combinations of AMP with other active compounds we applied the same principle based on the Loewe additivity paradigm (Greco et al., 1992) that was used in the analysis of the combined antibacterial action. We calculated Fractional Effective Concentration Index (FECI), which could be seen as a particular case of the interaction index (I) proposed by Berenbaum (1977) or of the similar combination index (CI) proposed by Chou and Talalay (1983), according to the equation below:

$$\text{FEC Index} = [A]/[\text{MEC A}] + [B]/[\text{MEC B}]. \quad (1)$$

Here, [MEC A] and [MEC B] are the minimum effective concentrations (MEC) of substances A and B, when they are used alone. MEC is defined as the minimum concentration of the compound, at which the statistically significant difference with the control samples containing intact cells (0% hemolysis for hemolytic activity assay or 100% cell survival for MTT-test) is found, concerning the studied effect (thereby it is called “effective”). [A] and [B] are respective concentrations of substances A and B in their combination, where the same statistically significant difference is detected. A non-parametric Mann-Whitney *U*-test ($p < 0.05$ or $p < 0.01$) was used for the mentioned statistical comparison.

We have chosen the same intervals as that of FICI to determine synergy, additivity, independent action, and antagonism based on the minimal FICI values. However, in case of cytotoxic or hemolytic effect we were interested mainly in testing the possibility of additive or synergistic interaction itself, and not in assessing the exact magnitude of such interaction. Thus, in contrast to the “checkerboard titration” method used for combined antimicrobial activity investigation, studying the combined cytotoxic effect, we considered only two combinations of concentrations for the substances A and B in the mixture:

($\frac{1}{2}$ MEC A + $\frac{1}{2}$ MEC B), which, if found effective, provides the FICI value of 1 (the threshold value for additivity);

($\frac{1}{4}$ MEC A + $\frac{1}{4}$ MEC B), which, if found effective, provides the FICI value of 0.5 (the threshold value for synergistic interaction).

The combined action of the test substances was classified as independent (in the absence of statistically significant difference found for both combinations of concentrations), additive (if the statistically significant difference was shown only for a combination of $\frac{1}{2}$ MEC A + $\frac{1}{2}$ MEC B), or synergistic (if there is a statistically significant difference from the control samples for both combinations of concentrations). When action on tumor cells was tested in combination with antitumor antibiotic the lower concentrations up to ($\frac{1}{16}$ MEC A + $\frac{1}{16}$ MEC B) as in checkerboard titration were additionally examined to assess the magnitude of synergistic effect more precisely. The final conclusion was made based on the three independent experiments.

Hemolysis Test

Hemolytic activity was investigated by incubating tested compounds in various concentrations and their combinations with a suspension of washed human red blood cells. Two hundred eighty microliters of erythrocyte precipitate obtained as described in section Eukaryotic Cells was added into the sterile 15 ml tube and its volume was adjusted to 10 ml with cooled PBS. Using 0.5 ml plastic tubes, 3 μ l of the tested compound serially diluted in PBS or of the combination of two compounds were mixed with the 27 μ l of the prepared erythrocyte suspension for each sample. For positive control (100% lysis of erythrocytes) 3 μ l of the detergent (10% Triton X-100 solution in PBS) were added to the 27 μ l of the erythrocyte suspension, and for negative control (0% lysis of erythrocytes) 3 μ l of the PBS were used instead of any cell-damaging compound. Resulting 2.5% (v/v) erythrocyte suspensions were incubated for 30 min at 37°C with periodical shaking. After incubation, the hemolysis process was stopped by the addition of 75 μ l of cooled PBS. The samples were centrifuged at 5,000 g and 4°C for 4 min. The optical density of the supernatants was measured at a wavelength of 540 nm using SpectraMax 250 Spectrophotometer (Molecular Devices, USA). The experiments were repeated three times. In each experiment all the test or control samples were made in triplicates. The percentage of hemolysis of erythrocytes was assessed by the following formula:

$$\text{Hemolysis}(\%) = (\text{OD}_{\text{sample}} - \text{OD}_{0\% \text{ lysis}}) / (\text{OD}_{100\% \text{ lysis}} - \text{OD}_{0\% \text{ lysis}}) \times 100\%, \quad (2)$$

where $\text{OD}_{\text{sample}}$, $\text{OD}_{0\% \text{ lysis}}$, and $\text{OD}_{100\% \text{ lysis}}$ are values of the OD at 540 nm for the test sample, negative (0% lysis) control, and positive (100% lysis) control, respectively. However, due to the design of the study of combined action, described above in Combined Hemolytic or Cytotoxic Action, the obtained $\text{OD}_{\text{sample}}$ and $\text{OD}_{0\% \text{ lysis}}$ values were rather used to determine MECs and FICI by the Mann-Whitney *U*-test ($p < 0.05$, n_1 , $n_2 = 3$).

MTT-Test

Standard MTT-test (Mosmann, 1983) was used for the examination of the cytotoxic activity of antimicrobial compounds and their combinations toward varied eukaryotic cells. Briefly, cell suspensions in RPMI-1640 prepared as described in

Eukaryotic Cells were dispensed into the 96-well microplates (2×10^5 cells/well). Then, serial dilutions of AMPs, or other antibiotic compounds, or their mixtures in RPMI-1640 were added. In positive controls (100% cell survival) the according volume of RPMI-1640 without test substances was added instead. The final volume in each well was 100 μ l. Negative controls (0% cell survival) were made with 100 μ l of the sterile RPMI-1640. The plates were incubated at 37°C under 5% CO₂ for 24 h. Four hours before the end of incubation, 10 μ l of metabolic marker MTT–3-(4,5-dimethylthiazol-2-yl)-2,5-diphenyltetrazolium bromide (5 mg/ml, diluted in PBS) was added to each well. Incubation was stopped by adding 90 μ l of isopropanol containing 0.04 M HCl. Content of the wells was thoroughly mixed, so that the formazan crystals, formed in case of the reduction of MTT in presence of actively metabolizing cells, were fully dissolved. The optical density of the samples was evaluated at 540 nm, subtracting the background absorbance at 690 nm, by SpectraMax 250 Spectrophotometer (Molecular Devices, USA). The experiments were repeated at least three times. In each experiment test samples were made in triplicates and control samples were made in hexaplicates. OD values of samples and of positive controls (100% cell survival) were statistically compared using the Mann-Whitney *U*-test ($p < 0.05$ or $p < 0.01$; $n_1 = 2-3$, $n_2 = 5-6$) to determine MECs and FECI (as previously defined). The % of surviving cells for test samples could be found as:

$$\text{Survival(\%)} = (\text{OD}_{\text{sample}} - \text{OD}_{0\% \text{ survival}}) / (\text{OD}_{100\% \text{ survival}} - \text{OD}_{0\% \text{ survival}}) \times 100\%, \quad (3)$$

where $\text{OD}_{\text{sample}}$, $\text{OD}_{0\% \text{ survival}}$, and $\text{OD}_{100\% \text{ survival}}$ are values of the OD at 540 nm minus the OD at 690 nm for the test sample, negative (0% cell survival) control, and positive (100% cell survival) control, respectively.

Ethics Statement

In this study erythrocytes, mononuclear cells and neutrophils, used for evaluation of cytotoxic activity of the peptides and antibiotics, were obtained from blood of healthy donors. Since authors of this article served as such the donors, ethical approval was not required by the Ethics Committee of the Institute of Experimental Medicine. All subjects/authors gave their written consent.

RESULTS

Effects on Bacterial Cells Combined Antibacterial Action

At the first stage of the study we explored the combined action of AMPs and lysozyme with antibiotics against drug-susceptible bacteria. MIC values for individual substances are displayed in **Table 1**. The individual antimicrobial activity of oxacillin, HNP-4 and hBD-2 against *E. coli* ML-35p and that of LL-37 and HNP-4 against MRSA ATCC 33591 is low. The combinations including named substances were not further tested against the corresponding microorganisms after it was verified that an addition of $\frac{1}{4}$ MIC of the second antimicrobial to the $\frac{1}{2}$ MIC of the component with low activity was not effective (data not

shown). For lysozyme, which also is not active against these two bacteria, that, however, was not the case, thus, it was not excluded. The minimal FICIs for tested combinations of AMPs or lysozyme with antibiotics are given in **Table 2**. Values corresponding to synergistic effect ($\text{FICI} \leq 0.5$) are shown in bold type.

The data are also represented as polygonograms (**Figure 1**) to better visualize the general picture of interactions. Given polygonograms are in fact complete bipartite graphs, which can be considered as labeled or even weighted, as the minimal FICI value for the particular combination is coded by thickness (the lesser – the thicker) and color of the edge connecting the nodes representing the components of the said combination. Pie charts reflecting various types of interactions for the selected compounds are placed in the corresponding nodes as in Cokol et al. (2011). The color coding used for both charts and edges is: green for synergy ($\text{FICI} \leq 0.5$), blue for additivity ($0.5 < \text{FICI} \leq 1$), violet for independent action ($1 < \text{FICI} \leq 2$) and red for antagonism ($\text{FICI} > 2$).

Synergistic effects are found for combinations of battenencin ChBac3.4 with rifampicin against Gram-negative bacteria *E. coli* ML-35p; with oxacillin against Gram-positive bacteria MRSA ATCC 33591, which has a relatively high resistance to this antibiotic; with ofloxacin against Gram-positive bacteria *M. luteus* CIP A270. Membranolytic AMP PG-1 demonstrates synergistic action with gentamicin against both Gram-negative microorganisms tested, and, albeit to a lesser extent, against the Gram-positive strain *M. luteus* CIP A270.

The mutual enhancement of antimicrobial activity occurs in case of the combined use of lysozyme and polymyxin B on Gram-negative bacteria. The action of lysozyme with some antibiotics against bacteria, which are highly resistant to the former, is also quite close to synergistic: namely, with gentamicin against *E. coli* ML-35p and with gentamicin, oxacillin, and polymyxin B against MRSA ATCC 33591.

Amongst tested human AMPs, synergistic effect is detected in following combinations: hBD-3 with gentamicin against Gram-negative bacteria; hBD-2 with rifampicin and polymyxin B against susceptible *A. baumannii*, as well as with polymyxin B against *M. luteus* CIP A270; HNP-1 or hBD-3 with rifampicin against MRSA ATCC 33591; LL-37, or HNP-1, or hBD-2, or hBD-3 with gentamicin against *M. luteus* CIP A270. Interaction close to synergy is observed for combinations of HNP-1 with rifampicin and hBD-3 with ofloxacin against *E. coli* ML-35p, as well as for LL-37 with polymyxin B and HNP-4 with gentamicin against *M. luteus* CIP A270.

In total, counting the combined action of each AMP/antibiotic combination on each tested bacteria separately, additivity is observed in 75.4% of cases (101 of 134), and synergy is found in 14.2% of cases (19 of 134). However, from 40 examined combinations of AMPs and conventional antibiotics 13 (that is 32.5%) shows synergistic effect against at least one of the tested bacterial strains. Ten of this thirteen combinations include gentamicin, rifampicin or ofloxacin, which affect intracellular biosynthesis of proteins and nucleic acids. No antagonistic interactions are found.

TABLE 1 | Antimicrobial activity of individual fractions of AMPs and antibiotics against Gram-negative and Gram-positive bacteria.

Sample	MIC ^a (μM) toward bacterial strains			
	Gram-negative		Gram-positive	
	<i>E. coli</i> ML-35p	<i>A. baumannii</i> (clin. isol.)	MRSA ATCC 33591	<i>M. luteus</i> CIP A270
LL-37	10	2.5	50	1.25
HNP-1	50	0.6	2.5	0.1
HNP-4	>100 [200]	0.8	12.5	0.2
hBD-2	>100 [200]	6.25	>100 [200]	1.0
hBD-3	30	1.2	6.8	0.6
PG-1	3.1	1.6	3.8	0.5
ChBac3.4	3.1	1.6	7.2	1.6
Lysozyme	>250 [500]	1.2	>250 [500]	0.08
Oxacillin	>250 [500]	25	7.5	3.1
Polymyxin B	0.4	1.25	12.5	0.6
Gentamicin	0.625	0.06	0.16	0.16
Rifampicin	10	0.125	0.003	0.003
Ofloxacin	0.125	0.3	0.625	5

^aMinimal inhibitory concentrations (MIC) values are medians of 3–6 independent experiments made in triplicates. If actual MIC value was out of the tested concentrations range, it was assessed as twice the maximal tested concentration; the corresponding value is given in square brackets.

TABLE 2 | Antimicrobial activity of combinations of AMPs with antibiotics against Gram-negative and Gram-positive bacteria.

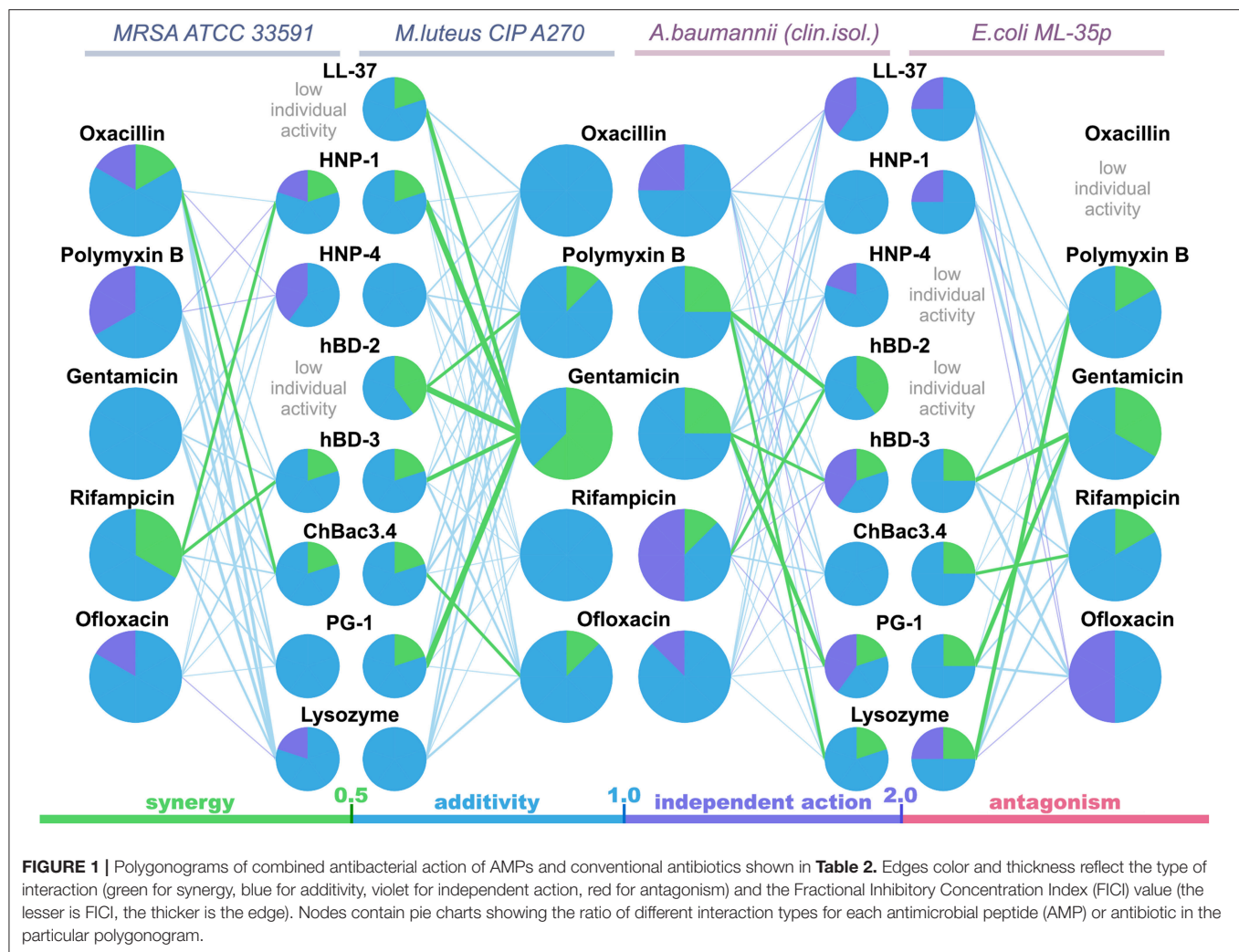
AMP\AB	Minimal FICIs ^a of AMP\antibiotic(AB) combinations against bacteria									
	Gram-negative					Gram-positive				
	RIF	PMB	GEN	OFL	OX	RIF	PMB	GEN	OFL	OX
<i>E. coli</i> ML-35p						MRSA ATCC 33591				
LL-37	0.75	0.75	0.75	1.12	–	HNP-4	0.75	1.12	1	1.12
HNP-1	0.56	1	0.62	1.12	–	HNP-1	0.5	1.12	0.75	1
hBD-3	0.75	0.75	0.28	0.53	–	hBD-3	0.5	1	0.75	0.75
ChBac3.4	0.5	1	1	0.75	–	ChBac3.4	0.75	0.62	0.75	0.5
PG-1	0.75	1	0.38	0.62	–	PG-1	0.75	0.62	1	0.75
Lysozyme	0.62	0.25	0.53	1.12	–	Lysozyme	0.62	0.56	0.53	0.53
<i>A. baumannii</i> (clin.isol.)						<i>M. luteus</i> CIP A270				
LL-37	1.12	1	0.75	1	1.5	LL-37	1	0.56	0.25	0.75
HNP-1	0.75	1	0.62	0.75	0.75	HNP-1	0.75	0.75	0.19	1
HNP-4	1.12	1	0.62	1	1	HNP-4	1	0.75	0.56	0.75
hBD-2	0.5	0.38	0.75	1	1	hBD-2	0.75	0.5	0.19	0.75
hBD-3	1.12	0.62	0.5	1.12	1	hBD-3	0.62	0.75	0.31	0.62
ChBac3.4	0.75	0.75	1	1	0.75	ChBac3.4	0.75	0.75	0.62	0.5
PG-1	1.12	0.75	0.38	1	1.12	PG-1	0.75	0.62	0.12	1
Lysozyme	1	0.5	0.75	1	1	Lysozyme	0.75	0.62	0.62	0.62

AMP, antimicrobial peptide; RIF, rifampicin; PMB, polymyxin B; GEN, gentamicin; OFL, ofloxacin; OX, oxacillin.

^aFractional Inhibitory Concentration Indices (FICI) values are medians of 3–4 independent experiments; FICI > 2 indicates antagonism, 1 < FICI ≤ 2 shows independent action, 0.5 < FICI ≤ 1 corresponds to additivity, FICI ≤ 0.5 denotes synergy; synergy cases are set off in bold type.

Interestingly, most of the synergy cases occur in combinations of AMPs with gentamicin (the effect is revealed for LL-37, PG-1, HNP-1, hBD-2, hBD-3). After this finding, measurements of combined antimicrobial action with listed AMPs were replicated using another aminoglycoside antibiotic – amikacin. Activity was examined against *M. luteus* CIP A270, where all these

combinations with gentamicin had previously shown synergy, and similar results with amikacin were obtained. Corresponding isobolograms are shown at **Figure 2A**. After the checkerboard titration test, the content of the wells was ten-fold diluted and putted onto the solid nutrient medium. Microbial growth was observed after a 24 h incubation at 37°C, showing that the



effects of combinations were not just bacteriostatic, but indeed bactericidal (examples are shown at **Figure 2B**).

For PG-1 and ChBac3.4, which were most active amongst tested AMPs, combined antibacterial effects with antibiotics were further explored against drug-resistant clinical isolates. The MICs and minimal FICIs values are shown in **Tables 3, 4**, respectively. As none synergistic interactions were previously found for combinations of either PG-1 or ChBac3.4 with polymyxin B, the latter was excluded from the list of tested antibiotics. Meropenem and erythromycin were examined instead.

Individually PG-1 is active against all of the antibiotic-resistant isolates (**Table 3**) in the same concentrations as against laboratory drug-sensitive strains (**Table 1**); for ChBac3.4 the MICs are just slightly higher. For combinations of AMPs with aminoglycoside amikacin, synergy is found in almost all cases with the exception of the action against *S. aureus* 1399/17 for PG-1 and against *E. coli* ESBL 521/17 for ChBac3.4. Though only *S. aureus* 1399/17 shows high resistance to amikacin itself as it can be seen in **Table 3**. Interestingly, the cases of synergy with erythromycin, to which all clinical isolates possesses significant

level of resistance, are also quite numerous. Rather similarly to amikacin, this antibiotic affects bacterial ribosomes, albeit binding to another subunit. The synergistic effect is found against *P. aeruginosa* MDR 522/17 and *K. pneumoniae* ESBL 344/17 for combination of the antibiotic with PG-1, and against all tested strains, except *A. baumannii* 7226/16, for combination with ChBac3.4. Combination of ofloxacin with PG-1 shows synergy only against *K. pneumoniae* ESBL 344/17, which is susceptible to this antibiotic. On the other hand, for such combination with ChBac3.4, synergistic action is detected against the ofloxacin-resistant strains *A. baumannii* 7226/16 and *S. aureus* 1399/17. The combined effect of both PG-1 and ChBac3.4 with meropenem is synergistic against *A. baumannii* 7226/16, which has a high level of resistance to this antibiotic, and against *S. aureus* 1399/17, for which MIC of meropenem is also higher than that for susceptible strains. The combination of ChBac3.4 and oxacillin, previously shown to be synergistic against the laboratory strain MRSA ATCC 33591, demonstrates similar effect against clinically isolated *S. aureus* 1399/17, which is highly resistant to oxacillin.

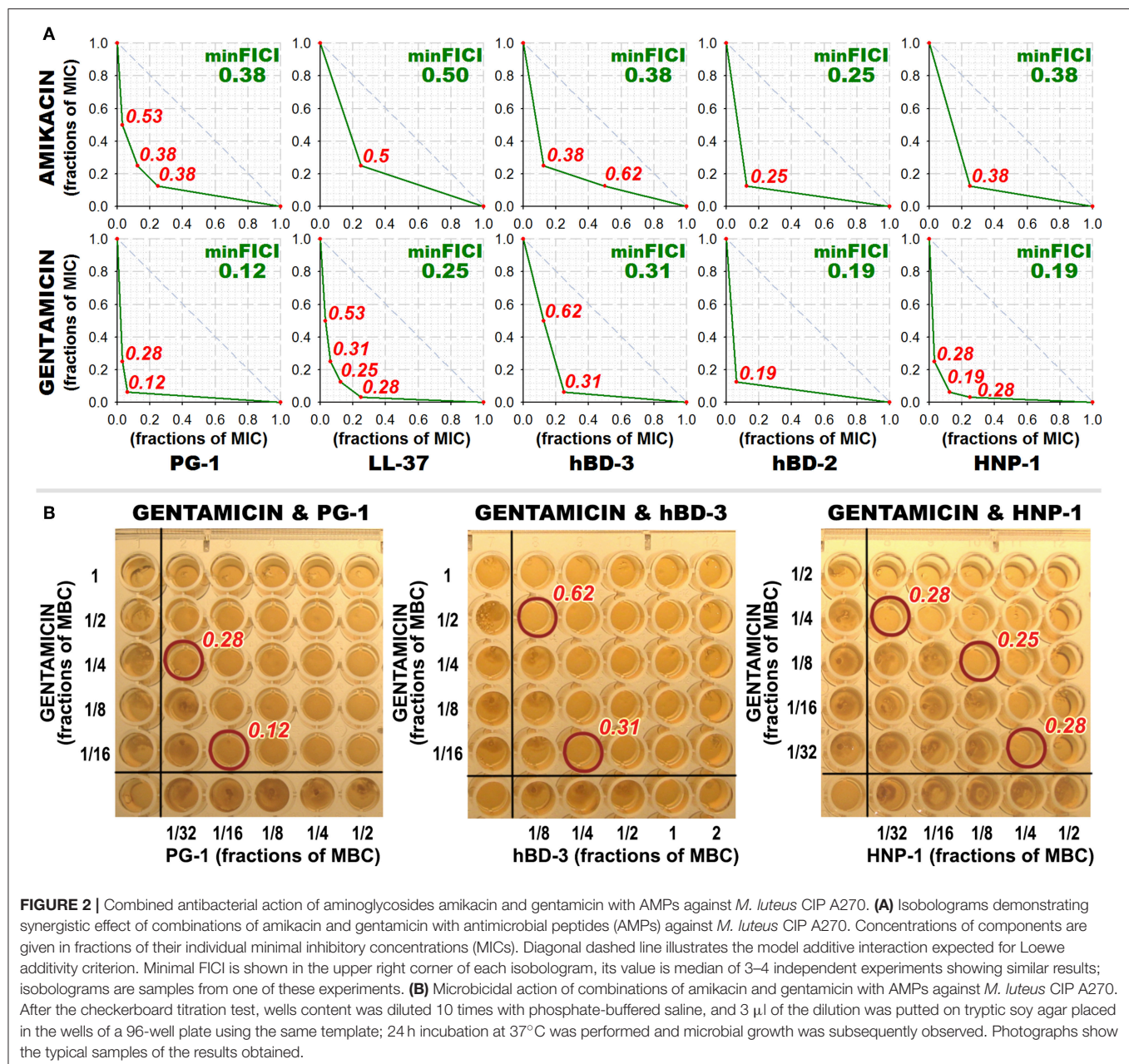


FIGURE 2 | Combined antibacterial action of aminoglycosides amikacin and gentamicin with AMPs against *M. luteus* CIP A270. **(A)** Isobolograms demonstrating synergistic effect of combinations of amikacin and gentamicin with antimicrobial peptides (AMPs) against *M. luteus* CIP A270. Concentrations of components are given in fractions of their individual minimal inhibitory concentrations (MICs). Diagonal dashed line illustrates the model additive interaction expected for Loewe additivity criterion. Minimal FICI is shown in the upper right corner of each isobologram, its value is median of 3–4 independent experiments showing similar results; isobolograms are samples from one of these experiments. **(B)** Microbicidal action of combinations of amikacin and gentamicin with AMPs against *M. luteus* CIP A270. After the checkerboard titration test, wells content was diluted 10 times with phosphate-buffered saline, and 3 μ l of the dilution was putted on tryptic soy agar placed in the wells of a 96-well plate using the same template; 24 h incubation at 37°C was performed and microbial growth was subsequently observed. Photographs show the typical samples of the results obtained.

Results of the checkerboard titrations for combinations of ChBac3.4, PG-1, and lysozyme with gelatin-stabilized silver nanoparticles against drug-susceptible bacteria are represented as isobolograms at **Figure 3**. Minimal FICIs are shown in the upper right corners of the corresponding plots. They are typed in green for synergy, in blue for additive effect, and in violet for independent action. Additional red numbers on the plots are FICIs calculated for combinations corresponding to red dots. MIC values for antimicrobial action of gelatin-stabilized silver nanoparticles alone are given under the isobolograms as medians of 3–4 independent broth microdilution tests.

According to the obtained data, combined effect of PG-1 and lysozyme with silver nanoparticles proves to be synergistic

in almost all cases, except that against *A. baumannii* for lysozyme. ChBac3.4 in combination with nanoparticles mainly shows additivity.

Although the combined action with AMPs for the gelatin-stabilized nanoparticles was not further examined against multidrug-resistant isolates, we carried out such experiments using the combinations of PG-1 or ChBac3.4 with poviargolum (**Table 5**), which is a preparation of polyvinylpyrrolidone-stabilized highly dispersed silver used as broad-spectrum bactericidal agent (Patent of the Russian Federation No 2088234, owned by the Institute of Macromolecular Compounds RAS). Synergy was found with PG-1 against Gram-negative clinical isolates *P.*

TABLE 3 | Antimicrobial activity of individual fractions of AMPs and antibiotics against drug-resistant clinical isolates.

Sample	MIC ^a (μM) against drug-resistant clinical isolates				
	Gram-negative				Gram-positive
	<i>E. coli</i> ESBL 521/17	<i>A. baumannii</i> 7226/16	<i>P. aeruginosa</i> MDR 522/17	<i>K. pneumoniae</i> ESBL 344/17	<i>S. aureus</i> 1399/17
PG-1	0.4	6.25	1.6	1.6	1.0
ChBac3.4	6.25	12.5	6.25	6.25	12.5
Oxacillin	>50 [100]	>50 [100]	>50 [100]	>50 [100]	>50 [100]
Meropenem	0.04	>50 [100]	25	0.04	6.25
Erythromycin	>50 [100]	>50 [100]	>50 [100]	50	>50 [100]
Amikacin	1.0	6.25	1.0	0.25	>50 [100]
Ofloxacin	50	25	>50 [100]	0.25	>50 [100]

^aMinimal inhibitory concentrations (MIC) values are medians of 3–6 independent experiments made in triplicates. If actual MIC value was out of the tested concentrations range, it was assessed as twice the maximal tested concentration; the corresponding value is given in square brackets.

TABLE 4 | Antimicrobial activity of combinations of AMPs with antibiotics against drug-resistant clinical isolates.

AB\AMP	Minimal FICIs ^a of antibiotic(AB)\AMP combinations against drug-resistant clinical isolates									
	Gram-negative								Gram-positive	
	<i>E. coli</i> ESBL 521/17		<i>A. baumannii</i> 7226/16		<i>P. aeruginosa</i> MDR 522/17		<i>K. pneumoniae</i> ESBL 344/17		<i>S. aureus</i> 1399/17	
	PG-1	ChBac3.4	PG-1	ChBac3.4	PG-1	ChBac3.4	PG-1	ChBac3.4	PG-1	ChBac3.4
OX	1.12	1.12	0.75	1.12	1.12	1.12	1.12	1.12	1.12	0.25*
MEM	1.0	1.0	0.38*	0.5*	1.0	0.62	1.0	1.0	0.25*	0.31*
ERY	0.62	0.38*	1.12	0.75	0.5*	0.38*	0.25*	0.25*	0.75	0.5*
AMK	0.38	0.62	0.38*	0.5*	0.5	0.5	0.31	0.38	1.0	0.125*
OFL	0.75	0.75	0.62	0.5*	1.12	0.75	0.5	0.75	0.56	0.125*

AMP, antimicrobial peptide; OX, oxacillin; MEM, meropenem; ERY, erythromycin; AMK, amikacin; OFL, ofloxacin.

^aFractional Inhibitory Concentration Indices (FICI) values are medians of 3–6 independent experiments; FICI > 2 indicates antagonism, 1 < FICI ≤ 2 shows independent action, 0.5 < FICI ≤ 1 corresponds to additivity, FICI ≤ 0.5 denotes synergy; synergy cases are set off in bold type.

*Bacterium has moderate or high resistance to the antibiotic being part of the synergistic combination.

aeruginosa MDR 522/17, *K. pneumoniae* ESBL 344/17 and *A. baumannii* 7226/16, and, interestingly, with ChBac3.4 as well: against Gram-negative strains *E. coli* ESBL 521/17, *K. pneumoniae* ESBL 344/17, and Gram-positive bacterium *S. aureus* 1399/17.

Analysis of the Bacterial Membrane Permeabilization

Plots at **Figure 4A** show obtained kinetic curves, illustrating the changes in the permeability of the cytoplasmic bacterial membrane caused by AMP/antibiotic combinations, which most often demonstrated synergy of antibacterial action, in comparison with the effect of individual compounds. We examined combined effect of ChBac3.4 with rifampicin, ofloxacin, or oxacillin; of PG-1 or LL-37 with gentamicin; of HNP-1 or hBD-3 with gentamicin or rifampicin; and of lysozyme with polymyxin B. However, it should be mentioned, that not all of these combinations demonstrated synergy specifically against *E. coli* ML-35p. In addition, a combination of two membranolytic agents PG-1 and polymyxin B, whose interaction was predictably additive, and a combination of lysozyme and gentamicin, whose effect was close to synergistic, were also considered.

For AMP/antibiotic pairs, where the peptide component demonstrates rapid membranolytic effect, such as hBD-3/gentamicin, hBD-3/rifampicin and PG-1/gentamicin, curves of combined action almost replicate those illustrating the action of the corresponding peptide alone. In case of the additive combination of PG-1 with polymyxin B, where both components are distinctly membranoactive, total effect is predictably equal to the individual action of PG-1, as it arises more quickly.

The effect of lysozyme and polymyxin B, when they are applied in combination, is noticeably intensified: its development rate doubles. Interestingly, the same phenomenon could be observed for the outer membrane of the tested bacteria (**Figure 4B**) using another chromogenic marker nitrocefin, which is a substrate of *E. coli* ML-35p periplasmic β-lactamase. The latter may indicate that the interaction between lysozyme and polymyxin B is not limited to the facilitation of lysozyme access to the peptidoglycan layer. It is possible that lysozyme in its turn contributes directly to the process of polymyxin interaction with the outer membrane of bacteria, and later with the inner membrane as well.

ChBac3.4 and HNP-1 show no substantial effect on the membrane permeability in concentrations equal to ¼ MIC, which is expected, as dimeric pores suggested for HNP-1 do not cause

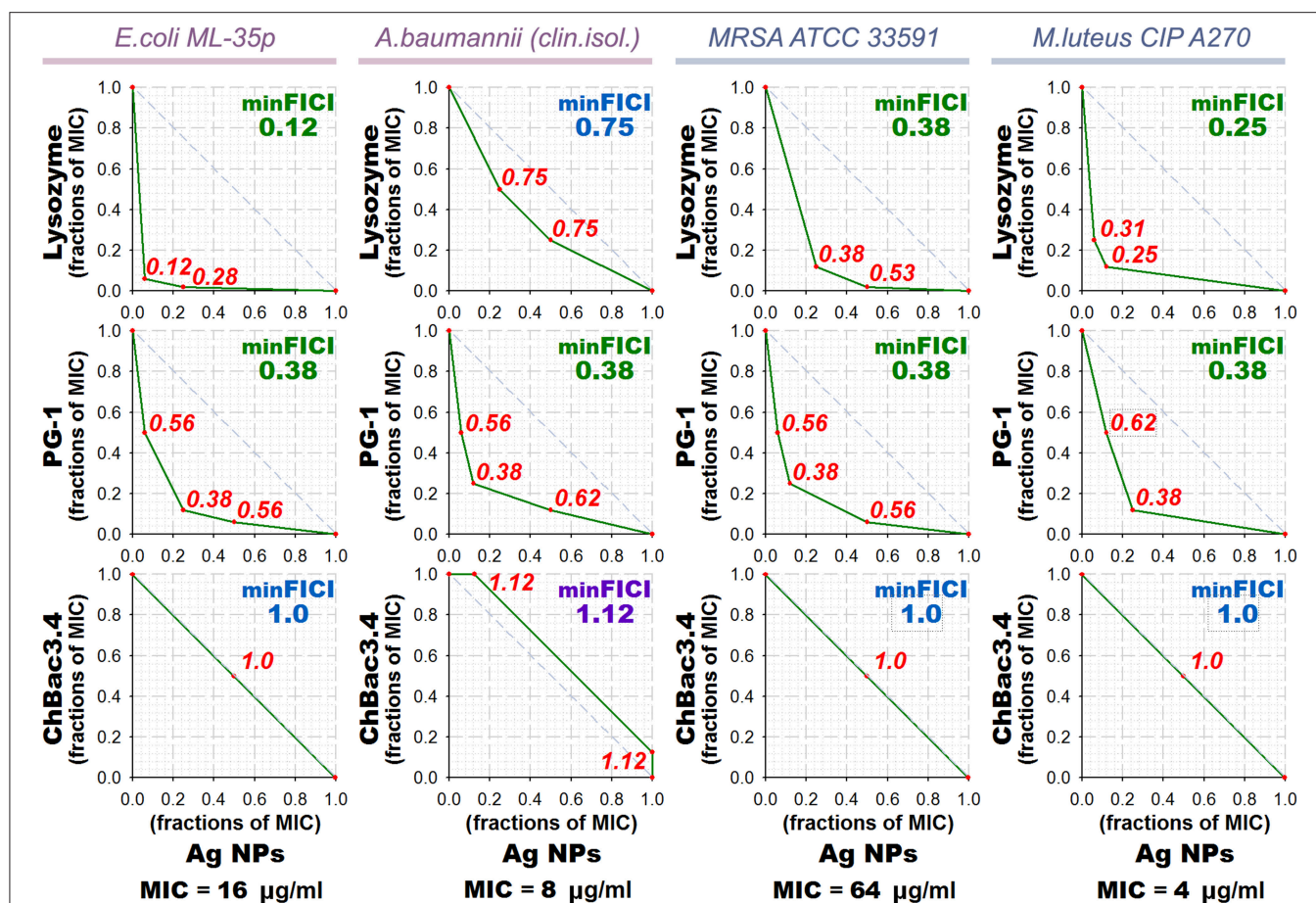


FIGURE 3 | Isobolograms of combined antibacterial action of gelatin-coated silver nanoparticles (Ag NPs) with lysozyme and AMPs. Concentrations of components are given in fractions of their individual minimal inhibitory concentrations (MICs). MICs values for silver nanoparticles alone are shown under the graphs. Diagonal dashed line illustrates the model additive interaction expected for Loewe additivity criterion. Minimal Fractional Inhibitory Concentration Index (FICI) is shown in the upper right corner of each isobologram, its value is median of 3–4 independent experiments showing similar results; it is green for synergy ($\text{FICI} \leq 0.5$), blue for additive effect ($0.5 < \text{FICI} \leq 1$), and violet for independent action ($1 < \text{FICI} \leq 2$). Isobolograms represent samples from one of the experiments. AMP, antimicrobial peptide.

significant membrane disruption (Lehrer and Lu, 2012), and ChBac3.4 in low concentrations is believed to act via non-membranolytic mechanism (Shamova et al., 2009). However, slight acceleration in the development of membrane-damaging effect of these peptides, when in combination with rifampicin, can be noted.

Significantly more prominent effect of this nature occurs for the combination of LL-37 with gentamicin. AMP alone is causing quite slow enhance of the membrane permeability, but in presence of gentamicin the process of membrane-damaging is developing rather quickly. In the tested concentration gentamicin alone causes no substantial increase in the permeability of the membrane. It means that a non-specific membrane damaging, which is possible at the late stages of aminoglycosides action on bacteria, when the protein synthesis is affected and incorrectly synthesized proteins are embedded into the membrane disturbing its stability (Taber et al., 1987), is out of the picture. Perhaps, aminoglycoside molecules can contribute to the lipid clusterization process and overall

membrane disturbance, thereby accelerating AMP integration into the bilayer and/or their aggregation.

For another combination with gentamicin, which includes α -defensin HNP-1, no changes are found comparing the action of the peptide alone or with the antibiotic. As it was mentioned, HNP-1 does not show prominent effect on the permeability of bacterial membrane in concentrations of $\frac{1}{4}$ MIC. Though, synergy between HNP-1 and gentamicin is observed not against *E. coli* ML-35p, but against Gram-positive bacteria *M. luteus* CIP A270. Probably, in this case a certain role in the realization of the synergistic effect can be attributed to the ability of defensins (in particular, HNP-1) to bind lipid II and block the biosynthesis of the cell wall, described not so long ago (de Leeuw et al., 2010).

In case of lysozyme, the addition of gentamicin in the mixture unexpectedly results in slower increase of permeability in comparison to the action of lysozyme alone. The effect of the combination against *E. coli* ML-35p is close to synergy, though the bacterium is highly resistant to lysozyme, as it is Gram-negative. It could be speculated, that after

TABLE 5 | Antimicrobial activity of colloidal silver preparation “Poviargolum” alone and in combinations with PG-1 or ChBac3.4 against drug-resistant clinical isolates.

Bacteria	Poviargolum MIC ^a (μg/ml)	Poviargolum and PG-1 FICI ^b	Poviargolum and ChBac3.4 FICI ^b
<i>E. coli</i> ESBL 521/17	78	0.56	0.375
<i>A. baumannii</i> 7226/16	78	0.5	0.75
<i>P. aeruginosa</i> MDR 522/17	78	0.5	0.625
<i>K. pneumoniae</i> ESBL 344/17	78	0.5	0.5
<i>S. aureus</i> 1399/17	156	0.62	0.5

^aMinimal inhibitory concentrations (MIC) values are medians of 4 independent experiments made in triplicates.

^bFractional Inhibitory Concentration Indices (FICI) values are medians of 3–4 independent experiments; $FICI > 2$ indicates antagonism, $1 < FICI \leq 2$ shows independent action, $0.5 < FICI \leq 1$ corresponds to additivity, $FICI \leq 0.5$ denotes synergy; synergy cases are set off in bold type.

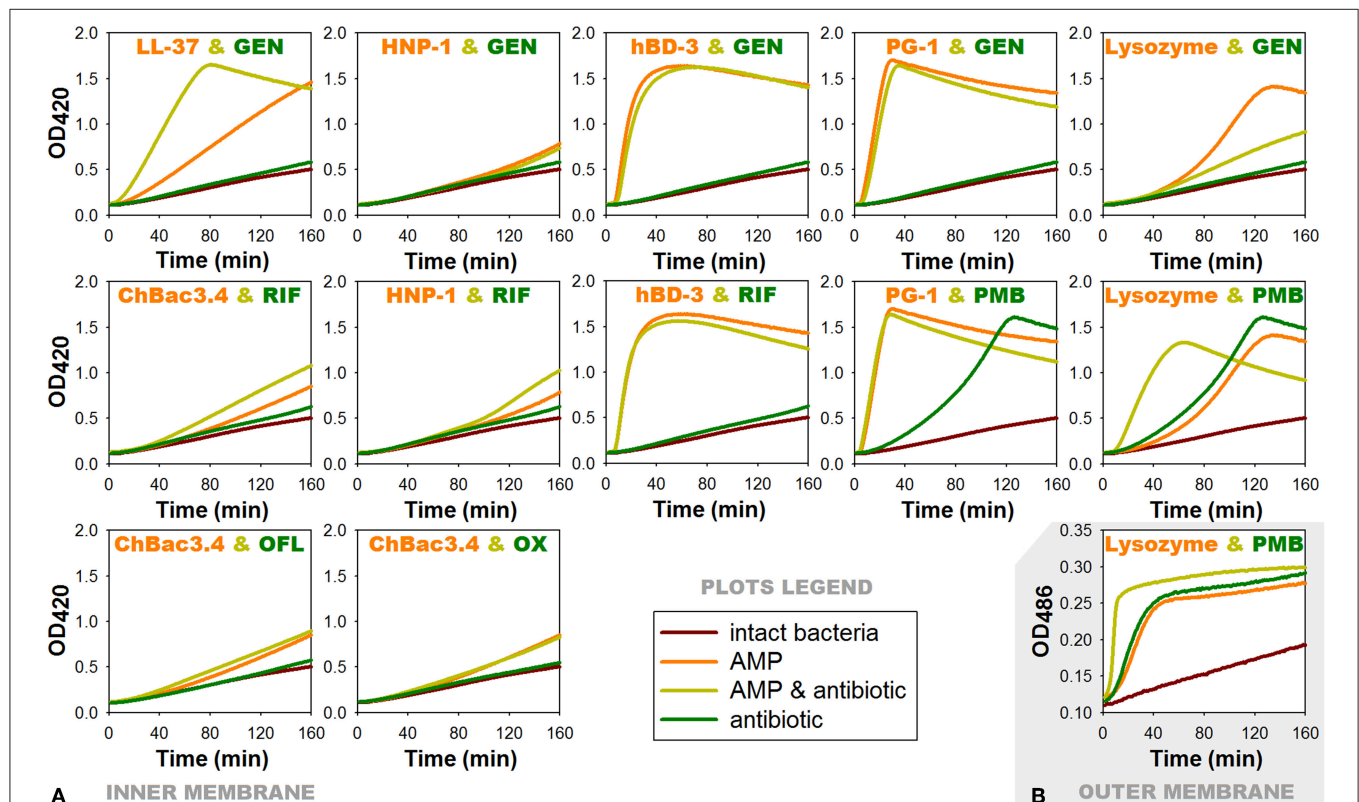


FIGURE 4 | Effects of combinations of AMPs with antibiotics showing antibacterial synergy on membrane permeability of *E. coli* ML-35p. **(A)** Permeability of the inner membrane for a chromogenic marker o-nitrophenyl-β-D-galactoside (ONPG). ¼ of minimal inhibitory concentrations (MICs) of antimicrobial peptides (AMPs) and antibiotics were used when alone, and ¼ MIC of AMP + ¼ MIC of antibiotic when in combination. Curves illustrate ONPG degradation by the cytoplasmic β-galactosidase of bacteria, when the membranes are damaged by test substances. Curves slope and the time of their rising to the plateau correspond to the extent of this damage. **(B)** Permeability of the outer membrane for a chromogenic marker nitrocefin under the effect of combination of lysozyme with polymyxin B. Outer membrane permeability was examined similarly to the inner membrane except for the chromogenic marker being used was nitrocefin in concentration of 20 μM and the OD measurement was performed at 486 nm. Nitrocefin is a substrate for the periplasmic β-lactamase of the bacteria. RIF, rifampicin; PMB, polymyxin B; GEN, gentamicin; OFL, ofloxacin; OX, oxacillin.

lysozyme penetrates through the outer membrane of *E. coli* ML-35p, it induces the cleavage of the cell wall, and the access of the gentamicin molecules to its targets is probably facilitated, similar to the mechanism described for aminoglycosides and β-lactam antibiotics. However, to explain observed changes in the dynamic of lysozyme-induced membrane permeability increase, further research is needed. Probably, the non-enzymatic mechanism, reported for

lysozyme (Laible and Germaine, 1985; Ibrahim et al., 2001) is involved.

Effects on Eukaryotic Cells

Combined Hemolytic Activity

Synergistic antimicrobial combinations of PG-1, ChBac3.4, lysozyme, and LL-37 with antibiotics (from Table 2) were tested for hemolytic activity. MECs for individual substances are

TABLE 6 | Cytotoxic action of individual fractions of AMPs and antibiotics toward normal or tumor mammalian cells and their hemolytic activity toward human erythrocytes.

Sample	MEC ^a (μM) of cytotoxic action toward					MEC ^a (μM) of hemolysis of human erythrocytes
	Normal Cells			Tumor Cells		
	Human PBMC	Human neutrophils	Murine peritoneal macrophages	K562	Murine EAC	
PG-1	5.0	2.5	2.5	1.25	1.25	2.0
LL-37	12	10	>20 [40]	5.0	10	5.0
Lysozyme	>50 [100]	>50 [100]	>50 [100]	>50 [100]	50	>50 [100]
ChBac3.4	20	>20 [40]	>20 [40]	20	5.0	>50 [100]
Gentamicin	>50 [100]	50	>50 [100]	50	>50 [100]	>50 [100]
Rifampicin	>20 [40]	20	>20 [40]	>20 [40]	>20 [40]	20
Oxacillin	>50 [100]	>50 [100]	>50 [100]	>50 [100]	>50 [100]	25
Ofloxacin	>50 [100]	>50 [100]	>50 [100]	>50 [100]	>50 [100]	>50 [100]
Polymyxin B	50	>50 [100]	50	25	50	>50 [100]

PBMC, peripheral blood mononuclear cells; EAC, Ehrlich ascites carcinoma.

^aMinimal effective concentrations (MEC) values are medians of 3–4 independent experiments made in triplicates. MECs are minimal concentrations where the statistically significant difference from the untreated (intact) cells is found with Mann-Whitney U-test ($p < 0.01$; $n_1 = 3$, $n_2 = 6$ –8 for cytotoxic action; $p < 0.05$, n_1 , $n_2 = 3$ for hemolysis). If actual MEC value was out of the tested concentrations range, it was assessed as twice the maximal tested concentration; the corresponding value is given in square brackets.

summarized in **Table 6**. Peptides PG-1 and LL-37 start to show hemolytic properties in quite low concentrations of $<10 \mu\text{M}$ in *in vitro* conditions in absence of blood serum; amongst the antibiotics only oxacillin and rifampicin demonstrate slight hemolytic action. Results for combinations in **Table 7** illustrate by “+” the presence or by “–” the absence of any statistically significant hemolytic effect of examined mixtures of AMPs with antibiotics in a series of three independent experiments. Based on these data the corresponding FECI value for each combination is assessed. Despite hemolytic properties possessed by some of the tested compounds, no cases of synergy or even additivity regarding combined hemolytic action are detected.

Combined Cytotoxic Action

To determine whether the cytotoxicity of combinations of AMPs and antibiotics against various normal and tumor eukaryotic cells is higher than that of individual substances, we used MTT-test. The effect was observed toward human PBMC and neutrophils of healthy donors, murine peritoneal macrophages of healthy mice, human erythromyeloid leukemia cell line K562 and murine EAC cells. Examined combinations were the same as for the hemolytic assay. Additionally, the combination of PG-1 and polymyxin B, where both compounds had explicit membranolytic action, was tested.

MECs of individual substances were determined before examining combined action (**Table 6**). Though AMPs are more toxic toward tumor cells, which correspond to the literature (Al-Benna et al., 2011; Gaspar et al., 2013), PG-1 also starts to damage normal cells in quite low concentrations. To the lesser extent it is true for LL-37 against human PBMC and neutrophils, and ChBac3.4 against human PBMC. Antibiotics are generally non-toxic toward both tumor and normal eukaryotic cells in concentrations below 25–50 μM .

Data on the toxicity of AMP/antibiotic combinations in three independent experiments and corresponding FECIs values are summarized in **Table 8** in the same manner as for the hemolysis. Despite the promising results of the hemolytic test, we identified synergy of cytotoxic action against tumor and/or normal cells in a number of cases. Thus, LL-37/gentamicin combination provides synergistic effect toward both types of tested tumor cells (human K562, murine EAC) and normal PBMC; toward human neutrophils and murine peritoneal macrophages it shows at least additive interaction. Combination of lysozyme with polymyxin B also demonstrates synergy against K562, EAC and PBMC cells, and additivity toward peritoneal macrophages of mice. PG-1 and gentamicin applied together exert synergistic cytotoxic action on human neutrophils; however, in other cases the effect is independent. Combination of PG-1 and polymyxin B shows synergy against K562 cells, and PMBC. The combined effect of lysozyme and gentamicin on eukaryotic cells is additive in the majority of the cases. For combinations of ChBac3.4 and antibiotics, combined action is mainly independent.

We noticed that in the identified synergistic combinations at least one component demonstrates a pronounced membranolytic action on bacterial membranes (PG-1, LL-37, polymyxin B). This fact corresponds with generally accepted conception that such mechanism contributes to non-specific toxicity toward eukaryotic cells as well.

The obtained data indicate that combined use of AMP and antimicrobial antibiotics in some cases can result in simultaneous enhancement of antibacterial action and of cytotoxic effects on eukaryotic cells. Therefore, to strengthen only the first kind of activity, the selection of effective combinations should be approached with caution. However, it should be noted that in the majority of cases the concentrations of conventional antibiotics used to examine the combined action on eukaryotic

TABLE 7 | Hemolytic action of combinations of AMP and conventional antibiotics toward human erythrocytes.

A and B combination	Hemolytic activity		FECI ^a
	(½ MEC A + ½ MEC B)	(¼ MEC A + ¼ MEC B)	
LL-37 and GEN	+ - - [-]	- - - [-]	>1.0
PG-1 and GEN	- - - [-]	- - - [-]	>1.0
Lysozyme and GEN	- - - [-]	- - - [-]	>1.0
Lysozyme and PMB	- - - [-]	- - - [-]	>1.0
ChBac3.4 and OX	- - - [-]	- - - [-]	>1.0
ChBac3.4 and OFL	- - - [-]	- - - [-]	>1.0
ChBac3.4 and RIF	- - - [-]	- - - [-]	>1.0

GEN, gentamicin; PMB, polymyxin B; OX, oxacillin; OFL, ofloxacin; RIF, rifampicin. + | - presence or absence of the statistically significant difference from intact cells (Mann-Whitney U-test $p < 0.05$, n_1 , $n_2 = 3$) in each of the three independent experiments; resulting assessment of the combination effect is given in square brackets.

^aAssessment of the minimal Fractional Effective Concentration Index (FECI) based on the results for (½ MEC A + ½ MEC B) and (¼ MEC A + ¼ MEC B) combinations of substances A and B; FECI > 1.0 shows independent action or antagonism, $0.5 < \text{FECI} \leq 1$ indicates additivity, $\text{FECI} \leq 0.5$ denotes synergy. MEC, minimal effective concentration.

cells significantly exceeded those used to study the combined effect on bacteria. Resulting difference in the molar ratios of the components between combinations tested on eukaryotic and bacterial cells probably makes the current assessment a bit more pessimistic than it should have been, if component ratios were preserved in accordance to antimicrobial assays.

At the same time, combined cytotoxic action of PG-1 with anticancer agent doxorubicin was determined to be synergistic against both doxorubicin-sensitive and doxorubicin-resistant K562 tumor cells with minimal FECIs being 0.25 and 0.38, respectively (median values based on three independent experiments). However, it must be noted, that this phenomenon was tested regarding minimal toxicity level, and at the 50%-effect level used to define IC_{50} in standard antitumor activity tests the type of interaction may differ. It is also of interest, that the enhancement in MEC values comparing susceptible and resistant cell lines is significantly higher for doxorubicin than for PG-1 (100 times, from 1 to 100 µg/ml, for doxorubicin against 4 times, from 1.25 to 5.0 µM, for PG-1). However, it may simply be due to the absence of cross-resistance.

DISCUSSION

AMPs of animals' host defense are widely acknowledged to effectively suppress the growth of microorganisms resistant to the clinically used drugs (Hancock and Lehrer, 1998; Deslouches et al., 2013; Kang et al., 2014). The synergy of various AMPs with different antibiotic compounds including other AMPs or proteins of neutrophil granules as well as clinically used antibiotics has been reported in numerous papers (Giacometti et al., 2000a,b,c; Yan and Hancock, 2001; Cassone and Otvos, 2010; Yu et al., 2016). Current research was aimed to study the combined effects of AMPs with other antibiotic agents considering their direct antibacterial and cytotoxic activity in order to reveal certain patterns in such interactions that can provide additional

TABLE 8 | Cytotoxic action of combinations of AMP and conventional antibiotics toward normal or tumor mammalian cells.

A and B	Toxicity of (½ MEC A + ½ MEC B) and (¼ MEC A + ¼ MEC B) combinations and corresponding FECIs ^a											
	Normal cells						Tumor cells					
	Human PBMC			Human neutrophils			K562			Murine peritoneal macrophages		
	½ A and ½ B	¼ A and ¼ B	FECI	½ A and ½ B	¼ A and ¼ B	FECI	½ A and ½ B	¼ A and ¼ B	FECI	½ A and ½ B	¼ A and ¼ B	FECI
LL-37 and GEN	+ + + [+]	+ + + [+]	0.5	+ + + [+]	+ + + [+]	1.0	+ + + [+]	+ + + [+]	0.5	+ + + [+]	+ + + [+]	0.5
PG-1 and GEN	- - - [-]	- - - [-]	>1.0	+ + + [+]	+ + + [+]	0.5	- - - [-]	- - - [-]	>1.0	- - - [-]	- - - [-]	>1.0
PG-1 and PMB	+ + + [+]	+ + + [+]	0.5	+ + + [+]	+ + + [+]	>1.0	+ + + [+]	+ + + [+]	0.5	+ + + [+]	+ + + [+]	1.0
LYZ and GEN	+ + + [+]	+ + + [+]	>1.0	+ + + [+]	+ + + [+]	1.0	- - - [-]	- - - [-]	>1.0	+ + + [+]	+ + + [+]	1.0
LYZ and PMB	+ + + [+]	+ + + [+]	0.5	+ + + [+]	+ + + [+]	>1.0	+ + + [+]	+ + + [+]	0.5	+ + + [+]	+ + + [+]	0.5
ChBac3.4 and OX	+ + + [+]	+ + + [+]	1.0	+ + + [+]	+ + + [+]	>1.0	- - - [-]	- - - [-]	>1.0	- - - [-]	- - - [-]	>1.0
ChBac3.4 and OFL	- - - [-]	- - - [-]	>1.0	+ + + [+]	+ + + [+]	>1.0	- - - [-]	- - - [-]	>1.0	- - - [-]	- - - [-]	>1.0
ChBac3.4 and RIF	- - - [-]	- - - [-]	>1.0	- - - [-]	- - - [-]	>1.0	- - - [-]	- - - [-]	>1.0	- - - [-]	- - - [-]	>1.0

GEN, gentamicin; PMB, polymyxin B; OX, oxacillin; OFL, ofloxacin; RIF, rifampicin; LYZ, lysozyme.

+ | - presence or absence of the statistically significant difference from intact cells (Mann-Whitney U-test $p < 0.01$; $n_1 = 3$, $n_2 = 6-8$) in each of the three independent experiments; resulting assessment of the combination effect is given in square brackets.

^aAssessment of the minimal Fractional Effective Concentration Index (FECI) based on the results for (½ MEC A + ½ MEC B) and (¼ MEC A + ¼ MEC B) combinations of substances A and B; FECI > 1.0 shows independent action or antagonism, $0.5 < \text{FECI} \leq 1$ indicates additivity, $\text{FECI} \leq 0.5$ denotes synergy; synergy cases are set off in bold type. MEC, minimal effective concentration.

information on the mechanisms standing behind the observed synergistic action, and to verify the effectiveness of such combinations against multidrug-resistant bacterial strains.

A number of different generalized models explaining synergy are in place. Some are specific to the mechanisms of action of both components. They apply to the cases when the ways in which interacting compounds perform their individual action converge at some specific site; for example, if two drugs are inhibiting alternative pathways producing the same essential metabolite (Jia et al., 2009; Yeh et al., 2009), or if they share the same target, but bind non-competitively, providing synergy on molecular level (Breitinger, 2012). In other scenarios synergistic action is contributed mostly to the mechanism of action of one of the components in the pair. In such cases this component provides to the other a better ability to exert its effect (Zimmerman et al., 2007). It can be either due to facilitating the access of the second component to its targets or due to inhibiting some mechanism, for example, biodegradation, that prevent the second component from taking its action (Zimmerman et al., 2007; Cokol et al., 2011). In case of this bioavailability model, the first compound which is a “provider” of said bioavailability can demonstrate synergistic interactions with a large number of substances having distinctly different mechanisms of action (Chou, 2006). On the other hand, some researchers point out a possible danger of increasing bioavailability not only for the desired drug, but also for other substances which were not taken into consideration (Cokol et al., 2011).

Synergy observed so far in AMP/antibiotic pairs or for AMPs with antimicrobial proteins co-located with them *in vivo* is generally attributed to AMPs' brand ability to enhance the permeability of bacterial membranes and by extent the access of other compounds into the periplasm and cytoplasm of bacterial cells (Cassone and Otvos, 2010; Yenugu and Narmadha, 2010; Singh et al., 2014; Feng et al., 2015; Gupta et al., 2015; Khara et al., 2015; Soren et al., 2015). However, it does not eliminate the possibility that synergistic interactions of AMPs with other antimicrobials are not limited to just that.

Most of the cases of synergistic interaction we found in present study were between AMPs having a pronounced effect on the permeability of bacterial membranes (PG-1, β -defensins, LL-37) and antibiotics affecting the biosynthesis of nucleic acids and proteins, which, in order to perform their microbicidal action, must penetrate inside the cell. This fact supports the existing bioavailability model proposed for such synergy, suggesting the crucial role of AMP-provided membranolytic action in it.

Most frequently synergy was observed in combinations of AMPs with aminoglycoside gentamycin affecting protein synthesis at ribosomes, whereas effects of combined action with antibiotics influencing nucleic acid synthesis (rifampicin and ofloxacin) were a bit less frequent (more so for ofloxacin). The rate of development of the damaging effect can play a certain role here: violation of the synthesis of nucleic acids affects cell viability in a more distant perspective and needs more time to make a significant contribution compared to the rapid damage caused by the peptide, and compared to the peptide synthesis blockage on ribosome as well. Another factor may be the presence of rigid structures of fused aromatic rings in ofloxacin and rifampicin

molecules which can limit to some extent their ability to penetrate through the pores formed by AMPs.

Synergy with gentamycin was reproduced with another aminoglycoside amikacin. According to existing knowledge, after the electrostatic binding of aminoglycoside molecules carrying large positive charge to the negatively charged structures distributed on the surface of bacteria, the energy-dependent uptake of antibiotic into the cell takes place, although no specific carrier proteins were reported (Taber et al., 1987). Frequently reported cases of synergy between aminoglycosides and β -lactam antibiotics (Rahal, 2006; Leibovici and Paul, 2007) are believed to occur due to the damaging of the cell wall by β -lactams, facilitating the access of aminoglycosides to their targets (Davis, 1982). Based on that, the antimicrobial synergy of aminoglycosides with AMPs can also be attributed to the main proposed model: membrane-damaging performed by peptide allows easier access into the cell for the antibiotic. The fact that the synergistic action of gentamicin and membranolytic AMP PG-1 is more pronounced against Gram-negative bacteria (Table 2; Figure 1), where besides the cytoplasmic membrane, an additional external one also exists, supports this theory.

The scenario of bioavailability increase is also applicable to the combination of lysozyme and polymyxin B found to exert synergy against Gram-negative bacteria. Our data correspond with the known fact, that the pretreatment with non-bactericidal doses of polymyxin B allows lysozyme to lyse bacterial wall of Gram-negative bacteria in concentrations which are otherwise ineffective (Warren et al., 1957), and supply further evidence for this synergy in formal terms of Loewe additivity model. However, in this case it is the antibiotic that presumably damages the outer membrane to provide lysozyme with the access to the peptidoglycan layer. This hypothesis is supported by the study of combined action of lysozyme and polymyxin B immobilized on agarose beads which prevented the latter from interacting with other bacterial structures except outer membrane (Rosenthal and Storm, 1977). Though, there are facts demonstrating that the bioavailability model here works the other way around as well. The report by Galizzi et al. (1975) indicates that the presence of low doses of lysozyme, which do not affect microbial growth, renders Gram-positive bacteria *Bacillus subtilis*, both polymyxin-resistant and sensitive strains, susceptible to 10 times lower concentrations of polymyxin B. And the dynamic of permeabilization of the cytoplasmic membrane of *E. coli* ML-35p by polymyxin B observed in current study shows significant acceleration in presence of lysozyme.

The effect of combinations on the permeability of bacterial membranes in comparison with the effects of individual substances in the same concentrations was investigated not only for lysozyme and polymyxin B, but also for other AMP/antibiotic pairs showing synergy, as the damage to bacterial membranes is simultaneously the main mechanism of antibacterial action of AMPs and the main estimated cause of their synergistic interaction with other antimicrobial compounds.

From mechanistic considerations if the synergy-providing interaction of AMP and antibiotic is limited to the easier access of the latter into the inner space of bacterial cells using AMP-formed pores in their membranes, the effect of AMP on the membrane

permeability should not be affected by the presence or absence of antibiotic, at least in the beginning when antibiotic impact on bacterial biosynthesis is yet to manifest. This assumption proved to be right for AMP/antibiotic pairs including PG-1 and hBD-3 which caused swift increase of membrane permeability.

On the other hand, observed synergy cases were not limited to combinations with AMPs demonstrating rapid membranolytic action in tested concentrations. Thus, ChBac3.4 and HNP-1 in tested concentrations caused only slight effect on cytoplasmic membrane permeability. In case of synergy between HNP-1 and gentamicin against Gram-positive bacteria, HNP-1 described ability to bind lipid II, thereby disturbing bacterial cell wall synthesis, can contribute to the interaction observed, as in mentioned synergy of aminoglycosides with β -lactams (Rahal, 2006; Leibovici and Paul, 2007) the latter also affect said synthesis. Some supplementary mechanisms could be involved for ChBac3.4 as well, as its action is believed to include intracellular targets in addition to membrane disruption, especially in low concentrations.

Another interesting observation is a prominent acceleration of the membrane damaging process compared to the action of AMP alone found for the combination of LL-37 with gentamicin. On a lesser scale such effect was also observed for combinations of ChBac3.4 and HNP-1 with rifampicin. It suggests that in some cases the interaction between AMP and antibiotic may be more complex than the penetration of the antibiotic through the pores formed by peptide, and can include some direct or indirect effect on the incorporation or orientation of AMP molecules in the bacterial membrane mediated by antibiotic.

Further examination of antibiotics combinations with PG-1 and ChBac3.4 against clinically isolated multidrug-resistant strains of *E.coli*, *A. baumannii*, *P. aeruginosa*, *K. pneumoniae*, and *S. aureus* confirmed the described above dependencies in synergistic interaction. Most numerous cases of synergy were found for both peptides with amikacin used instead of gentamicin in these tests, and with erythromycin. This two antibiotics both affect protein synthesis by binding to bacterial ribosomes. Other studies also report synergy of AMPs with antibiotics targeting this process, such as chloramphenicol (Zhang et al., 1999; Yenugu and Narmadha, 2010; Sanchez-Gomez et al., 2011; Rajasekaran et al., 2017); tetracyclines (Giacometti et al., 2000c; Yenugu and Narmadha, 2010; Sanchez-Gomez et al., 2011); aminoglycosides gentamicin (Yenugu and Narmadha, 2010; Wu et al., 2017), tobramycin (Payne et al., 2017; Pollini et al., 2017), kanamycin (Anantharaman et al., 2010; Yenugu and Narmadha, 2010), streptomycin (Yenugu and Narmadha, 2010); macrolides azithromycin (Wu et al., 2017), erythromycin (Vaara and Porro, 1996; Ulvatne et al., 2001; Moerman et al., 2002; Sanchez-Gomez et al., 2011; Gopal et al., 2014; Jindal et al., 2017), clarithromycin (Giacometti et al., 1999, 2000a,b,c). Synergistic interactions with rifampicin affecting transcription and hence RNA synthesis are also frequently described (Vaara and Porro, 1996; Giacometti et al., 2000a; Ulvatne et al., 2001; Cirioni et al., 2008; Anantharaman et al., 2010; Yenugu and Narmadha, 2010; Khara et al., 2014, 2015; Gupta et al., 2015; Soren et al., 2015; Pollini et al., 2017).

Synergy with ofloxacin disturbing DNA-replication process was also shown against drug-resistant isolates, thought for PG-1 only against ofloxacin-susceptible *K. pneumoniae*. Synergistic interactions with different quinolone antibiotics are indicated in various publications: with naladixic acid (Scott et al., 1999; Zhang et al., 1999; Sanchez-Gomez et al., 2011), with ciprofloxacin (Scott et al., 1999; Giacometti et al., 2000a; Yenugu and Narmadha, 2010; Gopal et al., 2014; Singh et al., 2014; Bessa et al., 2018), with levofloxacin (Feng et al., 2015), and with norfloxacin (Niu et al., 2013); as well as synergy with novobiocin which also inhibit DNA-gyrase activity (Vaara and Porro, 1996).

Although the indications are quite vague, synergy between ChBac3.4 and oxacillin seems to manifest specifically against *S. aureus* strains resistant to this antibiotic. Further study is required to clarify if there are some unique features underlying AMP/antibiotic interaction in this case. Noteworthy, not only ChBac3.4, but also PG-1 was found to be synergistic with meropenem, another β -lactam antibiotic, against resistant *A. baumannii* and moderately resistant *S.aureus*; however, against meropenem-resistant *P. aeruginosa* this effect wasn't shown. Nevertheless, the obtained data look promising in the light of recent challenges posed by carbapenem-resistant bacteria. For both oxacillin and meropenem, synergy was found against bacteria which had enhanced MIC levels to these antibiotics, and was not found against those more sensitive; thereby it may be suspected, that some resistance mechanism can be affected by AMPs, thought further investigation is needed. Cases of AMPs synergy with β -lactam antibiotics against multidrug-resistant bacteria (including those resistant to this particular β -lactam) are also demonstrated in numerous works for ampicillin (Yenugu and Narmadha, 2010; Sanchez-Gomez et al., 2011), amoxicillin (Giacometti et al., 2000c; Moerman et al., 2002; Sanchez-Gomez et al., 2011; Wu et al., 2017), carbenicillin (Scott et al., 1999; Yenugu and Narmadha, 2010), ticarcillin (Sanchez-Gomez et al., 2011), aztreonam (Pollini et al., 2017), piperacillin (Giacometti et al., 2000b,c), cephalosporins ceftazidime (Giacometti et al., 2000b,c; Soren et al., 2015; Bessa et al., 2018), cefuroxime (Moerman et al., 2002), ceftriaxone (Giacometti et al., 2000c; Singh et al., 2014; Soren et al., 2015; Jindal et al., 2017), cefepime (Feng et al., 2015), cefotaxime (Gopal et al., 2014; Singh et al., 2014); carbapenems meropenem (Giacometti et al., 2000b,c; Sanchez-Gomez et al., 2011; Pollini et al., 2017), and imipenem (Sanchez-Gomez et al., 2011; Feng et al., 2015). In addition, AMPs are reported to synergize with vancomycin (Giacometti et al., 2000a; Shin et al., 2002; Feng et al., 2015; Wu et al., 2017) which also disturbs cell wall synthesis. He et al. (2015) indicate that wide synergy between magainin II and β -lactam antibiotics, also observed by Giacometti et al. (2000c), seems to be unusual, and may be provided by some unique mechanism. Giacometti et al. (2000a,b) mention the hypothesis that AMPs may trigger the activity of bacterial murein hydrolases, hence contributing to the peptidoglycan degradation in cooperation with β -lactams. Regarding possible resistance mechanisms attenuation, Sanchez-Gomez et al. (2011) suggest that some AMPs can counteract efflux pump overexpression. Soren et al. (2015) also refer to efflux pump systems as possible targets of AMPs action in Gram-negative bacteria.

Interestingly, in as much as 72.8 % (16 of 22) of all synergy cases observed in clinical isolates in the current study, bacteria indeed showed moderate or high level of resistance toward the antibiotic taking part in the synergistic pair. Thus, combined use of AMPs and antibiotics could be a valuable tool to decrease MIC levels of antibiotics in resistant strains, even if only 4–16 times. The ability of AMPs to prevent biofilm formation or affect those already formed (Algburi et al., 2017; Chung and Khanum, 2017) can also contribute to overcoming bacterial resistance to antibiotics. This kind of potentiation of antimicrobial activity was suggested in several reports (Gopal et al., 2014; de la Fuente-Núñez et al., 2015; Bessa et al., 2018) further substantiating possible benefits of combination antimicrobial therapy including AMPs. However, our study and previous works (Pollini et al., 2017) indicate that observed synergy is not universal for combating bacterial strains and species with different resistance profiles. Hence, such combination therapy will not allow avoiding susceptibility testing procedures even if applied in healthcare practice.

It is also of note, that in synergy cases with conventional antibiotics we observed *in vitro* for human AMPs their concentrations were around 150 nM for LL-37, 12.5–125 nM for HNP-1, 0.2–1.6 μ M for hBD-2, and 0.08–3.75 μ M for hBD-3. Some of these values fall within the range of concentrations of said peptides in different body fluids of healthy individuals reported in literature. It is mostly true for LL-37, which was detected in concentration of 0.15–6.1 μ M in saliva, of 0.16–1.9 μ M in bronchoalveolar lavage (BAL), and of 0.2–0.5 μ M in plasma (Byfield et al., 2011), and to the lesser extent for α -defensin, which was found in plasma in concentration of around 80–95 nM [13.5 ± 1.2 ng/50 μ L according to Mattar et al. (2016) and 323.3 ± 173.1 ng/ml according to Mukae et al. (2002)] and in BAL in concentration of 3.7 nM (12.9 ± 15 ng/ml according to Mukae et al. (2002)). However, for β -defensins reported concentrations were lower, in saliva their detected levels were 2.2 (0.3–4.8) nM [9.5 (1.2–21) μ g/L] for hBD-2 and 63 (10–182) nM [326 (50–931) μ g/L] for hBD-3 (Ghosh et al., 2007), hBD-2 concentration in serum was reported to be only 8.3 ± 3.9 pM (36.1 ± 17.0 pg/ml) (Arimura et al., 2004), and hBD-3 was not detected in BAL (Ghosh et al., 2007). Though, local concentrations of AMPs in the site of inflammation are supposed to become significantly higher, than these mean values.

We also found synergy of antibacterial action in combinations of the membranolytic AMP PG-1 and of the antimicrobial protein lysozyme with gelatin-stabilized silver nanoparticles, when tested on laboratory strains. This effect was observed in the majority of cases, against both Gram-positive and Gram-negative bacteria, and was quite pronounced providing 8–16 times decrease of effective concentrations. Synergy was previously described for silver nanoparticles with polymyxin B (Ruden et al., 2009), which acts rather similarly to the membranolytic AMPs. However, for ChBac3.4 interaction was additive as in some reported cases for other AMPs (Ruden et al., 2009; Mohanty et al., 2013). The impact of silver nanoparticles used in our study on bacterial membranes permeability was rather slow for the outer and absent for the inner one (Supplementary Figure S1A), but their effect on metabolic activity of bacteria was swift

(Supplementary Figure S1B), suggesting that they exert their action without penetrating through the cytoplasmic membrane. However, based on the observed synergy cases, we assume that membranolytic activity of AMPs plays a certain role in the realization of synergistic interaction. We could also hypothesize, that wide-scale oxidative effects provided by silver compounds can contribute to this outcome, as it has been reported that oxidation of membrane lipids potentiated bactericidal activity of membranoactive AMPs (Libardo et al., 2017).

The preparation of colloid silver stabilized with polyvinylpyrrolidone, currently used as a bactericidal agent in Russian Federation, also exerted synergistic effect of antimicrobial action in combination with AMPs against multidrug-resistant clinical isolates, including Gram-negative carbapenem-resistant strains of *A. baumannii* and *P. aeruginosa*, when with PG-1, and mildly meropenem-resistant Gram-positive strain *S. aureus* 1399/17, when with ChBac3.4; though only 4 times dose reduction was achieved in these cases.

Overall, the phenomenon of mutual potentiation of antibacterial activity for combinations of silver nanoparticles or colloids with antimicrobial polypeptides manifests rather abundantly. As well as AMPs, silver nanoparticles are believed to provide wide-scale damage for bacterial cells (Dakal et al., 2016). Bacterial resistance to silver preparations is rarely induced (Yang et al., 2018). Both AMPs (Algburi et al., 2017; Chung and Khanum, 2017), and nanoparticles (Blanchette and Wenke, 2018) are reported to prevent biofilm formation. Considering all these facts, the possibility of combined use of these two classes of compounds against multidrug-resistant pathogens looks very promising. As the penetration within bacterial cytoplasm do not appear to be necessarily required for the successful action of named substances, the idea of developing AMP-capped silver nanoparticles also has a prospect of practical use, as it was already suggested for polymyxin B stabilized ones (Lambadi et al., 2015).

Though hints on the additional mechanisms behind the synergy of AMPs with other antimicrobial compounds were found, their effect on bacterial membranes permeability seems to be the main (or at least very important) cause of said interaction. The wide-scale effect provided by AMPs on membrane bilayers has its downside of comparatively low selectivity and is believed to be the cause of some cytotoxic effects toward eukaryotic cells, for instance, hemolytic activity, observed in many AMPs (Matsuzaki, 2009; Takahashi et al., 2010). Hence, we considered possible amplification of toxicity in combinations, as several cases where antibiotic presence enhanced the rate of membrane damaging caused by AMP in bacteria had been revealed in previous experiments. The results of hemolytic test for AMP/antibiotic combinations showing antimicrobial synergy were promising: no evidence of synergy or even additivity of hemolytic action was detected, supporting the notion that combined use may indeed reduce toxicity and increase selectivity. The same is reported for AMPs and silver nanoparticles (Ruden et al., 2009). However, when cytotoxicity was tested against different eukaryotic cells using MTT-test, combinations including membranoactive components were found synergistic in a number of cases. Though the proportion of components in tested combinations was significantly different

than that in the antimicrobial assays, as the range between toxic and antimicrobial concentrations is wider for antibiotics than for AMPs, observed synergy indicates that this factor should be closely considered when choosing the optimal antimicrobial compositions containing AMPs. On the other hand, ability of AMPs to synergistically enhance cytotoxic effects in combinations with other compounds can be of use regarding possible antitumor applications, as the effect was also found for PG-1 and anticancer drug doxorubicin against both doxorubicin-sensitive and doxorubicin-resistant human erythromyeloid leukemia cells (K562 cell line).

CONCLUSION

The results obtained in current study together with data published by other researchers indicate that synergistic combinations of AMPs with antibiotics as well as with silver nanoparticles are effective tools against multidrug-resistant bacterial strains, including carbapenem-resistant clinical isolates. The most abundant synergy, including the interactions with human endogenous AMPs, is observed for antibiotics targeting protein biosynthesis, such as aminoglycosides and macrolids. Thus, these antibiotics may enhance the antimicrobial activity of host defensive molecules as well as can be used in combinations with AMP-derived antimicrobial drugs.

Our study confirms that the ability of AMPs to permeabilize bacterial membranes plays central role in their synergy with other antimicrobial compounds, but also indicates that this ability could be in turn modulated by the second substance in the combination contributing to the combined effect. Certain cases of synergy with non-membranolytic AMPs suggest that additional mechanisms also exist and require further exploration.

Some cases of increasing cytotoxic activity toward host cells *in vitro* found for AMPs used in combinations with conventional antibiotics point to the importance of further investigation of these effects *in vivo* to avoid them upon a practical application of AMPs against bacteria. However, synergistic action of PG-1 with an antitumor drug doxorubicin indicates the prospect for AMPs in the development of new approaches for combination anticancer therapy.

Taken together our data contribute to the conception of the prospect of an application of antimicrobial peptides of the innate

immune systems as non-traditional tools for counteracting drug-resistant bacteria, in particular by their usage in combination with conventional antibiotics.

AUTHOR CONTRIBUTIONS

OS and DO contributed conception and design of the study. MZ performed all antimicrobial testing experiments, the statistical analysis of the obtained data, wrote the first draft of the manuscript. DO participated in the experiments on the evaluation of the effects of AMP/antibiotics combination on bacterial membrane permeabilization. TG elaborated doxorubicin-resistant K562 erythroleukemia cell line; IE examined the hemolytic activity of the studied substances, OC carried out MTT tests. OG synthesized and characterized silver nanoparticles. All authors contributed to manuscript revision, read, and approved the submitted version.

FUNDING

This work was supported by RFBR grants No 18-315-00333 and No 17-04-02177a.

ACKNOWLEDGMENTS

We would like to acknowledge Prof. R. Lehrer (University of California, Los Angeles, USA), Prof. A. Tossi (University of Trieste, Italy), Prof. G. Afinogenov (St. Petersburg State University, Russia), Dr. A. Afinogenova (Research Institute of Epidemiology and Microbiology named after L. Pasteur, St. Petersburg, Russia), Dr. E. Ermolenko (Institute of Experimental Medicine, St. Petersburg, Russia) for providing bacteria used in this study and characterization of their antibiotic resistance; Dr. A. Kolobov (State Research Institute of Highly Pure Biopreparations, St. Petersburg, Russia) for the synthesized batenecin ChBac 3.4.

SUPPLEMENTARY MATERIAL

The Supplementary Material for this article can be found online at: <https://www.frontiersin.org/articles/10.3389/fcimb.2019.00128/full#supplementary-material>

REFERENCES

- Al-Benna, S., Shai, Y., Jacobsen, F., and Steintraesser, L. (2011). Oncolytic activities of host defense peptides. *Int. J. Mol. Sci.* 12, 8027–8051. doi: 10.3390/ijms12118027
- Aldred, K. J., Kerns, R. J., and Osheroff, N. (2014). Mechanism of quinolone action and resistance. *Biochemistry* 53, 1565–1574. doi: 10.1021/bi5000564
- Alexander, J. W. (2009). History of the medical use of silver. *Surg. Infect.* 10, 289–292. doi: 10.1089/sur.2008.9941
- Algburi, A., Comito, N., Kashtanov, D., Dicks, L. M., and Chikindas, M. L. (2017). Control of biofilm formation: antibiotics and beyond. *Appl. Environ. Microbiol.* 83:e02508–16. doi: 10.1128/AEM.02508–16
- Anantharaman, A., Rizvi, M. S., and Sahal, D. (2010). Synergy with rifampin and kanamycin enhances potency, kill kinetics, and selectivity of *de novo*-designed antimicrobial peptides. *Antimicrob. Agents Chemother.* 54, 1693–1699. doi: 10.1128/AAC.01231–09
- Arimura, Y., Ashitani, J., Yanagi, S., Tokojima, M., Abe, K., Mukae, H., et al. (2004). Elevated serum beta-defensins concentrations in patients with lung cancer. *Anticancer Res.* 24, 4051–4057. Available online at: <http://ar.iiarjournals.org/content/24/6/4051.long>
- Aumelas, A., Mangoni, M., Roumestand, C., Chiche, L., Despau, E., Grassy, G., et al. (1996). Synthesis and solution structure of the antimicrobial peptide protegrin-1. *Eur. J. Biochem.* 237, 575–583. doi: 10.1111/j.1432-1033.1996.0575p.x
- Berenbaum, M. C. (1977). Synergy, additivism and antagonism in immunosuppression. A critical review. *Clin. Exp. Immunol.* 28, 1–18.
- Bessa, L. J., Eaton, P., Dematei, A., Plácido, A., Vale, N., Gomes, P., et al. (2018). Synergistic and antibiofilm properties of ocellatin peptides against

- multidrug-resistant *Pseudomonas aeruginosa*. *Future Microbiol.* 13, 151–163. doi: 10.2217/fmb-2017-0175
- Blanchette, K. A., and Wenke, J. C. (2018). Current therapies in treatment and prevention of fracture wound biofilms: why a multifaceted approach is essential for resolving persistent infections. *J. Bone Jt. Infect.* 3, 50–67. doi: 10.7150/jbji.23423
- Bolintineanu, D. S., and Kaznessis, Y. N. (2011). Computational studies of protegrin antimicrobial peptides: a review. *Peptides* 32, 188–201. doi: 10.1016/j.peptides.2010.10.006
- Breiting, H.-G. (2012). “Drug synergy – mechanisms and methods of analysis,” in *Toxicity and Drug Testing*, ed B. Acree (InTech), 143–166. doi: 10.5772/30922. Available online from: <http://www.intechopen.com/books/toxicity-and-drug-testing/drug-synergy-mechanisms-and-methods-of-analysis>
- Brogden, K. A. (2005). Antimicrobial peptides: pore formers or metabolic inhibitors in bacteria? *Nat. Rev. Microbiol.* 3, 238–250. doi: 10.1038/nrmicro1098
- Byfield, F. J., Wen, Q., Leszczynska, K., Kulakowska, A., Namiot, Z., Janmey, P. A., et al. (2011). Cathelicidin LL-37 peptide regulates endothelial cell stiffness and endothelial barrier permeability. *Am. J. Physiol. Cell. Physiol.* 300, C105–C112. doi: 10.1152/ajpcell.00158.2010
- Carmona-Ribeiro, A. M., and de Melo Carrasco, L. D. (2014). Novel formulations for antimicrobial peptides. *Int. J. Mol. Sci.* 15, 18040–18083. doi: 10.3390/ijms151018040
- Carretero, M., Escamez, M. J., Garcia, M., Duarte, B., Holguin, A., Retamosa, L., et al. (2008). *In vitro* and *in vivo* wound healing-promoting activities of human cathelicidin LL-37. *J. Invest. Dermatol.* 128, 223–236. doi: 10.1038/sj.jid.5701043
- Cassone, M., and Otvos, L. Jr. (2010). Synergy among antibacterial peptides and between peptides and small-molecule antibiotics. *Expert Rev. Anti Infect. Ther.* 8, 703–716. doi: 10.1586/eri.10.38
- Cavassin, E. D., de Figueiredo, L. F. P., Otoch, J. P., Seckler, M. M., de Oliveira, R. A., Franco, F. F., et al. (2015). Comparison of methods to detect the *in vitro* activity of silver nanoparticles (AgNP) against multidrug resistant bacteria. *J. Nanobiotechnol.* 13:64. doi: 10.1186/s12951-015-0120-6
- Chen, X. J., Niyonsaba, F., Ushio, H., Okuda, D., Nagaoka, I., Ikeda, S., et al. (2005). Synergistic effect of antibacterial agents human beta-defensins, cathelicidin LL-37 and lysozyme against *Staphylococcus aureus* and *Escherichia coli*. *J. Dermatol. Sci.* 40, 123–132. doi: 10.1016/j.jdermsci.2005.03.014
- Chou, T. C. (2006). Theoretical basis, experimental design and computerized simulation of synergism and antagonism in drug combination studies. *Pharmacol. Rev.* 58, 621–681. doi: 10.1124/pr.58.3.10
- Chou, T. C., and Talalay, P. (1983). Analysis of combined drug effects: a new look at a very old problem. *Trends Pharmacol. Sci.* 4, 450–454. doi: 10.1016/0165-6147(83)90490-x
- Chung, P. Y., and Khanum, R. (2017). Antimicrobial peptides as potential anti-biofilm agents against multidrug-resistant bacteria. *J. Microbiol. Immunol. Infect.* 50, 405–410. doi: 10.1016/j.jmii.2016.12.005
- Cirioni, O., Silvestri, C., Ghiselli, R., Orlando, F., Riva, A., Mocchegiani, F., et al. (2008). Protective effects of the combination of alpha-helical antimicrobial peptides and rifampicin in three rat models of *Pseudomonas aeruginosa* infection. *J. Antimicrob. Chemother.* 62, 1332–1338. doi: 10.1093/jac/dkn393
- Close, B., Banister, K., Baumans, V., Bernoth, E.-M., Bromage, N., Bunyan, J., et al. (1996). Recommendations for euthanasia of experimental animals: Part 1. *Lab Anim.* 30, 293–316. doi: 10.1258/002367796780739871
- Cokol, M., Chua, H. N., Tasan, M., Mutlu, B., Weinstein, Z. B., Suzuki, Y., et al. (2011). Systematic exploration of synergistic drug pairs. *Mol. Syst. Biol.* 7:544. doi: 10.1038/msb.2011.71
- Dakal, T. C., Kumar, A., Majumdar, R. S., and Yadav, V. (2016). Mechanistic basis of antimicrobial actions of silver nanoparticles. *Front Microbiol.* 7:1831. doi: 10.3389/fmicb.2016.01831
- Dale, B. A., and Fredericks, L. P. (2005). Antimicrobial peptides in the oral environment: expression and function in health and disease. *Curr. Issues Mol. Biol.* 7, 119–133. doi: 10.21775/cimb.007.119
- Davis, B. D. (1982). Bactericidal synergism between beta-lactams and aminoglycosides: mechanism and possible therapeutic implications. *Rev. Infect. Dis.* 4, 237–245. doi: 10.1093/clinids/4.2.237
- Davis, B. D. (1987). Mechanism of bactericidal action of aminoglycosides. *Microbiol. Rev.* 51, 341–350.
- de la Fuente-Núñez, C., Reffuveille, F., Mansour, S. C., Reckseidler-Zenteno, S. L., Hernández, D., Brackman, G., et al. (2015). D-Enantiomeric peptides that eradicate wild-type and multidrug-resistant biofilms and protect against lethal *Pseudomonas aeruginosa* infections. *Chem. Biol.* 22, 196–205. doi: 10.1016/j.chembiol.2015.01.002
- de Leeuw, E., Li, C., Zeng, P., Li, C., Diepvee-de Buin, M., Lu, W. Y., et al. (2010). Functional interaction of human neutrophil peptide-1 with the cell wall precursor lipid II. *FEBS Lett.* 584, 1543–1548. doi: 10.1016/j.febslet.2010.03.004
- Deslouches, B., Steckbeck, J. D., Craig, J. K., Doi, Y., Mietzner, T. A., and Montelaro, R. C. (2013). Rational design of engineered cationic antimicrobial peptides consisting exclusively of arginine and tryptophan, and their activity against multidrug-resistant pathogens. *Antimicrob. Agents Chemother.* 57, 2511–2521. doi: 10.1128/aac.02218-12
- Durán, N., Marcato, P. D., De Conti, R., Alves, O. L., Costab, F. T. M., and Brocchib, M. (2010). Potential use of silver nanoparticles on pathogenic bacteria, their toxicity and possible mechanisms of action. *J. Braz. Chem. Soc.* 21, 949–959. doi: 10.1590/S0103-50532010000600002
- Durán, N., Silveira, C. P., Durán, M., and Martinez, D. S. (2015). Silver nanoparticle protein corona and toxicity: a mini-review. *J. Nanobiotechnol.* 13:55. doi: 10.1186/s12951-015-0114-4
- Fábián, T. K., Hermann, P., Beck, A., Fejérdy, P., and Fábián, G. (2012). Salivary defense proteins: their network and role in innate and acquired oral immunity. *Int. J. Mol. Sci.* 13, 4295–4320. doi: 10.3390/ijms13044295
- Fehri, L. F., Wróblewski, H., and Blanchard, A. (2007). Activities of antimicrobial peptides and synergy with enrofloxacin against *Mycoplasma pulmonis*. *Antimicrob. Agents Chemother.* 51, 468–474. doi: 10.1128/aac.01030-06
- Feng, Q., Huang, Y., Chen, M., Li, G., and Chen, Y. (2015). Functional synergy of alpha-helical antimicrobial peptides and traditional antibiotics against Gram-negative and Gram-positive bacteria *in vitro* and *in vivo*. *Eur. J. Clin. Microbiol. Infect. Dis.* 34, 197–204. doi: 10.1007/s10096-014-2219-3
- Fleming, A. (1922). On a remarkable bacteriolytic element found in tissues and secretions. *Proc. Roy. Soc. Ser. B.* 93, 306–317. doi: 10.1098/rspb.1922.0023
- Galizzi, A., Cacco, G., Siccardi, A. G., and Mazza, G. (1975). Mode of action of polymyxin B: physiological studies with *Bacillus subtilis*-resistant mutant. *Antimicrob. Agents Chemother.* 8, 366–369. doi: 10.1128/aac.8.3.366
- Gallo, R. L., and Hooper, L. V. (2012). Epithelial antimicrobial defence of the skin and intestine. *Nat. Rev. Immunol.* 12, 503–516. doi: 10.1038/nri3228
- Gaspar, D., Veiga, A. S., and Castanho, M. A. R. B. (2013). From antimicrobial to anticancer peptides. A review. *Front. Microbiol.* 4:294. doi: 10.3389/fmicb.2013.00294
- Ghosh, S. K., Gerken, T. A., Schneider, K. M., Feng, Z., McCormick, T. S., and Weinberg, A. (2007). Quantification of human beta-defensin-2 and -3 in body fluids: application for studies of innate immunity. *Clin. Chem.* 53, 757–765. doi: 10.1373/clinchem.2006.081430
- Giacometti, A., Cirioni, O., Barchiesi, F., Fortuna, M., and Scalise, G. (1999). *In-vitro* activity of cationic peptides alone and in combination with clinically used antimicrobial agents against *Pseudomonas aeruginosa*. *J. Antimicrob. Chemother.* 44, 641–645. doi: 10.1093/jac/44.5.641
- Giacometti, A., Cirioni, O., Barchiesi, F., and Scalise, G. (2000a). *In-vitro* activity and killing effect of polycationic peptides on methicillin-resistant *Staphylococcus aureus* and interactions with clinically used antibiotics. *Diagn. Microbiol. Infect. Dis.* 38, 115–118. doi: 10.1016/s0732-8893(00)00175-9
- Giacometti, A., Cirioni, O., Del Prete, M. S., Barchiesi, F., Fortuna, M., Drenaggi, D., et al. (2000b). *In vitro* activities of membrane-active peptides alone and in combination with clinically used antimicrobial agents against *Stenotrophomonas maltophilia*. *Antimicrob. Agents Chemother.* 44, 1716–1719. doi: 10.1128/aac.44.6.1716-1719.2000
- Giacometti, A., Cirioni, O., Del Prete, M. S., Paggi, A. M., D’Errico, M. M., and Scalise, G. (2000c). Combination studies between polycationic peptides and clinically used antibiotics against Gram-positive and Gram-negative bacteria. *Peptides* 21, 1155–1160. doi: 10.1016/s0196-9781(00)00254-0
- Gopal, R., Kim, Y. G., Lee, J. H., Lee, S. K., Chae, J. D., Son, B. K., et al. (2014). Synergistic effects and antibiofilm properties of chimeric peptides against multidrug-resistant *Acinetobacter baumannii* strains. *Antimicrob. Agents Chemother.* 58, 1622–1629. doi: 10.1128/AAC.02473-13
- Gordon, Y. J., Romanowski, E. G., and McDermott, A. M. (2005). A review of antimicrobial peptides and their therapeutic potential as anti-infective drugs. *Curr. Eye Res.* 30, 505–515. doi: 10.1080/02713680590968637

- Greco, W., Unkelbach, H.-D., Pösch, G., Sühnel, J., Kundi, M., and Bödeker, W. (1992). Consensus on concepts and terminology for combined-action assessment: the Saarisekka agreement. *Arch. Complex Environmen. Studies*. 4, 65–69.
- Grinchuk, T. M., Pavlenko, M. A., Lipskaya, L. A., Sorokina, E. A., Tarunina, M. V., Berjokina, E. V., et al. (1998). Resistance to adriamycin in human chronic promyeloleukemia line K562 correlates with directed genome destabilization–amplification of MDR1 gene and nonrandom changes in karyotype structure. *Cytology*. 40, 652–660.
- Guaní-Guerra, E., Santos-Mendoza, T., Lugo-Reyes, S. O., and Terán, L. M. (2010). Antimicrobial peptides: general overview and clinical implications in human health and disease. *Clin. Immunol.* 135, 1–11. doi: 10.1016/j.clim.2009.12.004
- Guilhelmelli, F., Vilela, N., Albuquerque, P., Derengowski Lda, S., Silva-Pereira, I., and Kyaw, C. M. (2013). Antibiotic development challenges: the various mechanisms of action of antimicrobial peptides and of bacterial resistance. *Front. Microbiol.* 4:353. doi: 10.3389/fmicb.2013.00353
- Gupta, K., Singh, S., and van Hoek, M. L. (2015). Short, synthetic cationic peptides have antibacterial activity against *Mycobacterium smegmatis* by forming pores in membrane and synergizing with antibiotics. *Antibiotics* 4, 358–378. doi: 10.3390/antibiotics4030358
- Hale, J. D., and Hancock, R. E. (2007). Alternative mechanisms of action of cationic antimicrobial peptides on bacteria. *Expert Rev. Anti. Infect. Ther.* 5, 951–959. doi: 10.1586/14787210.5.6.951
- Hancock, R. E., and Lehrer, R. (1998). Cationic peptides: a new source of antibiotics. *Trends Biotechnol.* 16, 82–88. doi: 10.1016/s0167-7799(97)01156-6
- Hancock, R. E., and Rozek, A. (2002). Role of membranes in the activities of antimicrobial cationic peptides. *FEMS Microbiol. Lett.* 206, 143–149. doi: 10.1111/j.1574-6968.2002.tb11000.x
- Haney, E. F., Mansour, S. C., and Hancock, R. E. W. (2017). “Antimicrobial peptides: an introduction,” in *Antimicrobial Peptides. Methods in Molecular Biology*, Vol. 1548, ed P. Hansen (New York, NY: Humana Press), 3–22. doi: 10.1007/978-1-4939-6737-7_1
- He, J., Starr, C. G., and Wimley, W. C. (2015). A lack of synergy between membrane-permeabilizing cationic antimicrobial peptides and conventional antibiotics. *Biochim. Biophys. Acta*. 1848, 8–15. doi: 10.1016/j.bbamem.2014.09.010
- Hsieh, M. H., Yu, C. M., Yu, V. L., and Chow, J. W. (1993). Synergy assessed by checkerboard. A critical analysis. *Diagn. Microbiol. Infect. Dis.* 16, 343–349. doi: 10.1016/0732-8893(93)90087-n
- Ibrahim, H. R., Matsuzaki, T., and Aoki, T. (2001). Genetic evidence that antibacterial activity of lysozyme is independent of its catalytic function. *FEBS Lett.* 506, 27–32. doi: 10.1016/s0014-5793(01)02872-1
- Jia, J., Zhu, F., Ma, X., Cao, Z., Li, Y., and Chen, Y. Z. (2009). Mechanisms of drug combinations: interaction and network perspectives. *Nat. Rev. Drug Discov.* 8, 111–128. doi: 10.1038/nrd2683
- Jindal, H. M., Zandi, K., Ong, K. C., Velayuthan, R. D., Rasid, S. M., Samudi Raju, C., et al. (2017). Mechanisms of action and *in vivo* antibacterial efficacy assessment of five novel hybrid peptides derived from Indolicidin and Ranalexin against *Streptococcus pneumoniae*. *PeerJ*. 5:e3887. doi: 10.7717/peerj.388
- Kang, S. J., Park, S. J., Mishig-Ochir, T., and Lee, B. J. (2014). Antimicrobial peptides: therapeutic potentials. *Expert Rev. Anti. Infect. Ther.* 12, 1477–1486. doi: 10.1586/14787210.2014.976613
- Keskar, M. R., and Jugade, R. M. (2015). Spectrophotometric investigations of macrolide antibiotics: a brief review. *Anal. Chem. Insights*. 10, 29–37. doi: 10.4137/ACIS31857
- Khara, J. S., Lim, F. K., Wang, Y., Ke, X.-Y., Voo, Z. X., Yang, Y. Y., et al. (2015). Designing α -helical peptides with enhanced synergism and selectivity against *Mycobacterium smegmatis*: discerning the role of hydrophobicity and helicity. *Acta Biomater.* 28, 99–108. doi: 10.1016/j.actbio.2015.09.015
- Khara, J. S., Wang, Y., Ke, X. Y., Liu, S., Newton, S. M., Langford, P. R., et al. (2014). Anti-mycobacterial activities of synthetic cationic alpha-helical peptides and their synergism with rifampicin. *Biomaterials*. 35, 2032–2038. doi: 10.1016/j.biomaterials.2013.11.035
- Knappe, D., Kabankov, N., Herth, N., and Hoffmann, R. (2016). Insect-derived short proline-rich and murine cathelicidin-related antimicrobial peptides act synergistically on Gram-negative bacteria *in vitro*. *Future Med. Chem.* 8, 1035–1045. doi: 10.4155/fmc-2016-0083
- Kokryakov, V. N., Harwig, S. S., Panyutich, E. A., Shevchenko, A. A., Aleshina, G. M., Shamova, O. V., et al. (1993). Protegrins: leukocyte antimicrobial peptides that combine features of corticostatic defensins and tachyplesins. *FEBS Lett.* 327, 231–236. doi: 10.1016/0014-5793(93)80175-T
- Kong, K. F., Schnepel, L., and Mathee, K. (2010). Beta-lactam antibiotics: from antibiosis to resistance and bacteriology. *APMIS*. 118, 1–36. doi: 10.1111/j.1600-0463.2009.02563.x
- Krizsan, A., Prahl, C., Goldbach, T., Knappe, D., and Hoffmann, R. (2015). Short proline-rich antimicrobial peptides inhibit either the bacterial 70S ribosome or the assembly of its large 50S subunit. *Chembiochem*. 16, 2304–2308. doi: 10.1002/cbic.201500375
- Lai, Y., and Gallo, R. L. (2009). AMPed Up immunity: how antimicrobial peptides have multiple roles in immune defense. *Trends Immunol.* 30, 131–141. doi: 10.1016/j.it.2008.12.003
- Laible, N. J., and Germaine, G. R. (1985). Bactericidal activity of human lysozyme, muramidase-inactive lysozyme and cationic polypeptides against *Streptococcus sanguis* and *Streptococcus faecalis*: inhibition by chitin oligosaccharides. *Infect. Immun.* 48, 720–728.
- Lambadi, P. R., Sharma, T. K., Kumar, P., Vasnani, P., Thalluri, S. M., Bisht, N., et al. (2015). Facile biofunctionalization of silver nanoparticles for enhanced antibacterial properties, endotoxin removal, and biofilm control. *Int. J. Nanomedicine* 10, 2155–2171. doi: 10.2147/IJN.S72923
- Lara, H. H., Garza-Treviño, E. N., Ixtepan-Turrent, L., and Singh, D. K. (2011). Silver nanoparticles are broad-spectrum bactericidal and virucidal compounds. *J. Nanobiotechnol.* 9:30. doi: 10.1186/1477-3155-9-30
- LaRock, C. N., and Nizet, V. (2015). Cationic antimicrobial peptide resistance mechanisms of streptococcal pathogens. *Biochim. Biophys. Acta*. 1848(11Pt B), 3047–3054. doi: 10.1016/j.bbamem.2015.02.010
- Le, C. F., Fang, C. M., and Sekaran, S. D. (2017). Intracellular targeting mechanisms by antimicrobial peptides. *Antimicrob. Agents Chemother.* 61, 02340–02316. doi: 10.1128/AAC.02340-16
- Lehrer, R. I., Barton, A., and Ganz, T. (1988). Concurrent assessment of inner and outer membrane permeabilization and bacteriolysis in *E. coli* by multiple-wavelength spectrophotometry. *J. Immunol. Methods*. 108, 153–158. doi: 10.1016/0022-1759(88)90414-0
- Lehrer, R. I., and Lu, W. (2012). α -defensins in human innate immunity. *Immunol. Rev.* 245, 84–112. doi: 10.1111/j.1600-065x.2011.01082.x
- Leibovici, L., and Paul, M. (2007). Aminoglycoside/beta-lactam combinations in clinical practice. *J. Antimicrob. Chemother.* 60, 911–912. doi: 10.1093/jac/dkm377
- Libardo, M. D. J., Wang, T. Y., Pellois, J. P., and Angeles-Boza, A. M. (2017). How does membrane oxidation affect cell delivery and cell killing? *Trends Biotechnol.* 35, 686–690. doi: 10.1016/j.tibtech.2017.03.015
- Machado, L. R., and Ottoloni, B. (2015). An evolutionary history of defensins: a role for copy number variation in maximizing host innate and adaptive immune responses. *Front. Immunol.* 6:115. doi: 10.3389/fimmu.2015.00115
- Mahlapuu, M., Hakansson, J., Ringstad, L., and Bjorn, C. (2016). Antimicrobial peptides: an emerging category of therapeutic agents. *Front Cell Infect Microbiol.* 6:194. doi: 10.3389/fcimb.2016.00194
- Mansour, S. C., Pena, O. M., and Hancock, R. E. (2014). Host defense peptides: front-line immunomodulators. *Trends Immunol.* 35, 443–450. doi: 10.1016/j.it.2014.07.004
- Markowska, K., Grudniak, A. M., and Wolska, K. I. (2013). Silver nanoparticles as an alternative strategy against bacterial biofilms. *Acta Biochim Pol.* 60, 523–530.
- Maróti, G., Kereszt, A., Kondorosi, E., and Mergaert, P. (2011). Natural roles of antimicrobial peptides in microbes, plants and animals. *Res. Microbiol.* 162, 363–374. doi: 10.1016/j.resmic.2011.02.005
- Marxer, M., Vollenweider, V., and Schmid-Hempel, P. (2016). Insect antimicrobial peptides act synergistically to inhibit a trypanosome parasite. *Philos. Trans. R. Soc. Lond. B. Biol. Sci.* 371:20150302. doi: 10.1098/rstb.2015.0302
- Masschalck, B., and Michiels, C. W. (2003). Antimicrobial properties of lysozyme in relation to foodborne vegetative bacteria. *Crit. Rev. Microbiol.* 29, 191–214. doi: 10.1080/713610448
- Matsuzaki, K. (2009). Control of cell selectivity of antimicrobial peptides. *Biochim. Biophys. Acta*. 1788, 1687–1692. doi: 10.1016/j.bbamem.2008.09.013
- Mattar, E. H., Almedhar, H. A., Aljaddawi, A. A., Abu Zeid, I. E., and Redwan, E. M. (2016). Elevated concentration of defensins in hepatitis C virus-infected patients. *J. Immunol. Res.* 2016:8373819. doi: 10.1155/2016/8373819

- Mattiuzzo, M., Bandiera, A., Gennaro, R., Benincasa, M., Pacor, S., Antcheva, N., et al. (2007). Role of the *Escherichia coli* SbmA in the antimicrobial activity of prolinerich peptides. *Mol. Microbiol.* 66, 151–163. doi: 10.1111/j.1365-2958.2007.05903.x
- Moerman, L., Bosteels, S., Noppe, W., Willems, J., Clynen, E., Schoofs, L., et al. (2002). Antibacterial and antifungal properties of alpha-helical, cationic peptides in the venom of scorpions from southern Africa. *Eur. J. Biochem.* 269, 4799–4810. doi: 10.1046/j.1432-1033.2002.03177.x
- Mohanty, S., Jena, P., Mehta, R., Pati, R., Banerjee, B., Patil, S., et al. (2013). Cationic antimicrobial peptides and biogenic silver nanoparticles kill mycobacteria without eliciting DNA damage and cytotoxicity in mouse macrophages. *Antimicrob. Agents Chemother.* 57, 3688–3698. doi: 10.1128/AAC.02475-12
- Mosmann, T. (1983). Rapid colorimetric assay for cellular growth and survival: application to proliferation and cytotoxicity assays. *J. Immunol. Methods.* 65, 55–63. doi: 10.1016/0022-1759(83)90303-4
- Mukae, H., Iiboshi, H., Nakazato, M., Hiratsuka, T., Tokojima, M., Abe, K., et al. (2002). Raised plasma concentrations of alpha-defensins in patients with idiopathic pulmonary fibrosis. *Thorax.* 57, 623–628. doi: 10.1136/thorax.57.7.623
- Nguyen, L. T., Haney, E. F., and Vogel, H. J. (2011). The expanding scope of antimicrobial peptide structures and their modes of action. *Trends Biotechnol.* 29, 464–472. doi: 10.1016/j.tibtech.2011.05.001
- Niu, M., Li, X., Gong, Q., Wang, C., Qin, C., Wang, W., et al. (2013). Expression of 4kD scorpion defensin and its *in vitro* synergistic activity with conventional antibiotics. *World J. Microbiol. Biotechnol.* 29, 281–288. doi: 10.1007/s11274-012-1181-4
- Orhan, G., Bayram, A., Zer, Y., and Balci, I. (2005). Synergy tests by E test and checkerboard methods of antimicrobial combinations against *Brucella melitensis*. *J. Clin. Microbiol.* 43, 140–143. doi: 10.1128/jcm.43.1.140-143.2005
- Otvos, L. (2002). The short proline-rich family. *Cell Mol. Life Sci.* 59, 1138–1150. doi: 10.1007/s00018-002-8493-8
- Pace, C. N., Vajdos, F., Fee, L., Grimsley, G., and Gray, T. (1995). How to measure and predict the molar absorption coefficient of a protein. *Protein Sci.* 4, 2411–2423. doi: 10.1002/pro.5560041120
- Papp-Wallace, K. M., Endimiani, A., Taracila, M. A., and Bonomo, R. A. (2011). Carbapenems: past, present, and future. *Antimicrob. Agents Chemother.* 55, 4943–4960. doi: 10.1128/AAC.00296-11
- Payne, J. E., Dubois, A. V., Ingram, R. J., Weldon, S., Taggart, C. C., Elborn, J. S., et al. (2017). Activity of innate antimicrobial peptides and ivacaftor against clinical cystic fibrosis respiratory pathogens. *Int. J. Antimicrob. Agents.* 50, 427–435. doi: 10.1016/j.ijantimicag.2017.04.014
- Pfalzgraff, A., Brandenburg, K., and Weindl, G. (2018). Antimicrobial peptides and their therapeutic potential for bacterial skin infections and wounds. *Front. Pharmacol.* 9:281. doi: 10.3389/fphar.2018.00281
- Phoenix, D. A., Dennison, S. R., and Harris, F. (2013). *Antibacterial Peptides*. Weinheim: Wiley-VCH Verlag GmbH & Co. KGaA. doi: 10.1002/9783527652853
- Pillai, S. K., Moellering, R. C., and Eliopoulos, G. M. (2005). “Antimicrobial Combinations” in *Antibiotics in Laboratory Medicine, 5th Edn*, ed V. Lorian (Philadelphia, PA: the Lippincott Williams & Wilkins Co.), 365–440.
- Pollini, S., Brunetti, J., Sennati, S., Rossolini, G. M., Bracci, L., Pini, A., et al. (2017). Synergistic activity profile of an antimicrobial peptide against multidrug-resistant and extensively drug-resistant strains of Gram-negative bacterial pathogens. *J. Pept. Sci.* 23, 329–333. doi: 10.1002/psc.2978
- Rahal, J. J. (2006). Novel Antibiotic Combinations against Infections with Almost Completely Resistant *Pseudomonas aeruginosa* and *Acinetobacter* Species. *Clin. Infect. Dis.* 43, S95–S99. doi: 10.1086/504486
- Rai, M. K., Deshmukh, S. D., Ingle, A. P., and Gade, A. K. (2012). Silver nanoparticles: the powerful nanoweapon against multidrug-resistant bacteria. *J. Appl. Microbiol.* 112, 841–852. doi: 10.1111/j.1365-2672.2012.05253.x
- Rajasekaran, G., Kim, E. Y., and Shin, S. Y. (2017). LL-37-derived membrane-active FK-13 analogs possessing cell selectivity, anti-biofilm activity and synergy with chloramphenicol and anti-inflammatory activity. *Biochim. Biophys. Acta.* 1859, 722–733. doi: 10.1016/j.bbame.2017.01.037
- Ramanathan, B., Davis, E. G., Ross, C. R., and Blecha, F. (2002). Cathelicidins: microbicidal activity, mechanisms of action, and roles in innate immunity. *Microbes Infect.* 4, 361–372. doi: 10.1016/s1286-4579(02)01549-6
- Rosenthal, K. S., and Storm, D. R. (1977). Disruption of the *Escherichia coli* outer membrane permeability barrier by immobilized polymyxin B. *J. Antibiot.* 30, 1087–1092. doi: 10.7164/antibiotics.30.1087
- Rossolini, G. M., Arena, F., Pecile, P., and Pollini, S. (2014). Update on the antibiotic resistance crisis. *Curr. Opin. Pharmacol.* 18, 56–60. doi: 10.1016/j.coph.2014.09.006
- Roy, R. N., Lomakin, I. B., Gagnon, M. G., and Steitz, T. A. (2015). The mechanism of inhibition of protein synthesis by the proline-rich peptide oncocin. *Nat. Struct. Mol. Biol.* 22, 466–469. doi: 10.1038/nsmb.3031
- Ruden, S., Hilpert, K., Berditsch, M., Wadhwani, P., and Ulrich, A. S. (2009). Synergistic interaction between silver nanoparticles and membrane-permeabilizing antimicrobial peptides. *Antimicrob. Agents Chemother.* 53, 3538–3540. doi: 10.1128/AAC.01106-08
- Sakoulas, G., Okumura, C. Y., Thienphrapa, W., Olson, J., Nonejuie, P., Dam, Q., et al. (2014). Nafcillin enhances innate immune-mediated killing of methicillin-resistant *Staphylococcus aureus*. *J. Mol. Med.* 92, 139–149. doi: 10.1007/s00109-013-1100-7
- Sanchez-Gomez, S., Japelj, B., Jerala, R., Moriyon, I., Fernandez, A. M., Leiva, J., et al. (2011). Structural features governing the activity of lactoferricin-derived peptides that act in synergy with antibiotics against *Pseudomonas aeruginosa* *in vitro* and *in vivo*. *Antimicrob. Agents Chemother.* 55, 218–228. doi: 10.1128/aac.00904-10
- Sass, V., Schneider, T., Wilmes, M., Körner, C., Tossi, A., Novikova, N., et al. (2010). Human beta-defensin 3 inhibits cell wall biosynthesis in *Staphylococci*. *Infect. Immun.* 78, 2793–2800. doi: 10.1128/iai.00688-09
- Scocchi, M., Lüthy, C., Decarli, P., Mignogna, G., Christen, P., and Gennaro, R. (2009). The proline-rich antibacterial peptide Bac7 Binds to and Inhibits *in vitro* the molecular chaperone DnaK. *Int. J. Pept. Res. Therapeut.* 15, 147–155. doi: 10.1007/s10989-009-9182-3
- Scott, M. G., Yan, H., and Hancock, R. E. (1999). Biological properties of structurally related alpha-helical cationic antimicrobial peptides. *Infect. Immun.* 67, 2005–2009.
- Shamova, O., Orlov, D., Stegemann, C., Czihal, P., Hoffmann, R., Brogden, K., et al. (2009). ChBac3.4: a novel proline-rich antimicrobial peptide from goat leukocytes. *Int. J. Pept. Res. Therap.* 15, 31–42. doi: 10.1007/s10989-009-9170-7
- Shin, S. Y., Yang, S. T., Park, E. J., Eom, S. H., Song, W. K., Kim, Y., et al. (2002). Salt resistance and synergistic effect with vancomycin of alpha-helical antimicrobial peptide P18. *Biochem. Biophys. Res. Commun.* 290, 558–562. doi: 10.1006/bbrc.2001.6234
- Singh, A. P., Prabha, V., and Rishi, P. (2014). Efficacy of cryptdin-2 as an adjunct to antibiotics from various generations against *Salmonella*. *Indian J. Microbiol.* 54, 323–328. doi: 10.1007/s12088-014-0463-y
- Soren, O., Brinch, K. S., Patel, D., Liu, Y., Liu, A., Coates, A., et al. (2015). Antimicrobial peptide novicidin synergizes with rifampin, ceftriaxone, and ceftazidime against antibiotic-resistant *Enterobacteriaceae* *in vitro*. *Antimicrobial Agents and Chemotherapy.* 59, 6233–6240. doi: 10.1128/AAC.01245-15
- Steinberg, D. A., Hurst, M. A., Fujii, C. A., Kung, A. H. C., Ho, J. F., Cheng, F. C., et al. (1997). Protegrin-1: a broad-spectrum, rapidly microbicidal peptide with *in vivo* activity. *Antimicrob. Agents Chemother.* 41, 1738–1742.
- Stensberg, M. C., Wei, Q., McLamore, E. S., Porterfield, D. M., Wei, A., and Sepúlveda, M. S. (2011). Toxicological studies on silver nanoparticles: challenges and opportunities in assessment, monitoring and imaging. *Nanomedicine* 6, 879–898. doi: 10.2217/nnm.11.78
- Taber, H. W., Mueller, J. P., Miller, P. F., and Arrow, A. S. (1987). Bacterial uptake of aminoglycoside antibiotics. *Microbiol. Rev.* 51, 439–457.
- Takahashi, D., Shukla, S. K., Prakash, O., and Zhang, G. (2010). Structural determinants of host defense peptides for antimicrobial activity and target cell selectivity. *Biochimie.* 92, 1236–1241. doi: 10.1016/j.biochi.2010.02.023
- Taylor, K., Barran, P. E., and Dorin, J. R. (2008). Structure-activity relationships in beta-defensin peptides. *Biopolymers* 90, 1–7. doi: 10.1002/bip.20900
- Teixeira, V., Feio, M. J., and Bastos, M. (2012). Role of lipids in the interaction of antimicrobial peptides with membranes. *Prog. Lipid Res.* 51, 149–177. doi: 10.1016/j.plipres.2011.12.005
- Tosi, M. F. (2005). Innate immune responses to infection. *J. Allergy. Clin. Immunol.* 116, 241–249. doi: 10.1016/j.jaci.2005.05.036
- Tossi, A., Scocchi, M., Zanetti, M., Genaro, R., Storici, P., and Romeo, D. (1997). “An approach combining cDNA amplification and chemical

- synthesis for the identification of novel, cathelicidin-derived, antimicrobial peptides" in *Antibacterial Peptide Protocols. Methods In Molecular Biology*, Vol. 78, ed W. Shafer (Totowa, NJ: Humana Press Inc.), 133–151. doi: 10.1385/0-89603-408-9:133
- Turnidge, J. (2014). "Drug-Drug combinations" in *Fundamentals of Antimicrobial Pharmacokinetics and Pharmacodynamics*, eds A. Vinks, H. Derendorf, and J. Mouton (New York, NY: Springer), 153–198. doi: 10.1007/978-0-387-75613-4_8
- Ulvatne, H., Karoliussen, S., Stiberg, T., Rekdal, O., and Svendsen, J. S. (2001). Short antibacterial peptides and erythromycin act synergistically against *Escherichia coli*. *J. Antimicrob. Chemother.* 48, 203–208. doi: 10.1093/jac/48.2.203
- Vaara, M., and Porro, M. (1996). Group of peptides that act synergistically with hydrophobic antibiotics against gram-negative enteric bacteria. *Antimicrob. Agents Chemother.* 40, 1801–1805.
- Vandamme, D., Landuyt, B., Luyten, W., and Schoofs, L. (2012). A comprehensive summary of LL-37, the factotum human cathelicidin peptide. *Cell. Immunol.* 280, 22–35. doi: 10.1016/j.cellimm.2012.11.009
- Ventola, C. L. (2015a). The antibiotic resistance crisis: part 1: causes and threats. *Pharm. Therap.* 40, 277–283.
- Ventola, C. L. (2015b). The antibiotic resistance crisis: part 2: management strategies and new agents. *Pharm. Therap.* 40, 344–352.
- Warren, G. H., Gray, J., and Yurchenko, J. A. (1957). Effect of polymyxin on the lysis of *Neisseria catarrhalis* by lysozyme. *J. Bacteriol.* 74, 788–793.
- Wehrli, W. (1983). Rifampin: mechanisms of action and resistance. *Rev. Infect. Dis.* 5, 407–411. doi: 10.1093/clinids/5.Supplement_3.S407
- Wiegand, I., Hilpert, K., and Hancock, R. E. W. (2008). Agar and broth dilution methods to determine the minimal inhibitory concentration (MIC) of antimicrobial substances. *Nat. Protocols* 3, 163–175. doi: 10.1038/nprot.2007.521
- Wiesner, J., and Vilcinskas, A. (2010). Antimicrobial peptides: the ancient arm of the human immune system. *Virulence* 1, 440–464. doi: 10.4161/viru.1.5.12983
- Wilmes, M., Cammue, B. P., Sahl, H. G., and Thevissen, K. (2011). Antibiotic activities of host defense peptides: more to it than lipid bilayer perturbation. *Nat. Prod. Rep.* 28, 1350–1358. doi: 10.1039/c1np00022e
- Wimley, W. C. (2010). Describing the mechanism of antimicrobial peptide action with the interfacial activity model. *ACS Chem. Biol.* 5, 905–917. doi: 10.1021/cb1001558
- World Health Organization (2015). *Global Action Plan on Antimicrobial Resistance*. Geneva: World Health Organization. Available online at: <http://www.who.int/antimicrobial-resistance/publications/global-action-plan/en/> (accessed April 17, 2019).
- World Health Organization (2017). *Global Priority List of Antibiotic-Resistant Bacteria to Guide Research, Discovery, and Development of New Antibiotics*. World Health Organization. Available online at: <http://www.who.int/medicines/publications/global-priority-list-antibiotic-resistant-bacteria> (accessed April 17, 2019).
- Wu, X., Li, Z., Li, X., Tian, Y., Fan, Y., Yu, C., et al. (2017). Synergistic effects of antimicrobial peptide DP7 combined with antibiotics against multidrug-resistant bacteria. *Drug Des. Dev. Ther.* 11, 939–946. doi: 10.2147/DDDT.S107195
- Yan, H., and Hancock, R. E. (2001). Synergistic interactions between mammalian antimicrobial defense peptides. *Antimicrob. Agents Chemother.* 45, 1558–1560. doi: 10.1128/aac.45.5.1558-1560.2001
- Yang, K., Han, Q., Chen, B., Zheng, Y., Zhang, K., Li, Q., et al. (2018). Antimicrobial hydrogels: promising materials for medical application. *Int. J. Nanomedicine* 13, 2217–2263. doi: 10.2147/IJN.S154748
- Yeh, P. J., Hegreness, M. J., Aiden, A. P., and Kishony, R. (2009). Drug interactions and the evolution of antibiotic resistance. *Nat. Rev. Microbiol.* 7, 460–466. doi: 10.1038/nrmicro2133
- Yenugu, S., and Narmadha, G. (2010). The human male reproductive tract antimicrobial peptides of the HE2 family exhibit potent synergy with standard antibiotics. *J. Pept. Sci.* 16, 337–341. doi: 10.1002/psc.1246
- Yu, G., Baeder, D. Y., Regoes, R. R., and Rolff, J. (2016). Combination effects of antimicrobial peptides. *Antimicrob. Agents Chemother.* 60, 1717–1724. doi: 10.1128/AAC.02434-15
- Zahn, M., Berthold, N., Kieslich, B., Knappe, D., Hoffmann, R., and Strater, N. (2013). Structural studies on the forward and reverse binding modes of peptides to the chaperone DnaK. *J. Mol. Biol.* 425, 2463–2479. doi: 10.1016/j.jmb.2013.03.041
- Zaslouff, M. (2002). Antimicrobial peptides of multicellular organisms. *Nature* 415, 389–395. doi: 10.1038/415389a
- Zhang, L., Benz, R., and Hancock, R. E. (1999). Influence of proline residues on the antibacterial and synergistic activities of alpha-helical peptides. *Biochemistry* 38, 8102–8111. doi: 10.1021/bi9904104
- Zhang, Y., Lu, W., and Hong, M. (2011). The membrane-bound structure and topology of a human alpha-defensin indicate a dimer pore mechanism for membrane disruption. *Biochemistry* 49, 9770–9782. doi: 10.1021/bi101512j
- Zimmerman, G. R., Lehar, J., and Keith, C. T. (2007). Multi-target therapeutics: when the whole is greater than the sum of the parts. *Drug. Discov. Today* 12, 34–42. doi: 10.1016/j.drudis.2006.11.008

Conflict of Interest Statement: The authors declare that the research was conducted in the absence of any commercial or financial relationships that could be construed as a potential conflict of interest.

Copyright © 2019 Zharkova, Orlov, Golubeva, Chakchir, Eliseev, Grinchuk and Shamova. This is an open-access article distributed under the terms of the Creative Commons Attribution License (CC BY). The use, distribution or reproduction in other forums is permitted, provided the original author(s) and the copyright owner(s) are credited and that the original publication in this journal is cited, in accordance with accepted academic practice. No use, distribution or reproduction is permitted which does not comply with these terms.



3-Benzyl-Hexahydro-Pyrrolo[1,2-a]Pyrazine-1,4-Dione Extracted From *Exiguobacterium indicum* Showed Anti-biofilm Activity Against *Pseudomonas aeruginosa* by Attenuating Quorum Sensing

OPEN ACCESS

Edited by:

Natalia V. Kirienko,
Rice University, United States

Reviewed by:

Bartolome Moya Canellas,
University of Florida, United States
Claus Moser,
Rigshospitalet, Denmark

*Correspondence:

Avinash Mishra
avinash@csmcni.res.in;
avinashmishra11@rediffmail.com;
avinashmishra.csmcni@gmail.com
Bhavanath Jha
jha.bhavanath@gmail.com

† Present address:

Vijay K. Singh,
Department of Microbiology and
Immunobiology, Harvard Medical
School, Boston, MA, United States;
Department of Surgery,
Massachusetts General Hospital,
Boston, MA, United States

Specialty section:

This article was submitted to
Antimicrobials, Resistance
and Chemotherapy,
a section of the journal
Frontiers in Microbiology

Received: 09 November 2018

Accepted: 22 May 2019

Published: 07 June 2019

Citation:

Singh VK, Mishra A and Jha B
(2019) 3-Benzyl-Hexahydro-
Pyrrolo[1,2-a]Pyrazine-1,4-Dione
Extracted From *Exiguobacterium*
indicum Showed Anti-biofilm Activity
Against *Pseudomonas aeruginosa* by
Attenuating Quorum Sensing.
Front. Microbiol. 10:1269.
doi: 10.3389/fmicb.2019.01269

Vijay K. Singh[†], Avinash Mishra^{*} and Bhavanath Jha^{*}

Division of Biotechnology and Phycology, CSIR – Central Salt and Marine Chemicals Research Institute, Bhavnagar, India

Bacterial cell-to-cell communication promotes biofilm formation and can potentially lead to multidrug resistance development. Quorum sensing inhibition (QSI) is an effective and widely employed strategy against biofilm formation. The extract from *Exiguobacterium indicum* SJ16, a gram-positive bacterium, isolated from the rhizosphere of *Cyperus laevigatus* showed significant anti-quorum sensing activity (about 99%) against the reference *Chromobacterium violaceum* CV026 strain without exerting any antibacterial effect. The potentially active QSI compound identified in the SJ16 extract was 3-Benzyl-hexahydro-pyrrolo[1, 2-a]pyrazine-1,4-dione. The SJ16 extract containing this active compound showed significant anti-quorum sensing activity against a model quorum sensing bacterium strain *Pseudomonas aeruginosa* PAO1 and a clinical isolate *P. aeruginosa* PAH by preventing biofilm formation without attenuating the cell growth within the biofilm. More specifically, the SJ16 extract changed the topography and architecture of the biofilm, thus preventing bacterial adherence and further development of the biofilm. Furthermore, it decreased virulence factors (rhamnolipid and pyocyanin), the bacterial motility, as well as the elastase, and protease activities in *P. aeruginosa*. Microarray analysis revealed the differential expression of quorum sensing regulatory genes. Based on these results, we herein propose a hypothetical model, characterizing the role of this QSI agent in the transcriptional regulation of quorum sensing in *P. aeruginosa* PAO1, demonstrating that this compound has significant drug-development potential. Further research is required to delineate its possible applications in therapeutics in the context of biofilm forming bacterial infections.

Keywords: anti-biofilm, anti-quorum, biofilm, *Exiguobacterium*, *Pseudomonas*, quorum quenching, quorum sensing

INTRODUCTION

The diseases caused by pathogenic bacteria are controlled, prevented, and treated with a number of antibiotics which inhibit essential bacterial processes, such as cell wall synthesis, DNA replication, or protein biosynthesis. Antibiotics have long become the commonplace in our effort to tackle infectious diseases (Chu et al., 2014). However, extensive use of these agents creates an evolutionary

pressure on bacteria which, in many cases, leads to antibiotics resistance. Therefore, alternative strategies with low potential for resistance emergence are required in order to combat pathogenic multidrug resistant bacteria (Chu et al., 2014; Singh et al., 2016b). Quorum sensing (QS) is directly involved in pathogenesis of infectious disease, by regulating the biofilm formation, the production of multiple virulence factors, as well as the motility of bacteria (Singh et al., 2017). In QS system, molecular cascades regulate the gene expression and determine the fate of bacterial biofilms (Ganin et al., 2015). In this context, gram-negative bacteria communicate through small diffusible molecules, such as acyl homoserine lactones, whereas gram-positive bacteria use autoinducer peptides for their communication (Galloway et al., 2011).

Biofilms are comprised of single or multiple microbial species and develop on different biotic and abiotic surfaces. In most of the cases, mixed species biofilms are predominant. However, single species biofilms are commonly associated with medical equipment-related infections, especially dental plaque and medical implants (O'Toole et al., 2000). *Pseudomonas aeruginosa*, a gram-negative bacterium, is considered to be the most important species of biofilm-forming bacteria. It can develop biofilms on a variety of biotic and abiotic surfaces; especially in immunocompromised patients (Driscoll et al., 2007). Moreover, this bacterium shows resistance to most of the conventional antibiotics, because it can form a biofilm matrix, which protects bacterial cells. Therefore, eradicating such infections poses a significant challenge (Driscoll et al., 2007; Lee and Zhang, 2015). QS regulatory networks control the virulence factors and biofilm formation in *P. aeruginosa* (Lee and Zhang, 2015). Therefore, utilization of anti-QS strategies could prove to be a promising way to tackle *P. aeruginosa* infections.

The rhizosphere is a region of soil adjacent to the plant roots that inhabits a number of microbes and facilitates various plant-microbe and microbe-microbe interactions. Many rhizospheric bacteria prevent the development of soilborne pathogens, while at the same time they protect the associated plants by activating the induced systemic resistance (Berendsen et al., 2012). Importantly, the rhizosphere supports different bacterial communities that exert QS and quorum quenching activities. Christiaen et al. (2011) isolated 59 bacterial species from 16 different environmental samples including plant rhizospheres and water, and found that 41 of them had anti-QS properties. Furthermore, *Stenotrophomonas maltophilia* and *Delftia tsuruhatensis*, isolated from the rhizosphere of *Cyperus laevigatus* showed anti-QS and anti-biofilm activities against *P. aeruginosa* (Singh et al., 2013, 2017). Moreover, a bacterium from the family of the *Acinetobacter* spp., isolated from the cucumber rhizosphere, inhibited the growth of *Pseudomonas chlororaphis* and *Burkholderia glumae* during co-cultivation by degrading acyl-homoserine lactones (AHLs), produced by these bacteria (Kang et al., 2004). Other AHL producing and degrading bacteria were isolated from the tobacco rhizosphere, including two newly identified species, *Sphingopyxis wifflariensis* and *Bosea thiooxidans*, belong to the *Bacillus* α -proteobacteria family (D'Angelo-Picard et al., 2005).

A three bacterial consortium comprised of *Acinetobacter* sp., *Burkholderia* sp. and *Klebsiella* sp. was isolated from the ginger rhizosphere, demonstrating significant AHL degrading activities and growth-inhibiting capabilities against *P. aeruginosa* and the plant pathogen *Erwinia carotovora* without affecting their planktonic growth (Chan et al., 2011). Last but not least, the AHL degrading bacterial consortia isolated from the potato rhizosphere showed significant biocontrol activity against *Pectobacterium atrosepticum* (Cirou et al., 2007). In most of these earlier studies, the above mentioned bacteria were isolated and characterized for their anti-QS properties; however, to the best of our knowledge there is no report, so far, on the isolation and characterization of the active compounds from these bacteria.

In the present study, a bacterium *Exiguobacterium indicum* SJ16 was isolated from the rhizosphere of a monocot *C. laevigatus*, amply growing in the coastal saline area and was tested for its anti-QS and anti-biofilm potential. The active fraction was collected, identified, and regulatory key genes were studied to elucidate a possible QSI mechanism.

MATERIALS AND METHODS

Isolation and Molecular Identification of Bacteria

Bacteria from the rhizosphere of *C. laevigatus* L. from the natural habitat of Bhavnagar, India (Latitude N 21°45.124", Longitude E 72°13.579") were isolated. Bacteria were screened by plate based bioassay, and two were found positive for anti-QS activity (Singh et al., 2017). The bacterial isolate SJ16, which showed anti-QS (but not antibacterial) activity was selected for further characterization. Genomic DNA of the bacterium was isolated, and the 16S rRNA gene was amplified by universal primers fD1-5'-AGA GTT TGA TCC TGG CTC AG -3' and rP2-5'-ACG GCT ACC TTG TTA CGA CTT -3' using optimized PCR conditions (Weisburg et al., 1991). The amplified PCR product was purified, sequenced (at Macrogen Inc., South Korea), analyzed and submitted to the NCBI GenBank. The phylogenetic analysis was performed using MEGA version 6.0 (Tamura et al., 2013), and a phylogenetic tree was inferred by neighbor-joining methods (Saitou and Nei, 1987). Bootstrap analysis was performed, and maximum composite likelihood algorithms were used for the determination of the evolutionary distances (Felsenstein, 1985; Tamura et al., 2004).

Fatty Acid Methyl Ester Profiling of Bacteria

Fatty acid methyl ester (FAME) profiling of *E. indicum* SJ16 was carried out using Microbial Identification System coupled with gas chromatography (MIDI, Microbial ID; GC system-6850, Agilent Technologies, United States). The bacterium was grown for 24 h at 30°C on Tryptic soy yeast agar, FAMES were prepared using MIDI manual, and peaks were identified with RTSBA6 6.10 database (Jha et al., 2015).

Preparation of the Bacterial Extract, Fractionation, and Identification of the Active Compound

Bacterial culture (*E. indicum* SJ16) was grown for 48 h at 30°C in 500 ml of nutrient broth, kept in an incubator shaker with agitation at 180 rpm. The culture was centrifuged for 15 min at $10,000 \times g$ (4°C), the supernatant was collected, and filtered through 0.22 μm filter for the complete removal of remaining bacterial cells. The supernatant was extracted with ethyl acetate (equal volume), evaporated to dryness under vacuum and the dried residue finally dissolved in methanol.

The methanol extract of SJ16 was further fractionated by solid phase extraction method using different cartridges including anion exchanger DAE, cation mixed Plexa PCX, polar SI, and non-polar C18 (Agilent, United States). Each fraction was tested for quorum sensing inhibition (QSI) activity (Singh et al., 2017). The positive fraction (collected through the C18 cartridge with 40% methanol) showing a maximum zone of QSI was used for the subsequent studies and was also subjected to GC-MS (GC-2010, Shimadzu, Japan) analysis. The probable active compound was identified by comparing the mass spectra with the reference spectra library. The mass of the probable active compound was further confirmed by electrospray ionization mass spectrometry (ESI-MS; Q-ToF micro TM, Micromass, United Kingdom).

Anti-quorum Sensing and Anti-biofilm Activities

The anti-QS activity was tested (i) by a plate-based bioassay using *Chromobacterium violaceum* CV026 as a tester strain, methanol as a negative control and cinnamaldehyde (Sigma-Aldrich, United States) as a positive control, and (ii) by quantifying the violacein production. Both the plate-based bioassay and the violacein quantification, were performed as per our previously optimized methods (Singh et al., 2013).

The anti-biofilm formation assay was performed with different concentrations of bacterial (strain SJ16) extracts (0.2, 0.4, 0.6, 0.8, 1.0, and 1.2 mg/ml) using two *P. aeruginosa* strains, PAO1 as well as the PAH clinical isolate (provided as a courtesy from the Government Medical College, Bhavnagar; Goswami et al., 2011). Briefly, 200 μl bacterial culture ($\text{OD}_{600 \text{ nm}} = 0.1$) dilute from overnight grown PAO1 and PAH cultures were added to a 96-well polystyrene microtiter plate with different concentrations of the SJ16 extracts. The plates were allowed to grow for 24 h (at 37°C with 100 rpm), and growth was measured at 600 nm. The biofilm formation was assayed using our previously optimized crystal violet staining method (Kavita et al., 2014). The experiments were performed three times with five replicates each time.

Fluorescence Microscopy

Pseudomonas aeruginosa (strains PAO1 and PAH) were grown in a 24 well polystyrene plate with or without SJ16 extract to assess the development of biofilm on a sterilized glass coverslip (11 mm). In a 24-well polystyrene plate 1 ml of NB media containing bacterial culture at $\text{OD}_{600 \text{ nm}} = 0.1$

(diluted from overnight grown culture) was added to each well with or without (control) 1.0 mg/ml of SJ16 extract. One glass coverslip/well was submerged and the plate was incubated in static condition at 37°C. The effect of the SJ16 extract (1.0 mg/ml) on the *P. aeruginosa* cell viability within biofilm was examined at different time points (24, 48, and 72 h) under a fluorescence microscope using FilmTracer LIVE/DEAD Biofilm Viability Kit (Invitrogen, United States) (Singh et al., 2013). The bacterial cells within the biofilm were labeled with a fluorescent dye (propidium iodide and SYTO 9), were further processed according to the manufacturer's instructions and were visualized under an epifluorescence microscope (Axio Imager, Carl Zeiss AG, Germany).

Scanning Electron and Atomic Force Microscopy

Scanning electron microscopy (SEM) and atomic force microscopy (AFM) were used to visualize the effect of the SJ16 extract on the topology of the biofilm developed by the *P. aeruginosa* strains. For the SEM, a previously described protocol was used (Andersson et al., 2009; Singh et al., 2013). In brief, biofilms of *P. aeruginosa* PAO1 and *P. aeruginosa* PAH were grown on glass coverslips submerged in nutrient broth in a 24-well polystyrene plate with (1.0 mg/ml) or without extract (control). The plate containing the culture and the coverslips were kept at 37°C for 24 h. After incubation, the planktonic culture was removed and coverslips were gently washed with 0.9% NaCl. The samples were treated with 2.5% glutaraldehyde for 20 min followed by 4% OsO_4 for 30 min and dehydrated using ethanol gradient (10 to 95%) treatment for 10 min for each concentration. The dehydrated and dried biofilms were coated with gold and observed under a scanning electron microscope (SEM, LEO series VP1430, Germany). For the AFM, overnight grown cultures of *P. aeruginosa* PAO1 and *P. aeruginosa* PAH were diluted to reach an $\text{OD}_{600 \text{ nm}} = 0.1$ in NB broth, sterile glass cover slips were submerged in 24-well polystyrene plate with (1.0 mg/ml) or without extract (control). The plate was kept for 24 h at 37°C. Following this incubation period, the biofilm that developed on the glass coverslip was rinsed gently with phosphate buffer saline (pH 7.4) and was kept under the desiccators until completely dry. Finally, the biofilm was scanned under AFM (NT-MDT, Russia) in a semi-contact mode (Oh et al., 2009; Singh et al., 2013).

Swarming Motility Assay

The swarming motility of PAO1 and PAH were tested in the presence (1.0 mg/ml) and absence of SJ16 extract. Overnight grown culture of *P. aeruginosa* PAO1 and *P. aeruginosa* PAH were diluted to $\text{OD}_{600 \text{ nm}} = 1.0$ and spotted on a plate containing BM2 swarming medium (62 mM PBS at pH 7, 2 mM MgSO_4 , 10 μM FeSO_4 , 0.4% glucose, 0.1% casamino acids and 0.5% agar) supplemented with 1.0 mg/ml SJ16 extract or without extract supplementation (control) (Overhage et al., 2007). The plates were incubated at 37°C for 24 h and swarming zones were observed.

Swimming Motility Assay

The overnight grown culture of PAO1 and PAH were diluted to $OD_{600\text{ nm}} = 1.0$ and spotted on a plate containing tryptone broth (10 g/l tryptone, 5 g/l NaCl and 0.3% agar) supplemented with 1.0 mg/ml SJ16 extract or without extract supplementation (control) (Rashid and Kornberg, 2000). The plates were incubated at 37°C and analyzed after 24 h.

Virulence Factor Analysis

The effect of the SJ16 bacterial extracts (1.0 mg/ml) on the production of virulence factors by reference *P. aeruginosa* strains (PAO1 and PAH) was studied by measuring the levels of pyocyanin and rhamnolipid, and by analyzing the elastase and protease activities. For pyocyanin assay, starter cultures of *P. aeruginosa* strains (PAO1 and PAH) were grown at 37 °C in an incubator shaker until $OD_{600\text{ nm}} = 3.0$ and diluted to $OD_{600\text{ nm}} = 0.1$ in PB medium (5 ml; 20 g/l peptone, 1.4 g/l $MgCl_2$, and 10 g/l K_2SO_4). The tubes containing 5 ml PB medium ($OD_{600\text{ nm}} = 0.1$) supplemented with 1.0 mg/ml SJ16 extract or without extract supplementation (control). Supernatants were collected by centrifuging cultures at $10,000 \times g$ for 10 min; pyocyanin was extracted in 3 ml of chloroform followed by 1 ml of 0.2 N HCl and quantified spectrophotometrically at 520 nm (Essar et al., 1990). For rhamnolipid assay, *P. aeruginosa* strains PAO1 and PAH ($OD_{600\text{ nm}} = 0.1$) were grown overnight at 37°C in NB medium, supplemented with 1.0 mg/ml SJ16 extract or without extract supplementation (control). The culture was centrifuged ($10,000 \times g$ for 10 min), the supernatant was collected and acidified to pH 2 (with HCl), and absorbance was measured at 570 nm (McClure and Schiller, 1992; Sarabhai et al., 2013).

Elastase Assay

To estimate the elastase activity, the supernatant (750 μ l) from overnight grown (with or without SJ16 extract) cultures of *P. aeruginosa* (PAO1 and PAH) were incubated with elastin congo red solution (250 μ l; 5 mg/ml in 0.1 M Tris-HCl pH 8; 1 mM $CaCl_2$) at 37°C for 16 h. Reaction-mixtures were centrifuged ($3,000 \times g$ for 10 min), the supernatant was collected, and the absorbance was read at 495 nm (Bjorn et al., 1979; Zhu et al., 2002).

Protease Assay

For the protease activity, 2% azocasein solution was prepared in 50 mM phosphate buffer saline (pH 7). The supernatant (400 μ l) from overnight grown (with or without SJ16 extract) cultures of *P. aeruginosa* (PAO1 and PAH) were incubated with an equal volume of azocasein solution (2%) at 37°C for 1 h. A measure of 500 μ l of 10% trichloroacetic acid was added to stop the reaction. Reaction-mixtures were centrifuged ($8,000 \times g$ for 5 min) to remove residual azocasein and the absorbance of the supernatant was measured at 400 nm (Adonizio et al., 2008).

Microarray

A single colony of the reference strain *P. aeruginosa* PAO1 was inoculated in a 5 ml NB tubes, was grown until $OD_{600\text{ nm}}$

3.0 and was then diluted to $OD_{600\text{ nm}} = 0.1$. Following dilution, *P. aeruginosa* PAO1 was grown in a tube containing 5 ml starter culture ($OD_{600\text{ nm}} = 0.1$) with or without bacterial extracts (1.0 mg/ml) at 37°C for 24 h in a shaker incubator at 200 rpm (Singh et al., 2017). Planktonic cells were harvested by centrifuge at $12,000 \times g$ for 5 min and total RNA was isolated using TRI reagent (Sigma, United States). Total RNA was analyzed on 2% agarose gel and quantified using ND-1000 spectrophotometer (Nanodrop Technologies, United States). Ten μ g RNA, extracted from control and treated samples were converted to cDNA, fragmented and labeled using previously optimized method (Singh et al., 2016a). Labeled cDNAs were hybridized with genome array gene chip (Gene Chip *P. aeruginosa* PAO1 containing total 5,886 gene probes), washed, stained, and scanned (Scanner 3000 7G, Affymetrix, United States) (Singh et al., 2017). Scanned chips were processed and analyzed using the expression console and the transcriptome analysis console (Affymetrix, United States). Microarray analysis was performed in duplicate and the genes showing significant differences in fold-change expression (ANOVA p -value < 0.05) were considered for the study.

Statistical Analysis

Statistical analysis was performed using GraphPad Prism software. One-way ANOVA followed by Tukey *post hoc* that was applied for the comparison of test samples and controls.

RESULTS

Isolation, Molecular Identification, Phylogeny and Fatty Acid Methyl Ester Profiling

Previously, out of 56 bacterial axenic cultures which were obtained from the rhizosphere of *C. laevigatus* L., two axenic cultures (SJ01 and SJ16) showed anti-QS activity (Singh et al., 2017). The 16S rRNA gene sequence (accession no. KX130768) of isolate SJ16 showed 99% similarity with *E. indicum* with 100% query coverage; therefore, this isolate was designated as *E. indicum* SJ16. The phylogenetic analysis showed the taxonomic position of the strain SJ16 (**Supplementary Figure S1**). The whole-cell FAME profile of the *E. indicum* SJ16 bacterium demonstrated an abundance of the iso-C_{17:0} (17.39%), iso-C_{15:0} (14.79%) and anteiso-C_{13:0} (11.36%) fatty acids (**Supplementary Figure S2**).

Identification of the Active Fraction/Compound

All fractions, collected from the various SPE cartridges (anion exchanger DAE, cation mixed Plexa PCX, polar SI, and non-polar C18) were individually screened for anti-QS activity using a biosensor plate containing the tester strain *C. violaceum* CV026. The fraction collected from the C18 cartridge (with 40% methanol) showed a maximum zone of QSI. This fraction was subjected to GC-MS analysis, and the chromatogram showed a single predominant peak at

the retention time 16.01 min (Figure 1). The detected peak resembled the 3-Benzyl-hexahydro-pyrrolo[1, 2-a]pyrazine-1,4-dione ($C_{14}H_{16}N_2O_2$; expected molecular mass 244.28) from the GC-MS library. The active fraction was also subjected to ESI-MS analysis, which showed a dominating spectral peak at m/z 249.29 (Figure 1). Thus, the experimental molecular mass of the active compound was determined to be 249.29, which is corresponding to the theoretical mass of the active fraction.

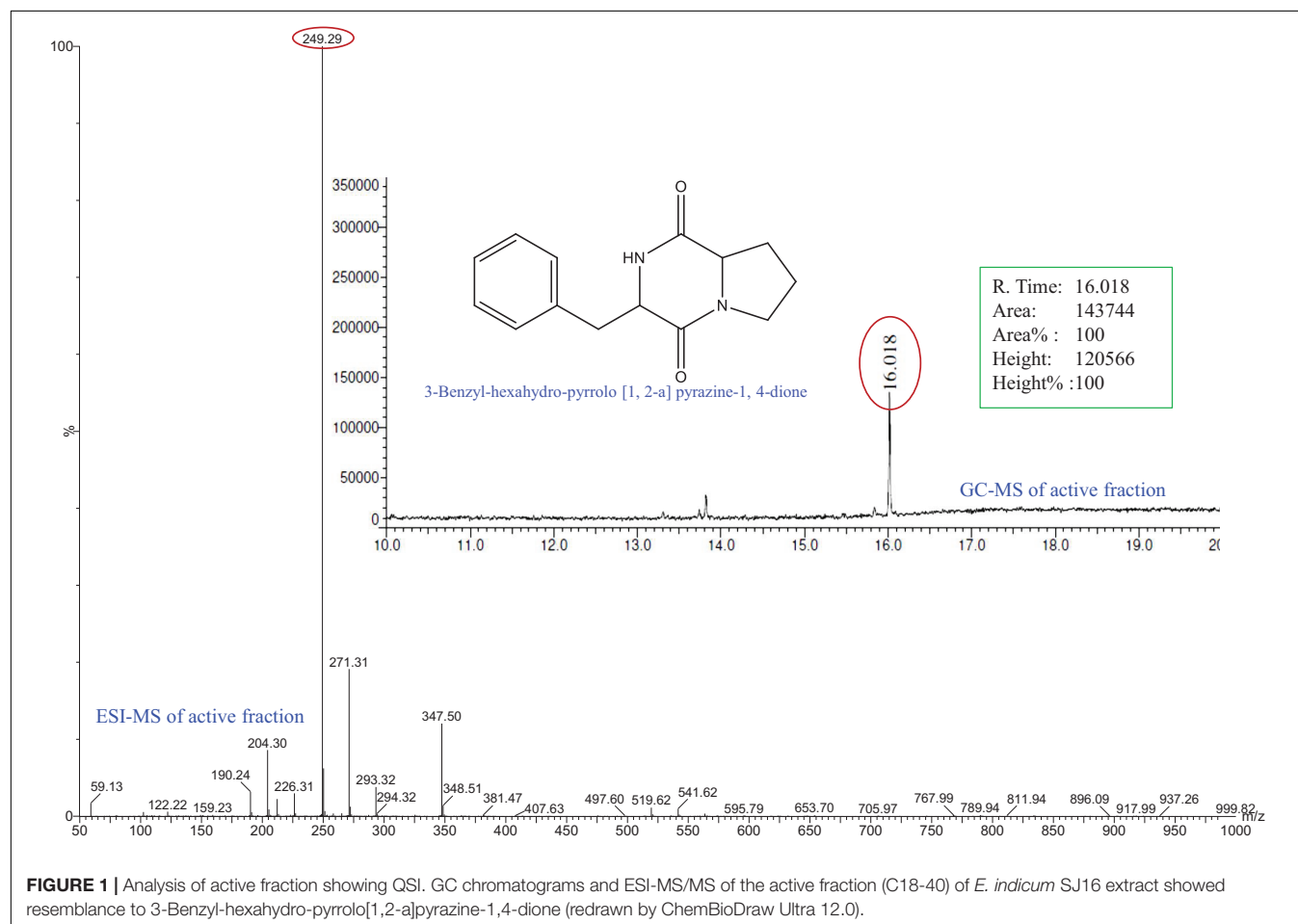
***Exiguobacterium indicum* SJ16 Showed Anti-quorum Sensing and Anti-biofilm Activities Without Inhibiting the Planktonic Growth**

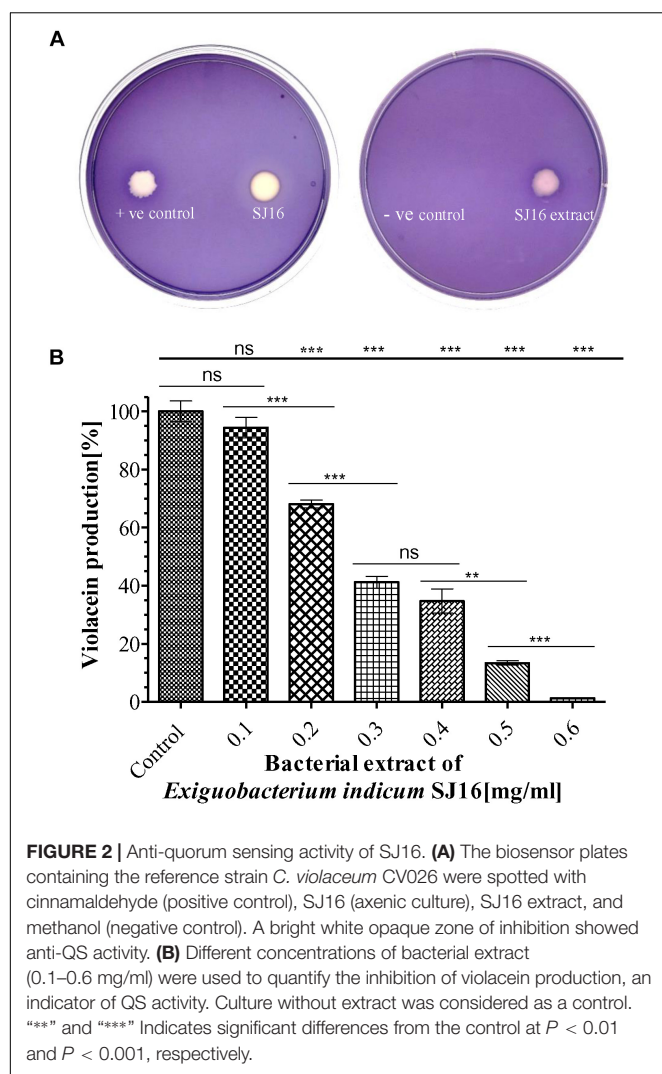
A clear white opaque zone was observed with the axenic culture and crude extract of the *E. indicum* strain SJ16 in the biosensor plate containing the reference strain *C. violaceum* CV026, result that was comparative to the positive control with cinnamaldehyde, a well-known QS inhibitor (Figure 2). The zone of inhibition was not detected with the extraction solvent methanol that was used as a negative control. As inhibition of violacein production is an indicator of QS activity, different concentrations (0.1–0.6 mg/ml) of the SJ16 extract were used to quantify the levels of this QSI marker. Indeed, the

violacein production decreased concomitantly with increasing concentrations of the extract, and about 99% inhibition was achieved with 0.6 mg/ml of the SJ16 extract (Figure 2). Furthermore, the antibacterial assay, performed by using the disc diffusion technique, confirmed that the bacterial isolate SJ16 did not halt the growth or the viability of the reference strain *C. violaceum* CV026 (Supplementary Figure S3).

The anti-biofilm activity of *E. indicum* SJ16 extract was performed with a different concentration (0.2–1.2 mg/ml) against PAO1 and PAH strains. The biofilm formation capability of both strains significantly decreased with increasing concentrations of the extract (Figure 3). About 50% inhibition of biofilm formation was noticed with 1.0 mg/ml extract. No significant effect of this compound was observed on the planktonic growth of either PAO1 or PAH even with highest extract concentrations used (0.2–1.2 mg/ml) (Figure 3).

The viability of the reference strains (*P. aeruginosa* PAO1 and PAH) within the biofilm was further analyzed with the SJ16 extract at 24, 48, and 72 h. The live cells of *P. aeruginosa* were labeled with SYTO 9, whereas dead cells were stained with propidium iodide using a Live/Dead staining kit. Live and dead cells produced green and red fluorescence, respectively, when visualized under an epi-fluorescence microscope (Figure 4A). *P. aeruginosa* (PAO1 and PAH) cells, treated with SJ16





extract were not tightly attached to the biofilm surface compared to the control. There was no difference between the control and treated biofilm when considering the cell viability within biofilm, and insignificant numbers of dead cells were detected in the biofilm at different time points (Figure 4A). Overall, these results indicate that the SJ16 extract does not exert any toxic effect on the growth or viability of the aforementioned reference strains, even after a longer duration, or higher concentrations of the compound, while at the same time it effectively inhibits the bacterial biofilm formation (Figure 4).

Exiguobacterium indicum SJ16 Extract Disrupts the Topology of the Biofilm

The effect of the SJ16 extract on the topology of the biofilm developed by the PAO1 and PAH was visualized under SEM and AFM. A biofilm along with adhering bacterial cells was developed by *P. aeruginosa* in the absence of SJ16 extract (control), whereas an immature biofilm with dispersed bacterial cells was observed when *P. aeruginosa* was grown with SJ16 extract (Figure 4B).

Similarly, AFM micrographs showed changes in the topology of the biofilm developed by *P. aeruginosa* in the presence of SJ16 extract compared to normal (control) biofilm (Figure 4C). AFM showed poor biofilm adherence on the surface of the glass cover slip, while height distribution profile showed the average thickness of the biofilm developed in the presence of SJ16 extract was significantly reduced compared to the control biofilm (Figure 4C).

Exiguobacterium indicum SJ16 Extract Downregulates the Motility of *P. aeruginosa*

Bacterial motility and initial attachment of bacterial cells to surfaces are key prerequisites for biofilm formation. Therefore, the effect of the *E. indicum* SJ16 extract on the motility of reference *P. aeruginosa* strains (PAO1 and PAH) was studied. Our results show that the swarming and swimming motility of PAO1 and PAH are significantly inhibited in the presence of the SJ16 extract (Figure 5A).

Exiguobacterium indicum SJ16 Extract Shows Inhibitory Effect on Virulence Activities

Virulence activities of the *P. aeruginosa* strains (PAO1 and PAH), including elastase and protease activities, as well as the production of virulence factors (pyocyanin and rhamnolipid) accelerate biofilm formation. Our data indicate that the SJ16 extract considerably reduced the production of virulence factors, with pyocyanin production decreasing about 50% in both PAO1 and PAH compared to the untreated samples (Figure 5B). Similarly, rhamnolipid production was also significantly decreased by 55% in PAO1 and 37% in PAH in the presence of the SJ16 extract compared to control (Figure 5B). Furthermore, the SJ16 extract led to a drastic inhibition of the elastase and protease activities in the above-mentioned *P. aeruginosa* strains. Specifically, elastase activity was decreased by 62% in PAO1 and by 31% PAH compared to untreated samples (Figure 5B). Similarly, protease activity was reduced by about 40% in PAO1 and by 28% in PAH in the presence of the SJ16 extract compared to control (Figure 5B). Overall, our results (Figures 3–5) strongly demonstrate that the SJ16 extract inhibits the cell-to-cell communication and thus prevents *P. aeruginosa* from developing a robust biofilm.

Differential Expression of Quorum Sensing Regulatory Genes

A *P. aeruginosa* PAO1 genome array chip, containing 5,886 gene-probe sets, was used to study the effect of 3-Benzyl-hexahydro-pyrrolo[1, 2-a]pyrazine-1,4-dione on QS regulatory genes. Scattered plot analysis showed that 1,237 out of 5,886 genes (Array-Express accession E-MTAB-6829) were differentially expressed (Figure 6), with a two-fold ($p < 0.05$) up- (>2) or down- (<-2) regulation at minimum (Supplementary Table S1). More specifically, a total of 868 genes were down-regulated, whereas 369 genes were up-regulated in the presence of the compound. Among these, we identified a plethora of genes

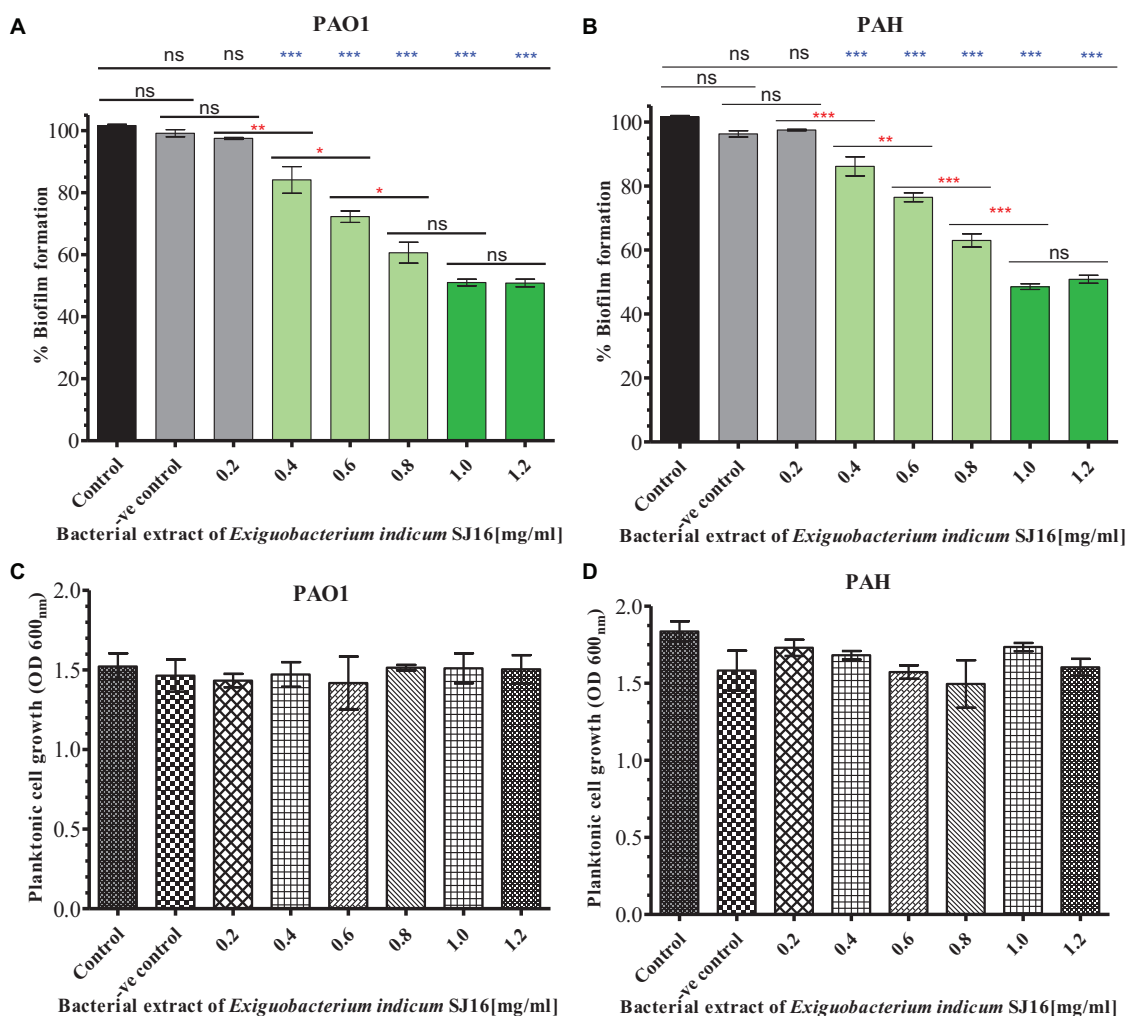


FIGURE 3 | Effect of *E. indicum* SJ16 extract on biofilm formation and planktonic growth of *P. aeruginosa*. Different concentration of bacterial extracts (0.2–1.2 mg/ml) were tested against the biofilm forming reference *P. aeruginosa* strains PAO1 (A) and PAH (B). The same concentrations of bacterial extracts were also tested for the inhibitory effect on the planktonic growth of PAO1 (C) and PAH (D) strains. Tests without extract and with methanol were considered as control and negative control, respectively. **, *** and **** indicates significant differences from the control at $P < 0.05$, $P < 0.01$, and $P < 0.001$, respectively.

that are key players in bacterial QS network of *P. aeruginosa* and exert crucial functions in general metabolic pathways in bacteria (Table 1).

DISCUSSION

The genus *Exiguobacterium* is comprised of 16 species, and *E. indicum* was isolated from meltwater of the Hamta glacier (Himalayan mountain ranges) of India (Chaturvedi and Shivaji, 2006). The present study is the second report on the isolation of *E. indicum* from a rhizosphere of the coastal area after Susilowati et al. (2015), who isolated this bacteria from rice rhizosphere and reported its plant growth promotion trait. To the best of our knowledge, there is no available study, so far reporting the anti-QS activity of the genus *Exiguobacterium*. We herein for the first time demonstrate the inhibitory effect

of *E. indicum* on bacterial quorum-sensing biofilm formation. In this study, the *E. indicum* SJ16 extract showed QSI activity (without any antibacterial activity; Supplementary Figure S3) against the reference strain *C. violaceum* CV026 on biosensor plates. This was also demonstrated by reduced levels of violacein in the violacein quantification assay (99% inhibition with 0.6 mg/ml SJ16 extract), which was a dose-dependent (Figure 2). A high concentration of methanolic extract (4 mg/ml) of an edible plant, *Melicope lunuankenda*, inhibited the response of *C. violaceum* CV026 to N-hexanoyl homoserine lactone (Tan et al., 2012). Similarly, Rodrigues et al. (2016) have shown that another plant methanol extract (*Eugenia uniflora*) showed inhibition of violacein production in *C. violaceum*, reaching up to 96% at the highest concentration tested. We have previously demonstrated a 98% decrease of violacein production in a dose-dependent manner with 3.7 mg/ml extract of *S. maltophilia*, as well as a 95% reduction with 0.1 mg/ml of *D. tsuruhatensis*

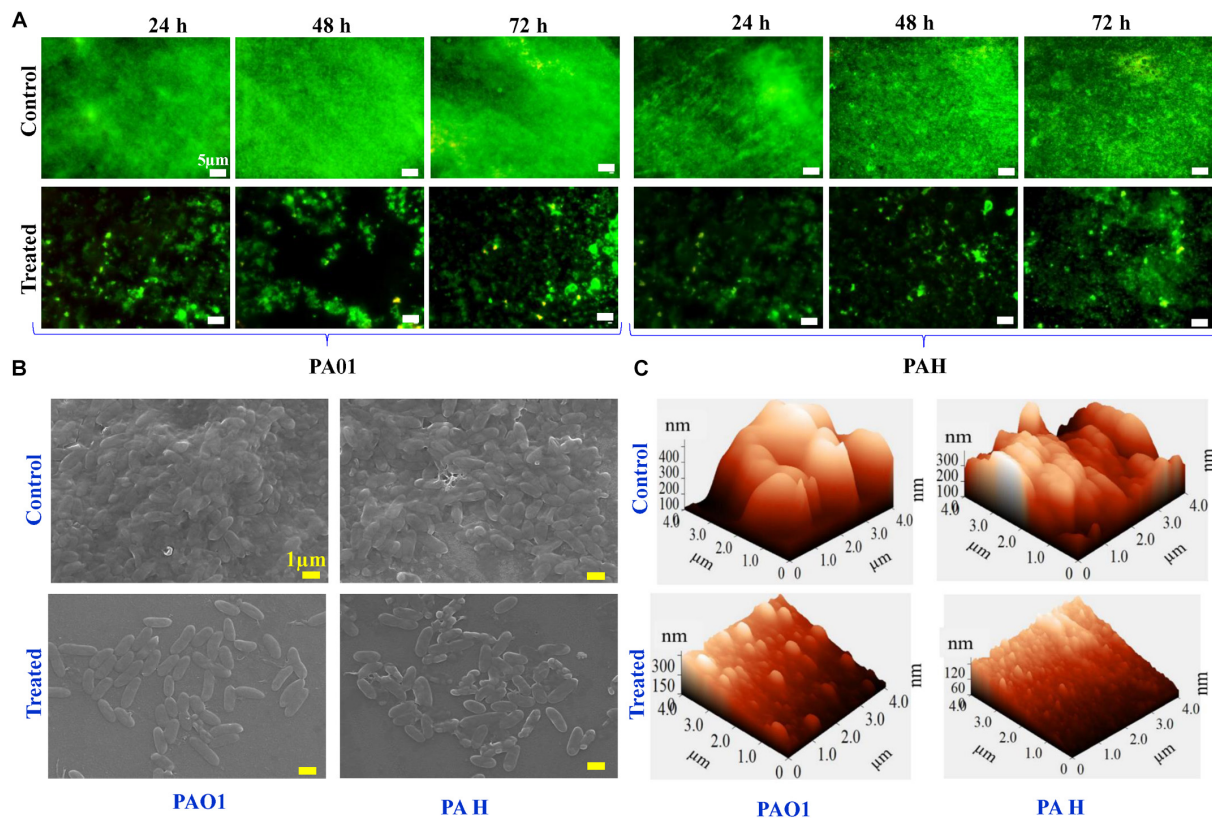


FIGURE 4 | Effect of *E. indicum* SJ16 extract on cell viability, and topology of biofilms developed by *P. aeruginosa*. **(A)** The effect of the bacterial extract (1.0 mg/ml) on the viability of reference *P. aeruginosa* strains (PAO1 and PAH) in the biofilm was examined under an epifluorescence microscope at different time points (24, 48 and 72 h) and compared with control. The dead bacterial cells were labeled with propidium iodide whereas live cells were stained with SYTO 9, which produced red and green fluorescence, respectively. SEM **(B)** and AFM **(C)** images illustrate the effect of the bacterial extract (1.0 mg/ml) on biofilm formation and topology. **(B)** A well-grown biofilm along with adhering bacterial cells was observed in the control samples (normal biofilm developed by *P. aeruginosa*), whereas dispersed bacterial cells were observed in treated samples under SEM. Similarly, AFM **(C)** showed a disrupted surface topology and a height distribution profile of the biofilm developed by the reference *P. aeruginosa* strains in the presence of the bacterial extract compared to the control biofilm.

extract, both isolated from the rhizosphere of *C. laevigatus* (Singh et al., 2013, 2017).

The treatment of biofilm-associated infections is extremely challenging, as biofilm-forming bacteria are commonly resistant to a broad spectrum of antibiotics (Høiby et al., 2010). *P. aeruginosa*, an opportunistic pathogen that causes severe infections in immunocompromised patients possesses a regulatory gene cascade that controls quorum-sensing and thus, biofilm formation and virulence factors productions. Quorum-sensing inhibition with potent QSI compounds shows promise in tackling biofilm formation in the setting of bacterial infections (Kalia, 2013; Singh et al., 2017; Quecán et al., 2018). In the field of drug discovery, extracts from natural products, especially those of microbial origin, have always been a tremendous source effective novel therapeutics (Gillespie et al., 2002; Courtois et al., 2003). These compounds have the ability to interfere with the QS system, inhibit the expression of virulence factors and prevent biofilm formation. In the present study, the *E. indicum* SJ16 extract robustly inhibits the biofilm formation of two reference *P. aeruginosa* strains (PAO1 and PAH) by modulating virulence factors

(Figure 5), without affecting the planktonic growth of these bacteria (Figure 3). It is possible that these observations are the effect of the active compound within the extract that hinder the *P. aeruginosa* QS regulatory cascade (Table 1). These results are in accordance to our previous work describing the quorum quenching and anti-biofilm forming activities of the extracts from *S. maltophilia* BJ01 and *D. tsuruhatensis* SJ01 that we isolated from the rhizosphere of *C. laevigatus* (Singh et al., 2013, 2017).

In this study, the active compound that we herein describe was fractionated and identified as 3-Benzyl-hexahydropyrrolo[1,2-a]pyrazine-1,4-dione with a theoretical mass of 244.28 (RT-16.018) and an experimental mass of 249.28 (*m/z*) (Figure 1). Interestingly, a similar to this molecule, Pyrrolo[1,2-a]pyrazine-1,4-dione, hexahydro compound that was extracted from the newly identified species of *Streptomyces mangrovisoli* showed significant antioxidant and free-radical scavenging activities (Ser et al., 2015). Furthermore, the Hexahydropyrrolo[1,2-a]pyrazine-1,4-dione compound, isolated from the *Shewanella* sp. Lzh-2 possessed algicidal activity against several cyanobacterial and algal strains (Li et al., 2014). Moreover,

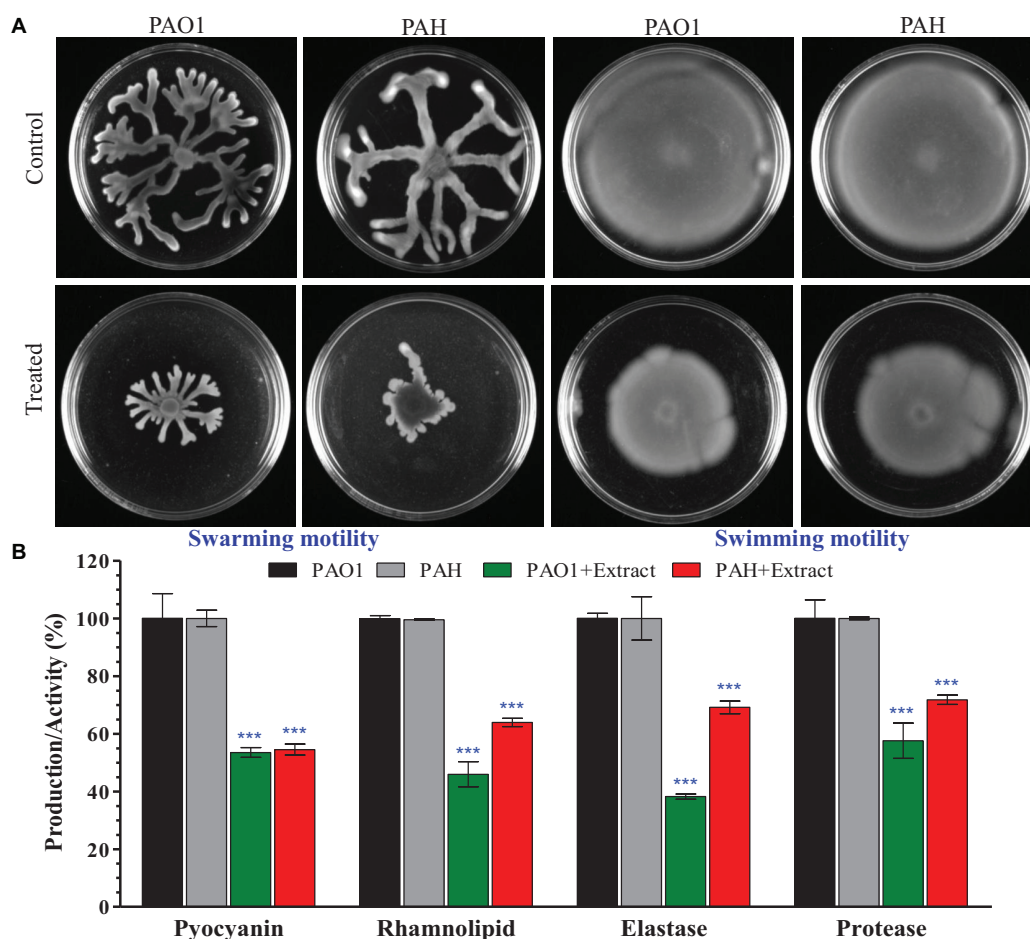
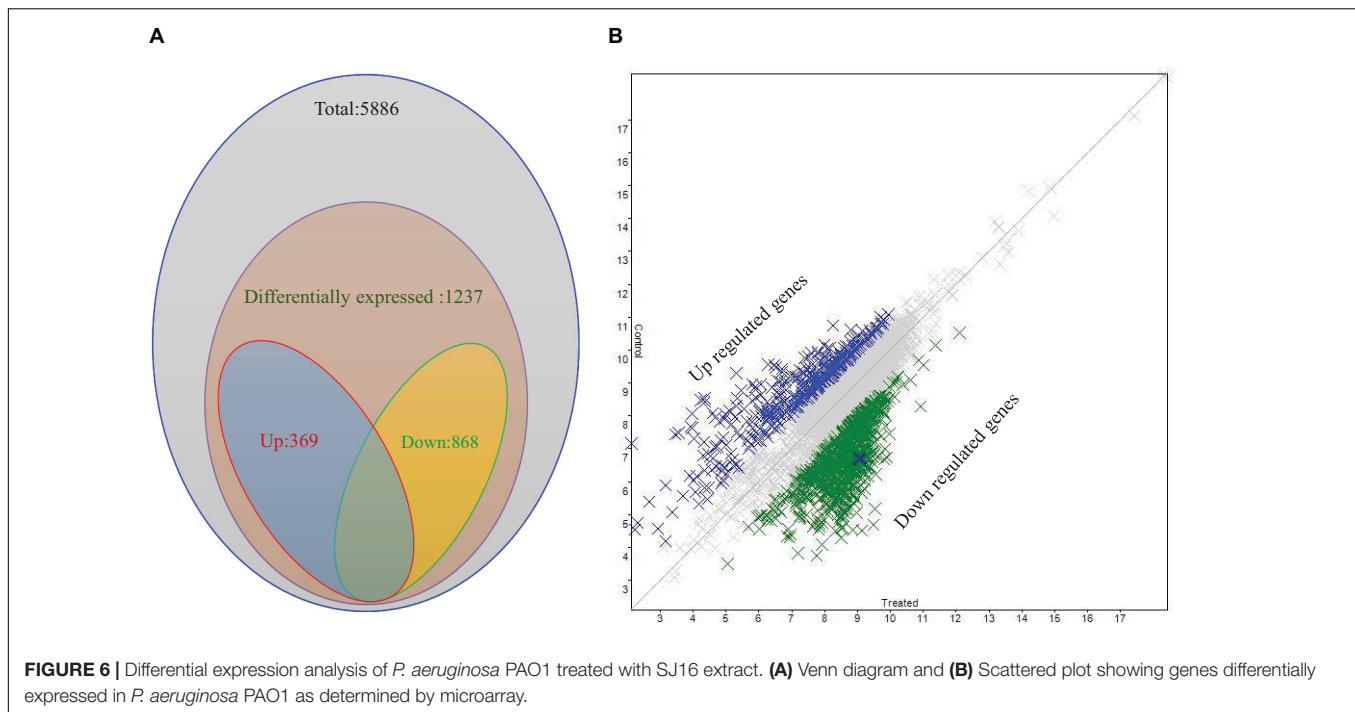


FIGURE 5 | Effect of *E. indicum* SJ16 extract on cell motility, and the virulence factors of *P. aeruginosa*. **(A)** The effect of the bacterial extract on the swarming and swimming motility of reference *P. aeruginosa* strains (PAO1 and PAH). *P. aeruginosa* was spotted on a plate supplemented with 1.0 mg/ml extract or without extract supplementation (control). Plates were analyzed after incubation of 24 h at 37°C; **(B)** The effect of the bacterial extracts (SJ16; 1.0 mg/ml) was determined based on the production of virulence factors of the reference *P. aeruginosa* strains by quantifying pyocyanin and rhamnolipid, as well as by analyzing the elastase and protease activities. “****” Indicates significant differences from the control at $P < 0.001$.

the compound Pyrrolo[1,2-a]pyrazine-1,4-dione,hexahydro-3-(phenylmethyl) compound, obtained from the *Streptomyces* sp. VITPK9 showed anticandidal activity against *Candida albicans*, *C. krusei*, and *C. tropicalis* (Sanjenbam et al., 2014). Additionally, the Pyrrolo[2,1-c][1,4]benzodiazepine compound was demonstrated to be an effective anti-tumor drugs (Cipolla et al., 2009), while the recently described hordenine compound that was obtained from sprouting barley showed significant QSI and anti-biofilm effects against *P. aeruginosa* (Zhou et al., 2018). Taken together, compounds that are similar to the one described in our study present great potential as bioactive molecules with diverse functions including antimicrobial, anti-cancer, antioxidant and now, anti-QS activity.

As stated above, the SJ16 extract inhibits the biofilm formation of the reference *P. aeruginosa* strains PAO1 and PAH in a concentration-dependent manner without affecting their planktonic growth (Figure 3). Furthermore, epi-fluorescence microscopy confirmed the viability of *P. aeruginosa* cells within

the biofilm (Figure 4A). Thus, the possibility of an inhibitory effect of the SJ16 extract on the growth of these reference strains (PAO1 and PAH) was ruled out. The SEM and AFM images suggest an alteration in the topology of the biofilm in the samples supplemented with the extract, compared to their corresponding controls, while a growing biofilm with dispersed bacterial cells was developed by *P. aeruginosa* strains in the presence of the SJ16 extract (Figures 4B,C). Disruption of biofilm architecture is a promising strategy to inhibit biofilm formation of drug-resistant *P. aeruginosa* strains. Importantly, in order for the bacteria to form a biofilm, they need to attach to a surface or substratum. Bacterial motility is crucial in the effort of the microbes to reach the substratum. Once attached to the surface, the bacteria spread all around via swarming and swimming type of motility, ultimately leading to biofilm formation over the surface (O’May and Tufenkji, 2011). Inhibition of the swarming and swimming motility of PAO1 and PAH was observed in the presence of the SJ16 extract (Figure 5A). It is possible that the SJ16 extract



may also have the capability to block the initial attachment of *P. aeruginosa* by preventing the bacterial motility toward the surface. This strategy could potentially open new avenue in the effort to halt bacterial spreading and thus minimize the ability of microbes to form biofilms (Singh et al., 2017).

The *P. aeruginosa* pathogenicity depends on the ability of this microbe to produce virulence factors. Pyocyanin, rhamnolipids, elastase, and protease are the key virulence factors which are highly expressed by *P. aeruginosa* during QS, infection and biofilm formation (Driscoll et al., 2007; Sarabhai et al., 2013). Elastase and protease are involved in the early steps of host colonization by the bacterial cells, pyocyanin is crucial for the demonstration of *P. aeruginosa* virulence, while rhamnolipids facilitate the bacterial motility. The combined effect of the afore-mentioned microbial factors eventually lead to biofilm formation (O'May and Tufenkji, 2011; Sarabhai et al., 2013). Elastase and protease activities, as well as the production of pyocyanin and rhamnolipid of both *P. aeruginosa* strains PAO1 and PAH were significantly reduced following SJ16 extract supplementation (**Figure 5B**), demonstrating the ability of the extract to attenuate the *P. aeruginosa* virulence functions, largely regulated by the *las* and *rhl* regulatory gene cascades (De Kievit and Iglewski, 2000). Similar results were obtained with the extract of *Terminalia chebula* and *D. tsuruhatusensis* (Sarabhai et al., 2013, Singh et al., 2017).

The microarray analysis revealed that at least 1,237 genes were differentially expressed following SJ16 extract supplementation, 868 out of which were down-regulated, whereas 369 were up-regulated (**Supplementary Table S1** and **Figure 6**). These microarray results demonstrated that a plethora of genes affected by the SJ16 extract are involved in QS regulation and biofilm formation. More specifically, these genes are crucial in the

control of bacterial QS, virulence, motility, cell metabolism, cell wall synthesis, and transcriptional regulation, while some others encode hypothetical proteins (**Table 1**). The expression profile of cells treated with the SJ16 extract containing the active 3-Benzyl-hexahydro-pyrrolo[1,2-a]pyrazine-1,4-dione compound showed that this agent downregulates genes responsible for the synthesis of the flagellar protein, the type III export apparatus protein, the flagellar basal-body rod protein, the pyochelin biosynthetic protein, the phenazine-modifying enzyme, the type III export protein, the twitching motility protein, as well as some hypothetical proteins. The extract also represses the expression of gene(s) which are involved in the biosynthesis of transcriptional regulators/ activators of QS network. These genes are controlled by QS systems and are closely associated with the pathogenicity of *P. aeruginosa* (Wagner et al., 2003). Similar results were obtained when *P. aeruginosa* PAO1 cells were treated with 1,2-benzenedicarboxylic acid, diisooctyl ester (Singh et al., 2017).

Based on the results that we herein report, we adopted a hypothetical model that elucidates the transcriptional regulation of *P. aeruginosa* virulence mediated by the by *E. indicum* SJ16 extract (**Figure 7**). We hypothesized that the identified active compound, 3-Benzyl-hexahydro-pyrrolo[1,2-a]pyrazine-1,4-dione lowers the expression of key regulatory genes including, *pqsA*, *pqsC*, *pscB*, *pstC*, *pqqA*, and *qor* (**Table 1**), in addition to the differential expression of other genes (**Supplementary Table S1**). Alteration in the transcript expression of these genes leads to lower levels of HHQ. Thus, it is possible that 3-Benzyl-hexahydro-pyrrolo[1,2-a]pyrazine-1,4-dione modulates the function of the *pqs* transcriptional regulatory system, hence controlling the production of MvfR (also known as PqsR). Inhibition of the MvfR system decreases the production of QS activators and signaling molecules, thus regulating the *las*

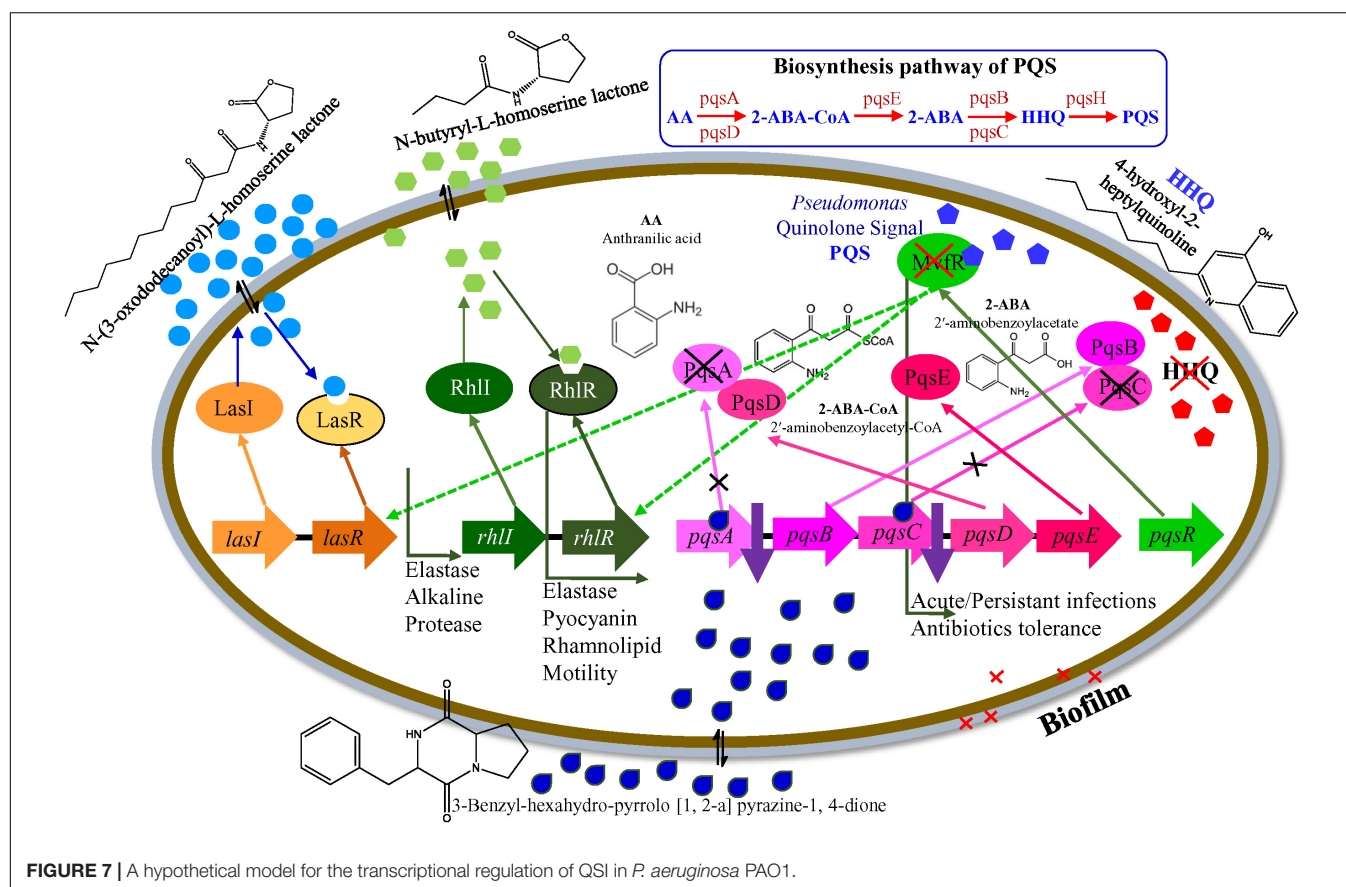
TABLE 1 | Selected transcripts that are differentially expressed (up- or down- regulated) in *P. aeruginosa* PAO1, treated with the bacterial (*E. indicum* SJ16) active fraction compared to control (untreated PAO1 strain).

Transcript ID	Gene Symbol	Description	Swiss Prot	Fold Change
PA0998	<i>pqsC</i>	Homologous to beta-keto-acyl-acyl-carrier protein synthase	Q9I4X1	−11.76
PA5493_polA	<i>polA</i>	DNA polymerase I	Q9HT80	−11.3
PA1105_fliJ	<i>fliJ</i>	flagellar protein FliJ	Q9I4N0	−7.31
PA1715_pscB	<i>pscB</i>	type III export apparatus protein	Q9I320	−6.94
PA5368_pstC	<i>pstC</i>	membrane protein component of ABC phosphate transporter	Q51544	−6.62
PA3064	<i>pelA</i>	hypothetical protein	Q9HZE4	−6.18
PA1985_pqqA	<i>pqqA</i>	pyrroloquinoline quinone biosynthesis protein A	Q9ZAA0	−6.18
PA0996	<i>pqsA</i>	probable coenzyme A ligase	Q9I4X3	−5.96
PA0520_nirQ	<i>nirQ</i>	regulatory protein NirQ	Q51481	−5.6
PA1077_flgB	<i>flgB</i>	flagellar basal-body rod protein FlgB	Q9I4Q2	−5.23
PA3824_queA	<i>queA</i>	S-adenosylmethionine:trna ribosyltransferase-isomerase	Q9HXX8	−5.15
PA5501_znuB	<i>znuB</i>	permease of ABC zinc transporter ZnuB	Q9HT72	−4.97
PA2236	<i>pslF</i>	hypothetical protein	Q9I1N3	−4.76
PA1082_flgG	<i>flgG</i>	flagellar basal-body rod protein FlgG	Q9I4P7	−4.75
PA4309_pctA	<i>pctA</i>	chemotactic transducer PctA	G3XD24	−4.35
PA4224	<i>pchG</i>	pyochelin biosynthetic protein PchG	G3XCL0	−4.17
PA3061	<i>pelD</i>	hypothetical protein	Q9HZE7	−3.97
PA5450_wzt	<i>wzt</i>	ABC subunit of A-band LPS efflux transporter	P72163	−3.62
PA4225_pchF	<i>pchF</i>	pyochelin synthetase	Q9HWG4	−3.39
PA5107_blc	<i>blc</i>	outer membrane lipoprotein Blc	Q9HU76	−3.26
PA1049_pdxH	<i>pdxH</i>	pyridoxine 5'-phosphate oxidase	—	−3.21
PA1704_pcrR	<i>pcrR</i>	transcriptional regulator protein PcrR	G3XCW4	−3.01
PA2238	<i>pslH</i>	hypothetical protein	Q9I1N1	−2.74
PA3701_prfB	<i>prfB</i>	peptide chain release factor 2	—	−2.73
PA1311_phnX	<i>phnX</i>	2-phosphonoacetaldehyde hydrolase	Q9I433	−2.71
PA4229_pchC	<i>pchC</i>	pyochelin biosynthetic protein PchC	Q9HWG2	−2.38
PA2686_pfeR	<i>pfeR</i>	two-component response regulator PfeR	Q04803	−2.25
PA1720_pscG	<i>pscG</i>	type III export protein PscG	P95435	−2.13
PA0023_qor	<i>qor</i>	quinone oxidoreductase	P43903	−2.12
PA4590_pra	<i>pra</i>	protein activator	G3XDA9	−2.09
PA0409_pilH	<i>pilH</i>	twitching motility protein PilH	P43501	−2.04
PA0051	<i>phzH</i>	potential phenazine-modifying enzyme	Q9I781	−2.01
PA2425	<i>pvdG</i>	PvdG	Q9I156	2.06
PA1544_anr	<i>anr</i>	transcriptional regulator Anr	P23926	2.13
PA2399_pvdD	<i>pvdD</i>	pyoverdine synthetase D	Q9I182	2.17
PA2054_cynR	<i>cynR</i>	transcriptional regulator CynR	Q9I261	2.36
PA1783_nasA	<i>nasA</i>	nitrate transporter	Q9I2V9	2.54
PA1904	<i>phzF</i>	phzF1 and phzF2 probable phenazine biosynthesis protein	Q69754	2.72
PA4034_aqpZ	<i>aqpZ</i>	aquaporin Z	Q9HWZ3	3.04
PA1723_pscJ	<i>pscJ</i>	type III export protein PscJ	Q9I314	3.39
PA1717_pscD	<i>pscD</i>	type III export protein PscD	Q9I318	3.43
PA2424	<i>pvdL</i>	PvdL	Q9I157	3.43
PA1097_fleQ	<i>fleQ</i>	transcriptional regulator FleQ	G3XCV0	4.91
PA4472_pmbA	<i>pmbA</i>	PmbA protein	Q9HVU9	5.13
PA2961_holB	<i>holB</i>	DNA polymerase III, delta prime subunit	—	7.97
PA2258_ptxR	<i>ptxR</i>	transcriptional regulator PtxR	P72131	9.11

“—” sign means down-regulation.

and *rhl* transcription cascades. Subsequently, *rhl* leads lower levels of pyocyanin and rhamnolipid, decreased protease and elastase activities as well as reduced bacterial motility (Déziel et al., 2005). Our results indicate that the active compound present in the SJ16 extract decreases the virulence activity

through modulating the *pqs* transcription regulation system. The proposed model is a schematic representation of the regulatory mechanism, illustrated based on the available literature. However, a comprehensive study is required to confirm the precise role of the identified compound,



3-Benzyl-hexahydro-pyrrolo[1,2-a]pyrazine-1,4-dione in the QSI regulation mechanism as well as its interacting partners.

CONCLUSION

The QS regulates virulence factor activities and biofilm formation, and disrupting the QS mechanism is an important strategy to inhibit pathogenicity of *P. aeruginosa* strains. Anti-QS compounds provides a useful tool in the effort to tackle infections caused by pathogenic bacteria. *E. indicum* SJ16, a microbe isolated from the rhizosphere of *C. laevigatus* showed promising anti-QS and anti-biofilm activities, without exhibiting any anti-bacterial properties. The 3-Benzyl-hexahydro-pyrrolo[1, 2-a]pyrazine-1,4-dione compound present in the SJ16 extract was identified as a potentially active agent inhibiting the biofilm formation of two references *P. aeruginosa* strains, PAO1 and PAH by decreasing their swimming and swarming motility and by regulating the production of virulence factors such as pyocyanin, rhamnolipid, elastase, and protease. Furthermore, it is possible that this compound controls the *pqs* QS system, thus regulating the bacterial QS mechanism as indicated by our proposed inhibitory model. Overall, our results indicate that the SJ16 extract did not have any toxic effect on the growth and viability of the reference *P. aeruginosa* strains (PAO1 and PAH), even after longer incubation periods. On the contrary, it exhibits a strong

inhibitory effects on the microbial motility, on the production of virulence factors as well as on biofilm formation. Importantly, our data indicate that the SJ16 extract is able to disrupt the cell-to-cell communication (QSI) by modulating a key component of the molecular cascade regulating the *P. aeruginosa* of QS systems (*las*, *rhl*, and *pqs*). Therefore, the identified compound has great potential for drug development in our efforts to enrich our antimicrobial armamentarium. Further research is necessary to explore and determine its pharmaceutical applications.

AUTHOR CONTRIBUTIONS

All authors conceived and designed the experiments. VS performed the experiments. VS and AM analyzed the data and wrote the manuscript.

ACKNOWLEDGMENTS

The authors would like to gratefully acknowledge Prof. Anton Hartmann (Helmholtz Zentrum, München, Germany) for providing the reference strain *C. violaceum* CV026. The authors are also thankful to the Government Medical College, Bhavnagar (India) for providing the clinical isolate *P. aeruginosa* PAH. The Analytical and Environmental Science Division and Centralized Instrument Facility of the Institute is duly acknowledged for

running the samples. Prof. Uelinton Manoel Pinto, University of Sao Paulo, Brazil and Dr. Marianna Almpiani, Harvard Medical School, Boston, United States are kindly acknowledged for their language editing and proofreading. CSIR-CSMCRI Communication No. PRIS-103/2018.

REFERENCES

- Adonizio, A., Kong, K. F., and Mathee, K. (2008). Inhibition of quorum sensing controlled virulence factor production in *Pseudomonas aeruginosa* by south florida plant extracts. *Antimicrob. Agents Chemother.* 52, 198–203. doi: 10.1128/AAC.00612-07
- Andersson, S., Dalhammar, G., Land, C., and Rajarao, G. (2009). Characterization of extracellular polymeric substances from denitrifying organism *Comamonas denitrificans*. *Appl. Microbiol. Biotechnol.* 82, 535–543. doi: 10.1007/s00253-008-1817-3
- Berendsen, R. L., Pieterse, C. M. J., and Bakker, P. A. (2012). The rhizosphere microbiome and plant health. *Trends Plant Sci.* 17, 478–486. doi: 10.1016/j.tplants.2012.04.001
- Bjorn, M. J., Sokol, P. A., and Iglewski, B. H. (1979). Influence of iron on yields of extracellular products in *Pseudomonas aeruginosa* cultures. *J. Bacteriol.* 138, 193–200.
- Chan, K., Atkinson, S., Mathee, K., Sam, C., Chhabra, S. R., Camara, M., et al. (2011). Characterization of N-acyl-homoserine lactone-degrading bacteria associated with the *Zingiber officinale* (ginger) rhizosphere: co-existence of quorum quenching and quorum sensing *Acinetobacter* and *Burkholderia*. *BMC Microbiol.* 11:51. doi: 10.1186/1471-2180-11-51
- Chaturvedi, P., and Shivaji, S. (2006). *Exiguobacterium indicum* sp. nov., a psychrophilic bacterium from the Hamta glacier of the Himalayan mountain ranges of India. *Int. J. Syst. Evol. Microbiol.* 56, 2765–2770. doi: 10.1099/ijs.0.64508-0
- Christiaen, S. E., Brackman, G., Nelis, H. J., and Coenye, T. (2011). Isolation and identification of quorum quenching bacteria from environmental samples. *J. Microbiol. Methods* 87, 213–219. doi: 10.1016/j.mimet.2011.08.002
- Chu, W., Zhou, S., Zhu, W., and Zhuang, X. (2014). Quorum quenching bacteria *Bacillus* sp. QSI-1 protect zebrafish (*Danio rerio*) from *Aeromonas hydrophila* infection. *Sci. Rep.* 4:5446. doi: 10.1038/srep05446
- Cipolla, L., Araújo, A. C., Airolidi, C., and Bini, D. (2009). Pyrrolo [2, 1-c] [1, 4] benzodiazepine as a scaffold for the design and synthesis of anti-tumour drugs. *AntiCancer Agents Med. Chem.* 9, 1–31. doi: 10.2174/187152009787047743
- Cirou, A., Diallo, S., Kurt, C., Latour, X., and Faure, D. (2007). Growth promotion of quorum-quenching bacteria in the rhizosphere of *Solanum tuberosum*. *Environ. Microbiol.* 9, 1511–1522. doi: 10.1111/j.1462-2920.2007.01270.x
- Courtois, S., Cappellano, C. M., Ball, M., Francou, F. X., Normand, P., Helynick, G., et al. (2003). Recombinant environmental libraries provide access to microbial diversity for drug discovery from natural products. *Appl. Environ. Microbiol.* 69, 49–55. doi: 10.1128/AEM.69.1.49-55.2003
- D'Angelo-Picard, C., Faure, D., Penot, I., and Dessaux, Y. (2005). Diversity of N-acyl homoserine lactone-producing and degrading bacteria in soil and tobacco rhizosphere. *Environ. Microbiol.* 7, 1796–1808. doi: 10.1111/j.1462-2920.2005.00886.x
- De Kievit, T. R., and Iglewski, B. H. (2000). Bacterial quorum sensing in pathogenic relationships. *Infect. Immun.* 68, 4839–4849. doi: 10.1128/IAI.68.9.4839-4849.2000
- Déziel, E., Gopalan, S., Tampakaki, A. P., Lépine, F., Padfield, K. E., Saucier, M., et al. (2005). The contribution of MvfR to *Pseudomonas aeruginosa* pathogenesis and quorum sensing circuitry regulation: multiple quorum sensing-regulated genes are modulated without affecting *lasRI*, *rhlRI* or the production of N-acyl-l-homoserine lactones. *Mol. Microbiol.* 55, 998–1014. doi: 10.1111/j.1365-2958.2004.04448.x
- Driscoll, J. A., Brody, S. L., and Kollef, M. H. (2007). The epidemiology, pathogenesis, and treatment of *Pseudomonas aeruginosa* infections. *Drugs* 67, 351–368. doi: 10.2165/00003495-200767030-00003
- Essar, D. W., Eberly, L., Hadero, A., and Crawford, I. P. (1990). Identification and characterization of genes for a second anthranilate synthase in *Pseudomonas aeruginosa*: interchangeability of the two anthranilate synthases and evolutionary implications. *J. Bacteriol.* 172, 884–900. doi: 10.1128/JB.172.2.884-900.1990
- Felsenstein, J. (1985). Confidence limits on phylogenesis: an approach using the bootstrap. *Evolution* 39, 783–791. doi: 10.1111/j.1558-5646.1985.tb00420.x
- Galloway, W. R., James, T. H., Bowden, S. D., Welch, M., and Spring, D. R. (2011). Quorum sensing in gram-negative bacteria: small-molecule modulation of AHL and AI-2 quorum sensing pathways. *Chem. Rev.* 111, 28–67. doi: 10.1021/cr100109t
- Gain, H., Yardeni, E. H., and Kolodkin-Gal, I. (2015). “Biofilms: maintenance, development, and disassembly of bacterial communities are determined by QS cascades,” in *Quorum Sensing vs Quorum Quenching: A Battle with No End in Sight*, ed. V. Kalia (New Delhi: Springer), 23–37. doi: 10.1007/978-81-322-1982-8_3
- Gillespie, D. E., Brady, S. F., Bettermann, A. D., Cianciotto, N. P., Liles, M. R., Rondon, M. R., et al. (2002). Isolation of antibiotics turbomycin A and B from metagenomic library of soil microbial DNA. *Appl. Environ. Microbiol.* 68, 4301–4306. doi: 10.1128/AEM.68.9.4301-4306.2002
- Goswami, N. N., Trivedi, H. R., Goswami, A. P. P., Patel, T. K., and Tripathi, C. B. (2011). Antibiotic sensitivity profile of bacterial pathogens in postoperative wound infections at a tertiary care hospital in Gujarat, India. *J. Pharmacol. Pharmacother.* 2:158. doi: 10.4103/0976-500X.83279
- Hoiby, N., Bjarnsholt, T., Givskov, M., Molin, S., and Ciofu, O. (2010). Antibiotic resistance of bacterial biofilms. *Int. J. Antimicrob.* 35, 322–332. doi: 10.1016/j.ijantimicag.2009.12.011
- Jha, B., Singh, V. K., Weiss, A., Hartmann, A., and Schmid, M. (2015). *Zhihengliuella somnathii* sp. nov., a halotolerant actinobacterium from the rhizosphere of a halophyte *Salicornia brachiata*. *Int. J. Syst. Evol. Microbiol.* 65, 3137–3142. doi: 10.1099/ijs.0.000391
- Kalia, V. C. (2013). Quorum sensing inhibitors: an overview. *Biotechnol. Adv.* 31, 224–245. doi: 10.1016/j.biotechadv.2012.10.004
- Kang, B. R., Lee, J. H., Ko, S. J., Lee, Y. H., Cha, J. S., Cho, B. H., et al. (2004). Degradation of acyl-homoserine lactone molecules by *Acinetobacter* sp. strain C1010. *Can. J. Microbiol.* 50, 935–941. doi: 10.1139/w04-083
- Kavita, K., Singh, V. K., Mishra, A., and Jha, B. (2014). Characterisation and anti-biofilm activity of extracellular polymeric substances from *Oceanobacillus iheyensis*. *Carbohydr. Polym.* 101, 29–35. doi: 10.1016/j.carbpol.2013.08.099
- Lee, J., and Zhang, L. (2015). The hierarchy quorum sensing network in *Pseudomonas aeruginosa*. *Protein Cell* 6, 26–41. doi: 10.1007/s13238-014-0100-x
- Li, Z., Lin, S., Liu, X., Tan, J., Pan, J., and Yang, H. (2014). A freshwater bacterial strain, *Shewanella* sp. *Lzh-2*, isolated from Lake Taihu and its two algicidal active substances, hexahydropyrrolo [1, 2-a] pyrazine-1, 4-dione and 2, 3-indolinedione. *Appl. Microbiol. Biotechnol.* 98, 4737–4748. doi: 10.1007/s00253-014-5602-1
- McClure, C. D., and Schiller, N. L. (1992). Effects of *Pseudomonas aeruginosa* rhamnolipids on human monocyte-derived macrophages. *J. Leukoc. Biol.* 51, 97–102. doi: 10.1002/jlb.51.2.97
- Oh, Y., Lee, N., Jo, W., Jung, W., and Lim, J. (2009). Effects of substrates on biofilm formation observed by atomic force microscopy. *Ultramicroscopy* 109, 874–880. doi: 10.1016/j.ultramic.2009.03.042
- O'May, C., and Tufenkji, N. (2011). The swarming motility of *Pseudomonas aeruginosa* is blocked by cranberry proanthocyanidins and other tannin-containing materials. *Appl. Environ. Microbiol.* 77, 3061–3067. doi: 10.1128/AEM.02677-10
- O'Toole, G., Kaplan, H. B., and Kolter, R. (2000). Biofilm formation as microbial development. *Annu. Rev. Microbiol.* 54, 49–79. doi: 10.1146/annurev.micro.54.1.49
- Overhage, J., Lewenza, S., Marr, A. K., and Hancock, R. E. (2007). Identification of genes involved in swarming motility using a *Pseudomonas aeruginosa* PAO1

SUPPLEMENTARY MATERIAL

The Supplementary Material for this article can be found online at: <https://www.frontiersin.org/articles/10.3389/fmicb.2019.01269/full#supplementary-material>

- Mini-Tn5-lux mutant library. *J. Bacteriol.* 189, 2164–2169. doi: 10.1128/JB.01623-06
- Quecán, B. X. V., Rivera, M. L. C., and Pinto, U. M. (2018). “Bioactive phytochemicals targeting microbial activities mediated by quorum sensing,” in *the Biotechnological Applications of Quorum Sensing Inhibitors*. ed. V. Kalia (Singapore: Springer), 397–416. doi: 10.1007/978-981-10-9026-4_19
- Rashid, M. H., and Kornberg, A. (2000). Inorganic polyphosphate is needed for swimming, swarming, and twitching motilities of *Pseudomonas aeruginosa*. *Proc. Natl. Acad. Sci. U.S.A.* 97, 4885–4890. doi: 10.1073/pnas.060030097
- Rodrigues, A. C., Zola, F. G., Ávila Oliveira, B. D., Sacramento, N. T. B., da Silva, E. R., Bertoldi, M. C., et al. (2016). Quorum quenching and microbial control through phenolic extract of *Eugenia uniflora* fruits. *J. Food Sci.* 81, M2538–M2544. doi: 10.1111/1750-3841.13431
- Saitou, N., and Nei, M. (1987). The neighbor-joining method: a new method for reconstructing phylogenetic trees. *Mol. Biol. Evol.* 4, 406–425. doi: 10.1093/oxfordjournals.molbev.a040454
- Sanjenbam, P., Gopal, J. V., and Kannabiran, K. (2014). Isolation and identification of anticandidal compound from *Streptomyces* sp. VITPK9. *Appl. Microbiol. Biotechnol.* 50, 492–499. doi: 10.1134/S0003683814050081
- Sarabhai, S., Sharma, P., and Capalash, N. (2013). Ellagic acid derivatives from terminalia chebula retz. Downregulate the expression of quorum sensing genes to attenuate *Pseudomonas aeruginosa* PAO1 virulence. *PLoS One* 8:e53441. doi: 10.1371/journal.pone.0053441
- Ser, H. L., Palanisamy, U. D., Yin, W. F., Malek, S. N. A., Chan, K. G., Goh, B. H., et al. (2015). Presence of antioxidative agent, Pyrrolo [1, 2-a] pyrazine-1, 4-dione, hexahydro-in newly isolated *Streptomyces mangrovisoli* sp. nov. *Front. Microbiol.* 6:854. doi: 10.3389/fmicb.2015.00854
- Singh, V. K., Kavita, K., Prabhakaran, R., and Jha, B. (2013). Cis-9-octadecenoic acid from the rhizospheric bacterium *Stenotrophomonas maltophilia* BJ01 shows quorum quenching and anti-biofilm activities. *Biofouling* 29, 855–867. doi: 10.1080/08927014.2013.807914
- Singh, V. K., Mishra, A., and Jha, B. (2016b). “Marine bacterial extracellular polymeric substances: characteristics and applications,” in *Marine Glycobiology: Principles and Applications*. ed. S. Kim (Boca Raton, FL: CRC Press), 369–377. doi: 10.1201/9781315371399-27
- Singh, V. K., Mishra, A., Haque, I., and Jha, B. (2016a). A novel transcription factor-like gene *SbSDR1* acts as a molecular switch and confers salt and osmotic endurance to transgenic tobacco. *Sci. Rep.* 6:31686. doi: 10.1038/srep31686
- Singh, V. K., Mishra, A., and Jha, B. (2017). Anti-quorum sensing and anti-biofilm activity of *Delftia tsuruhatensis* extract by attenuating the quorum sensing-controlled virulence factor production in *Pseudomonas aeruginosa*. *Front. Cell. Infect. Microbiol.* 7:337. doi: 10.3389/fcimb.2017.00337
- Susilowati, D. N., Sudiana, I. M., Mubarik, N. R., and Suwanto, A. (2015). Species and functional diversity of rhizobacteria of rice plant in the coastal soils of Indonesia. *Indones. J. Agric. Sci.* 16, 39–50. doi: 10.21082/ijas.v16n1.2015.p39-50
- Tamura, K., Nei, M., and Kumar, S. (2004). Prospects for inferring very large phylogenies by using the neighbor-joining method. *Proc. Natl. Acad. Sci. U.S.A.* 101, 11030–11035. doi: 10.1073/pnas.0404206101
- Tamura, K., Stecher, G., Peterson, D., Filipski, A., and Kumar, S. (2013). MEGA6: molecular evolutionary genetics analysis version 6.0. *Mol. Biol. Evol.* 30, 2725–2729. doi: 10.1093/molbev/mst197
- Tan, L. Y., Yin, W. F., and Chan, K. G. (2012). Silencing quorum sensing through extracts of *Melicope lunuankenda*. *Sensors* 12, 4339–4351. doi: 10.3390/s120404339
- Wagner, V. E., Bushnell, D., Passador, L., Brooks, A. I., and Iglewski, B. H. (2003). Microarray analysis of *Pseudomonas aeruginosa* quorum-sensing regulons: effects of growth phase and environment. *J. Bacteriol.* 185, 2080–2095. doi: 10.1128/JB.185.7.2080-2095.2003
- Weisburg, W. G., Barns, S. M., Pelletier, D. A., and Lane, D. J. (1991). 16S ribosomal DNA amplification for phylogenetic study. *J. Bacteriol.* 173, 697–703. doi: 10.1128/jb.173.2.697-703.1991
- Zhou, J. W., Luo, H. Z., Jiang, H., Jian, T. K., Chen, Z. Q., and Jia, A. Q. (2018). Hordenine, a novel quorum sensing inhibitor and anti-biofilm agent against *Pseudomonas aeruginosa*. *J. Agric. Food Chem.* 66, 1620–1628. doi: 10.1021/acs.jafc.7b05035
- Zhu, H., Thuruthyl, S. J., and Willcox, M. D. P. (2002). Determination of quorum-sensing signal molecules and virulence factors of *Pseudomonas aeruginosa* isolates from contact lens-induced microbial keratitis. *J. Med. Microbiol.* 51, 1063–1070. doi: 10.1099/0022-1317-51-12-1063

Conflict of Interest Statement: The authors declare that the research was conducted in the absence of any commercial or financial relationships that could be construed as a potential conflict of interest.

Copyright © 2019 Singh, Mishra and Jha. This is an open-access article distributed under the terms of the Creative Commons Attribution License (CC BY). The use, distribution or reproduction in other forums is permitted, provided the original author(s) and the copyright owner(s) are credited and that the original publication in this journal is cited, in accordance with accepted academic practice. No use, distribution or reproduction is permitted which does not comply with these terms.



The Anti-virulence Efficacy of 4-(1,3-Dimethyl-2,3-Dihydro-1H-Benzimidazol-2-yl)Phenol Against Methicillin-Resistant *Staphylococcus aureus*

Nagendran Tharmalingam, Rajamohammed Khader, Beth Burgwyn Fuchs and Eleftherios Mylonakis*

Department of Medicine, Division of Infectious Diseases, Warren Alpert Medical School of Brown University, Rhode Island Hospital, Providence, RI, United States

OPEN ACCESS

Edited by:

Natalia V. Kirienko,
Rice University, United States

Reviewed by:

Polly H. M. Leung,
Hong Kong Polytechnic University,
Hong Kong
You-Hee Cho,
Cha University, South Korea
Rustam Aminov,
University of Aberdeen,
United Kingdom

*Correspondence:

Eleftherios Mylonakis
emylonakis@lifespan.org

Specialty section:

This article was submitted to
Antimicrobials, Resistance and
Chemotherapy,
a section of the journal
Frontiers in Microbiology

Received: 02 November 2018

Accepted: 21 June 2019

Published: 17 July 2019

Citation:

Tharmalingam N, Khader R, Fuchs BB
and Mylonakis E (2019) The Anti-
virulence Efficacy of 4-(1,3-Dimethyl-
2,3-Dihydro-1H-Benzimidazol-2-yl)
Phenol Against Methicillin-Resistant
Staphylococcus aureus.
Front. Microbiol. 10:1557.
doi: 10.3389/fmicb.2019.01557

Antimicrobial drug discovery against drug-resistant bacteria is an urgent need. Beyond agents with direct antibacterial activity, anti-virulent molecules may also be viable compounds to defend against bacterial pathogenesis. Using a high throughput screen (HTS) that utilized *Caenorhabditis elegans* infected with methicillin-resistant *Staphylococcus aureus* (MRSA) strain of MW2, we identified 4-(1,3-dimethyl-2,3-dihydro-1H-benzimidazol-2-yl)phenol (BIP). Interestingly, BIP had no *in vitro* inhibition activity against MW2, at least up to 64 $\mu\text{g/ml}$. The lack of direct antimicrobial activity suggests that BIP could inhibit bacterial virulence factors. To explore the possible anti-virulence effect of the identified molecule, we first performed real-time PCR to examine changes in virulence expression. BIP was highly active against MRSA virulence factors at sub-lethal concentrations and down-regulated virulence regulator genes, such as *agrA* and *codY*. However, the benzimidazole derivatives omeprazole and pantoprazole did not down-regulate virulence genes significantly, compared to BIP. Moreover, the BIP-pretreated MW2 cells were more vulnerable to macrophage-mediated killing, as confirmed by intracellular killing and live/dead staining assays, and less efficient in establishing a lethal infection in the invertebrate host *Galleria mellonella* ($p = 0.0131$). We tested the cytotoxicity of BIP against human red blood cells (RBCs), and it did not cause hemolysis at the highest concentration tested (64 $\mu\text{g/ml}$). Taken together, our findings outline the potential anti-virulence activity of BIP that was identified through a *C. elegans*-based, whole animal based, screen.

Keywords: anti-virulent molecules, *agrA*, bacterial virulence, *codY*, methicillin-resistant *Staphylococcus aureus*

INTRODUCTION

Fatal infections from antibiotic-resistant bacteria are predicted to rise and expected to exceed deaths caused by cancer by the year 2050 (de Kraker et al., 2016), therefore putting forth a critical need for novel antibiotics (Zaman et al., 2017). The infection process is a multifaceted process with the interplay between the invading bacteria and host. Most bacterial pathogens

rely on virulence factors, inclusive of toxins, adhesins, secreted proteins, secretion systems, lytic enzymes, invasins, etc. to establish an infection (Defoirdt, 2017). Targeting these virulence mechanisms can be a means of thwarting the microbial attack (Wilson et al., 2002).

A possible benefit to developing anti-virulence agents is the potential to reduce antibiotic resistance from overexposure to antibiotic compounds (Hauser et al., 2016). Anti-virulence compounds neither kill nor inhibit bacterial growth, but disable the infection process (Heras et al., 2015; Totsika, 2017). The fundamental principle behind blocking virulence factors is to make the pathogen more vulnerable to host immune responses (Longdon et al., 2015). Currently, anti-virulence compounds present a potentially untapped strategy in controlling or treating bacterial infections.

Virulence factors are already a target exploited by nature to curb microbial infections. Natural products exist that target microbial virulence factors. Examples include garlic, menthol, clove, and black pepper which inhibit enterotoxins, the type III secretion system (T3SS), and biofilm (Maura et al., 2016; Silva et al., 2016). Anti-virulence compounds can also be found among orphaned United States-Food and Drug Administration (FDA)-approved drugs and existing therapeutic agents by engaging in “drug repurposing” (Rampioni et al., 2017). For example, anthelmintic drug niclosamide was found to have a potential “anti-quorum sensing” activity against the Gram-Negative pathogen *Pseudomonas aeruginosa* (Imperi et al., 2013). Recently, the FDA approved a therapy that targets virulence factors using immunoglobulins, while other anti-virulence molecules are in preclinical evaluation (Dickey et al., 2017).

In search of new antimicrobial agents, we performed a high throughput screen (HTS) to find compounds that prolong the survival of *C. elegans* infected with methicillin-resistant *Staphylococcus aureus* (Rajamuthiah et al., 2014; Kim et al., 2018). In this screen, the molecule BIP was identified as a hit. The compound is a benzimidazole derivative linked with phenol. Benzimidazole is a heterocyclic aromatic organic compound consisting of a fusion of benzene and imidazole (Shrivastava et al., 2017) and its derivatives exhibit a diverse biological activity including, anthelmintic, antibacterial, anticancer, anti-inflammatory, etc. (Singh et al., 2012). Because the compound did demonstrate *in vitro* inhibition activity against the MW2, we hypothesized that BIP exhibits anti-virulence activity.

MATERIALS AND METHODS

Compound Information

4-(1,3-Dimethyl-2,3-dihydro-1H-benzimidazol-2-yl)phenol (Chembridge # 5534382) (BIP) was purchased from Chembridge (Chembridge Corporation, San Diego, CA, USA). BIP was prepared by dissolving in DMSO (Sigma Aldrich, St. Louis, MO, USA) at 10 mg/ml and diluting as required for experiments. Hits were identified from the screen based on the Z-score. The Z-score was calculated from the ratio of live versus dead worms after treatment with investigational compounds, and the score is defined as the number of standard deviations (SD) by

which the investigational compound is separated from the mean using the formula $Z = (x - \mu)/\sigma$, where x is the raw sample score, μ is the mean of the population, and σ is the standard deviation of the population. Samples with $Z > 2\sigma$ were considered as hits (Rajamuthiah et al., 2014). Other approved clinical drugs were purchased from Sigma Aldrich.

Bacterial and Nematode Strains

All reference and clinical bacterial strains were from our laboratory collection (Table 1). For all experiments, bacteria were grown at 37°C. *S. aureus* (MRSA strain MW2) (clinical strains BF 9 and BF 10) *agr* mutant *S. aureus* RN 4220, *Enterococcus faecium*, *Klebsiella pneumoniae*, *Acinetobacter baumannii*, *Pseudomonas aeruginosa*, *Enterobacter aerogenes*, and *Candida albicans* were grown in tryptic soy broth (TSB) (BD Biosciences, Franklin Lakes, NJ, USA). The *C. elegans* *glp-4(bn2);sek-1(km4)* strain was maintained at 15°C on a lawn of *Escherichia coli* strain HB101 on 10-cm plates, as previously described (Rajamuthiah et al., 2014). The *glp-4(bn2)* mutation renders the strain unable to produce progeny at 25°C (Beanan and Strome, 1992), and the *sek-1(km4)* mutation increases sensitivity to several pathogens (Tanaka-Hino et al., 2002), thereby reducing assay time.

Antimicrobial Susceptibility Testing

In vitro, antibiotic susceptibility assays were carried out using a broth microdilution assay using Müller-Hinton broth (BD Biosciences) in 96-well plates (BD Biosciences) with a total assay volume of 100 µl (Wikler, 2006). Two-fold serial dilutions of BIP were prepared over the concentration range 0.01– 64 µg/ml. The initial bacterial inoculum was adjusted to OD₆₀₀ = 0.06 and assays were incubated at 35°C for 18 h. To determine the minimum inhibitory concentration (MIC), OD₆₀₀ was measured and visual inspection was made after incubation, and the lowest concentration of test compound that suppressed bacterial growth was reported as the MIC. The choice of medium for *C. albicans* was RPMI and 10³–2.5 × 10³ of initial inoculum was used to determine the MIC. The assays were carried out in triplicate.

Time to Kill Assays

The strain MW2 was used to probe the killing effects of BIP, as previously described (Rajamuthiah et al., 2015). The assays were carried out in 10-ml tubes (BD Biosciences) in duplicate. Briefly, log-phase cultures of MW2 were diluted in fresh TSB to a density of 10⁸ cells/ml. BIP was added at sub-lethal

TABLE 1 | Antimicrobial activity of BIP against the major pathogens.

Pathogen	MIC (µg/ml)
<i>Staphylococcus aureus</i> MW2	>64
<i>Enterococcus faecium</i> ATCC E007	>64
<i>Acinetobacter baumannii</i> ATCC 17978	>64
<i>Enterobacter aerogenes</i> EAE 2625	>64
<i>Klebsiella pneumoniae</i> ATCC 77326	>64
<i>Pseudomonas aeruginosa</i> PA14	>64
<i>Candida albicans</i> SC 5314	>64

concentrations (64, 32 µg/ml), and the tubes were incubated at 37°C with agitation. At periodic intervals, aliquots from each tube were serially diluted in TSB and plated onto tryptic soy agar (TSA, BD Biosciences). CFU was enumerated after overnight incubation at 37°C (Tharmalingam et al., 2017). Gentamicin at 0.5 µg/ml (MIC: 1.0 µg/ml) was used as a control agent.

An independent experiment was carried out to test the hypothesis of post-antibiotic effect. The MW2 cells were treated with BIP (64 µg/ml) for 4 h, and the cells were washed with sterile PBS. The washed cells were suspended in fresh MHB (0.05 OD₆₀₀) and incubated for 2 h with agitation. After 2 h, the total viable count was enumerated as described earlier in this section.

Human Red Blood Cell Hemolysis

Human erythrocytes (Rockland Immunochemicals, Limerick, PA, USA) were used to test the hemolytic properties of BIP, as described previously (Isnansetyo and Kamei, 2003). BIP was serially diluted in PBS, and an equal volume of 4% RBCs were added in 96-well plates. After incubating at 37°C for 1 h, the plates were centrifuged at 500 × g for 5 min, and an aliquot of 100 µl of the supernatant from each well was transferred to a second 96-well plate. Triton-X (0.0025–1.0%) was used as a positive control. Visual inspection and absorbance at 540 nm were used to measure hemolysis.

Real-Time Quantitative PCR Assays

An overnight culture of MW2 was grown in TSB to evaluate the effects of BIP on bacterial gene expression. The culture was harvested when the OD₆₀₀ had reached 0.4. The cells were washed with PBS and exposed to the sub-lethal concentration of BIP (32 or 64 µg/ml), vancomycin (0.5 µg/ml), or DMSO for 4 h. RNA was prepared using RNeasy mini kit (Qiagen, Hilden, Germany) according to the manufacturer's instructions. The Verso cDNA synthesis kit (Thermo Fisher Scientific, MA, USA) was used for cDNA synthesis. Real-time quantitative polymerase chain reaction (RT-qPCR) was performed as described in the manufacturer's instructions (Bio-Rad, CA, USA) using the primers reported by Liu et al. (2018) and the iCycler iQ real-time detection system (Bio-Rad). No-RT control was included as a negative control. According to Mitchell et al. (2011), the relative expression ratios were calculated as follows: $n\text{-fold expression} = 2^{-\Delta\Delta Ct}$, $\Delta\Delta Ct = \Delta Ct (\text{drug-treated}) / \Delta Ct (\text{untreated})$, where ΔCt represents the difference between the cycle threshold (Ct) of the gene studied and the Ct of housekeeping 16S rRNA gene (internal control). Primer sequences used in this study were: 5-GGGACCCGCACAAGCGGTGG-3 and 5-GGGTTGCGCTCGTTGCGGGA-3 (Atshan et al., 2013). Statistical significance was calculated using Student's *t*-test.

Intracellular Killing Assays

RAW 264.7 macrophages were used to evaluate the intracellular killing of BIP-pretreated *S. aureus*. Assays were performed in triplicate as described by Schmitt et al. (2013). Briefly, macrophages were cultured and maintained as described previously (Jayamani et al., 2017). Macrophages (5×10^5) were

seeded in 24-well plates 24 h before infection. The multiplicity of infection (MOI) of 25 (i.e., 25 bacterial cells per macrophage) was used for the assay in which BIP-pretreated MW2, untreated MW2 alone, or *agr* mutant *S. aureus* RN4220 cells were added to macrophage cultures for 2 h to interrogate phagocytosis. After the incubation period, planktonic bacteria were removed, and DMEM containing 200 µg/ml gentamicin was added for 2 h to inhibit/kill remaining extracellular bacteria. The cells were incubated under 5% CO₂ for 20 h with gentamicin (1X MIC, 1 µg/ml) to prevent the multiplication of bacterial cells released from burst macrophages. After incubation, the macrophages were lysed by adding SDS to a final concentration of 0.02% (i.e., lysing only macrophages and not ingested bacteria). Cell lysates were diluted serially and the CFUs were enumerated by plating on TSA plates (Tharmalingam et al., 2017).

Live/Dead Staining Assay

The macrophage phagocytosis assay was performed as discussed in the intracellular killing assay above, except cells were not lysed. Instead, after 20 h of incubation, the cells were washed twice with 0.1 M 3-(N-morpholino) propanesulfonic acid (MOPS), pH 7.2, containing 1 mM MgCl₂ (MOPS/MgCl₂). Then, the cells were stained with live/dead staining solution (5 µM SYTO9, 30 µM propidium iodide and 0.1% saponin in MOPS/MgCl₂) and incubated for 15 min in the dark. The cells were then rinsed with MOPS/MgCl₂ and observed using a Nikon C1si 141 confocal microscope (Nikon, Melville, NY, USA) with 488- and 561-nm diode lasers and images were captured (Zheng et al., 2017b).

Checkerboard Assay

Compounds were arrayed in serial concentrations, vertically for one molecule and horizontally for the other molecule in 96-well plate. The bacterial inoculation and measurement of growth were carried out as described earlier in the antimicrobial susceptibility assay. The synergy was measured by calculating the fractional inhibitory concentration index (FICI) using the formula $FICI = (A/MICA) + (B/MICB)$, whereby MICA and MICB are the MIC's individual molecules, and (A) and (B) are the lowest concentration of the molecule in combination with another molecule that inhibits bacterial growth. An FICI of <0.5 indicated synergism and scores between 0.51 and 1.0 suggest a partial synergy between the compounds being tested (Odds, 2003).

Galleria mellonella Methicillin-Resistant *Staphylococcus aureus* Infection Assay

Sixteen *G. mellonella* larvae (Vanderhorst Wholesale, St. Mary's, OH, USA), which were randomly selected and weigh between 300 and 350 mg, were used for each group in the experiment interrogated group (Gibreel and Upton, 2013). Overnight, MW2 cells were diluted at 1:2,000 in a cation-adjusted MHB in the presence of a sub-lethal concentration of BIP (64 µg/ml) or vancomycin (0.5 µg/ml). After incubation with agitation for 12 h, the cells were washed and suspended in PBS at an optical density of absorbance 600 (OD₆₀₀) of 0.3. A 10-µl

(2×10^6 cells/ml) inoculum was injected into the last left proleg using a Hamilton syringe and incubated at 37°C. Five test groups were included, and the same dose of bacteria was injected into the corresponding infection groups: (1) PBS alone (no bacteria control), (2) BIP-pretreated MW2 cells, (3) vancomycin-pretreated MW2 cells, (4) DMSO-pretreated MW2 cells, and (5) no injection and no bacteria (quality control). *G. mellonella* survival was assessed up to 120 h, with larvae considered dead if unresponsive to touch using sterile tips. Killing curves and differences in survival were analyzed by the Kaplan–Meier method using GraphPad Prism version 6.04 (GraphPad Software, La Jolla, CA, USA). All of the statistical analysis was carried out using the same program, and $p < 0.05$ was considered significant.

RESULTS AND DISCUSSION

Antibacterial Susceptibility

We previously reported several direct antibacterial molecules that were discovered using a whole organism *C. elegans*-based HTS (Rajamuthiah et al., 2014, 2015; Gwisai et al., 2017; Jayamani et al., 2017; Tharmalingam et al., 2017, 2018a,b; Zheng et al., 2017a). In this work, we report a molecule 4-(1,3-dimethyl-2,3-dihydro-1H-benzimidazol-2-yl)phenol (BIP) (Figure 1) that produced an average Z-score of 9.61 and rescued the nematode *C. elegans* from MW2 infection. The benzimidazole derivatives have potent antibacterial activity against Gram-positive (Göker et al., 2005; Tunçbilek et al., 2009; Karataş et al., 2012) and certain Gram-negative bacteria (Picconi

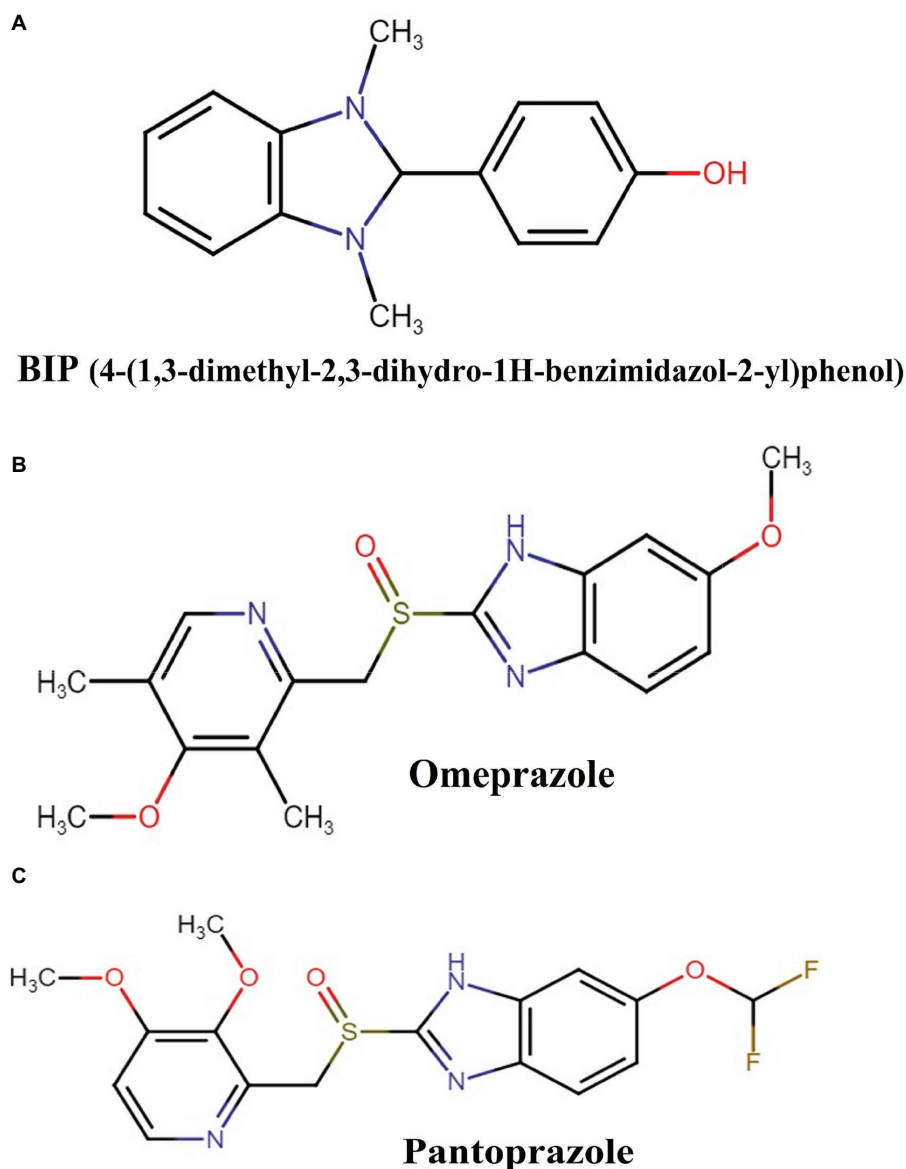


FIGURE 1 | Chemical structures of: **(A)** BIP (4-(1,3-dimethyl-2,3-dihydro-1H-benzimidazol-2-yl)phenol), **(B)** omeprazole, and **(C)** pantoprazole.

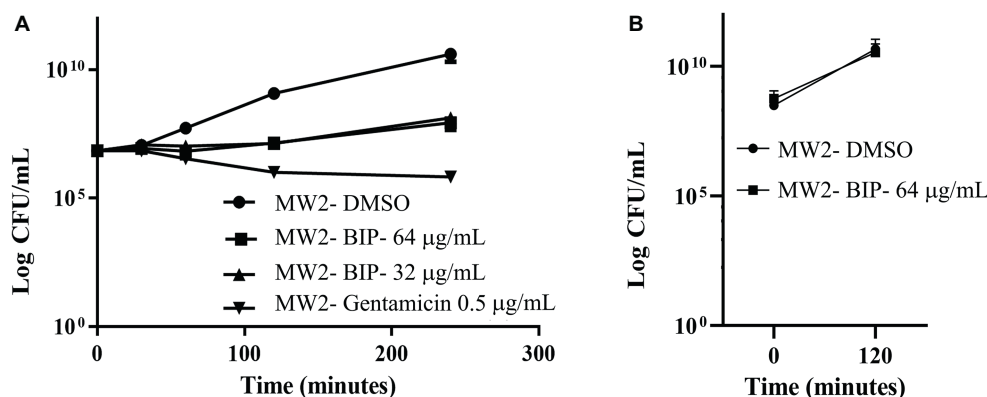


FIGURE 2 | Killing kinetics. Growth curves were generated using *S. aureus* cells. **(A)** After BIP treatment, MW2 cells continued to grow, although at a slower rate than cells exposed to DMSO. **(B)** After BIP was removed by washing, the MW2 cells exhibited normal growth comparable to DMSO pre-treated cells. Data represent the mean \pm SD ($n = 3$).

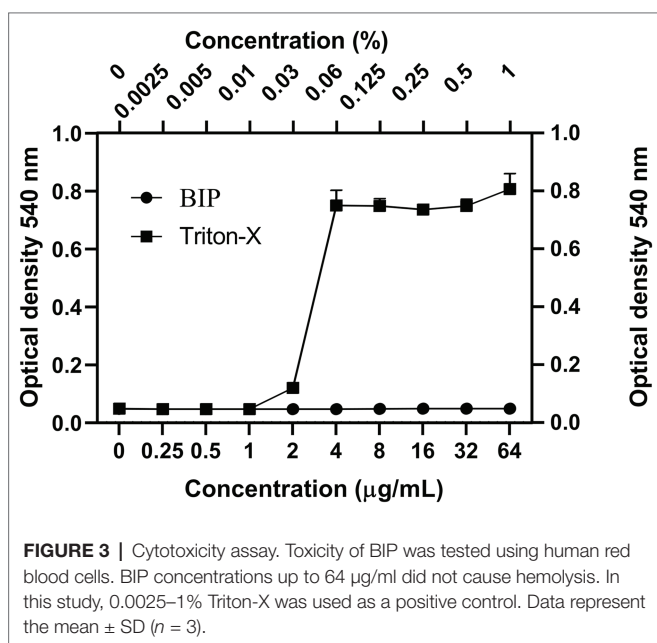


FIGURE 3 | Cytotoxicity assay. Toxicity of BIP was tested using human red blood cells. BIP concentrations up to 64 µg/ml did not cause hemolysis. In this study, 0.0025–1% Triton-X was used as a positive control. Data represent the mean \pm SD ($n = 3$).

et al., 2017; Vashist et al., 2018). Also, studies have reported that the benzimidazole derivatives exhibit an anti-biofilm and anti-virulence role (Kim et al., 2009; Sambanthamoorthy et al., 2011; Kong et al., 2018). Interestingly, although BIP was identified as a hit from the screen, the broth microdilution assay revealed that BIP did not inhibit the growth of *S. aureus* or any other organisms tested (Table 1). The seemingly contradictory results from HTS and broth-microdilution assay generated the hypothesis that the molecule may prolong host survival by either inhibiting bacterial virulence or modulating host immunity. We also tested the antibacterial activity of the benzimidazole derivatives omeprazole and pantoprazole. As previously reported (Sjöström et al., 1996; Ni et al., 2014),

neither compound inhibited MW2 growth at the highest concentration tested (64 µg/ml).

Exploring the Role of 4-(1,3-Dimethyl-2,3-Dihydro-1H-Benzimidazol-2-yl)Phenol on MW2 Growth

First, we aimed to evaluate whether BIP can decrease the bacterial cell numbers at the concentration of 32 or 64 µg/ml from an initial inoculum. The killing kinetics assay determined that the total viable bacterial count was about 5-logCFU at 0 h. After 4 h, the total viable count of BIP-pretreated cells was about 6-logCFU (Figure 2A). The DMSO-treated MW2 cells at the later time point were measured at 10-logCFU. The data suggest that BIP treatment resulted in slower bacterial growth compared to DMSO treatment but did not exert either bacteriostatic or bactericidal activity. As a positive control, we included the antibacterial agent gentamicin at 0.5 MIC (0.5 µg/ml). Gentamicin decreased the initial inoculum by 1-logCFU during the same time period (Figure 2A). In addition, a post-antibiotic effect assay determined that the bacterial cells grew normally compared to DMSO control after the cells were washed post drug treatment (Figure 2B). Taken together, we found that BIP did not decrease overall cell number from an initial inoculum and BIP-pretreated cells grew normally upon drug removal indicating that the effect of the compound is related to altered growth dynamic and not viability.

Toxicity of 4-(1,3-Dimethyl-2,3-Dihydro-1H-Benzimidazol-2-yl)Phenol on Human Red Blood Cells

We tested the hemolysis potential of BIP with human RBCs and found that the BIP treatment did not cause hemolysis up to 64 µg/ml (Figure 3). We used 0.0025–1.0% of Triton-X as a positive control. The lack of detectable RBC cytotoxicity was confirmed in this assay.

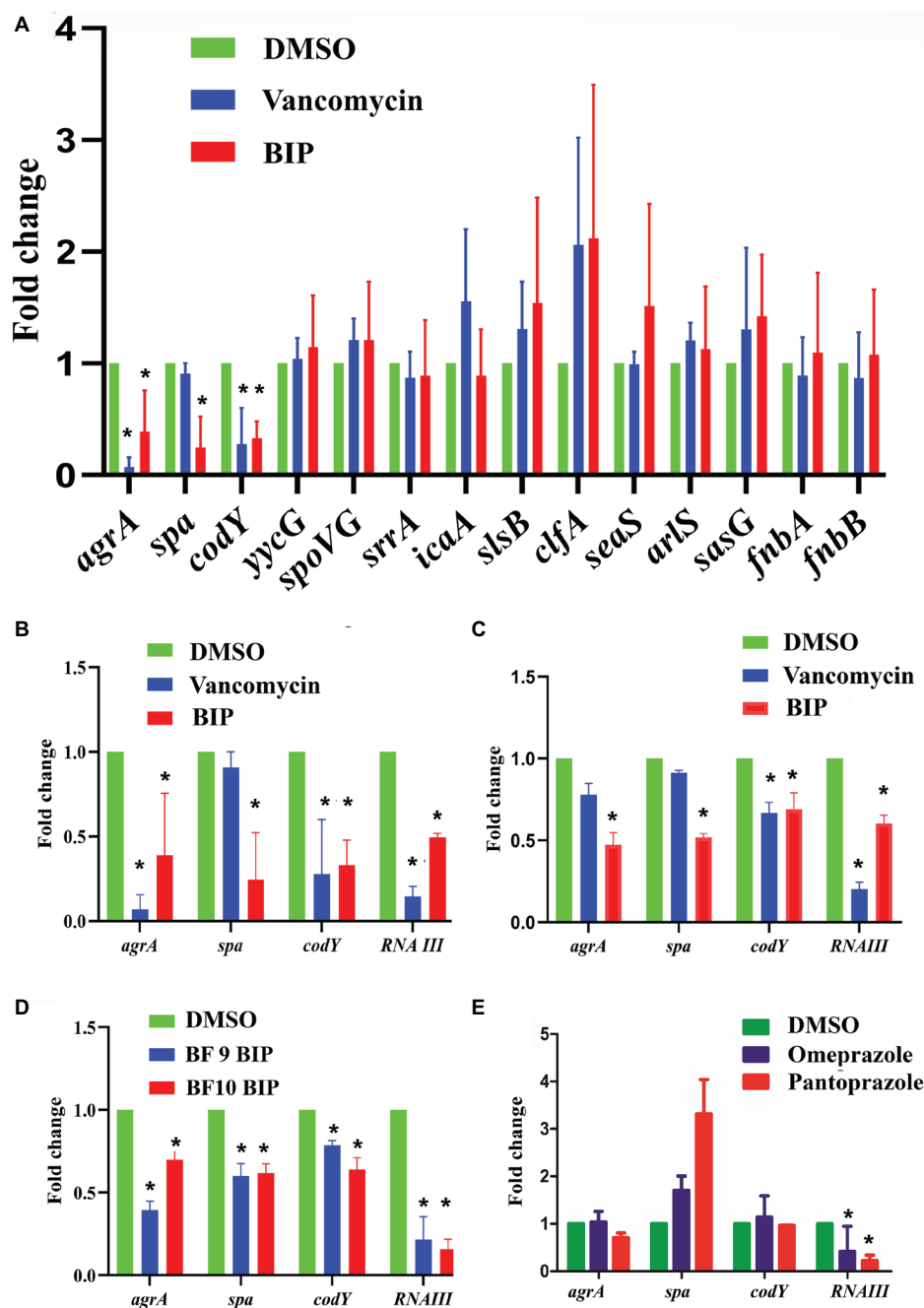


FIGURE 4 | Effect of BIP on virulence genes. *S. aureus* MW2 cells were treated with BIP (64 μ g/ml) for 4 h. RNA was isolated and used as a template for cDNA synthesis and was analyzed using real-time PCR. **(A)** Exposure to BIP was associated with down-regulation of major virulence regulator genes, including *agrA*, *spa*, and *codY*. **(B,C)** The expression of virulence genes *agrA*, *spa*, *codY*, *RNA III* was examined during the 4- and 24-h treatments of BIP, respectively. Drug treatment down-regulated *agrA*, *spa*, *codY*, and *RNA III* expression. **(D)** Two clinical strains of *S. aureus* (BF 9, BF 10) were also evaluated for changes to *agrA*, *spa*, *codY*, and *RNA III* expression. **(E)** MW2 cells were exposed with the benzimidazole derivatives omeprazole and pantoprazole (64 μ g/ml) for 4 h. Data represent the mean \pm SD ($n = 3$). * $p < 0.05$, Student's *t*-test comparing DMSO control.

Exploring the Anti-virulence Role of 4-(1,3-Dimethyl-2,3-Dihydro-1H-Benzimidazol-2-yl)Phenol

We examined a panel of known virulence genes (*agrA*, *spa*, *codY*, *yycG*, *spoVG*, *srrA*, *icaA*, *slsB*, *clfA*, *saeS*, *arlS*, *sasG*, *fnbA*,

fnbB) to evaluate if they were affected by BIP. Since RNA III is known to control several virulence factors, we also included it in the panel of examined genes. After exposing bacteria to BIP, we monitored the expression of MW2 virulence genes through a real-time PCR assay. The presence of the BIP

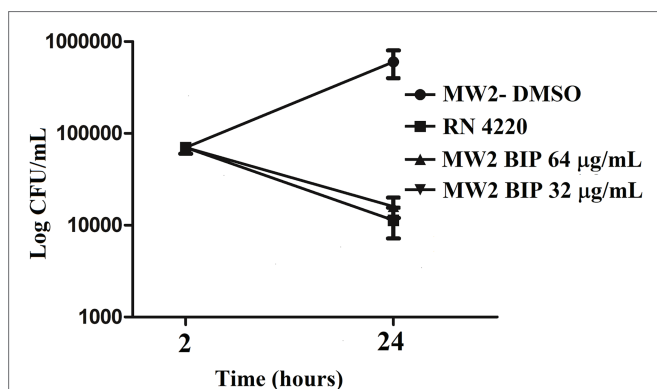


FIGURE 5 | The effect of BIP in the killing of *S. aureus* MW2 cells by mouse macrophages. Raw 264.7 cells were co-incubated with BIP-pretreated MW2 cells, and the viable bacterial cells were enumerated after lysis release. Mouse macrophages killed the BIP-pretreated cells, while DMSO-pretreated cells survived and increased to 1.5-logCFU from the initial inoculation. The *agr* mutant strain *S. aureus* RN4220 was used as a positive control.

down-regulated virulence genes such as accessory gene regulator A (*agrA*), staphylococcal protein A (*spa*), and GTP-sensing transcriptional pleiotropic repressor (*codY*) with statistical significance (Figure 4A). Virulence gene expression after the BIP treatment was examined in reference and non-reference strains of *S. aureus*, including two clinical isolates in order to evaluate the effect of conservation. Interestingly, BIP induced down-regulation of *agrA*, *spa*, *codY*, and *RNA III* genes in all the isolates tested, (Figure 4D) demonstrated that the effect is not a strain-specific. To exclude the possibility of a time-dependent effect of BIP treatment, we examined the prolonged treatment (24 h) of BIP and observed a down-regulation of *agrA*, *spa*, and *codY* (Figures 4B,C) in MW2. Benzimidazole derivatives are majorly known for their antimicrobial action (Singh et al., 2012). However, few studies show that these compounds target virulence determinants by inhibiting multiple adaptational response (MAR) transcription factor in various pathogens without targeting bacterial growth (Kim et al., 2009; Grier et al., 2010). These previous studies support our findings that the BIP down-regulates bacterial virulence without targeting bacterial growth *in vitro*.

In *S. aureus*, the *agr* system plays a central control in the regulation of virulence gene expression and is involved in the production of multiple virulence factors (Tan et al., 2018). Also, *agrA* is a response regulator of the *agr* system, and it binds to the recognition site in *RNA III* and *RNA II* (Tan et al., 2018). *RNA III* controls several virulence factors, including the *spa* gene (Huntzinger et al., 2005), supporting our finding that down-regulation of *agrA* by BIP is coupled with down-regulation of the *spa* gene. Shrestha et al. reported that the benzimidazole derivative (ABC-1) down-regulated *spa* primarily, but not *fnbA*, *fnbB*, *clfA*, and *clfB* (Shrestha et al., 2016) supports our study with a similar kind of observation. Exposure to BIP also caused reduced expression of *codY* that produces a global regulator protein known to repress *agrBDCA* and *RNA III* transcription (Roux et al., 2014). By comparison, vancomycin treatment caused down-regulation of *agrA* and

codY (Figure 4A) but not *spa*, demonstrating that the sub-MIC level of vancomycin exerted limited influences on *S. aureus* virulence genes expression (Cázares-Domínguez et al., 2015; Hodille et al., 2017). In addition, we tested the anti-virulence activity of the benzimidazole derivatives omeprazole and pantoprazole (Kromer, 1995). Omeprazole at 64 µg/ml did not down-regulate the expression of the major staphylococcal virulence genes *agrA*, *spa*, and *codY* (Figure 4E). Pantoprazole at 64 µg/ml down-regulated the gene expression of *RNA III* (Figure 4E). These results, along with published reports, indicate that some benzimidazole derivatives down-regulate bacterial virulence (Kim et al., 2009; Sambanthamoorthy et al., 2011; Kong et al., 2018), while other benzimidazole derivatives, such as omeprazole, and pantoprazole, do not appear to influence staphylococcal virulence. The two approved drugs, omeprazole and pantoprazole, are proton pump inhibitors (PPIs) and reduce the gastric pH (Axon and Moayyedi, 1996). Structural activity relationship (SAR) studies demonstrated that the omeprazole and methoxy or fluorine-substituted analogs affect urease activity (Kühler et al., 1995). Vidaillac et al. demonstrated that the addition of one methoxy group in the benzimidazole nucleus resulted in improved activity (Vidaillac et al., 2007).

Macrophage Assay

O'Keeffe et al. reported that the *agr* gene is associated with autophagosome protection of bacterial cells that leads to intracellular survival within phagocytes (O'Keeffe et al., 2015). As shown above, BIP causes down-regulation of *agr* and we investigated whether exposure to BIP affects the susceptibility of MRSA cells during phagocytosis by mouse macrophage cells. In this macrophage assay, MW2 cells were treated with BIP for 4 h, before being introduced into wells with RAW 264.7 cells. Untreated cells and the *agr* mutant strain *S. aureus* RN 4220 were included as controls. The *agrA* mutant strain RN4220 was used as a control in order to contrast the down-regulation of *agrA* in BIP-treated MW2 cells. After 20 h of incubation, live bacterial cells inside the macrophages were enumerated by total viable count and bacterial live/dead stain.

We found that the DMSO-pretreated MW2 cells survived and grew inside the macrophages. After 20 h of incubation, the 1.5-logCFU of DMSO-pretreated cells increased from the initially phagocytosed MW2 cells (Figure 5). However, BIP-pretreated cells and *agr* mutant *S. aureus* RN4220 were killed by macrophages, resulting in a 1-logCFU decrease from the initially phagocytosed MW2 cells inside the macrophages (Figure 5). Kong et al. reported that the new benzimidazole derivative (UM-C162) exhibits a strong anti-virulence role by down-regulating the major biofilm forming genes, including the genes responsible for intracellular multiplications (*clpB*, *clpC*, *ctsR*) (Kong et al., 2018). Hence, targeting genes responsible for intracellular bacterial survival directly or indirectly results in hindered intracellular multiplication, supporting our observation that the role of BIP on *agrA* down-regulation might contribute in making bacteria more prone to macrophage-mediated killing.

S. aureus cells can survive inside macrophages (Fraunholz and Sinha, 2012). In order to confirm the reduction of

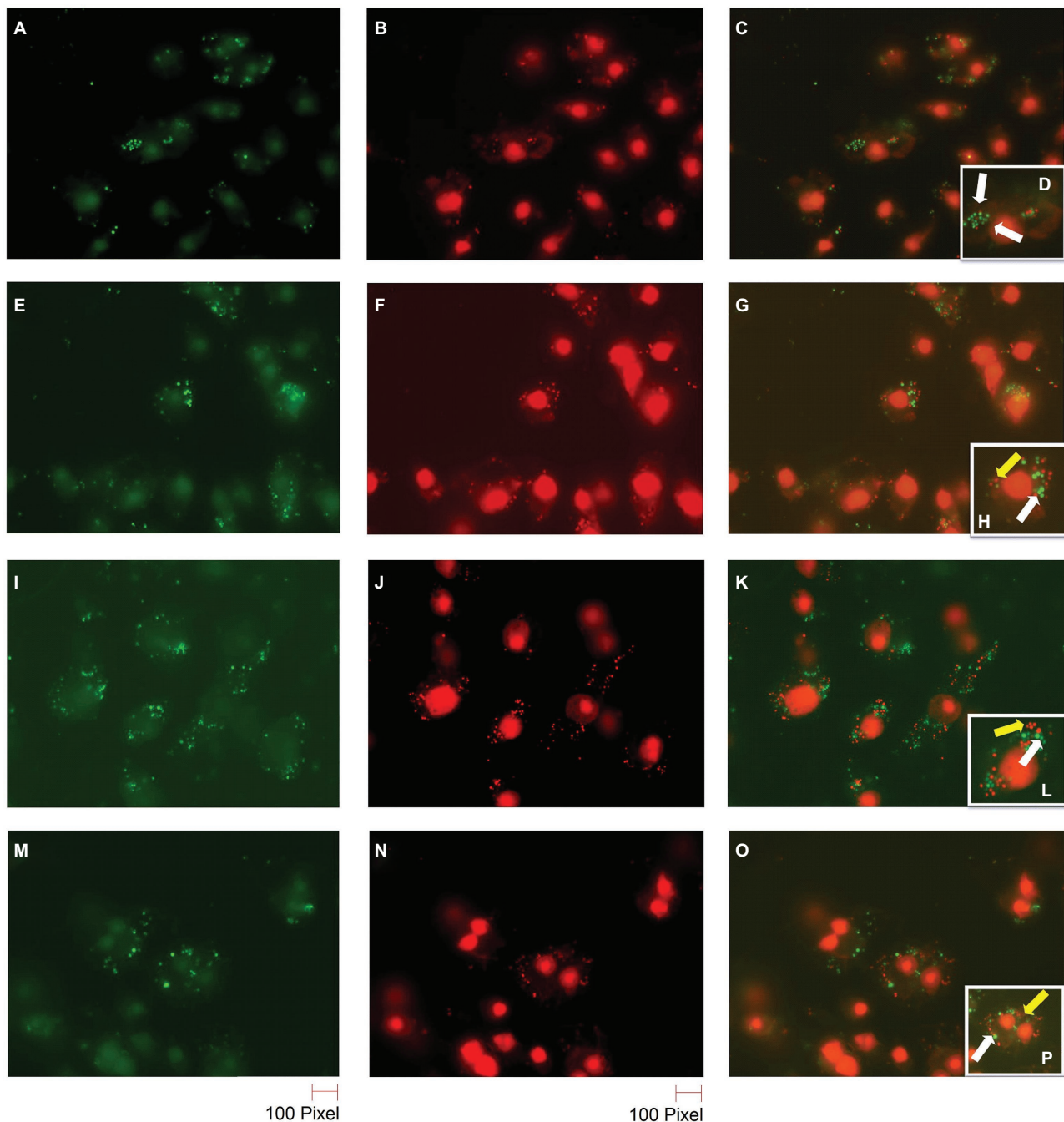
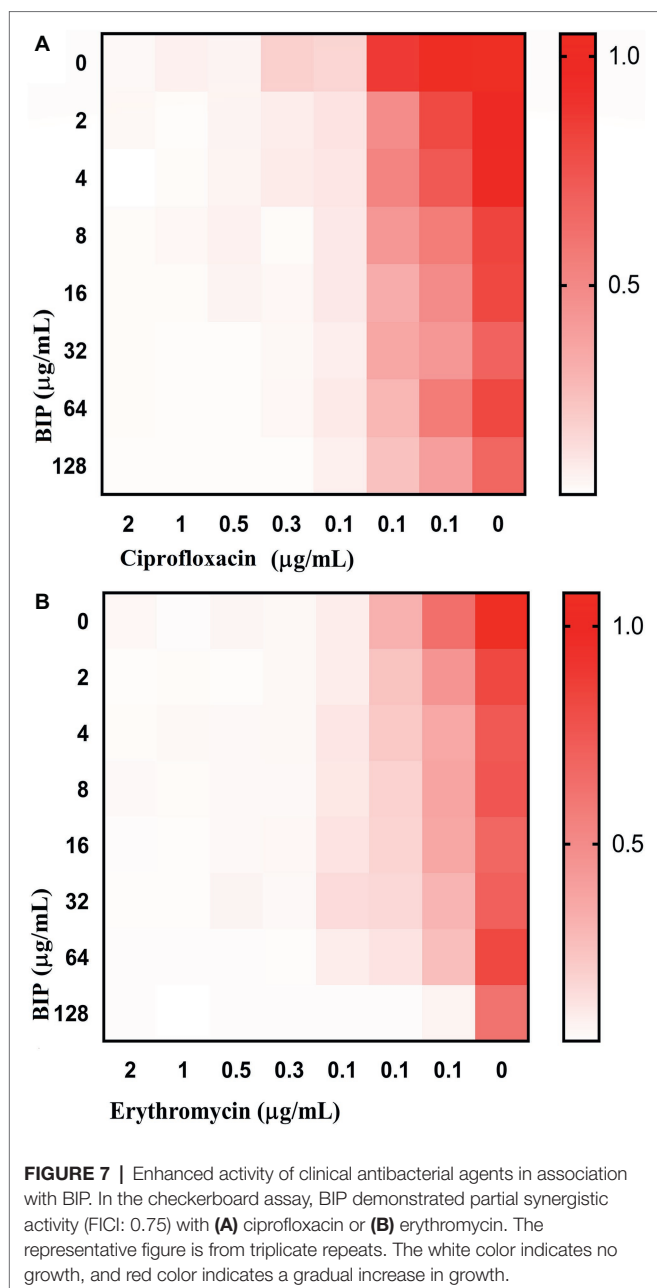


FIGURE 6 | Live/dead staining of BIP-pretreated *S. aureus* MW2 cells within macrophages. Raw 264.7 cells were allowed to phagocytose MW2 cells that were pretreated with either DMSO or BIP. After 20 h, the cells were washed and stained with a bacterial live/dead stain. The fluorescence figures were imaged using two different channels. Live cells are depicted with green fluorescent images (**A,E,I,M**), and dead cells are represented in red fluorescent images (**B,F,J,N**) (magnification 65 \times). Images taken in two different channels were merged (**C,G,K,O**) and enlarged images are presented in the panel (**D,H,L,P**). Live bacterial cells were marked with a white arrow, and dead bacterial cells were marked with a yellow arrow. DMSO-treated bacterial cells (**A–D**) were stained green, while BIP-pretreated bacterial cells (**E–H** – 64 $\mu\text{g/ml}$ and **I–L** – 32 $\mu\text{g/ml}$) were stained red suggesting that pretreatment with BIP made cells susceptible to macrophage killing. The *agr* mutant strain *S. aureus* RN4220 (**M–P**) was used as a positive control.

BIP-pretreated bacterial cells and the greater susceptibility of the *agr* mutant strain, we performed bacterial live/dead stain (green/red color) to differentiate viable versus dead cells inside the macrophages (**Figures 6A–D**). We found that the DMSO-pretreated

MW2 cells fluoresced green (**Figures 6A–D**), indicating bacterial survival, and BIP-pretreated bacterial cells (64 $\mu\text{g/ml}$, **Figures 6E–H**; 32 $\mu\text{g/ml}$, **Figures 6I–L**) stained red, indicating death. These studies confirmed our findings observed through CFU-based



data. We also used the *S. aureus* RN 4220 (an *agrA* mutant strain) to confirm the hypothesis that down-regulation of *agrA* makes bacteria more susceptible to macrophage-mediated killing (O’Keeffe et al., 2015). Indeed, the strain RN 4220 was more susceptible to macrophage-mediated killing (Figures 6M–P), than a wild strain of MW2.

4-(1,3-Dimethyl-2,3-Dihydro-1H-Benzimidazol-2-yl)Phenol Potentiates Antibiotic Activity

Anti-virulence molecules work synergistically with conventional antibiotics to impair bacterial cells (van Tilburg Bernardes et al., 2017). For example, Abraham et al. reported that the

tick anti-virulence protein IAFGP demonstrated a synergistic role with conventional antibiotics (Abraham et al., 2017). Hence, we evaluated if BIP was synergistic with other conventional antibiotics, testing a representative from the most common antibiotics, including β -lactam, fluoroquinolones, peptide antibiotics, tetracyclines, macrolides, and aminoglycosides. In a checkerboard assay, BIP enhanced the antibiotic activity of ciprofloxacin and erythromycin (Figure 7) with a FICI of 0.75, a value that indicates partial synergy (Martin et al., 1996). Fractional Inhibitory Concentration Index (FICI) = (A/MICA) + (B/MICB), where MICA and MICB are the MIC’s individual molecules, and (A) and (B) are the lowest concentration of the molecule in combination with another molecule that inhibits bacterial growth. An FICI of <0.5 indicates synergism, while scores between 0.51 and 1.0 suggest a partial synergy between the compounds being tested (Odds, 2003).

Insect Survival

G. mellonella is used widely to investigate various pathogens (Gibreel and Upton, 2013; Giannouli et al., 2014; Yang et al., 2017), and test new investigational compounds (Desbois and Coote, 2012). Given that BIP-pretreated cells were more susceptible to macrophage killing, we hypothesized that they would be less efficient in killing an infected host. We injected DMSO-treated MW2 cells versus BIP-pretreated MW2 cells into *G. mellonella* larvae. After 24 h, all larvae injected with DMSO-treated MW2 cells were dead (100%). However, at the same time point, 80% of BIP-pretreated (64 μ g/ml) MW2 injected larvae survived ($p = 0.131$; Figure 8). Starkey et al. reported that the benzamide-benzimidazole phenoxy substituted benzamide ring that contains a benzimidazole moiety rescue mice from *P. aeruginosa* infection by reducing its acute virulence without reducing bacterial CFU (Starkey et al., 2014). Garrity et al. demonstrated that non-antibacterial LcrF inhibitors protected mice significantly from lethal *Yersinia pseudotuberculosis* lung infection (Garrity-Ryan et al., 2010). These reports support our insect survival data and, taken together, these observations suggest that the anti-virulence molecules harboring the benzimidazole moiety can prevent the invertebrate/vertebrate animals from lethal bacterial infection. Vancomycin is known to prolong the survival of *S. aureus*-infected *G. mellonella* (Tharmalingam et al., 2017). However, in the presented assay, a sub-MIC concentration was provided to *G. mellonella* as a positive control to induce a moderate inhibition of bacteria within the host. The provision of vancomycin at sub-MIC levels was shown to reduce expression of *agrA*, *spa*, and *codY* as was also seen with BIP treatment (Figure 4). However, a distinction between vancomycin and BIP treatment was noted with *G. mellonella* survival in which BIP prolonged survival, whereas vancomycin treatment did not.

The finding suggests that exposure of MW2 cells to BIP results in down-regulation of major virulence factors, such as *agrA*, *spa*, *codY*. Moreover, the MW2 cells become more vulnerable to phagocytosis-mediated bacterial killing and, in turn, less virulent in a model host. Based on our findings, we conclude that BIP is an anti-virulence candidate compound that deserves further study. The current data lead us to believe that BIP acts in a capacity to inhibit *S. aureus* virulence

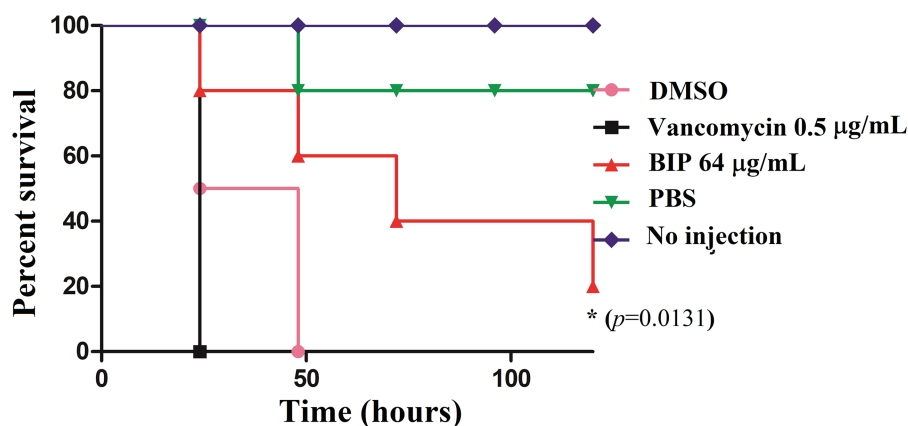


FIGURE 8 | *In vivo* killing efficacy of BIP-pretreated *S. aureus* MW2 cells in the *G. mellonella* model. MW2 cells were pretreated with BIP or DMSO for 12 h prior to injection to *G. mellonella* larva ($n = 16$). After 24 h, the group of larvae that received the BIP-pretreated cells survived longer than the group that received the DMSO-pretreated bacterial cells ($p = 0.0131$). As a control, the group of larvae that received vancomycin-pretreated MW2 cells also killed the larvae within 24 h from incubation. The figure is a representative graph from three independent replicates.

factors. The fact that BIP treatment contributes to staphylococcal killing by macrophages and results in prolonged survival of the infected alternative host suggests that the compound might act through host immune modulation (which we do not rule out as a contributing influence) and/or inhibition of virulence attributes needed during the infection process. Apart from an anti-virulence role, BIP might modulate host immunity, but this is beyond the scope of this report. Nevertheless, the effects of benzimidazole derivatives to host immunity are noted in the literature. Wildenberg et al. reported that six benzimidazole derivatives induced regulatory macrophages (Wildenberg et al., 2017). Rickard et al. reported that the benzimidazole diamide GSK 669 inhibits NOD2, an intracellular pattern recognition receptor involved in the induction of pro-inflammatory cytokines (Rickard et al., 2013). Moreover, the benzimidazole derivatives are reported to have an analgesic action (Srivastava et al., 2012). In another study, the benzimidazole derivatives are a potential candidate for the management of opioid-induced paradoxical pain (Idris et al., 2019). As demonstrated by Alpan et al., BIP compounds can also bind with mammalian DNA (Alpan et al., 2007). Further SAR studies demonstrated that the methylated BIP (5-methyl-4-(1H-benzimidazole-2-yl)phenol) derivative exerts increased topo-isomerase I inhibition (Alpan et al., 2007). Interestingly, Gul et al. reported that the benzimidazole phenol derivative (4-(1H-benzimidazol-2-yl)phenol) inhibits human carbonic

anhydrase (hCA) activity and addition of more phenol side group decreases the level of inhibition (Gul et al., 2016). Taken together, these reports suggest that the benzimidazole compounds potentially have multiple targets (Singh et al., 2012). In drug discovery, we often find that compounds do not have a singular effect or target; indeed, effects can be multifaceted. This withstanding, our current research does provide strong evidence that BIP inhibits known virulence genes. Future work is needed to determine the specific mechanisms that convey the anti-virulence effect.

AUTHOR CONTRIBUTIONS

NT and EM conceived the idea and designed the study. NT designed the project, performed the experiments, and analyzed the data. RK performed the RT-qPCR and insect survival assays. NT drafted the manuscript with revisions and final approval by BF and EM. EM supervised the project.

FUNDING

This study was funded by NIH grants P01 AI083214 to EM and grant P20 GM121344 from the COBRE Center for Antimicrobial Resistance and Therapeutic Discovery, awarded to BF.

REFERENCES

- Abraham, N. M., Liu, L., Jutras, B. L., Murfin, K., Acar, A., Yarovsky, T. O., et al. (2017). A tick antivirulence protein potentiates antibiotics against *Staphylococcus aureus*. *Antimicrob. Agents Chemother.* 61, e00113–e00117. doi: 10.1128/AAC.00113-17
- Alpan, A. S., Gunes, H. S., and Topcu, Z. (2007). 1H-benzimidazole derivatives as mammalian DNA topoisomerase I inhibitors. *Acta Biochim. Pol.-English Edition* 54, 561–565. Available at: http://www.actabp.pl/pdf/3_2007/561.pdf
- Atshan, S. S., Shamsudin, M. N., Karunanidhi, A., Van Belkum, A., Lung, L. T. T., Sekawi, Z., et al. (2013). Quantitative PCR analysis of genes expressed during biofilm development of methicillin resistant *Staphylococcus aureus* (MRSA). *Infect. Genet. Evol.* 18, 106–112. doi: 10.1016/j.meegid.2013.05.002
- Axon, A., and Moayyedi, P. (1996). Eradication of *Helicobacter pylori*: omeprazole in combination with antibiotics. *Scand. J. Gastroenterol.* 31, 82–89.
- Beanan, M. J., and Strome, S. (1992). Characterization of a germ-line proliferation mutation in *C. elegans*. *Development* 116, 755–766.
- Cázares-Domínguez, V., Ochoa, S. A., Cruz-Córdova, A., Rodea, G. E., Escalona, G., Olivares, A. L., et al. (2015). Vancomycin modifies the expression of the agr system in multidrug-resistant *Staphylococcus aureus* clinical isolates. *Front. Microbiol.* 6:369. doi: 10.3389/fmicb.2015.00369

- de Kraker, M. E., Stewardson, A. J., and Harbarth, S. (2016). Will 10 million people die a year due to antimicrobial resistance by 2050? *PLoS Med.* 13:e1002184. doi: 10.1371/journal.pmed.1002184
- Defoirdt, T. (2017). Quorum-sensing systems as targets for antivirulence therapy. *Trends Microbiol.* 26, 313–328. doi: 10.1016/j.tim.2017.10.005
- Desbois, A. P., and Coote, P. J. (2012). "Utility of greater wax moth larva (*Galleria mellonella*) for evaluating the toxicity and efficacy of new antimicrobial agents". *Adv. Appl. Microbiol.* 78, 25–53. doi: 10.1016/B978-0-12-394805-2.00002-6
- Dickey, S. W., Cheung, G. Y., and Otto, M. (2017). Different drugs for bad bugs: antivirulence strategies in the age of antibiotic resistance. *Nat. Rev. Drug Discov.* 16, 457–471. doi: 10.1038/nrd.2017.23
- Fraunholz, M., and Sinha, B. J. F. I. C. (2012). Intracellular *Staphylococcus aureus*: live-in and let die. *Front. Cell. Infect. Microbiol.* 2:43. doi: 10.3389/fcimb.2012.00043
- Garrity-Ryan, L. K., Kim, O. K., Balada-Llasat, J.-M., Bartlett, V. J., Verma, A. K., Fisher, M. L., et al. (2010). Small molecule inhibitors of LcrF, a *Yersinia pseudotuberculosis* transcription factor, attenuate virulence and limit infection in a murine pneumonia model. *Infect. Immun.* 78, 4683–4690. doi: 10.1128/IAI.01305-09
- Giannouli, M., Palatucci, A. T., Rubino, V., Ruggiero, G., Romano, M., Triassi, M., et al. (2014). Use of larvae of the wax moth *Galleria mellonella* as an in vivo model to study the virulence of *Helicobacter pylori*. *BMC Microbiol.* 14:228. doi: 10.1186/s12866-014-0228-0
- Gibrel, T. M., and Upton, M. (2013). Synthetic epidermicin NI01 can protect *Galleria mellonella* larvae from infection with *Staphylococcus aureus*. *J. Antimicrob. Chemother.* 68, 2269–2273. doi: 10.1093/jac/dkt195
- Göker, H., Özden, S., Yildiz, S., and Boykin, D. W. (2005). Synthesis and potent antibacterial activity against MRSA of some novel 1, 2-disubstituted-1H-benzimidazole-N-alkylated-5-carboxamides. *Eur. J. Med. Chem.* 40, 1062–1069. doi: 10.1016/j.ejmech.2005.05.002
- Grier, M. C., Garrity-Ryan, L. K., Bartlett, V. J., Klausner, K. A., Donovan, P. J., Dudley, C., et al. (2010). N-Hydroxybenzimidazole inhibitors of ExsA MAR transcription factor in *Pseudomonas aeruginosa*: in vitro anti-virulence activity and metabolic stability. *Bioorg. Med. Chem. Lett.* 20, 3380–3383. doi: 10.1016/j.bmcl.2010.04.014
- Gul, H. I., Yazici, Z., Tanc, M., and Supuran, C. T. (2016). Inhibitory effects of benzimidazole containing new phenolic Mannich bases on human carbonic anhydrase isoforms hCA I and II. *J. Enzyme Inhib. Med. Chem.* 31, 1540–1544. doi: 10.3109/14756366.2016.1156675
- Gwisai, T., Hollingsworth, N., Cowles, S., Tharmalingam, N., Mylonakis, E., Fuchs, B., et al. (2017). Repurposing niclosamide as a versatile antimicrobial surface coating against device-associated, hospital-acquired bacterial infections. *Biomed. Mater.* 12, 1–13. doi: 10.1088/1748-605X/aa7105
- Hauser, A. R., Mecasas, J., and Moir, D. T. (2016). Beyond antibiotics: new therapeutic approaches for bacterial infections. *Clin. Infect. Dis.* 63, 89–95. doi: 10.1093/cid/ciw200
- Heras, B., Scanlon, M. J., and Martin, J. L. (2015). Targeting virulence not viability in the search for future antibacterials. *Br. J. Clin. Pharmacol.* 79, 208–215. doi: 10.1111/bcp.12356
- Hodille, E., Rose, W., Diep, B. A., Goutelle, S., Lina, G., and Dumitrescu, O. J. C. M. R. (2017). The role of antibiotics in modulating virulence in *Staphylococcus aureus*. *Clin. Microbiol. Rev.* 30, 887–917. doi: 10.1128/CMR.00120-16
- Huntzinger, E., Boisset, S., Saveanu, C., Benito, Y., Geissmann, T., Namane, A., et al. (2005). *Staphylococcus aureus* RNAIII and the endoribonuclease III coordinately regulate spa gene expression. *EMBO J.* 24, 824–835. doi: 10.1038/sj.emboj.7600572
- Idris, Z., Abbas, M., Nadeem, H., and Khan, A.-U. (2019). The benzimidazole derivatives, B1 (N-[(1H-benzimidazol-2-yl) methyl]-4-methoxyaniline) and B8 (N-[4-[(1H-benzimidazol-2-yl) methoxy] phenyl] acetamide) attenuate morphine-induced paradoxical pain in mice. *Front. Neurosci.* 13, 1–9. doi: 10.3389/fnins.2019.00101
- Imperi, F., Massai, F., Pillai, C. R., Longo, F., Zennaro, E., Rampioni, G., et al. (2013). New life for an old drug: the anthelmintic drug niclosamide inhibits *Pseudomonas aeruginosa* quorum sensing. *Antimicrob. Agents Chemother.* 57, 996–1005. doi: 10.1128/AAC.01952-12
- Isnansetyo, A., and Kamei, Y. (2003). MC21-A, a bactericidal antibiotic produced by a new marine bacterium, *Pseudoalteromonas phenolica* sp. nov. O-BC30(T), against methicillin-resistant *Staphylococcus aureus*. *Antimicrob. Agents Chemother.* 47, 480–488. doi: 10.1128/AAC.47.2.480-488.2003
- Jayamani, E., Tharmalingam, N., Rajamuthiah, R., Coleman, J. J., Kim, W., Okoli, I., et al. (2017). Characterization of a *Francisella tularensis*-*Caenorhabditis elegans* pathosystem for the evaluation of therapeutic compounds. *Antimicrob. Agents Chemother.* 61, e00310–e00317. doi: 10.1128/AAC.00310-17
- Karatas, H., Alp, M., Yildiz, S., and Göker, H. (2012). Synthesis and potent in vitro activity of novel 1H-benzimidazoles as anti-MRSA agents. *Chem. Biol. Drug Des.* 80, 237–244. doi: 10.1111/j.1747-0285.2012.01393.x
- Kim, O. K., Garrity-Ryan, L. K., Bartlett, V. J., Grier, M. C., Verma, A. K., Medjanis, G., et al. (2009). N-hydroxybenzimidazole inhibitors of the transcription factor LcrF in *Yersinia*: novel antivirulence agents. *J. Med. Chem.* 52, 5626–5634. doi: 10.1021/jm9006577
- Kim, W., Zhu, W., Hendricks, G. L., Van Tyne, D., Steele, A. D., Keohane, C. E., et al. (2018). A new class of synthetic retinoid antibiotics effective against bacterial persisters. *Nature* 556:103. doi: 10.1038/nature26157
- Kong, C., Chee, C.-F., Richter, K., Thomas, N., Rahman, N. A., and Nathan, S. (2018). Suppression of *Staphylococcus aureus* biofilm formation and virulence by a benzimidazole derivative, UM-C162. *Sci. Rep.* 8:2758. doi: 10.1038/s41598-018-21141-2
- Kromer, W. (1995). Similarities and differences in the properties of substituted benzimidazoles: a comparison between pantoprazole and related compounds. *Digestion* 56, 443–454.
- Kühler, T. C., Fryklund, J., Bergman, N.-K., Weilitz, J., Lee, A., and Larsson, H. (1995). Structure-activity relationship of omeprazole and analogs as *Helicobacter pylori* urease inhibitors. *J. Med. Chem.* 38, 4906–4916.
- Liu, Q., Zheng, Z., Kim, W., Burgwyn Fuchs, B., and Mylonakis, E. (2018). Influence of subinhibitory concentrations of NH125 on biofilm formation & virulence factors of *Staphylococcus aureus*. *Future Med. Chem.* 10, 1319–1331. doi: 10.4155/fmc-2017-0286
- Longdon, B., Hadfield, J. D., Day, J. P., Smith, S. C., McGonigle, J. E., Cogni, R., et al. (2015). The causes and consequences of changes in virulence following pathogen host shifts. *PLoS Pathog.* 11:e1004728. doi: 10.1371/journal.ppat.1004728
- Martin, S. J., Pendland, S. L., Chen, C., Schreckenberger, P., and Danziger, L. H. (1996). In vitro synergy testing of macrolide-quinolone combinations against 41 clinical isolates of *Legionella*. *Antimicrob. Agents Chemother.* 40, 1419–1421.
- Maura, D., Ballok, A. E., and Rahme, L. G. (2016). Considerations and caveats in anti-virulence drug development. *Curr. Opin. Microbiol.* 33, 41–46. doi: 10.1016/j.mib.2016.06.001
- Mitchell, G., Lafrance, M., Boulanger, S., Séguin, D. L., Guay, I., Gattuso, M., et al. (2011). Tomatidine acts in synergy with aminoglycoside antibiotics against multidrug-resistant *Staphylococcus aureus* and prevents virulence gene expression. *J. Antimicrob. Chemother.* 67, 559–568. doi: 10.1093/jac/dkr510
- Ni, W., Cai, X., Liang, B., Cai, Y., Cui, J., and Wang, R. (2014). Effect of proton pump inhibitors on in vitro activity of tigecycline against several common clinical pathogens. *PLoS One* 9:e86715. doi: 10.1371/journal.pone.0086715
- Odds, F. C. (2003). Synergy, antagonism, and what the checkerboard puts between them. *J. Antimicrob. Chemother.* doi: 10.1093/jac/dkg301
- O'Keeffe, K. M., Wilk, M. M., Leech, J. M., Murphy, A. G., Laabei, M., Monk, I. R., et al. (2015). Manipulation of autophagy in phagocytes facilitates *Staphylococcus aureus* bloodstream infection. *Infect. Immun.* 83, 3445–3457. doi: 10.1128/IAI.00358-15
- Picconi, P., Hind, C., Jamshidi, S., Nahar, K., Clifford, M., Wand, M. E., et al. (2017). Triaryl benzimidazoles as a new class of antibacterial agents against resistant pathogenic microorganisms. *J. Med. Chem.* 60, 6045–6059. doi: 10.1021/acs.jmedchem.7b00108
- Rajamuthiah, R., Fuchs, B. B., Conery, A. L., Kim, W., Jayamani, E., Kwon, B., et al. (2015). Repurposing salicylanilide anthelmintic drugs to combat drug resistant *Staphylococcus aureus*. *PLoS One* 10:e0124595. doi: 10.1371/journal.pone.0124595
- Rajamuthiah, R., Fuchs, B. B., Jayamani, E., Kim, Y., Larkins-Ford, J., Conery, A., et al. (2014). Whole animal automated platform for drug discovery against multi-drug resistant *Staphylococcus aureus*. *PLoS One* 9:e89189. doi: 10.1371/journal.pone.0089189
- Rampioni, G., Visca, P., Leoni, L., and Imperi, F. (2017). Drug repurposing for antivirulence therapy against opportunistic bacterial pathogens. *Emerging Top. Life Sci.* 1, 13–22. doi: 10.1042/ETLS20160018

- Rickard, D. J., Sehon, C. A., Kasparcova, V., Kallal, L. A., Zeng, X., Montoute, M. N., et al. (2013). Identification of benzimidazole diamides as selective inhibitors of the nucleotide-binding oligomerization domain 2 (NOD2) signaling pathway. *PLoS One* 8:e69619. doi: 10.1371/journal.pone.0069619
- Roux, A., Todd, D. A., Velázquez, J. V., Cech, N. B., and Sonenshein, A. L. (2014). CodY-mediated regulation of the *Staphylococcus aureus* Agr system integrates nutritional and population density signals. *J. Bacteriol.* 196, 1184–1196. doi: 10.1128/JB.00128-13
- Sambanthamoorthy, K., Gokhale, A. A., Lao, W., Parashar, V., Neiditch, M. B., Semmelhack, M. F., et al. (2011). Identification of a novel benzimidazole that inhibits bacterial biofilm formation in a broad-spectrum manner. *Antimicrob. Agents Chemother.* 55, 4369–4378. doi: 10.1128/AAC.00583-11
- Schmitt, D. M., O'dee, D. M., Cowan, B. N., Birch, J. W., Mazzella, L. K., Nau, G. J., et al. (2013). The use of resazurin as a novel antimicrobial agent against *Francisella tularensis*. *Front. Cell. Infect. Microbiol.* 3:93. doi: 10.3389/fcimb.2013.00093
- Shrestha, L., Kayama, S., Sasaki, M., Kato, F., Hisatsune, J., Tsuruda, K., et al. (2016). Inhibitory effects of antibiofilm compound 1 against *Staphylococcus aureus* biofilms. *Microbiol. Immunol.* 60, 148–159. doi: 10.1111/1348-0421.12359
- Shrivastava, N., Naim, M. J., Alam, M. J., Nawaz, F., Ahmed, S., and Alam, O. (2017). Benzimidazole scaffold as anticancer agent: synthetic approaches and structure–activity relationship. *Arch. Pharm.* 350, 1–80. doi: 10.1002/ardp.201700040
- Silva, L. N., Zimmer, K. R., Macedo, A. J., and Trentin, D. S. (2016). Plant natural products targeting bacterial virulence factors. *Chem. Rev.* 116, 9162–9236. doi: 10.1021/acs.chemrev.6b00184
- Singh, N., Pandurangan, A., Rana, K., Anand, P., Ahamad, A., and Tiwari, A. K. (2012). Benzimidazole: a short review of their antimicrobial activities. *Int. Curr. Pharm. J.* 1, 119–127. doi: 10.3329/icpj.v1i5.10284
- Sjöström, J., Fryklund, J., Kühler, T., and Larsson, H. (1996). In vitro antibacterial activity of omeprazole and its selectivity for *Helicobacter* spp. are dependent on incubation conditions. *Antimicrob. Agents Chemother.* 40, 621–626.
- Srivastava, S., Pandeya, S., Yadav, M. K., and Singh, B. (2012). Synthesis and analgesic activity of novel derivatives of 1,2-substituted benzimidazoles. *J. Chem.* 2013. doi: 10.1155/2013/694295
- Starkey, M., Lepine, F., Maura, D., Bandyopadhyaya, A., Lesic, B., He, J., et al. (2014). Identification of anti-virulence compounds that disrupt quorum-sensing regulated acute and persistent pathogenicity. *PLoS Pathog.* 10:e1004321. doi: 10.1371/journal.ppat.1004321
- Tan, L., Li, S. R., Jiang, B., Hu, X. M., and Li, S. (2018). Therapeutic targeting of the *Staphylococcus aureus* accessory gene regulator (agr) system. *Front. Microbiol.* 9:55. doi: 10.3389/fmicb.2018.00055
- Tanaka-Hino, M., Sagasti, A., Hisamoto, N., Kawasaki, M., Nakano, S., Ninomiya-Tsuji, J., et al. (2002). SEK-1 MAPKK mediates Ca²⁺ signaling to determine neuronal asymmetric development in *Caenorhabditis elegans*. *EMBO Rep.* 3, 56–62. doi: 10.1093/embo-reports/kvf001
- Tharmalingam, N., Jayamani, E., Rajamuthiah, R., Castillo, D., Fuchs, B. B., Kelso, M. J., et al. (2017). Activity of a novel protonophore against methicillin-resistant *Staphylococcus aureus*. *Future Med. Chem.* 9, 1401–1411. doi: 10.4155/fmc-2017-0047
- Tharmalingam, N., Port, J., Castillo, D., and Mylonakis, E. (2018a). Repurposing the anthelmintic drug niclosamide to combat *Helicobacter pylori*. *Sci. Rep.* 8:3701. doi: 10.1038/s41598-018-22037-x
- Tharmalingam, N., Rajmuthiah, R., Kim, W., Fuchs, B. B., Jayamani, E., Kelso, M. J., et al. (2018b). Antibacterial properties of four novel hit compounds from a methicillin-resistant *Staphylococcus aureus*–*Caenorhabditis elegans* high-throughput screen. *Microb. Drug Resist.* 24, 666–674. doi: 10.1089/mdr.2017.0250
- Totsika, M. (2017). Disarming pathogens: benefits and challenges of antimicrobials that target bacterial virulence instead of growth and viability. *Future Med. Chem.* 9, 267–269. doi: 10.4155/fmc-2016-0227
- Tunçbilek, M., Kiper, T., and Altanlar, N. (2009). Synthesis and in vitro antimicrobial activity of some novel substituted benzimidazole derivatives having potent activity against MRSA. *Eur. J. Med. Chem.* 44, 1024–1033. doi: 10.1016/j.ejmech.2008.06.026
- van Tilburg Bernardes, E., Charron-Mazenod, L., Reading, D., Reckseidler-Zenteno, S. L., and Lewenza, S. (2017). Exopolysaccharide repressing small molecules with antibiofilm and antivirulence activity against *Pseudomonas aeruginosa*. *Antimicrob. Agents Chemother.* 61:e01997-16. doi: 10.1128/AAC.01997-16
- Vashist, N., Sami, S. S., Narasimhan, B., Kumar, S., Lim, S. M., Shah, S. A. A., et al. (2018). Synthesis and biological profile of substituted benzimidazoles. *Chem. Cent. J.* 12:125. doi: 10.1186/s13065-018-0498-y
- Vidaillac, C., Guillon, J., Arpin, C., Forfar-Bares, I., Ba, B. B., Grellet, J., et al. (2007). Synthesis of omeprazole analogues and evaluation of these as potential inhibitors of the multidrug efflux pump NorA of *Staphylococcus aureus*. *Antimicrob. Agents Chemother.* 51, 831–838. doi: 10.1128/AAC.01306-05
- Wikler, M. A. (2006). *Methods for dilution antimicrobial susceptibility tests for bacteria that grow aerobically; approved standard—eleventh edition*. CLSI document M07-A9. 1–18. Clinical and Laboratory Standards Institute; 2012.
- Wildenberg, M. E., Levin, A. D., Ceroni, A., Guo, Z., Koelink, P. J., Hakvoort, T. B., et al. (2017). Benzimidazoles promote anti-TNF mediated induction of regulatory macrophages and enhance therapeutic efficacy in a murine model. *J. Crohn's Colitis* 11, 1480–1490. doi: 10.1093/ecco-jcc/jjx104
- Wilson, J., Schurr, M., Leblanc, C., Ramamurthy, R., Buchanan, K., and Nickerson, C. A. (2002). Mechanisms of bacterial pathogenicity. *Postgrad. Med. J.* 78, 216–224. doi: 10.1136/pmj.78.918.216
- Yang, H.-F., Pan, A.-J., Hu, L.-F., Liu, Y.-Y., Cheng, J., Ye, Y., et al. (2017). *Galleria mellonella* as an in vivo model for assessing the efficacy of antimicrobial agents against *Enterobacter cloacae* infection. *J. Microbiol. Immunol. Infect.* 50, 55–61. doi: 10.1016/j.jmii.2014.11.011
- Zaman, S. B., Hussain, M. A., Nye, R., Mehta, V., Mamun, K. T., and Hossain, N. (2017). A review on antibiotic resistance: alarm bells are ringing. *Cureus* 9:e1403. doi: 10.7759/cureus.1403
- Zheng, Z., Liu, Q., Kim, W., Tharmalingam, N., Fuchs, B. B., and Mylonakis, E. (2017a). Antimicrobial activity of 1,3,4-oxadiazole derivatives against planktonic cells and biofilm of *Staphylococcus aureus*. *Future Med. Chem.* 10, 283–296. doi: 10.4155/fmc-2017-0159
- Zheng, Z., Tharmalingam, N., Liu, Q., Jayamani, E., Kim, W., Fuchs, B. B., et al. (2017b). The synergistic efficacy of *Aedes aegypti* antimicrobial peptide cecropin A2 and tetracycline against *Pseudomonas aeruginosa*. *Antimicrob. Agents Chemother.* 61:e00686-17. doi: 10.1128/AAC.00686-17

Conflict of Interest Statement: The authors declare that the research was conducted in the absence of any commercial or financial relationships that could be construed as a potential conflict of interest.

Copyright © 2019 Tharmalingam, Khader, Fuchs and Mylonakis. This is an open-access article distributed under the terms of the Creative Commons Attribution License (CC BY). The use, distribution or reproduction in other forums is permitted, provided the original author(s) and the copyright owner(s) are credited and that the original publication in this journal is cited, in accordance with accepted academic practice. No use, distribution or reproduction is permitted which does not comply with these terms.

Advantages of publishing in Frontiers



OPEN ACCESS

Articles are free to read
for greatest visibility
and readership



FAST PUBLICATION

Around 90 days
from submission
to decision



HIGH QUALITY PEER-REVIEW

Rigorous, collaborative,
and constructive
peer-review



TRANSPARENT PEER-REVIEW

Editors and reviewers
acknowledged by name
on published articles

Frontiers

Avenue du Tribunal-Fédéral 34
1005 Lausanne | Switzerland

Visit us: www.frontiersin.org

Contact us: info@frontiersin.org | +41 21 510 17 00



REPRODUCIBILITY OF RESEARCH

Support open data
and methods to enhance
research reproducibility



DIGITAL PUBLISHING

Articles designed
for optimal readership
across devices



FOLLOW US

@frontiersin



IMPACT METRICS

Advanced article metrics
track visibility across
digital media



EXTENSIVE PROMOTION

Marketing
and promotion
of impactful research



LOOP RESEARCH NETWORK

Our network
increases your
article's readership